CANCER RESEARCH UK | OXFORD CENTRE

Small Molecule Colorimetric and Fluorescent Probes for Specific Protein Detection

A thesis submitted in part requirement for the degree of Doctor of Philosophy



James Edward Egleton

Department of Organic Chemistry, University of Oxford

July 2015

To my grandmothers, Marie and Beatrice,

who are dearly missed and to whom I am eternally grateful.

Abstract

This thesis describes the design, synthesis, analysis, mechanistic evaluation and optimisation of small molecule probes for the specific detection of proteins, focusing on the target protein human arylamine *N*-acetyltransferase type 1 (HUMAN(NAT1)) and its murine homologue, mouse arylamine *N*-acetyltransferase type 2 (MOUSE(NAT2)).[1] The *HUMAN(NAT1)* gene is reported to be one of the most highly overexpressed genes in estrogen-receptor-positive (ER+) breast tumours, leading to its potential use as both a novel diagnostic biomarker and a novel therapeutic target for this disease.[2]

Chapter 1 reviews the literature on optical methods for the specific detection of a protein target, exploring strategies both based on biosensors and on chemical probes, before introducing the arylamine *N*-acetyltransferases as a family of enzymes. In **Chapter 2**, a family of naphthoquinone inhibitors of HUMAN(NAT1) are introduced, which undergo a colour change from red to blue upon binding specifically to the enzyme. The mechanism of this colour change, a proton transfer-mediated process, is discussed *via* the synthesis, pharmacological and colorimetric evaluation of close analogues of the hit compound lacking a key acidic sulfonamide-N*H* proton. During these studies, it was found that direct *O*-methylation of a sulfonamide is possible under certain conditions; such a reaction has not previously been reported. Furthermore, upon heating in polar solvents the *O*-methylated sulfonamide was observed to undergo rearrangement, and the mechanism of this process is investigated *via* NMR and kinetic studies.

In **Chapter 3**, the design, synthesis and evaluation of HUMAN(NAT1) inhibitors with improved pharmacological and colorimetric profiles over the initial hit are described. From this optimisation, structure-activity relationships and an *in silico* model of interactions between the inhibitors and enzyme are evaluated. Testing of these compounds in cellular environments, however, exposes some limitations of this approach, notably the lack of sensitivity of the probes when dosed at low concentrations in cellular samples.

Abstract

In order to overcome this limitation, in **Chapter 4** fluorescent analogues of the hit compound are designed and synthesised. Initial compounds developed in this series possess promising properties, but each compound generated suffers from either a low fluorescent intensity, lack of a *p*H-dependent switch in fluorescence or a low fluorescence excitation wavelength, which overlaps with those of tryptophan or tyrosine residues in proteins. Insights into the mechanism of molecular fluorescence and application of some simple quantum mechanical principles, however, lead to the design of a species which possesses all the required properties. The fluorescent emission intensity of this probe correlates linearly with [MOUSE(NAT2)] in *E. coli* cell extracts, and can quantify as little as 0.64% MOUSE(NAT2) in the samples; furthermore, the probe is capable of unambiguously detecting HUMAN(NAT1) within a cell extract from the ER+ breast cancer cell line ZR-75-1; future work on this probe may therefore enable its clinical use in improved early diagnosis of breast tumours. This study also represents, to the best of our knowledge, the first ever example of a small molecule, non-covalent probe capable of quantifying the concentration of a target protein in cellular extracts.

In **Chapter 5**, the series of naphthoquinone probes is further optimised in order to study the roles of HUMAN(NAT1) in a cellular environment. Firstly, structure-activity relationships are utilised to design inhibitors with improved physical properties such as aqueous solubility and cell membrane permeability, in order to test the effect of HUMAN(NAT1) inhibitors in tumour cell models, which could have implications for the future use of a HUMAN(NAT1) inhibitor as a therapeutic agent in oncology. Secondly, the effect of the cofactor folic acid on the function and activity of HUMAN(NAT1) is explored. Finally, in **Chapter 6**, the conclusions of this study are outlined and a hypothesis as to how the concepts developed in this thesis might be applied to alternative, more ubiquitous biological targets is discussed, paving the way for future investigations.

1. Kawamura, A. *et al.*, *Biochem Pharm*, **2008**, *75* (7), 1550-1560.
2. (a) Tozlu, S. *et al.*, *Endrocr Relat Cancer*, **2006**, *13* (4), 1109-1120; (b) Adam, P. J. *et al.*, *Mol Cancer Res*, **2003**, *1* (11), 826-835.

Declaration

This thesis and the work of which it is a record were carried out by myself unless otherwise acknowledged. Three undergraduate students under my supervision, Kate S. Hadavizadeh (KSH), Robert Barker (RB) and Robyn Zorab (RZ), have contributed to this work; their contributions are clearly acknowledged where appropriate. No part of this thesis has been submitted in any other previous application for a higher degree.

James Edward Egleton

Oxford, Friday 24th July 2015

Acknowledgements

Firstly, I would like to express a huge gratitude to Prof. Angela Russell and Prof. Edith Sim for advising me over the past 4 (5!) years. **Angie**, I appreciate the freedom you have given me and trust you have shown for me to develop this project in my own directions – I hope this thesis does you proud. I can only apologise that I still can't draw hexagons! **Edith**, thank-you for all the support, wise words, an enjoyable conference and efficiency in getting papers published – it has been a pleasure to work with you and I wish you and Bob all the best for retirement.

My biggest and most heartfelt thanks go to three exceptionally talented people: Kate, Rob and Robyn (Z), what amazing Part II students you have been and I cannot thank you enough for all you have done. **Kate**, thanks for trusting my inexperienced self, the best (Iranian, obviously) pistachios, not being as clumsy in the lab as me, instigating a trend in hilarious thesis acknowledgements, and for being the most efficient person I know! Super-Jeggy enjoyed rescuing you from "The Master" and our fun times in "pharmalology"… **Rob**, the Timone to my Pumba, thanks for all your excited ideas and all those TLCs. I had radio, but you got me music: thanks for teaching me how to count to five. Every time I walk down George St I now hear the words "it's his first Hannukah away from home" and I laugh uncontrollably. I can't say I'm surprised we've ended up choosing the same career, and I look forward to all those drinks in the big city. **Robyn**, part-time colleague, full-time friend: it's been really special to teach/supervise you from Prelims to Part II, and I could not have wished for a more genuine and lovely person to do so with. You're a total (prize-winning!) star and I am beyond proud of you. I'm sure the alarm clock will come in handy in the real world…

To my G7 family: you've been amazing. **Lucia**, our little hungry caterpillar – you brightened up the lab with Spanish wit and charm, through all the lows (like that time we made Gu mad) and highs (helium?!). I think you might have even found time to play some sort of sport, but I can't for the life of me remember what. Whenever I hear Pitbull, the Ting Tings or a stereotypical Mexican song – or I catch sight of a snowman – I think of you and smile. I hope you've learnt

on your travels how to cook noodles that aren't blue. But above all, thanks for being a true friend – you're most definitely a butterfly now. **Fernando-dog**, the older brother I never had, there simply are no words to express how fantastic you are. No-one can match your levels of patience, generosity and willingness to help in any situation. Every time I watch the Algerian football team play (come on!) I will wear my Angelina Jolie T-shirt and have a plate of buenos nachos. Just remember that Malta is better than Spain, and that YOU. CANNOT. TOUCH. THIS. To **Marcus**, for the entertainment you brought to the lab – we liked you really (x 67). I enjoyed our games of "around the world with Marcus", and thanks for not killing Robyn when you blew the lab up! And of course, to the modern-day Chinese Jesus herself, Dr Linlu Liu, otherwise known as our dear leader Kim. Or just plain old Gu. **Gu**, not only have you been the source of all lab wisdom and knowledge, you have managed to cheer me up when things were bad (well, except when you made them worse) and always had something entertaining to say. Thanks for teaching me the best way to kill people (ice, rope, heat gun), for advice on how to take care of hedgehogs, and for all the Gu-isms: today has definitely been a total rip-off. Thanks for the karaoke, the most bizarre "would you rather" conversations, your good humour over the G7 map, and for proof-reading. I hope in return I have taught you the way to Oxford train station, and that 92% of people make up statistics.

To my fellow D.Phils., I know I have made friends for life. **Fit Amy**, jungle woman Amazonian extraordinaire, what can I say? You've been the best of friends, best of colleagues, hilarious beyond belief and have the most ridiculous stories. And you were just so strong. It's almost as if you believed in yourself... How you balanced doing chemistry and the thing with oars I don't know. Hell, you even methylated arginine. I think. I promise I'll keep quiet about that time you swigged gin under my desk… **Caitlin**, "story of the day" is an institution, and don't think that because I'm leaving you're getting any less spam/tumblr/vine/DM/BuzzFeed in your inbox, because e-mail, satire, wit and stupid people know no boundaries. When we are filthy rich we will eat in every Michelin-starred restaurant in London. And if it all goes wrong, we'll get drunk and it'll be OK. **Aini**, our little forest/city/lab elf, thanks for bringing your Scandinavian humour, language (nulla mustikoida!) and drinking habits to the lab; Friday night UC-Spoons-

Maxwells wouldn't be the same without you. I hope you can move on after your divorce from Josh without too many tears (of joy). To **Becky (H)**, for all the enjoyable tea breaks and dinners. And to **Gammack**, for being Gammack.

To the other Part IIs, with whom I have shared many good times. **"Baby" Bethy**, Fridays aren't the same without your cakes!! It really was some effort to keep that up for a year (*cough* Rob *cough*), and thanks for our sweets from abroad: overeaters anonymous 4eva. Thanks for bringing the world's finest rants and Simlish to the lab – dis wompf es fredesche. If I fall on hard times, I'll remember how to fake dystonia. To **Joe**, for your questionable humour and ability to even push Amy to the limits of her dirty mind. To **Robyn (H)**, for being such a great friend and uni club drinking buddy: I will forever be indebted to you for introducing me to Breaking Bad, chilli cheese bites, GeoGuessr, MiniMetro and so many other gems. And for mini Jeg! To **Hannah (B)**, for the laughs, and proving that you can literally break yourself but still get through a lab project… To **Oakley**, for the joakleys. To **Angelica**, for our shared love of awful TV. To **Phil**, for bringing Shakira to the lab. To **Becky (C)**, **Wenye**, **Ceri**, **Josh** and **Jess** – I have enjoyed working with you all. And to **Ulrich**, for singing Happy Birthday.

To all the post-docs who have taught me so much. **Carole**, it staggers me how generous you are and how you will always go above and beyond to lend a hand. For all the funny stories, your brutally honest advice, everything Alice-in-Wonderland related and for always being up for a drink when I needed one most, thank you so much. In particular I will never forget the support you have given me over the past few challenging months, and for proof-reading this thesis I am eternally grateful. To **Camilo**, just because I'm leaving, don't think that Super-Jeggy isn't watching you. There will always be damsels in distress to rescue! Thanks (or perhaps not?) for introducing Jeggles of the week, and THAT Christmas carol. To **Noelia**, for always being willing to help, for your calming aura and for generally just being ridiculously lovely in every way. To **Pete**, for helping me through the early days and teaching me all I know about practical chemistry; a million thanks for your patience when things went wrong at 6pm on a Friday. To **Alan** – sorry for turning your fume hood purple on day 1. To **James**, for help with all

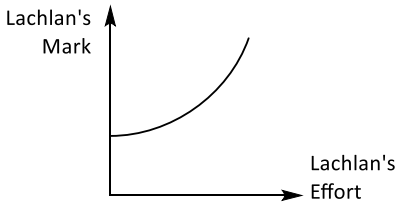
manner of reaction and mechanistic troubleshooting, for being a great colleague in teaching, and for all the puns and tea break banter. To **Helen (N)**, for always bringing a smile to the lab and for being game for just about any social activity we could conjure up. To **Rod**, for good cheer, wit, humour and for being a huge help with cells. To **Kristina**, for your no-nonsense approach and encyclopaedic knowledge of organic chemistry. To **Dave**, for having no idea how helpful the comment "aren't fluorenes planar?" would be. To **Nicky**, for good banter – it's a shame I didn't have the opportunity to work with you for longer. To **Méabh**, for your Irish charm. To **Graham**, I still don't really know what you do….but sincerest thanks for all the many helpful discussions. We'll have to have a 10k rematch at some point (where you don't cheat). To **Ali**, for help with protein purification and solving my biology woes! I know you're going to make a great academic. To **Nicola**, you are an inspiration and I feel privileged to have learnt from you. To the NMR and MS staff, particularly **Barbara**: thank-you for your help and time. To **Hayden**, for assistance with HPLC. And to everyone in pharmacology: **Abby**, **Helen (S)**, **Katherine**, **Diana**, **Hilary**, **Ant**, **Grant**, **Inês**….and **Stuart**, for good cheer and good conversation.

To all at New College and Corpus, thanks for six enjoyable years; to Hertford, for a scholarship; and to CRUK for funding! Thanks to all my colleagues at NC and SEH: to **David Manolopolous** and **Steve Davies** for giving me the opportunity to teach, **Paul Roberts** for helpful discussions, **Rob Jacobs** for maths help, **John McGrady**, **Philip Mountford**, **Mike Laidlaw**, **Matt Rattley** and most of all, **Chris Timmel**: Chris, thank-you for being such a great mentor to me, and I leave Oxford considering you not just an excellent tutor and colleague, but also a friend.

To the Teddy Hall chemists: **Katie**, it's been the most rewarding thing to see you become such a good and confident chemist and I couldn't be prouder of you. Thanks for all the sweets, diet cokes, laughs and strong chat! **Emma**, you've been a joy – I'm going to miss your bubbly nature, pictures of cats, rants about Oxford/men/life, and being put in my place. **Will**, congrats on being equally good at Chemistry and Tinder. **Rhiannon**, I hope I've managed to impart a tiny fondness of organic chemistry in you! You'll miss it... **Marie**, your dedication is second to none – I look forward to reading all your *Nature* papers. **Alex**…glad you finished

your labs. **Jake**, you're incredibly gifted and I'm sure you're going to enjoy the CDT! **Sophie** and **Henry**, I enjoyed teaching you a lot and I wish you the best for the future. **Greg**, **Tom**, **Lucy**, **Anny** and **Gareth** – your good banter was unwavering. **Parky**, you're unique.

To the NC class of 2015: **Katie**, you might be terrible at hangovers, but you're "flipping brilliant at chelation control" (your words not mine!). I promise I won't forget that benzene is not a chair... **Andy**, I'm not sure gown-wearing in tutes will ever be a "thing", but bismuth certainly is. **Adam**, you pushed me to the limits of my knowledge, and were never "workshy"! I know all three of you are going to make a great success of your doctorates. **Dohmnall**, you're going to be successful in life and I really hope you make it as a singer. **Alicia**, I hope you find teaching as rewarding as I did, and that the teenagers aren't too troublesome! **Henry**, you're going to make one hell of a doctor – best of luck with the further study. **George**, your cheeky banter will serve you well in the city! **Lachlan**, here's a quick graph:



Finally, thank-you to all outside the lab who have made these past four years special too. To my OMO friends – thank-you for the music, many a pub evening and the best tours ever. To my fellow tour manager, housemate and partner in crime **Hannah (H)**: you're amazing. To my other wonderful housemates: **Zoë**, I'm really going to miss the daily adventures of someone who leads a spookily parallel life to mine…and all the cakes and sound words of advice!! **Michaela**, I hope I've taken in some knowledge about stone-age man, and I look forward to seeing you fronting a reality TV show at some point. To **Johnathan**, **Krishna**, **Dan**, **Jemma** and **Lizzie**, I'm so glad "Best of Britain" night became a reality. To **Hannah (F)**, for deciding one day to start playing the violin again, because I can't imagine life without you. And to all my family and friends, for being the most amazing people, and always being there when I needed you.

Feliz Navidad.

Abbreviations

4AS	4-aminosalicyclic acid
4AV	4-aminoveratrole
4BA	4-bromoaniline
4CA	4-chloroaniline
5AS	5-aminosalicylic acid
A	Ampere; acceptor
Å	Ångström
A to B	apical to basolateral
A_x	absorption at wavelength x nm
a.u.	arbitrary units
Ab	antibody
Ab_2	secondary antibody
ABPP	activity based protein profiling
Ac	acetyl
AcCoA	acetyl coenzyme A
ACD	Advanced Chemistry Development
ACT	α_1-antichymotrypsin
AFB_1	aflatoxin-B_1
AFP	alpha-fetoprotein
Ag	antigen
AGD	affinity-guided DMAP
Ala	alanine
AMC	7-amino-4-methylcoumarin
ANL	aniline
app.	apparent
APS	3-aminopropyltriethoxysilane
APTEC	aptamer-tethered enzyme capture
aq.	aqueous
Ar	aryl
Arg	arginine
ASL	anisole
Asp	aspartic acid
atm.	atmosphere
AuNP	gold nanoparticle
AuNR	gold nanorods
ax	axial
B to A	basolateral to apical
B_2R	bradykinin B_2 receptor
$B_{AC}2$	basic ester hydrolysis, second order, with acyl-O bond cleavage
BCA	bicinchoninic acid
bFGF	basic fibroblast growth factor
BFP	blue fluorescent protein
BirA	biotin ligase
BlaC	β-lactamase C

Bn	benzyl
Boc	*tert*-butyl carbamate
BODIPY	boron-dipyrromethene
BPH	benign prostate hyperplasia
bpy	bipyridyl
br.	broad
BSA	bovine serum antigen
BZ	benzethonium chloride
c	concentration in g/100 mL
c.	concentrated
c.	about
C	concentration
CA	cancer antigen; California
cal	calorie
CAP	catabolite activator protein
CAPS	*N*-cyclohexyl-3-aminopropanesulfonic acid
cat.	catalytic
CB	conjugate base
CDI	1,1'-carbonyldiimadazole
CE	capillary electrophoresis
CEA	carcinoembryonic antigen
cf.	see, by way of comparison; compared to
CHES	*N*-cyclohexyltaurine
cLogP	calculated LogP
cm^{-1}	wavenumber
CNT	carbon nanotube
CoA	coenzyme A
Con A	concanavalin A
Cond.	conditions
Cong II	congerin II
Cpd	compound
CT	charge transfer
CTAB	cetyltrimethylammonium bromide
CuAAC	copper-catalysed azide-alkyne 1,3-dipolar cycloaddition
Cys	cysteine
d	doublet
d	distance
D	diffusion coefficient
D	dextrorotatory
Da	Dalton
DBF	dibenzo[*b*,*d*]furan
DCE	dichloroethane
dd	doublet of doublets
ddd	doublet of doublet of doublets
deg	degree
DFT	density functional theory
DhaA	haloalkane dehalogenase

DHFR	dihydrofolate reductase
DIAD	di-*iso*-propyl azodicarboxylate
DLS	dynamic light scattering
DMA	*N*,*N*-dimethylacetamide
DMAB	*para*-dimethylaminobenzoic aicd
DMAP	4-dimethylaminopyridine
DMF	dimethylformamide
DMSO	dimethyl sulfoxide
DNA	deoxyribonucleic acid
dq	doublet of quartets
dquin	doublet of quintets
dt	doublet of triplets
DTNB	5,5'-dithio-*bis*(2-nitrobenzoic acid)
DTT	dithiothreitol
e^-	electron
E	energy
E. coli	*Escherichia coli*
e.g.	for example
***Ec*DHFR**	DHFR from *E. coli*
ECL	electrochemiluminescence
EDC	1-ethyl-3-(3-dimethylaminopropyl)carbodiimide
EDT_2	di(ethylene dithiol)
EDTA	ethylenediaminetetraacetic acid
EGFR	epidermal growth factor receptor
ELISA	enzyme-linked immunosorbent assay
ELONA	enzyme-linked oligonucleotide assay
em	emission
EOA	4-ethoxyaniline
eq.	equivalents
equ	equatorial
ER	estrogen receptor
ER+	estrogen-receptor-positive
ESI	electrospray ionisation
Et	ethyl
EWS	evanescent wave spectroscopy
ex	excitation
F	phenylalanine
FA	folic acid
FB_1	fumonisin B_1
FBS	foetal bovine serum
FGE	formylglycine-generating enzyme
FI	field ionisation
FITC	fluorescein isothiocyanite conjugate
FlAsH	fluorescein arsenical helix binder
fluor	fluorophore
FR	folate receptor
FRET	fluorescent resonant energy transfer

g	gram; gaseous
G	glycine
G_2/M	pre-mitotic/mitotic phase
GAD	glutamic acid decarboxylase
GFP	green fluorescent protein
Gln	glutamine
Glu	glucagon
Glu	glutamic acid
Gly	glycine
GNAT	Gcn5-related *N*-acetyltransferase
GOx	glucose oxidase
GPCR	G-protein coupled receptor
h	hour
h	Planck's constant
hAGT	human O^6-alkylguanine-DNA alkyltransferase
HAT	histone acetyltransferase
HATU	1-[*bis*(dimethylamino)methylene]-1*H*-1,2,3-triazolo[4,5-*b*]pyridinium 3-oxide hexafluorophosphate
Hb	haemoglobin
hCAII	human carbonic anhydrase II
hCG	human chorionic gonadotrophin
HDZ	hydralazine
HEPES	4-(2-hydroxyethyl)-1-piperazineethanesulfonic acid
HER	human epidermal growth factor receptor
His	histidine
HIV	human immunodeficiency virus
HMBC	heteronuclear multiple bond correlation
HOMO	highest occupied molecular orbital
HPLC	high performance liquid chromatography
HRMS	high resolution mass spectrometry
HRP	horseradish peroxidase
HAS	human serum albumin
HSQC	heteronuclear single quantum correlation
HUMAN(NAT1)	human arylamine *N*-acetyltransferase 1
HUMAN(NAT2)	human arylamine *N*-acetyltransferase 2
Hz	Hertz
I	luminescence intensity
I_0	intensity of incident beam
IC_{50}	half-maximal inhibitory potency
i.e.	that is
IgG	immunoglobulin G
IMPDH	inosine monophosphate dehydrogenase
INH	isoniazid
i_p	peak current
^{i}Pr	*iso*-propyl
IPTG	*iso*-propyl β-D-1-thiogalactopyranoside
IR	infrared

J	coupling constant
k	rate constant
k	geometric constant
k_2	second order rate constant
K_a	acid dissociation constant
K_d	dissociation constant
K_i	affinity constant
KPS	potassium persulfate
L	litre; leucine
L	laevorotatory
l	path length
LAT	large amino acid transporter
LB	Luria-Bertani
LDA	lithium di-*iso*-propyl amide
LDAI	ligand-directed acyl imidazole
LDH	lactate dehydrogenase
LDT	ligand-directed tosyl
LED	light-emitting diode
LIF	laser-induced fluorescence
lit.	literature value
LLE	lipophilic ligand efficiency
LOD	limit of detection
LogP	water/octanol partition coefficient
LRMS	low resolution mass spectometry
LSPR	localised surface plasmon resonance
LUMO	lowest unoccupied molecular orbital
Lys	lysine
m	metre; multiplet
M	molar
m/z	mass/charge ratio
mAb	monoclonal antibody
MAB	molecular aptamer beacon
MALDI	matrix-assisted laser desorption ionisation
Me	methyl
MES	2-(*N*-morpholino)ethanesulfonic acid
min	minute
MMIP	magnetic molecularly imprinted polymer
mNAT2	MOUSE(NAT2)
mol	mole
MOUSE(NAT1)	mouse arylamine *N*-acetyltransferase 1
MOUSE(NAT2)	mouse arylamine *N*-acetyltransferase 2
mp	melting point
MPTES	mercaptopropyltriethoxysilane
mRNA	messenger RNA
MS	mass spectrometry
MW	molecular weight
N	neutral

n	number of electrons
N/A	not applicable
N.D.	not determined
NADH	nicotinamide adenine dinucleotide
NADPH	nicotinamide adenine dinucleotide phosphate
NAT	arylamine *N*-acetyltransferase
NATP	NAT pseudogene
NB	note well
^{n}Bu	*normal*-butyl
NHS	*N*-hydroxysuccinamide
NIR	near infrared
NMR	nuclear magnetic resonance
nOe	nuclear Overhauser effect
NOESY	nucelar Overhauser effect spectroscopy
NP	nanoparticle
NQO	NAD(P)H:quinone oxidoreductase
NT	nanotube
NTA	nitrilotriacetic acid
Nu	nucleophile
OD_x	optical density at wavelength x nm
OEG	oligo(ethylene glycol) thiol
OmpC	outer membrane protein C
Orn	ornithine
P	confidence interval
***p*ABA**	*para*-aminobenzoic acid
***p*ABAglu**	*para*-aminobenozyl-L-glutamate
P-ALM	post-affinity labelling modification
PAP	prostatic acid phosphatase
PBS	phosphate-buffered saline
pdb	protein data bank
PDDA	poly(dimethyldiallylammonium chloride)
PdNP	palladium nanoparticle
PEG	poly(ethylene glycol)
PEG-400	poly(ethylene glycol), mean weight 400 Da
PET	photoinduced electron transfer
pet	Petroleum
***Pf*LDH**	LDH from *Plasmodium falciparum*
***p*H**	$-\log_{10}[H^+]$
Ph	phenyl
Phe	phenylalanine
pK_a	$-\log[K_a]$
pK_{aH}	pK_a of the corresponding conjugate base species
plc	public limited company
***p*LDH**	LDH from *Plasmodium*
POA	4-phenoxyaniline
PoI	protein of interest
P-PALM	post-photoaffinity labelling modification

PPB	plasma protein binding
ppm	parts per million
Pro	proline
PSA	prostate specific antigen
PSS	poly(styrene sulfonate)
***Pv*LDH**	LDH from *Plasmodium vivax*
PYP	photoactive yellow protein
q	quartet
quant.	quantitative
QD	quantum dot
qd	quartet of doublets
qt	quartet of triplets
quin	quintet
quind	quintet of doublets
R	arginine
R	coefficient of multiple correlation
R^2	coefficient of determination
RCF	relative centrifugal force
RDS	rate-determining step
RhoBo	rhodanine *bis*-boronic acid
RIU	refractive index units
RPMI	Roswell Park Memorial Institute
RNA	ribonucleic acid
RP-HPLC	reverse phase HPLC
rpm	revolutions per minute
RSD	relative standard deviation
RT	room temperature
s	second; singlet
S	surface area; serine
S_0	ground electronic state of fluorophore
S_1	first excited electronic state of fluorophore
SAR	structure-activity relationship
sat.	saturated
SBDS	sodium dedecylbenzenesulfonate
SCE	standard calomel electrode
SDS	sodium dodecyl sulfate
SDS-PAGE	sodium dodecyl sulfate-poly(acrylamide) gel electrophoresis
S_EAr	electrophilic substitution, aromatic
SELEX	selective evolution of ligands by exponential enrichment
sep	septet
Ser	serine
SERM	selective estrogen receptor modulator
SET	single electron transfer
shRNA	short hairpin RNA
S_N1	nucleophilic substitution, first order
S_N2	nucleophilic substitution, second order
S_NAr	nucleophilic substitution, aromatic

SPR	surface plasmon resonance
SPW	surface plasmon wave
ssDNA	single-stranded DNA
Sulf	sulfonamide
t	triplet
t	time
$t_{1/2}$	half-life
T3P	propylphosphonic anhydride
^{t}Bu	*tert*-butyl
td	triplet of doublets
tdd	triplet of doublet of doublets
TEMED	tetramethylenediamine
TFA	trifluoroacetic acid
THF	tetrahydrofuran
TIRF	total internal reflection fluorescence
TLC	thin layer chromatography
TMB	3,3',5,5'-tetramethylbenzidine
TMEDA	tetramethylethylenediamine
TMP	trimethoprim
TMS	trimethylsilyl
TNB	thionitrobenzoate
TOF	time of flight
Tol	*para*-methylphenyl
t_R	retention time
Tris	2-amino-2-(hydroxymethyl)-1,3-propanediol
Trt	trityl
Ts	tosyl
TSPO	translocator protein
tt	triplet of triplets
Tyr	tyrosine
U	enzyme unit (1 µmol/min)
UDPGA	uridine diphosphate glucuronic acid
UK	United Kingdom
USR	ultrafast shape recognition
UV	ultraviolet
V	volts; voltage
v	scan rate
v.	version
v/v	volume per volume
VA	Virginia
VEGF	vascular endothelial growth factor
vs.	versus
w.r.t.	with respect to
w/v	weight per volume
WT	wild type
XantPhos	4,5-*bis*(diphenylphosphine)-9,9-dimethylxanthene
XNA	xeno nucleic acid

XPhos	2-dicyclohexylphosphino-2',4',6'-triisopropylbiphenyl
$\alpha_D^{[x]}$	optical rotation at x ^oC
δ	chemical shift
Δ	difference in
ε_{CB}	absorption coefficient of conjugate base species
ε_N	absorption coefficient of neutral species
ε(x)	absorption coefficient at wavelength x nm
θ	torsional angle
λ	wavelength
λ_{em}	wavelength of emission
λ_{ex}	wavelength of excitation
λ_{max}	wavelength of maximum absorption
ν	frequency
ν_{max}	frequency of maximum absorption
φ_f	quantum yield of fluorescence
*	excited state
^oC	degrees Celsius
[x]	concentration of x

Table of Contents

Abstract i

Declaration iii

Acknowledgements v

Abbreviations xi

Table of Contents xxi

1. Introduction 1

1.1. Optical Methods for Specific Protein Detection in Solution 1

1.1.1. Non-Specific Methods for Quantification of Protein Levels 1

1.1.2. The Development of Biosensor Technology 3

1.1.2.1. Protein as the Analyte: Biosensors for Specific Protein Recognition 4

1.1.2.2. Immunosensors for Specific Proteins 5

1.1.2.2.1. Optical Immunosensors Based on Sandwich Modes of Action 7

1.1.2.2.2. Optical Immunosensors Based on Competitive Modes of Action 12

1.1.2.2.3. Optical Immunosensors Based on Direct Binding Modes of Action 14

1.1.2.3. Homogeneous Systems for Protein Detection 19

1.1.2.4. Aptasensors for Protein Detection 21

1.1.3. Covalent Optical Tagging of Specific Proteins: From Fusion Proteins to Small Molecules 26

1.1.3.1. Protein and Peptide Fusion Tags 26

1.1.3.2. Protein Labelling *via* Incorporation of Unnatural Amino Acids 36

1.1.3.3. Covalent Labelling of Native Proteins: Ligation Probes 44

1.1.4. Non-Covalent Probes for Detection of Specific Native Proteins: Substrate Mimics 48

1.1.5. Non-Covalent Probes for Detection of Specific Native Proteins: Towards a Non-Covalent Inhibitory Probe? 51

1.2. Arylamine *N*-Acetyltransferases 53

1.2.1. NATs in Human Function and Disease 54

1.2.2. Known Inhibitors of HUMAN(NAT1) 58

1.3. Aims of the Current Project 60

2. Investigating the Requirements of a Colorimetric HUMAN(NAT1) Probe 61

2.1. Elucidation of the Mechanism of Colour Change of Naphthoquinone **32** in the Presence of HUMAN(NAT1) 61

2.1.1. Evaluation of the *in silico* Model using Molecular Dynamics 63

2.1.2. Synthesis and Evaluation of Sulfonate Ester **36** 67

2.1.3. Studies on the Formation of *O*-Methylated Sulfonamide **35** 72

2.1.4. Studies on the Stability and Rearrangement of *O*-Methylated Sulfonamide **35** 77

2.1.5. Conclusions from Mechanistic Investigations 88

2.2. Determination of the Required Sensitivity of a Colorimetric Probe for HUMAN(NAT1) 89

3. Optimisation of Colorimetric HUMAN(NAT1) Probes 95

3.1. Overview of Structure-Activity Relationship Studies 95

3.2. SAR at C_3 of the Naphthoquinone Core 96

3.2.1. Design and Synthesis of an Inhibitor Library Containing Arylamino-, Alkylamino-, Aryloxy- and Aryl-Substituted Species at C_3 96

3.2.2. Pharmacological Evaluation of the Initial Compound Library 100

3.2.3. Colorimetric Evaluation of the Initial Compound Library 106

3.3. SAR at C_2 of the Naphthoquinone Core 109

3.3.1. Design and Synthesis of Sulfonamido-Substituted Species at the C_2 Position 109

3.3.2. Pharmacological Evaluation of the Sulfonamido-Substituted Library 114

3.3.3. Colorimetric Evaluation of the Sulfonamido-Substituted Library 115

3.3.4. Synthesis and Evaluation of Benzylamido-Substituted Species at the C_2 Position 117

3.3.5. Synthesis and Evaluation of Larger Amide Derivatives at the C_2 Position: Cinnamoyl, Hydrocinnamoyl, 2-Oxo-2-Phenyl and Cyclopropanecarboxy Amides 125
3.3.6. Evaluation of the Pharmacological and Colorimetric Properties of the 2-Amido-3-Chloro-Substituted Intermediates in Inhibitor Synthesis 132
3.4. SAR at C_5-C_8 of the Naphthoquinone Core 135
3.5. A Return to the C_3 Position: Biaryl Derivatives 140
3.6. Evaluation of Probes in Cell Extracts from the Breast Cancer Cell Line ZR-75-1 148
3.7. Conclusions from SAR Studies on Colorimetric Probes 151
4. Development of Fluorescent HUMAN(NAT1) Probes 153
4.1. Conception of Fluorescent Derivatives of Naphthoquinone **32** 153
4.1.1. Synthesis and Evaluation of the Second Generation Lead Compound **238** 154
4.1.2. Synthesis and Evaluation of a Biaryl-Based Library Derived from Compound **238** 158
4.1.3. Determining the Molecular Mechanism of Fluorescence: A Screen of the Naphthoquinone Library 166
4.2. Pursuit of a PET-Quenched System: Inserting a Linker 169
4.2.1. Synthesis of the Methylene-Linked Biaryls **279-281** and Naphthyl **282** 173
4.2.2. Pharmacological and Optical Evaluation of the Methylene-Linked Species 175
4.3. Changing the Fluorophore: Coumarin and Quinolinone C_3 Derivatives 178
4.3.1. Synthesis of Coumarin Derivative **300** 179
4.3.2. Pharmacological and Optical Evaluation of Coumarin Derivative **300** 183
4.3.3. Synthesis of the Coumarin and Quinolinone Analogue Library 186
4.3.4. Evaluation of the Coumarin and Quinolinone Analogue Library 188
4.4. Back to the Biaryls : Rigidified Fluorene Analogues 193
4.4.1. Pharmacological and Fluorescent Evaluation of Fluorene Derivative **323** 195
4.4.2. Increasing the Excitation Wavelength: Design and Synthesis of a Target Library of Fluorene and Dibenzofuran Derivatives 198
4.4.3. Evaluation of the Library of Fluorene and Dibenzofuran Derivatives 202

4.4.4. Evaluation of Ester **326** and Acid **349** in Cellular Samples 207
4.5. Conclusions from Fluorescent Probe Development 211
5. Development of Inhibitors to Study the Endogenous Roles of HUMAN(NAT1) 215
5.1. HUMAN(NAT1) as a Potentially Therapeutic Target in Cancer 215
5.1.1. Introduction of Solubilising Groups at the C_3 Position 217
5.1.2. Evaluation of the Pharmacological and Physical Properties of Derivatives **350-353** 221
5.1.3. Solubilising the Biaryls: Replacement of the Second Aromatic Ring with Heterocycles and Amino Acid Derivatives 228
5.1.4. Strategies to Overcome the Instability of Phenylenediamine C_3 Substituents 240
5.1.4.1. Synthesis and Evaluation of Dipeptide-Substituted **412** 241
5.1.4.2. Attempted Synthesis of Serine-Derived **413** 243
5.1.4.3. Synthesis and Evaluation of Phenylalanine-Derived Species 244
5.1.5. Conclusions from Physical Property Optimisation Studies 252
5.2. The Role of HUMAN(NAT1) in Folate Metabolism 255
6. Concluding Remarks and Future Directions 265
6.1. Concluding Remarks 265
6.2. Future Directions 271
6.2.1. Further Characterisation and Development of Fluorescent Fluorene Probe **326** 271
6.2.2. Elucidation of the Role of HUMAN(NAT1) in NAT +ve Tumour Cell Lines 273
6.2.3. Extension of the Novel Sensing Paradigm to other Targets: Detection of Lysine Acetylation Status 277
7. Experimental 285
7.1. General Experimental 285
7.2. General Synthetic Procedures 287
7.3. Preparation and Characterisation of Compounds Reported in **Chapter 2** 290
7.4. Preparation and Characterisation of Compounds Reported in **Chapter 3** 301

7.5. Preparation and Characterisation of Compounds Reported in **Chapter 4** 372

7.6. Preparation and Characterisation of Compounds Reported in **Chapter 5** 379

7.7. Preparation and Characterisation of Compounds Reported in **Chapter 6** 432

7.8. Expression and Purification of MOUSE(NAT2)_WT 437

7.9. Purification of HUMAN(NAT1)_WT 440

7.10. Growth of ZR-75-1 Breast Cancer Cell Line 441

7.11. Alkylation of the Cys68 Residue of MOUSE(NAT2)_WT 443

7.12. BCA Assay 444

7.13. Protocols for Compound Evaluation 445

7.13.1. Acetyl CoA Hydrolysis Assay 445

7.13.2. Cytotoxicity Studies Against the ZR-75-1 Cell Line 446

7.13.3. Spectrophotometry 447

7.13.4. Titration Experiments to Determine pK_a Values 447

7.13.5. Determination of Absorption Coefficients 448

7.13.6. Fluorescence Studies 449

7.13.7. Docking Studies 449

7.13.8. DFT Modelling Studies 450

Bibliography **451**

Chapter 1: Introduction

1.1. Optical Methods for Specific Protein Detection in Solution

A range of technologies have been developed for the *in vitro* or *in vivo* detection of proteins in the solution phase which make use of either biosensors or chemical probes. In this chapter, the development and use of such methods will be reviewed, with an emphasis on those which give an optical output. The detection of immobilised proteins, by techniques such as western blotting and the many variants thereof, lies outside the scope of this review, although it is a well-established field and has been reviewed extensively in the scientific literature.[1]

1.1.1. Non-Specific Methods for Quantification of Protein Levels

For many decades, several assays have been exploited to quantify levels of protein, non-specifically, present in biological samples such as cell extracts. Many of these are based on optical detection systems, the simplest being an absorbance measurement at 280 nm, since aromatic amino acids – principally tryptophan – strongly absorb radiation of this wavelength.[2] If the absorption coefficient (ε) of the protein in question is known, the absorbance readout correlates directly with protein concentration according to Beer and Lambert's law:[3]

$$A_{280} = (\varepsilon_{280}) \times (\text{path length}) \times (\text{protein concentration})$$

ε values do, however, vary between proteins depending upon their aromatic residue content, and so the use of this method is limited where solutions of protein mixtures are concerned.[2] Hence several reagent-based colorimetric or fluorescent assays which can more accurately quantitate protein concentrations regardless of protein identity have been developed and are widely used.[4] **Table 1.1** summarises some of the main methods available and any particular advantages or disadvantages which these might present. The importance and widespread use of these assays is underlined by the fact that the paper in which Lowry's method was first described[5] is the most highly-cited ever in scientific literature, with over 305,000 citations.[6]

Method (Year)	Reagents	Readout	Linear Range for HSA (mg/L)	Characteristic Advantages	Potential Disadvantages
Biuret Assay (1949)[7]	$CuSO_4$, NaOH and potassium sodium tartrate	Absorption at 565 nm	100-5000*	First chemical method in which protein levels in samples can be quantified	Large amounts of protein sample required
Lowry *et al.* (1951)[5]	$CuSO_4$, NaOH and Folin-Ciocalteu's reagent (Mo^{VI})[8]	Absorption at 750 nm	5-25	More sensitive than Biuret test due to strong absorption from Mo^{IV} formed in redox processes	Standard regression plot dependent on aromatic amino acid composition of protein
Bradford (1976)[9]	Coomassie Brilliant Blue G-250, H^+	Absorption at 595 nm	2-10	Less susceptible to interference from chemicals, except detergents or high buffer concentrations	Nonlinearity between [protein] and absorption above 2 mg/mL
BCA Assay (1985)[10]	$CuSO_4$, NaOH and bicinchoninic acid (BCA)	Absorption at 562 nm	10-1000 0.5-10 ("micro" variant)	100x more sensitive than Biuret method; wide linear range; compatible with samples containing up to 5% surfactant	Sensitive to interference from reducing sugars; anomalous response with Cys-rich proteins
Guo *et al.* (2000)[11]	Dibromohydroxy-fluorone-Mo^{VI}	Absorption at 533 nm	0-8	Complexes stable for up to 15 h after incubation; high sensitivity	Surfactants added to aid water solubility
Capitán-Vallvey *et al.* (2001)[12]	BZ, fibreglass support, Folin-Ciocalteu's reagent[8]	Solid phase absorption at 750 nm	25-200	Higher sensitivity than Lowry's method; less dependent on protein nature; samples stable up to 2 years after incubation	Lesser reproducibility than solution-phase measurements
Chen *et al.* (2004)[13]	2-acrylamidoglycolic acid, KPS and CdS nanoclusters	Synchronous fluorescence at 280 nm ($\Delta\lambda$ = 270 nm)	0.03-2	Very high levels of sensitivity for detecting low concentrations of protein accurately	Different proteins have different properties and may require different standard regression plots
Tsukagoshi *et al.* (2004)[14]	Luminol, H_2O_2 and Cu^{2+}	Chemiluminescence measurement	1.2×10^{-7} to 1×10^{-5}†	Capillary electrophoresis prior to measurement allows simultaneous detection of several samples	Different proteins may give different responses; some not detected
Jiang and Lo (2004)[15]	Doxycycline, Eu^{3+}	Fluorescence λ_{ex} at 612 nm (λ_{em} = 385 nm)	0-9.2 and 9.2-34.5	Enables detection of trace amounts of HSA, e.g. in urine samples	Fluorescent output is highly sensitive to temperature and *p*H
Chen *et al.* (2007)[16]	Toluidine Blue, SBDS (surfactant)	Fluorescence λ_{em} at 648 nm (λ_{ex} = 624 nm)	0.5-50	Simple operation; accurate, reproducible results; no buffer solution required	Sensitive to factors such as ionic strength and temperature
Dong *et al.* (2007)[17]	Methyl Blue, Walpole (acidic) buffer	Resonance Light Scattering at 333 nm	2.0-37.3	Sensitive, reproducible results over relatively large linear range	Can require flow injection for reliable results
Kang *et al.* (2011)[18]	$K_2S_2O_8$, Tb^{3+} and NaOH	Chemiluminescence measurement	3.3-665	High sensitivity and selectivity; wide linear response range compared to other methods	Can require dialysis of samples to remove other interfering metal ions

Table 1.1: Summary of selected methods for non-specific determination of protein concentration, and their relative advantages and disadvantages. *for chicken egg albumin; †for haemoglobin. BCA = bicinchoninic acid; BZ = benzethonium chloride; HSA = human serum albumin; KPS = potassium persulfate; SBDS = sodium dodecylbenzenesulfonate.

1.1.2. The Development of Biosensor Technology

In the broadest sense, a biosensor can be defined as "a device that intimately associates a biological sensing element and a transducer";[19] in other words, these are analytical devices which enable detection of a biological or biologically-derived phenomenon by recording a physical output. Biosensors have found uses in a range of industries, from agriculture to pollution control;[20] however, of particular interest to the present study is their application to clinical healthcare, where the development of point-of-care devices has been instrumental in improving patient health outcomes across a broad spectrum of disease areas.[4, 21]

The development of an electrochemical glucose sensor by Clark and Lyons in 1962 is commonly regarded as the first known example of a biosensing device.[22] This device couples the oxidation of glucose by glucose oxidase (the biological sensing element) with an amperometric readout detailing either the consumption of O_2 or the formation of H_2O_2 (the transduction element). Such glucose sensing devices are still vital today for monitoring blood glucose concentrations in the 5% of the global population who suffer from diabetes.[23] In the following years, many researchers investigated catalytic biosensor systems based on enzyme immunoassays employing bioconjugates.[24] The term "enzyme electrode" was coined in *Nature* by Updike and Hicks in 1967,[25] relating to their invention of an amperometric glucose sensor comprising an oxygen electrode coated in a polyacrylamide gel that entrapped glucose oxidase. Potentiometric examples followed soon after, such as Guilbault and Matalvo's development of a urea-specific enzyme electrode.[26]

The field has subsequently expanded rapidly and detection methods now include not just electrochemical transducers, but optical, thermal and piezoelectric ones amongst others. Catalytic turnover systems for biomolecular recognition were developed into affinity-based systems, in which initiation of detection is dependent on an affinity interaction between the analyte and the immobilised biomolecule, rather than a catalysed reaction. The general configuration of a biosensor as we would acknowledge one today is shown in **Figure 1.1**.

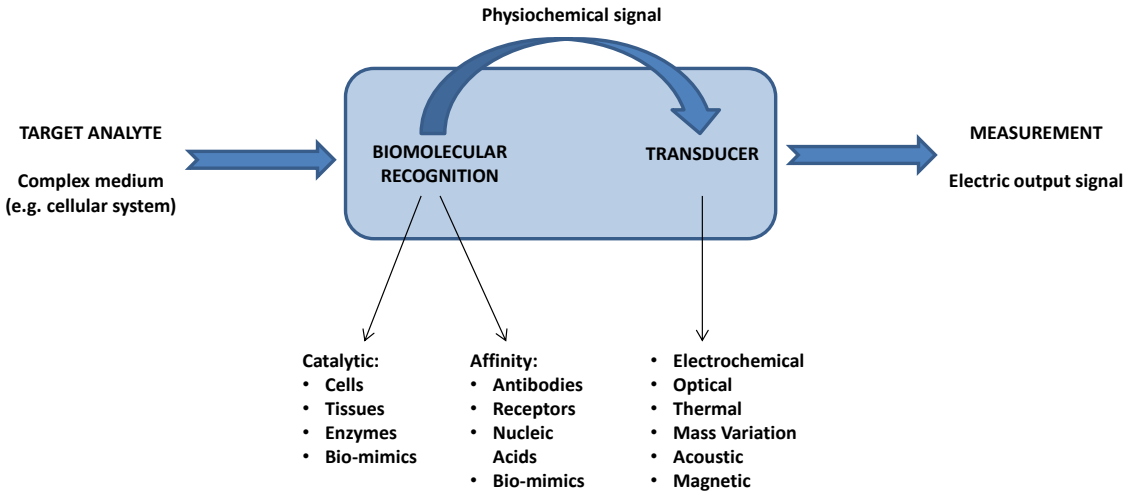


Figure 1.1: Schematic configuration of a biosensor (adapted from *Biosensor Principles and Applications*).[19]

When designing a biosensing device, several practical challenges must be overcome.[19] The first of these is bioamplification: varying degrees of amplification can be obtained when molecular recognition of the analyte occurs. For instance, in catalytic sensing systems one might encounter variability in reaction rates, and hence in the quantity of reagent consumed or product derived in a given time period; meanwhile, in affinity-based systems a 1:1 ratio between analyte and bioreceptor gives no amplification of transduced signal which can lead to sensitivity problems in complex media. Another key issue is that of intrinsic specificity of the biological sensing element. In catalytic sensing elements, if enzymes have anything other than strict specificity[27] then off-target activity may arise and affect the reliability of the transduced biosensor output. Optimisation of specificity is more readily possible with affinity-based sensing systems; for example, the use of monoclonal antibodies (mAbs) can greatly enhance specificity in antibody-antigen (Ab-Ag) recognition interactions.[19]

1.1.2.1. Protein as the Analyte: Biosensors for Specific Protein Recognition

Analytes detected by various types of biosensor include toxins,[28] drugs,[29] pesticides,[30] neurotransmitters,[31] inorganic ions,[32] gaseous species,[33] metabolites,[34] saccharides,[22, 35] oligonucleotides[36] and bacterial cells[37] amongst others. A comprehensive review of optical biosensors for detection of a wide variety of species is given by Borisov & Wolfbeis.[21a]

However, of particular interest to this study is the recognition of proteins at the molecular level. Proteins comprise *c.* 20% of total cell mass,[38] and changes in or misregulation of protein expression, structure or function have been implicated in a vast spectrum of diseases.[39] Thus the ability to accurately and specifically determine the cellular concentration of particular proteins could lead to new advances in the diagnosis and prognosis of disease, more accurate stratification of patients in the quest for "personalised" therapies, and novel biochemical techniques to study disease at the molecular level.

1.1.2.2. Immunosensors for Specific Proteins

The highly specific non-covalent molecular interactions between an antigen (Ag) and an antibody (Ab) have been exploited in the design of many biosensors in which the antigen is a protein. Antibodies are Y-shaped proteins of around 150 kDa in weight which are used by the body's immune system to recognise and eliminate foreign species such as bacteria. **Figure 1.2** illustrates the different possible assays which could be employed in such biosensors. The labelled element in these systems might be, for example, an enzyme, a metal nanoparticle, a fluorescent probe or an electrochemical probe.[4]

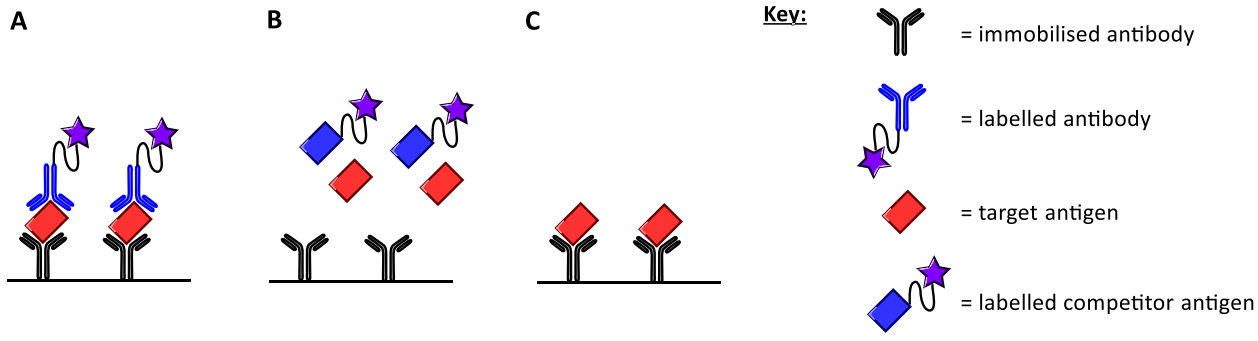


Figure 1.2: Cartoon representations of different possible configurations of immunosensors (adapted from Borisov & Wolfbeis, 2008).[21a] **A:** Sandwich model, whereby the target Ag binds to both an immobilised Ab and an added labelled Ab_2; **B:** Competitive model, whereby the target Ag competes with added labelled Ag for the Ab – readout from the label is inversely proportional to native Ag concentration; **C:** Direct binding model, whereby the direct interaction of Ag and immobilised Ab can be detected without the need for a label.

Immobilisation of antibodies on surfaces can be carried out chemically *via* one of several different techniques; the common strategies employed are as follows:[21a, 21c]

- Formation of a covalent linkage such as an amide or ester bond between the support and the protein, by tagging each of the components with a reactive group;
- Immobilisation of polyhistidine-tagged antibodies *via* complexation to a surface coated in Ni^{2+} or Cu^{2+};
- Formation of a strong noncovalent interaction between biotin (attached to either the solid support or the antibody) and (strept)avidin (conjugated to the other component);
- Attachment of Protein A to the support, which has a high affinity for the Fc region of mammalian antibodies.

A large number of immunosensors for proteins containing an optical transduction element have been developed.[4, 21a, 21b, 40] Readouts based on absorbance, reflectance or fluorescence emissions in the ultraviolet (UV), visible or near-infrared (NIR) ranges are possible. Of these, fluorescence is often the system of choice, because of its higher intrinsic sensitivity as a technique and because of less background noise at key wavelengths in complex biological media such as cellular extracts. However, single-wavelength fluorescence readouts can prove problematic, since these do not contain an internal standard, and this can lead to unreproducible results.[21a] Parker's Law states that the luminescence intensity (I) of an antigen is not only proportional to its concentration (c), but also to several other variables: the intensity of the excitation beam (I_o); the molar absorption coefficient (ε) of the antigen; the path length (l); the quantum yield of fluorescence (φ_f); and a geometrical constant (k).

$$I = I_o \varepsilon c l \varphi_f k$$

In designing an experimental set-up containing an internal reference, the compounding effect of these other variables is neutralised. Therefore, ratiometric fluorescent systems, involving measurements at two wavelengths, have become increasingly common in sensing applications,[41] such as the inclusion of an inert reference fluorophore or using a system based on fluorescent resonant energy transfer (FRET) between a donor and an acceptor. Self-

referencing can also be achieved by the measurement of fluorescence decay time;[32a, 32c] however, measurement on nanosecond or even picosecond timescales can prove difficult.

Below are outlined some specific examples of optical immunosensors for specific protein detection, grouped by their configurations.

1.1.2.2.1. Optical Immunosensors Based on Sandwich Modes of Action

In sandwich configurations, the secondary antibody must be labelled to give an optical readout. Often this is achieved by coupling the antibody to an enzyme; this technique is commonly referred to as an enzyme-linked immunosorbent assay (ELISA). One such sensing system was achieved by Papkovsky *et al.* for detection of murine immunoglobulin G (IgG).[42] The solid support was a glass fibre membrane linked to a phosphorescent metalloporphyrin which is an optical transducer for oxygen sensing; anti-IgG Abs were immobilised onto the surface. The secondary anti-IgG Ab was labelled with glucose oxidase (GOx), and so the ELISA was able to detect oxygen consumption by GOx in the presence of glucose as a measure for the concentration of mouse IgG present with a detection limit of 500 pg/mL; the luminescence decay time of the metalloporphyrin was measured as the internal reference. A similar ELISA protocol was used to detect human lactate dehydrogenase isoenzyme (LDH-1) with anti-LDH-1 antibodies, to a detection limit of 2500 pg/mL.

A major advancement in the field was the recognition that the solid support for the immobilised antibody could itself be used as the optical transduction element. One method by which this is possible is the use of evanescent wave spectroscopy (EWS).[21a] The intensity of an evanescent wave decays exponentially with increasing distance from the surface at which it is generated **(Figure 1.3)**. Therefore, if the immunosensor solid support contains an optical fibre, total internal reflection of a beam of light of a specific wavelength through this fibre generates evanescent waves at the surface where it reflects; these waves travel away from the surface but decay exponentially. Any fluorophore-labelled antibodies or antigens within a very short

distance from the surface (*i.e.* bound to the sensing device) can absorb this light, the frequency of which is specific to excite the fluorophore in their labels. The evanescent waves will however decay before being able to excite fluorophores in any antibodies/antigens not directly bound to the sensor, ensuring that background fluorescence from other species in the media is minimised. Narang *et al.* reported a sandwich assay for ricin detection that relied on this technique:[43] anti-ricin IgG was immobilised onto an optic fibre surface *via* an avidin-biotin interaction and cy5-labelled anti-ricin antibody, which was induced to fluoresce in the presence of an evanescent wave, was used as the secondary antibody. The detection limit of 100 pg/mL is of a comparable order of magnitude to the most sensitive ELISA systems.

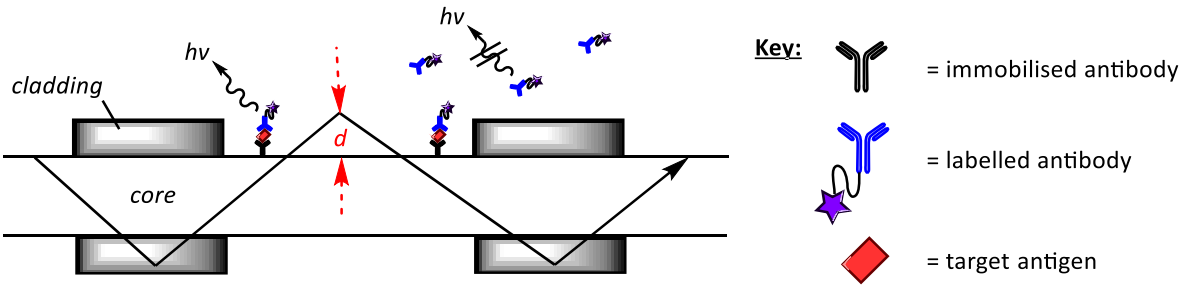
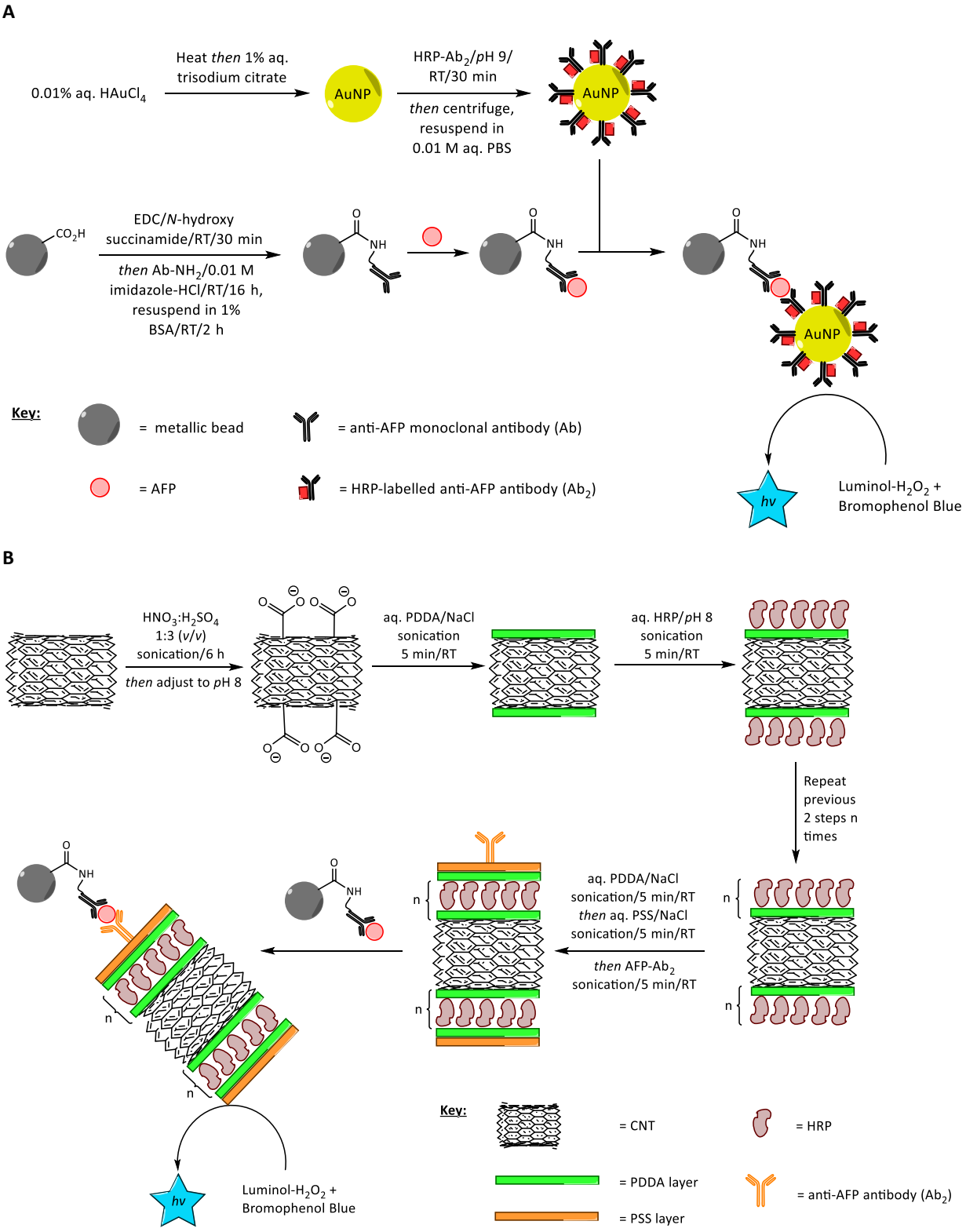


Figure 1.3: Principle of total internal reflection fluorescence (adapted from Borisov & Wolfbeis, 2008).[21a] As a light beam passes through the core of an optical fibre a component of it is totally internally reflected whilst another penetrates into a second medium with a lower refractive index. The evanescent wave generated at the interface of the two dielectric media decays exponentially over a penetrating depth *d*. Any fluorophores present within the distance *d* in a declad zone will be excited by the evanescent wave whilst those further away will not.

Nanotechnology has also been employed in the development of sandwich biosensors.[40] Bi *et al.* have reported two different immunochemiluminescent strategies for detection of the cancer biomarker alpha-fetoprotein (AFP), found in liver conditions including hepatocellular carcinoma and hepatoblastoma.[44] In both cases, the primary anti-AFP antibody is immobilised to a carboxyl-modified metallic bead. Metallic beads are useful immobilisation platforms for biosensors as they have potentially large surface areas, giving a high antibody density, and they enable the direct capture, easy separation and even concentration of target antigens from clinical samples.[45] Ab_2 is labelled with horseradish peroxidase (HRP) and is immobilised either to a gold nanoparticle (AuNP)[46] or a carbon nanotube (CNT)[47] **(Scheme 1.1)**.



Scheme 1.1: Immunochemiluminescence assays for detection of the cancer biomarker alpha-fetoprotein (AFP). **A:** System in which anti-AFP Ab_2 is immobilised on an AuNP;[46] **B:** System in which Ab_2 is immobilised on a CNT.[47] Ab = antibody; AuNP = gold nanoparticle; BSA = bovine serum albumin; CNT = carbon nanotube; EDC = *N*-(3-dimethylaminopropyl)-*N*'-ethylcarbodiimide; HRP = horseradish peroxidase; PBS = phosphate-buffered saline; PDDA = poly(dimethyldiallylammonium chloride); PSS = poly(styrene sulfonate).

Formation of the sandwich complex and subsequent addition of luminol and H_2O_2 with bromophenol blue as a signal enhancer generates a quantifiable chemiluminescent output *via* reaction catalysed by HRP. Use of AuNPs gives both enhanced sensitivity and reduced assay duration over ELISA techniques, with an AFP detection limit of 10 pg/mL **(Scheme 1.1A)**. Use of CNTs further decreases the detection limit to 8 pg/mL, since enzyme multilayers can be constructed on CNT surfaces using an electrostatic layer-by-layer construction approach with anionic HRP and polycationic poly(dimethyldiallylammonium chloride) (PDDA), leading to a large amplification of the chemiluminescent signal upon binding of a single secondary antibody to AFP **(Scheme 1.1B)**. Jokerst *et al.* meanwhile developed an immunofluorimetric assay for the detection of the cancer biomarkers carcinoembryonic antigen (CEA), cancer antigen 125 (CA125) and Her-2/*Neu* in serum or saliva samples using semiconductor nanoparticle quantum dots (QDs) as the label on the secondary antibody,[48] giving a thirty-fold signal amplification over standard molecular fluorophores.

Nanoparticles can also be used to improve the sensitivity of classical ELISA tests themselves, as demonstrated by Ambrosi *et al.*:[49] immobilisation of HRP-Ab_2 conjugates for detection of the breast cancer glycoprotein marker CA15-3 to AuNPs gave two-fold increased sensitivity, a lower detection limit and a shorter assay time in a colorimetric assay using 3,3',5,5'-tetramethylbenzidine (TMB) than in the absence of AuNPs, attributed to the "concentrating" effect that AuNPs have on the signalling antibodies.

In a recent development of the sandwich configuration, Zhou *et al.* have replaced the first antibody with a magnetic molecularly imprinted polymer (MMIP) as the antigen capture probe, for haemoglobin (Hb) detection **(Figure 1.4)**.[50] The second antibody uses $Ru(bpy)_3^{2+}$-doped silica-doped Au ($Ru@SiO_2@Au$) as its label; upon sandwich formation an electrochemiluminescent readout can detect haemoglobin in as low a concentration as 0.023 pg/mL, due to the ability of MMIPs to enrich trace concentrations of antigens from a solution sample. An extension of this methodology from the same laboratory has enabled detection of the anti-human immunodeficiency virus-1 (HIV-1) antibody as the protein

analyte,[51] by creating a sandwich complex from MMIPs, anti-HIV-1 and HIV-1 conjugated to horseradish peroxidase as the label (HRP-HIV-1) and optically detecting this complex *via* chemiluminescence after addition of luminol and H_2O_2. The ability to detect anti-HIV-1 to a dilution factor of 1:60,000 is promising for the improvement of early diagnosis of HIV-1 infection, since the window for anti-HIV-1 detection is 4-8 weeks after infection.[52]

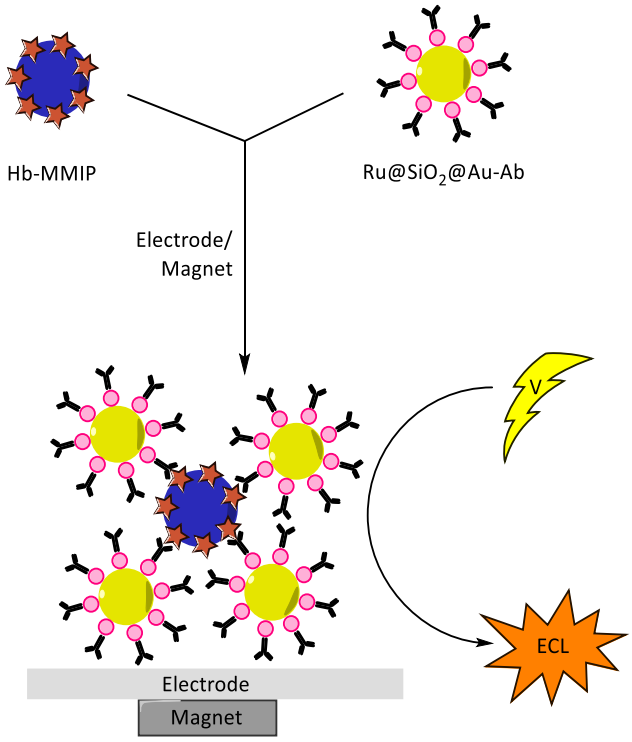


Figure 1.4: A "single antibody sandwich" model, in which use of MMIPs as the antigen capture probe for Hb in solution enables a large increase in the effective concentration of antigen when Ab, bound to an AuNP doped with $Ru(bpy)_3^{2+}$-doped silica, is added and the particles are brought to an electrode surface by a magnet. Application of a voltage generates an [Hb]-dependent electrochemiluminescent signal from the Ru^{2+} label.[50] Ab = antibody; AuNP = gold nanoparticle; ECL = electrochemiluminescence; Hb = haemoglobin; MMIP = magnetic molecularly imprinted polymer.

Cecchin *et al.* have also used a modified ELISA protocol to detect the HIV-1 protein gp120 in ultralow concentrations; the elegance of their particular strategy is that concentrations of gp120 as low as 10^{-17} g/mL could be detected and clearly distinguished from the control test with BSA *by the naked eye*.[53] In their experimental setup, Ab_2 is biotinylated and after the

assay, plates are treated with a streptavidin-catalase conjugate. After washing, H_2O_2 solution is added to the wells and incubated for 30 min before 0.2 mM $AuCl_3 \cdot 3H_2O$ solution was added. This results in nanoparticle growth which is highly sensitive to tiny concentration changes in H_2O_2: lower concentrations of H_2O_2 found in wells where catalase (and by extension, gp120) is present cause the solution in the wells to take on a blue hue instead of a red one, which is detectable both by visible spectroscopy and by eye with an LOD of 10^{-17} g/mL.

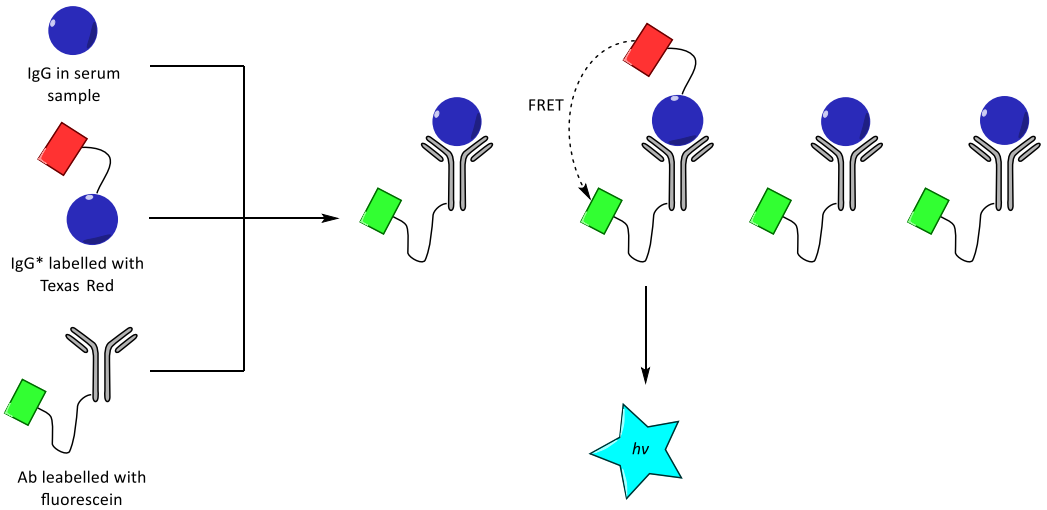
1.1.2.2.2. Optical Immunosensors Based on Competitive Modes of Action

Optical immunosensors based on competitive binding between a wild-type antigen and a labelled analogue (see **Figure 1.2**) offer some advantages over those based on a sandwich model involving secondary antibodies: it may be possible to reuse the sensing element; antigen levels could be continuously detected over a period of time; and assays might be more rapid. In 1999, Maragos & Thompson developed a flow cell consisting of a capillary tube with fibre-optic sensors in the capillary wall and antibodies against fumonisin B_1 (FB_1) attached to the inner surface of the tube.[54] FB_1 is a toxin found in maize plants. Solution samples from maize plants were spiked with known concentrations of synthetically-prepared FB_1-fluorescein isothiocyanite conjugate solution (FB_1-FITC), which competes with FB_1 for the antibodies in the sensor. When light of λ_{ex} = 490 nm is incident on the sensor, FB_1-FITC fluoresces at λ_{ex} = 520 nm and the output signal is measured; thus the fluorescence intensity is inversely proportional to the concentration of natural FB_1 present in the sample. By comparison to standard curves, the concentration of FB_1 in maize samples over the range of 10-1000 ng/mL could be determined.

Capillary electrophoresis (CE) has also been employed in some competitive immunoassays, to separate mixtures of free antigen and antigen-antibody conjugates in solution prior to optical measurements. One example is German & Kennedy's sensor for detection of the peptide glucagon:[55] to pancreatic samples were added a known concentration of fluorescein-labelled glucagon (Glu*), and after separation of the components by CE, laser-induced fluorescence

(LIF) was used to record the amount of Ab-Glu* complex, the concentration of which is inversely proportional to that of native glucagon in the samples. A similar CE-LIF protocol has been used by Babu *et al.* for the detection of the opioid peptide methionine-enkephalin.[56]

However, the requirement for fast separation of solution components, before the Ab-Ag conjugates can separate, is a downside of CE-LIF techniques, as is protein binding to the capillary walls.[57] One development to mitigate these issues is to immobilise the antibodies on magnetic beads, e.g. packed into a capillary tube over which the test solution flows.[58] Magnets can be used to rapidly separate the beads from the supernatant solution for analysis. One example of this setup is Zhao & Shippy's quantification of IgG in serum samples.[59] Labelled and unlabelled IgG compete for antibodies immobilised on magnetic beads in a capillary tube, which are then separated from the supernatant. The supernatant is blotted onto a membrane and NIR fluorescence is used to detect the concentration of labelled IgG present, which correlates directly to the concentration of unlabelled IgG in the initial serum sample. This technique enables analysis of a single µL of serum with an LOD of 400 pg/mL.



Scheme 1.2: Competitive FRET assay for IgG quantification.[60] Serum samples containing an unknown concentration of IgG were spiked with a known concentration of Texas Red-labelled IgG*. Competition between IgG and IgG* for a fluorescein-labelled antibody results in a fluorescence readout due to FRET between Texas Red and fluorescein, which is directly proportional to [Ab-IgG*] and hence inversely proportional to [IgG]. FRET = fluorescent resonance energy transfer; IgG = immunoglobulin G.

FRET sensing has also been used as the optical readout of choice in analogous immunosensors. Barnard and Walt developed a FRET-based competitive immunosensor for IgG which had the advantage that it could be used to make measurements continuously over a period of up to a month.[60] In this case, the antibody itself is fluorescein-labelled, and the modified IgG antigen (IgG*) was labelled with the dye Texas Red. Competition between labelled IgG* and non-labelled IgG in serum samples thus generated an equilibrium mixture of Ab-IgG and Ab-IgG*. FRET between Texas Red and fluorescein enabled Ab-IgG* to fluoresce; the fluorescence output correlates directly to the concentration of Ab-IgG* and hence inversely to that of IgG **(Scheme 1.2)**. Controlled release of the components was achieved by incorporating them into a poly(ethylene-co-vinyl acetate) matrix.

1.1.2.2.3. Optical Immunosensors Based on Direct Binding Modes of Action

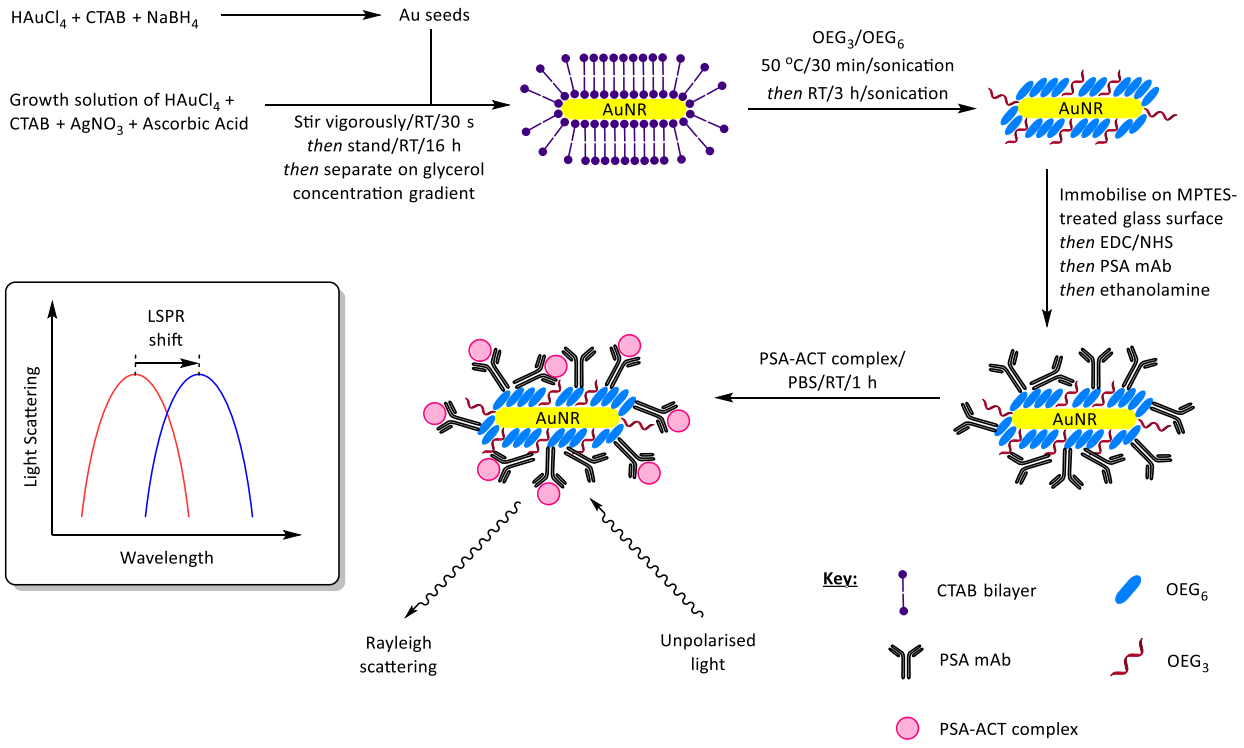
Development of immunosensors which directly measure the interaction between an antibody and the antigen of interest is clearly advantageous in many cases over the techniques described thus far, because labelling of reagents can prove troublesome and time-consuming, and direct methods of quantification are often more reliable than indirect ones. Maragos & Thompson were able to modify their sensors for detecting the toxin FB_1 in maize (see **Section 1.2.2.2.2.** above) for the detection of aflatoxin-B_1 (AFB_1), another naturally-occurring toxin found in their maize samples.[54] Unlike FB_1, AFB_1 is inherently fluorescent (λ_{ex} = 360 nm; λ_{ex} = 427 nm). Use of a dichroic mirror which reflects light at 360 nm in the sensor therefore enabled detection of light generated from AFB_1 bound to anti-AFB_1 antibodies in the sensor, as the emitted light from AFB_1 is partially coupled back into the fibre-optic sensor and transmitted through the dichroic mirror for detection. AFB_1 could be detected at concentrations as low as 2 ng/mL.

Many optical immunosensors based on direct binding rely on their solid support to also act as the transduction element, and hence use of techniques such as evanescent wave spectroscopy (EWS) and surface plasmon resonance (SPR) predominate in these devices. SPR

is a technique which was pioneered in biosensing by Liedberg *et al.* in 1983;[61] its basis is that changes in a surface plasmon wave (SPW) are monitored as an analyte binds to an immobilised antibody. The SPW is an oscillating wave set up at the interface between two materials of dielectric constants of opposite signs, such as a metal (e.g. gold/silver) and a dielectric medium. SPWs can be excited by one of several techniques, such as prism coupling,[62] waveguide coupling,[63] fibre optic coupling[64] or grating coupling.[65] Each of these techniques is reviewed thoroughly by Fan *et al.*;[21b] broadly speaking though, at a particular angle, wavelength or momentum of incident electromagnetic radiation, the propagation constant of this incident radiation will match that of the SPW and a photon will be coupled into the SPW. Upon binding of the target analyte to the antibody, changes in the resonant angle, wavelength or intensity of the SPW are monitored to give a quantifiable readout of analyte concentration.

Most commercially available SPR sensors have a typical LOD of 1×10^{-6} to 1×10^{-7} refractive index units (RIU) and are based on the prism coupling mechanism of action, such as those produced by Biacore.[66] Haasnoot *et al.* used such an instrument (Biacore 3000) in a direct immunoassay for quantifying plant proteins in milk powders.[67] Four assays could be performed simultaneously as four different polyclonal antibodies (reference, anti-soy, anti-pea and anti-soluble wheat protein) were immobilised *via* amide bond coupling on the four different channels of the chip. Methods have subsequently been established for improving the sensitivity of SPR-based biosensors. As SPR methods rely on a change in refractive index on a thin gold film when modified with different components, building a suitable surface monolayer onto the gold film has been found to be crucial to their utility.[68] Using a mixed thiol monolayer improves the surface coverage of the chip by antibodies,[69] and use of a streptavidin-biotin mediated immobilisation strategy enhances the orientation of the protein on the surface.[70] This experimental setup was successfully used by Lee *et al.* in 2005 to detect levels of the autoantibody anti-glutamic acid decarboxylase (anti-GAD) in samples with as low a concentration as 0.5 μM anti-GAD,[71] which is an important tool for predicting, diagnosing and monitoring patients suffering from type I diabetes.[72] Sensitivity of this technique was

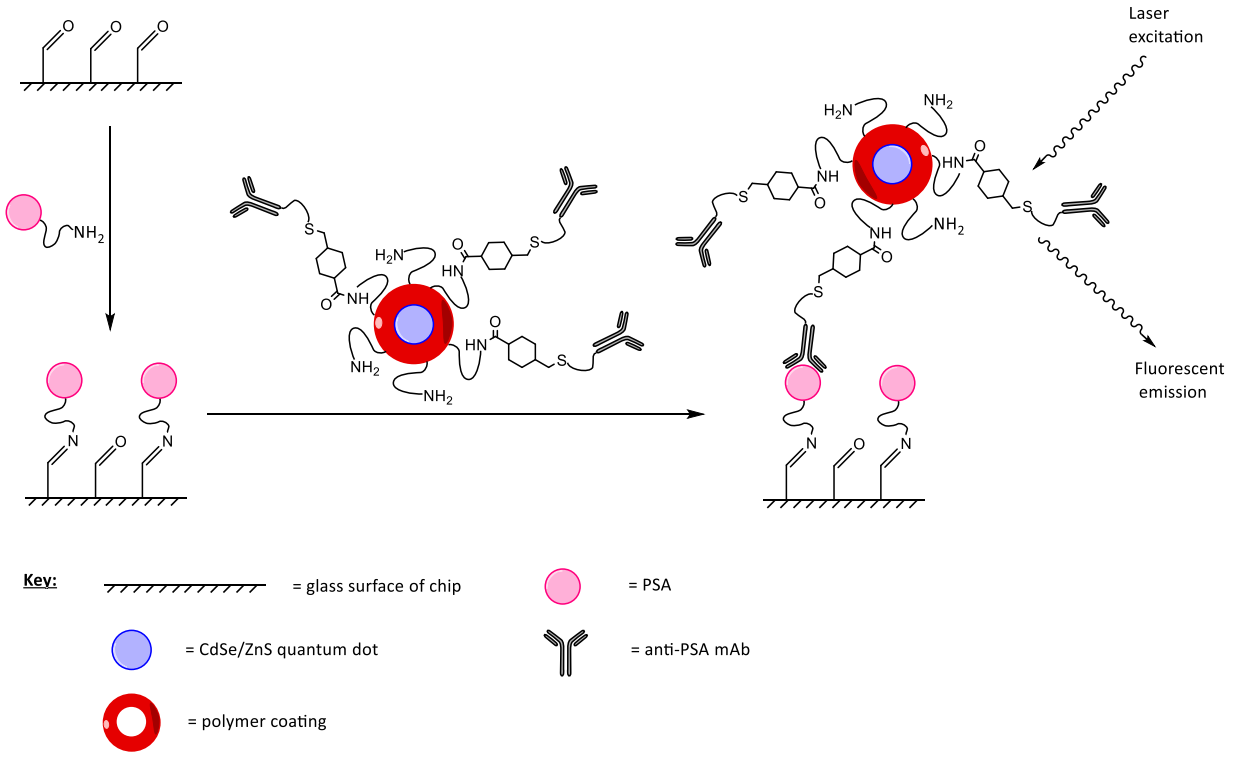
further improved by increasing the *p*H of the buffer solution from 4.0 to 5.5, as this enhanced the immobilisation of positively-charged streptavidin to the gold film as the carboxylic acid groups on the surface monolayer were deprotonated.[73]



Scheme 1.3: Preparation of AuNRs for ultra-sensitive detection of PSA-ACT complex.[74] After initial growth of the nanorods, they are functionalised with OEG_3 and OEG_6 which are cross-linked to the PSA mAbs by amide bonds, and unreacted sites are blocked by ethanolamine. **Inset:** Optical readout is plotted as Rayleigh scattering as a function of wavelength for the AuNR in the absence (red line) and presence (blue line) of PCT-ACT complex. The binding of PSA-ACT complex to the mAbs results in a measurable LSPR shift, proportional to [PSA-ACT] present. Ab = antibody; ACT = α_1-antichymotrypsin; AuNR = gold nanorod; CTAB = cetyltrimethylammonium bromide; LSPR = localised surface plasmon resonance; MPTES = mercaptopropyltriethoxysilane; NHS = *N*-hydroxysuccinamide; OEG_3 = oligo(ethylene glycol) thiol, $HS(CH_2)_{11}(OCH_2CH_2)_3OH$; OEG_6 = oligo(ethylene glycol) thiol, $HS(CH_2)_{11}(OCH_2CH_2)_3OCH_2CO_2H$; PBS = phosphate-buffered saline; PSA = prostate specific antigen.

Nanotechnology has also had a large impact on the development of direct immunosensors, as it has with sandwich-type systems.[40] Nanomaterials such as gold nanorods (AuNRs) possess unique Rayleigh scattering properties which enable the generation of collective electron charge oscillations of a certain wavelength called localised SPRs (LSPRs) when excited with

incident light.[75] As the scattering properties are a function of the dielectric environment of the nanoparticle, AuNRs coated in monoclonal antibodies against prostate specific antigen-α_1-antichymotrypsin (PSA-ACT complex) have been developed which undergo a shift in LSPR λ_{max} upon binding of PSA-ACT complex,[74] a well-established biomarker in prostate cancer patients **(Scheme 1.3)**.[76] The limit of detection is an astonishing 1 aM (*c.* 600 molecules/mL) corresponding to an LSPR λ_{max} shift of 4.20 nm; however, interference from other proteins at high concentrations in complex media still remains a barrier to clinical application.



Scheme 1.4: Use of a CdSe/ZnS QD in a direct immunosensor for PSA.[77] Free amine groups on PSA condense with aldehyde groups on the surface of the sensor; the anti-PSA mAb is conjugated to the QD *via* a 4-(thiomethyl)cyclohexane carbonyl linkage. After washing the surface of the chip, excitation of the quantum dot gives a fluorescent output which is directly proportional to [PSA]. Ab = antibody; PSA = prostate-specific antigen; QD = quantum dot.

Aćimović *et al.* have recently reported a 'lab-on-a-chip' LSPR technique which enables parallel, real-time detection of 32 sensing sites across 8 independent microfluidic channels; they have

demonstrated detection of cancer biomarkers such as PSA and AFP with an LOD of 500 pg/mL in a buffered solution containing 50% human serum.[78] QDs have also been employed as a direct sensing strategy for PSA: PSA in a sample reacts with free aldehyde groups on the surface of the biochip, before anti-PSA-mAb-conjugated CdSe/ZnS (core/shell) QDs are added and bind to any PSA on the surface; subsequent washing and laser excitation causes fluorescence of the QDs which is proportional to the PSA concentration **(Scheme 1.4)**.[77] However, the off-target reactivity of other biomolecules containing primary amine functionality (e.g. lysine side chains or *N*-termini of proteins) with the aldehyde groups on the chip may result in the blocking of sites which could reduce the accuracy of this method.

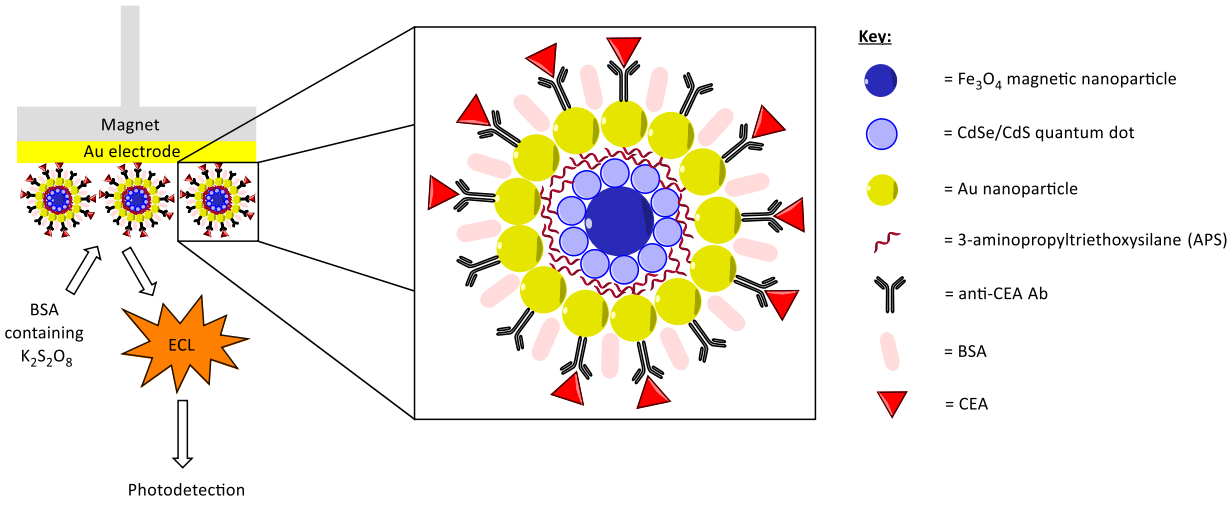


Figure 1.5: Experimental setup of Jie *et al.*'s electrochemiluminescent immunosensor for the cancer biomarker CEA.[79] The CdSe/CdS quantum dot sensing elements are bound to a magnetic iron oxide nanoparticle, which enables them to be localised on a gold electrode using a magnetic field. The QDs are coated in an APS film with terminal cationic ($-NH_3^+$) groups, which: (a) enhance the ECL signal from the nanocomposite; (b) facilitate conjugation of AuNPs *via* ionic interactions; and (c) facilitate immobilisation of the nanocomposite on the Au electrode. The AuNPs themselves enhance the ECL signal too, and enable anti-CEA Abs to be bound onto the nanocomposite. Nonspecific binding sites on the AuNPs are blocked with BSA. When a serum sample containing CEA is added to the nanocomposites at the Au electrode, CEA binds to the anti-CEA Abs, and the ECL signal, which displays strong inversely proportionality to [CEA] present (R = -0.992), is measured using a photodetector. Ab = antibody; APS = 3-aminopropyltriethoxysilane; BSA = bovine serum antigen; CEA = carcinoembryonic antigen; ECL = electrochemiluminescence; QD = quantum dot.

Electrochemiluminescence (ECL) of QDs has also been used in cancer biomarker detection, specifically of CEA, elevated levels of which are associated with cancers of the gastrointestinal tract such as colorectal tumours.[80] Composite nanoparticle hybrid superstructures were developed which consisted of a magnetic Fe_3O_4 core coated in CdSe/CdS QDs and a surface layer of 3-aminopropyltriethoxysilane (APS); these were then immobilised to a thin film of gold and coated with AuNPs **(Figure 1.5)**.[79] Anti-CEA Abs were then immobilised to the AuNPs and the chip washed with BSA to block any vacant nonspecific binding sites on the AuNPs. Addition of the samples containing CEA thus led to Ab-Ag interactions which could be detected after the nanoparticle superstructures were removed using a magnetic field and treated with both light and a buffer solution containing $K_2S_2O_8$, which enabled ECL from the QDs to occur. The binding of CEA to the Abs increases the steric hinderance towards the transfer of electrons and $K_2S_2O_8$ to the surface of the gold electrode, and hence decreases the ECL signal generated. The probable mechanism of ECL is given by equations (A)-(D):[81]

$CdSe\text{-}CdS + e^- \rightarrow CdSe\text{-}CdS^{\cdot\cdot}$ (A)

$S_2O_8^{2-} + e^- \rightarrow SO_4^{2-} + SO_4^{\cdot\cdot}$ (B)

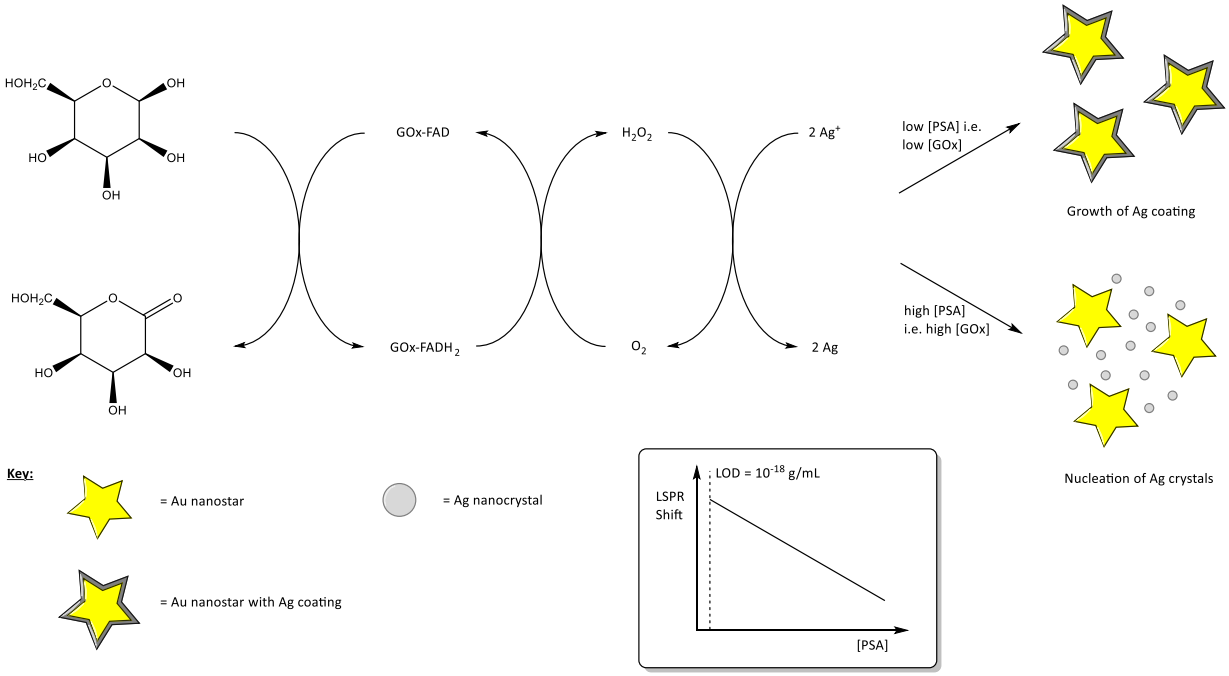
$CdSe\text{-}CdS^{\cdot\cdot} + SO_4^{\cdot\cdot} \rightarrow CdSe\text{-}CdS^* + SO_4^{2-}$ (C)

$CdSe\text{-}CdS^* \rightarrow CdSe\text{-}CdS + h\nu$ (D)

1.1.2.3. Homogenous Systems for Protein Detection

All of the immunosensors described above are examples of heterogeneous systems, *i.e.* systems in which the sensing element for the protein in a solution sample is immobilised onto a solid-phase support. Traditional heterogeneous assays sometimes containing several incubation, separation and washing steps can however be time-consuming, taking hours or days to carry out. Recently, some sophisticated assays have been reported which enable optical assays to be performed directly in a homogeneous solution.[40] Liu *et al.* developed a system based on AuNPs coated in PSA-Ab and AuNRs coated in PSA-Ab_2, whereby in the presence of PSA, AuNP-Ab-PSA-Ab_2-AuNR dimers are formed; after dilution, the technique of dynamic light scattering (DLS), which determines particle size distribution in a solution, can

then be used to accurately determine the dimer:monomer ratio in solution and hence the concentration of PSA.[82] DLS can also be used to detect protein complexes/aggregates in solution. This has been exploited by Huo: through developing a nanoparticle aggregation immunoassay, he found that some proteins known to be overexpressed in tumour tissue *vs.* normal tissue were also substantially more complexed/aggregated in the cancerous tissues than in normal tissue.[83] Most interestingly, he noted that prostate tumours could clearly be distinguished from normal tissue and benign prostate hyperplasia (BPH) on the basis of levels of aggregated prostatic acid phosphatase (PAP). Other techniques, such as determination of PSA concentration, are limited in their ability to distinguish prostate cancers from BPH.



Scheme 1.5: Key redox processes in an inversely sensitive homogeneous sandwich immunoassay for PSA.[84] At low PSA concentrations, low [GOx] is present and so the rate of deposition of Ag is slow, leading to a uniform coating on the Au nanostars and causing a large shift in LSPR. At higher PSA concentrations, high [GOx] is present and so the deposition rate of Ag is faster, causing nucleation of Ag crystals and less deposition of Ag on the surface of the Au nanostars, thus giving a smaller shift in LSPR. GOx = glucose oxidase; LSPR = localised surface plasmon resonance; PSA = prostate-specific antigen.

One other noteworthy example is the work of Rodriguez-Lorenzo *et al.*, who have developed a nanosensor with "inverse sensitivity", whereby low levels of the analyte yield a greater optical

response than higher levels.[84] Gold nanostars were coated with polyclonal antibodies against PSA and added to a solution containing samples of PSA and a secondary monoclonal PSA antibody labelled with GOx. Addition of glucose initiated H_2O_2 production; subsequently, $AgNO_3$ and NH_3 were added which triggered the reduction of Ag^+ to Ag around the nanostars **(Scheme 1.5)**. At low GOx concentrations the nucleation rate is slow, leading to growth of a uniform silver coating on the nanostars; at higher GOx concentations the nucleation rate is faster, resulting in the formation of silver nanocrystals and fewer silver deposits on the nanostars themselves. Thus in the former case, a larger shift in LSPR wavelength can be detected than in the latter, resulting in a superbly sensitive system, capable of detecting PSA in human serum at 10^{-18} g/mL.

1.1.2.4. Aptasensors for Protein Detection

Advances in nucleic acid chemistry have led to the development of oligonucleotide aptamers, which are fragments of RNA, DNA or XNA (*c.* 25-80 nucleotides in length) that can bind to target molecules with high affinity and specificity. The fragments are selected from a large pool of 10^{15} random sequences by an *in vitro* selection process known as SELEX (selective evolution of ligands by exponential enrichment).[85] Aptamers have found various biochemical uses, ranging from target validation to therapy and use in high-throughput screening.[86] Moreover, aptamers can also be utilised as recognition elements in biosensors: to generate an optical readout, a useful approach is to tag different sections of the aptamer(s) in the system with a fluorescence donor and a fluorescence acceptor, such that binding of the aptamer(s) to the target protein results in the donor and acceptor being brought close together in space, quenching fluorescence. Such sensors are often referred to as molecular aptamer beacons (MABs). Aptamers are particularly attractive alternatives to antibodies for use in biosensors because of their exceptional stability, their smaller size, the elimination of the need to use animals in their generation, the relative ease of their synthesis and derivatisation, and the ability to alter their specificity and selectivity based on the selection conditions under which they are derived.[87]

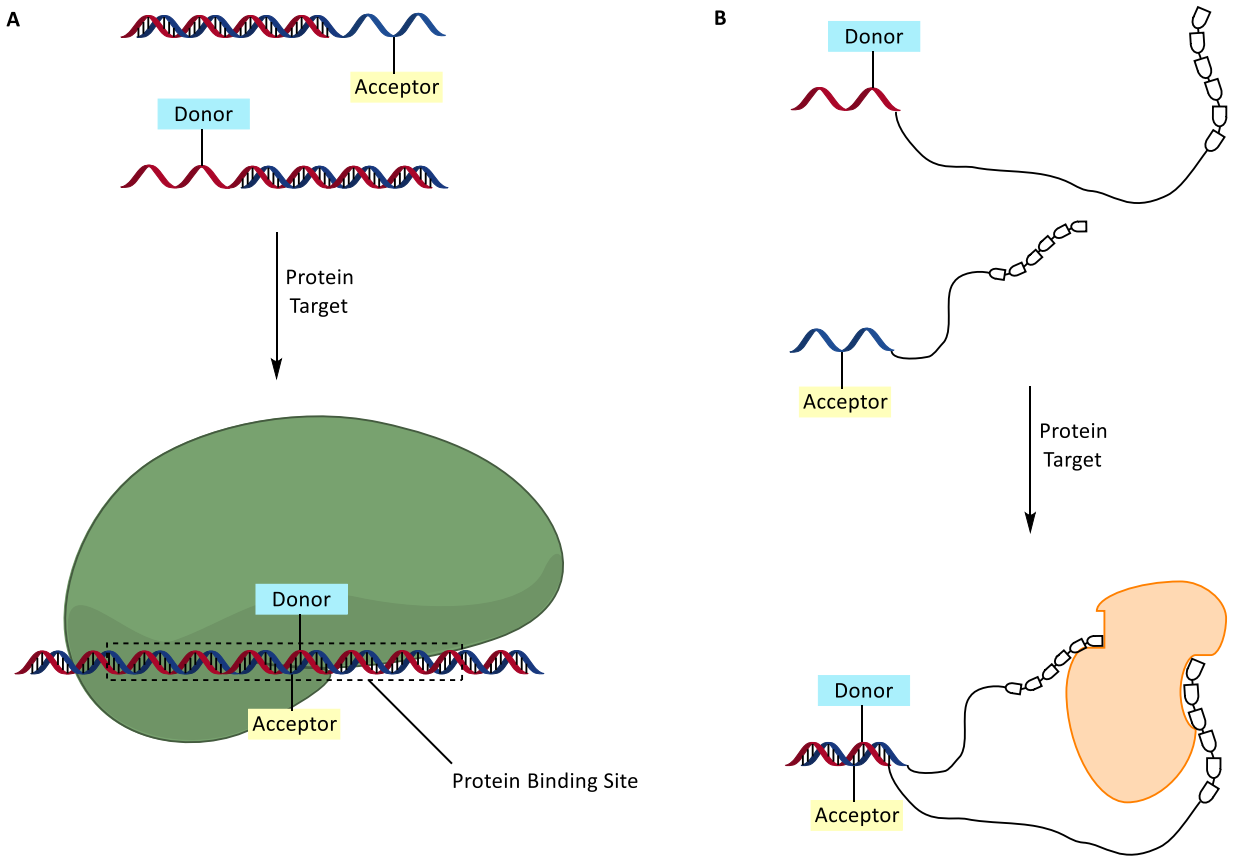


Figure 1.6: A: MAB consisting of two "half-site" aptamer binders; one "half" carries a fluorescence donor on a single-stranded section of DNA and the other "half" a fluorescence acceptor. Binding of both fragments to the protein binding site results in annealing of the DNA and fluorescence quenching *via* FRET.[88] **B:** MAB in which the ssDNA carrying the fluorescence donor and the ssDNA carrying the fluorescence acceptor are conjugated *via* a non-DNA linker to two aptamers which specifically bind to different epitopes of the target protein.[89] FRET = fluorescence resonant energy transfer; MAB = molecular aptamer beacon; ssDNA = single-stranded DNA.

Several examples of MABs for detection of proteins have been reported in the literature. Heyduk & Heyduk developed a system in which two DNA aptamers each bind to a "half-site" on the bacterial transcription activator CAP (catabolite activator protein), one of which was labelled with the fluorescence donor fluorescein, and the other with the fluorescence acceptor dabcyl **(Figure 1.6A)**; when both aptamers bind to the protein, short single-stranded complementary sections at the end of each aptamer anneal *via* hydrogen bond formation.[88] The fluorescence signal is quenched in a linear fashion as the target protein concentration is increased. The same authors subsequently designed a system in which the two labelled

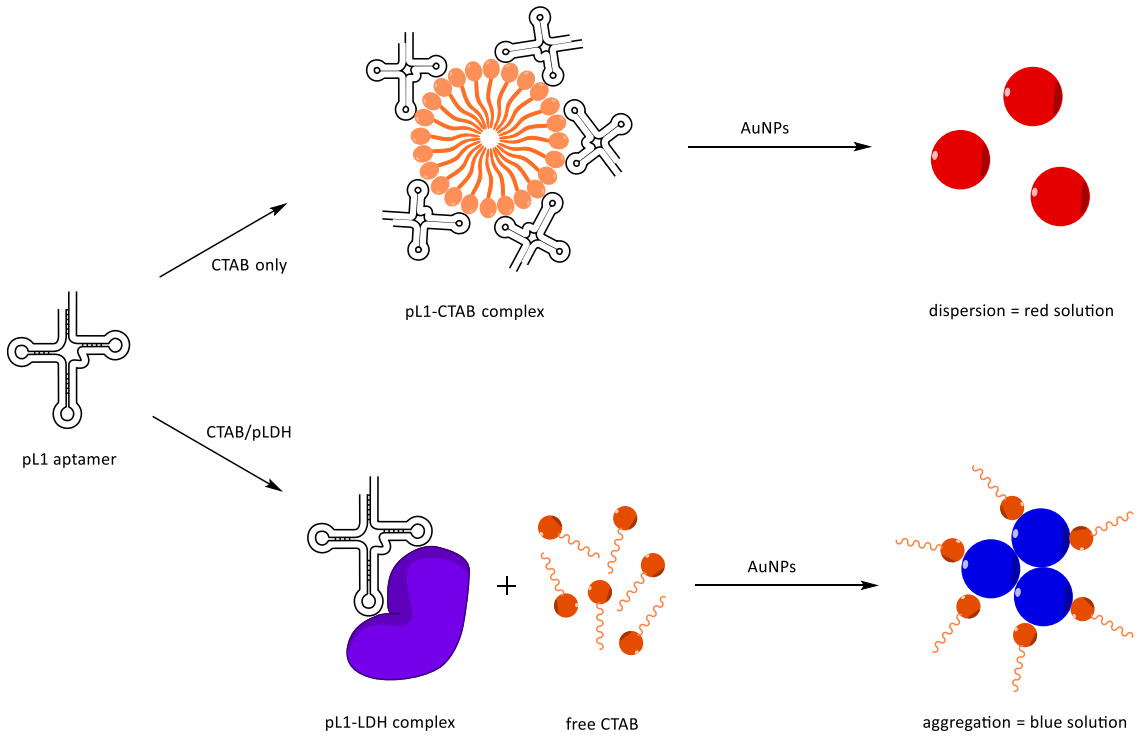
aptamer fragments bind to two distinct epitopes of the protein, using thrombin as a model system. The fluorophore-labelled complementary single-stranded DNA (ssDNA) oligomers are joined to the respective aptamers *via* a non-DNA linker **(Figure 1.6B)**, and fluorescence quenching occurs upon co-association of the two aptamers with the target protein.[89]

Aptamer systems which more closely resemble the immunoassay formats outlined in **Figure 1.2** have also been utilised in protein detection. Drolet *et al.* reported an oligonucleotide analogue of an ELISA, which they termed an "ELONA" (enzyme-linked oligonucleotide assay); in their system, a plate coated in anti-VEGF (vascular endothelial growth factor) Abs was able to bind VEGF in solution before addition of a fluorescein-tagged aptamer which recognises VEGF.[87c] After washing, addition of an anti-fluorescein fragment conjugated to alkaline phosphatase enables a chemiluminescent assay to be performed which quantifies VEGF levels. Furthermore, the aptamers could be modified to be selective binders for the predominant $VEGF_{165}$ isoform and to be resistant to nuclease activity by the addition of triphosphate groups. Whilst the ELISA and ELONA protocols gave very high levels of agreement with many of the VEGF serum samples tested, in some cases the two assay protocols gave very different values for [VEGF]; the authors speculate that this could be due to serum-specific interference effects in one or both assays.

Potyrailo *et al.* also worked on an assay for thrombin detection, but based on EWS, in which anti-thrombin DNA aptamers labelled with FITC were covalently attached to a glass slide, and changes in the evanescent-wave-induced fluorescence anisotropy of the aptamer selectively upon its binding to thrombin in solution were monitored.[90] Thrombin could be detected using this method over a dynamic range of three orders of magnitude, ranging from 5 nM to several μM; repeat readings from a single glass slide gave a relative standard deviation (RSD) of <1% over a concentration range of 0.2-200 nM, whilst those from different slides gave an RSD of <4%. McCauley *et al.* extended this label-free chip technology to develop a multiplex chip for simultaneous detection of several cancer biomarkers;[91] however, the chips are not reusable as some of the aptamers are based on RNA and were susceptible to degredation.

Nanotechnology has also enabled the development of some very sensitive aptamer-based assay systems for protein detection. Aptasensors in which AuNPs are used as the sensing device are widely reported in the literature,[92] and sensors in which assay procedures rely on non-crosslinking aggregation of AuNPs are thought to be cheaper and more convenient than systems in which complex (and often expensive) thiol-containing ligands are used to cross-link AuNPs.[93] One elegant example of this type of assay was reported in 2014 by Lee *et al.*, in which LDH from the malarial parasites *Plasmodium falciparum* (*Pf*LDH) and *Plasmodium vivax* (*Pv*LDH) could be detected in human serum samples with respective LODs of 14 pM and 10 pM.[94] In this assay, the pL1 aptamer for *Plasmodium* LDH (pLDH) was incubated with pLDH-containing samples, AuNPs and the cationic surfactant CTAB. In the absence of pLDH, CTAB binds to pL1 and the AuNPs are freely dispersed in the sample solution, which is therefore red in colour. However, competitive binding of LDH to pL1 frees CTAB molecules, which stabilise the formation of blue-coloured AuNP aggregates **(Scheme 1.6)**. Colorimetric measurements were made by UV-visible spectroscopy, and the size of AuNP aggregates confirmed by transmission electron microscopy.

Use of nanotechnology in sensing devices does however have its disadvantages: AuNP-based colorimetric assays, for instance, can be time-consuming[92a] and give false positive results in certain environments (e.g. in the presence of proteases).[95] An alternative promising technique for rapid clinical diagnostic testing is that of aptamer-tethered enzyme capture (APTEC), illustrated by a recent assay reported by Dirkzwager *et al.* for *Pf*LDH.[96] A chip with 2008s aptamers bound to its surface selectively captures *Pf*LDH from solution and after washing, incubation with L-lactate and nitotetrazolium blue results in [*Pf*LDH]-dependent production of diformazan dye, which is blue and can be quantified colorimetrically. The LOD for recombinant *Pf*LDH was found to be 5.9 ng/mL, and in 80% of clinical blood samples tested from patients infected with *P. falciparum* the APTEC test correctly diagnosed infection; in all three false negative results the parasitemia level was very low (< 0.06%).



Scheme 1.6. Colorimetric assay for *Plasmodium* LDH based on AuNP aggregation.[94] In the absence of LDH, the pL1 aptamer associates with CTAB allowing free dispersion of the AuNPs in solution, which is red in colour; when LDH is added to the solution, it binds to pL1 leaving CTAB free in solution, which in turn promotes aggregation of AuNPs which turns the solution blue. AuNP = gold nanoparticle; CTAB = cetyl trimethylammonium bromide; LDH = lactate dehydrogenase.

Amino acid analogues of aptamers, known as Affirmers®, have also been developed for use in analogous assays for protein detection. Affirmers® are 12-36 amino acid fragments derived from cystatins,[97] protein inhibitors of cysteine proteases;[98] their structure comprises an α-helix stacked on top of an antiparallel β-sheet.[99] Loop lengths between adjacent strands of the β-sheet can be varied in length to alter the shape and/or size of the recognition surface. Affirmers® benefit from generally higher stability over aptamers since the amide bonds in peptides are less prone to degredation than the phosphodiester bonds in oligonucleotides; Affirmers® are stable to temperatures up to 80 °C and over a *p*H range from 2 to 12.[100] The ability to produce Affirmers® in a recombinant fashion means that their generation could be more reliable, more rapid and cheaper than that of antibodies, but to date the technology is in its infancy and although they have demonstrated promise in ELISA, SPR and immunohistochemical systems,[100] a widespread utility is yet to be realised.

1.1.3. Covalent Optical Tagging of Specific Proteins: From Fusion Proteins to Small Molecules

The optical biosensors developed for protein detection discussed thus far possess some very favourable properties, most notably very high specificities for the proteins of interest and the ability to detect very low concentrations of protein in a clinical sample. However, there are several drawbacks to the use of such biosensors, not least that for the detection of molecules as complex as proteins, antibodies are required in the majority of experimental setups. Abs can be difficult to work with, the analysis can be both expensive and time-consuming, and because of the complex nature of the protein analyte, the optimisation of the immobilisation and labelling strategy is unique for each Ab-Ag conjugate pair selected.[21a] Aptamers, although often easier to generate against a target than antibodies, have their own limitations. Notably, aptamers (particularly RNA aptamers) are prone to degradation by nucleases, can in many cases only be generated by SELEX if a purified protein target is available (which precludes their use against many membrane-associated receptors), and can have significant levels of cross-reactivity.[101] Therefore, in recent years many researchers have begun to investigate the possibility of detecting and measuring specific proteins in a solution sample using optical *chemical* probes – small molecules which interact directly with a protein of interest giving a measurable change in optical properties upon binding, with no need for a biological sensing element – a story which begins with the discovery of green fluorescent protein (GFP).

1.1.3.1. Protein and Peptide Fusion Tags

GFP, first isolated from the jellyfish *Aequorea victoria*, is a protein which fluoresces with λ_{ex} = 395 nm and λ_{em} = 509 nm.[102] In *A. victoria* it is found in complex with the fluorescent protein aequorin; aequorin absorbs UV light and from its excited state transfers this absorbed energy to the associated GFP *via* FRET, enabling the excited state of GFP to relax to its ground state *via* fluorescent emission of green light which gives the jellyfish cells their characteristic colour **(Figure 1.7)**.

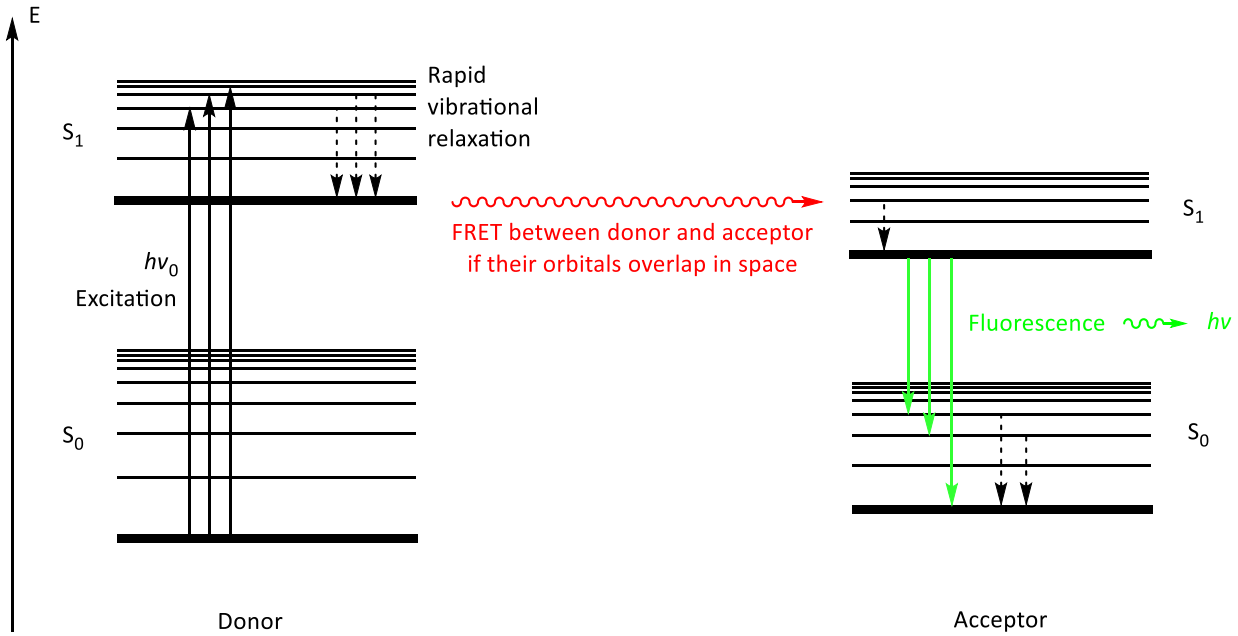


Figure 1.7: Jablonski diagram showing FRET from the first excited (S_1) electronic state of a donor fluorophore (e.g. aequorin) to that of an acceptor fluorophore (e.g. GFP), which enables fluorescence of the acceptor to be observed upon relaxation of the excited photon from the S_1 state to the S_0 (ground) electronic state. FRET = fluorescent resonance energy transfer; GFP = green fluorescent protein.

Pioneering work by Prasher *et al.* enabled cloning of the gene coding for GFP,[103] and subsequent studies by Chalfie *et al.* and Inouye & Tsuji demonstrated that expression of the gene in other organisms generates fluorescence, without the need for exogenous substrates or cofactors.[104] Hence GFP expression could be used to monitor gene expression *in vivo*.[104a] However, GFP requires strong promoters to be sufficiently expressed and suffers from a lack of sensitivity as a so-called gene-tag because of an inherent lack of signal amplification.[102c, 105] Some limitations can be overcome through re-engineering GFP *via* mutagenesis, as pioneered by Tsien and co-workers.[105] GFP and its mutants have subsequently been applied widely and successfully in the generation of so-called fusion proteins. In this technique, the gene encoding GFP is fused into a frame encoding a separate endogenous protein in order to generate the fusion protein, which in an ideal embodiment has the same function and localisation as the endogenous protein but is fluorescent. Such fusion proteins have found widespread use in establishing the localisation and fate of endogenous proteins in cells; they have been used to target a wide range of eukaryotic organelles.[102c, 106]

Additionally, applications of GFP have been established which rely on active changes to the GFP fluorescence under different biochemical conditions. The most commonly exploited technique in this regard is FRET between fluorescent proteins of different colours. The first demonstrated case of this involved fusing a GFP to a blue-emitting GFP mutant (a BFP) *via* a protease-sensitive spacer.[107] This fusion protein initially glows bright green due to FRET from the BFP to the GFP, but after exposure to trypsin, the fluorescence intensity diminishes. Similar techniques have been used to monitor intracellular [Ca^{2+}], an essential ion in many metabolic processes.[108]

GFP is, however, a rather bulky protein containing 238 amino acids with a molecular weight of 26.9 kDa, which can be problematic as its folding is not instantaneous and it can affect the structure and/or function of the endogenous protein to which it is fused.[109] Furthermore, GFP can only be fused at the $–NH_2$ or $–CO_2H$ terminus of an endogenous protein, and studies with GFP are limited to fluorescent readouts up to a maximum λ_{em} of 529 nm (although red-emitting fluorescent proteins are known, their use is restricted by their obligate tetramerisation and the slow maturation of their fluorescent signal).[110] Therefore, Tsien's lab developed an alternative genetic approach to generating fluorescent proteins, which involves the insertion of a short sequence of as few as six natural amino acids (Cys-Cys-Xaa-Xaa-Cys-Cys, where Xaa is any amino acid except cysteine) into recombinant DNA coding for the protein, to enable recognition by arsenic-based ligands such as fluorescein arsenical helix binder-di(ethylene dithiol), FlAsH-EDT_2 **1 (Figure 1.8A)**.[111]

These arsenic ligands have high specificity, binding to the designed cysteine-containing peptide fragment with nanomolar dissociation constants but having few other binding partners in nontransfected mammalian cells as the tetracysteine motif is absent from the endogenous proteome.[112] Serendipitously, it was discovered that **1** is almost non-fluorescent when free in solution, but fluoresces 50,000 times more strongly when bound to the peptide target; it is believed that the increased rigidity of the complex with the peptide prevents excited state quenching by vibrational energy transfer or photoinduced electron transfer

(PET).[111a] Initially it was hypothesised that the preferred hexapeptide conformation was an α-helix;[111a] however, the highest ligand affinities were found when Xaa-Xaa = Pro-Gly, suggesting that the preferred conformation is in fact that of a hairpin turn.[113] Subsequently, a range of As(III)-based ligands have been developed which fluoresce at different excitation and emission wavelengths, such as the red-fluorescing ReAsH-EDT$_2$ **2** and the blue-fluorescing HoXAsH-EDT$_2$ **3 (Figure 1.8B)**. These biarsenical dyes can however only bind to reduced forms of cysteine, and so complications arise in oxidising environments. They also suffer from off-target reactivity with other biological thiols and nonspecific hydrophobic interactions (e.g. with BSA), both of which can lead to undesirable background fluorescence.[114] Suppression techniques developed to prevent this fluorescence include adding an excess of EDT to compete with biological thiols, and adding hydrophobic molecules to compete for nonspecific binding sites.[111b]

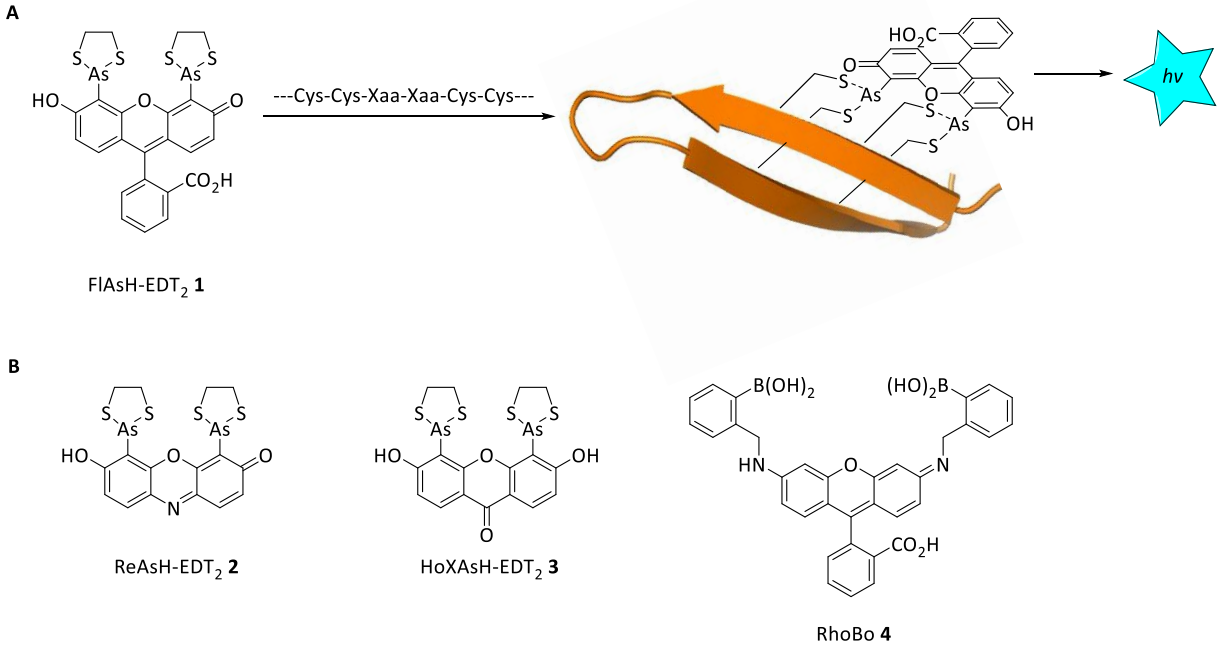
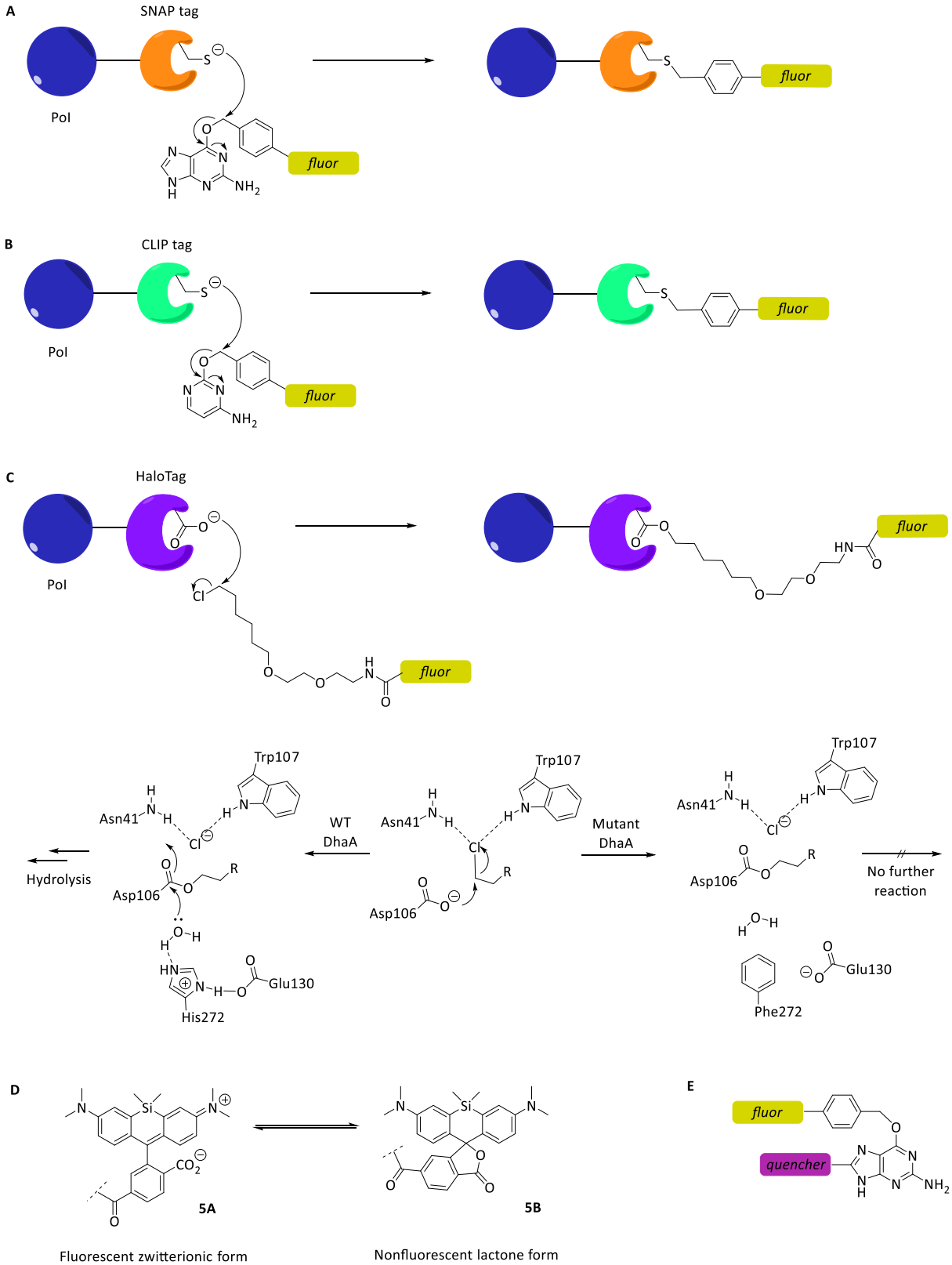


Figure 1.8: A: Structure of FLAsH-EDT$_2$ **1** and one possible orientation of binding (*i, i+4* and *i+1*, *i+5*) to the hexapeptide amino acid sequence Cys-Cys-Xaa-Xaa-Cys-Cys in a β-turn, where Xaa is any amino acid other than cysteine. An alternative orientation involving *i*, *i+1* and *i+4*, *i+5* binding of the arsenics is also possible. **B:** Structure of the second generation ligands ReAsH-EDT$_2$ **2** and HoXAsH-EDT$_2$ **3**, which also bind to the Cys-Cys-Xaa-Xaa-Cys-Cys sequence, and RhoBo **4**, which recognises the sequence Ser-Ser-Xaa-Xaa-Ser-Ser in a similar fashion.

Schepartz's lab have developed an analogous binder for a tetraserine motif, the rhodamine *bis*-boronic acid reagent RhoBo **1.4 (Figure 1.8B)**, which exhibits a switch-on fluorescence in the presence of a Ser-Ser-Xaa-Xaa-Ser-Ser sequence in peptides.[115] **4**, like the biarsenical dyes, is cell-permeable and has a nanomolar association constant against its target, but does not suffer from competitive binding to thiols and does not contain toxic arsenic. However, over 100 other proteins contain a tetraserine motif and may bind to the probe resulting in off-target fluorescence. Other researchers have tried to exploit chelation effects to transition metals in probe design, e.g. the use of fluorophores conjugated to Ni^{2+} for detection of proteins containing a polyhistidine (commonly His_6 or His_{10}) tag;[116] however, these probes release toxic Ni^{2+} in cells[117] and can be quenched by free Ni^{2+} since it is paramagnetic ($3d^2$).[118] Greater success has been obtained using non-toxic, d^0 Zn^{2+} chelators, examples of which have been reported by Tsien's lab[119] for hexhistidine tags and Hamachi's lab[120] for tetraaspartate tags. Lanthanide-binding peptide sequences have also been elucidated, and have been useful *in vitro* for studying protein-protein interactions and detecting tagged ubiquitin;[121] however, toxicity and poor membrane permeability remains a barrier to *in vivo* use of such probes.[122]

The tagged proteins discussed thus far only allow recognition by one or a very limited number of chemical probes. The development of fusion proteins which ligate an intermediate "linker" enzyme to the protein of interest have enabled recognition by a wide range of reporter molecules, which can react and form covalent bonds to the linker protein. Johnsson and co-workers developed a system they called SNAP tags, in which the linker protein is the human DNA repair protein O^6-alkylguanine-DNA alkyltransferase (hAGT) and reporters based on guanine can attach *via* an S_N2 displacement to install a variety of fluorophores **(Scheme 1.7A)**.[123] Subsequently, Johnsson's lab developed CLIP tags, in which the linker protein is an hAGT variant which acts on O^2-benzylcytosine derivatives **(Scheme 1.7B)**.[124] The substrate orthogonality between SNAP and CLIP tags enables simultaneous and specific labelling of two different proteins of interest in living cells. Promega have developed their own variant known as HaloTag, which utilises mutated bacterial haloalkane dehalogenase (DhaA) as the linker, enabling tagging of the enzyme by alkyl chloride probes **(Scheme 1.7C)**.[125]

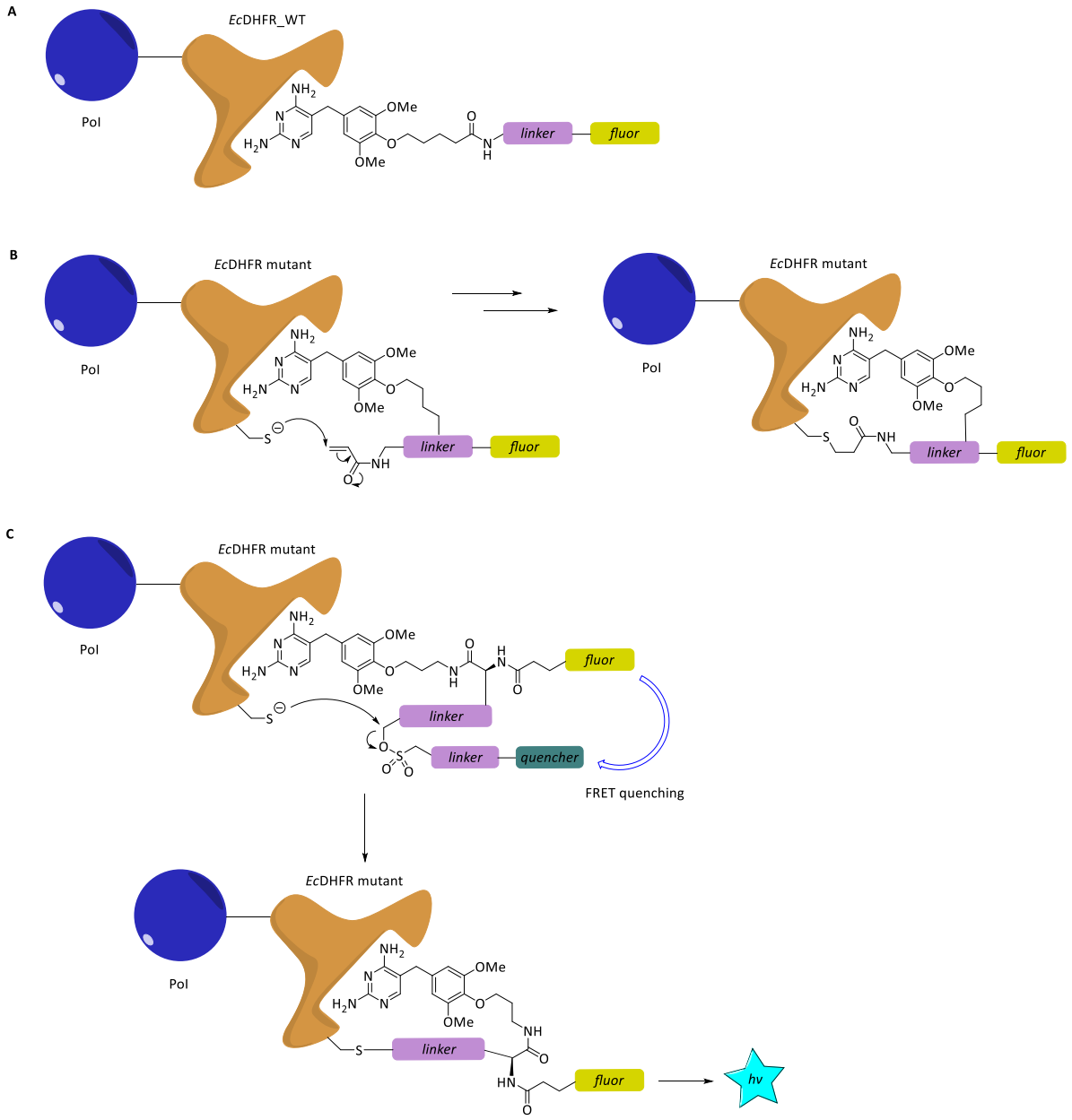


Scheme 1.7: A: General mechanism of action of a SNAP tag.[123] **B:** General mechanism of action of a CLIP tag.[124] **C:** General mechanism of action of a HaloTag (above) and differences in the reactivity of wild type (WT) and mutant DhaA when His272 is replaced by Phe272 (below).[125] **D:** Fluorescent and non-fluorescent forms of an optimised fluorophore **5**.[126] **E:** Class of self-quenching SNAP tag probe.[127] *fluor* = fluorophore; PoI = protein of interest.

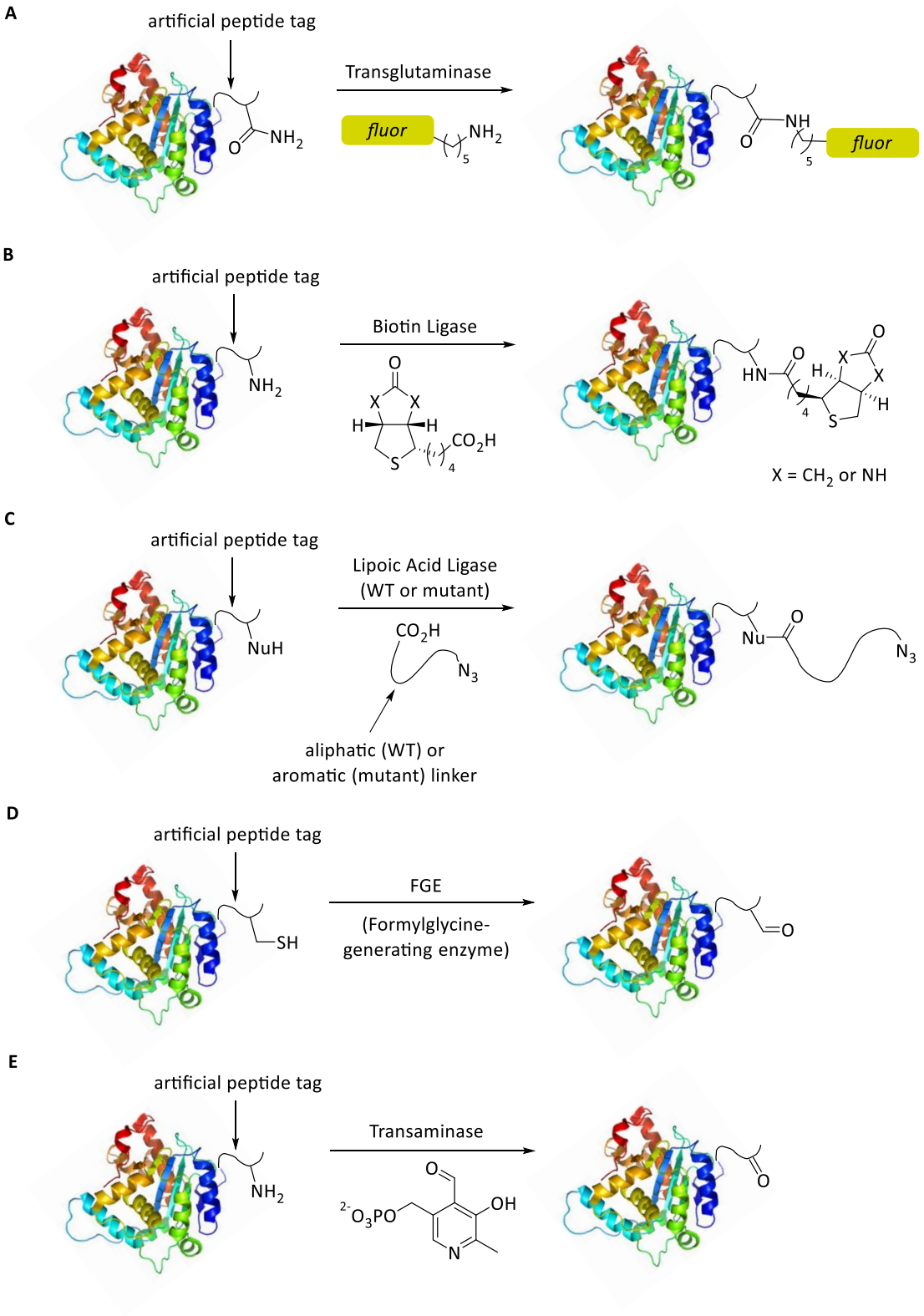
The point mutation which replaces His272 in the active site with Phe272 prevents catalysis of the attack of water on the covalent adduct to Asp106, stabilising this adduct. Recently, a near-IR fluorophore **5** has been developed which is suitable for live cell imaging due to its low toxicity, high λ_{ex}, high membrane permeability and low background fluorescence thanks to its ability to form a non-fluorescent lactone **(Scheme 1.7D)**.[126, 128] New smart probes for use with SNAP tag fusion proteins have also been reported, which incorporate a fluorescence quencher onto the guanine ring such that any unreacted probe self-quenches, reducing background fluorescence levels in cells **(Scheme 1.7E)**; this eliminates the need for laborious washing steps to boost the fluorescence intensity.[127] A similar system has been designed by Hori *et al.* utilising photoactive yellow protein (PYP) as their "linker" enzyme.[129]

Another strategy which can be employed with fusion proteins is that of proximity-induced reactivity. This is where recognition between two chemical entities – e.g. noncovalent interactions between a ligand and a receptor – brings the reactive groups of the entities close to one another in space and hence facilitates a reaction. One such system was developed by Cornish and co-workers, in which the affinity of the enzyme *E. coli* dihydrofolate reductase (*Ec*DHFR) for folate analogues such as trimethoprim (TMP) was exploited. Cornish's lab initially reported a membrane-permeable fluorophore-tagged TMP derivative which binds noncovalently to *Ec*DHFR with high affinity (K_i = *c.* 1 nM) and high specificity (>1,000-fold specificity for *Ec*DHFR over human isoforms) **(Scheme 1.8A)**;[130] this enabled efficient and specific labelling of protein both *in vitro* and within living cells.[131] A variant for two-photon imaging in live cells was also developed.[132] Perhaps surprisingly given the noncovalent nature of these probes, the background fluorescence was low, probably ensured by the favourable binding kinetics. Subsequently an electrophilic Michael acceptor was incorporated into the probes, which has the potential to react with nucleophilic residues in proteins. Mutation of *Ec*DHFR to install a cysteine residue adjacent to the active site enables proximity-induced conjugate addition to form a covalent bond between enzyme and probe **(Scheme 1.8B)**,[133] and further optimisation of both the Michael acceptor probe and the *Ec*DHFR mutant led to a more suitable probe for live cell imaging with a shorter labelling half-life.[134] More recently,

Jing & Cornish reported a self-quenching TMP-based tag in which the quencher is cleaved upon interaction with the cysteine residue of mutant *Ec*DHFR, thereby giving a more sensitive "switch-on" fluorescent system **(Scheme 1.8C)**.[135]



Scheme 1.8: A: Noncovalent fluorescent probe which binds strongly to WT *Ec*DHFR in a fusion protein *via* a TMP motif.[130] **B:** Introduction of an acrylamide on the probe and a cysteine residue adjacent to the *Ec*DHFR active site enables bond formation between protein and tag *via* proximity-induced reactivity.[133] **C:** Self-quenching TMP-based probe, which only fluoresces in the presence of mutant *Ec*DHFR-tagged fusion protein, as bond formation to the key cysteine residue cleaves the quenching group.[135] *Ec*DHFR = *E. coli* dihydrofolate reductase; *fluor* = fluorophore; PoI = protein of interest; TMP = trimethoprim; WT = wild type.



Scheme 1.9: Representative examples of post-translational modifications of tagged proteins by enzymes, which generate products that can be detected optically. **A:** Transglutaminase conjugates primary amines onto certain glutamine residues;[136] **B:** Biotin ligase conjugates biotin or its ketone derivative to a lysine residue;[137] **C:** Lipoic acid ligase can specifically modify certain nucleophilic residues with fatty acids;[138] **D & E:** FGE and transaminase can respectively convert cysteine and amino functionalities into carbonyl moieties.[139]

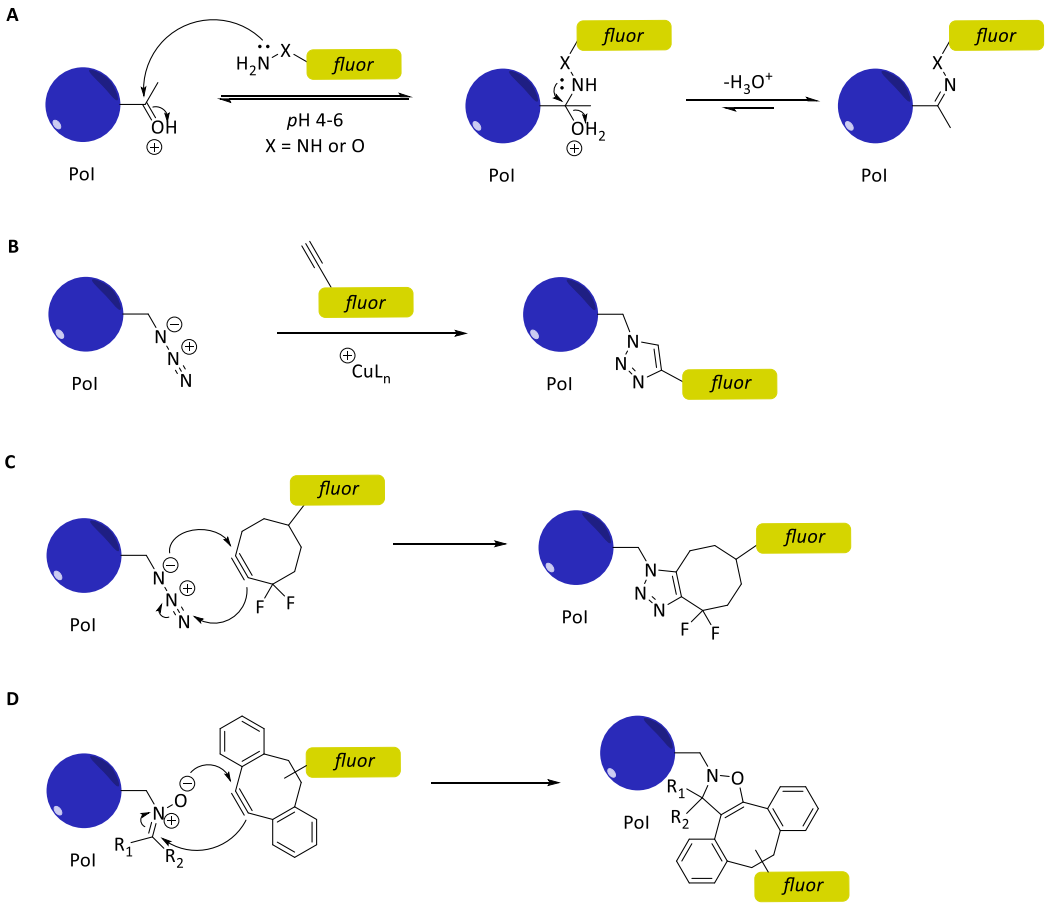
In a related approach, enzymes whose endogenous role is to covalently modify proteins containing certain peptide motifs with small molecule cofactors can be persuaded to make the same post-translational modification to any protein of choice that is genetically modified to incorporate the relevant peptide recognition motif.[140] Representative systems which have been developed are illustrated in **Scheme 1.9**. Some such systems directly link a fluorescent tag to the modified protein of interest, such as labelling glutamine residues with a fluorophore-linked primary amine using the enzyme transglutaminase **(Scheme 1.9A)**.[136] Others install functionality which is not itself fluorescent **(Schemes 1.9B-E)**,[137-139] but can undergo a further reaction with added optical probes (that are kinetically, thermodynamically and metabolically stable) which is exquisitely selective *in vitro* or *in vivo* and does not interfere with any other biological processes. Such reactions are termed *bioorthogonal* reactions.[140c]

Ting and co-workers utilised the biotin ligase from *E. coli*, BirA, which biotinylates a lysine residue within a 15-residue fusion peptide, to tag proteins with either biotin **(Scheme 1.9B; X = NH)** or a ketone derivative **(Scheme 1.9B; X = CH_2)**.[137a] Proteins tagged with biotin can be visualised with strepatividin-conjugated QDs,[137b] whilst those tagged with the ketone derivative can undergo a bioorthogonal reaction with fluorescent hydroxylamines or hydrazines to selectively form fluorescent oximes or hydrazones respectively.[137a] Subsequently, the group developed systems using either wild type or mutant lipoic acid ligase to tag a fusion peptide with an azide group **(Scheme 1.9C)**.[138] Azides can undergo several bioorthogonal reactions with fluorescent small molecule probes, a type of so-called "click" reaction with alkynes (see **Section 1.1.3.2.** below). Some post-translational modifications can be orthogonally modified by a particular enzyme without conjugation of a substrate; this is the case for the oxidation of cysteine to formylglycine **(Scheme 1.9D)**[139a, 139b] and the transamination of amino functionalities **(Scheme 1.9E)**.[139c] In both cases, the modified proteins contain an electrophilic carbonyl group which can be fluorescently labelled using similar means to the ketone derivatives of biotin. Whilst this small collection of examples illustrates the principles and breadth of this tagging method, there are other elegant systems reported in the literature too.[141]

1.1.3.2. Protein Labelling *via* Incorporation of Unnatural Amino Acids

An alternative approach to using fusion proteins to introduce specific tag-recognising functionality to a system is to incorporate an unnatural amino acid containing the desired functionality (a reactive "handle") into the native protein.[131, 140c, 142] A diverse range of unnatural amino acids have been developed for this purpose, incorporating aldehyde, ketone, azide, alkyne, alkene, haloarene or boronic acid functionalities amongst others.[142a] There are several well-established methods for incorporation of such amino acids into protein sequences, including chemical, enzymatic and genetic techniques: an excellent account of these methods is given by Lang & Chin.[142a]

Schemes 1.10-1.13 detail some of the most commonly utilised bioorthogonal reactions in protein labelling with fluorophores. Crucially, for a bioorthogonal reaction to be effective it must possess a high intrinsic second-order rate constant (k_2), to avoid the need for using a large excess of the fluorescently-labelled tag, which might have off-target activity or poor solubility at higher concentrations.[142a] Carbonyl moieties were among the first to be used in this type of protein labelling strategy. Aldehydes have too high an intrinsic reactivity with amine groups to be useful bioorthogonal reagents (*cf.* off-target effects for analogous antibody-based systems discussed in **Section 1.1.2.2.3.**), but ketones are less reactive under physiological conditions and this, alongside their ease of incorporation into proteins *via* residue-specific[143] or site-specific[144] methods, makes them useful reactive handles. Reaction of a ketone with a fluorescent hydroxylamine or hydrazine under mildly acidic conditions (*p*H 4-5) forms a fluorescent oxime or hydrazone product respectively, with the α-effect nucleophile ensuring the position of equilibrium lies to the side of the product **(Scheme 1.10A)**.[145] Whilst such reactions have proved useful *in vitro* or for cell surface labelling,[137a, 146] relatively slow kinetics[147] and the requirement for acidic conditions restricts the intracellular use of this technique. Addition of aniline as a nucleophilic catalyst, however, has been reported to increase k_2 by 5-7 orders of magnitude,[148] which has enabled labelling of the intracellular receptor LasR in bacteria.[149]



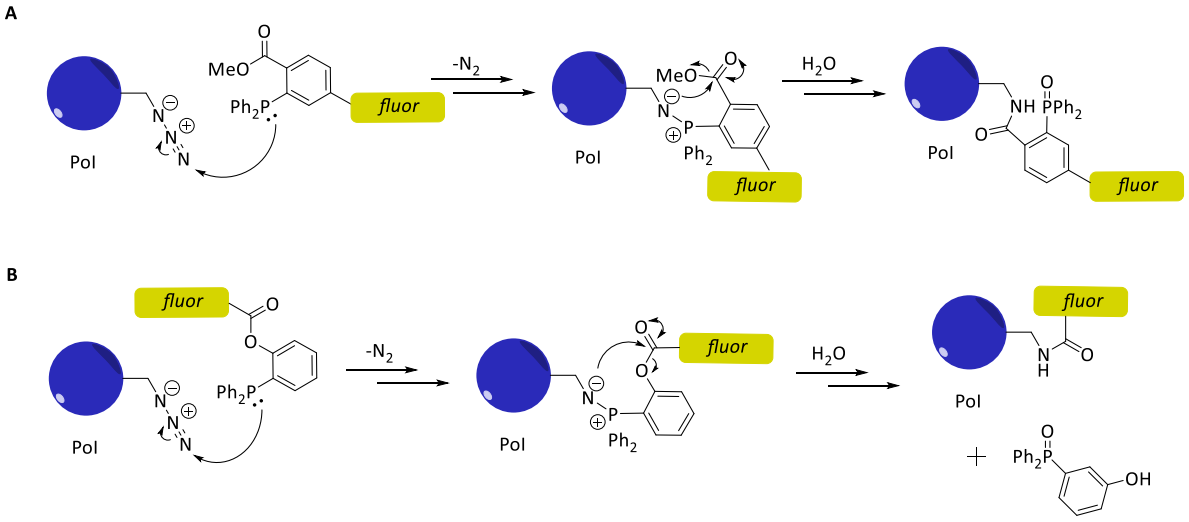
Scheme 1.10: Methods for covalently modifying unnatural amino acids within engineered proteins in order to label or otherwise modify the protein of interest (PoI), utilising condensation and cycloaddition reactions. **A:** Condensation of a fluorescent hydroxylamine or hydrazine with a ketone-containing amino acid to form a fluorescent oxime or hydrazine tag;[145] **B:** Cu-catalysed azide-alkyne cycloaddition (CuAAC) reaction between an azido-containing amino acid and a fluorescent alkyne;[150] **C:** A strain-promoted Cu-free click reaction using a fluorescent strained alkyne, a cyclooctyne derivative;[151] **D:** 1,3-dipolar cycloaddtion between a nitrone and a fluorescent strained alkyne.[152] *fluor* = fluorophore; L = ligand.

A more genuinely bioorthogonal handle than a carbonyl is the azide group,[153] and its small size and high kinetic stability enable azido-substituted amino acids to be incorporated into proteins.[154] Azido-tagged proteins can react as 1,3-dipoles in a [3+2]-dipolar cycloaddition[155] with a fluorescent terminal alkyne in order to be optically labelled as a triazole derivative. In the absence of a catalyst, however, the reaction is slow and requires high temperatures and pressures,[150] conditions which are not biocompatible. The discovery that Cu(I) salts can catalyse the process to regioselectively give a 1,4-disubstituted triazole in aqueous media in

high yield[156] has enabled such copper-catalysed azide-alkyne 1,3-dipolar cycloadditions (CuAACs) to be performed *in vitro* or *in vivo* on functionalised cowpea mosaic virus proteins,[157] yeast proteins[158] and *E. coli* cell surface proteins.[159] CuAAC is now widely referred to as the archetypal "click reaction", a term coined by Sharpless to refer to facile, high-yielding stereospecific reactions which are insensitive to oxygen or water, do not require an organic solvent and the products of which do not require chromatographic purification.[160] The proposed stepwise mechanism for the reaction invokes a six-membered Cu(III) intermediate which explains the observed regioselectivity **(Scheme 1.10B)**.[150] It has also been shown that the reaction partners of CuAAC may be reversed, *i.e.* alkyne functionality can be incorporated into the protein of interest, and the added probe can contain an azide group.[158, 161]

The principle disadvantage of using CuAAC *in vivo* is the toxicity of many Cu(I) salts,[162] possibly due to the formation of reactive oxygen species from O_2.[163] It is possible to mitigate this toxicity by using water-soluble Cu-chelating ligands which both facilitate the cycloaddition reaction and act as a reductant to protect against reactive oxygen species; such ligands have been used in cell surface labelling of live cells.[163-164] Alternatively, azide tags for proteins have been developed containing a donor nitrogen, oxygen or sulfur atom β or γ to the azide, which chelate Cu and hence increase its effective concentration at the site of reaction.[165] One other elegant approach has been developed by Bertozzi and co-workers, which eradicates the need for Cu(I) salts altogether.[166] If the alkyne employed in the cycloaddition is highly strained, e.g. a cyclooctyne derivative, the activation barrier to reaction with an azide is dramatically lowered, enabling cycloaddition to occur at ambient temperature in an aqueous environment in the absence of a catalyst **(Scheme 1.10C)**. Several such strained alkynes have been developed,[151] and unnatural amino acids bearing a strained alkyne have also been successfully incorporated into proteins;[167] k_2 values for the most reactive cases are however low, at *c.* 0.1-1.0 M^{-1} s^{-1} (*cf.* 10-200 M^{-1} s^{-1} for ligand-assisted CuAAC). Nonetheless, such probes have been used successfully for *in vivo* imaging of membrane-associated glycoproteins in mammalian cells[168] and zebrafish embryos.[169] k_2 values up to 39 M^{-1} s^{-1} are achievable by using a nitrone derivative as the unnatural amino acid with which the strained alkyne reacts in a 1,3-dipolar

cycloaddition **(Scheme 1.10D)**, since nitrones are inherently more reactive than azides.[152, 170] Strain-promoted alkyne-nitrone cycloaddition has been used to image epidermal growth factor receptors (EGFRs) that are overexpressed on the surface of human breast tumours.[171]



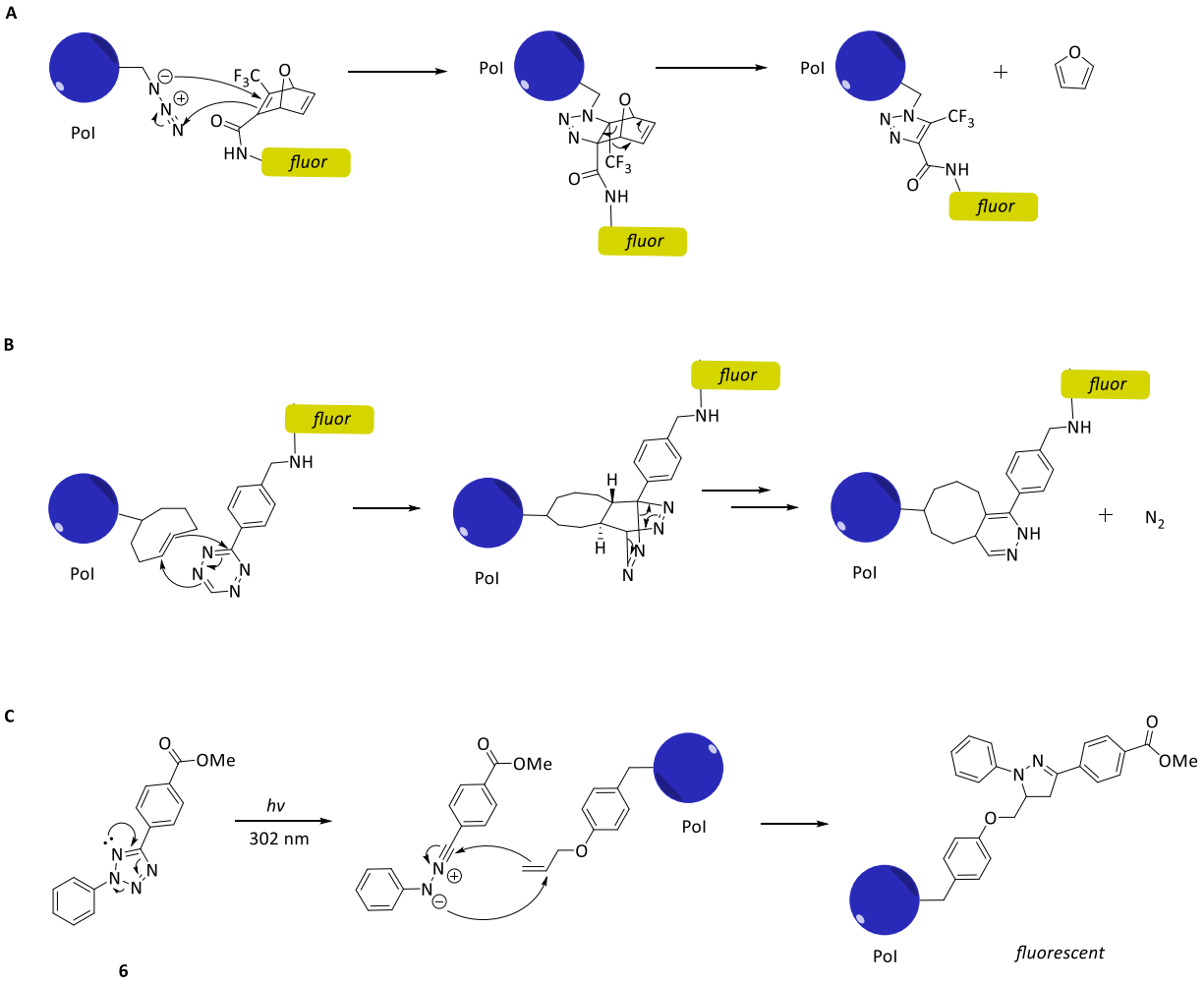
Scheme 1.11: Methods for covalently modifying unnatural amino acids within engineered proteins in order to label or otherwise modify the protein of interest (PoI), utilising Staudinger-type reactions. **A:** Staudinger-Bertozzi ligation to incorporate a fluorescent tag onto an azido-containing amino acid;[172] **B:** Traceless Staudinger-Bertozzi ligation, in which the phosphorous-containing group is cleaved and not incorporated into the final fluorescent product.[173] *fluor* = fluorophore.

Another key use of azido-labelled unnatural amino acids is in a variant of the Staudinger reduction,[174] which is classically the reduction of an azide to a primary amine using a phosphine in the presence of water. Bertozzi's group were able to develop a ligating variant of the Staudinger reaction by using an aromatic phosphine bearing both a fluorophore (or other such tag) and an electrophilic ester group which can trap the initial aza-ylide adduct **(Scheme 1.11A)**.[172] This process has recently become known as the Staudinger-Bertozzi ligation, and has been utilised to label azido-tagged proteins or cell surface glycans, both in live cell cultures[175] and living organisms,[176] and has also proved useful in proteomic analysis,[177] studying fatty-acylation of proteins in eukaryotic cells[178] and for site-selective protein immobilisation.[179] A "traceless" variant has also been developed by reversal of the ester motif in the phosphine probe, such that the phosphine oxide moiety becomes detached from the

labelled protein conjugate during the reaction **(Scheme 1.11B)**.[173] Recently, Gobbo *et al.* have developed AuNP-labelled phosphine probes which are compatible with a Staudinger-Bertozzi ligation to azido-functionalised peptides;[180] this method could show promise for imaging if applicable to a live cell environment due to the ease with which the optical properties of AuNPs can be tuned.[181] The major limitation of the Staudinger-Bertozzi method is the slow kinetics of the ligation; k_2 values are *c.* 10^{-3} M^{-1} s^{-1}, with the rate-limiting step believed to be initial nucleophilic attack of the phosphine on the azide.[172] This limitation, in addition to competing oxidation of phosphines and their off-target reactivity with disulfides, means that high concentrations of phosphines are often required, which can lead to high levels of background noise. The development of second generation phosphine probes, which either only become fluorescent upon oxidation to the phosphine oxide[182] or which contain an intramolecular quenching moiety which is cleaved upon ligation,[175c] have helped to mitigate against these limitations.

Another important chemoselective functionality which can be incorporated into proteins is the olefin group. Olefins do occur naturally in cells (e.g. in cofactors or lipids), and so elegant methods have been developed to make the engineered olefins more reactive than their endogenous counterparts.[183] Initially, a strained derivative of oxonorbornadiene was utilised as a small molecule probe to react with an azido-modified protein **(Scheme 1.12A)**;[184] the reaction proceeds *via* a 1,3-dipolar cycloaddition followed by a retro-[4+2] cycloaddition, liberating furan as a byproduct and forming a stable triazine. However, the reaction is slow (k_2 = *c.* 10^{-4} M^{-1} s^{-1}) and some nucleophilic amino acid residues have the potential to undergo a competing conjugate addition with the electron-deficient olefin in the oxonorbornadiene; both of these limit the widespread use of this methodology.[184] However, incorporation of a strained olefin into a protein as an unnatural amino acid residue has proved more promising. A *trans*-cyclooctene-containing protein has been demonstrated to react with 1,2,4,5-tetrazines in aqueous media at ambient temperature in an inverse electron-demand [4+2] cycloaddition-retro-[4+2] cycloaddition reaction sequence to liberate dinitrogen; the initial product then undergoes isomerisation in a protic solvent **(Scheme 1.12B)**.[185] The k_2 values for

such reactions are remarkably high, at *c.* 10^3-10^4 M^{-1} s^{-1}, which has enabled its use in modifying and imaging proteins both *in vitro* and *in vivo*.[185c, 186]

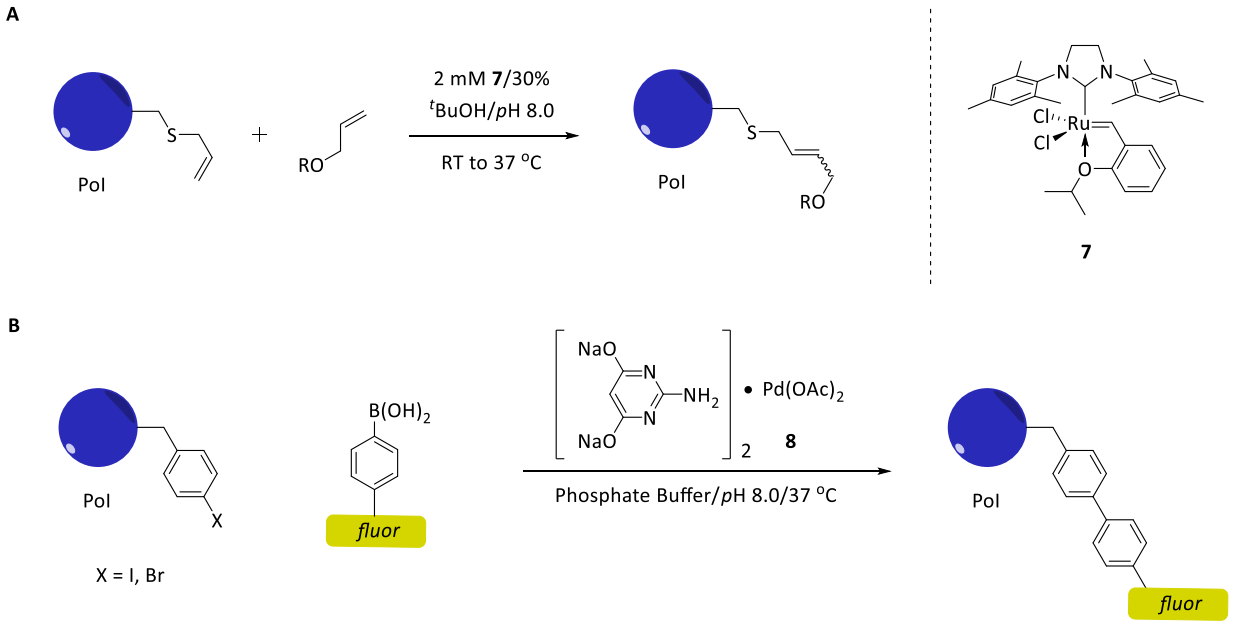


Scheme 1.12: Methods for covalently modifying unnatural amino acids within engineered proteins in order to label or otherwise modify the protein of interest (PoI), utilising cycloaddition reactions of olefins. **A:** 1,3-dipolar cycloaddition of an azido-containing amino acid with a strained fluorophore-labelled alkene, followed by a retro-[4+2]-cycloaddition to liberate furan;[184] **B:** Inverse-electron-demand [4+2] cycloaddition with a fluorescent 1,2,4,5-tetrazine followed by a retro-[4+2] cycloaddition to liberate nitrogen gas;[185] **C:** Photoinduced click reaction between 2,5-diaryltetrazole **6** and an allyl ether.[187] *fluor* = fluorophore.

Norborenes have also been incorporated into proteins and undergo similar reactions with tetrazines, but with lower k_2 values (*c.* 2 M^{-1} s^{-1}); however, this k_2 value is still higher than that for most Cu-free click reactions and the reaction has been used to image proteins in live

bacterial and mammalian cells.[188] Usefully, if the tetrazine moiety is conjugated to a red fluorophore, the tetrazine itself acts as a fluorescence quencher and thus suppresses background fluorescence; however, after reaction with the desired strained alkene target the fluorescence is restored.[189] This chemistry has recently been used for some promising medical imaging applications. Rossin *et al.* developed a system whereby a *trans*-cyclooctene-tagged mAb against the solid state tumour marker TAG72 undergoes a click reaction with a tetrazine linked to a chelating agent for the positron emitting radioisotope ^{111}In, which enables imaging of the tumours.[190] Zeglis *et al.* reported a similar strategy, based on a norborene-tagged anti-HER2 antibody and using ^{64}Cu or ^{89}Zr as the radioisotope;[191] both of these examples are of particular note as they enable a diverse range of radiopharmaceuticals to interact with a single antibody stock.

Other cycloaddition reactions for labelling of modified proteins include Ni-catalysed [2+2+2] cycloadditions[192] and a [4+1] cycloaddition between an isonitrile and a tetrazine,[193] which has been used to image cell surface glycoproteins on tumour cells.[194] A photoinduced 1,3-dipolar cycloaddition (a "photoclick" reaction) between a 2,5-diaryltetrazole, **6**, and an olefin-tagged protein has also been effected: irradation at 302 nm promotes a retro-1,3-dipolar cycloaddition of **6** to liberate dinitrogen and a nitrile-imine, which can undergo rate-limiting 1,3-dipolar cycloaddition with the olefin **(Scheme 1.12C)**.[187] Electron-donating groups on the aryl substituents of the tetrazole raise the HOMO energy of the nitrile-imine and hence speed up the reaction:[195] k_2 values of up to 60 M^{-1} s^{-1} have been reported, making these processes faster than Staudinger-Bertozzi or Cu-free click reactions. The most useful facets of this reaction, however, are that: (a) both starting materials are non-fluorescent but the product pyrazoline is; and (b) the induction of the reaction by light gives spatiotemporal control over the reaction. These features make this system (or the corresponding reaction whereby the protein is tetrazole-labelled and the probe contains olefin functionality) attractive for live cell imaging and perturbation studies.[196] However, the extent of undesirable side reactions of tetrazoles with endogenous olefins under these conditions has not yet been fully determined.



Scheme 1.13: Methods for covalently modifying unnatural amino acids within engineered proteins in order to label or otherwise modify the protein of interest (PoI), utilising biocompatible organometallic-catalysed reactions. **A:** Biocompatible olefin metathesis between an *S*-allylcysteine with allyl ethers using catalyst **7**;[197] **B:** Biocompatible Suzuki-Miyuara coupling, in which a fluorescent boronic acid is coupled to a haloarene-containing amino acid under aqueous conditions.[198] *fluor* = fluorophore.

An alternative interesting reaction of olefin-containing unnatural amino acids is olefin metathesis,[199] which Davis and co-workers have shown can be carried out in a water/*tert*-butanol mixture with a 50-90% conversion rate using the Hoyveda-Grubbs catalyst **7**[200] and $MgCl_2$ **(Scheme 1.13A)**.[197] The protein tag initially chosen was an allyl sulfide, which can be incorporated into a protein either chemically or genetically,[197, 201] but subesqeuently allyl selenides were found to be more optimal substrates.[202] A range of modifications were carried out *in vivo* such as glycosylation and PEGylation. Further developments could lead to catalysts which are capable of installing fluorescent groups and act effectively *in vivo*.

The Davis group have also successfully developed biocompatible catalytic conditions for the labelling of haloarene-containing unnatural amino acids *via* a Suzuki-Miyaura[203] cross-coupling reaction catalysed by the Pd-complex **8 (Scheme 1.13B)**.[198] By incorporation of *para*-iodophenylalanine into the *E. coli* porin channel protein OmpC, the bacterial cell surface could

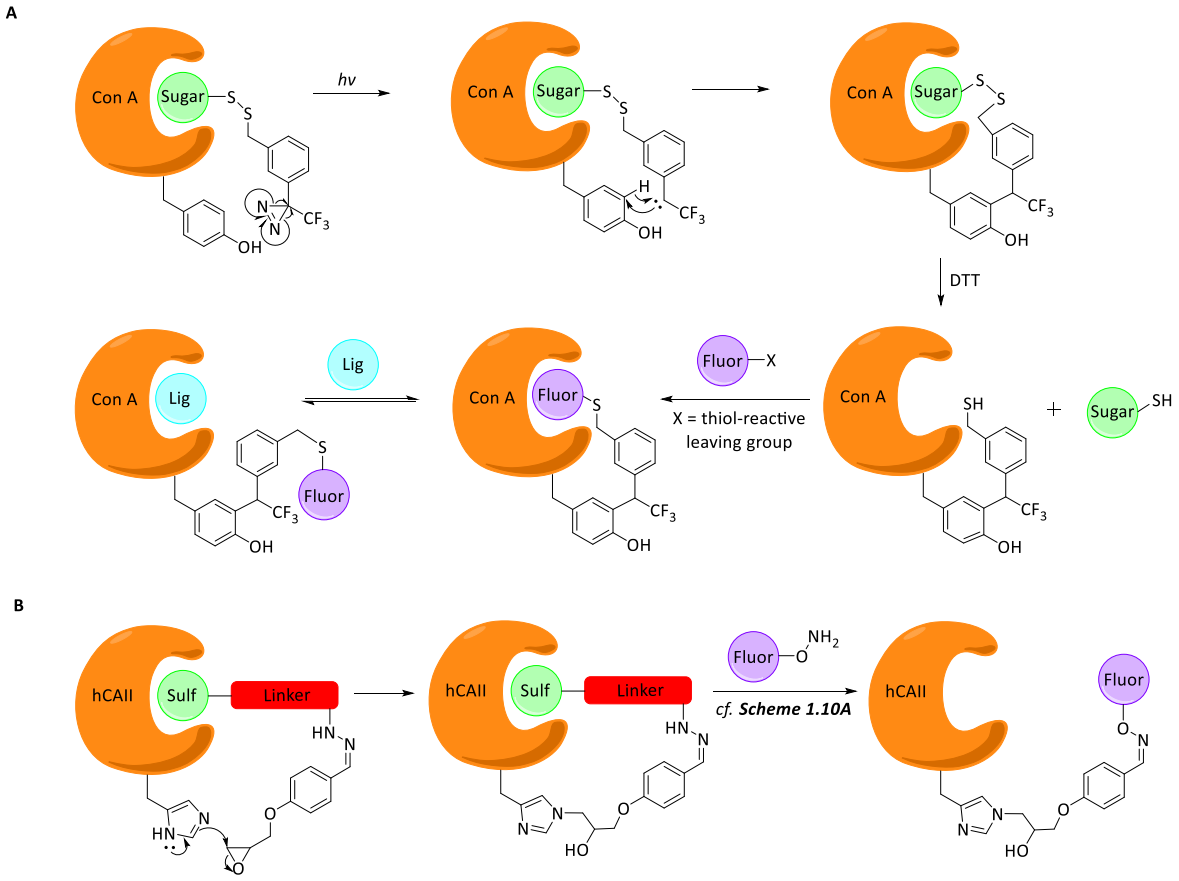
be labelled with a fluorescent boronic acid.[204] Cu-free Sonogashira-type[205] couplings have also been used to functionalise metabolically encoded alkyne-containing proteins in *E. coli* using a similar catalyst.[206] More recently, Chen and co-workers have developed a ligand-free variant in which water-soluble PdNPs generated from $Pd(NO_3)_2$ *in situ* act as the catalyst, and have used this reaction to site-specifically label modified proteins from pathogenic Gram-negative bacteria.[207] One of the strengths of this system is that it is truly bioorthogonal due to the absence of palladium from biological systems. However, care must be taken when designing metal-based systems for use *in vivo* due to the cytotoxicity of many *d*-block metals and metal-based complexes.

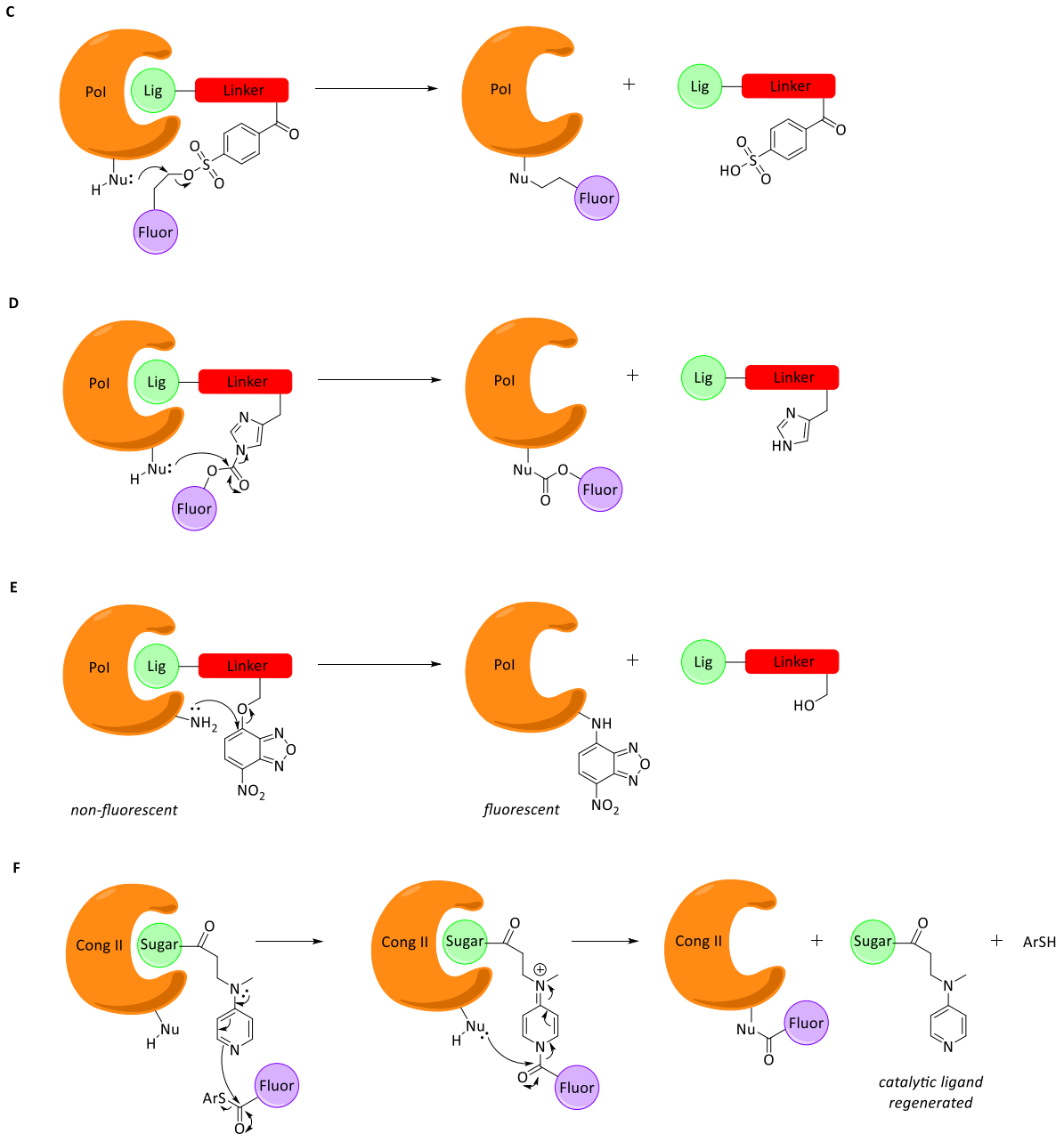
1.1.3.3. Covalent Labelling of Native Proteins: Ligation Probes

The techniques discussed in the previous two sections all add vastly to the repertoire of the chemical biologist and have played key roles in elucidating aspects of protein structure, function and dynamics *in vivo*, and will continue to do so, particularly considering the advent of methods for genetic code expansion.[142a] However, none of these methods are of use in the clinic for disease diagnosis, given the prerequisite of a modified protein. Alternative techniques have also been developed for covalent labelling of *native* proteins with optical chemical probes.[208] These are broadly termed "ligand-directed" labelling methods, as they rely on a noncovalent recognition between the probe ligand and the protein active site followed by proximity-induced formation of a covalent linkage between a reactive group on the probe and a residue on the target protein neighbouring the active site; removal of the recognition ligand from the active site enables "traceless" labelling **(Scheme 1.14)**.

Hamachi and co-workers pioneered a system called post-photoaffinity labelling modification (P-PALM) on the model protein concanavalin A (Con A), a lectin which recognises saccharide moieties.[208] A Con A inhibitor was developed which contained three key functionalities: an α-D-mannoside for enzyme recognition; a cleavable disulfide linker; and a photo-reactive diazirine group **(Scheme 1.14A)**.[209] After binding of the saccharide to the Con A active site,

irradiation with UV light (λ_{ex} = 330-400 nm) extrudes nitrogen from the diazirine, forming a reactive carbene species which reacts specifically with the Tyr100 residue of Con A proximal to the active site. Once attached, the disulfide tether is cleaved with a reducing agent such as dithiothreitol (DTT), and the free α-toluenethiol group can chemoselectively ligate to an added thiol-reactive fluorophore. The fluorescent output of the tag is dependent on its solvation environment, and fluoresces more strongly within the active site of Con A than in the more polar aqueous environment around the protein; therefore, if a saccharide is added which can compete with the fluorophore for the active site **(Scheme 1.14A)**, fluorescence titration enables an accurate quantification of the binding constant of the added saccharide. In this example, labelled Con A itself therefore acts as a biosensing device. This is a particularly ingenious development as it mitigates against any non-specific interactions of the thiol-reactive fluorophores (e.g. with cysteine-containing proteins),[208] which is a common limitation of the use of the P-PALM method to *in vitro* or *in vivo* protein detection. The other major limitation of all P-PALM strategies is the often low yield of the photoaffinity step (*c.* 20%).[208]





Scheme 1.14: Methods of covalently modifying native proteins. **A:** Post-photoaffinity labelling modification (P-PALM);[209] **B:** Post-affinity labelling modification (P-ALM);[210] **C:** Ligand-directed tosyl (LDT) chemistry;[211] **D:** Ligand-directed acyl imidazole (LDAI) chemistry;[212] **E:** Use of an *O*-nitro-benzoxadiazole probe;[213] **F:** Catalytic strategy based on affinity-guided DMAP (AGD) chemistry.[214] Con A = concanavalin A; Cong II = congerin II; Fluor = fluorophore; hCAII = human carbonic anhydrase II; Lig = ligand; PoI = protein of interest; Sulf = sulfonamide.

Subsequently, a non-photoactivated system known as post-affinity labelling modification (P-ALM) was developed. The tags used in P-ALM contain an electrophilic moiety linked to the ligand; the electrophilic moiety can then react with a nucleophilic amino acid residue to form

a covalent link to the protein. In a model system, a sulfonamide ligand for human carbonic anhydrase II (hCAII) was attached to a reactive epoxide *via* a hydrazone linkage.[210] After ligand binding to the active site, a histidine residue attacks the terminal carbon of the epoxide to form a covalent linkage. Enzymatic activity is restored by cleavage of the hydrazone using an excess of a fluorescent hydroxylamine **(Scheme 1.14B)**.

A one-step procedure for protein labelling termed ligand-directed tosyl (LDT) chemistry was subsequently developed, eliminating the intermediate steps required in P-PALM and P-ALM. Proximity-induced attack of a nucleophilic amino acid residue in an S_N2 fashion on a reactive tosyl linker both tags the protein with a functional reporter (e.g. a fluorophore) and cleaves the ligand in a single step **(Scheme 1.14C)**. His, Tyr and Glu are all suitable nucleophilic residues for LDT labelling, and site-specific labelling of a variety of endogenous proteins has been reported in intracellular environments.[211] LDT labelling of FKBP12 has also enabled study of its molecular interactions both *in vitro* and in living cells using FRET imaging.[215] LDT is however limited by its slow rate *in vivo*, and hence more reactive approaches have recently been employed. In ligand-directed acyl imidazole (LDAI) chemistry, the key step is acyl transfer from the acyl imidazole probe to a nucleophilic amino acid residue on the target protein **(Scheme 1.14D)**;[212] LDAI has enabled functional studies on a host of membrane proteins in living cells.[212-216] LDAI reagents are complementary to LDT reagents as they react with Ser, Tyr and Lys residues.[217] One other ligation strategy of interest uses non-fluorescent *O*-nitro-benoxadiazole derivatives as ligands: displacement of the *O*-substituent by a Lys residue in an S_NAr-type reaction results in "switch-on" fluorescence **(Figure 1.14E)**.[213] The technique has been used to visualise mitrochondria which express translocator protein (TSPO) in living cells.

In a further variant on these strategies known as affinity-guided DMAP (AGD) chemistry, a protein of interest can be selectively acylated using a ligand-tethered DMAP catalyst. Hamachi and co-workers initially used a DMAP-tethered saccharide and a fluorescent thioester as the acyl donor for labelling the lectin congerin II (Cong II) **(Scheme 1.14F)**.[214] The strategy proved effective for labelling Cong II in bacterial cell extracts and animal tissue. Use of a multivalent

AGD catalyst enabled labelling and imaging of proteins on the surface of live cells, such as the G-protein coupled receptor (GPCR) bradykinin B_2 (B_2R).[218] The fluorescence output of modified B_2R can be quenched *via* FRET by the addition of a B_2R ligand containing a quenching moiety, but restored upon binding of a competitor antagonist of B_2R; this highlights the potential use of AGD systems in cellular screening and testing of potential drug candidates against receptors. In another recently developed catalytic system, Nakamura and co-workers have developed a protein modification system based on proximal single electron transfer (SET) catalysis, using a ligand which is conjugated to $[Ru(bpy)_3]^{2+}$.[219]

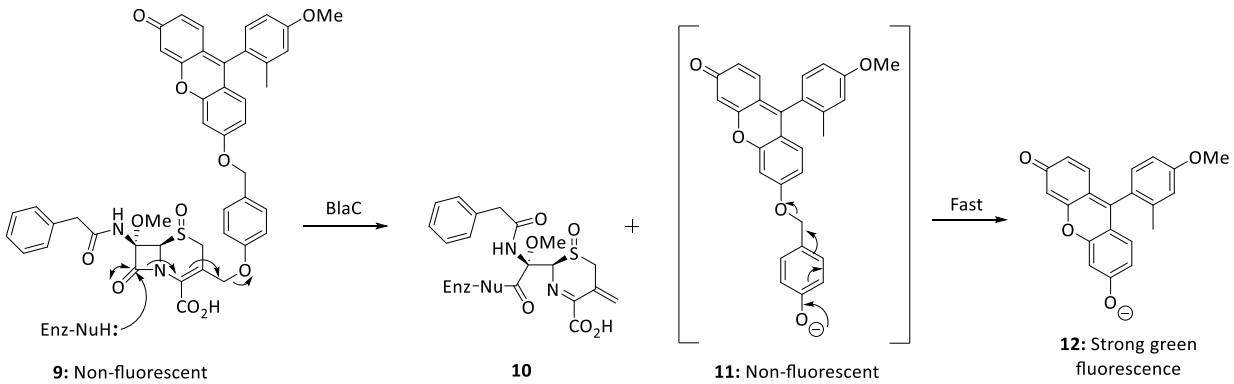
One other technique of note involving covalent protein tagging is activity-based protein profiling (ABPP), pioneered by the Cravatt lab,[220] which aims to identify and assign roles to numerous newly predicted gene products. In ABPP, reactive probes ligate to only the active form of an enzyme.[221] The probes are linked to fluorophores or biotin and can be detected by in-gel fluorescence scanning;[221a] subsequent affinity purification and MS analysis enables identification of the protein target.[221b] The key advantage of ABPP over other proteomic techniques is the ability to only detect active protein and exclude any inactive (e.g. inhibitor-bound or mis-folded) forms; ABPP probes have been developed for enzyme classes including metalloproteases,[222] serine proteases[221b, 223] and oxidoreductases;[224] enzyme activity can even be profiled *in vivo* by utilisation of click chemistry methods.[225] Whilst useful for elucidating protein function and for discovering novel protein inhibitors *via* competition experiments,[226] the need for a purification step limits the utility of ABPP in a point-of-care diagnostic device.

1.1.4. Non-Covalent Probes for Detection of Specific Native Proteins: Substrate Mimics

Two major challenges arise in covalent labelling of proteins: firstly, many of the developed systems are not truly “bioorthogonal” and do suffer from the possibility of off-target effects; and secondly, covalent modifications are irreversible, which might preclude any desired *in vivo* studies due to potential modulations of protein structure or function. No covalently-modifying system has yet been developed to sensitively quantify levels of a target protein.

Both of these limitations could be overcome if ligands which bind to specific proteins in a non-covalent fashion could be engineered to give a distinctive optical readout in the presence solely of their protein target. Several laboratories have researched the possibility that such a ligand could be a substrate mimic of the target enzyme; for instance, a substrate mimic might be nonfluorescent, but its reaction products in the presence of the enzyme might emit a concentration-dependent fluorescent signal, enabling quantification of enzymatic activity.

One of the most promising recently reported systems features a substrate mimic for the *M. tuberculosis* protein β-lactamase C (BlaC) **(Scheme 1.15)**.[227] The mimic, CDC-OMe **9**, contains a β-lactam ring at its core which is hydrolysed by BlaC, and the byproduct of the reaction, **12**, shows a strong green fluorescence. The mimic was specific for detecting activity of BlaC over the common TEM-1 β-lactamase found in Gram negative bacteria, and could be used to detect *M. tuberculosis* in unprocessed human sputum with an LOD of just 10 colony units. Furthermore, the real elegance of this system is that the product fluorescence can be accurately quantified using only a cardboard box, a light-emitting dioide (LED) light source, excitation and emission filters and a camera phone with a lux intensity app, which makes it a rapid and cheap diagnostic test suitable for use in developing countries. Subsequently, similar prinicples have been used to develop a near-IR probe for quantification of BlaC in various strains of *S. aureus*,[228] a far-red probe for quantification of esterase activity,[229] and a green fluorescent probe for imaging mammalian thioredoxin reductase activity in living cells.[230]



9: Non-fluorescent **10** **11:** Non-fluorescent **12:** Strong green fluorescence

Scheme 1.15: Reaction of CDC-OMe **9** and BlaC to generate a "turn-on" fluorescent sensor for detection of tuberculosis pathogens in human sputum samples.[227]

Another "switch-on" optical system of interest is that based on quenching *via* photoelectron transfer (PET).[231] This principle is illustrated by Terai *et al.*, who developed a luminescent probe to monitor the activity of human arylamine *N*-acetyltransferase 2 (HUMAN(NAT2)),[232] an enzyme implicated in phase II metabolism which plays an important role in detoxification of xenobiotic arylamines, hydroxylamines and hydrazines, notably the drug isoniazid.[233] The substrate mimic is an aniline-bearing Tb^{3+} complex, **13**, which is non-luminescent due to intramolecular transfer of a photoelectron from the electron-rich aniline group to the quinolinone moiety; however, upon HUMAN(NAT2)-mediated acetylation to **14**, the aniline group becomes less electron-rich, PET is no longer possible and the complex becomes luminescent **(Figure 1.9A)**. Time-dependent luminescence activity was observed *in vivo* in HUMAN(NAT2)-expressing HepG2, A549 and HeLa cells.[234] Subsequently Wang *et al.* reported a switch-on fluorescent probe **15** for HUMAN(NAT2) which operates *via* an analogous mechanism, and was utilised in *in vivo* murine studies in which the fluorescent signal of product **16** could be detected through the skin of non-shaved live mice **(Figure 1.9B)**.[235] PET-based systems for detection of other enzymatic activity *in vitro* and *in vivo* have also been reported, both based on luminescent[236] and fluorescent[237] probes; enzymes targeted by these studies range from other metabolising enzymes such as glutathione *S*-transferase, alkaline phosphatase and β-galactosidase to enzymes reported to be biomarkers for tumorigenesis, such as carbonic anhydrase, cyclooxygenase-2 and human NAD(P)H:quinone oxidoreductase.

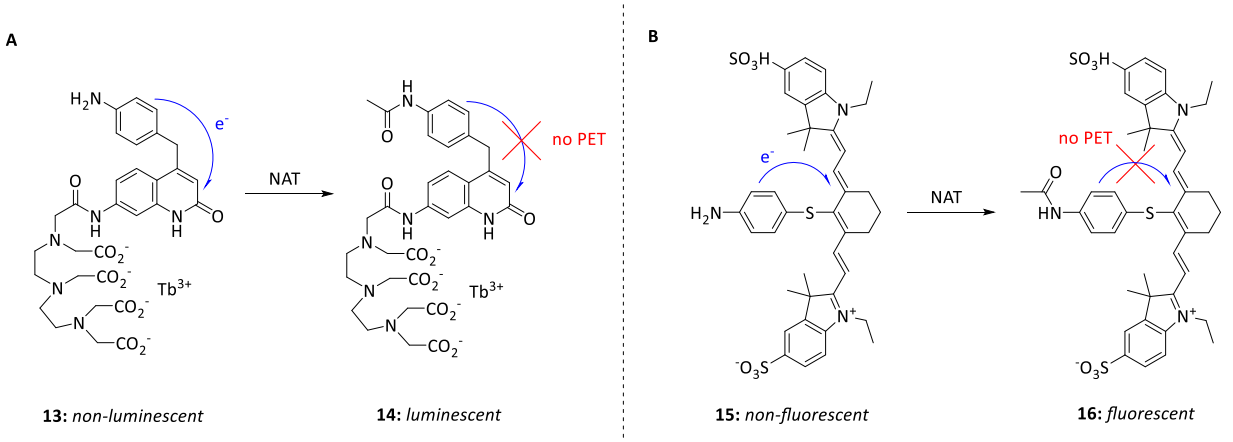


Figure 1.9: Switchable PET sensors for detection of HUMAN(NAT2) activity *in vitro* and *in vivo*, giving a quantifiable luminescent **(A)**[232] or fluorescent **(B)**[235] optical output. PET = photoelectron transfer.

1.1.5. Non-Covalent Probes for Detection of Specific Native Proteins: Towards a Non-Covalent Inhibitory Probe?

Substrate mimics have, for the first time, led to the development of rapid diagnostic tests using small molecules with a real possibility of clinical application.[227] Whilst the sensitivities of such systems might not yet be as impressive as those of biosensors, their relative simplicity, lower cost and the ease of assay procedure makes them promising for widespread use. However, substrate mimics too have their limitations. Since they rely on catalytic activity and substrate turnover to generate an optical output, their use is restricted to detection of proteins with a catalytic function. Moreover, substrate mimics can give a reliable quantification of enzymatic activity, but not of enzyme concentration – both the intrinsic turnover rate of the enzyme and whether it is correctly folded will dramatically affect the readout from these assays. What would ultimately be highly desirable in a small molecule protein sensor is a molecule which binds non-covalently and selectively to its target protein, with low levels of nonspecific binding, and which generates a change in optical readout upon binding that could enable quantification of the protein concentration.

Cravatt and co-workers have reported a non-covalent fluorescent probe (JW576, **19**) for the serine hydrolase KIAA1363, which they developed by fusing a known inhibitor (JW480, **17**) for the enzyme with the fluorophore boron-dipyrromethene (BODIPY) **18 (Figure 1.10A)**.[238] KIAA1363 regulates pro-tumorigenic lipids in cancer cells, and through spatiotemporal imaging *in vivo* using **19** it was found that KIAA1363 is largely localised to the endoplasmic reticulum in these cells and has a half-life of 14-23 h. In other examples, a coumarin-labelled probe was used for in-gel fluorescence detection of human cysteine cathepsins,[239] and a biotin-tagged antagonist of cannabinoid receptors was used for imaging of cell cultures.[240] These non-covalent sensors are useful and effective in the particular systems studied because they have incredibly high potencies for the target enzyme; however, as they are not switchable, in any system where such a probe displays non-specific or non-absolute binding to its target, there will be high background fluorescence and false positive readouts.

In 2010, a promising lead[241] for a switchable non-covalent probe was reported by Russell and co-workers.[242] Naphthoquinone **20** was identified in a medium-throughput screen[243] as a potent and selective inhibitor for the putative cancer biomarker human arylamine *N*-acetyltransferase 1 (HUMAN(NAT1)); serendipitously, it was noted that naphthoquinone **20** undergoes a colour change from red to blue in the presence of HUMAN(NAT1) and its murine homologue MOUSE(NAT2), but not in the presence of any other NAT isoform tested, even MOUSE(NAT1), for which partial inhibition was observed **(Figure 1.10B)**. As a similar colour change was observed in a basic aq. 1 M NaOH solution, it was hypothesised that the observed colour change might arise due to deprotonation of naphthoquinone **20** within the active site of its target protein; titration revealed a pK_a of *c.* 9.5 for the acidic sulfonamide-N*H*. This result gave rise to the possibility that a probe based on naphthoquinone **20** might able to accurately quantify levels of HUMAN(NAT1) in a biopsy sample in order to diagnose early-stage cancers, and this is the premise to which the remainder of this thesis is devoted.

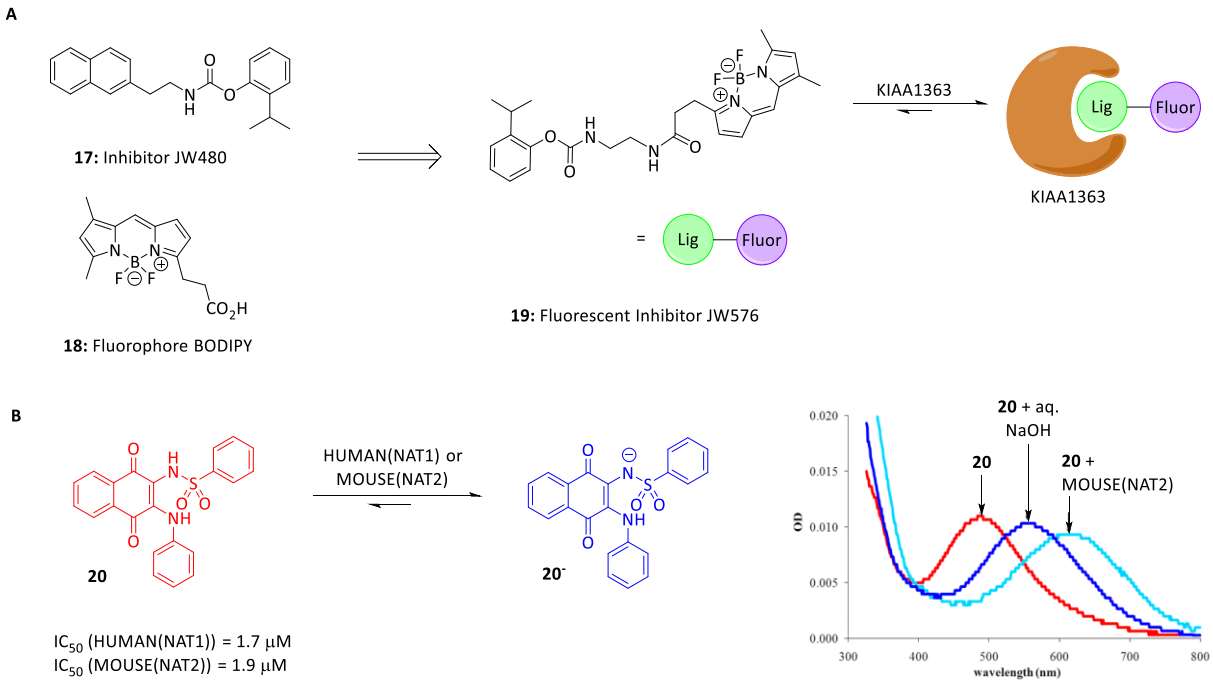
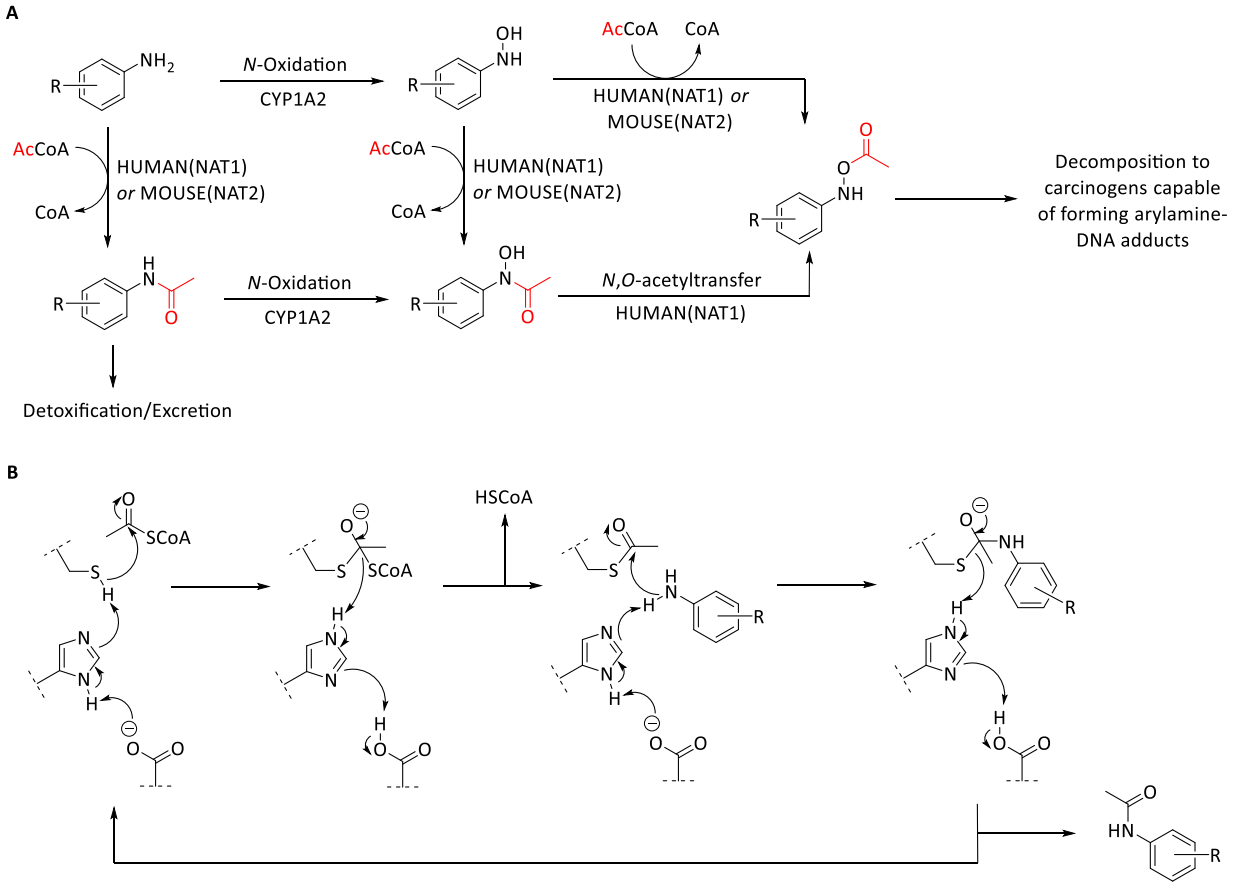


Figure 1.10: A: Non-covalent fluorescent inhibitor of the serine hydrolase KIAA1363, which displays favourable thermodynamics and kinetics of binding to its target protein.[238] **B: Left:** Naphthoquinone inhibitor **20**, a switchable colorimetric probe for HUMAN(NAT1); **Right:** UV-visible spectrum of **20** at 10 µM in 95% aq. Tris•HCl (*p*H 8.0)/5% DMSO (*v/v*) (red line, λ_{max} = 489 nm), 95% aq. NaOH/5% DMSO (*v/v*) (dark blue line, λ_{max} = 561 nm) and 95% aq. Tris•HCl (*p*H 8.0)/5% DMSO (*v/v*) + 20 µM MOUSE(NAT2) (light blue line, λ_{max} = 610 nm).[242]

1.2. Arylamine *N*-Acetyltransferases

The arylamine *N*-acetyltransferases (NATs) are a family of enzymes between 30-35 kDa in molecular weight, found in a wide variety of both prokaryotic and eukaryotic species.[244] Their catalytic function is to transfer an acetyl group from the biological cofactor acetyl Coenzyme A (AcCoA) to a xenobiotic arylamine, alkylarylamine, arylhydroxylamine or arylhydrazine; *N*-, *O*- and *N*,*O*-acetylation have all been reported in the literature.[245] *N*-acetylation of these species results in detoxification, whilst *O*-acetylation of *N*-arylhydroxylamines can generate highly reactive species which are capable of forming adducts with DNA **(Scheme 1.16A)**.[246] Crystallographic studies reveal that the key catalytic triad comprises of an aspartic acid, a histidine and a cysteine,[247] and kinetic studies suggest that the catalysis is mediated *via* a Ping-Pong bi-bi mechanism, as outlined in **Scheme 1.16B**.[248]



Scheme 1.16: A: Metabolic pathways showing the potential fates of arylamines in a NAT-producing organism.[246] **B:** Ping-pong bi-bi mechanism of catalysis by NATs, utilising the Cys-His-Asp catalytic triad.

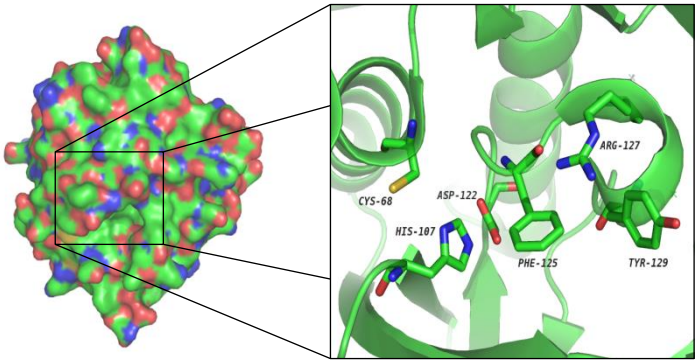
1.2.1. NATs in Human Function and Disease

In humans there are two known functional paralogues of the *NAT* gene, *HUMAN(NAT1)* and *HUMAN(NAT2)*, which are found adjacent to one another on chromosome 8 at the 8p22 locus, in addition to a third pseudogene (*NATP*).[249] The functional genes both encode enzymes which catalyse acetyl transfer from AcCoA to xenobiotic substrates, but the tissue distribution and substrate specificities of the two enzymes differ. Different polymorphisms of the *HUMAN(NAT2)* gene exist,[250] and individuals may be broadly classified as having either a "rapid" or "slow" acetylation phenotype with regard to their metabolism of isoniazid, hydralazine and other so-called polymorphic drugs;[245b] the slow acetylation phenotype was found to predominate amongst patients suffering from isoniazid-induced toxicity or hydralazine-induced lupus.[251] A slow acetylation phenotype was also postulated as a risk factor for bladder cancers amongst industrial workers exposed to carcinogenic aniline dyes.[252] *HUMAN(NAT1)* too has subsequently been found to have different alleles due to point mutations.[253] An interesting case is that of the *NAT1*10* allele, which has been associated with an enhanced colon cancer risk;[254] however, this is controversial as the mutation is not within the coding exon – rather, there are insertions and deletions at the 3' end of the gene.

As far as the gene products themselves are concerned, HUMAN(NAT2) is abundant in liver and intestinal cells, and is implicated in Phase II drug metabolism.[245a] The endogenous role of HUMAN(NAT1), however, is unclear: it possesses a widespread tissue distribution and is reported to play a role in cofactor homeostasis, notably folate catabolism,[255] and its eukaryotic homologues are implicated in growth and embryogenesis.[256] Rodent NATs have been reported in several studies to be good models for studying the corresponding human proteins; in particular, MOUSE(NAT2) shares a substrate profile, tissue distribution and 82% sequence identity with HUMAN(NAT1), and is a useful mimic for the human protein in *in vitro* investigations because of its higher stability and greater yields from recombinant expression in *E. coli* and subsequent purification.[257] In 2007, a crystal structure of HUMAN(NAT1) was generated through selective chemical modification of the catalytic Cys68 residue by the

irreversible inhibitor 2-bromoacetanilide,[247b] as had previously been used successfully to determine the first crystal structure of an arylamine *N*-acetyltransferase.[247a] **Figure 1.11A** shows the active site of HUMAN(NAT1) with key active site residues highlighted. Similarities and differences in these residues between the two human and murine versions of the gene are shown in **Figure 1.11B**, with a whole sequence comparison outlined in **Figure 1.11C**.

A



B

Residue	HUMAN (NAT1)	HUMAN (NAT2)	MOUSE (NAT1)	MOUSE (NAT2)
68	Cys	Cys	Cys	Cys
107	His	His	His	His
122	Asp	Asp	Asp	Asp
125	Phe	Ser	Tyr	Phe
127	Arg	Ser	Gly	Arg
129	Tyr	Ser	Tyr	Tyr

C

```
HUMAN(NAT2)     MDIEAYFERIGYKNSRNKLDLETLTDILEHQIRAVPFENLNMHCGQAMELGLEAIFDHIV   60
MOUSE(NAT1)     MDIEAYFERIGYKNSVNKLDLATLTEVLQHQMRAVPFENLNMHCGEAMHLDLQDIFDHIV   60
HUMAN(NAT1)     MDIEAYLERIGYKKSRNKLDLETLTDILQHQIRAVPFENLNIHCGDAMDLGLEAIFDQVV   60
MOUSE(NAT2)     MDIEAYFERIGYQSTRSKLDLKTLTEILQHQIRAIPFENLNIHCGESMELSLEAIFDQIV   60

HUMAN(NAT2)     RRNRGGWCLQVNQLLYWALTTIGFQTTMLGGYFYIPPVNKYSTGMVHLLLQVTIDGRNYI  120
MOUSE(NAT1)     RKKRGGWCLQVNHLLYWALTKMGFETTMLGGYVYITPVSKYSSEMVHLLVQVTISDRKYI  120
HUMAN(NAT1)     RRNRGGWCLQVNHLLYWALTTIGFETTMLGGYVYSTPAKKYSTGMIHLLLQVTIDGRNYI  120
MOUSE(NAT2)     RKKRGGWCLQVNHLLYWALTKLGFETTMLGGYVFNTPANKYSSGMIHLLVQVTISGKDYI  120

HUMAN(NAT2)     VDAGSGSSSQMWQPLELISGKDQPQVPCIFCLTEERGIWYLDQIRREQYITNKEFLNSHL  180
MOUSE(NAT1)     VDSAYGGSYQMWEPLELTSGKDQPQVPAIFLLTEENGTWYLDQIRREQYVPNEEFVNSDL  180
HUMAN(NAT1)     VDAGFGRSYQMWQPLELISGKDQPQVPCVFRLTEENGFWYLDQIRREQYIPNEEFLHSDL  180
MOUSE(NAT2)     VDAGFGRSYQMWEPLELTSGKDQPQVPAIFRLTEENGTWYLDQIRREQYVPNQEFINSDL  180

HUMAN(NAT2)     LPKKKHQKIYLFTLEPRTIEDFESMNTYLQTSPTSSFITTSFCSLQTPEGVYCLVGFILT  240
MOUSE(NAT1)     LEKNKYRKIYSFTLEPRVIEDFEYVNSYLQTSPASVFVSTSFCSLQTSEGVHCLVGSTFT  240
HUMAN(NAT1)     LEDSKYRKIYSFTLKPRTIEDFESMNTYLQTSPSSVFTSKSFCSLQTPDGVHCLVGFTLT  240
MOUSE(NAT2)     LEKNKYRKIYSFTLEPRTIEDFESMNTYLQTSPASVFTSKSFCSLQTPEGVHCLVGSTLT  240

HUMAN(NAT2)     YRKFNYKDNTDLVEFKTLTEEEVEEVLKNIFKISLGRNLVPKPGDGSLTI            290
MOUSE(NAT1)     SRRFSYKDDVDLVEFKYVNEEEIEDVLKTAFGISLERKFVPKHGELVFTI            290
HUMAN(NAT1)     HRRFNYKDNTDLIEFKTLSEEEIEKVLKNIFNISLQRKLVPKHGDRFFTI            290
MOUSE(NAT2)     YRRFSYKDNVDLVEFKSLTEEEIEDVLRTIFGVSLERKLVPKHGDRFFTI            290
```

Figure 1.11: A: Surface representation of the HUMAN(NAT1) protein (pdb: 2PQT);[247b] red represents regions of positive charge, blue regions of negative charge, and green neutral regions. **Inset:** Cartoon representation of the active site, with key residues involved in catalysis or ligand binding highlighted in stick representation. **B:** Similarities and differences in key active site residues between the human and murine NAT1 and NAT2 proteins. **C:** Sequence alignment of HUMAN(NAT2), MOUSE(NAT1), HUMAN(NAT1) and MOUSE(NAT2), using Clustal Omega. A sky blue background highlights the conserved catalytic triad residues; a yellow background differences in residues at a given position between the isoenzymes HUMAN(NAT1) and HUMAN(NAT2); and red lettering differences in residues at a given position between the homologous HUMAN(NAT1) and MOUSE(NAT2).

The substrate selectivity of both human and murine NATs have been studied extensively, and representative substrates for each isoform are shown in **Table 1.2**. Generally, HUMAN(NAT1)/ MOUSE(NAT2) substrates are more polar or charged arylamines, whilst arylhydrazines and less polar arylamines are more readily metabolised by HUMAN(NAT2)/MOUSE(NAT1).[258]

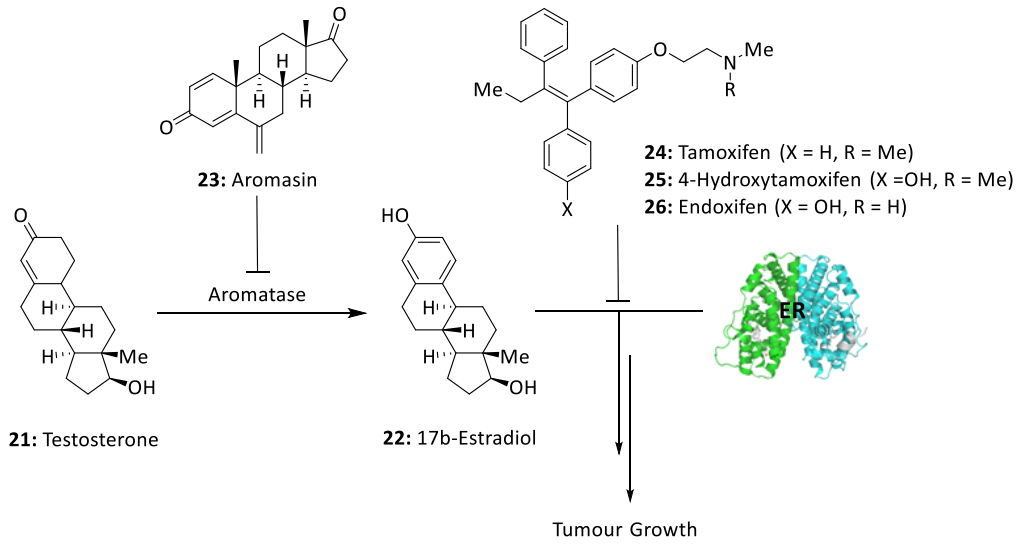
NAT Isoform	Charged Arylamines at *p*H 8				Neutral Arylamines at *p*H 8							Hydrazines	
	*p*ABAglu	*p*ABA	4AS	5AS	ANL	4CA	4BA	ASL	4AV	EOA	POA	INH	HDZ
HUMAN(NAT1)	-	++	+	+	-	-	-	+	-	-	--	--	--
MOUSE(NAT2)	++	++	+	-	+	-	--	++	++	++	--	--	--
MOUSE(NAT1)	--	-	+	+	++	--	--	-	--	--	--	++	+
HUMAN(NAT2)	--	--	--	-	++	+	+	--	+	+	+	+	++

Table 1.2: Substrate specificities of HUMAN(NAT1), MOUSE(NAT2), MOUSE(NAT1) and HUMAN(NAT2).[258] The symbols show % specific activity for each substrate/enzyme combination as follows: ++ for 75-100%; + for 50-74.9%; - for 25-49.9%; -- for 0-24.9%. ANL = aniline; 4AS = 4-aminosalicylic acid; 5AS = 5-aminosalicyclic acid; ASL = anisole; 4AV = 4-aminoveratrole; 4BA = 4-bromoaniline; 4CA = 4-chloroaniline; EOA = 4-ethoxyaniline; glu = glutamate; HDZ = hydralazine; INH = isoniazid; *p*ABA = *para*-aminobenzoic acid; POA = 4-phenoxyaniline.

Over the last decade, efforts have been made to investigate the emerging role of HUMAN(NAT1) in breast cancers.[259] Breast cancer is the second most common cancer worldwide, with over a million new cases reported each year. In the UK it accounts for 30% of female cancers, and the lifetime risk of a woman developing the disease is 1 in 8.[260] There are several subtypes of breast tumour, of which the most prevalent are estrogen-receptor-positive (ER+) tumours, in which the nuclear estrogen receptor (ER) is overexpressed. It is believed that overexpression of ERs can lead to carcinogenesis either due to the fact that increased binding of estrogen to ERs stimulates proliferation of mammary cells (which in turn gives rise to an increased probability of replication errors), or that the by-products of increased estrogen metabolism are genotoxic.[261]

Current treatments for ER+ tumours include aromatase inhibitors, which inhibit the final step in the biosynthesis of estrogen from testosterone, and selective ER modulator (SERM) therapies, such as Tamoxifen **24**, the downstream metabolites of which (4-hydroxytamoxifen **25** and endoxifen **26**) are antagonists of ERs **(Scheme 1.17)**.[262] However, treatment can fail

due to intrinsic or acquired resistance,[263] highlighting the need for alternative therapies for ER+ cancers. Early detection of tumours is known to be vital for increasing the chances of long-term patient survival;[264] however, current immuno-histochemical staining tests to detect ERs are expensive, time-consuming and can suffer from standardisation problems.[265]



Scheme 1.17: Final step in the biosynthesis of 17b-estradiol, and mechanisms of action of the drugs Aromasin **23** and Tamoxifen **24** in the treatment of ER+ breast tumours. ER = estrogen receptor.

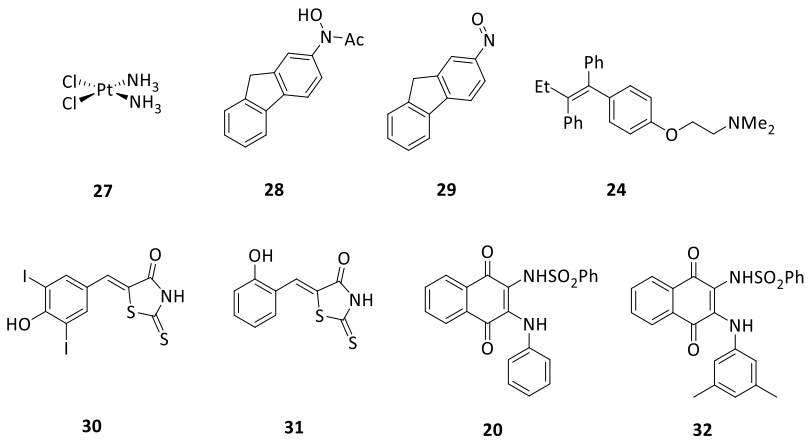
Microarray[266] and proteomic[267] studies have independently reported *HUMAN(NAT1)* as one of the ten most overexpressed genes in ER+ breast tumours relative to healthy tissue; this overexpression correlates inversely with tumour grade.[268] More recently, *HUMAN(NAT1)* overexpression in ER+ male breast cancers has also been reported,[269] and expression levels of NAT1 are shown to be positively correlated to those of ERα (P <0.0001).[270] Estrogen levels themselves are believed to play a role in HUMAN(NAT1) overexpression.[271] Interestingly, lymph node-positive breast cancer patients with tumours expressing high levels of NAT1 were observed to have better disease-free survival (P = 0.0025) and overall survival (P = 0.0007) than those expressing lower NAT1 levels.[270] These data suggest that HUMAN(NAT1) could be a potential surrogate diagnostic or prognostic marker for the estrogen receptor in ER+ tumours.

In addition, shRNA knockdown experiments have demonstrated that knockdown of the *HUMAN(NAT1)* gene in the triple-negative breast cancer cell line MDA-MB-231 (which

expresses high levels of HUMAN(NAT1)) results in a reduction in both the proliferative and invasive capabilities of the cells,[272] accompanied by a change in cell morphology and loss of cell surface filopodia.[273] When MDA-MB-231 cells were injected into nude mice, those expressing anti-NAT1 shRNA led to the formation of significantly fewer colonies in the lungs of the mice than those not expressing anti-NAT1 shRNA.[273] shRNA knockdown of NAT1 in the non-invasive colon cancer cell line HT-29 also led to a reduction in cell proliferation in cultures due to an upregulation of E-cadherin, a membrane protein which promotes cell-cell contact inhibition of growth.[274] Furthermore, hallmarks of oncogenic potential have been reported in the non-cancerous breast cell line HB4a after the cells were induced to overexpress *HUMAN(NAT1)*,[267] and overexpression of HUMAN(NAT1) in mice has been demonstrated to be detrimental in development, and may well act through a reduction in folate levels.[275] These studies suggest that HUMAN(NAT1) should be further investigated as a potentially novel therapeutic target in several cancer subtypes.

1.2.2. Known Inhibitors of HUMAN(NAT1)

Several small molecules **(Figure 1.12)** have been reported to act as inhibitors of HUMAN(NAT1). Many of these, however, are non-specific inhibitors, which preclude them from being useful tools for studying HUMAN(NAT1) in cells or in the diagnosis and treatment of disease. The chemotherapeutic agent *cis*-platin **27** is reported to bind covalently and irreversibly to Cys68 of NAT1, with a fast on-rate of 700 M^{-1} min^{-1},[276] and species such as the *N*-substituted hydroxamic acid **28** and nitrosoarene **29** were also reported to bind covalently but reversibly to Cys68.[277] The SERM Tamoxifen **24** was shown to inhibit HUMAN(NAT1) non-covalently,[278] although in a non-specific fashion. Recently, certain nanoparticles have been observed to bind to HUMAN(NAT1), affecting its behaviour: negatively-charged nanoparticles such as ZnO and SiO_2 were shown to have an inhibitory effect, whilst thermo-responsive diblock copolymers of poly(dimethylacrylamide) and poly(*N*-isopropylacrylamide) enhanced enzymatic activity.[279]



Compound	IC_{50} (μM) HUMAN(NAT1)	IC_{50} (μM) MOUSE(NAT2)
30	0.33	1.80
31	1.10	N.D.
20	1.65	1.86
32	N.D.	0.99

Figure 1.12: Compounds which are reported to be either covalent **(27-29)** or non-covalent **(20, 24, 30-32)** inhibitors of HUMAN(NAT1) activity *in vitro* or *in vivo*, and IC_{50} values for compounds **20** and **30-32** against HUMAN(NAT1) and its murine homologue MOUSE(NAT2), as reported in studies by Russell *et al.*[243] and Laurieri *et al.*[242]; N.D. = not determined in these particular studies.

In a medium-throughput screen of 5016 compounds, naphthoquinone **20** and rhodanine **30** were found to inhibit both recombinant HUMAN(NAT1) and NAT1 activity in the ER+ breast cancer cell line ZR-75-1, and were selective for NAT1 over NAT2 and prokaryotic NATs.[243] Optimisation of rhodanine **30** generated the more stable inhibitor Rhod-*o*-hp **31**,[174] which in a study by Minchin and co-workers exhibited dose-dependent inhibition of cell growth in the MDA-MB-231 cancer cell line;[272] however, rhodanines are known to be "promiscuous" protein inhibitors[280] and the concentrations used in this study vastly exceeded the IC_{50} value of **31** against HUMAN(NAT1), and so a NAT-dependent mechanism could not be proved.

Naphthoquinone **20**, meanwhile, is of great interest due to the fact that it undergoes a distinct, visible colour change from red to blue specifically in the presence of HUMAN(NAT1), as described above **(Section 1.1.5.)**;[242] this type of non-covalent, switchable optical probe for specific protein detection represents, to the best of our knowledge, a completely novel paradigm in protein sensing. A small initial optimisation study on **20** led to the discovery of dimethylated species **32** with modestly enhanced potency and optical sensitivity;[127] this species **32** is considered to be the lead compound for further investigations into developing small molecule optical probes for specific detection and inhibition of HUMAN(NAT1).

1.3. Aims of the Current Project

The discovery of compounds **20** and **32** as specific, non-covalent, reversible inhibitors of HUMAN(NAT1) and MOUSE(NAT2) which undergo a colour change from red to blue in the presence of these homologous proteins leads to the possibility that such switchable probes could be used to quantify levels of HUMAN(NAT1) in patient samples for more effective diagnosis and prognosis of ER+ breast cancers. Furthermore, the development of a potent and specific HUMAN(NAT1) inhibitor could enable us to establish the role of small molecule HUMAN(NAT1) inhibition in cancer cell lines, as well to further investigate the poorly-defined endogenous function(s) of the protein. The central aims of this thesis are therefore:

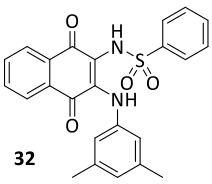
- To establish the mechanism by which the observed colour change is effected in the presence of HUMAN(NAT1) and its murine homologue MOUSE(NAT2), which is used extensively throughout this study as a model for the human protein;
- To develop a binding model for derivatives of compound **32** to HUMAN(NAT1) and MOUSE(NAT2), based on structure-activity relationship studies and *in silico* modelling;
- To develop analogues of compound **32** with increased potency and sensitivity, but retained selectivity, for HUMAN(NAT1) and its murine homologue, such that levels of HUMAN(NAT1) can be accurately detected and quantified in cell extracts from cell lines overexpressing NAT1;
- To develop potent, specific inhibitors of HUMAN(NAT1) and MOUSE(NAT2) with sufficiently high aqueous solubility and cell membrane permeability to enable testing of the effects of a small molecule HUMAN(NAT1) inhibitor on NAT1-expressing cancer cell lines;
- To utilise developed probes to explore the role of HUMAN(NAT1) in folate metabolism;
- To investigate the potential for extending this novel sensing paradigm to other targets.

Some initial studies on understanding the mechanism of the colour change and structure-activity relationships have been undertaken previously and will be described in **Chapters 2 and 3**.[281]

Chapter 2: Investigating the Requirements of a Colorimetric HUMAN(NAT1) Probe

2.1. Elucidation of the Mechanism of Colour Change of Naphthoquinone 32 in the Presence of HUMAN(NAT1)

In the previous chapter **(Sections 1.1.5. and 1.2.2.)** it was reported that the non-covalent reversible inhibitor of HUMAN(NAT1) naphthoquinone **20** and its dimethylated analogue **32** undergo a striking visible colour change from red to blue specifically in the presence of this isoenzyme and its functional homologues, notably the murine protein MOUSE(NAT2), which is used throughout this study as a model for HUMAN(NAT1).[242, 257] Since a similar colour change was observed in 1 M aq. NaOH solution, it was hypothesised that the underlying mechanism of colour change was deprotonation of the acidic sulfonamide-N*H* (pK_a = 9.5 for **20** and 9.2 for **32**)[281a] within the enzyme active site. *In silico* modelling studies were therefore performed which predicted an interaction between the sulfonamide moiety of naphthoquinone **32** and the arginine residue 127 (Arg127) within the HUMAN(NAT1) active site **(Figure 2.1)**, although this model considers only the neutral form of the ligand and does not take charge into account.[281a]



32

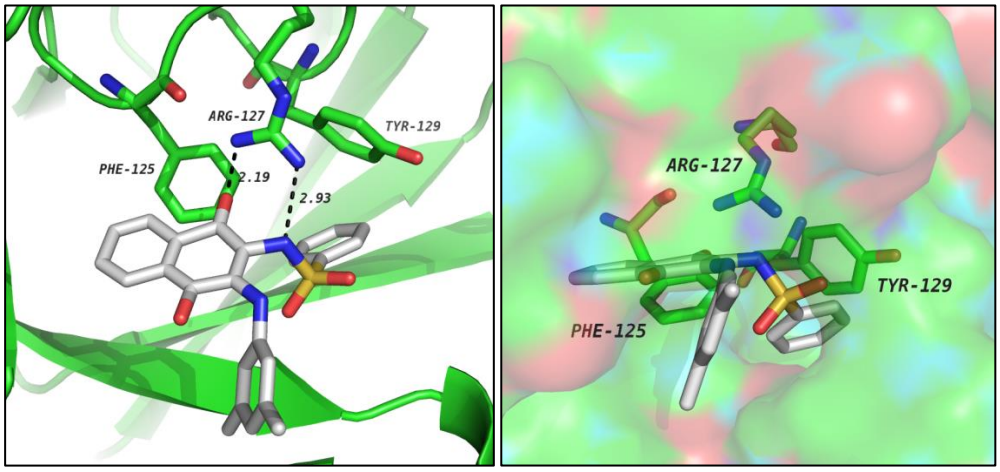


Figure 2.1: *In silico* modelling of naphthoquinone **32 (left)** in the active site of HUMAN(NAT1) (pdb: 2PQT).[247b] Analysis performed using GOLD® (v.5.2).[282] **Centre:** Cartoon representation showing the hypothesised interaction between the sulfonamide moiety of **32** and Arg127; polar contacts are shown by dashed lines with distances in Ångströms. **Right:** Surface representation showing the anilino-C_3 substituent protruding from the active site.

Under the assay conditions of *p*H 8.0, it is predicted that Arg127 will be protonated (pK_{aH} = 12.48),[283] and therefore the hypothesis was modified to accommodate this: if the *in silico* model is correct and an interaction between Arg127 and the sulfonamide moiety of **32** is important in molecular recognition, then the conjugate base of **32**, [**32**]$^-$, could reasonably be expected to bind more strongly to Arg127 *via* an ionic interaction than the neutral species **32**; thus the enzyme might sequester the conjugate base [**32**]$^-$ from an equilibrium mixture of **32** and [**32**]$^-$, driving a concomitant colour change of the solution from red to blue **(Figure 2.2A)**.

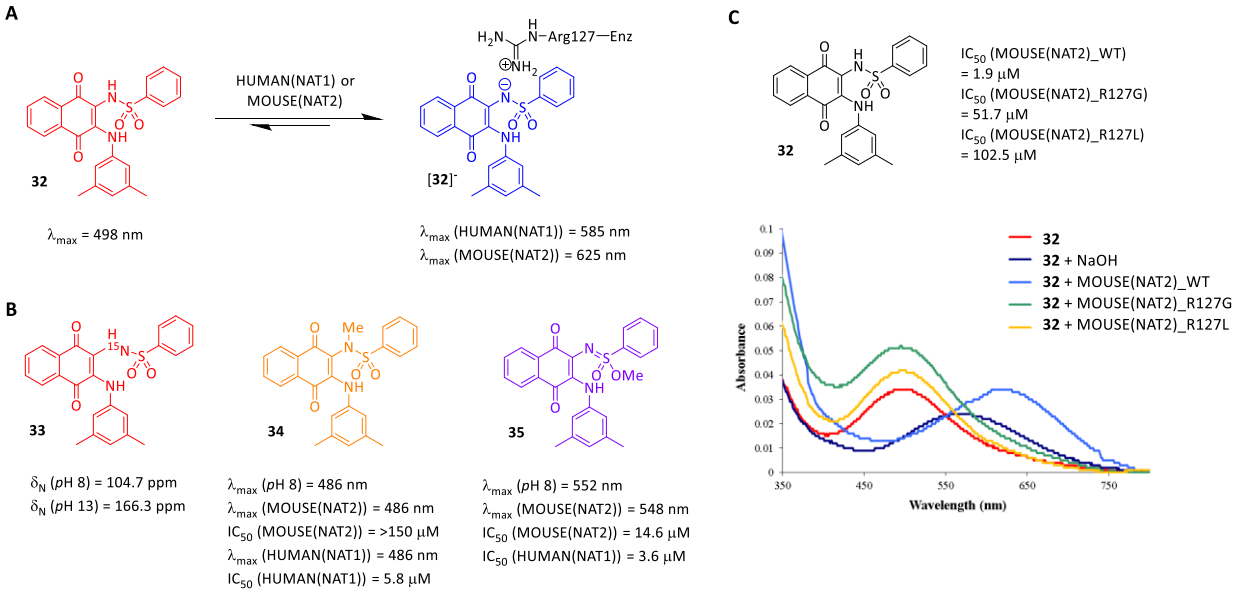


Figure 2.2: A: Hypothesised sequestration of the conjugate base of naphthoquinone **32**, [**32**]$^-$, by Arg127 to drive the observed colour change from red to blue; **B:** Structures of ^{15}N-labelled species **33**, *N*-methylated species **34** and *O*-methylated species **35**, the properties of which lend weight to the deprotonation hypothesis; **C:** Visible absorption spectra of **32** at *p*H 8.0 (red line), *p*H 13.75 (dark blue line), and in the presence of wild type (WT) MOUSE(NAT2) (sky blue line), glycine mutant R127G (green line) and leucine mutant R127L (yellow line); IC_{50} values for **32** against the wild type and mutant proteins are also given. Enz = enzyme.

Some previous studies have provided some key evidence in support of this hypothesis **(Figures 2.2B and 2.2C)**:

- An ^{15}N-labelled analogue of naphthoquinone **32**, **33**, was synthesised which displayed a large shift in δ_N in its ^{15}N-NMR spectrum in the presence of base (from 104.7 ppm to 166.3 ppm) – however the solubility of this analogue was not high enough in a 5%

DMSO-d_6/95% H_2O mixture to enable NMR studies to be conducted in the presence of protein;[281b]

- *N*-Methyl sulfonamide **34** and *O*-methyl sulfonamide **35** were synthesised, both of which display dose-dependent binding to HUMAN(NAT1) and MOUSE(NAT2) but without showing a concomitant instantaneous colour change;[281a]
- Mutants of wild-type MOUSE(NAT2) (MOUSE(NAT2)_WT) were generated *via* single point mutations in which the Arg127 residue was replaced with either glycine (MOUSE(NAT2)_R127G) or leucine (MOUSE(NAT2)_R127L) – naphthoquinone **32** displayed dose-dependent binding to these mutants, but with significantly higher IC_{50} values and with no concomitant colour change.[284]

Moreover, alternative hypotheses have also been ruled out. Treatment of naphthoquinone **32** with a variety of reducing agents led to an observed decolourisation, which suggests that the observed red to blue colour change is not caused by reduction of the naphthoquinone core,[242] and treatment of naphthoquinone **32** with thiolates did not lead to any observed adduct formation, which suggests it is unlikely that conjugate addition to the α,β-unsaturated carbonyl in the naphthoquinone core by the catalytic Cys68 residue of HUMAN(NAT1)/MOUSE(NAT2) is possible within the enzyme active site.[281a]

Below, two further pieces of evidence in support of the current hypothesis are described, which enable us to better evaluate the proposed *in silico* model of binding.

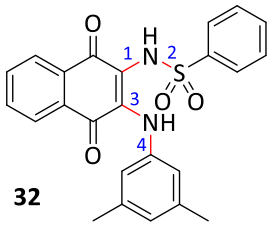
2.1.1. Evaluation of the *in silico* Model using Molecular Dynamics

HUMAN(NAT1) has proved to be a difficult protein to crystallise, and a selective chemical modification of the catalytic Cys68 residue by the irreversible inhibitor 2-bromoacetanilide was required in order to obtain a crystal structure of the protein.[247b] Previous attempts to co-crystallise naphthoquinone **32** with MOUSE(NAT2) have also failed, possibly due to the difficulty of crystallising MOUSE(NAT2) itself or the poor water solubility of naphthoquinone

32, which had been observed qualitatively.[284] Therefore, key hypotheses about the orientation of binding of naphthoquinone **32** to the enzyme, including the prediction of an ionic interaction between the sulfonamide moiety of the naphthoquinone and Arg127 of the enzyme, have been derived from an *in silico* docking model using GOLD® software (v.5.2).[282]

Whilst generation of a co-crystal structure between naphthoquinone **32** and HUMAN(NAT1)/MOUSE(NAT2) would be the only validation of the *in silico* model, conformational modelling studies on naphthoquinone **32** can be used to infer whether the proposed binding model is based on an energetically reasonable conformer of the ligand. To this end, modelling studies were carried out on naphthoquinone **32** to determine the optimum geometry of the molecule about four key rotatable bonds in its structure. Several computational methods exist for performing such calculations, with some of the most popular being density functional theory (DFT) methods. DFT methods are based on electronic structure theory, which takes into account the stationary electronic state of a molecule as described by a wavefunction that satisfies the many-electron time-independent Schrödinger equation, but simplifies the problem into a single-body problem by excluding the electron-electron interaction energy. Whilst this makes DFT methods less accurate than *ab initio* calculations, it reduces the amount of computational power required to carry out the calculations and thus makes DFT methods popular for this type of modelling problem. The DFT calculations described below were performed at the M06-2X/6-31G* level of theory[285] using the Gaussian09 package,[286] in collaboration with Dr Fernando Martínez.[287] **Figure 2.3A** illustrates the four key rotatable bonds within molecule **32** which were evaluated in this study, whilst **Figures 2.3B-2.3E** show the variation in the energy of the molecule as the torsional angle about each of these four bonds is varied and the torsional angles of all other bonds in the molecule remain fixed. The lowest energy conformer in each case is visualised as a 3D model (images manipulated in ChemBioDraw3D®), and in **Figure 2.3F** the conformation of **32** as predicted by the *in silico* model **(Figure 2.1)** is shown and labelled with relevant torsional angles to enable comparisons with the optimal conformations.

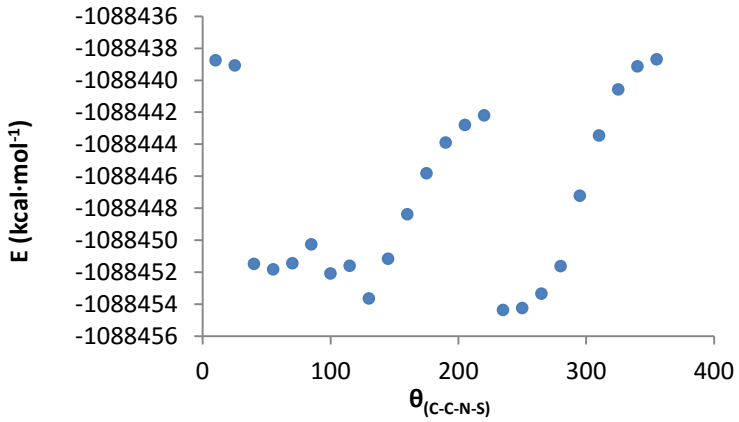
A

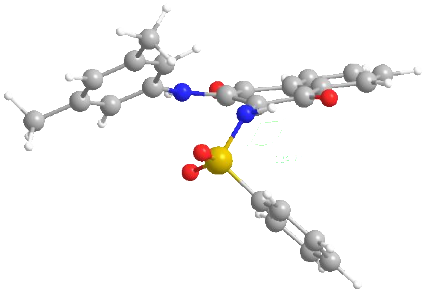


32

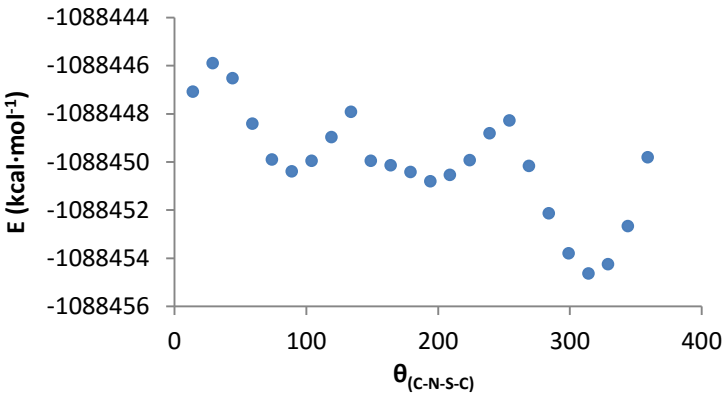
1 = θ (C-C-N-S)
2 = θ (C-N-S-C)
3 = θ (C-C-N-C)
4 = θ (C-N-C-C)

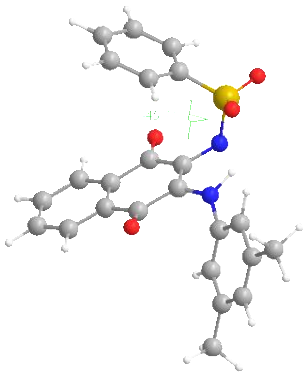
B



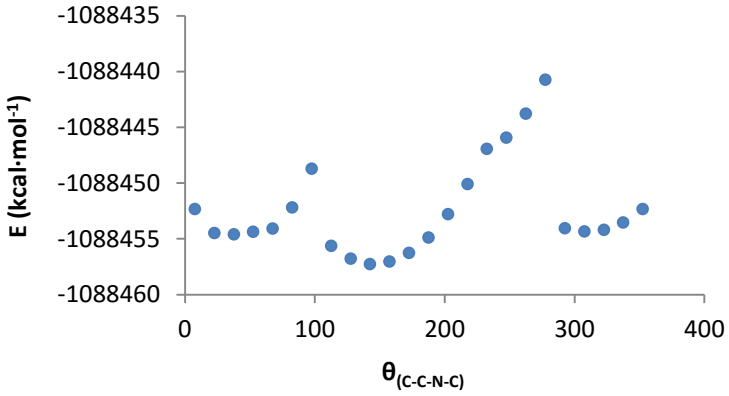


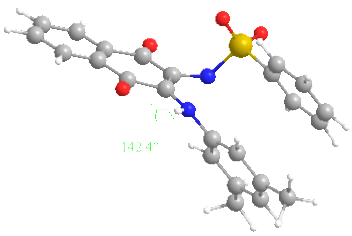
C



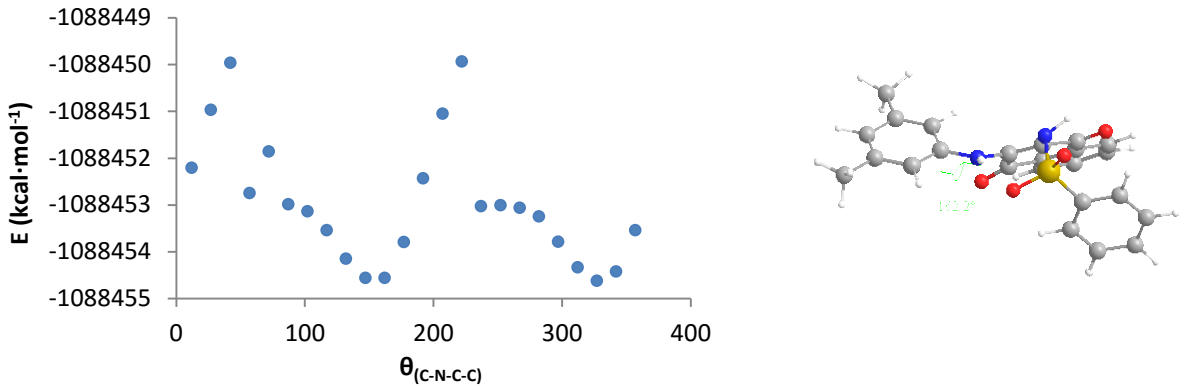


D





E



F

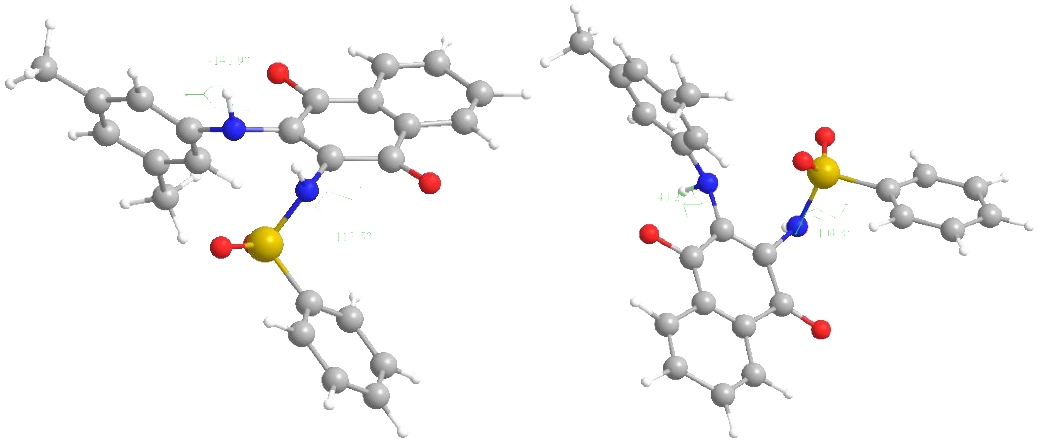


Figure 2.3: DFT modelling studies showing the variation of energy with torsional angle, θ, about the each of the four key rotatable bonds in naphthoquinone **32**. **A:** Structure of **32** with the key bonds highlighted in red; **B-E:** Plots of energy *vs.* torsional angle for each of the bonds 1-4, respectively, with images to show the optimal torsional angle for each bond generated in ChemBioDraw3D®; **F:** Images to show the torsional angles about all four key bonds in the conformation of **32** predicted by the *in silico* model in **Figure 2.1**.

These data reveal that the docked conformer of naphthoquinone **32** is indeed predicted to be an energetically reasonable conformer of the molecule:

- About bonds 1 and 4, the docked conformer sits approximately at the global minimum energy conformer according to the torsional energy profiles **(Figures 2.3B and 2.3E)**, with torsional angles of 246.5° and 219.1° respectively;
- About bond 2, the docked conformer does not sit at the calculated minimum energy torsional angle of 314.3° (a relatively unextended conformer which one might not

expect to be particularly favourable within a protein environment), but does sit close to a local energy minimum in the torsional angle profile, at 104.8° **(Figure 2.3C)**;

- About bond 3, the docked conformer also sits at a local energy minimum at a torsional angle of 40.2°, which lies only approximately 2.7 kcal/mol above the global minimum **(Figure 2.3D)**.

These studies, therefore, support the use of this *in silico* model in evaluation of the mechanism of molecular recognition between naphthoquinone **32** and HUMAN(NAT1), and imply that a key interaction between the sulfonamide moiety in **32** and the Arg127 residue of the protein is a reasonable hypothesis, particularly in light of the accompanying chemical and biochemical evidence described above.

2.1.2. Synthesis and Evaluation of Sulfonate Ester 36

The synthesis of sulfonate ester **36 (Figure 2.4)** would provide further valuable evidence in support of the deprotonation hypothesis. Unlike methylated species **34** and **35**, sulfonate ester **36** is both isosteric and isoelectronic to compound **32**, and is therefore more likely to have the same preferred binding orientation as **32** in the enzyme active site. However, as for methylated species **34** and **35**, if the deprotonation hypothesis is correct, it would be anticipated that sulfonate ester **36** would display no observable colour change upon binding to HUMAN(NAT1) or MOUSE(NAT2).

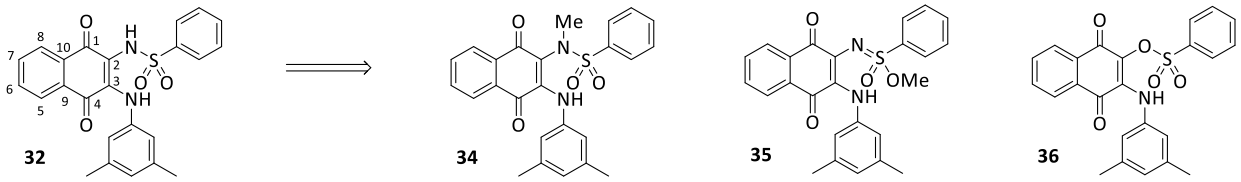
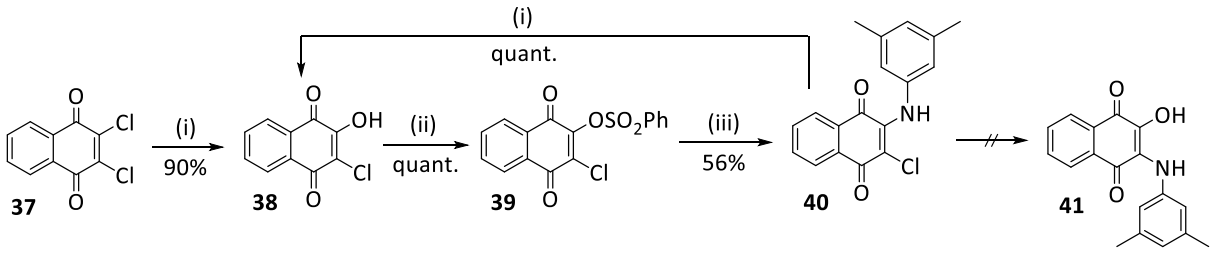


Figure 2.4: Structures of possible analogues of **32** which do not bear an acidic sulfonamide proton: *N*-methylated **34**, *O*-methylated **35** and sulfonate ester **36**. Note the numbering of the naphthoquinone core of **32**, which is used in all subsequent discussions in this thesis.

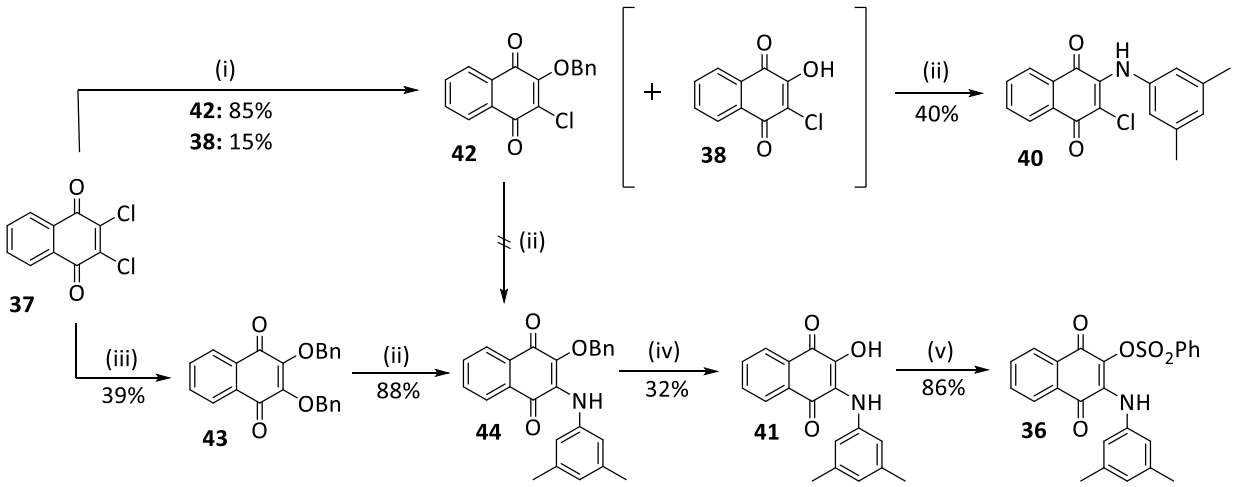
A previously attempted synthesis of sulfonate ester **36** which proved unsuccessful is outlined in **Scheme 2.1**.[281a] In this strategy, the sulfonate ester moiety was installed in two steps from 2,3-dichloro-1,4-naphthoquinone **37**: firstly, a conjugate addition-elimination of chloride with hydroxide gave 2-hydroxy-3-chloro-1,4-naphthoquinone **38** in 90% yield, which subsequently underwent a nucleophilic addition-elimination reaction with benzenesulfonyl chloride under basic conditions to yield sulfonate ester **39** in a quantitative fashion. It was envisaged that a Buchwald-type cross-coupling reaction[288] between compound **39** and 3,5-dimethylaniline would give the desired target **36**; however, the only isolated product from this reaction was species **40**, in which 3,5-dimethylaniline displaces the tosylate rather than the chloride. This could possibly be due to a conjugate addition-elimination reaction outcompeting the desired cross-coupling. A further attempt to install the sulfonate ester moiety on species **40** failed, as treatment of **40** with hydroxide yielded only 2-hydroxy-3-chloro-1,4-naphthoquinone **38**, in which the aniline is displaced by hydroxide in preference to the chloride.



Scheme 2.1: Previously attempted synthesis of sulfonate ester **36**.[281a] *Reagents and conditions:* (i) 0.5 M aq. NaOH (excess), 60 °C, 4 h; (ii) $PhSO_2Cl$ (excess), Et_3N (3.0 eq.), RT, 16 h; (iii) 3,5-dimethylaniline (1.2 eq.), $Pd(OAc)_2$ (0.01 eq.), XPhos (0.03 eq.), K_2CO_3 (1.4 eq.), H_2O (0.04 eq.), ^{t}BuOH, 100 °C, 16 h.

In this study, an alternative route to access sulfonate ester **36** was therefore sought **(Scheme 2.2)**. It was hypothesised that if 2,3-dichloro-1,4-naphthoquinone **37** was singly substituted with benzyl alcohol instead of hydroxide, then an addition-elimination reaction could be carried out on the resulting adduct **42** to yield 2-benzoxy-3-anilino-1,4-naphthoquinone **44**; this route was predicted to be more successful than the previously attempted route *via* sulfonate ester **39** as benzyl alcohol was expected to be less amenable to displacement than benzenesulfonic acid. **42** was therefore synthesised in 85% yield by treatment of 2,3-dichloro-

1,4-naphthoquinone **37** with benzyl alcohol and Cs_2CO_3 in DMF at RT. 2-hydroxy-substituted **38** was observed as a significant by-product (15% yield) and might be formed *via* an S_N2-type cleavage at the benzylic position by either excess benzyl alkoxide or hydroxide generated *in situ* from Cs_2CO_3; alternatively, hydroxide could displace the benzyl alkoxide *via* an addition-elimination type process with attack at C_2. Upon heating of **42** with $CeCl_3 \bullet 7H_2O$ and 3,5-dimethylaniline in methanol, once again only 2-anilino-3-chloro-1,4-naphthoquinone **40** could be isolated, in 40% yield after losses attributable to the purification step. This would be consistent with a rate-determining attack of the aniline on **42**, since the relative electronegativities of oxygen and chlorine might favour nucleophilic attack at the more electropositive C_2 position; the rate-determining step of Michael-type additions is reported to vary with the identity of the nucleophile.[289]

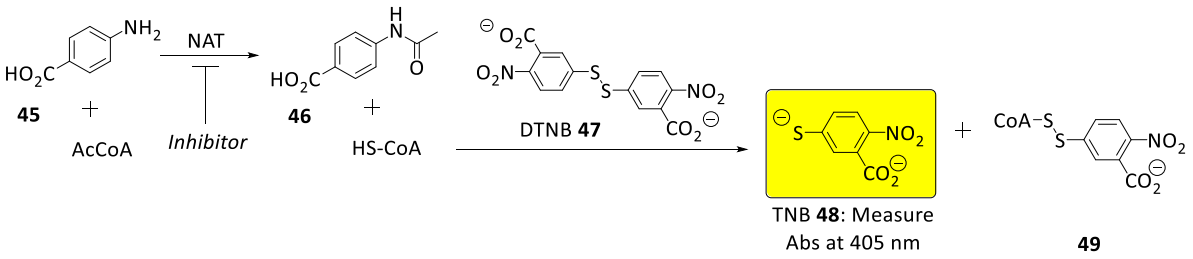


Scheme 2.2: Attempted and successful synthetic routes to sulfonate ester **36**. *Reagents and conditions:* (i) Benzyl alcohol (1.2 eq.), Cs_2CO_3 (1.0 eq.), THF, RT, 72 h; (ii) $CeCl_3 \bullet 7H_2O$ (1.0 eq.), MeOH, RT, 1.5 h *then* add 3,5-dimethylaniline, 110 ^{o}C, 16 h; (iii) Benzyl alcohol (2.2 eq.), Cs_2CO_3 (2.2 eq.), THF, reflux, 18 h; (iv) H_2 (1 atm.), 10% Pd/C (0.2 eq.), MeOH, RT, 16 h; (v) Benzenesulfonyl chloride (excess), Et_3N (3.0 eq.), RT, 16 h.

Therefore, it was decided that the most accessible route to 2-benzoxy-3-anilino-1,4-naphthoquinone **44** might be *via* the di-benzloxy-substituted species **43**, which was formed from 2,3-dichloro-1,4-naphthoquinone **37** in 39% yield by refluxing **37** with 2.2 eq. of benzyl alcohol and Cs_2CO_3 in THF for 18 h. As predicted, an addition-elimination reaction with 3,5-

dimethylaniline resulted in the displacement of a single benzyl alcohol group to give the desired naphthoquinone **44** in excellent yield. From this species, the target sulfonate ester **36** could be accessed in 28% yield over two further steps: firstly, removal of the benzyl protecting group using a catalytic hydrogenation on 10% Pd/C to give hydroxyl-substituted intermediate **41**; and secondly, a nucleophilic addition-elimination reaction with benzenesulfonyl chloride under basic conditions. HMBC analysis of sulfonate ester **36** is consistent with the proposed 1,4-dione structure and not that of a 1,2-dione as the carbonyl resonance at 182.2 ppm (C_4) shows interactions with both the anilino-N*H* and naphthoquinone C_5-*H* protons.

The activity of sulfonate ester **36** against both MOUSE(NAT2) and HUMAN(NAT1) was subsequently determined in an acetyl CoA hydrolysis assay. Recombinant MOUSE(NAT2) was expressed and purified as outlined in **Section 7.8.** and as described in previous studies.[257] A pellet of *E. coli* cells induced to overexpress HUMAN(NAT1) was kindly supplied by Dr Julien Dairou and Prof. Fernando Rodrigues-Lima (University Paris-Diderot), from which recombinant HUMAN(NAT1) was purified (for protocol see **Section 7.9.**).[290] NAT activity in the presence of an inhibitor was determined by monitoring the rate of acetyl CoA hydrolysis when the relevant NAT was incubated with *para*-aminobenzoic acid (*p*ABA) **45** (a substrate of HUMAN(NAT1) and MOUSE(NAT2), *cf.* **Section 1.2.1.**), acetyl CoA and inhibitor in 5% DMSO (*v/v*). Free CoA generated by NAT-mediated acetylation of *p*ABA was then quantified by addition of the quenching reagent 5,5'-dithio-*bis*(2-nitrobenzoic acid) (DTNB) **47** *via* formation of the yellow-coloured species thionitrobenzoate (TNB) **48**, which could be detected by absorbance measurements at 405 nm **(Scheme 2.3)**. The full assay protocol is outlined in **Section 7.13.1**.



Scheme 2.3: Acetyl CoA hydrolysis assay used to determine the potency of synthesised inhibitors against NATs.

In the acetyl CoA hydrolysis assay, sulfonate ester **36** was observed to display weak dose-dependent binding to both MOUSE(NAT2) and HUMAN(NAT1), with IC_{50} values of >150 µM and 93 µM respectively. However, as with *N*-methylated species **34** and *O*-methylated species **35**, sulfonate ester **36** neither undergoes a colour change in aq. NaOH solution nor in the presence of either the human or murine protein **(Figure 2.5)**; this lends further support to the hypothesis that sulfonamide-N*H* deprotonation and sequestration of the conjugate base by the protein is the mechanism by which the observed colour change occurs.

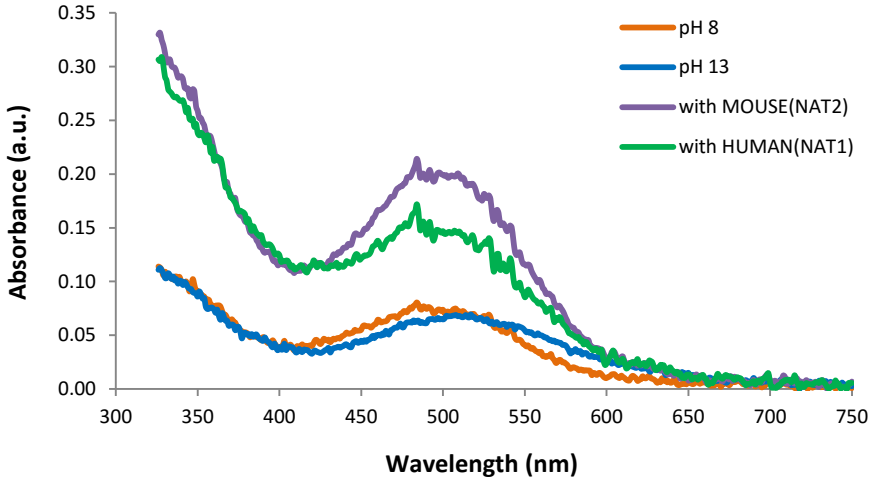
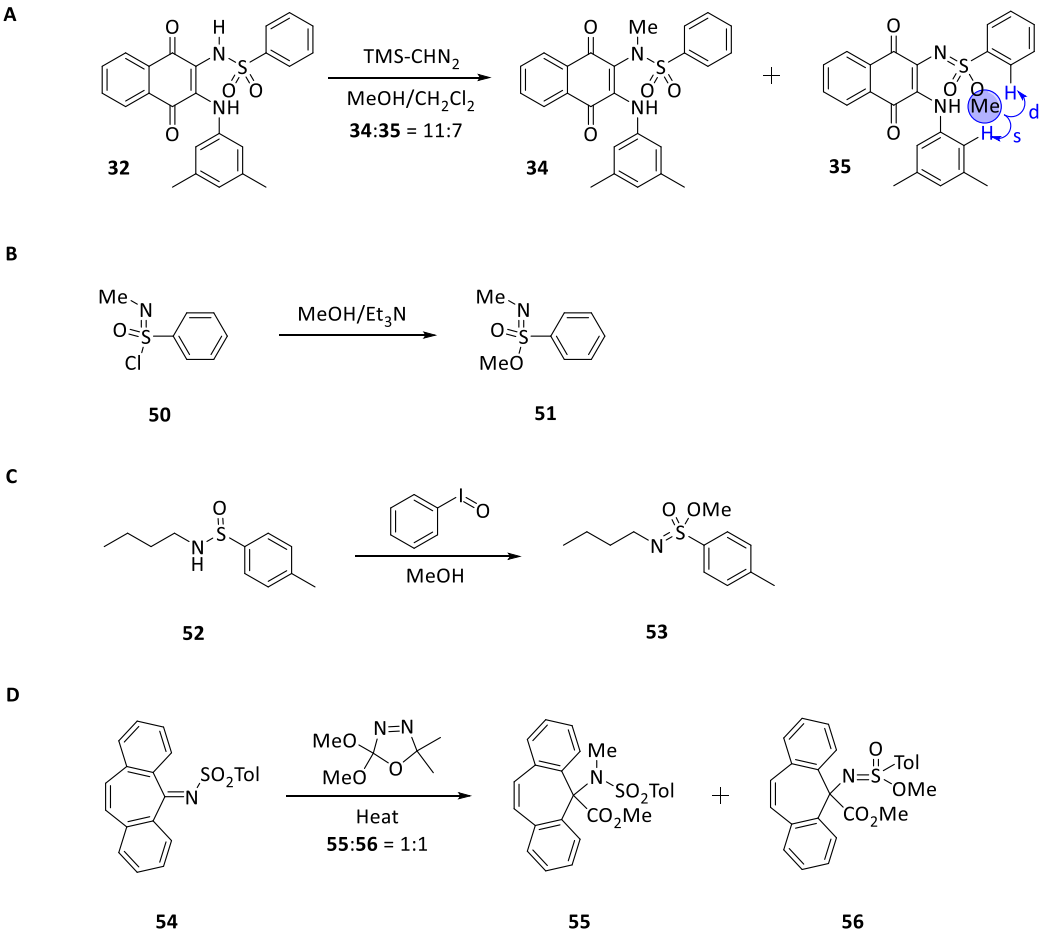


Figure 2.5: Visible spectra of sulfonate ester **36** (15 µM) in the presence of 5% DMSO and 95% 20 mM Tris•HCl (*p*H 8) (orange line), 35 mM Na_2HPO_4•NaOH (*p*H 13) (blue line), MOUSE(NAT2) in 20 mM Tris•HCl (*p*H 8) (purple line) or HUMAN(NAT1) in 20 mM Tris•HCl (*p*H 8) (green line) (*v/v*). a.u. = arbitrary units.

Furthermore, it is interesting to note the high IC_{50} values of sulfonate ester **36** against both HUMAN(NAT1) and MOUSE(NAT2) (>150 µM and 93 µM respectively) in comparison to those of sulfonamide **32** (3.1 µM and 4.1 µM respectively). Unlike with *N*-methylated **34** and *O*-methylated **35**, it is an improbable hypothesis that steric factors are responsible for its poor binding affinity; rather, the key difference between sulfonate ester **36** and sulfonamide **32** is the inability of the former to ionise in the presence of enzyme, and this provides the strongest evidence to date that an ionic interaction between the ligand and enzyme active site is crucial for high inhibition potency.

2.1.3. Studies on the Formation of *O*-Methylated Sulfonamide 35

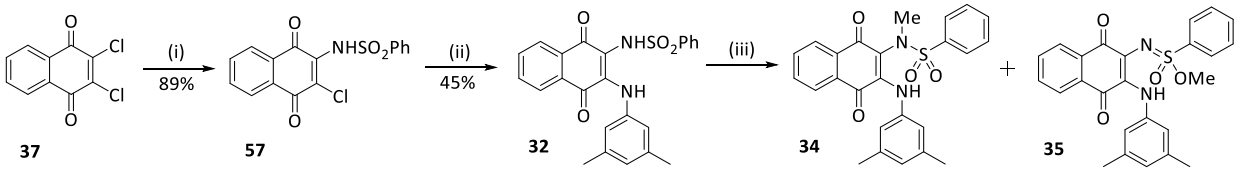
In previous investigations, the methylation of sulfonamide **32** to give both *N*-methylated **34** and *O*-methylated **35** proved surprising **(Scheme 2.4A)**, since such a direct alkylation is, to the best of our knowledge, without precedent in the literature, although examples of *O*-arylation of tertiary or secondary[291] sulfonamides with very electrophilic diazonium salts are known. Methyl iminosulfonates have been previously reported; however, their formation is limited to addition-elimination of iminosulfonyl chlorides,[292] methanolic oxidation of sulfinamides[293] or reaction of *N*-tosylated imines with dimethoxycarbene[294] **(Schemes 2.4B-D)**.



Scheme 2.4: Reported synthetic routes to methyl iminosulfonates. **A:** Methylation of **32** to give both *N*-methylated **34** and *O*-methylated **35** adducts – the identity of **35** was confirmed by the nOe signal enhancements shown in blue;[281a] **B:** Addition-elimination of methanol on iminosulfonyl chloride **50**;[292] **C:** Example of a methanolic oxidation of a sulfinamide **52**, utilising iodosylbenzene as the oxidant;[293] **D:** Reaction of an *N*-tosylated imine **54** with a precursor of dimethoxycarbene.[294] d = doublet; s = singlet; Tol = *para*-methylphenyl.

The formation of *O*-methylated **35** raised an intriguing question: is *O*-methylation the kinetic product of sulfonamide methylation, and *N*-methylation the thermodynamic product? It is possible that no previous reports of *O*-methylation exist because the conjugate bases of most sulfonamides are too unstable and short-lived a species under the reaction conditions of methylation. The high stability of the conjugate base of sulfonamide **32**, however, might offer a system in which this question can be further investigated.

An authentic sample of naphthoquinone **32** was synthesised in two Michael-type addition-elimination steps from 2,3-dichloro-1,4-naphthoquinone **37**, as previously reported,[242] in an overall isolated yield of 40% **(Scheme 2.5)**. Subsequent methylation of **32** with 1 eq. of TMS-diazomethane (as a 2 M solution in hexanes) was effected under various conditions and the product distribution in the crude reaction mixtures were determined by ^{1}H-NMR in DMSO-d_6 as solvent **(Table 2.1)**.



Scheme 2.5: Synthesis of *N*-methylated **34** and *O*-methylated **35**. *Reagents and conditions:* (i) $PhSO_2NH_2$ (1.0 eq.), Cs_2CO_3 (1.4 eq.), DMF, RT, 5 h; (ii) $CeCl_3 \bullet 7H_2O$ (1.0 eq.), MeOH, RT, 1.5 h *then* 3,5-dimethylaniline (3.0 eq.), 110 ^{o}C, 16 h; (iii) TMS-CHN_2 (2 M in hexanes, 1.0 eq.), MeOH (17.0 eq.), CH_2Cl_2, for reaction temperatures and times see **Table 2.1**.

Entry	mmol of 32	[32] in solvent (mmol/mL)	Temperature	Reaction Time	Relative Proportion of Products			
					Unmethylated 32	*N*-methyl 34	*O*-methyl 35	34:35
(i)	2.200	0.134	RT	16 h	60	30	5	6:1
(ii)	0.116	0.056	RT	16 h	35	55	15	3.7:1
(iii)	0.116	0.091	RT	16 h	15	70	15	4.7:1
(iv)	0.116	0.200	RT	16 h	0	80	20	4:1
(v)	0.116	0.038	-78 ^{o}C	3 h	100	0	0	N/A
(vi)	0.116	0.038	0 ^{o}C	3 h	50	40	10	4:1
(vii)	0.116	0.038	RT	3 h	50	40	10	4:1
(viii)	0.116	0.038	40 ^{o}C	3 h	20	70	10	7:1

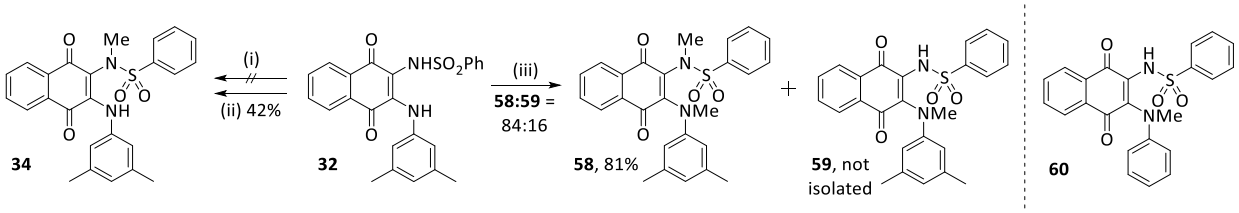
Table 2.1: Ratios of unmethylated **32**, *N*-methylated **34** and *O*-methylated **35** observed under different conditions for methylation step (iii) in **Scheme 2.5**. RT = room temperature; proportions recorded to nearest 5%.

The data in **Table 2.1** show some notable trends. Firstly, the distribution of products when the methylation was repeated under the same conditions initially reported (entry (i)), namely reaction of 2.2 mmol of **32** in 15 mL CH_2Cl_2, gives a 6:1 ratio of adducts **34**:**35**, which is vastly different to the 1.6:1 ratio previously reported. This was believed most likely to be due to the use of a different source of TMS-diazomethane, which could have differed in its active concentration. Entries (ii)-(iv) show that, on a smaller reaction scale, a slightly greater proportion of the *O*-methylated adduct can be observed *cf.* the *N*-methylated adduct; however, altering the concentration of **32** used does not significantly affect the product ratio – only the amount of starting material which is converted to product over the 16 h reaction duration, as expected.

Entries (v)-(viii) show that, as would be anticipated, the rate of methylation increases with increasing temperature; no reaction is observed at -78 ^{o}C, but increasing conversion of starting material is seen at reaction temperatures from 0 ^{o}C to 40 ^{o}C. The data reveal that at 0 ^{o}C and RT, similar proportions of *O*-methylated **35** and *N*-methylated **34** are formed (**34**:**35** = 4:1) and a similar conversion rate of **32** to products is observed within 16 h (50%). However, at 40 ^{o}C the proportion of *N*-methylated **34** formed relative to that of *O*-methylated **35** becomes even greater than at lower temperature (**34:35** = 7:1); this is consistent with the hypothesis that *O*-methylated **35** is the kinetic product of the reaction and *N*-methylated **34** the thermodynamic product.

Methylation of naphthoquinone **32** was also attempted with different methylating reagents; if the hypothesis is correct, it would be anticipated that decreasing the electrophilicity of the methylating reagent would result in an increased proportion of the *N*-methylated adduct **34** being formed. Methylation was firstly attempted with excess MeI in the presence of 3 eq. Et_3N as a base; however, under these conditions no methylation was observed (conditions (i) in **Scheme 2.6**). Subsequently, **32** was treated with 1 eq. of NaH followed by 1 eq. of dimethyl sulfate (conditions (ii)). Under these conditions, solely *N*-methylation was observed, with a conversion rate of 42% at RT after 16 h. Furthermore, when **32** was treated with 2 eq. of NaH

followed by 2 eq. of dimethyl sulfate (conditions (iii)), two products were isolated: the major product **58** was methylated on both the anilino and sulfonamido nitrogen atoms, and the minor product **59** was methylated solely on the anilino nitrogen. The identity of species **58** and **59** were confirmed by ^{1}H-NMR and HMBC analysis: the proton spectrum of **58** in DMSO-d_6 contains a 3H singlet at δ = 2.94 ppm, which is consistent with the shift of a sulfonamide-N*Me* (*cf.* δ = 2.83 ppm for the sulfonamide-N*Me* in **34**) and the protons of this methyl group exhibit a coupling interaction with C_2 of the naphthoquinone core in an HMBC experiment; furthermore, the proton spectra of **58** and **59** contain 3H singlets at δ = 3.39 and 3.13 ppm respectively that display strong interactions with both the corresponding C_3 and $C_{1''}$ carbons in the HMBC spectrum, indicative of an aniline-N*Me* group (*cf.* δ = 3.10 for the aniline-N*Me* in the known analogous species **60**).[281a]



Scheme 2.6: Left: Methylation of naphthoquinone **32** under various conditions. *Reagents and conditions:* (i) MeI (excess), Et_3N (3.0 eq.), RT, 16 h; (ii) NaH (1.0 eq.), dimethyl sulfate (1.0 eq.), THF, RT, 16 h; (iii) NaH (2.0 eq.), dimethyl sulfate (2.0 eq.), THF, RT, 16 h. **Right:** Previously reported aniline *N*-methylated species **60**, synthesised from 2-benzenesulfonamido-3-chloro-1,4-naphthoquinone **57** and *N*-methylaniline.[281a]

These data are consistent with the hypothesis that *O*-methylated **35** is the kinetic adduct of methylation. It is of particular note that **35** is only observed as a product when methylation is carried out with TMS-diazomethane, since in the anticipated mechanism of methylation with this reagent, the reactive electrophile is generated in close proximity to the nucleophile. In a future study, it would be desirable to replace TMS-diazomethane with diazomethane as the methylating reagent, since if the hypothesis is correct, this would be predicted to increase the proportion of *O*-methylated **35** formed relative to *N*-methylated **34**.

Changing the substrate would also be predicted to affect the ratio of *O*-methylated to *N*-methylated product when TMS-diazomethane is the methylating agent due to a change in relative stability of the conjugate base species. To test this hypothesis, a series of secondary sulfonamides were treated with 1 eq. of TMS-diazomethane and 17 eq. of anhydrous MeOH in anhydrous CH_2Cl_2 at RT for 16 h **(Table 2.2)**; sulfonamides are listed in the anticipated decreasing order of stability of their conjugate bases, and with naphthoquinone **32** included for comparison.

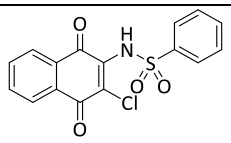
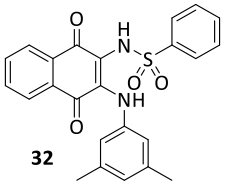
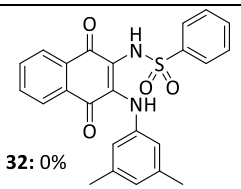
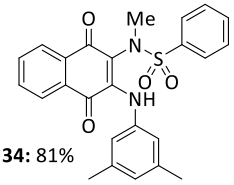
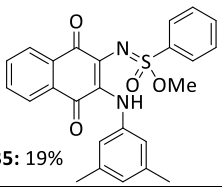
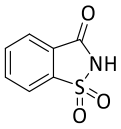
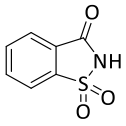
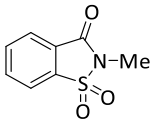
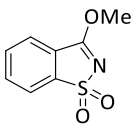
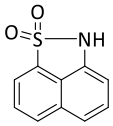
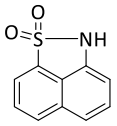
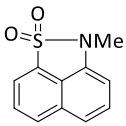
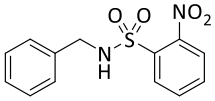
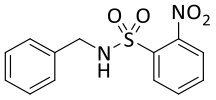
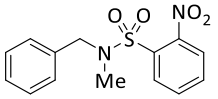
Entry	Sulfonamide	Structures and Relative Proportion of Products of Methylation
(i)	 **57**	Complex Mixture
(ii)	 **32**	 **32:** 0% +  **34:** 81% +  **35:** 19%
(iii)	 **61**	 **61:** 0% +  **62:** 78% +  **63:** 22%
(iv)	 **64**	 **64:** 31% +  **65:** 69%
(v)	 **66**	 **66:** 82% +  **67:** 18%

Table 2.2: Outcome of methylation of a range of different secondary sulfonamides using 3.5 mmol/mL of substrate in CH_2Cl_2, 1 eq. TMS-diazomethane and 17 eq. MeOH at RT for 16 h.

Unfortunately, methylation of chloro-substituted **57** under these conditions, which is reported to have a more stable conjugate base than **32** (pK_a of **57** = *c.* 4),[281a] produced a complex mixture of products from which the anticipated products of methylation could not be isolated

(entry (i)). Methylation of saccharin **61** under these conditions did produce a mixture of *N*- and *O*-methylated products **62** and **63** (entry (iii)); however, in *O*-methylated **63**, the chemical shift of the O*Me* group (δ = 4.20 ppm) is consistent with the chemical shift of an amide *O*-methylated species rather than a sulfonamide *O*-methylated species, and moreover, in the HMBC spectrum of **63**, the methyl protons show a correlation with the amide carbonyl carbon at δ = 169.7 ppm. Finally, as anticipated, methylation of either 1,8-naphthalinsultam **64** or *N*-benzyl-2-nitrobenzenesulfonamide **66** furnished solely the *N*-methylated adducts **65** or **67** respectively (entries (iv) and (v)).

2.1.4. Studies on the Stability and Rearrangement of *O*-Methylated Sulfonamide 35

In a previous study in which species **34** and **35** were synthesised in order to demonstrate that an acidic sulfonamide-N*H* functionality is a prerequisite of observing the characteristic colour change of **32** in the presence of HUMAN(NAT1) or MOUSE(NAT2), it was shown that initially upon treatment of either **34** or **35** with MOUSE(NAT2) in 95% 20 mM Tris•HCl (*p*H 8)/5% DMSO (*v/v*), no colour change of either inhibitor was observed.[281a] However, if **35** is incubated with MOUSE(NAT2) at 37 ^{o}C for 5 h, a colour change in **35** could be observed after this time; moreover, the spectrum recorded matched closely with the known spectrum of [**32**]$^{-}$ in the presence of MOUSE(NAT2).[281a] A mass spectrum of a sample of **35** which had been left to stand in 95% 20 mM Tris•HCl (*p*H 8)/5% DMSO (*v/v*) at RT for 16 h additionally revealed an *m/z* (ESI^{-}) peak at 431 Da.[281a] These data would be consistent with demethylation of **35** to **32** occurring under these conditions.

This observation therefore led to an investigation of the thermal stability of the *N*-methylated and *O*-methylated adducts **34** and **35** *via* ^{1}*H*-NMR. Upon heating to 100 ^{o}C, it was observed that *N*-methyl **34** was thermally stable in all solvents tested when heated for >5 days. However, *O*-methyl **35** was found to be stable in benzene-d_6 but not in any of DMSO-d_6, DMF-d_7 and THF-d_8 **(Table 2.3)**. When heated in DMSO-d_6, within 2 h **35** was observed to primarily undergo demethylation to **32** as well as a small extent of decomposition to further

unidentifiable products. The results in DMF-d_7 were even more intriguing: within 2 h, no *O*-methylated **35** remained, but this time both demethylated **32** and *N*-methylated **34** were observed as components of the reaction mixture, in a ratio of 11.5:1. In THF-d_8, again both demethylated **32** and *N*-methylated **34** were observed, but the formation of both products was much slower, with the reaction still incomplete after 48 h, and the relative proportion of **34** was found to be higher than in the reaction in DMF-d_7, with a **32**:**34** ratio of 4.4:1.

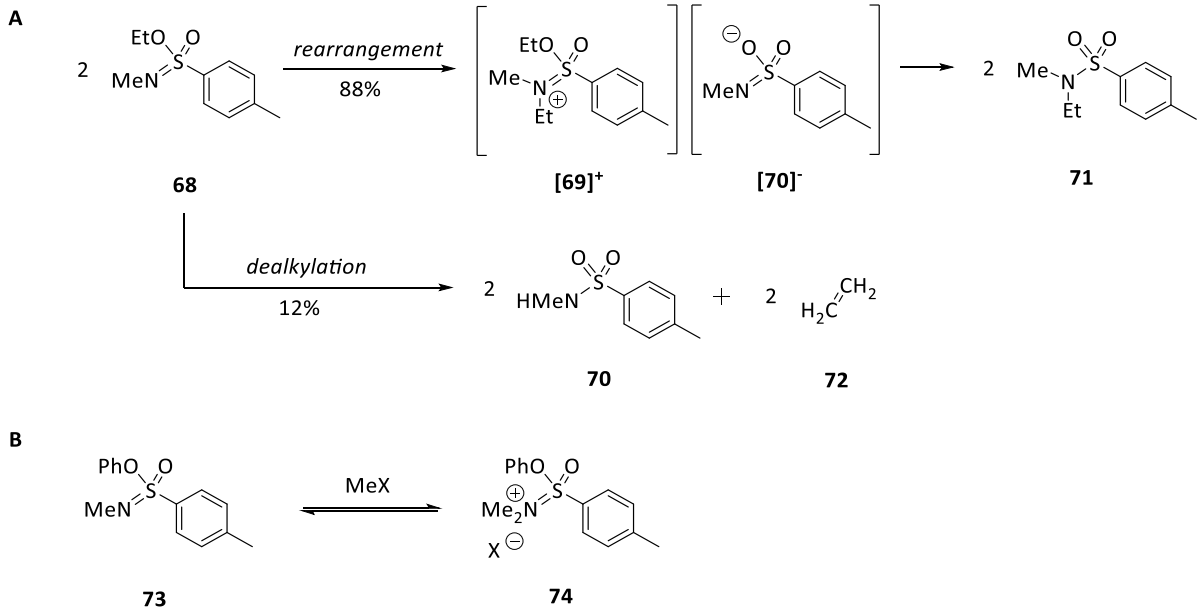
Solvent	Reaction Time	Relative Proportion of Observed Products		
		***O*-Methylated 35**	**Demethylated 32**	***N*-Methylated 34**
DMSO-d_6	2 h	0	100	0
DMF-d_7	2 h	0	92	8
THF-d_8	48 h	35	53	12
benzene-d_6	12 days	100	0	0

Table 2.3: Relative proportions of *O*-methylated **35**, demethylated **32** and *N*-methylated **34** observed by ^1H-NMR when a sample of *O*-methylated **35** (10 mg/mL) was heated in the stated deuterated solvent for the stated time at 100 ^oC.

A survey of the literature revealed that rearrangements of *O*-methylated sulfonamides have been previously reported;[291, 295] however, such a reaction within this short a timescale is unprecedented. Challis & Iley reported the rearrangement of ethyl sulfonimidate **68** into *N*-ethyl **71** (88%) and dealkylated **70** (12%) when heated in acetonitrile-d_3 or acetone-d_6 at 100 ^oC, with a half-life of *c.* 20 days **(Scheme 2.7A)**.[291] Ethene was deduced to be the byproduct of dealkylation by the appearance of a peak in the ^1H-NMR spectrum at δ = 5.48 ppm.

It was observed that the rate of loss of *O*-alkylated **68** with time increased five-fold when [**68**] was increased by a factor of 2.26, from which they concluded that both the dealkylation and the rearrangement were second-order processes; they hypothesise a mechanism for rearrangement in which an ion pair is formed from ethylation of a molecule of **68** by another molecule of **68** followed by a more rapid transfer of the second ethyl group between the ions in this pair, but do not offer a mechanistic proposal for dealkylation which would be

consistent with a second order process.[291] Evidence for their proposed rearrangement mechanism comes from the fact that addition of alkyl halides accelerates the rate of rearrangement, and under these conditions the reaction is first order with respect to both [**68**] and [alkyl halide]; faster reaction in more polar solvents also supported the formation of an ion pair intermediate.[291] Furthermore, treatment of phenyl sulfonimidate **73**, which cannot undergo phenyl group transfer by the proposed mechanism, with methyl iodide in acetonitrile-d_3 at 100 °C gives a structure for which the ^1H-NMR data are consistent with the sulfonimidonium salt **74 (Scheme 2.7B)**.[291]



Scheme 2.7: A: Rearrangement of ethyl sulfonimidate **68** to *N*-ethyl **71** and dealkylated **70**, *via* a bimolecular pathway hypothesised by Challis & Iley (1985). *Conditions:* Acetonitrile-d_3 (excess), 100 °C, $t_{1/2}$ = *c.* 20 days.[291] **B:** Reaction of phenyl sulfonimidate with MeI can be observed by ^1H-NMR and goes to *c.* 20% completion. *Conditions:* Acetonitrile-d_3 (excess), 100 °C.[291]

The rearrangement of *O*-methylated species **35** observed in DMF-d_7, however, differs from Challis & Iley's (1985) system in three notable ways: (a) when **35** is heated, a far higher proportion of demethylated **32** is generated compared to *N*-methylated **34**; (b) it is not possible for demethylated **32** to be generated from **35** *via* β-elimination, and an α-elimination is improbable as it would require the generation of a high-energy carbene; and (c) the anion

generated by demethylation of **35**, [**32**]$^-$, is anticipated to be far more stable than that generated by dealkylation of **68** due to resonance stabilisation of [**32**]$^-$ by the naphthoquinone core. As a corollary of these points, we cannot assume that the mechanism of reaction of *O*-methylated **35** follows the pathway proposed by Challis & Iley.

Given the strong solvent dependence of the stability of **35**, it is first important to consider the fate of the methyl group in the demethylation of **35** in DMSO-d_6, DMF-d_7 or THF-d_8. Considering the absence of reaction in benzene-d_6, it is hypothesised that demethylation is effected directly by either the solvent or adventitious water present acting as the nucleophile.

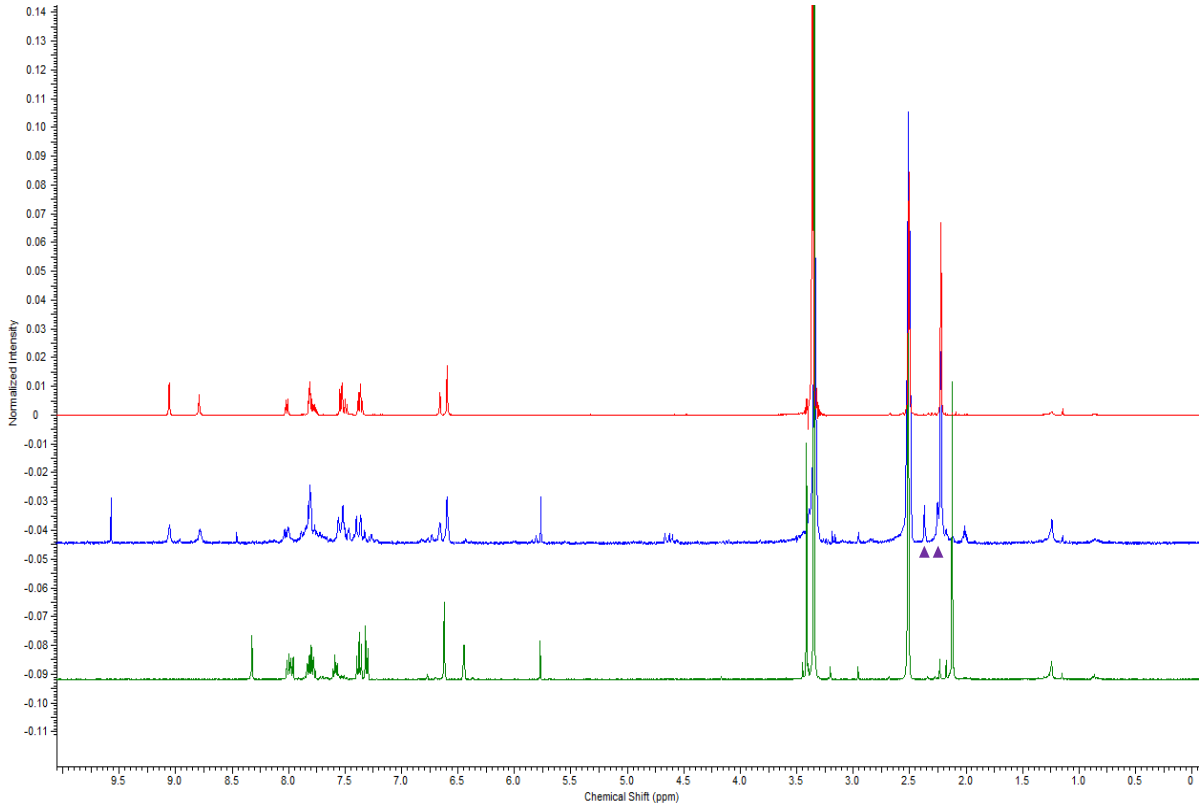


Figure 2.6: ^{1}*H*-NMR spectra of *O*-methylated **35** in DMSO-d_6 (green), *O*-methylated **35** in DMSO-d_6 after heating at 100 ^{o}C for 2 h (blue), and demethylated **32** in DMSO-d_6 (red), which show that **32** is the major product obtained under these conditions. There is a small solvent impurity of CH_2Cl_2 in the sample at δ = 5.78 ppm. The purple triangles represent singlets that are the likely fate of the methyl group of **35** in this reaction.

Analysis of the demethylation in DMSO-d_6 after 2 h by ^1H-NMR **(Figure 2.6)** shows almost the total disappearance of the peaks corresponding to **35** and appearance of peaks corresponding to demethylated **32**. However, also of importance is the appearance of a pair of singlets at δ = 2.27 and 2.38 ppm, which together integrate to 3H when referenced against the known 1H peaks in **32**. These peaks likely represent the fate of the methyl group of **35**; however, unfortunately it was not possible to determine the species to which these peaks correlate since they correspond to neither the anticipated chemical shift for methyl protons in methanol (3.16 ppm) nor those of the trimethylsulfonium cation (3.91 ppm).[296]

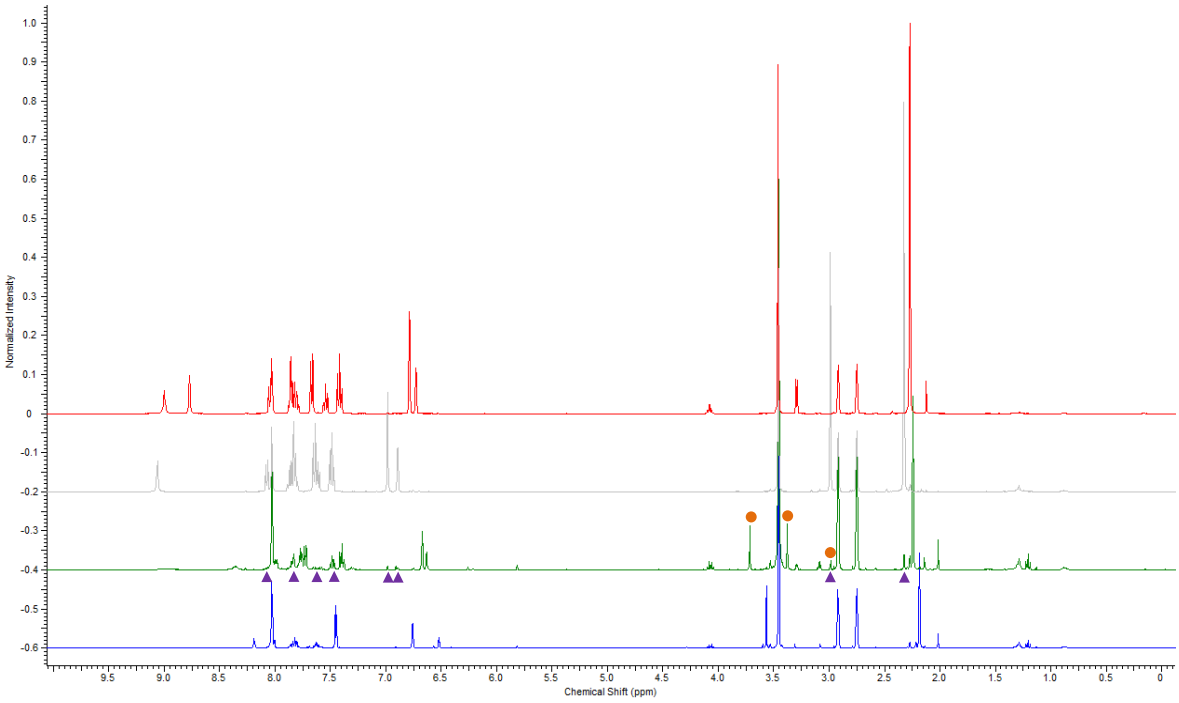


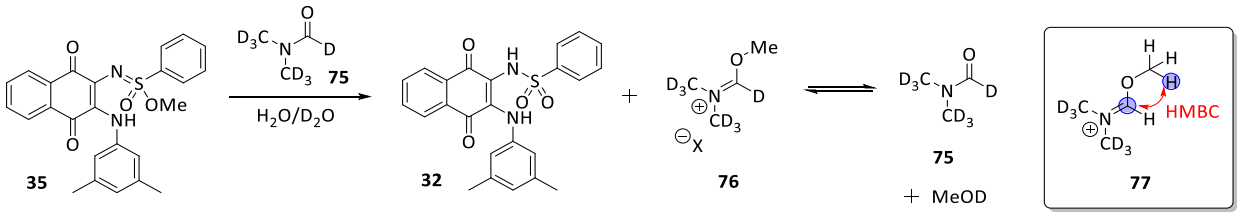
Figure 2.7: ^1H-NMR spectra of *O*-methylated **35** in DMF-d_7 (blue), *O*-methylated **35** in DMF-d_7 after heating at 100 °C for 2 h (green), *N*-methylated **34** in DMF-d_7 (grey) and demethylated **32** in DMF-d_7 (red), which show that **32**:**34** are obtained in a 92:8 ratio under these conditions. The purple triangles show peaks that correspond to formation of the minor product **34**; the orange circles show the three peaks which represent the fate of the methyl group of **35**.

More tractable results are observed in the reaction of **35** in DMF-d_7. The ^1H-NMR spectrum after 2 h **(Figure 2.7)** shows a complete disappearance of the 3H sulfonamide-O*Me* singlet at δ = 3.57 ppm and appearance of three singlets at δ = 3.72, 3.38 and 2.99 ppm, which together

integrate to give a relative intensity of 2.80 when the known 1H singlet in **32** at δ = 6.73 ppm is set to 0.92 (since 92% of **35** is observed to demethylate under these conditions).

The singlet at δ = 2.99 ppm clearly corresponds to the sulfonamide-N*Me* group in the rearranged product **34**, and integrates accordingly. The peak at δ = 3.38 ppm could be consistent with the chemical shift of the methyl protons of MeOD, since DMF-d_7 spiked with MeOH shows evolution of a new signal at δ = 3.31 ppm. Its sole correlation in 2D NMR experiments is in the HSQC spectrum, which shows that the carbon these protons are bonded to has a chemical shift of δ = 54.6 ppm, again consistent with that of an *O*-methylated carbon.

Meanwhile, the peak at δ = 3.72 ppm intriguingly exhibits a correlation both in the HSQC spectrum with a carbon at δ = 50.2 ppm and in the HMBC spectrum with a singlet carbon at δ = 162.6 ppm, which coincides with the 1:1:1 triplet of the carbonyl carbon in DMF-d_7 **75**; it is proposed that this species is the *O*-methylated imidate salt of DMF **76**, and only the species which has undergone hydrogen-deuterium exchange at the imidate carbon, **77**, is observable in the ^{13}C-NMR spectrum as any triplet or higher order multiplet carbons would give peak heights that are not intense enough to resolve above background noise **(Scheme 2.8)**.



Scheme 2.8: Proposed mechanism of demethylation of **35** in DMF-d_7; X^- = $[HO]^-$, $[DO]^-$ or $[\mathbf{32}]^-$. **Inset:** Imidate **77**, which has undergone proton-deuteron exchange at the imidate carbon, enabling an HMBC interaction to be observed between the singlet imidate carbon and the methyl protons.

The proposed mechanism of demethylation, therefore, is that DMF-d_7 **75** effects an S_N2-type attack on **35** to form imidate salt **76**, which in the presence of water is in equilibrium with DMF-d_7 **75** and MeOD, giving rise to both of the observed singlets. This is thought to be more

likely than a competing attack between DMF-d_7 and H_2O or D_2O directly acting as a nucleophile on **35**, due to the vast difference in the rates of demethylation in DMF-d_7 and THF-d_8. A time-course experiment in DMF-d_7 showed that reaction of **35** was complete in just 8 min at 100 °C, whilst in THF-d_8, the reaction had only proceeded 65% to completion even after 48 h of heating at 100 °C. THF itself is not capable of acting as a nucleophile, and in this case it is believed that adventitious water present in the NMR solvent is responsible for effecting the demethylation; the ^1H-NMR of the reaction in THF-d_8 clearly shows the formation of a singlet peak at δ = 3.14 ppm, which is consistent with the expected chemical shift of methanol **(Figure 2.8)**. These data suggest that water is capable of demethylating **35** in a polar solvent medium by a direct S_N2 attack, but at a relatively slow rate that does not account for the speed of reaction observed in DMF-d_7.

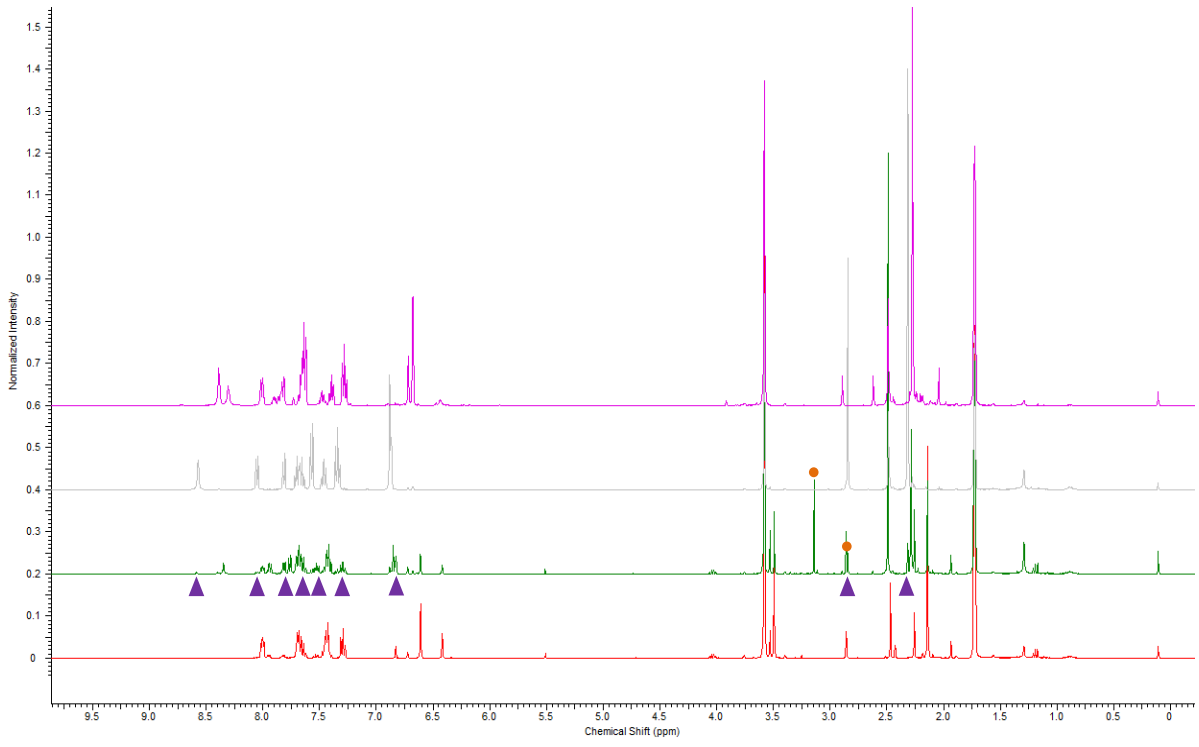


Figure 2.8: ^1H-NMR spectra of *O*-methylated **35** in THF-d_8 (red), *O*-methylated **35** in THF-d_8 after heating at 100 °C for 48 h (green), *N*-methylated **34** in THF-d_8 (grey) and demethylated **32** in THF-d_8 (magenta), which show that **35**:**32**:**34** are present after this time in a 35:53:12 ratio under these conditions. The purple triangles show peaks that correspond to formation of the minor product **34**; the orange circles show the two peaks which represent the fate of the methyl group of **35**.

Having established that in the reaction of **35** in DMF-d_7 demethylation likely occurs as a result of a direct solvent-mediated attack on **35**, it can be assumed, given that the solvent is in vast excess, that the kinetics of formation of **32** are pseudo-first order with respect to [**35**], *i.e.*

35 + DMF-d_7 → **32** + imidate salt **76**;

Rate = k_1[**35**] where k_1 is the pseudo-first order rate constant $k_{1'}$[DMF-d_7]

The mechanism of rearrangement of *O*-methylated **35** to *N*-methylated **34** is less obvious. There are three reasonable mechanisms for this process which could be proposed:

(a) An intramolecular [1,3]-sigmatropic methyl shift **(Scheme 2.9A)**;

(b) The bimolecular process analogous to that proposed by Challis & Iley (1985) for the dealkylation of **68**, or a subtle variation on this in which an initial bimolecular reaction between two molecules of **35** produces the ion pair [**78**]$^+$[**32**]$^-$ but is subsequently followed by a propagating chain reaction, in which another molecule of **35** is methylated by [**78**]$^+$ to give **34** and another molecule of [**78**]$^+$ – this possibility is more likely in this case than in Challis & Iley's due to the stability of the ion [**32**]$^-$ which makes its immediate methylation after ion pair formation less likely **(Scheme 2.9B)**;

(c) A mechanism in which demethylated **32** is actually an intermediate that subsequently reacts with another molecule of **35** to give **34**; this is also an example of a propagating chain reaction **(Scheme 2.9C)**.

Of all the possible mechanisms, kinetically (a) presents a trivial case whilst (b) and (c) are far more complex. In the case of (a), it can be noted that:

$$d[\mathbf{35}]/dt = -k_1[\mathbf{35}] - k_2[\mathbf{35}]$$

$$[\mathbf{35}] = [\mathbf{35}]_o e^{-(k_1+k_2)t}$$

where: k_1 and k_2 are the rate constants for demethylation and [1,3]-shift respectively

$[\mathbf{35}]_o$ is the concentration of **35** at time $t = 0$

Hence: $$d[\mathbf{32}]/dt = k_1[\mathbf{35}] = k_1[\mathbf{35}]_o e^{-(k_1+k_2)t}$$

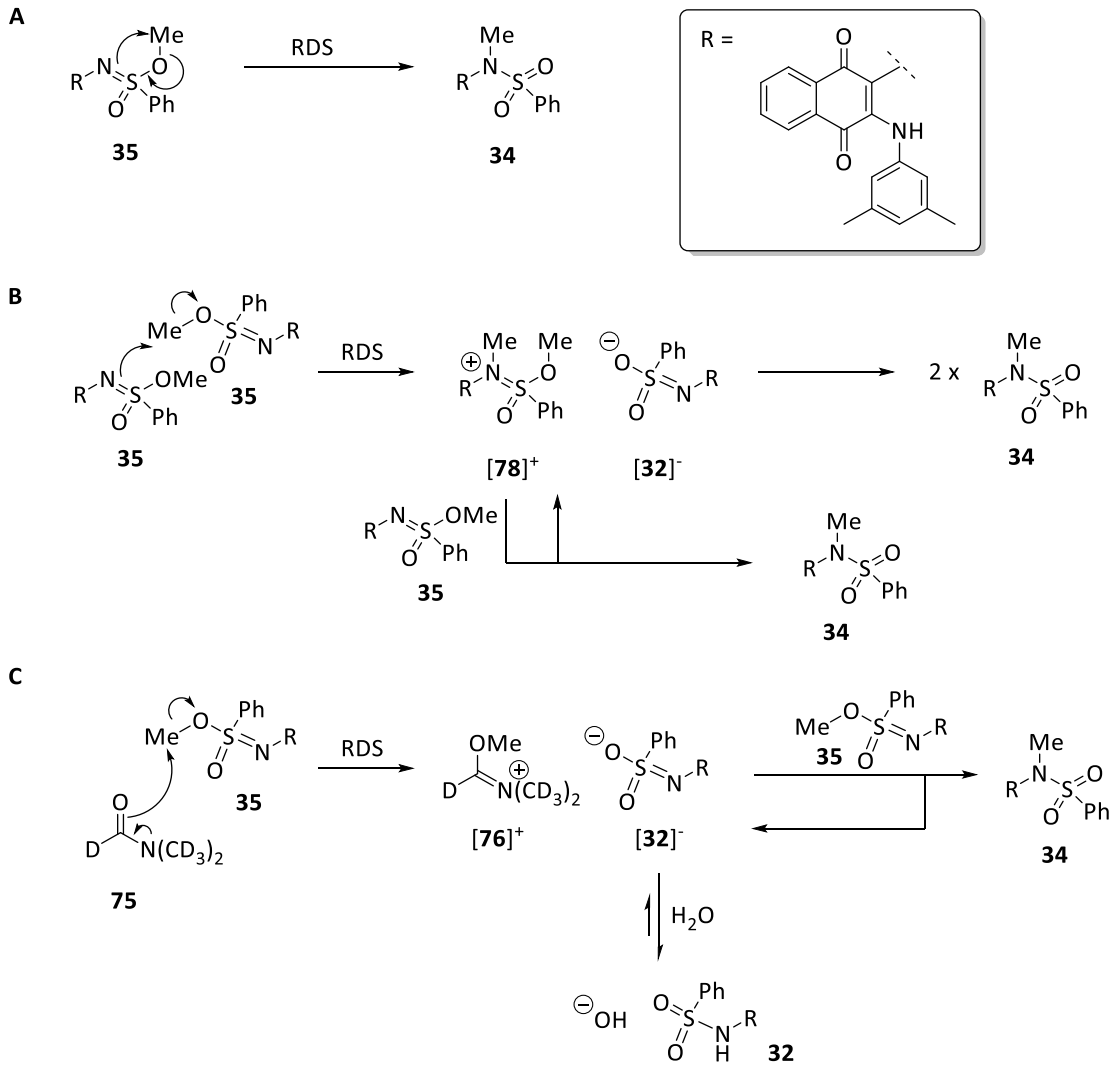
$$[\mathbf{32}] = (-[k_1[\mathbf{35}]_o/(k_1+k_2)]e^{-(k_1+k_2)t}) + [k_1[\mathbf{35}]_o/(k_1+k_2)]$$

Analogously: $[\mathbf{34}] = (-[k_2[\mathbf{35}]_o/(k_1+k_2)]e^{-(k_1+k_2)t}) + [k_2[\mathbf{35}]_o/(k_1+k_2)]$

Therefore, in the limit of complete reaction of **35** (*i.e.* as *t* tends to infinity):

$$[\mathbf{34}]/[\mathbf{32}] = k_2/k_1$$

i.e. the ratio of rearranged **34** and demethylated **32** observed as products should be independent of the initial concentration of **35**.



Scheme 2.9: Proposed possible mechanisms for the rearrangement of *O*-methylated **35** into *N*-methylated **34**. **A:** [1,3]-sigmatropic rearrangement. **B:** Bimolecular reaction of two molecules of **35** to form an ion pair which either subsequently exchange a methyl group to make two molecules of **34**, or undergo a propagation step with a further molecule of **35**. **C:** Mechanism in which demethylation first occurs to give **32**, followed by a bimolecular reaction of **32** and **35** to give **34** and a further molecule of **32** in a propagating step.

Thus the rearrangement of **35** was carried out in DMF-d_7 at 100 °C for different starting concentrations of **35**; the relative proportions of demethylated **32** and rearranged **34** were monitored by ^1H-NMR and the results are presented in **Table 2.4** and **Figure 2.9**.

$[35]_o$ (mg/mL)	2.2	4.2	8.3	11.8	16.7	19.2	22.2
% 32 observed	94.3	93.7	91.7	88.2	87.2	85.0	81.0
% 34 observed	5.7	6.3	8.3	11.8	12.8	15.0	19.0

Table 2.4: Relative proportions of demethylated **32** and *N*-methylated **34** observed by ^1H-NMR when *O*-methylated **35** is heated in DMF-d_7 for 2 h as the initial concentration of **35**, $[35]_o$, is varied.

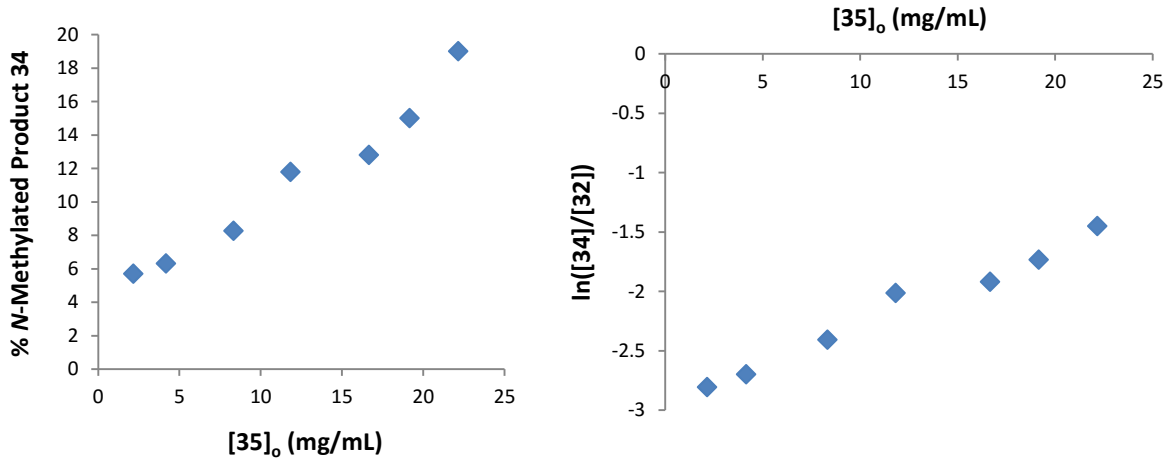


Figure 2.9: Left: Dependence of the relative % of *N*-methylated **34** formed on the initial concentration of **35**, $[35]_o$. **Right:** Apparent linear dependence of ln([**34**]/[**32**]) on $[35]_o$.

These experiments clearly demonstrate that the ratio **34**:**32** is $[35]_o$-dependent, and moreover, the dependence appears to be exponential, with the natural logarithm of the ratio having an approximately linear dependence on $[35]_o$ for the chosen range of $[35]_o$ values. This rules out the intramolecular mechanism (a) as the primary mechanism by which the rearrangement of **35** to **34** occurs.

To determine whether the demethylated species **32** is an intermediate in the formation of *N*-methylated **34** or not, time-course NMR studies were devised in which different amounts of demethylated **32** were added to *O*-methylated **35** at time t = 0 and the initial rates of

formation of both demethylated **32** and *N*-methylated **34** were determined. Given the reaction at 100 °C proceeds to completion within 8 minutes, it was not possible to carry out the time-course NMR experiments at this temperature; however, demethylation and rearrangement of **35** were also observed in DMF-d_7 at room temperature, and so the reactions were monitored at this temperature for 95 h **(Table 2.5; Figure 2.10)**.

mmol of 32 added	0.0 µmol			8.8 µmol			15.5 µmol		
Initial rate of change of each species (µmol h^{-1})	**35**	**32**	**34**	**35**	**32**	**34**	**35**	**32**	**34**
	-0.093	+0.082	+0.010	-0.062	+0.049	+0.011	-0.067	+0.055	+0.011

Table 2.5: Initial rate of change in concentration of each of *O*-methylated **35**, demethylated **32** and *N*-methylated **34** present in a DMF-d_7 sample (0.6 mL) left to stand at RT, when the samples are spiked with different amounts of demethylated **32** at time t = 0.

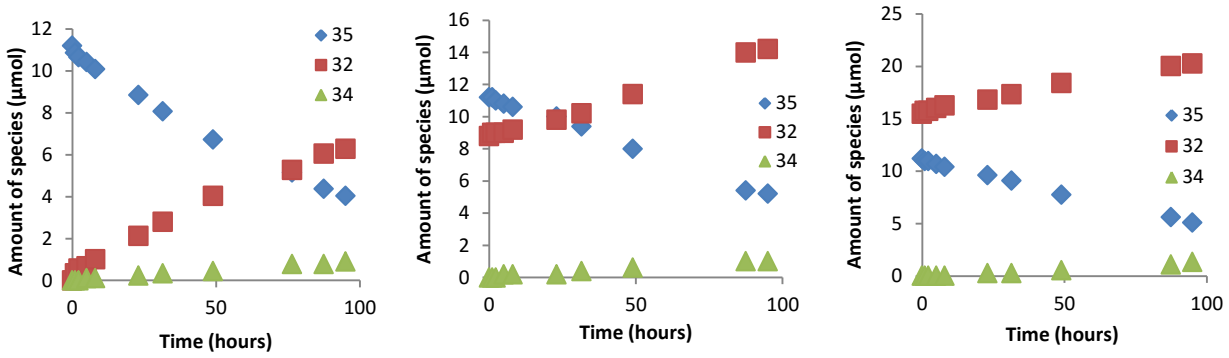


Figure 2.10: Kinetics of formation or depletion of **35**, **32** and **34** over time in DMF-d_7 (0.6 mL) at RT for 95 h, with, from left to right: no added **32**; 8.8 µmol **32** added at t = 0 h; 15.5 µmol **32** added at t = 0 h.

These experiments clearly demonstrate that increasing the concentration of demethylated species **32** at time t = 0 does not increase the rate of formation of *N*-methylated **34**. Therefore, these data suggest that the *N*-methylated species **34** is not formed from the direct reaction of **32** and **35** in a bimolecular step, and hence mechanism (c) for the formation of **34** appears unlikely.

Therefore, *N*-methylated **34** is most probably formed from a bimolecular reaction of *O*-methylated **35** to generate the ion pair intermediate [**78**]$^+$[**32**]$^-$, from which a methyl group is

either transferred from [**78**]$^+$ either directly onto [**32**]$^-$ or onto another molecule of **35** in a propagation step. Given a competing, and in fact dominant, pseudo first order reaction of **35** to form demethylated **32**, the kinetics of these two cases are expected to be far more complex than the simple second order case discussed by Challis & Iley. One possible experiment, however, which might be able to distinguish between these two subtly different mechanistic possibilities, is to monitor the relative rates of reaction of **35** and [**32**]$^-$ with MeI in DMF-d_7 by NMR; both species would be predicted to react to give *N*-methylated **34** under such conditions. Such an experiment would not, however, take into account the fact that the high effective concentrations of species [**32**]$^-$ present in the tight ion pair intermediate [**78**]$^+$[**32**]$^-$.

2.1.5. Conclusions from Mechanistic Investigations

Studies on naphthoquinone analogues of hit compound **32**, a selective inhibitor of HUMAN(NAT1) and MOUSE(NAT2) that changes colour from red to blue specifically in the presence of the target enzyme, suggest that this colour change is effected by the deprotonation of the acidic sulfonamide-N*H* in **32**, mediated by sequestration of the conjugate base of **32**, [**32**]$^-$, by the active site of the enzyme. *In silico* modelling supports an ionic interaction between the sulfonamide functionality of [**32**]$^-$ and the Arg127 residue of HUMAN(NAT1); DFT modelling of the free ligand in the gas phase shows that the docked conformer of **32** in this *in silico* model is energetically reasonable. Furthermore, synthesis of *N*-methylated sulfonamide **34**, *O*-methylated sulfonamide **35** and sulfonate ester **36** all support this hypothesis: all three analogues show dose-dependent binding to the HUMAN(NAT1) active site as measured by their inhibitory potencies, but with significantly higher IC_{50} values than **32** and without a concomitant colour change. These observations are in accord with an ionic interaction with Arg127 being key for ligand recognition by the enzyme active site, and a proton transfer being responsible for the colour change.

Subsequent mechanistic investigations into the unprecedented methylation of sulfonamide **32** to give both *N*-methylated **34** and *O*-methylated **35** suggest that *O*-methylation is the kinetic

product of the reaction; the *O*-methylated product is likely observed in this case due to the particularly high stability of the conjugate base of **32**. Furthermore, **35** was found to be unstable with respect to both demethylation to **32** and rearrangement to **34** in polar solvents; NMR and kinetic studies support the hypothesis that demethylation is effected directly by either the reaction solvent or adventitious water, whilst rearrangement occurs *via* the ion pair intermediate [**78**]$^+$[**32**]$^-$, formed from self-methylation of **35** in a bimolecular reaction step.

2.2. Determination of the Required Sensitivity of a Colorimetric Probe for HUMAN(NAT1)

In order for a colorimetric probe based on naphthoquinone **32** to be useful in the quantification of HUMAN(NAT1) in cell extracts (such as biopsy samples), it must possess the following key molecular properties:

- A **high potency** against HUMAN(NAT1), to ensure that in the presence of the protein, the equilibrium between the neutral species and conjugate base species lies as far to the side of the conjugate base species as possible;
- A **high absorption coefficient** of the conjugate base species, ε_{CB}, such that absorption from the probe would be detectable above background absorption in cell extracts;
- A **high degree of selectivity** for binding to HUMAN(NAT1) over other proteins, both plasma proteins and the isoenzyme HUMAN(NAT2);
- A **suitable *p*K$_a$ value**: the *p*K$_a$ must be above the assay buffer *p*H of 8.0 (since otherwise the probe will be deprotonated before being added to the cell extract), but below the *p*K$_{aH}$ of arginine, 12.48,[283] as this is expected to be a requirement for sequestration of the conjugate base from solution by Arg127.

Studies to date have shown that naphthoquinone **32** displays both a high degree of selectivity for binding to HUMAN(NAT1) over HUMAN(NAT2) and a suitable *p*K$_a$ for a colour change against HUMAN(NAT1) to be observed.[242] However, the IC$_{50}$ values of naphthoquinone **32** against both HUMAN(NAT1), 5.1 μM, and MOUSE(NAT2), 1.9 μM, show scope for

improvement. This leaves the question of intrinsic sensitivity: what is the highest concentration of naphthoquinone **32** that can be used in diagnostic tests for HUMAN(NAT1) levels in a typical HUMAN(NAT1)-overexpressing cancer cell line, and can this concentration of **32** be detected optically above background absorption in cell samples?

A previous study by Lee and Laurieri determined the approximate HUMAN(NAT1) concentration in the representative breast cancer cell line ZR-75-1 using immunoblotting techniques.[297] An antibody was generated which selectively recognises both HUMAN(NAT1) and MOUSE(NAT2),[256a, 298] with comparable levels of sensitivity,[299] since the *C*-terminal dodecapeptide of HUMAN(NAT1) and MOUSE(NAT2) are identical but differ from that of HUMAN(NAT2). A Western blot carried out against both varying dilutions of ZR-75-1 cell extracts and varying concentrations of pure recombinant MOUSE(NAT2) gave an upper bound for the HUMAN(NAT1) concentration of the cells to be 62.5 ng/μL (with 5 x 10^4 cells per μL), whilst dot blotting studies under both native and denatured conditions gave a lower bound for the HUMAN(NAT1) concentration of 19.5 ng/μL.[297] Therefore, the approximate HUMAN(NAT1) concentration in ZR-75-1 cells is 20-60 ng/μL, or in units of molarity, *c.* 0.6-1.2 μM.

Kinetic studies have previously shown that naphthoquinone **32** binds to MOUSE(NAT2) in a 1:1 ratio,[242] and thus given the similarity between the murine and human protein active sites, we can hypothesise that **32** binds to HUMAN(NAT1) in a similar fashion. In solution not all molecules of **32** may be bound to the target protein, and it would be anticipated that an excess of protein would be required to ensure that all of the inhibitor molecules in solution are present as their conjugate base (blue). If a sizeable proportion of inhibitor molecules remain protonated (red), overlapping visible spectra from the blue and red species in solution may make determination of NAT presence ambiguous. The fold excess of protein required to fully sequester the conjugate base species [**32**]$^-$ from the equilibrium between **32** and [**32**]$^-$ is particularly important to determine given that the calculated K_d for **32** against MOUSE(NAT2) is a relatively modest 4.9 μM.

Figure 2.11 shows the results of an experiment in which the inhibitor **32**:enzyme ratio was varied incrementally from 1:2 to 1:1 and a visible absorption spectrum of the solution recorded. This experiment demonstrates that λ_{max} for a ratio of 1:1 is ambiguous; however, for a ratio of 1:1.2 or higher, λ_{max} of these spectra clearly correlates to the spectrum of the conjugate base of **32** (585 nm) rather than that of the neutral species (498 nm).

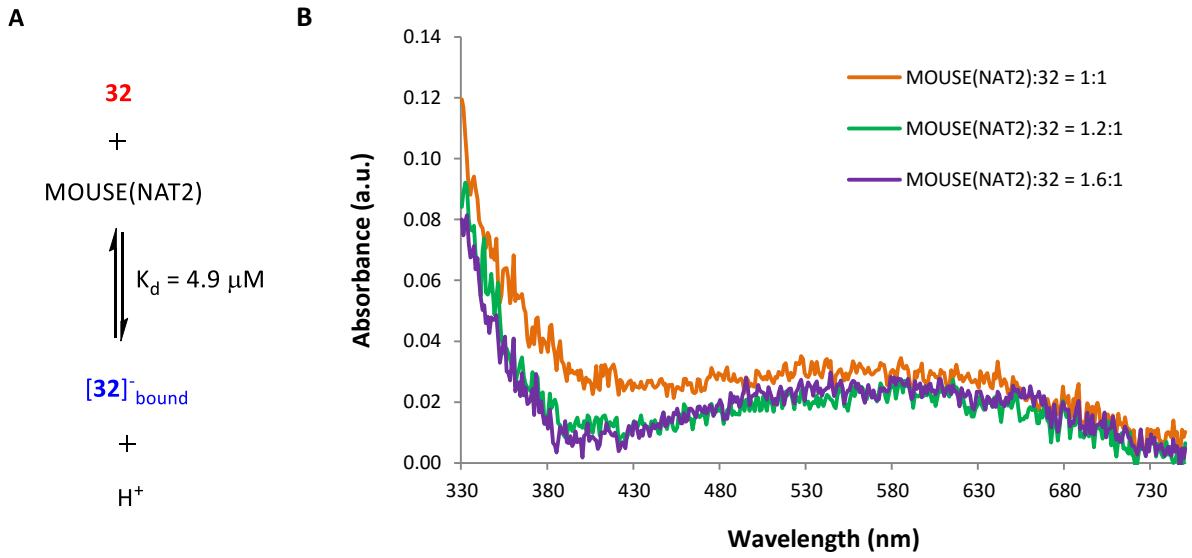


Figure 2.11: **A:** Binding equilibrium of **32** to MOUSE(NAT2). **B:** Visible spectra of compound **32** (15 µM) at MOUSE(NAT2):inhibitor ratios of 1:1 (orange line), 1.2:1 (green line) and 1.6:1 (purple line) in 95% 20 mM Tris•HCl (*p*H 8)/5% DMSO (*v/v*); MOUSE(NAT2) concentration was varied from 30 µM to 15 µM in 2.5 µM intervals. a.u. = arbitrary units.

Given that the approximate concentration of HUMAN(NAT1) in ZR-75-1 cell extracts is 0.6-1.2 µM, this means that the maximum concentration of inhibitor **32** that could be applied to the cell extracts to record an unambiguous shift in λ_{max} would lie in the region of 0.5-1.0 µM. Visible absorption spectra of **32** were therefore recorded at a range of different concentrations between 20 µM and 0.5 µM in order to determine whether the absorption coefficient of **32** is high enough for λ_{max} of its neutral and conjugate base species to be detected in the required concentration range **(Figure 2.12)**. The minimum detectable concentration under the conditions used lies between 2.5 and 5 µM, concentrations which are significantly in excess of the concentration of HUMAN(NAT1) in the ZR-75-1 cell extracts.

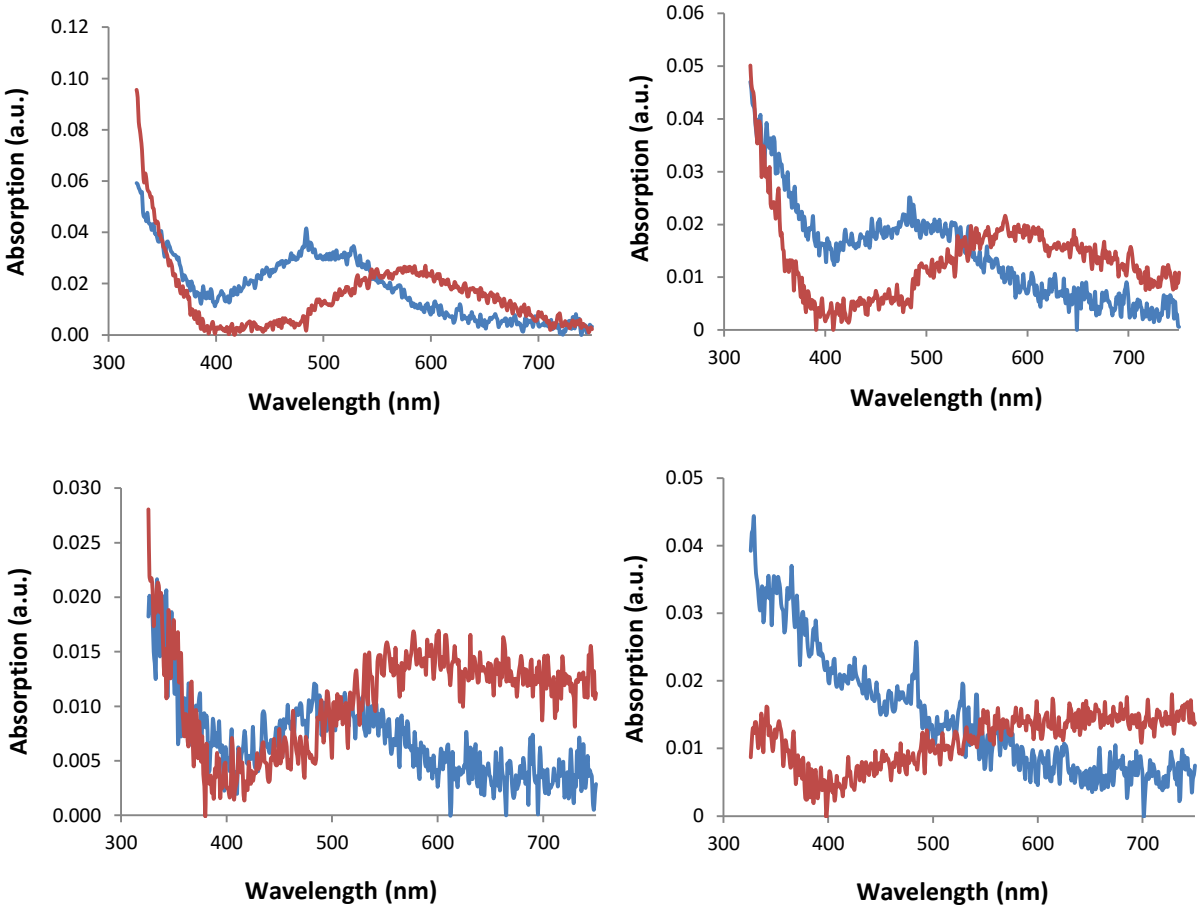


Figure 2.12: Visible spectra of compound **32** at *p*H 8 (red lines) and *p*H 13.75 (blue lines). Spectra were recorded in 95% buffer (20 mM Tris•HCl for *p*H 8, 4 M aq. NaOH for *p*H 13.75)/5% DMSO (*v/v*). Concentrations of **32** are as follows: 10 µM (top left); 5 µM (top right); 2.5 µM (bottom left); 1.25 µM (bottom right). a.u. = arbitrary units.

Cells from the human ER+ breast cancer cell line ZR-75-1 were subsequently grown and harvested to prepare a cell extract with a final concentration of 5 x 10^7 cells/mL (for protocol see **Section 7.10.**). Compound **32** was added to these ZR-75-1 cell extracts at concentrations ranging from 0.6 to 2.5 µM, but no λ_{max} peak could be detected at these low concentrations above background absorbance from the cells **(Figure 2.13)**. A negative control concentration of 20 µM **32** was also used, in which λ_{max} for the neutral species is detectable at *c.* 500 nm.

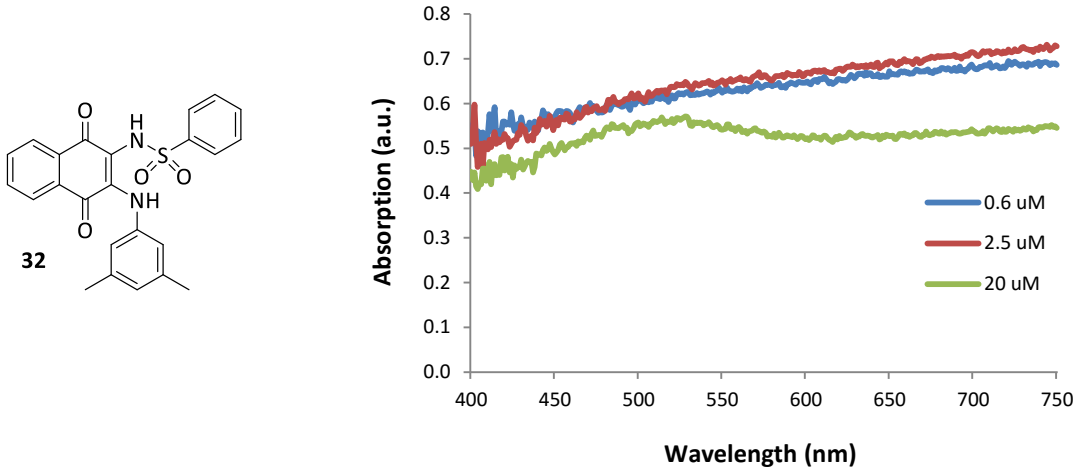


Figure 2.13: Left: Structure of naphthoquinone **32**. **Right:** Visible spectra of naphthoquinone **32** at 0.6 µM (blue line), 2.5 µM (red line) and 20 µM (green line) in 95% ZR-75-1 cell extract (5 x 10^7 cells/mL)/5% DMSO (*v/v*). a.u. = arbitrary units.

These data imply that the intrinsic sensitivity, *i.e.* the absorption coefficient, of **32** must be improved for this family of probes to exhibit clinical utility in cancer diagnosis. Additionally, increasing the potency of **32** would also be predicted to aid NAT detection in cell extracts, since the minimum required enzyme:inhibitor ratio for unambiguous detection of the conjugate base would be predicted to decrease in line with increasing active site occupancy of the inhibitor. Therefore, in **Chapter 3**, structure-activity relationships around the core of naphthoquinone **32** will therefore be described, with the aims of increasing the sensitivity and potency of HUMAN(NAT1) inhibitors based on **32** whilst maintaining its desirable selectivity and pK_a value.

Chapter 3: Optimisation of Colorimetric HUMAN(NAT1) Probes

3.1. Overview of Structure-Activity Relationship (SAR) Studies

The naphthoquinone core of inhibitor **32** is believed to be crucial for the unique colorimetric properties of the molecule in the presence of HUMAN(NAT1) or its murine homologue MOUSE(NAT2) for two reasons. Firstly, the α,β-unsaturated carbonyl system is a good electron acceptor, which stabilises the conjugate base of **32** *via* resonance and hence ensures the pK_a of the inhibitor lies within the required range. Secondly, it has been hypothesised that π-π stacking of the naphthoquinone core with the Phe125 residue in the active site is required for inhibitor binding: naphthoquinone **32** shows poor levels of inhibition of a mutant MOUSE(NAT2) protein in which Phe125 was replaced with serine (MOUSE(NAT2)_F125S).[258]

Therefore, in structure-activity relationship (SAR) studies to improve the potency and sensitivity of naphthoquinone **32**, whilst retaining its selectivity for HUMAN(NAT1) over HUMAN(NAT2), it was decided to leave the naphthoquinone core unmodified, and to systematically alter the substituents at various positions, as outlined in **Figure 3.1**. The modifications made were guided throughout by the *in silico* model of binding between the naphthoquinone inhibitors and the HUMAN(NAT1) active site.

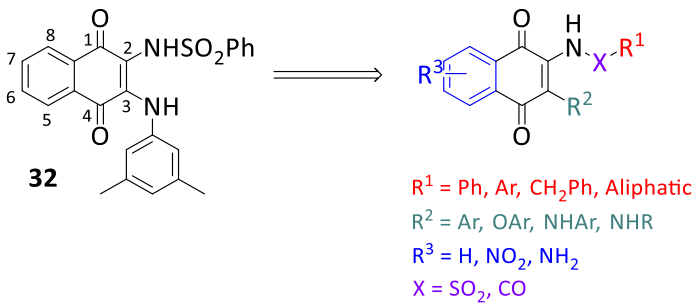


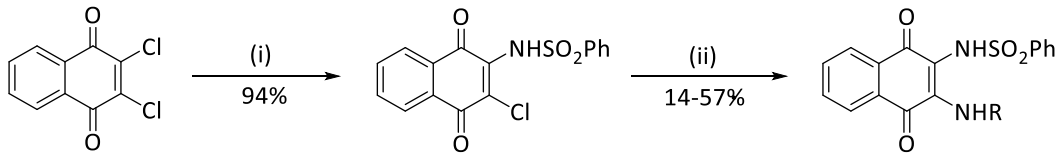
Figure 3.1: Modifications to naphthoquinone **32** which form the basis of SAR studies in this chapter; note the numbering of the naphthoquinone core, which is referred to throughout this thesis.

3.2. SAR at C_3 of the Naphthoquinone Core

At the C_3 position of the naphthoquinone core, anilino and 3,5-dimethylanilino groups have thus far been shown to be tolerated.[242, 281a] In this study, a wider range of arylamino substituents and analogous alkylamino, aryloxy and aryl substituents were investigated at this position, to determine their effect on inhibitory and optical properties of the molecules.

3.2.1. Design and Synthesis of an Inhibitor Library Containing Arylamino-, Alkylamino-, Aryloxy- and Aryl-substituted Species at C_3

An initial library of compounds was generated bearing different anilino substituents at the C_3 position. These compounds were synthesised by Kate S. Hadavizadeh (KSH) using an analogous protocol to the synthesis of hit compound **32** comprising two sequential Michael-type addition-elimination steps **(Scheme 3.1)**.[300] A wide range of substituents were selected: *ortho*-bromo **79**, *meta*-bromo **80** and *para*-bromo **81** were chosen to enable the investigation of substitution pattern on pharmacological properties, with the bromo group acting as an isostere for a phenyl group. *para*-Methoxy **82** and *para*-trifluoromethoxy **83** allow a direct comparison between the effects of electron-donating and electron-withdrawing groups on the aniline ring respectively, whilst dimethoxy **84** and trimethoxy **85** show the effect of introducing multiple electron-donating substituents onto the ring. Methoxy substituents were selected due to their auxochromic properties, which were predicted to increase the absorption coefficients of the inhibitors.



37 **57** **32, 79-85**

Scheme 3.1: Synthesis of a C_3 anilino-substituted library. *Reagents and conditions:* (i) $PhSO_2NH_2$ (1.0 eq.), Cs_2CO_3 (1.4 eq.), DMF, RT, 5 h; (ii) $CeCl_3 \bullet 7H_2O$ (1.0 eq.), MeOH, RT, 1.5 h *then* requisite aniline (3.0 eq.), 110 ^oC, 16 h. For identities of R groups and the respective yields of step (ii), see **Table 3.1**.

Compound	R	Yield of Step (ii)	Compound	R	Yield of Step (ii)
32	3,5-Dimethylphenyl	57%	**82**	4-Methoxyphenyl	49%
79	2-Bromophenyl	14%	**83**	4-Trifluoromethoxyphenyl	53%
80	3-Bromophenyl	22%	**84**	3,4-Dimethoxyphenyl	23%
81	4-Bromophenyl	30%	**85**	3,4,5-Trimethoxyphenyl	48%

Table 3.1: Identities of the R group and corresponding yields of step (ii) in **Scheme 3.1**.

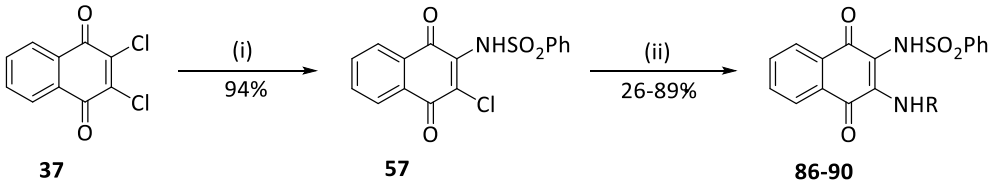
As some of the anilines used as nucleophiles in the Michael-type step (ii) gave poor yields, efforts were made to optimise the conditions for this step, using 3,5-dimethylaniline as a model nucleophile **(Table 3.2)**.

Entry	Equivalents of 3,5-dimethylaniline	Other Reagents and Conditions	Isolated Yield of 32
(i)	3.0	$CeCl_3 \bullet 7H_2O$ (1.0 eq.), MeOH, 110 ^oC, 16 h	57%
(ii)	3.0	$CeCl_3$ (1.0 eq.), Anhydrous toluene, 110 ^oC, 16 h	66%
(iii)	3.0	$CeCl_3 \bullet 7H_2O$ (1.0 eq.), MeOH, 90 ^oC, 16 h	62%
(iv)	3.0	$InCl_3$ (1.0 eq.), MeOH, 90 ^oC, 16 h	78%
(v)	2.0	$Pd(OAc)_2$ (0.01 eq.), XPhos (0.03 eq.), K_2CO_3 (1.4 eq.), H_2O (0.04 eq.), ^{t}BuOH, 110 ^oC, 16 h	14%

Table 3.2: Attempts to improve the yield of the Michael-type addition-elimination step (ii) in **Scheme 3.1** above, using 3,5-dimethylaniline as a model aniline nucleophile. Data for entries (i)-(iii) and (v) generated by KSH.[300]

It was observed that this reaction can also proceed in good yield under anhydrous conditions (entry (ii)); anhydrous $CeCl_3$ was prepared from the corresponding heptahydrate salt by heating under vacuum for 2 h at 130 ^oC. Interestingly, improved isolated yields could be obtained when the reaction temperature was reduced from 110 ^oC to 90 ^oC or when $InCl_3$ replaced $CeCl_3 \bullet 7H_2O$ as the Lewis acid (entries (iii) and (iv) respectively). These enhanced yields were attributed to a greater ease of purification in these cases; qualitative TLC analysis suggests that fewer by-products are formed under both sets of reaction conditions *cf.* entry (i). A palladium-mediated cross-coupling methodology was also trialled (entry (v)), and this did lead to formation of some desired product, but in a low isolated yield of 14%. These observations are of interest to other syntheses which utilise the Michael-type addition-elimination reaction between an aniline and a naphthoquinone described later in this thesis.

A small series of aliphatic amino groups were also introduced at the C_3 position by substitution of chloride from intermediate **57** with aliphatic amines **(Scheme 3.2)**. Aliphatic amines are generally more conformationally flexible than their aromatic counterparts, and are unable to form π-π interactions with the NAT active site upon binding. The analogues chosen for study enable comparison of effects of chain extension, inclusion of polar heteroatoms and aromatic moieties. 2-Methoxyethyl **86** and cyclopentyl **87** analogues had been prepared in a previous study,[281b] whilst benzyl **88** and ethylphenyl **90** were synthesised by KSH.[300] In contrast to the corresponding addition-elimination reactions with anilines, these reactions with aliphatic amines proceeded in good yield in 6 h at 110 °C in toluene as a solvent; in fact, reaction of benzylamine (as a representative amine) in MeOH at this temperature formed a complex mixture of products in which the desired adduct could not be detected.



37 **57** **86-90**

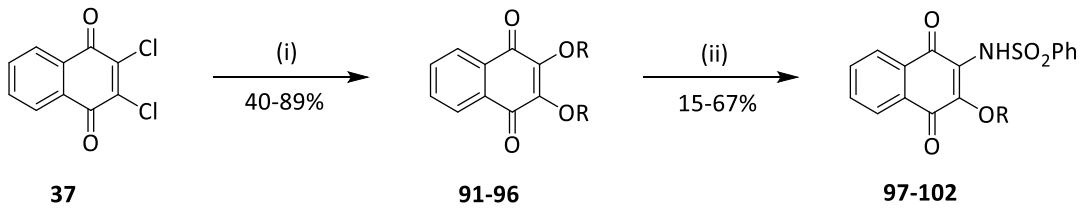
Scheme 3.2: Synthesis of a C_3 alkylamino-substituted library. *Reagents and conditions:* (i) $PhSO_2NH_2$ (1.0 eq.), Cs_2CO_3 (1.4 eq.), DMF, RT, 5 h; (ii) $CeCl_3 \bullet 7H_2O$ (1.0 eq.), toluene, RT, 1.5 h *then* requisite amine (3.0 eq.), 110 °C, 6 h. For identities of R groups and the respective yields of step (ii), see **Table 3.3**.

Compound	R	Yield of Step (ii)
86	2-Methoxyethyl	87%^
87	Cyclopentyl	89%^
88	Benzyl	42%*
89	(±)-α-Methylbenzyl	26%
90	Phenylethyl	29%*

Table 3.3: Identities of the R group and corresponding yields of step (ii) in **Scheme 3.2**. * = data generated by KSH;[300] ^ = synthesised in a previous study.[281b]

Aryloxy-substituted analogues of **32** were also synthesised, as these were predicted to have similar conformational preferences to the corresponding anilino-substituted species, but lack H-bond donor properties. Synthesis of these derivatives was inspired by that of sulfonate

ester **36**, which has been described previously in **Section 2.1.2.**: 2,3-dichloro-1,4-naphthoquinone **37** was treated with 2.2 eq. of the requisite arylalcohol and 2.2. eq. of Cs_2CO_3 under reflux in THF for 16 h to generate *bis*-substituted-2,3-aryloxy-1,4-naphthoquinones **91-96**, which subsequently underwent displacement of a single aryloxy substituent by benzenesulfonamide when refluxed in THF for 1 h in the presence of Cs_2CO_3 **(Scheme 3.3)**. Analogues **97**, **98** and **100**, bearing phenoxy-, 3,5-dimethylphenoxy- and 4-bromophenoxy-C_3 substituents respectively, were synthesised to enable a direct comparison with anilino-substituted **20**, **32** and **81**, whilst formyl derivatives **99** and **101** and methoxy derivate **102** were of respective interest as examples of highly electron-withdrawing and electron-donating moieties.



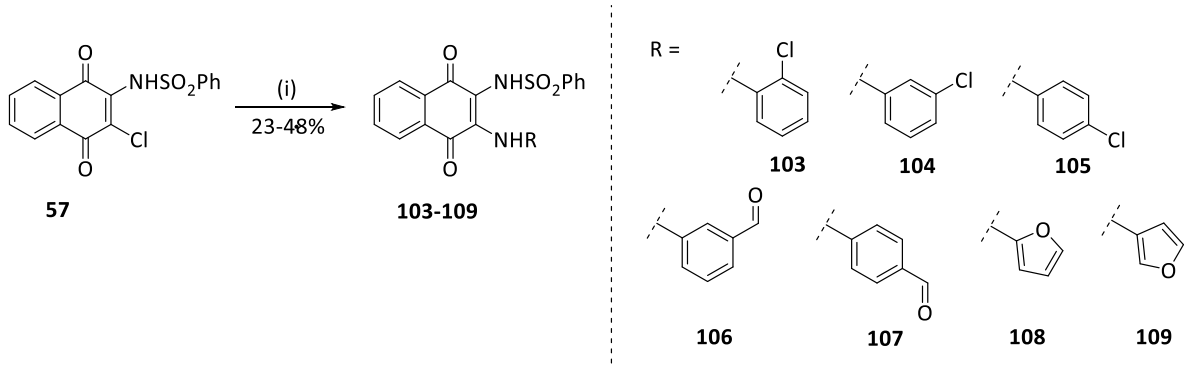
Scheme 3.3: Synthesis of a library of compounds containing a C_3 aryloxy substituent. *Reagents and conditions:* (i) requisite arylalcohol (2.2 eq.), Cs_2CO_3 (2.2 eq.), THF, reflux, 16 h; (ii) $PhSO_2NH_2$ (1.0 eq.), Cs_2CO_3 (1.2 eq.), THF, reflux, 1 h. For the identity of R and yields of each step, refer to **Table 3.4**.

R	Compound	Yield Step (i)	Compound	Yield Step (ii)
Phenyl	**91**	63%	**97**	67%
3,5-Dimethylphenyl	**92**	89%	**98**	57%
3-Formylphenyl	**93**	81%	**99**	15%
4-Bromophenyl	**94**	72%	**100**	43%
4-Formylphenyl	**95**	40%	**101**	23%
4-Methoxyphenyl	**96**	87%	**102**	37%

Table 3.4: Identity of the R group and corresponding yields of steps (i) and (ii) in **Scheme 3.3** above.

Finally, C_3 aryl-substituted analogues were also investigated. These compounds are predicted to have different conformational preferences to the anilino and aryloxy derivatives, and additionally lack both H-bond donor and acceptor properties. A library of such C_3 aryl-substituted analogues had been prepared in a previous study *via* Suzuki-Miyaura-type cross-

coupling reactions[203] on 2-benzenesulfonamido-3-chloro-1,4-naphthoquinone **57 (Scheme 3.4)**;[281b] however, the MOUSE(NAT2) and HUMAN(NAT1) samples available at the time of this study showed very low levels of specific activity and hence some doubt was cast about the pharmacological conclusions drawn. ^{1}H-NMR, ^{13}C-NMR, LRMS and HPLC analysis showed that these samples had retained their structural integrity and thus some of this series were selected for further evaluation in this study; those examples selected are illustrated in **Scheme 3.4** and encompass both electron-rich and electron-poor aryl derivatives, as well as groups which are *ortho*-, *meta*- and *para*-substituted.



Scheme 3.4: Aryl-substituted C_3 analogues synthesised *via* a Suzuki-Miyaura-type cross-coupling reaction in a previous study.[281b] *Reagents and conditions:* (i) requisite boronic acid (2.0 eq.), $Pd(PPh_3)_2Cl_2$ (0.1 eq.), THF:sat. aq. $NaHCO_3$ (22:5), reflux, 18 h.

3.2.2. Pharmacological Evaluation of the Initial Compound Library

All of the anilino-, alkylamino-, aryloxy- and aryl-substituted analogues of hit compound **32** were initially tested for inhibitory potency against recombinant MOUSE(NAT2) and HUMAN(NAT1) in the acetyl CoA hydrolysis assay (previously described in **Section 2.1.2.**), in triplicate at a single-point concentration of 30 μM. **Figure 3.2** shows the mean % residual enzyme activity observed when each compound was applied, ± one standard deviation. Student's *T*-Tests were performed to determine whether the results against the murine and human proteins were significantly different from one another.

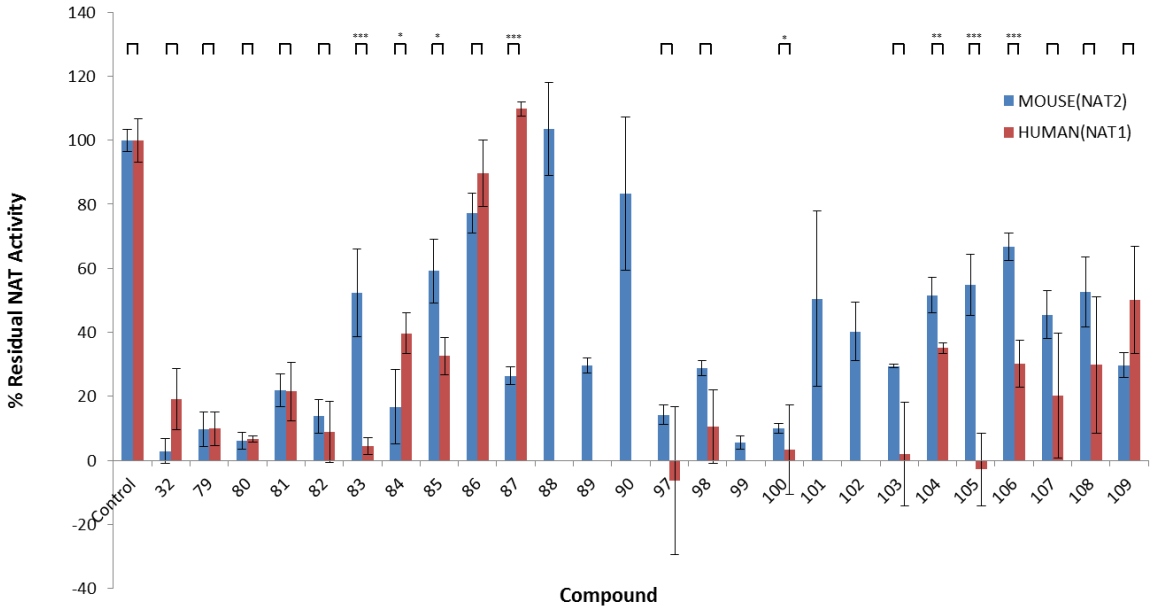
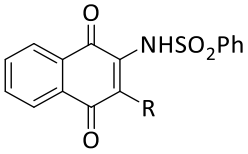


Figure 3.2: % Residual activity, ± one standard deviation, when MOUSE(NAT2) (blue columns) or HUMAN(NAT1) (red columns) were dosed with 30 µM of compounds **32**, **79-90** and **97-109** in the acetyl CoA hydrolysis assay. Experiments were conducted in triplicate and the final DMSO concentration was 5% (*v/v*). Data on compounds **79-85**, **88** and **90** generated by KSH.[300] The stars and brackets above the bars show the significance of the difference between the MOUSE(NAT2) and HUMAN(NAT1) data when a Student's *T*-Test was performed: no stars = $P > 0.05$; * = $P < 0.05$; ** = $P < 0.01$; *** = $P < 0.005$.

For any of the inhibitors which displayed >50% inhibition at 30 µM, IC_{50} values were calculated by applying ten different concentrations of each inhibitor to the enzyme **(Table 3.5)**. The % residual enzyme activity was plotted against inhibitor concentration, and KyPlot® software was used to calculate IC_{50} values based on the method of least squares; squared correlation coefficient (R^2) values and significance limits (P) for each data set are also reported.

From these data, we can see that a wide variety of aromatic substituents are tolerated at the C_3 position, with examples of anilino-, aryloxy- and aryl-substituted species giving comparable levels of potency against both MOUSE(NAT2) and HUMAN(NAT1). This suggests that neither N-*H* hydrogen bond donor nor acceptor capabilities are a crucial requirement for binding of the inhibitors to the enzyme active site. Furthermore, examples of both electron-rich and electron-poor aromatic substituents (e.g. methoxy-susbtituted **82** and **102**, formyl-substituted

106 and **107**, and furanyl derivatives **108** and **109**) show similar levels of binding to the enzyme as the hit compound **32**.



32, 79-90, 97-109

Compound	R	IC_{50} MOUSE(NAT2) (μM)	R^2 Value	*P*	IC_{50} HUMAN(NAT1) (μM)	R^2 Value	*P*
32	NH-3,5-Me-C_6H_3	3.1 ± 0.69	0.8972	***	4.1 ± 0.56	0.9658	***
79	NH-2-Br-C_6H_4	5.7 ± 0.90	0.9124	***	2.8 ± 0.37	0.9673	***
80	NH-3-Br-C_6H_4	1.3 ± 0.28	0.9124	***	0.96 ± 0.21	0.9343	***
81	NH-4-Br-C_6H_4	1.7 ± 0.36	0.9030	***	0.89 ± 0.25	0.8781	**
82	NH-4-OMe-C_6H_4	6.6 ± 1.9	0.7429	**	2.3 ± 0.58	0.8961	***
83	NH-4-OCF_3-C_6H_4	3.8 ± 1.3	0.6271	**	0.57 ± 0.14	0.9039	***
84	NH-3,4-OMe-C_6H_3	23.3 ± 4.5	0.7220	***	8.2 ± 1.9	0.8504	***
85	NH-3,4,5-OMe-C_6H_2	>30	N/A	N/A	26.6 ± 4.4	0.8482	***
86	$NHCH_2CH_2OMe$	>30	N/A	N/A	>30	N/A	N/A
87	Cyclopentylamine	>30	N/A	N/A	>30	N/A	N/A
88	$NHCH_2Ph$	>30	N/A	N/A	>30	N/A	N/A
89	NHCH(Me)Ph	>30	N/A	N/A	N.D.	N/A	N/A
90	$NHCH_2CH_2Ph$	>30	N/A	N/A	N.D.	N/A	N/A
97	OPh	5.7 ± 1.4	0.8264	***	2.8 ± 0.26	0.9594	***
98	O-3,5-Me-C_6H_3	5.2 ± 1.4	0.2925	**	12.1 ± 0.87	0.9602	***
99	O-3-CHO-C_6H_4	17.1 ± 4.5	0.8119	**	N.D.	N/A	N/A
100	O-4-Br-C_6H_4	1.1 ± 0.38	0.3814	**	1.9 ± 0.25	0.9654	***
101	O-4-CHO-C_6H_4	18.5 ± 6.3	0.7155	*	N.D.	N/A	N/A
102	O-4-OMe-C_6H_4	8.3 ± 2.2	0.7592	**	N.D.	N/A	N/A
103	2-Cl-C_6H_4	3.7 ± 0.57	0.8416	***	8.0 ± 0.66	0.9648	***
104	3-Cl-C_6H_4	5.1 ± 0.98	0.8213	***	14.5 ± 1.2	0.9500	***
105	4-Cl-C_6H_4	8.3 ± 2.2	0.2414	**	12.1 ± 1.7	0.9030	***
106	3-CHO-C_6H_4	9.2 ± 1.9	0.7080	***	8.4 ± 0.79	0.9397	***
107	4-CHO-C_6H_4	6.9 ± 1.5	0.5529	***	10.3 ± 1.1	0.9385	***
108	Furan-2-yl	4.3 ± 0.88	0.7914	***	9.6 ± 1.3	0.9098	***
109	Furan-3-yl	1.4 ± 0.25	0.8385	***	10.0 ± 0.76	0.9671	***

Table 3.5: IC_{50} values for compounds **32**, **79-90** and **97-109** in the C_3 analogue library against MOUSE(NAT2) and HUMAN(NAT1) in the acetyl CoA hydrolysis assay, with squared correlation coefficients (R^2) and significance levels (*P*); * = *P* <0.05; ** = *P* <0.01; *** = *P* <0.005. IC_{50} values for compounds **79-85**, **88** and **90** determined by KSH.[300] Data calculated using KyPlot® software. N.D. = not determined; N/A = not applicable.

In silico modelling was carried out on compounds **79-85** and **97-109**, which predicts that all the compounds in this library have a similar binding mode to the HUMAN(NAT1) active site. Representative examples from this modelling study, namely compounds **97** and **109**, are displayed in **Figure 3.3**, overlaid with the model of hit compound **32** for comparison.

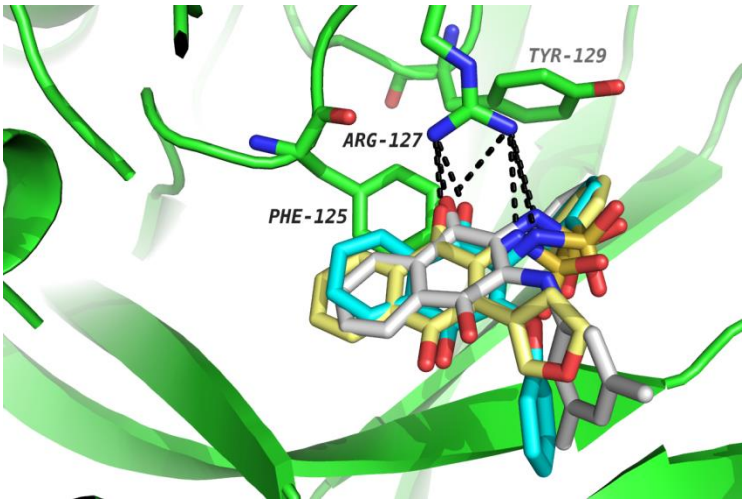
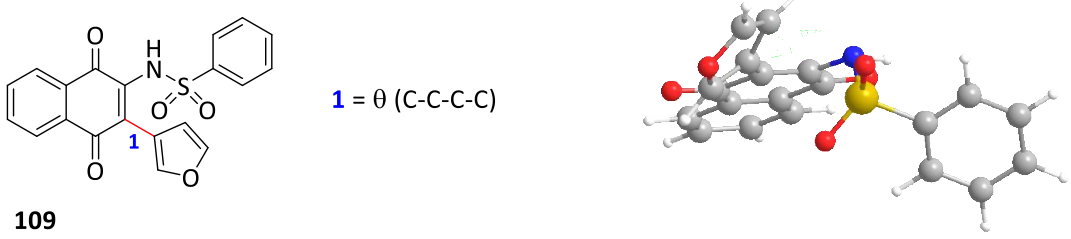


Figure 3.3: *In silico* modeling of compounds **32** (carbon atoms in grey), **97** (carbon atoms in cyan) and **109** (carbon atoms in yellow) in the active site of HUMAN(NAT1) (pdb: 2PQT).[247b] Analysis performed using GOLD® (v.5.2).[282] Inhibitors are displayed using stick representation and HUMAN(NAT1) is displayed in cartoon representation, with key active site residues Phe125, Arg127 and Tyr129 highlighted in stick representation (carbon atoms in green).

It can be observed from the *in silico* models in **Figure 3.3** that aryloxy-substituted **97** and aryl-substituted **109** are predicted to have similar torsional angles about the C-N and N-S bonds in the C_2 sulfonamide moiety as that of hit anilino-substituted compound **32**, torsional angles which were previously determined through DFT modelling of the free ligands to be low-energy conformers. Furthermore, the conformations about the rotatable C_3-O and O-Ar bonds in the docked phenoxy-substituted **97** are analogous to those about the C_3-N and N-Ar bonds in hit compound **32**, which were also previously shown to be energetically favourable. To evaluate the docked conformation of aryl-substituted **109** about the C_3-Ar bond, the docked conformer is compared to the minimum energy conformer as predicted by DFT modelling on **109** in the gas phase **(Figure 3.4)**. It can be observed that whilst the docked conformer of **109** is not the

lowest energy conformer about the C_3-aryl bond as predicted by the DFT model, the torsional angle of 37.5° in the docked conformer does represent a local energy minimum in the DFT calculations and hence could be a reasonable conformer for the ligand to adopt in the active site.

A



109

B

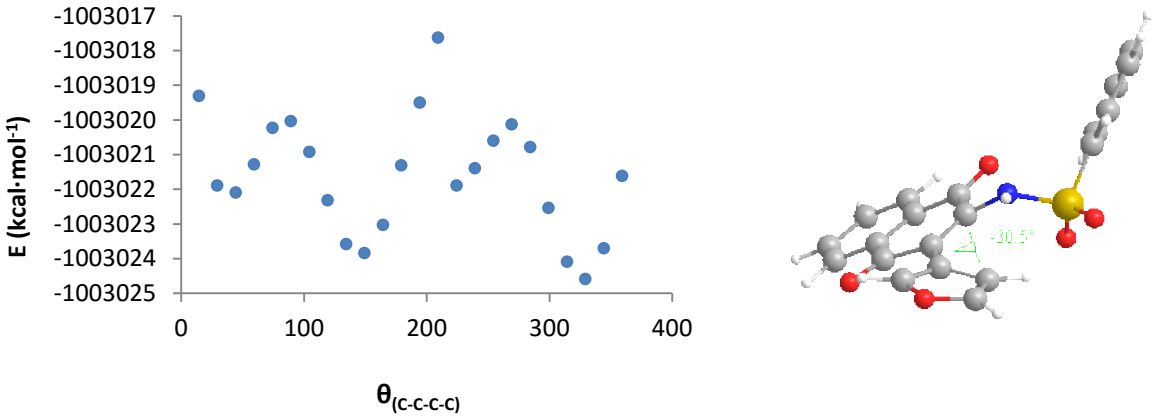


Figure 3.4: DFT modelling studies showing the variation of energy with torsional angle, θ, about the rotatable bonds of the C_3 position in representative aryl-substituted naphthoquinone **109**. **A:** Structure of aryl-substituted **109** with the rotatable bond highlighted in red, and an image to show the torsional angle about this bond in the conformation of **109** predicted by the *in silico* model in **Figure 3.3**; **B:** Plot of energy *vs.* torsional angle for the rotatable bond in **109** with an image to show the optimal torsional angle for this bond. All images generated in ChemBioDraw3D®.

It can also be noted from the inhibitory data in **Figure 3.2** and **Table 3.5** that all of the synthesised analogues bearing an alkylamino substituent at the C_3 position are poor inhibitors of both MOUSE(NAT2) and, where tested, HUMAN(NAT1). Docking studies do not reveal any residues around the entrance to the active site which might be capable of forming π-π

interactions with the C_3 substituent; however, any of the hydrophobicity, electron density or preferred conformations of such aromatic substituents may be required for binding. Entropy changes upon binding might also play a role, since the ground state conformations of alkylamino-substituted species are likely to have a higher flexibility than their aromatic counterparts, leading to a greater concomitant loss of entropy upon binding to the protein. However, the fact that the more rigid cyclopentyl derivative **87** also exhibits poor inhibition of MOUSE(NAT2) and HUMAN(NAT1) suggests that this is unlikely to be the only explanation for the observed trend.

Examination of the IC_{50} values of the anilino-substituted inhibitors **79-85** in more detail also reveals some interesting trends. Firstly, it should be noted that bromo-substitution at all three positions on the aniline ring leads to IC_{50} values comparable to that of dimethyl-substituted **32**; this implies that there is scope for further substitution around the ring. The electron-poor *para*-trifluoromethoxy-substituted **83** shows slightly lower IC_{50} values of 3.8 and 0.57 μM against the murine and human proteins respectively than the more electron-rich *para*-methoxy-substituted **82**, with IC_{50} values of 6.6 and 2.3 μM; however, a Student's *T*-test carried out on these data sets suggests that the difference is not statistically significant.

Finally, the inhibition data on di-methoxy-substituted **84** and tri-methoxy-substituted **85** suggests that multiple substituents on the anilino ring are less well-tolerated than a single substituent; **84** and **85** possess IC_{50} values against both the murine and human proteins which are approximately one order of magnitude greater than the corresponding values for mono-methoxy-substituted **82**. *In silico* modelling suggests that the multiple -OMe substituents might lead to undesirable steric repulsions with the residues around the entrance to the active site. In the modelled ligand conformers, the multiple O-Me bonds in **84** and **85** oppose one another, which suggests that the preferred conformations of these bonds might be induced by one another **(Figure 3.5)**.

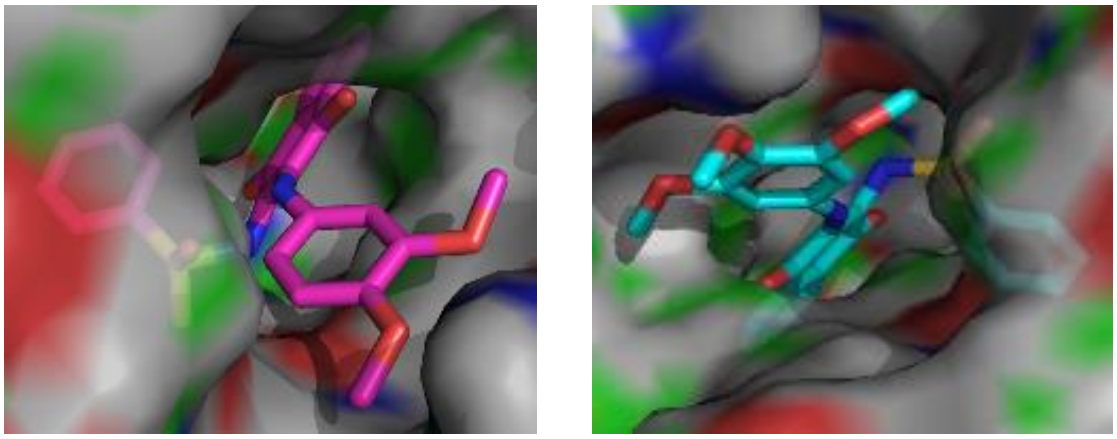


Figure 3.5: *In silico* modelling of dimethoxy-anilino-substituted **84 (left)** and trimethoxy-anilino-substituted **85 (right)** in the active site of HUMAN(NAT1) (pdb: 2PQT).[247b] Analysis performed using GOLD® (v.5.2).[282] The ligands are shown in stick representation, with carbon atoms in magenta for **84** and cyan for **85**; the protein is shown in surface representation.[300] The modelling simulations show that the methyl groups are conformationally induced to oppose one another, which might lead to repulsive steric interactions with the residues lining the opening to the enzyme active site.

3.2.3. Colorimetric Evaluation of the Initial Compound Library

A useful colorimetric probe for quantification of HUMAN(NAT1) in biological samples must not only be a potent and selective inhibitor of the enzyme, but also display a distinct and unambiguous shift in λ_{max} in the presence of the protein, and consequently must also possess an appropriate *p*K_a value. As such, the *p*K_a of each of the synthesised compounds in the initial compound library was determined *via* titration: a plot of λ_{max} against *p*H was measured and a method of least squares used to fit a sigmoidal curve to the data, from which the *p*K_a could be determined as the point of inflexion (see **Section 7.13.4.** for detailed protocol) **(Table 3.6)**.

These data tell us that despite the reasonable potency of many of the aryloxy-substituted species **97-102** and aryl-substituted species **103-109** against the human and murine proteins, these species all have unsuitable *p*K_a values for use as colorimetric HUMAN(NAT1) probes; the *p*K_a values for these compounds are all below 8 and therefore the compounds would be deprotonated in the assay buffer or under physiological conditions.

Compound	*p*K_a	Compound	*p*K_a	Compound	*p*K_a
32	9.2 ± 0.05	**87**	10.1 ± 0.2	**102**	5.0 ± 0.8
79	8.1 ± 0.4	**88**	10.4 ± 0.2	**103**	4.9 ± 0.2
80	8.5 ± 0.7	**89**	9.7 ± 0.05	**104**	4.5 ± 0.1
81	10.4 ± 0.2	**90**	10.4 ± 0.2	**105**	5.0 ± 0.2
82	9.2 ± 0.3	**97**	5.0 ± 0.2	**106**	5.0 ± 0.1
83	9.5 ± 0.01	**98**	5.0 ± 0.1	**107**	4.6 ± 0.1
84	7.9 ± 0.1	**99**	5.0 ± 1.9	**108**	5.1 ± 0.3
85	8.7 ± 0.1	**100**	5.0 ± 0.1	**109**	5.0 ± 0.1
86	9.8 ± 0.2	**101**	5.3 ± 0.6		

Table 3.6: *p*K_a values for compounds in the C_3 analogue library, determined *via* colorimetric titration experiments and calculated using GraphPad Prism®, using a variable slope non-linear regression model; the R^2 value for each compound is >0.95. Values are quoted ± one standard deviation. Data on compounds **79-85**, **88** and **90** generated by KSH.[300]

Conversely, all the anilino-substituted species (**32** and **79-85**) and alkylamino-substituted species (**86-90**) have *p*K_a values in a desirable range (from 7.9 for **84** to 10.4 for **81** and **88**); this is consistent with nitrogen being a stronger mesomeric electron donor into the naphthoquinone core than either the oxygen or carbon atoms at C_3 in the aryloxy-substituted and aryl-substituted species respectively. Therefore, further colorimetric parameters of each of the inhibitors **32** and **79-90** were measured, namely: λ_{max} in Tris•HCl assay buffer (*p*H 8), λ_{max} under basic conditions (*p*H 13.0), λ_{max} in the presence of MOUSE(NAT2), absorption coefficient of the neutral species at *p*H 8 (ε_N) and absorption coefficient of the conjugate base species at *p*H 13 (ε_{CB}) **(Table 3.7)**. These parameters were calculated *via* spectrophotometric measurements recorded as described in **Sections 7.13.3.-7.13.5**.

The first key observation to draw from these data is that all of the tested compounds display a clear shift in λ_{max} under basic conditions. Anilino-substituted species **32** and **79-85** show a similar shift in λ_{max} in the presence of MOUSE(NAT2), which is consistent with the theory that the enzyme sequesters the conjugate base of these inhibitors from solution. Notably, however, the majority of alkylamino-substituted species **86-90** do not display such a shift in λ_{max} in the presence of MOUSE(NAT2); this might be explained by their comparatively weaker inhibitory potencies against the enzyme (IC_{50} >30 μM) than their anilino-substituted

counterparts. Within the anilino-substituted series itself, compounds **83-85** display a smaller λ_{max} shift than compounds **32** and **79-82**, which have IC_{50} values that are one order of magnitude lower.

Unfortunately, however, the conjugate bases of none of the synthesised analogues display significantly enhanced absorption coefficients over hit compound **32**, despite the addition of auxochromic groups (e.g. -OMe) in some examples.

Compound	*p*K_a	λ_{max} *p*H 8 (nm)	$\Delta\lambda_{max}$ *p*H 13 (nm)	$\Delta\lambda_{max}$ MOUSE(NAT2) (nm)	ε_N ($M^{-1}cm^{-1}$)	$\varepsilon_N/\varepsilon_N(32)$	ε_{CB} ($M^{-1}cm^{-1}$)	$\varepsilon_{CB}/\varepsilon_{CB}(32)$
32	9.2	498	+ 79	+ 112	11960	1.00	6590	1.00
79	8.1 ± 0.4	490	+ 61	+ 78	31110	2.60	7790	1.14
80	8.5 ± 0.7	503	+ 59	+ 95	15560	1.30	5800	0.88
81	10.4 ± 0.2	500	+ 70	+ 93	13330	1.11	7790	1.18
82	9.2 ± 0.3	509	+ 61	+ 64	17780	1.49	7500	1.14
83	9.5 ± 0.01	509	+ 51	+ 32	13330	1.11	7220	1.10
84	7.9 ± 0.1	510	+ 69	+ 42	8890	0.74	7220	1.10
85	8.7 ± 0.1	503	+ 87	+ 52	32380	2.71	5770	0.88
86	9.8 ± 0.2	469	+ 89	N.D.	1330	0.11	1010	0.15
87	10.1 ± 0.2	471	+ 82	+ 3	10080	0.84	4470	0.68
88	10.4 ± 0.2	486	+ 74	+ 5	10480	0.88	5770	0.88
89	9.7 ± 0.05	472	+ 78	+ 11 And emerging shoulder at +137	16150	1.35	5070	0.77
90	10.4 ± 0.2	489	+ 71	+ 2	13020	1.09	5770	0.88

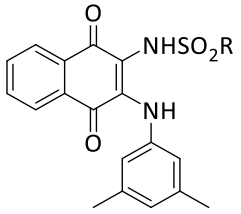
Table 3.7: Colorimetric data for compounds **32** and **79-90**: *p*K_a values (calculated using GraphPad Prism® and quoted ± one standard deviation; R^2 >0.95 for all compounds); wavelengths of maximum absorption at *p*H 8, *p*H 13 and in the presence of MOUSE(NAT2); and absorption coefficients of the neutral (N) and conjugate base (CB) species. Data for **79-85**, **88** and **90** generated by KSH.[300] N.D. = not determined.

3.3. SAR at C_2 of the Naphthoquinone Core

Thus far, all the synthesised analogues described bear a bezenesulfonamide moiety at the C_2 position of the naphthoquinone core. Here, the synthesis and evaluation of a library of both sulfonamido- and amido-substituted C_2 derivatives will be discussed, in further attempts to increase the potency and sensitivity of colorimetric HUMAN(NAT1) probes (*cf.* **Figure 3.1**).

3.3.1. Design and Synthesis of Sulfonamido-Substituted Species at the C_2 Position

In a previous study, a small library of compounds was generated which comprised of six analogues of **32** each bearing different aliphatic or aromatic sulfonamide moieties at the C_2 position of the naphthoquinone core and a 3,5-dimethylanilino substituent at the C_3 position.[281a] The structures, pharmacological and colorimetric properties of these compounds are summarised in **Table 3.8**.



32, 110-116

Compound	R	IC_{50} MOUSE(NAT2) (μM)	pK_a	λ_{max} *p*H 8 (nm)	$\Delta\lambda_{max}$ *p*H 13 (nm)	$\varepsilon_N/\varepsilon_N$(32)	$\varepsilon_{CB}/\varepsilon_{CB}$(32)
32	Ph	2.4 ± 0.61	9.2 ± 0.1	498	+ 79	1.00	1.00
110	Me	>30	9.5 ± 0.1	491	+ 87	0.84	1.03
111	^{i}Pr	>30	9.8 ± 0.1	498	+ 86	0.92	1.16
112	4-Me-C_6H_4	>30	9.7 ± 0.1	505	+ 73	1.17	1.09
113	3-Me-2-pyridyl	>30	N.D.	535	0	0.69	1.15
114	2-Me-C_6H_4	>100	9.3 ± 0.2	512	+ 17	1.23	0.82
115	2-NO_2-C_6H_4	28.7 ± 11.1	7.9 ± 0.1	528	+ 32	1.04	1.16
116	2-NH_2-C_6H_4	>100	9.2 ± 0.3	503	+ 82	0.94	0.98

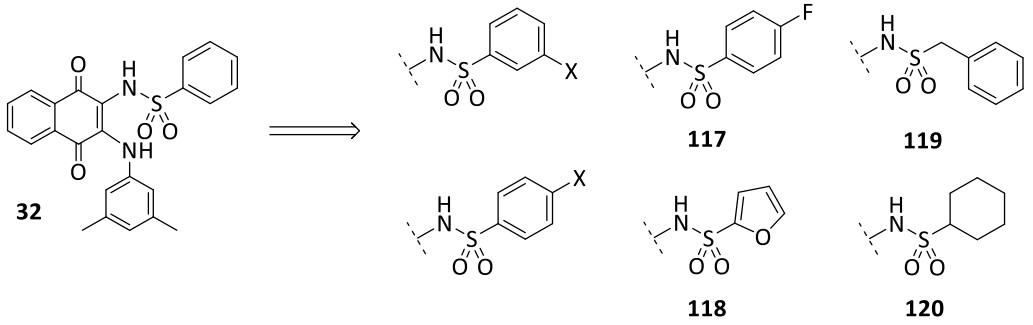
Table 3.8: Summary of the pharmacological and optical properties of a series of analogues of **32** bearing different sulfonamido substituents at the C_2 position, synthesised in a previous study.[281a]

The data on these compounds suggested that neither aliphatic sulfonamides, even the sterically similar isopropyl analogue, nor substituted aromatic sulfonamides were as well tolerated in the MOUSE(NAT2) active site as the phenyl sulfonamide **32**; the only substituted aromatic sulfonamide to display an IC_{50} value below 30 μM was the strongly electron-withdrawing 2-nitrophenyl analogue. These observations led to the hypothesis that the benzenesulfonamide substituent in hit compound **32** interacts with an electron-rich, aromatic amino acid within the enzyme active site, possibly *via* edge-face π-π interactions, which is consistent with the proposed *in silico* model (**Figure 2.1,** *vide infra*) that predicts a potential interaction between the benzenesulfonamide substituent and Tyr129. Furthermore, an interesting study was carried out on the homologous protein to HUMAN(NAT1) from the Syrian hamster, HAMSTER(NAT2), in which 81% residues including the Cys-His-Asp catalytic triad and many active site residues, such as Phe125 and Arg127, are conserved from HUMAN(NAT1) but at the 129 position a Leu residue is found in place of Tyr.[301] Hit compound **32** was found to exhibit only weak dose-dependent binding to HAMSTER(NAT2) (IC_{50} = 89 μM) despite showing some evidence of a colour change: this implies the Tyr129 is important in ligand recognition for the naphthoquinone family based on **32**.[281a]

To add further weight to this hypothesis, it was decided to synthesise a larger library of compounds in which the C_2 sulfonamido substituent is varied; in particular, it was deemed desirable to expand the library to include bezenesulfonamido analogues bearing either mesomerically electron-withdrawing or electron-donating groups on the *para* and *meta* positions of the aromatic ring, to enable comparison with *ortho*-nitro- and amino-substituted derivatives **115** and **116 (Figure 3.6A)**. Furthermore, given that none of the substituted aromatic sulfonamide substituents yielded an IC_{50} value against MOUSE(NAT2) of less than 30 μM, smaller aromatic groups, such as fluorobenzenesulfonamido and furanylsulfonamido substituents were also considered valuable additions to the library. *In silico* modelling studies suggested that 4-fluorobenzenesulfonamido-subsituted naphthoquinone **117** and furan-2-ylsulfonamido-substituted naphthoquinone **118** would be tolerated within the HUMAN(NAT1) active site **(Figure 3.6B)**. Benzyl sulfonamide **119** was also considered a

valuable target since this analogue was predicted to have greater conformational flexibility due to the presence of an additional rotatable bond. Finally, it was also decided to synthesise the aliphatic cyclohexylsulfonamido derivative **120** as this compound, like isopropylsulfonamido **111**, is predicted to be approximately isosteric to hit compound **32** and should provide further evidence about the importance of the C_2 substituent bearing aromatic functionality.

A



B

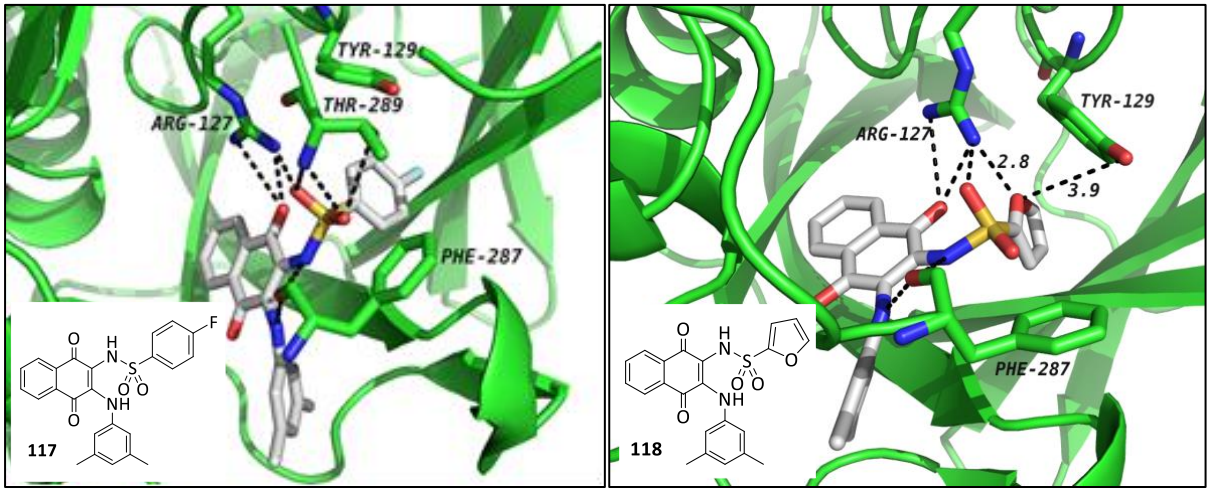
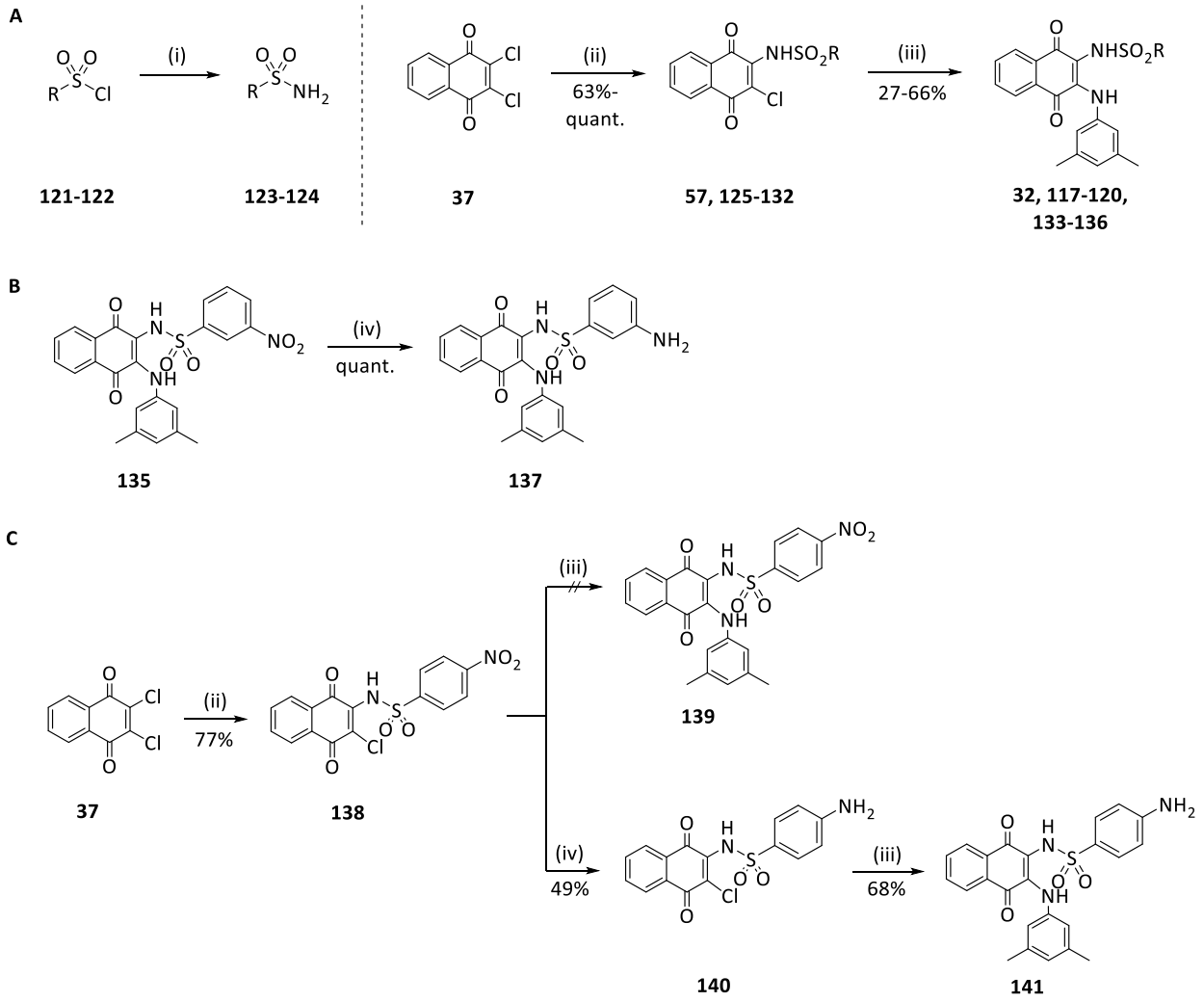


Figure 3.6: A: Desired C_2-sulfonamido-subsituted targets; X = electron-donating or electron-withdrawing group. **B:** *In silico* modelling of 4-fluorobenzenesulfonamido derivative **117 (left)** and furan-2-ylsulfonamido derivative **118 (right)** in the active site of HUMAN(NAT1) (pdb: 2PQT).[247b] Analysis performed using GOLD® (v.5.2).[282] Inhibitors are shown in stick representation (carbon atoms in grey); the protein is shown in cartoon representation with active site residues Arg127, Tyr129, Phe287 and Thr289 highlighted in stick representation (carbon atoms in green). Predicted polar contacts are represented by dashed lines, with inter-atomic distances given in Ångströms.

The majority of desired analogues were synthesised *via* an analogous two-step protocol to that of hit compound **32**, in which 2,3-dichloro-1,4-naphthoquinone **37** was first treated with the requisite sulfonamide and Cs_2CO_3 in DMF at RT to give 2-sulfonamido-3-chloro-1,4-naphthoquinone intermediates **125-132**; all sulfonamides were commercially available except for cyclohexylsulfonamide **123** and furan-2-ylsulfonamide **124**, which were synthesised from the corresponding sulfonyl chlorides in excellent yield (>90%). Intermediates **125-132** subsequently underwent a further Michael-type addition-elimination reaction with 3,5-dimethylaniline in the presence of $CeCl_3 \bullet 7H_2O$ in MeOH at 110 ^{o}C to give the desired products **117-120** and **133-136** in overall yields between 20-56% for the two steps **(Scheme 3.5A)**.

meta-Aminobenzenesulfonamido-substituted analogue **137** was accessed from the corresponding nitro-derivatised analogue **135** in a final catalytic hydrogenation step **(Scheme 3.5B)**. One exception to this protocol was the synthesis of *para*-aminobenzenesulfonamido-substituted **141**: the corresponding *para*-nitrobenezenesulfonamido adduct **139** was not observed in the reaction of chloro-substituted intermediate **138** with 3,5-dimethylaniline; therefore, a catalytic hydrogenation of intermediate **138** was instead effected to give species **140**, which was able to undergo addition-elimination with 3,5-dimethylaniline to give *para*-aminobenzenesulfonamido **141** in good yield **(Scheme 3.5C)**.



Scheme 3.5: A: Synthesis of a library of analogues of **32** bearing different sulfonamido substituents at the C_2 position. For the identity of R and yields of each step, see **Table 3.9**. **B:** Reduction of 3-nitrophenylsulfonamido derivative **135** to 3-aminophenylsulfonamido derivative **137**. **C:** Synthesis of an analogue of **32** bearing a 4-aminophenylsulfonamido substituent at the C_2 position. *Reagents and conditions:* (i) 33% aq. NH_4OH, RT, 0.5-1.5 h; (ii) Requisite sulfonamide (1.0 eq.), Cs_2CO_3 (1.4 eq.), DMF, RT, 5-16 h; (iii) $CeCl_3 \bullet 7H_2O$, MeOH, RT, 1.5 h *then* add 3,5-dimethylaniline, 110 ^oC, 16-48 h; (iv) H_2 (1 atm.), 10% Pd/C (0.1 eq.), MeOH, RT, 16 h.

R	Compound	Yield Step (i)	Compound	Yield Step (ii)	Compound	Yield Step (iii)
Cyclohexyl	**123**	91%	**125**	64%	**120**	32%
Phenyl	N/A	N/A	**57**	89%	**32**	45%
2,6-Difluorophenyl	N/A	N/A	**126**	67%	**133**	33%
3-Methoxyphenyl	N/A	N/A	**127**	Quant.	**134**	49%
3-Nitrophenyl	N/A	N/A	**128**	97%	**135**	27%
4-Methoxyphenyl	N/A	N/A	**129**	Quant.	**136**	38%
4-Fluorophenyl	N/A	N/A	**130**	63%	**117**	59%
Benzyl	N/A	N/A	**131**	81%	**119**	53%
Furan-2-yl	**124**	Quant.	**132**	85%	**118**	66%

Table 3.9: Identities of R groups and yields for each step in **Scheme 3.5A** above.

3.3.2. Pharmacological Evaluation of the Sulfonamido-Substituted Library

The synthesised library of C_2-sulfonamide-substituted derivatives was evaluated in the acetyl CoA hydrolysis assay against MOUSE(NAT2) and, in most cases, against HUMAN(NAT1) also. Initial single-point tests were conducted at 30 μM, and subsequently at a range of concentrations for those inhibitors displaying >50% inhibition in order to determine IC_{50} values **(Figure 3.7; Table 3.10)**. Methylsulfonamido **110**, 4-methylbenzenesulfonamido **112**, 2-methylbenzene-sulfonamido **114** and 2-nitrobenzenesulfonamido **115**, synthesised in a previous study,[281a] were also re-tested for comparative purposes.

It can be observed from these data that the IC_{50} values for all these derivatives are >30 μM, with the exception of compounds **114**, **115**, **117**, **118** and **133**. 2-Methylbenzenesulfonamido **114** and 2-nitrobenzenesulfonamido **115** both display weak potency against HUMAN(NAT1) of 23.1 and 21.8 μM respectively, whilst the only derivatives in this series to exhibit comparable levels of activity to the hit phenylsulfonamido **32** are the bioisosteric 4-fluorophenylsulfonamido **117** and 2,6-difluorophenylsulfonamido **133** as well as the furanylsulfonamido analogue **118**. These data do indeed agree with the hypothesis and the *in silico* modelling, suggesting that an aryl or heteroaryl substituent is required for binding to the MOUSE(NAT2) or HUMAN(NAT1) active site, since the cyclohexyl derivative **120** displays very poor potency against both enzymes. Substitution on the aromatic moiety is also poorly tolerated, with the only substitution patterns to show comparable activity to the unsubstituted phenyl sulfonamide **32** against one or both enzymes being the isosteric 4-fluoro and 2,6-difluoro analogues **117** and **133**. This suggests that the aromatic group occupies a tight pocket within the enzyme active site; synthesis of the benzyl derivative **119** appears to confirm this as it too is a poor inhibitor of both the human and murine proteins.

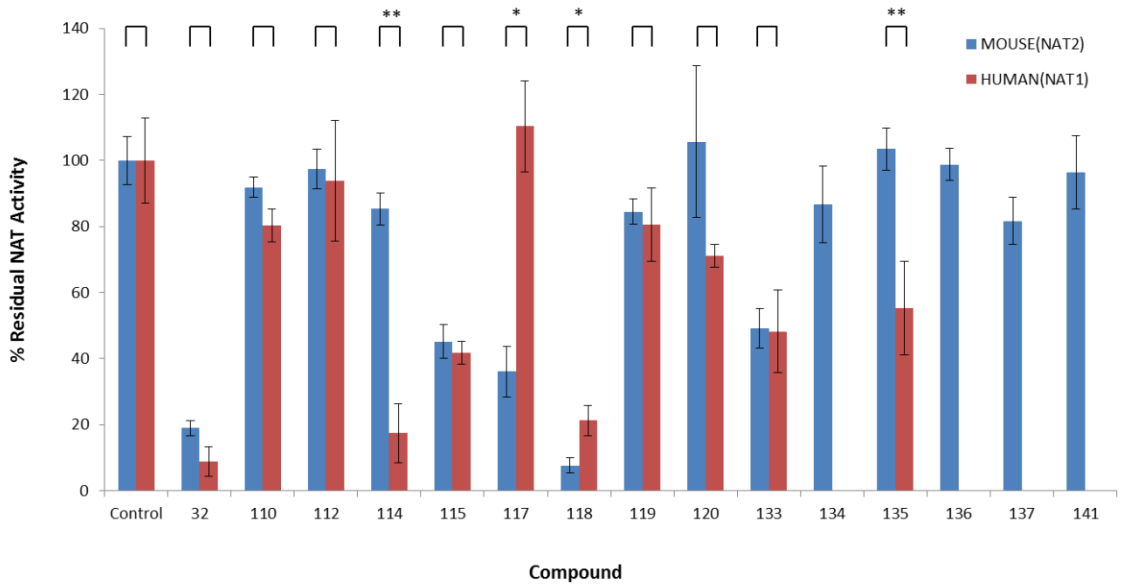


Figure 3.7: % Residual activity, ± one standard deviation, when MOUSE(NAT2) (blue columns) or HUMAN(NAT1) (red columns) were dosed with 30 µM of compounds **32**, **110**, **112**, **114-115**, **117-120**, **133-137** and **141** in the acetyl CoA hydrolysis assay. Experiments were conducted in triplicate and the final DMSO concentration was 5% (*v/v*). The stars and brackets above the bars show the significance of the difference between the MOUSE(NAT2) and HUMAN(NAT1) data when a Student's *T*-Test was performed: no stars = $P > 0.05$; * = $P < 0.05$; ** = $P < 0.01$.

Compound	C_2 Sulfonamido Substituent	IC_{50} MOUSE(NAT2) (µM)	R^2	*P*	IC_{50} HUMAN(NAT1) (µM)	R^2	*P*
32	Phenyl	2.4 ± 0.59	0.5843	***	4.1 ± 0.56	0.9658	***
114	2-Methylphenyl	>30	N/A	N/A	23.1 ± 4.8	0.4736	***
115	2-Nitrophenyl	>30	N/A	N/A	21.8 ± 4.0	0.5665	***
117	4-Fluorophenyl	3.9 ± 0.54	0.9420	***	>30	N/A	N/A
118	Furan-2-yl	1.9 ± 0.08	0.9936	***	7.0 ± 0.43	0.9799	***
133	2,6-Difluorophenyl	10.0 ± 1.6	0.9231	***	10.0 ± 1.7	0.8176	***

Table 3.10: IC_{50} values for compounds **32**, **114-115**, **117-118** and **133** in the C_2 sulfonamido library against MOUSE(NAT2) and HUMAN(NAT1) in the acetyl CoA hydrolysis assay, with squared correlation coefficients (R^2) and significance levels (*P*) as given; *** = $P < 0.005$. Data calculated using KyPlot® software. N.D. = not determined; N/A = not applicable.

3.3.3. Colorimetric Evaluation of the Sulfonamido-Substituted Library

Analogous colorimetric tests were carried out on the sulfonamide-substituted library as for the earlier C_3 library **(Section 3.2.3.)**; the data are presented in **Table 3.11**.

Compound	pK_a	λ_{max} *p*H 8 (nm)	$\Delta\lambda_{max}$ *p*H 13 (nm)	$\Delta\lambda_{max}$ MOUSE(NAT2) (nm)	ε_N ($M^{-1}cm^{-1}$)	$\varepsilon_N/\varepsilon_N(32)$	ε_{CB} ($M^{-1}cm^{-1}$)	$\varepsilon_{CB}/\varepsilon_{CB}(32)$
32	9.2 ± 0.05	498	+ 79	+ 112	11960	1.00	6590	1.00
117	9.9 ± 0.1	497	+ 59	+ 122	6580	0.55	3490	0.53
118	8.3 ± 0.2	509	+ 32	+ 99	7770	0.65	8440	1.28
119	10.0 ± 0.2	507	+ 61	+ 57	17580	1.47	6660	1.01
120	10.6 ± 0.2	505	+ 53	- 7	19850	1.66	6790	1.03
133	8.4 ± 0.1	509	+ 39	+ 79	7420	0.62	7780	1.18
134	9.6 ± 0.1	512	+ 48	N.D.	11120	0.93	4090	0.62
135	8.6 ± 0.05	509	+ 42	N.D.	8730	0.73	5670	0.86
136	10.1 ± 0.1	507	+ 46	N.D.	16500	1.38	6260	0.95
137	9.6 ± 0.2	495	+ 63	N.D.	7420	0.62	6590	1.00
141	9.5 ± 0.1	509	+ 42	N.D.	21650	1.81	6060	0.92

Table 3.11: Colorimetric data for compounds **32**, **117-120**, **133-137** and **141**: pK_a values (calculated using GraphPad Prism® and quoted ± one standard deviation; R^2 >0.95 for all compounds); wavelengths of maximum absorption at *p*H 8, *p*H 13 and in the presence of MOUSE(NAT2); and absorption coefficients of the neutral (N) and conjugate base (CB) species. N.D. = not determined.

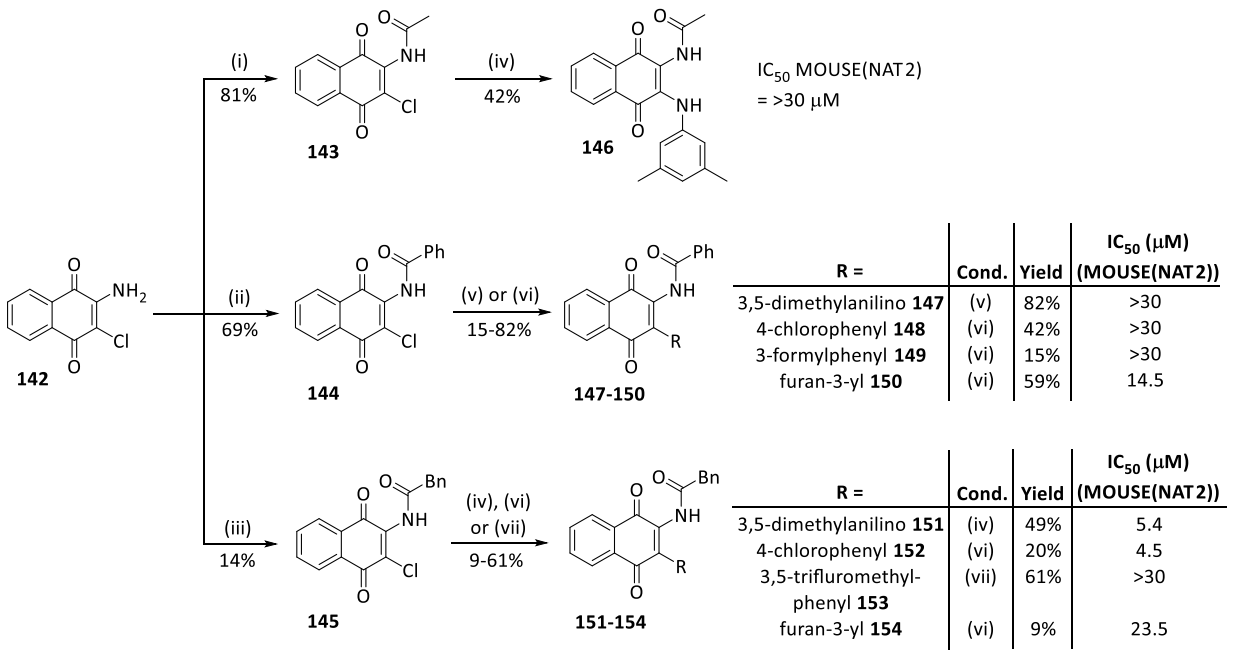
All of the analogues in this series possess pK_a values in the range 8.3-10.6, with more strongly electron-donating substituents predictably resulting in higher pK_a values than corresponding examples bearing electron-withdrawing substituents (e.g. 3-methoxyphenyl **134** and 3-aminophenyl **137** both have pK_a values of 10.6, whilst 3-nitrophenyl **135** has a pK_a of 8.6). The most potent analogues, 2,6-difluorophenyl **133**, 4-fluorophenyl **117** and 2-furyl **118** as well as hit compound **32**, all possess pK_a values towards the lower end of the range for this series, which is consistent with sequestration of the conjugate base species by the enzyme active site for potent inhibition.

Other than variation in pK_a values, however, it is notable from the data in **Table 3.11** how little colorimetric variation there is between members of this series. All the tested analogues display remarkably similar λ_{max} values at both *p*H 8 and *p*H 13, and the variation in λ_{max} in the presence of MOUSE(NAT2) can be accounted for by a variation in potency, since $\Delta\lambda_{max}$ correlates inversely to IC_{50} values. Furthermore, none of this series offers a significant improvement in intrinsic sensitivity over hit compound **32**, with the highest ε_{CB} value achieved only a factor of 1.28 greater than that of **32**.

3.3.4. Synthesis and Evaluation of Benzylamido-Substituted Species at the C_2 Position

Given that altering the sulfonamido C_2 substituent was unable to lead to any significant increases in either potency or sensitivity, it was hypothesised that an amide motif might be a suitable complementary binding partner for the guanidinium group of Arg127 to replace the sulfonamide. Amide functionality would not only be predicted to have a different preferred conformation to a sulfonamide, which might affect the binding potency, but additionally amido-substituted derivatives might have significantly different colorimetric properties, such as λ_{max} and ε_{CB} values. The amido derivatives would also be expected to have increased *p*K_a values of around 7-8 log units compared to their sulfonamide counterparts.[302] In a previous study, a small number of such amido derivatives were synthesised and their IC_{50} values against MOUSE(NAT2) measured **(Scheme 3.6)**.[281a]

The results of this study suggested that benzyl amides are potentially promising inhibitors of MOUSE(NAT2), whilst phenyl and methyl amides are relatively poor inhibitors; in the case of phenyl amides, a C_3 aryl substituent gave a higher level of potency than a C_3 3,5-dimethylanilino substituent. However, crucially, the acetyl CoA hydrolysis assays carried out on benzylamido-C_2 derivatives **151-154** were carried out in the presence of Triton X100 detergent due to complications caused by enzyme aggregation for the particular batch of MOUSE(NAT2) used;[281a] therefore in this study, it was decided to synthesise an authentic sample of compound **151** to enable a repeat of this test, alongside a greater range of benzyl amides bearing a C_3 aryl substituent, which would be predicted to have lower *p*K_a values and hence potentially more favourable binding potencies. Computational modelling studies support the proposal of a benzyl amide group as an isostere for the phenyl sulfonamide in **32**, due to the shorter bond lengths in an amide functional group compared to a sulfonamide **(Figure 3.8)**.

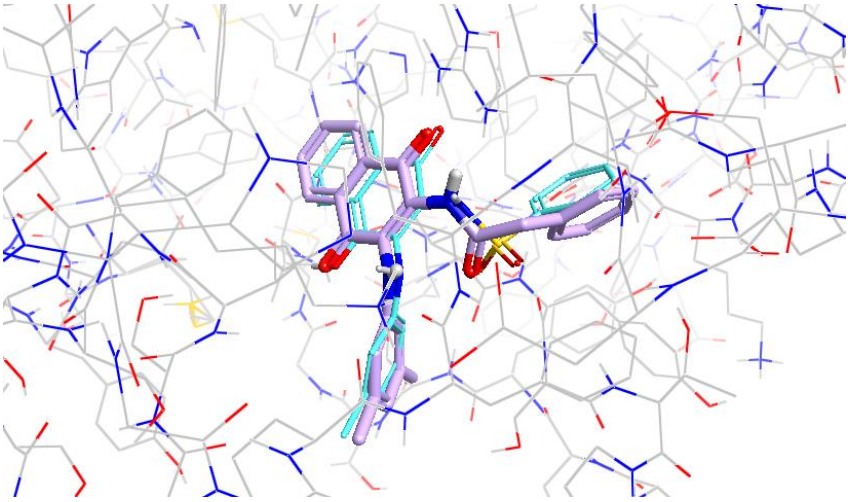


R =	Cond.	Yield	IC_{50} (μM) (MOUSE(NAT2))
3,5-dimethylanilino **147**	(v)	82%	>30
4-chlorophenyl **148**	(vi)	42%	>30
3-formylphenyl **149**	(vi)	15%	>30
furan-3-yl **150**	(vi)	59%	14.5

R =	Cond.	Yield	IC_{50} (μM) (MOUSE(NAT2))
3,5-dimethylanilino **151**	(iv)	49%	5.4
4-chlorophenyl **152**	(vi)	20%	4.5
3,5-trifluromethyl-phenyl **153**	(vii)	61%	>30
furan-3-yl **154**	(vi)	9%	23.5

Scheme 3.6: Previous synthesis of C_2 amido-substituted derivatives and their reported IC_{50} values against MOUSE(NAT2).[281a] *Reagents and conditions:* (i) MeCOCl (excess), c. H_2SO_4 (cat.), 50 °C, 1 h; (ii) NaH (3.3 eq.), THF, RT, 30 min *then* PhCOCl 1.3 eq.), RT, 1 h; (iii) BnCOCl (excess), HCl (g), 100 °C, 2 h; (iv) $CeCl_3 \cdot 7H_2O$ (1.0 eq.), MeOH, RT, 1.5 h *then* 3,5-dimethylaniline (3.0 eq.), 110 °C, 16 h; (v) 3,5-dimethylaniline (1.2 eq.), $Pd(OAc)_2$ (0.01 eq.), XPhos (0.03 eq.), K_2CO_3 (1.4 eq.), H_2O (0.04 eq.), ^{t}BuOH, 100 °C, 16 h; (vi) requisite boronic acid (2.0 eq.), $Pd(PPh_3)_2Cl_2$ (0.1 eq.), THF:sat. aq. $NaHCO_3$ (22:5), 100 °C, 16 h; (vii) requisite boronic acid (2.0 eq.), $Pd(PPh_3)_2Cl_2$ (0.1 eq.), Na_2CO_3 (3.0 eq.), toluene, 130 °C, 16 h. Cond. = conditions.

A



B

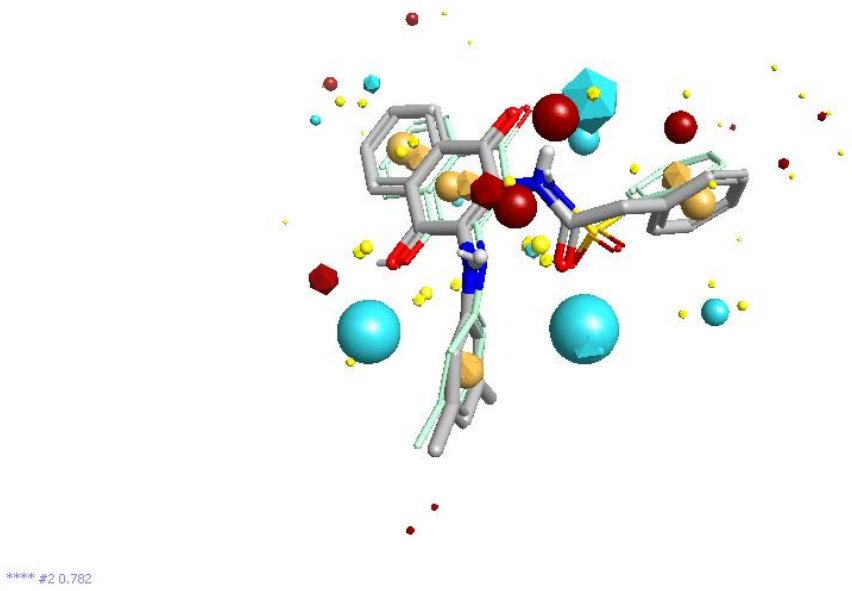
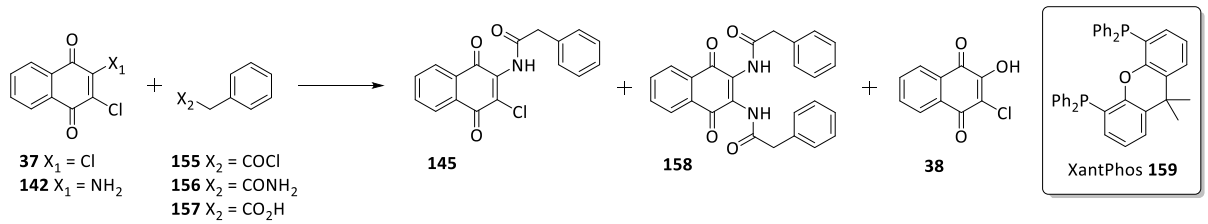


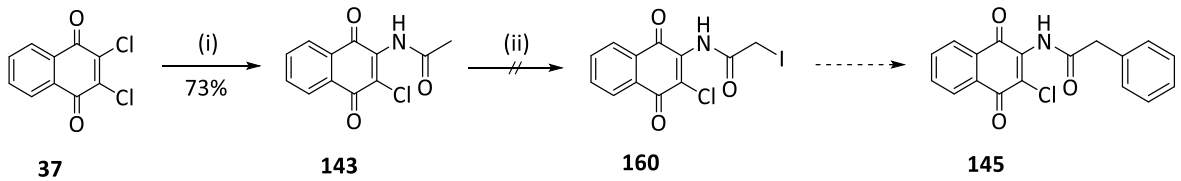
Figure 3.8: Modelling of a benzyl amide substituent as an isostere of a phenyl sulfonamide substituent using FORGE® (Cresset Group, Litlington, Cambridgeshire, UK).[303] Modelling was carried out using the structure of sulfonamide **32** docked into the crystal structure of HUMAN(NAT1) (pdb: 2PQT)[247b] as a reference ligand, benzyl amide **151** as the test ligand, and HUMAN(NAT1) as an excluded volume. **A:** Predicted spatial alignment between compounds **32** (carbons in cyan) and **151** (carbons in lilac) with HUMAN(NAT1) (carbons in light grey) as an excluded volume; **B:** Predicted electronic density distribution alignment between compounds **32** (carbons in light green) and **151** (carbons in grey). Regions of negative charge are shown in cyan, regions of neutral charge in yellow and regions of positive charge in dark red. Icosahedra correspond to the electronic fields of compound **32** and spheres to the electronic fields of compound **151**.

The major synthetic challenge in generating the desired library of benzyl amides lies in the first step of the synthesis; in the only previous synthesis of such species a laborious procedure involving the generation of HCl gas *in situ* from c. H_2SO_4 and NaCl and bubbling this through a solution of 2-amino-3-chloro-1,4-naphthoquinone **142** and phenyl acetyl chloride **155** before refluxing was required for formation of the desired 2-benzylamido-3-chloro-1,4-naphthoquinone intermediate **145**, which could only be obtained in 14% yield after a difficult separation by column chromatography on silica gel.[281a] Thus efforts were made to optimise this step, not only to increase the obtained yield of product but also to simplify both the reaction and purification procedures; these efforts are summarised in **Table 3.12** and **Scheme 3.7**.



Entry	X_1	X_2	Reagents	Conditions	Product(s) and Yield
(i)[281a]	NH_2	COCl	c. H_2SO_4	Up to 110 °C, Up to 72 h	No reaction
(ii)[281a]	NH_2	COCl	NaH, THF	Stir **142** with NaH/RT, 30 min *then* add **155**/RT, 1 h	No reaction
(iii)[281a]	NH_2	COCl	HCl (g)	Reflux, 6 h	**145** (14%)
(iv)	NH_2	COCl	LiI, EtOAc	70 °C, 48 h	No reaction
(v)	Cl	$CONH_2$	BuLi, THF	Stir **156** with BuLi/-78 °C, 30 min *then* add **37**/RT, 1 h	**38** (not isolated)
(vi)	Cl	$CONH_2$	$Pd(OAc)_2$, Xantphos **159**, Na_2CO_3, 1,4-dioxane	100 °C, 24 h	No reaction
(vii)	Cl	$CONH_2$	$Pd(OAc)_2$, Xantphos **159**, Cs_2CO_3, 1.4-dioxane	100 °C, 24 h	No reaction
(viii)	Cl	$CONH_2$	$Pd(OAc)_2$, Xantphos **159**, KO^tBu, 1,4-dioxane	100 °C, 24 h	**145** (10%) + **158** (10%)
(ix)	Cl	$CONH_2$	CuI, $(MeNHCH_2)_2$, Cs_2CO_3, 1,4-dioxane *or* toluene	100 °C, 16 h	No reaction
(x)	Cl	$CONH_2$	CuI, $(MeNHCH_2)_2$, K_2CO_3, 1,4-dioxane *or* toluene	100 °C, 16 h	No reaction
(xi)	Cl	$CONH_2$	CuI, $(MeNHCH_2)_2$, KO^tBu, 1,4-dioxane *or* toluene	100 °C, 16 h	No reaction
(xii)	NH_2	CO_2H	CDI, THF	70 °C, 72 h	No reaction
(xiii)	NH_2	CO_2H	EDC, DMAP, DMF	110 °C, 72 h	No reaction
(xiv)	NH_2	CO_2H	HATU, dipea, DMF	110 °C, 72 h	No reaction
(xv)	NH_2	COCl	BF_3•OEt_2, toluene	110 °C, 2.5 h	Complex Mixture
(xvi)	NH_2	COCl	BF_3•OEt_2, toluene	90 °C, 4 h	**145** (57%)

Table 3.12: Attempted methods for synthesis of benzyl amide intermediate **145**, showing reagents used, reaction conditions and product outcomes. "No reaction" refers to reaction of the naphthoquinone starting material.



Scheme 3.7: Attempted synthesis of benzyl amide **145** *via* iodo-substituted intermediate **160**. *Reagents and conditions:* (i) MeCOCl (excess), c. H_2SO_4 (cat.), 60 °C, 1 h; (ii) TMSCl (2.0 eq.), TMEDA (3.0 eq.), CH_2Cl_2, -15 °C, 15 min *then* I_2, 0 °C, 3 h.

Use of c. H_2SO_4 as a catalyst for the reaction between 2-amino-3-chloro-1,4-naphthoquinone **142** and phenyl acetyl chloride **155** failed (entry (i) in **Table 3.12**), as did prior deprotonation of **142** with NaH in THF (entry (ii)), conditions which were used successfully in previous syntheses of the corresponding methyl and phenyl amides respectively.[281a] Use of LiI as a nucleophilic catalyst (entry (iv)) also failed to yield any of the desired product. The difficulty in the condensation reaction with phenyl acetyl chloride, compared with other acid chlorides, lies not only in the expected poor nucleophilicity of the vinologous amide naphthoquinone **142**, but also in the possible alternative reactivity of phenyl acetyl chloride under either acidic or basic conditions in which ketene formation is possible *via* elimination of HCl.

To overcome both of these potential problems, reversal of reactivity in this system was trialled, with the use of 2,3-dichloro-1,4-naphthoquinone **37** as an electrophilic component and phenyl acetamide **156** as the nucleophilic component. When phenyl acetamide **156** was first deprotonated using ^{n}BuLi as a strong base, it was observed to undergo reaction with naphthoquinone **37** (entry (v)). However, ^{1}H-NMR analysis of the reaction suggested that **37** had been converted to 2-hydroxy-3-chloro-1,4-naphthoquinone **38**, of which an authentic sample was available for comparison (*vide infra*), rather than the desired product **145**. This suggested that sodium 2-phenylacetylamide reacted nucleophilically through oxygen in preference to through nitrogen (*i.e.* as the sodium 2-phenylacetimidate).

Subsequently, metal-mediated coupling conditions were investigated to encourage reaction between 2,3-dichloro-1,4-naphthoquinone **37** and phenyl acetamide **156**, since Buchwald-Hartwig-type cross-couplings have been reported extensively in the literature using an amide as the nucleophilic species in the presence of bidentate phosphine ligands with particularly large bite angles, such as Xantphos **159**. Initial attempts at a Buchwald-type reaction using Na_2CO_3 or Cs_2CO_3 as the base and $Pd(OAc)_2$ as the metal source failed to produce any reaction of naphthoquinone **37** (entries (vi) and (vii)); however, substituting the carbonate base for the more bulky, non-nucleophilic base KO^{t}Bu proved more promising, with the desired product **145** being isolated in a 10% yield (entry (viii)). Interestingly, in this reaction the *bis*-substituted

adduct **158** was also isolated in 10% yield; this was unexpected since the amide-N*H* in the presumed mono-substituted intermediate **145** ought to be deprotonated under the basic reaction conditions, rendering the C_3-Cl less prone to a subsequent oxidative addition step with palladium. Alternative conditions were then trialled using copper as the metal source instead of palladium, since Buchwald's lab have demonstrated that cross-coupling reactions between aryl halides and amides can occur under such conditions. However, no reaction was observed between naphthoquinone **37** and phenyl acetamide **156** with CuI and $(MeNHCH_2)_2$ using any of K_2CO_3, Cs_2CO_3 or KO^tBu as the base and either toluene or 1,4-dioxane as the solvent (entries (ix)-(xi)).

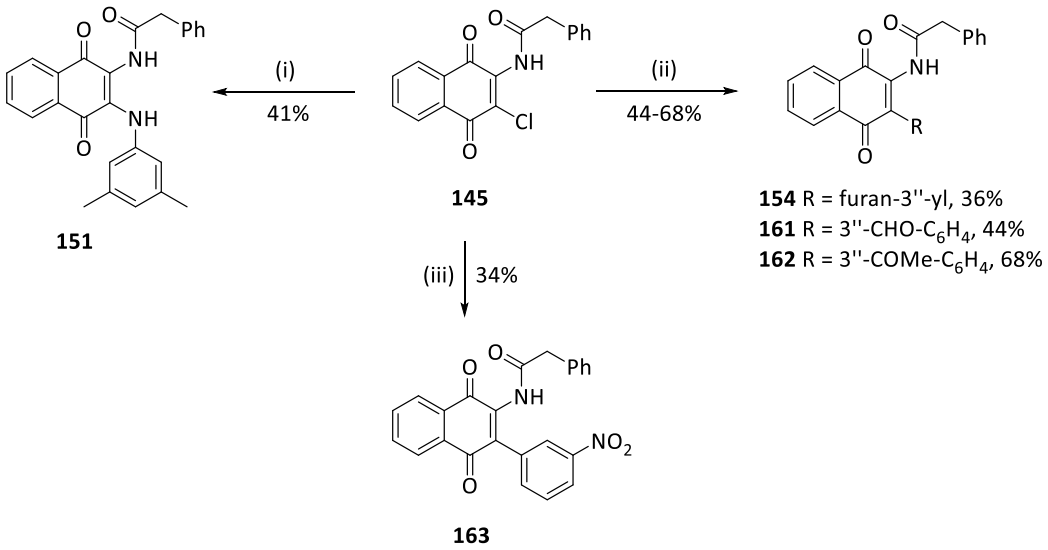
At this point, attention returned to use of the naphthoquinone moiety as the nucleophilic component of the reaction. If reaction of 2-amino-3-chloro-1,4-naphthoquinone **142** and phenyl acetyl chloride **155** was indeed problematic due to the ability of the latter to form ketene intermediates, then use of 2-phenylacetic acid **157** and an activating agent in place of the acid chloride might overcome this difficulty. Hence reaction between naphthoquinone **37** and acid **157** was attempted in the presence of CDI (entry (xii)), EDC (entry (xiii)) or HATU (entry (xiv)) as coupling agents; however, no desired reaction was observed in any case. In an alternative strategy, the acetyl-substituted intermediate **143** was instead synthesised under the acidic conditions used in previous studies **(Scheme 3.7)**. It was hypothesised that if a good leaving group could be introduced α to the carbonyl, a phenyl moiety could subsequently be installed at this position *via* Grignard-type chemistry. However, attempted α-iodination of acetamide **143** failed and this strategy was abandoned.

In a final attempt to optimise this reaction, it was realised that for a successful reaction between the poorly nucleophilic amino-naphthoquinone **142** and phenylacetyl chloride **155**, conditions which effected a strong activation of the carbonyl but which did not compromise the integrity of phenylacetyl chloride would be required; anhydrous, gaseous HCl meets this requirement, but so might a hard, anhydrous Lewis acid. Therefore, a reaction was attempted between **142** and **155** using a stoichiometric amount of $BF_3 \bullet OEt_2$. Consumption of the

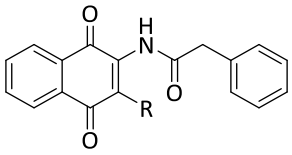
naphthoquinone starting material was observed to occur at 110 ^{o}C, but after 2.5 h both TLC and ^{1}*H*-NMR analysis of the crude reaction mixture showed a complex mixture of products had formed (entry (xv)). However, by reducing the reaction temperature to 90 ^{o}C and increasing the reaction time to 4 h (entry (xvi)), the desired product **145** could be obtained in a 57% yield after a recrystallisation of the crude reaction mixture from acetone.

Thus, the formation of the required benzyl amide intermediate was ultimately optimised on all counts: the yield of the reaction was improved from 14% to 57%, the experimental procedure was much simplified and a laborious purification was replaced by a facile recrystallisation. With the required intermediate now in hand, the desired substitutions at the C_3 position were effected either *via* a Michael-type addition-elimination reaction or a Suzuki-type cross-coupling reaction **(Scheme 3.8)**.

The activity of benzyl amide analogues **151**, **154** and **161-163**, in addition to a sample of 4-chlorophenyl derivative **152** synthesised in a previous study,[281a] were evaluated against MOUSE(NAT2) and HUMAN(NAT1) in the acetyl CoA hydrolysis assay **(Table 3.13)**. Unfortunately, these assay results suggest that these benzyl amides are not as potent a series inhibitors of inhibitors of MOUSE(NAT2) as previous studies suggested, with none of the compounds displaying as low an IC_{50} value against the murine protein as hit compound **32**. Furthermore, none of the tested analogues display any more than modest potency against HUMAN(NAT1).



Scheme 3.8: Synthesis of C_3-anilino and -aryl analogues from the 2-benzylamido intermediate **145**. *Reagents and conditions:* (i) $CeCl_3 \bullet 7H_2O$ (1.0 eq.), MeOH, RT, 1.5 h *then* 3,5-dimethylaniline (3.0 eq.), 110 ^oC, 16 h; (ii) requisite boronic acid (2.0 eq.), $Pd(PPh_3)_2Cl_2$ (0.1 eq.), Na_2CO_3 (3.0 eq.), toluene, 120 ^oC, 16 h; (iii) 3-nitrophenylboronic acid (1.0 eq.), $Pd(PPh_3)_4$ (0.1 eq.), KCl (3 eq.), toluene:EtOH:sat. aq. $NaHCO_3$ (4:1:1), 100 ^oC, 3 h.



151-152, 154, 161-163

Compound	R	IC_{50} MOUSE(NAT2) (μM)	R^2	*P*	IC_{50} HUMAN(NAT1) (μM)	R^2	*P*
151	NH-3,5-Me-C_6H_3	29.6 ± 5.64	0.8731	***	>30	N/A	N/A
152	4-Cl-C_6H_4	>30	N/A	N/A	N.D.	N/A	N/A
154	Furan-3-yl	23.5 ± 2.28	0.9413	***	19.6 ± 4.66	0.5022	**
161	3-CHO-C_6H_4	36.8 ± 10.5	0.7271	**	22.1 ± 3.62	0.7379	***
162	3-COMe-C_6H_4	25.6 ± 5.00	0.7549	***	N.D.	N/A	N/A
163	3-NO_2-C_6H_4	>30	N/A	N/A	N.D.	N/A	N/A

Table 3.13: IC_{50} values for the C_2 benzylamido derivatives against both MOUSE(NAT2) and HUMAN(NAT1) in the acetyl CoA hydrolysis assay, with squared correlation coefficients (R^2 values) and significance levels (*P*); * = $P < 0.05$; ** = $P < 0.01$; *** = $P < 0.005$. Data calculated using KyPlot® software. N/A = not applicable; N.D. = not determined.

Subsequently, colorimetric properties of this series of amides were determined **(Table 3.14)**; crucially, it was observed that the pK_a of each of the analogues was over 11, and none of these analogues showed a colour change in the presence of MOUSE(NAT2). These observations suggest that the conjugate bases of the benzyl amides are not being formed to a significant extent in the presence of MOUSE(NAT2), which would preclude the formation of any stabilising ionic interaction with Arg127. Additionally, it was observed that the absorption coefficients of the conjugate bases of the amides are generally lower than those of the analogous phenyl sulfonamide **32** and benzyl sulfonamide **119**.

Compound	pK_a	λ_{maz} *p*H 8 (nm)	$\Delta\lambda_{maz}$ *p*H 13 (nm)	$\Delta\lambda_{maz}$ MOUSE(NAT2) (nm)	ε_N ($M^{-1}cm^{-1}$)	$\varepsilon_N/\varepsilon_N$ (32)	ε_{CB} ($M^{-1}cm^{-1}$)	$\varepsilon_{CB}/\varepsilon_{CB}$ (32)
32	9.2 ± 0.05	498	+ 79	+ 112	11960	1.00	6590	1.00
119	10.0 ± 0.1	507	+ 61	+ 57	17580	1.47	6660	1.01
151	>14	489	+ 24	N.D.	N.D.	N.D.	N.D.	N.D.
152*	12.6 ± 0.3	410^	+ 74	0	12350	1.03	3650	0.55
154	12.5 ± 0.2	400^	+ 112	0	3230	0.27	2440	0.37
161	11.4 ± 0.1	396^	+ 56	0	18060	1.51	4680	0.71
162	11.7 ± 0.2	400^	+ 50	0	10050	0.84	4940	0.75
163	12.2 ± 0.2	401^	+ 66	+ 2[b]	26860	2.25	4360	0.66

Table 3.14: Colorimetric data for benzyl amide derivatives **151-152**, **154** and **161-163**, with data for phenyl sulfonamide **32** and benzyl sulfonamide **119** included for comparison. pK_a values were calculated using GraphPad Prism® and quoted ± one standard deviation; R^2 >0.95 for all compounds. * = Data obtained in a previous study.[281a] ^ = λ_{max} not well defined.

3.3.5. Synthesis and Evaluation of Larger Amide Derivatives at the C_2 Position: Cinnamoyl, Hydrocinnamoyl, 2-Oxo-2-phenyl and Cyclopropanecarboxy Amides

One alternative possible explanation for the lack of potency of the benzyl amide derivatives is that, despite the computationally predicted isosteric and isoelectronic relationship between the benzyl amide and phenyl sulfonamide derivatives, the different conformational preferences of the amide and sulfonamide groups mean that the spatial positioning of the amide derivatives within the enzyme active site are shifted in relation to those of the sulfonamide derivatives. Indeed, the computational model in **Figure 3.8** (*vide infra*) does suggest that the aromatic ring in the benzyl amide C_2 substituent might prefer to adopt a

different conformation to that in the phenyl sulfonamide. Since phenyl amides were also observed to display poor potency against MOUSE(NAT2) and HUMAN(NAT1), it was hypothesised that increasing the steric bulk of the C_2 amido group might help to restore the levels of activity observed in the sulfonamide series. Analogues bearing cinnamoyl, hydrocinnamoyl, 2-oxo-2-phenyl and cyclopropane-carboxy amides were therefore conceived as desirable targets **(Figure 3.9)**.

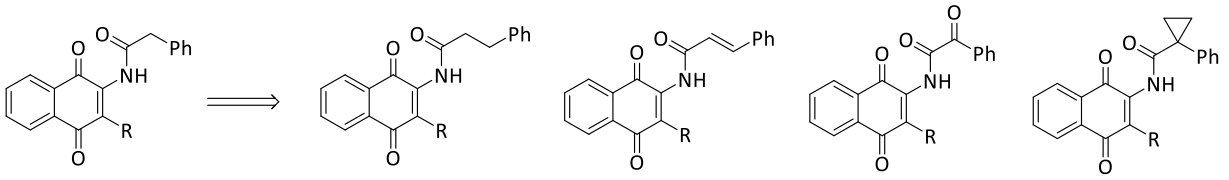
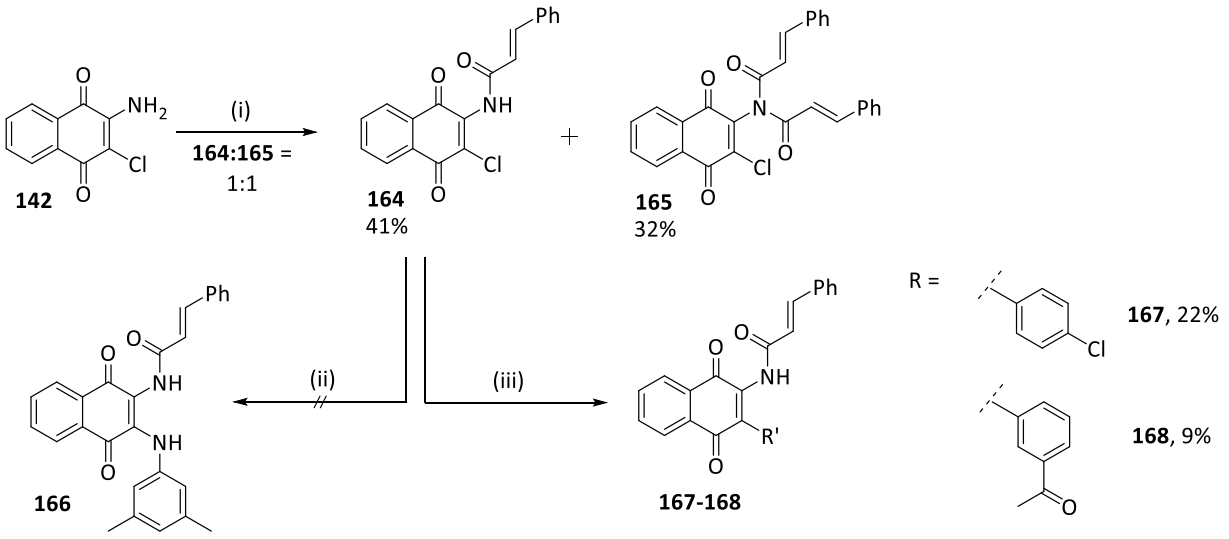


Figure 3.9: Alternative amido derivatives to be synthesised; R = anilino or aryl.



Scheme 3.9: Synthesis of *trans*-cinnanamido C_2 analogues. *Reagents and conditions:* (i) NaH (2.0 eq.), THF, 0 ^{o}C, 30 min *then* cinnamoyl chloride (1.3 eq.), RT, 1 h; (ii) $CeCl_3 \bullet 7H_2O$ (1.0 eq.), MeOH, RT, 1.5 h *then* 3,5-dimethylaniline (3.0 eq.), 110 ^{o}C, 16 h; (iii) requisite boronic acid (2.0 eq.), $Pd(PPh_3)_2Cl_2$ (0.1 eq.), THF:sat. aq. $NaHCO_3$ (22:5), 100 ^{o}C, 16 h.

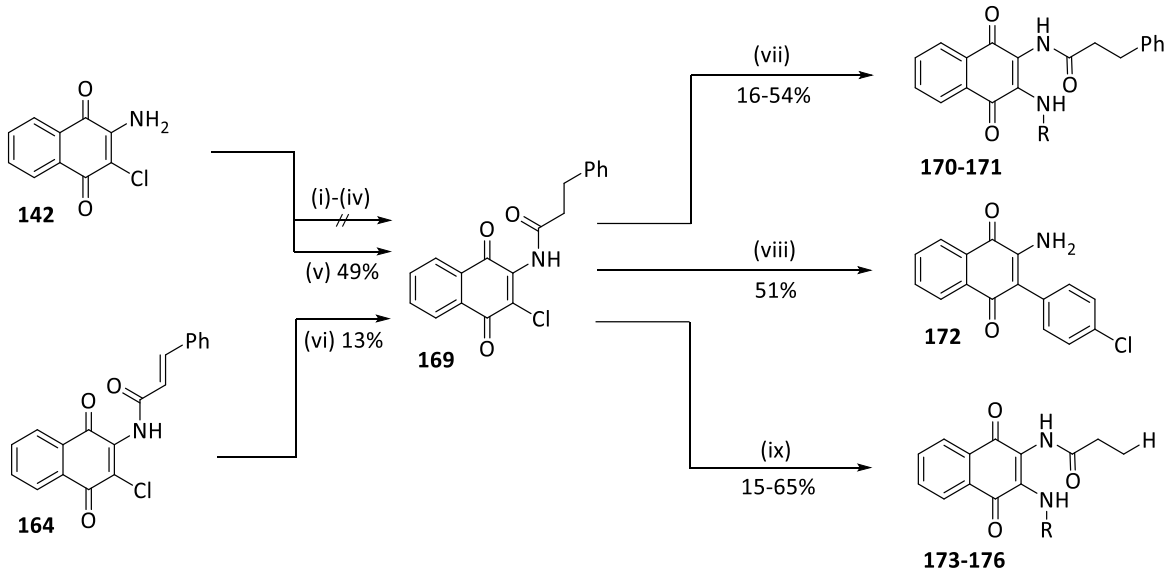
In order to synthesise cinnamoyl derivatives, 2-amino-3-chloronaphthoquinone **142** was reacted with cinnamoyl chloride in the presence of NaH **(Scheme 3.9)**; basic conditions (i) were selected by analogy to the previously reported reaction between naphthoquinone **142** and benzoyl chloride, given that both cinnamoyl and benzoyl chlorides contain a carbonyl

moiety which is conjugated to (C=C)π bonds. Under such conditions, both the desired 2-cinnanamido intermediate **164** and also the di-substituted byproduct **165** were produced in a 1:1 ratio; however, after column chromatography it was possible to separate these two species in isolated yields of 41% and 32% respectively.

Subsequently, the mono-substituted intermediate **164** underwent derivatisation at the C_3 position: a Michael-type addition-elimination reaction with 3,5-dimethylaniline was unable to yield any of the desired 3-anilino substituted product **166**, possibly due to the presence of multiple electrophilic sites in **164** which might compete for the aniline nucleophile; however, Suzuki-type cross-coupling reactions were successfully effected to give aryl-substituted derivatives **167** and **168** in moderate yield after purification.

Subsequently, saturated hydrocinnamoyl analogues were also synthesised **(Scheme 3.10)**: initially, it was hypothesised that the required 2-hydrocinnanamide-3-chloro-1,4-naphthoquinone intermediate **169** could be produced from the corresponding cinnamoyl equivalent **164** *via* a hydrogenation catalysed by 10% palladium on carbon (conditions (vi)). However, although such a reaction of **164** was indeed observed, the isolated yield obtained of 14% was poor, and therefore a direct route to hydrocinnamoyl intermediate **169** was sought from 2-amino-3-chloro-1,4-naphthoquinone **142**. Reaction of **142** with hydrocinnamoyl chloride was observed under neither protic acid nor basic conditions (conditions (i)-(iv)); however, use of the optimised protocol to access the benzyl analogue **(Table 3.12)** in which stoichiometric BF_3•OEt_2 was used as a Lewis acid catalyst gave the desired product in a reasonable yield of 49% after recrystallisation (conditions (v)). The hydrocinnamoyl intermediate **169** successfully underwent Michael-type reactions with aniline and 3,5-dimethylaniline to generate the corresponding C_3-anilino derivatives **170** and **171** in good yield (conditions (vii); **Table 3.15**). An attempted Suzuki-type cross-coupling reaction with 4-chlorobenzeneboronic acid under aqueous basic conditions resulted in the hydrolysis of the amide group to give 2-amino-3-aryl-1,4-naphthoquinone **172** in 51% yield (conditions (viii)); however, use of anhydrous conditions utilising toluene as the solvent and Na_2CO_3 as the base

gave the desired 2-amido-3-aryl-1,4-naphthoquinone **173** in 52% yield (conditions (ix)). Subsequently this methodology was also applied to the successful synthesis of the corresponding aryl derivatives **174-176 (Table 3.15)**.



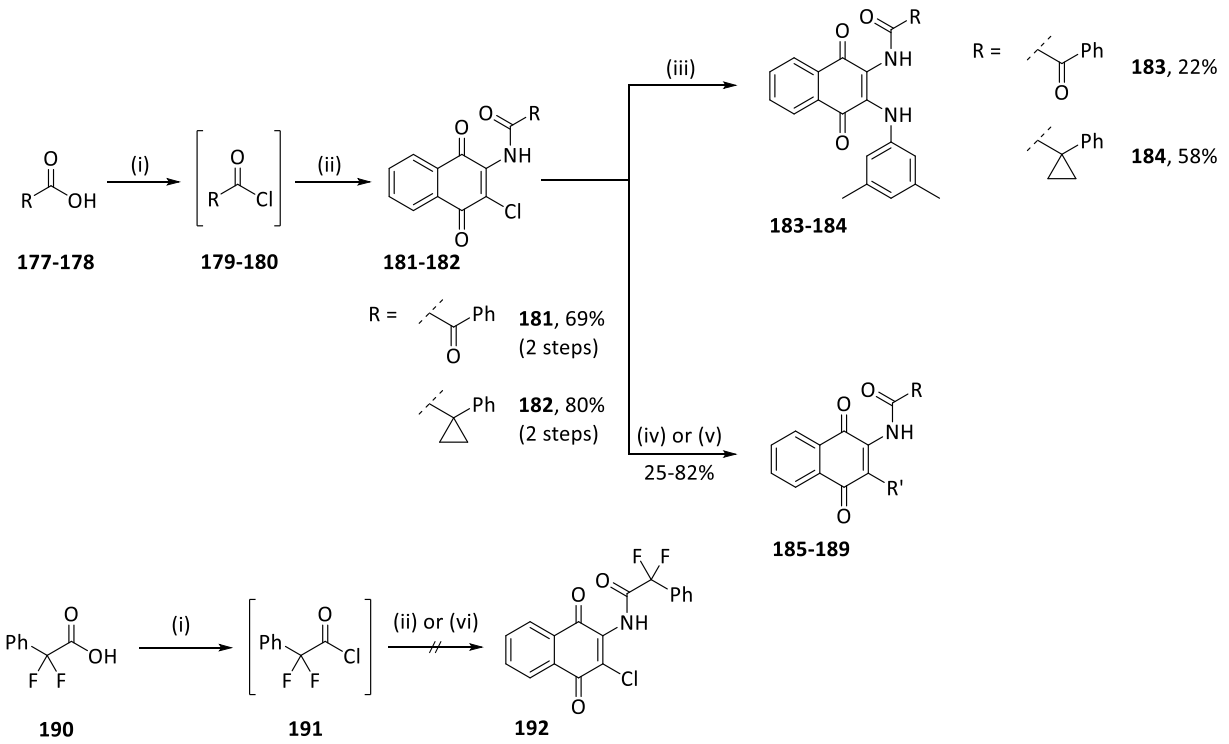
Scheme 3.10: Synthesis of hydrocinnanamido C_2 analogues. *Reagents and conditions:* (i) hydrocinnaomyl chloride (excess), c. H_2SO_4 (cat.), 50-100 ^oC, 24 h; (ii) hydrocinnamoyl chloride (3.0 eq.), c. H_2SO_4 (cat.), THF, 50 ^oC, 24 h; (iii) NaH (2.0 eq.), THF, 0 ^oC, 30 min *then* add hydrocinnamoyl chloride (1.3 eq.), RT, 1 h; (iv) NaH (2.0 eq.), THF, 0 ^oC, 30 min *then* add premixed hydrocinnamoyl chloride (1.3 eq.) and Et_3N (1.3 eq.) in THF, RT, 1 h; (v) hydrocinnamoyl chloride (4.0 eq.), $BF_3{\bullet}OEt_2$ (1.0 eq.), toluene, reflux, 24 h; (vi) H_2 (1 atm.), 10% Pd/C (0.4 eq.), EtOAc:MeOH (5:1), 48 h; (vii) $CeCl_3{\bullet}7H_2O$ (1.0 eq.), MeOH, RT, 1.5 h *then* requisite aniline (3.0 eq.), 110 ^oC, 16 h; (viii) 4-chlorobenzeneboronic acid (2.0 eq.), $Pd(PPh_3)_2Cl_2$ (0.1 eq.), THF:sat. aq. $NaHCO_3$ (22:5), 100 ^oC, 16 h; (ix) requisite boronic acid (2.0 eq.), $Pd(PPh_3)_2Cl_2$ (0.1 eq.), Na_2CO_3 (3.0 eq.), toluene, 130 ^oC, 16 h. For the identities of R and yields of steps (vii) and (ix) please refer to **Table 3.15**.

Compound	R	Yield Step (vii)	Yield Step (ix)
170	Phenyl	16%	N/A
171	3,5-Dimethylphenyl	54%	N/A
173	4-Chlorophenyl	N/A	52%
174	3,5-Trifluoromethylphenyl	N/A	15%
175	3-Formylphenyl	N/A	56%
176	3-Acetylphenyl	N/A	65%

Table 3.15: Identities of R groups and yields for steps (vii) and (ix) in **Scheme 3.10**. N/A = not applicable.

Use of the optimised amide bond-forming reaction between naphthoquinone **142** and acyl chlorides with $BF_3{\bullet}OEt_2$ catalysis also enabled generation of 2-oxo-2-phenylamido and 2-cyclopropanecarboxyamido intermediates **181** and **182 (Scheme 3.11)**. In these cases, the

required acid chlorides were not commercially available, and were prepared from the corresponding carboxylic acids using oxalyl chloride; the amidonaphthoquinone intermediates were produced in excellent yields over the two steps (conditions (i)-(ii)). From these intermediates, a variety of C_3-anilino and C_3-aryl substituents were appended *via* Michael-type or Suzuki-type reactions respectively (conditions (iii)-(v); **Table 3.16**). However, compound **183**, bearing a 2-oxo-2-phenyl amide at the C_2 position and 3,5-dimethylaniline at the C_3 position, was observed to undergo decomposition after several days of standing at room temperature; this could be due to the presence of both an electrophilic carbonyl moiety and a nucleophilic anilino nitrogen within the molecule in close proximity to one another.



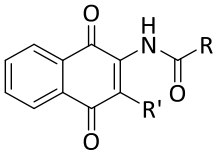
Scheme 3.11: Synthesis of 2-oxo-2-phenylacetamido and cyclopropanecarboxamido C_2 analogues. *Reagents and conditions:* (i) oxalyl chloride (1.0 eq.), DMF (3 drops), CH_2Cl_2, RT, 3 h; (ii) 2-amino-3-chloro-1,4-naphthoquinone **142** (0.25 eq.), BF_3•OEt_2 (0.25 eq.), toluene, 90 °C, 4 h (**181**) *or* 90 °C, 30 min *then* 110 °C, 1 h (**182**); (iii) $CeCl_3$•$7H_2O$ (1.0 eq.), MeOH, RT, 1.5 h *then* 3,5-dimethylaniline (3.0 eq.), 110 °C, 16 h; (iv) requisite boronic acid (2.0 eq.), $Pd(PPh_3)_2Cl_2$ (0.1 eq.), THF:sat. aq. $NaHCO_3$ (22:5), 100 °C, 16 h; (v) requisite boronic acid (2.0 eq.), $Pd(PPh_3)_2Cl_2$ (0.1 eq.), Na_2CO_3 (3.0 eq.), toluene, 130 °C, 16 h; (vi) 2-amino-3-chloro-1,4-naphthoquinone **142** (0.25 eq.), NaH (0.83 eq.), THF, RT, 30 min *then* **181** (1.0 eq.), RT, 1 h. For the identities of R and R' and yields of steps (iv) and (v) refer to **Table 3.16**.

Compound	R	R'	Yield Step (iv)	Yield Step (v)
185	COPh	4-Chlorophenyl	N/A	25%
186	COPh	3-Formylphenyl	N/A	28%
187	1,1-Phenylcyclopropyl	4-Chlorophenyl	77%	N/A
188	1,1-Phenylcyclopropyl	Furan-3-yl	36%	N/A
189	1,1-Phenylcyclopropyl	3-Formylphenyl	82%	N/A

Table 3.16: Identities of R and R' groups and yields for steps (iv) and (v) in **Scheme 3.11**. N/A = not applicable.

Synthesis of difluoro-substituted intermediate **192** was also desirable, as the two fluorine atoms were predicted to lower the pK_a of the amide-N*H* by inductive stabilisation of the conjugate base, which might lead to an increase in potency of the amide inhibitors. As fluorine is isosteric to hydrogen, it was also predicted that C_3-anilino and C_3-aryl analogues derived from intermediate **192** would be sterically tolerated within the HUMAN(NAT1)/MOUSE(NAT2) active site. However, formation of **192** from difluorophenylacetic acid **190** was unsuccessful when **190** was treated with oxalyl chloride in CH_2Cl_2 followed by either 2-amino-3-chloronaphthoquinone **142** and $BF_3 \bullet OEt_2$ at either 90 ^oC or 110 ^oC (conditions (ii)) or sodium 2-amido-3-chloronaphthoquninone (conditions (vi)). IR analysis of the reaction mixture of the first step clearly showed the presence of two carbonyl stretching frequencies at 1753 cm^{-1} and 1580 cm^{-1}; these suggest respectively that the desired acyl chloride **191** is being formed in this step but that some carboxylic acid starting material is still present after 3 h. No further attempts were made to access the difluoro intermediate **192**.

Subsequently, the final amido-substituted products **167-168**, **170-171**, **173-176** and **184-189** were all evaluated for activity against MOUSE(NAT2) and their colorimetric properties were determined **(Table 3.17)**. Unfortunately, it can be observed that only one member of this series effects >50% inhibition of MOUSE(NAT2) when dosed at 30 µM, the C_2-cyclopropylcarboxyamido-C_3-furanyl substituted derivative **188**; this species was subsequently determined to possess an IC_{50} value of 10.6 ± 2.2 µM against the murine protein (R^2 = 0.8664, P = <0.005).



167-168, 170-171, 173-176, 184-189

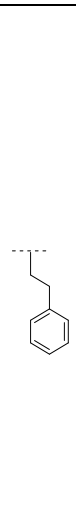
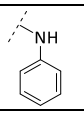
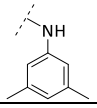
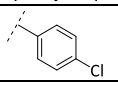
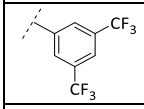
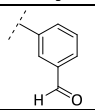
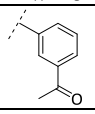
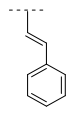
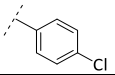
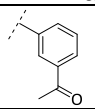
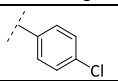
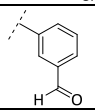
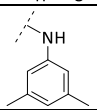
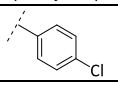
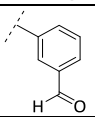
Cpd	R	R'	IC_{50} MOUSE (NAT2) (μM)	*p*K_a	λ_{max} *p*H 8 (nm)	$\Delta\lambda_{max}$ *p*H 13 (nm)	ε_N ($M^{-1}cm^{-1}$)	ε_N/ ε_N (32)	ε_{CB} ($M^{-1}cm^{-1}$)	ε_{CB}/ ε_{CB} (32)
170			>30	>14	N.D.	N.D.	N.D.	N.D.	N.D.	N.D.
171			>30	>14	N.D.	N.D.	N.D.	N.D.	N.D.	N.D.
173			>30	>12	~400^	*	N.D.	N.D.	N.D.	N.D.
174			>30	>12	~400^	*	N.D.	N.D.	N.D.	N.D.
175			>30	11.2 ± 0.3	~409^	+ 35	12200	1.02	2970	0.45
176			>30	11.8 ± 0.2	~405^	+ 47	27030	2.26	4280	0.65
167			>30	12.1 ± 0.1	~401^	+ 38	9570	0.80	2040	0.31
168			>30	11.4 ± 0.1	~406^	+ 51	14710	1.23	3620	0.55
185			>30	10.2 ± 0.1	~393^	+ 70	19970	1.67	5340	0.81
186			>30	9.2 ± 0.2	~402^	+ 61	29180	2.44	6520	0.99
184			>30	>14	N.D.	N.D.	N.D.	N.D.	N.D.	N.D.
187			>30	*	~405^	+ 13	22840	1.91	4740	0.72
188			11.2 ± 2.2	*c.*12.5	443	+ 37	8730	0.73	3560	0.54
189			>30	12.5 ± 0.3	~401^	+ 81	20930	1.75	5210	0.79

Table 3.17: Pharmacological and colorimetric properties of C_2-amido derivatives. * = Not possible to determine; ^ = No clear λ_{max} value – rather, an emerging shoulder is observed. *p*K_a values were calculated using GraphPad Prism® and quoted ± one standard deviation; R^2 >0.95 for all compounds. Cpd = compound; ε_N = absorption coefficient of neutral species; ε_{CB} = absorption coefficient of conjugate base species; N.D. = not determined.

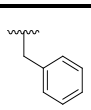
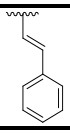
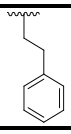
These data suggest that cinnamoyl, hydrocinnamoyl, 2-oxo-2-phenyl and cyclopropylcarboxy amides at the C_2 position are likely too sterically cumbersome to bind effectively to the MOUSE(NAT2) active site, particularly given the relatively low *p*K_a values of cinnamoyl-substituted species **167** and **168** (10.2 and 9.2 respectively), which should not preclude formation of the conjugate base species in the presence of the target enzyme.

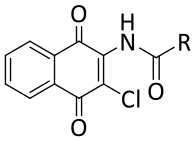
The anomalously high potency of furanyl derivative **188** might be explained by the lower steric bulk of the furan substituent, which might enable adoption of a conformation within the active site which better accommodates the bulky C_2 substituent – a conformation inaccessible to inhibitors with a larger C_3 substituent. The IC_{50} value for this compound is consistent with those for the corresponding phenyl amide **150** and benzyl amide **154** which bear a C_3 furanyl substituent – each of these compounds is the most potent in their respective amide series.

Finally, it should be noted that, as with other amide derivatives, the ε_{CB} values of this series of compounds are all lower than for hit compound **32**, some significantly so.

3.3.6. Evaluation of the Pharmacological and Colorimetric Properties of the 2-Amido-3-chloro-Substituted Intermediates in Inhibitor Synthesis

Given the hypothesis that the disappointing pharmacological and colorimetric properties of the C_2 amido-substituted library are at least in part due to their high *p*K_a values, and that the highest IC_{50} values were observed when the C_3 substituent was the relatively small furanyl moiety, it was decided to investigate the properties of the 2-amido-3-chloro-1,4-naphthoquinone intermediates in the synthesis of this inhibitor library. These chloro-substituted intermediates would be predicted to have lower *p*K_a values than either the corresponding C_3 anilino- or aryl-substituted final products, and the chloro group is predicted to be even less bulky than a furanyl substituent. For each intermediate synthesised, IC_{50} values against MOUSE(NAT2) and *p*K_a values are reported in **Table 3.18**.

Compound	143	144	145	164	169	181	182
R	Me	Ph					
IC_{50} MOUSE(NAT2) (μM)	1.0 ± 0.14	2.3 ± 0.20	2.1 ± 0.15	19.7 ± 5.1	6.6 ± 1.1	4.1 ± 0.64	2.2 ± 0.51
R^2	0.9428	0.9618	0.9789	0.8155	0.9088	0.9304	0.7488
P	***	***	***	***	***	***	***
***p*K_a**	10.0 ± 0.2	9.0 ± 0.05	10.4 ± 0.1	*c.* 11.0	10.6 ± 0.2	6.0 ± 0.4	*c.* 10.5



143-145, 164, 169, 181-182

Table 3.18: IC_{50} values against MOUSE(NAT2) in the acetyl CoA hydrolysis assay and *p*K_a values for the 2-amido-3-chloro-1,4-naphthoquinone intermediates. IC_{50} values were calculated using KyPlot® software, and are quoted as ± one standard deviation, with squared correlation coefficients (R^2) and significance levels (*P*) as given; *** = P <0.005. *p*K_a values were calculated using GraphPad Prism® and quoted ± one standard deviation; R^2 for each compound is >0.95.

The most striking observation from the data in **Table 3.18** is that all of these intermediates, with the exception of cinnamoyl amide intermediate **164**, possess more potent IC_{50} values against MOUSE(NAT2) (6.6 μM or below) than any of the C_3 anilino- or aryl-substituted final products evaluated in **Section 3.3.5**. Tellingly, every one of these potent inhibitors has a *p*K_a value of 10.6 or less; the less potent cinnamoyl amido species **164** is found to have a slightly higher *p*K_a value of *c.* 11.0. This adds further weight to the hypothesis that *p*K_a is a crucial parameter in the design of a potent MOUSE(NAT2)/HUMAN(NAT1) inhibitor and that an ionic interaction with Arg127 drives ligand recognition. Interestingly, the potency of these intermediates appears not to be dependent on the steric bulk of the R group at the C_2 position of the naphthoquinone core; this is at first glance a peculiar observation given the earlier reported steepness of the SAR at the C_2 position for the sulfonamide derivatives (*cf.* **Section 3.3.2.**). One possible explanation for this is that because the chloro group is far smaller than the aryl, aryloxy and anilino substituents considered earlier, the naphthoquinone core is able to bind deeper into the MOUSE(NAT2) active site when the C_3 substituent is chloro rather than anilino, which enables the accommodation of a larger C_2 substituent such as 2-oxo-2-phenyl **181** and cyclopropanecarboxy **182** amides.

One alternative hypothesis that could explain both the higher potency of the chloro-substituted intermediates compared to the anilino-substituted final products would be that the chloro-substituted intermediates are in fact acting as irreversible MOUSE(NAT2) inhibitors, reacting with the catalytic Cys68 residue *via* a Michael-type addition-elimination of the C_3 chloride. In order to test this alternate hypothesis, two experiments were carried out. In the first, three samples of MOUSE(NAT2) were each incubated with an excess of one of chloro-substituted intermediates **143**, **144** or **145** in Tris•HCl (*p*H 8) buffer at 37 ^{o}C for 30 min; subsequent MS-MALDI analysis showed a molecular ion *m/z* peak of 33988 Da in all three cases in addition to a control sample containing only MOUSE(NAT2). This suggests that these chloro-substituted intermediates are not capable of binding covalently to MOUSE(NAT2) under the assay conditions.

Furthermore, a sample of MOUSE(NAT2) was incubated with 2-iodoacetamide, which previous studies have demonstrated results in the selective alkylation of only the catalytic Cys68 residue in an S_N2-like fashion (for protocol see **Section 7.11.**); the successful monoalkylation was demonstrated by an increase in the molecular ion *m/z* peak in the MS-MALDI spectrum by 48 Da. Samples of the chloro-substituted intermediates **143-145**, **169** and **181-182** were then treated with this alkylated MOUSE(NAT2) protein, and visible absorption spectra show that a similar shift in λ_{max} occurs in the presence of Cys68-alkylated protein as in the presence of wild type MOUSE(NAT2), suggesting that the chloro-substituted intermediates are still capable of binding to MOUSE(NAT2) even after alkylation of the nucleophilic active site thiol; spectra are shown in **Figure 3.10** for the representative cyclopropanecarboxyamido-substituted example **182**. This evidence also suggests that the chloro-substituted intermediates bind to MOUSE(NAT2) in a non-covalent fashion analogous to that of hit compound **32**.

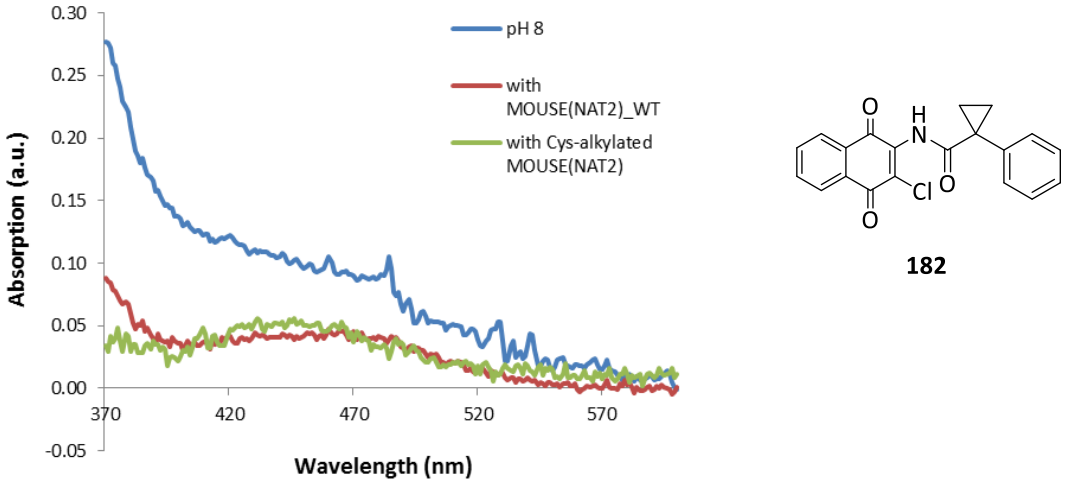
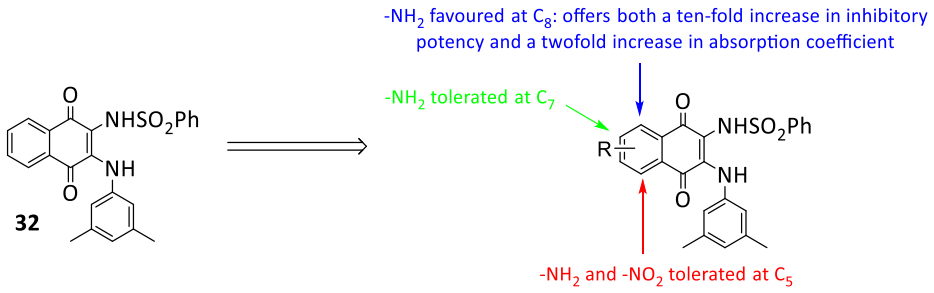


Figure 3.10: Visible absorption spectrum of amide intermediate **182** at *p*H 8.0 (blue line), *p*H in the presence of wild type (WT) MOUSE(NAT2) (green line) and in the presence of MOUSE(NAT2) with an alkylated Cys68 residue (green line). a.u. = arbitrary units.

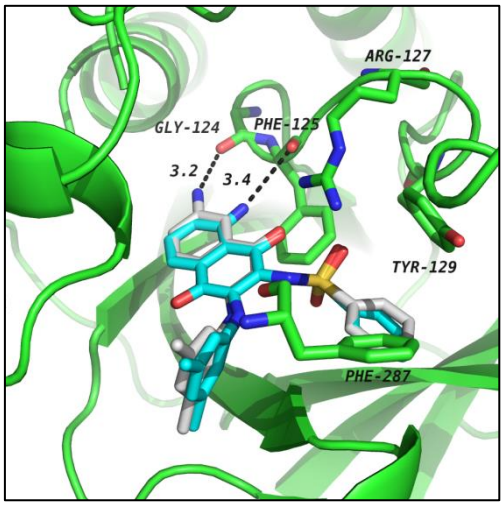
3.4. SAR at C_5-C_8 of the Naphthoquinone Core

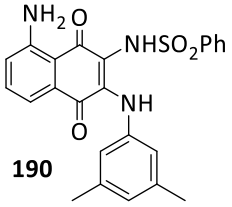
In an SAR study around the naphthoquinone core of **32**, the other key positions on which to consider functionalisation are carbons 5-8 of the core. Previous work has described the addition of nitro- and amino-groups to each of these positions as examples of electron-poor and electron-rich groups respectively **(Figure 3.11A)**;[281a] it was observed that addition of an auxochromic amino-group at C_8 to give compound **190** both increased potency ten-fold and absorption coefficient two-fold over hit compound **32** (IC_{50} for **190** = 0.43 µM and 0.54 µM against MOUSE(NAT2) and HUMAN(NAT1) respectively), whilst an amino substituent at C_7 was also well-tolerated (IC_{50} for **191** = 2.5 µM against MOUSE(NAT2)).[281a] Conversely, addition of a nitro group to the naphthoquinone core led to a loss of potency in all cases, except for at the C_5 position. Furthermore, it was reported that **190** retained high levels of selectivity for HUMAN(NAT1) over the homologous HUMAN(NAT2).[281a] *In silico* modelling suggests that both 8-amino- and 7-amino-substituted naphthoquinones have the potential to form a stabilising hydrogen-bond interaction to the backbone carbonyl of Phe125 or Gly124 respectively **(Figure 3.11B)**; this is hypothesised to be the origin of their additional potency.

A



B





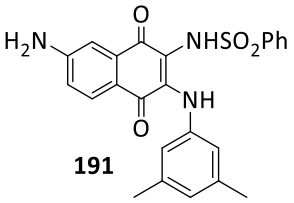
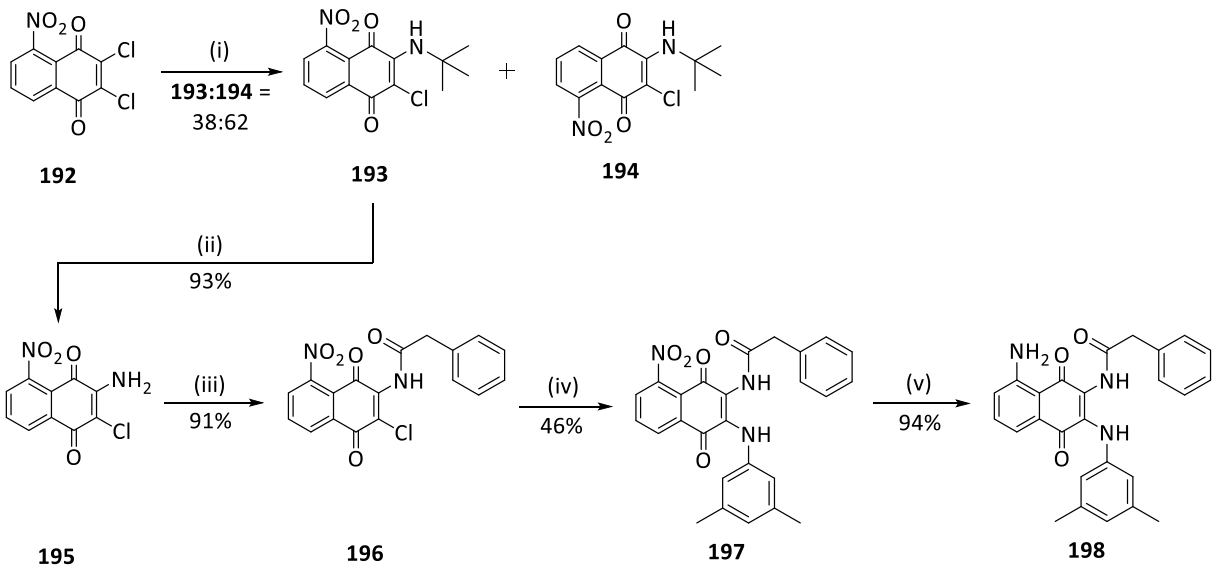


Figure 3.11: A: Diagram to show tolerated and favourable substitutions of nitro and amino groups on the naphthoquinone core at $C_{5\text{-}8}$. **B:** *In silico* modelling of 8-amino-substituted **190** (carbon atoms in grey) and 7-amino-substituted **191** (carbon atoms in cyan) in the active site of HUMAN(NAT1) (pdb: 2PQT).[247b] Analysis performed using GOLD® (v.5.2).[282] The protein is shown in cartoon representation with active site residues Gly124, Phe125, Arg127, Tyr129 and Phe287 shown in stick representation (carbon atoms in green). Predicted polar contacts are represented by dashed lines with inter-atomic distances given in Ångströms.

Given these findings, it was decided to synthesise a benzyl amido analogue of 8-amino sulfonamide **190**, to see if an 8-amino substituent could mitigate against the higher *p*K_a of the amide derivatives and notably increase potency **(Scheme 3.12)**. The desired compound **198** was successfully synthesised from commercially available 5-nitro-2,3-dichloro-1,4-naphthoquinone **192** in 5 steps in an overall yield of 14%.



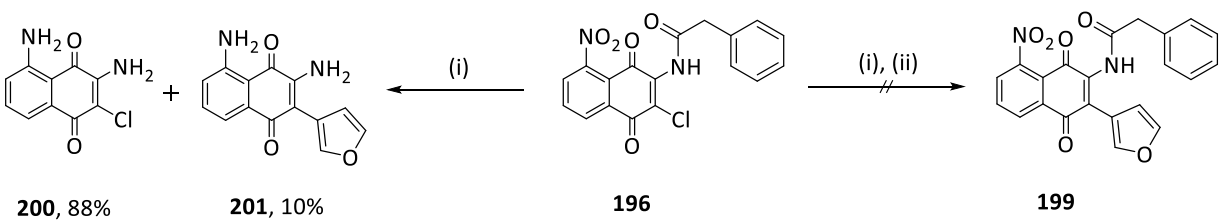
Scheme 3.12: Synthesis of a 3-anilino-8-amino substituted benzyl amide. *Reagents and conditions:* (i) *tert*-butylamine (1.0 eq.), 2,6-lutidene (1.4 eq.), DMF, RT, 2 h; (ii) TFA:CH_2Cl_2 (1:1), 0 ^oC to RT, 30 min; (iii) phenyl acetyl chloride (4.0 eq.), BF_3•OEt_2 (4.0 eq.), 90 ^oC, 4 h; (iv) $CeCl_3$•$7H_2O$ (1.0 eq.), MeOH, RT, 1.5 h *then* 3,5-dimethylaniline (3.0 eq.), 110 ^oC, 16 h; (v) H_2 (1 atm.), 10% Pd/C (0.1 eq.), MeOH, RT, 16 h.

Firstly, **192** was treated with *tert*-butylamine and Cs_2CO_3 in DMF to effect overall substitution of one of the chloro substituents with the amine; the reaction was found to give a 38:62 crude mixture of 8-nitro **193**:5-nitro **194**, the regiochemical preference for the latter likely to arise from the inductive and mesomeric electron-withdrawing effects of the nitro group. **193** could be successfully deprotected within 2 h at 0 ^oC in a 1:1 mixture of CH_2Cl_2:TFA in good yield to give amino-naphthoquinone **195**. Subsequently, **195** was subjected to the optimised conditions for amide formation with phenyl acetyl chloride utilising BF_3•OEt_2, which gave 2-benzylamido-8-nitro derivative **196** in an excellent yield of 91%. With the key intermediate in hand, Michael-type reaction of **196** with 3,5-dimethylaniline and $CeCl_3$•$7H_2O$ enabled isolation of a reasonable yield of 3-anilino adduct **197**, before in the final step, the nitro group was reduced to amine functionality using 10% Pd/C in MeOH in a 94% yield.

8-Nitro-substituted **197** and 8-amino-subsituted **198** were evaluated for activity against MOUSE(NAT2). **197** displayed poor potency against the enzyme, with an IC_{50} of >30 μM; this is consistent with the poor potency of other 8-nitro-substituted analogues. 8-amino **198**,

however, was found to have an IC_{50} of 7.5 µM (R^2 = 0.6895; P <0.01), which demonstrates a statistically significant increase in potency compared to unsubstituted benzyl amide **151**. Testing of 8-amino **198** against HUMAN(NAT1) meanwhile revealed an IC_{50} value of *c.* 30 µM. Additionally, chloro-substituted intermediate **196** was found to have an IC_{50} value against MOUSE(NAT2) of 2.6 ± 0.33 µM (R^2 = 0.8584, P = <0.005), which is consistent with the observations on other chloro-substituted intermediates outlined in **Section 3.3.6.**

Given the increase in potency effected by an 8-amino group on 2-benzylamido-3-anilino **198**, it was of interest to synthesise an 8-amino-2-benzylamido-3-aryl derivative, since a C_3 aryl group would be predicted to significantly lower pK_a *cf.* compound **198** and hence might give an additional increase in potency; 3-furanyl was chosen as the desired C_3 aryl group due to favourable potency of other 3-furanyl analogues. However, attempts to synthesise such a derivative *via* a Suzuki-type cross-coupling on 2-benzylamido-8-nitro intermediate **196** proved unsuccessful: when **196** was treated with 3-furanyl boronic acid and $Pd(PPh_3)_2Cl_2$ in THF and sat. aq. $NaHCO_3$ in THF, no trace of the desired adduct **199** could be detected. Rather, the rate of cross-coupling was found to be lower than both the rate of hydrolysis of the benzyl amide functionality and, more surprisingly, the rate of reduction of the 8-nitro group to an amino group under the conditions, to give 2,8-diamino-3-chloro **200** and 2,8-diamino-3-furan-3'-yl **201** in isolated yields of 88% and 10% respectively **(Scheme 3.13)**. Two key pieces of evidence confirm the reduction of the nitro functionality to an amino group in **200** and **201**: (a) the predominant *m/z* peaks in the MS (ESI^+) spectra for **200** and **201** appear at 245:247 (3:1) and 277 respectively, corresponding to the respective $[M+Na]^+$ ion peaks; and (b) the δ values for H_5, H_6 and H_7 in the ^1H-NMR spectra of **200** and **201** appear within the range 6.8-7.5 ppm, which is consistent with 8-substitution by the mesomeric electron donor $-NH_2$ – δ values for these protons in the presence of an 8-nitro substituent would be higher, and are in the range 7.6-8.3 ppm for analogous derivatives.



200, 88% **201**, 10% **196** **199**

Scheme 3.13: Attmepted synthesis of a C_2-benzylamido-C_3-aryl-C_8-amino naphthoquinone derivative. *Reagents and conditions:* (i) 3-furanylboronic acid (2.0 eq.), $Pd(PPh_3)_2Cl_2$ (0.1 eq.), THF:sat. aq. $NaHCO_3$ (22:5), 100 ^oC, 16 h; (ii) 3-furanylboronic acid (2.0 eq.), $Pd(PPh_3)_2Cl_2$ (0.1 eq.), Na_2CO_3 (3.0 eq.), toluene, 130 ^oC, 16 h.

Whilst unanticipated, an analogous arylnitro to arylamino reduction in a Suzuki-type cross-coupling has previously been reported, when DMF/H_2O[304] or DMF alone[305] was used as the reaction solvent. As reactions in *N*,*N*-dimethylacetamide (DMA) do not lead to any such reduction, it was hypothesised that under the basic reaction conditions, an ammonium formate derivative could be generated from DMF which subsequently acts as a reductant.[305] No previous studies have investigated the potential for such a reduction to occur in THF, and the mechanism of generation of a hydrogen source is unclear; it is possible that homocoupling of the furanylboronic acid could generate a palladium hydride species, and that this process outcompetes oxidative addition of palladium into the carbon-chlorine bond. By switching the reaction system from THF/sat. aq. $NaHCO_3$ to Na_2CO_3 in anhydrous toluene, both hydrolysis of the benzyl amide and reduction of the nitro group in **196** were suppressed; however, the desired cross-coupling was not observed either and only starting material was returned.

Given the relatively poor pharmacological and colorimetric properties of the amide series as a whole, no further time was invested in the synthesis of target **199**; however, future work could involve the screening of a greater range of solvents, bases, Pd sources and phosphine ligands in effecting a successful Suzuki-type cross-coupling on intermediate **196**.

3.5. A Return to the C_3 Position: Biaryl Derivatives

Following the successful increase in both potency and absorption coefficient of both the sulfonamide and amide series by addition of an 8-amino auxochromic substituent on the naphthoquinone core, efforts were focussed once again on the C_3 position of the core, since the SAR established at both the C_2 and C_5-C_8 positions around the naphthoquinone appears to be very steep, with little potential for change in substituents. Conversely, the initial C_3 analogue library generated **(Section 3.2.)** demonstrates that a wide range of aromatic groups are tolerated at the C_3 position.

Of the initially synthesised library **(Section 3.2.1.)**, 4-bromoanilino-substituted **81** and 3-bromoanilino-substituted **80** proved particularly interesting, since they both display high potency against the human and murine proteins, and the bromine atoms are sterically large; furthermore, *in silico* modelling suggests that the C_3 substituent points out of the enzyme active site **(Figure 3.12)**. Given this information, it was hypothesised that in order to further increase the absorption coefficients of the inhibitors, the molecular chromophore could be extended at either the *meta* or *para* positions of a C_3-anilino substituent.

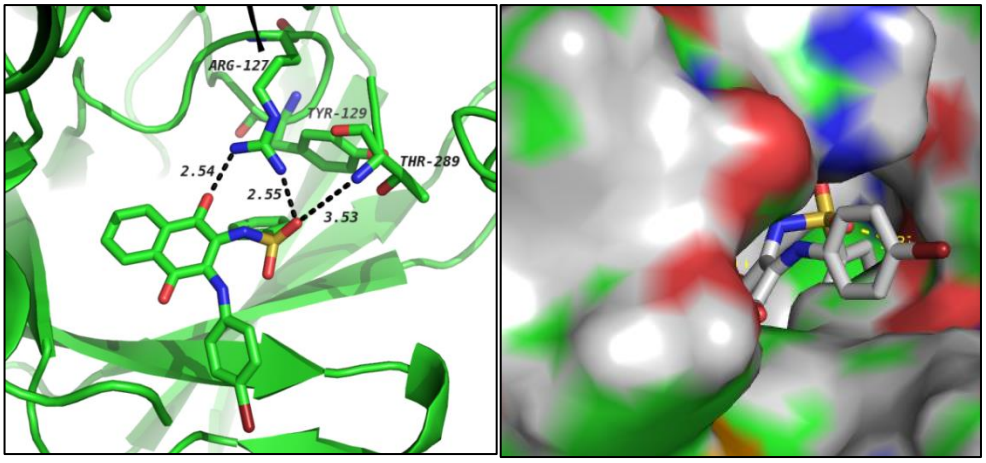
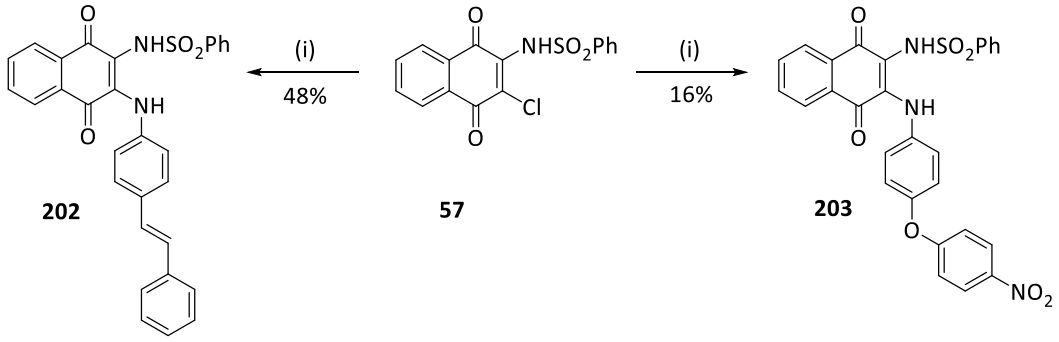


Figure 3.12: *In silico* modelling of 4-bromoanilino-substituted **81** in the active site of HUMAN(NAT1) (pdb: 2PQT);[247b] analysis performed using GOLD (v.5.2).[282] **Left:** Protein shown in cartoon representation, with key polar contacts and active site residues Arg127, Tyr129 and Thr289 highlighted in stick representation; predicted polar contacts are represented by dashed lines and inter-atomic distances are given in Ångströms. **Right:** Protein shown in surface representation, showing the 4-bromoaniline substituent of **81** protruding from the active site.

Therefore, a library of analogues was designed to include aminobiaryl, aminostilbene and aminodiphenyl ether C_3 substituents. Stilbene **202** and diphenyl ether **203** were readily prepared from the corresponding commercially available anilines and 3-chloro-2-benzenesulfonamidonaphthoquinone **57** *via* a Michael-type reaction in moderate isolated yields **(Scheme 3.14)**.

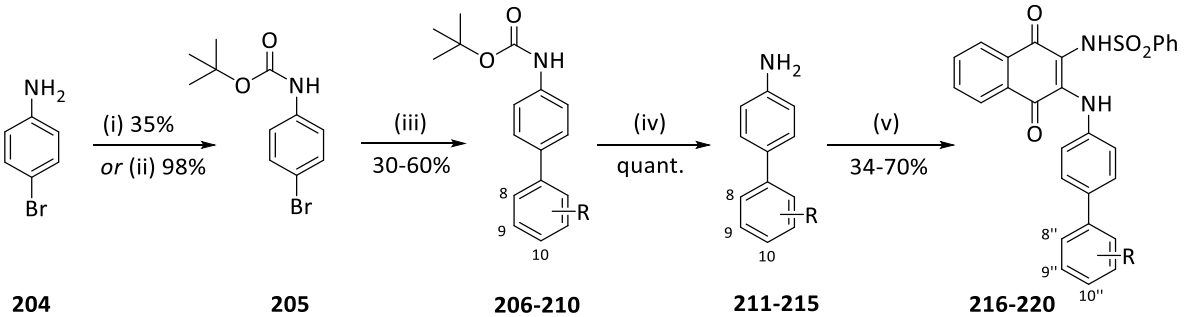


Scheme 3.14: Synthesis of amino-stilbene derivative **202** and 4-amino-4'-nitrodiphenyl ether derivative **203**; data for compound **202** generated by KSH.[300] *Reagents and conditions:* (i) $CeCl_3 \bullet 7H_2O$ (1.0 eq.), MeOH, RT, 1.5 h *then* requisite aniline (3.0 eq.), 90 ^oC, 16 h.

To prepare C_3-aminobiaryl derivatives, the requisite biaryl amines first had to be synthesised from *tert*-butyl (4-bromophenyl)carbamate **205** and a phenylboronic acid derivative in a Suzuki-type cross-coupling[203] reaction **(Scheme 3.15)**. *N*-Boc species **205** was itself synthesised from *para*-bromoaniline **204** and Boc_2O in only a modest yield of 35% when heated overnight at 60 ^oC in a 1:1 mix of THF:H_2O in the presence of NaOH (conditions (i)); however, use of an alternative procedure in which $InCl_3$ was used as a Lewis acid catalyst resulted in a vastly improved isolated yield of 98% for the reaction, with both a lower reaction temperature and shorter reaction time employed (conditions (ii)).

The subsequent Suzuki-type cross-couplings (conditions (iii)) were effected in good yield; methoxy-substituted phenylboronic acids were chosen as the coupling partners due to the auxochromic nature of the OMe group. The biaryl products were next subjected to Boc group deprotection in 1:5 TFA:CH_2Cl_2 at 0 ^oC (conditions (iv)) to give anilines **211-215** in good to

excellent yield; these anilines then underwent a Michael-type reaction with naphthoquinone **57** in MeOH catalysed by $CeCl_3 \bullet 7H_2O$ (conditions (v)) to furnish the desired final products in 34-70% yield.

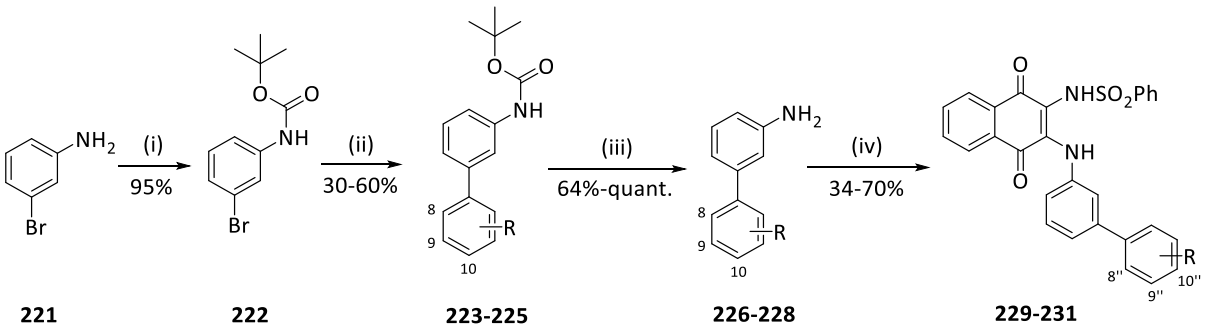


Scheme 3.15: Synthesis of a *para*-substituted anilino biaryl library. *Reagents and conditions:* (i) Boc_2O (1.2 eq.), NaOH (2.2 eq.), THF:H_2O (1:1), 60 ^oC, 24 h; (ii) Boc_2O (1.2 eq.), $InCl_3$ (0.01 eq.), 40 ^oC, 2 h; (iii) requisite arylboronic acid (2.0 eq.), $Pd(PPh_3)_2Cl_2$ (0.1 eq.), THF:sat. aq. $NaHCO_3$ (22:5), 100 ^oC, 16 h; (iv) TFA:CH_2Cl_2 (1:5), RT, 2 h; (v) 2-benzenesulfonamido-3-chloro-1,4-naphthoquinone **57** (0.5 eq.), $CeCl_3 \bullet 7H_2O$ (0.5 eq.), MeOH, 90 ^oC, 16 h, *yields quoted w.r.t. naphthoquinone **57***. For yields of steps (ii), (iii) and (iv), refer to **Table 3.19**.

R =	Cpd	Yield Step (ii)	Cpd	Yield Step (iii)	Cpd	Yield Step (iv)
All H	**206**	69%*	**211**	96%*	**216**	70%*
8''-OMe	**207**	16%	**212**	69%	**217**	34%*
9''-OMe	**208**	50%*	**213**	75%*	**218**	50%*
10''-OMe	**209**	53%*	**214**	70%*	**219**	63%*
8'',9'',10''-tri-OMe	**210**	67%	**215**	76%	**220**	40%*

Table 3.19: Yields for steps (ii), (iii) and (iv) in the synthesis of *para*-substituted biaryls from **Scheme 3.15**. * = data generated by KSH.[300]

An entirely analogous synthetic route to *meta*-substituted biaryl products was also effected **(Scheme 3.16; Table 3.20)**. In synthesis of the *para* derivatives, it had been noted qualitatively that use of phenylboronic acid and 4-methoxybenzeneboronic acid in the coupling steps led to final products which had particularly low solubility under the assay conditions of 95% 20 mM Tris•HCl (*p*H 8)/5% DMSO (*v/v*), and so these two analogues were omitted from the *meta*-substituted library.



221 **222** **223-225** **226-228** **229-231**

Scheme 3.16: Synthesis of a *meta*-substituted anilino biaryl library. *Reagents and conditions:* (i) Boc_2O (1.2 eq.), $InCl_3$ (0.01 eq.), 40 ^oC, 2 h; (ii) Requisite arylboronic acid (2.0 eq.), $Pd(PPh_3)_2Cl_2$ (0.1 eq.), THF:sat. aq. $NaHCO_3$ (22:5), 100 ^oC, 16 h; (iii) TFA:CH_2Cl_2 (1:5), RT, 2 h; (iv) 2-benzenesulfonamido-3-chloro-1,4-naphthoquinone **57** (0.5 eq.), $CeCl_3 \bullet 7H_2O$ (0.5 eq.), MeOH, 90 ^oC, 16 h, *yields quoted w.r.t. naphthoquinone **57***. For yields of steps (ii), (iii) and (iv), refer to **Table 3.20**.

R =	Cpd	Yield Step (ii)	Cpd	Yield Step (iii)	Cpd	Yield Step (iv)
8''-OMe	**223**	18%	**226**	Quant.	**229**	27%
9''-OMe	**224**	60%	**227**	64%	**230**	32%
8'',9'',10''-tri-OMe	**225**	33%	**228**	92%	**231**	21%

Table 3.20: Yields for steps (ii), (iii) and (iv) in the synthesis of *meta*-substituted biaryls from **Scheme 3.16**.

The pharmacological and optical properties of these synthesised derivatives containing extended chromophores were subsequently evaluated; the data are presented in **Figure 3.13** and **Tables 3.21 and 3.22**.

It can be noted that the *meta*-biaryl derivatives have relatively low potency against MOUSE(NAT2), with only tri-methoxy-substituted **231** displaying an IC_{50} value of less than 30 µM. The unsubstituted *para*-biaryl species **216** also has low potency against MOUSE(NAT2) at 30 µM; however, **216** was observed to have a low solubility under the assay conditions and precipitated out of the wells. *para*-Methoxy-substituted *para*-biaryl **219** and stilbene **202** were also qualitatively observed to have low solubilities under the assay conditions; both show reasonable IC_{50} values against MOUSE(NAT2) of 3.0 and 3.1 µM respectively, but the confidence limit of the result (*P*) and the goodness of fit of the data to the regression curve (R^2) for compound **219** were poor.

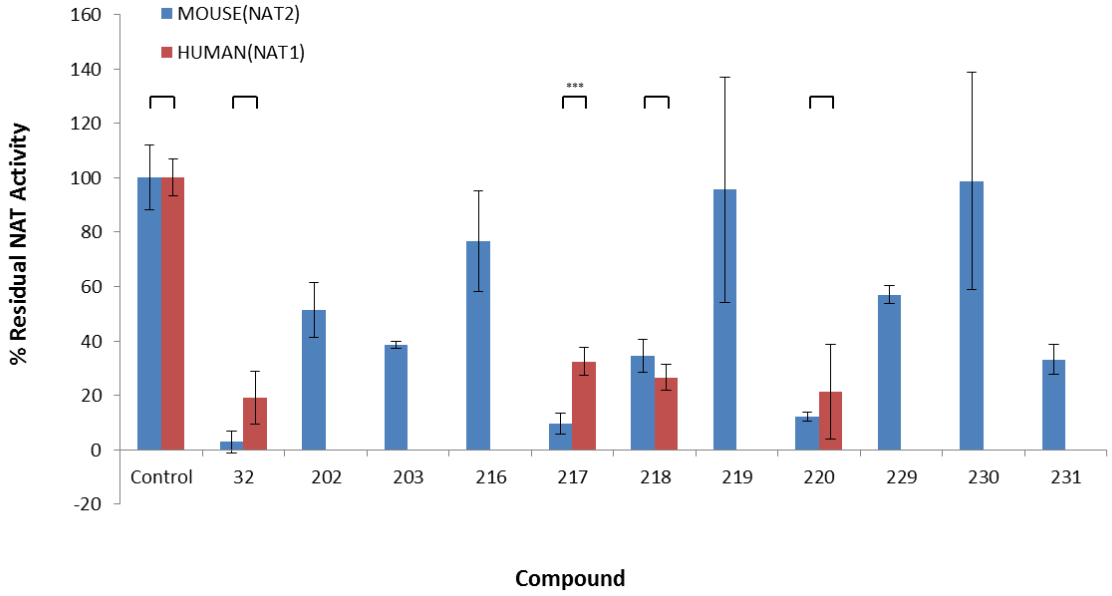


Figure 3.13: % Residual activity, ± one standard deviation, when MOUSE(NAT2) (blue columns) or HUMAN(NAT1) (red columns) were dosed with 30 µM of compounds **202-203**, **216-220** and **229-231** in the acetyl CoA hydrolysis assay. Experiments were conducted in triplicate and the final DMSO concentration was 5% (*v/v*). Stars and brackets above the bars show the significance of the difference between the MOUSE(NAT2) and HUMAN(NAT1) data when a Student's *T*-Test was performed: no stars = $P > 0.05$; *** = $P < 0.005$.

Compound	C_3 Anilino Substituent	IC_{50} MOUSE(NAT2) (µM)	R^2	*P*	IC_{50} HUMAN(NAT1) (µM)	R^2	*P*
32	3,5-Dimethylamino	3.1 ± 0.69	0.8972	***	4.1 ± 0.56	0.9658	***
202	4-Aminostilbene	3.1 ± 0.69	0.8972	***	N.D.	N.D.	N.D.
203	4-Amino-4'-nitrodiphenyl ether	5.3 ± 1.4	0.6705	**	N.D.	N.D.	N.D.
217	8-Methoxy-[4,7]-biaryl-1-amine	0.46 ± 0.11	0.9044	***	0.15 ± 0.02	0.9641	***
218	9-Methoxy-[4,7]-biaryl-1-amine	0.71 ± 0.23	0.8521	**	0.27 ± 0.05	0.9394	***
219	10-Methoxy-[4,7]-biaryl-1-amine	3.0 ± 1.1	0.2618	*	N.D.	N.D.	N.D.
220	8,9,10-Trimethoxy-[4,7]-biaryl-1-amine	0.42 ± 0.11	0.8912	***	0.12 ± 0.02	0.9554	***
231	8,9,10-Trimethoxy-[3,7]-biaryl-1-amine	12.2 ± 3.3	0.3168	***	N.D.	N.D.	N.D.

Table 3.21: IC_{50} values for compounds **202-203**, **217-220** and **231** in the C_3 biaryl library against MOUSE(NAT2) and HUMAN(NAT1) in the acetyl CoA hydrolysis assay, with squared correlation coefficients (R^2) and significance levels (*P*) as given; * = $P < 0.05$; ** = $P < 0.01$; *** = $P < 0.005$. Data on compounds **202** and **217-220** generated by KSH.[300] Data calculated using KyPlot® software. N.D. = not determined; N/A = not applicable.

Compound	pK_a	λ_{max} *p*H 8 (nm)	$\Delta\lambda_{max}$ *p*H 13 (nm)	$\Delta\lambda_{max}$ MOUSE(NAT2) (nm)	ε_N ($M^{-1}cm^{-1}$)	$\varepsilon_N/\varepsilon_N(32)$	ε_{CB} ($M^{-1}cm^{-1}$)	$\varepsilon_{CB}/\varepsilon_{CB}(32)$
32	9.2 ± 0.05	498	+ 79	+ 112	11960	1.00	6590	1.00
202	10.1 ± 0.3	542	+ 60	+ 9	32380	1.79	3180	0.46
216	9.3 ± 0.2	528	+ 57	+ 34	17780	1.47	14430	2.17
217	10.3 ± 0.3	534	+ 47	+ 15	20950	1.74	10100	1.52
218	10.5 ± 0.1	526	+ 60	+ 6	17460	1.45	6930	1.04
219	10.2 ± 0.5	555	+ 33	- 4	16190	1.34	14430	2.17
220	10.1 ± 0.1	531	+ 53	- 31	24760	2.05	8080	1.22
229	9.6 ± 0.05	509	+ 64	+ 94	N.D.	N.D.	N.D.	N.D.
230	10.2 ± 0.1	508	+ 62	+ 120	21550	1.80	5160	0.43
231	9.7 ± 0.1	507	+51	N.D.	5750	0.48	2210	0.34

Table 3.22: Colorimetric data for compounds **32**, **202**, **216-220** and **229-231**: pK_a values (calculated using GraphPad Prism® and quoted ± one standard deviation; R^2 >0.95 for all compounds); wavelengths of maximum absorption at *p*H 8, *p*H 13 and in the presence of MOUSE(NAT2); and absorption coefficients of the neutral (N) and conjugate base (CB) species. Data for **202** and **216-220** generated by KSH.[300] N.D. = not determined.

Far more pleasingly, the IC_{50} values for *para*-substituted biaryl derivatives **217**, **218** and **220** against both MOUSE(NAT2) and HUMAN(NAT1) are an order of magnitude lower than those for hit compound **32**. This effect could be due to an increase in the number of binding contacts between the biaryl substiuent and the residues around the entrance to the enzyme active site.

One alternative explanation for the low IC_{50} values of biaryl species **217**, **218** and **220** could be an entropic effect resulting from their anticipated hydrophobicity: upon desolvation and binding to the target enzyme active site, it would be predicted that the entropy of the solvent molecules would increase significantly. However, a plot of calculated HUMAN(NAT1) pIC_{50} values against lipophilic ligand efficiency (LLE) for compounds **32**, **217**, **218** and **220** shows a non-linear relationship **(Table 3.23; Figure 3.14)**, which suggests that the increased potency of

these biaryl derivatives is not merely an entropic effect and that these ligands also offer an increased enthalpic contribution in binding to the HUMAN(NAT1) active site.

Compound	IC_{50} HUMAN(NAT1) (nM)	pIC_{50} HUMAN(NAT1)	cLogP	LLE
32	4100	6.39	4.90	1.44
217	150	7.82	5.71	2.11
218	270	7.57	5.71	1.86
220	120	7.92	5.34	2.58

Table 3.23: Calculation of pIC_{50} values and lipophilic ligand efficiencies (LLEs) for hit compound **32** and biaryls **217**, **218** and **220**.[300] cLogP values calculated using Virtual Computational Chemistry Laboratory software (accessed online at http://www.vcclab.org/).

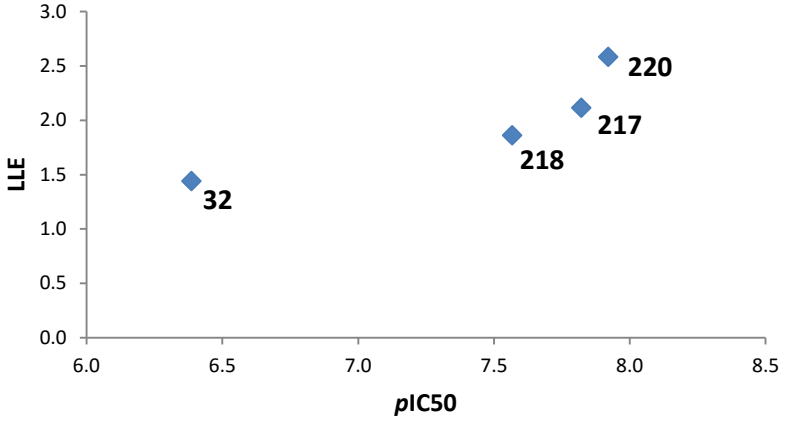
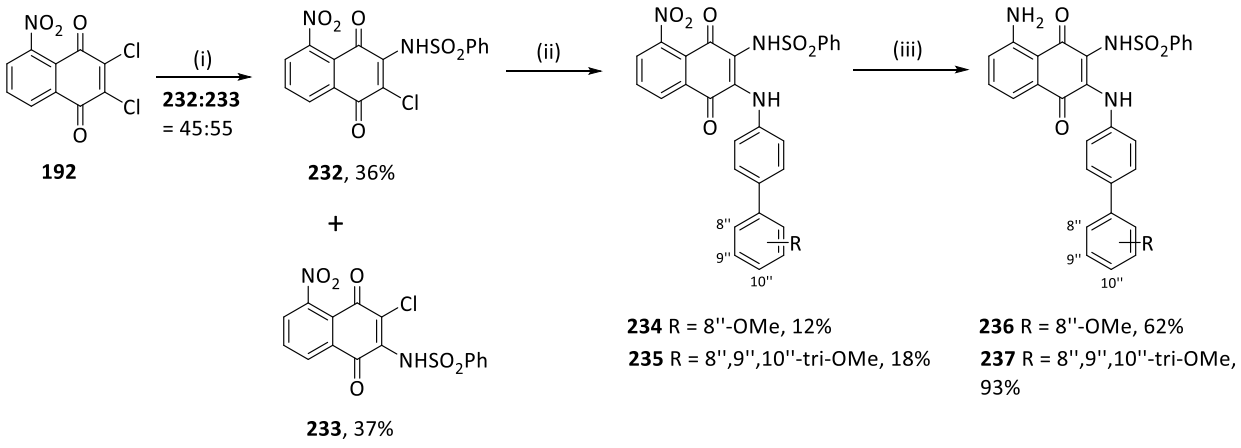


Figure 3.14: Non-linear plot of pIC_{50} against lipophilic ligand efficiency for C_3 biaryl-substituted analogues.[300]

Colorimetric evaluation of the biaryl derivatives **(Table 3.22)** shows that many of the species in this series possess larger absorption coefficients than hit compound **32**, with the ε_{CB} values of compounds **216** and **219** calculated as over twice as large as that of **32**; these data support the hypothesis that extending the molecular chromophore at the C_3 position might increase the sensitivity of the ligand. However, the most potent members of this compound library (namely **217**, **218** and **220**) display disappointingly small shifts in λ_{max} in the presence of MOUSE(NAT2). There are three plausible explanations for this behaviour: firstly, these compounds could be binding in a different fashion to that predicted by the *in silico* model, without forming an ionic salt bridge to Arg127; secondly, the pK_a values of these particular species (all >10) are too high for complete conversion to their respective conjugate bases

under the assay conditions (*cf.* the earlier synthesised derivative cyclohexyl **120**, which has a pK_a of 10.1 and a λ_{max} shift of only -7 nm in the presence of MOUSE(NAT2)); or thirdly, the increased enthalpic and entropic driving forces for binding of these derivatives enables the neutral species to bind to the active site without its prior deprotonation.

Given that both a *para*-biaryl amine substituent at the C_3 position and an NH_2 group at the C_8 position each independently give approximately a twenty-fold and ten-fold increase respectively in potency against HUMAN(NAT1) *cf.* hit compound **32**, it was decided to synthesise inhibitors containing both of these structural motifs. Furthermore, based on the findings of previous work, addition of a C_8 amino substituent would be predicted to lower the pK_a of the C_3 biaryl-substituted species and so might enable a clear shift in λ_{max} to be observed in the presence of MOUSE(NAT2). Analogues **236** and **237** were synthesised from 2,3-dichloro-5-nitro-1,4-naphthoquinone **192** and 4-bromoaniline **204** in a longest linear sequence of five steps; the linear sequence from starting material **192** is outlined in **Scheme 3.17** and the synthesis of the requisite amines for step (iii) has been previously shown in **Scheme 3.15** and **Table 3.19**.



Scheme 3.17: Synthesis of naphthoquinones bearing both a C_3 *para*-substituted anilino biaryl substituent and a C_8 amino substituent. *Reagents and conditions:* (i) Benzenesulfonamide (1.0 eq.), Cs_2CO_3 (1.4 eq.), DMF, RT, 16 h; (ii) $CeCl_3 \bullet 7H_2O$ (1.0 eq.), MeOH, RT, 1.5 h *then* aniline **234** or **235** (2.0 eq.), 90 ^oC, 16 h; (iii) H_2 (1 atm.), 10% Pd/C (0.1 eq.), MeOH, RT, 16 h.

Pharmacological evaluation of compounds **236** and **237** reveal disappointing IC_{50} values against MOUSE(NAT2) of >30 μM and 2.5 ± 0.4 μM respectively (R^2 = 0.9139; P = <0.005 for **237**). This suggests that the beneficial effects on potency conferred by each of the C_3-biaryl and C_8-amino substituents individually are not additive. One possible reason for this is that compounds **236** and **237** containing both these structural features cannot adopt a conformation in the active site of the enzyme which is optimal for interactions between either the C_3-biaryl substituent or the C_8-amino substituent and the key enzyme active site residues.

Given the disappointingly low potencies of compounds **236** and **237**, no further attempts were made to combine a C_3 biaryl and a C_8 amino substituent within the same inhibitor.

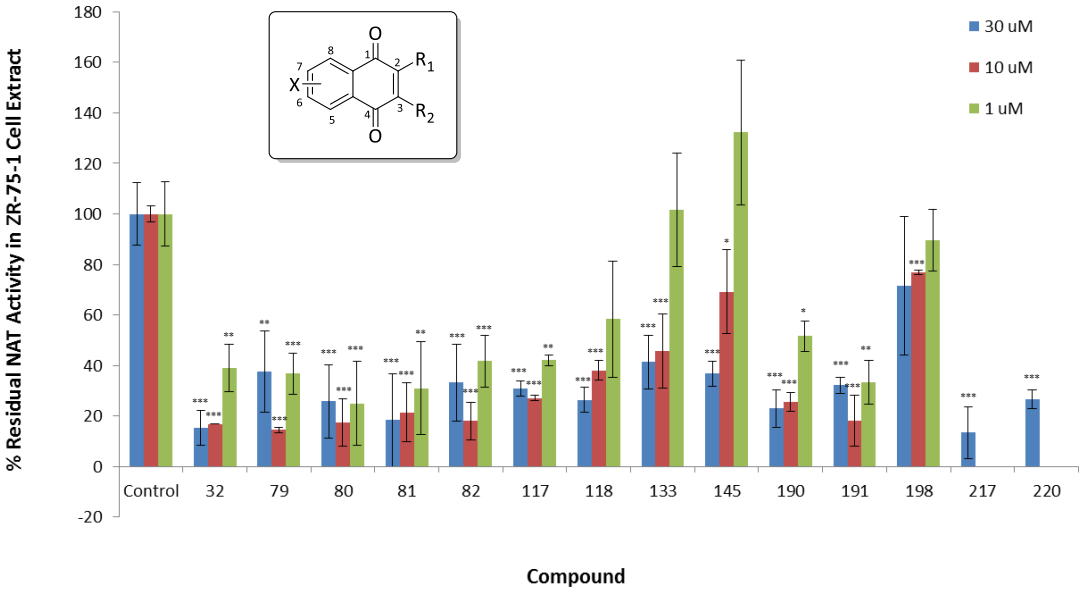
3.6. Evaluation in Cell Extracts from the Breast Cancer Cell Line ZR-75-1

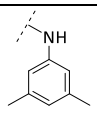
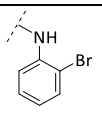
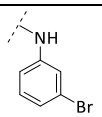
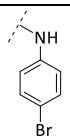
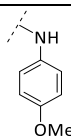
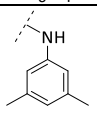
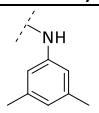
Some of the most potent HUMAN(NAT1)/MOUSE(NAT2) inhibitors developed in this SAR study were tested for activity against cell extracts from the ER+ breast cancer cell line ZR-75-1, which overexpresses HUMAN(NAT1). The cell line was grown and harvested to create a cell extract as outlined in **Section 7.10**. Representative compounds which display a range of structural functionality were selected for this study, and were tested for inhibitory activity of HUMAN(NAT1) within the cell extract at concentrations of 30 μM, 10 μM and 1 μM **(Figure 3.15A)**. All of the representative sulfonamides which showed high levels of potency against recombinant HUMAN(NAT1) also showed high levels of inhibition of HUMAN(NAT1) in the cell extracts, with compounds **32**, **79-82**, **117** and **191** exhibiting >50% inhibition of HUMAN(NAT1) at an inhibitor concentration of 1 μM.

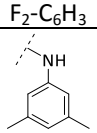
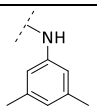
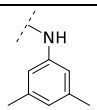
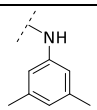
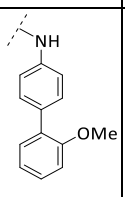
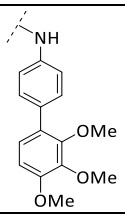
A small amount of recombinant HUMAN(NAT2) was also kindly made available by Prof. Fernando Rodrigues-Lima and Dr Julian Dairou, colleagues at the University of Paris-Diderot (Paris, France). This was used to test for cross-inhibition of some of the C_3 anilino-substituted and biaryl amino-substituted analogues synthesised; compounds were tested at a single-point concentration of 30 μM in triplicate **(Figure 3.15B)**. The majority of compounds appeared not

to show any appreciable levels of HUMAN(NAT2) inhibition; although those bearing C_3 biaryl amino substituents may appear to show some inhibition, the low specific activity of the HUMAN(NAT2) protein used led to large standard deviations in the data sets, and when Student's *T*-tests were performed, none of the test data points were shown to be statistically significantly different to the control. In future, inhibition studies on HUMAN(NAT2) should be repeated in order to be able to draw firmer conclusions about any possible cross-inhibition.

A



Compound	32	79	80	81	82	117	118
R_1	$NHSO_2Ph$	$NHSO_2Ph$	$NHSO_2Ph$	$NHSO_2Ph$	$NHSO_2Ph$	$NHSO_2$-4-F-C_6H_4	$NHSO_2$-furan-2-yl
R_2							
X	H	H	H	H	H	H	H

Compound	133	145	190	191	198	217	220
R_1	$NHSO_2$-2,6-F_2-C_6H_3	$NHCOCH_2Ph$	$NHSO_2Ph$	$NHSO_2Ph$	$NHCOCH_2Ph$	$NHSO_2Ph$	$NHSO_2Ph$
R_2		Cl					
X	H	H	C_8-NH_2	C_7-NH_2	C_8-NH_2	H	H

B

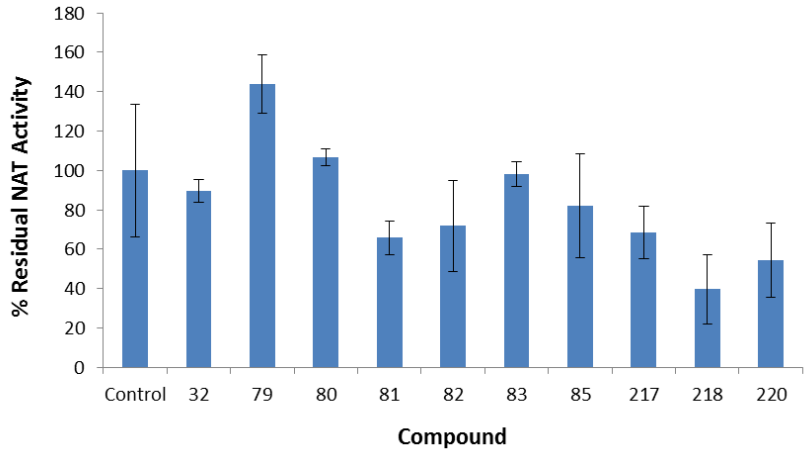


Figure 3.15: A: % Residual activity of HUMAN(NAT1) in ZR-75-1 cell extracts when dosed with representative inhibitors from each of the C_3 analogue library, the C_2 sulfonamido and amido libraries, the C_5-C_8 substituted library and the C_3 biaryl library, the structures of which are given. Compounds were dosed at 30, 10 and 1 µM in triplicate, and the final DMSO concentration in the assays was 5% (*v/v*), and % activity values are quoted relative to a control experiment (vehicle only). Results are presented as average values ± one standard deviation, and the stars above the columns show the significance of the difference between the test data and its respective control when a Student's *T*-test was performed: no stars = P >0.05; * = P <0.05; ** = P <0.01; *** = P <0.005. **B:** % Residual activity of HUMAN(NAT2) when dosed with 30 µM of representative compounds from the C_3 anilino and biaryl amine libraries, relative to a control experiment (vehicle only). Assays were performed in triplicate with a final DMSO concentration of 5% (*v/v*); results are presented as average values ± one standard deviation.

Subsequently, C_8 amino-substituted **190**, C_7 amino-substituted **191** and C_3 biaryl-substituted **217** and **220** were examined in spectroscopic experiments with ZR-75-1 cell extracts in an attempt to detect HUMAN(NAT1) present in the cells. These compounds were selected because they display both improved potency against HUMAN(NAT1) and improved ε_{CB} values over **32**, as well as show high levels of inhibition of HUMAN(NAT1) in the ZR-75-1 cell extracts.

In the spectroscopic experiments, each probe was tested at concentrations ranging from 0.6 µM to 2.5 µM, but as was the case with similar experiments performed on hit compound **32** (*cf.* **Section 2.2.**), no λ_{max} peak could be detected at these concentrations due to a poor signal-to-noise ratio. A negative control concentration of 20 µM was used, clearly showing λ_{max} corresponding to the neutral (protonated) species in each case. This demonstrates that further improvements to the sensitivity of the probes are required for their clinical use,

although the SAR studies outlined in this chapter have provided key underpinning insights to demonstrate at which positions around the naphthoquinone core of **32** there is scope for structural variation in order to achieve this.

3.7. Conclusions from SAR Studies on Colorimetric Probes

In this chapter, an extensive SAR study has been conducted around the naphthoquinone core of hit compound **32**, in order to try to increase both the potency and sensitivity of HUMAN(NAT1) inhibitors, whilst maintaining a suitable *p*K_a value for detection of the target protein in cell media. Variations have been made at the C_2, C_3 and C_5-C_8 positions around the core, and the effects on compound activity are summarised in **Figure 3.16**.

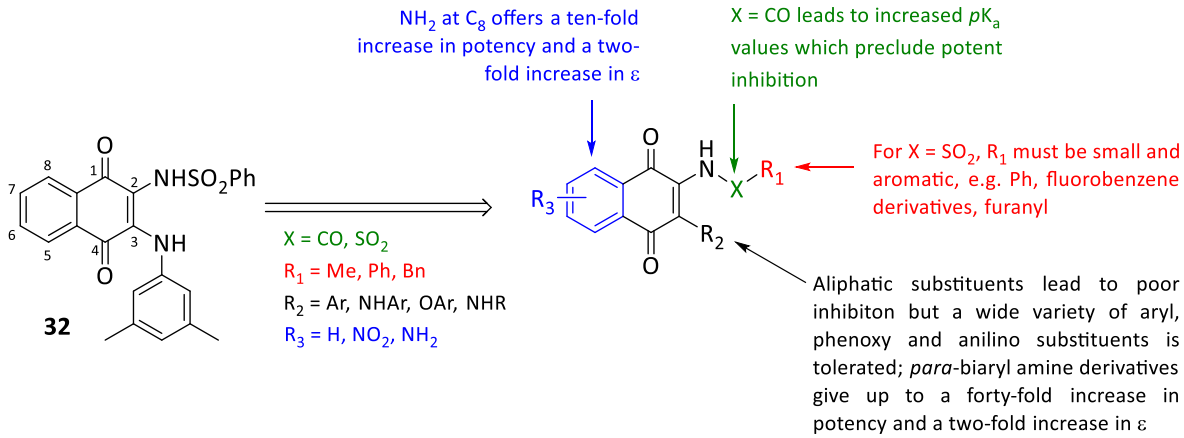


Figure 3.16: Summary of the SAR elucidated around the naphthoquinone core of hit compound **32**.

At the C_2 position, SAR for the sulfonamide derivatives is very steep, with only small, aromatic substituents such as phenyl (**32**), 4-fluorophenyl (**117**), 2-furyl (**118**) and 2,6-difluorophenyl (**133**) being tolerated, and none of the alterations at this position effected the desired increase in sensitivity of detection. Furthermore, replacement of the sulfonamide functionality with an amide motif led for most examples to a significant decrease in potency, despite the predicted isosteric and isoelectronic nature of benzyl amide and phenyl sulfonamide functionalities; the difference in observed properties is likely due to the high *p*K_a values of the amide derivatives.

At the C_3 position, a wide variety of aromatic groups is tolerated, although C_3-aryl and C_3-aryloxy analogues possess low *p*K_a values which render them unsuitable as cellular probes. Many anilino substituents possess favourable properties, and *para*-biaryl amines such as **217**, **218** and **220** were shown to be up to forty times more potent against HUMAN(NAT1) than **32**, as well as exhibit up to a two-fold increase in absorption coefficient. Qualitatively, however, it was noted that the solubility of these biaryl derivatives was low under the assay conditions employed; therefore, in order to generate HUMAN(NAT1) inhibitors which might be of greater use in cellular studies, this issue will be returned to in **Chapter 5**, where efforts to replace the second aryl ring of these derivatives with alternative functionalities will be discussed.

At the C_5-C_8 positions around the naphthoquinone ring, it was previously observed that appending an amino group at the C_8 position led to a ten-fold increase in potency and two-fold increase in sensitivity over compound **32**. However, synthesised derivatives containing both a C_3 *para*-biaryl amino substituent and a C_8 amino group possessed higher IC_{50} values against MOUSE(NAT2) than any of compounds **190**, **217**, **218** or **220**, suggesting that the beneficial effects of these two structural features are not additive.

Crucially, in this chapter it has been discovered that despite the generation of HUMAN(NAT1) inhibitors with up to a forty-fold increased potency and two-fold increased absorption coefficient over compound **32**, and which also inhibit HUMAN(NAT1) activity in cell extracts from the ER+ breast cancer cell line ZR-75-1, none of the improved inhibitors are capable of detecting the presence of HUMAN(NAT1) in the cell extracts *via* shifts in their λ_{max} values because of high levels of background noise. Fundamentally, we can conclude from the studies in this chapter that the technique of colorimetry itself is a limiting factor in using such probes to accurately detect HUMAN(NAT1). More desirable, therefore, would be the generation of fluorescent HUMAN(NAT1) inhibitors, since fluorescence is a far more sensitive optical detection technique in biological systems than colorimetry due to less background noise at key wavelengths. In **Chapter 4**, efforts to synthesise fluorescent HUMAN(NAT1) probes based on naphthoquinone **32** will be described.

Chapter 4: Development of Fluorescent HUMAN(NAT1) Probes

4.1. Conception of Fluorescent Derivatives of Naphthoquinone 32

In **Chapter 3**, an extensive SAR study was described with the aim of optimising colorimetric probes that might be used to detect and quantify the levels of HUMAN(NAT1) present in cellular samples.[266] However, despite displaying up to a forty-fold increase in potency and a two-fold increase in absorption coefficient over the hit compound **32**, the optimised inhibitors were not capable of detecting HUMAN(NAT1) in cell extracts from the ER+ breast cancer cell line ZR-75-1. It is believed that the high background noise levels in colorimetric absorption spectra of cellular extract samples contribute significantly to the insensitivity of probe detection.

Fluorescence spectroscopy, on the other hand, is a far more sensitive technique to use in biological systems than colorimetry, because of less background noise at key wavelengths.[306] It was therefore decided to design, synthesise and test analogues of naphthoquinone **32** which would be anticipated to fluoresce, and which exhibit all of the following properties:

- A high potency against HUMAN(NAT1);
- A high fluorescence intensity;
- A fluorescence wavelength at which background noise in cellular extracts is low;
- A suitable pK_a such that its conjugate base can be selectively sequestered by HUMAN(NAT1), but is not the predominant ionisation form in solution at *p*H 8;
- A "switch" in either fluorescence intensity or wavelength in the presence of HUMAN(NAT1).

In this regard, the HUMAN(NAT1) inhibitors **217**, **218** and **220** described in **Chapter 3**, which bear a *para*-biaryl amino substituent at the C_3 position of the naphthoquinone core, present a useful starting point, since they are the most potent inhibitors of HUMAN(NAT1) yet synthesised, and small molecule fluorophores based on a biaryl core have been widely

reported in the scientific literature **(Figure 4.1)**.[307] One of the key limitations of using a C_3 *para*-biaryl amino derivative as a probe for HUMAN(NAT1) detection, however, is the observation that species **217**, **218** and **220** all displayed relatively small λ_{max} shifts in the presence of MOUSE(NAT2): if a colorimetric shift is not observed in the presence of the target protein, then it is improbable that a fluorescent one will be either.

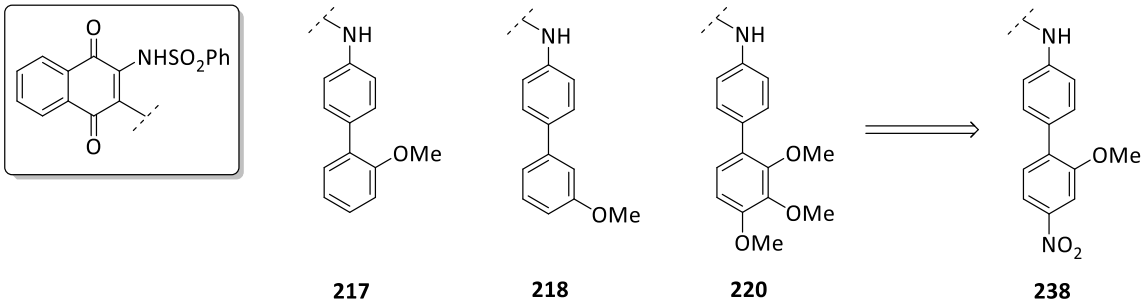


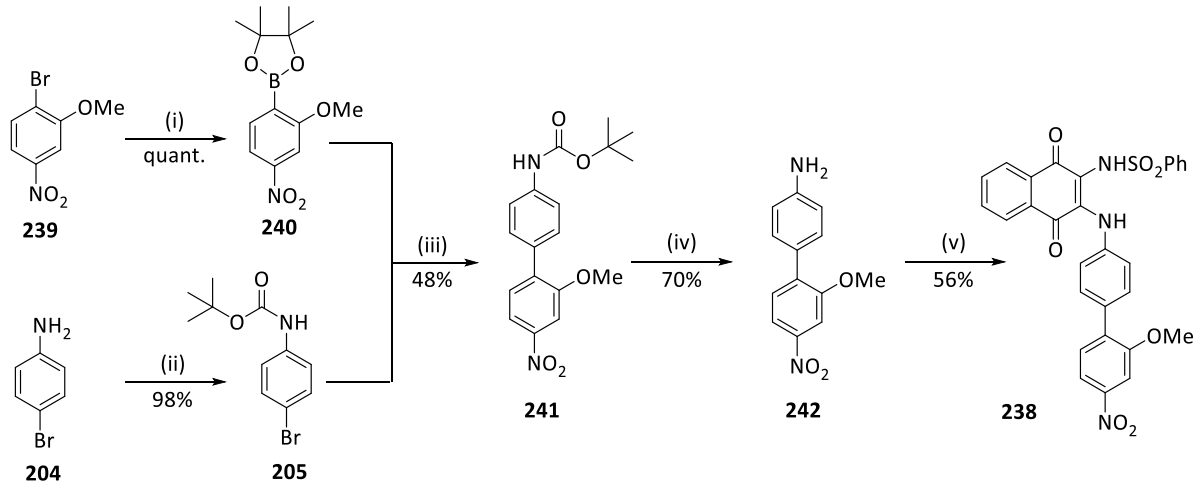
Figure 4.1: C_3-Biaryl amino derivatives **217**, **218** and **220**, which display high potency against MOUSE(NAT2) and HUMAN(NAT1), and proposed derivative **238**, which contains both an electron-withdrawing nitro group and an electron-donating methoxy group.

4.1.1. Synthesis and Evaluation of the Second Generation Lead Compound 238

One of the possible reasons suggested for the low λ_{max} shifts observed for compounds **217**, **218** and **220** is that these species all possess *p*K_a values over 10, which might prevent effective formation of the conjugate base species; this could well be compounded by a high affinity of the neutral (protonated) species for the enzyme active site. **217**, **218** and **220** all contain very electron-rich aryl moieties due to the presence of methoxy substituents. Therefore, it was reasoned that a more electron-poor biaryl moiety might possess a lower *p*K_a value and hence might show a greater λ_{max} shift in the presence of MOUSE(NAT2) than any of **217**, **218** and **220**, whilst still retaining a high potency against the target enzyme.

The species designed to test this hypothesis was **238**, containing an 8-methoxy-10-nitro-[4,7]-biaryl-1-amine substituent at the C_3 position of the naphthoquinone core **(Figure 4.1)**. This was chosen because: (a) it was hypothesised that the addition of a nitro group *cf.* **217** might

lower the *p*K_a value; (b) retaining the 8-methoxy functionality might be beneficial for potency; and (c) biaryl moieties with both an electron donor and an electron acceptor group are anticipated to be more fluorescent than those with only one or other of these groups.



Scheme 4.1: Synthesis of second generation lead compound **238**. *Reagents and conditions:* (i) B_2Pin_2 (1.5 eq.), KOAc (3.0 eq.), $Pd(PPh_3)_2Cl_2$ (0.05 eq.), 1,4-dioxane, 100 ^oC, 3 h; (ii) Boc_2O (1.2 eq.), $InCl_3$ (0.01 eq.), 35 ^oC, 3 h; (iii) boronic ester **240** (2.0 eq.), carbamate **241** (1.0 eq.), $Pd(PPh_3)_2Cl_2$ (0.1 eq.), THF:sat. aq. $NaHCO_3$ (22:5), 100 ^oC, 16 h, yield quoted *w.r.t.* carbamate **205**; (iv) TFA:CH_2Cl_2 (1:5), RT, 2 h; (v) 2-benzenesulfonamido-3-chloro-1,4-naphthoquinone **57** (1.0 eq.), $CeCl_3 \bullet 7H_2O$ (1.0 eq.), MeOH, RT, 16 h *then* amine **242** (3.0 eq.), 90 ^oC, 16 h.

The synthetic route to access this test compound **238** is outlined in **Scheme 4.1**. Essentially, the scheme follows the same synthetic route as for the biaryl derivatives discussed in **Chapter 3**, with initial *N*-Boc protection of 4-bromoaniline effected by $InCl_3$ catalysis (conditions (ii)) followed by a Suzuki-type cross-coupling[203] with boronic ester **240** utilising $Pd(PPh_3)_2Cl_2$ as the catalyst in THF:sat. aq. $NaHCO_3$ (22:5) (conditions (iii)), which proceeded in moderate yield. Neither boronic ester **240** nor the corresponding boronic acid are commercially available, and so **240** was obtained quantitatively in a single step from 2-methoxy-4-nitrobromobenzene **239** using 1.5 eq. *bis*(pinacolato)diboron in the presence of potassium acetate and catalytic $Pd(PPh_3)_2Cl_2$ in 1,4-dioxane (conditions (i)). Subsequently, the carbamate protecting group in **241** was readily deprotected to give biaryl amine **242** (conditions (iv)), which was subjected to a Michael-type reaction with naphthoquinone intermediate **57** (conditions (v)).

When tested in the acetyl CoA hydrolysis assay against MOUSE(NAT2), compound **238** was determined to have an IC_{50} value of 2.7 ± 0.54 μM (R^2 = 0.8545; P <0.005). Although this is an order of magnitude higher than the IC_{50} values determined for the more electron-rich biaryl derivatives **217**, **218** and **220**, pleasingly this value is still comparable with that of initial hit compound **32**. Unfortunately, at the time of this study, no HUMAN(NAT1) was available, as the human protein has poor stability even when stored at -78 °C, and the samples used in the studies outlined in **Chapter 3** proved inactive in the trialled acetyl CoA hydrolysis assays. Multiple attempts were made to express and purify a new batch of HUMAN(NAT1), but these all failed: SDS-PAGE gels suggested that whilst HUMAN(NAT1) expression occurred under the trialled conditions, all of the desired expressed protein was present in the insoluble fraction after cell lysis and thus could not be obtained *via* Ni-NTA column chromatography. However, many studies highlight the similarity between the behaviour of HUMAN(NAT1) and MOUSE(NAT2)[257] and hence in the interests of time, MOUSE(NAT2) was used as a model for HUMAN(NAT1) in this particular series of experiments.

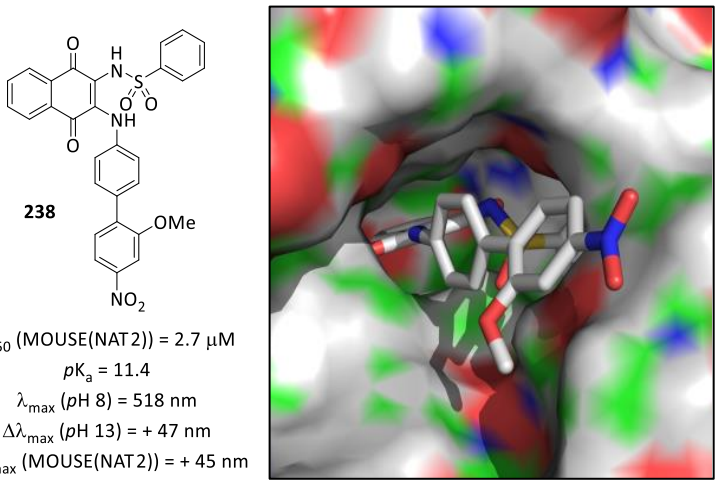


Figure 4.2: Left: Key pharmacological and colorimetric data on compound **238**. **Centre and Right:** *In silico* modelling of biaryl derivative **238** in the active site of HUMAN(NAT1) (pdb: 2PQT).[247b] Protein is shown in both surface representation **(centre)** and cartoon representation **(right)**. Analysis performed using GOLD® (v.5.2).[282] Predicted polar contacts are highlighted by dashed black lines with inter-atomic distances given in Ångströms; key active site residues Arg127 and Tyr129 are highlighted in stick representation (carbon atoms in green).

In silico modelling of compound **238** in the active site of HUMAN(NAT1) suggests that **238** is capable of binding in an analogous fashion to that of previously synthesised naphthoquinone derivatives, with the C_3 biaryl amino subsituent protruding out of the active site into bulk solvent **(Figure 4.2)**. Interestingly, colorimetric evaluation of **238** revealed a pK_a of 11.4, which is unexpectedly higher than those of derivatives **217**, **218** and **220**; however, in the presence of MOUSE(NAT2) a shift in the λ_{max} value of +45 nm relative to that in a *p*H 8 buffer solution is observed (*cf.* a shift of +47 nm in *p*H 13 buffer solution). This not only suggests that **238** does indeed bind in the fashion predicted by the *in silico* model, but also that the pK_a values of previously reported biaryl derivatives **217**, **218** and **220** (10.5, 10.3 and 10.1 respectively) are unlikely to preclude a colour change of these compounds in the MOUSE(NAT2) active site; rather, it seems more probable that these species do in fact adopt a different binding mode in the active site in which there is no ionic interaction between their sulfonamide moieties and the Arg127 residue of MOUSE(NAT2) which can drive the colour change.

Analysis of the fluorescence properties of biaryl derivative **238** was subsequently carried out by Robert Barker (RB). **238** was initially evaluated at a 150 µM concentration in a 95% Tris•HCl (*p*H 8.0)/5% DMSO (*v/v*) solution of total volume 100 µL (for protocol see **Section 7.13.6.**); this high concentration was used to ensure that no low-intensity fluorescent peaks were overlooked. After systematic excitation of **238** over a range of wavelengths (beginning at λ_{ex} = 200 nm and increasing λ_{ex} by a 5 nm increment each time), an emission peak was identified at λ_{em} = 424 nm, which corresponds to excitation peaks of λ_{ex} = 372 nm and 408 nm **(Figure 4.3)**. These peaks are also observed if the buffer solution is acidified to *c. p*H 2 by the addition of 1 M aq. HCl, but not if the buffer solution is basified to *c. p*H 14 by the addition of 1 M aq. NaOH. If the basic solution is reacidified to *p*H 8 by the addition of an equal volume of 1 M aq. HCl, the fluorescent excitation and emission peaks are restored to their initial intensities.

This result offers the exciting indication that compound **238** acts as a reversible "off-on" *p*H-dependent fluorescent switch; however, the fluorescence intensity of the compound is relatively low and must be increased before studies in the presence of MOUSE(NAT2) can be

carried out. In further investigations, **238** is considered a "second generation" lead compound due to its progressive development from the initial hit compound **32**.

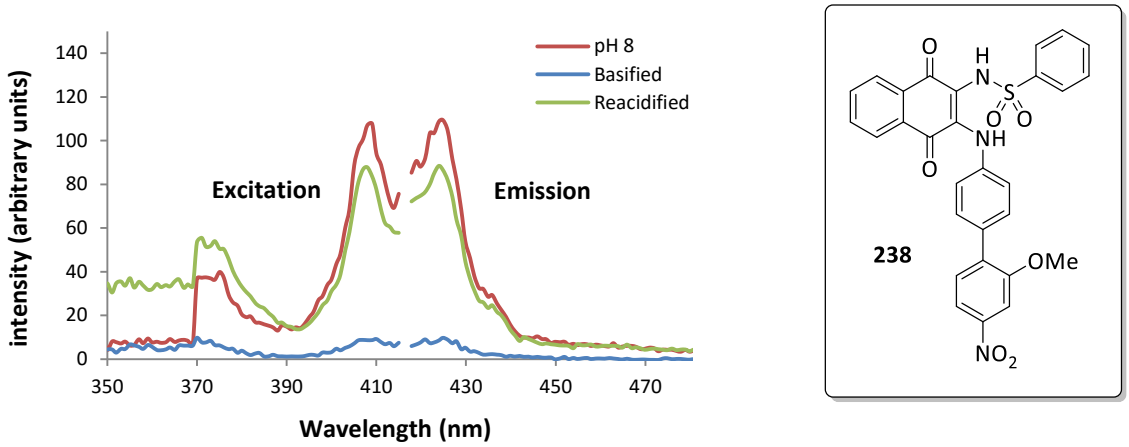


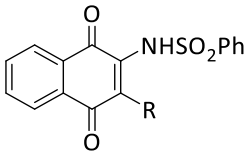
Figure 4.3: Blank-corrected excitation (λ_{em} = 424 nm) and emission (λ_{ex} = 408 nm) fluorescence spectra of **238** measured in Tris•HCl (*p*H 8) buffer solution (red lines), after basification with 5 µL 1 M aq. NaOH (blue lines), and after subsequent reacidification to *c. p*H 8 by the addition of 5 µL 1 M aq. HCl (green lines).[308] The concentration of **238** was 150 µM and of DMSO was 5% (*v/v*); sensitivity voltage = 800 V.

4.1.2. Synthesis and Evaluation of a Biaryl-Based Library Derived from Compound 238

In order to learn more about the fluorescent properties of biaryl amino-substituted naphthoquinone derivatives such as **238**, a library of target biaryl substituents was designed **(Table 4.1)** with two main investigations envisaged:

(a) Does substitution of the methoxy group on the biaryl at differing positions relative to the nitro group (targets **243-245**) affect properties such as fluorescence intensity, λ_{em}, λ_{ex}, pK_a and potency against MOUSE(NAT2)?

(b) Are both an electron-donating group and an electron-withdrawing group required for observation of the *p*H-dependent fluorescent switch, or is it possible to observe such behaviour with either only one electron-poor (**246**) or electron-rich group (**247**) present – or, in fact, if two of each such substituent are present (**248** and **249** respectively)?



238, 243-249

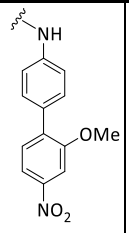
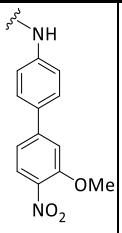
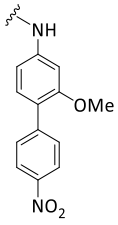
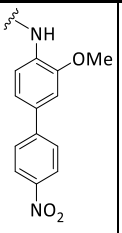
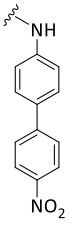
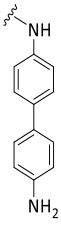
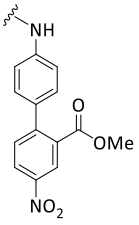
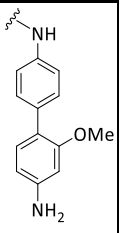
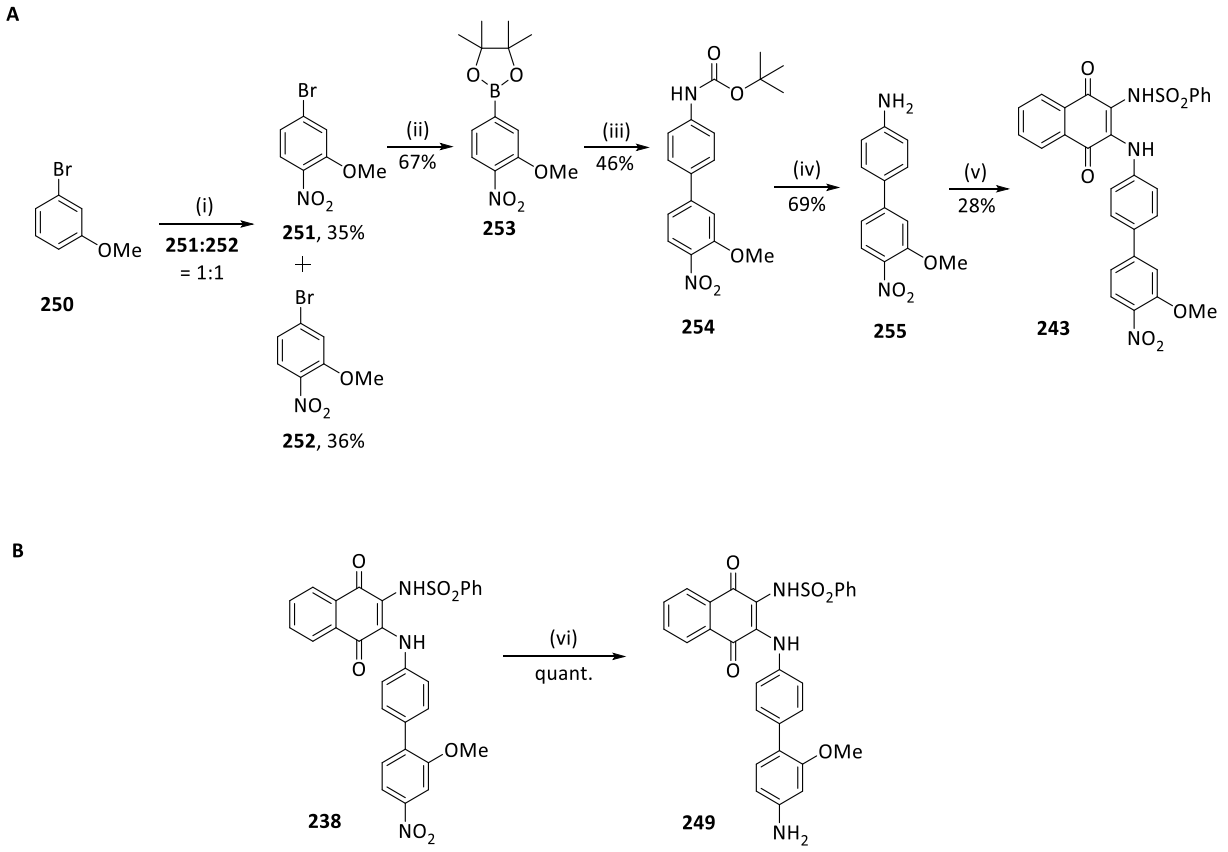
Compound	238	243	244	245	246	247	248	249
C_3 Substituent								

Table 4.1: Target biaryl derivatives to be synthesised, to explore the effect of different biaryl substitution patterns on pharmacological and optical properties.

Target derivative **243**, in which the nitro and methoxy groups are bound to the same aromatic ring in the biaryl moiety with an *ortho* relationship, was synthesised by RB utilising an analogous procedure to the second generation lead **238 (Scheme 4.2A)**. However, in this case, the required 3-methoxy-4-nitrobromobenzene **251** was not commercially available, and was hence synthesised by a nitration of 3-methoxybromobenzene **250** (conditions (i)).[309] The isolated yield of **251** was modest (35%) due to the formation of both the 4-nitro **251** and 6-nitro **252** regioisomers in the nitration step which were challenging to separate *via* column chromatography on silica gel; analysis of the crude reaction mixture by ^1H-NMR suggests that **251** and **252** are formed in a 1:1 ratio. Yields for the subsequent steps (ii)-(v) to give the desired target **243** were all lower than those reported for the analogous synthesis of **238 (Scheme 4.1)**.

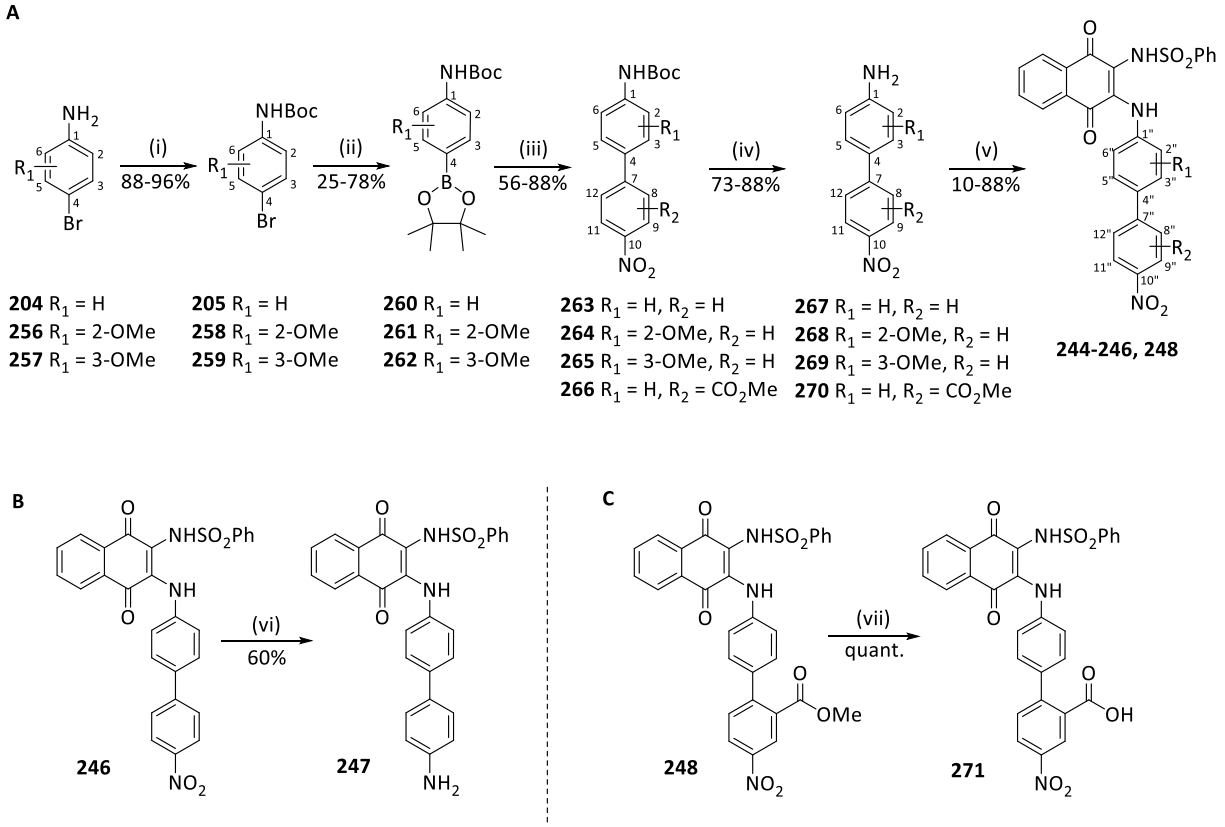
In addition, it was possible to access target compound **249**, which bears two electron-donating substituents on the biaryl moiety, in a single catalytic hydrogenation step from second generation lead **238** in a quantitative yield **(Scheme 4.2B)**.



Scheme 4.2: A: Synthesis of biaryl derivative **243**; data generated by RB.[308] **B:** Synthesis of biaryl derivative **249**. *Reagents and conditions:* (i) 70% HNO_3:c. H_2SO_4 (5:4), 50 ^oC, 16 h; (ii) B_2Pin_2 (1.5 eq.), KOAc (3.0 eq.), $Pd(PPh_3)_2Cl_2$ (0.05 eq.), 1,4-dioxane, 100 ^oC, 3 h; (iii) *tert*-butyl (4-bromophenyl)carbamate **205** (0.5 eq.), $Pd(PPh_3)_2Cl_2$ (0.05 eq.), THF:sat. aq. $NaHCO_3$ (22:5), 100 ^oC, 16 h, yield quoted *w.r.t.* carbamate **205**; (iv) TFA:CH_2Cl_2 (1:5), RT, 2 h; (v) 2-benzenesulfonamido-3-chloro-1,4-naphthoquinone **57** (1.0 eq.), $CeCl_3 \bullet 7H_2O$ (1.0 eq.), MeOH, RT, 16 h *then* biaryl amine **255** (3.0 eq.), 90 ^oC, 16 h; (vi) H_2 (1 atm.), 10% Pd/C (0.1 eq.), MeOH, RT, 16 h.

Attempts to access singly-substituted nitro derivative **246** *via* an analogous synthetic route however proved challenging due to a poor conversion to the desired biaryl species in the cross-coupling step (iii).[308] Therefore, it was hypothesised that the Suzuki-type cross-coupling step might proceed more efficiently if the coupling partners were switched, *i.e.* if *tert*-butyl (4-bromopehnyl)carbamate **205** was converted to its corresponding boronic pinacol ester **260** and subsequently coupled to 4-bromonitrobenzene. This exploits the inherent preference for electron-poor halides to undergo oxidative addition with Pd(0) and more electron-rich boronic esters to undergo efficient transmetallation.[203] This strategy proved successful, with the Suzuki-type cross-coupling between **260** and *para*-bromonitrobenzene effected in 56% yield,

and was subsequently utilised by RB not only for the synthesis of target compound **246**, but also of **244**, **245** and **248**, all of which contain biaryl moieties in which one of the two aromatic rings is very electron poor **(Scheme 4.3A; Table 4.2)**.

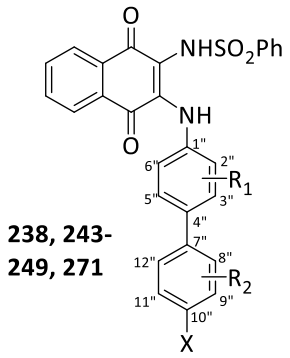


Scheme 4.3: A: Synthetic route to access biaryl derivatives containing one very electron-poor aromatic ring; data generated by RB.[308] **B:** Synthesis of amino-substituted biaryl derivative **247** from the corresponding nitro-substituted analogue **246**; data generated by RB.[308] **C:** Synthesis of carboxylic acid **271** from methyl ester **248**; data generated by RB.[308] *Reagents and conditions:* (i) Boc_2O (1.0 eq.), $InCl_3$ (0.01 eq.), 35 ^oC, 45 min; (ii) B_2Pin_2 (1.5 eq.), KOAc (3.0 eq.), $Pd(PPh_3)_2Cl_2$ (0.05 eq.), 1,4-dioxane, 120 ^oC, 3 h; (iii) requisite arylbromide (0.5 eq.), $Pd(PPh_3)_2Cl_2$ (0.05 eq.), THF:sat. aq. $NaHCO_3$ (22:5), 100 ^oC, 16 h, yield quoted *w.r.t.* arylbromide; (iv) TFA:CH_2Cl_2 (1:5), RT, 2 h; (v) 2-benzenesulfonamido-3-chloro-1,4-naphthoquinone **57** (1.0 eq.), $CeCl_3 \bullet 7H_2O$ (1.0 eq.), MeOH, RT, 16 h *then* add requisite biaryl amine (3.0 eq.), 90 ^oC, 16 h; yields for these steps are given in **Table 4.2**; (vi) H_2 (1 atm.), 10% Pd/C (0.1 eq.), MeOH, RT, 16 h; (vii) 1 M aq. NaOH (5.0 eq.), MeOH, 60 ^oC, 48 h *then* HCl, RT.

Target Compound	R_1	R_2	Yield for Step				
			(i)	(ii)	(iii)	(iv)	(v)
246	H	H	89%	78%	56%	86%	23%
244	2''-OMe	H	96%	72%	72%	73%	86%
245	3''-OMe	H	88%	25%	73%	88%	10%
248	H	8''-CO_2Me	89%	78%	45%	77%	88%

Table 4.2: Yields for steps (i)-(v) from the synthesis of target derivatives outlined in **Scheme 4.3**.[308]

Furthermore, target compound **247**, bearing a single amino group on the biaryl moiety, was accessed from nitro-substituted **246** in a catalytic hydrogenation step **(Scheme 4.3B)**. The formation of ester-substituted **248** also provided the opportunity to access carboxylic acid **271** *via* a basic ester hydrolysis **(Scheme 4.3C)**. Since it is predicted that the biaryl moiety of these ligands extends out of the enzyme active site, the presence of a carboxylic acid group might enable stabilising interactions to solvent molecules which could increase inhibitory potency.



238, 243-249, 271

Compound	238	243	244	245	246	247	248	249	271
R_1	All H	All H	3''-OMe	2''-OMe	All H	All H	All H	All H	All H
R_2	8''-OMe	9''-OMe	All H	All H	All H	All H	8''-CO_2Me	8''-OMe	8''-CO_2H
X	NO_2	NO_2	NO_2	NO_2	NO_2	NH_2	NO_2	NH_2	NO_2
IC_{50} MOUSE(NAT2) (μM)	2.7 ± 0.54	1.9 ± 0.6	27.9 ± 7.6	1.0 ± 0.63	2.7 ± 0.6	0.64 ± 0.08	>30	1.6 ± 0.35	0.51 ± 0.06
R^2	0.8545	0.5600	0.5673	0.8668	0.7706	0.9503	N/A	0.7779	0.9792
P	***	**	***	***	***	***	N/A	***	***

Table 4.3: IC_{50} values against MOUSE(NAT2) for biaryl derivatives **238, 243-249** and **271** in the acetyl CoA hydrolysis assay; data calculated using KyPlot® software by RB.[308] IC_{50} values are quoted ± one standard deviation, with squared correlation coefficients (R^2) and significance levels (*P*) as given; ** = P <0.01; *** = P <0.005.

All of the synthesised biaryl derivatives were evaluated in the acetyl CoA hydrolysis assay against MOUSE(NAT2); the calculated IC_{50} values are given in **Table 4.3**.

The data reveal that many of these biaryl derivatives display promising potency against MOUSE(NAT2). Substitution of the methoxy group at any of the 2'', 8'' or 9'' positions on the biaryl moiety leads to a comparable inhibitory potency, although the 3''-methoxy substituted analogue **244** is an order of magnitude less potent; this could be due to the methoxy group at this position forcing the two rings of the biaryl to twist relative to one another into an unfavourable conformation for binding to MOUSE(NAT2). Derivative **246**, which does not possess a methoxy substituent at all, also has a similar IC_{50} to the second generation lead **238**. Furthermore, by comparison of compounds **246** and **247**, it can be observed that conversion of this electron-withdrawing nitro group to an electron-donating amino group leads to approximately a four-fold increase in potency. This result is consistent with the findings of **Chapter 3**, in which electron-rich biaryl analogues **217**, **218** and **220** all possessed IC_{50} values <1 μM against MOUSE(NAT2) in the acetyl CoA hydrolysis assay. However, the effect of adding a second electron-donating substituent does not appear to confer an additive increase in potency, as compound **249** with an additional methoxy substituent is less potent an inhibitor than compound **247**; when a Student's *T*-Test is performed, the difference between the IC_{50} values of **247** and **249** is shown to be statistically significant (P = <0.01).

Finally, it can be noted that derivative **248**, bearing two electron-withdrawing groups, is a poor MOUSE(NAT2) inhibitor, with an IC_{50} value of greater than 30 μM. However, conversion of the ester functionality in **271** to a carboxylic acid functionality gives an increase in potency of at least two orders of magnitude; **271** has an IC_{50} value of 0.51 μM against the target protein. *In silico* modelling of **271** in the HUMAN(NAT1) active site suggests a similar mode of binding to second generation lead **238**, and that the carboxylic acid derivative might be capable of forming stabilising hydrogen-bonding interactions both with solvent molecules outside of the enzyme active site and with the hydroxyl group of the Ser214 residue which lines the entrance channel to the active site **(Figure 4.4)**.

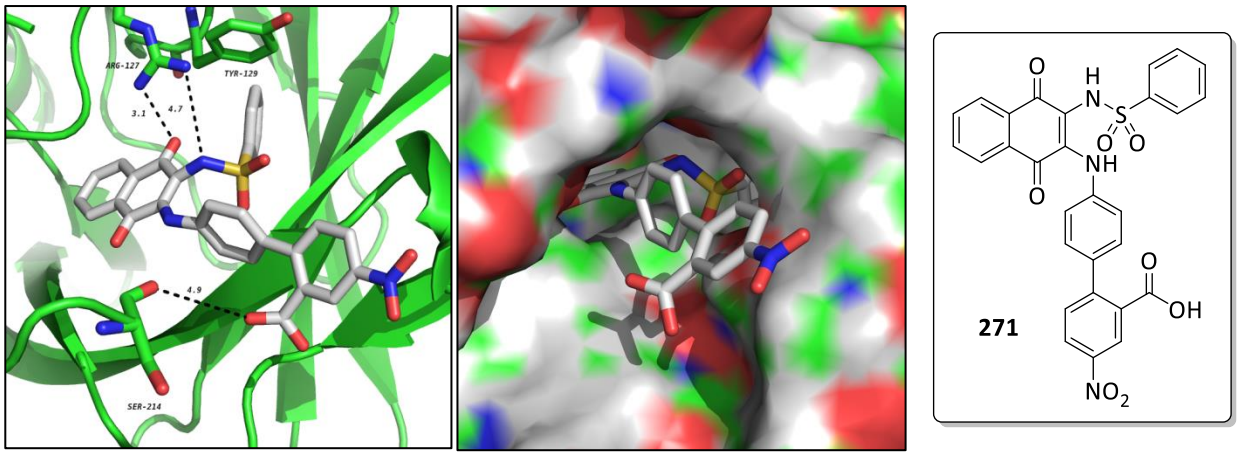


Figure 4.4: *In silico* modelling of carboxylic acid derivative **271** in the active site of HUMAN(NAT1) (pdb: 2PQT)[247b], showing a potential interaction between the acid moiety and the hydroxyl group of Ser214. The protein is shown in both surface representation **(centre)** and cartoon representation **(left)**. Analysis performed using GOLD® (v.5.2).[282] Key polar contacts are highlighted by dashed black lines with inter-atomic distances given in Ångströms; key active site residues Arg127 and Tyr129, in addition to Ser214 which lines the entrance to the active site, are highlighted in stick representation (carbon atoms in green).

Subsequently, the optical properties of this library of biaryl derivatives were investigated. Initially, the colorimetric properties of the compounds were determined, and crucially, it was found that most of the inhibitors in this series possess appropriate *p*K_a values for use as probes, and all show a shift in λ_{max} in the presence of MOUSE(NAT2). This suggests a mode of binding for these compounds which involves sequestration of the conjugate base to form an ionic interaction with Arg127 **(Table 4.4)**. The exception is ester-substituted **248**, which contains two electron-withdrawing groups on the biaryl moiety, lowering its *p*K_a (7.7) relative to the rest of the series; however, this species still shows a clear shift in λ_{max} in the presence of MOUSE(NAT2) of +93 nm. Furthermore, the absorption coefficients of these species are generally comparable with those of the biaryl derivatives evaluated in **Chapter 3**. Notably, however, the carboxylic acid derivative **271** possesses very low sensitivity, with ε_N and ε_{CB} values of only 4540 $M^{-1}cm^{-1}$ and 2530 $M^{-1}cm^{-1}$ respectively.

Compound	238	243	244	245	246	247	248	249	271
pK_a	11.4 ± 0.5	10.5 ± 0.3	9.5 ± 0.2	10.7 ± 0.3	9.9 ± 0.3	8.9 ± 0.4	7.7 ± 0.3	9.2 ± 0.4	8.1 ± 0.3
λ_{max} *p*H 8 (nm)	518	513	504	528	484	528	529	529	484
$\Delta\lambda_{max}$ *p*H 13 (nm)	+47	+53	-41	+38	+64	+44	+13	+54	+78
$\Delta\lambda_{max}$ MOUSE(NAT2) (nm)	+45	+86	N.D.	+40	+112	+106	+93	+104	+148
ε_N ($M^{-1}cm^{-1}$)	21500	18300	2130	14700	7760	7060	8010	8990	4540
ε_N /ε_N (32)	1.80	1.53	0.18	1.23	0.65	0.59	0.67	0.75	0.38
ε_{CB} ($M^{-1}cm^{-1}$)	8320	7280	1213	6590	3780	4410	4290	4730	2530
ε_{CB} /ε_{CB} (32)	1.26	1.10	0.18	1.00	0.57	0.67	0.65	0.72	0.38

Table 4.4: Colorimetric properties of the biaryl derivative library. N.D. = not determined. Data generated by RB.[308]

Following this, the library was screened for fluorescence activity at *p*H 8 and under basic conditions, using the same protocol as for compound **238 (Table 4.5)**; first generation hit compound **32** was also included in these experiments as a control. Interestingly, all members of the biaryl library fluoresce with the same excitation and emission wavelengths as compound **238** (λ_{ex} = 372 and 408 nm; λ_{em} = 424 nm), except for carboxylic acid derivative **271**, which displays no fluorescence at all. Each of these fluorescent peaks is reversibly quenchable, *i.e.* the initial peak intensities are restored upon reacidification of the basic samples with 5 µL 1 M aq. HCl. Furthermore, as initially hypothesised, it would appear that the species with the highest fluorescence intensities are those bearing both an electron-donating group and an electron-withdrawing group on the biaryl moiety: the most strongly fluorescent compound is the second generation lead **238**, followed by compounds **246** and **244**, which also bear one methoxy and one nitro substituent each. Perhaps the most important result, however, is that the 3,5-dimethylanilino-substituted initial hit compound **32** is also found to fluoresce in a similar fashion, with an intensity of approximately half that of biaryl **238**. This gives rise to speculation about the origin of the fluorescence, and suggests that the biaryl moiety does not alone confer fluorescent properties on this series of compounds.

Compound		32	238	243	244	245	246	247	248	249	271
pK_a		9.2 ± 0.05	11.4 ± 0.5	10.5 ± 0.3	9.5 ± 0.2	10.7 ± 0.3	9.9 ± 0.3	8.9 ± 0.4	7.7 ± 0.3	9.2 ± 0.4	8.1 ± 0.3
Fluorescence Emission Intensity at 424 nm (λ_{ex} = 408 nm) (a.u.)	***p*H 8**	61	126	67	8	75	27	26	61	16	0
	+ Base	0	0	0	0	0	0	0	0	0	0

Table 4.5: Comparison of fluorescence emission intensities observed for 3,5-dimethylanilino-substituted species **32** and the members of the biaryl-substituted library, **238**, **243-249** and **271**, at *p*H 8 and under basic conditions; data generated by RB.[308] Experiments at *p*H 8 were carried out in 95% 20 mM Tris•HCl (*p*H 8)/5% DMSO (*v/v*); basification was effected by addition of 5% 1 M aq. NaOH to these solutions. Sensitivity voltage = 800 V; a.u. = arbitrary units.

4.1.3. Determining the Molecular Mechanism of Fluorescence: A Screen of the Naphthoquinone Library

In light of the finding that 3,5-dimethylanilino-substituted species **32** fluoresces in a similar manner to the biaryl-substituted derivatives, further compounds selected from the SAR libraries described in **Chapter 3** that do not contain a biaryl moiety were also screened for fluorescent properties in a similar fashion **(Table 4.6)**. Each of these species was found to possess the same distinctive fluorescent peaks at λ_{ex} = 372 and 408 nm and λ_{em} = 424 nm, and in each case only the neutral form of the compound was found to fluoresce and not the conjugate base species.

These findings suggest that the biaryl unit in compounds **238** and **243-249** is not the structural motif which leads rise to their fluorescent properties. Indeed, the only moiety common to all of the fluorescent molecules is the naphthoquinone core itself; naphthoquinones have been reported in the literature to fluoresce, albeit with generally low intensities.[310] The data in **Tables 4.5 and 4.6** also suggest that an increase in electron density on the naphthoquinone core, brought about by deprotonation of the acidic sulfonamide-N*H*, causes a quenching of the fluorescence, since the *p*H at which fluorescence is quenched correlates with the pK_a of each tested species, as measured by colorimetric titration. Indeed, when a fluorescent

titration experiment on second generation lead compound **238** was carried out, plotting *p*H against fluorescent emission intensity, the pK_a value generated of 10.5 ± 0.8 was found to be approximately consistent with that generated *via* the colorimetric method (11.4 ± 0.4).

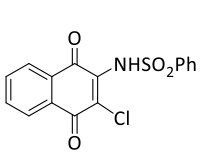
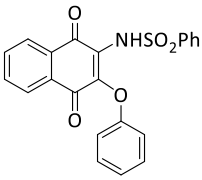
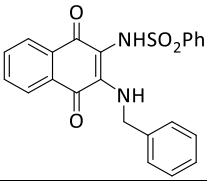
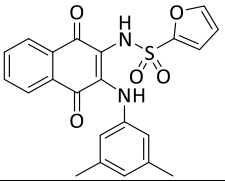
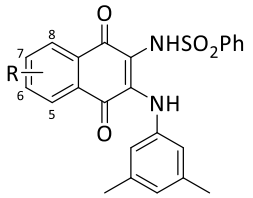
Compound		**57**	**97**	**88**	**118**
Structure					
pK_a		3.0	5.0	10.4	8.3
Fluorescence Emission Intensity at 424 nm (λ_{ex} = 408 nm) (a.u.)	**+ Acid**	50	108	197	68
	***p*H 8**	0	0	99	32
	+ Base	0	0	0	0

Table 4.6: Fluorescent emission properties of a selection of representative naphthoquinones lacking a C_3 biaryl substituent under various conditions of *p*H; data on compounds **57**, **97** and **118** generated by RB.[308] Experiments at *p*H 8 were carried out in 95% 20 mM Tris•HCl (*p*H 8)/5% DMSO (*v/v*); basification was effected by addition of 5% 1 M aq. NaOH to these solutions and acidification by addition of 5 µL 1 M aq. HCl. Sensitivity voltage = 800 V; a.u. = arbitrary units.

The variation in fluorescence emission intensities for each member of the tested compound library may well reflect the variation of electron density on the naphthoquinone core. To investigate this hypothesis in more detail, analogues of the initial hit compound **32** which bear nitro or amino substituents directly on the C_5-C_8 positions of the naphthoquinone core, which were synthesised in a previous study[281a] and discussed in **Chapter 3**, were evaluated for their fluorescence properties **(Table 4.7; Figure 4.5)**. As anticipated, each member of this series displayed the characteristic fluorescent emission at λ_{ex} = 372, 408 nm and λ_{em} = 424 nm, and these peaks are reversibly quenched above the pK_a of each compound. Interestingly, there appears to be a positive correlation between how electron-withdrawing each substituent (H, NO_2 or NH_2) is and the fluorescence intensity of the molecule under acidic conditions. This supports the hypothesis that increasing the electron density on the naphthoquinone core reduces the intensity of fluorescence.



32, 190-191, 272-277

Compound	R	pK_a	Fluorescence Emission Intensity at 424 nm (a.u.)		
			Acidic conditions	*p*H 8	Basic conditions
32	H	9.2	61	61	0
272	5-NO_2	8.2	99	77	0
273	5-NH_2	N.D.	47	47	0
274	6-NO_2	7.5	43	35	0
275	6-NH_2	N.D.	21	32	0
276	7-NO_2	8.0	115	106	0
191	7-NH_2	N.D.	44	49	0
277	8-NO_2	8.6	94	85	0
190	8-NH_2	8.4	78	86	0

Table 4.7: Fluorescence intensities of C_5-C_8 nitro- and amino-substituted derivatives of compound **32** at *p*H 8 and under acidic and basic conditions; data generated by RB.[308] Experiments at *p*H 8 were carried out in 95% 20 mM Tris•HCl (*p*H 8)/5% DMSO (*v/v*); basification was effected by addition of 5% 1 M aq. NaOH to these solutions and acidification by addition of 5% 1 M aq. HCl. pK_a values are those determined in a previous study by colorimetric titration.[281a] Sensitivity voltage = 800 V; λ_{ex} = 408 nm; a.u. = arbitrary units; N.D. = not determined.

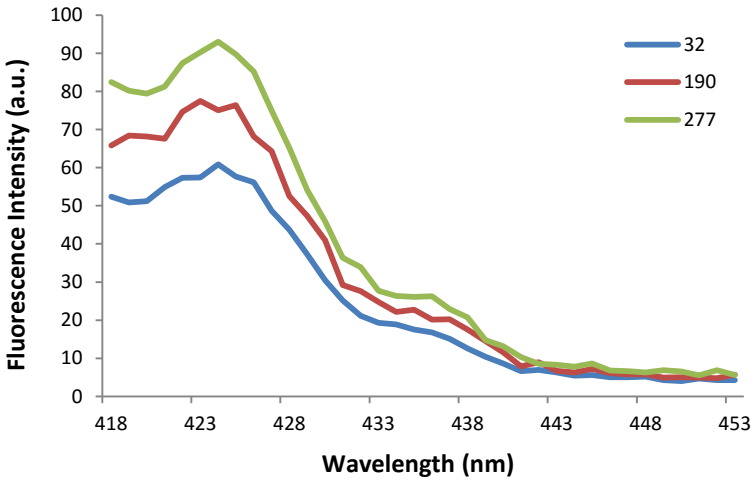


Figure 4.5: Fluorescence emission spectra of unsubstituted **32** (blue line), 8-amino substituted **190** (red line) and 8-nitro substituted **277** (green line) under acidic conditions, as a representative example to show the correlation between electron density on the naphthoquinone core and the intensity of emission; data generated by RB.[308] Sensitivity voltage = 800 V; λ_{ex} = 408 nm; a.u. = arbitrary units.

The studies described thus far have yielded key mechanistic insights into the mechanism of molecular fluorescence of naphthoquinone analogues based on lead compounds **32** and biaryl-susbtituted **238**. Promisingly, it has been identified that compounds containing an acidic sulfonamide-N*H* undergo a reversible quenching of fluorescence under basic conditions,

suggesting that they have the potential to be used as *p*H-dependent "on-off" fluorescent molecular switches. However, none of the compounds evaluated thus far possess a high enough intrinsic fluorescent sensitivity to enable *in vitro* assays to be carried out with the desired target proteins MOUSE(NAT2) or HUMAN(NAT1), since the highest reported fluorescent emission intensity amongst the tested library is 126 a.u. at 150 μM for the second generation lead compound **238**.

Therefore, efforts were turned to further development of the C_3 substituent to determine whether it is possible to significantly enhance the fluorescent output of molecules based on compounds **32** and **238**, whilst retaining a *p*H-dependent switch in fluorescent intensity brought about by deprotonation of the sulfonamide-N*H* on the C_2 substituent.

4.2. Pursuit of a PET-Quenched System: Inserting a Linker

Many molecular fluorescent switches reported in the scientific literature are reliant on the principle of photoelectron transfer (PET). PET is a light-induced intramolecular electron transfer from an electron donor moiety to an electron acceptor moiety **(Figure 4.6A)**; this generates a charge-separated species which can undergo non-radiative relaxation to return to the ground electronic state. As a result, PET is a reduction potential-dependent process, *i.e.* if the reduction potential of the electron acceptor moiety within the molecule of interest is decreased, PET will less readily occur from the electron donor moiety upon light-induced electronic excitation.

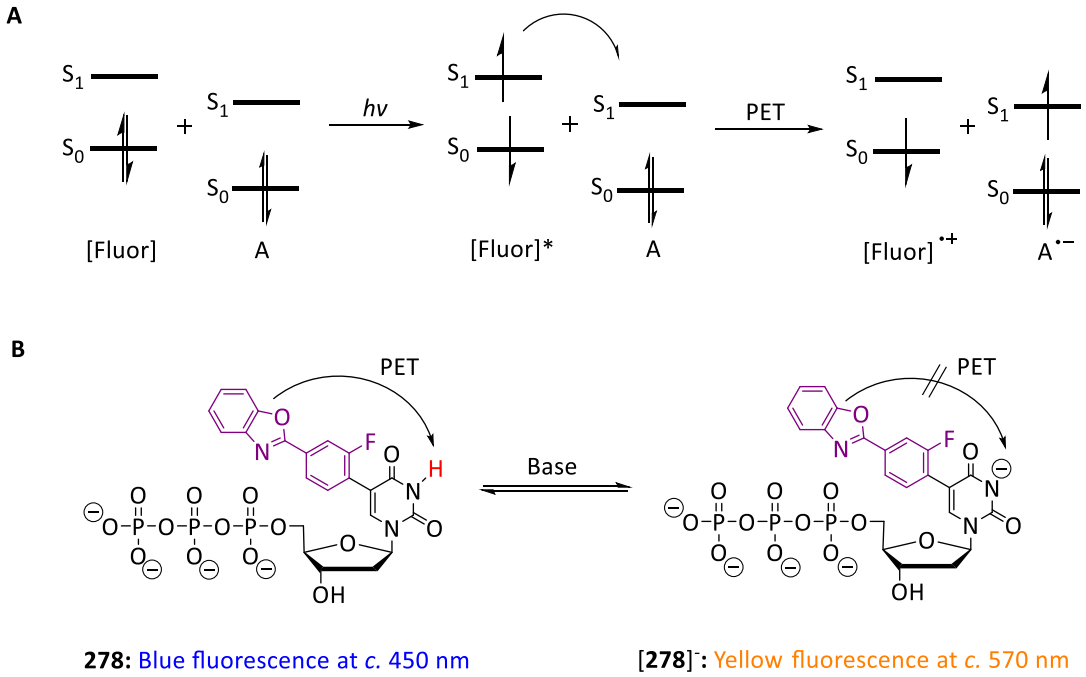


Figure 4.6: A: Energy level diagram to show the electronic processes involved in a PET-quenched fluorescent probe. [Fluor] = fluorophore; A = acceptor; * indicates an excited state. **B:** Uracil-based *p*H-dependent ratiometric fluorescent probe **278** developed by Riedl *et al.* (2012), which shows a shift in λ_{em} upon deprotonation of the acidic uracil-N*H*.[311]

The reduction potential dependence of PET has recently been exploited by Riedl *et al.* in order to generate the *p*H-dependent fluorescent probe **278** based on a uracil oligonucleotide **(Figure 4.6B)**.[311] Under acidic conditions, an electron from the benzoxazole fluorophore in **278** can be excited and subsequently undergoes PET to the uracil moiety; this species displays a blue fluorescence with λ_{em} = *c.* 450 nm. However, upon deprotonation of the acidic N*H* (highlighted in red) to give [**278**]$^-$, the uracil moiety becomes more electron rich and hence possesses a decreased reduction potential. This ensures that PET quenching can no longer occur when an electron in the benzoxaaole group is photochemically excited, and so this electron relaxes to the ground state in a radiative fashion, giving rise to a shifted fluorescent λ_{em} of *c.* 570 nm. Thus this system constitutes a "ratiometric" *p*H-dependent fluorescent probe, whereby the ratio of the fluorescent emission peak heights at *c.* 450 and 570 nm is correlated to the *p*H of the medium the probe is in. Relative fluorescent emissions at these two wavelengths can thus be measured to determine the *p*H of a biological medium.

Taking inspiration from Riedl's system, a PET-quenched probe for HUMAN(NAT1) or MOUSE(NAT2) based on biaryl-substituted **238** was designed **(Figure 4.7)**. It was reasoned that if a linker was inserted between the naphthoquinone core and the C_3 biaryl substituent, such that the two groups were no longer directly conjugated to one another, photoexcitation might become possible from the biaryl moiety. It was envisaged that in such a neutral (*i.e.* protonated) species, PET of this excited electron from the biaryl moiety to the naphthoquinone core, which is a good electron acceptor, might occur, leading to little or no fluorescence of the neutral species; however, upon deprotonation of the sulfonamide-N*H*, the electron density on the naphthoquinone core might be sufficiently increased so as to preclude PET quenching, and hence fluorescence might be observed from the biaryl moiety. It was hoped that this strategy could lead to the generation of a fluorescent "off-on" *p*H-dependent switch which could also be dependent on the concentration of HUMAN(NAT1) or MOUSE(NAT2) present in a solution.

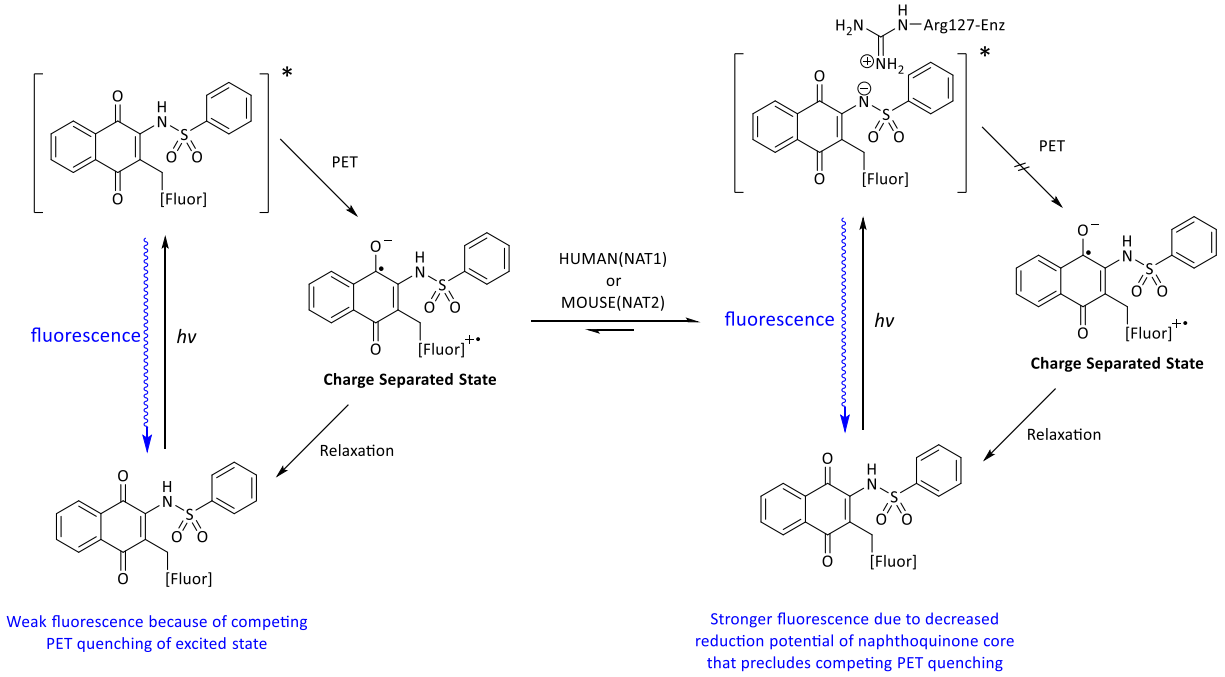


Figure 4.7: Proposed mechanism of action for an "off-on" fluorescent probe for HUMAN(NAT1) or MOUSE(NAT2), in which the neutral (protonated) species undergoes PET quenching but the conjugate base (deprotonated) species sequestered by the enzyme contains a more electron-rich naphthoquinone core, which is less able to accept an electron and thus might prevent PET quenching, leading to an increase in fluorescence intensity. [Fluor] = fluorophore; * indicates an excited state.

It was decided to use a methylene unit as the required linker: this could ensure that the biaryl and naphthoquinone moieties are in close proximity to one another, which ought to facilitate PET; and furthermore, a methylene linker is not too sterically cumbersome. Compounds **279**, **280** and **281** were therefore all conceived as target probes **(Figure 4.8)**; [2,7]-, [3,7]- and [4,7]-linked biaryls were all considered desirable targets as each would be predicted to present a very different conformation in solution, and hence their ability to bind to the HUMAN(NAT1) or MOUSE(NAT2) active site might vary considerably. A methoxy substituent was also designed into each probe, since other methoxy-susbtituted biaryl derivatives have been shown to have high potencies (*cf.* **Chapter 3**), and unsubstituted biaryls were previously found to be highly insoluble. Furthermore, by ensuring that a nitrogen atom remains directly bonded to the C_3 position of the naphthoquinone core, probes **279**, **280** and **281** ought to retain pK_a values within the desirable range.

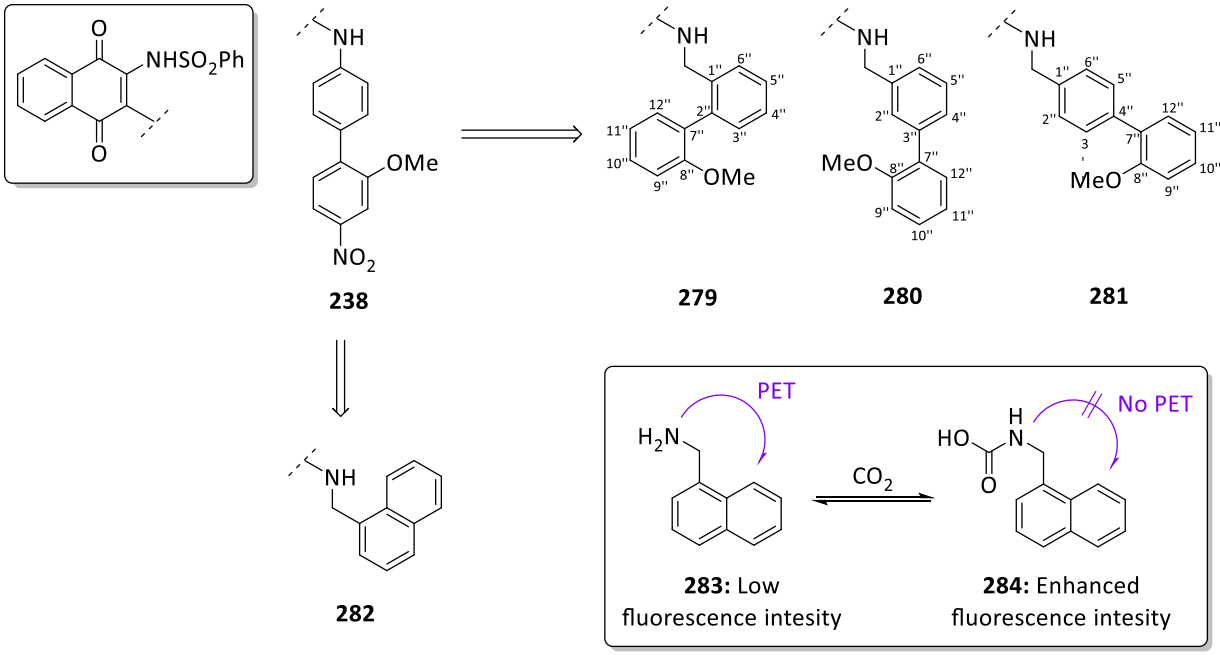
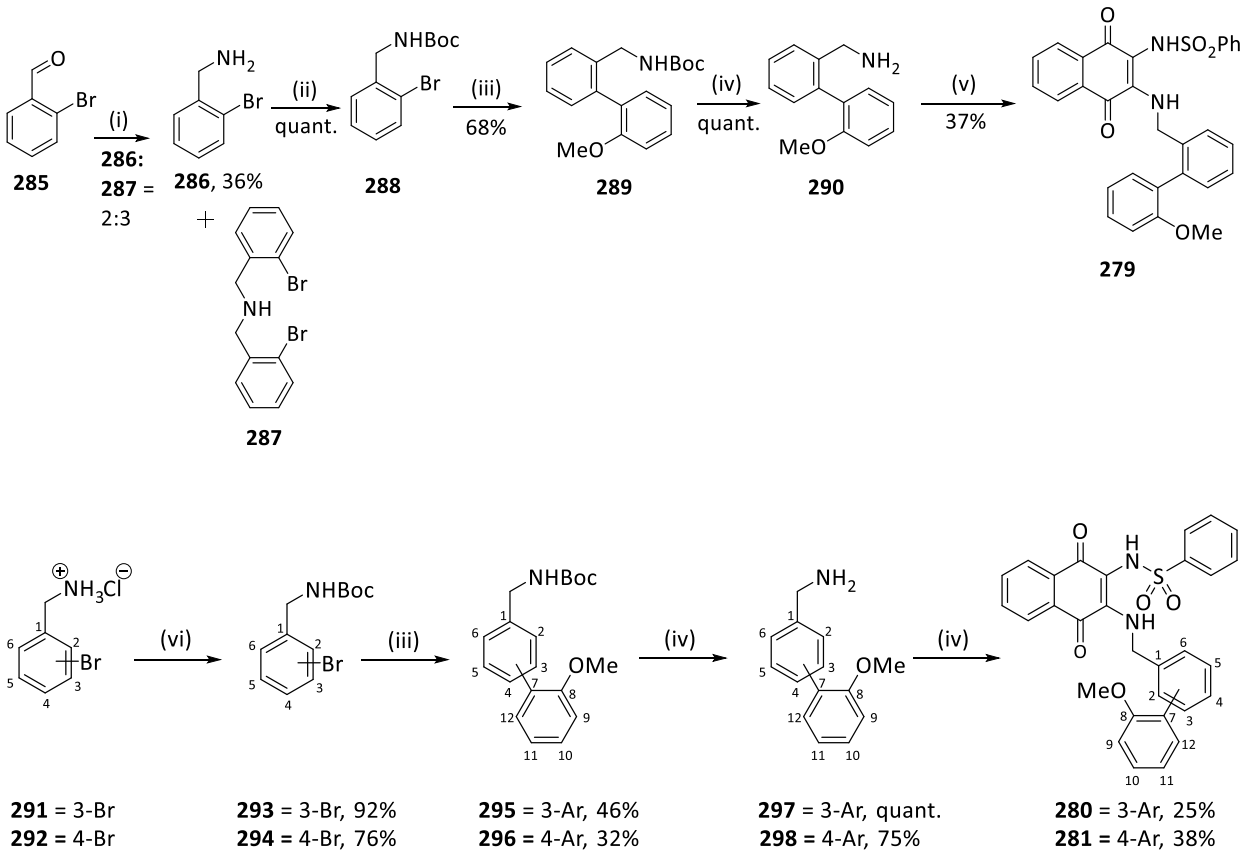


Figure 4.8: Second-generation lead compound **238**, and proposed derivatives in which a methylene linker is inserted to ensure a break in conjugation between the biaryl and naphthoquinone systems within the molecules. **Inset:** Naphthalene-based PET sensor **283** for CO_2 sensing, reported by Herman *et al.* (1999).[312]

One other target of interest is methylnaphthyl derivative **282**, since naphthalenes are also reported in the literature to fluoresce and are of a similar size to a biaryl substituent;[313] however, they possess less conformational flexibility in solution than biaryl moieties and are necessarily planar, which may be of benefit to their fluorescence properties. Furthermore, 1-naphthylmethylamine **283** is reported in the literature as a PET-based fluorescent sensor for CO_2:[312] in the absence of CO_2, the amine lone pair can undergo PET to the aromatic core of the naphthyl group, preventing **283** from being highly fluorescent; however, in the presence of CO_2, an equilibrium is established between **283** and carbamate **284**, which cannot undergo PET and hence is more highly fluorescent, with the fluorescent output correlating with the concentration of CO_2 present.

4.2.1. Synthesis of the Methylene-Linked Biaryls 279-281 and Naphthyl 282

Methylene-linked [2,7]-biaryl **279** was synthesised by RB in five steps from *ortho*-bromobenzaldehyde **285 (Scheme 4.4A)**. Reductive amination of arylaldehyde **285** with aqueous ammonia and sodium cyanoborohydride (conditions (i))[314] gave a mixture of the mono- and di-substituted *ortho*-bromobenzylamines **286** and **287** in a 2:3 ratio; the desired mono-substituted adduct **286** could subsequently be cleanly isolated in a 36% yield. Amine **286** was next protected to give *tert*-butyl carbamate **288** in a quantitative yield utilising the previously described procedure with catalytic $InCl_3$ (conditions (ii)). Suzuki-type cross-coupling[203] of carbamate **288** with 2-methoxybezeneboronic acid (conditions (iii)) gave [2,7]-biaryl **289** in good yield, and subsequent facile *N*-carbamate deprotection (conditions (iv)) followed by Michael-type reaction of amine **290** with 2-benzenesulfonamido-3-chloro-1,4-naphthoquinone **57** using anhydrous $CeCl_3$ as the Lewis acid and anhydrous toluene as solvent (conditions (v)) furnished the desired methylene-linked [2,7]-biaryl derivative **279** in 37% yield over the two steps.



291 = 3-Br
292 = 4-Br

293 = 3-Br, 92%
294 = 4-Br, 76%

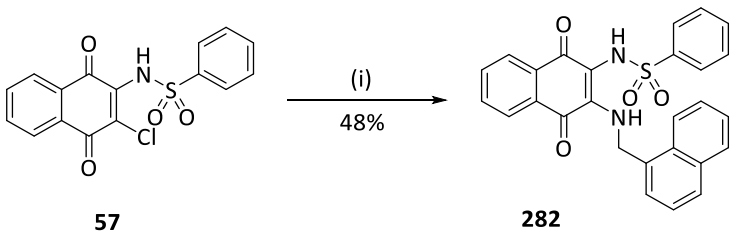
295 = 3-Ar, 46%
296 = 4-Ar, 32%

297 = 3-Ar, quant.
298 = 4-Ar, 75%

280 = 3-Ar, 25%
281 = 4-Ar, 38%

Scheme 4.4: A: Synthesis of methylene-linked [2,7]-biaryl analogue **279**; data generated by RB.[308] **B:** Synthesis of methylene-linked [3,7]- and [4,7]-biaryl analogues **280** and **281**; data generated by RB.[308] *Reagents and conditions:* (i) 30% aq. NH_3, sat. aq. NH_4OAc, $NaBH_3CN$ (3.0 eq.), 90 ^oC, 18 h; (ii) Boc_2O (1.0 eq.), $InCl_3$ (0.01 eq.), 35 ^oC, 45 min; (iii) requisite boronic acid (2.0 eq.), $Pd(PPh_3)_2Cl_2$ (0.1 eq.), THF:sat. aq. $NaHCO_3$ (22:5), 100 ^oC, 16 h; (iv) TFA:CH_2Cl_2 (1:5), RT, 2 h; (v) 2-benzenesulfonamido-3-chloro-1,4-naphthoquinone **57** (1.0 eq.), $CeCl_3$ (1.0 eq.), toluene, RT, 1.5 h *then* requisite amine (3.0 eq.), 110 ^oC, 16 h; (vi) Boc_2O (1.0 eq.), Et_3N (1.7 eq.), $InCl_3$ (0.01 eq.), 35 ^oC, 45 min.

Analogous procedures were subsequently used by RB to access both the desired [3,7]- and [4,7]-linked biaryl derivatives **280** and **281** in four steps from the commercially available benzylamine hydrochloride salts **291** and **292 (Scheme 4.4B**). Meanwhile, access to the naphthyl-substituted target **282** proved trivial, with commercially available amine **283** readily undergoing Michael-type reaction with naphthoquinone **57** to afford **282** in a moderate isolated yield of 48% **(Scheme 4.5)**.



57 **282**

Scheme 4.5: Synthesis of naphthyl derivative **282** from naphthoquinone **57**. *Reagents and conditions:* (i) $CeCl_3 \bullet 7H_2O$ (1.0 eq.), toluene, RT, 1.5 h *then* 1-naphthylmethylamine **283** (3.0 eq.), 110 ^oC, 6 h.

4.2.2. Pharmacological and Optical Evaluation of the Methylene-Linked Species

Evaluation of the inhibitory potency of compounds **279-282** against MOUSE(NAT2) in the acetyl CoA hydrolysis assay revealed that both [2,7]- and [3,7]-biaryl analogues **279** and **280**, in addition to naphthyl derivative **282**, were poor inhibitors with IC_{50} values >30 µM; however, [4,7]-biaryl analogue **281** proved to be significantly more potent, with a calculated IC_{50} value of 2.1 ± 0.51 µM (R^2 = 0.5034, P <0.005) **(Table 4.8)**.

Subsequently, colorimetric and fluorescence tests analogous to those performed on the initial biaryl library were also carried out. Two striking observations can be made from the colorimetric data: firstly, all of the methylene-linked biaryl and naphthyl species possess higher pK_a values (in the range 11.6-12.0) than the corresponding biaryl derivatives without a methylene linker (in the range 7.7-11.4; *cf.* **Section 4.1.2.**); and secondly, analogues **279** and **281** show far smaller shifts in λ_{max} in the presence of MOUSE(NAT2) (+20 and +12 nm respectively) than in the presence of a *p*H 13 buffer solution (+77 and +84 nm respectively). The two observations are likely linked: the high pK_a values may preclude complete formation of the conjugate base species in the presence of MOUSE(NAT2); however, for [2,7]-biaryl **279**, its low inhibitory potency against MOUSE(NAT2) may also play a role. The high pK_a values themselves are likely attributable to the fact that the lone pair on the nitrogen atom bonded to C_3 of the naphthoquinone core is more strongly conjugated with the naphthoquinone core than when there is an additional conjugating aromatic substituent on this nitrogen.

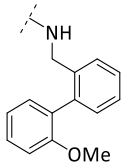
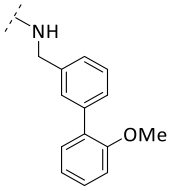
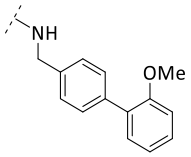
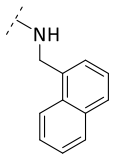
Compound		**279**	**280**	**281**	**282**
Structure					
IC_{50} MOUSE(NAT2) (μM)		>30	>30	2.1 ± 0.51	>30
pK_a		11.6 ± 0.3	11.6 ± 0.4	11.7 ± 0.8	*c.* 12.0
λ_{max} *p*H 8 (nm)		483	474	471	492
$\Delta\lambda_{max}$ *p*H 13 (nm)		+77	+86	+84	+60
$\Delta\lambda_{max}$ MOUSE(NAT2) (nm)		+20	N.D.	+12	N.D.
Fluorescence Intensity at 424 nm (λ_{ex} = 408 nm) (a.u.)	***p*H 8**	204	69	152	148
	+ Base	0	0	0	49
Fluorescence Intensity at 344 nm (λ_{ex} = 252 nm) (a.u.)	***p*H 8**	0	102	55	0
	+ Base	0	107	55	0

Table 4.8: Summary of pharmacological, colorimetric and fluorescent properties of methylene-linked biaryl derivatives **279-281** and naphthyl derivative **282**; data on the biaryl species generated by RB.[308] IC_{50} values were calculated from the acetyl CoA hydrolysis assay and were carried out in triplicate; analysis was performed using KyPlot® software. Fluorescence experiments at *p*H 8 were carried out at a final concentration of 150 μM in 95% 20 mM Tris•HCl/5% DMSO (*v/v*); basification was effected by addition of 5% 1 M aq. NaOH to these solutions and acidification by addition of 5 μL 1 M aq. HCl. Sensitivity voltage = 800 V; a.u. = arbitrary units; N.D. = not determined.

Evaluation of compounds **279-282** *via* fluorescence spectroscopy revealed that all four compounds displayed the characteristic fluorescent peaks at λ_{ex} = 372 and 408 nm and λ_{em} = 424 nm that correspond to fluorescence of the naphthoquinone core; as for all the previous analogues tested, these fluorescent peaks are quenched reversibly upon basification. Naphthyl derivative **282** appears less sensitive to basification than the biaryl derivatives, as although there is an observed reduction in the fluorescence intensity of the emission peak, the quenching is not total under these conditions. Interestingly, for the [3,7]- and [4,7]-biaryl derivatives **280** and **281**, an additional peak in each of the excitation and emission spectra were also observed, with an excitation wavelength of 252 nm and an emission wavelength of 344 nm **(Figure 4.9)**. Crucially, these peaks were not quenched by the basification of the solutions.

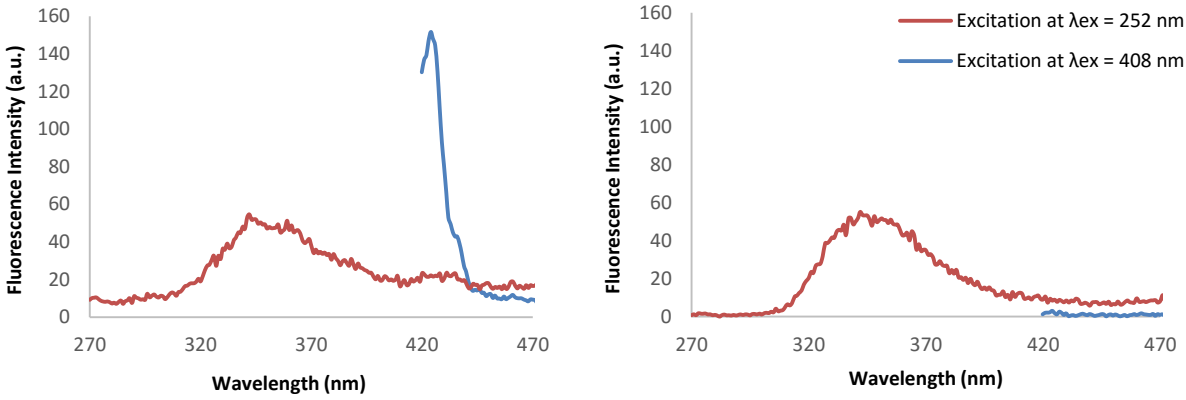


Figure 4.9: Fluorescence emission spectra for compound **281** (150 µM) at *p*H 8 in 95% 20 mM Tris•HCl/5% DMSO (*v/v*) **(left)** and after addition of 5% 1 M aq. NaOH **(right)**; data generated by RB.[308] Red lines correspond to excitation at 252 nm and blue lines to excitation at 408 nm. Sensitivity voltage = 800 V; a.u. = arbitrary units.

Intriguingly, when fluorescence spectra of the [3,7]- and [4,7]-biaryl methyl amine precursors to the final products, **297** and **298**, were recorded, very similar excitation and emission peaks were observed at 247 nm and 350 nm respectively; no such peaks could be observed in the fluorescence spectra of the [2,7]-biaryl methyl amine precursor **290**. This suggests that the additional peaks in the fluorescence spectra of **280** and **281** are attributable to the biaryl appendage; however, the appearance of these peaks at the same intensity in both the neutral and conjugate base forms of the molecule suggests that no change in the ability of the compounds to undergo intramolecular PET quenching occurs upon deprotonation of the acidic sulfonamide-N*H*. It is possible that the [2,7]-biaryl derivative **279** and its precursor amine **290** do not exhibit such fluorescence because steric repulsions prevent the formation of a planar electronically excited state from which fluorescent emission can occur.[315] Surprisingly, given its necessary planarity, naphthyl deriviative **282** was also not observed to fluoresce at wavelengths other than those attributable to the naphthoquinone core.

Compounds **280** and **281** therefore represent examples of fluorescent *p*H-dependent probes which are somewhat ratiometric, because the intensity of the emission peaks at 344 nm remain constant in base whilst those at 424 nm are quenched; however, since the biaryl peak itself does not change in intensity, these probes are of limited use for specific protein

detection in a cellular environment. Furthermore, both the peaks corresponding to biaryl and naphthoquinone fluorescence are of low intensity.

4.3. Changing the Fluorophore: Coumarin and Quinolinone C_3 Derivatives

The data generated for the methylene-linked biaryl and naphthyl derivatives suggest that for a *p*H-dependent switch in fluorescence to be observed in derivatives of naphthoquinone **238**, the fluorescent moiety most likely needs to be directly conjugated to the naphthoquinone core. It was therefore decided to replace the biaryl substituent in **238** with a substituent of similar steric bulk but which is predicted to be a significantly brighter fluorophore. A search of the literature revealed the known fluorophore 7-amino-4-methylcoumarin (AMC) **299**, which is reported to have a particularly high brightness:size ratio **(Figure 4.10)**.[316] Compound **300**, bearing an AMC substituent at the C_3 position, was thus designed as a target molecule which was predicted to be highly fluorescent and possess an appropriate *p*K_a to observe a switch in fluorescence intensity over the desired *p*H range; furthermore, *in silico* modelling of **300** in the HUMAN(NAT1) active site predicts that such a species is capable of binding to the enzyme.

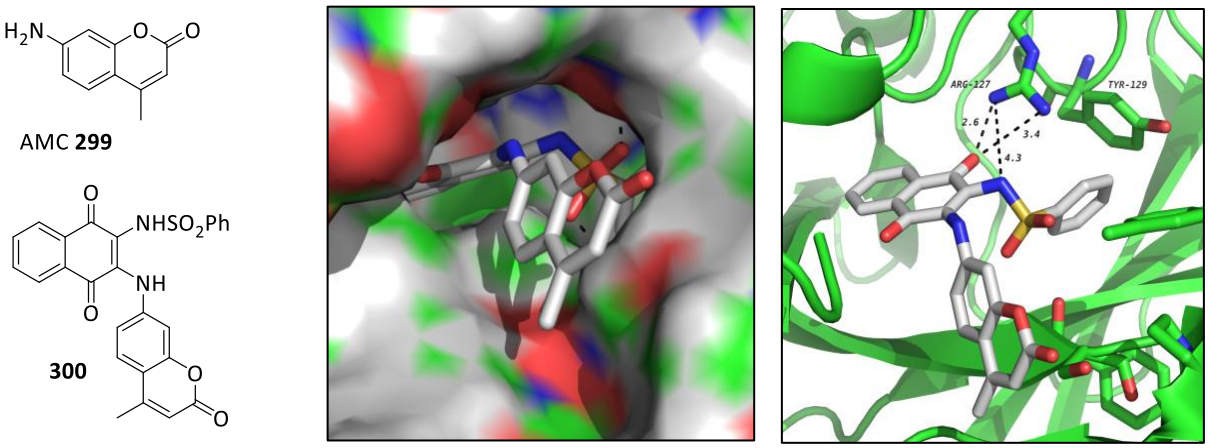
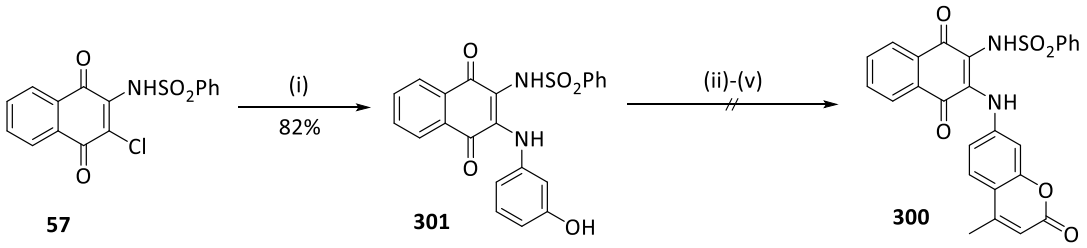


Figure 4.10: Left: Known fluorophore 7-amino-4-methylcoumarin (AMC) **299** and proposed coumarin-substituted naphthoquinone derivative **300**. **Centre and right:** *In silico* modelling of proposed coumarin derivative **300** in the active site of HUMAN(NAT1) (pdb: 2PQT);[247b] the protein is shown in both surface representation **(centre)** and cartoon representation **(right)**. Analysis performed using GOLD® (v.5.2).[282] Predicted polar contacts are highlighted by dashed black lines with inter-atomic distances given in Ångströms; key active site residues Arg127 and Tyr129 are highlighted in stick representation (carbon atoms in green).

4.3.1. Synthesis of Coumarin Derivative 300

The synthesis of coumarin derivative **300** proved far more challenging than anticipated. Initially, a Michael-type addition-elimination reaction between 2-benzenesulfonamido-3-chloro-1,4-naphthoquinone **57** and 3-aminophenol under standard reaction conditions was used by RB to generate intermediate **301** in an excellent yield of 82% (conditions (i) in **Scheme 4.6**). It was envisaged that this species might undergo a Pechmann condensation[317] to yield the target species **300** directly; however, treatment of **301** with excess ethyl acetoacetate and c. H_2SO_4 led to no observed reaction at RT and degradation of the starting materials at 80 ^oC (conditions (ii) and (iii)). Use of Lewis acids $BiCl_3$ or $InCl_3$ to catalyse the reaction[318] led to some evidence of product formation *via* HRMS (ESI^-) analysis; however, attempted isolation of the desired product failed.

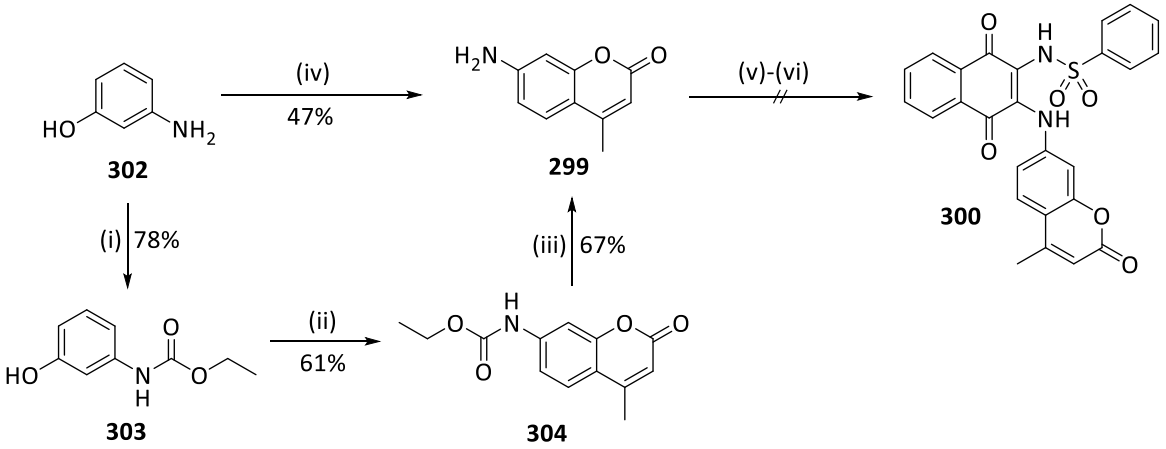


57 **301** **300**

Scheme 4.6: Attempted synthesis of coumarin derivative **300** by RB *via* 3-hydroxyanilino-substituted intermediate **301**.[308] *Reagents and conditions:* (i) $CeCl_3 \bullet 7H_2O$ (1.0 eq.), MeOH, RT, 1.5 h *then* 3-aminophenol (3.0 eq.), 90 ^oC, 16 h; (ii) ethyl acetoacetate (1.2 eq.), 70% ethanolic H_2SO_4 (excess), RT, 6 h; (iii) ethyl acetoacetate (1.2 eq.), 70% ethanolic H_2SO_4 (excess), 80 ^oC, 6 h; (iv) ethyl acetoacetate (excess), $BiCl_3$ (2.0 eq.), 110 ^oC, 16 h; (v) ethyl acetoacetate (excess), $InCl_3$ (0.1 eq.), 110 ^oC, 16 h.

Due to the intractability of this synthetic route, it was subsequently decided to synthesise AMC **299** before attempting to append this onto naphthoquinone intermediate **57** directly *via* a Michael-type addition-elimination reaction **(Scheme 4.7)**. AMC **299** was successfully synthesised in three steps by RB from 3-aminophenol **302** in an overall yield of 32% (conditions (i)-(iii)).[317] It was also demonstrated by Robyn Zorab (RZ) that AMC **299** could be

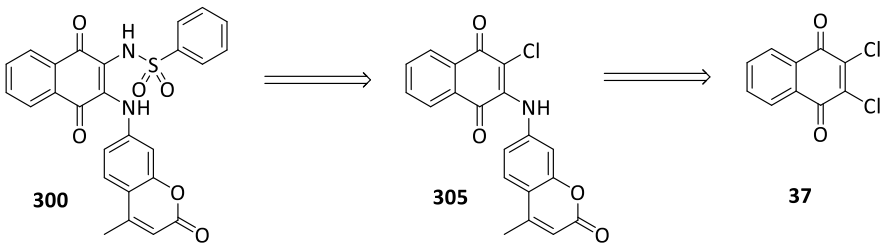
synthesised from 3-aminophenol **302** in a single Pechmann condensation step using 0.1 eq. $InCl_3$ as a Lewis acid catalyst in 47% yield (conditions (iv)).



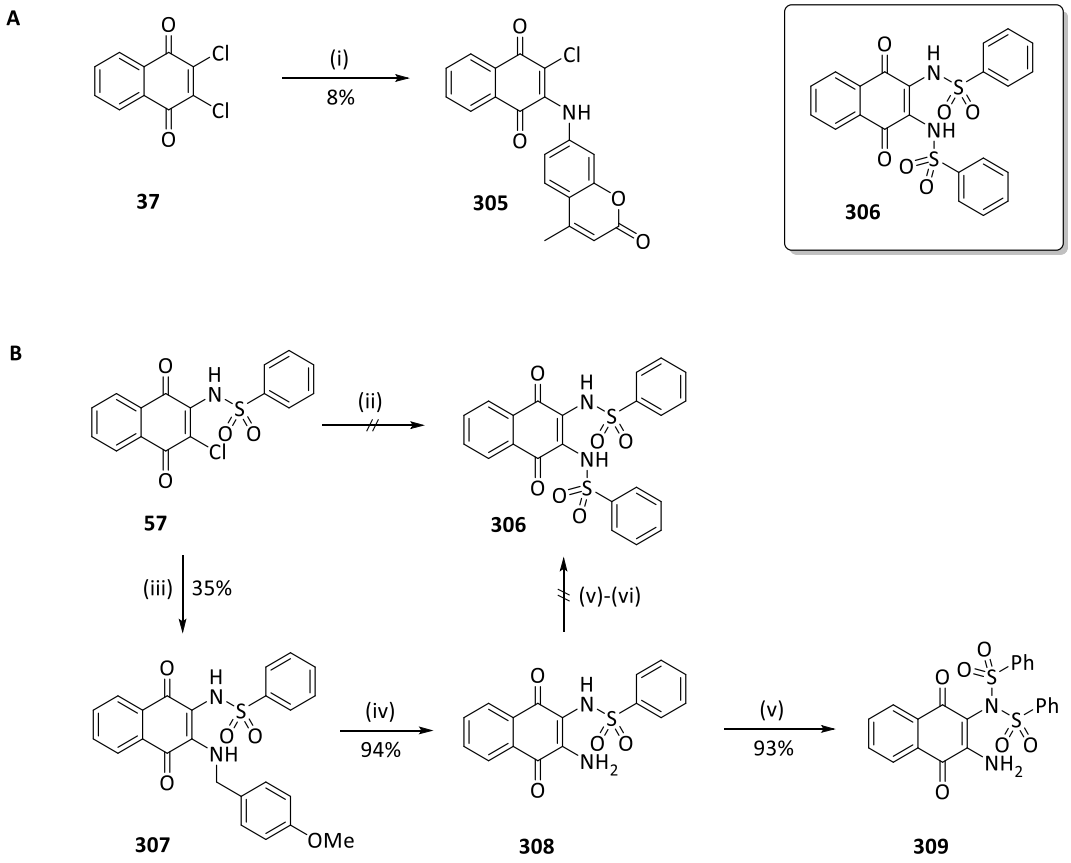
Scheme 4.7: Attempted synthesis of coumarin derivative **300** *via* Michael-type addition-elimination methodology; data generated by RB[308] and RZ.[319] *Reagents and conditions:* (i) ethyl chloroformate (1.0 eq.), Et_2O, RT, 2 h; (ii) ethyl acetoacetate (1.2 eq.), 70% ethanolic H_2SO_4 (excess), RT, 6 h; (iii) glacial acetic acid:c. H_2SO_4 (1:1), 120 ^oC, 4 h; (iv) ethyl acetoacetate (excess), $InCl_3$ (0.1 eq.), 75 ^oC, 48 h; (v) naphthoquinone **57** (1.0 eq.), $CeCl_3 \bullet 7H_2O$ (1.0 eq.), MeOH, RT, 1.5 h *then* AMC **299** (3.0 eq.), 90 ^oC, 16 h; (vi) naphthoquinone **57** (1.0 eq.), $CeCl_3$ (1.0 eq.), toluene, RT, 1.5 h *then* AMC **299** (3.0 eq.), 110 ^oC, 16 h.

Although hydroxyl-substituted analogues of AMC **299** have been reported to act as nucleophiles,[320] Michael-type addition-elimination reaction between AMC **299** and naphthoquinone intermediate **57** was not effected with either $CeCl_3 \bullet 7H_2O$ in MeOH or with anhydrous $CeCl_3$ in anhydrous toluene (conditions (v)-(vi)). This is likely due to the poor nucleophilicity of AMC **299** as the lone pair on the amine nitrogen is predicted to be highly conjugated with the aromatic π-electron system.

The next efforts employed to access **300** involved a different retrosynthetic strategy, in which it was envisaged that the coumarin substituent could be appended to the naphthoquinone core of 2,3-dichloro-1,4-naphthoquinone **37** before the addition of the benzenesulfonamide moiety **(Scheme 4.8)**; this would exploit the increased propensity for naphthoquinone **37** to undergo addition-elimination reactions with nucleophiles *cf.* naphthoquinone **57**.



Scheme 4.8: Alternative proposed retrosynthetic route to coumarin derivative **300**, in which the coumarin moiety is installed prior to the benzenesulfonamide.

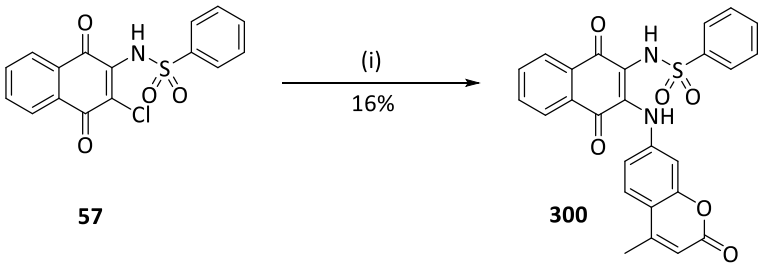


Scheme 4.9: A: Synthesis of C_2-chloro-C_3-coumarin substituted intermediate **305**. **B:** Attempted synthesis of *bis*(benzenesulfonamido) **306** as a model reaction system. *Reagents and conditions:* (i) AMC **299** (2.2 eq.), NaO^{t}Bu (2.2 eq.), THF, reflux, 16 h; (ii) $CeCl_3 \bullet 7H_2O$ (1.0 eq.), MeOH, RT, 1.5 h *then* benzenesulfonamide (3.0 eq.), 90 ^oC, 16 h; (iii) $CeCl_3 \bullet 7H_2O$ (1.0 eq.), toluene, RT, 1.5 h *then para*-methoxybenzylamine (3.0 eq.), 110 ^oC, 6 h; (iv) H_2 (1 atm.), 10% Pd/C (0.2 eq.), RT, 16 h; (v) benzenesulfonyl chloride (excess), Et_3N (3.0 eq.), RT, 16 h; (vi) NaH (as a 60% dispersion in oil, 2.0 eq.), THF, RT, 0.25 h *then* benzenesulfonyl chloride (1.0 eq.), RT, 16 h.

Formation of intermediate **305** from dichloronaphthoquinone **37** and AMC **299** was observed under basic conditions (conditions (i) in **Scheme 4.9A**). Unfortunately, intermediate **305** proved challenging to separate from unreacted AMC **299** *via* column chromatography, and **305** was therefore only isolated in a poor yield of 8%. Due to the low amount of material available, it was therefore decided to optimise the remainder of the synthetic route on a different, analogous substrate. It was noted that intermediate **305** has a pK_a value of *c.* 5.0, and hence it was predicted that electronically, **305** might possess similar properties to the well-used benzenesulfonamido-substituted intermediate **57** (pK_a = 3.0). Hence it was postulated that if it proved possible to synthesise *bis*(benzenesulfonamido)-substituted species **306** from intermediate **57**, an analogous synthetic route might be used to access coumarin **300** from intermediate **305**.

Michael-type addition elimination between intermediate **57** and benzenesulfonamide was therefore attempted using $CeCl_3 \bullet 7H_2O$ (conditions (ii) in **Scheme 4.9B**); however, this procedure returned only starting materials. Taking inspiration from the earlier described synthesis of sulfonate ester **36** (*cf.* **Section 2.1.2.**), it was postulated that if an $-NH_2$ group could be installed at the C_3 position of intermediate **57**, it might be possible to form the desired target in a final addition-elimination step on benzenesulfonyl chloride. The desired amino-substituted intermediate **308** was accessed in two facile steps from chloro-substituted **57**: firstly, Michael-type reaction of *para*-methoxybenzyl amine with **57** and $CeCl_3 \bullet 7H_2O$ in toluene yielded C_3-benzylamino substituted **307**, which subsequently underwent a quantitative catalytic hydrogenation to remove the electron-rich benzyl protecting group. However, treatment of amino-substituted intermediate **308** with excess benzenesulfonyl chloride and 3.0 eq. trimethylamine unexpectedly yielded adduct **309**, formed from preferential reaction of the secondary sulfonamide nitrogen with the electrophilic sulfonyl chloride over reaction of the C_3-NH_2 group. In an attempt to overcome this undesired reactivity, intermediate **308** was instead treated with 2.0 eq. NaH in THF, followed by a single equivalent of benzenesulfonyl chloride; after 16 h of stirring at RT, however, only starting materials could be recovered from the reaction mixture.

Given both the inability to form *bis*(benzenesulfonamido) adduct **306** from intermediate **57**, and the low isolated yield of coumarin-substituted intermediate **305** obtained, no further efforts were made to access coumarin **300** from **305**. Instead, one final attempt was made by RB to encourage Michael-type addition elimination reaction of naphthoquinone **57** and AMC **299**. In this case, anhydrous reaction conditions were used, but MeOH retained as the solvent, since it would be anticipated that formation of a charge-separated intermediate would be more favourable in a polar solvent **(Scheme 4.10)**. Moreover, the concentrations of the reagents were increased and the reaction time extended to 72 h. After a challenging purification *via* both column chromatography and preparatory TLC, the desired compound **300** was finally cleanly obtained in 16% yield.

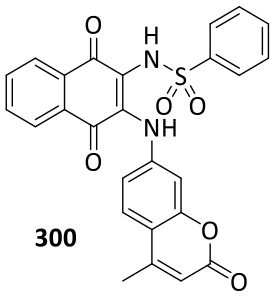


Scheme 4.10: Successful synthesis of coumarin derivative **300** from chloro-substituted naphthoquinone **57**; data generated by RB.[308] *Reagents and conditions:* (i) $CeCl_3$ (1.0 eq.), MeOH (0.24 mmol **57**/mL), RT, 1.5 h *then* AMC **299** (3.0 eq.), 110 ^{o}C, 72 h.

4.3.2. Pharmacological and Optical Evaluation of Coumarin Derivative 300

The obtained sample of coumarin derivative **300** was subjected to the same pharmacological and optical evaluation as previously synthesised compounds **(Table 4.9)**. Pleasingly, **300** displayed dose-dependent inhibition of MOUSE(NAT2), with a calculated IC_{50} value of 6.7 ± 1.4 μM (R^2 = 0.6270, P <0.005), and also demonstrated the characteristic shift in λ_{max} both in the presence of MOUSE(NAT2) and in a basic buffer solution. However, these observed shifts in λ_{max} are appreciably lower than corresponding values for many of the colorimetric probes previously reported; this is most probably due to the low pK_a value of 7.3 which was

calculated for **300** *via* titration. It is hypothesised that the strong electron-withdrawing nature of the coumarin moiety at the C_3 position is responsible for this low pK_a.



IC_{50} MOUSE(NAT2) (μM)		6.7 ± 1.4
pK_a		7.3 ± 0.3
λ_{max} *p*H 8 (nm)		549
$\Delta\lambda_{max}$ *p*H 12.8 (nm)		+6
$\Delta\lambda_{max}$ MOUSE(NAT2) (nm)		+55
Fluorescence emission intensity at 424 nm (λ_{ex} = 408 nm) (a.u.)	***p*H 8.0**	10
	+ Acid	103
	+ Base	0
	***p*H 12.8**	0
Fluorescence emission intensity at 440 nm (λ_{ex} = 344 nm) (a.u.)	***p*H 8.0**	149
	+ Acid	30
	+ Base	54
	***p*H 12.8**	147

Table 4.9: Summary of pharmacological and optical properties of coumarin derivative **300**; data generated by RB[308] and RZ.[319] IC_{50} values were calculated from the acetyl CoA hydrolysis assay and were carried out in triplicate; analysis was performed using KyPlot® software. Fluorescence experiments at *p*H 8 were carried out at a final concentration of 150 μM in 95% 20 mM Tris•HCl/5% DMSO (*v/v*); basification was effected by addition of 5% 1 M aq. NaOH to these solutions and acidification by addition of 5 μL 1 M aq. HCl. Fluorescence experiments at *p*H 12.8 were carried out in 95% 35 mM Na_2HPO_4•NaOH/5% DMSO (*v/v*). Sensitivity voltage = 800 V; a.u. = arbitrary units.

Fluorescence spectroscopy showed that, as for the other naphthoquinone derivatives tested previously, **300** displays an emission peak at 424 nm when excited at 408 nm, which corresponds to fluorescence of the naphthoquinone core and is reversibly quenched above the pK_a of **300**. Notably, however, compound **300** displays a second, more intense fluorescent peak at *p*H 8 with λ_{ex} = 344 nm and λ_{em} = 440 nm, which is attributed to the fluorescence of the coumarin moiety. Interestingly, this fluorescent peak is reversibly quenched both upon acidification to *c. p*H 2 with 5 μL 1 M aq. HCl and upon basification to *c. p*H 14 with 5 μL 1 M aq. NaOH, but not in a 35 mM Na_2HPO_4•NaOH buffer solution at *p*H 12.8, a *p*H at which the sulfonamide-N*H* of **300** would be fully deprotonated **(Figure 4.11)**. One possible explanation for these observations is that the change in electron density in **300** which results from sulfonamide-N*H* deprotonation is too remote to affect the fluorescence intensity of the coumarin moiety; the quenching of fluorescence observed after the addition of 1 M aq. NaOH

to the sample might be due to deprotonation of the coumarin-N*H* above *p*H 13. Indeed, when up to 10 µL recombinant MOUSE(NAT2) solution (which was determined to have an approximate concentration of 3450 µg/mL, or 100 µM, in a BCA assay; [10] see **Section 7.12.**) was added to a 15 µM sample of **300** in 95 µL 20 mM Tris•HCl and 5 µL DMSO at *p*H 8, no reduction in fluorescence intensity was recorded, again suggesting that the coumarin fluorescence is insensitive to sulfonamide-N*H* deprotonation **(Figure 4.11)**.

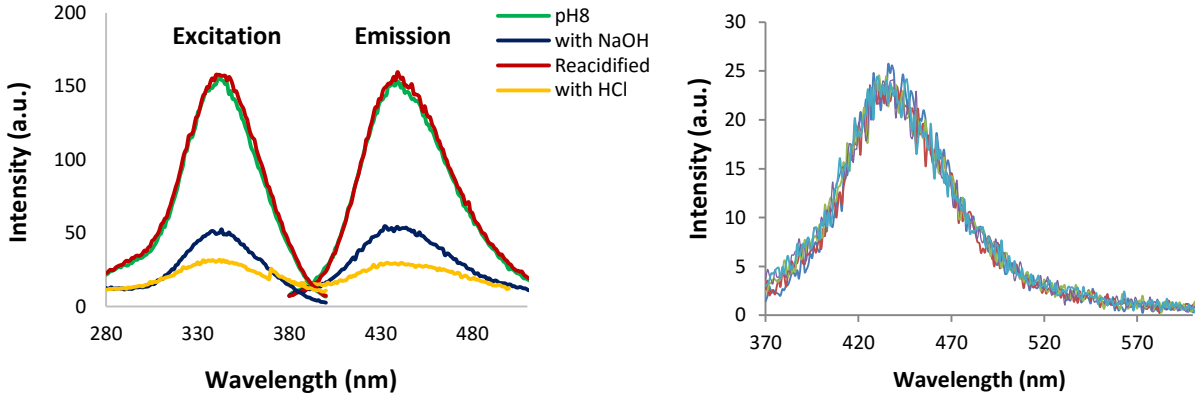


Figure 4.11: Left: Excitation and emission spectra for coumarin derivative **300** at 150 µM (λ_{ex} = 344 nm) in 95% 20 mM Tris•HCl (*p*H 8)/5% DMSO (*v/v*) (green lines), with the addition of 5% 1 M aq. NaOH (blue lines), upon reacidification with 5% 1M aq. HCl (red lines), and with the addition of 5% 1 M aq. HCl (yellow lines). Data generated by RZ;[319] sensitivity voltage = 800 V; a.u. = arbitrary units. **Right:** Emission spectra for coumarin derivative **300** at 15 µM in 95% 20 mM Tris•HCl (*p*H 8)/5% DMSO (*v/v*) with the addition of the following volumes of recombinant MOUSE(NAT2): 0 µL (dark blue line); 4 µL (red line), 6 µL (green line), 8 µL (purple line), 10 µL (sky blue line). Data generated by RB;[308] sensitivity voltage = 800 V; a.u. = arbitrary units.

One hypothesis for the lack of observed sensitivity to sulfonamide-N*H* deprotonation of the coumarin fluorescence is that because the coumarin is such a strongly electron-withdrawing substituent, the propensity for the lone pair electrons on the C_3 nitrogen to be delocalised over the coumarin moiety in preference to the naphthoquinone core is high, even when the molecule is protonated; hence sulfonamide-N*H* deprotonation might not greatly affect the overall electron density on the coumarin moiety. However, if electron rich groups were appended to the coumarin moiety, this might increase the propensity for the C_3 nitrogen to donate its lone pair into the naphthoquinone core when the molecule is protonated. In turn, it

is postulated that this could lead to a sufficient change in electron density on the coumarin when the sulfonamide-N*H* is deprotonated for the fluorescence intensity of the coumarin to become sensitive to sulfonamide-N*H* deprotonation.

To test this hypothesis, a small library of analogues of coumarin **300** was designed **(Figure 4.12)**. Target compounds **310** and **311** bear hydroxy and methoxy substituents on the coumarin moiety respectively, which are predicted to be mesomeric electron donors, whilst in quinolinone **312**, the lactone functionality is replaced by a lactam; this might not only alter the electron density distribution over the C_3 appendage, but would also be anticipated to be more stable than coumarin **300** with respect to base-catalysed ring opening.

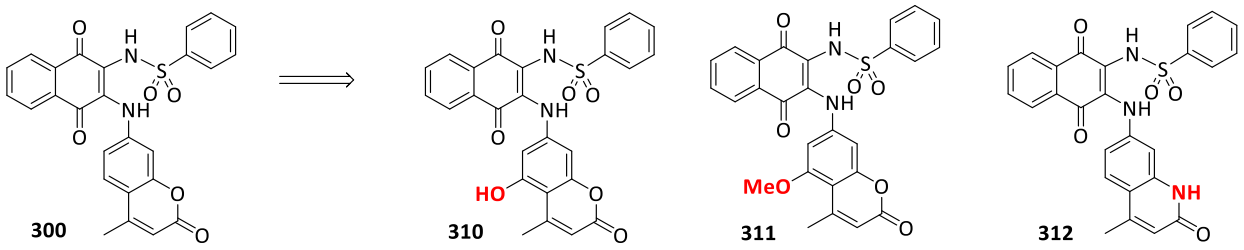


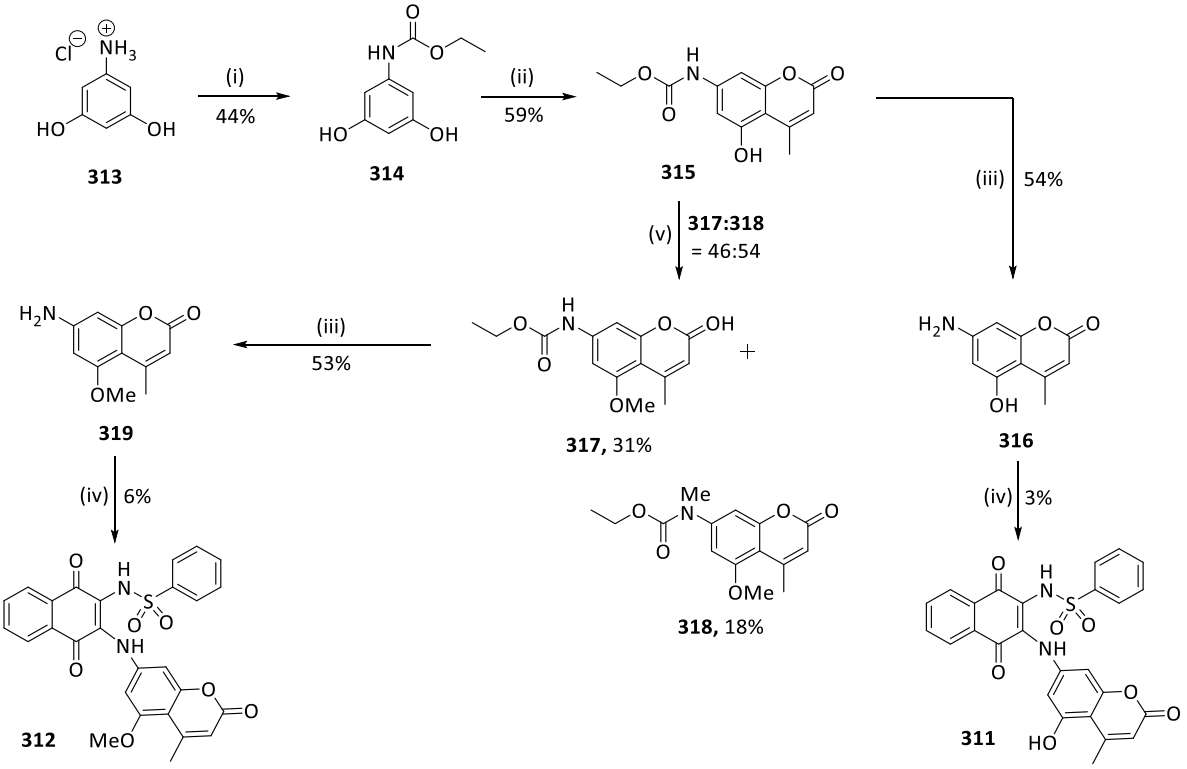
Figure 4.12: Designed library of more electron-rich coumarin and quinolinone derivatives of compound **300**.

4.3.3. Synthesis of the Coumarin and Quinolinone Analogue Library

It was anticipated that the desired electron-rich variants of coumarin **300** would be more readily accessible from chloro-substituted naphthoquinone **57** *via* a Michael-type addition-elimination reaction than was the case for coumarin **300** itself, because the corresponding precursor amino-coumarins are predicted to be more strongly nucleophilic than AMC **299**.

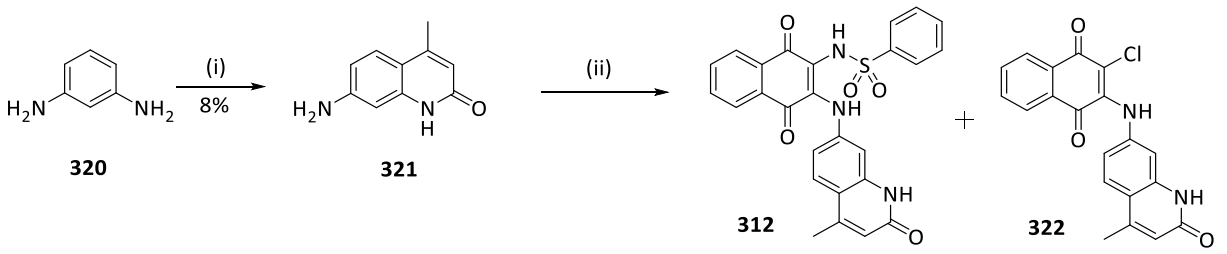
Therefore, in order to synthesise coumarins **310** and **311**, the requisite amines 7-amino-5-hydroxy-4-methylcoumarin **316** and 7-amino-5-methoxy-4-methylcoumarin **319** were first synthesised by RZ from the common starting material 5-aminobenzene-1,3-diol hydrochloride **313 (Scheme 4.11)**.

N-Ethyl carbamate protection of **313** was achieved using $NaHCO_3$ as a base in a 1:1 mixture of THF and H_2O (conditions (i)), and a subsequent Pechmann condensation furnished intermediate **315** in good yield (conditions (ii)). Acid-catalysed *N*-carbamate deprotection of **315** gave one of the required amines, 7-amino-5-hydroxy-4-methylcoumarin **316**, in a 54% yield (conditions (iii)), which was subjected to Michael-type addition-elimination with naphthoquinone **57** to give coumarin **311** in a poor isolated yield after a challenging purification. Meanwhile, methylation of intermediate **315** in which two equivalents of MeI were added portionwise in the presence of NaO^tBu (conditions (v)) yielded a 46:54 ratio of monomethylated **317** and dimethylated **318**, which could be isolated in respective yields of 31% and 18%. Subsequent carbamate deprotection of monomethylated **317** and Michael-type reaction with **57** afforded the desired methoxy-substituted coumarin derivative **312**.



Scheme 4.11: Synthesis of hydroxy- and methoxy-substituted coumarin derivatives **311** and **312**; data generated by RZ.[319] *Reagents and conditions:* (i) ethyl chloroformate (3.0 eq.), $NaHCO_3$ (5.0 eq.), THF:H_2O (1:1), RT, 12 h; (ii) ethyl acetoacetate (1.2 eq.), 70% ethanolic H_2SO_4, RT, 6 h; (iii) c. H_2SO_4:glacial AcOH (1:1), 120 ^oC, 4 h; (iv) naphthoquinone **57** (1.0 eq.), $CeCl_3$ (1.0 eq.), MeOH, RT, 1.5 h *then* requisite coumarin amine **316** or **319** (3.0 eq.), 100 ^oC, 48 h; (v) MeI (2.1 eq.); NaO^tBu (1.0 eq.), MeCN, reflux, 16 h.

A similar strategy was utilised by RZ for the synthesis of quinolinone derivative **312**; the requisite amine for the Michael-type step in this case was 7-amino-4-methylquinolin-2(1*H*)-one **321 (Scheme 4.12)**, which could be accessed in a single step from *meta*-phenylenediamine **320** (conditions (i)).[317] Subsequently, a Michael-type reaction between **321** and naphthoquinone **57** was effected by $CeCl_3$ in MeOH (conditions (vii)), with ^{1}*H*-NMR and *m/z* (ESI^-) analysis indicating formation of the desired product. However, attempted purification of **312** *via* column chromatography led only to the isolation of the by-product **322** in a 2% yield, in which quinolinone **321** had substituted for the bezenesulfonamide substituent of **57** in preference to the chloro substituent. 2D-TLC analysis indicated that the major product **312** within the reaction mixture was unstable on both silica and alumina; therefore, sequential recrystallisations – firstly from DMSO/H_2O and secondly from MeOH – yielded a 4:1 mixture of **312**:**322**, which could not be further purified. This mixture was used in subsequent analysis alongside the purified sample of by-product **322** for comparison.



Scheme 4.12: Synthesis of quinolinone derivative **312**; data generated by RZ.[319] *Reagents and conditions:* (i) ethyl acetoacetate (1.0 eq.), 150 °C, 18 h *then* H_2O, 100 °C, 0.5 h; (ii) naphthoquinone **57** (1.0 eq.), $CeCl_3$ (1.0 eq.), MeOH, RT, 1.5 h *then* amine **321** (3.0 eq.), 110 °C, 48 h.

4.3.4. Evaluation of the Coumarin and Quinolinone Analogue Library

The IC_{50} values for the synthesised coumarins against MOUSE(NAT2) in the acetyl CoA hydrolysis assay are presented in **Table 4.10**. All of the modifications made to the coumarin moiety led to an approximately four-fold decrease in inhibitory potency; an *in silico* model of methoxy-substituted **311** in the active site of the homologous HUMAN(NAT1) suggests that

additional substituents on the coumarin moiety might lead to unfavourable steric interactions with residues lining the entrance channel to the active site **(Figure 4.13)**.

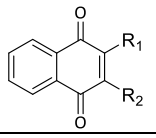
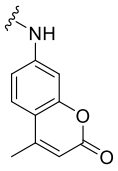
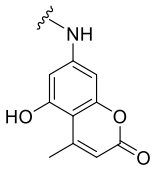
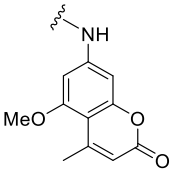
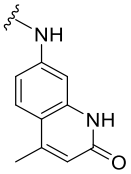
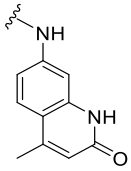
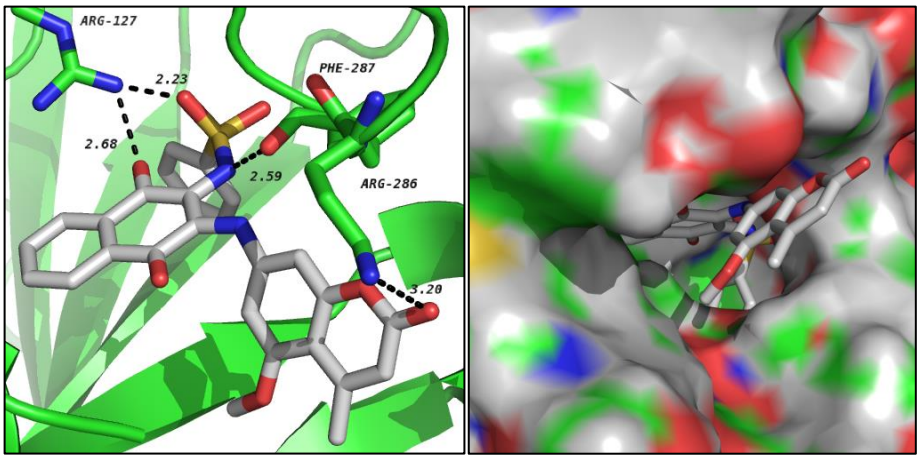
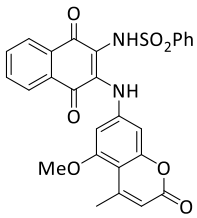
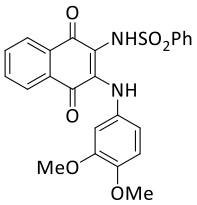
	**300**	**310**	**311**	**312:322 (4:1)**	**322**
R_1	$NHSO_2Ph$	$NHSO_2Ph$	$NHSO_2Ph$	$NHSO_2Ph$:Cl	Cl
R_2					
IC_{50} MOUSE(NAT2) (μM)	6.7 ± 1.4	27.4 ± 6.9	22.5 ± 8.4	23.1 ± 5.6	>30
R^2	0.6270	0.1563	^	0.5908	N/A
P	***	***	*	***	N/A

Table 4.10: IC_{50} values for the library of coumarin and quinolinone derivatives against MOUSE(NAT2) in the acetyl CoA hydrolysis assay, with squared correlation coefficients (R^2) and significance levels (P) as given; * = P <0.05; *** = P <0.005. Data generated by RZ with KyPlot® software using the IC50%FUN model.[319] N/A = not applicable; ^ = data does not fit regression model well enough for a calculated value of R^2 to be obtained.





311



84

Figure 4.13: Left and Centre: *In silico* modelling of methoxy-substituted coumarin derivative **311** in the active site of HUMAN(NAT1) (pdb: 2PQT);[247b] the protein is shown in both surface representation **(centre)** and cartoon representation **(left)**. Analysis performed using GOLD® software (v.5.2).[282] Predicted polar contacts are highlighted by dashed black lines with inter-atomic distances given in Ångströms; residues Arg127, Arg286 and Phe287 are highlighted in stick representation. **Right:** The conformation of the methoxy substituent in **311** is likely to be induced in a similar manner to that in anilino derivative **84**, which displays a similar IC_{50} value to **311**.

The lactone ring within the coumarin will likely influence the conformation of the adjacent methoxy substituent, in much the same way as the presence of multiple O-Me bonds in C_3 di- and tri-methoxyanilino derivatives **84** and **85** (*cf.* **Section 3.2.2.**) induced the conformation of one another; indeed, the similarity in IC_{50} values between methoxy-substituted coumarin derivative **311** and dimethoxy-substituted anilino derivative **84** is striking. The activity of the 4:1 mixture of quinolinones **312** and **322** likely arises from the major species **312**, since minor species **322** alone does not display dose-dependent inhibition of MOUSE(NAT2) below 30 μM. The observed disparity in potency between coumarin **300** and quinolinone **312** is unlikely due to any steric effects; however, it is possible that the replacement of an oxygen sp^2-hybridised lone pair, a hydrogen bond acceptor, with an N-H bond, a hydrogen-bond donor, leads to an electronic destabilisation of the bound conformer.

Subsequently, the colorimetric and fluorescent properties of coumarin derivatives **310** and **311** and the 4:1 mixture of quinolinones **312** and **322** were also evaluated **(Tables 4.11 and 4.12)**.

pK_a data for compounds **310**, **311** and **312** reveal that, despite an anticipated increase in electron density over the coumarin moiety in these compounds, the modifications made do not significantly affect the acidity of the sulfonamide-N*H*; the observed *p*K_a values between 7.0 and 7.7 are similar to that of the unsubstituted coumarin **300** (7.3). It is also of note that hydroxyl-substituted **310** displays two different *p*K_a values over the range tested; the first of these (7.0) is consistent with sulfonamide-N*H* deprotonation, and the second (10.4) is predicted to be due to deprotonation of the hydroxyl functionality. Pleasingly, all three compounds show a significant shift in λ_{max} in the presence of MOUSE(NAT2), despite only exhibiting a relatively small shift λ_{max} in a 35 mM Na_2HPO_4•NaOH buffer solution at *p*H 12.8, a *p*H which is basic enough to ensure sulfonamide-N*H* deprotonation.

Compound	310	311	312:322 (4:1)
pK_a	7.0 ± 0.1 (1^{st}) 10.4 ± 0.3 (2^{nd})	7.2 ± 0.1	7.7 ± 0.3
λ_{max} *p*H 8 (nm)	543	545	526
$\Delta\lambda_{max}$ *p*H 12.8 (nm)	+17	+6	+33
$\Delta\lambda_{max}$ MOUSE(NAT2) (nm)	+53	+85	+63

Table 4.11: Colorimetric properties of the coumarin and quinolinone derivatives. Wavelength scans were conducted at a final concentration of 15 µM in 5% DMSO (*v/v*); data generated by RZ.[319]

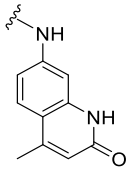
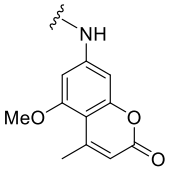
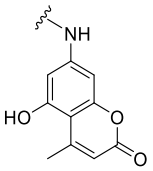
Compound		4:1 312:322		311		310	
C_2 Substituent		$NHSO_2Ph$:Cl		$NHSO_2Ph$		$NHSO_2Ph$	
C_3 Substituent							
Wavelength (nm)		λ_{ex} = 343	λ_{em} = 422	λ_{ex} = 342	λ_{em} = 446	λ_{ex} = 344	λ_{em} = 451
Fluorescence Emission Intensity at *p*H 8 (150 µM) (a.u.)		312	318	259	259	251	248
Δ Fluorescence Intensity from *p*H 8 (a.u.)	+ 5 µL 1 M aq. NaOH	-241	-253	-191	-176	-184	-181
	Reacidified	+13	+14	-71	-74	-28	-25
	+ 5 µL Na_2HPO_4•NaOH buffer (*p*H 12.8)	-6	-5	-29	-42	-146	-161
Fluorescence Emission Intensity at *p*H 8 (15 µM) (a.u.)		N.D.	N.D.	97	96	57	56
Δ Fluorescence Intensity from *p*H 8 (a.u.)	+2 µL MOUSE(NAT2)	N.D.	N.D.	-24	-23	-23	-21
	+4 µL MOUSE(NAT2)	N.D.	N.D.	-28	-27	-24	-23
	+6 µL MOUSE(NAT2)	N.D.	N.D.	-28	-27	-24	-23

Table 4.12: Fluorescent properties of coumarins **310** and **311** and quinolinone **312**; data at 150 µM generated by RZ.[319] Spectra at *p*H 8 were recorded in 95% 20 mM Tris•HCl/5% DMSO (*v/v*); reacidification was effected by addition of 5 µL 1 M aq. HCl subsequent to basification. Sensitivity voltage = 800 V for compounds **310** and **312**, 600 V for compound **311**; a.u. = arbitrary units; N.D. = not determined.

Fluorescence spectroscopy revealed that the coumarin moieties in **310** and **311** and the quinolinone moiety in **312** possess very similar λ_{ex} values to one another (342-344 nm), whilst λ_{em} for quinolinone **312** (422 nm) is at a lower wavelength than λ_{em} for coumarins **310** and **311** (446-451 nm). The fluorescent intensity of the peaks for methoxy-substituted coumarin **311** were found to be orders of magnitude greater than those for either unsubstituted coumarin

300 or hydroxy-substituted coumarin **310**, with intensity values of >1000 a.u. at a sensitivity voltage of 800 V; hence a reduced voltage of 600 V was used for all measurements pertaining to compound **311**. The origin of this increased fluorescent intensity might be due to the propensity for the methoxy substituent to donate its lone pair electrons into the coumarin π-electron system.

Intriguingly, all three compounds **310**, **311** and **312** exhibited reversible quenching of their fluorescent peaks when basified with 1 M aq. NaOH, but only compound **310** displayed such behaviour when treated with *p*H 12.8 buffer solution **(Figure 4.14)**. It is thought that the latter observation is due to deprotonation of the hydroxyl substituent on the coumarin moiety (pK_a = 10.4), and that the florescence quenching in the presence of NaOH might be associated with coumarin-N*H* deprotonation above *p*H 13, as for the previously tested coumarin **300**.

Furthermore, when 15 μM of compounds **310** and **311** were treated with increasing volumes of MOUSE(NAT2), a small but significant decrease in fluorescent intensity of the excitation and emission peaks was observed upon initial addition of a small volume of enzyme (2 μL), but any further addition of enzyme did not lead to any further concomitant quenching of fluorescence in either case **(Figure 4.14)**. It is hypothesised that, whilst these experiments suggest that increasing the electron density on the coumarin moiety has indeed increased the sensitivity of this appendage and its associated fluorescence to remote sulfonamide-N*H* deprotonation within the molecule *cf.* unsubstituted coumarin **300**, the low pK_a values of the synthesised derivatives preclude their effective use as probes for accurately quantifying the levels of MOUSE(NAT2) in solution at *p*H 8. With pK_a values in the range 7.0-7.7, it would be anticipated that the majority of molecules are already deprotonated in solution at *p*H 8, meaning that addition of only a small amount of MOUSE(NAT2) is required to entirely sequester the conjugate base species from the acid-base equilibrium. Therefore, whilst addition of a small amount of MOUSE(NAT2) leads to a measurable change in the molecular fluorescence of **310** and **311**, the range of MOUSE(NAT2) concentrations to which **310** and **311** are sensitive is very narrow.

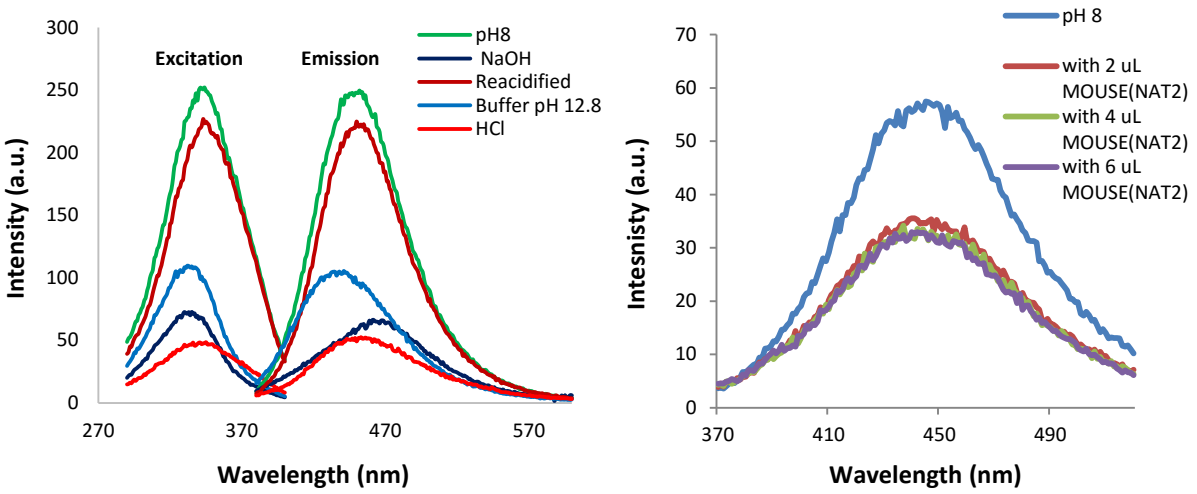


Figure 4.14: Left: Excitation and emission spectra for hydroxy-substituted coumarin derivative **310** at 150 µM (λ_{ex} = 344 nm) in 95% 20 mM Tris•HCl (*p*H 8)/5% DMSO (*v/v*) (green lines), with the addition of 5% 1 M aq. NaOH (dark blue lines), upon reacidification with 5% 1M aq. HCl (dark red lines), with the addition of 5% 1 M aq. HCl (red lines), and in 95% 35 mM Na_2HPO_4•NaOH (*p*H 12.8)/5% DMSO (*v/v*) (sky blue lines). Data generated by RZ;[319] sensitivity voltage = 800 V; a.u. = arbitrary units. **Right:** Emission spectra for coumarin derivative **310** at 15 µM in 95% 20 mM Tris•HCl (*p*H 8)/5% DMSO (*v/v*) with the addition of the following volumes of recombinant MOUSE(NAT2): 0 µL (sky blue line); 2 µL (red line), 4 µL (green line) and 6 µL (purple line). Sensitivity voltage = 800 V; a.u. = arbitrary units.

Nonetheless, the results of these fluorescence experiments are tantalising, since they suggest that if a strongly fluorescing moiety is appended to the C_3 position of the naphthoquinone core such that the fluorophore and the naphthoquinone are in direct conjugation with one another, and if the resultant compound both possesses an appropriate *p*K_a and is an inhibitor of MOUSE(NAT2), then the fluorescent output of such a probe might be acutely sensitive to MOUSE(NAT2) concentration in solution.

4.4. Back to the Biaryls: Rigidified Fluorene Analogues

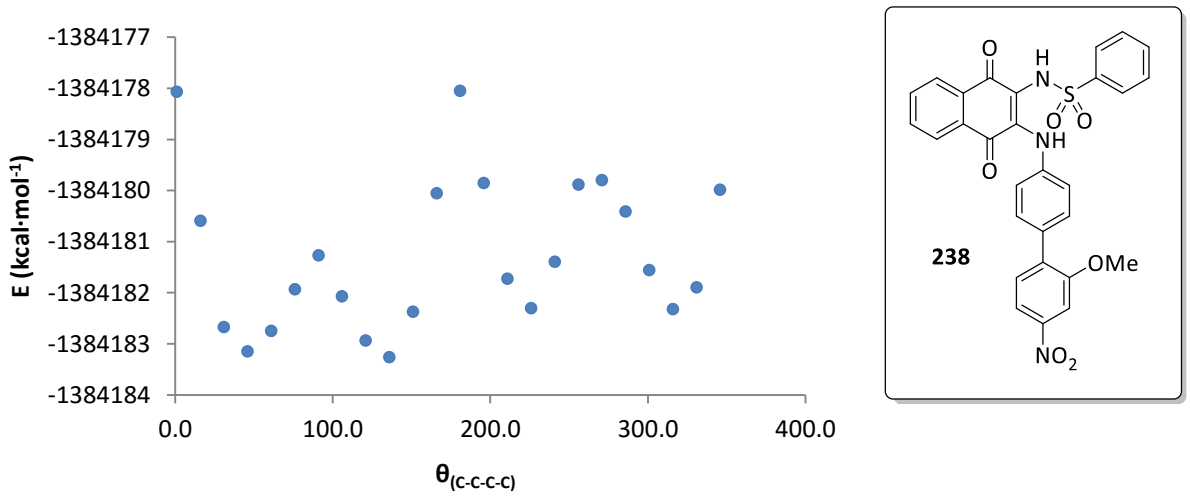
Given the results of fluorescence evaluation on coumarin derivatives **310** and **311**, it was reasoned that a C_3 substituent had to be developed which conferred not only a good

inhibitory potency against MOUSE(NAT2) (and by extension, HUMAN(NAT1)) and a high fluorescent intensity, but also a pK_a value above 8.

Given the favourable pK_a and IC_{50} values observed for the initial biaryl library of compounds (*cf.* **Section 4.1.2.**), optimisation of a biaryl-based system was reconsidered. One possible explanation for the lack of a fluorescent signal emanating from the biaryl moiety in compounds such as the second generation lead **238** is that in the preferred conformation of such biaryl substituents both in solution and in the MOUSE(NAT2) active site, the two aromatic rings of the biaryl are not in the same plane and hence fluorescence from the system is either weak or non-existent.[315] DFT modelling studies on compound **238** support this theory **(Figure 4.15)**: the lowest-energy conformations about the aryl-aryl bond in the biaryl moiety of **238** correspond to torsional angles of 46° and 136°, whilst torsional angles of 1° and 181° correspond to energy maxima.

It was therefore hypothesised that to encourage the biaryl appendage to emit fluorescence, the two aromatic rings of the biaryl should be forced into coplanarity by the addition of a second linker between the rings. 2-aminofluorene was used as an appropriate substituent to test this hypothesis, and was introduced at the C_3 position by RB *via* a Michael-type reaction with naphthoquinone **57**, which proceeded in quantitative fashion to yield **323 (Scheme 4.13)**.

A



B

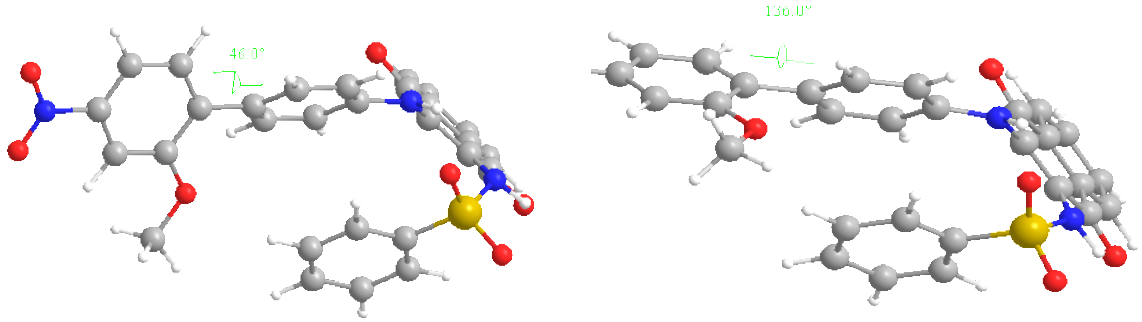
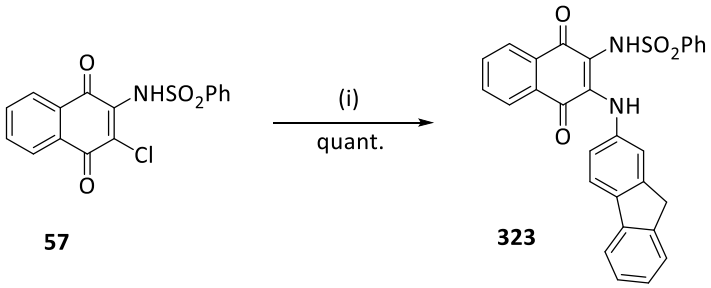


Figure 4.15: DFT modelling studies showing the variation of energy with torsional angle, θ, about the each of the four key rotatable bonds in naphthoquinone **238**. **A:** Structure of **238** with the key bond highlighted in red **(right)**, and a calculated plot of energy *vs.* torsional angle about this bond **(left)**; **B:** Images to show the optimal torsional angles about the aryl-aryl bond, generated in ChemBioDraw3D®.

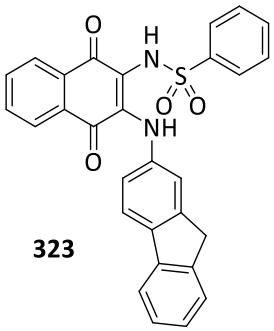


57 **323**

Scheme 4.13: Synthesis of fluorene-substituted **323** from naphthoquinone **57** *via* a Michael-type reaction; data generated by RB.[308] *Reagents and conditions:* (i) $CeCl_3 \cdot 7H_2O$ (1.0 eq.), MeOH, RT, 1.5 h *then* 2-aminofluorene (3.0 eq.), 90 °C, 16 h.

4.4.1. Pharmacological and Fluorescent Evaluation of Fluorene Derivative 323

In the acetyl CoA hydrolysis assay, fluorene derivative **323** was observed to be a potent MOUSE(NAT2) inhibitor, with a calculated IC_{50} value of 1.2 ± 0.1 µM (R^2 = 0.965, P <0.005) **(Table 4.13)**; moreover, **323** undergoes a distinctive shift in λ_{max} in the presence of MOUSE(NAT2) of +32 nm, indicative of a similar mode of binding within the enzyme active site to hit compound **32** and second generation lead **238**.



323

IC_{50} MOUSE(NAT2) (μM)		1.2 ± 0.1
***p*K_a**		10.2 ± 0.4
λ_{max} *p*H 8 (nm)		530
$\Delta\lambda_{max}$ *p*H 12.8 (nm)		+43
$\Delta\lambda_{max}$ MOUSE(NAT2) (nm)		+35
Fluorescence emission intensity at 424 nm (λ_{ex} = 408 nm) (a.u.)	***p*H 8.0**	54
	+ Base	0
	Reacidified	51
Fluorescence emission intensity at 374 nm (λ_{ex} = 279 nm) (a.u.)	***p*H 8.0**	503
	+ Base	275
	Reacidified	465

Table 4.13: Summary of pharmacological and optical properties of fluorene derivative **323**; data generated by RB.[308] IC_{50} values were calculated from the acetyl CoA hydrolysis assay and were carried out in triplicate; analysis was performed using KyPlot® software. Fluorescence experiments at *p*H 8 were carried out at a final concentration of 150 μM in 95% 20 mM Tris•HCl/5% DMSO (*v/v*); basification was effected by addition of 5% 1 M aq. NaOH to these solutions and acidification by addition of 5 μL 1 M aq. HCl. Fluorescence experiments at *p*H 12.8 were carried out in 95% 35 mM Na_2HPO_4•NaOH/5% DMSO (*v/v*). Sensitivity voltage = 800 V; a.u. = arbitrary units.

Unlike the coumarin derivatives, fluorene **323** also possesses a *p*K_a above 8, which suggests that any fluorescent peaks might be more sensitive to basification than those of the coumarin derivatives. The characteristic naphthoquinone fluorescence at λ_{em} = 424 nm was once again observed for compound **323**, and once again this fluorescence was reversibly quenched upon the addition of aq. 1 M NaOH. However, as predicted, an additional fluorescence peak was also observed in the emission spectrum of **323** following a zero order scan, which was attributed to fluorescence of the fluorene moiety. This fluorescence was observed at λ_{ex} = 279 nm and λ_{em} = 374 nm **(Figure 4.16)**. Crucially, a partial quenching of fluorescence is observed in both the excitation and emission spectra upon basification, and this quenching is also observed to be reversible, with the peak heights returning to near-original intensities upon reacidification.

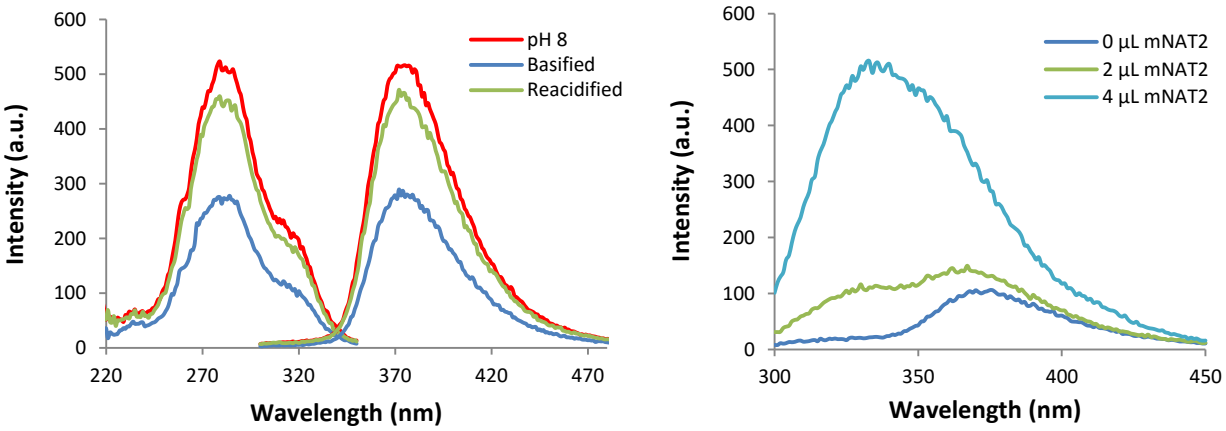


Figure 4.16: Left: Excitation and emission spectra for fluorene derivative **323** at 150 µM (λ_{ex} = 279 nm; λ_{em} = 374 nm) in 95% 20 mM Tris•HCl (*p*H 8)/5% DMSO (*v/v*) (red lines), with the addition of 5% 1 M aq. NaOH (blue lines) and upon reacidification with 5% 1 M aq. HCl (green lines). Data generated by RB;[308] sensitivity voltage = 800 V; a.u. = arbitrary units. **Right:** Emission spectra for fluorene derivative **323** at 15 µM in 95% 20 mM Tris•HCl (*p*H 8)/5% DMSO (*v/v*) with the addition of the following volumes of recombinant MOUSE(NAT2): 0 µL (dark blue line); 2 µL (green line) and 4 µL (sky blue line). Data generated by RB;[308] Sensitivity voltage = 800 V; a.u. = arbitrary units; mNAT2 = MOUSE(NAT2).

Furthermore, the peak heights corresponding to fluorescence of the fluorene moiety in **323** are approximately ten-fold more intense than those corresponding to fluorescence of the naphthoquinone moiety in **323** (518 a.u. and 54 a.u. at *p*H 8 respectively). This ensures that these peaks are clearly resolvable at far lower concentrations of **323** in solution than 150 µM, and hence a fluorescence titration experiment with increasing amounts of MOUSE(NAT2) was carried out at 15 µM **323 (Figure 4.16)**. In the emission spectrum (for λ_{ex} = 279 nm), initially the characteristic emission peak at 374 nm is clearly visible; however, upon the addition of 2 µL 100 µM recombinant MOUSE(NAT2) solution, new peaks begin to appear at lower wavelength. Upon addition of a further 2 µL of enzyme, the intensity of this peak increased significantly, completely obscuring the fluorescent peak corresponding to **323**. This new peak was attributed to fluorescence of tyrosine and tryptophan residues within MOUSE(NAT2); the fluorescence of aromatic amino acid residues with λ_{ex} = *c.* 280 nm and λ_{em} = 300-350 nm are widely reported.[321] Therefore, whilst fluorene derivative **323** is a potent MOUSE(NAT2) inhibitor and displays an intense, *p*H-dependent fluorescence over the required range of *p*H,

the excitation and emission wavelengths of **323** are too low for **323** to be a useful probe in the detection and quantification of MOUSE(NAT2) in solution.

4.4.2. Increasing the Excitation Wavelength: Design and Synthesis of a Target Library of Fluorene and Dibenzofuran Derivatives

Based on the fluorescence properties of fluorene derivative **323**, efforts were focussed on developing a close analogue of fluorene **323** which possessed a fluorescence excitation wavelength orthogonal to that of tryptophan and tyrosine residues. Treating the π-electrons of fluorene as particles in a one-dimensional box, the laws of quantum mechanics suggest that a longer wavelength of excitation is achievable by increasing the length of our "box", *i.e.* adding a conjugating acceptor group to the fluorene appendage at the opposite end to the naphthoquinone.

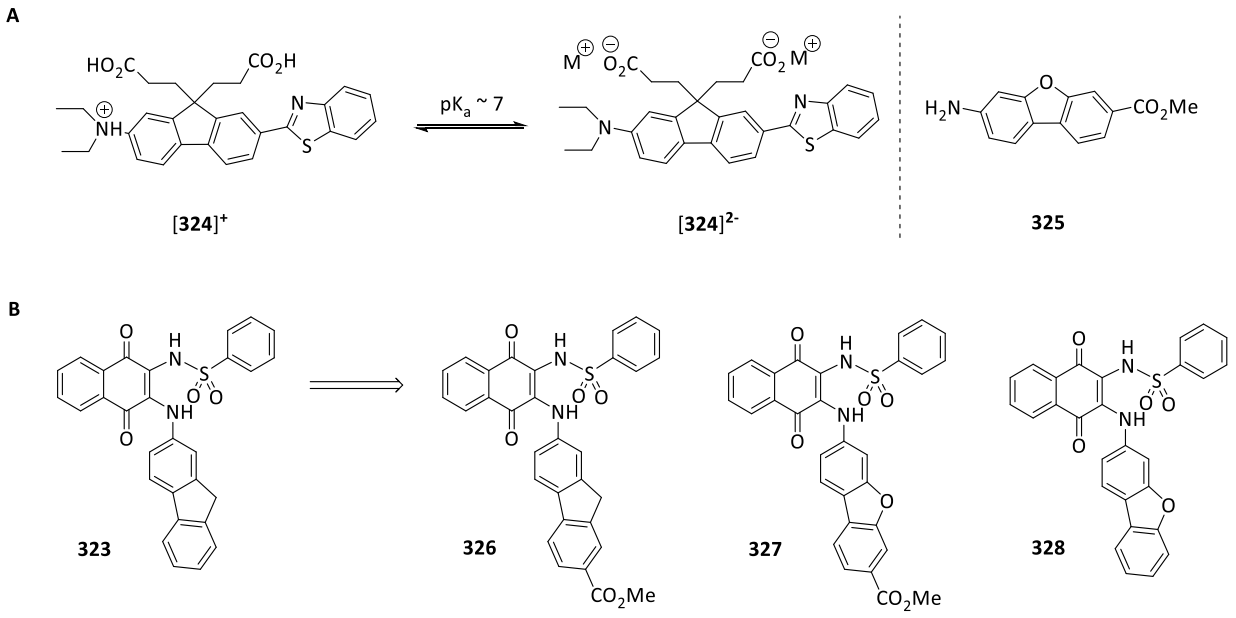


Figure 4.17: A: Water-soluble *p*H-dependent fluorophore **324**[322] and the less sterically cumbersome **325**.[323] **B:** Target library of derivatives based on MOUSE(NAT2) inhibitor **323**, which shows *p*H-dependent fluorescence.

Two interesting fluorophores sharing structural similarities to 2-aminofluorene have recently been reported in the literature **(Figure 4.17A)**. Compound **324** is a cell-permeable, *p*H-

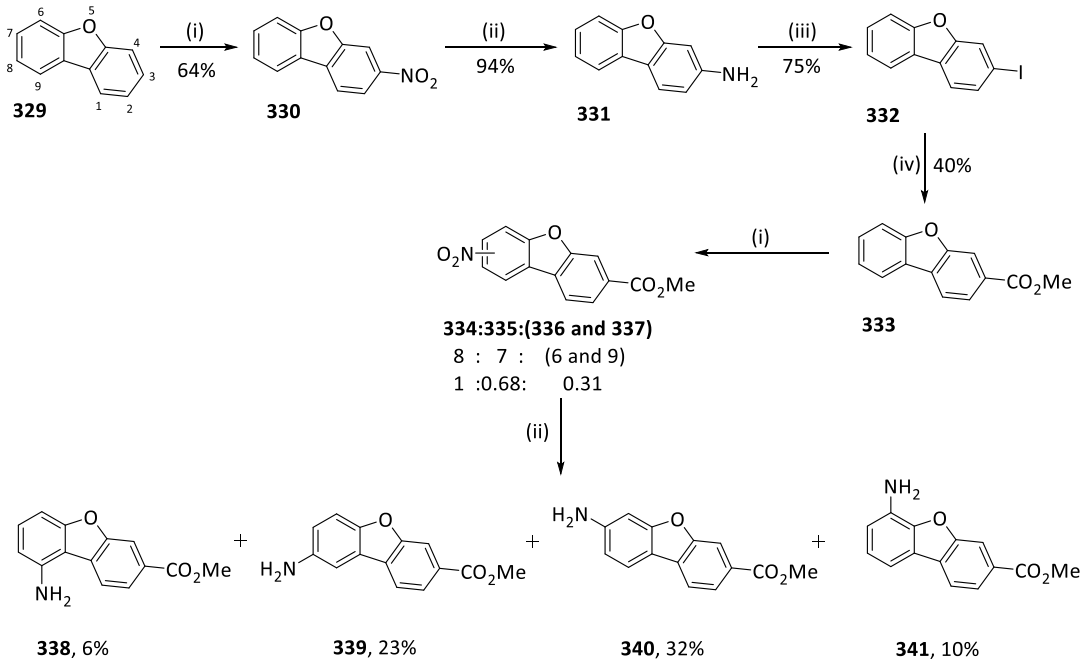
dependent fluorophore, with the acceptor-π-acceptor species [**324**]$^{+}$ exhibiting λ_{ex} = 341 nm and λ_{em} = 391 nm at *p*H <7 and the donor-π-acceptor species [**324**]$^{2-}$ exhibiting λ_{ex} = 382 nm and λ_{em} = *c.* 550 nm at *p*H >10.[322] Compound **325**, meanwhile, exhibits fluorescence in aqueous solution with an excitation wavelength of 335 nm, and contains a relatively small methyl ester as the acceptor group:[323] it is anticipated that the smaller the acceptor group which is appended to fluorene **323**, the more likely the resultant species is to retain inhibitory potency against MOUSE(NAT2).

On the basis of both these literature findings and the data generated from compound **323**, compounds **326** and **327** were designed as target compounds which might possess *p*H-dependent fluorescence with an excitation wavelength orthogonal to those of tryptophan and tyrosine, and given the reported behaviour of compound **324**, might even display a shift in λ_{ex} or λ_{em} upon deprotonation **(Figure 4.17B)**. Compound **328**, the unsubstituted analogue of methyl ester **327**, is also a desirable target to enable comparisons to be drawn between the two species.

The synthesis of amines **331** and **340**, the precursors to desired targets **328** and **327** respectively, from dibenzo[*b*,*d*]furan (DBF) was carried out by RZ and is outlined in **Scheme 4.14**. Nitration of DBF with nitric acid in TFA (conditions (i)) furnished solely 3-substituted nitro derivative **330**, which could be isolated in a 64% yield; the origin of the observed regiochemistry is postulated to derive from a charge-transfer (CT) mechanism of nitration, in which the rate-determining step involves electron transfer from electron-rich DBF to the nitronium ion formed from reaction of nitric acid and TFA.[319]

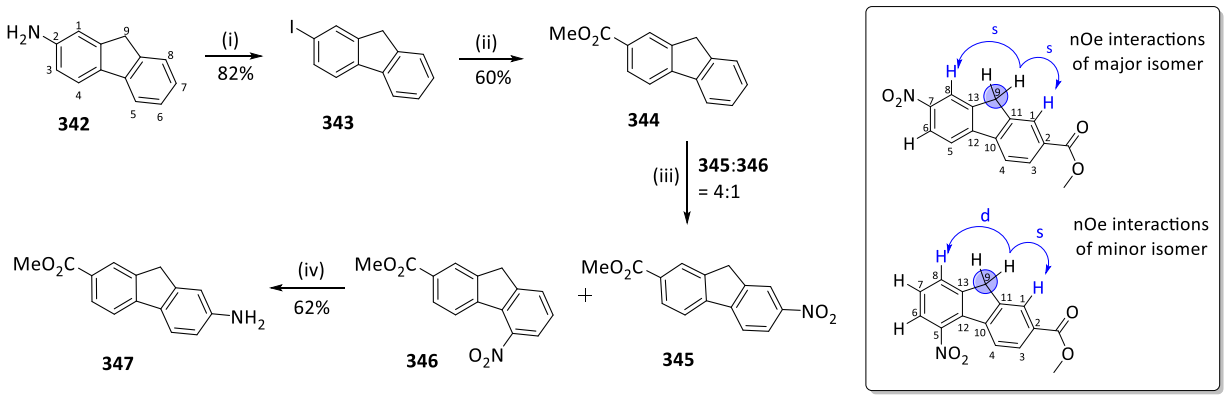
Nitrated species **330** was then reduced to aromatic amine **331** in 94% yield *via* catalytic hydrogenation on 10% Pd/C (conditions (ii)). Diazotisation and subsequent iodination was successfully effected on **331** to give 3-iodo-substituted **332** (conditions (iii)), which underwent Pd-mediated carbonylation[324] to furnish methyl ester **333** in a 40% yield (conditions (iv)). Nitration of methyl ester **333** under analogous conditions to the initial nitration of DBF **329**

yielded a 50:34:16 ratio of 8-nitro:7-nitro:(6-nitro and 9-nitro) substituted regioisomers; the 6- and 9-substituted isomers **336** and **337** were indistinguishable in the ^{1}H-NMR spectrum of the crude reaction mixture. The predominant isomer is the 8-substituted species **334**, the formation of which is consistent with an S_EAr-type mechanism proceeding *via* a σ-complex with preferential substitution of NO_2^+ *para* to oxygen. Hydrogenation of this mixture of nitrated species to the corresponding anilines was effected to furnish the four regiomeric aromatic amines **338**, **339**, **340** and **341** in respective isolated yields of 10%, 32%, 23% and 6%.

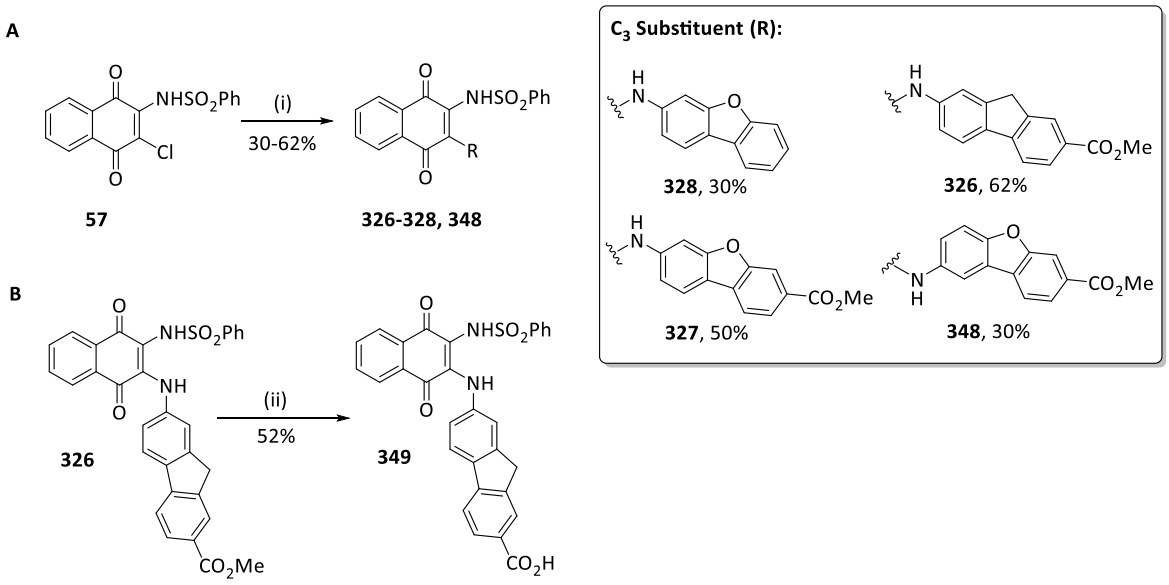


Scheme 4.14: Synthesis of aniline precursors to target dibenzo[*b*,*d*]furan derivatives **331** and **340**; data generated by RZ.[319] *Reagents and conditions:* (i) HNO_3 (1.2 eq.), TFA (excess), 0 ^{o}C, 1.5 h; (ii) H_2 (1 atm.), 10% Pd/C (0.2 eq.), MeOH, RT, 16 h; (iii) 1 M aq. $NaNO_2$ (1.5 eq.), 18% aq. HCl (excess), 0 ^{o}C, 0.5 h *then* 2 M aq. NaI (1.8 eq.), RT, 4 h; (iv) $Pd(OAc)_2$ (0.02 eq.), Xantphos (0.04 eq.), CO (1 atm.), MeOH:Et_3N (2:1), 70 ^{o}C, 5 days.

Aromatic amine **347**, the precursor to the desired target **326**, was synthesised by RZ in an analogous fashion **(Scheme 4.15)**, although without requiring the first two corresponding steps since 2-aminofluorene **342** was commercially available. The regioisometic identities of the key nitrated intermediates **345** and **346** were established by a combination of ^{1}H-NMR, HMBC and nOe spectroscopic experiments.



Scheme 4.15: Left: Synthesis of aromatic amine **347** from 2-aminofluorene **342**; data generated by RZ.[319] *Reagents and conditions:* (i) 1 M aq. $NaNO_2$ (1.5 eq.), 18% aq. HCl (excess), 0 °C, 0.5 h *then* 2 M aq. NaI (1.8 eq.), RT, 4 h; (ii) $Pd(OAc)_2$ (0.02 eq.), Xantphos (0.04 eq.), CO (1 atm.), MeOH: Et_3N (2:1), 70 °C, 5 days; (iii) HNO_3 (1.2 eq.), TFA (excess), 0 °C, 1.5 h; (iv) H_2 (1 atm.), 10% Pd/C (0.2 eq.), MeOH, RT, 16 h. **Right:** nOe irradiation of the C_9 protons give signal enhancements of H_1 and H_8 which confirms the regiochemical identity of nitration products **345** and **346**.



Scheme 4.16: A: Michael-type addition-elimination reaction of synthesised anilines **331**, **339**, **340** and **347** with naphthoquinone intermediate **57**; data generated by RZ.[319] **B:** Hydrolysis of methyl ester **326** to carboxylic acid **349**; data generated by RZ.[319] *Reagents and conditions:* (i) $CeCl_3 \bullet 7H_2O$ (1.0 eq.), MeOH, RT, 1.5 h *then* requisite aromatic amine (3.0 eq.), 90 °C, 16 h, yields for each adduct are given in the inset box to the right-hand side; (ii) LiOH (5 eq.), THF:H_2O (1:1), RT, 16 h *then* HCl, RT.

The synthesised anilines **331**, **340** and **347** were all subjected to Michael-type reaction with naphthoquinone **57** by RZ to give the desired target compounds **328**, **327** and **326** respectively

in moderate to good yield (conditions (i) in **Scheme 4.16A**). Sufficient quantities of aniline **339** had also been produced to enable formation of 8-nitro dibenzo[*b*,*d*]furan analogue **348** *via* a similar protocol.

Finally, it was also possible to furnish carboxylic acid **349** in 52% yield from the hydrolysis of the corresponding methyl ester **326** (conditions (ii) in **Scheme 4.16B**). Carboxylic acid **349** was a particularly desirable species to synthesise for two reasons: firstly, the analogous carboxylic acid biaryl derivative **271** possessed higher potency against MOUSE(NAT2) than many of the other biaryl derivatives synthesised; and secondly, it was predicted that the carboxylic acid functionality might confer an increase in aqueous solubility on the probe, which would be advantageous for downstream cellular studies.

4.4.3. Evaluation of the Library of Fluorene and Dibenzofuran Derivatives

The synthesised fluorene and dibenzofuran derivatives were all evaluated against MOUSE(NAT2) in the acetyl CoA hydrolysis assay, alongside the initial fluorene-substituted compound **323 (Table 4.14)**. Surprisingly, in these assays compound **323** displayed an IC_{50} value of >30 μM, and therefore the assay on compound **323** was repeated a further twice on two separate samples of the compound; all three sets of data conflict with the initially reported IC_{50} value for this species and suggest that **323** is a poor MOUSE(NAT2) inhibitor. Likewise, all of the species containing an oxygen atom (**327**, **328** and **348**) in place of the fluorene CH_2 group displayed poor IC_{50} values, above 30 μM. However, both ester **326** and carboxylic acid **349** possessed much more favourable potencies, with IC_{50} values of 8.3 μM and 3.1 μM respectively. It is hypothesised that replacement of the CH_2 group with an oxygen atom might therefore lead to the loss of a favourable interaction to the enzyme or the gain of a repulsive electronic interaction; the two oxygen lone pairs are predicted to adopt a similar spatial orientation to the two C-H σ-bonds which they are replacing.

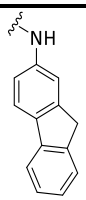
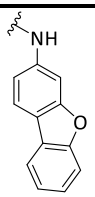
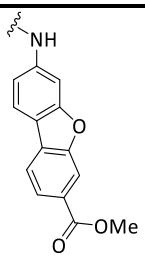
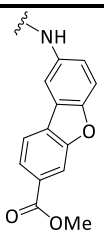
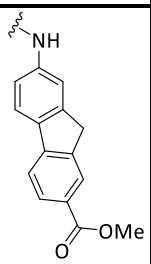
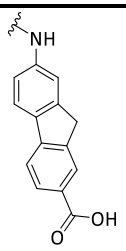
Compound	323	328	327	348	326	349
C_3 Substituent						
IC_{50} MOUSE(NAT2) (μM)	>30	>30	>30	>30	8.3 ± 2.2	3.1 ± 0.8
R^2	N/A	N/A	N/A	N/A	0.5648	0.6750
P	N/A	N/A	N/A	N/A	***	**
***p*K_a**	10.6 ± 0.2	10.1 ± 0.1	10.5 ± 0.1	11.2 ± 0.3	11.0 ± 0.05	8.5 ± 0.1
λ_{max} *p*H 8 (nm)	530	520	512	507	525	524
$\Delta\lambda_{max}$ *p*H 12.8 (nm)	+54	+40	+55	+73	+54	+68
$\Delta\lambda_{max}$ MOUSE(NAT2) (nm)	+50	+52	N.D.	+83	+95	N.D.

Table 4.14: IC_{50} values and key colorimetric parameters for fluorene derivatives **323**, **326-328** and **348-349** against MOUSE(NAT2) in the acetyl CoA hydrolysis assay, with squared correlation coefficients (R^2) and significance levels (*P*) as given; ** = $P < 0.01$; *** = $P < 0.005$. Data generated by RZ;[319] N.D. = not determined.

The carboxylic acid functionality in **349** appears to confer additional potency on this compound, as was observed to be the case for species **271** in the initial biaryl series (*cf.* **Section 4.1.1.**) – this supports the hypothesis that a polar substituent on the C_3 moiety might protrude from the active site and make additional enthalpic contributions to binding *via* interactions with the aqueous solvent medium. Furthermore, the kinetic solubility of carboxylic acid **349** and methyl ester **326** were measured in 99% 0.01 M aq. PBS/1% DMSO (*v/v*), and were found to be 65 μM and <1 μM respectively. This suggests that hydrolysis of the methyl ester group of **326** has, as predicted, had a hugely beneficial effect on the solubility of the species within an aqueous medium. The solubility limit of **349** is also approximately twenty-fold higher than that of hit compound **32**, which was calculated to be 3.75 μM.

Colorimetric evaluation of the fluorene-derived library shows that, unlike for the coumarin and quinolinone derivatives, these species possess desirable *p*K_a values within the range of 8.5-11.2 **(Table 4.14)**. These values are consistent with those reported earlier (*cf.* **Section**

3.2.3.) for C_3-anilino substituted species. Moreover, all of the derivatives tested display a similar shift in λ_{max} in the presence of MOUSE(NAT2) to that in the presence of a basic buffer solution; carboxylic acid **349** could not, however, be detected above background noise at 15 µM in the presence of MOUSE(NAT2) due to its low absorption coefficients (ε_N = 773 $M^{-1}cm^{-1}$ and ε_{CB} = 431 $M^{-1}cm^{-1}$). These data are consistent with the proposed model of binding of the fluorene analogues and, pleasingly, suggest that the optical properties of the molecules are sensitive to sulfonamide-N*H* deprotonation.

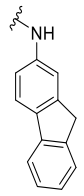
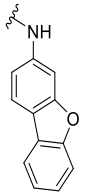
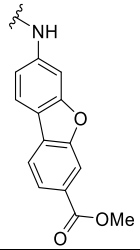
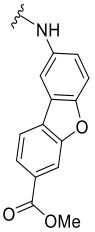
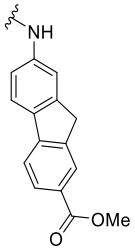
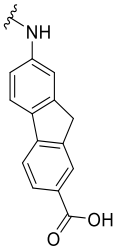
Compound		**323**		**328**		**327**	
C_3 Substituent							
Wavelength (nm)		λ_{ex} = 279	λ_{em} = 374	λ_{ex} = 309	λ_{em} = 368	λ_{ex} = 332	λ_{em} = 423
Fluorescence Intensity (a.u.)	***p*H 8**	667	663	741	734	426	352
	+ Base	207	213	127	140	116	85
	Reacidified	537	491	51	35	164	103
Compound		**348**		**326**		**349**	
C_3 Substituent							
Wavelength (nm)		λ_{ex} = 339	λ_{em} = 473	λ_{ex} = 333	λ_{em} = 493	λ_{ex} = 327	λ_{em} = 446
Fluorescence Intensity (a.u.)	***p*H 8**	37	37	349	343	325	319
	+ Base	18	17	191	188	194	294
	Reacidified	34	31	413	432	315	309

Table 4.15: Fluorescent properties of fluorene and dibenzofuran derivatives **323**, **326-328** and **348-349** at 150 µM; data generated by RZ.[319] Spectra at *p*H 8 were recorded in 95% 20 mM Tris•HCl/5% DMSO (*v/v*); basification was effected by addition of 5 µL 1 M aq. NaOH and reacidification was susbequently effected by addition of 5 µL 1 M aq. HCl. Sensitivity voltage = 800 V; a.u. = arbitrary units.

In light of these encouraging pharmacological and colorimetric data sets, the fluorescence properties corresponding to the fluorene or dibenzofuran moieties within compounds **326-328** and **348-349** were evaluated **(Table 4.15)**. Unsubstituted fluorene derivative **323** was also

re-evaluated in these studies and the fluorescence data on this compound was found to be consistent with that obtained previously (*cf.* **Section 4.4.1.**).

Encouragingly, these data show that as anticipated, adding an acceptor group to the fluorene or dibenzofuran moieties increases its fluorescent excitation and emission wavelengths, with methyl ester derivative **326** displaying λ_{ex} = 333 nm and λ_{em} = 493 nm *cf.* λ_{ex} = 279 nm and λ_{em} = 374 nm for unsubstituted derivative **323**; this ensures that the excitation wavelengths of these newly synthesised derivatives are orthogonal to those of tyrosine and tryptophan residues.

Each of the tested derivatives display relatively intense fluorescence peaks at 150 µM with the exception of compound **348**, which is regioisomeric to the other analogues and bears the -NH- linker to the naphthoquinone core at the 8-position of dibenzofuran rather than the 7-position. Upon basification, it can be observed that the fluorescence of all the fluorene derivatives is partially quenched; however, upon reacidification the dibenzofuran analogues **327** and **328** do not regain their original fluorescence intensities, unlike the fluorene analogues **323**, **326** and **349**.

The fluorescence properties of methyl ester **326** and carboxylic acid **349** were subsequently evaluated in the presence of recombinant MOUSE(NAT2), given that these two species both display the required combination of high inhibitory potency against the enzyme, a desirable *p*K_a value, and intense fluorescent excitation and emission peaks which are reversibly quenched in the presence of base and are at orthogonal wavelengths to those of typtophan and tyrosine residues in proteins.

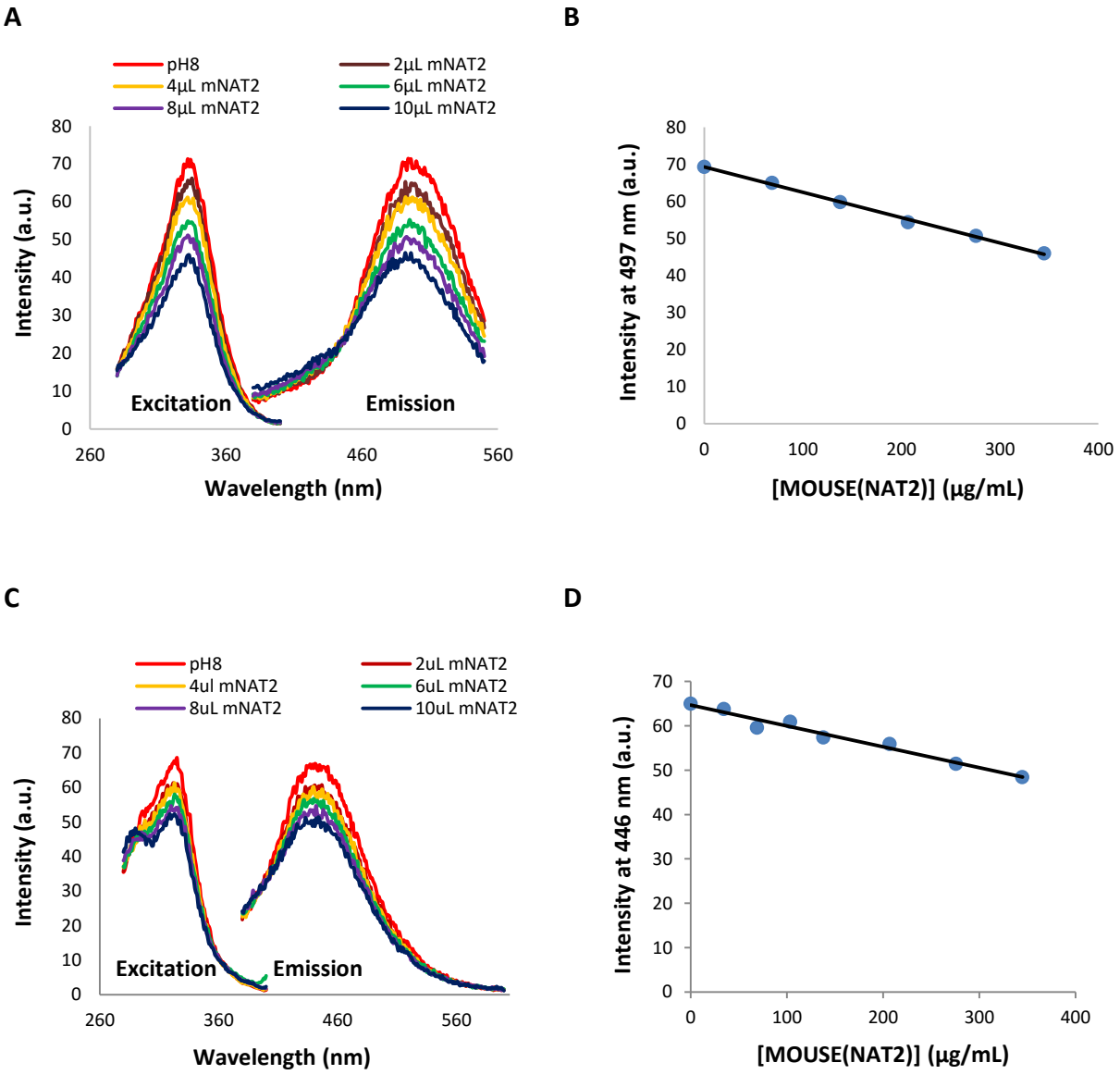


Figure 4.18: A: Excitation and emission spectra of methyl ester derivative **326** in 95% Tris•HCl (*p*H 8)/5% DMSO (*v/v*) (red line) and with increasing volumes of MOUSE(NAT2): 2 µL (brown line), 4 µL (yellow line), 6 µL (green line), 8 µL (purple line) and 10 µL (dark blue line); data generated by RZ.[319] **B:** Variation of fluorescence emission intensity of methyl ester **326** at 497 nm with the added concentration of MOUSE(NAT2). **C:** Excitation and emission spectra of carboxylic acid derivative **349** in 95% Tris•HCl (*p*H 8)/5% DMSO (*v/v*) (red line) and with increasing volumes of MOUSE(NAT2): 2 µL (brown line), 4 µL (yellow line), 6 µL (green line), 8 µL (purple line) and 10 µL (dark blue line); data generated by RZ.[319] **D:** Variation of fluorescence emission intensity of carboxylic acid **349** at 446 nm with the added concentration of MOUSE(NAT2). The concentration of the stock MOUSE(NAT2) solution as determined by a BCA assay was 3450 µg/mL (*c.* 100 µM) and the concentration of **326** and **349** used in the experiments was 15 µM. Sensitivity voltage = 800 V; a.u. = arbitrary units; mNAT2 = MOUSE(NAT2).

Excitingly, when methyl ester **326** was treated with increasing concentrations of recombinant MOUSE(NAT2) up to 345 μg/mL (10 μM) in a 95% Tris•HCl (*p*H 8)/5% DMSO (*v/v*) solution, a linear, [MOUSE(NAT2)]-dependent quenching of fluorescence was observed that was clearly visible above background noise **(Figures 4.18A and 4.18B)**. The smallest concentration of MOUSE(NAT2) sensitively detected in this experiment is therefore 34.5 μg/mL, or 1 μM. This result represents, to the best of our knowledge, the first example of a non-covalent, small molecule fluorescent probe which is capable of quantifying the concentration of its target protein within solution *via* a rapid optical measurement. When the same experiments were repeated on carboxylic acid derivative **349**, a similar [MOUSE(NAT2)]-dependent quenching of fluorescence was also observed **(Figures 4.18C and 4.18D)**, albeit with a slightly lower sensitivity than for methyl ester **326**.

4.4.4. Evaluation of Ester 326 and Acid 349 in Cellular Samples

Following the successful generation of a linear plot of fluorescence emission intensity of compounds **326** and **349** against the concentration of recombinant MOUSE(NAT2), experiments were conducted to determine whether probes **326** and **349** are capable of detecting MOUSE(NAT2) above background noise in a cellular extract sample. An *E. coli* cell culture was therefore grown and harvested (analogously to the procedure outlined in **Section 7.8.**), and compounds **326** or **349** were independently added to solutions containing 10% of this cell extract and 5% DMSO in 20 mM Tris•HCl (*p*H 8) (*v/v/v*). Fluorescent peaks for both **326** and **349** were observed in such an environment, with both compounds displaying quenching of their fluorescent peaks upon the addition of 5% 1 M aq. NaOH solution.

Subsequently, the cell extract solutions containing **326** or **349** were spiked with increasing concentrations of MOUSE(NAT2). In the case of methyl ester **326**, a very clear quenching of fluorescence emission is observed at 497 nm, and this quenching is approximately linearly dependent upon the concentration of MOUSE(NAT2), as observed in the experiments using recombinant enzyme **(Figures 4.19A and 4.19C)**.

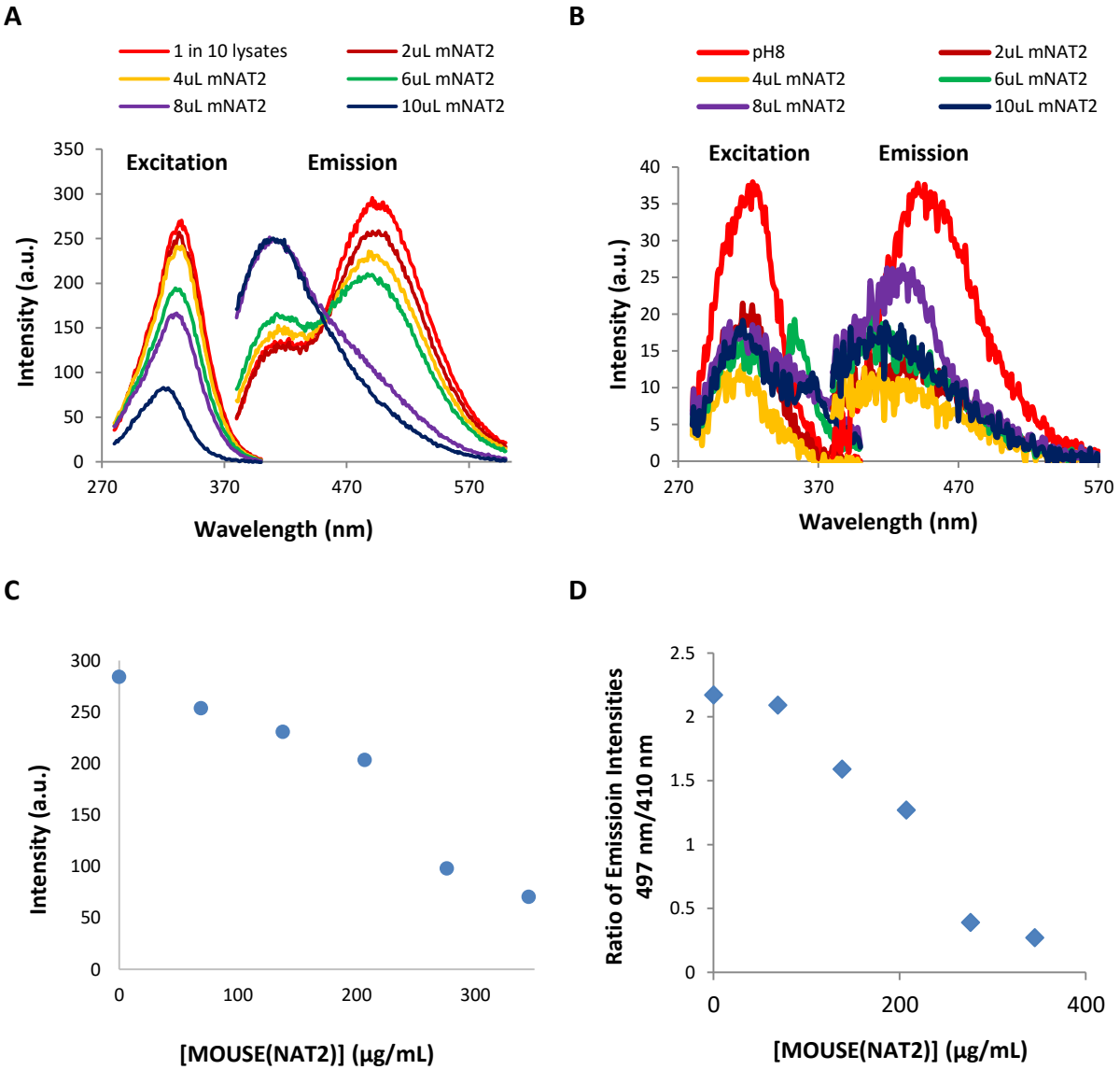


Figure 4.19: A: Excitation and emission spectra of methyl ester derivative **326** in 85% Tris•HCl (*p*H 8)/10% *E. coli* cell extract/5% DMSO (*v/v/v*) (red line) and with increasing volumes of MOUSE(NAT2): 2 µL (brown line), 4 µL (yellow line), 6 µL (green line), 8 µL (purple line) and 10 µL (dark blue line); data generated by RZ.[319] **B:** Excitation and emission spectra of carboxylic acid derivative **349** in 85% Tris•HCl (*p*H 8)/10% *E. coli* cell extract/5% DMSO (*v/v/v*) (red line) and with increasing volumes of MOUSE(NAT2): 2 µL (brown line), 4 µL (yellow line), 6 µL (green line), 8 µL (purple line) and 10 µL (dark blue line); data generated by RZ.[319] **C:** Variation of fluorescence emission intensity of methyl ester **326** at 497 nm with the added concentration of MOUSE(NAT2). **D:** Variation of the ratio of fluorescence emission intensities of **326** at 497 nm and 410 nm with the added concentration of MOUSE(NAT2). The final concentration of **326** and **349** used was 15 µM and the concentration of the stock MOUSE(NAT2) solution was 3450 µg/mL (*c.* 100 µM); sensitivity voltage = 800 V; a.u. = arbitrary units; mNAT2 = MOUSE(NAT2).

Fascinatingly, in these experiments, the appearance of a new emission peak is observed at 410 nm in these spectra in a [MOUSE(NAT2)]-dependent fashion, giving us a truly ratiometric probe for MOUSE(NAT2) detection with a fluorescent "on" switch in addition to a fluorescent "off" switch. If the ratio of the intensity of the emission peaks at 497 nm and 410 nm is plotted against MOUSE(NAT2) concentration, an approximately linear relationship also appears to exist between these two variables **(Figure 4.19D)**.

The fluorescent emission peak of carboxylic acid **349** at 446 nm also appears to be quenched by the addition of MOUSE(NAT2), and a new emission peak generated at a lower wavelength, *c.* 400-410 nm; however, the emission intensities of these peaks are considerably lower than the corresponding peaks for methyl ester **326 (Figure 4.19B)**. This effect could possibly be due to higher levels of non-specific binding of carboxylic acid **349** in cellular extracts than of methyl ester **326**: in a protein binding experiment against 50% murine plasma, it was determined that the mean unbound fraction of ester **326** was 0.38, whilst for acid **349** this fraction was only 0.08.

To determine the sensitivity limit of detection of methyl ester **326** in these cell extract experiments, a BCA assay was carried out, which determined the total protein concentration in the ten-fold diluted *E. coli* cell extract to be 1350 μg/mL. Therefore, the smallest added concentration of MOUSE(NAT2) in these experiments which was sensitively detected by compound **326**, 69 μg/mL, corresponds to MOUSE(NAT2) comprising 5% of the total protein concentration in the samples. A subsequent experiment was carried out in which probe **326** was applied to a solution containing twice as much *E. coli* cell extract as previously (*i.e.* a solution comprising 75% 20 mM Tris•HCl (*p*H 8)/20% *E. coli* cell extract/5% DMSO (*v/v/v*)) and a four-fold smaller volume of MOUSE(NAT2) was added**.** This corresponded to a MOUSE(NAT2) concentration of 17.25 μg/mL (0.5 μM) and a total protein concentration of 2700 μg/mL, *i.e.* MOUSE(NAT2) comprised 0.6% of the total protein present. Under such conditions, a clear reduction in the intensity of the fluorescent emission peak at 497 nm could still be observed upon MOUSE(NAT2) addition.

This result is significant because **326** is therefore capable of detecting the presence of MOUSE(NAT2) at both a concentration and a proportion of total cellular protein which are very similar to that of HUMAN(NAT1) in the ER+ breast cancer cell line ZR-75-1; Western and dot blotting studies have estimated the concentration of HUMAN(NAT1) in ZR-75-1 cells to be within the range 0.6-1.2 µM and the proportion of total cellular protein which HUMAN(NAT1) comprises as 0.17-0.52%.[258]

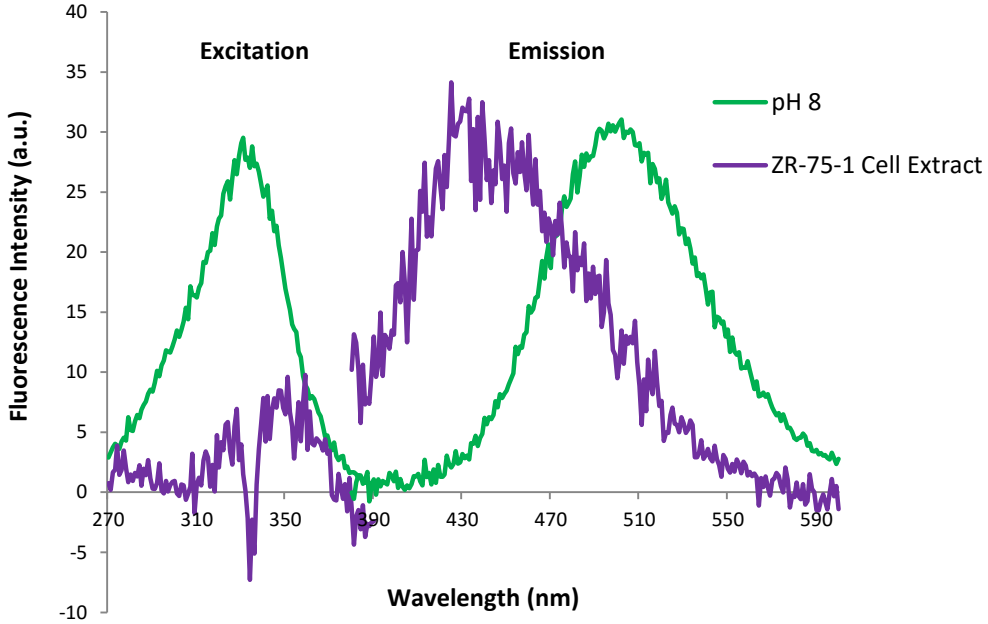


Figure 4.20: Excitation and emission spectra of fluorene **326** in 95% Tris•HCl (*p*H 8)/5% DMSO (*v/v*) (green lines) and in 95% ZR-75-1 cell extract/5% DMSO (*v/v*) (purple lines). The final concentration of **326** used was 15 µM and the cell extract solution contained the extract of 5 x 10^7 ZR-75-1 cells/mL. Sensitivity voltage = 800 V; a.u. = arbitrary units.

Therefore, a ZR-75-1 ER+ tumour cell line was grown (for protocol see **Section 7.10.**) and harvested to make an extract containing 5 x 10^7 cells/mL; the cell density was determined *via* cell counting using a haemocytometer. Compound **326** was added to neat extract to a final concentration of 15 µM in a solution containing 5% DMSO (*v/v*), and the fluorescence spectra recorded; the blank-corrected spectra are displayed in **Figure 4.20**. Fascinatingly, under these conditions, the excitation peak of **326** at 333 nm is significantly quenched, and the emission peak at 493 nm is shifted to a lower wavelength of *c.* 430 nm. This behaviour is analogous to

the behaviour of **326** in the previous *E. coli* doping experiments when the highest concentrations of MOUSE(NAT2) (345 mg/mL) were added, and so suggests that this is a NAT-dependent effect. In a future study, a ZR-75-1 cell line should be grown in which HUMAN(NAT1) is either knocked out by shRNA or removed by immunoprecipitation; this would give an adequate control experiment to determine if the measurable changes in the fluorescence spectrum of **326** in the presence of ZR-75-1 cell extracts are mediated by the presence of HUMAN(NAT1).

Nonetheless, the data collected in this study give a promising indication that we have successfully developed the first known example of a small molecule, non-covalent optical probe which is capable of detecting its native protein target in extracts from human cell samples. This represents a novel paradigm in protein detection which might enable the future development of a reliable and sensitive test for detecting the concentration of HUMAN(NAT1) in patient biopsy samples, for the accurate and rapid diagnosis and prognosis of ER+ breast cancers.

4.5. Conclusions from Fluorescent Probe Development

In this chapter, efforts have been described to utilise the structure-activity relationships elucidated in **Chapter 3** to develop a fluorescent probe for HUMAN(NAT1) detection in cells. SAR studies had suggested that a wide range of substituents were tolerated at the C_3 position of the naphthoquinone core of compound **32** and an *in silico* model suggested that this was due to the C_3 appendage pointing out of the active site into bulk solvent. C_3 biaryl amino substituents had displayed particularly promising potencies against both HUMAN(NAT1) and MOUSE(NAT2), and hence given the propensity for biaryl moieties to fluoresce in certain environments, a larger library of biaryl derivatives was synthesised, bearing a wide variety of electron-donating and electron-withdrawing substituents at different positions on the aromatic ring system.

Each of these derivatives was found to exhibit a characteristic fluorescence with λ_{ex} = 372 and 408 nm and λ_{em} = 424 nm; moreover, these fluorescent peaks are reversibly quenched under basic conditions. However, other analogues of hit compound **32** which are devoid of a biaryl moiety also display this characteristic fluorescence, and hence the presence of these peaks was attributed to fluorescence of the naphthoquinone core of the inhibitors itself. Unfortunately, the fluorescence observed was not intense enough to enable studies at lower concentrations of the probes in the presence of the target protein.

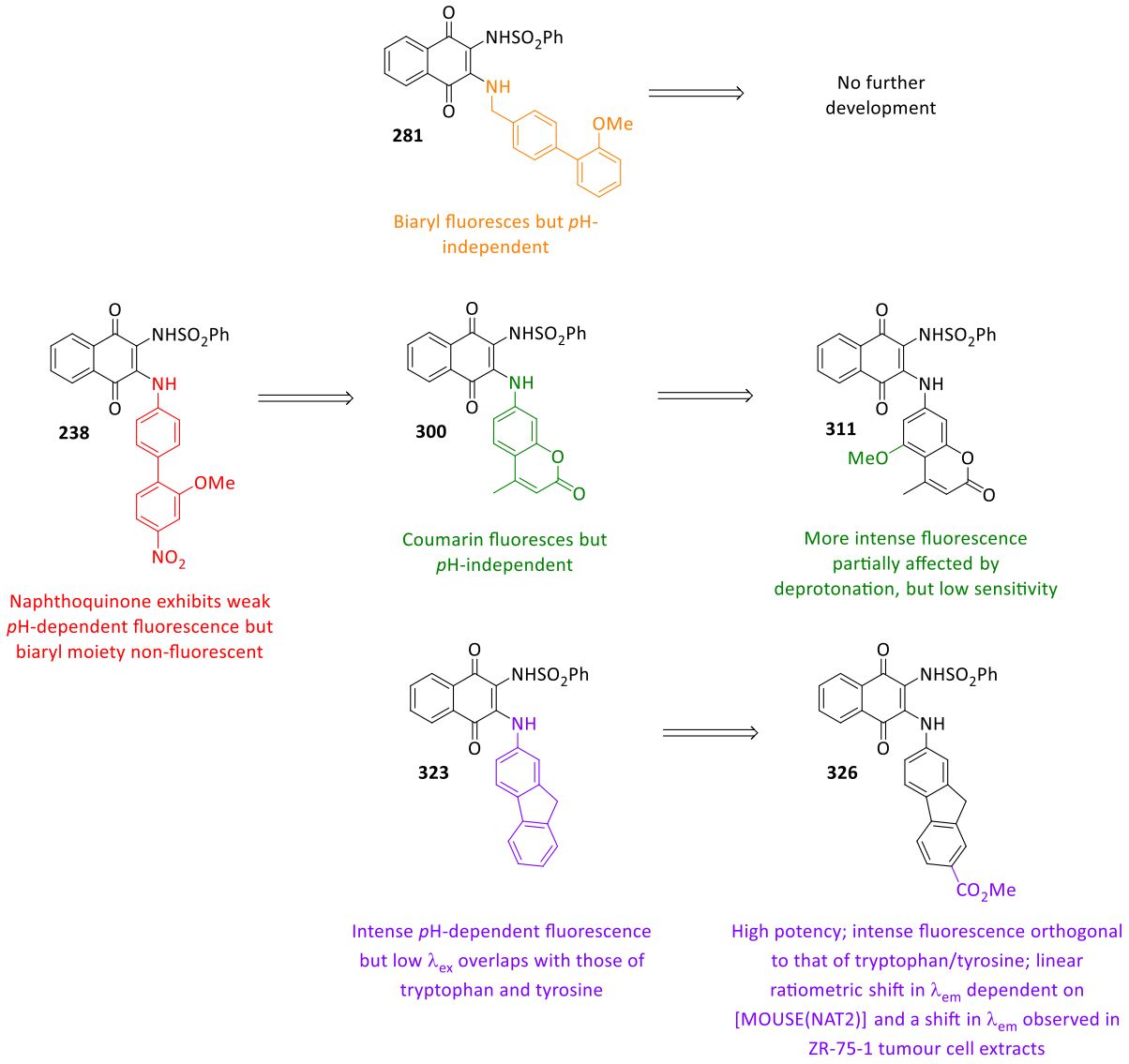


Figure 4.21: Progressive development of a fluorescent probe for HUMAN(NAT1) detection, culminating in the discovery of methyl ester-substituted fluorene **326**, the first developed non-covalent ratiometric fluorescent probe for quantification of a target protein in a cellular extract.

Three strategies were subsequently employed to generate more intense fluorescence peaks emanating from the C_3 substituent **(Figure 4.21)**. Firstly, a methylene linker was inserted between the nitrogen atom directly bonded to C_3 and the biaryl moiety; this led to the generation of species **281**, which was a potent MOUSE(NAT2) inhibitor and which possessed an additional fluorescent peak corresponding to the biaryl appendage; however, the fluorescence intensity was insensitive to remote sulfonamide-N*H* deprotonation.

Subsequently, the biaryl group was replaced with a coumarin moiety directly conjugated to the naphthoquinone core, since coumarins are reported to have a high fluorescence brightness:size ratio. Coumarin **300** was found to be a good inhibitor of MOUSE(NAT2) and possessed intense fluorescence at λ_{ex} = 344 nm and λ_{em} = 440 nm; however, this fluorescence too was found to be insensitive to sulfonamide-N*H* deprotonation. It was hypothesised that this might be due to the strong electron-withdrawing nature of the coumarin moiety resulting in only a small variation in electron density over the moiety with changing *p*H. Therefore, more electron rich coumarin and quinolinone analogues of **300**, such as methoxy-substituted **311**, were synthesised. **311** displayed both a higher fluorescence intensity and a greater sensitivity to sulfonamide-N*H* deprotonation than unsubstituted **300**, and in the presence of small quantities of MOUSE(NAT2) a partial quenching of its fluorescent emission was observed. However, addition of larger concentrations of MOUSE(NAT2) did not lead to any further perturbation of fluorescence intensity; the low sensitivity of derivatives such as **311** was attributed to their low *p*K_a values in the range 7.0-7.7 (*i.e.* below the assay buffer *p*H).

Given the more favourable *p*K_a values of the biaryl amine derivatives, an attempt was made to restore fluorescence by rigidifying the biaryl moiety. Synthesis of fluorene analogue **323** afforded a probe which possessed an intense, *p*H-dependent fluorescent peak which was reversibly quenched in base. However, the fluorescence excitation wavelength of **323**, 279 nm, overlaps with that of tryptophan and tyrosine residues in proteins,[321] which precluded enzymatic studies with MOUSE(NAT2). Addition of an electon-withdrawing ester substituent, however, led to formation of species **326** with increased fluorescence

wavelengths of λ_{ex} = 333 nm and λ_{em} = 493 nm. These peaks were found to be *p*H-dependent and were reversibly quenched in base; excitingly, a quenching of fluorescence which was linearly dependent on [MOUSE(NAT2)] was also observed. This led to studies in which **326** was added to *E. coli* cell extracts spiked with increasing concentrations of MOUSE(NAT2). As the MOUSE(NAT2) concentration was increased, not only was a linear quenching of fluorescence at 493 nm observed, but a fluorescent "on" switch at 410 nm was also observed. Excitingly, similar behaviour was also observed in the emission spectrum of **326** in the presence of cell extract from the human ER+ breast cancer cell line ZR-75-1, which overexpresses HUMAN(NAT1).

Therefore, **326** represents the first known example of a small molecule, non-covalent optical probe which is capable of quantifying the concentration of a target protein in its native state within a cell extract; furthermore, **326** is capable of detecting the presence of HUMAN(NAT1) in extracts from a representative human tumour cell line which overexpresses this protein.

Chapter 5: Development of Inhibitors to Study the Endogenous Roles of HUMAN(NAT1)

5.1. HUMAN(NAT1) as a Potentially Novel Therapeutic Target in Cancer

Recent work in the laboratory of Minchin and Butcher (University of Queensland, Brisbane, Australia) has offered a tantalising indication that inhibition of HUMAN(NAT1) *in vivo* might offer an alternative therapy for cancers in which HUMAN(NAT1) is overexpressed, if other treatments fail due to intrinsic or acquired resistance. shRNA knockdown of *HUMAN(NAT1)* in the triple-negative breast cancer cell line MDA-MB-231, which overexpresses *HUMAN(NAT1)*, leads to a reduction in both cell proliferation and invasiveness;[272] when this cell line was injected into nude mice, the cells expressing anti-NAT1 shRNA led to the formation of significantly fewer colonies in the lungs of the mice than those not expressing anti-NAT1 shRNA.[273] shRNA knockdown of NAT1 in the non-invasive colon cancer cell line HT-29 also led to a reduction in cell proliferation *via* upregulation of E-cadherin.[274] Additionally, Adam *et al.* showed that hallmarks of oncogenic potential can be observed in the non-cancerous breast cell line HB4a if the cells are induced to overexpress *HUMAN(NAT1)*.[267]

However, no specific small molecule inhibitors of HUMAN(NAT1) with a suitable balance of pharmacological and physical properties have ever been available to enable informative inhibition studies in NAT1 +ve cell lines, either *in vitro* or *in vivo*. Studies have shown that when MDA-MB-231 cells were treated with a rhodanine-based inhibitor[243] of HUMAN(NAT1), a dose-dependent reduction in cell proliferation and invasiveness was observed; the reduction in proliferation was attributed to blocking cells in the G_2/M phase of the cell cycle.[272] However, the inhibitor had to be dosed at concentrations well in excess of its IC_{50} value against HUMAN(NAT1) and so a NAT-dependent mechanism of action could not be proved, especially given the well-reported promiscuity of the rhodanine drug scaffold.[280]

The HUMAN(NAT1) inhibitors synthesised and evaluated in SAR studies in **Chapter 3** of this study have been qualitatively observed to possess low solubility in 95% Tris•HCl (*p*H 8)/5% DMSO (*v/v*), which preclude their utility in any cell-based studies. It was also hypothesised that the hydrophobicity of the naphthoquinone-derived species might prevent their effective transport across epithelial cell membranes,[325] and potentially lead to high levels of non-specific binding to other proteins within cells or in plasma.[326]

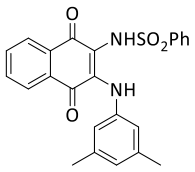
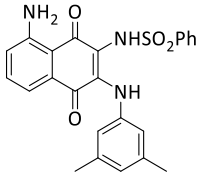
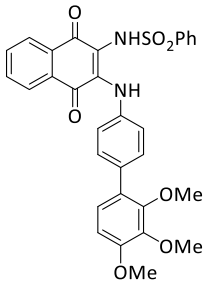
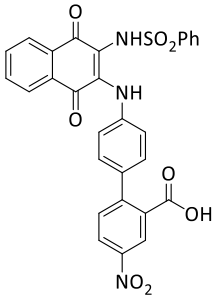
Compound		**32**	**190**	**220**	**271**
Structure					
IC_{50} MOUSE(NAT2) (µM)		3.1 ± 0.69	0.43 ± 0.06	0.42 ± 0.11	0.51 ± 0.06
IC_{50} HUMAN(NAT1) (µM)		4.1 ± 0.56	0.54 ± 0.13	0.15 ± 0.02	N.D.
Kinetic Solubility (µM)		3.8	2.0	3.8	6.5
Caco-2 Membrane Permeability	**Flux A to B (10^{-6} cms^{-1})**	7.7 ± 1.6	3.0 ± 0.97	3.0 ± 2.0	0.84 ± 0.06
	% Recovery	19	12	57	70
	Efflux Ratio	0.74	1.2	0.20	9.4
Fraction Unbound to Plasma Protein		0.038 ± 0.017	N.D.	0.007 ± 0.002	0.013

Table 5.1: Key physical parameters for hit compound **32** and developed analogues **190**, **220** and **271**, measured by Cyprotex plc (Macclesfield, UK). Kinetic solubility was determined *via* turbidimetric measurement in a solution containing 99% 0.01 M PBS (*p*H 7.4)/1% DMSO (*v/v*); data are presented as the calculated mid-range of three repeat readings. Permeability in both the apical to basolateral direction (A to B) and *vice versa* across a Caco-2 intestinal epithelial cell monolayer[327] was determined at a concentration of 1 µM (**32** and **190**) or 10 µM (**220** and **271**) at 37 ^{o}C with an incubation time of 2 h; data are presented as the mean of two repeat readings ± one standard deviation. The % recovery of compound in the experiment is also given as a mean value. Efflux ratios are calculated as the rate of B to A flux divided by the rate of A to B flux. The extent of binding to plasma proteins was determined by equilibrium dialysis, using 5 µM (**32**) or 1 µM (**220** and **271**) compound in a 50% mouse plasma solution; data are presented as the mean of two repeat readings ± one standard deviation (**32** and **220**) or as a single experimental reading (**271**). N.D. = not determined.

Therefore, the key physical parameters of kinetic solubility, transport rates across a model epithelial cell monolayer, Caco-2,[327] and levels of binding to plasma proteins were measured for hit compound **32**, 8-amino substituted **190**, which had been observed to possess a ten-fold higher potency against HUMAN(NAT1) than **32**, and the representative C_3-biaryl amino analogues **220** and **271 (Table 5.1)**.

These data do indeed suggest that there is a large scope for improvement of the physical properties of these inhibitors, particularly with regard to kinetic solubility: compound **32** is soluble in 99% 0.01 M PBS/1% DMSO (*v/v*) at a concentration approximately equal to its IC_{50} value against recombinant HUMAN(NAT1), and the other improved inhibitors are soluble at no more than one order of magnitude greater than their corresponding IC_{50} values. Given non-specific binding levels to plasma proteins, which are particularly high for biaryl derivative **220** (mean fraction unbound = 0.007), to accurately evaluate the effect of HUMAN(NAT1) inhibition in cell lines, it is necessary to dose the test compounds up to concentrations at least two orders of magnitude in excess of their IC_{50} values against the human protein, and preferably higher. Therefore, it was decided to design and synthesise analogues of compound **32** which would be anticipated to have increased solubility in aqueous media, whilst retaining favourable and specific binding to HUMAN(NAT1), and the ability to traverse cell membranes.

5.1.1. Introduction of Solubilising Groups at the C_3 Position

Given the high potencies of analogues of **32** bearing an aromatic amine at the C_3 position (*cf.* **Section 3.2.2**, **Section 3.5.** and **Chapter 4**), and the wide range of appendages tolerated at this position, it was hypothesised that the most fruitful strategy would be to introduce a hydrophilic substituent within the C_3 moiety. Further support for this approach comes from the encouraging potency of carboxylic acid-containing **271** and **349** against MOUSE(NAT2), and the well-reported hydrophobicity of the HUMAN(NAT1) and MOUSE(NAT2) active sites,[247b, 258] in which particularly polar substituents might be poorly tolerated; *in silico*

modelling however suggests that the C_3 appendage extends out of the active site into bulk solvent.

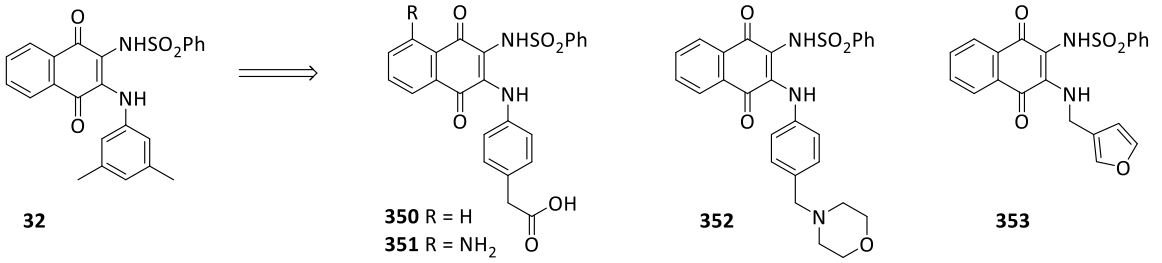
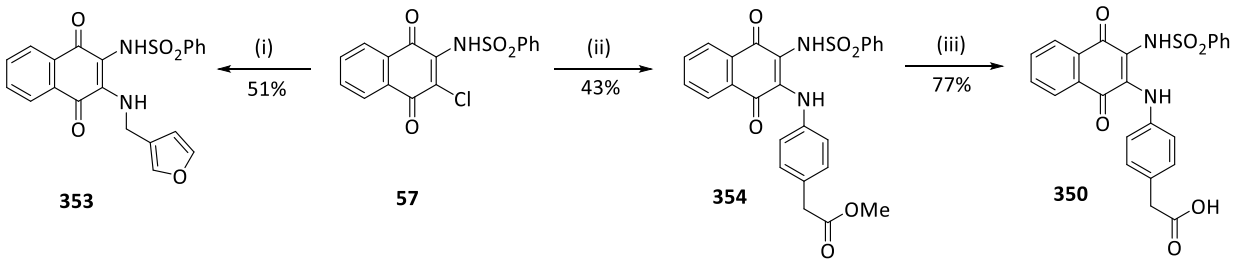


Figure 5.1: Initial library of compounds designed to be more soluble analogues of hit compound **32**.

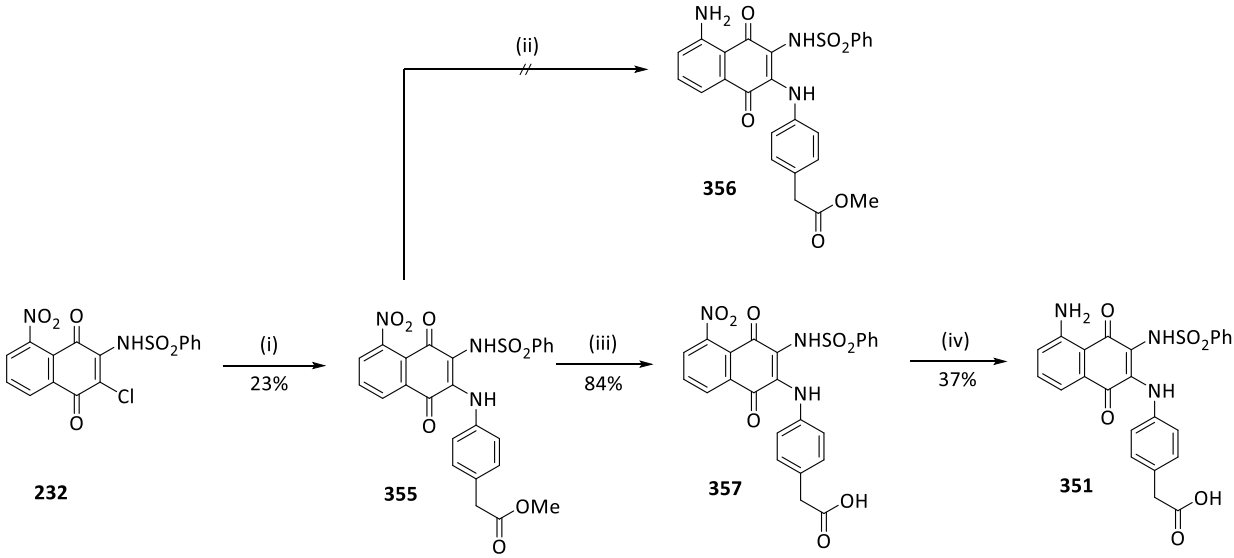
To this extent, a small initial target library of compounds was designed **(Figure 5.1)**. Compounds **350** and **351** were of interest due to the favourable potencies and solubility of the previously synthesised carboxylic acids **271** and **349**; however, **350** and **351** are even smaller examples of carboxylic-acid containing ligands with fewer aromatic rings, and hence are predicted to have superior aqueous solubility. Target **351** additionally contains an 8-amino substituent which SAR studies reveal to confer up to a ten-fold increase in potency on other analogues (*cf.* **Section 3.4.**). Morpholino derivative **352** is also a desirable target as the morpholine unit is a well-reported solubilising group in drug discovery programs,[328] such as in Pfizer's dual serotonin/noradrenaline reuptake inhibitors[329] and norepinephrine reuptake inhibitors.[330] Moreover, the morpholine unit is predicted to be predominantly uncharged at the assay *p*H of 8 (the reported pK_{aH} values for the analogous *N*-methyl morpholine and *N*-allyl morpholine are 7.41 and 7.05 respectively),[283] which enables an interesting comparison to be made with the negatively charged carboxylates [**350**]$^-$ and [**351**]$^-$. Meanwhile, compound **353**, bearing an alkylamino furyl C_3 substituent, was designed as a small substituent containing both an increased number of rotatable bonds and an additional heteroatom *cf.* compound **32**.

The syntheses of the target furanyl derivative **353** and methyl ester **354** were both readily effected by KSH from chloro-substituted naphthoquinone **57** *via* Michael-type reactions of furfuryl amine and methyl (4-aminophenyl)acetate respectively in moderate yield (conditions

(i) and (ii) in **Scheme 5.1**); the desired carboxylic acid **350** was subsequently readily accessed from methyl ester **354** in 77% yield in a facile basic hydrolysis (conditions (iii)).



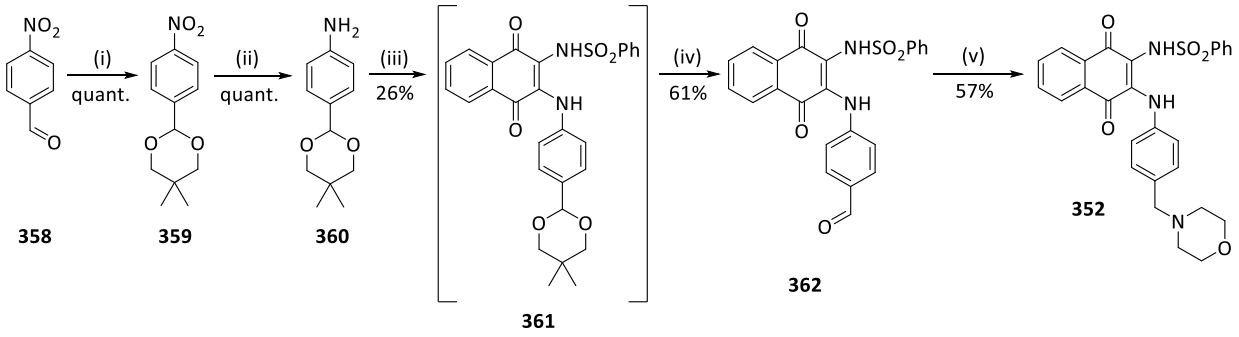
Scheme 5.1: Synthesis of furanyl amine **35**, methyl ester **354** and carboxylic acid **350**; data generated by KSH.[300] *Reagents and conditions:* (i) $CeCl_3 \bullet 7H_2O$ (1.0 eq.), toluene, RT, 1.5 h *then* furfuryl amine (3.0 eq.), 100 ^oC, 6 h; (ii) $CeCl_3 \bullet 7H_2O$ (1.0 eq.), MeOH, RT, 1.5 h *then* methyl (4-aminophenyl)acetate (3.0 eq.), 90 ^oC, 16 h; (iii) 1 M aq. NaOH (5.0 eq.), MeOH, RT, 1 h *then* HCl, RT.



Scheme 5.2: Synthesis of 8-amino-substituted carboxylic acid **351**. *Reagents and conditions:* (i) $CeCl_3 \bullet 7H_2O$ (1.0 eq.), MeOH, RT, 1.5 h *then* methyl (4-aminophenyl)acetate (3.0 eq.), 90 ^oC, 16 h; (ii) H_2 (1 atm.), 10% Pd/C (0.2 eq.), MeOH, RT, 16 h; (iii) 1,4-dioxane:1 M aq. NaOH (4:1), RT, 2 h *then* HCl, RT; (iv) H_2 (1 atm.), 10% Pd/C (0.2 eq.), MeOH, RT, 4 h.

Synthesis of the 8-amino substituted carboxylic acid derivative **351** was initially attempted *via* an analogous route to that for target **350 (Scheme 5.2)**. 8-Nitro-substituted naphthoquinone **232** (see **Section 3.5.**) was treated with methyl (4-aminophenyl)acetate and cerium trichloride heptahydrate in a Michael-type reaction to give intermediate **355** in 23% yield (conditions (i)).

It was envisaged that the ready ionisation of carboxylic acids above *c. p*H 5 would make these species difficult to handle in purification, and hence catalytic hydrogenation of the nitro group to yield 8-amino **356** was attempted prior to hydrolysis of the methyl ester (conditions (ii)); however, under these conditions a complex mixture of products was formed from which **356** could not be cleanly isolated. Therefore, hydrolysis was performed directly on **355** and this furnished the desired carboxylic acid **357** in an excellent yield of 84% (conditions (iii)). Catalytic hydrogenation of **357** in order to effect a reduction of the C_8 nitro group to the corresponding primary amine did not proceed cleanly (conditions (iv)); however, target compound **351** was successfully isolated in 37% yield following column chromatography on silica gel.



Scheme 5.3: Synthesis of morpholino derivative **352** *via* a reductive amination strategy; data generated by KSH.[300] *Reagents and conditions:* (i) 2,2-dimethylpropane-1,3-diol (2.25 eq.), TsOH (0.02 eq.), toluene, 135 ^{o}C, 2 h; (ii) H_2 (1 atm.), 10% Pd/C (0.1 eq.), EtOH, RT, 3 h; (iii) Naphthoquinone **57** (1.0 eq.), $CeCl_3 \bullet 7H_2O$ (1.0 eq.), MeOH, RT, 1.5 h *then* aniline **360** (3.0 eq.), 90 ^{o}C, 16 h; (iv) TFA:H_2O:CH_2Cl_2 (3:2:10), RT, 24 h; (v) morpholine (3.0 eq.), 3 Å molecular sieves, glacial AcOH:DCE (1:100), RT, 10 min *then* $NaHB(OAc)_3$ (2.5 eq.), RT, 16 h.

Synthesis of the morpholino-substituted species **352** was effected by KSH, using a retrosynthetic pathway that employed a reductive amination as the final step from aldehyde intermediate **362 (Scheme 5.3)**. To synthesise the requisite aldehyde intermediate **362** from chloro-substituted naphthoquinone **57**, the aldehyde functionality was masked as an acetal, since *para*-amino benzaldehyde is prone to rapid polymerisation *via* imine formation. The gem-dimethyl substituted cyclic acetal intermediate **359** was utilised as the acetal of choice due to its stability under the reaction conditions of reduction (conditions (ii)) and subsequent

Michael-type reaction with naphthoquinone **57** (conditions (iii)); it is believed that gem-dimethyl substitution makes ring-opening of the acetal both thermodynamically and kinetically unfavourable, since the resulting 2,2-dimethylpropane-1,3-diol possesses low conformational freedom in solution. Deprotection of the acetal functionality using TFA in H_2O and CH_2Cl_2 (3:2:10, conditions (vi)) afforded aldehyde **362** in excellent yield, which was subsequently subjected to reductive amination *via* a stepwise method to furnish **352** in good yield (conditions (v)).

5.1.2. Evaluation of the Pharmacological and Physical Properties of Derivatives 350-353

The synthesised target derivatives **350-353** were all evaluated for inhibitory activity in the acetyl CoA hydrolysis assay against MOUSE(NAT2) and, where the requisite enzyme was available, HUMAN(NAT1); the precursors to compounds **350** and **352** (methyl ester **354** and aldehyde **362** respectively) were also tested for comparison **(Table 5.3)**.

Interestingly, all of the compounds in this series possess moderate or good potency against both enzymes, with the exception of morpholino-substituted **352** and 8-amino substituted **351**, which display IC_{50} values of >30 μM against HUMAN(NAT1) and MOUSE(NAT2) respectively. The potency of carboxylic acid **350** against HUMAN(NAT1) is particularly promising, and is consistent with the high activity observed for other analogues of hit compound **32** bearing a carboxylic acid functionality within the C_3 moiety. Unfortunately, as proved the case with the biaryl substituted series (*cf.* **Section 3.5.**), the effects of adding both a carboxylic acid group to the C_3-anilino moiety and an amino group to C_8 of the naphthoquinone core on the potency of inhibition are not additive.

Important physical parameters of the compounds in this series – namely kinetic solubility, transport rates across a Caco-2 monolayer[327] at 10 μM, and the mean fraction of the compound unbound in a 50% plasma solution – were evaluated using the same methods as for previous analogues (*cf.* **Table 5.2**).

Compound		354	350	351	353	362	352
IC_{50} MOUSE(NAT2) (μM)		6.3 ± 2.1	15.8 ± 3.3	>30	2.6 ± 0.57	4.1 ± 0.74	4.1 ± 0.82
R^2		0.7124	0.8128	N/A	0.8980	0.9080	0.8860
P		**	***	N/A	***	***	***
IC_{50} HUMAN(NAT1) (μM)		2.6 ± 0.57	0.71 ± 0.23	N.D.	9.9 ± 2.6	0.41 ± 0.14	>30
R^2		0.8979	0.8251	N.D.	0.7450	0.8323	N/A
P		***	**	N.D.	**	**	N/A
Kinetic Solubility (μM)		N.D.	65.0	2.0	6.5	N.D.	2.0
Caco-2 Membrane Permeability	Rate of Flux A to B (10^{-6} cms^{-1})	N.D.	10.0 ± 1.4	1.1 ± 0.04	25.0 ± 0.25	N.D.	18.0 ± 0.01
	% Recovery	N.D.	46	70	49	N.D.	45
	Efflux Ratio	N.D.	0.56	9.80	0.50	N.D.	0.82
Fraction Unbound to Plasma Protein		N.D.	0.095 ± 0.006	0.044 ± 0.0004	0.120 ± 0.002	N.D.	0.098 ± 0.025

Table 5.3: Summary of pharmacological and physical data of compounds **350-354** and **362**; IC_{50} data on compounds **350**, **352-354** and **362** generated by KSH,[300] and all physical property data generated by Cyprotex plc (Macclesfield, UK). IC_{50} values were calculated from the acetyl CoA hydrolysis assay and were carried out in triplicate; values are quoted ± one standard deviation and analysis was performed using KyPlot® software. Confidence limits are denoted by the number of stars: ** = *P* <0.01; *** = *P* <0.005. Kinetic solubility was determined *via* turbidimetric measurement in a solution containing 99% 0.01 M PBS (*p*H 7.4)/1% DMSO (*v/v*); data are presented as the calculated mid-range of three repeat readings. Permeability in both the apical to basolateral direction (A to B) and *vice versa* across a Caco-2 intestinal epithelial cell monolayer[327] was determined at a concentration of 10 μM at 37 ^{o}C with an incubation time of 2 h; data are presented as the mean of two repeat readings ± one standard deviation. The % recovery of compound in the experiment is also given as a mean value. Efflux ratios are calculated as the rate of B to A flux divided by the rate of A to B flux. The extent of binding to plasma proteins was determined by equilibrium dialysis, using 5 μM compound in a 50% mouse plasma solution; data are presented as the mean of two repeat readings ± one standard deviation. N.D. = not determined.

The most striking observation from this data set is the high kinetic solubility of carboxylic acid **350** (65 μM), which demonstrates a twenty-fold improvement in solubility in a 1% DMSO (*v/v*) buffer solution containing 0.01 M PBS *cf.* hit compound **32** (3.8 μM). **350** also demonstrates a similarly favourable rate of A to B flux across a Caco-2 monolayer to **32**, but with a higher recovery of compound, which most probably reflects the significantly enhanced hydrophilicity of **350** over **32**; no significant amounts of efflux are observed for **350**. Furthermore, the mean fraction of **350** unbound in a plasma protein binding experiment (0.095) also compares favourably with the metric for **32** (0.038).

Similarly favourable rates of flux from A to B compartments across the Caco-2 monolayer were observed for furanyl derivative **353** and morpholino derivative **352**; however, disappointingly, neither of these species exhibit significantly enhanced kinetic solubility over hit compound **32**: it would appear that inclusion of neither additional rotatable bonds nor polar groups into the structure are sufficient to generate the desired improvement in physical properties.

Perhaps the most surprising data are that for C_8-amino substituted **351**, bearing an aniline at the C_3 position with a carboxylic acid appendage. Unlike the analogous carboxylic acid **350**, **351** possesses a low kinetic solubility (2 μM) offering little or no improvement over hit compound **32**; worse still, **351** possesses a low rate of apical to basolateral (A to B) flux across the Caco-2 cell monolayer leading to a high efflux ratio. Therefore, not only does addition of an 8-amino substituent result in a decrease in potency against MOUSE(NAT2) *cf.* carboxylic acid **350**, it would also appear that this substituent gives rise to some markedly unfavourable physical properties in combination with a carboxylic acid moiety elsewhere in the molecule.

On the basis of their pharmacological and physical properties, it was decided to advance carboxylic acid **350** and furanyl **353** to studies in the ER+ breast cancer cell line ZR-75-1, alongside biaryl derivative **220**, which demonstrates a forty-fold higher potency against HUMAN(NAT1) but a comparable kinetic solubility. Biaryl **220** had previously been demonstrated to inhibit NAT activity in cell extracts from a ZR-75-1 cell line in the acetyl CoA hydrolysis assay at 30 μM (see **Section 3.6.**); analogous tests were performed on carboxylic acid **350** and furanyl **353 (Figure 5.2)**, with data for hit compound **32** and biaryl **220** included for comparison. Pleasingly, both **350** and **353** demonstrate high levels of inhibition of HUMAN(NAT1) within the cell extracts at all tested concentrations. Additionally, compounds **350** and **353** were screened for activity against HUMAN(NAT2) in the DTNB assay at a 30 μM concentration in triplicate against recombinant HUMAN(NAT2) using 5-aminosalicyclic acid (5AS) as substrate; at this concentration neither compound leads to a statistically significant decrease in HUMAN(NAT2) activity *cf.* a control experiment in which no inhibitor is present.

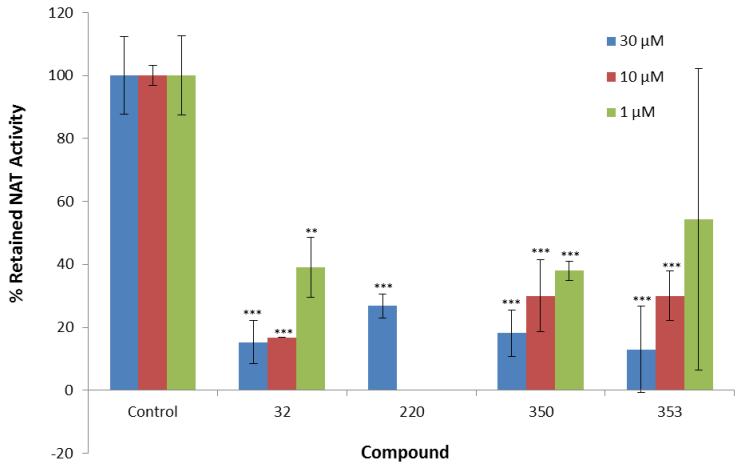


Figure 5.2: Residual activity of HUMAN(NAT1) in ZR-75-1 cell extracts when dosed with compounds **32**, **220**, **350** and **353** at 30, 10 and 1 µM. Compounds were dosed in triplicate, the final DMSO concentration in the assays was 5% (*v/v*), and % activity values are quoted relative to a control experiment (vehicle only). Results are presented as average values ± one standard deviation, and the stars above the columns show the significance of the difference between the test data and its respective control when a Student's *T*-Test was performed: no stars = P >0.05; ** = P <0.01; *** = P <0.005.

Following this, the potential effects of compounds **220**, **350** and **353** on the growth of a ZR-75-1 cell line were investigated. ZR-75-1 cells were incubated with inhibitor at a final concentration of 10 µM and 0.5% DMSO (*v/v*) for 48 h. After this time, the cells were counted using Trypan Blue exclusion and the total numbers of dead and live cells were calculated (**Figure 5.3**; for protocol see **Section 7.13.2.**). Tamoxifen **24** was chosen as a positive control as it has been reported to inhibit the growth of ZR-75-1 cells at a 10 µM concentration.[331] Whilst the data does provide some evidence of cytotoxicity of the synthesised compounds (the increased % in dead cells relative to the control is found to be statistically significant for compound **220** when a Student's *T*-Test is carried out (*P* = <0.05)), the results are not reliable due to the poor growth of the negative control cells relative to the test samples, and the lack of difference in cell growth between the negative and positive controls. In the future, a more robust assay should be developed in order to reliably examine the effects of compounds **220**, **350** and **353** on the growth of ZR-75-1 and other HUMAN(NAT1) +ve cell lines *cf.* cell lines in which HUMAN(NAT1) is not overexpressed.

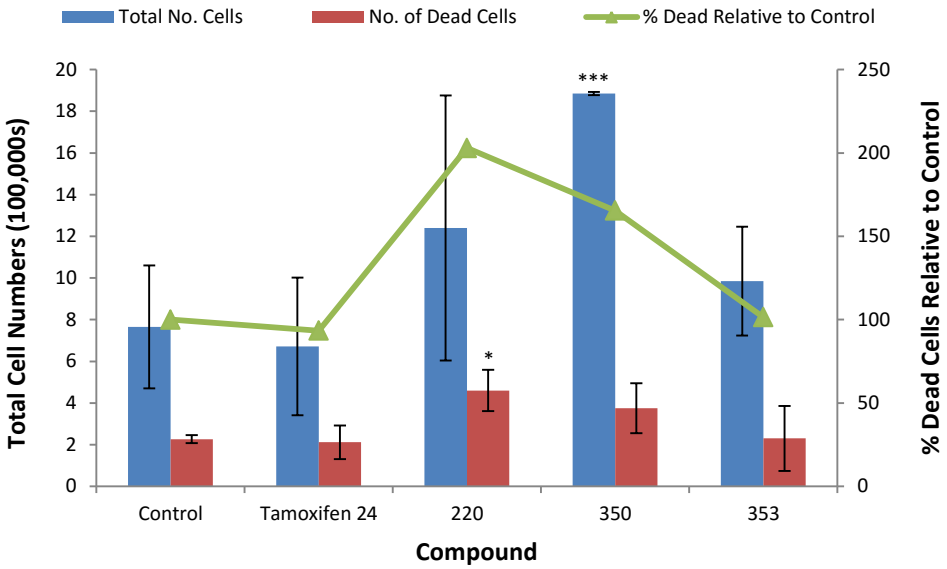


Figure 5.3: Total number of ZR-75-1 cells and number of dead ZR-75-1 cells after 48 h of incubation of ZR-75-1 cells with 10 μM tamoxifen, **220**, **350** or **353** or in a control experiment (vehicle only). The final DMSO concentration was 0.5% (*v/v*), experiments were conducted in triplicate and results are expressed as mean values ± one standard deviation. The mean % dead cells in each case is also given relative to the control (vehicle only) experiment. The stars above the columns show the significance of the difference between the number of cells counted *vs.* the control when a Student's *T*-Test was performed: no stars = P >0.05; * = P <0.05; *** = P <0.005.

In proposing the advancement of these compounds to cellular studies, one of the other key considerations is the possibility for the naphthoquinone core to be reduced under cellular conditions. To this extent, electrochemical studies were carried out on hit compound **32** to investigate the behaviour of a representative C_3 anilino-substituted naphthoquinone under reducing conditions. A cyclic voltammogram of a 0.1 mM solution of **32** in 95% 50 mM KH_2PO_4, 50 mM K_2HPO_4/5% DMSO (*v/v*) on a glassy carbon electrode clearly shows the two anticipated one-electron reduction peaks of the naphthoquinone in the forward sweep, and two corresponding peaks in the reverse direction **(Figure 5.4A)**. The area of the back-peak was observed to be smaller than that of the forwards peak, which suggests that either the reduced species diffuses away from the electrode surface before oxidation can occur or that the reduced species undergoes decomposition.

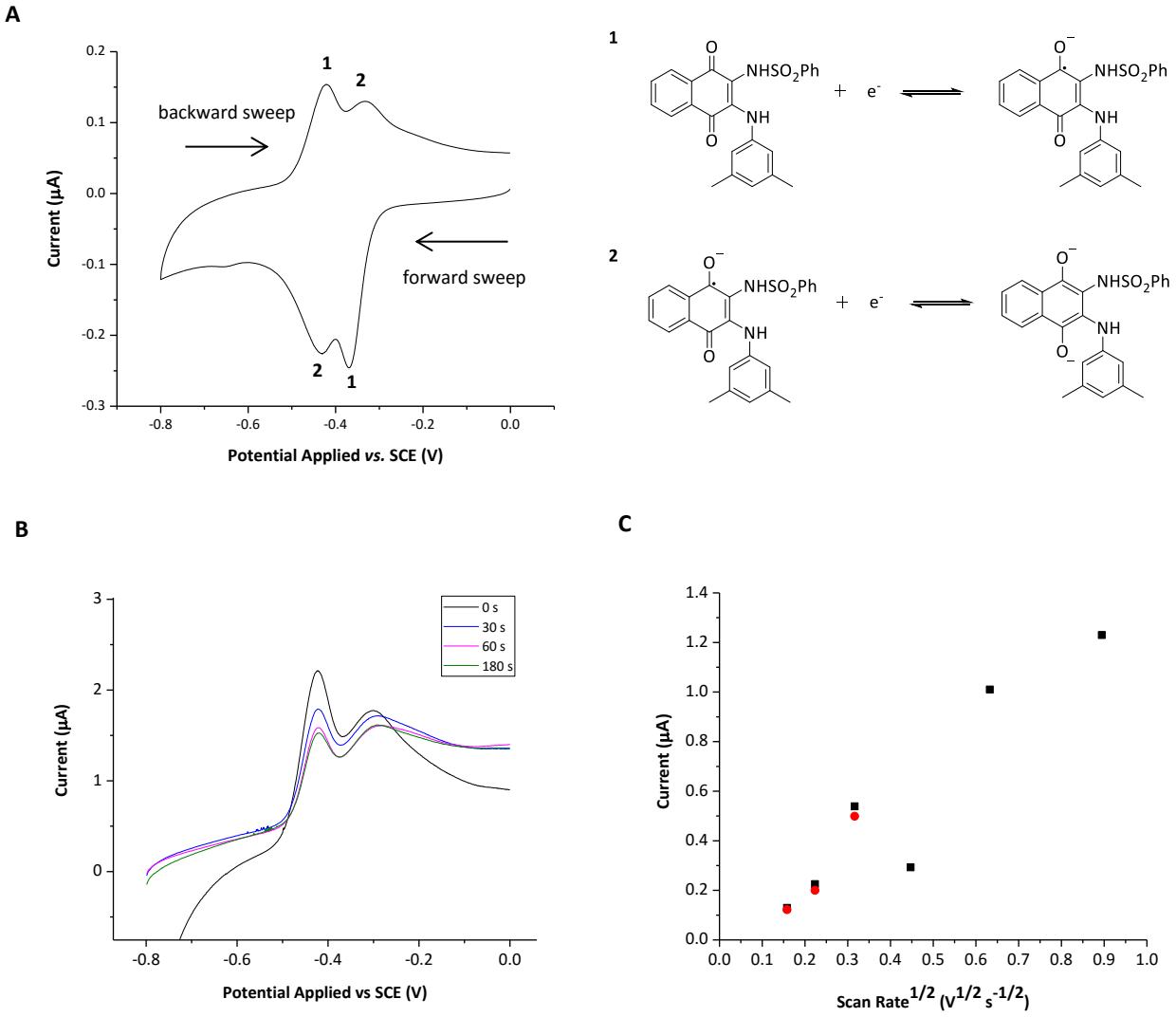


Figure 5.4: Electrochemical experiments performed on naphthoquinone **32**. Working electrode = glassy carbon; reference electrode = standard calomel electrode (SCE); counter electrode = platinum. **A:** Cyclic voltammogram of 0.1 mM **32** in 95% 50 mM KH_2PO_4, 50 mM K_2HPO_4/5% DMSO (*v/v*) recorded over the applied potential range of 0 V to -0.8 V witg a scan rate of 50 mVs^{-1} **(left)** and the reversible half-equations corresponding to the one-electron reduction and oxidation peaks labelled **1** and **2 (right)**. **B:** Linear sweep voltammogram of 0.1 mM **32** in 95% 50 mM KH_2PO_4, 50 mM K_2HPO_4/5% DMSO (*v/v*) over the applied potential range of -0.8 V to 0 V, with the potential applied held at -0.8 V for 0 s (black line), 30 s (blue line), 60 s (pink line) or 180 s (green line) prior to commencement of the sweep. **C:** Plot of the square root of scan rate against the peak current observed for reduction peaks **1** (black squares) and **2** (red circles, where observable).

Subsequently, linear sweep voltammetry experiments were conducted in which the potential at the electrode surface was held at -0.8 V (relative to the standard calomel electrode (SCE)) for varying lengths of time before oxidation of the reduced naphthoquinone in solution was

measured **(Figure 5.4B)**. These data show that as the area of the back-peak initially decreases as the holding time is increased from 0 s; however, after about 60 s, no further decrease in the area of this peak is observed with a further increase in holding time. This observation is consistent with establishment of an equilibrium between surface-bound and solution-phase reduced **32**, and not with the decomposition of **32** following reduction. Furthermore, the peak current for the forward peak has an approximately linear dependence on the square root of the applied scan rate **(Figure 5.4C)**, which is a further indication of a system operating under diffusion control. The corresponding diffusion coefficient can be calculated as 7.9×10^{-10} m^2s^{-1} from the gradient of this plot, since Fick's law[332] for mass transfer diffusion in such situations can be simplified to:

$$i_p = (2.69 \times 10^5) \bullet n^{3/2} \bullet S \bullet D^{1/2} \bullet C \bullet v^{1/2}$$

in which i_p is the measured peak current, n is the number of electrons gained in the reduction (in this case, 2), S is the surface area of the working electrode (in this case, 7.07×10^{-6} m^2), D is the diffusion coefficient, C is the concentration of **32** in solution and v is the scan rate.

These observations therefore suggest that **32** is stable when reduced; furthermore, the measured reduction potential under the experimental conditions used of -0.38 V *vs.* SCE suggests that a relatively strong reductant would be required to effect reduction of the naphthoquinone, presumably due to the electron-donating effect conferred by the C_3 anilino substituent. Evidence obtained in previous studies suggest that no change in the coloration of a solution of **32** is observed when treated with a range of different reducing agents, including the thiol DTT;[242] naphthoquinones undergo a characteristic decolorisation when reduced. One set of conditions used extensively in this study under which the naphthoquinone core of **32** and its analogues is observed to undergo reduction is under treatment with 1 atm. H_2 and 10% Pd/C in MeOH; however, this reduction is fully reversible when the product is exposed to oxygen and no decomposition of the naphthoquinones is observed.

As a corollary of these points, it would be anticipated that close analogues of **32** are resistant to reduction in biological systems, e.g. by the thiol functionality of glutathione or cysteine

residues in proteins. The resistance of **220**, **350** and **353** to reduction in the presence of thiols such as glutathione should, however, be tested prior to commencement of studies on these compounds in tumour cell lines. It would also be instructive to test representative examples of the developed inhibitors for activity against NAD(P)H:quinone oxidoreductases (NQOs) since these are widely reported to reduce quinone derivatives in a cellular environment.[333] Encouragingly, when 1 μM carboxylic acid **350** was incubated with murine hepatic (S9) microsomes (1 mg/mL protein in solution containing NADPH + UDPGA as cofactors and 0.25% DMSO (*v/v*)), **350** displayed promising metabolic stability with a half-life of 193 min and clearance of 3.6 μL/min/mg protein (taken as mean values from 5 repeat readings). This compares favourably with the stability of hit compound **32**, which under identical conditions was observed to have a half-life of 20 min and clearance of 36 μL/min/mg protein.

5.1.3. Solubilising the Biaryls: Replacement of the Second Aromatic Ring with Heterocycles and Amino Acid Derivatives

An alternative strategy to generate compounds with the required balance of both favourable pharmacological and physical properties might be to use biaryl derivatives such as **220** as a starting point as opposed to compound **32**: **220** and **32** possess similar kinetic solubilities, but **220** is forty-fold more potent against HUMAN(NAT1). It was reasoned that if the aromatic ring of such biaryl derivatives furthest from the naphthoquinone core were to be replaced with a saturated ring system containing a greater degree of conformational flexibility and/or ring systems containing heteroatoms, the resultant species might retain favourable interactions with the enzyme active site but display improved physical properties. A library of targets was designed to encompass a range of structural motifs containing varying degrees of aromaticity, different ring sizes, different heteroatoms and different substitution patterns **(Figure 5.5)**. Anticipated to be of particular interest was proline derivative **369**, since cell membranes contain transporter proteins which recognise amino acids and actively transport them across membranes;[334] it was hypothesised that if a structural motif could be incorporated into the NAT inhibitors that would allow recognition by such transporters, the membrane permeability

of the inhibitors might be increased. Alanine derivative **371** was also designed as an example of an aliphatic amino acid derivative for comparison with cyclic proline derivative **369**.

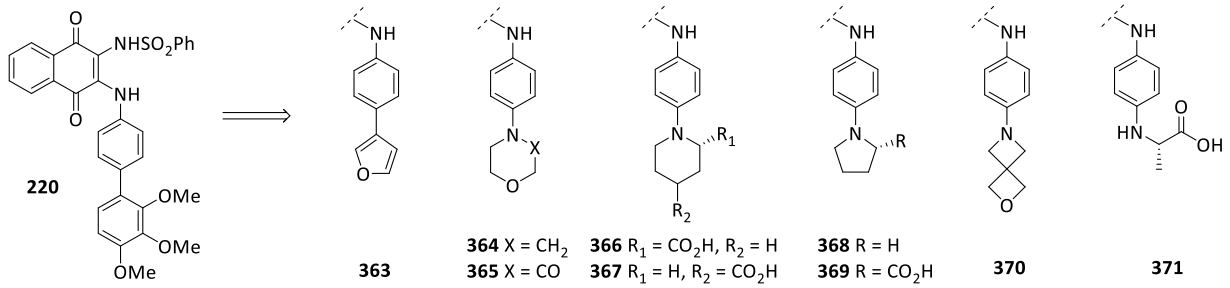
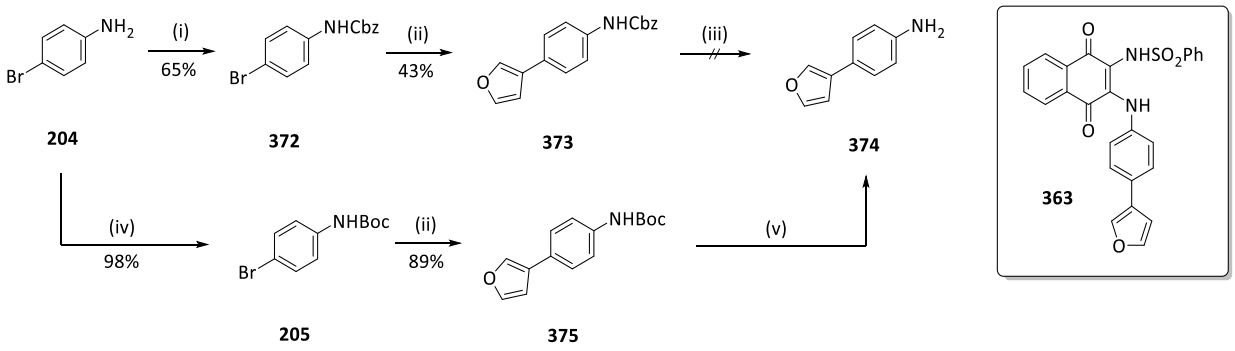


Figure 5.5: Structures of the C_3 moieties in target derivatives **363-371**.

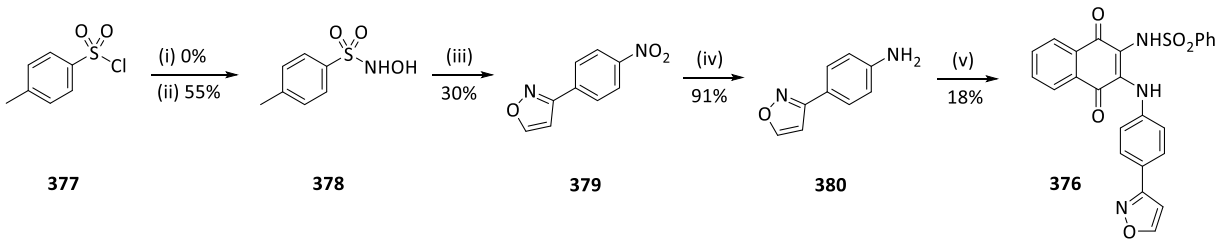
The first attempted synthesis was that of furan derivative **363 (Scheme 5.4)**. Protection of 4-bromoaniline **204** as the corresponding *N*-benzyl carbamate **372** was readily achieved in 65% yield (conditions (i)), and subsequent Suzuki-type coupling[203] with 3-furanylboronic acid furnished biaryl species **373** in moderate yield. However, the catalytic hydrogenation effected on **373** in order to cleave the benzyl carbamate did not proceed cleanly (conditions (iii)), necessitating a purification of the aniline **374** by column chromatography on silica gel. None of the desired product could be isolated *via* this method, and it was postulated that electron-rich **374** was unstable on silica.



Scheme 5.4: Attempted synthesis of furanyl derivative **363**. *Reagents and conditions:* (i) benzyl chloroformate (1.2 eq.), PEG-400, RT, 1 h; (ii) 3-furanylboronic acid (2.0 eq.), $Pd(PPh_3)_2Cl_2$ (0.1 eq.), sat. aq. $NaHCO_3$:THF (5:22), 100 ^oC, 16 h; (iii) H_2 (1 atm.), 10% Pd/C (0.2 eq.), MeOH, RT, 16 h; (iv) Boc_2O (1.2 eq.), $InCl_3$ (0.01 eq.), 40 ^oC, 2 h; (v) TFA:CH_2Cl_2 (1:5), 0 ^oC, 2 h *then* sat. aq. $NaHCO_3$, RT.

Therefore, an alternative route to **363** was sought which was envisaged not to require purification of the requisite aniline **374**. In this strategy, a *tert*-butyl carbamate protecting group was used in place of the benzyl carbamate. Initial protection of 4-bromoaniline was readily effected (conditions (iv)) to give intermediate **205**, before a Suzuki-type cross-coupling was utilised to install the furanyl ring in 89% yield. Subsequently, TLC analysis suggested that carbamate deprotection of **375** in TFA:CH_2Cl_2 (1:5) occurred cleanly, with an *m/z* (ESI^+) peak at 160 Da, suggesting formation of the required amine **374** had been successful. However, **374** degrades within hours on standing at room temperature, and hence it was not possible to effect the required Michael-type reaction on naphthoquinone **57**.

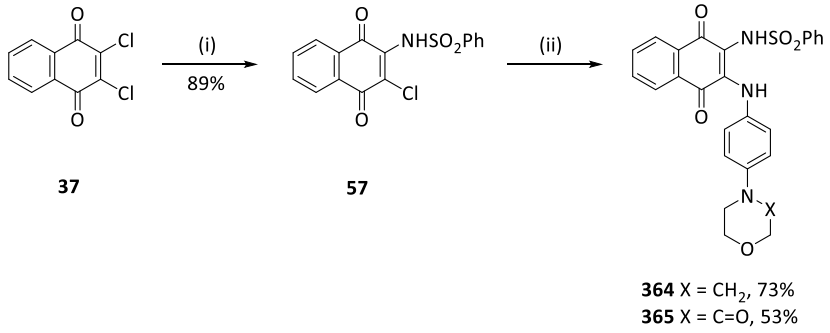
As an alternative target to the intractable furyl derivative **363**, isoxazole **376** was designed **(Scheme 5.5)**. Both **376** and its precursor amine **380** were postulated to be less susceptible to decomposition than furyl-substituted **363** or its precursor amine **374** due to the presence of the additional electronegative nitrogen in the aromatic ring system. The nitrogen was introduced into the ring at the 2-position since isoxazoles are prone to ring-opening *via* elimination if they bear a proton α to nitrogen; this is thought to be the mechanism by which the isoxazole-containing prodrug for rheumatoid arthritis, leflunomide,[335] is converted to its active metabolite.[336]



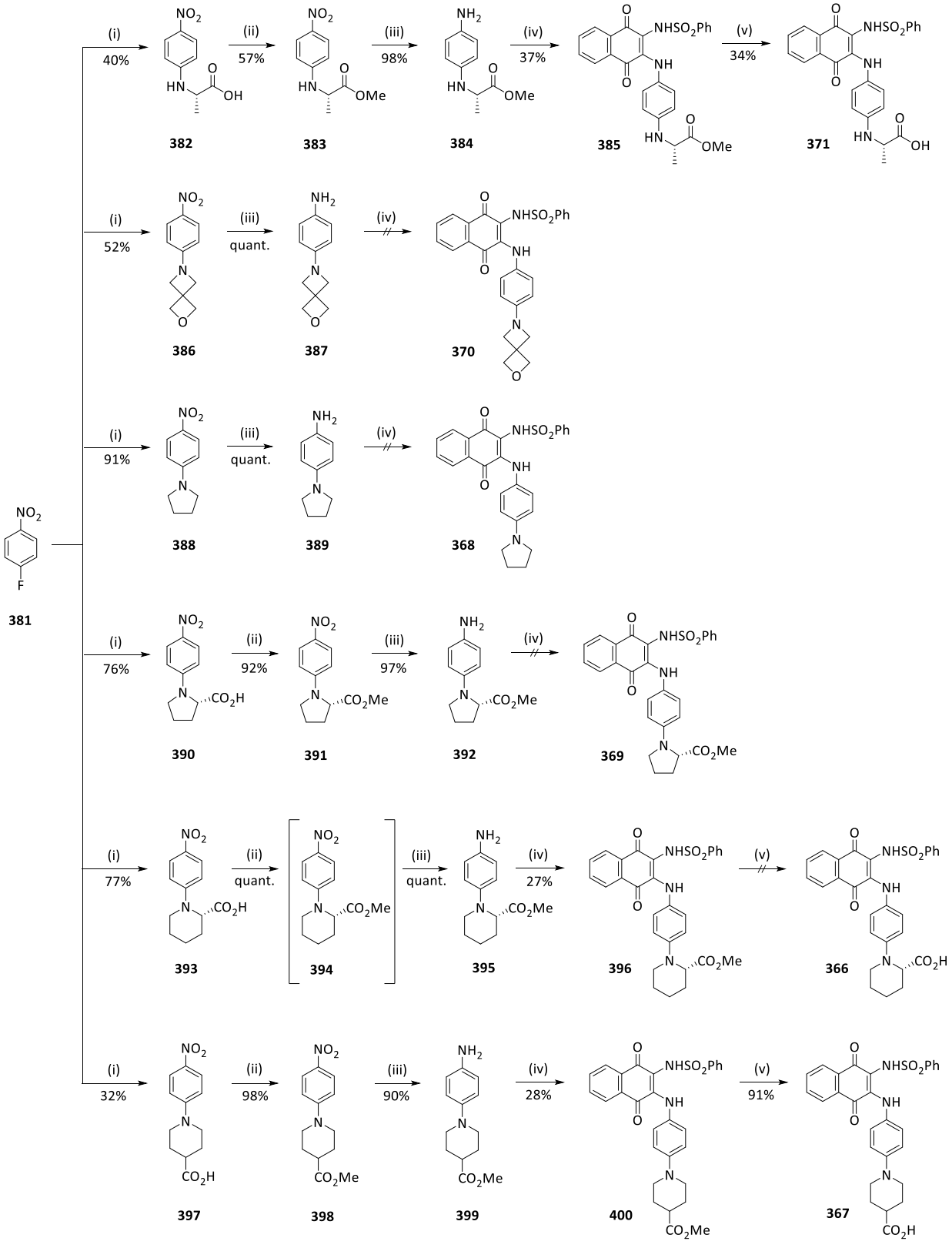
Scheme 5.5: Synthesis of isoxazole derivative **376**. *Reagents and conditions:* (i) NH_2OH•HCl (2.5 eq.), MgO (3.0 eq.), MeOH:H_2O:THF (3:2:30), RT, 16 h; (ii) NH_2OH•HCl (1.1 eq.), CH_2Cl_2:pyridine (2:1), RT, 16 h; (iii) *para*-nitrocinnamaldehyde (0.25 eq.), K_2CO_3 (1.25 eq.), MeOH:H_2O (6:1), RT, 2 h *then* K_2CO_3 (0.625 eq.), 60 ^oC, 1 h, yield quoted *w.r.t. para*-nitrocinnamaldehyde; (iv) H_2 (1 atm.), 10% Pd/C (0.1 eq.), MeOH, RT, 16 h; (v) naphthoquinone **57** (1.0 eq.), $CeCl_3$•$7H_2O$ (1.0 eq.), MeOH, RT, 1.5 h *then* aniline **380** (3.0 eq.), 90 ^oC, 16 h.

Isoxazole derivative **376** was successfully prepared from *para*-toluenesulfonyl chloride **377** in four linear steps. Use of literature conditions employing MgO to convert **377** to the corresponding hydroxylamine failed (conditions (i));[337] however, use of hydroxylamine hydrochloride in a pyridine:CH_2Cl_2 (1:2) solvent system (conditions (ii)) furnished the desired adduct **378** in 55% yield. Treatment of *para*-nitrophenylcinnamaldehyde with **378** under basic conditions led to successful isoxazole ring formation (conditions (iii)),[338] and **379** could be isolated in a moderate yield. The subsequent reduction of the nitro functionality in **379** to the corresponding primary amine **380** under hydrogenolysis conditions proved facile (conditions (iv)), and unlike the corresponding furyl derivative, isoxazole **380** was indeed found to be stable upon standing for months at room temperature. Subsequent Michael-type reaction of **380** with naphthoquinone **57** under standard conditions (conditions (v)) gave the desired target **376** in 18% yield after purification both by column chromatography and recrystallisation from MeOH.

Subsequently, the syntheses of the target species bearing a fully saturated ring system to replace the second aromatic ring of the biaryl appendage were attempted. Compounds **364** and **365**, bearing morpholine and oxomorpholine substituents respectively, were readily accessed from naphthoquinone **57** *via* Michael-type addition-elimination since the requisite anilines were commercially available (conditions (ii) in **Scheme 5.6**).



Scheme 5.6: Synthesis of derivatives **364** and **365** containing an alicyclic 6-membered ring substituent. *Reagents and conditions:* (i) benzenesulfonamide (1.0 eq.), Cs_2CO_3 (1.4 eq.), DMF, RT, 5 h; (ii) $CeCl_3 \bullet 7H_2O$ (1.0 eq.), MeOH, RT, 1.5 h *then* requisite aniline (3.0 eq.), 90 ^oC, 16 h.



Scheme 5.7: Efforts towards the synthesis of **366-371**. *Reagents and conditions:* (i) requisite amine (1.0 eq.), K_2CO_3 (3.0 eq.), EtOH:H_2O (3:1), reflux, 48 h; (ii) $SOCl_2$ (1.34 eq.), MeOH, RT, 0.5 h *then* reflux, 3-16 h; (iii) H_2 (1 atm.), 10% Pd/C (0.1 eq.), MeOH, RT, 16 h; (iv) naphthoquinone **57** (1.0 eq.), $CeCl_3 \bullet 7H_2O$ (1.0 eq.), MeOH, RT, 1.5 h *then* requisite aniline (3.0 eq.), 90 ^{o}C, 16 h; (v) 1,4-dioxane:1 M aq. NaOH (4:1), RT, 4-5 h *then* HCl, RT.

Formation of the other desired 6-membered ring analogues based on pipecolic acid (**366**) and isonipecotic acid (**367**), as well as formation of the 5-membered ring analogues based on pyrrolidine (**368**) and L-proline (**369**), the 4-membered ring analogue based on a spirocyclic oxetane (**370**) and the acyclic target based on alanine (**371**), all required the prior preparation of the precursor amines **(Scheme 5.7)**. These were accessed from 4-fluoronitrobenzene **381**: in the first step, **381** was treated with the requisite amine under basic conditions to effect S_NAr-type displacement of fluoride by the amine (conditions (i)); these reactions proceeded in yields ranging from 32% to 91%. Derivatives possessing a carboxylic acid functionality (**382**, **390**, **393** and **397**) were subsequently converted to the corresponding methyl esters (**383**, **391**, **394** and **398** respectively) in generally excellent yields by treatment with $SOCl_2$ in refluxing MeOH (conditions (ii)). Catalytic hydrogenation of the nitro functionalities then furnished the desired amines (conditions (iii)).

However, it was noted that following reduction, the 4- and 5-membered cyclic species **387**, **389** and **392** were unstable with respect to decomposition if left to stand at room temperature for 2-3 days; the 6-membered cyclic species **395** and **399** and the aliphatic-substituted **384** were however stable at RT for over 6 months.

Analogously, when all six of these anilines were subjected to Michael-type addition-elimination with naphthoquinone **57** (conditions (iv)), the adducts substituted with a 4- or 5-membered cyclic amine were unisolable, although TLC, *m/z* and ^1H-NMR analysis did provide some evidence that the desired products were being formed in the reaction but rapidly decomposed, with half-lives of <1 day. Adducts **385**, **396** and **400**, meanwhile, could be successfully isolated and subsequently, basic hydrolysis of the ester moieties in these species was attempted in order to reveal the desired carboxylic acid functionality (conditions (v)).

Ester hydrolysis of pipecolic acid derivative **396** proved intractable, even after heating to 60 ^oC for 1 h; further heating at 70 ^oC for 16 h led to decomposition of the starting material. Analysis of the coupling constants in the ^1H-NMR spectrum of methyl ester **396** suggests that the

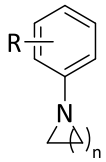
methyl ester group sits in a pseudo-axial position on the ring, since the proton α to the ester group appears as a doublet of doublets with coupling constants of 5.4 Hz and 2.4 Hz, consistent with equatorial-axial and equatorial-equatorial dihedral relationships. This would be anticipated to lead to a sterically crowded tetrahedral intermediate in the supposed $B_{AC}2$ mechanism of hydrolysis, giving rise to an activation energy which is too high to surmount under the reaction conditions.

However, the methyl esters of the alanine and isonipecotic acid derivatives **385** and **400** underwent facile ester hydrolysis under basic conditions, giving rise to isolated yields of 34% and 91% for the corresponding carboxylic acids **371** and **367** respectively; coupling constant analysis of the ^{1}H-NMR spectrum of methyl ester **400** suggests that the 6-membered ring preferentially adopts a conformation in which the ester group is in a pseudo-equatorial position. Disappointingly, yet intriguingly, both carboxylic acid derivatives **371** and **367** were found to decompose after *c.* 1 week of standing at room temperature.

The origin of the observed instability of compounds **368**, **369** and **370**, their corresponding precursor anilines **389**, **392** and **387**, and carboxylic acids **367** and **371** is hypothesised to be related to the oxidation potential of the respective C_3-phenylene-*para*-diamine moieties. Aniline **392** is reported in the literature to be unstable in air with respect to oxidation,[339] and hence it is proposed that phenylenediamines **387** and **389** also undergo a similar oxidative decomposition process. The propensity of the phenylenediamines to oxidise is believed to be related to the electron density on the aromatic ring, which in turn is related to how strongly the lone pair of the tertiary nitrogen atom (or secondary in the case of the alanine derivatives) is conjugated with the aromatic π-electron system.

A study by Rozeboom *et al.* utilised photoelectron spectroscopy to determine the conformations of various *N*-aryl cyclic amines; the extent of coplanarity of the nitrogen lone pair with the π-electrons of the aromatic ring was determined by comparing the measured photoelectron ionisation potentials arising from the three HOMOs in each amine with the

predicted computational values for a range of conformational angles.[340] They discovered that the smaller the ring size in which the nitrogen was located, the more coplanar the nitrogen lone pair and the aromatic π-electrons become; introducing *ortho*-methyl groups onto the aromatic ring decreases the propensity for coplanarity for every tested ring size, but addition of *para*-methyl groups has only a minimal effect **(Table 5.3)**.



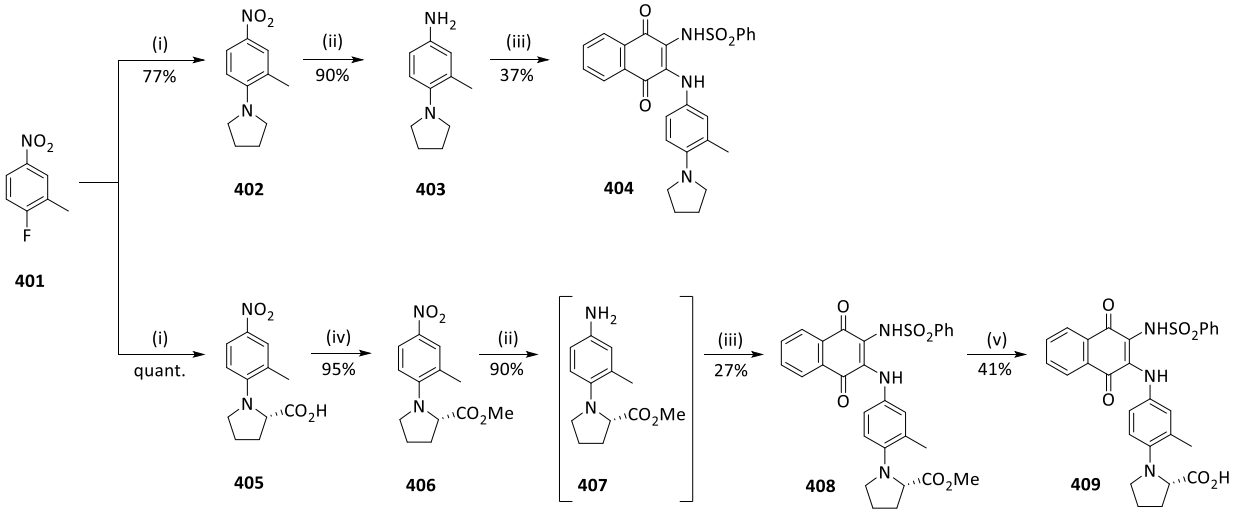
Aromatic Substituent	Angle between N lone pair and aromatic π system			
	n = 1	n = 2	n = 3	n = 4
R = H	0^o	0^o	0^o	48^o
R = *o*-Me	0^o	28^o	52^o	68^o
R = *o,p*-Me_2	0^o	30^o	58^o	72^o
R = *o,o'*-Me_2	0^o	34^o	83^o	86^o

Table 5.3: General structure of tested *N*-aryl cyclic amines **(left)** and dependence of the angle between the N lone pair, assumed to have sp^3 hybridisation, and aromatic π-system on the ring size and identity of R **(right)** (adapted from Rozeboom *et al.*, 1982).[340]

If we consider anilines **387**, **389**, **392**, **395** and **399** and their corresponding naphthoquinone adducts **370**, **368**, **369**, **396** and **400** to adopt similar conformations to those of the species studied by Rozeboom *et al.* (assuming that the *para*-amino or -aminonaphthoquinone substituent has little effect on the conformation of the *N*-cyclic amine), then the striking observation can be made that all of the anilines and aminonaphthoquinones found to be unstable are predicted to contain an *N*-cyclic amine group in which the N lone pair is coplanar with the adjacent aromatic π-system. In other words, the species anticipated to contain more electron-rich phenylenediamine moieties are less stable: this is consistent with the hypothesis that oxidation of the phenylenediamine group leads to the observed decomposition.

To further test this hypothesis, it was decided to synthesise analogues of pyrrolidine derivative **368** and proline derivative **369** in which a methyl group was installed *ortho* to the *N*-cyclic amine on the phenylenediamine moiety; according to Rozeboom *et al.*, addition of such a methyl group should induce a conformational switch from coplanarity (*c.* 0^o) to non-coplanarity (*c.* 52^o). The synthesis of target derivatives **404** and **409** were carried out in an

analogous fashion to previous analogues, using commercially available 2-fluoro-5-nitrotoluene as the starting material **(Scheme 5.8)**.



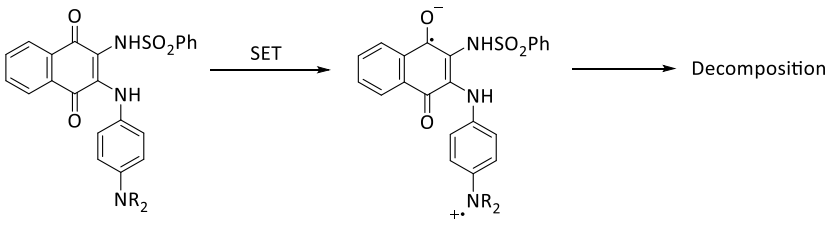
Scheme 5.8: Synthesis of 5-membered *N*-cyclic amine derivatives **404** and **409** bearing an *ortho*-methyl group. *Reagents and conditions:* (i) requisite amine (1.0 eq.), K_2CO_3 (3.0 eq.), EtOH:H_2O (3:1), reflux, 48 h; (ii) H_2 (1 atm.), 10% Pd/C (0.1 eq.), MeOH, RT, 16 h; (iii) naphthoquinone **57** (1.0 eq.), $CeCl_3 \bullet 7H_2O$ (1.0 eq.), MeOH, RT, 1.5 h *then* requisite aniline (3.0 eq.), 90 ^oC, 16 h; (iv) $SOCl_2$ (1.34 eq.), MeOH, RT, 0.5 h *then* reflux, 16 h; (v) 1,4-dioxane:1 M aq. NaOH (4:1), RT, 4 h *then* HCl, RT.

In accord with the hypothesis, it was found that both anilines **403** and **407** and anilinonaphthoquinones **404** and **408** were isolable and stable at RT for periods in excess of 6 months; this suggests that the conformation about the *N*-aryl bond, and hence the resulting electron density on the phenylenediamine ring, is indeed crucial to the observed stability of such species. Once again, however, it was observed that carboxylic acid **409** (prepared from methyl ester **408** in a 41% yield; conditions (v)) decomposed within *c.* 1 week of standing at room temperature; this is consistent with the observed stabilities of isonipecotic acid derivative **367** and alanine derivative **371**.

The observed instabilities of the carboxylic acids **367**, **371** and **409** pose an interesting puzzle, since hydrolysis of the methyl ester functionalities would not be predicted to significantly alter the conformation about the tertiary nitrogen-aryl bond. It is possible that ionisation of the

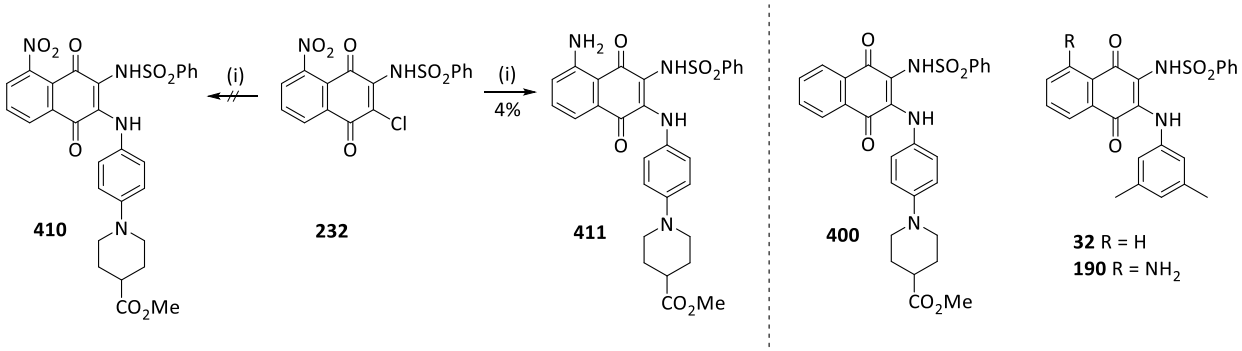
carboxylic acid group gives rise to an electron-rich carboxylate: this could increase the electron density on the phenylenediamine *via* a through-space interaction, leading to an increase in the propensity for the phenylenediamine to oxidise. However, one other mechanistic possibility also exists that might explain all of the reported observations. If oxidation of the phenylenediamine moiety by atmospheric oxygen is the mechanism of decomposition of anilinonaphthoquinones **368**, **369** and **370**, it might be anticipated that each of these species would have a significantly longer half-life than their corresponding precursor anilines **389**, **392** and **387** respectively, since the naphthoquinone group would withdraw electron density from the phenylenediamine; however, this is not observed to be the case (*vide infra*). In adducts **368**, **369** and **370** we have species which contain both a good electron donor (the phenylenediamine moiety) and a good electron acceptor (the naphthoquinone moiety). One alternative mechanism of decomposition of these species, therefore, is *via* single electron transfer (SET) from the phenylenediamine to the naphthoquinone, giving a charge-separated species which subsequently decomposes **(Scheme 5.9)**.

Such a decomposition mechanism would be consistent with all the experimental observations described thus far: the more electron-rich the phenylenediamine moiety is (influenced by the conformation of the *N*-cyclic amino substituent), the greater its oxidation potential and hence the greater the propensity for SET to the naphthoquinone core becomes. Additionally, this might also explain the unexpected instability of the carboxylic acid derivatives: ionisation of the carboxylic acid functionality might enable protonation of one of the naphthoquinone carbonyl groups, which could increase the reduction potential of the naphthoquinone sufficiently to enable SET from the phenylenediamine to occur.



Scheme 5.9: Possible decomposition pathway for phenylenediamine-substituted naphthoquinones *via* single electron transfer (SET).

To obtain further evidence of an SET mechanism of decomposition, aniline **399**, which generated a stable adduct **400** upon reaction with naphthoquinone **57**, was reacted with 8-nitro-substituted naphthoquinone **232 (Scheme 5.10)**. It was hypothesised that the electron-withdrawing nature of the nitro group would increase the reduction potential of the naphthoquinone, and hence reduce the stability of adduct **410** compared to **400** if SET is responsible for decomposition.



Scheme 5.10: **Left:** Reaction of the aniline derived from isonipecotic acid, **399**, with 8-nitro-substituted naphthoquinone **232**. *Reagents and conditions:* (i) $CeCl_3 \bullet 7H_2O$ (1.0 eq.), MeOH, RT, 1.5 h *then* aniline **399** (3.0 eq.), 110 ^{o}C, 16 h. **Right:** Structures of ester **400**, which is unsubstituted at C_5-C_8 of the naphthoquinone core, hit compound **32** and its 8-amino-substituted analogue **190**.

The outcome of this experiment, however, proved fascinating: none of the desired 8-nitro-susbtituted product **410** could be isolated from the reaction, but a product could be obtained with an *m/z* (ESI^+) peak at 560 Da and distinctive naphthoquinone-type ^{1}*H*-NMR shifts at 6.98 and 7.27-7.38 ppm, data consistent with the formation of 8-amino-substituted species **411** (*cf.* naphthoquinone ^{1}*H*-NMR shifts in the range 7.6-8.3 ppm for 8-nitro-substituted analogues). Full characterisation of this species was, however, precluded by its short half-life of <1 day; the ready decomposition of this species, which was also observed on silica TLC plates, is presumably responsible for the poor isolated yield after column chromatography.

This result is striking, since the mechanism of reduction of an aromatic nitro group to an aromatic amine is known, in the majority of cases, to involve SET. In the absence of any other reductants, a logical explanation for this finding is that phenylenediamine **399** acts as both a

nucleophile and a single-electron reductant in this reaction, suggesting SET from such amines to the naphthoquinone core is indeed thermodynamically feasible. Moreover, an 8-amino substituent has previously been found to exert a net electron-withdrawing force on the naphthoquinone core, since the pK_a values of species **32** and **190** are reported as 9.2 and 8.4 respectively.[281a] Therefore, it would be anticipated that the presence of the 8-amino group might increase the propensity for the naphthoquinone to be reduced compared with an unsubstituted analogue, and so the markedly decreased stability of 8-amino-substituted **411** *cf.* unsubstituted **400** adds further weight to the hypothesis that the instability of such species is due to SET.

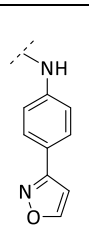
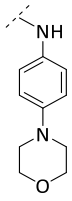
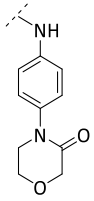
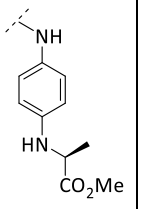
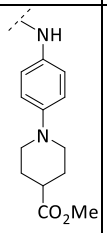
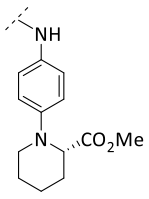
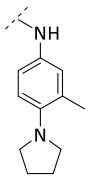
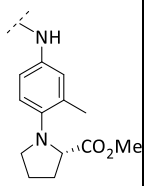
Compound	**376**	**364**	**365**	**385**	**400**	**396**	**404**	**408**
C_3 Substituent								
IC_{50} MOUSE(NAT2) (μM)	11.4 ± 5.3	>30	>30	16.3 ± 2.7	13.6 ± 3.2	>30	>30	>30
R^2	0.4271	N/A	N/A	0.8523	0.7643	N/A	N/A	N/A
P	*	N/A	N/A	***	***	N/A	N/A	N/A

Table 5.4: IC_{50} values against MOUSE(NAT2) for isoxazole **376** and compounds containing a phenylenediame C_3 substituent, determined from the acetyl CoA hydrolysis assay. Readings were carried out in duplicate; values are quoted ± one standard deviation and analysis was performed using KyPlot® software. Confidence limits are denoted by the number of stars: * = P <0.05; *** = P <0.005.

Although the desired carboxylic acid derivatives **367**, **371** and **409** proved unstable, the stable compounds in this synthesised library were evaluated for inhibitory activity against MOUSE(NAT2) **(Table 5.4)**. It can be observed that only the heteroaromatic isoxazole derivative **376**, isonipecotic methyl ester derivative **400** and alanine methyl ester derivative **385** exhibit IC_{50} values below 30 μM. Whilst promisingly, this demonstrates that saturated substituents on the C_3 anilino moiety are tolerated in the MOUSE(NAT2) active site, even the most potent such analogue (**400**) has an IC_{50} value over one order of magnitude greater than

that of the parent biaryl species **220** (0.42 μM). The discrepancy between the observed potencies in this particular series of compounds is predicted to be due to steric repulsions with the entrance to the MOUSE(NAT2) active site, since the three examples possessing IC_{50} values below 30 μM are the three which contain the least sterically demanding and most geometrically linear C_3 substituents.

5.1.4. Strategies to Overcome the Instability of Phenylenediamine C_3 Substituents

Following the observation that aliphatic substituents on the C_3 anilino moiety can be tolerated in the MOUSE(NAT2) active site, but that the potency of all of the examples synthesised thus far are low compared to the most potent biaryl derivatives, attention turned to the design of an amino acid-containing C_3 moiety which would be anticipated to be stable when appended to the naphthoquinone core, unlike carboxylic acids **367**, **371** and **409 (Figure 5.6)**.

Two different strategies were employed. Firstly, if carboxylic acids **367**, **371** and **409** are unstable due to a through-space interaction between the negatively-charged carboxylate functionality and the phenylenediamine ring, then increasing the distance between the ring and the carboxylate might be expected to increase stability; therefore, dipeptide-substituted compound **412** was proposed as the additional glycine spacer removes the carboxylate functionality from the vicinity of the phenylenediamine.

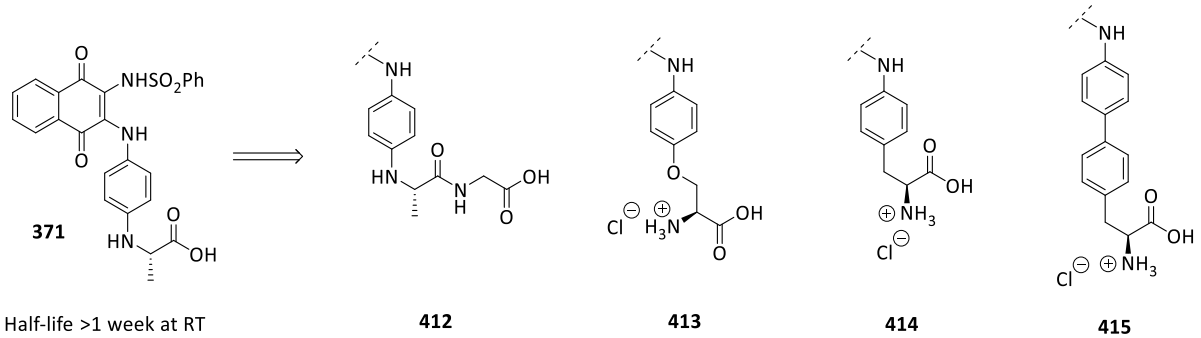


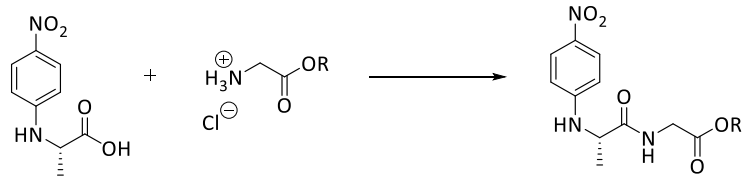
Figure 5.6: New target species containing an amino acid substituent on the C_3 anilino moiety which are predicted to have higher stability than alanine derivative **371**.

Secondly, if the *para* substituent on the C_3 anilino moiety is linked to the aromatic ring *via* either oxygen or carbon instead of nitrogen, then it would be anticipated that the electron density, and hence the oxidation potential, of the anilino moiety would decrease dramatically. Therefore, analogues based on either serine (**413**) or phenylalanine (**414**) were devised. Carbon-linked targets based on phenylalanine are of particular interest, because large amino acid transporters (LATs) are reported to be highly expressed in the membranes of epithelial tissues such as those in the intestine;[341] LATs are selective for the active transport of large amino acids with neutral R groups, such as phenylalanine, across cell membranes. Additionally, due to the high potency of biaryl amine derivatives, the further species **415** based on phenylalanine containing an additional aromatic ring *cf.* **414** was also proposed.

5.1.4.1. Synthesis and Evaluation of Dipeptide-Substituted 412

In order to synthesise dipeptide-derived target species **412**, appropriate methodology for formation of a peptide bond between *N*-(4-nitrophenyl)-L-alaninate **382** and an ester of glycine had to be established. A range of peptide coupling conditions were trialled for this reaction **(Table 5.5)**, and it was found that the optimum conditions were the use of HATU and Et_3N in the presence of catalytic DMAP, which were effective for coupling both the methyl and ethyl esters of glycine to alaninate **382**.

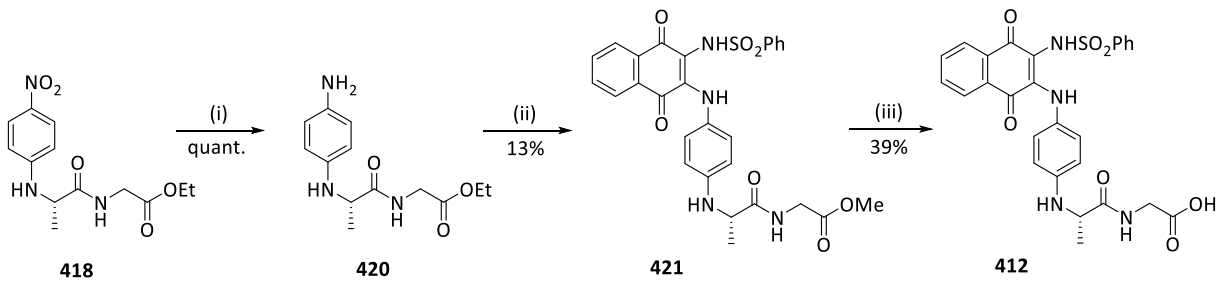
N-(4-Nitrophenyl) dipeptide ethyl ester **418** was then subjected to nitro group reduction and subsequent Michael-type addition to naphthoquinone **57**, to yield methyl ester **421** in 13% over two steps, the ethyl ester group having undergone transesterification in the presence of the Lewis acid $CeCl_3$ and MeOH as solvent (conditions (i) and (ii) respectively in **Scheme 5.11**). Basic hydrolysis of the methyl ester of **421** then led to the isolation of carboxylic acid **412** in 39% yield after purification *via* column chromatography. Crucially, **412** was found to be stable at RT for over 6 months; this suggests that increasing the through-space distance between the phenylenediamine moiety and the carboxylate group does indeed help to lower the oxidative potential of the phenylenediamine.



382 **416** R = Et, **417** R = Me, **418** R = Et, **419** R = Me

Entry	R	Coupling Reagents	Solvent	Temperature	Reaction Time	Conversion of 382	Isolated Yield
(a)	Et	T3P (4.0 eq.), *N*-methyl morpholine (6.0 eq.)	CH_2Cl_2	0 °C to RT	16 h	100%	62%
(b)	Et	EDC (1.0 eq.), Et_3N (1.0 eq.), DMAP (0.1 eq.)	CH_2Cl_2	RT	16 h	78%	Not isolated
(c)	Et	CDI (1.0 eq.), Et_3N (1.0 eq.)	THF	70 °C	16 h	35%	Not isolated
(d)	Et	HATU (1.0 eq.), Et_3N (1.0 eq.), DMAP (0.1 eq.)	CH_2Cl_2	RT	16 h	100%	64%
(e)	Me	HATU (1.0 eq.), Et_3N (1.0 eq.), DMAP (0.1 eq.)	CH_2Cl_2	RT	2 h	100%	75%

Table 5.5: Optimisation of conditions for coupling of glycine methyl or ethyl ester hydrochloride to *N*-(4-nitrophenyl)-L-alaninate **382**; conversion of **382** was determined by ^{1}*H*-NMR analysis.



418 **420** **421** **412**

Scheme 5.11: Synthesis of dipeptide-substituted target species **412**. *Reagents and conditions:* (i) H_2 (1 atm.), 10% Pd/C (0.1 eq.), MeOH, RT, 16 h; (ii) naphthoquinone **57** (1.0 eq.), $CeCl_3 \bullet 7H_2O$ (1.0 eq.), MeOH, RT, 1.5 h *then* aniline **420** (3.0 eq.), 90 °C, 16 h; (iii) 1,4-dioxane:1 M aq. NaOH (4:1), RT, 1 h *then* HCl, RT.

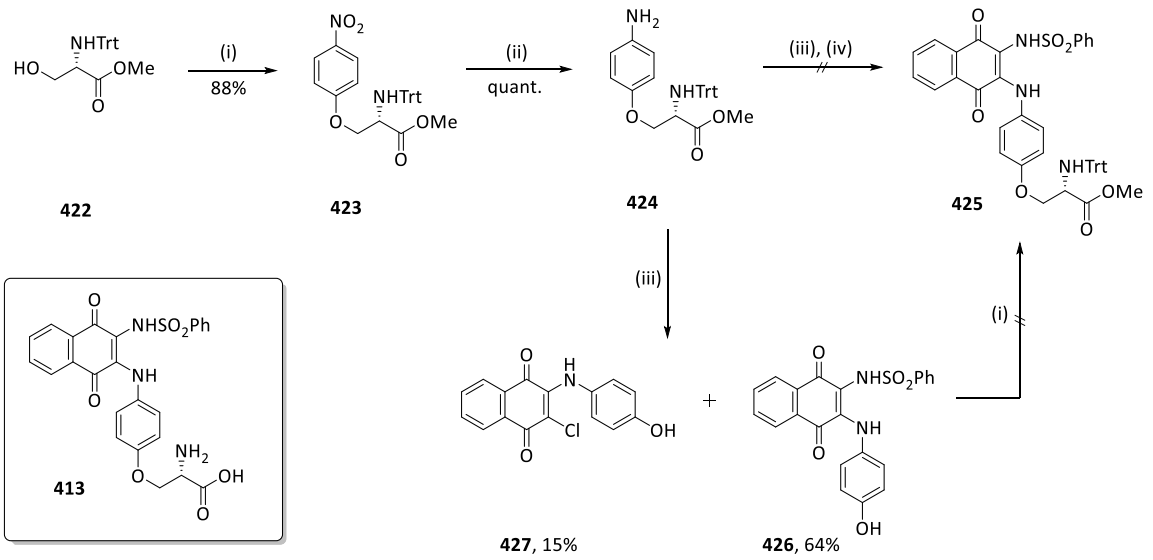
Both carboxylic acid **412** and its methyl ester precursor **421** were tested for their inhibitory potency against MOUSE(NAT2) in the acetyl CoA hydrolysis assay. Both compounds show very similar levels of inhibition which are comparable to that of the initial hit compound **32** but an order of magnitude above that of biaryl-substituted **220**: methyl ester **421** has an IC_{50} value of 6.9 ± 1.4 μM (R^2 = 0.7804, P = <0.005), whilst that of carboxylic acid **412** is 5.7 ± 2.1 μM (R^2 = 0.6512, P = <0.05). It is hypothesised that the polar dipeptide substituents point out of

the active site of MOUSE(NAT2) and are capable of forming stabilising interactions with solvent molecules.

Subsequently, the physical properties of carboxylic acid **412** were determined. Disappointingly, the kinetic solubility of **412** was found to be <2 μM in 99% 0.01 M PBS/1% DMSO (*v/v*), although this result should be treated with caution since **412** is a deep blue colour in DMSO and the wavelengths of visible light at which it absorbs interfere with the turbidimetric measurements used to determine solubility limits. It is, however, notable that the reported solubility limit is approximately 30-fold lower than that for carboxylic acid **350**; furthermore, a slow rate of A to B flux across the Caco-2 cell monolayer was measured, of $(0.98 \pm 0.27) \times 10^{-6}$ cms^{-1} (mean recovery = 18%; efflux ratio = 11.1). Compound **412**, therefore, would appear to be an unsuitable candidate for progression to studies in tumour cell models.

5.1.4.2. Attempted Synthesis of Serine-Derived 413

The synthesis of serine-derived analogue **413** was attempted from *N*-trityl L-serine methyl ester **422 (Scheme 5.12)**. Initially, a Mitsunobu reaction[342] between **422** and 4-nitrophenol furnished intermediate **423** in excellent yield (conditions (i)), which was subsequently reduced *via* catalytic hydrogenation with 10% Pd/C to give aniline **424** (conditions (ii)). Attempted Michael-type reaction of **424** with naphthoquinone **57** however did not yield the desired adduct **413** (conditions (iii)); rather, the major isolated product was **426**, bearing a *para*-hydroxyanilino moiety at the C_3 position. Under the Lewis acidic conditions in a polar solvent, it was assumed that cleavage of the serine group might have occurred *via* either nucleophilic substitution or elimination. The serine-containing by-product from the reaction could not be isolated; however, if in a future experiment the identity and enantiopurity of this by-product could be established, it could be possible to determine which is the predominant mechanism of cleavage. Additionally, by-product **427** was also isolated from the Michael-type step, in which the benzenesulfonamide substituent in **57** is substituted in preference to chloride.



Scheme 5.12: Attempted synthesis of serine-derived target species **413**. *Reagents and conditions:* (i) DIAD (1.35 eq.), PPh_3 (1.35 eq.), THF, RT, 1 h *then* *N*-trityl-L-serine **422** (1.0 eq.), 4-nitrophenol (1.35 eq.), RT, 48 h; (ii) H_2 (1 atm.), 10% Pd/C (0.1 eq.), MeOH, RT, 16 h; (iii) naphthoquinone **57** (1.0 eq.), $CeCl_3 \bullet 7H_2O$ (1.0 eq.), MeOH, RT, 1.5 h *then* aniline **424** (3.0 eq.), 90 ^oC, 16 h; (iv) naphthoquinone **57** (1.0 eq.), $CeCl_3$ (1.0 eq.), toluene, RT, 1.5 h *then* aniline **424** (3.0 eq.), 110 ^oC, 16 h.

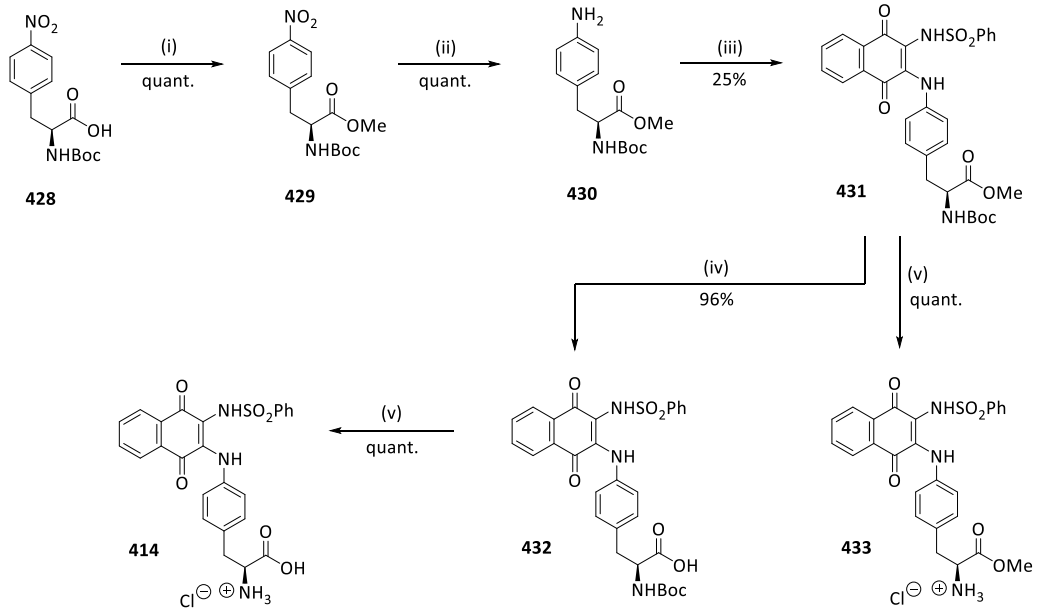
In an attempt to prevent cleavage of the serine group during the Michael-type step, anhydrous reaction conditions were trialled, using anhydrous $CeCl_3$ (formed from $CeCl_3 \bullet 7H_2O$ by heating under vacuum at 170 ^oC for 2 h) in toluene as solvent (conditions (iv)). These reaction conditions, however, led to a complex mixture of products from which **413** could not be isolated. In a final attempt to access **413**, *para*-hydroxyanilino species **426** was subjected to a Mitsunobu reaction with *N*-trityl L-serine methyl ester **422**. TLC, *m/z* (ESI^+) and ^1H-NMR analysis of the reaction all indicated signs of desired product formation; however, **413** could not be isolated. At this point, in the interests of time, no further attempts were made to synthesise serine derivative **413** and focus was turned to analogues bearing a methylene linker to the anilino ring in place of the oxygen linker in **413**.

5.1.4.3. Synthesis and Evaluation of Phenylalanine-Derived Species

Synthesis of phenylalanine-derived target **414** proved more tractable, and **414** was furnished successfully from *N*-Boc-4-nitro-L-phenylalanine **428** in five linear steps **(Scheme 5.13)**. An

initial methylation of **428** with 1.0 eq. TMS-diazomethane yielded methyl ester **429**, which could subsequently be reduced to aniline **430** in a quantitative fashion (conditions (i) and (ii) respectively). The subsequent Michael-type step gave intermediate **431** in a 25% isolated yield (conditions (iii)), which was then subjected to quantitative deprotection of firstly the methyl ester functionality *via* basic hydrolysis, and secondly the *tert*-butyl carbamate functionality *via* treatment with TFA in CH_2Cl_2 (conditions (iv) and (v) respectively). The final product **414** was isolated as the hydrochloride salt after azeotropic removal of TFA and treatment with c. HCl.

Additionally, intermediate **431** was also treated with TFA in CH_2Cl_2, followed by c. HCl, to yield methyl ester **433** as its hydrochloride salt, to prevent the possibility of undesirable diketopiperazine formation from the α-amino esters. This enabled a direct comparison of the pharmacological properties of **414**, in which both the amine and carboxylic acid functionalities are present, and the precursors **432** and **433**, in which one of these groups is protected (as a *tert*-butyl carbamate or as a methyl ester respectively).



Scheme 5.13: Synthesis of phenylalanine-derived species **414**, and precursors **432** and **433** in which one of the amino acid functionalities remains protected. *Reagents and conditions:* (i) TMS-CHN_2 (2 M in hexanes, 1.0 eq.), MeOH (17.0 eq.), CH_2Cl_2, RT, 16 h; (ii) H_2 (1 atm.), 10% Pd/C (0.1 eq.), MeOH, RT, 16 h; (iii) naphthoquinone **57** (1.0 eq.), $CeCl_3 \bullet 7H_2O$ (1.0 eq.), MeOH, RT, 1.5 h *then* requisite aniline (3.0 eq.), 90 ^{o}C, 16 h; (iv) 1,4-dioxane:1 M aq. NaOH (4:1), RT, 1.5 h; (v) TFA:CH_2Cl_2 (1:5), 0 ^{o}C, 0.5 h *then* c. HCl, toluene, RT.

The pharmacological and physical properties of compounds **431-433** and **414** were subsequently evaluated **(Table 5.6)**. All four compounds display dose-dependent inhibition of MOUSE(NAT2), with IC_{50} values below 30 μM. However, when a Student's *T*-Test is performed, it can be noted that final compound **414**, containing both primary ammonium chloride and carboxylic acid functionalities, possesses a statistically significant higher IC_{50} value (17.0 μM) than its precursor **432**, in which the amine group is protected as the corresponding *tert*-butyl carbamate (2.0 μM) (*P* = <0.05). In the assay buffer at *p*H 8, **414** would be anticipated to be zwitterionic in nature, and this may give rise to unfavourable interactions with residues lining the opening of the MOUSE(NAT2) active site.

Compound		**431**	**432**	**433**	**414**
IC_{50} MOUSE(NAT2) (μM)		8.4 ± 1.3	2.0 ± 0.5	9.4 ± 3.0	17.0 ± 4.2
R^2		0.8813	0.8708	0.7647	0.5998
P		***	***	**	***
Kinetic Solubility (μM)		N.D.	N.D.	<2	<2.4
Caco-2 Membrane Permeability	**Rate of Flux A to B (10^{-6} cms^{-1})**	N.D.	N.D.	0.33 ± 0.01	0.06 ± 0.01
	% Recovery	N.D.	N.D.	4	75
	Efflux Ratio	N.D.	N.D.	4.1	2.7

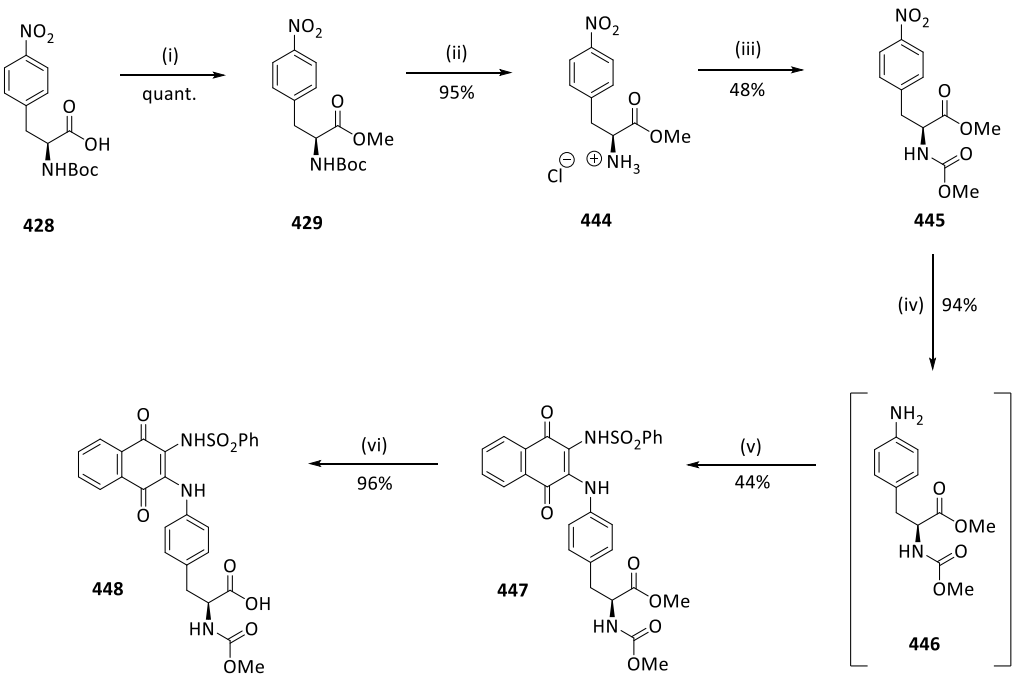
Table 5.6: Summary of pharmacological and physical data for compounds **414** and **431-433**; physical property data generated by Cyprotex plc (Macclesfield, UK). IC_{50} values were calculated from the acetyl CoA hydrolysis assay and were carried out in duplicate; values are quoted ± one standard deviation and analysis was performed using KyPlot® software. Confidence limits are denoted by the number of stars: ** = *P* <0.01; *** = *P* <0.005. Kinetic solubility was determined *via* turbidimetric measurement in a solution containing 99% 0.01 M PBS (*p*H 7.4)/1% DMSO (*v/v*); data are presented as the calculated mid-range of three repeat readings. Permeability in both the apical to basolateral direction (A to B) and *vice versa* across a Caco-2 intestinal epithelial cell monolayer[327] was determined at a concentration of 10 μM at 37 ^{o}C with an incubation time of 2 h; data are presented as the mean of two repeat readings ± one standard deviation. The % recovery of compound in the experiment is also given as a mean value. Efflux ratios are calculated as the rate of B to A flux divided by the rate of A to B flux. N.D. = not determined.

Meanwhile, it can also be observed that, contrary to the initial hypothesis, **414** possesses very poor kinetic solubility (<2.4 μM) and membrane permeability (A to B flux = 0.06 x 10^{-6} cms^{-1}). The poor kinetic solubility at *p*H 7.4 may well arise from the presence of the zwitterionic amino acid functionality in **414**, which in combination with the hydrophobic naphthoquinone

core will cause the molecule to be highly amphiphilic; indeed, **414** was also qualitatively observed to have poor solubility in organic solvents, proving insoluble in solvents of low polarity and only partially soluble in DMSO and MeOH. Unfortunately, it would also appear that despite the presence of an amino acid moiety, **414** has a low permeability across a Caco-2 monolayer, which does express LATs within its plasma membranes, for which phenylalanine is a good substrate.[343] This may be a consequence of the poor solubility of **414**, or because **414** is not a good substrate for such amino acid transporters. Furthermore, the kinetic solubility of ammonium chloride **433** is equally poor (<2 μM), and although **433** appears to have a higher membrane permeability than **414**, the observed rate of A to B flux (0.3×10^{-6} cms^{-1}) is still an order of magnitude lower than the corresponding value for hit compound **32**.

Of the four compounds synthesised in **Scheme 5.13**, arguably the most promising compound is carboxylic acid **432**, due to its high potency and the unfavourable physical properties which the ammonium chloride functionality appears to confer on analogues **414** and **433**. The physical properties of **432** were not however evaluated, since the *tert*-butyl carbamate functionality was not predicted to be conducive to a favourable kinetic solubility in aqueous media. Therefore, it was decided to synthesise the direct analogue of **432**, **448**, in which the *tert*-butyl carbamate was replaced with the corresponding methyl carbamate **(Scheme 5.14)**.

Carboxylic acid **448** was synthesised in a broadly analogous fashion to **432** in six linear steps from *N*-Boc-4-nitro-L-phenylalanine **428**. **428** was methylated as previously (conditions (i)), and subsequently the *tert*-butyl carbamate protecting group was removed in TFA and CH_2Cl_2 to generate, after work-up, hydrochloride salt **444** in a quantitative fashion (conditions (ii)). Preparation of methyl carbamate **445** could be effected in a facile manner using $InCl_3$ as a catalyst (conditions (iii); see **Section 3.5.**); subsequent reduction, Michael-type addition and ester hydrolysis using the standard procedures then allowed access to the desired carboxylic acid **448** in a yield of 40% over the three steps (conditions (iv), (v) and (vi) respectively).



Scheme 5.14: Synthesis of methyl carbamate analogue **448**. *Reagents and conditions:* (i) TMS-CHN_2 (2 M in hexanes, 1.0 eq.), MeOH (17.0 eq.), CH_2Cl_2, RT, 16 h; (ii) TFA:CH_2Cl_2 (1:5), 0 ^oC, 2 h *then* c. HCl, toluene, RT; (iii) methyl chloroformate (excess), Et_3N (1.0 eq.), $InCl_3$ (0.01 eq.), RT, 1 h; (iv) H_2 (1 atm.), 10% Pd/C (0.1 eq.), MeOH, RT, 16 h; (v) naphthoquinone **57** (1.0 eq.), $CeCl_3 \bullet 7H_2O$ (1.0 eq.), MeOH, RT, 1.5 h *then* requisite aniline (3.0 eq.), 90 ^oC, 16 h; (vi) 1,4-dioxane:1 M aq. NaOH (4:1), RT, 1.5 h *then* c. HCl, RT.

Pharmacological analysis of carboxylic acid **448** reveals that it has an IC_{50} value against MOUSE(NAT2) of 0.73 ± 0.18 μM (R^2 = 0.8764; P = <0.005), whilst its precursor methyl ester **447** has an IC_{50} value of 3.7 ± 1.6 μM (R^2 = 0.6317; P = <0.05). These data are very promising, and an *in silico* model of **448** in the active site of HUMAN(NAT1) suggests that the C_3 moiety extends out of the active site as predicted, but the small size of the methyl carbamate ensures that there are few unfavourable steric repulsions with the residues lining the entrance to the active site **(Figure 5.7)**. The acid **448** is likely more potent than the ester **447** due to the potential for ionic-dipole interactions between the charged carboxylate group and the bulk solvent.

However, when the physical properties of carboxylic acid **447** were determined, it was found to have a surprisingly low kinetic solubility of <2.8 μM in 99% 0.01 M PBS (*p*H 7.4)/1% DMSO (*v/v*), which offers no improvement over hit compound **32**; furthermore, it has a low A to B

flux rate across the Caco-2 monolayer of (0.28 ± 0.01) x 10^{-6} cms^{-1} (mean recovery = 81%; efflux ratio = 6.6), approximately one order of magnitude lower than that of compound **32**.

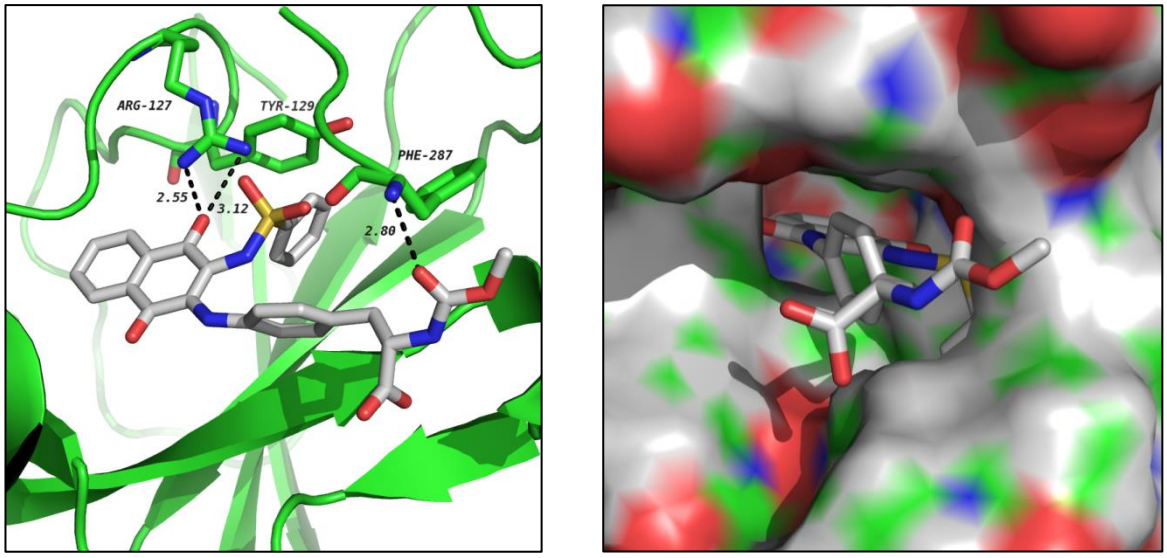
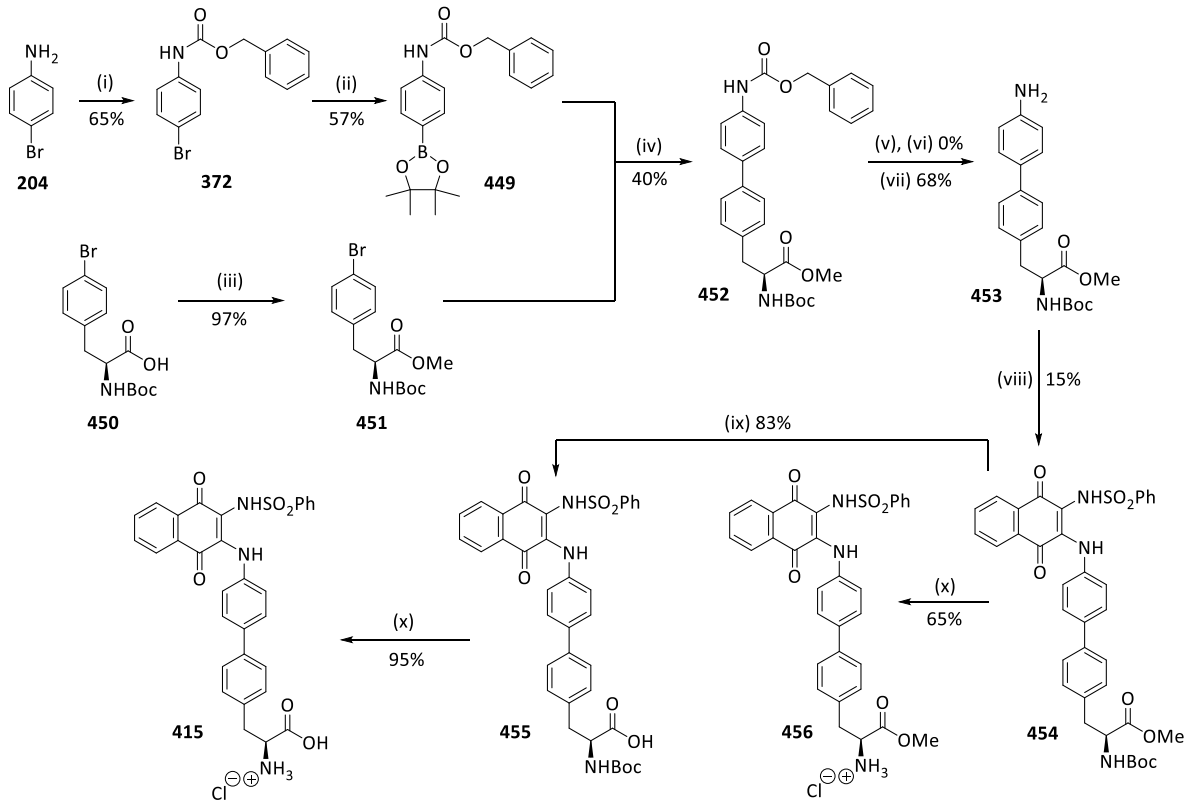


Figure 5.7: *In silico* modelling of methyl carbamate **448** within the active site of HUMAN(NAT1) (pdb: 2PQT);[247b] the protein is shown in both cartoon representation **(left)** and surface representation **(right)**. Analysis performed using GOLD® software (v.5.2).[282] Predicted polar contacts are highlighted by black dashed lines with inter-atomic distances given in Ångströms; key active site residues Arg127, Tyr129 and Phe287 are highlighted in stick representation (carbon atoms in green).

The final target compound chosen, biaryl phenylalanine derivative **415**, was also synthesised **(Scheme 5.15)**, although following the poor pharmacological and physical properties of species **414**, the precursors **455** and **456** in which the carboxylic acid or primary amine functionality are protected respectively are likely of greater interest.

para-Bromoaniline **204** was firstly *N*-protected as benzyl carbamate **372** as described previously (conditions (i)), before conversion of the bromo substituent to a boronic pinacol ester in a Pd-mediated cross-coupling step to give **449** in 57% yield (conditions (ii)). Intermediate **449** subsequently underwent Suzuki-type cross-coupling[203] with *para*-bromophenylalanine derivative **451** in moderate yield (conditions (iv)); **451** was itself

prepared in excellent yield by methylation of carboxylic acid **450** with 1.0 eq. TMS-diazomethane and 17.0 eq. MeOH in CH_2Cl_2.



Scheme 5.15: Synthesis of C_3-biaryl phenylalanine derivatives. *Reagents and conditions:* (i) benzyl chloroformate (1.2 eq.), PEG-400, RT, 1 h; (ii) B_2Pin_2 (1.5 eq.), KOAc (3.0 eq.), $Pd(PPh_3)_2Cl_2$ (0.1 eq.), 1.4-dioxane, 100 ^oC, 3 h; (iii) TMS-CHN_2 (2 M in hexanes, 1.0 eq.), MeOH (17.0 eq.), CH_2Cl_2, RT, 16 h; (iv) $Pd(PPh_3)_2Cl_2$ (0.1 eq.), sat. aq. $NaHCO_3$:THF (5:22), 100 ^oC, 16 h; (v) H_2 (1 atm.), 10% Pd/C (0.2 eq.), MeOH, RT, 16 h; (vi) H_2 (1 atm.), 10% Pd/C (0.2 eq.), EtOH:THF (1:1), RT, 16 h; (vii) ammonium formate (3.0 eq.), 10% Pd/C (0.2 eq.), MeOH, reflux, 1 h; (viii) naphthoquinone **57** (1.0 eq.), $CeCl_3 \bullet 7H_2O$ (1.0 eq.), MeOH, RT, 1.5 h *then* requisite aniline (3.0 eq.), 90 ^oC, 16 h; (ix) 1,4-dioxane:1 M aq. NaOH (4:1), RT, 2 h; (x) TFA:CH_2Cl_2 (1:5), 0 ^oC, 1 h *then* c. HCl, toluene, RT.

Reductive cleavage of the benzyl carbamate in biaryl intermediate **452** initially proved challenging, however, with no observed reaction in the presence of 0.1 eq. 10% Pd/C in MeOH after 16 h of stirring at room temperature (conditions (v)). The starting material **452** was poorly soluble in MeOH, and so the hydrogenation was instead attempted in 1:1 EtOH:THF, a solvent mixture in which **452** was soluble (conditions (vi)); however, once again no consumption of starting material was observed. Therefore, an alternative literature procedure

was trialled in which **452** was refluxed for 1 h with 3.0 eq. ammonium formate and 0.2 eq. 10% Pd/C in MeOH (conditions (vii));[344] this procedure successfully furnished the desired biaryl aniline **453** in 68% yield. The subsequent Michael-type reaction with naphthoquinone **57** (conditions (viii)), ester hydrolysis (conditions (ix)) and *tert*-butyl carbamate deprotection (conditions (x)) to generate the target compounds of interest all proceeded in comparable yields to analogous examples of these reactions described previously.

Compound		**454**	**455**	**456**	**415**
IC_{50} MOUSE(NAT2) (μM)		0.46 ± 0.11	0.29 ± 0.12	8.4 ± 3.8	N.D.
R^2		0.5910	0.2397	0.3562	N/A
P		***	*	*	N.A
Kinetic Solubility (μM)		N.D.	N.D.	6.5	<2
Caco-2 Membrane Permeability	**Rate of Flux A to B (10^{-6} cms^{-1})**	N.D.	N.D.	0.096	0.29 ± 0.04
	% Recovery	N.D.	N.D.	0.58	74
	Efflux Ratio	N.D.	N.D.	0.69	7.4

Table 5.7: Summary of pharmacological and physical data for compounds **415** and **454-456**; physical property data generated by Cyprotex plc (Macclesfield, UK). IC_{50} values were calculated from the acetyl CoA hydrolysis assay and were carried out in duplicate; values are quoted ± one standard deviation and analysis was performed using KyPlot® software. Confidence limits are denoted by the number of stars: * = *P* <0.05; *** = *P* <0.005. Kinetic solubility was determined *via* turbidimetric measurement in a solution containing 99% 0.01 M PBS (*p*H 7.4)/1% DMSO (*v/v*); data are presented as the calculated mid-range of three repeat readings. Permeability in both the apical to basolateral direction (A to B) and *vice versa* across a Caco-2 intestinal epithelial cell monolayer[327] was determined at a concentration of 10 μM at 37 ^{o}C with an incubation time of 2 h; data are presented as the mean of two repeat readings ± one standard deviation (**415**), or as a single experimental reading (**456**). Efflux ratios are calculated as the rate of B to A flux divided by the rate of A to B flux. The % recovery of compound in the experiment is also given as a mean value. N.D. = not determined.

Pharmacological analysis of compounds **415** and **454-456** reveals that as for previously synthesised biaryl derivatives, diprotected **454** and *N*-carbamate carboxylic acid **455** give very potent inhibition of MOUSE(NAT2), with IC_{50} values in the nanomolar range **(Table 5.7)**. Values for acid **455** should however be treated with caution due to its low R^2 value and confidence limit of *P* = <0.05. Carbamate deprotection to yield the free amine functionality appears to lead somewhat to loss of inhibition, with ammonium chloride **456** displaying an IC_{50} value which is an order of magnitude greater than those of **454** and **455**. Furthermore,

analysis of the physical properties of ammonium chloride **456** shows that it possesses only a two-fold increased kinetic solubility over hit compound **32** in 99% 0.01 M PBS (*p*H 7.4)/1% DMSO (*v/v*) of 6.5 μM, and a rate of A to B flux across the Caco-2 monolayer of 0.096 cms^{-1}, which is two orders of magnitude less than that of **32**. Interestingly, the kinetic solubility of ammonium chloride **456** is approximately three-fold higher than that of analogous ammonium chloride **433** containing one fewer aromatic ring. This is consistent with the earlier hypothesis that the biaryl moiety is not planar in its preferred conformation; the non-planarity of the biaryl ring system might lead to decreased π-π stacking between molecules of **456** and hence be responsible for the observed increase in solubility relative to that of **433**.

As for the analogous unprotected amino acid derivative **414**, compound **415** also has a very low kinetic solubility of <2 μM in 99% 0.01 M PBS (*p*H 7.4)/1% DMSO (*v/v*), most probably due to its ampiphilicity; in fact, its solubility in the assay buffer of 95% 20 mM Tris•HCl (*p*H 8.0)/5% DMSO (*v/v*) was so low that it precluded determination of its IC_{50} value against MOUSE(NAT2).

Therefore, unfortunately, attempts to generate amino acid-based analogues of hit compound **32** for use in cellular assays against HUMAN(NAT1) +ve cell lines have proved challenging. Although amino acid derivatives with either *N*-carbamate or carboxylic ester protecting groups such as **448**, **454** and **455** have been demonstrated to be highly potent against MOUSE(NAT2), with IC_{50} values <1 μM, none of these analogues have displayed significantly improved kinetic solubilities over hit compound **32**, and contrary to the initial hypothesis, all have exhibited very poor rates of A to B flux across the Caco-2 epithelial cell monolayer, indicative of poor membrane permeability.

5.1.5. Conclusions from Physical Property Optimisation Studies

In this chapter, efforts to improve the physical properties of selective HUMAN(NAT1) and MOUSE(NAT2) inhibitors have been described, with a particular focus on increasing both kinetic solubility in aqueous media and membrane permeability; such optimised inhibitors

were envisaged to be useful tools in studying the consequence of inhibiting HUMAN(NAT1) in NAT1+ tumour cell lines. Initial hit compound **32** and biaryl derivative **220** were used as starting points, and a variety of strategies were used in order to increase solubility, such as introduction of polar carboxylic acid and primary amine functionalities, increasing the number of rotatable bonds in the C_3 substituent or replacing one of the aromatic rings in a biaryl-derived species with a more highly saturated ring system **(Figure 5.8)**.

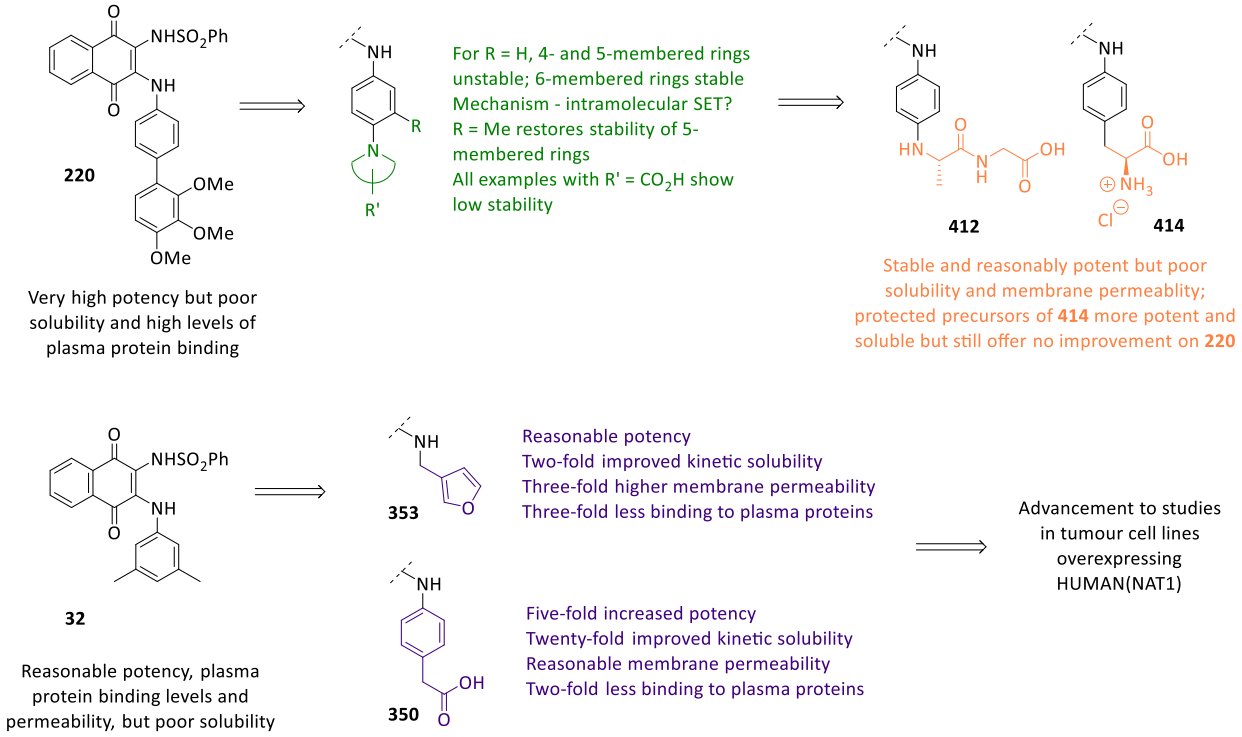


Figure 5.8: Summary of efforts to improve the physical properties of naphthoquinone inhibitors **32** and **220** for use in tumour cell line studies.

Interestingly, many of the aliphatic phenylenediamine-type derivatives of biaryl **220** proved to be unstable at RT; preliminary investigations suggest that the origin of their instability might be due to the possibility of an intramolecular single electron transfer from the phenylenediamine moiety to the naphthoquinone core, and that oxidation of the phenylenediamine subsequently leads to decomposition. Building upon the initial cyclic voltammetry experiments carried out on compound **32**, a comprehensive study of the

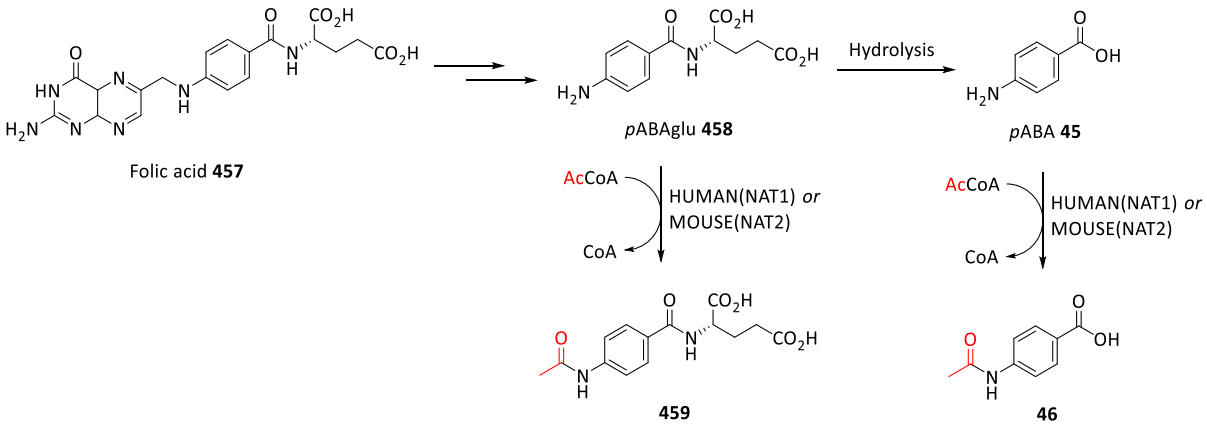
electrochemical properties of these molecules could provide further insights into these observations.

One key strategy to increase the solubility and membrane permeability of the inhibitors was to incorporate amino acid groups into the C_3 moiety. Of particular interest was the synthesis of species bearing a phenylalanine-derived C_3 substituent, due to the possibility that such compounds might be able to hijack large amino acid transporters (LATs) expressed in cell membranes, potentially leading to increased membrane permeability. However, compounds such as **414** displayed no improvement in potency against MOUSE(NAT2), kinetic solubility and membrane permeability over hit compound **32**, possibly due to their amphiphilicity. More promising levels of potency were achieved by precursors in which the primary amine functionality was protected as a carbamate; however, these species also offered little increase in kinetic solubility over hit compound **32**, and possessed poor membrane permeability.

However, the most promising results were given by the addition of the smallest and simplest solubilising groups trialled, and in carboxylic acid derivative **350** a molecule has been generated which possesses the correct balance of desired properties. **350** is a highly potent inhibitor of HUMAN(NAT1), with an IC_{50} value of 0.71 μM in the acetyl CoA hydrolysis assay, is selective for the inhibition of HUMAN(NAT1) at 30 μM over its isoenzyme HUMAN(NAT2), and is observed to inhibit NAT activity in cell extracts from the ER+ breast cancer cell line ZR-75-1, with the extent of inhibition at 1 μM demonstrated to be statistically significant from that of a control (vehicle only) experiment. Furthermore, **350** additionally displays a thirty-fold improved kinetic solubility over hit compound **32**, at 65 μM, a value which is two orders of magnitude higher than its IC_{50} value against HUMAN(NAT1), is cell membrane-permeable and was found to be 10% unbound in a plasma protein binding experiment. Additionally, studies on hit compound **32** suggest that close analogues such as **350** are unlikely to be reduced within a cellular environment. Carboxylic acid **350** therefore represents the first example of a small molecule inhibitor of HUMAN(NAT1) which might be able to offer a useful insight into the consequences of HUMAN(NAT1) inhibition in NAT1+ tumour cell lines in future studies.

5.2. The Role of HUMAN(NAT1) in Folate Metabolism

One intriguing endogenous role of HUMAN(NAT1) is its known involvement in the metabolic cycle of folate.[255b, 255c, 345] Both of the folate metabolites *para*-aminobenzoyl-L-glutamate (*p*ABAglu, **458**) and *para*-aminobenzoic acid (*p*ABA, **45**) are substrates of HUMAN(NAT1) **(Scheme 5.16)**,[257] and intracellular levels of folate in human erythrocytes have been reported to be inversely correlated with measured levels of *N*-acetylation of *p*ABA within the cells.[346] Furthermore, both folate and its analogues have been shown to reduce the rate of arylamine acetylation by recombinant HUMAN(NAT1) *in vitro*.[255c, 346] In recent years, knockout studies in murine models suggest a link between MOUSE(NAT2) and folate catabolism,[347] since the NAT2 null mice, whilst phenotypically normal, display no detectable amounts of *N*-acetyl-*p*ABAglu in their liver, kidneys or urine; additionally, the mice were shown to possess biochemical abnormalities in 5-methyl tetrahydrofolate and *S*-adenosylmethionine homeostasis.[255a, 348]



Scheme 5.16: Proposed involvement of HUMAN(NAT1) or MOUSE(NAT2) in the folate catabolic pathway.

HUMAN(NAT1) is highly expressed in the embryo and placenta, as early as the four-cell stage,[349] and its potential role in folate catabolism during development is of pathological significance because of the reported beneficial effects of folic acid supplementation on the prevention of neural tube defects[350] and oral clefts.[351] Rare loss of function mutations in *HUMAN(NAT1)* are also linked to a reduced risk of spina bifida.[352] Interestingly,

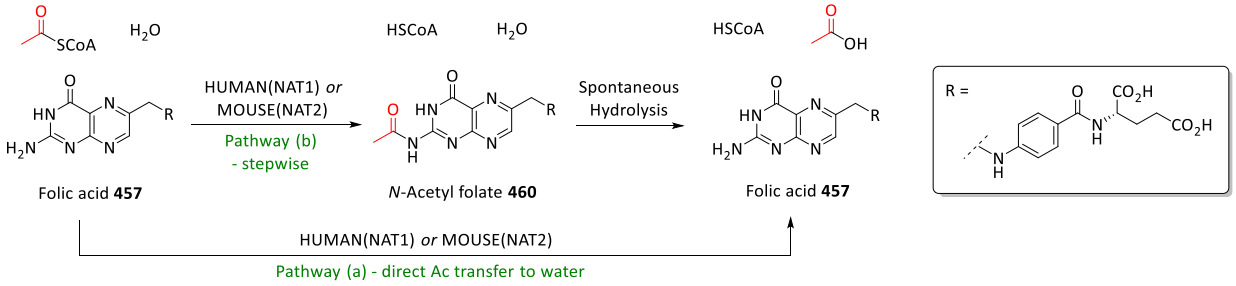
overexpression of HUMAN(NAT1) within mice results in an increased incidence of neural tube defects associated with folate deficiency,[353] and has complex reported effects on the incidence and severity of oral clefts.[354] Folate-dependent methylation is also believed to play a role in the epigenetic regulation of MOUSE(NAT2) expression,[355] which is of importance not just to developmental defects but also to tumorigenesis: in humans, hypomethylation of the promoter region associated with increased *HUMAN(NAT1)* mRNA expression has been reported in breast ductal carcinomas.[356]

Therefore, a fuller understanding of the link between HUMAN(NAT1) and folate is of importance to elucidating the endogenous roles of HUMAN(NAT1), and whether it might be a viable therapeutic target in treatment of cancers or developmental defects. One particularly interesting question surrounds the direct effect of folate levels on HUMAN(NAT1) or MOUSE(NAT2) activity: might HUMAN(NAT1) or its murine homologue still be able to hydrolyse acetyl coenzyme A in the presence of folate, even in the absence of arylamines? Truncated forms of both HUMAN(NAT1) and NAT from *S. typhimurium* with shortened *C*-termini have been reported to catalyse the hydrolysis of AcCoA without transfer of the acetyl group to an arylamine,[357] but such behaviour had not been previously observed using full length mammalian NATs.

Laurieri demonstrated *via* HPLC experiments that if HUMAN(NAT1) is treated with AcCoA and folate, over time the amount of folate remains constant, but AcCoA is depleted into its hydrolysis product, CoA.[258] This behaviour was also observed, with lower efficiency, in the presence of analogues of folate such as methotrexate, pterin and pteroic acid; furthermore, no such reaction was observed to occur when HUMAN(NAT1) was replaced with the orthologous enzyme HUMAN(NAT2).[258] Following this, the ability of MOUSE(NAT2) to catalyse this process was investigated *via* enzymatic assays. Acetyl CoA hydrolysis assays indicated that MOUSE(NAT2) but no other murine or prokaryotic enzyme tested was capable of hydrolysing AcCoA in the presence of folate but absence of arylamine; however, if an arylamine is present, a combination of an acetyl CoA hydrolysis assay and an arylamine acetylation assay shows

that the presence of folate does not affect or inhibit the acetylation of the arylamine by MOUSE(NAT2).[258]

Subsequently, monitoring of the hydrolysis of AcCoA by MOUSE(NAT2) in the presence of folate *via* ^{1}H-NMR suggested that the ultimate fate of the acetyl group in the reaction was a transfer to bulk solvent, *i.e.* AcOH was formed as the acetyl-containing by-product of the reaction **(Scheme 5.17)**.[258] However, it was not possible in these experiments to determine whether the mechanism of the reaction proceeds *via* a direct hydrolysis of the presumed Ac-Cys68 covalent intermediate in the NAT active site by a molecule of water (pathway (a)) or whether the acetyl group is initially transferred to folate, giving *N*-acetyl folate **460** which then spontaneously hydrolyses on a timescale too rapid for **460** to be detectable in an NMR experiment (pathway (b)).



Scheme 5.17: Possible mechanisms for folate-mediated hydrolysis of AcCoA by HUMAN(NAT1) or MOUSE(NAT2): a direct acetyl transfer to water (pathway (a)) or a stepwise process *via* *N*-acetyl folate **460** (pathway (b)).

All of the evidence gathered suggests that folate acts as a cofactor in the HUMAN(NAT1)/ MOUSE(NAT2)-mediated hydrolysis of AcCoA; experiments in which the initial rates of AcCoA hydrolysis were determined for varying concentrations of folate showed that the measured hydrolytic activities were consistent with Michaelis-Menten kinetics and enabled the estimation of dissociation constants of folate as 75 µM for HUMAN(NAT1) and 71 µM for MOUSE(NAT2).[258]

One key remaining question surrounds the mechanism by which folate acts as a cofactor in the hydrolysis reaction: does it bind directly to the active site of HUMAN(NAT1) and its murine homologue? In an attempt to dissect this question, both acetyl CoA hydrolysis assays with naphthoquinone inhibitor **32** and computational modelling studies were carried out.

In an initial test at 30 μM, compound **32** was found to almost entirely inhibit folate-induced hydrolysis of AcCoA by MOUSE(NAT2). Subsequent experiments demonstrated that **32** has a dose-dependent effect on inhibition of this enzymatic reaction, with a calculated IC_{50} value of 0.14 ± 0.03 (R^2 = 0.7043, P = <0.005), which is approximately twenty-fold lower than the calculated IC_{50} value for **32** when *p*ABA is present in the assay in place of folate (3.1 μM).

In the Ping-Pong bi-bi mechanism of acetyl transfer from AcCoA to an arylamine, the first step in the mechanism is the reaction of AcCoA with the Cys68 residue in the NAT active site to form a covalent Ac-Cys68 intermediate, releasing free CoA; the acetyl group is subsequently transferred to the arylamine nitrogen (see **Scheme 1.16B** in **Section 1.2.**).[248] In the folate-mediated hydrolysis of AcCoA, it is hypothesised that formation of the Ac-Cys68 intermediate occurs in an analogous fashion, but in the absence of arylamine and presence of folate, a molecule of water is able to deacetylate this covalent intermediate to form AcOH. Previous studies have reported the HUMAN(NAT1) and MOUSE(NAT2) active sites to be highly hydrophobic and inaccessible to water molecules;[247b] the observation that neither enzyme can hydrolyse AcCoA to an appreciable extent in the absence of both arylamine and folate supports this hypothesis.[358]

It is therefore postulated that the binding of folate as a cofactor to HUMAN(NAT1) or MOUSE(NAT2) might alter the hydrophobicity of the enzyme active site, so as to allow water molecules to access the active site and react with the Ac-Cys68 covalent intermediate. Such an alteration might be effected by a change in the folding of the protein induced by the binding of folate.

It was therefore deemed instructive to undertake *in silico* modelling studies in which folate was docked into the crystal structure of HUMAN(NAT1) **(Figure 5.9)**. Intriguingly, repeatable simulations suggest a number of hydrogen-bonding contacts might be formed between folate and a host of key residues within the active site, including the extensively discussed residues Arg127 and Gly124, and catalytic triad residues Cys68 and His107, amongst others. Furthermore, the model suggests that folate might also be able to form π-π stacking interactions at close range with residues Phe125 and Tyr129. The ability of folate to bind non-covalently to the HUMAN(NAT1) active site is also a reasonable hypothesis given that the structure of folate incorporates the *p*ABA and *p*ABAglu moieties, both of which are known to be selective substrates for HUMAN(NAT1).

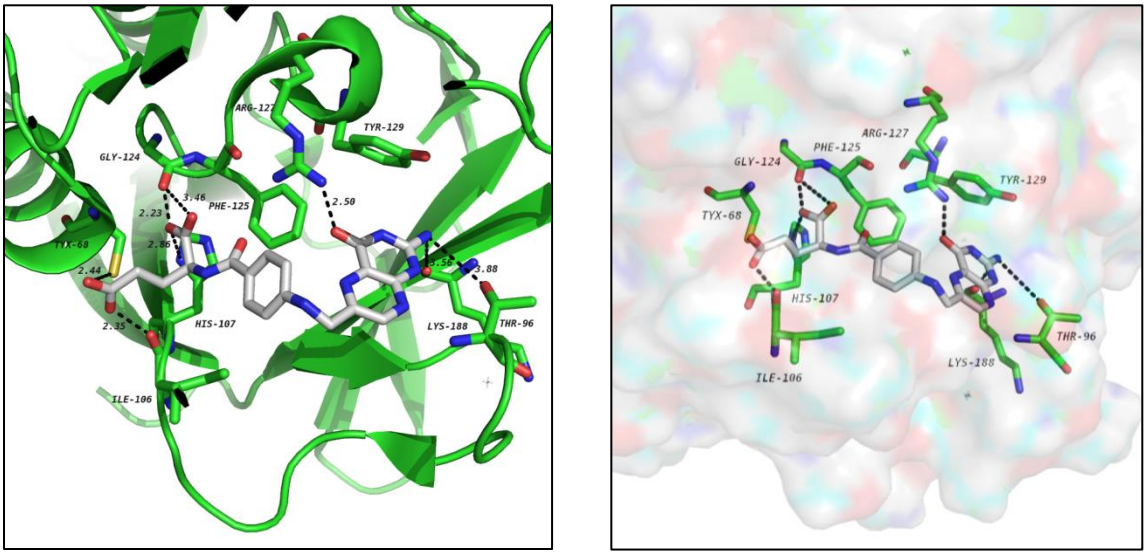
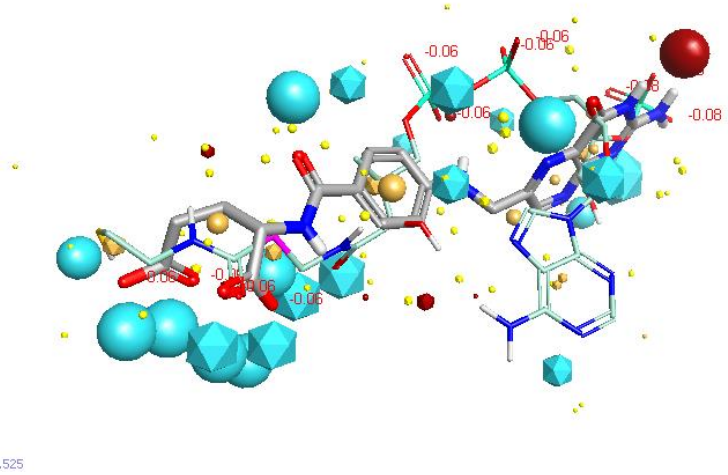
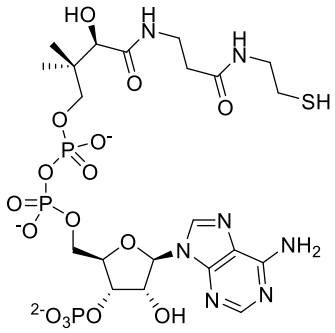


Figure 5.9: *In silico* modelling of folate **457** within the active site of HUMAN(NAT1) (pdb: 2PQT);[247b] the protein is shown in both cartoon representation **(left)** and surface representation **(right)**. Analysis performed using GOLD® software (v.5.2).[282] Predicted polar contacts are highlighted by black dashed lines with inter-atomic distances given in Ångströms; key active site residues Cys68 (labelled as Tyx68 due to the required modification of the residue in generation of the crystal structure), Thr96, His107, Gly124, Phe125, Arg127, Tyr129 and Lys188 are highlighted in stick representation (carbon atoms in green).

A





461

B

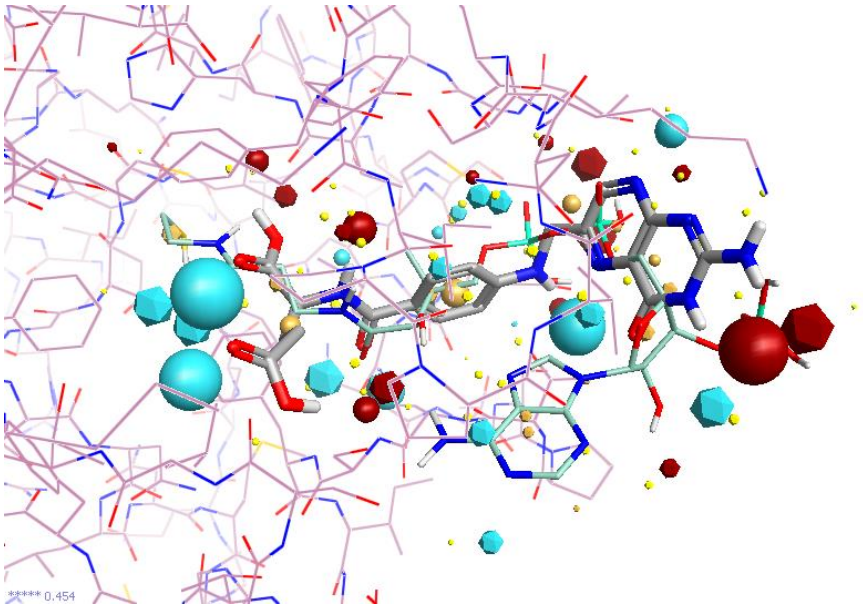


Figure 5.10: Modelling of the structural similarity between folate **457** and CoA **461** using FORGE® (Cresset Group, Litlington, Cambridgeshire, UK).[303] Modelling was carried out using the structure of CoA as bound in a co-crystal structure with HUMAN(NAT2) (pdb: 2PFR)[247b] as a reference ligand and folate **457** as the test ligand. **A:** Predicted spatial and electron density distribution alignment between folic acid **457** (carbons in grey) and CoA **461** (carbons in light green) in free space **(left)** with the structure of CoA **461** given **(right)**. Regions of negative charge are shown in cyan, regions of neutral charge in yellow and regions of positive charge in dark red. Icosahedra correspond to the electronic fields of CoA **461** and spheres to the electronic fields of folic acid **457**. **B:** Predicted spatial and electron density distribution alignment between folic acid **457** (carbons in grey) and CoA **461** (carbons in light green) using HUMAN(NAT2) (carbons in lilac) as an excluded volume. Folic acid **457**, CoA **461** and their respective electron density distributions are represented as in **(A)**.

Furthermore, a comparison of the conformation of free folate **457** with that of CoA **461**, in the conformation in which it is bound to the active site of HUMAN(NAT2) in the available co-crystal structure,[247b] suggests noticeable similarities between the shape and electron density distribution of the two species **(Figure 5.10A)**. Repeatable simulations show that regions of positive charge, negative charge and neutral regions for the two ligands align well in space.

When HUMAN(NAT2) was used as an excluded volume in this modelling, similar alignments were predicted **(Figure 5.10B)**. It should be noted that these experiments involve a comparison between the conformation of CoA as bound to HUMAN(NAT2) and that of free folate; thus the simulations pertain to free folate, and not to the predicted conformation of hypothetical enzyme-bound conformations of folate. HUMAN(NAT2) was utilised as an excluded volume to ensure that folate and CoA were excluded from the same space, permitting a reliable comparison between the shapes of the two molecules. Interestingly, when folate is docked into the active site of HUMAN(NAT2) it does give a good predicted fit **(Figure 5.11)**, but this does not necessarily imply binding of folate to HUMAN(NAT2) and even if folate does bind to HUMAN(NAT2), it may not induce the conformational changes required for AcCoA hydrolysis.

For a more complete description of the binding site of folate within HUMAN(NAT1) or MOUSE(NAT2), a crystal structure of either protein co-complexed with folate would be desirable, and future studies should seek to obtain such a structure. Another interesting future study would be to screen some of the HUMAN(NAT1) and MOUSE(NAT2) inhibitors developed in this study for inhibitory potency against the folate-mediated AcCoA hydrolysis assay, particularly some of the more polar analogues developed in this chapter such as carboxylic acid **350**. If, as hypothesised, binding of folate to HUMAN(NAT1) or MOUSE(NAT2) induces a significant change in the structure and hydrophobicity of the enzyme active site, it might be anticipated that the SAR for the developed library of naphthoquinone inhibitors against the AcCoA hydrolyase activity of the enzyme reveals some differences *cf.* the SAR against the arylamine *N*-acetyltransferase activity of the enzyme.

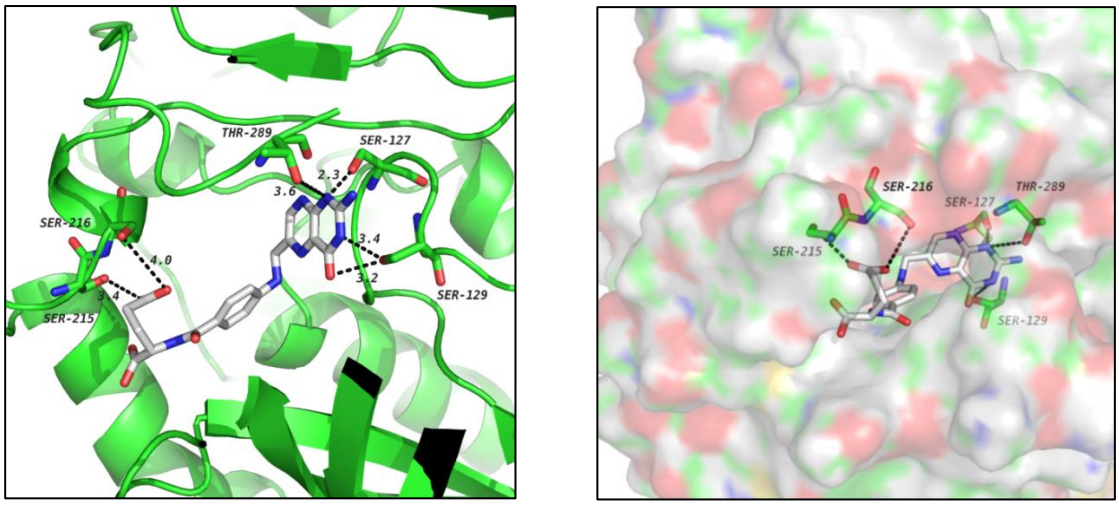


Figure 5.11: *In silico* modelling of folate **457** within the active site of HUMAN(NAT2) (pdb: 2PFR);[247b] the protein is shown in both cartoon representation **(left)** and surface representation **(right)**. Analysis performed using GOLD® software (v.5.2).[282] Predicted polar contacts are highlighted by black dashed lines with inter-atomic distances given in Ångströms; key active site residues Ser127, Ser129, Ser215, Ser216 and Thr289 are highlighted in stick representation (carbon atoms in green).

Nonetheless, the computational modelling studies presented here, in conjunction with the result that compound **32** inhibits folate-mediated AcCoA hydrolysis in a dose-dependent fashion, lend support to the hypothesis that folate is capable of binding to HUMAN(NAT1) – and by analogy, MOUSE(NAT2). This might induce a change in the conformation of the enzyme active site such as to allow a water molecule access to the Ac-Cys68 covalent intermediate, facilitating overall hydrolysis of AcCoA to CoA and AcOH. In the future, a more detailed kinetic analysis could be carried out to determine whether folate is a competitive binder to *p*ABA and AcCoA in the active site of HUMAN(NAT1) and MOUSE(NAT2), or whether it mediates the observed effects on the enzyme function *via* allosteric binding.

More broadly, the data enhance our understanding of the endogenous roles of HUMAN(NAT1) and MOUSE(NAT2), suggesting that they are not simply xenobiotic metabolising enzymes, but are likely to play a role in cellular metabolic cycles. In particular, these studies give rise to questions about the possible role of HUMAN(NAT1) and MOUSE(NAT2) in mediating AcCoA/CoA homeostasis. As AcCoA is a key metabolic

intermediate in the synthesis of a wide variety of macromolecules, the potential link between the reported overexpression of HUMAN(NAT1) in cell types associated with development (e.g. embryonic, placental, stem and tumour cells) and AcCoA levels in these cells is a fascinating one which should be the subject of future investigations. In particular, the potent and selective naphthoquinone-based inhibitors of HUMAN(NAT1) and MOUSE(NAT2) developed in this study provide a unique toolkit with which to further study the endogenous roles of these enzymes, particularly in light of the improved physicochemical profile of carboxylic acid **350** and the unique and sensitive fluorescent properties of fluorene **326**.

Chapter 6: Concluding Remarks and Future Directions

6.1. Concluding Remarks

This study was based on the observation that naphthoquinone **32** underwent an unprecedented colour change from red to blue specifically in the presence of the protein HUMAN(NAT1), a putative breast cancer biomarker, and its murine homologue MOUSE(NAT2). Previous investigations had provided evidence that the mechanism of colour change was due to selective recognition of the conjugate base of **32**, [**32**]$^-$, by the active site of HUMAN(NAT1)/MOUSE(NAT2) and its concomitant sequestration from solution, mediated by a key ionic interaction between [**32**]$^-$ and the Arg127 residue **(Figure 6.1)**.

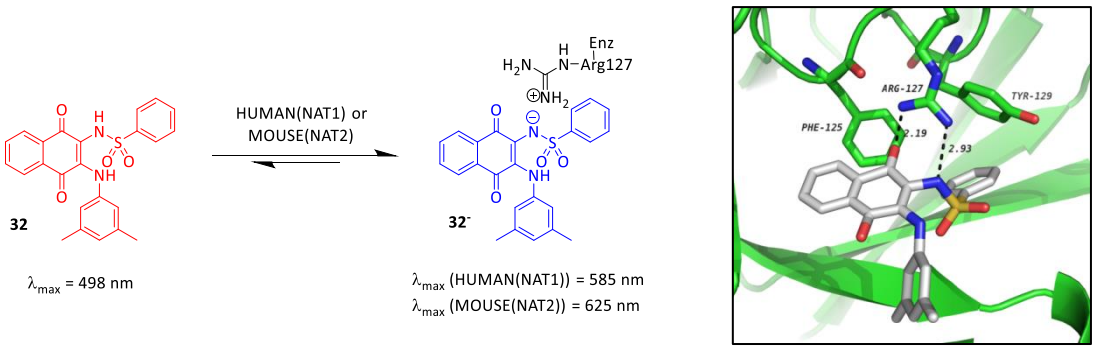


Figure 6.1: Compound **32** undergoes a distinctive colour change from red to blue selectively in the presence of HUMAN(NAT1) and its murine homologue MOUSE(NAT2), believed to be driven by an ionic interaction between the sulfonamide anion of the conjugate base of **32**, [**32**]$^-$, and the Arg127 residue of the enzyme.

Given the reported overexpression of HUMAN(NAT1) in ER+ breast cancers (amongst others), and the dependence of its expression level on tumour grade, the central aim of this thesis was to develop a probe based on **32** which might be capable of detecting and quantifying HUMAN(NAT1) in tumour cell extracts; such a probe could be used in improved diagnosis and prognosis of NAT1+ cancers. Additionally, development of probes based on **32** with an improved physicochemical profile was undertaken, in order to generate compounds which could be used in studies to elucidate the potential endogenous roles of HUMAN(NAT1) in tumorigenesis and folate metabolism.

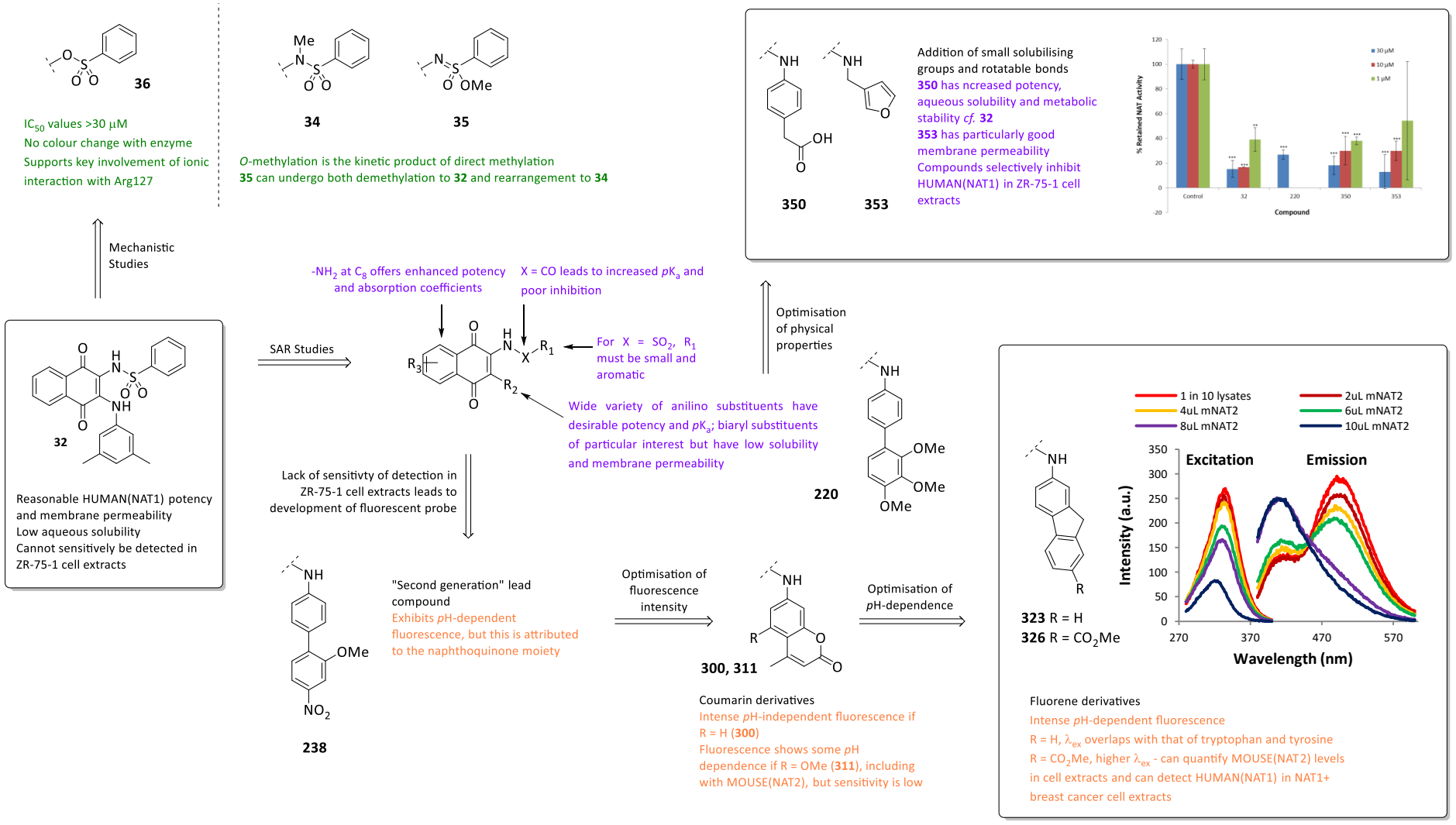


Figure 6.2: Summary of the key developments made in this thesis from the initial hit compound **32** to fluorescent fluorene probe **326** and derivatives **350** and **353** with improved physical properties which enable future inhibition studies to be carried out in HUMAN(NAT1)+ tumour cell lines. a.u. = arbitrary units; mNAT2 = MOUSE(NAT2).

Initially, further evidence was obtained in support of the proposed mechanism of colour change of **32** in the presence of HUMAN(NAT1) and MOUSE(NAT2) (green text in **Figure 6.2**). DFT modelling of **32** in free space showed that the bound conformation of **32** to HUMAN(NAT1) as predicted by an *in silico* model was an energetically reasonable conformer, as the bond angles about the four key rotatable bonds in **32** were all predicted to lie at either global or local energy minima. The successful synthesis of sulfonate ester **36** suggested that the ability of the sulfonamide functionality to ionise was crucial both for high binding potency and for observation of a colour change, which is consistent with data previously obtained on *N*- and *O*-methylated derivatives of the hit compound, **34** and **35**. A detailed mechanistic study on the unprecedented *O*-methylation of sulfonamide **32** revealed that *O*-methylation is the kinetic product of sulfonamide methylation, and *N*-methylation the thermodynamic product; furthermore, *O*-methylated **35** is observed to undergo competing demethylation to **32** and rearrangement to *N*-methylated **34** in solvents which are nucleophilic or contain adventitious water. ^{1}H-NMR studies suggest that demethylation occurs *via* a direct solvent-mediated attack on **35**, whilst rearrangement occurs *via* an initial bimolecular reaction between two molecules of **35** to form an ion pair intermediate.

Sensitivity studies on hit compound **32** demonstrate that in absorption experiments, it cannot be detected above background noise in the presence of cell extracts from the ER+ breast cancer cell line ZR-75-1, which overexpresses HUMAN(NAT1), at the concentrations of HUMAN(NAT1) present in the extracts. Therefore, an SAR study was undertaken around the naphthoquinone core of **32** in order to improve inhibitory potency and sensitivity of the compounds, whilst retaining specificity for HUMAN(NAT1) over its isoenzyme HUMAN(NAT2) (lilac text in **Figure 6.2**). At the C_3 position, a wide variety of aromatic substituents were tolerated, although aryl- and aryloxy-substituents possessed pK_a values which were below the assay buffer of *p*H 8, which precludes their use as aromatic probes. Anilino substituents did however possess more favourable potencies and pK_a values, with *para*-biaryl amine moieties displaying up to forty-fold improved IC_{50} values against HUMAN(NAT1) and up to two-fold higher absorption coefficients *cf.* **32**. The *in silico* model suggests that large C_3 appendages are

tolerated since they extend out of the enzyme active site into bulk solvent. At C_2 a very steep SAR was observed, with only small, aromatic substituents such as phenyl, fluorophenyl and furanyl sulfonamide tolerated, and none of the alterations at this position gave the desired increase in potency. Replacement of the sulfonamide functionality with an amide group led to a large increase in inhibitor *p*K_a and a concomitant decrease in potency. Around the C_5-C_8 positions on the naphthoquinone core, 8-amino substituents lead to up to a ten-fold increase in potency and three-fold increase in absorption coefficient *cf.* **32**. However, the promising effects of both 8-amino substitution and a C_3 biaryl amine substiuent are not additive.

A screen of the most promising compounds from this SAR study against cell extracts from the ZR-75-1 cell line encouragingly demonstrated that these species could effectively inhibit HUMAN(NAT1) activity in the extracts at concentrations as low as 1 μM. However, the sensitivity of these colorimetric probes had still not been sufficiently increased in order to be able to detect the probes above background noise at this concentration in the presence of the cell extracts. It was therefore decided to design and synthesise fluorescent analogues of **32**, since fluorescence is known to be a more sensitive optical detection technique at key wavelengths in biological environments (orange text in **Figure 6.2**). The promising potency of biaryl amine derivatives such as **220** was harnessed in the design of a biaryl moiety containing both electron donor and acceptor groups. This led to the synthesis of second generation lead compound **238**, which was observed to undergo an "on-off" *p*H-dependent fluorescent switch, with the excitation peaks at 372 and 408 nm and the emission peak at 424 nm being quenched in base. However, a screen of a wider library of compounds showed that this fluorescence is attributable to the naphthoquinone core itself, rather than the biaryl appendage, and has low sensitivity.

Three strategies were therefore employed to generate more intense fluorescent peaks emanating from the C_3 substituent. Addition of a methylene linker between the C_3-NH and the biaryl led rise to species which possessed an additional peak in each of their excitation and emission spectra corresponding to the biaryl moiety; however, this peak was *p*H-independent,

suggesting that the fluorophore had to be directly conjugated to the C_3 position of the naphthoquinone core in order for deprotonation of the remote sulfonamide-N*H* to have an effect on its fluorescent emission. Therefore, the biaryl group was replaced with a coumarin moiety; compound **300** was found to have intense fluorescence at λ_{ex} = 344 nm and λ_{em} = 440 nm; however, this fluorescence too was insensitive to basification. It was hypothesised that sensitivity to basification might be increased if electron-donating substituents were added to the coumarin; addition of a methoxy substituent yielded compound **311**, which displayed more intense fluorescent peaks that underwent a small extent of quenching upon treatment with MOUSE(NAT2). However, the low sensitivity of **311** to sulfonamide-N*H* deprotonation still precludes its utility as a probe for quantifying the target protein in cellular samples.

Subsequently, the biaryl scaffold was revisited. It was postulated that the lack of an observable fluorescent peak emanating from the biaryl in compounds such as **238** was due to the non-planarity of the biaryl moiety in its preferred solution conformation. However, synthesis of fluorene derivative **323** enabled rigidification of the moiety and concomitantly gave rise to a strong, observable fluorescence at λ_{ex} = 279 nm, λ_{em} = 374 nm (orange text in **Figure 6.2**, inset). However, the excitation wavelength of this species overlaps with that of tryptophan and tyrosine residues in proteins and so precludes detection of MOUSE(NAT2) or HUMAN(NAT1) *in vitro*. The design and synthesis of ester-substituted fluorene **326**, however, circumnavigated this problem as the ester functionality caused an increase in λ_{ex} and λ_{em} to 333 nm and 493 nm respectively. These peaks were found to be *p*H-dependent and were quenched reversibly in base. Moreover, the fluorescence quenching of **326** was observed to be linearly dependent on [MOUSE(NAT2)] when tested against the recombinant enzyme. In *E. coli* cell lysates spiked with increasing concentrations of MOUSE(NAT2), **326** displayed a quenching of fluorescence at 493 nm which was approximately linear with increasing [MOUSE(NAT2)], and additionally showed the appearance of a new emission peak at 410 nm; the ratio of fluorescence at 493 nm/410 nm also shows an approximately linear dependence

on [MOUSE(NAT2)], which demonstrates that the developed probe exemplifies a truly ratiometric "on-off" fluorescent switch in the presence of the target protein.

Excitingly, when **326** was treated with ZR-75-1 cell extracts, a similar quenching of the excitation peak and a shift in wavelength of the excitation peak (from 493 nm to 430 nm) was observed. This study therefore represents, to the best of our knowledge, the first known example of a small molecule, non-covalent optical probe which is capable of quantifying the concentration of a specific target protein, MOUSE(NAT2), in solution, and moreover is capable of detecting the homologous HUMAN(NAT1) protein unambiguously within the ER+ breast cancer cell line ZR-75-1. Not only is this a novel paradigm in specific protein detection, but also offers hope for a new, rapid and reliable test for earlier diagnosis and improved prognosis of ER+ tumours from patient biopsy samples.

Analogues of hit compound **32** with improved physical properties were also synthesised in order to study the endogenous roles of HUMAN(NAT1), with a particular emphasis on the role that HUMAN(NAT1) might play in the development of tumours. Interestingly, many of the synthesised derivatives in this library, based on a phenylenediamine C_3 moiety, were found to be unstable, and evidence was obtained that these compounds undergo an intramolecular single electron transfer from the phenylenediamine to the naphthoquinone core; oxidation of the phenylenediamine is likely what ultimately leads to the observed decomposition. Synthesised analogues of **32** based on amino acid building blocks, specifically phenylalanine and alanine derivatives, were found to display disappointingly poor aqueous solubility and cell membrane permeability; these effects were attributed to the amphiphilicity of such species. Addition of much smaller and simpler solubilising groups to the C_3 moiety however proved more fruitful (lilac text in **Figure 6.2**, inset), with furanyl **353** having a particularly high cell membrane permeability whilst retaining comparable levels of aqueous solubility and cell membrane permeability to compound **32**, and carboxylic acid **350** showing a twenty-fold increase in aqueous solubility, a five-fold increase in potency against HUMAN(NAT1) and a ten-fold increase in metabolic stability *cf.* **32**. These compounds also retain selectivity for

HUMAN(NAT1) over the isoenzyme HUMAN(NAT2) and therefore represent examples of optimised analogues which are suitable for progression to subsequent studies in tumour cell lines.

Finally, a combination of biochemical assays and computational modelling studies suggest that HUMAN(NAT1) and MOUSE(NAT2) are far from simply xenobiotic metabolising enzymes and the they likely play a role in AcCoA/CoA homeostasis in cells, perhaps regulated by the cofactor folic acid **457**. Given the reported links between *HUMAN(NAT1)* overexpression and both cancer and developmental defects, these studies, in combination with the synthesis of optimised probes for studying the target enzymes at a cellular level, give a foundation for the exploration of HUMAN(NAT1) as a possible novel therapeutic target in disease.

6.2. Future Directions

The observations reported in this study raise several further interesting questions for future studies. Broadly speaking, future work is proposed in three main areas: further characterisation of the biological and optical properties of fluorene **326**; analysis of specific HUMAN(NAT1) inhibitors with optimised physical properties in tumour cell lines; and efforts to extend the novel paradigm in protein detection developed in this thesis to other biological targets.

6.2.1. Further Characterisation and Development of Fluorescent Fluorene Probe 326

In **Chapter 4** the development and evaluation of fluorene probe **326** was discussed extensively, and it was shown that in the presence of cell extracts from the ER+ breast cancer cell line ZR-75-1, which overexpresses HUMAN(NAT1), the excitation peak of **326** at 333 nm was quenched and the emission peak of **326** at 493 nm was shifted to a lower wavelength of 430 nm, behaviour which mirrors the observations made on compound **326** in the presence of *E. coli* cell extracts spiked with increasing concentrations of MOUSE(NAT2).

However, in order to ensure that the observations reported are a NAT-dependent effect, a control ZR-75-1 cell line in which HUMAN(NAT1) is removed either *via* shRNA knockdown or immunoprecipitation should be carried out; it would be anticipated that, as with the *E. coli* cell extracts alone, the fluorescence properties of **326** remain unchanged in these NAT-negative ZR-75-1 cell extracts *cf.* its properties in a Tris•HCl buffer solution at *p*H 8. If, as anticipated, the effect on fluorescence properties prove to be NAT-mediated, fluorescence scans of compound **326** in the presence of ZR-75-1 cell extracts should be carried out at varying concentrations of both probe **326** and cell extract, in order to determine: (a) whether the observed changes in the fluorescence of **326** are linearly dependent on the concentration of **326** and the total protein concentration – and by extension, the HUMAN(NAT1) concentration – applied; (b) what the limit of detection of HUMAN(NAT1) using fluorescent probe **326** is; and (c) how accurately [HUMAN(NAT1)] in ZR-75-1 cell extracts can be quantitated.

Subsequent to this, it would also be instructive to grow other cell lines reported to overexpress HUMAN(NAT1) and to use compound **326** to determine the concentration of HUMAN(NAT1) present in each of these cell lines. One particularly interesting experiment would be to compare the concentration of HUMAN(NAT1) measured in each of the cell lines with the specific activity of HUMAN(NAT1), since the two are not necessarily related, and this might highlight some notable differences between the different types of NAT1-overexpressing cell lines. Additionally, values for the concentration of HUMAN(NAT1) present in cell extracts calculated using the newly-developed fluorescence method ought to be compared with estimates obtained *via* antibody staining, to determine how much more sensitive a fluorescence measurement is compared to the current "gold-standard" staining methods.

One other important study which could be carried out is to investigate the behaviour of compound **326** in growing NAT1 +ve cell lines. **326** is highly hydrophobic and is predicted to have poor aqueous solubility; however, it might be possible to encourage transport of **326** across cell membranes by the use of an additive such as cyclodextrin.[359] Within both NAT1 +ve

and NAT1 -ve cell populations, it would be fascinating to observe and compare the behaviour of compound **326** using fluorescence microscopy, as this might provide new insights into the molecular mechanism of fluorescence and generate new opportunities for developing a sensitive method for HUMAN(NAT1) quantification in whole cells.

6.2.2. Elucidation of the Role of HUMAN(NAT1) in NAT1 +ve Tumour Cell Lines

Another future study which should be undertaken on the basis of the conclusions of this thesis is using some of the optimised HUMAN(NAT1) inhibitors to investigate the consequences of NAT inhibition in growing tumour cell lines. Samples of carboxylic acid **350** and furanyl **353**, possessing improved physicochemical profiles over that of hit compound **32**, whilst retaining high potency for HUMAN(NAT1) and selectivity over HUMAN(NAT2), will be made available to our colleagues Minchin and Butcher (University of Queensland, Brisbane, Australia) in order for studies to test the effects of these compounds on cell proliferation and invasiveness in the ZR-75-1 ER+ breast cancer cell line and the MDA-MB-231 triple-negative breast cancer cell line. Such studies could potentially add weight to the growing evidence in the field that HUMAN(NAT1) might be a viable therapeutic target against various cancer subtypes.

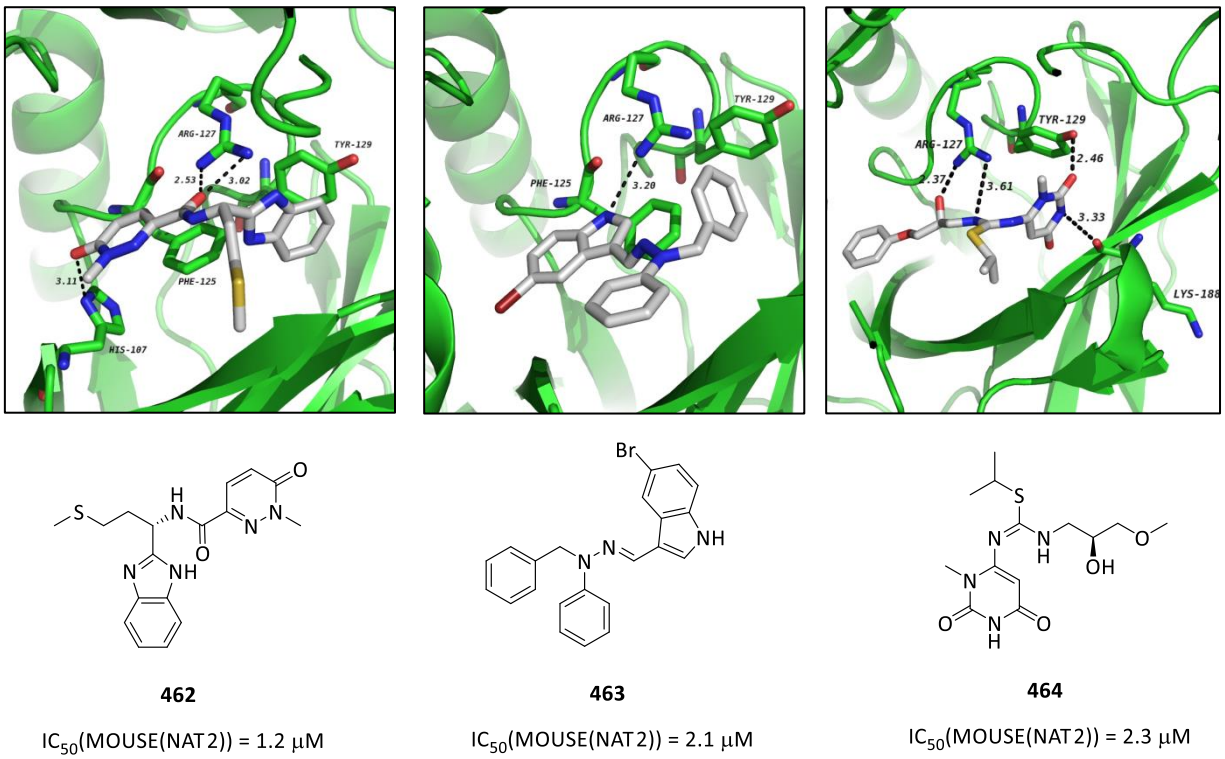
In parallel to these studies, it is imperative that the activity of compounds **350** and **353** is tested against NAD(P)H:quinone oxidoreductase 1 (NQO1); not only might this enzyme be able to reduce the naphthoquinone-based probes, leading to their instability in cellular environments containing high NQO1 levels, but **350** and **353** might possibly act as inhibitors of NQO1. Inhibition of NQO1 has been determined by other studies to result in cytotoxicity in tumour cell lines;[360] therefore, the interactions between naphthoquinones **350** and **353** and this enzyme must be fully characterised before any effects of **350** and **353** in NAT1 +ve tumour cell lines can be attributed to a NAT1-dependent mechanism.

The interactions of some of the potent HUMAN(NAT1) inhibitors developed in this study with two other important enzyme families should also be studied: specifically, data pertaining to their effects on histone acetyltransferases (HATs) would be of great interest. Analogously to NATs, HATs use AcCoA as a cofactor to acetylate conserved lysine residues on histone proteins; histone acetylation is an epigenetic transformation which is associated with transcriptional activation,[361] possibly mediated by the creation of a binding site for specific protein-protein interaction domains such as bromodomains.[362] The mechanism of acetyl transfer by both the Gcn5-related *N*-acetyltransferase (GNAT) and MYST subfamilies of HATs have been reported to occur *via* a direct attack of a histone lysine group on enzyme-bound AcCoA facilitated by general base catalysis,[363] although some conflicting reports have proposed a Ping-Pong bi-bi mechanism for MYST HATs.[364] Nonetheless, the HUMAN(NAT1) inhibitors developed in this study ought to be screened against HATs, as any cross-inhibition is important to note in the interpretation of data from tumour cell assays. Perhaps more fascinatingly, any inhibitor which displays both HUMAN(NAT1) and HAT inhibition might be an invaluable tool in investigating whether there are any links between the NAT and HAT enzyme families in AcCoA/CoA regulation and homeostasis in cellular environments.

Throughout this study, it has been observed that inhibitors based on hit compound **32** mostly have poor physical properties such as low aqueous solubility and low cell membrane permeability. This is possibly due to a combination of the use of the naphthoquinone core and the hydrophobicity of the enzyme active site necessitating multiple aromatic substituents around this core for potent inhibition. The naphthoquinone core was retained throughout this study due to the important optical properties it conferred upon the series of molecules under investigation. However, in future studies which have the aim solely of developing a more "drug-like" HUMAN(NAT1) inhibitor, the naphthoquinone core could be replaced with a core that confers more beneficial physicochemical properties to the molecules.

Recently, a prospective virtual screen of over 5.3 million molecules using Ultrafast Shape Recognition (USR), a computational technique which compares the three-dimensional spatial

arrangement of atoms in different molecules, identified 23 compounds which might be predicted to occupy a similar space in shape to that of compound **32**.[365] Purchase and testing of these 23 compounds in the acetyl CoA hydrolysis assay gave a hit rate of 40%, and three of the compounds, **462**, **463** and **464**, gave particularly potent IC_{50} values against MOUSE(NAT2).[365] *In silico* modelling of these three structures in the active site of HUMAN(NAT1) yield some interesting results **(Figure 6.3)**.



462

IC_{50}(MOUSE(NAT2)) = 1.2 μM

463

IC_{50}(MOUSE(NAT2)) = 2.1 μM

464

IC_{50}(MOUSE(NAT2)) = 2.3 μM

Figure 6.3: *In silico* modelling of compounds **462 (left)**, **463 (centre)** and **464 (right)** within the active site of HUMAN(NAT1) (pdb: 2PQT).[247b] The protein is shown in both cartoon representation and **a**nalysis was performed using GOLD® software (v.5.2).[282] Predicted polar contacts are highlighted by black dashed lines with inter-atomic distances given in Ångströms; key active site residues His107, Phe125, Arg127, Tyr129 and Lys188 are highlighted in stick representation (carbon atoms in green).

Of all three compounds, it can be observed that compound **463** is predicted to give the fewest polar contacts within the enzyme active site. Furthermore, the docked conformer of **463** gives a dihedral angle of *c.* 30° about the indole-hydrazone C-C bond, which is not anticipated to be a low energy-conformer about this bond. Compound **463** might also be expected to possess

low aqueous solubility as it contains several hydrophobic aromatic rings; the hydrazone functionality within the molecule is also liable to hydrolysis within a cellular environment. For all of these reasons, **463** is not anticipated to be a good candidate HUMAN(NAT1) inhibitor for further development.

Compounds **462** and **464**, however, appear more promising. *In silico* modelling of both compounds predicts similar interactions to those identified as key in the binding of naphthoquinone-based HUMAN(NAT1) inhibitors, such as hydrogen-bonded interactions with Arg127, π-π stacking with Phe125 and edge-face π-π interactions with Tyr129. Both species contain heterocyclic rings which are predicted to be more polar, and hence possibly more soluble, than those in the developed family of naphthoquinone inhibitors. The ability of more polar functionalities to be tolerated is perhaps unsurprising, given the polarity of the HUMAN(NAT1) substrates *p*ABA and *p*ABAglu, as well as that of folate, which is believed capable of binding to the active site of HUMAN(NAT1). The amino-uracil and β-amino alcohol functionalities within compound **464** are particularly notable as potential isosteres for the pterdine and amide functionalities in folate **457** respectively, and it is striking that the *in silico* models for compounds **464** and folate **454** predict very similar spatial alignments of these respective groups (*cf.* **Figure 5.9** for predicted binding orientation of folate in the HUMAN(NAT1) active site).

If the docking model is accurate, then there is also likely to be great scope for further improvements in the molecular solubility since **462** and **464** contain thioether and *S*-alkylthiourea moieties respectively which are predicted to project out of the active site; the present study has determined that polar groups which can form ion-dipole or hydrogen bonds to bulk solvent are well tolerated in this spatial position. Furthermore, both compounds contain high numbers of rotatable bonds and a stereogenic centre; in each case, one enantiomer was reported for the modelling studies, but the optical purity of neither compound is confirmed in the study in which they were tested against MOUSE(NAT2).

Therefore, in a future study it would be instructive to synthesise authentic samples of compounds **462** and **464**, and their corresponding enantiomers, and to test these compounds for MOUSE(NAT2) activity. The kinetics of binding to HUMAN(NAT1) and MOUSE(NAT2) should also be thoroughly investigated for both of these compounds, since both contain a moiety which might be susceptible to nucleophilic attack by the catalytic Cys68 residue (the α,β-unsaturated ketone in **462** and the *S*-alkylthiourea in **464**) leading to potential covalent inhibition of the enzymes. This is of particular note for compound **462**, since the predicted orientation of binding places the Michael-type acceptor functionality adjacent to the catalytic triad in space. The physicochemical properties of these compounds – specifically their kinetic solubility in aqueous media, cell membrane permeability, levels of binding to plasma proteins and microsomal stability – should also be measured and compared to the values obtained for the naphthoquinone family of inhibitors developed in this study. A combination of this pharmacological and physicochemical data might give rise to a new lead in the quest for a potent and selective inhibitor of HUMAN(NAT1) for use in cellular studies.

6.2.3. Extension of the Novel Sensing Paradigm to other Targets: Detection of Lysine Acetylation Status

The mechanism by which fluorene **326** is able to sensitivity quantify levels of recombinant MOUSE(NAT2) in buffer solution or *E. coli* cell extracts, and furthermore detect the presence of native HUMAN(NAT1) in cell extracts from the ER+ breast cancer cell line ZR-75-1, represents an entirely novel paradigm in the field of specific protein detection. Therefore, one key question that arises from this study pertains to the applicability of this technique outside of the NAT field: can small molecules be developed against other protein targets of interest which also show a reversible, [target]-dependent “switch” in their fluorescent wavelength and intensity?

Given both the potential role of HUMAN(NAT1) in folate metabolism and AcCoA homeostasis, and the central importance of epigenetics in oncology, one particularly inviting avenue for

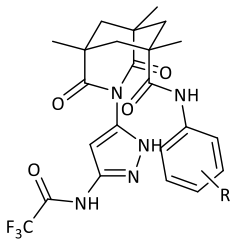
future research is the development of a reversible probe which can distinguish lysine acetylation status of a specific protein within a cell environment. Whether a specific protein is acetylated on a certain lysine residue might in many cases be indicative of a particular cell environment, or type, in which the protein is present.[366] Development of a fluorescent probe which is able to distinguish between Lys and Ac-Lys variants of such a protein could therefore be a valuable tool both in determination of biochemical functions and localisation of the target protein, and also potentially in disease diagnosis, prognosis and stratification.

Before attempting to develop such probes to target a specific protein, it would be useful to determine such an approach is experimentally viable using a dipeptide model system. In 2006, Schrader's lab reported a novel conformationally rigid scaffold based on Kemp's triacid which was capable of recognising and non-covalently binding to *N*-acetyl dipeptide methyl ester entities in solution; moreover, variation of the aryl substituent on the probe led to selective affinity of the probe for dipeptides containing a particular class of amino acid residue at the *N*-terminal end **(Figure 6.4A)**.[367] A binding model was computationally generated which predicts that the backbone of the dipeptide binds to the cleft between the aryl and pyrazole moieties of the host probe, driven by the formation of hydrogen bonds; this places the side chain of the *N*-terminal amino acid residue close in space to the aryl substituent of the probe.[367]

Given the selectivity of Schrader's probe containing a benzoic acid substituent for recognising and binding to basic amino acids such as ornithine, it was hypothesised that replacement of the carboxylate group on the probe with an aldehyde functionality to give probe **471** might lead to a similar recognition of an ornithine-containing dipeptide, but that subsequently, a proximity-induced imine formation might occur between the primary amine group of the ornithine and the aldehyde functionality of **471 (Figure 6.4B)**. Furthermore, if a fluorophore was also appended to the aromatic moiety on the probe, it was speculated that imine formation might lead to a measurable change in its fluorescence. Such a shift in fluorescence should enable a quick and reliable method by which to differentiate between dipeptides

containing ornithine and those containing acetylated ornithine, since the latter would be anticipated to be incapable of imine formation with the probe. This would be a useful model system with which to work; however, ultimately it is lysine acetylation that is of relevance in human disease. Analogously, therefore, it was postulated that addition of an extra methylene linker to give probe **472** and its fluorophore-conjugated analogues might lead to formation of appropriate binding partners for lysine residues **(Figure 6.4C)**.

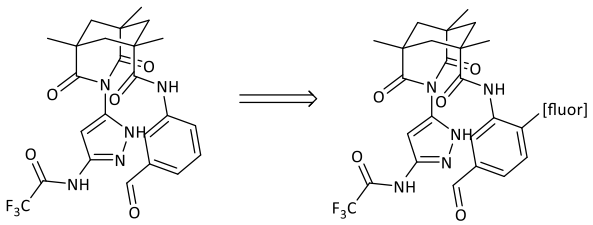
A



465-470

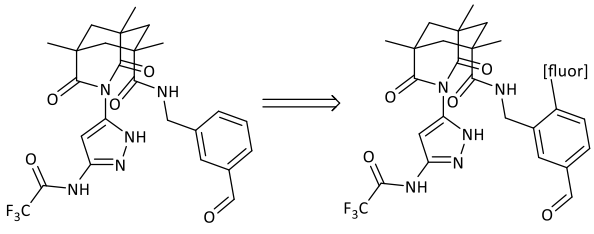
Compound	R	Class of amino acid side chain specifically recognised	Example dipeptide binding partner
465	*m*-C_2H_5	Reference compound: poor selectivity	N/A
466	*m*-$COCH_3$	Hydrogen bonding donor	Ac-Ser-Ala-OMe
467	*m*-NO_2	Aromatic	Ac-Phe-Ala-OMe
468	*m*-CO_2^-	Cationic	Ac-Orn-Ala-OMe
469	*m*-CH_2Ph	Alkyl	Ac-Val-Ala-Ac
470	*p*-$CH_2NH_3^+$	Acidic	Ac-Glu-Ala-OMe

B



471

C



472

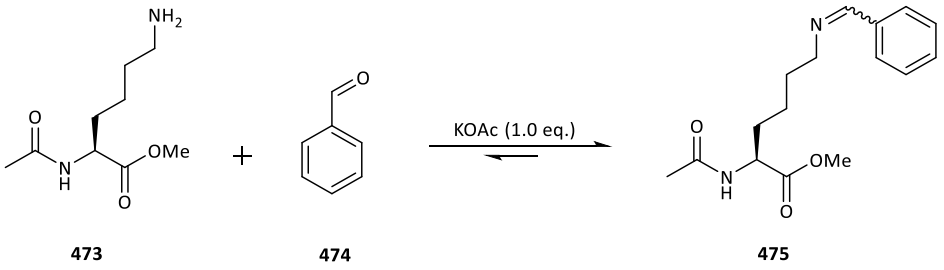
Figure 6.4: A: Schrader's family of probes for selective binding to N_α-acetyl-dipeptide methyl esters; the variation of R enables the selective recognition of dipeptides containing different classes of amino acid at the *N*-terminal end of the dipeptide. **B:** Proposed target probe **471** which might undergo reversible proximity-induced imine formation in the presence of ornithine-containing dipeptides, but not acetyl-ornithine-containing dipeptides, and variants thereof which might enable fluorescent quantification of the imine formation. **C:** Proposed target probe **472** derived by insertion of a methylene linker compared to **471**, and fluorescent derivatives thereof, which are predicted to be optimal binding partners for lysine-containing dipeptides. N/A = not applicable.

In order to determine whether the proposed type of proximity-induced imine formation might be capable of occurring, a preliminary study was carried out in which N_α-acetyl-L-lysine methyl ester hydrochloride **473** was added to either 1.0 eq. benzaldehyde **474** or 1.0 eq. *para*-

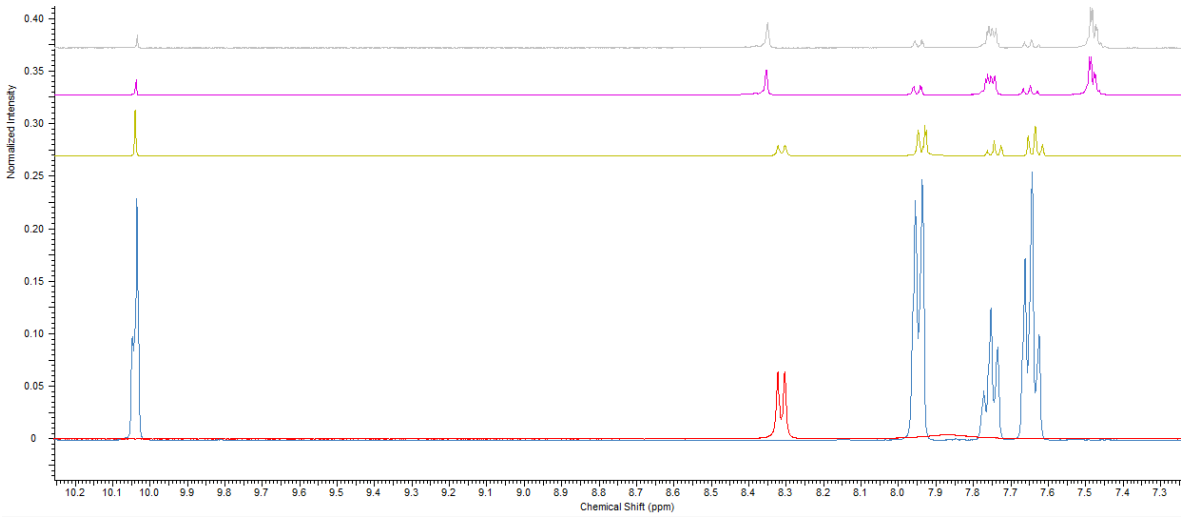
dimethylaminobenzaldehyde (DMAB) **476** in DMSO-d_6 and the reaction followed by ^1H-NMR spectroscopy (**Figures 6.5A and 6.5B** respectively).

No reaction is observed in either case prior to the addition of 1.0 eq. KOAc, which ensures that the solution is buffered to the correct *p*H (*c.* 4-5) for imine formation to occur. In the case of benzaldehyde, once KOAc is added it can be observed that imine formation occurs rapidly, within 0.5 h. Reaction of the more electron-rich aldehyde, DMAB, is however observed to be slow at RT; however, over time the presence of peaks corresponding to the imine product can be seen, and is accelerated upon heating the reaction, firstly to 40 ^{o}C, and subsequently to 60 ^{o}C. These experiments therefore suggest that N_{α}-acetyl-L-lysine methyl ester is capable of forming an imine even with electron-rich aldehydes in the absence of any induction by proximity; therefore, this suggests that imine formation between the proposed probe-peptide pairing is viable.

A



473 **474** **475**



B

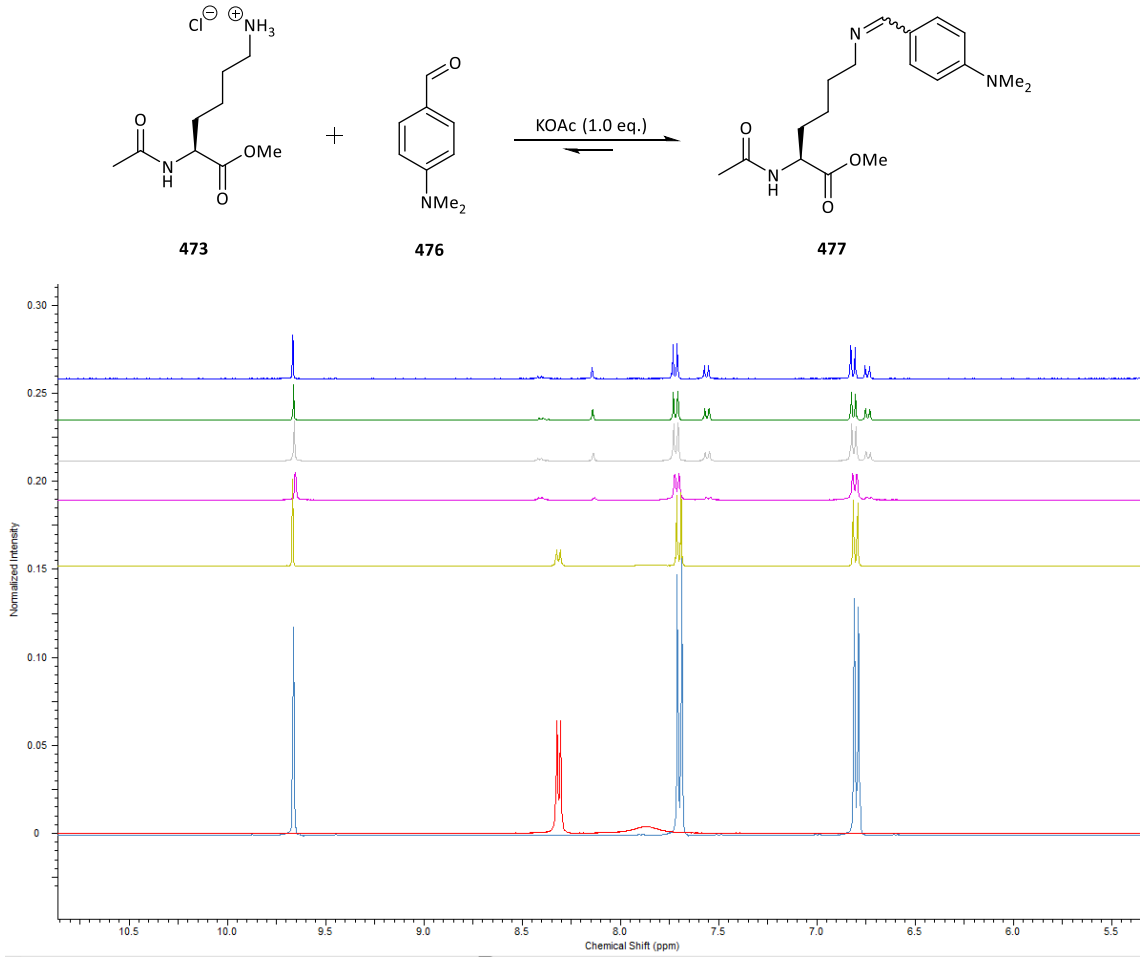
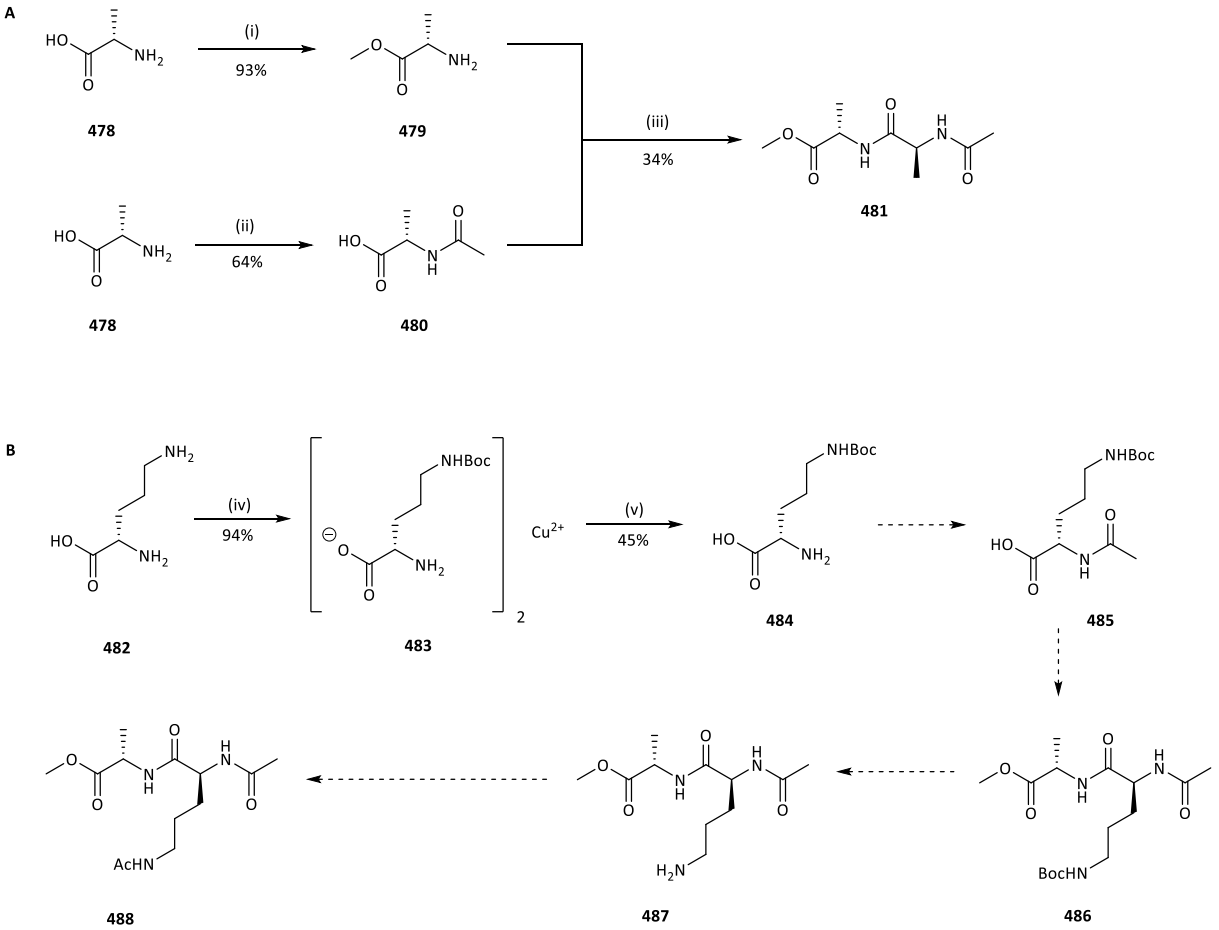
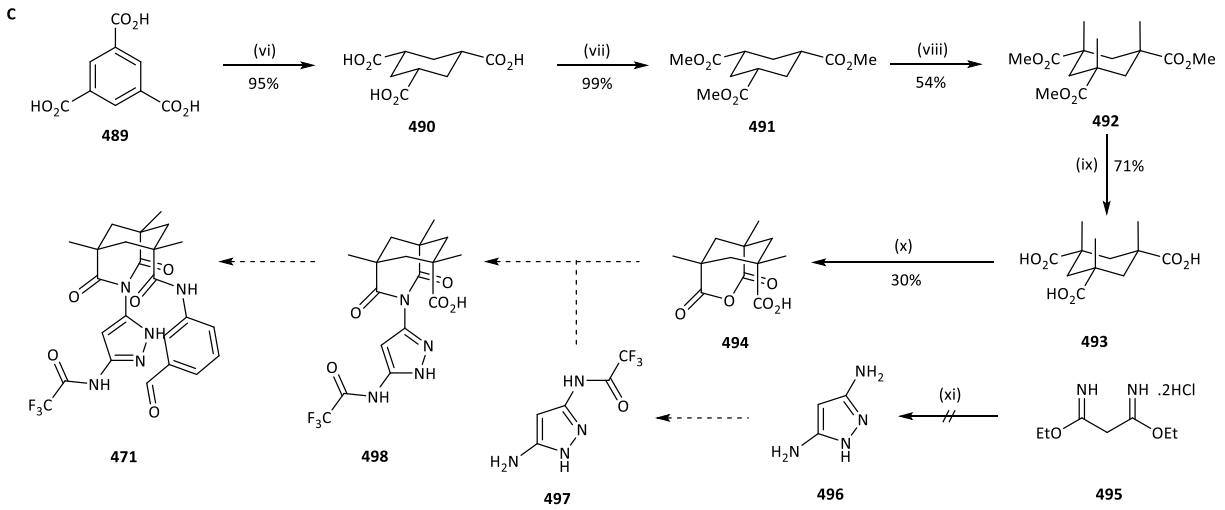


Figure 6.5: A: ^{1}H-NMR spectra to show the progression of the reaction between N_{α}-acetyl-L-lysine methyl ester hydrochloride **473** (red spectrum) and benzaldehyde **474** (blue spectrum) after 0.5 h (gold line), after 1.5 h (pink line) and after 5 h (grey line); 1.0 eq. KOAc was added to the reaction after 1 h. **B:** ^{1}H-NMR spectra to show the progression of the reaction between N_{α}-acetyl-L-lysine methyl ester hydrochloride **473** (red spectrum) and *para*-dimehtylaminobenzaldehyde **476** (blue spectrum) after 0.5 h (gold line), after 1.5 h (pink line), after 5 h (grey line), after 27 h (green line) and after 47 h (blue line); 1.0 eq. KOAc was added to the reaction after 1 h, the reaction was heated to 40 ^{o}C after 26 h and the reaction was further heated to 60 ^{o}C after 27 h.

It was therefore decided to synthesise the target aldehyde probe **471** and its anticipated binding partner Ac-Orn-Ala-OMe **487**; the N_{δ}-acetylated derivative Ac-Orn(Ac)-Ala-OMe **488** and the dialanine dipeptide Ac-Ala-Ala-OMe **481** were also desired as control peptides. The designed synthetic routes to these targets are outlined in **Scheme 6.1**.

Independent esterification and *N*-acylation of alanine **478** were effected in excellent yield (conditions (i) and (ii) respectively), and the Ac-Ala-Ala-OMe **481** dipeptide product of coupling utilising T3P as the coupling reagent could be isolated in 30% yield (conditions (iii)). In an attempt to make the desired ornithine-containing peptides **487** and **488**, the side chain nitrogen was first selectively Boc-protected utilising complexation of the C_α-CO_2H and C_α-NH_2 groups by Cu^{2+} ions, followed by decomplexation of Cu^{2+} in the presence of 8-quinolinol (conditions (iv) and (v)). Time constraints prevented an attempt at the subsequent *N*-acylation and coupling reaction with alanine methyl ester **479**, but in the future the coupling step should be attempted using either T3P or the conditions optimised in **Section 5.1.4.1.** utilising HATU as the coupling agent. Subsequent *tert*-butyl carbmate deprotection should afford Ac-Orn-Ala-OMe **487**, which could then be acetylated to give Ac-Orn(Ac)-Ala-OMe **488**.





Scheme 6.1: A: Synthesis of control dipeptide Ac-Ala-Ala-OMe **481**. **B:** Attempted synthesis of test peptides Ac-Orn-Ala-OMe **487** and Ac-Orn(Ac)-Ala-OMe **488**. **C:** Attempted synthesis of target aldehyde probe **471**. *Reagents and conditions:* (i) $SOCl_2$ (1.34 eq.), MeOH, RT, 0.5 h *then* reflux, 3 h *then* RT, 16 h; (ii) Ac_2O (1.2 eq.), AcOH, RT, 16 h; (iii) T3P (50% wt. in EtOAc, 4.3 eq.), *N*-methyl morpholine (6.2 eq.), CH_2Cl_2, 0 ^oC, 3 h *then* RT, 4 days; (iv) $Cu_2SO_4•5H_2O$ (0.5 eq.), Boc_2O (1.3 eq.), $NaHCO_3$ (1.0 eq.), 2 M aq. $NaHCO_3$:H_2O:acetone (11 parts:11 parts:15 parts), RT, 24 h *then* MeOH (3 parts), RT, 12 h; (v) 8-quinolinol (2.6 eq.), H_2O, RT, 5 h; (vi) H_2 (1 atm.), 5% Rh/Al (0.2 eq.), H_2O, 70 ^oC, 72 h; (vii) $SOCl_2$ (4.5 eq.), MeOH, 70 ^oC, sealed tube, 5 h; (viii) ^{n}BuLi (2.5 M in hexanes, 3.3 eq.), $^i Pr_2NH$ (3.3 eq.), Et_2O, 0 ^oC, 0.5 h *then* tricarboxylic ester **491** (1.0 eq.), 0 ^oC, 2 h *then* dimethylsulfate (5.0 eq.), RT, 16 h; (ix) 1 M aq. NaOH: MeOH (6:5), 65 ^oC, 12 h *then* HCl, RT; (x) 190 ^oC under vacuum, 5 h; (xi) sat. aq. K_2CO_3, 0 ^oC, 5 min *then* $N_2H_4•H_2O$ (1.03 eq.), reflux, 15 min *then* 5 ^oC, 18 h.

The preparation of Kemp's triacid **493** as a key intermediate in the synthesis of probe **471** was undertaken following a literature procedure in 4 linear steps from mesitic acid **489** (conditions (vi)-(ix)). Catalytic hydrogenation of **489** afforded the *cis*,*cis* species **490** as the major product in excellent yield, which subsequently underwent tri-esterification and tri-methylation following treatment with LDA, made *in situ* from di-*iso*-propylamine and ^{n}BuLi, and dimethylsulfate to give intermediate **492** in 54% yield. A facile basic ester hydrolysis led to the successful formation of Kemp's triacid **493**. This was subsequently converted to anhydride **494** by heating under vacuum (conditions (x)); however, the followed literature procedure gave no indication of the desirable reaction time or temperature, and it was discovered that if heated under vacuum at 190 ^oC, the yield of **494** is depleted over time by sublimation, which is responsible for the low mass return of this step. It was intended to react anhydride **494** with

2,5-diamino-pyrazole derivative **497** in order to furnish intermediate **498**, which is the precursor to the desired target **471**. However, in the time available, synthesis of **497** proved intractable, since the reported literature conditions for assembly of 2,5-diaminopyrazole **496** failed (conditions (xi)). In a future effort to synthesise target probe **471**, the conditions for formation of diamino pyrazole **496** should be optimised, possibly by increasing the number of equivalents of hydrazine employed or by altering the reaction temperature.

If in a future study intermediate **498** is successfully synthesised, this could give access to a wide variety of target probes *via* amide coupling reactions. Subsequently, the behaviour of these probes in the presence of dipeptides Ac-Orn-Ala-OMe **487**, Ac-Orn(Ac)-Ala-OMe **488** and Ac-Ala-Ala-OMe **481** could be investigated by ^{1}H-NMR spectroscopy and, for any fluorescent probes developed, by fluorescence spectroscopy. Synthesis of the lysine-derived peptides Ac-Lys-Ala-OMe and Ac-Lys(Ac)-Ala-OMe would also enable the specificity of probes such as **487** for binding to ornithine-containing dipeptides over lysine-containing dipeptides to be determined; in turn it is anticipated that this could lead to the generation of probes which conversely are selective for the lysine-containing dipeptides. Probes that specifically bind to lysine-containing dipeptides would then constitute a useful model system for studying interactions with lysine residues present in proteins that are the ultimate targets of this study.

Chapter 7: Experimental

7.1. General Experimental

Chemicals were purchased from Sigma-Aldrich UK, TCI UK, Apollo Scientific UK, Alfa Aesar UK, Fluorochem UK or Fisher Scientific UK unless otherwise stated. Where appropriate and if not stated otherwise, all reactions involving moisture-sensitive reagents were carried out under a nitrogen or argon atmosphere using anhydrous solvents, standard vacuum line techniques and glassware that was flame-dried before use. Anhydrous DMF, anhydrous MeOH and anhydrous dioxane were purchased from Sigma-Aldrich UK in SureSeal^{TM} bottles and used without further purification; other anhydrous solvents were dried following the procedure outlined by Grubbs and co-workers.[368] Water was purified by an Elix® UV-10 system. All other solvents and reagents were used as supplied (analytical or HPLC grade) without prior purification.

Organic layers were dried over anhydrous $MgSO_4$. Brine refers to a saturated aqueous solution of sodium chloride. *In vacuo* refers to the use of a rotary evaporator attached to a diaphragm pump. Pet ether refers to the fraction of petroleum spirit boiling between 30 and 40 ^{o}C, unless otherwise stated.

Thin layer chromatography was performed on Merck silica gel 60 F_{254} aluminium-supported thin layer chromatography sheets. Plates were visualised either under UV light (254 nm and 370 nm) or thermal development after dipping in 1% aq. $KMnO_4$ or ninhydrin.

Flash column chromatography was performed on Kieselgel 60 silica in a glass column.

Melting points were recorded on a Gallenkamp Hot Stage apparatus. Where relevant, the recrystallisation solvent is reported in parentheses.

Optical rotations were recorded on a Perkin-Elmer 241 polarimeter with a water-jacketed 10 cm cell at either 20 or 25 ^{o}C, as stated. Specific rotations are reported in 10^{-1} deg cm^{2} g^{-1} and concentrations in g/100 mL.

Infrared spectra were recorded on a Bruker Tensor 27 FT-IR spectrometer as thin film samples. Selected characteristic peaks above 1500 cm^{-1} are reported in wavenumbers (cm^{-1}).

NMR spectra were recorded on Bruker Avance spectrometers (DPX200, DPX400, AV II 400, AV II 500 or AV 700) in the deuterated solvent stated. The field was locked by external referencing to the relevant deuteron resonance. Chemical shifts (δ) are reported in parts per million (ppm). The multiplicity of each signal is indicated by: s (singlet); br. s (broad singlet); d (doublet); t (triplet); q (quartet); quin (quintet); sep (septet); dd (doublet of doublets); td (triplet of doublets); qd (quartet of doublets); quind (quintet of doublets); dt (doublet of triplets); tt (triplet of triplets); qt (quartet of triplets); dq (doublet of quartets); dquin (doublet of quintets); ddd (doublet of doublets of doublets); tdd (triplet of doublets of doublets); or m (multiplet). The number of protons or fluorines (n) for a given resonance signal is indicated by nH or nF respectively. In acyclic ring systems, axial and equatorial protons are represented by the abbreviations ax and equ respectively. Coupling constants (*J*) are quoted in Hz and are reported to the nearest 0.1 Hz. The coupling constants are determined by analysis using ACD Labs software.

Low-resolution mass spectra were recorded on either a VG MassLab 20-250 or a Micromass Platform 1 spectrometer, operating in positive or negative mode, from solutions of MeOH. Accurate mass measurements were run on either a Bruker MicroTOF internally calibrated with polyalanine, or a Micromass GCT instrument fitted with a Scientific Glass Instruments BPX5 column (15 m $\times$ 0.25 mm) using amyl acetate as a lock mass, by the mass spectrometry department of the Chemistry Research Laboratory, University of Oxford, UK. *m/z* values are reported in Daltons and followed by their percentage abundance in parentheses.

Reverse-phase high-performance liquid chromatography (RP-HPLC) was performed using a 1525 pump, 2707 autosampler and 2849 detector, all from Waters. Separations were performed on a Phenomonex Luma C18 (analytical) column (5 µm particle size, 250.0 mm x 4.6 mm). Experiments were performed under gradient elution (eluent H_2O containing 0.1% (*v/v*) TFA:MeCN 95:5 to 5:95 over 20 min then isocratic for 15 min). Sample injections consisted of 40 µL of 2 mg/mL sample solution in MeCN. The flow rate was 1.0 mL/min and detection was at a wavelength of 215 nm. For each compound, retention times (t_R) are quoted to the nearest minute and are followed by the % purity.

7.2. General Synthetic Procedures

General Procedure 1: Substitution of 2,3-dichloronaphthalene-1,4-dione or 2,3-dichloro-5-nitronaphthalene-1,4-dione with sulfonamides

2,3-Dichloronaphthalene-1,4-dione or 2,3-dichloro-5-nitronaphthalene-1,4-dione (1.0 eq.), the requisite sulfonamide (1.0 eq.) and Cs_2CO_3 (1.4 eq.) were stirred in DMF in a sealed microwave vial at RT for 5 h (unless otherwise stated). 1 M aq. HCl (50 mL) was added and the product extracted with EtOAc (3 x 50 mL). The organic layers were collected, washed with brine (3 x 50 mL), dried, filtered and concentrated *in vacuo* to give the crude product.

General Procedure 2: Substitution of *N*-(3-chloro-[x-nitro-]1,4-dioxo-1,4-dihydronaphthalen-2-yl)sulfonamides or amides with anilines (x = 5 or 8)

The sulfonamide or amide (1.0 eq.) was stirred with cerium trichloride heptahydrate (1.0 eq.) in MeOH or toluene, as stated, at RT for 1.5 h in a sealed microwave vial. The requisite aniline (2.0 eq. or 3.0 eq., as stated) was added and the reaction mixture heated to 90 ^{o}C or 110 ^{o}C for 16 h (as stated). The solution was cooled to RT, sat. aq. NH_4Cl (20 mL) was added and the product was extracted with EtOAc (3 x 20 mL). The organic layers were collected, washed with brine (3 x 20 mL), dried, filtered and concentrated *in vacuo* to give the crude product.

General Procedure 3: Disubstitution of 2,3-dichloronaphthalene-1,4-dione with phenols

2,3-Dichloronaphthalene-1,4-dione (1.0 eq.), the requisite phenol (2.2 eq.) and Cs_2CO_3 (2.2 eq.) were refluxed in THF for 16 h. The solution was cooled to RT and partitioned between EtOAc (50 mL) and 0.1 M aq. NaOH (30 mL). The organic layer was washed with sat. aq. NH_4Cl (2 x 20 mL) and brine (3 x 20 mL), before being dried, filtered and concentrated *in vacuo* to give the crude product.

General Procedure 4: Substitution of diphenols with benzenesulfonamide

The requisite diphenol (1.0 eq.), benzenesulfonamide (1.0 eq.) and Cs_2CO_3 (1.2 eq.) were refluxed in THF for 1 h, unless otherwise stated. The solution was cooled to RT and partitioned between EtOAc (50 mL) and 1 M aq. HCl (30 mL). The organic layer was washed with brine (3 x 20 mL), before being dried, filtered and concentrated *in vacuo* to give the crude product.

General Procedure 5: Reduction of aromatic nitro species to arylamines

The aromatic nitro species (1.0 eq.) and 10% Pd/C catalyst (0.1 eq. or 0.2 eq., as stated) were stirred in MeOH in a sealed microwave vial under H_2 (1 atm.) for 16 h. The mixture was subsequently filtered through Celite® and the filtrate concentrated *in vacuo* to give the crude product.

General Procedure 6: Suzuki-type cross-coupling of *N*-(3-chloro-1,4-dioxo-1,4-dihydronaphthelen-2-yl)arylamides with arylboronic acids under aqueous conditions

The amide (1.0 eq.), the requisite boronic acid (2.0 eq.) and $Pd(PPh_3)_2Cl_2$ (0.1 eq.) were stirred in sat. aq. $NaHCO_3$:THF (5:22) in a sealed microwave vial under N_2 and heated to 100 ^oC for 16 h (unless otherwise stated). The solution was cooled to RT, filtered through Celite® and partitioned between EtOAc (50 mL) and sat. aq. NH_4Cl (20 mL). The organic layer was collected, washed with brine (3 x 20 mL), dried, filtered and concentrated *in vacuo* to give the crude product.

General Procedure 7: Suzuki-type cross-coupling of *N*-(3-chloro-1,4-dioxo-1,4-dihydronaphthelen-2-yl)arylamides with arylboronic acids under anhydrous conditions

The amide (1.0 eq.), the requisite boronic acid (2.0 eq.), $Pd(PPh_3)_2Cl_2$ (0.1 eq.) and Na_2CO_3 (3.0 eq.) were stirred in toluene in a sealed microwave vial under N_2 and heated to 120 ^oC for 16 h (unless otherwise stated). The solution was cooled to RT, filtered through Celite® and partitioned between EtOAc (50 mL) and sat. aq. NH_4Cl (20 mL). The organic layer was collected, washed with brine (3 x 20 mL), dried, filtered and concentrated *in vacuo* to give the crude product.

General Procedure 8: *tert*-Butyl carbamate deprotection of protected anilines

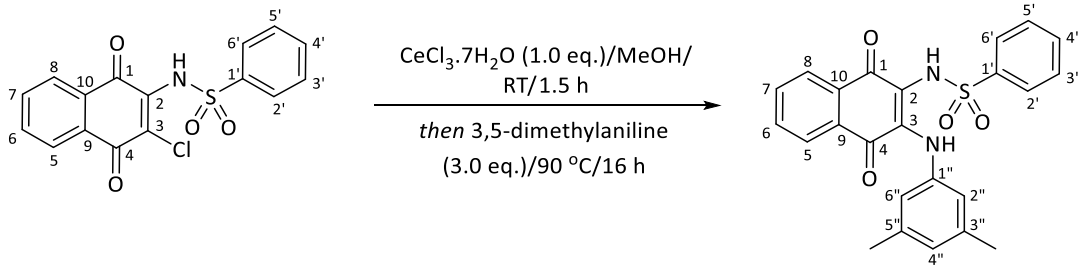
Trifluoroacetic acid (1 part) was added slowly to the *tert*-butyl carbamate (1 eq.) in CH_2Cl_2 (5 parts) at 0 ^oC. The solution was stirred at RT for 2 h. The reaction was then poured onto H_2O (50 mL) and extracted into CH_2Cl_2 (3 x 20 mL). The combined organic layers were washed with sat. aq. $NaHCO_3$ (3 x 20 mL), brine (2 x 10 mL), dried, filtered and concentrated *in vacuo* to give the crude product.

General Procedure 9: Nucleophilic aromatic substitution reaction on 1-fluoro-4-nitrobenzene or 1-fluoro-3-methyl-4-nitrobenzene

1-Fluoro-4-nitrobenzene (1.0 eq.) or 1-fluoro-3-methyl-4-nitrobenzene (1.0 eq.), the requisite nucleophile (1.0 eq.), K_2CO_3 (3.0 eq.) and H_2O (2.5 mL) were stirred in EtOH (7.5 mL) at 90 ^oC for 48 h. The solution was cooled to RT, poured onto ice water (50 mL) and 1 M aq. HCl (20 mL) was added. The reaction mixture was extracted with EtOAc (4 x 50 mL) and the organic extracts were combined, dried, filtered and concentrated *in vacuo* to give the crude product.

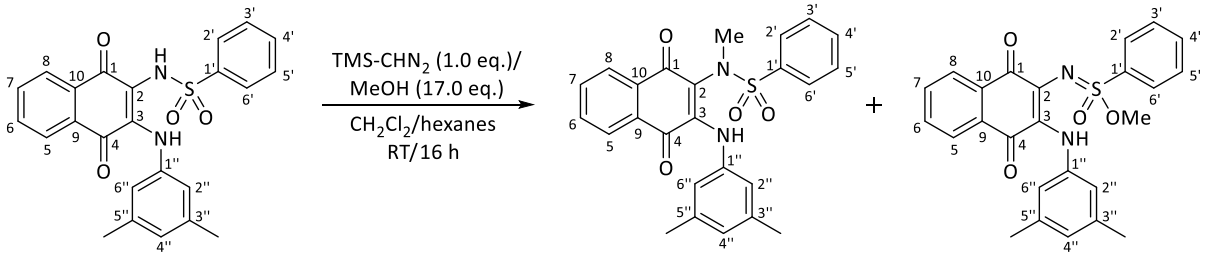
7.3. Preparation and Characterisation of Compounds Reported in Chapter 2

N-(3-((3”,5”-Dimethylphenyl)amino)-1,4-dioxo-1,4-dihydronaphthalen-2-yl) benzenesulfonamide 32[242]



Following *General Procedure 2,* using naphthoquinone **57** (200 mg, 0.576 mmol), 3,5-dimethylaniline (215 µL, 1.730 mmol) and cerium trichloride heptahydrate (214 mg, 0.576 mmol) in MeOH (5 mL) at 90 °C. Purification *via* column chromatography on silica gel (eluent pet ether:acetone 90:10 to 50:50) and subsequent recrystallisation from boiling toluene gave 3-anilinonaphthoquinone **32** as a dark red solid (112 mg, 45%). mp 184-186 °C (toluene) (lit. 178-182 °C);[242] δ_H (400 MHz, $CDCl_3$) 2.33 (6H, s, 2 x Ar-*Me*), 6.68 (2H, s, $H_{2''}$ and $H_{6''}$), 6.80 (1H, s, sulfonamide-N*H*), 6.83 (1H, s, $H_{4''}$), 7.31-7.38 (2H, m, $H_{3'}$ and $H_{5'}$), 7.44-7.50 (1H, m, $H_{4'}$), 7.62-7.72 (4H, m, H_6, H_7, $H_{2'}$ and $H_{6'}$), 7.90 (1H, dd, *J* 7.1, 1.5, H_8), 8.01 (1H, s, N*H*), 8.05-8.09 (1H, m, H_5); *m/z* (ESI^-) 431 ($[M-H]^-$, 100%).

N-(3-(3’’,5’’-Dimethylphenylamino)-1,4-dioxo-1,4-dihydronaphthalen-2-yl)-*N*-methylbenzenesulfonamide 34[281a] and Methyl-*N*-3-(3’’,5’’-dimethylphenylamino)-1,4-dioxo-1,4-dihydronaphthalen-2-ylbenzenesulfonimidate 35[281a]

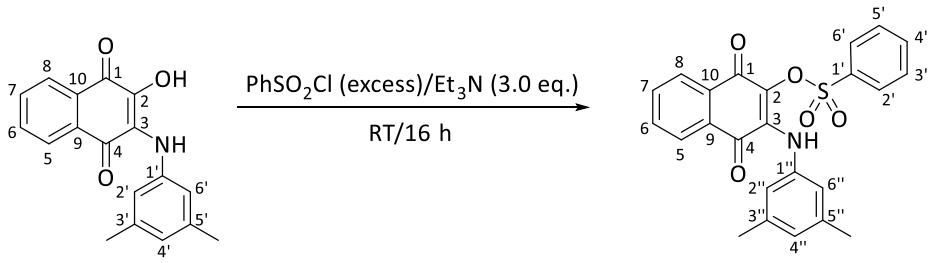


CH_2Cl_2 (15 mL) and MeOH (1.59 mL, 39.3 mmol) were added to naphthoquinone **32** (1.00 g, 2.31 mmol) at 0 ^oC under an argon atmosphere. This mixture was stirred until **32** had dissolved completely. 2 M Trimethylsilyldiazomethane in hexanes solution (1.16 mL, 2.31 mmol) was then added dropwise to the solution, which was stirred at RT for 16 h. After this time, the reaction was quenched by adding 20% aq. AcOH (20 mL), and then partitioned between EtOAc (50 mL) and H_2O (50 mL). The organic layer was collected, washed with sat. aq. $NaHCO_3$ (20 mL) and brine (3 x 20 mL), dried, filtered and concentrated *in vacuo* to give the crude product. Purification *via* column chromatography on silica gel (eluent pet ether:EtOAc 95:5) gave:

N-methylated sulfonamide **34** as an orange solid (547 mg, 53%). mp 215-218 ^oC (lit. 217-219 ^oC);[281a] HPLC t_R 14 min, 98%; δ_H (400 MHz, DMSO-d_6) 2.27 (6H, s, 2 x Ar-*Me*), 2.83 (3H, s, N*Me*), 6.84 (3H, s, $H_{2''}$, $H_{4''}$ and $H_{6''}$), 7.43 (2H, app. t, *J* 7.4, $H_{3'}$ and $H_{5'}$), 7.50-7.54 (2H, m, $H_{2'}$ and $H_{6'}$), 7.56-7.61 (1H, app. t, *J* 7.4, $H_{4'}$), 7.73-7.85 (3H, m, H_6, H_7 and H_8), 8.03 (1H, d, *J* 7.6, H_5), 9.13 (1H, s, N*H*); δ_H (400 MHz, DMF-d_7) 2.32 (6H, s, 2 x Ar-*Me*), 2.99 (3H, s, N*Me*), 6.89 (1H, s, $H_{4''}$), 6.98 (2H, s, $H_{2''}$ and $H_{6''}$), 7.49 (2H, app. t, *J* 7.9, $H_{3'}$ and $H_{5'}$), 7.59-7.67 (3H, m, $H_{2'}$, $H_{4'}$ and $H_{6'}$), 7.78-7.90 (3H, m, H_6, H_7 and H_8), 8.07 (1H, d, *J* 7.3, H_5), 9.06 (1H, s, N*H*); *m*/*z* (ESI^+) 447 ($[M+H]^+$, 100%), 469 ($[M+Na]^+$, 75%).

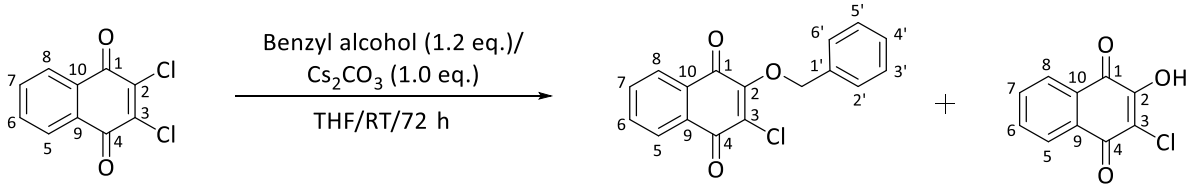
O-methylated sulfonamide **35** as a purple solid (330 mg, 32%). mp 66-68 ^oC (lit. 71-74 ^oC);[281a] HPLC t_R 15 min, 96%; δ_H (500 MHz, DMSO-d_6) 2.11 (6H, s, 2 x Ar-*Me*), 3.40 (3H, s, O*Me*), 6.43 (1H, s, $H_{4''}$), 6.61 (2H, s, $H_{2''}$ and $H_{6''}$), 7.27-7.31 (2H, m, $H_{3'}$ and $H_{5'}$), 7.34-7.40 (3H, m, $H_{2'}$ and $H_{6'}$), 7.54-7.60 (1H, m, $H_{4'}$), 7.74-7.83 (2H, m, H_6 and H_7), 7.93-8.01 (2H, m, H_5 and H_8), 8.31 (1H, s, N*H*); δ_H (400 MHz, DMF-d_7) 2.18 (6H, s, 2 x Ar-*Me*), 3.57 (3H, s, O*Me*), 6.52 (1H, s, $H_{4''}$), 6.76 (2H, s, $H_{2''}$ and $H_{6''}$), 7.43-7.47 (4H, m, $H_{2'}$, $H_{3'}$, $H_{5'}$ and $H_{6'}$), 7.60-7.66 (1H, m, $H_{4'}$), 7.77-7.87 (2H, m, H_6 and H_7), 7.99-8.06 (2H, m, H_5 and H_8, obscured by solvent resonance), 8.19 (1H, s, N*H*); *m*/*z* (ESI^+) 469 ($[M+Na]^+$, 100%); nOe irradiation of the O*Me* proton resonance shows an enhancement in the signal of both the $H_{2'}/H_{6'}$ and $H_{2''}/H_{6''}$ peaks, but no enhancement of the naphthoquinone peaks H_5 or H_8.

3-((3'',5''-Dimethylphenyl)amino)-1,4-dioxo-1,4-dihydronaphthalen-2-ylbenzenesulfonate 36



Naphthoquinone **41** (40 mg, 0.137 mmol) was added to benzenesulfonyl chloride (5 mL) and triethylamine (57 µL, 0.410 mmol) and stirred at RT for 16 h. The reaction mixture was quenched with MeOH (8 mL) and then partitioned between 1 M aq. HCl (20 mL) and EtOAc (20 mL). The organic layer was collected, washed with brine (3 x 20 mL), filtered and concentrated *in vacuo* to give the crude product. Purification *via* column chromatography on silica gel (eluent pet ether:EtOAc 95:5 to 75:25) gave sulfonate ester **36** as a red solid (51 mg, 86%). mp 200-203 ^{o}C; HPLC t_R 15 min, 94%; υ_{max} (thin film) 3288 (N-H), 1680 (C=O), 1616 (C=O), 1598, 1576, 1530; δ_H (500 MHz, $CDCl_3$) 2.22 (6H, s, 2 x Ar-*Me*), 6.51 (2H, s, $H_{2''}$ and $H_{6''}$), 6.70 (1H, s, $H_{4''}$), 7.35 (2H, app. t, *J* 7.9, $H_{3'}$ and $H_{5'}$), 7.48 (1H, s, N*H*), 7.54-7.62 (3H, m, $H_{2'}$, $H_{4'}$ and $H_{6'}$), 7.70 (1H, t, app. *J* 7.4, H_7), 7.79 (1H, app. t, *J* 7.4, H_6), 8.13 (1H, d, *J* 7.4, H_8), 8.18 (1H, d, *J* 7.4, H_5); δ_C (125 MHz, $CDCl_3$) 21.2 (2 x Ar-*Me*), 120.6 ($C_{2''}$ and $C_{6''}$), 126.8 (C_8), 126.8 ($C_{4''}$), 126.9 (C_5), 127.2 (C_2), 127.9 ($C_{2'}$ and $C_{6'}$), 128.6 ($C_{3'}$ and $C_{5'}$), 129.8 (C_{10}), 131.8 (C_9), 132.9 (C_7), 133.5 ($C_{4'}$), 135.4 (C_6), 135.8 (C_3), 136.3 ($C_{1'}$), 136.3 ($C_{1''}$), 137.9 ($C_{3''}$ and $C_{5''}$), 177.2 (C_1), 182.2 (C_4); HMBC analysis confirms that the product is the 1,4-dione and not the 1,2-dione as C_4 shows interactions with both N*H* and C_5-*H*; *m/z* (ESI$^+$) 456 ([M+Na]$^+$, 100%); HRMS (ESI$^+$) $C_{24}H_{19}NNaO_5S^+$ ([M+Na]$^+$) requires 456.0876, found 456.0859.

2-(Benzyloxy)-3-chloronaphthalene-1,4-dione 42[369] and 3-Chloro-2-hydroxy-naphthalene-1,4-dione 38[370]

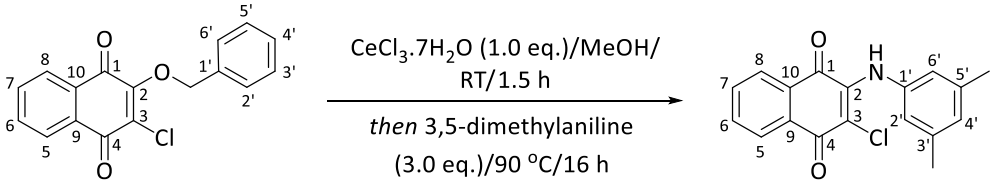


2,3-Dichloro-1,4-naphthoquinone **37** (1.00 g, 4.40 mmol), benzyl alcohol (547 µL, 5.29 mmol) and Cs_2CO_3 (1.44 g, 4.40 mmol) were stirred in THF (20 mL) at RT for 72 h. 1 M aq. HCl (50 mL) was then added and the organic product extracted with EtOAc (3 x 50 mL). The organic extracts were combined, washed with brine (3 x 20 mL), dried, filtered and concentrated *in vacuo* to give the crude reaction mixture. Purification *via* column chromatography on silica gel (eluent pet ether:acetone 90:10 to 20:80) gave:

2-benzyloxynaphthoquinone **42** as a yellow solid (1.11 g, 85%). mp 118 ^{o}C (lit. 115-116 ^{o}C);[369] δ_H (400 MHz, $CDCl_3$) 5.66 (2H, s, CH_2Ph), 7.31-7.41 (3H, m, Ph), 7.46-7.50 (2H, m, Ph), 7.72-7.77 (2H, m, H_6 and H_7), 8.07-8.15 (2H, m, H_5 and H_8); *m/z* (ESI$^+$) 321 ([M(^{35}Cl)+Na]$^+$, 100%), 323 ([M(^{37}Cl)+Na]$^+$, 33%).

2-hydroxynaphthoquinone **38** as a red solid (130 mg, 15%). mp 215-217 ^{o}C (lit. 215-216 ^{o}C);[370] δ_H (400 MHz, DMSO-d_6) 7.56 (1H, app. td, *J* 7.5, 1.2, H_6 or H_7), 7.69 (1H, app. td, *J* 7.5, 1.2, H_6 or H_7), 7.78-7.82 (1H, m, H_5 or H_8), 7.89-7.93 (1H, m, H_5 or H_8), *OH not observed*; *m/z* (ESI$^-$) 207 ([M(^{35}Cl)-H]$^-$, 100%), 209 ([M(^{37}Cl)-H]$^-$, 33%).

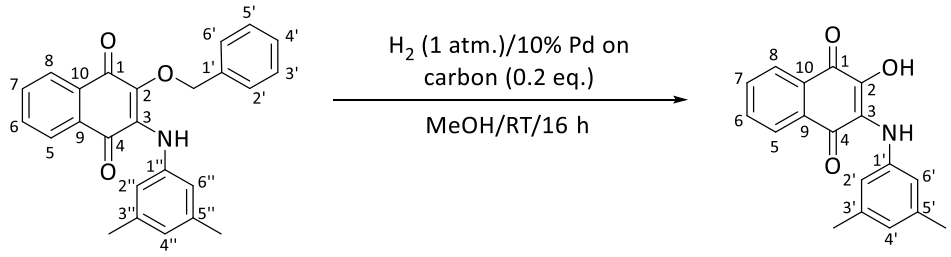
3-Chloro-2-(3',5'-dimethylphenylamino)naphthalene-1,4-dione 40[281a]



Following *General Procedure 2,* using naphthoquinone **42** (500 mg, 1.68 mmol), 3,5-dimethylaniline (626 µL, 5.03 mmol) and cerium trichloride heptahydrate (624 mg, 1.68 mmol) in MeOH (8 mL). Purification *via* column chromatography on silica gel (eluent pet ether:acetone 90:10 to 70:30) and subsequent recrystallisation from boiling MeOH gave 2-anilinonaphthoquinone **40** as a red solid (210 mg, 40%). mp 190-191 ^{o}C (MeOH) (lit. 187-188 ^{o}C);[281a] δ_H (400 MHz, $CDCl_3$) 2.32 (6H, s, 2 x Ar-*Me*), 6.70 (2H, s, $H_{2'}$ and $H_{6'}$), 6.85 (1H, s,

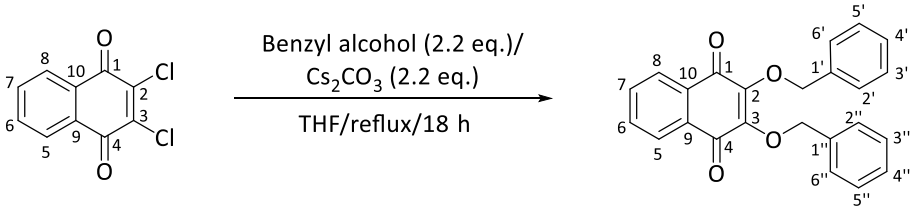
$H_{4'}$), 7.62-7.72 (2H, m, H_7 and N*H*), 7.77 (1H, app. td, *J* 7.5, 1.0, H_6), 8.11 (1H, d, *J* 7.5, H_8), 8.20 (1H, d, *J* 7.5, H_5); *m/z* (ESI$^+$) 312 ([M(^{35}Cl)+H]$^+$, 100%), 314 ([M(^{37}Cl)+H]$^+$, 33%).

2-((3',5'-Dimethylphenyl)amino)-3-hydroxynaphthalene-1,4-dione 41



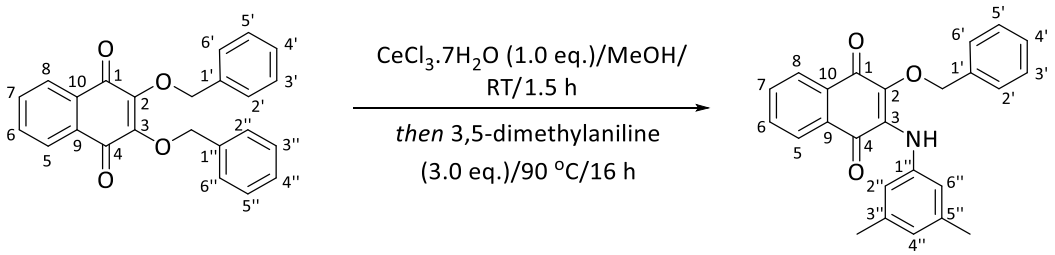
Naphthoquinone **44** (200 mg, 0.522 mmol) and 10% Pd/C (11 mg, 0.104 mmol) were stirred in MeOH (15 mL) in a sealed microwave vial under H_2 (1 atm.) for 16 h. The mixture was then filtered through Celite® and the filtrate concentrated *in vacuo* to give the crude product. Purification *via* column chromatography on silica gel (eluent pet ether:acetone 90:10 to 75:25) gave 2-hydroxynaphthoquinone **41** as a purple solid (49 mg, 32%). mp 212-215 ^{o}C; HPLC t_R 14 min, 95%; υ_{max} (thin film) 3316 (N-H/O-H), 2922 (C-H), 1655 (C=O), 1640 (C=O), 1594, 1572, 1517; δ_H (500 MHz, $CDCl_3$) 2.31 (6H, s, 2 x Ar-*Me*), 6.65 (2H, s, $H_{2'}$ and $H_{6'}$), 6.74 (1H, s, $H_{4'}$), 6.94 (1H, br. s, O*H*), 6.99 (1H, s, N*H*), 7.64-7.71 (2H, m, H_6 and H_7), 8.05-8.08 (2H, m, H_5 and H_8); δ_C (125 MHz, $CDCl_3$) 21.3 (2 x Ar-*Me*), 119.3 ($C_{2'}$ and $C_{6'}$), 125.0 (C_2), 125.3 ($C_{4'}$), 125.9 (C_5 or C_8), 126.6 (C_5 or C_8), 130.5 (C_9 or C_{10}), 130.8 (C_9 or C_{10}), 133.5 (C_6 or C_7), 134.0 (C_6 or C_7), 136.2 (C_3), 138.0 ($C_{3'}$ and $C_{5'}$), 138.6 ($C_{1'}$), 179.4 (C_4), 182.4 (C_1); *m/z* (ESI$^-$) 292 ([M-H]$^-$, 100%); HRMS (ESI$^-$) $C_{16}H_{14}NO_3^-$ ([M-H]$^-$) requires 292.0979, found 292.0976.

2,3-*bis*(Benzyloxy)naphthalene-1,4-dione 43



2,3-Dichloro-1,4-naphthoquinone **37** (1.00 g, 4.40 mmol), benzyl alcohol (1.00 mL, 9.69 mmol) and Cs_2CO_3 (3.16 g, 9.69 mmol) were stirred in THF (20 mL) and heated to reflux for 18 h. 1 M aq. HCl (50 mL) was then added and the organic product extracted with EtOAc (3 x 50 mL). The organic extracts were combined, washed with brine (3 x 20 mL), dried, filtered and concentrated *in vacuo* to give the crude reaction mixture. Purification *via* column chromatography on silica gel (eluent pet ether:EtOAc 95:5 to 75:25) gave 2,3-*bis*(benzyloxy)naphthoquinone **43** as a yellow solid (503 mg, 39%). mp 87-91 ^{o}C; υ_{max} (thin film) 3033 (C-H), 1660 (C=O), 1595, 1573; δ_H (500 MHz, C_6D_6) 5.30 (4H, s, 2 x CH_2), 7.06-7.10 (2H, m, H_6 and H_7), 7.14-7.18 (2H, m, $H_{4'}$ and $H_{4''}$), 7.20-7.24 (4H, m, $H_{3'}$, $H_{5'}$, $H_{3''}$ and $H_{5''}$), 7.48-7.51 (4H, m, $H_{2'}$, $H_{6'}$, $H_{2''}$ and $H_{6''}$), 8.05-8.05 (2H, m, H_5 and H_8); δ_C (125 MHz, C_6D_6) 75.3 (2 x *C*H_2), 126.3 (C_5 and C_8), 127.7-128.5 ($C_{2'}$, $C_{3'}$, $C_{4'}$, $C_{5'}$, $C_{6'}$, $C_{2''}$, $C_{3''}$, $C_{4''}$, $C_{5''}$ and $C_{6''}$, obscured under solvent resonance), 131.4 (C_9 and C_{10}), 133.3 (C_6 and C_7), 137.3 (C_2 and C_3), 148.4 ($C_{1'}$ and $C_{1''}$), 181.9 (C_1 and C_4); *m/z* (ESI$^+$) 393 ([M+Na]$^+$, 100%); HRMS (ESI$^+$) $C_{24}H_{18}NaO_4^+$ ([M+Na]$^+$) requires 393.1097, found 393.1082.

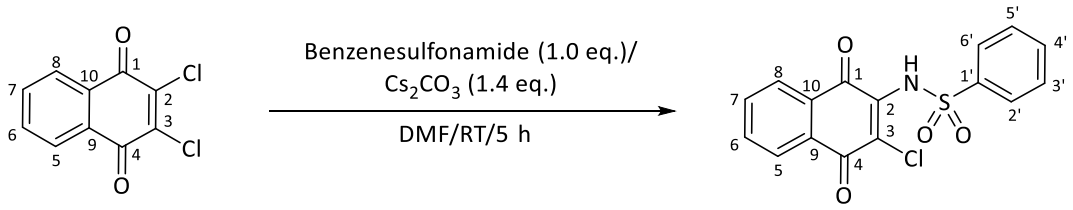
2-(Benzyloxy)-3-((3'',5''-dimethylphenyl)amino)naphthalene-1,4-dione 44



Following *General Procedure 2*, using naphthoquinone **43** (250 mg, 0.676 mmol), 3,5-dimethylaniline (252 µL, 2.028 mmol) and cerium trichloride heptahydrate (252 mg, 0.676 mmol) in MeOH (8 mL) at 90 ^{o}C. Purification *via* column chromatography on silica gel (eluent pet ether:EtOAc 95:5 to 75:25) and subsequent recrystallisation from boiling MeOH gave 3-anilinonaphthoquinone **44** as a red solid (227 mg, 88%). mp 152-153 ^{o}C (MeOH); υ_{max} (thin film) 3312 (N-H), 1705, 1663 (C=O), 1637 (C=O), 1597, 1570, 1521; δ_H (500 MHz, DMSO-d_6) 2.18 (6H, s, 2 x Ar-*Me*), 4.75 (2H, s, CH_2Ph), 6.67 (1H, s, $H_{4''}$), 6.72 (2H, s, $H_{2''}$ and

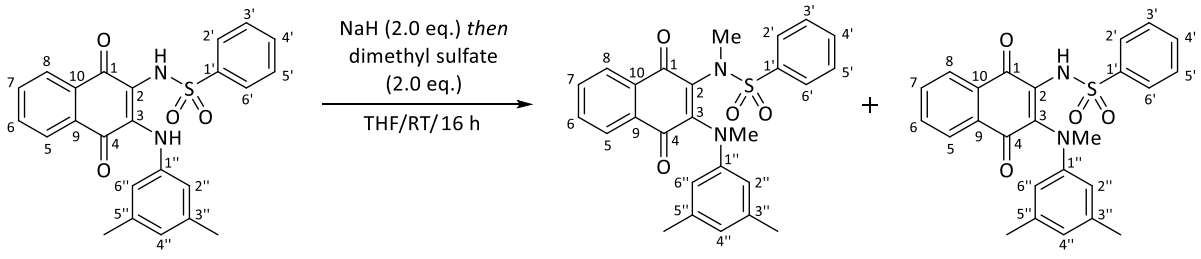
$H_{6''}$), 6.89-6.92 (2H, m, $H_{2'}$ and $H_{6'}$), 7.16-7.24 (3H, m, $H_{3'}$, $H_{4'}$ and $H_{5'}$), 7.77 (1H, app. td, *J* 7.8, 1.2, H_6 or H_7), 7.85 (1H, app. td, *J* 7.8, 1.2, H_6 or H_7), 7.97-8.01 (2H, m, H_5 and H_8), 8.42 (1H, s, N*H*); δ_C (125 MHz, DMSO-d_6) 20.9 (2 x Ar-*Me*), 72.7 (*C*H_2Ph), 120.2 ($C_{2''}$ and $C_{6''}$), 124.7 ($C_{4''}$), 125.5 (C_5 or C_8), 125.8 (C_5 or C_8), 127.5 ($C_{2'}$ and $C_{6'}$), 127.5 ($C_{4'}$), 127.8 ($C_{3'}$ and $C_{5'}$), 130.1 (C_9 or C_{10}), 131.7 (C_9 or C_{10}), 132.9 (C_6 or C_7), 134.6 (C_6 and C_7), 135.6 (C_3), 136.8 ($C_{1'}$), 136.8 ($C_{3''}$ and $C_{5''}$), 138.3 (C_2), 139.8 ($C_{1''}$), 178.7 (C_1), 182.7 (C_4); *m/z* (ESI^+) 252 (100%), 384 ($[M+H]^+$, 40%), 406 ($[M+Na]^+$, 50%); HRMS (ESI^+) $C_{25}H_{21}NNaO_3^+$ ($[M+Na]^+$) requires 406.1414, found 406.1395.

N-(3-Chloro-1,4-dioxo-1,4-dihydronaphthalen-2-yl)benzenesulfonamide 57[242]



Following *General Procedure 1*, using 2,3-dichloro-1,4-naphthoquinone **37** (3.00 g, 13.2 mmol), benzenesulfonamide (2.07 g, 13.2 mmol) and Cs_2CO_3 (6.03 g, 18.5 mmol) in DMF (30 mL). Purification *via* column chromatography on silica gel (eluent pet ether:acetone 80:20 to 50:50) gave sulfonamide **57** as a yellow solid (4.072 g, 89%). mp 218-220 ^oC (lit. 219-223 ^oC);[242] δ_H (400 MHz, DMSO-d_6) 7.54-7.67 (3H, m, $H_{3'}$, $H_{4'}$ and $H_{5'}$), 7.77-7.87 (2H, m, H_6 and H_7), 7.90-7.98 (3H, m, $H_{2'}$, $H_{6'}$ and H_8), 7.98-8.04 (1H, m, H_5); *m/z* (ESI^-) 138 (40%), 346 ($[M(^{35}Cl)-H]^-$, 100%), 348 ($[M(^{37}Cl)-H]^-$, 40%).

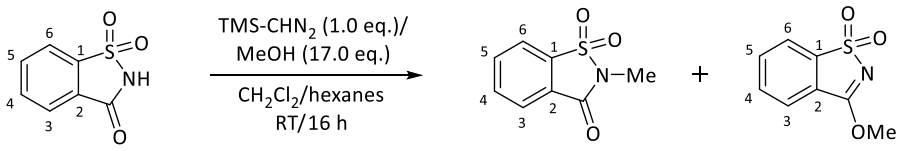
_N_-(3-(3'',5''-Dimethylphenyl(methyl)amino)-1,4-dioxo-1,4-dihydronaphthalen-2-yl)-_N_-methylbenzenesulfonamide 58 and _N_-(3-(3'',5''-Dimethylphenyl(methyl)amino)-1,4-dioxo-1,4-dihydronaphthalen-2-yl)benzenesulfonamide 59



Naphthoquinone **32** (100 mg, 0.231 mmol) was stirred at RT in THF (3 mL) under an argon atmosphere. Sodium hydride (as a 60% dispersion in oil, 19 mg, 0.462 mmol) was added and the reaction stirred for 5 min; subsequently, dimethyl sulfate (44 µL, 0.462 mmol) was added dropwise. The reaction was stirred at RT for 16 h before being quenched by the addition of 20% aq. AcOH (3 mL) and H_2O (5 mL). The organic products were extracted into EtOAc (2 x 10 mL), washed with brine (3 x 10 mL), dried, filtered and concentrated *in vacuo* to give the crude product. ^{1}*H*-NMR analysis of the crude reaction mixture showed that both *N*,*N*-dimethylated **58** and *N*-monomethylated **59** were formed in a ratio of 84:16. Purification *via* column chromatography on silica gel (eluent pet ether:EtOAc 95:5 to 80:20) subsequently afforded *N*,*N*-dimethylated **58** as a purple solid (86 mg, 81%). mp 35-39 ^{o}C; υ_{max} (thin film) 3408 (N-H), 2917 (C-H), 1675, 1641, 1593 (C=O), 1548 (C=O); δ_H (400 MHz, DMSO-d_6) 2.22 (6H, s, 2 x Ar-*Me*), 2.94 (3H, s, sulfonamide-N*Me*), 3.39 (3H, s, aniline-N*Me*), 6.68 (1H, s, $H_{4''}$), 6.76 (2H, s, $H_{2''}$ and $H_{6''}$), 7.52 (2H, app. t, *J* 7.8, $H_{3'}$ and $H_{5'}$), 7.62-7.72 (3H, m, $H_{2'}$, $H_{4'}$ and $H_{6'}$), 7.77-7.84 (3H, m, H_6, H_7 and H_8), 7.88-7.93 (1H, m, H_5); δ_C (100 MHz, DMSO-d_6) 21.0 (2 x Ar-*Me*), 36.5 (sulfonamide-N*Me*), 41.1 (aniline-N*Me*), 118.9 ($C_{2''}$ and $C_{6''}$), 124.6 ($C_{4''}$), 125.6 (C_8), 126.4 (C_5), 127.5 ($C_{2'}$ and $C_{6'}$), 128.8 ($C_{3'}$ and $C_{5'}$), 131.2 (C_2), 131.2 (C_9 or C_{10}), 131.5 (C_9 or C_{10}), 132.9 ($C_{4'}$), 133.6 (C_6), 134.4 (C_7), 137.7 ($C_{3''}$ and $C_{5''}$), 138.4 ($C_{1'}$), 147.5 ($C_{1''}$), 151.4 (C_3), 179.9 (C_1), 182.3 (C_4); *m/z* (ESI$^+$) 461 ([M+H]$^+$, 80%), 483 ([M+Na]$^+$, 100%); HRMS (ESI$^+$) $C_{26}H_{24}N_2NaO_4S^+$ ([M+Na]$^+$) requires 483.1349, found 483.1350. The structure of the minor product, *N*-monomethylated **59**, was unambiguously determined from a combination of ^{1}*H*-NMR, HMBC,

NOESY and *m/z* analysis. δ_H (400 MHz, DMSO-d_6) 2.18 (6H, s, 2 x Ar-*Me*), 3.12 (3H, s, N*Me*), 6.42 (2H, s, $H_{2''}$ and $H_{6''}$), 6.51 (1H, s, $H_{4''}$), 7.42-7.47 (2H, m, $H_{3'}$ and $H_{5'}$), 7.52-7.57 (1H, m, $H_{4'}$), 7.70-7.75 (2H, m, $H_{2'}$ and $H_{6'}$), 7.77-7.81 (2H, m, H_6 and H_7), 7.86-7.89 (2H, m, H_5 and H_8), 9.75 (1H, br. s, N*H*); in an HMBC experiment both the N*Me* protons and $H_{2''}$ and $H_{6''}$ show a correlation to a common carbon, $C_{1''}$; in a NOESY experiment, irradiation of the N*Me* protons shows only an enhancement of the signal corresponding to $H_{2''}$ and $H_{6''}$ and not to any of the protons on the sulfonamide or naphthoquinone moieties; *m/z* (ESI^-) 445 ($[M-H]^-$, 100%); HRMS (ESI^+) $C_{25}H_{22}N_2NaO_4S^+$ ($[M+Na]^+$) requires 469.1193, found 469.1192.

N-Methyl saccharin 62[371] and *O*-Methyl saccharin 63



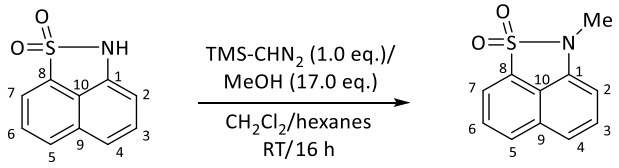
CH_2Cl_2 (9.5 mL) and MeOH (1.88 mL, 46.4 mmol) were added to saccharin **61** (500 mg, 2.73 mmol) at 0 °C under an argon atmosphere. 2 M Trimethylsilyldiazomethane in hexanes solution (1.37 mL, 2.73 mmol) was then added dropwise to the solution, which was stirred at RT for 16 h. After this time, the reaction was quenched by adding 20% aq. AcOH (10 mL), and then partitioned between EtOAc (30 mL) and H_2O (30 mL). The organic layer was collected, washed with sat. aq. $NaHCO_3$ (20 mL) and brine (3 x 20 mL), dried, filtered and concentrated *in vacuo* to give the crude product. Purification *via* column chromatography on silica gel (eluent pet ether:acetone 80:20) gave:

N-methyl saccharin **62** as a white solid (370 mg, 69%). mp 130-131 °C (lit. 132-133 °C);[371] δ_H (400 MHz, DMSO-d_6) 3.17 (3H, s, N*Me*), 8.00 (1H, app. t, *J* 7.7, H_4), 8.05 (1H, app. t, *J* 7.7, H_5), 8.11 (1H, d, *J* 7.7, H_3), 8.32 (1H, d, *J* 7.7, H_6); *m/z* (ESI^+) 172 (100%), 220 ($[M+Na]^+$, 20%).

O-methyl saccharin **63** as a white solid (100 mg, 19%). mp 179-180 °C; υ_{max} (thin film) 1739 (C=O), 1618, 1562; δ_H (400 MHz, DMSO-d_6) 4.21 (3H, s, O*Me*), 7.84-7.97 (3H, m, H_3, H_4 and H_5),

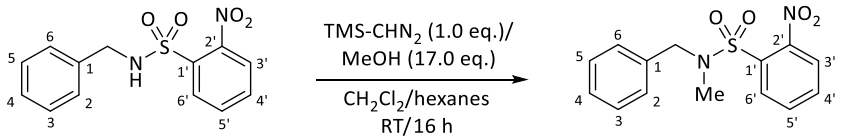
8.14 (1H, d, *J* 7.3, H_6); δ_C (100 MHz, DMSO-d_6) 58.6 (O*Me*), 122.0 (C_6), 123.8 (C_3), 126.0 (C_2), 134.4 (C_4), 135.0 (C_5), 142.7 (C_1), 169.7 (imidate-*C*N); *m/z* (ESI$^+$) 198 ([M+H]$^+$, 30%), 417 ([2M+Na]$^+$, 100%); HRMS (ESI$^+$) $C_8H_8NO_3S^+$ ([M+H]$^+$) requires 198.0219, found 198.0221.

_N_-Methyl 1,8-naphthalinsultam 65



CH_2Cl_2 (8.5 mL) and MeOH (1.38 mL, 34.0 mmol) were added to 1,8-naphthalinsultam **64** (500 mg, 2.31 mmol) at 0 ^oC under an argon atmosphere. 2 M Trimethylsilyldiazomethane in hexanes solution (1.22 mL, 2.44 mmol) was then added dropwise to the solution, which was stirred at RT for 16 h. After this time, the reaction was quenched by adding 20% aq. AcOH (10 mL), and then partitioned between EtOAc (30 mL) and H_2O (30 mL). The organic layer was collected, washed with sat. aq. $NaHCO_3$ (20 mL) and brine (3 x 20 mL), dried, filtered and concentrated *in vacuo* to give the crude product. Purification *via* column chromatography on silica gel (eluent pet ether:acetone 90:10) gave *N*-methylated **65** as a beige solid (320 mg, 60%). mp 112-118 ^oC; υ_{max} (thin film) 1627, 1589; δ_H (400 MHz, DMSO-d_6) 3.33 (3H, s, N*Me*), 7.06 (1H, d, *J* 7.0, H_2), 7.59-7.70 (2H, m, H_3 and H_4), 7.89 (1H, app. t, *J* 7.6, H_6), 8.24-8.32 (2H, m, H_5 and H_7); δ_C (100 MHz, DMSO-d_6) 26.6 (N*Me*), 104.0 (C_2), 118.2 (C_9 or C_{10}), 118.4 (C_4), 120.4 (C_5 or C_7), 128.7 (C_6), 129.7 (C_9 or C_{10}), 129.8 (C_3), 130.0 (C_8), 131.6 (C_5 or C_7), 136.5 (C_1); *m/z* (ESI$^+$) 242 ([M+Na]$^+$, 70%), 413 (70%), 461 ([2M+Na]$^+$, 100%); HRMS (ESI$^+$) $C_{11}H_9NNaO_2S^+$ ([M+Na]$^+$) requires 242.0246, found 242.0247.

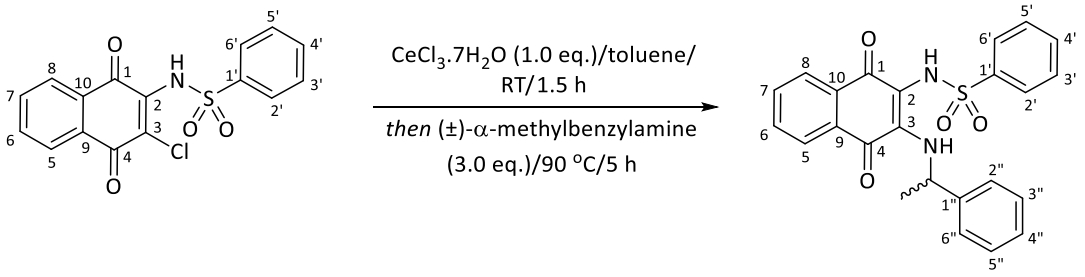
_N_-Benzyl-_N_-methyl-2'-nitrobenzenesulfonamide 67[372]



CH_2Cl_2 (6 mL) and MeOH (1.18 mL, 29.1 mmol) were added to *N*-benzyl-2'-nitrobenzene **66** (500 mg, 1.71 mmol) at 0 ^oC under an argon atmosphere. 2 M Trimethylsilyldiazomethane in hexanes solution (856 μL, 1.71 mmol) was then added dropwise to the solution, which was stirred at RT for 16 h. After this time, the reaction was quenched by adding 20% aq. AcOH (10 mL), and then partitioned between EtOAc (30 mL) and H_2O (30 mL). The organic layer was collected, washed with sat. aq. $NaHCO_3$ (20 mL) and brine (3 x 20 mL), dried, filtered and concentrated *in vacuo* to give the crude product. Purification *via* column chromatography on silica gel (eluent pet ether:acetone 90:10) gave *N*-methylated **67** as a beige solid (84 mg, 16%). mp 58 ^oC (lit. 56-57 ^oC);[372] δ_H (400 MHz, DMSO-d_6) 2.72 (3H, s, N*Me*), 4.40 (2H, s, CH_2), 7.29-7.35 (3H, m, H_2, H_4 and H_6), 7.35-7.41 (2H, m, H_3 and H_5), 7.88 (1H, app. t, *J* 7.8, $H_{4'}$), 7.93 (1H, app. t, *J* 7.8, $H_{5'}$), 8.03 (1H, d, *J* 7.8, $H_{6'}$), 8.07 (1H, d, *J* 7.8, $H_{2'}$); *m/z* (ESI^+) 329 ($[M+Na]^+$, 60%), 635 ($[2M+Na]^+$, 100%).

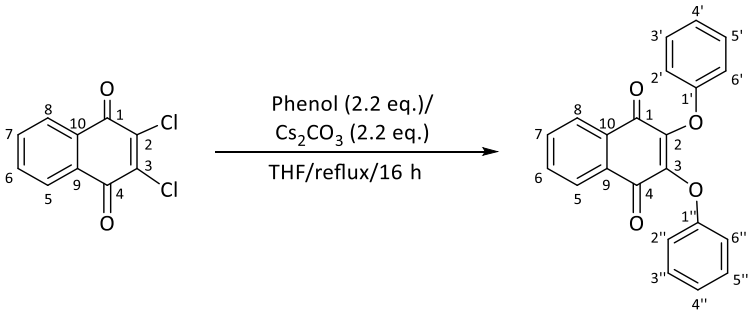
7.4. Preparation and Characterisation of Compounds Reported in Chapter 3

N-(1,4-Dioxo-3-((±)-α-methylbeznylamino)-1,4-dihydronaphthalen-2-yl)benzenesulfonamide 89



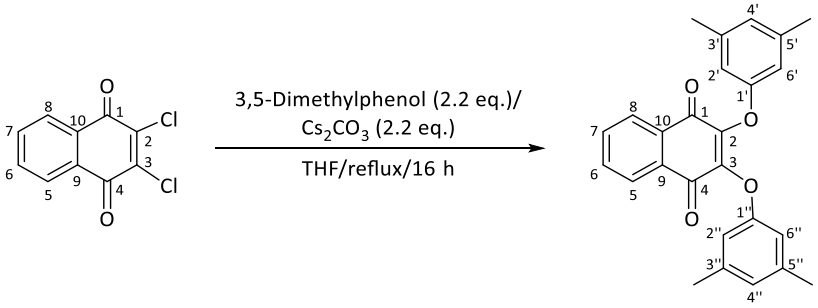
Following *General Procedure 2*, using naphthoquinone **57** (200 mg, 0.576 mmol), (±)-α-methylbenzylamine (220 µL, 1.727 mmol) and cerium trichloride heptahydrate (214 mg, 0.576 mmol) in toluene (8 mL) for 5 h at 90 ^{o}C. Purificiation *via* column chromatography on silica gel (eluent pet ether:acetone 90:10 to 70:30) afforded 3-aminonaphthoquinone **89** as an orange solid (65 mg, 26%). mp 163-165 ^{o}C; υ_{max} (thin film) 3325 (N-H), 3252 (N-H), 1711, 1671, 1608 (C=O), 1572 (C=O), 1508; δ_H (500 MHz, $CDCl_3$) 1.65 (3H, d, *J* 6.8, CH*Me*), 5.91 (1H, dq, *J* 7.9, 6.8, C*H*Me), 6.48 (1H, s, sulfonamide-N*H*), 6.65 (1H, d, *J* 7.9, amine-N*H*), 7.25 (1H, tt, *J* 7.3, 1.3, $H_{4''}$), 7.30-7.40 (6H, m, $H_{3'}$, $H_{5'}$, $H_{2''}$, $H_{3''}$, $H_{5''}$ and $H_{6''}$), 7.45-7.50 (1H, m, $H_{4'}$), 7.55-7.61 (2H, m, H_6 and H_7), 7.62-7.68 (1H, m, H_8), 7.78-7.81 (2H, m, $H_{2'}$ and $H_{6'}$), 8.00-8.04 (1H, m, H_5); δ_C (125 MHz, $CDCl_3$) 23.7 (CH*Me*), 52.7 (*C*HMe), 110.0 (C_2), 125.9 (C_8), 126.1 ($C_{2''}$ and $C_{6''}$), 126.8 (C_5), 127.4 ($C_{4''}$), 127.7 ($C_{2'}$ and $C_{6'}$), 128.6 ($C_{3'}$ and $C_{5'}$ or $C_{3''}$ and $C_{5''}$), 128.8 ($C_{3'}$ and $C_{5'}$ or $C_{3''}$ and $C_{5''}$), 130.0 (C_9), 131.6 (C_{10}), 132.5 (C_6), 133.1 ($C_{4'}$), 134.8 (C_7), 138.3 ($C_{1'}$), 142.8 (C_3), 144.0 ($C_{1''}$), 178.8 (C_1), 181.9 (C_4); *m/z* (ESI$^+$) 433 ([M+H]$^+$, 100%), 455 ([M+Na]$^+$, 95%); HRMS (ESI$^+$) $C_{24}H_{21}O_4N_2S^+$ ([M+H]$^+$) requires 433.1217, found 433.1218.

2,3-Diphenoxynaphthalene-1,4-dione 91



Following *General Procedure 3,* using 2,3-dichloronaphthalene-1,4-dione **37** (454 mg, 2.00 mmol), phenol (414 mg, 4.40 mmol) and Cs_2CO_3 (1430 mg, 4.40 mmol) in THF (30 mL) gave diphenoxy **91** as an orange solid (430 mg, 63%); this material was subsequently used without further purification. mp 188-193 ^{o}C; υ_{max} (thin film) 1662 (C=O), 1591 (C=O); δ_H (400 MHz, $CDCl_3$) 6.88-6.94 (4H, m, $H_{2'}$, $H_{6'}$, $H_{2''}$ and $H_{6''}$), 7.02-7.09 (2H, m, $H_{4'}$ and $H_{4''}$), 7.21-7.28 (4H, m, $H_{3'}$, $H_{5'}$, $H_{3''}$ and $H_{5''}$), 7.75-7.81 (2H, m, H_6 and H_7), 8.10-8.16 (2H, m, H_5 and H_8); δ_C (100 MHz, $CDCl_3$) 116.6 ($C_{2'}$, $C_{6'}$, $C_{2''}$ and $C_{6''}$), 123.6 ($C_{4'}$ and $C_{4''}$), 126.8 (C_5 and C_8), 129.4 ($C_{3'}$, $C_{5'}$, $C_{3''}$ and $C_{5''}$), 130.8 (C_9 and C_{10}), 134.3 (C_6 and C_7), 146.1 (C_2 and C_3), 156.5 ($C_{1'}$ and $C_{1''}$), 180.4 (C_1 and C_4); *m/z* (ESI$^+$) 139 (100%), 343 ([M+H]$^+$, 40%), 365 ([M+Na]$^+$, 50%); HRMS (ESI$^+$) $C_{22}H_{14}NaO_4^+$ ([M+Na]$^+$) requires 365.0784, found 365.0768.

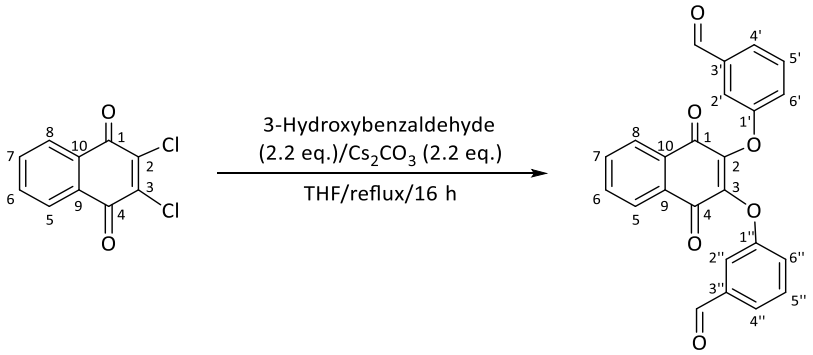
2,3-*bis*(3',5'-Dimethylphenoxy)naphthalene-1,4-dione 92



Following *General Procedure 3,* using 2,3-dichloronaphthalene-1,4-dione **37** (454 mg, 2.00 mmol), 3,5-dimethylphenol (537 mg, 4.40 mmol) and Cs_2CO_3 (1430 mg, 4.40 mmol) in THF (30 mL) gave diaryloxy **92** as an orange solid (709 mg, 89%); this material was

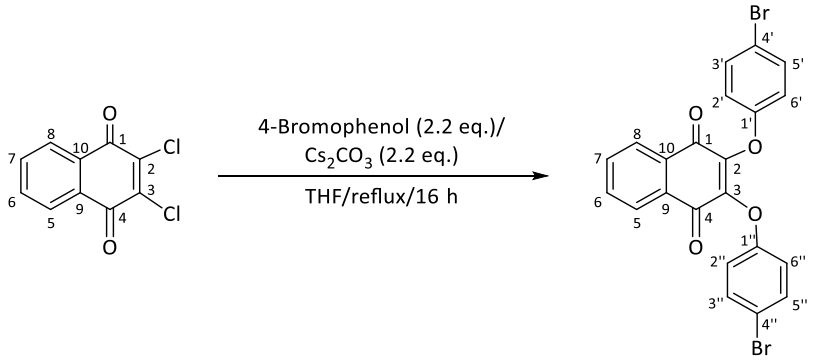
subsequently used without further purification. mp 175-177 ^{o}C; υ_{max} (thin film) 1665 (C=O), 1590 (C=O); δ_H (500 MHz, $CDCl_3$) 2.18 (12H, s, 4 x Ar-*Me*), 6.65 (2H, s, $H_{4'}$ and $H_{4''}$), 6.73 (4H, s, $H_{2'}$, $H_{6'}$, $H_{2''}$ and $H_{6''}$), 7.88-7.93 (2H, m, H_6 and H_7), 8.01-8.06 (2H, m, H_5 and H_8); δ_C (125 MHz, $CDCl_3$) 20.7 (4 x Ar-*Me*), 113.6 ($C_{2'}$, $C_{6'}$, $C_{2''}$ and $C_{6''}$), 124.3 ($C_{4'}$ and $C_{4''}$), 126.0 (C_5 and C_8), 131.0 (C_9 and C_{10}), 134.3 (C_6 and C_7), 138.8 ($C_{3'}$, $C_{5'}$, $C_{3''}$ and $C_{5''}$), 146.2 (C_2 and C_3), 156.7 ($C_{1'}$ and $C_{1''}$), 180.2 (C_1 and C_4); *m/z* (ESI$^+$) 399 ([M+H]$^+$, 100%), 421 ([M+Na]$^+$, 20%); HRMS (ESI$^+$) $C_{26}H_{22}NaO_4^+$ ([M+Na]$^+$) requires 421.1410, found 421.1391.

2,3-*bis*(3'-Formylphenoxy)naphthalene-1,4-dione 93



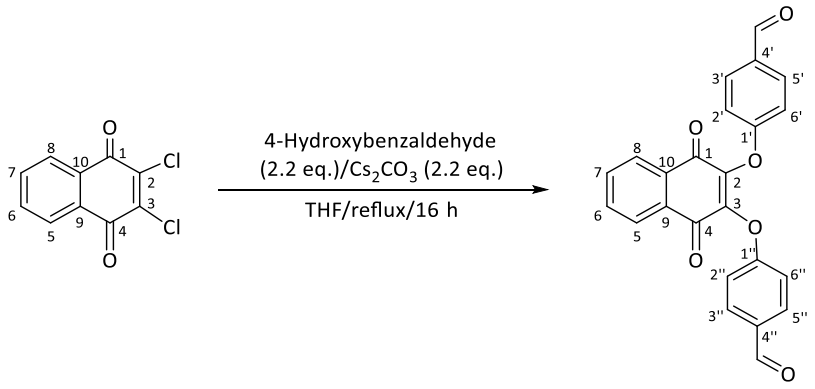
Following *General Procedure 3,* using 2,3-dichloronaphthalene-1,4-dione **37** (454 mg, 2.00 mmol), 3-hydroxybenzaldehyde (537 mg, 4.40 mmol) and Cs_2CO_3 (1430 mg, 4.40 mmol) in THF (30 mL) gave diaryloxy **93** as a yellow solid (648 mg, 81%); this material was subsequently used without further purification. mp 185-187 ^{o}C; υ_{max} (thin film) 1692 (C=O), 1662 (C=O), 1640, 1585; δ_H (500 MHz, $CDCl_3$) 7.22 (2H, ddd, *J* 7.9, 2.7, 1.1, $H_{6'}$ and $H_{6''}$), 7.36 (2H, dd, *J* 2.7, 1.1, $H_{2'}$ and $H_{2''}$), 7.44 (2H, app. t, *J* 7.9, $H_{5'}$ and $H_{5''}$), 7.57 (2H, app. dt, *J* 7.9, 1.1, $H_{4'}$ and $H_{4''}$), 7.80-7.85 (2H, m, H_6 and H_7), 8.12-8.17 (2H, m, H_5 and H_8), 9.90 (2H, s, 2 x C*H*O); δ_C (125 MHz, $CDCl_3$) 115.7 ($C_{2'}$ and $C_{2''}$), 123.0 ($C_{6'}$ and $C_{6''}$), 126.0 ($C_{4'}$ and $C_{4''}$), 127.0 (C_5 and C_8), 130.4 ($C_{5'}$ and $C_{5''}$), 130.6 (C_9 and C_{10}), 134.7 (C_6 and C_7), 137.7 ($C_{3'}$ and $C_{3''}$), 145.7 (C_2 and C_3), 156.9 ($C_{1'}$ and $C_{1''}$), 179.9 (C_1 and C_4), 191.0 (2 x *C*HO); *m/z* (ESI$^+$) 421 ([M+Na]$^+$, 100%); HRMS (ESI$^+$) $C_{24}H_{14}NaO_6^+$ ([M+Na]$^+$) requires 421.0683, found 421.0672.

2,3-*bis*(4'-Bromophenoxy)naphthalene-1,4-dione 94



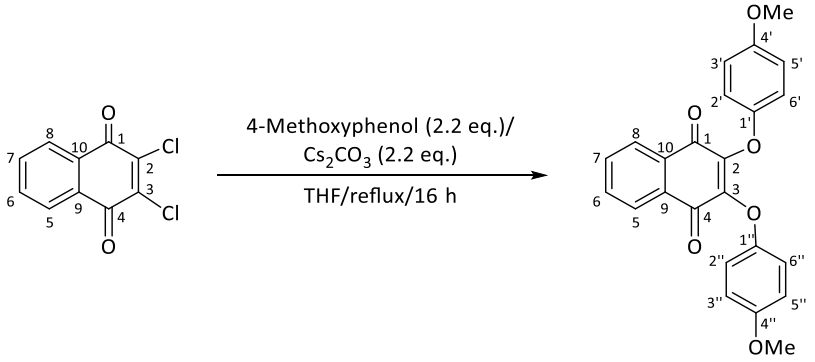
Following *General Procedure 3,* using 2,3-dichloronaphthalene-1,4-dione **37** (454 mg, 2.00 mmol), 4-bromophenol (761 mg, 4.40 mmol) and Cs_2CO_3 (1430 mg, 4.40 mmol) in THF (30 mL) gave diaryloxy **94** as a yellow solid (715 mg, 72%); this material was subsequently used without further purification. mp 182-185 ^{o}C; υ_{max} (thin film) 1677 (C=O), 1659 (C=O), 1624; δ_H (500 MHz, $CDCl_3$) 6.78-6.82 (4H, m, $H_{2'}$, $H_{6'}$, $H_{2''}$ and $H_{6''}$), 7.34-7.39 (4H, m, $H_{3'}$, $H_{5'}$, $H_{3''}$ and $H_{5''}$), 7.78-7.82 (2H, m, H_6 and H_7), 8.10-8.15 (2H, m, H_5 and H_8); δ_C (125 MHz, $CDCl_3$) 116.4 ($C_{4'}$ and $C_{4''}$), 118.3 ($C_{2'}$, $C_{6'}$, $C_{2''}$ and $C_{6''}$), 126.9 (C_5 and C_8), 130.6 (C_9 and C_{10}), 132.4 ($C_{3'}$, $C_{5'}$, $C_{3''}$ and $C_{5''}$), 134.5 (C_6 and C_7), 145.7 (C_2 and C_3), 155.4 ($C_{1'}$ and $C_{1''}$), 180.0 (C_1 and C_4); *m/z* (FI^+) 498 ([M(^{79}Br^{79}Br)]$^{+\cdot}$, 50%), 500 ([M(^{79}Br)(^{81}Br)]$^{+\cdot}$, 100%), 502 ([M(^{81}Br)(^{81}Br)]$^{+\cdot}$, 50%); HRMS (FI^+) $C_{22}H_{12}O_4Br_2^+$ ([M(^{79}Br^{79}Br)]$^{+\cdot}$) requires 497.9092, found 497.9102.

2,3-*bis*(4'-Formylphenoxy)naphthalene-1,4-dione 95



Following *General Procedure 3,* using 2,3-dichloronaphthalene-1,4-dione **37** (454 mg, 2.00 mmol), 4-hydroxybenzaldehyde (537 mg, 4.40 mmol) and Cs_2CO_3 (1430 mg, 4.40 mmol) in THF (30 mL) gave diaryloxy **95** as a yellow solid (315 mg, 40%); this material was subsequently used without further purification. mp 68-72 ^{o}C; υ_{max} (thin film) 2963 (C-H), 1673 (C=O), 1592 (C=O); δ_H (500 MHz, $CDCl_3$) 7.04-7.08 (4H, m, $H_{2'}$, $H_{6'}$, $H_{2''}$ and $H_{6''}$), 7.79-7.85 (6H, m, H_6, H_7, $H_{3'}$, $H_{5'}$, $H_{3''}$ and $H_{5''}$), 8.11-8.16 (2H, m, H_5 and H_8), 9.91 (2H, s, 2 x C*H*O); δ_C (125 MHz, $CDCl_3$) 116.9 ($C_{2'}$, $C_{6'}$, $C_{2''}$ and $C_{6''}$), 127.1 (C_5 and C_8), 130.5 (C_9 and C_{10}), 131.7 ($C_{3'}$, $C_{5'}$, $C_{3''}$ and $C_{5''}$), 132.3 ($C_{4'}$ and $C_{4''}$), 134.8 (C_6 and C_7), 145.6 (C_2 and C_3), 160.7 ($C_{1'}$ and $C_{1''}$), 179.5 (C_1 and C_4), 190.4 (2 x *C*HO); *m/z* (ESI$^+$) 421 ([M+Na]$^+$, 100%); HRMS (ESI$^+$) $C_{24}H_{14}NaO_6^+$ ([M+Na]$^+$) requires 421.0683, found 421.0674.

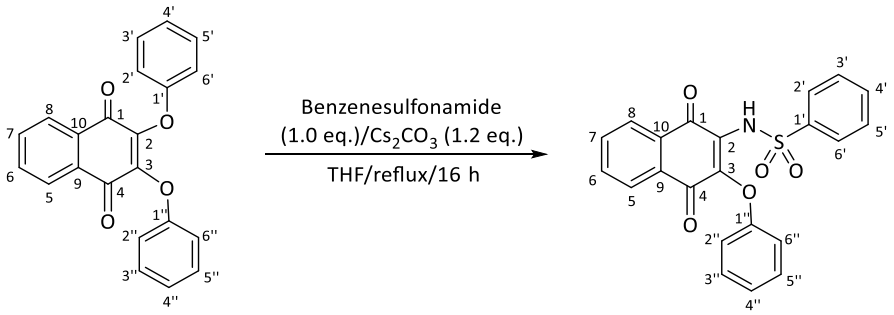
2,3-*bis*(4'-Methoxyphenoxy)naphthalene-1,4-dione 96



Following *General Procedure 3,* using 2,3-dichloronaphthalene-1,4-dione **37** (454 mg, 2.00 mmol), 4-methoxyphenol (546 mg, 4.40 mmol) and Cs_2CO_3 (1430 mg, 4.40 mmol) in THF (30 mL) gave diaryloxy **96** as a yellow solid (697 mg, 87%); this material was subsequently used without further purification. mp 128-130 °C; υ_{max} (thin film) 1662 (C=O), 1616 (C=O), 1593, 1502; δ_H (500 MHz, $CDCl_3$) 3.75 (6H, s, 2 x O*Me*), 6.73-6.79 (4H, m, $H_{2'}$, $H_{6'}$, $H_{2''}$ and $H_{6''}$ or $H_{3'}$, $H_{5'}$, $H_{3''}$ and $H_{5''}$), 6.83-6.88 (4H, m, $H_{2'}$, $H_{6'}$, $H_{2''}$ and $H_{6''}$ or $H_{3'}$, $H_{5'}$, $H_{3''}$ and $H_{5''}$), 7.74-7.79 (2H, m, H_6 and H_7), 8.08-8.13 (2H, m, H_5 and H_8); δ_C (125 MHz, $CDCl_3$) 55.6 (2 x O*Me*), 114.4 ($C_{2'}$, $C_{6'}$, $C_{2''}$ and $C_{6''}$ or $C_{3'}$, $C_{5'}$, $C_{3''}$ and $C_{5''}$), 117.7 ($C_{2'}$, $C_{6'}$, $C_{2''}$ and $C_{6''}$ or $C_{3'}$, $C_{5'}$, $C_{3''}$ and $C_{5''}$), 126.7 (C_5 and C_8), 130.8 (C_9 and C_{10}), 134.2 (C_6 and C_7), 146.3 (C_2 and C_3), 150.5 ($C_{1'}$ and $C_{1''}$),

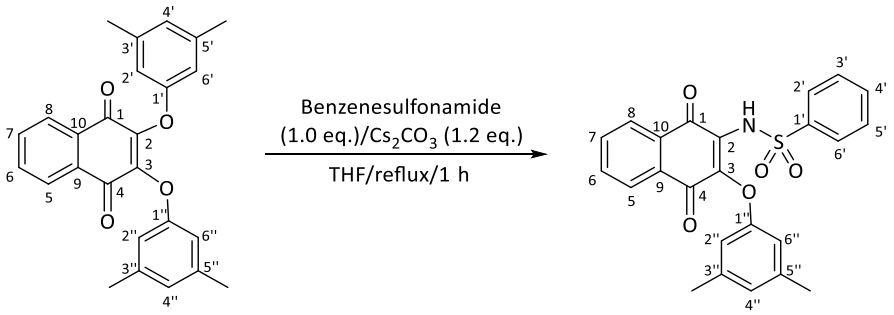
155.7 ($C_{4'}$ and $C_{4''}$), 180.7 (C_1 and C_4); *m/z* (ESI^+) 403 ($[M+H]^+$, 100%); HRMS (ESI^+) $C_{24}H_{18}NaO_6^+$ ($[M+Na]^+$) requires 425.0996, found 425.0986.

N-(3-Phenoxy-1,4-dioxo-1,4-dihydronaphthalen-2-yl)benzenesulfonamide 97



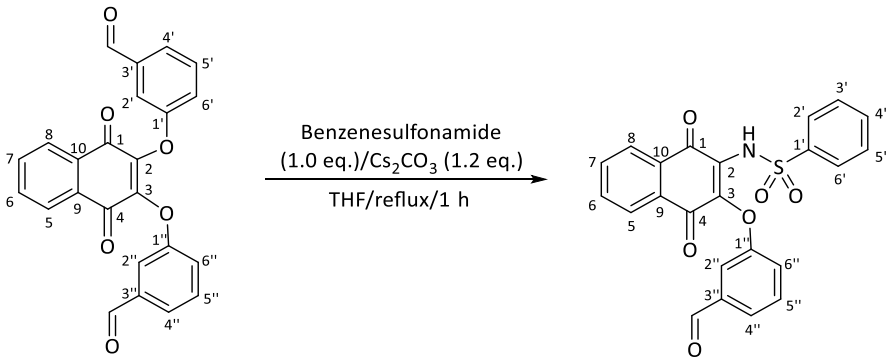
Following *General Procedure 4*, using naphthoquinone **91** (400 mg, 1.17 mmol), benzenesulfonamide (184 mg, 1.17 mmol) and Cs_2CO_3 (458 mg, 1.40 mmol) in THF (30 mL) for 16 h and subsequent recrystallisation from toluene gave 2-sulfonamidonaphthoquinone **97** as a yellow solid (175 mg, 67%). mp 216-219 ^oC (toluene); HPLC t_R 18 min, 95%; υ_{max} (thin film) 3235 (N-H), 1668 (C=O), 1655 (C=O), 1639; δ_H (500 MHz, DMSO-d_6) 6.82-6.86 (2H, m, $H_{2''}$ and $H_{6''}$), 6.99-7.04 (1H, m, $H_{4''}$), 7.18-7.24 (2H, m, $H_{3''}$ and $H_{5''}$), 7.46-7.51 (2H, m, $H_{3'}$ and $H_{5'}$), 7.53-7.57 (1H, m, $H_{4'}$), 7.81-7.92 (5H, m, H_5, H_6, H_7, $H_{2'}$ and $H_{6'}$), 8.03-8.06 (1H, m, H_8), 10.30 (1H, br. s, N*H*); δ_C (125 MHz, DMSO-d_6) 116.4 ($C_{2''}$ and $C_{6''}$), 122.7 ($C_{4''}$), 126.1 (C_5, C_8 or $C_{2'}$ and $C_{6'}$), 126.1 (C_5, C_8 or $C_{2'}$ and $C_{6'}$), 126.3 (C_5, C_8 or $C_{2'}$ and $C_{6'}$), 128.7 ($C_{3'}$ and $C_{5'}$), 129.1 ($C_{3''}$ and $C_{5''}$), 130.6 (C_9), 130.6 (C_{10}), 132.3 ($C_{4'}$), 132.4 (C_2 or C_3), 134.4 (C_6 or C_7), 134.5 (C_6 or C_7), 141.7 ($C_{1'}$), 145.1 (C_2 or C_3), 156.4 ($C_{1''}$), 179.1 (C_1 or C_4), 180.6 (C_1 or C_4); *m/z* (ESI^-) 405 ($[M-H]^-$, 100%); HRMS (ESI^+) $C_{22}H_{15}NNaO_5S^+$ ($[M+Na]^+$) requires 428.0563, found 428.0565.

***N*-(3-(3'',5''-Dimethylphenoxy)-1,4-dioxo-1,4-dihydronaphthalen-2-yl)benzenesulfonamide 98**



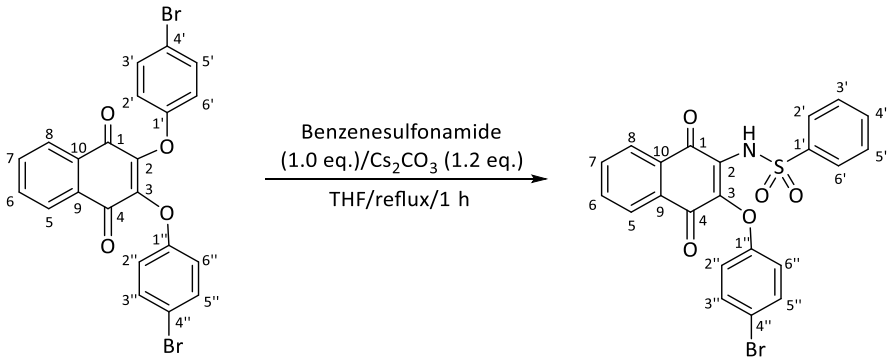
Following *General Procedure 4*, using naphthoquinone **92** (400 mg, 1.01 mmol), benzenesulfonamide (158 mg, 1.01 mmol) and Cs_2CO_3 (393 mg, 1.21 mmol) in THF (30 mL) and subsequent recrystallisation from toluene gave 2-sulfonamidonaphthoquinone **98** as an orange-brown solid (248 mg, 57%). mp 218-223 ^{o}C (toluene); HPLC t_R 18 min, 96%; υ_{max} (thin film) 3242 (N-H), 1662 (C=O), 1641 (C=O), 1613 1592; δ_H (500 MHz, $CDCl_3$) 2.22 (6H, s, 2 x Ar-*Me*), 6.28 (2H, s, $H_{2''}$ and $H_{6''}$), 6.66 (1H, s, $H_{4''}$), 7.32-7.37 (2H, m, $H_{3'}$ and $H_{5'}$), 7.43-7.49 (1H, m, $H_{4'}$), 7.72-7.77 (3H, m, H_6, H_7 and N*H*), 7.80-7.85 (2H, m, $H_{2'}$ and $H_{6'}$), 7.94-7.99 (1H, m, H_5), 8.12-8.18 (1H, m, H_8); δ_C (125 MHz, $CDCl_3$) 21.2 (2 x Ar-*Me*), 114.5 ($C_{2''}$ and $C_{6''}$), 125.3 ($C_{4''}$), 126.8 (C_5 or C_8), 126.9 (C_5 or C_8), 127.1 ($C_{2'}$ and $C_{6'}$), 128.5 ($C_{3'}$ and $C_{5'}$), 129.8 (C_{10}), 131.1 (C_9), 131.1 (C_2 or C_3), 132.7 ($C_{4'}$), 133.9 (C_7), 134.9 (C_6), 138.8 ($C_{3''}$ and $C_{5''}$), 140.1 ($C_{1'}$), 141.2 (C_2 or C_3), 156.0 ($C_{1''}$), 178.8 (C_1), 180.5 (C_4); *m/z* (ESI$^+$) 434 ([M+H]$^+$, 100%), 456 ([M+Na]$^+$, 60%); HRMS (ESI$^+$) $C_{24}H_{19}NNaO_5S^+$ ([M+Na]$^+$) requires 456.0876, found 456.0857.

***N*-(3-(3''-Formylphenoxy)-1,4-dioxo-1,4-dihydronaphthalen-2-yl)benzenesulfonamide 99**



Following *General Procedure 4*, using naphthoquinone **93** (400 mg, 1.01 mmol), benzenesulfonamide (158 mg, 1.01 mmol) and Cs_2CO_3 (393 mg, 1.21 mmol) in THF (30 mL) and subsequent recrystallisation from firstly toluene and then MeOH gave 2-sulfonamidonaphthoquinone **99** as a yellow solid (66 mg, 15%). mp 237-240 ^{o}C (MeOH); υ_{max} (thin film) 3242 (N-H), 1696 (C=O), 1655 (C=O), 1585; δ_H (500 MHz, $CDCl_3$) 7.03 (1H, dd, *J* 7.9, 1.9, $H_{6''}$), 7.09 (1H, s, $H_{2''}$), 7.32-7.38 (2H, m, $H_{3'}$ and $H_{5'}$), 7.40 (1H, app. t, *J* 7.9, $H_{5''}$), 7.43-7.47 (1H, m, $H_{4'}$), 7.57 (1H, d, *J* 7.9, $H_{4''}$), 7.74-7.81 (4H, m, H_6, H_7, $H_{2'}$ and $H_{6'}$), 7.87 (1H, s, N*H*), 7.93-7.97 (1H, m, H_5), 8.17-8.21 (1H, m, H_8), 9.91 (1H, s, C*H*O); δ_C (125 MHz, $CDCl_3$) 116.2 ($C_{2''}$), 123.2 ($C_{6''}$), 125.7 ($C_{4''}$), 126.8 ($C_{2'}$ and $C_{6'}$), 127.0 (C_5), 127.1 (C_8), 128.8 ($C_{3'}$ and $C_{5'}$), 129.7 (C_{10}), 129.9 ($C_{5''}$), 130.8 (C_9), 131.3 (C_2), 133.0 ($C_{4'}$), 134.2 (C_7), 135.2 (C_6), 137.4 ($C_{3''}$), 140.0 (C_3 or $C_{1'}$), 140.1 (C_3 or $C_{1'}$), 156.6 ($C_{1''}$), 178.5 (C_4), 180.2 (C_1), 191.2 (*C*HO); *m/z* (ESI$^-$) 432 ([M-H]$^-$, 100%); HRMS (ESI$^+$) $C_{23}H_{15}NNaO_6S^+$ ([M+Na]$^+$) requires 456.0512, found 456.0509.

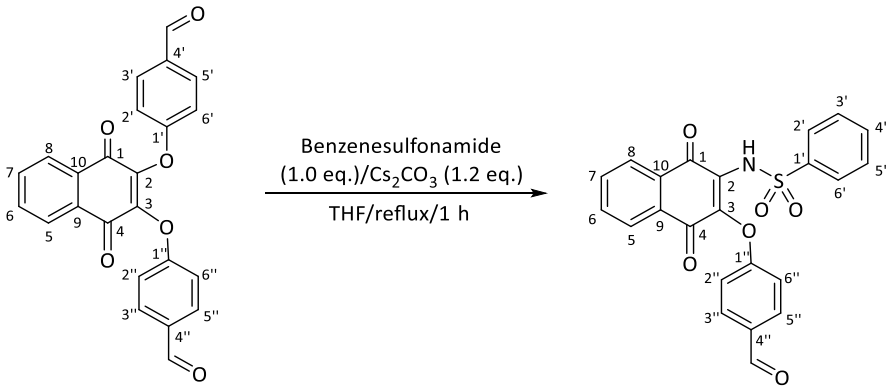
_N_-(3-(4''-Bromophenoxy)-1,4-dioxo-1,4-dihydronaphthalen-2-yl)benzenesulfonamide 100



Following *General Procedure 4*, using naphthoquinone **94** (400 mg, 0.800 mmol), benzenesulfonamide (126 mg, 0.800 mmol) and Cs_2CO_3 (313 mg, 0.960 mmol) in THF (30 mL) and subsequent recrystallisation from toluene gave 2-sulfonamidonaphthoquinone **100** as a yellow solid (210 mg, 43%). mp 215-218 ^{o}C (toluene); HPLC t_R 19 min, 97%; υ_{max} (thin film) 3251 (N-H), 1675 (C=O), 1649 (C=O), 1619; δ_H (500 MHz, $CDCl_3$) 6.57-6.62 (2H, m, $H_{2''}$ and $H_{6''}$), 7.29-7.34 (2H, m, $H_{3''}$ and $H_{5''}$), 7.36-7.42 (2H, m, $H_{3'}$ and $H_{5'}$), 7.48-7.53 (1H, m, $H_{4'}$), 7.72-7.84 (5H, m, H_6, H_7, $H_{2'}$, $H_{6'}$ and N*H*), 7.93-7.98 (1H, m, H_5), 8.13-8.18 (1H, m, H_8); δ_C (125 MHz, $CDCl_3$) 116.1 ($C_{4''}$), 118.7 ($C_{2''}$ and $C_{6''}$), 126.9 ($C_{2'}$ and $C_{6'}$), 126.9 (C_5 or C_8), 127.0 (C_5 or C_8),

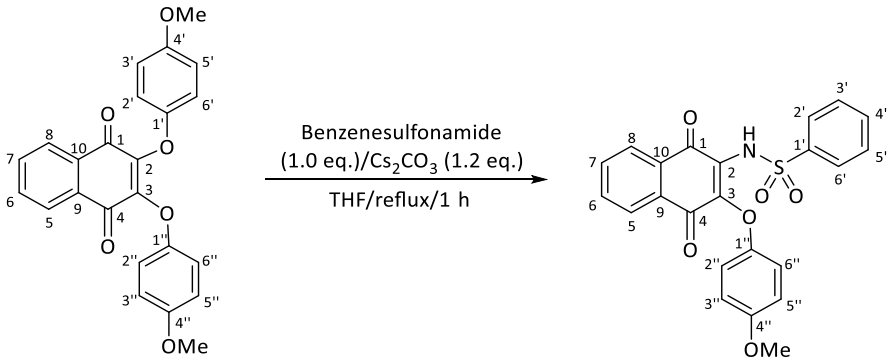
128.8 ($C_{3'}$ and $C_{5'}$), 129.7 (C_{10}), 130.9 (C_9), 131.0 (C_2), 132.1 ($C_{3''}$ and $C_{5''}$), 133.0 ($C_{4'}$), 134.1 (C_7), 135.1 (C_6), 140.2 ($C_{1'}$), 140.4 (C_3), 155.0 ($C_{1''}$), 178.5 (C_4), 180.3 (C_1); *m/z* (ESI^-) 482 ([M(^{79}Br)-H]$^-$, 100%), 484 ([M(^{81}Br)-H]$^-$, 100%); HRMS (ESI^+) $C_{22}H_{14}BrNNaO_5S^+$ ([M(^{81}Br)+Na]$^+$) requires 507.9649, found 507.9666.

_N_-(3-(4''-Formylphenoxy)-1,4-dioxo-1,4-dihydronaphthalen-2-yl)benzenesulfonamide 101



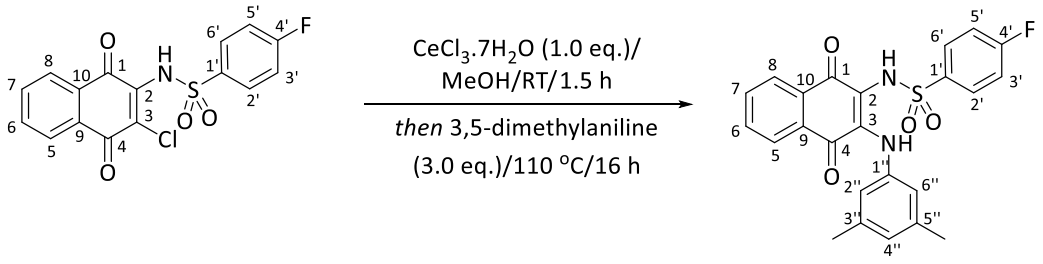
Following *General Procedure 4*, using naphthoquinone **95** (350 mg, 0.879 mmol), benzenesulfonamide (138 mg, 0.879 mmol) and Cs_2CO_3 (344 mg, 1.055 mmol) in THF (30 mL) for 16 h and subsequent recrystallisation from toluene gave 2-sulfonamidonaphthoquinone **101** as a yellow solid (89 mg, 23%). mp 190-193 ^oC (toluene); υ_{max} (thin film) 3300 (N-H), 1671 (C=O), 1652 (C=O), 1633, 1589; δ_H (500 MHz, $CDCl_3$) 6.80-6.84 (2H, m, $H_{2''}$ and $H_{6''}$), 7.37-7.42 (2H, m, $H_{3'}$ and $H_{5'}$), 7.48-7.53 (1H, m, $H_{4'}$), 7.75-7.81 (6H, m, H_6, H_7, $H_{2'}$, $H_{6'}$, $H_{3''}$ and $H_{5''}$), 7.89 (1H, s, N*H*), 7.94-8.00 (1H, m, H_5), 8.16-8.21 (1H, m, H_8), 9.92 (1H, s, C*H*O); δ_C (125 MHz, $CDCl_3$) 117.4 ($C_{2''}$ and $C_{6''}$), 126.8 ($C_{2'}$ and $C_{6'}$), 127.0 (C_5), 127.1 (C_8), 128.9 ($C_{3'}$ and $C_{5'}$), 129.6 (C_{10}), 130.8 (C_9), 131.2 (C_2 or C_3), 131.3 ($C_{3''}$ and $C_{5''}$), 132.0 ($C_{4''}$), 133.1 ($C_{4'}$), 134.3 (C_7), 135.3 (C_6), 139.7 (C_2 or C_3), 140.1 ($C_{1'}$), 160.6 ($C_{1''}$), 178.2 (C_4), 180.2 (C_1), 190.6 (*C*HO); *m/z* (ESI^-) 432 ([M-H]$^-$, 100%); HRMS (ESI^+) $C_{23}H_{15}NNaO_6S^+$ ([M+Na]$^+$) requires 456.0512, found 456.0506.

N-(3-(4''-Methoxyphenoxy)-1,4-dioxo-1,4-dihydronaphthalen-2-yl)benzenesulfonamide 102



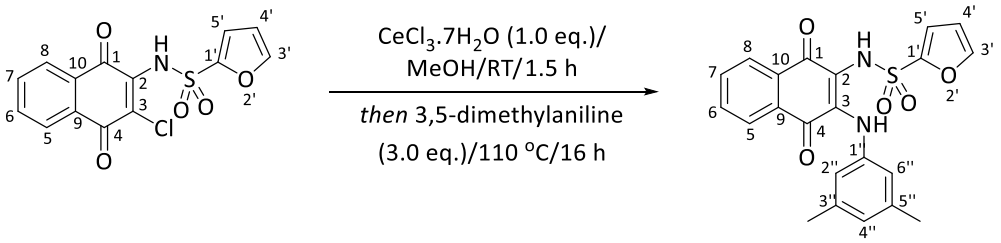
Following *General Procedure 4*, using naphthoquinone **96** (402 mg, 1.00 mmol), benzenesulfonamide (157 mg, 1.00 mmol) and Cs_2CO_3 (391 mg, 1.20 mmol) in THF (30 mL) and subsequent recrystallisation from firstly toluene and then MeOH gave 2-sulfonamidonaphthoquinone **102** as a yellow solid (160 mg, 37%). mp 210-216 ^{o}C (MeOH); υ_{max} (thin film) 3247 (N-H), 1669 (C=O), 1643 (C=O), 1592; δ_H (500 MHz, $CDCl_3$) 3.77 (3H, s, O*Me*), 6.63-6.68 (2H, m, $H_{2''}$ and $H_{6''}$ or $H_{3''}$ and $H_{5''}$), 6.71-6.75 (2H, m, $H_{2''}$ and $H_{6''}$ or $H_{3''}$ and $H_{5''}$), 7.34-7.39 (2H, m, $H_{3'}$ and $H_{5'}$), 7.45-7.50 (1H, m, $H_{4'}$), 7.70-7.75 (2H, m, H_6 and H_7), 7.76 (1H, s, N*H*), 7.80-7.84 (2H, m, $H_{2'}$ and $H_{6'}$), 7.92-7.96 (1H, m, H_5), 8.12-8.16 (1H, m, H_8); δ_C (125 MHz, $CDCl_3$) 55.5 (O*Me*), 114.2 ($C_{2''}$ and $C_{6''}$ or $C_{3''}$ and $C_{5''}$), 117.9 ($C_{2''}$ and $C_{6''}$ or $C_{3''}$ and $C_{5''}$), 126.8 (C_5), 126.8 (C_8), 127.0 ($C_{2'}$ and $C_{6'}$), 128.6 ($C_{3'}$ and $C_{5'}$), 129.7 (C_{10}), 130.8 (C_9), 131.0 (C_2 or C_3), 132.8 ($C_{4'}$), 133.9 (C_7), 134.9 (C_6), 140.3 ($C_{1'}$), 141.6 (C_2 or C_3), 149.9 ($C_{1''}$), 155.7 ($C_{4''}$), 178.9 (C_4), 180.5 (C_1); *m/z* (ESI$^-$) 434 ([M-H]$^-$, 100%); HRMS (ESI$^+$) $C_{23}H_{17}NNaO_6S^+$ ([M+Na]$^+$) requires 458.0669, found 458.0651.

***N*-(3-((3'',5''-Dimethylphenyl)amino)-1,4-dioxo-1,4-dihydronaphthalen-2-yl)-4'-fluorobenzenesulfonamide 117**



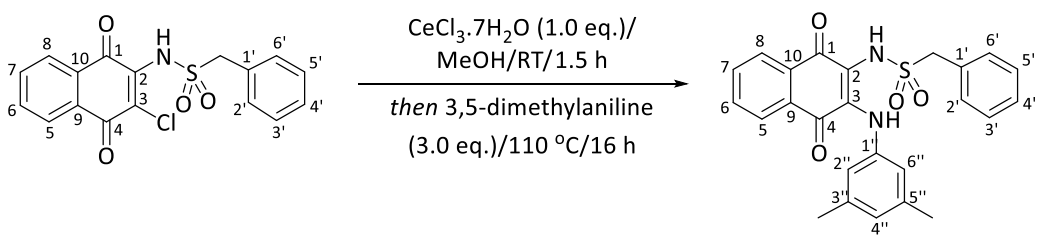
Following *General Procedure 2*, using naphthoquinone **130** (200 mg, 0.55 mmol), 3,5-dimethylaniline (205 µL, 1.64 mmol) and cerium trichloride heptahydrate (204 mg, 0.55 mmol) in MeOH (10 mL) at 110 °C. Purification *via* column chromatography on silica gel (eluent pet ether:acetone 80:20) and subsequent recrystallisation from boiling toluene gave 3-anilinonaphthoquinone **117** as a red solid (146 mg, 59%). mp 211-217 °C (toluene); HPLC t_R 22 min, 96%; υ_{max} (thin film) 3278 (N-H), 1674 (C=O), 1595, 1574; δ_H (500 MHz, $CDCl_3$) 2.32 (6H, s, 2 x Ar-*Me*), 6.67 (2H, s, $H_{2''}$ and $H_{6''}$), 6.77 (1H, s, sulfonamide-N*H*), 6.84 (1H, s, $H_{4''}$), 6.98-7.03 (2H, m, $H_{3'}$ and $H_{5'}$), 7.65-7.73 (4H, m, H_6, H_7, $H_{2'}$ and $H_{6'}$), 7.91-7.94 (1H, m, H_8), 7.97 (1H, s, aniline-N*H*), 8.07-8.10 (1H, m, H_5); δ_F (470 MHz, $CDCl_3$) -104.5 (1F, s, Ar-*F*); δ_C (125 MHz, $CDCl_3$) 21.3 (2 x Ar-*Me*), 112.8 (C_2), 115.9 (d, *J* 11.5, $C_{3'}$ and $C_{5'}$), 121.1 ($C_{2''}$ and $C_{6''}$), 126.4 (C_8), 126.9 (C_5 or $C_{4''}$), 127.0 (C_5 or $C_{4''}$), 130.1 (d, *J* 9.5, $C_{2'}$ and $C_{6'}$), 130.4 (C_9), 131.4 (C_{10}), 133.1 (C_6), 134.9 (C_7), 135.0 (d, *J* 2.8, $C_{1'}$), 137.1 ($C_{1''}$), 138.0 ($C_{3''}$ and $C_{5''}$), 139.1 (C_3), 165.2 (d, *J* 255.1, $C_{4'}$), 179.2 (C_1), 181.9 (C_4); *m/z* (ESI^-) 449 ($[M-H]^-$, 100%); HRMS (ESI^-) $C_{24}H_{18}FN_2O_4S^-$ ($[M-H]^-$) requires 449.0977, found 449.0967.

***N*-(3-((3'',5''-Dimethylphenyl)amino)-1,4-dioxo-1,4-dihydronaphthalen-2-yl)furan-2'-sulfonamide 118**



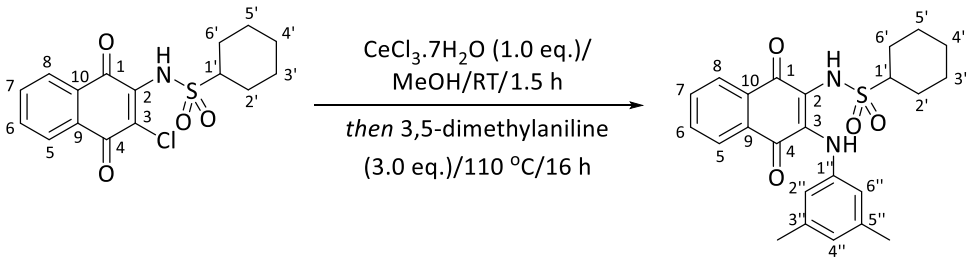
Following *General Procedure 2*, using naphthoquinone **132** (200 mg, 0.49 mmol), 3,5-dimethylaniline (222 µL, 1.78 mmol) and cerium trichloride heptahydrate (222 mg, 0.49 mmol) in MeOH (5 mL) at 110 ^{o}C. Purification *via* column chromatography on silica gel (eluent pet ether:acetone 90:10) and subsequent recrystallisation from boiling toluene gave 3-anilinonaphthoquinone **118** as a red solid (164 mg, 66%). mp 205-206 ^{o}C (toluene); HPLC t_R 23 min, 96%; υ_{max} (thin film) 3273 (N-H), 1674 (C=O), 1596, 1572, 1529; δ_H (500 MHz, $CDCl_3$) 2.34 (6H, s, 2 x Ar-*Me*), 6.34 (1H, dd, *J* 3.5, 1.6, $H_{4'}$), 6.73 (2H, s, $H_{2''}$ and $H_{6''}$), 6.78 (1H, s, sulfonamide-N*H*), 6.84 (1H, dd, *J* 3.5, 0.7, $H_{5'}$), 6.86 (1H, s, $H_{4''}$),7.43 (1H, dd, *J* 1.6, 0.7, $H_{3'}$), 7.68 (1H, app. td, *J* 7.6, 1.3, H_6), 7.72 (1H, app. td, *J* 7.6, 1.3, H_7), 7.95 (1H, s, aniline-N*H*), 7.98 (1H, dd, *J* 7.6, 1.3, H_8), 8.11 (1H, dd, *J* 7.6, 1.3, H_5); δ_C (125 MHz, $CDCl_3$) 21.4 (2 x Ar-*Me*), 111.1 (C_2), 111.5 ($C_{4'}$), 116.7 ($C_{5'}$), 121.6 ($C_{2''}$ and $C_{6''}$), 126.4 (C_8), 127.0 (C_5), 127.4 ($C_{4''}$), 130.4 (C_9), 131.6 (C_{10}), 133.0 (C_6), 135.0 (C_7), 136.8 ($C_{1''}$), 137.9 ($C_{3''}$ and $C_{5''}$), 139.8 (C_3), 146.3 ($C_{3'}$), 147.7 ($C_{1'}$), 179.5 (C_1), 181.9 (C_4); *m/z* (ESI$^+$) 445 ([M+Na]$^+$, 100%); HRMS (ESI$^+$) $C_{22}H_{18}N_2NaO_5S^+$ ([M+Na]$^+$) requires 445.0829, found 445.0819.

***N*-(3-((3'',5''-Dimethylphenyl)amino)-1,4-dioxo-1,4-dihydronaphthalen-2-yl)-α-toluenesulfonamide 119**



Following *General Procedure 2*, using naphthoquinone **131** (100 mg, 0.28 mmol), 3,5-dimethylaniline (103 µL, 0.83 mmol) and cerium trichloride heptahydrate (103 mg, 0.28 mmol) in MeOH (5 mL) at 110 ^{o}C. Purification *via* column chromatography on silica gel (eluent pet ether:acetone 85:15) and subsequent recrystallisation from boiling toluene gave 3-anilinonaphthoquinone **119** as a red solid (66 mg, 53%). mp 152-156 ^{o}C (toluene); HPLC t_R 25 min, 96%; υ_{max} (thin film) 3279 (N-H), 1708 (C=O), 1671 (C=O), 1595, 1571, 1523; δ_H (500 MHz, DMSO-d_6) 2.22 (6H, s, 2 x Ar-*Me*), 4.05 (2H, s, CH_2Ph), 6.70 (1H, s, $H_{4''}$), 6.72 (2H, s, $H_{2''}$ and $H_{6''}$), 7.22-7.26 (2H, m, $H_{2'}$ and $H_{6'}$), 7.28-7.33 (3H, m, $H_{3'}$, $H_{4'}$ and $H_{5'}$), 7.81 (1H, app. td, *J* 7.6, 1.9, H_6), 7.89 (1H, app. td, *J* 7.6, 1.9, H_7), 8.03 (1H, dd, *J* 7.6, 1.9, H_5), 8.06 (1H, dd, *J* 7.6, 1.9, H_8), 8.54 (1H, s, sulfonamide-N*H*), 8.84 (1H, s, aniline-N*H*); δ_C (125 MHz, DMSO-d_6) 20.9 (2 x Ar-*Me*), 58.7 (*C*H_2Ph), 115.1 (C_2), 121.3 ($C_{2''}$ and $C_{6''}$), 125.4 ($C_{4''}$), 126.0 (C_5 or C_8), 126.2 (C_5 or C_8), 128.0 ($C_{4'}$), 128.2 ($C_{3'}$ and $C_{5'}$), 129.6 ($C_{1'}$), 130.5 (C_9), 130.9 ($C_{2'}$ and $C_{6'}$), 131.8 (C_{10}), 133.1 (C_6), 134.9 (C_7), 136.7 ($C_{3''}$ and $C_{5''}$), 138.3 ($C_{1''}$), 141.1 (C_3), 179.6 (C_1), 182.3 (C_4); *m/z* (ESI$^-$) 445 ([M-H]$^-$, 100%); HRMS (ESI$^+$) $C_{25}H_{22}N_2NaO_4S^+$ ([M+Na]$^+$) requires 469.1192, found 469.1190.

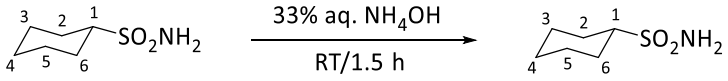
_N_-(3-((3'',5''-Dimethylphenyl)amino)-1,4-dioxo-1,4-dihydronaphthalen-2-yl)cyclohexanesulfonamide 120



Following *General Procedure 2*, using naphthoquinone **125** (100 mg, 0.28 mmol), 3,5-dimethylaniline (106 µL, 0.85 mmol) and cerium trichloride heptahydrate (105 mg, 0.28 mmol) in MeOH (5 mL) at 110 ^{o}C. Purification *via* column chromatography on silica gel (eluent pet ether:acetone 90:10) and subsequent recrystallisation from boiling toluene gave 3-anilinonaphthoquinone **120** as a red solid (40 mg, 32%). mp 192-197 ^{o}C (toluene); HPLC

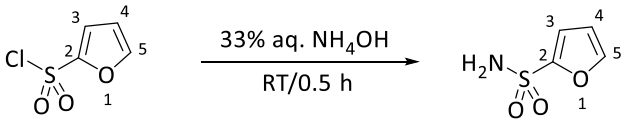
t_R 20 min, 97%; υ_{max} (thin film) 3280 (N-H), 2932 (C-H), 2857 (C-H), 1711 (C=O), 1670 (C=O), 1612, 1598, 1573, 1522; δ_H (500 MHz, $CDCl_3$) 0.98-1.17 (3H, m, $H_{3'}$(ax), $H_{4'}$(ax) and $H_{5'}$(ax)), 1.41 (2H, qd, *J* 12.1, 3.2, $H_{2'}$(ax) and $H_{6'}$(ax)), 1.62 (1H, app. d, *J* 12.6, $H_{4'}$(equ)), 1.77-1.83 (2H, m, $H_{3'}$(equ) and $H_{5'}$(equ)), 2.02 (2H, app. d, *J* 12.1, $H_{2'}$(equ) and $H_{6'}$(equ)), 2.14 (1H, tt, *J* 12.1, 4.3, $H_{1'}$(ax)), 2.32 (6H, s, 2 x Ar-*Me*), 6.53 (1H, s, sulfonamide-N*H*), 6.69 (2H, s, $H_{2''}$ and $H_{6''}$), 6.85 (1H, s, $H_{4''}$), 7.69 (1H, app. td, *J* 7.6, 1.3, H_6), 7.76 (1H, app. td, *J* 7.6, 1.3, H_7), 7.81 (1H, s, aniline-N*H*), 8.10 (1H, dd, *J* 7.6, 1.3, H_5), 8.15 (1H, dd, *J* 7.6, 1.3, H_8); δ_C (125 MHz, $CDCl_3$) 21.3 (2 x Ar-*Me*), 25.0 ($C_{3'}$ and $C_{5'}$), 25.0 ($C_{4'}$), 25.8 ($C_{2'}$ and $C_{6'}$), 61.4 ($C_{1'}$), 115.0 (C_2), 121.1 ($C_{2''}$ and $C_{6''}$), 126.7 (C_5 or C_8), 126.8 ($C_{4''}$), 126.9 (C_5 or C_8), 130.5 (C_9), 131.7 (C_{10}), 133.1 (C_6), 134.8 (C_7), 136.8 (C_3 or $C_{1''}$), 137.0 (C_3 or $C_{1''}$), 138.1 ($C_{3''}$ and $C_{5''}$), 180.1 (C_1), 182.1 (C_4); *m/z* (ESI^-) 303 (40%), 437 ($[M-H]^-$, 100%), 438 (40%); HRMS (ESI^-) $C_{24}H_{25}N_2O_4S^-$ ($[M-H]^-$) requires 437.1541, found 437.1536.

Cyclohexenesulfonamide 123[373]



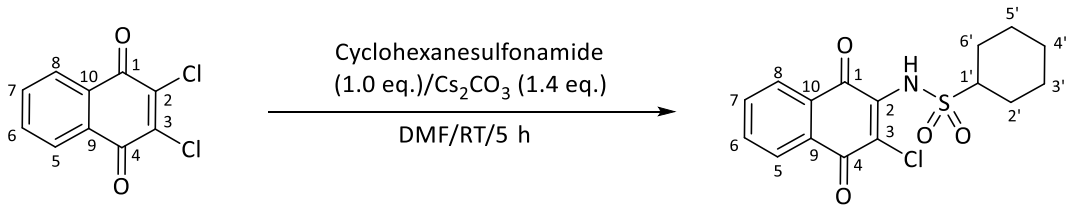
To a solution of 33% ammonia in water (12 mL), cyclohexenesulfonyl chloride **121** (580 µL, 4.00 mmol) was added dropwise over a period of 10 min at RT whilst the solution was stirred continuously. The solution was then left to stir at RT for a further 90 min before 1 M aq. HCl was added dropwise until the *p*H of the solution was *c.* 7. The organic product was then extracted into EtOAc (30 mL) and concentrated *in vacuo* to give sulfonamide **123** as a white solid (592 mg, 91%). mp 165-167 ^oC (lit. 94-95 ^oC);[373] δ_H (400 MHz, $CDCl_3$) 1.14-1.38 (3H, m, H_3(ax), H_4(ax) and H_5(ax)), 1.51 (2H, qd, *J* 12.2, 3.0, H_2(ax) and H_6(ax)), 1.74 (1H, app. d, *J* 12.2, H_4(equ)), 1.92 (2H, dt, *J* 13.4, 3.0, H_3(equ) and H_5(equ)), 2.25 (2H, app. d, *J* 12.2, H_2(equ) and H_6(equ)), 2.93 (1H, tt, *J* 12.2, 3.4, H_1(ax)), 4.58 (2H, br. s, NH_2); *m/z* (ESI^+) 186 ($[M+Na]^+$, 100%), 218 (70%), 349 ($[2M+Na]^+$, 85%).

Furan-2-sulfonamide 124[374]



To a solution of 33% ammonia in water (12 mL), furan-2-sulfonyl chloride **122** (600 mg, 3.60 mmol) was added dropwise over a period of 15 min at 0 °C whilst the solution was stirred continuously. The solution was then stirred at RT for a further 30 min before 1 M aq. HCl was added dropwise until the *p*H of the solution was *c.* 7. The organic product was then extracted into EtOAc (30 mL) and concentrated *in vacuo* to give sulfonamide **124** as a white solid (520 mg, quant.). mp 118-119 °C (lit. 120-122 °C)[374]; δ_H (500 MHz, DMSO-d_6) 6.64 (1H, dd, *J* 3.4, 1.7, H_4), 6.96 (1H, dd, *J* 3.4, 0.7, H_3), 7.74 (2H, s, NH_2), 7.91-7.93 (1H, m, H_5); *m/z* (ESI^-) 146 ($[M-H]^-$, 100%).

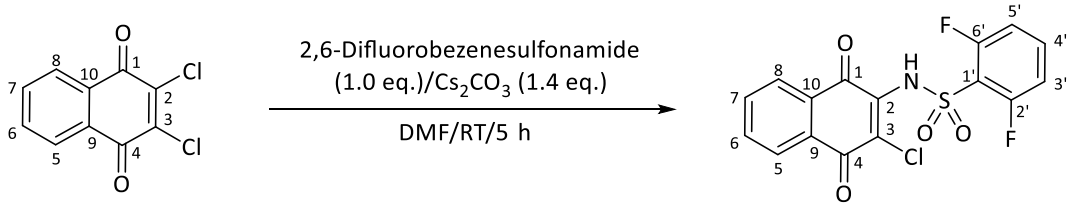
***N*-(3-Chloro-1,4-dioxo-1,4-dihydronaphthalen-2-yl)-cyclohexanesulfonamide 125**



Following *General Procedure 1*, using naphthoquinone **37** (400 mg, 1.76 mmol), cyclohexanesulfonamide **123** (287 mg, 1.76 mmol) and Cs_2CO_3 (804 mg, 2.46 mmol) in DMF (5 mL). Purification *via* column chromatography on silica gel (eluent pet ether:acetone 90:10 to 75:25 then pet ether:EtOAc 80:20 to 50:50) gave sulfonamide **125** as a yellow solid (396 mg, 64%). mp 178-179 °C; υ_{max} (thin film) 3254 (N-H), 2931 (C-H), 2856 (C-H), 1679 (C=O), 1595, 1573; δ_H (500 MHz, $CDCl_3$) 1.24-1.34 (1H, m, $H_{4'}$(ax)), 1.44 (2H, qt, *J* 12.9, 3.4, $H_{3'}$(ax) and $H_{5'}$(ax)), 1.71 (2H, qd, *J* 12.9, 3.4, $H_{2'}$(ax) and $H_{6'}$(ax)), 1.76-1.82 (1H, m, $H_{4'}$(equ)), 1.99 (2H, dt, *J* 12.9, 3.4, $H_{3'}$(equ) and $H_{5'}$(equ)), 2.37 (2H, app. d, *J* 12.6, $H_{2'}$(equ) and $H_{6'}$(equ)), 4.14 (1H, tt, *J* 12.9, 3.4, $H_{1'}$(ax)), 6.93 (1H, s, N*H*), 7.76-7.82 (2H, m, H_6 and H_7), 8.12-8.14 (1H, m, H_8), 8.17-8.19 (1H, m, H_5); δ_C (125 MHz, $CDCl_3$) 25.0 ($C_{3'}$ and $C_{5'}$), 25.0 ($C_{4'}$), 26.4 ($C_{2'}$ and $C_{6'}$), 64.0 ($C_{1'}$),

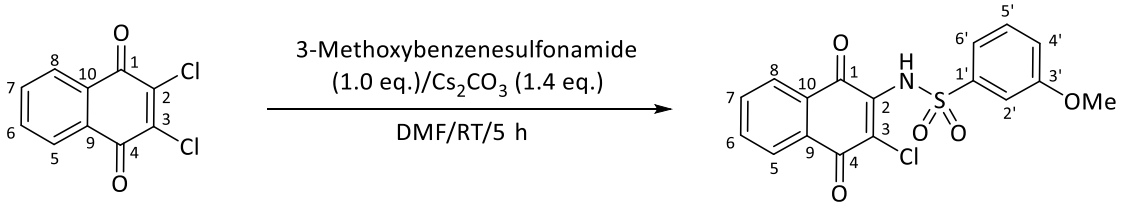
127.3 (C_5 or C_8), 127.4 (C_5 or C_8), 128.8 (C_3), 130.4 (C_{10}), 131.0 (C_9), 134.2 (C_7), 134.8 (C_6), 141.1 (C_2), 177.0 (C_4), 178.6 (C_1); *m/z* (ESI^-) 352 ([M(^{35}Cl)-H]$^-$, 100%), 354 ([M(^{37}Cl)-H]$^-$, 33%); HRMS (ESI^+) $C_{16}H_{16}ClNNaO_4S^+$ ([M(^{35}Cl)+Na]$^+$) requires 376.0381, found 376.0366.

N-(3-Chloro-1,4-dioxo-1,4-dihydronaphthalen-2-yl)-2',6'-difluorobenzenesulfonamide 126



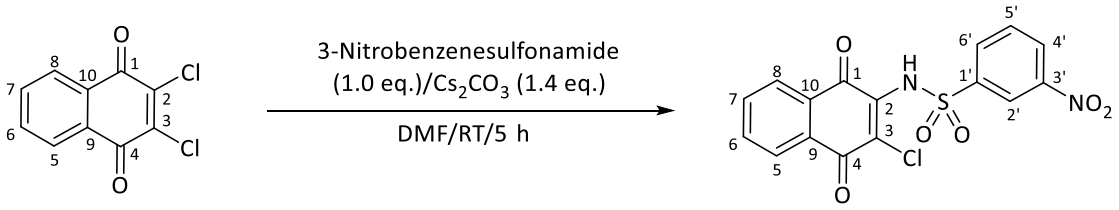
Following *General Procedure 1*, using naphthoquinone **37** (500 mg, 2.20 mmol), 2,6-difluorobenzenesulfonamide (425 mg, 2.20 mmol) and Cs_2CO_3 (1000 mg, 3.08 mmol) in DMF (5 mL). Purification *via* column chromatography on silica gel (eluent pet ether:acetone 70:30) gave sulfonamide **126** as a yellow solid (620 mg, 67%). mp 261-267 ^oC; υ_{max} (thin film) 3444 (N-H), 1657 (C=O), 1611 (C=O), 1588, 1515; δ_H (500 MHz, DMSO-d_6) 7.09-7.13 (2H, m, $H_{3'}$ and $H_{5'}$), 7.45-7.52 (1H, m, $H_{4'}$), 7.70 (1H, app. td, *J* 7.5, 1.4, H_6 or H_7), 7.78 (1H, app. td, *J* 7.5, 1.4, H_6 or H_7), 7.82 (1H, dd, *J* 7.5, 1.4, H_5 or H_8), 7.95 (1H, dd, *J* 7.5, 1.4, H_5 or H_8), 7.96 (1H, s, N*H*); δ_F (470 MHz, DMSO-d_6) -108.8 (2F, s, Ar-*F*); δ_C (125 MHz, DMSO-d_6) 112.4 (dd, *J* 22.4, 4.8, $C_{3'}$ and $C_{5'}$), 125.1 (m, $C_{1'}$), 125.6 (C_5 or C_8), 126.3 (C_5 or C_8), 126.5 (C_2 or C_3), 129.4 (C_2 or C_3), 130.8 (C_9 or C_{10}), 131.6 (m, $C_{4'}$), 131.8 (C_9 or C_{10}), 132.7 (C_6 or C_7), 134.0 (C_6 or C_7), 158.1 (dd, *J* 252.3, 5.2, $C_{2'}$ and $C_{6'}$), 176.6 (C_1 or C_4), 180.1 (C_1 or C_4); *m/z* (ESI^-) 382 ([M(^{35}Cl)-H]$^-$, 100%), 384 ([M(^{37}Cl)-H]$^-$, 50%); HRMS (ESI^-) $C_{16}H_7ClF_2NO_4S^-$ ([M(^{35}Cl)-H]$^-$) requires 381.9758, found 381.9765.

N-(3-Chloro-1,4-dioxo-1,4-dihydronaphthalen-2-yl)-3'-methoxybenzenesulfonamide 127



Following *General Procedure 1*, using naphthoquinone **37** (500 mg, 2.20 mmol), 3-methoxybenzenesulfonamide (412 mg, 2.20 mmol) and Cs_2CO_3 (1000 mg, 3.08 mmol) in DMF (5 mL). Purification *via* column chromatography on silica gel (eluent pet ether:acetone 80:20 to 50:50) gave sulfonamide **127** as a yellow solid (823 mg, quant.). mp 164-166 ^{o}C; υ_{max} (thin film) 3237 (N-H), 1668 (C=O), 1595; δ_H (500 MHz, DMSO-d_6) 3.82 (3H, s, O*Me*), 7.16-7.21 (1H, m, $H_{4'}$ or $H_{6'}$), 7.47-7.51 (3H, m, $H_{3'}$, $H_{5'}$ and $H_{4'}$ or $H_{6'}$), 7.82 (1H, app. td, *J* 7.3, 1.6, H_6 or H_7), 7.86 (1H, app. td, *J* 7.3, 1.6, H_6 or H_7), 7.95 (1H, dd, *J* 7.3, 1.6, H_5 or H_8), 8.03 (1H, dd, *J* 7.3, 1.6, H_5 or H_8); δ_C (125 MHz, DMSO-d_6) 55.5 (O*Me*), 111.3 ($C_{2'}$), 117.8 ($C_{4'}$ or $C_{6'}$), 118.3 ($C_{4'}$ or $C_{6'}$), 126.3 (C_5 or C_8), 126.6 (C_5 or C_8), 129.9 ($C_{5'}$), 130.6 (C_9 or C_{10}), 131.1 (C_9 or C_{10}), 133.9 (C_6 or C_7), 134.4 (C_6 or C_7), 143.5 (C_2 or C_3), 144.8 ($C_{1'}$), 159.0 ($C_{3'}$), 162.4 (C_2 or C_3), 177.0 (C_1 or C_4), 179.0 (C_1 or C_4); *m/z* (ESI$^-$) 376 ([M(^{35}Cl)-H]$^-$, 100%), 378 ([M(^{37}Cl)-H]$^-$, 40%); HRMS (ESI$^+$) $C_{17}H_{12}ClNNaO_5S^+$ ([M(^{35}Cl)+Na]$^+$) requires 400.0017, found 400.0012.

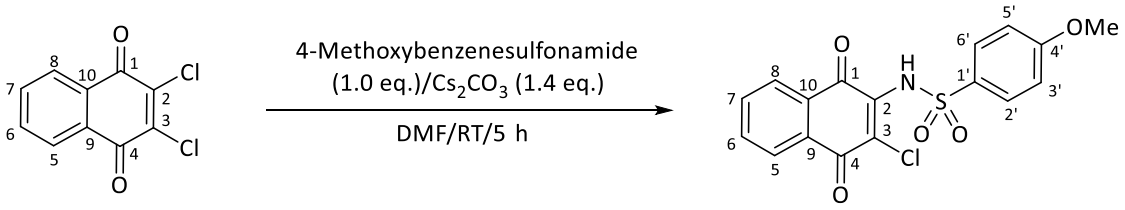
_N_-(3-Chloro-1,4-dioxo-1,4-dihydronaphthalen-2-yl)-3'-nitrobenzenesulfonamide 128



Following *General Procedure 1*, using naphthoquinone **37** (500 mg, 2.20 mmol), 3-nitrobenzenesulfonamide (445 mg, 2.20 mmol) and Cs_2CO_3 (1.00 g, 3.08 mmol) in DMF (5 mL). Purification *via* column chromatography on silica gel (eluent pet ether:acetone 80:20 to 50:50) gave sulfonamide **128** as a yellow solid (837 mg, quant.). mp 258-263 ^{o}C; υ_{max} (thin film) 3430 (N-H), 1678 (C=O), 1588, 1509; δ_H (500 MHz, DMSO-d_6) 7.71 (1H, app. td, *J* 7.6, 1.3, H_6 or H_7), 7.78 (1H, app. td, *J* 7.6, 1.3, H_6 or H_7), 7.79 (1H, app. t, *J* 8.1, $H_{5'}$), 7.88 (1H, dd, *J* 7.6, 1.3, H_5 or H_8), 7.96 (1H, dd, *J* 7.6, 1.3, H_5 or H_8), 8.28 (1H, ddd, *J* 8.1, 2.0, 0.9, $H_{4'}$ or $H_{6'}$), 8.32 (1H, ddd, *J* 8.1, 2.0, 0.9, $H_{4'}$ or $H_{6'}$), 8.66 (1H, app. t, *J* 2.0, $H_{2'}$); δ_C (125 MHz, DMSO-d_6) 120.1 ($C_{2'}$), 124.5 ($C_{4'}$ or $C_{6'}$), 125.5 (C_5 or C_8), 126.3 (C_5 or C_8), 130.1 ($C_{5'}$), 130.8 (C_9 or C_{10}), 131.7 ($C_{4'}$ or $C_{6'}$), 132.1 (C_9 or C_{10}), 132.5 (C_6 or C_7), 134.0 (C_6 or C_7), 147.3 ($C_{3'}$), 149.7 ($C_{1'}$), 176.3 (C_1 or C_4),

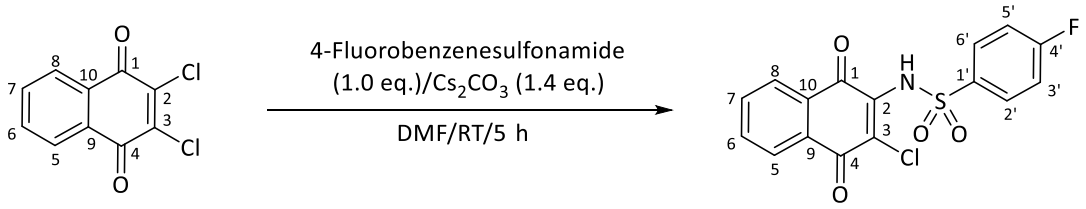
179.8 (C_1 or C_4), *C_2 and C_3 not observed*; *m/z* (ESI^-) 391 ([M(^{35}Cl)-H]$^-$, 100%), 393 ([M(^{37}Cl)-H]$^-$, 33%); HRMS (ESI^-) $C_{16}H_8ClN_2O_6S^-$ ([M(^{35}Cl)-H]$^-$) requires 390.9797, found 390.9801.

N-(3-Chloro-1,4-dioxo-1,4-dihydronaphthalen-2-yl)-4'-methoxybenzenesulfonamide 129



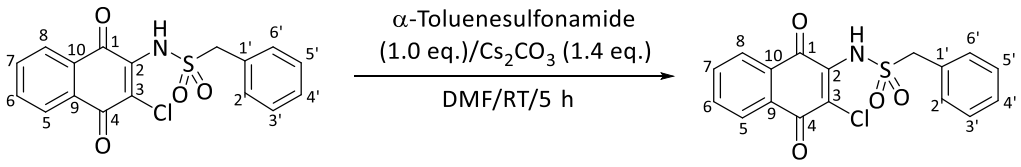
2,3-Dichloronaphthalene-1,4-dione **37** (500 mg, 2.20 mmol), 4-methoxybenzenesulfonamide (412 mg, 2.20 mmol) and Cs_2CO_3 (1.00 g, 3.08 mmol) were stirred in DMF (5 mL) in a microwave vial at RT for 16 h. 1 M aq. HCl (20 mL) was added and the organic product was extracted with EtOAc (3 x 20 mL) and washed with brine (3 x 20 mL). The precipitate formed in this organic layer was collected by suction filtration and washed with cold water (5 mL) and cold EtOAc (5 mL) to give sulfonamide **129** as a yellow solid (820 mg, quant.). mp 205-211 ^oC; υ_{max} (thin film) 3225 (N-H), 1666 (C=O), 1657 (C=O), 1610, 1595; δ_H (500 MHz, DMSO-d_6) 3.86 (3H, s, O*Me*), 7.13 (2H, d, *J* 9.0, $H_{3'}$ and $H_{5'}$), 7.85-7.91 (4H, m, H_6, H_7, $H_{2'}$ and $H_{6'}$) 7.96-8.00 (1H, m, H_5 or H_8), 8.04-8.08 (1H, m, H_5 or H_8), *NH not observed*; δ_C (125 MHz, DMSO-d_6) 55.7 (O*Me*), 114.0 ($C_{3'}$ and $C_{5'}$), 126.6 (C_5 or C_8), 126.7 (C_5 or C_8), 129.0 ($C_{2'}$ and $C_{6'}$), 130.5 (C_9 or C_{10}), 130.8 (C_9 or C_{10}), 133.3 ($C_{1'}$), 134.7 (C_3), 134.7 (C_6), 134.7 (C_7), 140.5 (C_2), 162.5 ($C_{4'}$), 177.6 (C_1 or C_4), 178.7 (C_1 or C_4); *m/z* (ESI^-) 376 ([M(^{35}Cl)-H]$^-$, 100%), 378 ([M(^{37}Cl)-H]$^-$, 40%); HRMS (ESI^+) $C_{17}H_{12}ClNNaO_5S^+$ ([M(^{35}Cl)+Na]$^+$) requires 400.0017, found 400.0003.

N-(3-Chloro-1,4-dioxo-1,4-dihydronaphthalen-2-yl)-4'-fluorobenzenesulfonamide 130



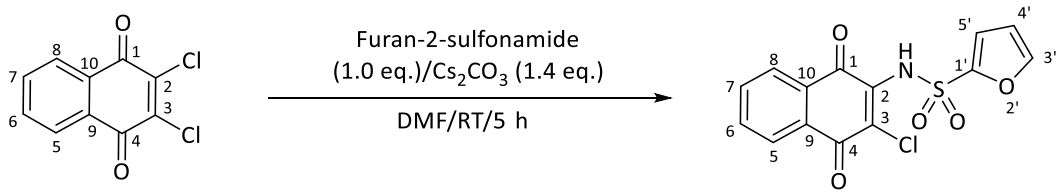
Following *General Procedure 1*, using naphthoquinone **37** (500 mg, 2.20 mmol), 4-fluorobenzenesulfonamide (386 mg, 2.20 mmol) and Cs_2CO_3 (1.00 g, 3.08 mmol) in DMF (5 mL). Purification *via* column chromatography on silica gel (eluent pet ether:acetone 75:25) gave sulfonamide **130** as a yellow solid (515 mg, 63%). mp >280 ^{o}C; υ_{max} (thin film) 1676 (C=O), 1591, 1543; δ_H (500 MHz, DMSO-d_6) 7.31 (2H, app. t, *J* 9.0, $H_{3'}$ and $H_{5'}$), 7.73 (1H, app. td, *J* 7.6, 1.4, H_6 or H_7), 7.79 (1H, app. td, *J* 7.6, 1.4, H_6 or H_7), 7.89 (1H, dd, *J* 7.6, 1.4, H_5 or H_8), 7.92-7.97 (3H, m, $H_{2'}$, $H_{6'}$ and H_5 or H_8); δ_F (470 MHz, DMSO-d_6) -110.4 (1F, s, Ar-*F*); δ_C (125 MHz, DMSO-d_6) 115.1 (d, *J* 21.9, $C_{3'}$ and $C_{5'}$), 125.6 (C_5 or C_8), 126.3 (C_5 or C_8), 128.3 (d, *J* 8.6, $C_{2'}$ and $C_{6'}$), 130.9 (C_9 or C_{10}), 132.1 (C_9 or C_{10}), 132.6 (C_6 or C_7), 134.0 (C_6 or C_7), 143.5 ($C_{1'}$), 162.9 (d, *J* 248.0, $C_{4'}$), 176.1 (C_1 or C_4), 179.7 (C_1 or C_4); *m/z* (ESI^-) 364 ([M(^{35}Cl)-H]$^-$, 100%), 366 ([M(^{37}Cl)-H]$^-$, 55%); HRMS (ESI^-) $C_{16}H_8ClFNO_4S^-$ ([M(^{35}Cl)-H]$^-$) requires 363.9852, found 363.9853.

_N_-(3-Chloro-1,4-dioxo-1,4-dihydronaphthalen-2-yl)-α-toluenesulfonamide 131



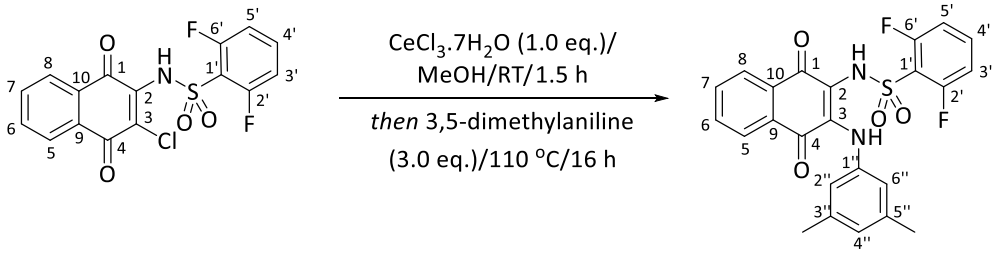
Following *General Procedure 1*, using naphthoquinone **37** (500 mg, 2.20 mmol), α-toluenesulfonamide (317 mg, 2.20 mmol) and Cs_2CO_3 (1.00 g, 3.08 mmol) in DMF (5 mL). Purification *via* column chromatography on silica gel (eluent pet ether:acetone 80:20) gave sulfonamide **131** as a yellow solid (643 mg, 81%). mp 176-179 ^{o}C; υ_{max} (thin film) 3259 (N-H), 1709 (C=O), 1663 (C=O); δ_H (500 MHz, $CDCl_3$) 4.92 (2H, s, CH_2Ph), 7.36-7.44 (3H, m, $H_{3'}$, $H_{4'}$ and $H_{5'}$), 7.47-7.51 (2H, m, $H_{2'}$ and $H_{6'}$), 7.90-7.94 (2H, m, H_6 and H_7), 8.06-8.09 (1H, m, H_5 or H_8), 8.09-8.13 (1H, m, H_5 or H_8); δ_C (125 MHz, $CDCl_3$) 60.5 (*C*H_2Ph), 126.6 (C_5 or C_8), 126.9 (C_5 or C_8), 128.2 (C_2 or C_3), 128.4 ($C_{3'}$ and $C_{5'}$), 128.4 ($C_{4'}$), 129.3 ($C_{1'}$), 130.7 (C_2 or C_3), 130.8 (C_9 or C_{10}), 130.9 (C_9 or C_{10}), 131.2 ($C_{2'}$ and $C_{6'}$), 134.5 (C_6 or C_7), 134.7 (C_6 or C_7), 177.4 (C_1 or C_4), 179.5 (C_1 or C_4); *m/z* (ESI^-) 360 ([M(^{35}Cl)-H]$^-$, 100%), 362 ([M(^{37}Cl)-H]$^-$, 33%); HRMS (ESI^+) $C_{17}H_{12}ClNNaO_4S^+$ ([M(^{35}Cl)+Na]$^+$) requires 384.0068, found 384.0068.

N-(3-Chloro-1,4-dioxo-1,4-dihydronaphthalen-2-yl)furan-2'-sulfonamide 132



Following *General Procedure 1*, using naphthoquinone **37** (500 mg, 2.20 mmol), furan-2-sulfonamide **124** (324 mg, 2.20 mmol) and Cs_2CO_3 (1.00 g, 3.08 mmol) in DMF (5 mL). Purification *via* column chromatography on silica gel (eluent pet ether:acetone 90:10 to 50:50) gave sulfonamide **132** as a yellow solid (634 mg, 85%). mp 259 ^{o}C; υ_{max} (thin film) 3388 (N-H), 1652 (C=O), 1590, 1560, 1514; δ_H (500 MHz, DMSO-d_6) 6.57 (1H, dd, *J* 3.1, 1.7, $H_{4'}$), 6.91 (1H, d, *J* 3.1, $H_{5'}$), 7.75-7.84 (3H, m, H_6, H_7 and $H_{3'}$), 7.94 (1H, dd, *J* 7.6, 1.3, H_5 or H_8), 7.99 (1H, dd, *J* 7.6, 1.3, H_5 or H_8); δ_C (125 MHz, DMSO-d_6) 110.7 ($C_{4'}$), 111.8 ($C_{5'}$), 125.8 (C_5 or C_8), 126.4 (C_5 or C_8), 130.8 (C_9 or C_{10}), 132.0 (C_9 or C_{10}), 133.0 (C_6 or C_7), 134.1 (C_6 or C_7), 144.6 ($C_{3'}$), 154.0 ($C_{1'}$), 176.5 (C_1 or C_4), 179.4 (C_1 or C_4), *C_2 and C_3 not observed*; *m/z* (ESI^-) 336 ([M(^{35}Cl)-H]$^-$, 100%), 338 ([M(^{37}Cl)-H]$^-$, 33%); HRMS (ESI^-) $C_{14}H_7ClNO_5S^-$ ([M(^{35}Cl)-H]$^-$) requires 335.9739, found 335.9748.

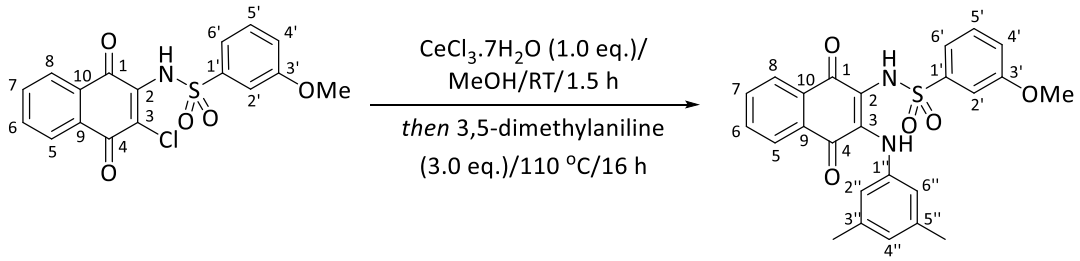
N-(3-((3'',5''-Dimethylphenyl)amino)-1,4-dioxo-1,4-dihydronaphthalen-2-yl)-2',6'-difluorobenzenesulfonamide 133



Following *General Procedure 2*, using naphthoquinone **126** (200 mg, 0.52 mmol), 3,5-dimethylaniline (195 µL, 1.57 mmol) and cerium trichloride heptahydrate (194 mg, 0.52 mmol) in MeOH (5 mL) at 110 ^{o}C. Purification *via* column chromatography on silica gel (eluent pet ether:EtOAc 85:15) and subsequent recrystallisation from boiling toluene gave 3-

anilinonaphthoquinone **133** as a red solid (81 mg, 33%). mp 222-225 ^{o}C (toluene); HPLC t_R 22 min, 98%; υ_{max} (thin film) 3347 (N-H), 3249 (N-H), 1679 (C=O), 1613 (C=O), 1588, 1564; δ_H (500 MHz, $CDCl_3$) 2.30 (6H, s, 2 x Ar-*Me*), 6.69 (2H, s, $H_{2''}$ and $H_{6''}$), 6.72 (1H, s, $H_{4''}$), 6.87-6.92 (2H, m, $H_{3'}$ and $H_{5'}$), 7.03 (1H, s, sulfonamide-N*H*), 7.37-7.43 (1H, m, $H_{4'}$), 7.67 (1H, app. td, *J* 7.5, 1.4, H_6), 7.71 (1H, app. td, *J* 7.5, 1.4, H_7), 7.87 (1H, s, aniline-N*H*), 8.00 (1H, dd, *J* 7.5, 1.4, H_8), 8.11 (1H, dd, *J* 7.5, 1.4, H_5); δ_F (470 MHz, $CDCl_3$) -106.6 (2F, s, Ar-*F*); δ_C (125 MHz, $CDCl_3$) 21.3 (2 x Ar-*Me*), 112.0 (C_2), 112.6 (dd, *J* 22.9, 3.9, $C_{3'}$ and $C_{5'}$), 118.2 (m, $C_{1'}$), 121.4 ($C_{2''}$ and $C_{6''}$), 126.6 (C_8), 126.9 (C_5), 127.4 ($C_{4''}$), 130.3 (C_9), 131.6 (C_{10}), 133.0 (C_6), 134.2 (m, $C_{4'}$), 134.9 (C_7), 136.3 ($C_{1''}$), 137.9 ($C_{3''}$ and $C_{5''}$), 138.8 (C_3), 159.3 (dd, *J* 258.5, 3.8, $C_{2'}$ and $C_{6'}$), 179.4 (C_1), 181.9 (C_4); *m/z* (ESI$^+$) 491 ([M+Na]$^+$, 100%); HRMS (ESI$^+$) $C_{24}H_{18}F_2N_2NaO_4S^+$ ([M+Na]$^+$) requires 491.0848, found 491.0842.

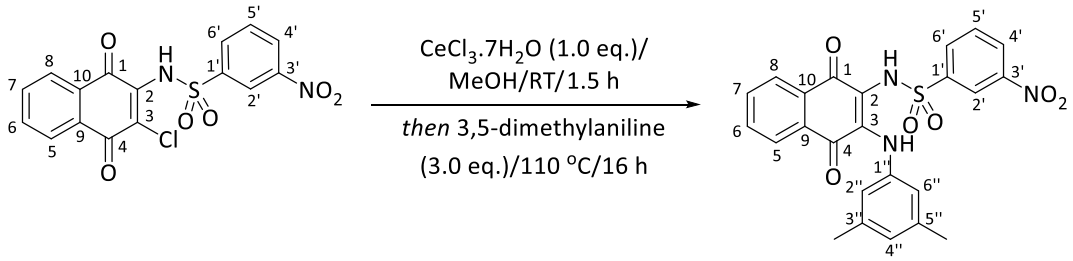
_N_-(3-((3'',5''-Dimethylphenyl)amino)-1,4-dioxo-1,4-dihydronaphthalen-2-yl)-3'-methoxybenzenesulfonamide 134



Following *General Procedure 2*, using naphthoquinone **127** (400 mg, 1.06 mmol), 3,5-dimethylaniline (395 µL, 3.18 mmol) and cerium trichloride heptahydrate (395 mg, 1.06 mmol) in MeOH (8 mL) at 110 ^{o}C. Purification *via* column chromatography on silica gel (eluent pet ether:EtOAc 85:15) gave 3-anilinonaphthoquinone **134** as a red solid (284 mg, 49%). mp 171-173 ^{o}C; υ_{max} (thin film) 3314 (N-H), 3232 (N-H), 1676 (C=O), 1599, 1574; δ_H (500 MHz, $CDCl_3$) 2.32 (6H, s, 2 x Ar-*Me*), 3.70 (3H, s, O*Me*), 6.66 (2H, s, $H_{2''}$ and $H_{6''}$), 6.80-6.83 (2H, m, $H_{4''}$ and sulfonamide-N*H*), 6.99 (1H, ddd, *J* 7.8, 2.4, 1.6, $H_{4'}$ or $H_{6'}$), 7.17 (1H, app. t, *J* 1.6, $H_{2'}$), 7.21-7.27 (2H, m, $H_{5'}$ and $H_{4'}$ or $H_{6'}$), 7.66 (1H, app. td, *J* 7.6, 1.5, H_6), 7.70 (1H, app. td, *J* 7.6, 1.5, H_7), 7.93 (1H, dd, *J* 7.6, 1.5, H_8), 7.97 (1H, s, aniline-N*H*), 8.08 (1H, dd, *J* 7.6, 1.5, H_5); δ_C (125 MHz,

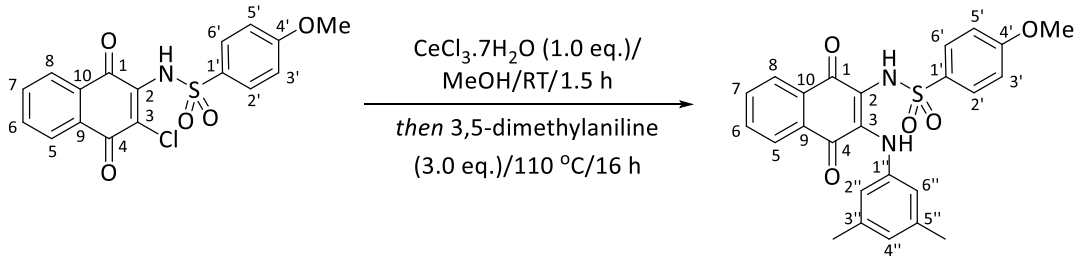
$CDCl_3$) 21.4 (2 x Ar-*Me*), 55.5 (O*Me*), 111.4 ($C_{2'}$), 113.5 (C_2), 119.5 ($C_{4'}$ or $C_{6'}$), 119.9 ($C_{4'}$ or $C_{6'}$), 121.0 ($C_{2''}$ and $C_{6''}$), 126.4 (C_8), 126.9 (C_5), 126.9 ($C_{4''}$), 129.7 ($C_{5'}$), 130.5 (C_9), 131.4 (C_{10}), 133.0 (C_6), 134.8 (C_7), 137.3 ($C_{1''}$), 138.0 ($C_{3''}$ and $C_{5''}$), 138.8 (C_3), 140.0 ($C_{1'}$), 159.5 ($C_{3'}$), 179.1 (C_1), 181.9 (C_4); *m/z* (ESI^-) 461 ($[M-H]^-$, 100%); HRMS (ESI^+) $C_{25}H_{22}N_2NaO_5S^+$ ($[M+Na]^+$) requires 485.1142, found 485.1122.

_N_-(3-((3'',5''-Dimethylphenyl)amino)-1,4-dioxo-1,4-dihydronaphthalen-2-yl)-3'-nitrobenzenesulfonamide 135



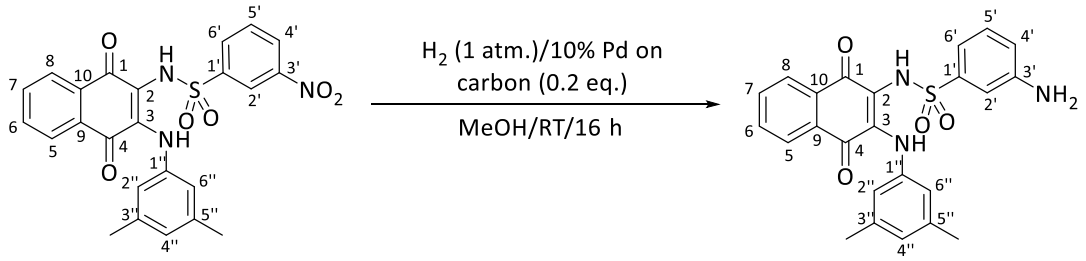
Following *General Procedure 2*, using naphthoquinone **128** (175 mg, 0.43 mmol), 3,5-dimethylaniline (162 µL, 1.23 mmol) and cerium trichloride heptahydrate (162 mg, 0.43 mmol) in MeOH (5 mL) at 110 °C. Purification *via* column chromatography on silica gel (eluent pet ether:EtOAc 80:20) gave 3-anilinonaphthoquinone **135** as a red solid (59 mg, 26%). mp 216-221 °C; HPLC t_R 22 min, 96%; υ_{max} (thin film) 3290 (N-H), 1708 (C=O), 1675 (C=O), 1596, 1573, 1529; δ_H (500 MHz, $CDCl_3$) 2.30 (6H, s, 2 x Ar-*Me*), 6.63 (2H, s, $H_{2''}$ and $H_{6''}$), 6.78 (1H, s, $H_{4''}$), 6.90 (1H, s, sulfonamide-N*H*), 7.55 (1H, app. t, *J* 8.0, $H_{5'}$), 7.68 (1H, app. td, *J* 7.6, 1.3, H_6), 7.72 (1H, app. td, *J* 7.6, 1.3, H_7), 7.89 (1H, s, aniline-N*H*), 7.93 (1H, dd, *J* 7.6, 1.3, H_8), 7.98-8.01 (1H, ddd, *J* 8.0, 1.9, 0.9, $H_{6'}$), 8.12 (1H, dd, *J* 7.6, 1.3, H_5), 8.30 (1H, ddd, *J* 8.0, 1.9, 0.9, $H_{4'}$), 8.45 (1H, app. t, *J* 1.9, $H_{2'}$); δ_C (125 MHz, $CDCl_3$) 21.3 (2 x Ar-*Me*), 112.0 (C_2), 121.0 ($C_{2''}$ and $C_{6''}$), 122.5 ($C_{2'}$), 126.5 (C_8), 127.0 (C_5), 127.1 ($C_{4'}$ or $C_{4''}$), 127.3 ($C_{4'}$ or $C_{4''}$), 129.7 ($C_{5'}$), 130.2 (C_9), 131.5 (C_{10}), 132.6 ($C_{6'}$), 133.2 (C_6), 135.2 (C_7), 136.5 ($C_{1''}$), 138.2 ($C_{3''}$ and $C_{5''}$), 139.2 (C_3), 141.6 ($C_{1'}$), 147.7 ($C_{3'}$), 179.5 (C_1), 181.8 (C_4); *m/z* (ESI^-) 476 ($[M-H]^-$, 100%); HRMS (ESI^-) $C_{24}H_{18}N_3O_6S^-$ ($[M-H]^-$) requires 476.0922, found 476.0922.

_N_-(3-((3'',5''-Dimethylphenyl)amino)-1,4-dioxo-1,4-dihydronaphthalen-2-yl)-4'-methoxybenzenesulfonamide 136



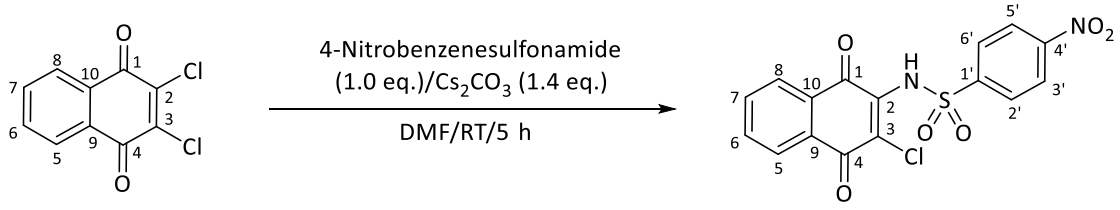
Following *General Procedure 2*, using naphthoquinone **129** (400 mg, 1.06 mmol), 3,5-dimethylaniline (395 µL, 3.18 mmol) and cerium trichloride heptahydrate (395 mg, 1.06 mmol) in MeOH (8 mL) at 110 °C. Purification *via* column chromatography on silica gel (eluent pet ether:acetone 90:10 to 33:67) and subsequent recrystallisation from boiling toluene gave 3-anilinonaphthoquinone **136** as a red solid (185 mg, 33%). mp 205-208 °C (toluene); υ_{max} (thin film) 3235 (N-H), 2924 (C-H), 1678 (C=O), 1638 (C=O), 1612, 1596, 1576; δ_H (500 MHz, $CDCl_3$) 2.32 (6H, s, 2 x Ar-*Me*), 3.79 (3H, s, O*Me*), 6.68 (2H, s, $H_{2''}$ and $H_{6''}$), 6.77-6.83 (3H, m, $H_{3'}$, $H_{5'}$ and $H_{4''}$), 6.83 (1H, br s, sulfonamide-N*H*), 7.59-7.63 (2H, m, $H_{2'}$ and $H_{6'}$), 7.65 (1H, app. td, *J* 7.6, 1.5, H_6), 7.69 (1H, app. td, *J* 7.6, 1.5, H_7), 7.93 (1H, dd, *J* 7.6, 1.5, H_8), 8.04 (1H, s, aniline-N*H*), 8.06 (1H, dd, *J* 7.6, 1.5, H_5); δ_C (125 MHz, $CDCl_3$) 21.4 (2 x Ar-*Me*), 55.5 (O*Me*), 113.8 ($C_{3'}$ and $C_{5'}$), 114.0 (C_2), 120.9 ($C_{2''}$ and $C_{6''}$), 126.4 (C_8), 126.8 (C_5), 126.8 ($C_{4''}$), 129.5 ($C_{2'}$ and $C_{6'}$), 130.4 (C_3 or C_9), 130.7 (C_3 or C_9), 131.3 (C_{10}), 133.0 (C_6), 134.7 (C_7), 137.6 ($C_{1''}$), 138.0 ($C_{3''}$ and $C_{5''}$), 139.0 ($C_{1'}$), 163.1 ($C_{4'}$), 179.1 (C_1), 181.8 (C_4); *m/z* (ESI^-) 461 ($[M-H]^-$, 100%); HRMS (ESI^-) $C_{25}H_{21}N_2O_5S^-$ ($[M-H]^-$) requires 461.1177, found 461.1160.

N-(3-((3'',5''-Dimethylphenyl)amino)-1,4-dioxo-1,4-dihydronaphthalen-2-yl)-3'-aminobenzenesulfonamide 137



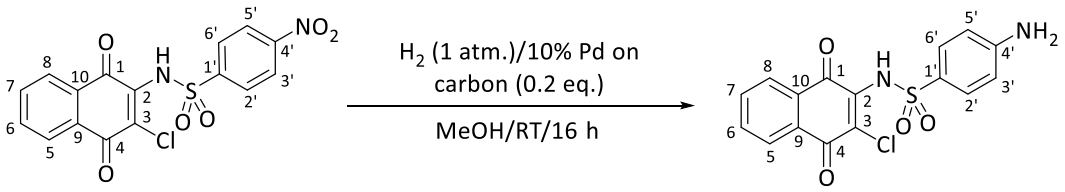
Following *General Procedure 5*, using naphthoquninone **135** (39 mg, 0.08 mmol) and 10% Pd/C (2 mg, 0.02 mmol) in MeOH (5 mL) at 110 ^{o}C. Purification *via* column chromatography on silica gel (eluent pet ether:acetone 80:20) gave aminobenzenesulfonamide **137** as a red solid (37 mg, quant.). mp 209-210 ^{o}C; υ_{max} (thin film) 3300 (N-H), 2922 (C-H), 1707 (C=O), 1671 (C=O), 1597, 1573, 1528; δ_H (500 MHz, $CDCl_3$) 2.32 (6H, s, 2 x Ar-*Me*), 6.68 (2H, s, $H_{2''}$ and $H_{6''}$), 6.72 (1H, ddd, *J* 7.8, 2.4, 0.9, $H_{4'}$ or $H_{6'}$), 6.82 (1H, s, $H_{4''}$), 6.83 (1H, s, sulfonamide-N*H*), 6.92 (1H, app. t, *J* 1.9, $H_{2'}$), 7.02-7.05 (1H, m, $H_{4'}$ or $H_{6'}$), 7.09 (1H, app. t, *J* 7.9, $H_{5'}$), 7.65 (1H, app. td, *J* 7.6, 1.3, H_6), 7.69 (1H, app. td, *J* 7.6, 1.3, H_7), 7.95 (1H, dd, *J* 7.6, 1.3, H_8), 8.03 (1H, s, aniline-N*H*), 8.07 (1H, dd, *J* 7.6, 1.3, H_5), *NH_2 not observed*; δ_C (125 MHz, $CDCl_3$) 21.4 (2 x Ar-*Me*), 113.0 ($C_{2'}$), 113.9 (C_2), 117.0 ($C_{4'}$ or $C_{6'}$), 119.2 ($C_{4'}$ or $C_{6'}$), 120.9 ($C_{2''}$ and $C_{6''}$), 126.4 (C_5), 126.8 (C_8), 126.8 ($C_{4''}$), 129.6 ($C_{5'}$), 130.7 (C_9), 131.4 (C_{10}), 133.0 (C_7), 134.7 (C_6), 137.6 ($C_{1''}$), 138.0 ($C_{3''}$ and $C_{5''}$), 138.8 (C_3), 139.4 ($C_{1'}$ or $C_{3'}$), 146.7 ($C_{1'}$ or $C_{3'}$), 179.1 (C_1), 181.9 (C_4); *m/z* (ESI^+) 139 (100%), 470 ($[M+Na]^+$, 40%); HRMS (ESI^+) $C_{24}H_{21}N_3NaO_4S^+$ ($[M+Na]^+$) requires 470.1145, found 470.1131.

N-(3-Chloro-1,4-dioxo-1,4-dihydronaphthalen-2-yl)-4'-nitrobenzenesulfonamide 138



2,3-Dichloronaphthalene-1,4-dione **37** (500 mg, 2.20 mmol), 4-nitrobenzenesulfonamide (445 mg, 2.20 mmol) and Cs_2CO_3 (1.00 g, 3.08 mmol) were stirred in DMF (5 mL) in a microwave vial at RT for 16 h. 1 M aq. HCl (20 mL) was added and the organic product was extracted with EtOAc (3 x 20 mL) and washed with brine (3 x 20 mL). The precipitate formed in the organic layer was collected by suction filtration and washed with cold water (5 mL) and cold EtOAc (5 mL) to give sulfonamide **138** as a yellow solid (667 mg, 77%). mp 266-267 ^{o}C; υ_{max} (thin film) 3238 (N-H), 1672 (C=O), 1612 (C=O), 1530; δ_H (500 MHz, DMSO-d_6) 7.85 (1H, app. td, *J* 7.6, 1.3, H_6 or H_7), 7.88 (1H, app. td, *J* 7.6, 1.3, H_6 or H_7), 7.94 (1H, dd, *J* 7.6, 1.3, H_5 or H_8), 8.05 (1H, dd, *J* 7.6, 1.3, H_5 or H_8), 8.17-8.20 (2H, m, $H_{2'}$ and $H_{6'}$ or $H_{3'}$ and $H_{5'}$), 8.44-8.47 (2H, m, $H_{2'}$ and $H_{6'}$ or $H_{3'}$ and $H_{5'}$), *NH not observed*; δ_C (125 MHz, DMSO-d_6) 124.2 ($C_{2'}$ and $C_{6'}$ or $C_{3'}$ and $C_{5'}$), 126.5 (C_5 or C_8), 126.7 (C_5 or C_8), 127.8 ($C_{2'}$ and $C_{6'}$ or $C_{3'}$ and $C_{5'}$), 130.4 (C_9 or C_{10}), 131.1 (C_9 or C_{10}), 133.6 (C_2 or C_3), 134.3 (C_6 or C_7), 134.6 (C_6 or C_7), 141.3 (C_2 or C_3), 148.2 ($C_{1'}$ or $C_{4'}$), 149.4 ($C_{1'}$ or $C_{4'}$), 177.3 (C_1 or C_4), 178.8 (C_1 or C_4); *m/z* (ESI$^-$) 391 ([M(^{35}Cl)-H]$^-$, 100%), 393 ([M(^{37}Cl)-H]$^-$, 33%); HRMS (ESI$^-$) $C_{16}H_8ClN_2O_6S^-$ ([M(^{35}Cl)-H]$^-$) requires 390.9797, found 390.9801.

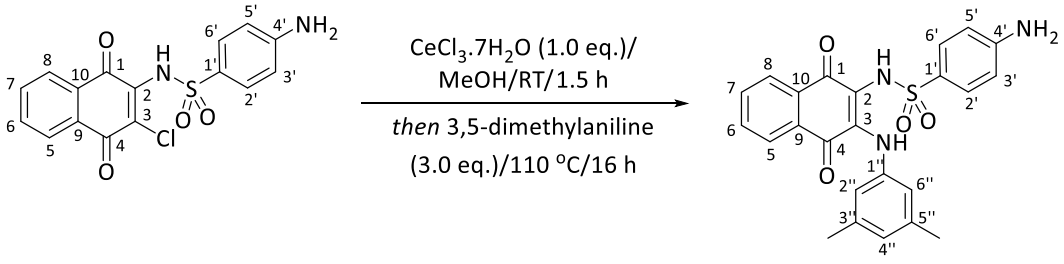
_N_-(3-Chloro-1,4-dioxo-1,4-dihydronaphthalen-2-yl)-4'-aminobenzenesulfonamide 140



Following *General Procedure 5*, using naphthoquninone **138** (150 mg, 0.38 mmol) and 10% Pd/C (8 mg, 0.08 mmol) in MeOH (5 mL). Purification *via* column chromatography on silica gel (eluent pet ether:acetone 80:20) gave aminobenzenesulfonamide **140** as a yellow solid (68 mg, 49%). mp 250-254 °C; υ_{max} (thin film) 3360 (N-H), 1666 (C=O), 1635 (C=O), 1528; δ_H (500 MHz, DMSO-d_6) 6.07 (2H, br. s, NH_2), 6.59-6.62 (2H, m, $H_{3'}$ and $H_{5'}$), 7.54-7.57 (2H, m, $H_{2'}$ and $H_{6'}$), 7.84-7.91 (2H, m, H_6 and H_7), 7.98-8.01 (1H, m, H_5 or H_8), 8.04-8.07 (1H, m, H_5 or H_8), *NH not observed*; δ_C (125 MHz, DMSO-d_6) 112.3 ($C_{3'}$ and $C_{5'}$), 126.5 (C_5 or C_8), 126.7 (C_5 or C_8),

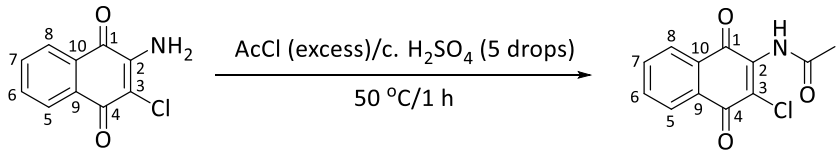
126.7 ($C_{4'}$), 128.9 ($C_{2'}$ and $C_{6'}$), 130.6 (C_9 or C_{10}), 131.0 (C_9 or C_{10}), 134.3 (C_6 or C_7), 134.5 (C_6 or C_7), 141.4 (C_2 or C_3; *other not observed*), 152.9 ($C_{1'}$), 177.5 (C_1 or C_4), 178.9 (C_1 or C_4); *m/z* (ESI^-) 361 ([M(^{35}Cl)-H]$^-$, 100%), 363 ([M(^{37}Cl)-H]$^-$, 40%); HRMS (ESI^-) $C_{16}H_{10}ClN_2O_4S^-$ ([M(^{35}Cl)-H]$^-$) requires 361.0050, found 361.0054.

_N_-(3-((3'',5''-Dimethylphenyl)amino)-1,4-dioxo-1,4-dihydronaphthalen-2-yl)-4'-aminobenzenesulfonamide 141



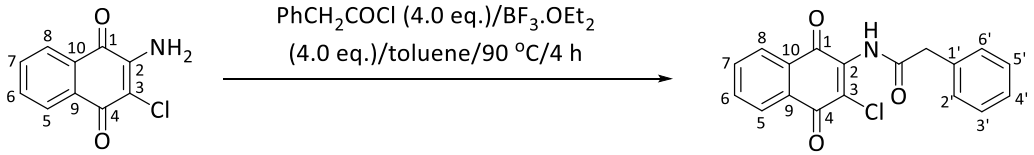
Following *General Procedure 2*, using naphthoquinone **140** (25 mg, 0.07 mmol), 3,5-dimethylaniline (26 µL, 0.21 mmol) and cerium trichloride heptahydrate (26 mg, 0.07 mmol) in MeOH (4 mL) at 110 °C. Purification *via* column chromatography on silica gel (eluent pet ether:acetone 90:10 to 80:20) and subsequent recrystallisation from boiling toluene gave 3-anilinonaphthoquinone **141** as a red solid (21 mg, 68%). mp 212-213 °C (toluene); υ_{max} (thin film) 3373 (N-H), 2923 (C-H), 1708 (C=O), 1671 (C=O), 1595, 1573, 1528; δ_H (500 MHz, $CDCl_3$) 2.31 (6H, s, 2 x Ar-*Me*), 6.49 (2H, d, *J* 8.5, $H_{3'}$ and $H_{5'}$), 6.67 (2H, s, $H_{2''}$ and $H_{6''}$), 6.81 (1H, s, $H_{4''}$), 6.83 (1H, s, sulfonamide-N*H*), 7.44 (2H, d, *J* 8.5, $H_{2'}$ and $H_{6'}$), 7.63 (1H, app. td, *J* 7.6, 1.3, H_6), 7.67 (1H, app. td, *J* 7.6, 1.3, H_7), 7.94 (1H, dd, *J* 7.6, 1.3, H_8), 8.03 (1H, dd, *J* 7.6, 1.3, H_5), 8.11 (1H, s, aniline-N*H*), *NH_2 not observed*; δ_C (125 MHz, $CDCl_3$) 21.4 (2 x Ar-*Me*), 113.6 ($C_{3'}$ and $C_{5'}$), 114.9 (C_2), 120.8 ($C_{2''}$ and $C_{6''}$), 126.3 (C_5 or C_8), 126.6 (C_5 or C_8), 126.7 ($C_{1'}$ or $C_{4''}$), 126.8 ($C_{1'}$ or $C_{4''}$), 129.5 ($C_{2'}$ and $C_{6'}$), 130.9 (C_9), 131.3 (C_{10}), 133.0 (C_6), 134.6 (C_7), 138.0 ($C_{1''}$), 138.0 ($C_{3''}$ and $C_{5''}$), 139.1 (C_3), 150.9 ($C_{4'}$), 179.1 (C_1), 181.8 (C_4); *m/z* (ESI^-) 113 (40%), 224 (30%), 446 ([M-H]$^-$, 100%), 447 (30%); HRMS (ESI^-) $C_{24}H_{20}N_3O_4S^-$ ([M-H]$^-$) requires 446.1180, found 446.1170.

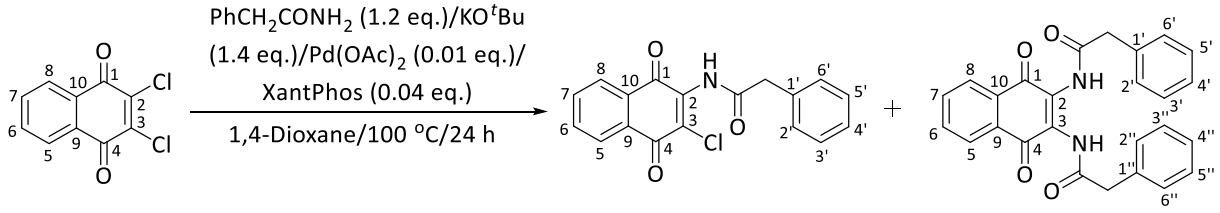
***N*-(3-Chloro-1,4-dioxo-1,4-dihydronaphthalen-2-yl)acetamide 143**



2-Amino-3-chloro-1,4-naphthoquinone **142** (1.00 g, 2.41 mmol) and 5 drops c. H_2SO_4 were stirred in acetyl chloride (10 mL) at 50 °C for 1 h. The reaction was then cooled to 0 °C and quenched by the dropwise addition of EtOH until gas liberation ceased, before being partitioned between 1 M aq. HCl (50 mL) and EtOAc (50 mL). The organic layer was collected, washed with brine (3 x 20 mL), dried, filtered and concentrated *in vacuo*. Purification *via* column chromatography on silica gel (eluent pet ether:EtOAc 90:10 to 80:20) gave acetamide **143** as a yellow solid (872 mg, 73%). mp 217-220 °C (lit. 215-218 °C); δ_H (400 MHz, DMSO-d_6) 2.14 (3H, s, *Me*), 7.87-7.94 (2H, m, H_6 and H_7), 8.02-8.06 (1H, m, H_8), 8.06-8.10 (1H, m, H_5), 10.17 (1H, s, N*H*); *m/z* (ESI^-) 248 ($[M(^{35}Cl)-H]^-$, 100%), 250 ($[M(^{37}Cl)-H]^-$, 33%).

***N*-(3-Chloro-1,4-dioxo-1,4-dihydronaphthalen-2-yl)phenylacetamide 145[375] and *N,N'*-(1,4-Dioxo-1,4-dihydronaphthalene-2,3-diyl)*bis*(phenylacetamide) 158**





Method A: 2-Amino-3-chloro-1,4-naphthoquinone **142** (2.00 g, 9.63 mmol) was stirred in toluene (25 mL) in a 2-necked round-bottomed flask at 90 °C. To a pressure-equalised dropping funnel was added phenylacetyl chloride (5.97 mL, 38.5 mmol) and boron trifluoride diethyl etherate (1.16 mL, 7.11 mmol) in toluene (15 mL). This solution was added dropwise to

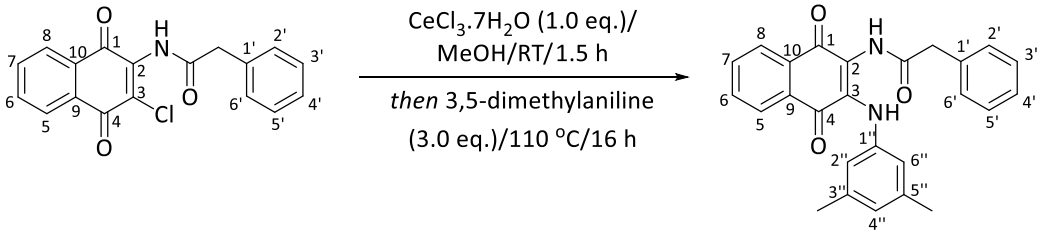
the flask over a period of 30 min and the reaction mixture stirred at 90 °C for a further 4 h. The reaction mixture was cooled to RT and then concentrated *in vacuo*. Acetone (20 mL) was added to the reaction and the beige precipitate that formed was collected by suction filtration. This precipitate was washed three further times with cold acetone (3 x 5 mL) to give phenylacetamide **145** as a beige solid (1.78 g, 57%).

Method B: 2-Amino-3-chloro-1,4-naphthoquinone **142** (100 mg, 0.441 mmol), 2-phenylacetamide (71 mg, 0.528 mmol), $Pd(OAc)_2$ (1 mg, 0.004 mmol), Xantphos **159** (4 mg, 0.007 mmol) and KO^{t}Bu (74 mg, 0.659 mmol) were stirred in 1,4-dioxane (1 mL) in a sealed microwave vial under argon and heated to 100 °C for 24 h. The solution was cooled to RT and partitioned between EtOAc (20 mL) and sat. aq. NH_4Cl (20 mL). The organic layer was collected, washed with brine (3 x 20 mL), dried, filtered and concentrated *in vacuo* to give the crude product. Purification *via* column chromatography on silica gel (eluent pet ether:EtOAc 75:25) gave phenylacetamide **145** as a beige solid (13 mg, 9%) and *bis*-amide **158** as a yellow solid (22 mg, 12%).

Phenylacetamide **145**: mp 211-213 °C (lit. 207-208 °C);[375] δ_H (400 MHz, $CDCl_3$) 3.86 (2H, s, C*H*$_2$Ph), 7.35-7.49 (5H, m, $H_{2'}$, $H_{3'}$, $H_{4'}$, $H_{5'}$ and $H_{6'}$), 7.62 (1H, br. s, N*H*), 7.71-7.81 (2H, m, H_6 and H_7), 8.05-8.09 (1H, m, H_5), 8.15-8.19 (1H, m, H_8); *m/z* (ESI$^+$) 348 ([M(^{35}Cl)+Na]$^+$, 100%), 350 ([M(^{37}Cl)+Na]$^+$, 35%).

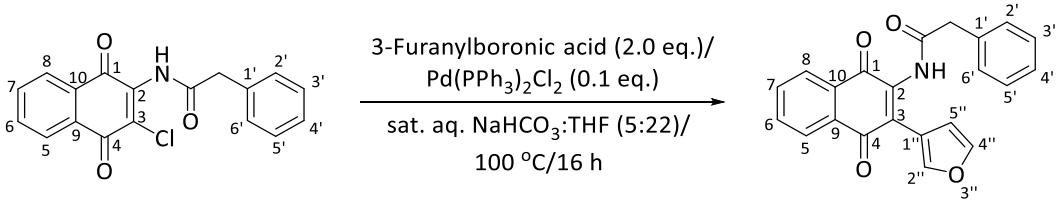
bis-Phenylacetamide **158**: mp 130-136 °C; υ_{max} (thin film) 3260 (N-H), 2962 (C-H), 1671 (C=O), 1595; δ_H (500 MHz, $CDCl_3$) 3.74 (4H, s, 2 x C*H*$_2$Ph), 7.32-7.39 (6H, m, $H_{2'}$, $H_{4'}$, $H_{6'}$, $H_{2''}$, $H_{4''}$ and $H_{6''}$), 7.40-7.45 (4H, m, $H_{3'}$, $H_{5'}$, $H_{3''}$ and $H_{5''}$), 7.67-7.71 (2H, m, H_6 and H_7), 8.01-8.05 (2H, m, H_5 and H_8), 8.32 (2H, s, 2 x N*H*); δ_C (125 MHz, $CDCl_3$) 43.9 (2 x *C*H$_2$Ph), 126.8 (C_5 and C_8), 127.7 ($C_{4'}$ and $C_{4''}$), 128.0 (C_2 and C_3), 129.1 ($C_{3'}$, $C_{5'}$, $C_{3''}$ and $C_{5''}$), 129.7 ($C_{2'}$, $C_{6'}$, $C_{2''}$ and $C_{6''}$), 130.7 (C_9 and C_{10}), 133.7 ($C_{1'}$ and $C_{1''}$), 134.3 (C_6 and C_7), 168.4 (2 x amide-*C*O), 180.6 (C_1 and C_4); *m/z* (ESI$^-$) 423 ([M-H]$^-$, 100%); HRMS (ESI$^-$) $C_{26}H_{19}N_2O_4^-$ ([M-H]$^-$) requires 423.1350, found 423.1337.

N-(3-(3'',5''-Dimethylphenylamino)-1,4-dioxo-1,4-dihydronaphthalen-2-yl)phenylacetamide 151[281a]



Following *General Procedure 2*, using naphthoquinone **145** (250 mg, 0.768 mmol), 3,5-dimethylaniline (288 µL, 2.304 mmol) and cerium trichloride heptahydrate (288 mg, 0.768 mmol) in MeOH (10 mL) at 110 °C. Purification *via* column chromatography on silica gel (eluent pet ether:acetone 90:10 to 70:30) and subsequent recrystallisation from boiling toluene gave 3-anilinonaphthoquinone **151** as a purple solid (128 mg, 41%). mp 214 °C (toluene) (lit. 216-217 °C);[281a] HPLC t_R 24 min, 98%; δ_H (500 MHz, $CDCl_3$) 2.31 (6H, s, 2 x Ar-*Me*), 3.20 (2H, s, CH_2Ph), 6.54 (2H, s, $H_{2''}$ and $H_{6''}$), 6.81 (1H, s, $H_{4''}$), 7.03 (2H, d, *J* 6.9, $H_{2'}$ and $H_{6'}$), 7.30-7.36 (3H, m, $H_{3'}$, $H_{4'}$ and $H_{5'}$), 7.47 (1H, s, amide-N*H*), 7.65 (1H, app. td, *J* 7.3, 1.0, H_6), 7.71 (1H, app. td, *J* 7.6, 1.3, H_7), 7.76 (1H, s, aniline-N*H*), 8.06 (1H, dd, *J* 7.6, 0.6, H_8), 8.08 (1H, dd, *J* 7.6, 0.9, H_5); *m*/*z* (ESI^-) 380 (60%), 409 ($[M-H]^-$, 100%).

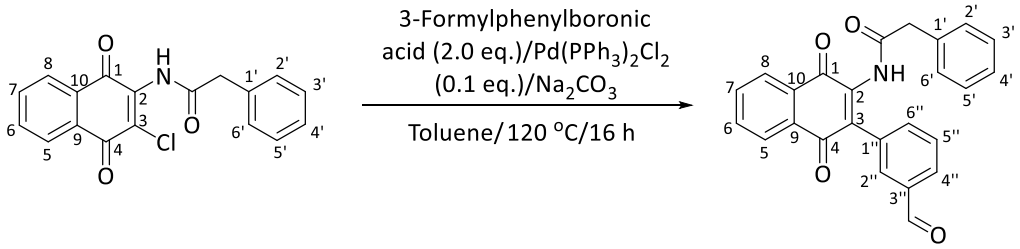
N-(3-(Furan-3''-yl)-1,4-dioxo-1,4-dihydronaphthalen-2-yl)phenylacetamide 154[281a]



Following *General Procedure 6*, using naphthoquinone **145** (250 mg, 0.768 mmol), 3-furanylboronic acid (172 mg, 1.536 mmol), $Pd(PPh_3)_2Cl_2$ (56 mg, 0.077 mmol) and sat. aq. $NaHCO_3$ (2.5 mL) in THF (11 mL). Purification *via* column chromatography on silica gel (eluent pet ether:acetone 90:10 then pet ether:EtOAc 80:20) and recrystallisation from boiling toluene gave 3-arylnaphthoquinone **154** as a copper brown solid (100 mg, 36%). mp 119-

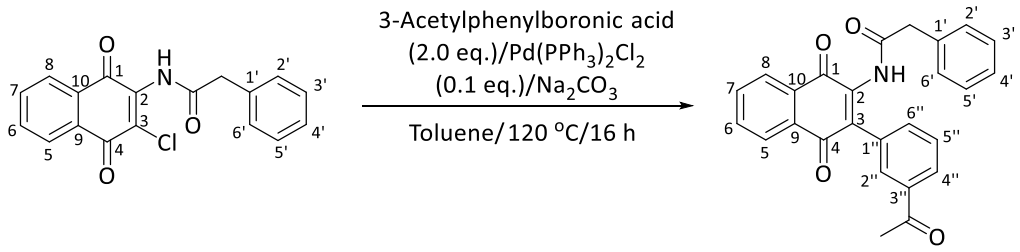
121 °C (toluene) (lit. 120-124 °C);[281a] HPLC t_R 25 min, 97%; δ_H (400 MHz, $CDCl_3$) 3.72 (2H, s, CH_2Ph), 6.39 (1H, d, *J* 1.3, $H_{5''}$), 7.33-7.40 (4H, m, $H_{2'}$, $H_{4'}$, $H_{6'}$ and $H_{4''}$), 7.42-7.47 (2H, m, $H_{3'}$ and $H_{5'}$), 7.68-7.77 (2H, m, H_6 and H_7), 7.86 (1H, br. s, N*H*), 8.04-8.08 (2H, m, $H_{2''}$ and H_5 or H_8), 8.13 (1H, dd, *J* 7.4, 1.1, H_5 or H_8); *m/z* (ESI^-) 356 ($[M-H]^-$, 100%).

N-(3-(3''-Formylphenyl)-1,4-dioxo-1,4-dihydronaphthalen-2-yl)phenylacetamide 161



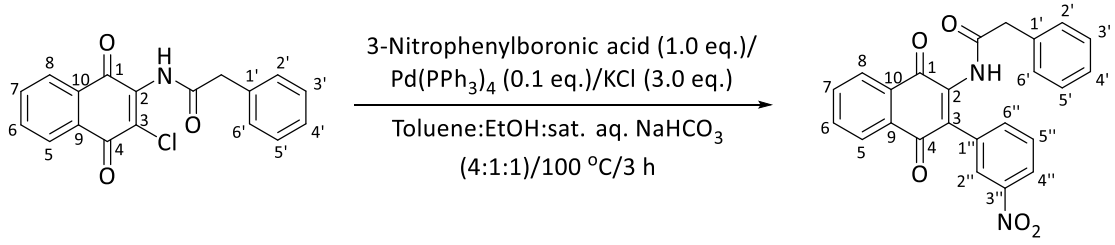
Following *General Procedure 7*, using naphthoquinone **145** (200 mg, 0.614 mmol), 3-formylphenylboronic acid (184 mg, 1.23 mmol), $Pd(PPh_3)_2Cl_2$ (43 mg, 0.061 mmol) and Na_2CO_3 (194 mg, 1.84 mmol) in toluene (10 mL). Purification *via* column chromatography on silica gel (eluent pet ether:EtOAc 90:10 to 70:30) gave 3-arylnaphthoquinone **161** as a yellow solid (107 mg, 44%). mp 158-162 °C; HPLC t_R 23 min, >99%; υ_{max} (thin film) 3272 (N-H), 1695 (C=O), 1665 (C=O), 1595; δ_H (500 MHz, $CDCl_3$) 3.51 (2H, s, CH_2Ph), 7.12 (2H, dd, *J* 7.4, 1.7, $H_{2'}$ and $H_{6'}$), 7.31-7.37 (3H, m, $H_{3'}$, $H_{4'}$ and $H_{5'}$), 7.53 (1H, app. t, *J* 7.7, $H_{5''}$), 7.58 (1H, app. dt, *J* 7.7, 1.5, $H_{6''}$), 7.72 (1H, app. t, *J* 1.5, $H_{2''}$), 7.75 (1H, app. td, *J* 7.6, 1.3, H_7), 7.79 (1H, app. td, *J* 7.6, 1.3, H_6), 7.85 (1H, app. dt, *J* 7.7, 1.5, $H_{4''}$), 7.94 (1H, s, N*H*), 8.11 (1H, dd, *J* 7.6, 1.3, H_8), 8.14 (1H, dd, *J* 7.6, 1.3, H_5), 9.93 (1H, s, C*H*O); δ_C (125 MHz, $CDCl_3$) 44.6 (*C*H_2Ph), 126.4 (C_8), 127.1 (C_5), 127.8 ($C_{4'}$), 128.6 ($C_{5''}$), 129.2 ($C_{2'}$ and $C_{6'}$), 129.2 ($C_{3'}$ and $C_{5'}$), 129.3 ($C_{4''}$), 130.2 (C_{10}), 130.2 ($C_{2''}$), 132.1 (C_9), 133.0 (C_3 or $C_{1'}$), 133.2 (C_3 or $C_{1'}$), 133.8 (C_7), 134.4 ($C_{1''}$), 134.9 (C_6), 135.6 ($C_{6''}$), 136.0 ($C_{3''}$), 137.3 (C_2), 166.9 (amide-*C*O), 182.1 (C_1), 183.0 (C_4), 191.9 (*C*HO); *m/z* (ESI^+) 111 (30%), 418 ($[M+Na]^+$, 100%), 434 (25%); HRMS (ESI^-) $C_{25}H_{16}NO_4^-$ ($[M-H]^-$) requires 394.1085, found 394.1076.

N-(3-(3''-Acetylphenyl)-1,4-dioxo-1,4-dihydronaphthalen-2-yl)phenylacetamide 162



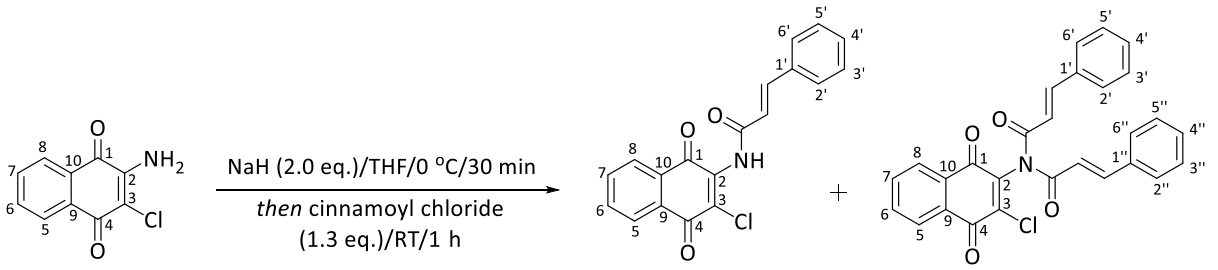
Following *General Procedure 7*, using naphthoquinone **145** (200 mg, 0.614 mmol), 3-acetylphenylboronic acid (200 mg, 1.23 mmol), $Pd(PPh_3)_2Cl_2$ (43 mg, 0.061 mmol) and Na_2CO_3 (194 mg, 1.84 mmol) in toluene (10 mL). Purification *via* column chromatography on silica gel (eluent pet ether:acetone 95:5 to 75:25) gave 3-arylnaphthoquinone **162** as a yellow solid (171 mg, 68%). mp 134-139 °C; υ_{max} (thin film) 3510 (N-H), 1707 (C=O), 1668 (C=O), 1595; δ_H (500 MHz, $CDCl_3$) 2.55 (3H, s, CO*Me*), 3.51 (2H, s, CH_2Ph), 7.12 (2H, dd, *J* 7.7, 1.7, $H_{2'}$ and $H_{6'}$), 7.30-7.36 (3H, m, $H_{3'}$, $H_{4'}$ and $H_{5'}$), 7.48 (1H, app. t, *J* 7.7, $H_{5''}$), 7.51-7.54 (1H, m, $H_{4''}$ or $H_{6''}$), 7.75 (1H, app. td, *J* 7.6, 1.4, H_7), 7.77 (1H, app. td, *J* 7.6, 1.4, H_6), 7.82 (1H, app. t, *J* 1.5, $H_{2''}$), 7.90 (1H, s, N*H*), 7.93 (1H, app. dt, *J* 7.7, 1.5, $H_{4''}$ or $H_{6''}$), 8.09 (1H, dd, *J* 7.6, 1.4, H_8), 8.13 (1H, dd, *J* 7.6, 1.4, H_5); δ_C (125 MHz, $CDCl_3$) 26.6 (CO*Me*), 44.5 (*C*H_2Ph), 126.3 (C_8), 127.1 (C_5), 127.8 ($C_{3'}$ and $C_{5'}$), 128.3 ($C_{5''}$), 128.3 ($C_{4''}$ or $C_{6''}$), 128.5 ($C_{2''}$), 129.2 ($C_{2'}$ and $C_{6'}$), 129.2 ($C_{4'}$), 130.3 (C_{10}), 132.1 (C_9), 133.3 ($C_{1'}$), 133.6 (C_3), 133.7 (C_7), 133.8 ($C_{1''}$), 134.4 ($C_{4''}$ or $C_{6''}$), 134.8 (C_6), 136.6 ($C_{3''}$), 137.3 (C_2), 167.0 (NH*C*O), 182.1 (C_1), 183.1 (C_4), 197.5 (*C*OMe); *m/z* (ESI^+) 432 ($[M+Na]^+$, 100%); HRMS (ESI^-) $C_{26}H_{18}NO_4^-$ ($[M-H]^-$) requires 408.1241, found 408.1238.

N-(3-(3''-Nitrophenyl)-1,4-dioxo-1,4-dihydronaphthalen-2-yl)phenylacetamide 163



Naphthoquinone **145** (300 mg, 0.922 mmol), 3-nitrophenyl boronic acid (145 mg, 0.922 mmol), potassium chloride (209 mg, 2.77 mmol) and $Pd(PPh_3)_4$ (107 mg, 0.092 mmol) were suspended in a solution of toluene:EtOH (4 mL:1 mL) under nitrogen. Sat. aq. $NaHCO_3$ (1 mL) was added and the reaction mixture was heated to 100 ^oC for 3 h. After cooling, the mixture was filtered through Celite® and partitioned between EtOAc (20 mL) and sat. aq. NH_4Cl (20 mL). The organic layer was subsequently washed with brine (3 x 20 mL), dried, filtered and concentrated *in vacuo*. Purification *via* column chromatography on silica gel (eluent pet ether:acetone 90:10 to 80:20) gave 3-arylnaphthoquinone **163** as a yellow solid (128 mg, 34%). mp 149-156 ^oC; υ_{max} (thin film) 3372 (N-H), 2923 (C-H), 1710 (C=O), 1657 (C=O), 1590 (C=O), 1526; δ_H (500 MHz, $CDCl_3$) 3.53 (2H, s, CH_2), 7.13 (2H, dd, *J* 7.6, 1.6, $H_{2'}$ and $H_{6'}$), 7.31-7.38 (3H, m, $H_{3'}$, $H_{4'}$ and $H_{5'}$), 7.54 (1H, t, *J* 7.9, $H_{5''}$), 7.67 (1H, app. dt, *J* 7.9, 1.6, $H_{6''}$), 7.77 (1H, app. td, *J* 7.6, 1.3, H_7), 7.81 (1H, app. td, *J* 7.6, 1.3, H_6), 8.03 (1H, s, N*H*), 8.06 (1H, app. t, *J* 1.6, $H_{2''}$), 8.12 (1H, dd, *J* 7.6, 1.3, H_8), 8.14-8.19 (2H, m, H_5 and $H_{4''}$); δ_C (125 MHz, $CDCl_3$) 44.6 (*C*H_2), 123.0 ($C_{4''}$), 123.4 ($C_{2''}$), 126.5 (C_8), 127.2 (C_5), 128.0 ($C_{4'}$), 128.7 ($C_{5''}$), 129.0 ($C_{2'}$ and $C_{6'}$), 129.2 ($C_{3'}$ and $C_{5'}$), 130.1 (C_{10}), 131.5 (C_3), 131.9 (C_9), 132.9 ($C_{1'}$), 133.9 (C_7), 135.1 ($C_{1''}$), 135.1 (C_6), 136.1 ($C_{6''}$), 137.4 (C_2), 147.7 ($C_{3''}$), 166.9 (amide *C*=O), 181.9 (C_1), 182.6 (C_4); *m/z* (ESI^-) 411 ($[M-H]^-$, 100%); HRMS (ESI^+) $C_{24}H_{16}N_2NaO_5^+$ ($[M+Na]^+$) requires 435.0951, found 435.0949.

_N_-(3-Chloro-1,4-dioxo-1,4-dihydronaphthalen-2-yl)*trans*-cinnamamide 164 and _N_-(3-Chloro-1,4-dioxo-1,4-dihydronaphthalen-2-yl)-_N_-*trans*-cinnamoyl-*trans*-cinnamamide 165



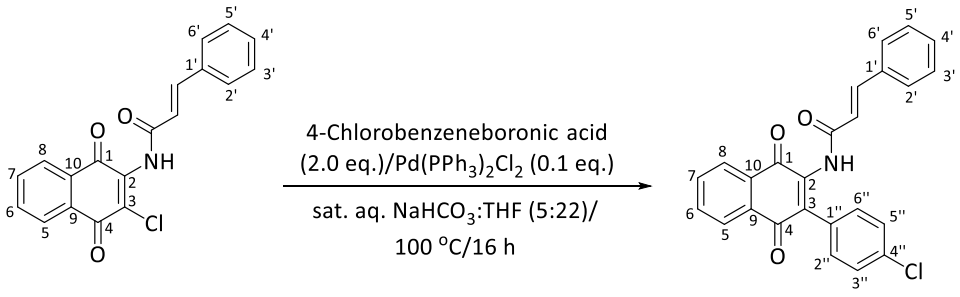
2-Amino-3-chloro-1,4-naphthoquinone **142** (500 mg, 2.41 mmol) was stirred under N_2 with sodium hydride (as a 60% dispersion in oil, 193 mg, 4.82 mmol) in THF (5 mL) at RT for 30 min.

Cinnamoyl chloride (522 mg, 3.13 mmol) was added portionwise and stirring continued under N_2 at RT for 1 h. The solution was then partitioned between EtOAc (20 mL) and sat. aq. NH_4Cl (20 mL). The organic layer was collected, washed with brine (3 x 20 mL), dried, filtered and concentrated *in vacuo* to give the crude product. Purification *via* column chromatography on silica gel (eluent pet ether:acetone 95:5) gave:

Amide **164** as a yellow solid (333 mg, 41%). Decomposes below mp; υ_{max} (thin film) 3250 (N-H), 1669 (C=O), 1627 (C=O), 1577; δ_H (500 MHz, $CDCl_3$) 6.68 (1H, d, *J* 15.7, C*H*(CO)=CHPh), 7.42-7.44 (3H, m, $H_{3'}$, $H_{4'}$ and $H_{5'}$), 7.58-7.61 (2H, m, $H_{2'}$ and $H_{6'}$), 7.78 (1H, app. td, *J* 7.5, 1.6, H_7), 7.81 (1H, app. td, *J* 7.5, 1.6, H_6), 7.82 (1H, d, *J* 15.7, C*H*(Ph)=CHCO), 7.92 (1H, s, N*H*), 8.14-8.16 (1H, m, H_8), 8.21-8.23 (1H, m, H_5); δ_C (125 MHz, $CDCl_3$) 119.1 (*C*H(CO)=CHPh), 127.1 (C_8), 127.6 (C_5), 128.3 ($C_{2'}$ and $C_{6'}$), 129.0 ($C_{3'}$ and $C_{5'}$), 130.2 (C_{10}), 130.7 ($C_{4'}$), 131.6 (C_9), 132.7 (C_3), 134.0 (C_7 or $C_{1'}$), 134.1 (C_7 or $C_{1'}$), 134.9 (C_6), 139.2 (C_2), 145.0 (*C*H(Ph)=CHCO), 162.2 (amide-*C*O), 177.6 (C_4), 180.0 (C_1); *m/z* (ESI^+) 360 ($[M(^{35}Cl)+Na]^+$, 80%), 362 ($[M(^{37}Cl)+Na]^+$, 30%), 697 ($[2M(^{35}Cl)+Na]^+$, 100%), 699 ($[M(^{35}Cl)M(^{37}Cl)+Na]^+$, 70%); HRMS ($ESI^-$) $C_{19}H_{11}ClNO_3^-$ ($[M(^{35}Cl)-H]^-$) requires 336.0433, found 336.0431.

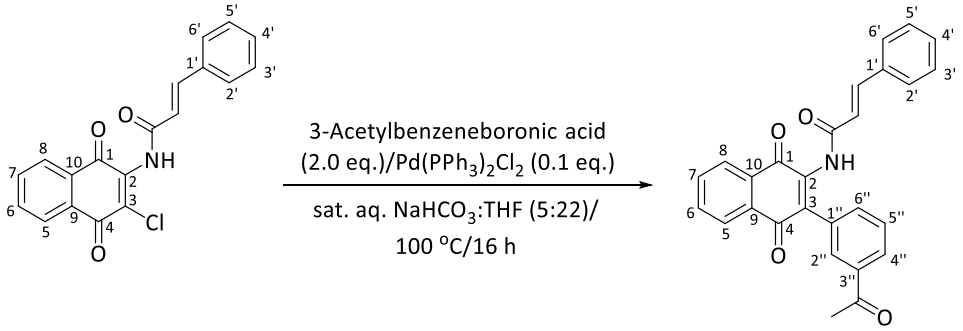
bis-Amide **165** as a yellow solid (356 mg, 32%). Decomposes below mp; υ_{max} (thin film) 1675 (C=O), 1612 (C=O), 1576; δ_H (500 MHz, $CDCl_3$) 6.98 (2H, d, *J* 15.5, C*H*(CO)=CHPh), 7.34-7.42 (6H, m, $H_{3'}$, $H_{4'}$, $H_{5'}$, $H_{3''}$, $H_{4''}$ and $H_{5''}$), 7.51-7.55 (4H, m, $H_{2'}$, $H_{6'}$, $H_{2''}$ and $H_{6''}$), 7.82-7.85 (2H, m, H_6 and H_7), 7.89 (2H, d, *J* 15.5, C*H*(Ph)=CHCO), 8.18-8.20 (1H, m, H_5 or H_8), 8.23-8.26 (1H, m, H_5 or H_8); δ_C (125 MHz, $CDCl_3$) 118.7 (*C*H(CO)=CHPh), 127.7 (C_5 or C_8), 127.8 (C_5 or C_8), 128.6 ($C_{2'}$, $C_{6'}$, $C_{2''}$ and $C_{6''}$), 128.9 ($C_{3'}$, $C_{5'}$, $C_{3''}$ and $C_{5''}$), 130.9 (C_9 or C_{10}), 131.0 ($C_{4'}$ and $C_{4''}$), 131.5 (C_9 or C_{10}), 134.1 ($C_{1'}$ and $C_{1''}$), 134.7 (C_6 or C_7), 134.9 (C_6 or C_7), 142.9 (C_2 or C_3), 144.3 (C_2 or C_3), 146.9 (*C*H(Ph)=CHCO), 166.8 (2 x amide-*C*O), 177.3 (C_1 or C_4), 178.3 (C_1 or C_4); *m/z* (FI^+) 148 (100%), 337 (50%), 467 ($[M(^{35}Cl)]^+$, 5%); HRMS (FI^+) $C_{28}H_{18}ClNO_4$ ($[M(^{35}Cl)]^+$) requires 467.0924, found 467.0352 (80%) and 467.1109 (100%).

N-(3-(4''-Chlorophenyl)-1,4-dioxo-1,4-dihydronaphthalen-2-yl)*trans*-cinnamamide 167



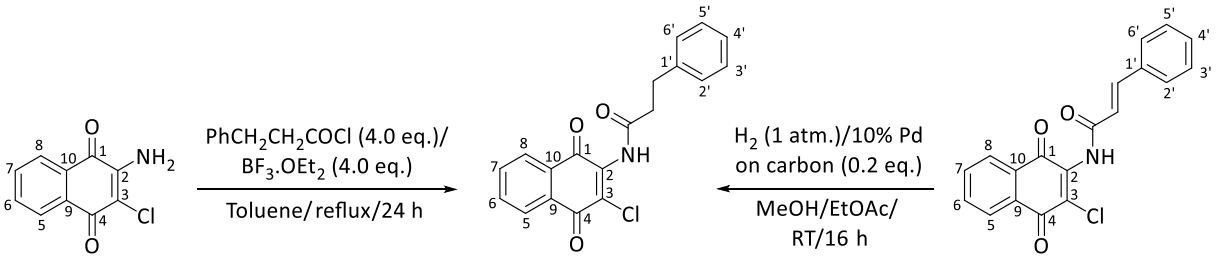
Following *General Procedure 6*, using naphthoquinone **164** (100 mg, 0.296 mmol), 4-chlorobenzeneboronic acid (93 mg, 0.593 mmol), $Pd(PPh_3)_2Cl_2$ (21 mg, 0.030 mmol) and sat. aq. $NaHCO_3$ (2.5 mL) in THF (11 mL). Purification *via* column chromatography on silica gel (eluent pet ether:acetone 95:5 to 90:10) gave 3-arylnaphthoquinone **167** as a yellow solid (27 mg, 22%). mp 185-190 ^{o}C; υ_{max} (thin film) 3260 (N-H), 2927 (C-H), 1709, 1663 (C=O), 1629 (C=O), 1592; δ_H (500 MHz, $CDCl_3$) 6.51 (1H, d, *J* 15.7, C*H*(CO)=CHPh), 7.34-7.40 (7H, m, $H_{3'}$, $H_{4'}$, $H_{5'}$, $H_{2''}$, $H_{3''}$, $H_{5''}$ and $H_{6''}$), 7.48-7.50 (2H, m, $H_{2'}$ and $H_{6'}$), 7.51 (1H, d, *J* 15.7, C*H*(Ph)=CHCO), 7.77 (1H, app. td, *J* 7.5, 1.5, H_6 or H_7), 7.81 (1H, app. td, *J* 7.5, 1.5, H_6 or H_7), 8.11 (1H, s, N*H*), 8.15-8.19 (2H, m, H_5 and H_8); δ_C (125 MHz, $CDCl_3$) 119.2 (*C*H(CO)=CHPh), 126.4 (C_5 or C_8), 127.2 (C_5 or C_8), 128.2 ($C_{2'}$ and $C_{6'}$), 128.3 ($C_{2''}$ and $C_{6''}$ or $C_{3''}$ and $C_{5''}$), 128.9 ($C_{2''}$ and $C_{6''}$ or $C_{3''}$ and $C_{5''}$), 128.9 ($C_{4'}$), 130.3 (C_9 or C_{10}), 130.5 ($C_{3'}$ and $C_{5'}$), 132.1 (C_9 or C_{10}), 132.3 ($C_{1''}$ or $C_{4''}$), 132.7 (C_2 or C_3), 133.6 (C_6 or C_7), 134.0 ($C_{1'}$), 134.5 ($C_{1''}$ or $C_{4''}$), 134.9 (C_6 or C_7), 137.3 (C_2 or C_3), 144.1 (*C*H(Ph)=CHCO), 162.0 (amide-*C*O), 182.3 (C_1 or C_4), 183.1 (C_1 or C_4); *m/z* (ESI^-) 412 ($[M(^{35}Cl)-H]^-$, 100%), 414 ($[M(^{37}Cl)-H]^-$, 33%); HRMS (ESI^-) $C_{25}H_{15}ClNO_3^-$ ($[M(^{35}Cl)-H]^-$) requires 412.0746, found 412.0742.

***N*-(3-(3''-Acetylphenyl)-1,4-dioxo-1,4-dihydronaphthalen-2-yl)*trans*-cinnamamide 168**



Following *General Procedure 6*, using naphthoquinone **164** (112 mg, 0.332 mmol), 3-acetylbenzeneboronic acid (109 mg, 0.664 mmol), $Pd(PPh_3)_2Cl_2$ (23 mg, 0.033 mmol) and sat. aq. $NaHCO_3$ (2.5 mL) in THF (11 mL). Purification *via* column chromatography on silica gel (eluent pet ether:acetone 95:5 to 90:10) gave 3-arylnaphthoquinone **168** as a yellow solid (12 mg, 9%). mp 108-110 ^{o}C; υ_{max} (thin film) 3270 (N-H), 2923 (C-H), 1666 (C=O), 1629 (C=O), 1595; δ_H (500 MHz, $CDCl_3$) 2.59 (3H, s, CO*Me*), 6.49 (1H, d, *J* 15.8, C*H*(CO)=CHPh), 7.34-7.43 (4H, m, $H_{3'}$, $H_{4'}$, $H_{5'}$ and C*H*(Ph)=CHCO), 7.44-7.47 (2H, m, $H_{2'}$ and $H_{6'}$), 7.55 (1H, app. t, *J* 7.8, $H_{5''}$), 7.68 (1H, app. dt, *J* 7.8, 1.4, $H_{6''}$), 7.78 (1H, app. td, *J* 7.6, 1.3, H_6 or H_7), 7.82 (1H, app. td, *J* 7.6, 1.3, H_6 or H_7), 7.93 (1H, app. dt, *J* 7.8, 1.4, $H_{4''}$), 7.99 (1H, app. t, *J* 1.4, $H_{2''}$), 8.11-8.20 (3H, m, H_5, H_8 and N*H*); δ_C (125 MHz, $CDCl_3$) 26.6 (CO*Me*), 119.3 (*C*H(CO)=CHPh), 126.4 (C_5 or C_8), 127.2 (C_5 or C_8), 128.1 ($C_{2'}$ and $C_{6'}$), 128.3 ($C_{4''}$ or $C_{5''}$), 128.4 ($C_{4''}$ or $C_{5''}$), 128.8 ($C_{2''}$), 128.9 ($C_{3'}$ and $C_{5'}$), 130.3 (C_9 or C_{10}), 130.5 ($C_{4'}$) 131.5 (C_2 or C_3), 132.3 (C_9 or C_{10}), 132.6 ($C_{1''}$), 133.7 (C_6 or C_7), 133.9 ($C_{1'}$), 134.3 ($C_{6''}$), 134.9 (C_6 or C_7), 136.7 ($C_{3''}$), 137.5 (C_2 or C_3), 144.0 (*C*H(Ph)=CHCO), 162.1 (amide-*C*O), 182.3 (C_1 or C_4), 183.1 (C_1 or C_4), 197.7 (*C*OMe); *m/z* (ESI^-) 420 ($[M-H]^-$, 100%); HRMS (ESI^+) $C_{27}H_{19}NNaO_4^+$ ($[M+Na]^+$) requires 444.1206, found 444.1189.

***N*-(3-Chloro-1,4-dioxo-1,4-dihydronaphthalen-2-yl)hydrocinnanamide 169**

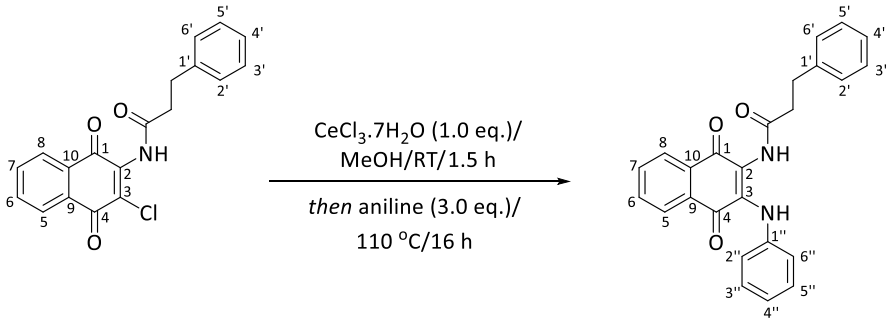


Method A: 2-Amino-3-chloro-1,4-naphthoquinone **142** (1.70 g, 8.19 mmol) and hydrocinnamoyl chloride (5.00 mL, 30.1 mmol) were stirred in boron trifluoride diethyl etherate (1 mL) in a round-bottomed flask and heated to reflux for 30 min. The reaction mixture was then cooled and toluene (10 mL) was added, before being heated to reflux for a further 24 h. The crude reaction mixture was concentrated *in vacuo* and the subsequent addition of acetone (20 mL) resulted in the precipitation of a yellow solid. This solid was collected by suction filtration and recrystallised from boiling acetone to give hydrocinnanamide **169** as a yellow solid (1.39 g, 50%).

Method B: Following *General Procedure 5*, using naphthoquinone **164** (300 mg, 0.889 mmol), 10% Pd/C (19 mg, 0.178 mmol) and MeOH (2 mL) in EtOAc (10 mL). Purification *via* column chromatography on silica gel (eluent pet ether:EtOAc 80:20 to 60:40) gave hydrocinnanamide **169** as a yellow solid (40 mg, 13%).

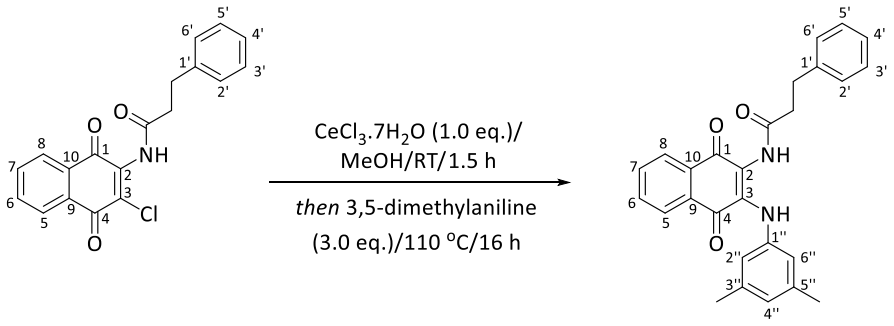
mp 162-167 ^{o}C (acetone); υ_{max} (thin film) 3284 (N-H), 1662 (C=O); δ_H (500 MHz, $CDCl_3$) 2.84 (2H, t, *J* 7.6, COC*H*$_2$CH$_2$Ph), 3.09 (2H, t, *J* 7.6, COCH$_2$C*H*$_2$Ph), 7.21-7.28 (3H, m, H$_{2'}$, H$_{4'}$ and H$_{6'}$), 7.30-7.34 (2H, m, H$_{3'}$ and H$_{5'}$), 7.61 (1H, s, N*H*), 7.74-7.81 (2H, m, H$_6$ and H$_7$), 8.10 (1H, dd, *J* 7.3, 1.5, H$_8$), 8.19 (1H, dd, *J* 7.3, 1.5, H$_5$); δ_C (125 MHz, $CDCl_3$) 31.1 (COCH$_2$C*H*$_2$Ph), 38.9 (CO*C*H$_2$CH$_2$Ph), 126.5 (C$_{4'}$), 127.0 (C$_8$), 127.5 (C$_5$), 128.4 (C$_{2'}$ and C$_{6'}$), 128.7 (C$_{3'}$ and C$_{5'}$), 130.2 (C$_{10}$), 131.5 (C$_9$), 133.2 (C$_3$), 134.1 (C$_7$), 134.8 (C$_6$), 138.9 (C$_2$), 139.9 (C$_{1'}$), 168.8 (amide-*C*O), 177.6 (C$_4$), 179.8 (C$_1$); *m/z* (ESI$^-$) 113 (30%), 249 (40%), 338 ([M(^{35}Cl)-H]$^-$, 100%); HRMS (ESI$^+$) $C_{19}H_{14}ClNNaO_3^+$ ([M(^{35}Cl)+Na]$^+$) requires 362.0554, found 362.0554.

***N*-(3-(Phenylamino)-1,4-dioxo-1,4-dihydronaphthalen-2-yl)hydrocinnanamide 170**



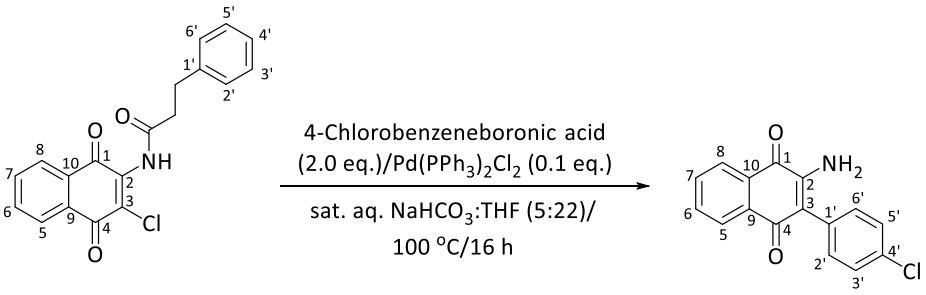
Following *General Procedure 2*, using naphthoquinone **169** (150 mg, 0.440 mmol), aniline (121 µL, 1.33 mmol) and cerium trichloride heptahydrate (165 mg, 0.440 mmol) in MeOH (5 mL) at 110 ^{o}C. Purification *via* column chromatography on silica gel (eluent pet ether:EtOAc 80:20 then pet ether:acetone 90:10) gave 3-anilinonaphthoquinone **170** as a red solid (28 mg, 16%). mp 198-202 ^{o}C; υ_{max} (thin film) 3326 (N-H), 2925 (C-H), 2854 (C-H), 1737 (C=O), 1670 (C=O), 1595; δ_H (500 MHz, $CDCl_3$) 2.16-2.20 (2H, m, C*H*$_2$CH$_2$Ph), 2.45-2.50 (2H, m, CH$_2$C*H*$_2$Ph), 6.94 (2H, d, *J* 7.6, H$_{2''}$ and H$_{6''}$), 7.06 (2H, d, *J* 7.4, H$_{2'}$ and H$_{6'}$), 7.13 (1H, app. t, *J* 7.6, H$_{4''}$), 7.18 (1H, app. t, *J* 7.4, H$_{4'}$), 7.25 (2H, app. t, *J* 7.4, H$_{3'}$ and H$_{5'}$), 7.29 (2H, app. t, *J* 7.6, H$_{3''}$ and H$_{5''}$), 7.59 (1H, s, amide-N*H*), 7.68 (1H, app. td, *J* 7.6, 1.3, H$_6$ or H$_7$), 7.74 (1H, app. td, *J* 7.6, 1.3, H$_6$ or H$_7$), 7.87 (1H, s, aniline-N*H*), 8.09-8.13 (2H, m, H$_5$ and H$_8$); δ_C (125 MHz, $CDCl_3$) 30.7 (CH$_2$*C*H$_2$Ph), 37.7 (*C*H$_2$CH$_2$Ph), 115.2 (C$_2$), 122.4 (C$_{2''}$ and C$_{6''}$), 124.1 (C$_{4''}$), 126.2 (C$_{4'}$), 126.3 (C$_5$ or C$_8$), 126.8 (C$_5$ or C$_8$), 127.9 (C$_{3''}$ and C$_{5''}$), 128.1 (C$_{2'}$ and C$_{6'}$), 128.5 (C$_{3'}$ and C$_{5'}$), 130.6 (C$_9$ or C$_{10}$), 131.7 (C$_9$ or C$_{10}$), 133.1 (C$_6$ or C$_7$), 134.0 (C$_3$), 134.6 (C$_6$ or C$_7$), 137.1 (C$_{1''}$), 140.5 (C$_{1'}$), 168.5 (amide-*C*O), 180.1 (C$_1$), 182.1 (C$_4$); *m/z* (ESI$^-$) 395 ([M-H]$^-$, 100%); HRMS (ESI$^+$) $C_{25}H_{20}N_2NaO_3^+$ ([M+Na]$^+$) requires 419.1366, found 419.1349.

N-(3-((3'',5''-Dimethylphenyl)amino)-1,4-dioxo-1,4-dihydronaphthalen-2-yl)hydrocinnanamide 171



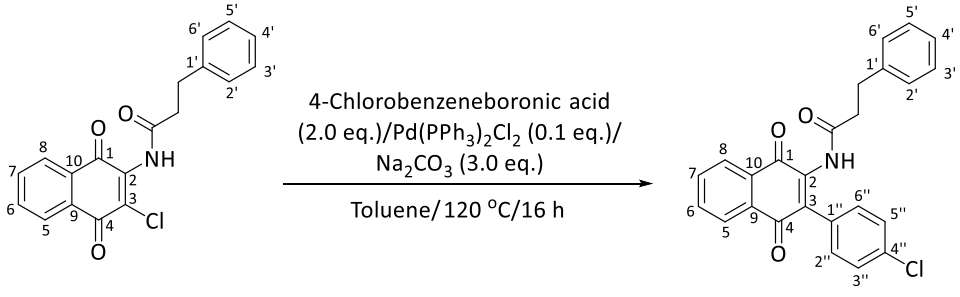
Following *General Procedure 2*, using naphthoquinone **169** (100 mg, 0.300 mmol), 3,5-dimethylaniline (110 μL, 0.890 mmol) and cerium trichloride heptahydrate (110 mg, 0.300 mmol) in MeOH (5 mL) at 110 ^{o}C. Purification *via* column chromatography on silica gel (eluent pet ether:acetone 90:10 to 75:25) gave 3-anilinonaphthoquinone **17** as a red solid (67 mg, 54%). mp 186-190 ^{o}C; HPLC t_R 23 min, 95%; υ_{max} (thin film) 3305 (N-H), 1669 (C=O), 1596, 1573, 1500; δ_H (500 MHz, $CDCl_3$) 2.19-2.24 (2H, m, C$H_2$$CH_2$Ph), 2.30 (6H, s, 2 x Ar-*Me*), 2.46-2.51 (2H, m, CH_2CH_2Ph), 6.57 (2H, s, $H_{2''}$ and $H_{6''}$), 6.78 (1H, s, $H_{4''}$), 7.06 (2H, d, *J* 7.3, $H_{2'}$ and $H_{6'}$), 7.19 (1H, app. t, *J* 7.3, $H_{4'}$), 7.24-7.29 (2H, m, $H_{3'}$ and $H_{5'}$), 7.60 (1H, s, amide-N*H*), 7.67 (1H, app. td, *J* 7.6, 1.3, H_6 or H_7), 7.73 (1H, app. td, *J* 7.6, 1.3, H_6 or H_7), 7.84 (1H, s, aniline-N*H*), 8.09-8.12 (2H, m, H_5 and H_8); δ_C (125 MHz, $CDCl_3$) 21.3 (2 x Ar-*Me*), 30.8 (CH_2*C*H_2Ph), 37.7 (*C*$H_2$$CH_2$Ph), 114.9 ($C_2$), 120.1 ($C_{2''}$ and $C_{6''}$), 125.9 ($C_{4''}$), 126.2 ($C_{4'}$), 126.3 (C_5 or C_8), 126.7 (C_5 or C_8), 128.1 ($C_{2'}$ and $C_{6'}$), 128.5 ($C_{3'}$ and $C_{5'}$), 130.6 (C_9 or C_{10}), 131.8 (C_9 or C_{10}), 133.0 (C_6 or C_7), 134.2 (C_3), 134.6 (C_6 or C_7), 136.9 ($C_{1''}$), 137.6 ($C_{3''}$ and $C_{5''}$), 140.6 ($C_{1'}$), 168.4 (amide-*C*O), 180.1 (C_1), 182.1 (C_4); *m/z* (ESI$^+$) 425 ([M+H]$^+$, 45%), 447 ([M+Na]$^+$, 80%), 871 ([2M+H]$^+$, 100%); HRMS (ESI$^+$) $C_{27}H_{24}N_2NaO_3S^+$ ([M+Na]$^+$) requires 447.1679, found 447.1672.

2-Amino-3-(4'-chlorophenyl)naphthalene-1,4-dione 172



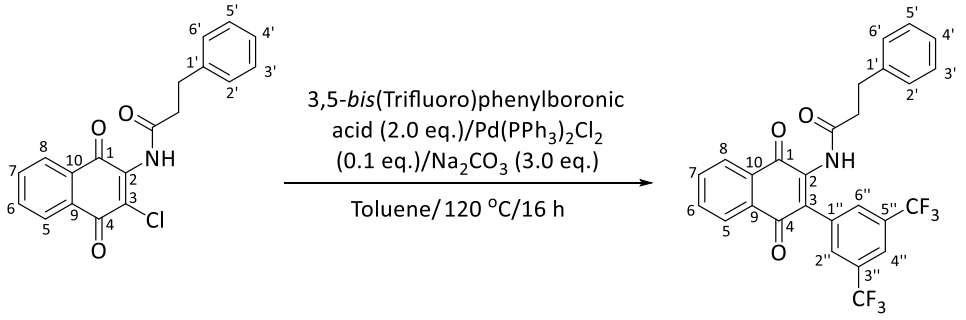
Following *General Procedure 6*, using naphthoquinone **169** (100 mg, 0.300 mmol), 4-chlorobenzeneboronic acid (92 mg, 0.590 mmol), $Pd(PPh_3)_2Cl_2$ (21 mg, 0.030 mmol) and sat. aq. $NaHCO_3$ (2.5 mL) in THF (11 mL). Purification *via* column chromatography on silica gel (eluent pet ether:acetone 90:10 to 75:25) gave 3-arylnaphthoquinone **172** as an orange solid (43 mg, 51%). mp 222-227 ^{o}C; υ_{max} (thin film) 3465 (N-H), 3353 (N-H), 2925 (C-H), 1674 (C=O), 1599, 1558; δ_H (500 MHz, $CDCl_3$) 5.22 (2H, br. s, NH_2), 7.32 (2H, d, *J* 8.5, $C_{2'}$ and $C_{6'}$), 7.48 (2H, d, *J* 8.5, $C_{3'}$ and $C_{5'}$), 7.67 (1H, app. td, *J* 7.6, 1.3, C_6 or C_7), 7.76 (1H, app. td, *J* 7.6, 1.3, C_6 or C_7), 8.11 (1H, dd, *J* 7.6, 1.3, C_5 or C_8), 8.15 (1H, dd, *J* 7.6, 1.3, C_5 or C_8); δ_C (125 MHz, $CDCl_3$) 115.7 (C_3), 126.0 (C_5 or C_8), 126.6 (C_5 or C_8), 129.2 ($C_{3'}$ and $C_{5'}$), 130.4 (C_9 or C_{10}), 130.8 ($C_{1'}$), 131.5 ($C_{2'}$ and $C_{6'}$), 132.3 (C_6 or C_7), 133.0 (C_9 or C_{10}), 134.1 ($C_{4'}$), 134.8 (C_6 or C_7), 145.0 (C_2), 181.5 (C_1), 181.5 (C_4); *m/z* (ESI$^+$) 284 ([M(^{35}Cl)+H]$^+$, 40%), 306 ([M(^{35}Cl)+Na]$^+$, 100%), 308 ([M(^{37}Cl)+Na]$^+$, 33%); HRMS (ESI$^+$) $C_{16}H_{10}ClNNaO_2^+$ ([M+Na]$^+$) requires 306.0292, found 306.0289.

***N*-(3-(4''-Chlorophenyl)-1,4-dioxo-1,4-dihydronaphthalen-2-yl)hydrocinnanamide 173**



Following *General Procedure 7*, using naphthoquinone **169** (150 mg, 0.440 mmol), 4-chlorobenzeneboronic acid (138 mg, 0.880 mmol), $Pd(PPh_3)_2Cl_2$ (31 mg, 0.040 mmol) and Na_2CO_3 (139 mg, 1.33 mmol) in toluene (7 mL). Purification *via* column chromatography on silica gel (eluent pet ether:EtOAc 80:20 to 60:40) gave 3-arylnaphthoquinone **173** as a yellow solid (95 mg, 52%). mp 162-166 ^{o}C; υ_{max} (thin film) 3269 (N-H), 1683 (C=O), 1663 (C=O), 1646 (C=O), 1612, 1591; δ_H (500 MHz, $CDCl_3$) 2.59 (2H, t, *J* 7.6, CH_2CH_2Ph), 2.83 (2H, t, *J* 7.6, CH_2CH_2Ph), 7.10 (2H, d, *J* 7.5, $H_{2'}$ and $H_{6'}$), 7.20-7.24 (1H, m, $H_{4'}$), 7.24-7.31 (4H, m, $H_{3'}$, $H_{5'}$, $H_{2''}$ and $H_{6''}$), 7.35 (2H, d, *J* 8.5, $H_{3''}$ and $H_{5''}$), 7.74-7.82 (3H, m, H_6, H_7 and N*H*), 8.13 (1H, dd, *J* 7.5, 1.4, H_8), 8.16 (1H, dd, *J* 7.5, 1.4, H_5); δ_C (125 MHz, $CDCl_3$) 30.7 (CH_2CH_2Ph), 38.7 (*C*H_2CH_2Ph), 126.3 (C_8 or $C_{4'}$), 126.4 (C_8 or $C_{4'}$), 127.1 (C_5), 128.2 ($C_{2'}$ and $C_{6'}$ or $C_{3''}$ and $C_{5''}$), 128.3 ($C_{2'}$ and $C_{6'}$ or $C_{3''}$ and $C_{5''}$), 128.6 ($C_{3'}$ and $C_{5'}$), 130.3 (C_{10}), 130.5 ($C_{2''}$ and $C_{6''}$), 131.8 (C_9 or $C_{1''}$), 132.2 (C_9 or $C_{1''}$), 133.3 (C_3), 133.6 (C_7), 134.5 ($C_{4''}$), 134.8 (C_6), 137.0 (C_2), 139.9 ($C_{1'}$), 168.4 (amide-*C*O), 182.2 (C_1), 183.1 (C_4); *m/z* (ESI$^+$) 301 (60%), 339 (35%), 393 (30%), 413 ([M(^{35}Cl)+H]$^+$, 35%), 438 ([M(^{35}Cl)+Na]$^+$, 100%), 440 ([M(^{37}Cl)+Na]$^+$, 40%), 853 ([2M(^{35}Cl)+Na], 45%), 855 ([M(^{35}Cl)M(^{37}Cl)+Na], 35%); HRMS (ESI$^+$) $C_{25}H_{18}ClNNaO_3^+$ ([M+Na]$^+$) requires 438.0867, found 438.0855.

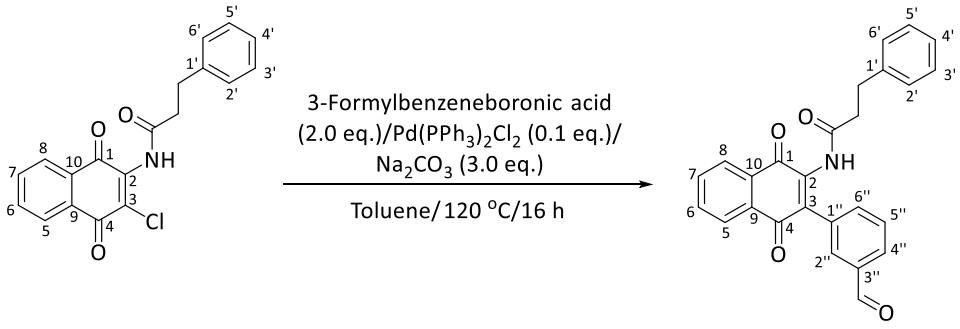
_N_-(3-(3'',5''-_bis_(Trifluoromethyl)phenyl)-1,4-dioxo-1,4-dihydronaphthalen-2-yl)hydrocinnanamide 174



Following *General Procedure 7*, using naphthoquinone **169** (100 mg, 0.300 mmol), 3,5-*bis*(trifluoro)phenylboronic acid (152 mg, 0.590 mmol), $Pd(PPh_3)_2Cl_2$ (21 mg, 0.030 mmol) and Na_2CO_3 (93 mg, 0.880 mmol) in toluene (5 mL). Purification *via* column chromatography on

silica gel (eluent pet ether:acetone 90:10 to 75:25 then pet ether:EtOAc 85:15 to 60:40) gave 3-arylnaphthoquinone **174** as a yellow solid (23 mg, 15%). mp 200 ^{o}C; υ_{max} (thin film) 3390 (N-H), 1668 (C=O); δ_H (500 MHz, $CDCl_3$) 2.57 (2H, t, *J* 8.2, C*H*$_2$CH$_2$Ph), 2.75 (2H, t, *J* 8.2, CH$_2$C*H*$_2$Ph), 7.10 (2H, d, *J* 7.5, H$_{2'}$ and H$_{6'}$), 7.21 (1H, app. t, *J* 7.5, H$_{4'}$), 7.25-7.29 (2H, m, H$_{3'}$ and H$_{5'}$), 7.80 (1H, app. td, *J* 7.6, 1.4, H$_7$), 7.83 (2H, s, H$_{2''}$ and H$_{6''}$), 7.83-7.87 (2H, m, H$_6$ and H$_{4''}$), 7.87 (1H, s, N*H*), 8.17 (1H, dd, *J* 7.6, 1.4, H$_8$), 8.19 (1H, dd, *J* 7.6, 1.4, H$_5$); δ_F (376 MHz, $CDCl_3$) -62.7 (6F, 2 x Ar-C*F*$_3$); δ_C (125 MHz, $CDCl_3$) 30.7 (CH$_2$*C*H$_2$Ph), 39.0 (*C*H$_2$CH$_2$Ph), 121.9 (m, C$_{4''}$), 123.3 (q, *J* 272.7, *C*F$_3$), 126.5 (C$_8$ or C$_{4'}$), 126.6 (C$_8$ or C$_{4'}$), 127.3 (C$_5$), 128.1 (C$_{2'}$ and C$_{6'}$), 128.6 (C$_{3'}$ and C$_{5'}$), 129.5 (m, C$_{2''}$ and C$_{6''}$), 130.0 (C$_{10}$), 130.2 (C$_3$), 131.1 (q, *J* 33.4, C$_{3''}$ and C$_{5''}$), 131.9 (C$_9$), 133.9 (C$_7$), 135.3 (C$_6$), 135.9 (C$_2$ or C$_{1''}$), 137.4 (C$_2$ or C$_{1''}$), 139.6 (C$_{1'}$), 168.3 (amide-*C*O), 181.8 (C$_1$), 182.4 (C$_4$); *m/z* (ESI$^+$) 301 (30%), 393 (30%), 413 (25%), 498 (30%), 540 ([M+Na]$^+$, 100%); HRMS (ESI$^+$) $C_{27}H_{17}F_6NNaO_3^+$ ([M+Na]$^+$) requires 540.1005, found 540.0991.

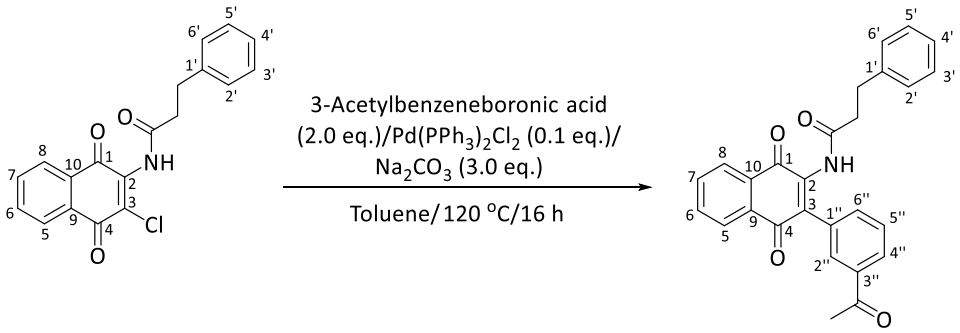
***N*-(3-(3''-Formylphenyl)-1,4-dioxo-1,4-dihydronaphthalen-2-yl)hydrocinnanamide 175**



Following *General Procedure 7*, using naphthoquinone **169** (150 mg, 0.440 mmol), 3-formylbenzeneboronic acid (132 mg, 0.880 mmol), Pd(PPh$_3$)$_2$Cl$_2$ (31 mg, 0.040 mmol) and Na$_2$CO$_3$ (139 mg, 1.33 mmol) in toluene (7 mL). Purification *via* column chromatography on silica gel (eluent pet ether:acetone 90:10 to 75:25) gave 3-arylnaphthoquinone **175** as a yellow solid (102 mg, 56%). mp 122-125 ^{o}C; υ_{max} (thin film) 3260 (N-H), 1706 (C=O), 1668 (C=O), 1596; δ_H (500 MHz, $CDCl_3$) 2.55 (2H, t, *J* 7.7 C*H*$_2$CH$_2$Ph), 2.73 (2H, t, *J* 7.7, CH$_2$C*H*$_2$Ph), 7.04 (2H, d, *J* 7.8, H$_{2'}$ and H$_{6'}$), 7.15-7.20 (1H, m, H$_{4'}$), 7.20-7.25 (2H, m, H$_{3'}$ and H$_{5'}$), 7.56 (1H, app. t, *J* 7.9, H$_{5''}$), 7.64 (1H, app. dt, *J* 7.9, 1.5, H$_{6''}$), 7.73 (1H, app. td, *J* 7.6, 1.4, H$_7$), 7.78 (1H,

app. td, *J* 7.6, 1.4, H_6), 7.82-7.85 (2H, m, $H_{2''}$ and $H_{4''}$), 8.04 (1H, s, N*H*), 8.10 (1H, dd, *J* 7.6, 1.4, H_8), 8.13 (1H, dd, *J* 7.6, 1.4, H_5), 9.99 (1H, s, C*H*O); δ_C (125 MHz, $CDCl_3$) 30.8 (CH_2CH_2Ph), 38.8 (CH_2CH_2Ph), 126.4 (C_8 or $C_{4'}$), 126.5 (C_8 or $C_{4'}$), 127.2 (C_5), 128.2 ($C_{2'}$ and $C_{6'}$), 128.7 ($C_{3'}$ and $C_{5'}$), 128.7 ($C_{5''}$), 129.7 ($C_{2''}$ or $C_{4''}$), 130.2 (C_{10}), 130.3 ($C_{2''}$ or $C_{4''}$), 132.1 (C_9), 132.9 (C_3), 133.8 (C_7), 134.8 ($C_{1''}$), 135.0 (C_6), 135.6 ($C_{6''}$), 136.1 ($C_{3''}$), 137.4 (C_2), 140.0 ($C_{1'}$), 168.6 (amide-*C*O), 182.2 (C_1), 183.1 (C_4), 192.1 (*C*HO); *m/z* (ESI^-) 408 ($[M-H]^-$, 100%); HRMS (ESI^+) $C_{26}H_{19}NNaO_4^+$ ($[M+Na]^+$) requires 432.1206, found 432.1193.

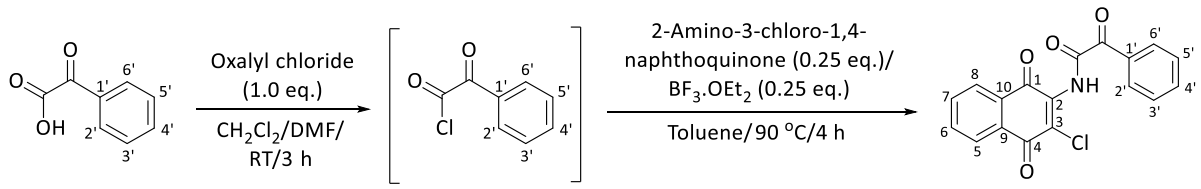
N-(3-(3''-Acetylphenyl)-1,4-dioxo-1,4-dihydronaphthalen-2-yl)hydrocinnanamide 176



Following *General Procedure 7*, using naphthoquinone **169** (150 mg, 0.440 mmol), 3-acetylbenzeneboronic acid (144 mg, 0.880 mmol), $Pd(PPh_3)_2Cl_2$ (31 mg, 0.040 mmol) and Na_2CO_3 (139 mg, 1.33 mmol) in toluene (7 mL). Purification *via* column chromatography on silica gel (eluent pet ether:acetone 90:10 to 75:25) gave 3-arylnaphthoquinone **176** as a yellow solid (121 mg, 65%). mp 144-148 °C; υ_{max} (thin film) 3305 (N-H), 2925 (C-H), 1666 (C=O), 1595; δ_H (500 MHz, $CDCl_3$) 2.54 (2H, t, *J* 7.8, CH_2CH_2Ph), 2.58 (3H, s, *Me*), 2.78 (2H, t, *J* 7.8, CH_2CH_2Ph), 7.05 (2H, d, *J* 7.4, $H_{2'}$ and $H_{6'}$), 7.15-7.19 (1H, app. t, *J* 7.4, $H_{4'}$), 7.20-7.25 (2H, app. t, *J* 7.4, $H_{3'}$ and $H_{5'}$), 7.51 (1H, app. t, *J* 7.9, $H_{5''}$), 7.59 (1H, app. dt, *J* 7.9, 1.3, $H_{6''}$), 7.73 (1H, app. td, *J* 7.6, 1.4, H_7), 7.77 (1H, app. td, *J* 7.6, 1.4, H_6), 7.90-7.94 (2H, m, $H_{2''}$ and $H_{4''}$), 8.00 (1H, s, N*H*), 8.09 (1H, dd, *J* 7.6, 1.4, H_8), 8.12 (1H, dd, *J* 7.6, 1.4, H_5); δ_C (125 MHz, $CDCl_3$) 30.8 (CH_2CH_2Ph), 38.8 (CH_2CH_2Ph), 126.4 (C_8), 126.4($C_{4'}$), 127.0 (C_5), 128.1 ($C_{2'}$ and $C_{6'}$), 128.2 ($C_{2''}$, $C_{4''}$ or $C_{5''}$), 128.4 ($C_{2''}$, $C_{4''}$ or $C_{5''}$), 128.6 ($C_{2''}$, $C_{4''}$ or $C_{5''}$), 128.6 ($C_{3'}$ and $C_{5'}$), 130.3 (C_{10}), 132.1 (C_9), 133.4 (C_3), 133.7 (C_7), 134.1 ($C_{1''}$), 134.4 ($C_{6''}$), 134.8 (C_6), 136.7 ($C_{3''}$), 137.4 (C_2), 140.0

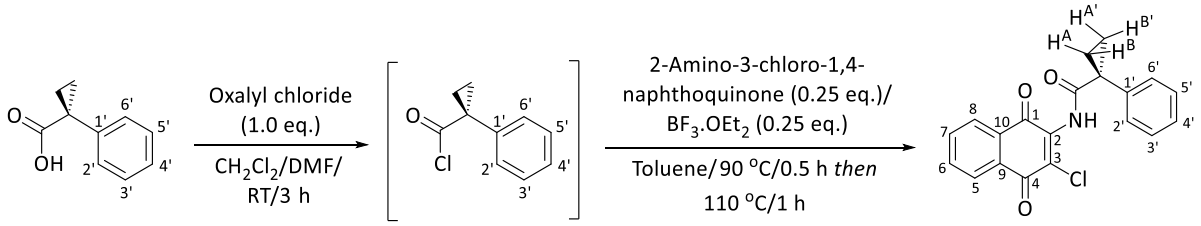
($C_{1'}$), 168.7 (amide-*C*O), 182.1 (C_1), 183.2 (C_4), 197.7 (*C*OMe); *m/z* (ESI^+) 446 ($[M+Na]^+$, 85%), 869 ($[2M+Na]^+$, 100%); HRMS (ESI^+) $C_{27}H_{21}NNaO_4^+$ ($[M+Na]^+$) requires 446.1363, found 446.1350.

***N*-(3-Chloro-1,4-dioxo-1,4-dihydronaphthalen-2-yl)-2-oxo-2-phenylacetamide 181**



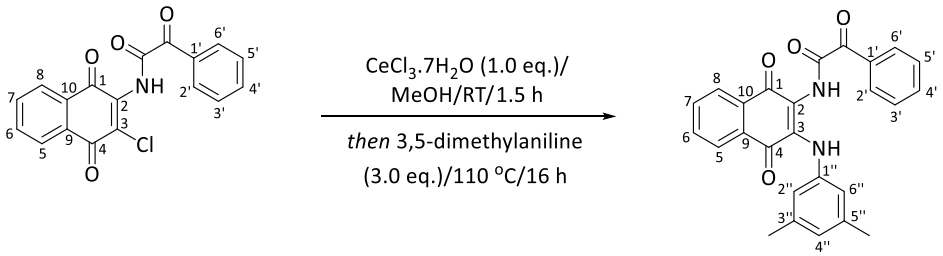
Benzoylformic acid **177** (2.70 g, 18.1 mmol) and DMF (3 drops) were stirred in CH_2Cl_2 (15 mL) at RT. Oxalyl chloride (2.07 mL, 21.7 mmol) was added to this solution and stirring continued at RT for 3 h. The reaction mixture was then concentrated *in vacuo*. 2-Amino-3-chloro-1,4-naphthoquinone **142** (0.94 g, 4.53 mmol), boron trifluoride diethyl etherate (0.545 mL, 3.34 mmol) and toluene (25 mL) were added and the mixture was stirred at 90 °C for 4 h. The crude reaction mixture was concentrated *in vacuo* and the subsequent addition of acetone (20 mL) resulted in the precipitation of a yellow solid. This solid was collected by suction filtration and washed with cold acetone to give oxophenylacetamide **181** as a yellow solid (1.07 g, 69%). mp 218-221 °C; υ_{max} (thin film) 3100 (N-H), 2950 (C-H), 1739 (C=O), 1673 (C=O), 1616, 1590, 1529; δ_H (500 MHz, DMSO-d_6) 7.66-7.70 (2H, m, $H_{3'}$ and $H_{5'}$), 7.79-7.83 (1H, m, $H_{4'}$), 7.91-7.96 (2H, m, H_6 and H_7), 8.07-8.14 (4H, m, H_5, H_8, $H_{2'}$ and $H_{6'}$), *NH not observed*; δ_C (125 MHz, DMSO-d_6) 126.8 (C_5 or C_8), 126.9 (C_5 or C_8), 129.2 ($C_{3'}$ and $C_{5'}$), 129.8 ($C_{2'}$ and $C_{6'}$), 130.7 (C_9 or C_{10}), 131.0 (C_9 or C_{10}), 132.4 ($C_{1'}$), 134.7 (C_6 or C_7), 134.8 (C_6 or C_7), 135.1 ($C_{4'}$), 136.3 (C_3), 139.8 (C_2), 164.1 (NH*C*O), 177.4 (C_4), 178.4 (C_1), 188.9 (*C*OPh); *m/z* (ESI^-) 338 ($[M(^{35}Cl)-H]^-$, 100%), 340 ($[M(^{37}Cl)-H]^-$, 33%); HRMS (ESI^+) $C_{18}H_{10}ClNNaO_4^+$ ($[M(^{35}Cl)+Na]^+$) requires 362.0191, found 362.0180.

N-(3-Chloro-1,4-dioxo-1,4-dihydronaphthalen-2-yl)-1-phenylcyclopropanecarboxamide 182



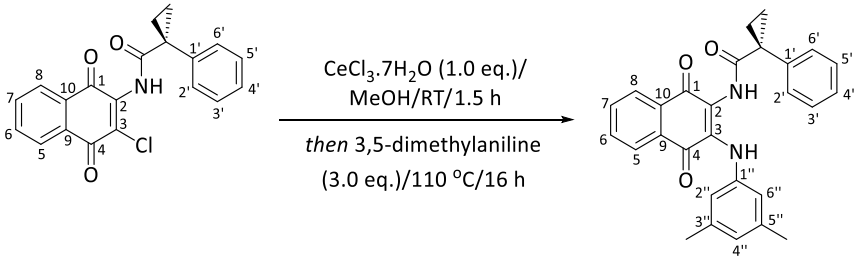
1-Phenyl-1-cyclopropanecarboxylic acid **178** (3.12 g, 19.3 mmol) and DMF (3 drops) were stirred in CH_2Cl_2 (10 mL) at RT. Oxalyl chloride (1.83 mL, 19.3 mmol) was added to this solution and stirring continued at RT for 3 h. The reaction mixture was then concentrated *in vacuo*. 2-Amino-3-chloro-1,4-naphthoquinone **142** (1.00 g, 4.82 mmol), boron trifluoride diethyl etherate (0.81 mL, 4.82 mmol) and toluene (15 mL) were added and the mixture was stirred at 90 °C for 30 min and subsequently at 110 °C for 1 h. The crude reaction mixture was concentrated *in vacuo* and the subsequent addition of acetone (20 mL) resulted in the precipitation of a yellow solid. This solid was collected by suction filtration and washed with cold acetone to give phenylcyclopropanecarboxamide **182** as a yellow solid (1.35 g, 80%). mp 214-215 °C; υ_{max} (thin film) 3338 (N-H), 1739 (C=O), 1713 (C=O), 1665 (C=O), 1615, 1589; δ_H (500 MHz, $CDCl_3$) 1.22-1.25 (2H, m, H_B and $H_{B'}$), 1.51-1.54 (2H, m, H_A and $H_{A'}$), 7.33-7.38 (1H, m, $H_{4'}$), 7.40-7.45 (2H, m, $H_{3'}$ and $H_{5'}$), 7.49-7.53 (2H, m, $H_{2'}$ and $H_{6'}$), 7.87-7.92 (2H, m, H_6 and H_7), 7.99-8.03 (1H, m, H_8), 8.05-8.08 (1H, m, H_5), 8.55 (1H, s, N*H*); δ_C (125 MHz, $CDCl_3$) 16.0 (2 x *C*H_2), 31.0 (NHCO*C*$(CH_2)_2$Ph), 126.6 (C_5 or C_8), 126.8 (C_5 or C_8), 127.8 ($C_{4'}$), 128.9 ($C_{3'}$ and $C_{5'}$), 130.1 ($C_{2'}$ and $C_{6'}$), 130.5 (C_9 or C_{10}), 130.9 (C_9 or C_{10}), 134.4 (C_3), 134.6 (C_6 or C_7), 134.7 (C_6 or C_7), 138.9 ($C_{1'}$), 140.9 (C_2), 170.9 (NH*C*O), 177.6 (C_4), 178.8 (C_1); nOe irradiation of H_A and $H_{A'}$ shows a signal enhancement of N*H*; nOe irradiation of H_B and $H_{B'}$ shows a signal enhancement of $H_{2'}$ and $H_{6'}$; *m/z* (ESI^+) 199 (100%), 352 ($[M(^{35}Cl)+H]^+$, 40%), 374 ($[M(^{35}Cl)+Na]^+$, 60%), 376 ($[M(^{37}Cl)+Na]^+$, 20%); HRMS (ESI^+) $C_{20}H_{14}ClNNaO_3^+$ ($[M(^{35}Cl)+Na]^+$) requires 374.0554, found 374.0549.

***N*-(3-((3'',5''-Dimethylphenyl)amino-1,4-dioxo-1,4-dihydronaphthalen-2-yl)-2-oxo-2-phenylacetamide 183**



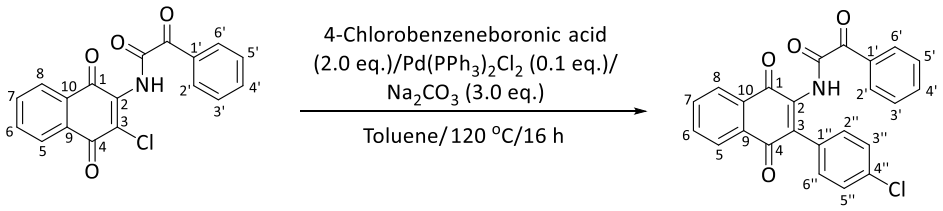
Following *General Procedure 2,* using naphthoquinone **181** (150 mg, 0.442 mmol), 3,5-dimethylaniline (165 µL, 1.33 mmol) and cerium trichloride heptahydrate (165 mg, 0.442 mmol) in MeOH (5 mL) at 110 ^{o}C. Purification *via* column chromatography on silica gel (eluent pet ether:acetone 95:5 to 80:20) gave 3-anilinonaphthoquinone **183** as a red solid (42 mg, 22%). mp 185-188 ^{o}C; υ_{max} (thin film) 2971 (N-H), 1739 (C=O); δ_H (500 MHz, C_6D_6) 2.06 (6H, s, 2 x Ar-*Me*), 6.64 (1H, s, $H_{4''}$), 6.80 (2H, s, $H_{2''}$ and $H_{6''}$), 6.98 (1H, app. td, *J* 7.6, 0.9, H_7), 7.02-7.09 (3H, m, H_6, $H_{2'}$ and $H_{6'}$), 7.14 (2H, app. t, *J* 7.9, $H_{3'}$ and $H_{5'}$), 7.78-7.84 (3H, m, H_5 or H_8, $H_{4'}$ and amide-N*H*), 8.08 (1H, dd, *J* 7.6, 0.9, H_5 or H_8), 8.64 (1H, s, aniline-N*H*); δ_C (125 MHz, C_6D_6) 21.1 (2 x Ar-*Me*), 121.4 (C_2 or C_3), 125.3 ($C_{2''}$ and $C_{6''}$), 125.6 (C_5 or C_8), 126.7 (C_5 or C_8), 127.7-128.4 ($C_{3'}$, $C_{4'}$, $C_{5'}$ and $C_{4''}$, obscured under solvent peak), 129.0 ($C_{2'}$ and $C_{6'}$), 130.3 (C_2 or C_3), 130.8 (C_9 or C_{10}), 132.6 (C_9 or C_{10}), 133.3 (C_6 or C_7), 133.4 (C_6 or C_7), 137.8 ($C_{3''}$ and $C_{5''}$), 139.4 ($C_{1'}$), 141.7 ($C_{1''}$), 161.5 (NH*C*O), 170.1 (*C*OPh), 176.0 (C_1 or C_4), 178.6 (C_1 and C_4); *m/z* (FI^+) 77 (90%), 105 (90%), 275 (70%), 288 (66%), 319 (38%), 331 (64%), 379 (60%), 408 (100%), 424 ($[M]^+$, 10%); HRMS (FI^+) $C_{26}H_{20}N_2O_4^+$ ($[M]^+$) requires 424.1423, found 423.9493.

_N_-(3-((3'',5''-Dimethylphenyl)amino)-1,4-dioxo-1,4-dihydronaphthalen-2-yl)-1-phenylcyclopropanecarboxamide 184



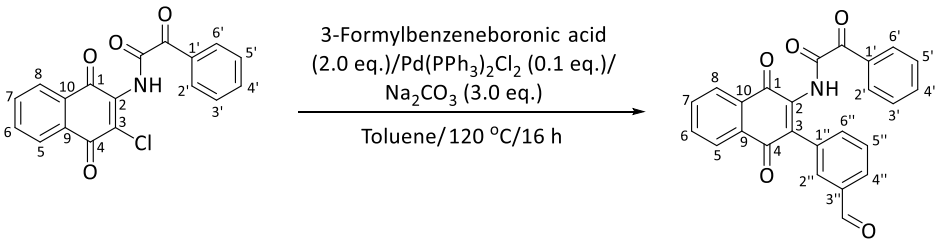
Following *General Procedure 2,* using naphthoquinone **182** (150 mg, 0.427 mmol), 3,5-dimethylaniline (160 µL, 1.28 mmol) and cerium trichloride heptahydrate (159 mg, 0.427 mmol) in MeOH (5 mL) at 110 ^{o}C. Purification *via* column chromatography on silica gel (eluent pet ether:EtOAc 95:5 to 75:25) gave 3-anilinonaphthoquinone **184** as a red solid (107 mg, 58%). mp 241-242 ^{o}C; HPLC t_R 23 min, >99%; υ_{max} (thin film) 3356 (N-H), 2924 (C-H), 2855 (C-H), 1734 (C=O), 1669 (C=O), 1596, 1526; δ_H (500 MHz, $CDCl_3$) 0.83-0.86 (2H, m, 2 x cyclopropyl-C*H*), 1.07-1.10 (2H, m, 2 x cyclopropyl-C*H*), 2.35 (6H, s, 2 x Ar-*Me*), 6.52 (2H, s, $H_{2''}$ and $H_{6''}$), 6.87 (1H, s, $H_{4''}$), 7.25-7.29 (2H, m, $H_{2'}$ and $H_{6'}$), 7.35-7.38 (1H, m, $H_{4'}$), 7.39-7.44 (2H, m, $H_{3'}$ and $H_{5'}$), 7.46 (1H, s, amide-N*H*), 7.62 (1H, app. td, *J* 7.5, 1.3, H_6), 7.65-7.70 (2H, m, H_7 and aniline-N*H*), 8.00 (1H, dd, *J* 7.5, 1.3, H_8), 8.05 (1H, dd, *J* 7.5, 1.3, H_5); δ_C (125 MHz, $CDCl_3$) 16.3 (2 x *C*H_2), 21.4 (2 x Ar-*Me*), 30.4 (NHCO*C*$(CH_2)_2$Ph), 115.5 (C_2), 120.4 ($C_{2''}$ and $C_{6''}$), 126.0 (C_8 or $C_{4''}$), 126.1 (C_8 or $C_{4''}$), 126.6 (C_5), 128.3 ($C_{4'}$), 129.1 ($C_{3'}$ and $C_{5'}$), 130.5 (C_9), 131.0 ($C_{2'}$ and $C_{6'}$), 131.8 (C_{10}), 132.8 (C_6), 134.3 (C_3 or C_7), 134.5 (C_3 or C_7), 137.2 ($C_{1''}$), 137.6 ($C_{3''}$ and $C_{5''}$), 139.0 ($C_{1'}$), 170.8 (amide-*C*O), 179.9 (C_1), 182.2 (C_4); *m/z* (ESI$^+$) 111 (100%), 437 ($[M+H]^+$, 50%), 459 ($[M+Na]^+$, 80%); HRMS (ESI$^+$) $C_{28}H_{24}N_2NaO_3^+$ ($[M+Na]^+$) requires 459.1679, found 459.1668.

***N*-(3-(4''-Chlorophenyl)-1,4-dioxo-1,4-dihydronaphthalen-2-yl)-2-oxo-2-phenylacetamide 185**



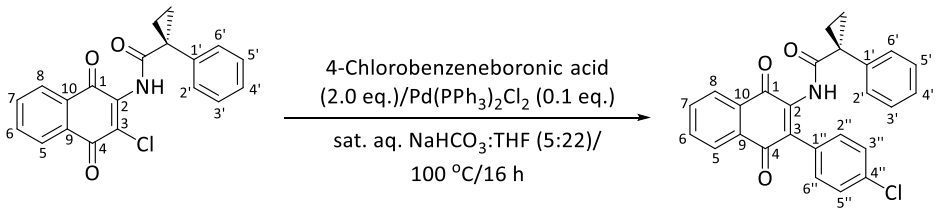
Following *General Procedure 7*, using naphthoquninone **181** (150 mg, 0.442 mmol), 4-chlorophenylboronic acid (138 mg, 0.884 mmol), $Pd(PPh_3)_2Cl_2$ (31 mg, 0.044 mmol) and Na_2CO_3 (139 mg, 1.33 mmol) in toluene (5 mL). Purification *via* column chromatography on silica gel (eluent pet ether:EtOAc 95:5 to 80:20) and subsequent recrystallisation from boiling MeOH gave 3-arylnaphthoquinone **185** as a yellow solid (46 mg, 25%). mp 157-159 ^{o}C (MeOH); υ_{max} (thin film) 3324 (N-H), 1667 (C=O), 1593; δ_H (500 MHz, $CDCl_3$) 7.36-7.40 (2H, m, $H_{2'}$ and $H_{6'}$), 7.42-7.47 (4H, m, $H_{3'}$, $H_{5'}$, $H_{2''}$ and $H_{6''}$), 7.62 (1H, app. tt, *J* 7.5, 1.4, $H_{4'}$), 7.78-7.86 (2H, m, H_6 and H_7), 7.86-7.89 (2H, m, $H_{3''}$ and $H_{5''}$), 8.19-8.22 (2H, m, H_5 and H_8), 9.30 (1H, br. s, N*H*); δ_C (125 MHz, $CDCl_3$) 126.6 (C_5 or C_8), 127.2 (C_5 or C_8), 128.7 ($C_{3'}$ and $C_{5'}$), 128.7 ($C_{2''}$ and $C_{6''}$ or $C_{3''}$ and $C_{5''}$), 130.5 (C_9 or C_{10}), 130.7 ($C_{2'}$ and $C_{6'}$), 131.0 ($C_{2''}$ and $C_{6''}$ or $C_{3''}$ and $C_{5''}$), 131.5 ($C_{1'}$, $C_{1''}$ or $C_{4''}$), 132.1 (C_9 or C_{10}), 132.1 ($C_{1'}$, $C_{1''}$ or $C_{4''}$), 133.9 (C_6 or C_7), 134.4 (C_2 or C_3), 134.9 (C_6 or C_7), 134.9 ($C_{4'}$), 135.1 ($C_{1'}$, $C_{1''}$ or $C_{4''}$), 136.6 (C_2 or C_3), 158.1 (NH*C*O), 181.5 (C_1 or C_4), 182.9 (C_1 or C_4), 186.1 (*C*OPh); *m/z* (ESI^-) 249 (20%), 338 (50%), 414 ($[M(^{35}Cl)-H]^-$, 100%), 416 ($[M(^{37}Cl)-H]^-$, 33%); HRMS (ESI^+) $C_{24}H_{14}ClNNaO_4^+$ ($[M(^{35}Cl)+Na]^+$) requires 438.0504, found 438.0500.

N-(3-(3''-Formylphenyl)-1,4-dioxo-1,4-dihydronaphthalen-2-yl)-2-oxo-2-phenylacetamide 186



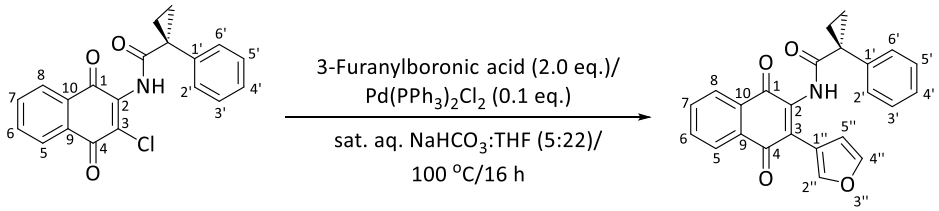
Following *General Procedure 7*, using naphthoquninone **181** (150 mg, 0.442 mmol), 3-formylbenzeneboronic acid (133 mg, 0.884 mmol), $Pd(PPh_3)_2Cl_2$ (31 mg, 0.044 mmol) and Na_2CO_3 (139 mg, 1.33 mmol) in toluene (5 mL). Purification *via* column chromatography on silica gel (eluent pet ether:EtOAc 95:5 to 80:20) gave 3-arylnaphthoquinone **186** as a yellow solid (51 mg, 28%). mp 169-175 ^{o}C; υ_{max} (thin film) 3339 (N-H), 2925 (C-H), 1668 (C=O), 1595; δ_H (500 MHz, $CDCl_3$) 7.36-7.40 (2H, m, $H_{3'}$ and $H_{5'}$), 7.59 (1H, app. tt, *J* 7.3, 1.3, $H_{4'}$), 7.63 (1H, app. t, *J* 7.7, $H_{5''}$), 7.71 (1H, app. dt, *J* 7.7, 1.5, $H_{6''}$), 7.79-7.86 (4H, m, H_6, H_7, $H_{2'}$ and $H_{6'}$), 7.93-7.97 (2H, m, $H_{2''}$ and $H_{4''}$), 8.19-8.22 (2H, m, H_5 and H_8), *NH not observed*; δ_C (125 MHz, $CDCl_3$) 126.7 (C_5 or C_8), 127.2 (C_5 or C_8), 128.6 ($C_{3'}$ and $C_{5'}$), 129.0 ($C_{5''}$), 129.3 ($C_{4''}$), 130.4 (C_9 or C_{10}), 130.9 ($C_{2'}$ and $C_{6'}$), 131.2 ($C_{2''}$), 132.0 (C_9 or C_{10}), 132.0 ($C_{1'}$), 133.8 (C_3), 134.0 (C_6 or C_7), 134.3 ($C_{1''}$), 134.9 (C_6 or C_7), 135.0 ($C_{4'}$), 135.2 ($C_{6''}$), 136.4 ($C_{3''}$), 136.7 (C_2), 158.0 (NH*C*O), 181.4 (C_1), 182.9 (C_4), 185.8 (*C*OPh), 191.8 (*C*HO); *m/z* (ESI$^+$) 410 ([M+H]$^+$, 100%); HRMS (ESI$^+$) $C_{25}H_{15}NNaO_5^+$ ([M+Na]$^+$) requires 432.0842, found 432.0841.

N-(3-(4''-Chlorophenyl)-1,4-dioxo-1,4-dihydronaphthalen-2-yl)-1-phenylcyclopropanecarboxamide 187



Following *General Procedure 6*, using naphthoquinone **182** (100 mg, 0.284 mmol), 4-chlorophenylboronic acid (89 mg, 0.569 mmol), $Pd(PPh_3)_2Cl_2$ (20 mg, 0.028 mmol) and sat. aq. $NaHCO_3$ (2.5 mL) in THF (11 mL). Purification *via* column chromatography on silica gel (eluent pet ether:EtOAc 95:5 to 80:20) gave 3-arylnaphthoquinone **187** as a yellow solid (94 mg, 77%). mp 166-169 ^{o}C; υ_{max} (thin film) 3352 (N-H), 2926 (C-H), 1706 (C=O), 1664 (C=O), 1611, 1592; δ_H (500 MHz, $CDCl_3$) 1.08-1.11 (2H, m, 2 x cyclopropyl-C*H*), 1.34-1.37 (2H, m, 2 x cyclopropyl-C*H*), 7.24-7.27 (2H, m, $H_{2''}$ and $H_{6''}$ or $H_{3''}$ and $H_{5''}$), 7.40-7.45 (5H, m, $H_{2'}$, $H_{4'}$, $H_{6'}$ and $H_{2''}$ and $H_{6''}$ or $H_{3''}$ and $H_{5''}$), 7.45-7.50 (2H, $H_{3'}$ and $H_{5'}$), 7.69-7.78 (3H, m, H_6, H_7 and N*H*), 8.04 (1H, dd, *J* 7.6, 1.3, H_8), 8.12 (1H, dd, *J* 7.6, 1.3, H_5); δ_C (125 MHz, $CDCl_3$) 16.9 (2 x *C*H_2), 31.7 (NHCO*C*$(CH_2)_2$Ph), 126.2 (C_8), 127.0 (C_5), 128.2 ($C_{2'}$ and $C_{6'}$), 128.6 ($C_{4'}$), 129.4 ($C_{3'}$ and $C_{5'}$), 130.4 (C_{10}) 130.4 ($C_{2''}$ and $C_{6''}$ or $C_{3''}$ and $C_{5''}$), 130.8 ($C_{2''}$ and $C_{6''}$ or $C_{3''}$ and $C_{5''}$), 131.8 (C_3, $C_{1''}$ or $C_{4''}$), 132.1 (C_9), 132.7 (C_3, $C_{1''}$ or $C_{4''}$), 133.6 (C_7), 134.4 (C_3, $C_{1''}$ or $C_{4''}$), 134.6 (C_6), 137.7 (C_2), 138.5 ($C_{1'}$), 170.5 (amide-*C*O), 182.0 (C_1), 183.1 (C_4); *m/z* (ESI^-) 426 ($[M(^{35}Cl)-H]^-$, 100%), 428 ($[M(^{37}Cl)-H]^-$, 33%); HRMS (ESI^+) $C_{26}H_{18}ClNNaO_3^+$ ($[M(^{35}Cl)+Na]^+$) requires 450.0851, found 450.0867.

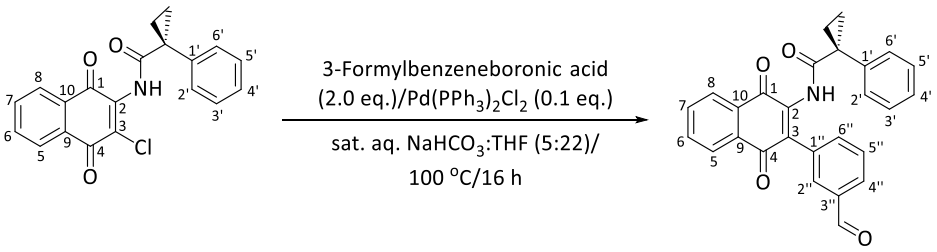
_N_-(3-(Furan-3''-yl)-1,4-dioxo-1,4-dihydronaphthalen-2-yl)-1-phenylcyclopropanecarboxamide 188



Following *General Procedure 6*, using naphthoquinone **182** (100 mg, 0.284 mmol), 3-furanylboronic acid (64 mg, 0.569 mmol), $Pd(PPh_3)_2Cl_2$ (20 mg, 0.028 mmol) and sat. aq. $NaHCO_3$ (2.5 mL) in THF (11 mL). Purification *via* column chromatography on silica gel (eluent pet ether:EtOAc 95:5 to 80:20) gave 3-arylnaphthoquinone **188** as a yellow-orange solid (39 mg, 36%). mp 139-142 ^{o}C; υ_{max} (thin film) 3325 (N-H), 2900 (C-H), 1665 (C=O), 1614, 1593, 1542; δ_H (500 MHz, $CDCl_3$) 1.18-1.21 (2H, m, 2 x cyclopropyl-C*H*), 1.56-1.59 (2H, m, 2 x cyclopropyl-C*H*), 6.59 (1H, dd, *J* 1.9, 0.6, $H_{5''}$), 7.43-7.48 (2H, m, $H_{4'}$ and $H_{4''}$), 7.50-7.54 (2H, m,

$H_{3'}$ and $H_{5'}$), 7.55-7.59 (2H, m, $H_{2'}$ and $H_{6'}$), 7.68 (1H, app. td, *J* 7.6, 1.3, H_7), 7.73 (1H, app. td, *J* 7.6, 1.3, H_6), 7.88 (1H, br. s, N*H*), 8.00 (1H, dd, *J* 7.6, 1.3, H_8), 8.11 (1H, dd, *J* 7.6, 1.3, H_5), 8.15-8.17 (1H, m, $H_{2''}$); δ_C (125 MHz, $CDCl_3$) 16.8 (2 x CH_2), 31.9 (NHCO*C*$(CH_2)_2$Ph), 109.5 ($C_{5''}$), 117.3 ($C_{1''}$), 126.1 (C_8), 127.0 (C_5), 127.7 (C_3), 128.7 ($C_{4'}$), 129.5 ($C_{3'}$ and $C_{5'}$), 130.3 (C_{10}), 131.0 ($C_{2'}$ and $C_{6'}$), 132.4 (C_9), 133.5 (C_7), 134.4 (C_6), 135.8 (C_2), 138.7 ($C_{1'}$), 142.1 ($C_{4''}$), 145.7 ($C_{2''}$), 171.0 (amide-*C*O), 181.8 (C_1), 183.3 (C_4); *m/z* (ESI^-) 382 ($[M-H]^-$, 100%); HRMS (ESI^+) $C_{24}H_{17}NNaO_4^+$ ($[M+Na]^+$) requires 406.1050, found 406.1035.

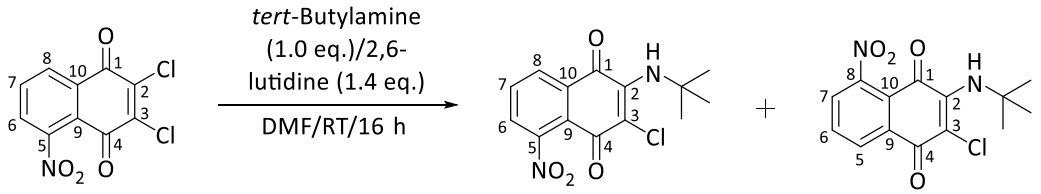
N-(3-(3''-Formylphenyl)-1,4-dioxo-1,4-dihydronaphthalen-2-yl)-1-phenylcyclopropanecarboxamide 189



Following *General Procedure 6*, using naphthoquinone **182** (100 mg, 0.284 mmol), 3-formylbenzeneboronic acid (85 mg, 0.569 mmol), $Pd(PPh_3)_2Cl_2$ (20 mg, 0.028 mmol) and sat. aq. $NaHCO_3$ (2.5 mL) in THF (11 mL). Purification *via* column chromatography on silica gel (eluent pet ether:acetone 95:5 to 80:20) gave 3-arylnaphthoquinone **189** as a yellow solid (98 mg, 82%). mp 143-145 °C; υ_{max} (thin film) 3351 (N-H), 1696 (C=O), 1664 (C=O), 1595; δ_H (500 MHz, $CDCl_3$) 1.03-1.07 (2H, m, 2 x cyclopropyl-C*H*), 1.20-1.24 (2H, m, 2 x cyclopropyl-C*H*), 7.41-7.45 (3H, m, $H_{2'}$, $H_{4'}$ and $H_{6'}$), 7.47-7.52 (2H, m, $H_{3'}$ and $H_{5'}$), 7.64-7.71 (2H, m, $H_{5''}$ and $H_{6''}$), 7.73 (1H, app. td, *J* 7.6, 1.3, H_7), 7.78 (1H, app. td, *J* 7.6, 1.3, H_6), 7.83 (1H, s, N*H*), 7.83-7.85 (1H, m, $H_{2''}$), 7.89-7.92 (1H, m, $H_{4''}$), 8.05 (1H, dd, *J* 7.6, 1.3, H_8), 8.14 (1H, dd, *J* 7.6, 1.3, H_5), 10.09 (1H, s, *CH*O); δ_C (125 MHz, $CDCl_3$) 16.9 (2 x CH_2), 31.9 (NHCO*C*$(CH_2)_2$Ph), 126.2 (C_8), 127.1 (C_5), 128.7 ($C_{4'}$), 128.7 ($C_{4''}$), 129.5 ($C_{3'}$ and $C_{5'}$), 129.6 ($C_{4''}$), 129.9 ($C_{2''}$), 130.3 (C_{10}), 130.8 ($C_{2'}$), 130.8 ($C_{6'}$), 131.9 (C_3 or C_9), 132.1 (C_3 or C_9), 133.7 (C_7), 134.8 (C_6), 134.8 ($C_{1''}$), 135.7 ($C_{6''}$), 136.1 (C_3), 137.7 (C_2), 138.3 ($C_{1'}$), 170.5 (amide-*C*O), 182.0 (C_1), 183.0 (C_4), 192.0

(*C*HO); *m/z* (ESI$^-$) 420 ([M-H]$^-$, 100%); HRMS (ESI$^+$) $C_{27}H_{19}NNaO_4^+$ ((M+Na)$^+$) requires 444.1206, found 444.1200.

2-(*tert*-Butylamino)-3-chloro-8-nitronaphthalene-1,4-dione 193 and 2-(*tert*-Butylamino)-3-chloro-5-nitronaphthalene-1,4-dione 194



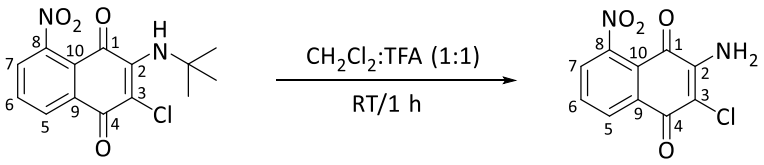
2,3-Dichloro-5-nitro-1,4-naphthoquninone **192** (500 mg, 1.84 mmol), *tert*-butylamine (193 µL, 1.84 mmol) and 2,6-lutidine (300 µL, 2.57 mmol) were stirred in DMF (5 mL) in a sealed microwave vial at RT for 16 h. 1 M aq. HCl (10 mL) was added and the organic product extracted with EtOAc (3 x 20 mL). The organic layers were combined, washed with brine (3 x 20 mL), dried, filtered and concentrated *in vacuo*. Purification *via* column chromatography on silica gel (eluent pet ether:EtOAc 95:5 to 85:15) gave:

2-*tert*-butylamino-3-chloro-8-nitro-1,4-naphthoquinone **193** as an orange solid (110 mg, 19%). mp 132-134 ^oC; υ_{max} (thin film) 3363 (N-H), 1687 (C=O), 1643 (C=O), 1587, 1539; δ_H (500 MHz, $CDCl_3$) 1.54 (9H, s, C*Me*$_3$), 5.83 (1H, br. s, N*H*), 7.73 (1H, dd, *J* 7.9, 1.3, H_7), 7.82 (1H, app. t, *J* 7.9, H_6), 8.33 (1H, dd, *J* 7.9, 1.3, H_5); δ_C (125 MHz, $CDCl_3$) 31.5 (C*Me*$_3$), 56.1 (*C*Me$_3$), 113.0 (C_3), 124.0 (C_{10}), 126.6 (C_7), 129.1 (C_5), 133.0 (C_9), 134.5 (C_6), 146.0 (C_2 or C_8), 146.5 (C_2 or C_8), 173.8 (C_4), 178.3 (C_1); *m/z* (ESI$^+$) 331 ([M(^{35}Cl)+Na]$^+$, 60%), 333 ([M(^{37}Cl)+Na]$^+$, 30%), 639 ([2M(^{35}Cl)+Na]$^+$, 100%), 641 ([M(^{35}Cl)M(^{37}Cl)+Na]$^+$, 70%); HRMS (ESI$^+$) $C_{14}H_{13}ClN_2NaO_4^+$ ([M(^{35}Cl)+Na]$^+$) requires 331.0456, found 331.0452.

2-*tert*-butylamino-3-chloro-5-nitro-1,4-naphthoquinone **194** as an orange solid (301 mg, 53%). mp 143-145 ^oC; υ_{max} (thin film) 3395 (N-H), 3320 (N-H), 1710 (C=O), 1688 (C=O), 1644, 1595; δ_H (500 MHz, $CDCl_3$) 1.57 (9H, s, C*Me*$_3$), 7.65 (1H, dd, *J* 7.8, 1.2, H_6), 7.76 (1H, app. t, *J* 7.8, H_7),

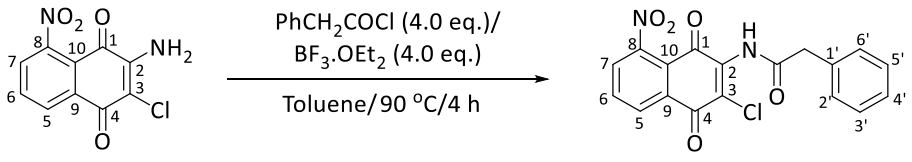
8.22 (1H, dd, *J* 7.8, 1.2, H_8), *NH not observed*; δ_C (125 MHz, $CDCl_3$) 31.5 (CMe_3), 55.6 (CMe_3), 112.9 (C_3), 123.2 (C_9), 128.0 (C_6), 129.0 (C_8), 131.4 (C_{10}), 133.2 (C_7), 145.6 (C_2), 148.4 (C_5), 172.7 (C_4), 178.9 (C_1); *m/z* (ESI^+) 331 ($[M(^{35}Cl)+Na]^+$, 90%), 333 ($[M(^{37}Cl)+Na]^+$, 40%), 368 (70%), 639 ($[2M(^{35}Cl)+Na]^+$, 100%), 641 ($[M(^{35}Cl)M(^{37}Cl)+Na]^+$, 70%); HRMS ($ESI^+$) $C_{14}H_{13}ClN_2NaO_4^+$ ($[M(^{35}Cl)+Na]^+$) requires 331.0456, found 331.0444.

2-Amino-3-chloro-8-nitronaphthalene-1,4-dione 195



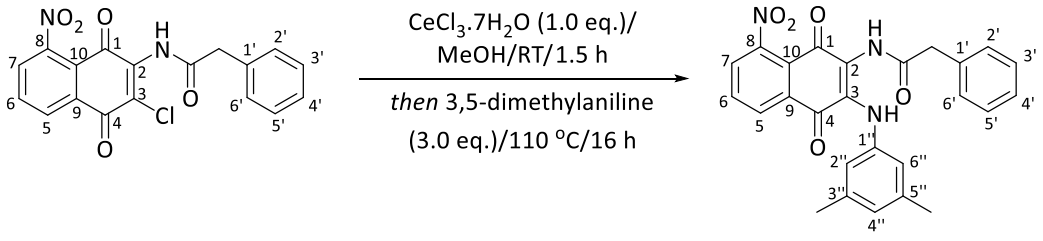
Naphthoquinone **194** (669 mg, 2.17 mmol) and trifluoroacetic acid (12 mL) were stirred in CH_2Cl_2 (12 mL) at RT for 1 h. The solution was partitioned between CH_2Cl_2 (50 mL) and sat. aq. $NaHCO_3$ (50 mL) and the organic later collected, washed with brine (3 x 20 mL), dried, filtered and concentrated *in vacuo*. Purification *via* column chromatography on silica gel (eluent pet ether:acetone 50:50) gave primary amine **195** as an orange solid (507 mg, 93%). mp 245-246 ^oC; υ_{max} (thin film) 3457 (N-H), 3345 (N-H), 2924, 1681 (C=O), 1606 (C=O), 1590, 1538; δ_H (500 MHz, DMSO-d_6) 7.76 (2H, br. s, NH_2), 7.99-8.06 (2H, m, H_6 and H_7), 8.20 (1H, dd, *J* 7.1, 1.8, H_5); δ_C (125 MHz, DMSO-d_6) 108.6 (C_3), 120.5 (C_{10}), 126.1 (C_7), 128.1 (C_5), 133.4 (C_9), 136.0 (C_6), 147.3 (C_2 or C_8), 147.7 (C_2 or C_8), 173.4 (C_4), 176.5 (C_1); *m/z* (ESI^-) 251 ($[M(^{35}Cl)-H]^-$, 100%), 253 ($[M(^{37}Cl)-H]^-$, 33%); HRMS (ESI^+) $C_{10}H_5ClN_2NaO_4^+$ ($[M(^{35}Cl)+Na]^+$) requires 274.9830, found 274.9830.

***N*-(3-Chloro-8-nitro-1,4-dioxo-1,4-dihydronaphthalen-2-yl)phenylacetamide 196**



2-Amino-3-chloro-8-nitro-1,4-naphthoquinone **195** (500 mg, 1.98 mmol) was stirred in toluene (15 mL) in a 2-necked round-bottomed flask at 90 ^{o}C. To a pressure-equalised dropping funnel was added phenylacetyl chloride (1050 µL, 7.92 mmol) and boron trifluoride diethyl etherate (244 µL, 7.11 mmol) in toluene (10 mL). This solution was added dropwise to the reaction flask over a period of 30 min and the reaction mixture was stirred at 90 ^{o}C for a further 4 h. The reaction mixture was cooled to RT and then concentrated *in vacuo*. Acetone (10 mL) was added to the reaction mixture and the yellow precipitate that formed was collected by suction filtration. This precipitate was washed with ice-cold toluene (3 x 2 mL) to give 2-phenylacetamide **196** as a yellow solid (667 mg, 91%). mp 208-209 ^{o}C; υ_{max} (thin film) 3166 (N-H), 1682 (C=O), 1667 (C=O), 1619, 1596, 1529; δ_H (500 MHz, DMSO-d_6) 3.79 (2H, s, CH_2Ph), 7.25-7.28 (1H, m, $H_{4'}$), 7.33-7.36 (4H, m, $H_{2'}$, $H_{3'}$, $H_{5'}$ and $H_{6'}$), 8.06 (1H, app. t, *J* 7.8, H_6), 8.19 (1H, dd, *J* 7.8, 1.2, H_7), 8.28 (1H, dd, *J* 7.8, 1.2, H_5), 10.48 (1H, s, N*H*); δ_C (125 MHz, DMSO-d_6) 41.9 (*C*H_2Ph), 122.1 (C_{10}), 126.7 ($C_{4'}$), 127.8 (C_7), 128.3 ($C_{2'}$ and $C_{6'}$ or $C_{3'}$ and $C_{5'}$), 129.1 (C_5), 129.2 ($C_{2'}$ and $C_{6'}$ or $C_{3'}$ and $C_{5'}$), 132.2 (C_9), 133.9 (C_3), 135.1 ($C_{1'}$), 135.6 (C_6), 141.2 (C_2), 147.9 (C_8), 168.8 (amide-*C*O), 175.8 (C_1), 176.1 (C_4); *m/z* (ESI$^-$) 369 ([M(^{35}Cl)-H]$^-$, 100%), 371 ([M(^{37}Cl)-H]$^-$, 40%); HRMS (ESI$^+$) $C_{18}H_{11}ClN_2NaO_5^+$ ([M(^{35}Cl)+Na]$^+$) requires 393.0249, found 393.0232.

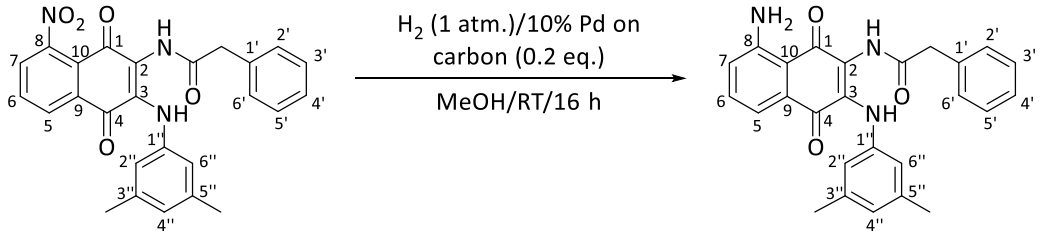
_N_-(3-((3'',5''-Dimethylphenyl)amino)-8-nitro-1,4-dioxo-1,4-dihydronaphthalen-2-yl)phenylacetamide 197



Following *General Procedure 2*, using naphthoquinone **196** (100 mg, 0.270 mmol), 3,5-dimethylaniline (101 µL, 0.810 mmol) and cerium trichloride heptahydrate (101 mg, 0.270 mmol) in MeOH (5 mL) at 110 ^{o}C. Purification *via* column chromatography on silica gel (eluent pet ether:acetone 95:5 to 70:30) gave 3-anilinonaphthoquinone **197** as a red solid

(56 mg, 46%). mp 232 ^{o}C; υ_{max} (thin film) 3321 (N-H), 1676 (C=O), 1611, 1595; δ_H (500 MHz, $CDCl_3$) 2.29 (6H, s, 2 x Ar-*Me*), 3.13 (2H, s, CH_2Ph), 6.52 (2H, s, $H_{2''}$ and $H_{6''}$), 6.82 (1H, s, $H_{4''}$), 6.92-6.95 (2H, m, $H_{2'}$ and $H_{6'}$), 7.25-7.31 (3H, m, $H_{3'}$, $H_{4'}$ and $H_{5'}$), 7.40 (1H, s, amide-N*H*), 7.63 (1H, dd, *J* 7.7, 1.1, H_7), 7.76 (1H, app. t, *J* 7.7, H_6), 7.79 (1H, s, aniline-N*H*), 8.25 (1H, dd, *J* 7.7, 1.1, H_5); δ_C (125 MHz, $CDCl_3$) 21.3 (2 x Ar-*Me*), 42.9 (*C*H_2Ph), 114.9 (C_2), 120.7 ($C_{2''}$ and $C_{6''}$), 122.7 (C_{10}), 126.8 ($C_{4''}$), 127.5 ($C_{4'}$), 127.9 (C_7), 128.8 (C_5), 128.9 ($C_{3'}$ and $C_{5'}$), 129.5 ($C_{2'}$ and $C_{6'}$), 131.4 (C_9), 133.4 ($C_{1'}$), 133.7 (C_6), 134.7 (C_3), 136.2 ($C_{1''}$), 137.8 ($C_{3''}$ and $C_{5''}$), 148.4 (C_8), 167.3 (amide-*C*O), 175.7 (C_1), 180.4 (C_4); *m/z* (ESI$^+$) 478 ([M+Na]$^+$, 100%); HRMS (ESI$^+$) $C_{26}H_{21}N_3NaO_5^+$ ([M+Na]$^+$) requires 478.1373, found 478.1367.

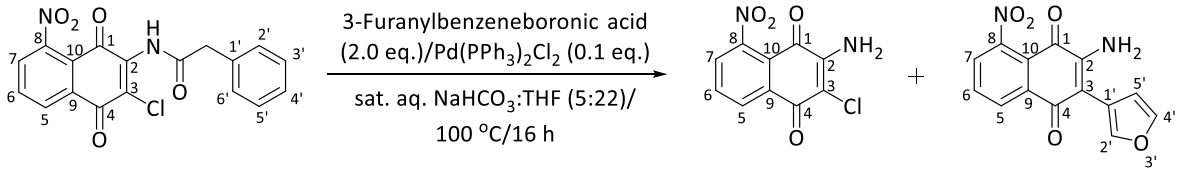
_N_-(8-Amino-3-((3'',5''-dimethylphenyl)amino)-1,4-dioxo-1,4-dihydronaphthalen-2-yl)-2-phenylacetamide 198



Following *General Procedure 5*, using naphthoquninone **197** (40 mg, 0.088 mmol) and 10% Pd/C (2 mg, 0.0018 mmol) in MeOH (5 mL). The crude product was filtered through Celite® and the residue concentrated *in vacuo* to give 8-aminonaphthoquinone **198** as a magenta solid (35 mg, 94%). mp 210-215 ^{o}C; υ_{max} (thin film) 3317 (N-H), 1662 (C=O), 1616 (C=O); δ_H (500 MHz, $CDCl_3$) 2.28 (6H, s, 2 x Ar-*Me*), 3.23 (2H, s, CH_2Ph), 6.48 (2H, s, $H_{2''}$ and $H_{6''}$), 6.50 (2H, br. s, NH_2), 6.76 (1H, s, $H_{4''}$), 6.88 (1H, app. d, *J* 8.2, H_7), 7.03 (2H, d, *J* 6.9, $H_{2'}$ and $H_{6'}$), 7.27-7.36 (4H, m, H_6, $H_{3'}$, $H_{4'}$ and $H_{5'}$), 7.46 (1H, dd, *J* 7.4, 0.8, H_5), 7.56 (1H, s, amide-N*H*), 7.58 (1H, s, aniline-N*H*); δ_C (125 MHz, $CDCl_3$) 21.3 (2 x Ar-*Me*), 43.2 (*C*H_2Ph), 110.8 (C_9), 115.7 (C_2), 117.6 (C_5), 119.8 ($C_{2''}$ and $C_{6''}$), 124.2 (C_7), 125.5 ($C_{4''}$), 127.4 ($C_{4'}$), 128.9 ($C_{3'}$ and $C_{5'}$), 129.6 ($C_{2'}$ and $C_{6'}$), 131.6 (C_{10}), 133.3 (C_3 or C_6), 133.5 (C_3 or C_6), 133.9 ($C_{1'}$), 137.4 ($C_{1''}$), 137.6 ($C_{3''}$ and $C_{5''}$), 149.6 (C_8), 167.1 (NH*C*O), 182.3 (C_1 or C_4), 182.6 (C_1 or C_4); *m/z* (ESI$^+$) 426 ([M+H]$^+$, 60%),

448 ([M+Na]$^+$, 100%); HRMS (ESI$^+$) $C_{26}H_{23}N_3NaO_3^+$ ([M+Na]$^+$) requires 448.1632, found 448.1622.

2,8-Diamino-3-chloronaphthalene-1,4-dione 200 and 2,8-Diamino-3-(furan-3''-yl)naphthalene-1,4-dione 201



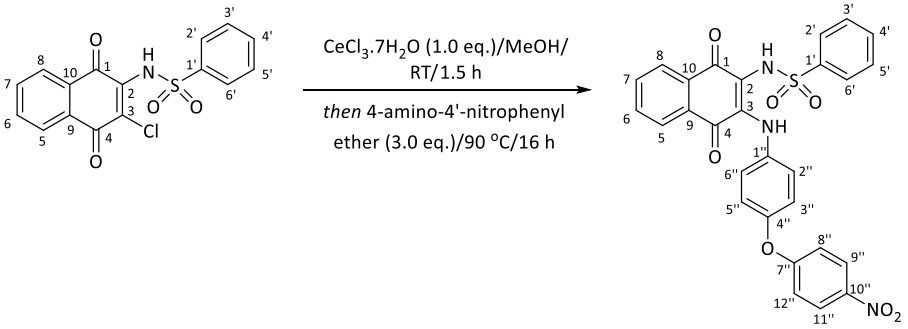
Following *General Procedure 6*, using naphthoquinone **196** (100 mg, 0.270 mmol), 3-furanylboronic acid (60 mg, 0.540 mmol), $Pd(PPh_3)_2Cl_2$ (19 mg, 0.027 mmol) and sat. aq. $NaHCO_3$ (2.5 mL) in THF (11 mL). Purification *via* column chromatography on silica gel (eluent pet ether:acetone 95:5 to 80:20) gave:

2,8-diamino-3-chloro-naphthoquinone **200** as an orange solid (53 mg, 88%). mp 178-180 ^oC; υ_{max} (thin film) 3430 (N-H), 3329 (N-H), 2925 (C-H), 1593 (C=O), 1544; δ_H (500 MHz, DMSO-d_6) 7.05 (1H, dd, *J* 8.5, 0.9, H_7), 7.21 (1H, dd, *J* 7.3, 0.9, H_5), 7.39 (2H, br. s, NH_2), 7.42 (1H, dd, *J* 8.5, 7.3, H_6), 7.90 (2H, br. s, NH_2); δ_C (125 MHz, DMSO-d_6) 107.2 (C_3), 108.5 (C_{10}), 115.5 (C_5), 122.2 (C_7), 133.0 (C_9), 135.1 (C_6), 147.9 (C_2), 151.9 (C_8), 174.9 (C_4), 179.0 (C_1); *m/z* (ESI$^+$) 139 (45%), 245 ([M(^{35}Cl)+Na]$^+$, 100%), 247 ([M(^{37}Cl)+Na]$^+$, 33%), 467 ([2M(^{35}Cl)+Na]$^+$, 40%); HRMS (ESI$^+$) $C_{10}H_7ClN_2NaO_2^+$ ([M(^{35}Cl)+Na]$^+$) requires 245.0088, found 245.0089.

2,8-diamino-3-arylnaphthoquinone **201** as an orange solid (7 mg, 10%). mp 187-189 ^oC; υ_{max} (thin film) 3329 (N-H), 1634 (C=O); δ_H (500 MHz, $CDCl_3$) 5.49 (2H, br. s, -NH_2), 6.65 (2H, br. s, NH_2), 6.69 (1H, app. d, *J* 1.6, $H_{5'}$), 6.84 (1H, dd, *J* 8.3, 1.0, H_7), 7.41 (1H, dd, *J* 8.3, 7.4, H_6), 7.50 (1H, dd, *J* 7.4, 1.0, H_5), 7.56 (1H, t, *J* 1.6, $H_{4'}$), 7.79 (1H, app. s, $H_{2'}$); δ_C (125 MHz, $CDCl_3$) 107.6 (C_3), 110.8 (C_{10} or $C_{5'}$), 111.0 (C_{10} or $C_{5'}$), 116.6 ($C_{1'}$), 117.1 (C_5), 121.3 (C_7), 134.1 (C_9), 135.5 (C_6), 142.4 ($C_{2'}$), 143.0 ($C_{4'}$), 146.1 (C_2), 150.2 (C_8), 181.3 (C_1 or C_4), 181.7 (C_1 or C_4); *m/z* (ESI$^+$)

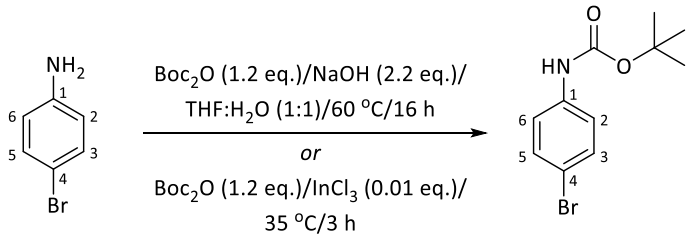
139 (100%), 181 (60%), 277 ([M+Na]$^+$, 85%); HRMS (ESI$^+$) $C_{14}H_{10}N_2NaO_3^+$ ([M+Na]$^+$) requires 277.0584, found 277.0587.

_N_-3-((4''-(10''-Nitrophenoxy)phenyl)amino)-1,4-dioxo-1,4-dihydronaphthalen-2-yl)benzenesulfonamide 203



Following *General Procedure 2*, using naphthoquinone **57** (130 mg, 0.374 mmol), 4-amino-4'-nitrophenyl ether (258 mg, 1.12 mmol) and cerium trichloride heptahydrate (139 mg, 0.374 mmol) in MeOH (7 mL) at 90 ^oC. Purification *via* column chromatography (eluent pet ether:acetone 90:10 to 75:25) and subsequent recrystallisation from boiling acetone gave 3-anilinonaphthoquninone **203** as a red solid (32 mg, 16%). mp >250 ^oC (acetone); υ_{max} (thin film) 3331 (N-H), 3231 (N-H), 1672 (C=O), 1607 (C=O), 1575, 1511; δ_H (500 MHz, DMSO-d_6) 7.07-7.11 (2H, m, $H_{3''}$ and $H_{5''}$), 7.15-7.20 (4H, m, $H_{2''}$, $H_{6''}$, $H_{8''}$ and $H_{12''}$), 7.38-7.43 (2H, m, $H_{3'}$ and $H_{5'}$), 7.49-7.54 (1H, m, $H_{4'}$), 7.61-7.65 (2H, m, $H_{2'}$ and $H_{6'}$), 7.74-7.81 (3H, m, H_6, H_7 and H_8), 8.03-8.07 (1H, m, H_5), 8.22-8.26 (2H, m, $H_{9''}$ and $H_{11''}$), 9.03 (1H, s, sulfonamide-N*H*), 9.24 (1H, s, aniline-N*H*); δ_C (125 MHz, DMSO-d_6) 112.8 (C_2), 116.9 ($C_{8''}$ and $C_{12''}$), 119.8 ($C_{3''}$ and $C_{5''}$), 125.7 (C_8), 126.0 ($C_{9''}$ and $C_{11''}$), 126.2 (C_5), 126.3 ($C_{2''}$ and $C_{6''}$), 126.5 ($C_{2'}$ and $C_{6'}$), 128.5 ($C_{3'}$ and $C_{5'}$), 130.2 (C_9), 131.6 (C_{10}), 132.2 ($C_{4'}$), 133.0 (C_6), 135.0 (C_7), 135.9 ($C_{1''}$), 141.3 ($C_{1'}$), 142.0 ($C_{7''}$). 142.3 (C_3), 150.0 ($C_{4''}$), 163.7 ($C_{10''}$), 178.5 (C_1), 182.4 (C_4); *m/z* (ESI$^-$) 540 ([M-H]$^-$, 100%); HRMS (ESI$^-$) $C_{28}H_{18}O_7N_3S^-$ ([M-H]$^-$) requires 540.0871, found 540.0881.

tert-Butyl (4-bromophenyl)carbamate 205[376]

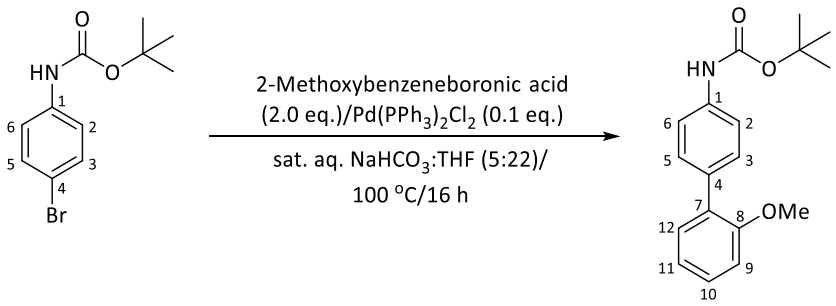


Method A: To a solution of 4-bromoaniline **204** (5.00 g, 29.0 mmol) in THF (120 mL) at RT, NaOH (2.56 g, 64.0 mmol) and Boc anhydride (7.63 g, 35.0 mmol) in H_2O (120 mL) were added dropwise over 30 min, and the solution was stirred at 60 °C for 16 h. The product was extracted with CH_2Cl_2 (3 x 50 mL) and the combined organic layers were washed with H_2O (2 x 50 mL), dried, filtered and concentrated *in vacuo*. Purification *via* column chromatography (eluent pet ether:EtOAc) gave *tert*-butyl carbamate **205** as a light yellow solid (2.75 g, 35%).

Method B: 4-Bromoaniline **204** (5.00 g, 29.0 mmol), Boc anhydride (7.61 g, 34.9 mmol) and indium trichloride (145 mg, 0.290 mmol) were added to a flask and stirred at 35 °C for 3 h. The reaction mixture was then partitioned between EtOAc (50 mL) and H_2O (50 mL); the organic layer was collected, washed with brine (3 x 20 mL), dried, filtered and concentrated *in vacuo*. Purification *via* column chromatography on silica gel (eluent pet ether:EtOAc 95:5) afforded *tert*-butyl carbamate **205** as a light yellow solid (7.76 g, 98%).

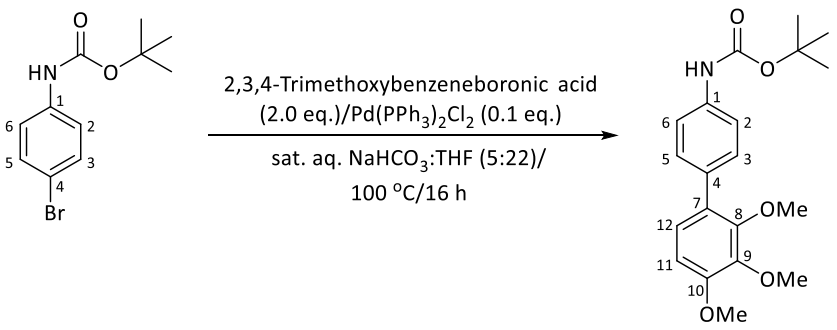
mp 106-107 °C (lit. 104 °C);[376] δ_H (400 MHz, $CDCl_3$) 1.52 (9H, s, OC*Me*$_3$), 6.58 (1H, br. s, N*H*), 7.26 (2H, d, *J* 8.0, H_3 and H_5), 7.39 (2H, d, *J* 8.0, H_2 and H_6); *m/z* (ESI^+) 216 (80%), 218 (80%), 295 ($[M(^{79}Br)+Na]^+$, 100%), 297 ($[M(^{81}Br)+Na]^+$, 100%).

tert-Butyl (8-Methoxy-[4,7-biphenyl]-1-yl)carbamate 207[300]



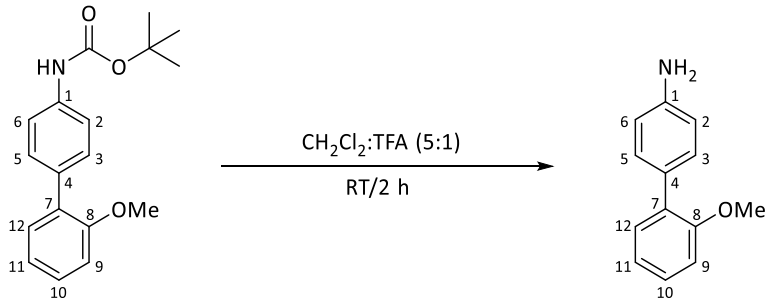
Following *General Procedure 6*, using *tert*-butyl (4-bromophenyl)carbamate **205** (1.00 g, 3.68 mmol), 2-methoxybenzeneboronic acid (1.12 g, 7.35 mmol), $Pd(PPh_3)_2Cl_2$ (257 mg, 0.368 mmol) and sat. aq. $NaHCO_3$ (2.5 mL) in THF (11 mL). Purification *via* column chromatography on silica gel (eluent pet ether:acetone 95:5 to 90:10) gave [4,7]-biphenyl **207** as a light yellow solid (177 mg, 16%). mp 92-94 ^oC (lit. 168-170 ^oC);[300] δ_H (400 MHz, $CDCl_3$) 1.54 (9H, s, C*Me*$_3$), 3.81 (3H, s, O*Me*), 6.57 (1H, br. s, N*H*), 6.98 (1H, d, *J* 8.5, H_9), 7.02 (1H, app, t, *J* 7.5, H_{11}), 7.28-7.33 (2H, m, H_{10} and H_{12}), 7.40 (2H, d, *J* 8.8, H_2 and H_6), 7.48 (2H, d, *J* 8.8, H_3 and H_5); *m/z* (ESI^+) 244 ($[M-^tBu+2H]^+$, 90%), 322 ($[M+Na]^+$, 100%).

tert-Butyl (8,9,10-trimethoxy-[4,7-biphenyl]-1-yl)carbamate 210[300]



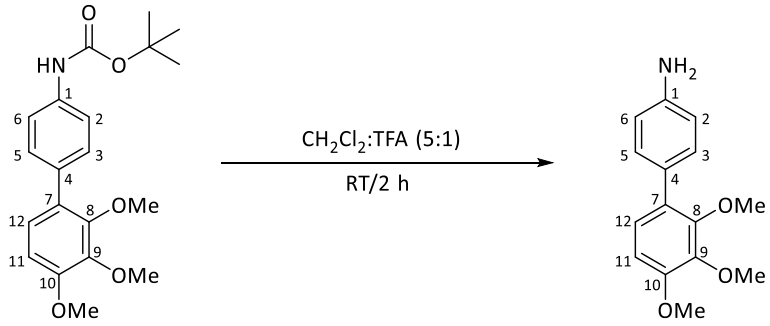
Following *General Procedure 6,* using *tert*-butyl carbamate **205** (738 mg, 2.71 mmol), 2,3,4-trimethoxyphenylboronic acid (1.15 g, 5.42 mmol), $Pd(PPh_3)_2Cl_2$ (190 mg, 0.271 mmol) and sat. aq. $NaHCO_3$ (2.5 mL) in THF (11 mL). Purification *via* column chromatography (eluent acetone:pet ether 5:95) gave biphenyl **210** as a yellow solid (648 mg, 67%). mp 147-148 ^oC (lit. 143-145 ^oC);[300] δ_H (500 MHz, $CDCl_3$) 1.53 (9H, s, OC*Me*$_3$), 3.65 (3H, s, C_8-O*Me*), 3.89 (3H, s, C_{10}-O*Me*), 3.93 (3H, s, C_9-O*Me*), 6.57 (1H, br. s, N*H*), 6.73 (1H, d, *J* 8.7, H_{11}), 7.01 (1H, d, *J* 8.7, H_{12}), 7.37-7.46 (4H, m, H_2, H_3, H_5 and H_6); *m/z* (ESI^+) 304 ($[M-^tBu+2H]^+$, 100%), 382 ($[M+Na]^+$, 75%).

8-Methoxy-[4,7-biphenyl]-1-amine 212[300]



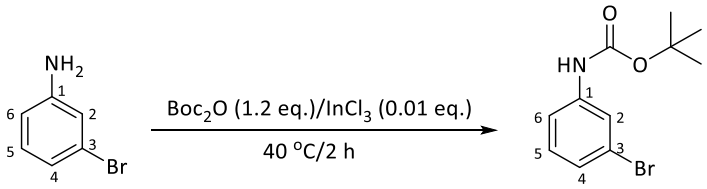
Following *General Procedure 8*, using carbamate **207** (200 mg, 0.669 mmol) and trifluoroacetic acid (3 mL) in CH_2Cl_2 (15 mL) to give amine **212** as a brown oil (92 mg, 69%) which was used subsequently without further purification. δ_H (400 MHz, $CDCl_3$) 3.82 (3H, s, O*Me*), 6.76-6.81 (2H, m, H_2 and H_6), 6.97 (1H, d, *J* 8.2, H_9), 7.01 (1H, app. td, *J* 7.5, 0.9, H_{11}), 7.25-7.33 (2H, m, H_{10} and H_{12}), 7.35-7.41 (2H, m, H_3 and H_5), *NH not observed*; *m/z* (ESI^+) 200 ($[M+H]^+$, 100%).

8,9,10-Trimethoxy-[4,7-biphenyl]-1-amine 215[300]



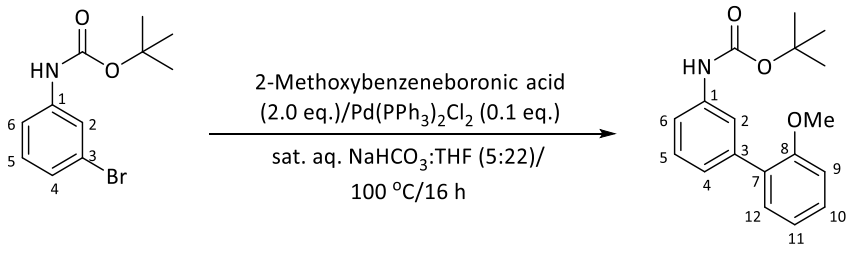
Following *General Procedure 8,* using carbamate **210** (640 mg, 1.78 mmol) and trifluoroacetic acid (6 mL) and in CH_2Cl_2 (30 mL) to give aniline **215** as a brown oil (350 mg, 76%) which was used subsequently without further purification. δ_H (500 MHz, $CDCl_3$) 3.67 (3H, s, C_9-O*Me*), 3.88-3.94 (6H, m, C_8-O*Me* and C_{10}-O*Me*), 6.70-6.79 (3H, m, H_2, H_6 and H_{11}), 7.00 (1H, d, *J* 8.5, H_{12}), 7.33 (2H, d, *J* 8.5, H_3 and H_5), *NH_2 not observed*; *m/z* (ESI^+) 260 ($[M+H]^+$, 100%).

tert-Butyl (3-bromophenyl)carbamate 222



3-Bromoaniline **221** (3.16 mL, 29.1 mmol), Boc anhydride (7.61 g, 34.9 mmol) and indium trichloride (145 mg, 0.29 mmol) were added to a flask and stirred at 40 ^{o}C for 2 h. The reaction mixture was then partitioned between EtOAc (50 mL) and H_2O (50 mL); the organic layer was collected, washed with brine (3 x 20 mL), dried, filtered and concentrated *in vacuo*. Purification *via* column chromatography on silica gel (eluent pet ether:EtOAc 98:2 to 90:10) afforded carbamate **222** as a white solid (7.50 g, 95%). mp 86-87 ^{o}C; υ_{max} (thin film) 3313 (N-H), 2976 (C-H), 1691 (C=O), 1589, 1536; δ_H (500 MHz, $CDCl_3$) 1.53 (9H, s, C*Me*$_3$), 6.49 (1H, br. s, N*H*), 7.11-7.18 (2H, m, H_5 and H_4 or H_6), 7.19-7.24 (1H, m, H_4 or H_6), 7.68 (1H, s, H_2); δ_C (125 MHz, $CDCl_3$) 28.3 (C*Me*$_3$), 81.0 (*C*Me$_3$), 116.8 (C_4 or C_6), 121.3 (C_2), 122.7 (C_3), 126.0 (C_4 or C_6), 130.2 (C_5), 139.7 (C_1), 152.4 (carbamate-*C*O); *m/z* (ESI$^+$) 294 ([M(^{79}Br)+Na]$^+$, 100%), 296 ([M(^{81}Br)+Na]$^+$, 100%); HRMS (ESI$^+$) $C_{11}H_{14}BrNNaO_2^+$ ([M(^{79}Br)+Na]$^+$) requires 294.0100, found 294.0101.

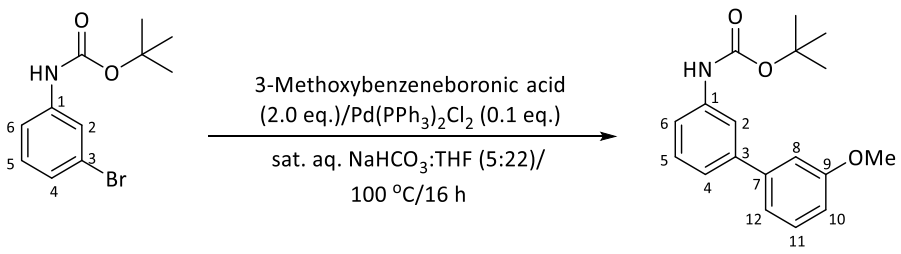
tert-Butyl (8-methoxy-[3,7]-biphenyl-1-yl)carbamate 223



Following *General Procedure 6*, using *tert*-butyl (3-bromophenyl)carbamate **222** (2.00 g, 7.35 mmol), 2-methoxybenzeneboronic acid (2.24 g, 14.7 mmol), $Pd(PPh_3)_2Cl_2$ (1.03 g, 1.47 mmol) and sat. aq. $NaHCO_3$ (5 mL) in THF (22 mL). Purification *via* column chormatogrpahy on silica gel (eluent pet ether:acetone 98:2) gave [3,7]-biphenyl **223** as a

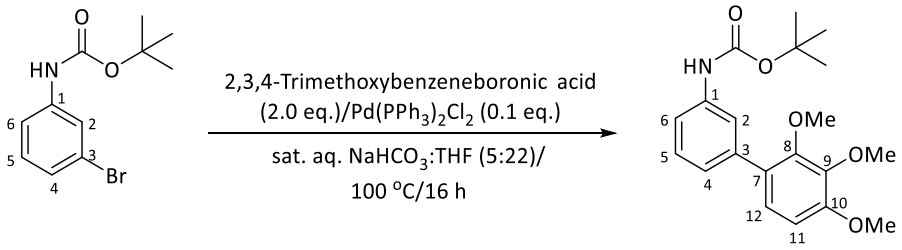
white solid (406 mg, 18%). mp 108-110 ^{o}C; υ_{max} (thin film) 3331 (N-H), 2976 (C-H), 1704 (C=O), 1591, 1535; δ_H (400 MHz, DMSO-d_6) 1.47 (9H, s, CMe_3), 3.75 (3H, s, O*Me*), 6.98-7.06 (2H, m, H_4 and H_{11}), 7.09 (1H, d, *J* 8.2, H_9), 7.19-7.28 (2H, m, H_5 and H_{12}), 7.33 (1H, app. td, *J* 7.6, 1.6, H_{10}), 7.42 (1H, d, *J* 8.1, H_6), 7.54 (1H, s, H_2), 9.32 (1H, s, N*H*); δ_C (100 MHz, DMSO-d_6) 28.1 (CMe_3), 55.5 (O*Me*), 79.0 (*C*Me$_3$), 111.8 (C_9), 116.7 (C_6), 119.2 (C_2), 120.7 (C_{11}), 123.1 (C_4), 128.1 (C_5), 128.8 (C_{10}), 130.1 (C_7), 130.2 (C_{12}), 138.6 (C_1 or C_3), 139.2 (C_1 or C_3), 152.8 (*C*=O), 156.1 (C_8); *m/z* (ESI$^+$) 244 ([M-^{t}Bu+2H]$^+$, 30%), 322 ([M+Na]$^+$, 90%), 621 ([2M+Na]$^+$, 100%); HRMS (ESI$^+$) $C_{18}H_{21}NNaO_3^+$ ([M+Na]$^+$) requires 322.1414, found 322.1415.

tert-Butyl (9-methoxy-[3,7]-biphenyl-1-yl)carbamate 224



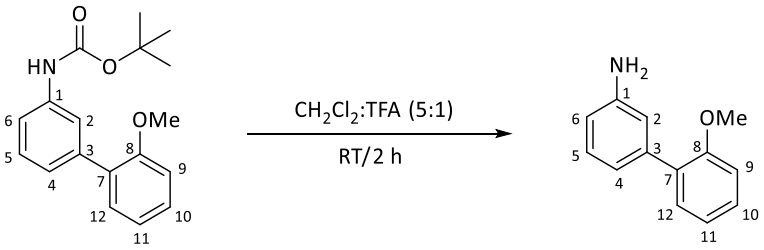
Following *General Procedure 6*, using *tert*-butyl carbamate **222** (458 mg, 1.68 mmol), 3-methoxyphenyl boronic acid (512 mg, 3.37 mmol), $Pd(PPh_3)_2Cl_2$ (117 mg, 0.168 mmol) and sat. aq. $NaHCO_3$ (2.5 mL) in THF (11 mL). Purification *via* column chromatography (eluent pet ether:acetone 95:5) afforded biphenyl **224** as a pale yellow solid (300 mg, 60%). mp 110-112 ^{o}C; υ_{max} (thin film) 3360 (N-H), 2983 (C-H), 1700 (C=O), 1583, 1542; δ_H (500 MHz, $CDCl_3$) 1.55 (9H, s, CMe_3), 3.87 (3H, s, O*Me*), 6.59 (1H, br. s, N*H*), 6.90 (1H, ddd, *J* 8.2, 2.5, 0.8, H_{10}), 7.12 (1H, app. t, *J* 2.5, H_8), 7.16-7.20 (1H, m, H_{12}), 7.25-7.28 (1H, m, H_4), 7.33-7.39 (3H, m, H_5, H_6 and H_{11}), 7.60 (1H, app. s, H_2); δ_C (125 MHz, $CDCl_3$) 28.3 (CMe_3), 55.3 (O*Me*), 80.6 (*C*Me$_3$), 112.8 (C_8 or C_{10}), 112.9 (C_8 or C_{10}), 117.3 (C_2), 117.5 (C_6), 119.7 (C_{12}), 121.9 (C_4), 129.3 (C_5), 129.7 (C_{11}), 138.7 (C_1), 142.0 (C_3), 142.4 (C_7), 152.7 (*C*=O), 159.8 (C_9); *m/z* (ESI$^+$) 244 ([M-^{t}Bu+2H]$^+$, 60%), 322 ([M+Na]$^+$, 70%), 621 ([2M+Na]$^+$, 100%); HRMS (ESI$^+$) $C_{18}H_{21}NNaO_3^+$ ([M+Na]$^+$) requires 322.1414, found 322.1413.

tert-Butyl (8,9,10-trimethoxy-[3,7-biphenyl]-1-yl)carbamate 225



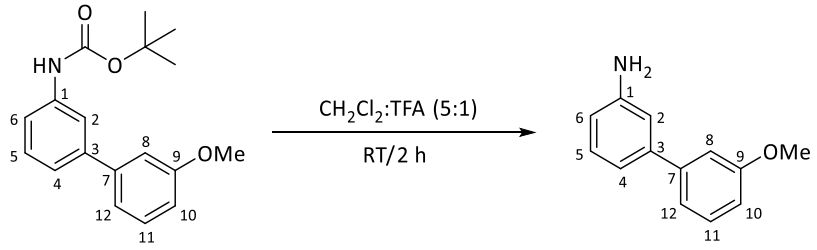
Following *General Procedure 6*, using *tert*-butyl carbamate **222** (1.00 g, 3.68 mmol), 2,3,4-trimethoxyphenylboronic acid (1.56 g, 7.35 mmol), $Pd(PPh_3)_2Cl_2$ (514 mg, 0.735 mmol) and sat. aq $NaHCO_3$ (2.5 mL) in THF (11 mL). Purification *via* column chromatography on silica gel (eluent pet ether:acetone 90:10 to 80:20 then pet ether:Et_2O 90:10 to 60:40) gave biphenyl **225** as a light yellow solid (441 mg, 33%). mp 122-125 ^oC; υ_{max} (thin film) 337 (N-H), 2977 (C-H), 2936 (C-H), 1707 (C=O), 1608, 1591, 1542; δ_H (500 MHz, $CDCl_3$) 1.53 (9H, s, C*Me*$_3$), 3.68 (3H, s, C_8-O*Me* or C_{10}-O*Me*), 3.90 (3H, s, C_8-O*Me* or C_{10}-O*Me*), 3.93 (3H, s, C_9-O*Me*), 6.52 (1H, br. s, N*H*), 6.73 (1H, d, *J* 8.6, H_{11}), 7.04 (1H, d, *J* 8.6, H_{12}), 7.19 (1H, d, *J* 7.6, H_4 or H_6), 7.32 (1H, app. t, *J* 7.6, H_5), 7.37-7.42 (1H, m, H_4 or H_6), 7.44 (1H, s, H_2); δ_C (125 MHz, $CDCl_3$) 28.3 (C*Me*$_3$), 56.0 (C_8-O*Me* or C_{10}-O*Me*), 61.0 (C_9-O*Me*), 61.0 (C_8-O*Me* or C_{10}-O*Me*), 80.4 (*C*Me$_3$), 107.4 (C_{11}), 117.0 (C_4 or C_6), 119.3 (C_2), 124.0 (C_4 or C_6), 124.8 (C_{12}), 128.4 (C_7), 128.7 (C_5), 138.1 (C_1), 139.0 (C_3), 142.5 (C_9), 151.4 (C_8 or C_{10}), 152.7 (*C*O$_2$^{t}Bu), 153.1 (C_8 or C_{10}); *m/z* (ESI$^+$) 304 ([M-^{t}Bu+2H]$^+$, 50%), 382 ([M+Na]$^+$, 100%), 741 ([2M+Na]$^+$, 70%); HRMS (ESI$^+$) $C_{20}H_{25}NNaO_5^+$ ([M+Na]$^+$) requires 382.1625, found 382.1622.

8-Methoxy-[3,7]-biphenyl-1-amine 226



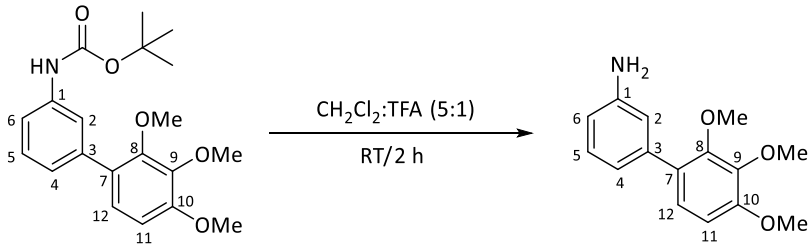
Following *General Procedure 8*, using *tert*-butyl carbamate **223** (335 mg, 1.12 mmol) and trifluoroacetic acid (6 mL) in CH_2Cl_2 (30 mL) to give aniline **226** as a white solid (223 mg, quant.) which was used subsequently without further purification. mp 62-65 ^oC; υ_{max} (thin film) 3450 (N-H), 3372 (N-H), 2917 (C-H), 1684, 1618, 1601; δ_H (400 MHz, $CDCl_3$) 3.81 (3H, s, O*Me*), 6.67 (1H, dd, *J* 7.8, 1.8, H_6), 6.87 (1H, s, H_2), 6.93 (1H, d, *J* 7.8, H_4), 6.96-7.05 (2H, m, H_9 and H_{11}), 7.20 (1H, app. t, *J* 7.8, H_5), 7.28-7.35 (2H, m, H_{10} and H_{12}), *NH_2 not observed*; δ_C (100 MHz, $CDCl_3$) 55.6 (O*Me*), 111.2 (C_9), 113.9 (C_6), 116.5 (C_2), 120.1 (C_4), 120.7 (C_{11}), 128.4 (C_{10} or C_{12}), 128.8 (C_5), 130.8 (C_{10} or C_{12}), 130.9 (C_7), 139.6 (C_3), 146.0 (C_1), 156.5 (C_8); *m/z* (ESI^+) 200 ($[M+H]^+$, 100%); HRMS (ESI^+) $C_{13}H_{14}NO^+$ ($[M+H]^+$) requires 200.1070, found 200.1072.

9-Methoxy-[3,7]-biphenyl-1-amine 227



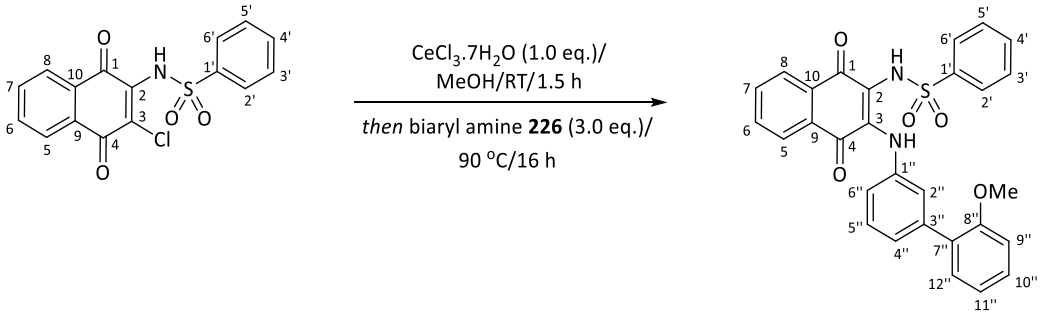
Following *General Procedure 8*, using *tert*-butyl carbamate **224** (250 mg, 0.836 mmol) and trifluoroacetic acid (6 mL) in CH_2Cl_2 (30 mL). This procedure afforded aniline **227** as an orange oil (106 mg, 64%) which was used subsequently without further purification. υ_{max} (thin film) 2920 (N-H), 1779, 1667, 1600, 1579; δ_H (500 MHz, $CDCl_3$) 3.87 (3H, s, O*Me*), 6.69 (1H, ddd, *J* 7.8, 2.1, 1.0, H_6), 6.89 (1H, ddd, *J* 8.1, 2.3, 0.9, H_{10}), 6.91 (1H, app. t, *J* 2.1, H_2), 6.99 (1H, app. dt, *J* 7.8, 1.0, H_4), 7.11 (1H, app. t, *J* 2.3, H_8), 7.16 (1H, app. dt, *J* 8.1, 0.9, H_{12}), 7.23 (1H, app. t, *J* 7.8, H_5), 7.34 (1H, app. t, *J* 8.1, H_{11}), *NH_2 not observed*; δ_C (125 MHz, $CDCl_3$) 55.3 (O*Me*), 112.7 (C_8 or C_{10}), 112.8 (C_8 or C_{10}), 113.9 (C_2), 114.2 (C_6), 117.7 (C_4), 119.6 (C_{12}), 129.6 (C_5), 129.6 (C_{11}), 142.3 (C_3), 142.9 (C_7), 146.7 (C_1), 159.8 (C_9); *m/z* (ESI^+) 200 ($[M+H]^+$, 100%); HRMS (ESI^+) $C_{13}H_{14}NO^+$ ($[M+H]^+$) requires 200.1070, found 200.1072.

8,9,10-Trimethoxy-[3,7-biphenyl]-1-amine 228



Following *General Procedure 8*, using *tert*-butyl biphenyl carbamate **225** (370 mg, 1.03 mmol) and trifluoroacetic acid (6 mL) in CH_2Cl_2 (30 mL). This procedure afforded aniline **228** as an orange oil (246 mg, 92%) which was used subsequently without further purification. υ_{max} (thin film) 3367 (N-H), 2936 (C-H), 1602; δ_H (500 MHz, $CDCl_3$) 3.68 (3H, s, C_8-O*Me* or C_{10}-O*Me*), 3.90 (3H, s, C_8-O*Me* or C_{10}-O*Me*), 3.93 (3H, s, C_9-O*Me*), 6.67 (1H, dd, *J* 7.9, 2.2, H_6), 6.73 (1H, d, *J* 8.7, H_{11}), 6.84-6.87 (1H, m, H_2), 6.90 (1H, d, *J* 7.9, H_4), 7.02 (1H, d, *J* 8.7, H_{12}), 7.19 (1H, app. t, *J* 7.9, H_5), *NH_2 not observed*; δ_C (125 MHz, $CDCl_3$) 56.0 (C_9-O*Me*), 61.0 (C_8-O*Me*), 61.0 (C_{10}-O*Me*), 107.3 (C_{11}), 113.7 (C_6), 116.0 (C_2), 119.7 (C_4), 124.7 (C_{12}), 128.9 (C_7), 129.0 (C_5), 139.3 (C_3), 142.4 (C_9), 146.1 (C_1), 151.4 (C_8 or C_{10}), 153.0 (C_8 or C_{10}); *m/z* (ESI^+) 260 ($[M+H]^+$, 100%); HRMS (ESI^+) $C_{15}H_{18}NO_3^+$ ($[M+H]^+$) requires 260.1287, found 260.1279.

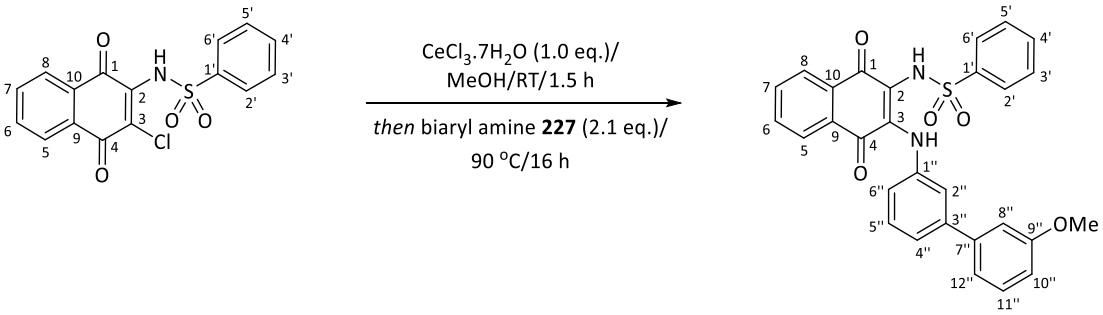
***N*-(3-((8''-Methoxy-[3'',7''-biphenyl]-1''-yl)amino)-1,4-dioxo-1,4-dihydronaphthalen-2-yl)benzenesulfonamide 229**



Following *General Procedure 2*, using naphthoquinone **57** (130 mg, 0.374 mmol), biaryl amine **226** (223 mg, 1.12 mmol) and cerium trichloride heptahydrate (139 mg, 0.374 mmol) in MeOH (7 mL) at 90 °C. Purification *via* column chromatography on silica gel (eluent pet ether:acetone

95:5 to 85:15) and subsequent recrystallisation from boiling MeOH afforded 3-anilinonaphthoquninone **229** as a red solid (52 mg, 27%). mp 176-181 ^{o}C (MeOH); υ_{max} (thin film) 3250 (N-H), 1673 (C=O), 1605 (C=O), 1571, 1526; δ_H (500 MHz, $CDCl_3$) 3.85 (3H, s, O*Me*), 6.75 (1H, s, sulfonamide-N*H*), 6.96-7.01 (2H, m, $H_{6''}$ and $H_{9''}$), 7.05 (1H, app. td, *J* 7.4, 1.0, $H_{11''}$), 7.19 (1H, app. t, *J* 1.8, $H_{2''}$), 7.31-7.40 (6H, m, $H_{3'}$, $H_{5'}$, $H_{4''}$, $H_{5''}$, $H_{10''}$ and $H_{12''}$), 7.46 (1H, app. tt, *J* 7.4, 1.1, $H_{4'}$), 7.64-7.73 (4H, m, H_6, H_7, $H_{2'}$ and $H_{6'}$), 7.93 (1H, dd, *J* 7.3, 1.4, H_8), 8.01 (1H, s, aniline-N*H*), 8.10 (1H, dd, *J* 7.3, 1.4, H_5); δ_C (125 MHz, $CDCl_3$) 55.6 (O*Me*), 111.3 ($C_{9''}$), 113.2 (C_2), 121.0 ($C_{11''}$), 121.9 ($C_{6''}$), 124.7 ($C_{2''}$), 126.4 ($C_{4''}$), 126.5 (C_8), 126.9 (C_5), 127.3 ($C_{2'}$ and $C_{6'}$), 128.2 ($C_{5''}$ or $C_{10''}$ or $C_{12''}$), 128.7 ($C_{3'}$ and $C_{5'}$), 128.9 ($C_{5''}$ or $C_{10''}$ or $C_{12''}$), 129.9 ($C_{7''}$), 130.4 (C_9), 130.9 ($C_{5''}$ or $C_{10''}$ or $C_{12''}$), 131.5 (C_{10}), 132.9 ($C_{4'}$), 133.0 (C_6), 134.9 (C_7), 137.0 ($C_{4''}$), 138.7 ($C_{1''}$), 139.2 ($C_{1'}$), 139.6 (C_3), 156.4 ($C_{8''}$), 179.4 (C_1), 182.0 (C_4); *m/z* (ESI$^-$) 257 (100%), 509 ([M-H]$^-$, 60%); HRMS (ESI$^+$) $C_{29}H_{22}N_2NaO_5S^+$ ([M+Na]$^+$) requires 533.1142, found 533.1141.

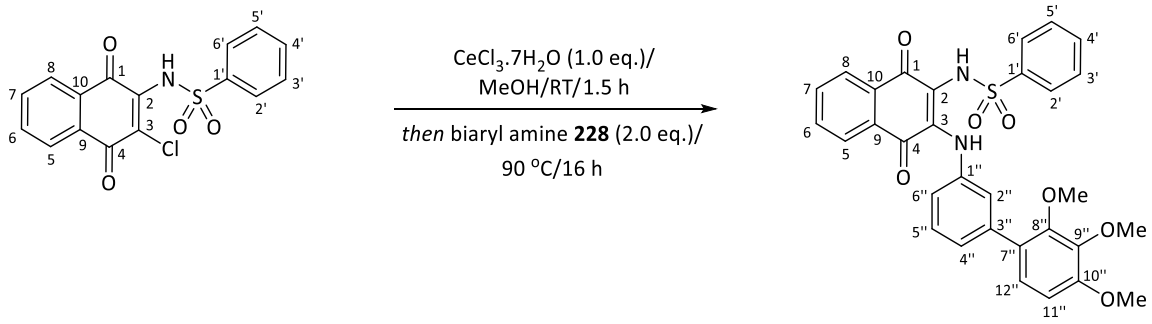
_N_-(3-((9''-Methoxy-[3'',7''-biphenyl]-1''-yl)amino)-1,4-dioxo-1,4-dihydronaphthalen-2-yl)benzenesulfonamide 230



Following *General Procedure 2*, using naphthoquinone **57** (87 mg, 0.251 mmol), biaryl amine **227** (100 mg, 0.521 mmol, 2.1 eq.) and cerium trichloride heptahydrate (94 mg, 0.251 mmol) in MeOH (7 mL) at 90 ^{o}C. Purification *via* column chromatography on silica gel (eluent pet ether:acetone 95:5 to 70:30) afforded 3-anilinonaphthoquninone **230** as a red solid (41 mg, 32%). mp 156-160 ^{o}C; υ_{max} (thin film) 3279 (N-H), 1709, 1672, 1599 (C=O), 1573 (C=O), 1526; δ_H (500 MHz, $CDCl_3$) 3.88 (3H, s, O*Me*), 6.89-6.93 (2H, m, $H_{10''}$ and sulfonamide-N*H*), 7.05-7.10 (1H, m, $H_{6''}$), 7.14-7.16 (1H, m, $H_{8''}$), 7.18-7.21 (1H, m, $H_{12''}$), 7.25 (1H, s, $H_{2''}$), 7.30-7.38 (3H, m,

$H_{3'}$, $H_{5'}$ and $H_{11''}$), 7.40-7.47 (3H, m, $H_{4'}$, $H_{4''}$ and $H_{5''}$), 7.64-7.71 (4H, m, H_6, H_7, $H_{2'}$ and $H_{6'}$), 7.88-7.91 (1H, m, H_8), 8.09-8.11 (1H, m, H_5), 8.14 (1H, s, aniline-N*H*); δ_C (125 MHz, $CDCl_3$) 55.3 (O*Me*), 113.0 ($C_{8''}$), 113.0 ($C_{10''}$), 113.5 (C_2), 119.8 ($C_{12''}$), 122.3 ($C_{2''}$), 122.3 ($C_{6''}$), 124.0 ($C_{4''}$), 126.4 (C_8), 127.0 (C_5), 127.3 ($C_{2'}$ and $C_{6'}$), 128.6 ($C_{5''}$), 128.7 ($C_{3'}$ and $C_{5'}$), 129.8 ($C_{11''}$), 130.5 (C_9), 131.3 (C_{10}), 133.1 (C_6 or $C_{4'}$), 133.2 (C_6 or $C_{4'}$), 134.9 (C_7), 137.8 ($C_{1''}$), 138.7 (C_3), 138.7 ($C_{1'}$), 141.4 ($C_{3''}$), 142.1 ($C_{7''}$), 159.9 ($C_{9''}$), 179.2 (C_1), 181.8 (C_4); *m/z* (ESI^-) 509 ($[M-H]^-$, 100%); HRMS (ESI^+) $C_{29}H_{22}NaN_2O_5S^+$ ($[M+Na]^+$) requires 533.1153, found 533.1129.

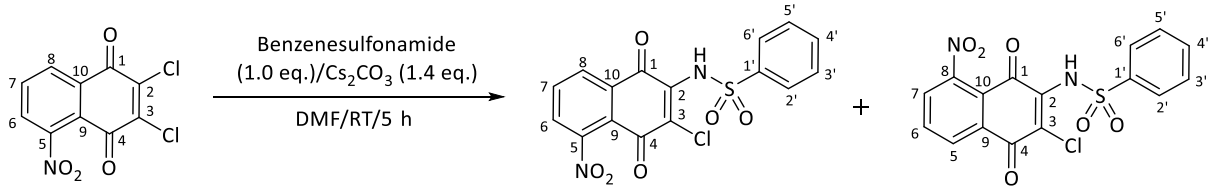
N-(3-((8'',9'',10''-Trimethoxy-[3'',7''-biphenyl]-1''-yl)amino)-1,4-dioxo-1,4-dihydronaphthalen-2-yl)benzenesulfonamide 231



Following *General Procedure 2*, using naphthoquinone **57** (80 mg, 0.230 mmol), biaryl amine **228** (119 mg, 0.460 mmol, 2 eq.) and cerium trichloride heptahydrate (86 mg, 0.230 mmol) in MeOH (6 mL), at 90 °C for 48 h. Purification *via* column chromatography on silica gel (eluent pet ether:EtOAc 90:10 to 70:30) afforded 3-anilinonaphthoquinone **231** as a red solid (28 mg, 21%). mp 182-186 °C; υ_{max} (thin film) 2928 (N-H), 1711 (C=O), 1600 (C=O), 1572; δ_H (500 MHz, $CDCl_3$) 3.70 (3H, s, $C_{8''}$-O*Me*), 3.91 (3H, s, $C_{10''}$-O*Me*), 3.94 (3H, s, $C_{9''}$-O*Me*), 6.76 (1H, d, *J* 8.6, $H_{11''}$), 6.77 (1H, br. s, sulfonamide-N*H*), 7.06 (1H, app. dt, *J* 8.0, 1.6, $H_{6''}$), 7.09 (1H, d, *J* 8.6, $H_{12''}$), 7.21 (1H, app. t, *J* 1.6, $H_{2''}$), 7.31-7.43 (4H, m, $H_{3'}$, $H_{5'}$, $H_{4''}$ and $H_{5''}$), 7.46 (1H, app. tt, *J* 7.4, 1.2, $H_{4'}$), 7.64-7.71 (4H, m, H_6, H_7, $H_{2'}$ and $H_{6'}$), 7.85-7.88 (1H, m, H_8), 8.07-8.11 (2H, m, H_5 and aniline-N*H*); δ_C (125 MHz, $CDCl_3$) 56.1 ($C_{10''}$-O*Me*), 61.1 ($C_{9''}$-O*Me*), 61.3 ($C_{8''}$-O*Me*), 107.5 ($C_{11''}$), 113.0 (C_2), 122.0 ($C_{6''}$), 124.5 ($C_{2''}$), 124.9 ($C_{12''}$), 126.1 ($C_{4''}$), 126.4 (C_8), 126.9 (C_5), 127.3 ($C_{2'}$ and $C_{6'}$), 128.0 ($C_{5''}$ or $C_{7''}$), 128.1 ($C_{5''}$ or $C_{7''}$), 128.7 ($C_{3'}$ and $C_{5'}$), 130.4 (C_9), 131.4 (C_{10}),

133.0 (C_6 or $C_{4'}$), 133.1 (C_6 or $C_{4'}$), 134.9 (C_7), 137.2 ($C_{1''}$), 138.4 ($C_{3''}$), 138.9 (C_3), 139.2 ($C_{1'}$), 142.5 ($C_{9''}$), 151.5 ($C_{8''}$), 153.3 ($C_{10''}$), 179.1 (C_1), 181.9 (C_4); *m/z* (ESI^-) 243 (100%), 455 (25%), 569 ($[M-H]^-$, 25%); HRMS (ESI^+) $C_{31}H_{27}N_2O_7S^+$ ($[M+H]^+$) requires 571.1534, found 571.1528.

_N_-(3-Chloro-8-nitro-1,4-dioxo-1,4-dihydronaphthalen-2-yl)benzenesulfonamide 232[377] and _N_-(3-Chloro-5-nitro-1,4-dioxo-1,4-dihydronaphthalen-2-yl)benzenesulfonamide 233[377]

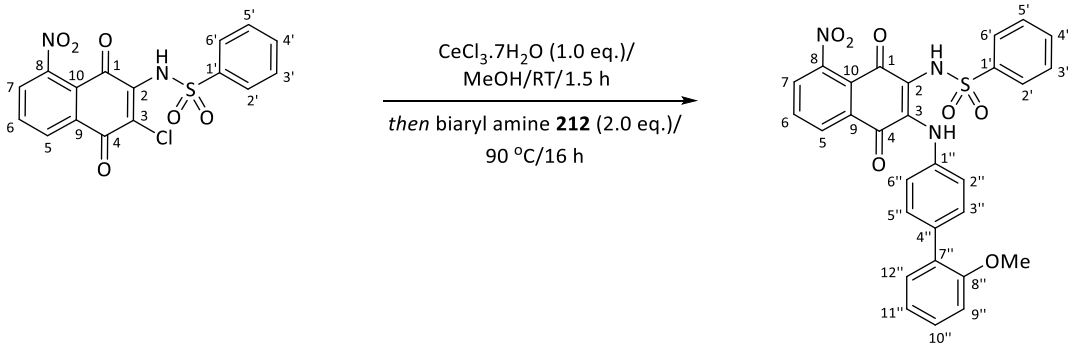


Following *General Procedure 1*, using 2,3-dichloro-5-nitro-1,4-naphthoquinone **192** (5.00 g, 18.4 mmol), benzenesulfonamide (2.89 g, 18.4 mmol) and Cs_2CO_3 (8.39 g, 25.7 mmol) in DMF (25 mL). Purification *via* column chromatography on silica gel (eluent pet ether:acetone 90:10 to 60:40) gave:

2-benzenesulfonamido-3-chloro-8-nitro-1,4-naphthoquinone **232** as a yellow solid (2.59 g, 36%). mp 224-225 ^oC (lit. 225-229 ^oC);[377] δ_H (400 MHz, DMSO-d_6) 7.48-7.62 (3H, m, $H_{3'}$, $H_{4'}$ and $H_{5'}$), 7.83-7.91 (2H, m, $H_{2'}$ and $H_{6'}$), 7.92-8.11 (2H, m, H_6 and H_5 or H_7), 8.22 (1H, dd, *J* 7.4, 1.4, H_5 or H_7), *NH not observed*; *m/z* (ESI^-) 391 ($[M(^{35}Cl)-H]^-$, 100%), 393 ($[M(^{37}Cl)-H]^-$, 33%).

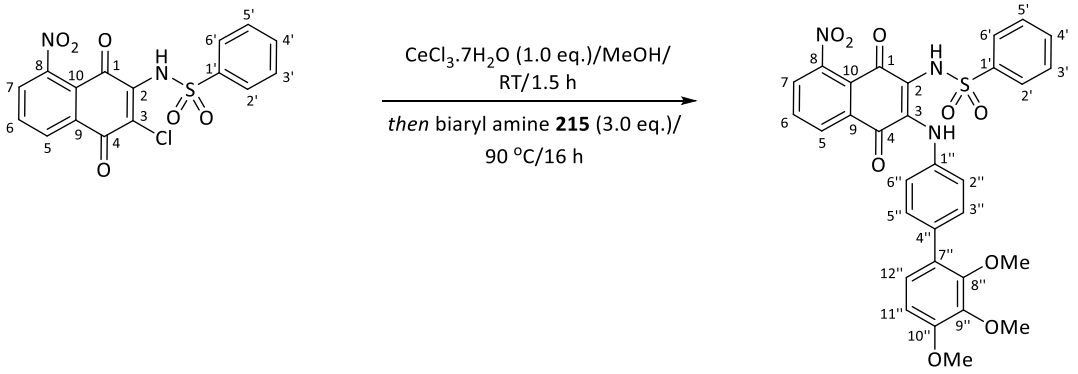
2-benzenesulfonamido-3-chloro-5-nitro-1,4-naphthoquinone **233** as a yellow solid (2.64 g, 37%). mp 227-228 ^oC (lit. 225-231 ^oC);[377] δ_H (400 MHz, DMSO-d_6) 7.42-7.50 (3H, m, $H_{3'}$, $H_{4'}$ and $H_{5'}$), 7.82-7.89 (3H, m, H_7, $H_{2'}$ and $H_{6'}$), 7.98 (1H, dd, *J* 7.8, 1.1, H_6 or H_8), 8.07 (1H, dd, *J* 7.8, 1.1, H_6 or H_8), *NH not observed*; *m/z* (ESI^-) 391 ($[M(^{35}Cl)-H]^-$, 100%), 393 ($[M(^{37}Cl)-H]^-$, 33%).

_N_-(3-((8''-Methoxy-[4'',7''-biphenyl]-1''-yl)amino)-1,4-dioxo-1,4-dihydro-8-nitro-naphthalen-2-yl)benzenesulfonamide 234



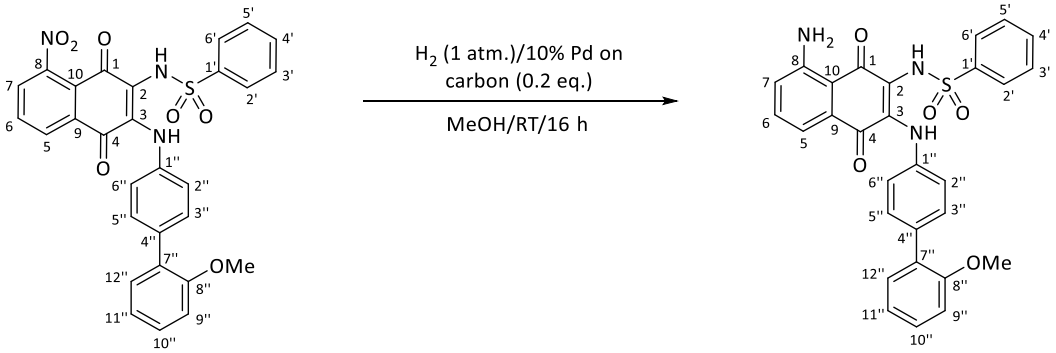
Following *General Procedure 2*, using naphthoquinone **232** (90 mg, 0.229 mmol), aniline **212** (92 mg, 0.462 mmol, 2.0 eq.) and cerium trichloride heptahydrate (85 mg, 0.229 mmol) in MeOH (5 mL) at 90 ^{o}C. Purification *via* column chromatography on silica gel (eluent pet ether:acetone 90:10 to 70:30 then pet ether:EtOAc 80:20 to 60:40) gave 3-anilinonaphthoquinone **234** as a purple solid (15 mg, 12%). mp 234-238 ^{o}C; υ_{max} (thin film) 3306 (N-H), 2962 (C-H), 2924 (C-H), 2853 (C-H), 1681, 1600 (C=O), 1571 (C=O), 1542, 1522; δ_H (500 MHz, $CDCl_3$) 3.85 (3H, s, O*Me*), 6.71 (1H, br. s, sulfonamide-N*H*), 7.01 (1H, d, *J* 8.5, $H_{9''}$), 7.06 (1H, app. t, *J* 8.0, $H_{11''}$), 7.13 (2H, d, *J* 8.5, $H_{2''}$ and $H_{6''}$), 7.32-7.42 (4H, m, $H_{3'}$, $H_{5'}$, $H_{10''}$ and $H_{12''}$), 7.50-7.55 (1H, m, $H_{4'}$), 7.57 (2H, d, *J* 8.5, $H_{3''}$ and $H_{5''}$), 7.60-7.63 (1H, m, H_7), 7.67 (2H, d, *J* 7.6, $H_{2'}$ and $H_{6'}$), 7.78 (1H, app. t, *J* 8.4, H_6), 8.17 (1H, s, aniline-N*H*), 8.26-8.29 (1H, m, H_5); δ_C (125 MHz, $CDCl_3$) 55.6 (O*Me*), 111.4 ($C_{9''}$), 113.7 (C_2), 120.9 ($C_{11''}$), 122.2 (C_{10}), 123.2 ($C_{2''}$ and $C_{6''}$), 127.3 ($C_{2'}$ and $C_{6'}$), 128.2 (C_7), 128.8 ($C_{10''}$), 128.9 ($C_{3'}$ and $C_{5'}$), 129.1 (C_5), 129.6 ($C_{3''}$ and $C_{5''}$), 129.7 ($C_{7''}$), 130.8 ($C_{12''}$), 131.6 (C_9), 133.5 ($C_{4'}$), 133.8 (C_6), 135.7 ($C_{1''}$), 136.1 ($C_{4''}$), 138.2 ($C_{1'}$), 139.0 (C_3), 148.3 (C_8), 156.5 ($C_{8''}$), 175.0 (C_1), 180.1 (C_4); *m/z* (ESI^-) 554 ($[M-H]^-$, 100%); HRMS (ESI^-) $C_{29}H_{20}N_3O_7S^-$ ($[M-H]^-$) requires 554.1027, found 554.1048.

***N*-(3-((8'',9'',10''-Trimethoxy-[4'',7''-biphenyl]-1''-yl)amino)-1,4-dioxo-1,4-dihydro-8-nitro-naphthalen-2-yl)benzenesulfonamide 235**



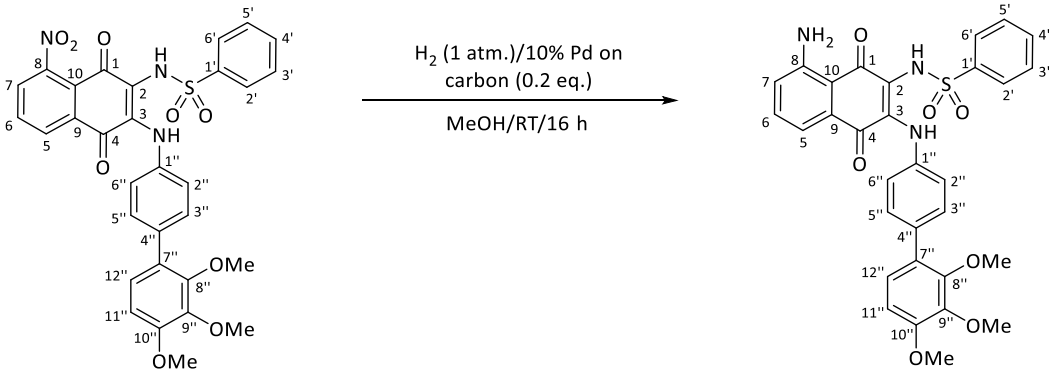
Following *General Procedure 2*, using naphthoquinone **232** (100 mg, 0.255 mmol), biaryl amine **215** (198 mg, 0.764 mmol) and cerium trichloride heptahydrate (95 mg, 0.255 mmol) in MeOH (8 mL) at 90 ^{o}C. Purification *via* column chromatography (eluent pet ether:EtOAc 80:20 to 70:30) gave 3-anilinonaphthoquinone **235** as a purple solid (28 mg, 18%). mp 209-210 ^{o}C; υ_{max} (thin film) 3305 (N-H), 2931 (C-H), 2853 (C-H), 1709 (C=O), 1680 (C=O), 1597 (N=O), 1542, 1525; δ_H (500 MHz, DMSO-d_6) 3.60 (3H, s, $C_{8''}$-O*Me* or $C_{10''}$-O*Me*), 3.80 (3H, s, $C_{9''}$-O*Me*), 3.84 (3H, s, $C_{8''}$-O*Me* or $C_{10''}$-O*Me*), 6.90 (1H, d, *J* 8.8, $H_{11''}$), 7.05 (1H, d, *J* 8.8, $H_{12''}$), 7.06-7.10 (2H, m, $H_{2''}$ and $H_{6''}$), 7.32-7.38 (4H, m, $H_{3'}$, $H_{5'}$, $H_{3''}$ and $H_{5''}$), 7.48-7.52 (1H, m, $H_{4'}$), 7.53-7.57 (2H, m, $H_{2'}$ and $H_{6'}$), 7.94 (1H, t, *J* 8.0, H_6), 8.04 (1H, app. d, *J* 8.0, H_7), 8.24 (1H, app. d, *J* 8.0, H_5), 9.09 (1H, s, sulfonamide-N*H*), 9.34 (1H, s, aniline-N*H*); δ_C (125 MHz, DMSO-d_6) 55.9 ($C_{8''}$-O*Me* or $C_{10''}$-O*Me*), 60.5 ($C_{9''}$-O*Me*), 60.7 ($C_{8''}$-O*Me* or $C_{10''}$-O*Me*), 108.2 ($C_{11''}$), 113.2 (C_2), 122.1 (C_{10}), 123.6 ($C_{2''}$ and $C_{6''}$), 124.4 ($C_{12''}$), 126.5 ($C_{2'}$ and $C_{6'}$), 127.4 ($C_{7''}$), 127.7 ($C_{3''}$ and $C_{5''}$), 128.1 (C_7), 128.5 ($C_{3'}$ and $C_{5'}$), 128.6 (C_5), 131.6 (C_9), 132.2 ($C_{4'}$), 133.4 ($C_{4''}$), 134.2 (C_6), 136.8 ($C_{1''}$), 140.8 ($C_{1'}$), 142.1 ($C_{9''}$), 142.5 (C_3), 147.7 (C_8), 151.0 ($C_{8''}$ or $C_{10''}$), 152.8 ($C_{8''}$ or $C_{10''}$), 175.0 (C_1), 180.7 (C_4); *m/z* (ESI$^-$) 257 (100%), 614 ([M-H]$^-$, 70%); HRMS (ESI$^+$) $C_{31}H_{25}N_3NaO_9S^+$ ([M+Na]$^+$) requires 638.1204, found 638.1202.

_N_-(3-((8''-Methoxy-[4'',7''-biphenyl]-1''-yl)amino)-1,4-dioxo-1,4-dihydro-8-amino-naphthalen-2-yl)benzenesulfonamide 236



Following *General Procedure 5*, using 8-nitronaphthoquinone **234** (12 mg, 0.022 mmol) and 10% Pd/C (0.5 mg, 0.0043 mmol) in MeOH (5 mL). Purification *via* column chromatography on silica gel gave 8-aminonaphthoquinone **236** as a magenta solid (7 mg, 62%). mp 78-79 ^{o}C; υ_{max} (thin film) 3463 (N-H), 3332 (N-H), 2918 (C-H), 2851 (C-H), 1735, 1665, 1619 (C=O), 1574, 1522; δ_H (500 MHz, DMSO-d_6) 3.79 (3H, s, O*Me*), 6.95 (2H, d, *J* 8.7, $H_{2''}$ and $H_{6''}$), 7.03 (1H, app. td, *J* 7.4, 1.0, $H_{11''}$), 7.08 (1H, dd, *J* 8.5, 1.1, H_7), 7.11 (1H, dd, *J* 8.4, 1.0, $H_{9''}$), 7.26 (1H, dd, *J* 7.3, 1.1, H_5), 7.28-7.41 (7H, m, H_6, $H_{3'}$, $H_{5'}$, $H_{3''}$, $H_{5''}$, $H_{10''}$ and $H_{12''}$), 7.47-7.51 (1H, m, $H_{4'}$), 7.54-7.57 (2H, m, $H_{2'}$ and $H_{6'}$), 8.61 (1H, s, aniline-N*H*), 9.00 (1H, s, sulfonamide-N*H*), *NH_2 not observed*; δ_C (125 MHz, DMSO-d_6) 55.5 (O*Me*), 109.2 (C_{10}), 111.9 ($C_{9''}$), 115.7 (C_2), 115.7 (C_5), 120.8 ($C_{11''}$), 121.7 ($C_{2''}$ and $C_{6''}$), 124.3 (C_7), 136.6 ($C_{2'}$ and $C_{6'}$), 128.4 ($C_{3''}$ and $C_{5''}$), 128.4 (C_{10} or C_{12}), 128.5 ($C_{3'}$ and $C_{5'}$), 129.6 ($C_{7''}$), 130.2 (C_{10} or C_{12}), 131.5 (C_9), 132.2 ($C_{4'}$), 132.3 ($C_{4''}$), 133.3 (C_6), 137.9 ($C_{1''}$), 140.0 (C_3), 140.8 ($C_{1'}$), 150.4 (C_8), 156.2 ($C_{8''}$), 181.6 (C_1), 182.5 (C_4); *m/z* (ESI^-) 313 (100%), 325 (100%), 524 ($[M-H]^-$, 80%); HRMS (ESI^-) $C_{29}H_{22}N_3O_5S^-$ ($[M-H]^-$) requires 524.1286, found 524.1295.

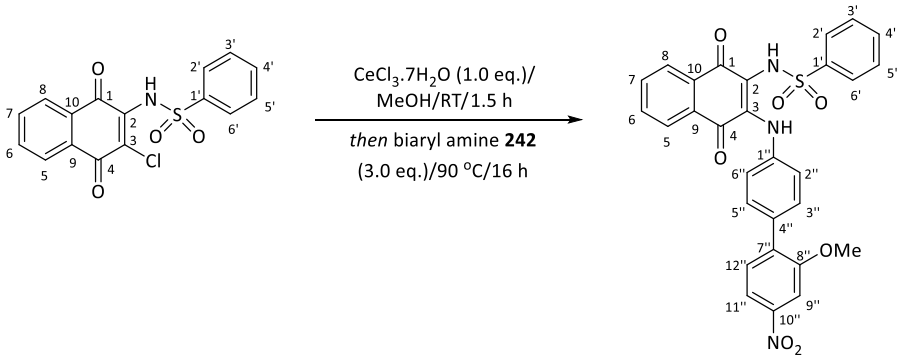
***N*-(3-((8'',9'',10''-Trimethoxy-[4'',7''-biphenyl]-1''-yl)amino)-1,4-dioxo-1,4-dihydro-8-amino-naphthalen-2-yl)benzenesulfonamide 237**



Following *General Procedure 5*, using 8-nitronaphthoquinone **235** (18 mg, 0.029 mmol) and 10% Pd/C (0.3 mg, 0.0029 mmol) in MeOH (5 mL). Purification *via* column chromatography (eluent pet ether:acetone 90:10 to 70:30) gave 8-aminonaphthoquinone **237** as a magenta solid (16 mg, 93%). mp 114-115 ^{o}C; υ_{max} (thin film) 3444 (br., N-H), 2927 (C-H), 1619 (C=O), 1524; δ_H (500 MHz, DMSO-d_6) 3.59 (3H, s, $C_{8''}$-O*Me*), 3.79 (3H, s, $C_{9''}$-O*Me*), 3.83 (3H, s, $C_{10''}$-O*Me*), 6.89 (1H, d, *J* 8.8, $H_{11''}$), 6.96 (2H, d, *J* 9.0, $H_{2''}$ and $H_{6''}$), 7.03 (1H, d, *J* 8.8, $H_{12''}$), 7.08 (1H, d, *J* 7.7, H_7), 7.25-7.31 (3H, m, H_5, $H_{3''}$ and $H_{5''}$), 7.34-7.41 (3H, m, H_6, $H_{3'}$ and $H_{5'}$), 7.47-7.52 (1H, m, $H_{4'}$), 7.55-7.58 (2H, m, $H_{2'}$ and $H_{6'}$), *NH_2 not observed*; δ_C (125 MHz, DMSO-d_6) 55.9 ($C_{10''}$-O*Me*), 60.1 ($C_{9''}$-O*Me*), 60.7 ($C_{8''}$-O*Me*), 108.2 ($C_{11''}$), 109.3 (C_{10}), 115.6 (C_5), 122.2 ($C_{2''}$ and $C_{6''}$), 124.2 (C_7), 124.4 ($C_{12''}$), 126.5 ($C_{2'}$ and $C_{6'}$), 127.6 ($C_{7''}$), 127.8 ($C_{3''}$ and $C_{5''}$), 128.4 ($C_{3'}$ and $C_{5'}$), 128.7 (C_2), 131.4 (C_9), 131.6 ($C_{4''}$), 132.0 ($C_{4'}$), 133.2 (C_6), 137.6 ($C_{1''}$), 140.0 (C_3), 141.0 ($C_{1'}$), 142.1 ($C_{9''}$), 150.4 (C_8), 150.9 ($C_{8''}$), 152.6 ($C_{10''}$), 181.6 (C_1), 182.5 (C_4); *m/z* (ESI^-) 257 (50%), 584 ($[M-H]^-$, 100%); HRMS (ESI^-) $C_{31}H_{26}N_3O_7S^-$ ($[M-H]^-$) requires 584.1497, found 584.1510.

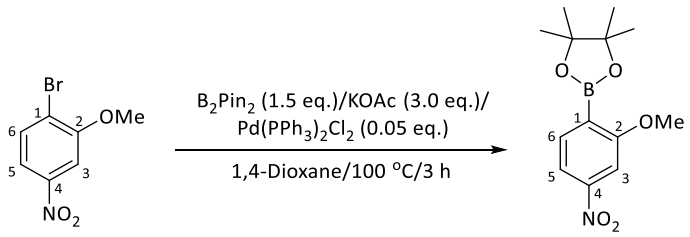
7.5. Preparation and Characterisation of Compounds Reported in Chapter 4

N-(3-((8''-Methoxy-10''-nitro-[4'',7''-biphenyl])amino)-1,4-dioxo-1,4-dihydronaphthalen-2-yl)benzenesulfonamide 238



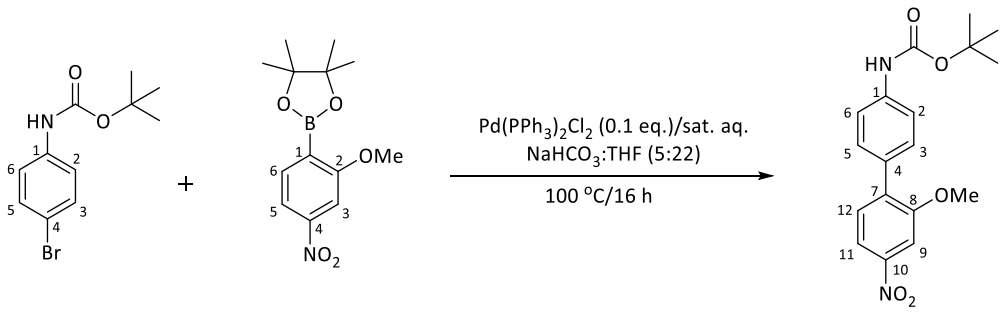
Following *General Procedure 2*, using naphthoquinone **57** (100 mg, 0.288 mmol), 8-methoxy-10-nitro-[4,7-biphenyl]amine **242** (211 mg, 0.863 mmol) and cerium trichloride heptahydrate (107 mg, 0.288 mmol) in MeOH (7 mL) at 90 ^{o}C. Upon workup 3-anilinonaphthoquinone **238** precipitated out of solution as a red solid; this precipitate was collected by suction filtration and washed with cold EtOAc (3 x 5 mL). Purification of the filtrate *via* column chromatography on silica gel (eluent pet ether:acetone 90:10 to 80:20) afforded further naphthoquinone **238** as a red solid; the precipitate from the workup and the purified product of column chromatography were combined (90 mg, 56%). mp 250-254 ^{o}C; υ_{max} (thin film) 3370 (N-H), 3315 (N-H), 3212 (N-H), 2956 (C-H), 2854 (C-H), 1726, 1671 (C=O), 1603 (C=O), 1587, 1513; δ_H (500 MHz, DMSO-d_6) 3.95 (3H, s, O*Me*), 7.08 (2H, d, *J* 8.5, $H_{2''}$ and $H_{6''}$), 7.34-7.38 (2H, m, $H_{3'}$ and $H_{5'}$), 7.44 (2H, d, *J* 8.5, $H_{3''}$ and $H_{5''}$), 7.47-7.51 (1H, m, $H_{4'}$), 7.56-7.61 (3H, m, $H_{2'}$, $H_{6'}$ and $H_{12''}$), 7.75-7.83 (3H, m, H_6, H_7 and H_8), 7.88 (1H, d, *J* 2.2, $H_{9''}$), 7.94 (1H, dd, *J* 8.4, 2.2, $H_{11''}$), 8.01-8.04 (1H, m, H_5), 9.08 (1H, br. s, aniline-N*H*), 9.16 (1H, s, sulfonamide-N*H*); δ_C (125 MHz, DMSO-d_6) 56.3 (O*Me*), 106.5 ($C_{9''}$), 115.0 (C_2), 116.0 ($C_{11''}$), 122.6 ($C_{2''}$ and $C_{6''}$), 125.7 (C_8), 126.2 (C_5), 126.5 ($C_{2'}$ and $C_{6'}$), 128.5 ($C_{3'}$ and $C_{5'}$), 128.5 ($C_{3''}$ and $C_{5''}$), 130.4 (C_9), 130.6 ($C_{4''}$), 130.9 ($C_{12''}$), 131.4 (C_{10}), 132.2 ($C_{4'}$), 133.1 (C_6), 134.9 (C_7), 136.5 ($C_{7''}$), 138.9 ($C_{1''}$), 141.0 ($C_{1'}$), 141.5 (C_3), 147.2 ($C_{10''}$), 156.6 ($C_{8''}$), 178.7 (C_1), 182.2 (C_4); *m/z* (ESI$^-$) 554 ([M-H]$^-$, 100%); HRMS (ESI$^-$) $C_{29}H_{20}N_3O_7S^-$ ([M-H]$^-$) requires 554.1027, found 554.1034.

2-Methoxy-4-nitrophenylboron pinacol ester 240[378]



To a solution of 1-bromo-2-methoxy-4-nitrobenzene **239** (2.00 g, 8.62 mmol) in 1,4-dioxane (12 mL) in a microwave vial under N_2 was added $Pd(PPh_3)_2Cl_2$ (300 mg, 0.430 mmol), *bis*(pinacolato)diboron (3.28 g, 12.9 mmol) and potassium acetate (2.53 g, 25.9 mmol). The vial was sealed and the reaction mixture was heated to 100 °C for 3 h. After cooling, H_2O (50 mL) was added and the organic product was extracted with EtOAc (2 x 50 mL). The combined organic layers were washed with brine (3 x 20 mL), dried over Na_2SO_4, filtered and concentrated *in vacuo* to give the crude product. Purification *via* column chromatography (eluent pet ether:EtOAc 90:10 to 50:50) gave pinacol ester **240** as a yellow solid (2.40 g, 100%). mp 81-83 °C (lit. 75-78 °C);[378] δ_H (500 MHz, $CDCl_3$) 1.38 (12H, s, 2 x C*Me*$_2$), 3.93 (3H, s, O*Me*), 7.66-7.68 (1H, m, H_3), 7.78-7.80 (2H, m, H_5 and H_6); *m/z* (ESI^+) 302 ($[M+Na]^+$, 100%).

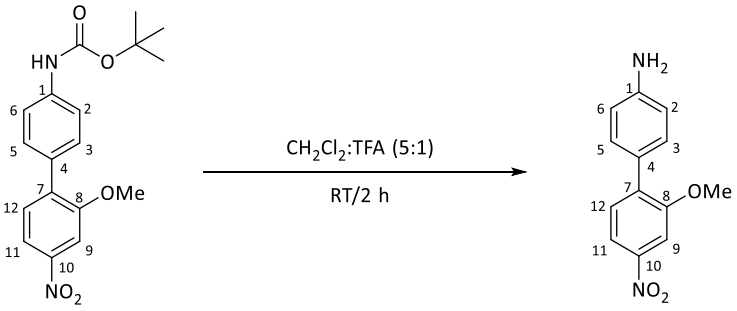
***tert*-Butyl (8-methoxy-10-nitro-[4,7-biphenyl])carbamate 241**



Following *General Procedure 6*, using *tert*-butyl(4-bromophenyl) carbamate **205** (700 mg, 2.57 mmol), 2-methoxy-4-nitrophenylboron pinacol ester **240** (1.43 g, 5.15 mmol), $Pd(PPh_3)_2Cl_2$ (180 mg, 0.257 mmol) and sat. aq. $NaHCO_3$ (2.5 mL) in THF (11 mL). Purification *via* column chromatography (eluent pet ether:acetone 95:5 to 80:20) and subsequent recrystallisation from boiling MeOH gave biphenyl carbamate **241** as a yellow solid (426 mg,

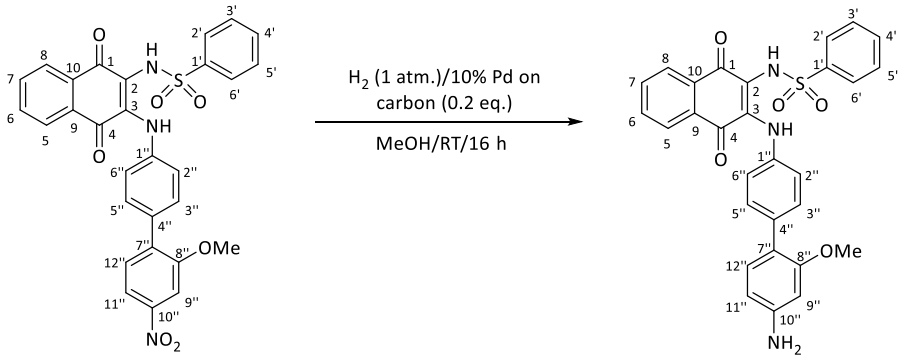
48%). mp 154-157 °C (MeOH); υ_{max} (thin film) 3382 (N-H), 2980 (C-H), 1731 (C=O), 1704, 1614, 1587 (N=O); δ_H (500 MHz, $CDCl_3$) 1.54 (9H, s, OC*Me*$_3$), 3.92 (3H, s, O*Me*), 6.60 (1H, br. s, N*H*), 7.42-7.47 (3H, m, H_2, H_6 and H_{12}), 7.48-7.51 (2H, m, H_3 and H_5), 7.82 (1H, d, *J* 2.2, H_9), 7.91 (1H, dd, *J* 8.3, 2.2, H_{11}); δ_C (125 MHz, $CDCl_3$) 28.3 (OC*Me*$_3$), 56.1 (O*Me*), 80.8 (O*C*Me$_3$), 106.2 (C_9), 116.1 (C_{11}), 118.1 (C_2 and C_6), 130.1 (C_3 and C_5), 130.7 (C_{12}), 130.8 (C_4), 136.9 (C_7), 138.5 (C_1), 147.7 (C_{10}), 152.6 (*C*O$_2$^{t}Bu), 156.7 (C_8); *m/z* (ESI$^+$) 289 (50%), 367 ([M+Na]$^+$, 100%); HRMS (ESI$^+$) $C_{18}H_{20}N_2NaO_5^+$ ([M+Na]$^+$) requires 367.1264, found 367.1261.

8-Methoxy-10-nitro-[4,7-biphenyl]amine 242



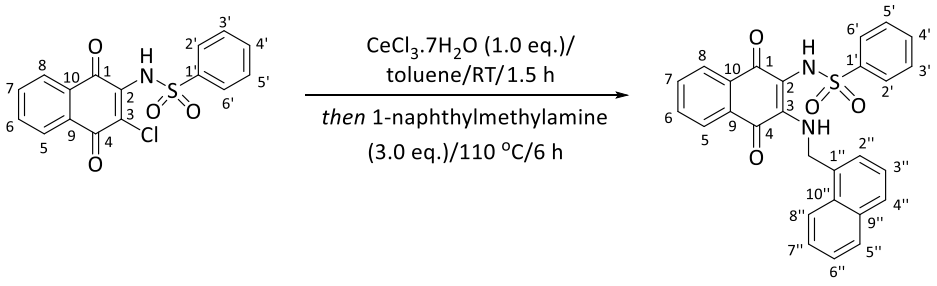
Following *General Procedure 8,* using carbamate **241** (600 mg, 1.74 mmol) and trifluoroacetic acid (8 mL) in CH_2Cl_2 (42 mL). Purification *via* column chromatography (eluent pet ether:acetone 80:20) gave aniline **242** as an orange solid (296 mg, 70%). mp 130-133 °C; υ_{max} (thin film) 3412 (N-H), 2006 (C-H), 1707, 1634, 1610, 1584 (N=O), 1516; δ_H (500 MHz, $CDCl_3$) 3.92 (3H, s, O*Me*), 6.73-6.77 (2H, m, H_2 and H_6), 7.37-7.41 (2H, m, H_3 and H_5), 7.43 (1H, d, *J* 8.4, H_{12}), 7.80 (1H, d, *J* 2.2, H_9), 7.89 (1H, dd, *J* 8.4, 2.2, H_{11}), *NH_2 not observed*; δ_C (125 MHz, $CDCl_3$) 56.0 (O*Me*), 106.1 (C_9), 114.6 (C_2 and C_6), 116.2 (C_{11}), 126.1 (C_4), 130.2 (C_{12}), 130.6 (C_3 and C_5), 137.6 (C_7), 146.7 (C_1), 147.1 (C_{10}), 156.6 (C_8); *m/z* (ESI$^+$) 245 ([M+H]$^+$, 100%), 267 ([M+Na]$^+$, 5%); HRMS (ESI$^+$) $C_{13}H_{12}N_2NaO_3^+$ ([M+Na]$^+$) requires 267.0740, found 267.0737.

_N_-(3-((8''-Methoxy-10''-amino-[4'',7''-biphenyl])amino)-1,4-dioxo-1,4-dihydronaphthalen-2-yl)benzenesulfonamide 249[308]



Following *General Procedure 5*, using naphthoquinone **238** (30 mg, 0.054 mmol) and 10% Pd/C (2 mg, 0.018 mmol) in MeOH (6 mL) gave amino-substituted **249** as a purple solid without the need for further purification (23 mg, 81%). mp 231-233 ^{o}C (lit. 226-229 ^{o}C);[308] δ_H (400 MHz, DMSO-d_6) 3.71 (3H, s, O*Me*), 5.21 (2H, br. s, NH_2), 6.25 (1H, dd, *J* 8.2, 1.9, $H_{11''}$), 6.32 (1H, d, *J* 1.9, $H_{9''}$), 6.90-7.00 (3H, m, $H_{2''}$, $H_{6''}$ and $H_{12''}$), 7.27 (2H, d, *J* 8.4, $H_{3''}$ and $H_{5''}$), 7.35 (2H, app. t, *J* 7.7, $H_{3'}$ and $H_{5'}$), 7.48 (1H, app. t, *J* 7.7, $H_{4'}$), 7.57 (2H, d, *J* 7.7, $H_{2'}$ and $H_{6'}$), 7.73-7.80 (3H, m, H_6, H_7 and H_8), 7.99 (1H, d, *J* 6.8, H_5), 8.86 (1H, br. s, N*H*), 9.05 (1H, br. s, N*H*); *m/z* (ESI$^+$) 526 ([M+H]$^+$, 100%), 548 ([M+Na]$^+$, 50%).

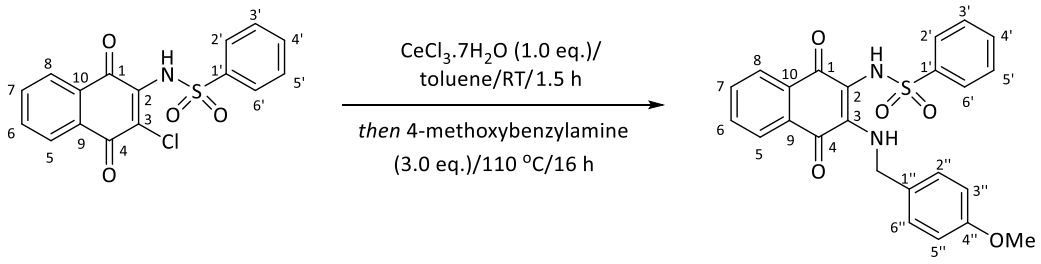
_N_-(3-((Naphthalene-1''-ylmethyl)amino)-1,4-dioxo-1,4-dihydronaphthalen-2-yl)benzenesulfonamide 282



Following *General Procedure 2*, using naphthoquinone **57** (150 mg, 0.430 mmol), 1-naphthalene methylamine (190 μL, 1.29 mmol) and cerium trichloride heptahydrate (161 mg,

0.430 mmol) in toluene (7 mL), at 110 °C for 6 h. Purification *via* column chromatography on silica gel (eluent pet ether:EtOAc 80:20) and subsequent recrystallisation from boiling MeOH gave 3-aminonaphthoquinone **282** as an orange solid (96 mg, 48%). mp 229-230 °C; υ_{max} (thin film) 3305 (N-H), 3280 (N-H), 2924 (C-H), 2853 (C-H), 1650 (C=O), 1597, 1567, 1508; δ_H (500 MHz, $CDCl_3$) 5.55 (2H, d, *J* 5.1, NHC*H*$_2$Ar), 6.45 (1H, br. t, *J* 5.1, N*H*CH$_2$Ar), 6.68 (1H, s, sulfonamide-N*H*), 7.39 (2H, m, $H_{3'}$ and $H_{5'}$), 7.45-7.61 (5H, m, $H_{4'}$, $H_{2''}$, $H_{3''}$, $H_{6''}$ and $H_{7''}$), 7.58 (1H, app. td, *J* 7.6, 1.4, H_6), 7.63 (1H, app. td, *J* 7.6, 1.4, H_7), 7.72 (1H, dd, *J* 7.6, 1.4, H_8), 7.85-7.90 (3H, m, $H_{2'}$, $H_{6'}$ and $H_{5''}$), 7.93 (1H, app. d, *J* 8.3, $H_{4''}$), 8.00 (1H, dd, *J* 7.6, 1.4, H_5), 8.14 (1H, app. d, *J* 8.5, $H_{8''}$); δ_C (125 MHz, $CDCl_3$) 47.5 (NH*C*H$_2$Ar), 109.6 (C_2), 123.6 ($C_{8''}$), 125.5 ($C_{3''}$), 126.0 (C_8 or $C_{6''}$), 126.1 (C_8 or $C_{6''}$), 126.8 (C_5), 127.0 ($C_{2''}$ or $C_{7''}$), 127.4 ($C_{2''}$ or $C_{7''}$), 127.9 ($C_{2'}$ and $C_{6'}$), 128.7 ($C_{3'}$ and $C_{5'}$), 128.8 ($C_{4''}$), 129.2 ($C_{5''}$), 130.0 (C_9), 131.5 ($C_{10''}$), 131.8 (C_{10}), 132.5 (C_6), 132.9 ($C_{4'}$ or $C_{1''}$), 133.2 ($C_{4'}$ or $C_{1''}$), 134.0 ($C_{9''}$), 135.0 (C_7), 138.3 ($C_{1'}$), 143.6 (C_3), 178.9 (C_1), 181.6 (C_4); *m/z* (ESI$^-$) 255 (60%), 467 ([M-H]$^-$, 100%), 468 (30%); HRMS (ESI$^-$) $C_{27}H_{19}N_2O_4S^-$ ([M-H]$^-$) requires 467.1071, found 467.1061.

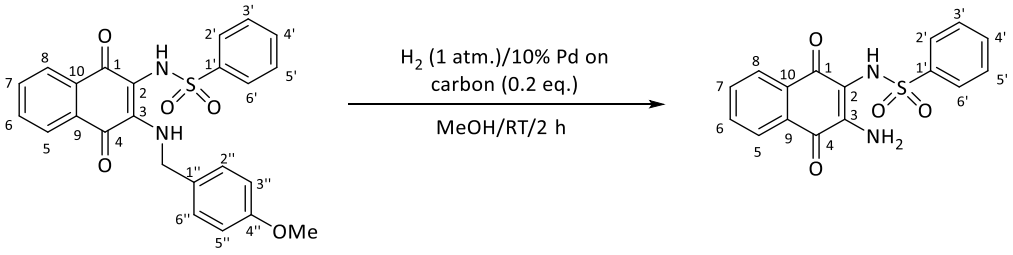
N-(3-((4''-Methoxybenzyl)amino)-1,4-dioxo-1,4-dihydronaphthalen-2-yl)benzenesulfonamide 307



Following *General Procedure 2*, using naphthoquinone **57** (200 mg, 0.576 mmol), 4-methoxybenzylamine (225 µL, 1.77 mmol) and cerium trichloride heptahydrate (214 mg, 0.576 mmol) in toluene (8 mL), at 110 °C. Purification *via* column chromatography on silica gel (eluent pet ether:acetone 90:10 to 80:20 then CH_2Cl_2:MeOH 90:10) gave naphthoquinone **307** as an orange solid (89 mg, 35%). mp 214-217 °C; υ_{max} (thin film) 3334 (N-H), 3231 (N-H), 1669 (C=O), 1615 (C=O), 1574, 1512; δ_H (400 MHz, $CDCl_3$) 3.83 (3H, s, O*Me*), 5.04 (2H, d, *J* 5.7, C*H*$_2$),

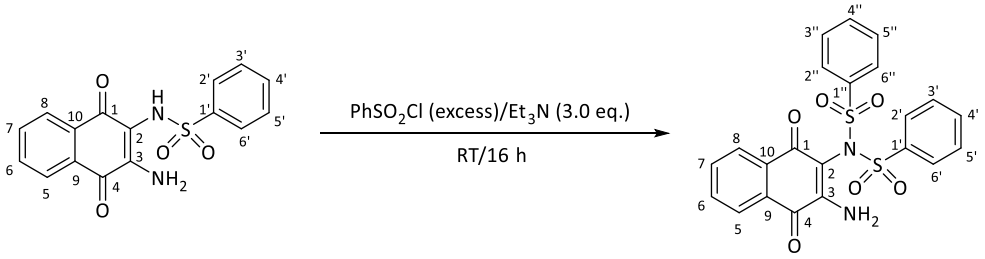
6.45-6.70 (2H, m, 2 x N*H*), 6.91 (2H, d, *J* 8.6, $H_{3''}$ and $H_{5''}$), 7.30-7.40 (4H, m, $H_{3'}$, $H_{5'}$, $H_{2''}$ and $H_{6''}$), 7.50 (1H, app. t, *J* 7.1, $H_{4'}$), 7.56-7.64 (2H, m, H_6 and H_7), 7.68-7.72 (1H, m, H_8), 7.82 (2H, d, *J* 7.6, $H_{2'}$ and $H_{6'}$), 8.01-8.06 (1H, m, H_5); δ_C (100 MHz, $CDCl_3$) 48.4 (*C*H_2), 55.3 (O*Me*), 109.7 (C_2), 114.3 ($C_{3''}$ and $C_{5''}$), 126.0 (C_8), 126.8 (C_5), 127.8 ($C_{2'}$ and $C_{6'}$), 128.6 ($C_{3'}$ and $C_{5'}$), 129.6 ($C_{2''}$ and $C_{6''}$), 129.9 (C_3), 130.1 (C_9), 131.8 (C_{10}), 132.5 (C_6), 133.1 ($C_{4'}$), 134.9 (C_7), 138.3 ($C_{1'}$), 143.6 ($C_{1''}$), 159.4 ($C_{4''}$), 178.7 (C_1), 181.9 (C_4); *m/z* (ESI^+) 471 ($[M+Na]^+$, 100%); HRMS (ESI^+) $C_{24}H_{20}N_2NaO_5S^+$ ($[M+Na]^+$) requires 471.0985, found 471.0985.

_N_-(3-Amino-1,4-dioxo-1,4-dihydronaphthalen-2-yl)benzenesulfonamide 308



Following *General Procedure 5*, using naphthoquinone **307** (80 mg, 0.179 mmol) and 10% Pd/C (4 mg, 0.036 mmol) in MeOH (15 mL) gave amino-substituted **308** as an orange solid without the need for further purification (55 mg, 94%). mp 207-210 ^oC; υ_{max} (thin film) 3374 (N-H), 3347 (N-H), 3243 (N-H), 1678, 1637, 1614 (C=O), 1595, 1574 (C=O); δ_H (500 MHz, $CDCl_3$) 6.33 (2H, br. s, NH_2), 6.94 (1H, s, sulfonamide-N*H*), 7.40-7.46 (2H, m, $H_{3'}$ and $H_{5'}$), 7.49-7.55 (1H, m, $H_{4'}$), 7.57-7.67 (2H, m, H_6 and H_7), 7.81-7.88 (3H, m, H_8, $H_{2'}$ and $H_{6'}$), 8.00-8.05 (1H, m, H_5); δ_C (125 MHz, $CDCl_3$) 111.4 (C_2), 126.3 (C_8), 126.5 (C_5), 127.5 ($C_{2'}$ and $C_{6'}$), 128.9 ($C_{3'}$ and $C_{5'}$), 130.1 (C_9), 131.3 (C_{10}), 132.8 (C_6), 133.5 ($C_{4'}$), 134.8 (C_7), 137.2 ($C_{1'}$), 142.6 (C_3), 177.9 (C_1), 180.8 (C_4); *m/z* (ESI^+) 329 ($[M+H]^+$, 50%), 351 ($[M+Na]^+$, 100%); HRMS (ESI^+) $C_{16}H_{13}N_2O_4S^+$ ($[M+H]^+$) requires 329.0591, found 329.0591.

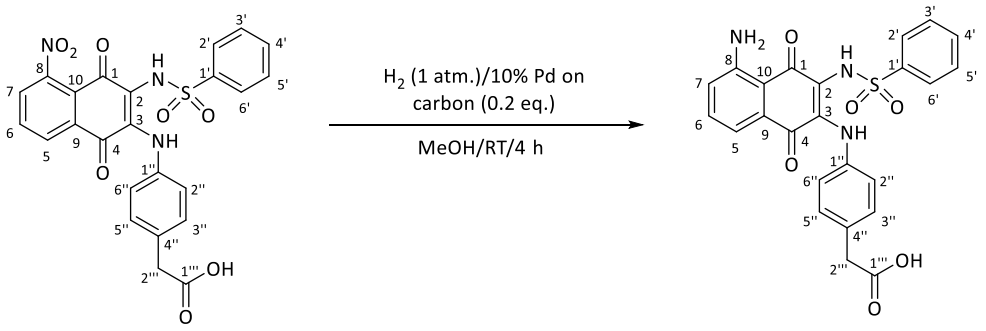
_N_-(3-Amino-1,4-dioxo-1,4-dihydronaphthalen-2-yl)-_N_-(phenylsulfonyl)benzenesulfonamide 309



Naphthoquinone **308** (50 mg, 0.152 mmol) was added to benzenesulfonyl chloride (5 mL) and triethylamine (63 µL, 0.457 mmol) and stirred at RT for 16 h. The reaction mixture was quenched with MeOH (8 mL) and then partitioned between 1 M aq. HCl (20 mL) and EtOAc (20 mL). The organic layer was collected, washed with brine (3 x 20 mL), filtered and concentrated *in vacuo* to give the crude product. Purification *via* column chromatography on silica gel (eluent pet ether:EtOAc 95:5 to 90:10) gave *N*-(phenylsulfonyl)benzenesulfonamide **309** as a yellow solid (66 mg, 93%). mp 172-176 ^{o}C; υ_{max} (thin film) 3320 (N-H), 1618 (C=O), 1579 (C=O); δ_H (500 MHz, $CDCl_3$) 5.74 (1H, br. s, N*H*), 6.19 (1H, br. s, N*H*), 7.48-7.53 (4H, m, $H_{3'}$, $H_{5'}$, $H_{3''}$ and $H_{5''}$), 7.63-7.70 (3H, m, H_6, $H_{4'}$ and $H_{4''}$), 7.73 (1H, dd, *J* 7.7, 1.3, H_7), 7.93-7.97 (5H, m, H_8, $H_{2'}$, $H_{6'}$, $H_{2''}$ and $H_{6''}$), 8.11 (1H, dd, *J* 7.7, 1.3, H_5); δ_C (125 MHz, $CDCl_3$) 109.9 (C_2), 126.7 (C_5), 126.9 (C_8), 128.8 ($C_{3'}$, $C_{5'}$, $C_{3''}$ and $C_{5''}$), 129.2 ($C_{2'}$, $C_{6'}$, $C_{2''}$ and $C_{6''}$), 130.1 (C_9), 132.4 (C_{10}), 132.7 (C_6), 134.2 ($C_{4'}$ and $C_{4''}$), 135.4 (C_7), 138.7 ($C_{1'}$ and $C_{1''}$), 150.0 (C_3), 177.6 (C_1), 180.5 (C_4); *m/z* (ESI$^-$) 467 ([M-H]$^-$, 100%); HRMS (ESI$^-$) $C_{22}H_{15}N_2O_6S_2^-$ ([M-H]$^-$) requires 467.0377, found 467.0383.

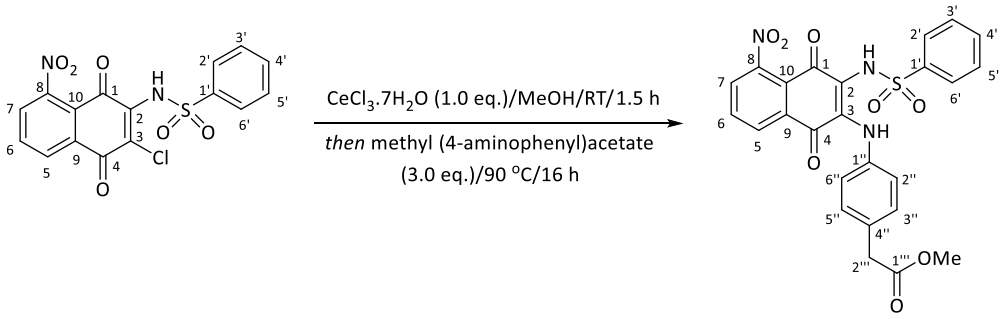
7.6. Preparation and Characterisation of Compounds Reported in Chapter 5

2'''-(*para*-((8-Amino-1,4-dioxo-2-(phenylsulfonamido)-1,4-dihydronaphthalen-3-yl)amino)phenyl)acetic acid 351



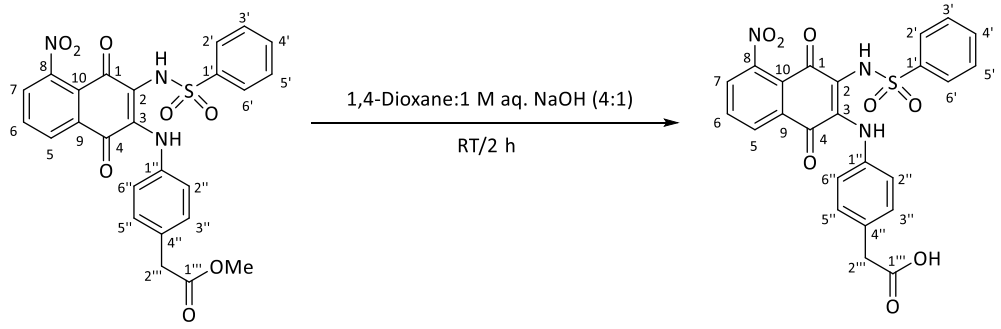
Following *General Procedure 5*, using naphthoquinone **357** (37 mg, 0.073 mmol) and 10% Pd/C (2 mg, 0.015 mmol) in MeOH (8 mL), for 4 h. Purification *via* column chromatography (eluent CH_2Cl_2:MeOH 100:0 to 80:20) gave 8-aminonaphthoquinone **351** as a magenta solid (13 mg, 37%). mp 175-177 ^{o}C; υ_{max} (thin film) 3455 (N-H), 3339 (O-H), 2924 (C-H), 1709, 1660 (C=O), 1516; δ_H (500 MHz, MeOD) 3.57 (2H, s, CH_2), 6.92 (2H, d, *J* 8.5, $H_{2''}$ and $H_{6''}$), 7.01 (1H, dd, *J* 8.2, 1.3, H_7), 7.19 (2H, d, *J* 8.5, $H_{3''}$ and $H_{5''}$), 7.30-7.38 (4H, m, H_5, H_6, $H_{3'}$ and $H_{5'}$), 7.45-7.50 (1H, m, $H_{4'}$), 7.60 (2H, dd, *J* 8.4, 1.2, $H_{2'}$ and $H_{6'}$); δ_C (125 MHz, MeOD) 42.2 (*C*H_2), 111.3 (C_{10}), 115.6 (C_2), 117.6 (C_5), 124.2 ($C_{2''}$ and $C_{6''}$), 125.6 (C_7), 128.5 ($C_{2'}$ amd $C_{6'}$), 129.8 ($C_{3'}$ and $C_{5'}$), 130.0 ($C_{3''}$ and $C_{5''}$), 131.7 ($C_{4''}$), 133/1 (C_9), 133.8 ($C_{4'}$), 134.4 (C_6), 138.8 ($C_{1''}$), 141.0 (C_3), 141.6 ($C_{1'}$), 176.7 (*C*O_2H), 183.6 (C_1), 184.0 (C_4); *m/z* (ESI$^-$) 476 ([M-H]$^-$, 100%); HRMS (ESI$^-$) $C_{24}H_{18}N_3O_6S^-$ ([M-H]$^-$) requires 476.0922, found 476.0923.

Methyl 2'''-(*para*-((8-nitro-1,4-dioxo-2-(phenylsulfonamido)-1,4-dihydronaphthalen-3-yl)amino)phenyl)acetate 355



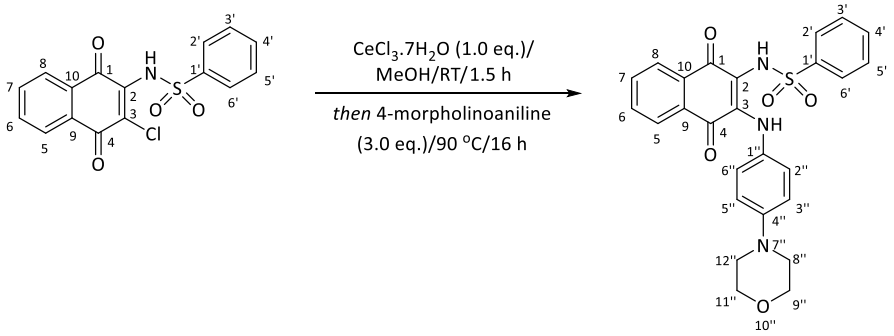
Following *General Procedure 2*, using naphthoquinone **232** (100 mg, 0.255 mmol), methyl (4-aminophenyl)acetate (126 mg, 0.764 mmol) and cerium trichloride heptahydrate (95 mg, 0.253 mmol) in MeOH, at 90 ^{o}C. Purification *via* column chromatography on silica gel (eluent pet ether:acetone 80:20 to 70:30) and subsequent recrystallisation from boiling toluene gave 3-anilinonaphthoquinone **355** as a purple solid (31 mg, 23%). mp 186-188 ^{o}C (toluene); υ_{max} (thin film) 3307 (N-H), 2925 (C-H), 2854 (C-H), 1734 (ester C=O), 1682, 1602 (C=O), 1572, 1542 (C=O), 1521; δ_H (500 MHz, DMSO-d_6) 3.63 (3H, s, O*Me*), 3.66 (2H, s, 2 x $H_{2'''}$), 6.98 (2H, d, *J* 8.4, $H_{2''}$ and $H_{6''}$), 7.12 (2H, d, *J* 8.4, $H_{3''}$ and $H_{5''}$), 7.33-7.38 (2H, m, $H_{3'}$ and $H_{5'}$), 7.48-7.53 (3H, m, $H_{2'}$, $H_{4'}$ and $H_{6'}$), 7.94 (1H, app. t, *J* 7.9, H_6), 8.02 (1H, dd, *J* 7.9, 1.1, H_7), 8.22 (1H, dd, *J* 7.9, 1.1, H_5), 9.03 (1H, s, sulfonamide-N*H*), 9.26 (1H, br. s, aniline-N*H*); δ_C (125 MHz, DMSO-d_6) 39.5 ($C_{2'''}$), 51.7 (O*Me*), 113.0 (C_2), 122.0 (C_{10}), 123.8 ($C_{2''}$ and $C_{6''}$), 126.5 ($C_{2'}$ and $C_{6'}$), 128.1 (C_7), 128.4 ($C_{3''}$ and $C_{5''}$), 128.5 ($C_{3'}$ and $C_{5'}$), 128.6 (C_5), 129.8 ($C_{4''}$), 131.6 (C_9), 132.1 ($C_{4'}$), 134.2 (C_6), 136.9 ($C_{1''}$), 140.7 ($C_{1'}$), 142.6 (C_3), 171.7 ($C_{1'''}$), 175.0 (C_1), 180.7 (C_4); *m/z* (ESI^+) 413 (100%), 544 ($[M+Na]^+$, 90%); HRMS (ESI^+) $C_{25}H_{19}N_3NaO_8S^+$ ($[M+Na]^+$) requires 544.0785, found 544.0784.

2'''-(*para*-((8-Nitro-1,4-dioxo-2-(phenylsulfonamido)-1,4-dihydronaphthalen-3-yl)amino)phenyl)acetic acid 357



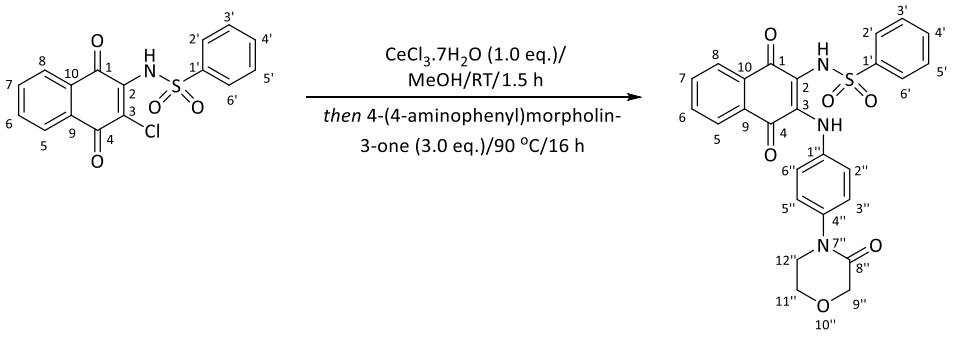
Methyl ester **355** (45 mg, 0.086 mmol) and 1 M aq. NaOH (2 mL) were stirred in 1,4-dioxane (8 mL) at RT for 2 h. After this time, the *p*H of the solution was adjusted to *c.* 2 with 1 M aq. HCl (10 mL) and the organic product was extracted into EtOAc (3 x 10 mL). The organic layers were combined, washed with brine (3 x 10 mL), dried over Na_2SO_4, filtered and concentrated *in vacuo*. Purification *via* column chromatography (eluent CH_2Cl_2:MeOH 100:0 to 80:20) gave carboxylic acid **357** as a purple solid (37 mg, 84%). mp 230-232 ^{o}C; υ_{max} (thin film) 3295 (N-H), 2956 (C-H), 2925 (C-H), 2855 (C-H), 1709 (C=O), 1685 (C=O), 1600 (C=O), 1572, 1541; δ_H (500 MHz, DMSO-d_6) 3.48 (2H, s, CH_2), 6.80 (2H, br. s, $C_{2''}$ and $C_{6''}$), 7.05 (2H, d, *J* 7.9, $H_{3''}$ and $H_{5''}$), 7.30-7.36 (2H, m, $H_{3'}$ and $H_{5'}$), 7.38-7.45 (1H, m, $H_{4'}$), 7.57 (2H, d, *J* 7.6, $H_{2'}$ and $H_{6'}$), 7.84-7.90 (1H, m, H_6), 7.94 (1H, d, *J* 7.3, H_5), 8.12 (1H, d, *J* 6.7, H_7); δ_C (125 MHz, DMSO-d_6) 69.8 (*C*H_2), 122.4 ($C_{2''}$ and $C_{6''}$), 125.6 (C_9 or C_{10}), 126.0 ($C_{2'}$ and $C_{6'}$), 126.5 (C_9 or C_{10}), 127.6 (C_5), 128.1 (C_5), 128.2 ($C_{3'}$ and $C_{5'}$), 128.6 ($C_{3''}$ and $C_{5''}$), 128.9 ($C_{4''}$), 129.7 ($C_{4'}$), 134.1 (C_6), 147.6 (C_8), 173.0 (*C*O_2H), *quality of spectra are poor due to poor solubility of* ***357*** *and C_1, C_2, C_3, C_4, $C_{1'}$ and $C_{1''}$ are not observed*; *m/z* (ESI$^-$) 252 (90%), 506 ([M-H]$^-$, 100%); HRMS (ESI$^-$) $C_{24}H_{16}N_3O_8S^-$ ([M-H]$^-$) requires 506.0664, found 506.0667.

_N_-(3-((4''-Morpholinophenyl)amino)-1,4-dioxo-1,4-dihydronaphthalen-2-yl)benzenesulfonamide 364



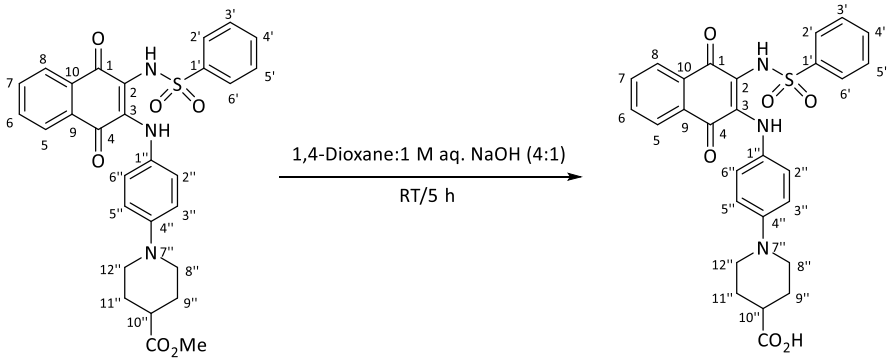
Following *General Procedure 2*, using naphthoquinone **57** (200 mg, 0.576 mmol), 4-morpholinoaniline (308 mg, 1.727 mmol) and cerium trichloride heptahydrate (214 mg, 0.576 mmol) in MeOH (8 mL), at 90 ^{o}C. Purification *via* column chromatography on silica gel (eluent pet ether:acetone 90:10 to 50:50) and subsequent recrystallisation from boiling toluene gave **364** as a purple solid (212 mg, 73%). mp 229 ^{o}C (toluene); υ_{max} (thin film) 3258 (N-H), 3209 (N-H), 2956 (C-H), 2922 (C-H), 2854 (C-H), 1667 (C=O), 1607 (C=O), 1572, 1518; δ_H (400 MHz, $CDCl_3$) 3.14 (4H, app. t, *J* 4.9, $H_{8''}$ and $H_{12''}$), 3.81 (4H, app. t, *J* 4.9, $H_{9''}$ and $H_{11''}$), 6.68 (1H, s, sulfonamide-N*H*), 6.81-6.86 (2H, m, $H_{3''}$ and $H_{5''}$), 6.95-7.00 (2H, m, $H_{2''}$ and $H_{6''}$), 7.26 (2H, app. t, *J* 7.6, $H_{3'}$ and $H_{5'}$), 7.39 (1H, app. t, *J* 7.6, $H_{4'}$), 7.53-7.63 (4H, m, H_6, H_7, $H_{2'}$ and $H_{6'}$), 7.75-7.79 (1H, m, H_8), 7.95 (1H, s, amide-N*H*), 7.98-8.02 (1H, m, H_5); δ_C (100 MHz, $CDCl_3$) 48.2 ($C_{8''}$ and $C_{12''}$), 65.9 ($C_{9''}$ and $C_{11''}$), 110.8 (C_2), 114.1 ($C_{3''}$ and $C_{5''}$), 123.9 ($C_{2''}$ and $C_{6''}$), 125.3 (C_8), 125.9 (C_5), 126.4 ($C_{2'}$ and $C_{6'}$), 127.7 ($C_{3'}$ and $C_{5'}$), 128.7 ($C_{1''}$), 129.4 (C_9), 130.6 (C_{10}), 131.8 (C_6 or $C_{4'}$), 132.0 (C_6 or $C_{4'}$), 133.8 (C_7), 137.9 (C_3 or $C_{1'}$), 138.1 (C_3 or $C_{1'}$), 148.0 ($C_{4''}$), 177.7 (C_1), 181.0 (C_4); *m/z* (ESI$^+$) 490 ([M+H]$^+$, 100%), 512 ([M+Na]$^+$, 15%); HRMS (ESI$^+$) $C_{26}H_{23}N_3NaO_5S^+$ ([M+Na]$^+$) requires 512.1251, found 512.1252.

***N*-(1,4-Dioxo-3-((4''-(8''-oxomorpholino)phenyl)amino)-1,4-dihydronaphthalen-2-yl)benzenesulfonamide 365**



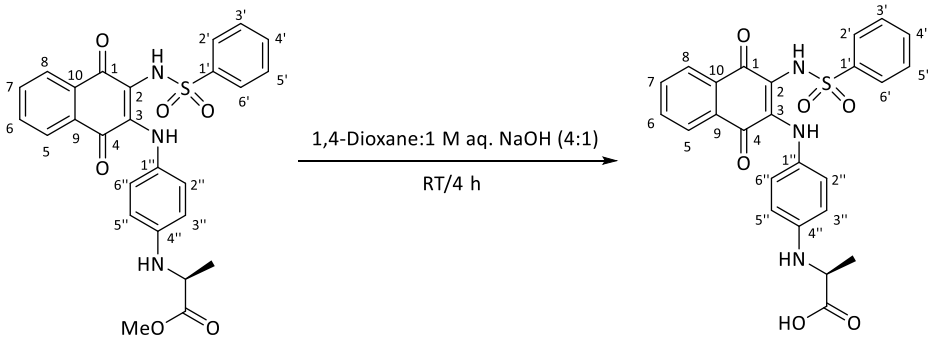
Following *General Procedure 2*, using naphthoquinone **57** (200 mg, 0.576 mmol), 4-(4-aminophenyl)morpholin-3-one (260 mg, 1.35 mmol) and cerium trichloride heptahydrate (214 mg, 0.576 mmol) in MeOH (8 mL), at 90 ^{o}C. Upon workup 3-anilinonaphthoquinone **365** precipitated as an orange solid; this precipitate was collected by suction filtration and washed with cold EtOAc (3 x 5 mL). Purification of the filtrate *via* column chromatography on silica gel (eluent pet ether:acetone 90:10 to 50:50) afforded further naphthoquinone **365** as an orange solid; the precipitate from the workup and the purified product of column chromatography were combined (153 mg, 53%). mp 225-226 ^{o}C; υ_{max} (thin film) 3302 (N-H), 3241 (N-H), 1688 (amide C=O), 1652 (naphthoquinone C=O), 1614 (naphthoquinone C=O), 1573, 1519; δ_H (400 MHz, $CDCl_3$) 3.85 (2H, app. t, *J* 5.0, $2H_{12''}$), 4.07 (2H, app. t, *J* 5.0, $2H_{11''}$), 4.37 (2H, s, $2H_{9''}$), 6.82 (1H, br. s, sulfonamide-N*H*), 7.11-7.16 (2H, m, $H_{2''}$ and $H_{6''}$), 7.33-7.40 (4H, m, $H_{3'}$, $H_{5'}$, $H_{3''}$ and $H_{5''}$), 7.45-7.50 (1H, m, $H_{4'}$), 7.64-7.72 (4H, m, H_6, H_7, $H_{2'}$ and $H_{6'}$), 7.83-7.89 (1H, m, H_8), 8.06 (1H, br. s, anilino-N*H*), 8.08-8.13 (1H, m, H_5); δ_C (100 MHz, $CDCl_3$) 49.7 ($C_{12''}$), 64.2 ($C_{11''}$), 68.6 ($C_{9''}$), 113.4 (C_2), 124.2 ($C_{2''}$ and $C_{6''}$), 125.1 ($C_{3''}$ and $C_{5''}$), 126.4 (C_8), 127.0 (C_5), 127.3 ($C_{2'}$ and $C_{6'}$), 128.8 ($C_{3'}$ and $C_{5'}$), 130.4 (C_9 or C_{10}), 131.2 (C_9 or C_{10}), 133.2 (C_6), 133.2 ($C_{4'}$), 134.9 (C_7), 136.0 ($C_{1''}$), 138.2 ($C_{4''}$), 138.6 (C_3 or $C_{1'}$), 138.7 (C_3 or $C_{1'}$), 166.7 ($C_{8''}$), 179.1 (C_1), 181.7 (C_4); *m/z* (ESI$^-$) 502 ([M-H]$^-$, 100%); HRMS (ESI$^+$) $C_{26}H_{21}N_3NaO_6S^+$ ([M+Na]$^+$) requires 526.1043, found 526.1040.

4''-(1''-((1,4-Dioxo-2-(phenylsulfonamido)-1,4-dihydronaphthalen-3-yl)amino)phenyl)piperidine-*para*-carboxylic acid 367



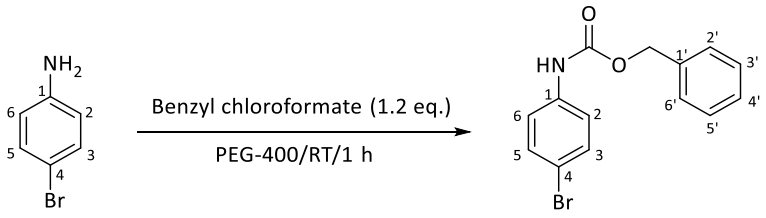
Methyl ester **400** (80 mg, 0.147 mmol) and 1 M aq. NaOH (2 mL) were stirred in 1,4-dioxane (8 mL) at RT for 5 h. The resultant mixture was partitioned between EtOAc (50 mL) and 1 M aq. HCl (20 mL). The aqueous layer was washed twice more with EtOAc (2 x 30 mL). The organic layers were combined, washed with H_2O (20 mL) and then brine (20 mL), dried over Na_2SO_4, filtered and concentrated *in vacuo* to give carboxylic acid **367** as a purple solid (71 mg, 91%), which was subsequently observed to undergo decomposition after *c.* 1 week of standing at RT. δ_H (500 MHz, DMSO-d_6) 1.67 (2H, qd, *J* 11.3, 3.8, $H_{9''}$(ax) and $H_{11''}$(ax)), 1.88-1.95 (2H, m, $H_{9''}$(equ) and $H_{11''}$(equ)), 2.40 (1H, tt, *J* 11.3, 3.8, $H_{10''}$(ax)), 2.75 (2H, td, *J* 11.3, 1.8, $H_{8''}$(ax) and $H_{12''}$(ax)), 3.59-3.65 (2H, m, $H_{8''}$(equ) and $H_{12''}$(equ)), 6.81 (2H, d, *J* 9.1, $H_{3''}$ and $H_{5''}$), 6.92 (2H, d, *J* 9.1, $H_{2''}$ and $H_{6''}$), 7.36 (2H, app. t, *J* 7.6, $H_{3'}$ and $H_{5'}$), 7.48 (1H, tt, *J* 7.6, 1.6, $H_{4'}$), 7.53-7.57 (2H, m, $H_{2'}$ and $H_{6'}$), 7.71-7.80 (3H, m, H_6, H_7 and H_8), 8.00 (1H, d, *J* 7.6, H_5), 8.86 (1H, s, sulfonamide-N*H*), 8.92 (1H, s, aniline-N*H*), 12.19 (1H, br. s, CO_2H); *m/z* (ESI^-) 530 ($[M-H]^-$, 100%).

***para*-((1,4-Dioxo-2-(phenylsulfonamido)1,4-dihydronaphthalen-3-yl)amino)phenyl)-L-alanine 371**



Methyl ester **385** (24 mg, 0.048 mmol) and 1 M aq. NaOH (1.5 mL) were stirred in 1,4-dioxane (6 mL) at RT for 4 h. After this time, the *p*H of the solution was adjusted to *c.* 2 with 1 M aq. HCl (10 mL) and the organic product was extracted into EtOAc (3 x 10 mL). The organic layers were combined, washed with brine (3 x 10 mL), dried over Na_2SO_4, filtered and concentrated *in vacuo*. Purification *via* column chromatography (eluent CH_2Cl_2:MeOH 95:5 to 80:20) gave carboxylic acid **371** as a red solid (8 mg, 34%), which was subsequently observed to undergo decomposition after *c.* 1 week of standing at RT. δ_H (400 MHz, MeOD) 1.46 (3H, d, *J* 6.4, CH*Me*), 3.87-3.95 (1H, m, C*H*Me), 6.60 (2H, d, *J* 8.2, $H_{2''}$ and $H_{6''}$ or $H_{3''}$ and $H_{5''}$), 6.88 (2H, d, *J* 8.2, $H_{2''}$ and $H_{6''}$ or $H_{3''}$ and $H_{5''}$), 7.34 (2H, app. t, *J* 7.8, $H_{3'}$ and $H_{5'}$), 7.44-7.50 (1H, m, $H_{4'}$), 7.60 (2H, d, *J* 7.8, $H_{2'}$ and $H_{6'}$), 7.64-7.74 (2H, m, H_6 and H_7), 7.77-7.82 (1H, m, H_8), 8.03-8.07 (1H, m, H_5), *NH and OH not observed*; *m/z* (ESI^-) 490 ($[M-H]^-$, 100%).

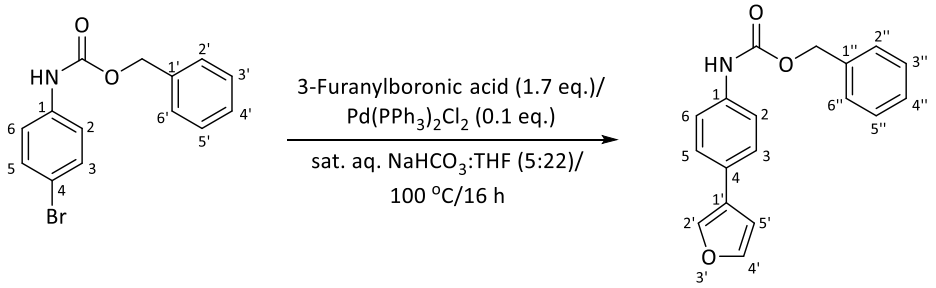
Benzyl (4-bromophenyl)carbamate 372[379]



4-Bromoaniline **204** (2.00 g, 11.6 mmol) and benzyl chloroformate (1.99 mL, 14.0 mmol) were added to a solution of PEG-400 (12 mL) and stirred at RT for 1 h. The crude reaction mixture

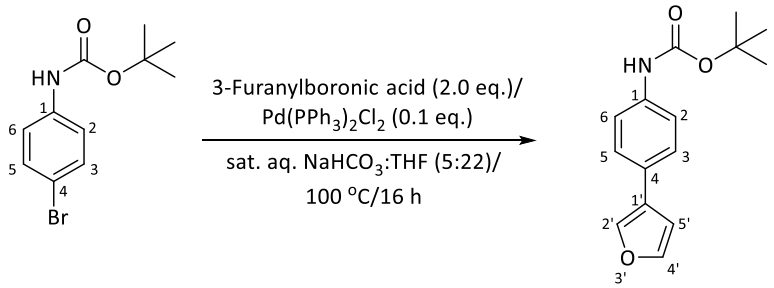
was partitioned between EtOAc (100 mL) and water (100 mL); the organic layer was then collected, dried, filtered and concentrated *in vacuo*. Purification *via* column chromatography on silica gel (eluent pet ether:EtOAc 95:5) afforded benzyl carbamate **372** as a white solid (2.32 g, 65%). mp 118-119 ^{o}C (lit. 123-124 ^{o}C);[380] δ_H (400 MHz, $CDCl_3$) 5.21 (2H, s, CH_2), 6.73 (1H, br. s, N*H*), 7.27-7.32 (2H, m, H_2 and H_6), 7.34-7.44 (7H, m, H_3, H_5, $H_{2'}$, $H_{3'}$, $H_{4'}$, $H_{5'}$ and $H_{6'}$); *m/z* (ESI$^-$) 304 ([M(^{79}Br)-H]$^-$, 100%), 306 ([M(^{81}Br)-H]$^-$, 100%).

Benzyl (4-(furan-3'-yl)phenyl)carbamate 373



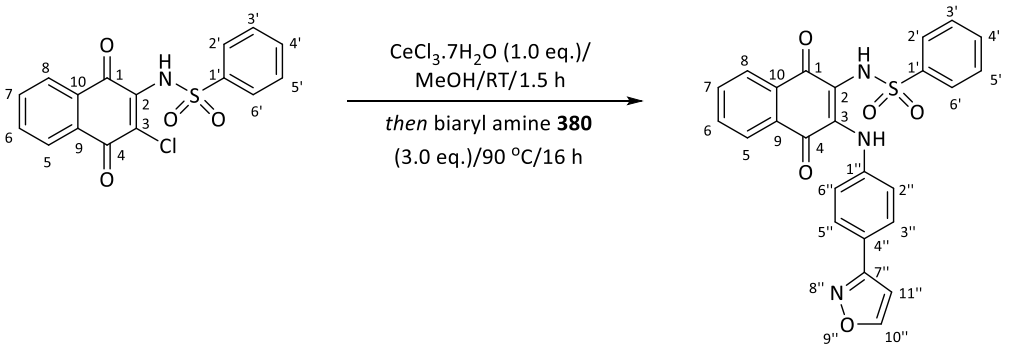
Following *General Procedure 6*, using benzyl (4-bromophenyl)carbamate **372** (500 mg, 1.64 mmol), 3-furanylboronic acid (317 mg, 2.83 mmol), $Pd(PPh_3)_2Cl_2$ (99 mg, 0.142 mmol) and sat. aq. $NaHCO_3$ (2.5 mL) in THF (11 mL). Purification *via* column chromatography on silica gel (eluent pet ether:acetone 90:10) afforded furan **373** as a pale yellow solid (207 mg, 43%). mp 153 ^{o}C; υ_{max} (thin film) 3528 (N-H), 3005 (C-H), 1709 (C=O), 1528; δ_H (400 MHz, $CDCl_3$) 5.23 (2H, s, CH_2Ph), 6.68 (1H, s, $H_{5'}$), 6.73 (1H, br. s, N*H*), 7.30-7.46 (9H, m, H_2, H_3, H_5, H_6, $H_{2''}$, $H_{3''}$, $H_{4''}$, $H_{5''}$ and $H_{6''}$), 7.47 (1H, s, $H_{4'}$), 7.70 (1H, s, $H_{2'}$); δ_C (100 MHz, $CDCl_3$) 67.1 (*C*H_2Ph), 108.8 ($C_{5'}$), 119.1 ($C_{4''}$), 152.9 ($C_{1'}$), 126.5 (C_2 and C_6), 127.8 (C_4), 128.3 ($C_{2''}$ and $C_{6''}$), 128.3 (C_3 and C_5 or $C_{3''}$ and $C_{5''}$), 128.6 (C_3 and C_5 or $C_{3''}$ and $C_{5''}$), 136.0 ($C_{1''}$), 136.6 (C_1), 138.1 ($C_{2'}$), 143.6 ($C_{4'}$), 153.3 (*C*O_2Bn); *m/z* (ESI$^+$) 316 ([M+Na]$^+$, 70%), 609 ([2M+Na]$^+$, 100%); HRMS (ESI$^+$) $C_{18}H_{15}NNaO_3^+$ ([M+Na]$^+$) requires 316.0944, found 316.0945.

tert-Butyl (4-(furan-3'-yl)phenyl)carbamate 375



Following *General Procedure 6*, using *tert*-butyl (4-bromophenyl)carbamate **205** (462 mg, 1.67 mmol), 3-furanylboronic acid (381 mg, 3.40 mmol), $Pd(PPh_3)_2Cl_2$ (119 mg, 0.167 mmol) and sat. aq. $NaHCO_3$ (2.5 mL) in THF (11 mL). Purification *via* column chromatography on silica gel (eluent pet ether:EtOAc 98:2 to 90:10) afforded furan **375** as a white solid (391 mg, 89%). mp 115 °C; υ_{max} (thin film) 3332 (N-H), 2979 (C-H), 1699 (C=O), 1582, 1524; δ_H (500 MHz, $CDCl_3$) 1.53 (9H, s, CMe_3), 6.51 (1H, br. s, N*H*), 6.67 (1H, s, $H_{5'}$), 7.34-7.44 (4H, m, H_2, H_3, H_5 and H_6), 7.46 (1H, s, $H_{4'}$), 7.68 (1H, s, $H_{2'}$); δ_C (125 MHz, $CDCl_3$) 28.4 (CMe_3), 80.6 (*C*Me$_3$), 108.8 ($C_{5'}$), 118.9 (C_2 and C_6), 126.0 ($C_{1'}$), 126.4 (C_3 and C_5), 127.3 (C_4), 137.3 (C_1), 138.0 ($C_{2'}$), 143.6 ($C_{4'}$), 152.7 ($CO_2{}^t$Bu); *m/z* (ESI$^+$) 282 ([M+Na]$^+$, 95%), 541 ([2M+Na]$^+$, 100%); HRMS (ESI$^+$) $C_{15}H_{17}NNaO_3{}^+$ ([M+Na]$^+$) requires 282.1101, found 282.1101.

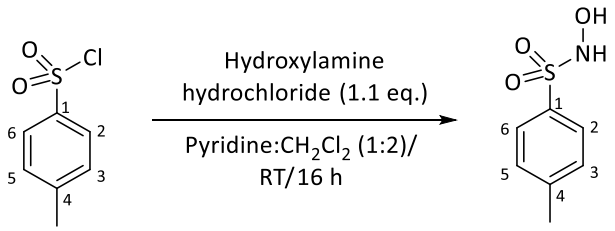
N-(3-((4''-(Isoxazol-7''-yl)phenyl)amino)-1,4-dioxo-1,4-dihydronaphthalen-2-yl)benzensulfonamide 376



Following *General Procedure 2*, using naphthoquinone **57** (76 mg, 0.219 mmol), 3-(4'-aminophenyl)isoxazole **380** (70 mg, 0.438 mmol) and cerium trichloride heptahydrate (82 mg,

0.219 mmol) in MeOH (7 mL), at 90 °C. Purification *via* column chromatography on silica gel (eluent petrol:acetone 80:20 to 70:30) gave 3-anilinonaphthoquninone **376** as a red solid (19 mg, 18%). mp 247-249 °C; υ_{max} (thin film) 3331 (N-H), 3261 (N-H), 1709 (C=O), 1663 (C=O), 1615, 1591, 1573, 1525; δ_H (500 MHz, DMSO-d_6) 7.10-7.18 (3H, m, $H_{2''}$, $H_{6''}$ and $H_{11''}$), 7.35 (2H, app. t, *J* 7.6, $H_{3'}$ and $H_{5'}$), 7.48 (1H, app. t, *J* 7.6, $H_{4'}$), 7.57 (2H, d, *J* 7.6, $H_{2'}$ and $H_{6'}$), 7.72-7.85 (5H, m, H_6, H_7, H_8, $H_{3''}$ and $H_{5''}$), 8.01-8.06 (1H, m, H_5), 8.98 (1H, s, $H_{10''}$), 9.12 (1H, s, sulfonamide-N*H*), 9.18 (1H, s, aniline-N*H*); δ_C (125 MHz, DMSO-d_6) 102.7 ($C_{11''}$), 114.7 (C_2), 123.0 ($C_{4''}$), 123.5 ($C_{2''}$ and $C_{6''}$), 125.7 (C_8), 125.9 ($C_{3''}$ and $C_{5''}$), 126.2 (C_5), 126.5 ($C_{2'}$ and $C_{6'}$), 128.5 ($C_{3'}$ and $C_{5'}$), 130.3 (C_9 or C_{10}), 131.4 (C_9 or C_{10}), 132.2 ($C_{4'}$), 133.1 (C_6), 134.9 (C_7), 140.3 ($C_{1''}$), 140.8 ($C_{1'}$), 141.5 (C_3), 160.4 ($C_{10''}$), 160.7 ($C_{7''}$), 178.7 (C_1), 182.2 (C_4); *m/z* (ESI^+) 139 (100%), 413 (30%), 472 ($[M+H]^+$, 15%), 494 ($[M+Na]^+$, 40%); HRMS (ESI^+) $C_{25}H_{17}N_3NaO_5S^+$ ($[M+Na]^+$) requires 494.0781, found 494.0780.

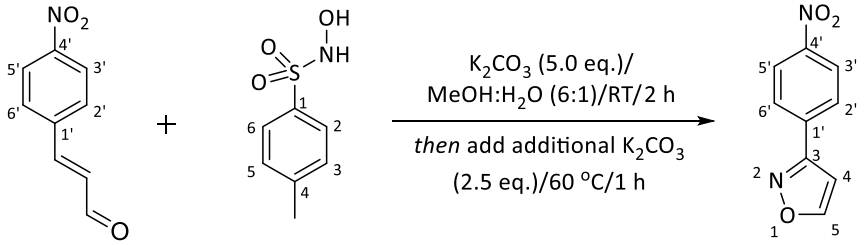
N-Hydroxy-4-methylbenzenesulfonamide 378[381]



To a solution of hydroxylamine hydrochloride (3.83 g, 55.0 mmol) in CH_2Cl_2 (60 mL) was added pyridine (30 mL) and then *para*-toluenesulfonyl chloride **377** (9.53 g, 50.0 mmol) at RT. The mixture was stirred for 16 h and then poured onto EtOAc:H_2O (500 mL:500 mL). The organic layer was subsequently collected, washed with 1 M aq. HCl (500 mL), H_2O (500 mL) and brine (500 mL), dried, filtered and concentrated *in vacuo*. Et_2O (100 mL) was then added to dissolve the concentrated residue and on subsequent addition of pentane (800 mL) a cream precipitate was formed. This was collected by suction filtration and purified *via* column chromatography on silica gel (eluent pet ether:acetone 50:50 to 25:75) to give sulfonamide **378** as a cream solid (5.180 g, 55%). mp 87-89 °C (lit. 82-84 °C);[381] δ_H (400 MHz, DMSO-d_6) 2.40

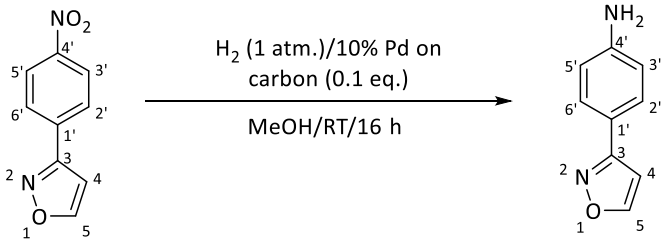
(3H, s, *Me*), 7.42 (2H, d, *J* 8.2, H_3 and H_5), 7.72 (2H, d, *J* 8.2, H_2 and H_6), 9.49 (1H, s, N*H* or O*H*), 9.55 (1H, br. s, N*H* or O*H*); *m/z* (ESI^+) 210 ($[M+Na]^+$, 100%), 397 ($[2M+Na]^+$, 95%).

3-(4'-Nitrophenyl)isoxazole 379[338]



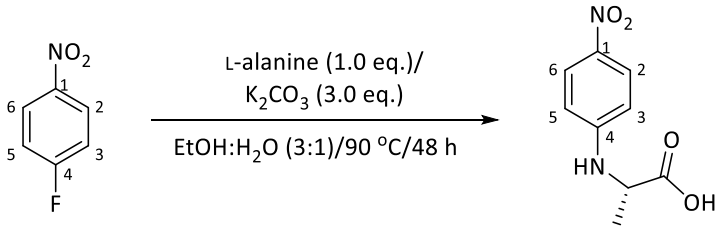
To a solution of *N*-hydroxy-4-methylbenzenesulfonamide **378** (1.500 g, 8.00 mmol) dissolved in MeOH:H_2O (10.8 mL:1.8 mL), K_2CO_3 (1.380 g, 10.00 mmol) was added portionwise. Subsequently, *para*-nitrocinnamaldehyde (0.354 g, 2.00 mmol) was added along with further MeOH (5.4 mL) and the reaction mixture was stirred at RT until the enal starting material was no longer observable by TLC (about 2 h). Next additional K_2CO_3 (0.900 g, 5.00 mmol) was added and the mixture was stirred at 60 °C for a further 1 h. On completion, the reaction mixture was diluted with EtOAc (40 mL), washed with H_2O (40 mL) and brine (2 x 40 mL), and the organic extracts were combined, dried, filtered and concentrated *in vacuo*. Purification *via* column chromatography on silica gel (eluent pet ether:acetone 95:5) afforded isoxazole **379** as a cream solid (87 mg, 23%). mp 175-176 °C (lit. decomposes 170-172 °C);[338] δ_H (400 MHz, DMSO-d_6) 7.35 (1H, d, *J* 1.5, H_4), 8.20 (2H, d, *J* 8.7, $H_{2'}$ and $H_{6'}$), 8.38 (2H, d, *J* 8.7, $H_{3'}$ and $H_{5'}$), 9.14 (1H, d, *J* 1.5, H_5); *m/z* (FI^+) 190 ($[M]^+$).

3-(4'-Aminophenyl)isoxazole 380



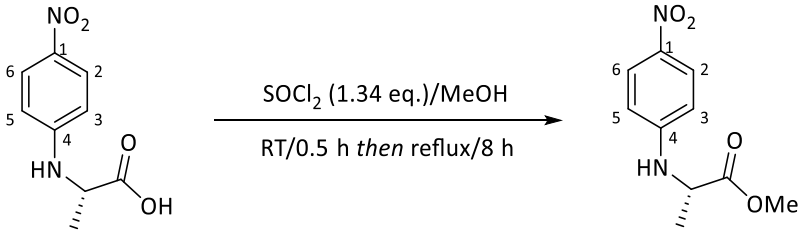
Following *General Procedure 5*, using 3-(4'-nitrophenyl)isoxazole **379** (94 mg, 0.492 mmol) and 10% Pd/C (5 mg, 0.049 mmol) in MeOH (6 mL). The crude product was filtered through Celite® and the residue concentrated *in vacuo* to give aniline **380** as a yellow oil (78 mg, quant.). υ_{max} (thin film) 3354 (N-H), 3225 (N-H), 2926 (C-H), 1610, 1557, 1527; δ_H (500 MHz, DMSO-d_6) 6.65 (2H, d, *J* 8.5, $H_{3'}$ and $H_{5'}$), 6.88 (1H, d, *J* 1.7, H_4), 7.52 (2H, d, *J* 8.5, $H_{2'}$ and $H_{6'}$), 8.78 (1H, d, *J* 1.7, H_5); δ_C (125 MHz, DMSO-d_6) 102.2 (C_4), 114.7 ($C_{3'}$ and $C_{5'}$), 116.6 ($C_{1'}$), 127.8 ($C_{2'}$ and $C_{6'}$), 148.9 ($C_{4'}$), 159.8 (C_5), 161.0 (C_3); *m/z* (ESI^+) 161 ($[M+H]^+$, 100%); HRMS (ESI^+) $C_9H_9N_2O^+$ ($[M+H]^+$) requires 161.0709, found 161.0708.

para-Nitrophenyl-L-alanine 382



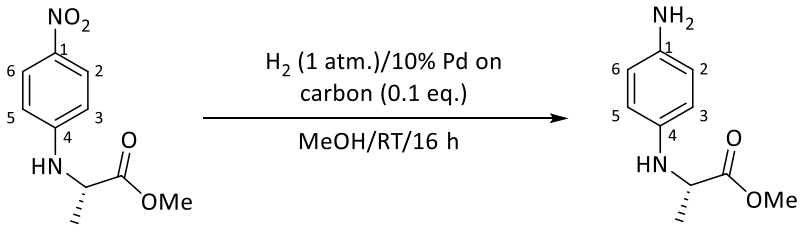
Following *General Procedure 9*, using 1-fluoro-4-nitrobenzene **381** (1.00 g, 7.09 mmol), L-alanine (631 mg, 7.09 mmol), K_2CO_3 (2.94 g, 21.3 mmol) and H_2O (2.5 mL) in EtOH (7.5 mL). Purification *via* column chromatography (eluent pet ether:actone 20:80) gave *para*-nitrophenyl-L-alanine **382** as a yellow solid (598 mg, 40%). mp 83-87 °C; υ_{max} (thin film) 3367 (N-H), 1705 (C=O), 1599 (N=O), 1529, 1505; $\alpha_D^{[25]}$ -80.9 (*c* 0.2, MeOH); δ_H (500 MHz, MeOD) 1.49 (3H, d, *J* 7.0, CH*Me*), 4.08 (1H, q, *J* 7.0, C*H*Me), 6.60-6.64 (2H, m, H_3 and H_5), 8.00-8.05 (2H, m, H_2 and H_6); δ_C (125 MHz, MeOD) 18.8 (CH*Me*), 53.7 (C*H*Me), 112.5 (C_3 and C_5), 127.3 (C_2 and C_6), 138.6 (C_1), 155.2 (C_4), 179.2 (CO_2H); *m/z* (ESI^-) 209 ($[M-H]^-$, 100%); HRMS (ESI^+) $C_9H_9O_4N_2^+$ ($[M+H]^+$) requires 209.0568, found 209.0571.

Methyl (*para*-nitrophenyl)-L-alaninate 383



To an ice-cold solution of *para*-nitrophenyl-L-alanine **382** (500 mg, 2.38 mmol) in MeOH (5 mL) was added thionyl chloride (233 µL, 3.19 mmol) dropwise. The solution was warmed to RT and stirred for 30 min before being heated under reflux for 8 h. The reaction mixture was then cooled to RT and concentrated *in vacuo*. Toluene (10 mL) was added and the solution was again concentrated *in vacuo*; this process was repeated twice more to give the crude product. Purification *via* column chromatography on silica gel (eluent pet ether:acetone 50:50) gave methyl L-alaninate **383** as a yellow solid (303 mg, 57%). mp 63 ^{o}C; υ_{max} (thin film) 3370 (N-H), 1735 (C=O), 1597 (N=O), 1531, 1504; $\alpha_D^{[25]}$ -87.1 (*c* 0.2, $CHCl_3$); δ_H (500 MHz, $CDCl_3$) 1.52 (3H, d, *J* 7.1, CH*Me*), 3.77 (3H, s, O*Me*), 4.22 (1H, t, *J* 7.1, C*H*Me), 5.13 (1H, d, *J* 7.1, N*H*), 6.51-6.55 (2H, m, H_3 and H_5), 8.04-8.08 (2H, m, H_2 and H_6); δ_C (125 MHz, $CDCl_3$) 18.4 (CH*Me*), 51.1 (*C*HMe), 52.6 (O*Me*), 111.5 (C_3 and C_5), 126.3 (C_2 and C_6), 138.5 (C_1), 151.6 (C_4), 173.5 (*C*O_2Me); *m/z* (ESI$^+$) 225 ([M+H]$^+$, 50%), 247 ([M+Na]$^+$, 100%); HRMS (ESI$^+$) $C_{10}H_{13}O_4N_2^+$ ([M+H]$^+$) requires 225.0870, found 225.0868.

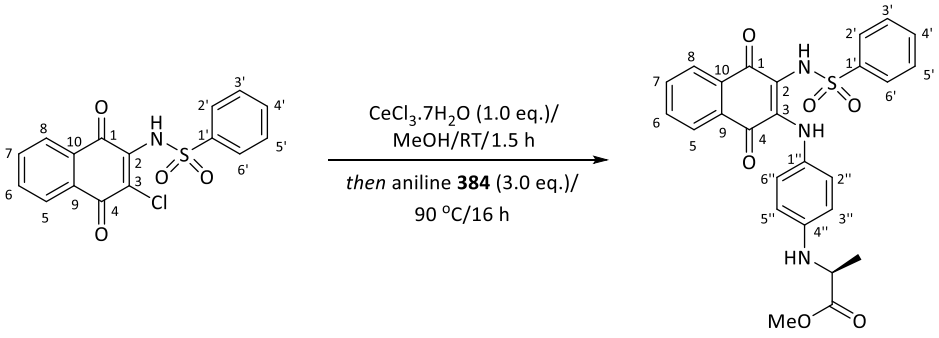
Methyl (*para*-aminophenyl)-L-alaninate 384



Following *General Procedure 5*, using methyl L-alaninate **383** (250 mg, 1.12 mmol) and 10% Pd/C (12 mg, 0.11 mmol) in MeOH (6 mL) gave aminophenyl **384** as a dark red oil (212 mg, 98%). υ_{max} (thin film) 3357 (N-H), 1733 (C=O), 1610, 1515; $[\alpha]_D^{25}$ -16.0 (*c* 0.025, $CHCl_3$);

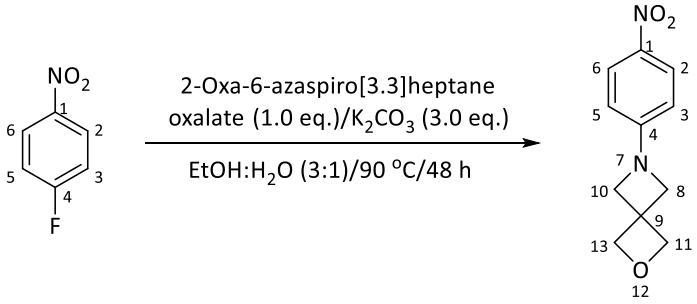
δ_H (500 MHz, $CDCl_3$) 1.45 (3H, d, *J* 6.9, CH*Me*), 3.71 (3H, s, O*Me*), 4.05 (1H, q, *J* 6.9, C*H*Me), 6.50-6.55 (2H, m, H_3 and H_5), 6.58-6.63 (2H, m, H_3 and H_5); δ_C (125 MHz, $CDCl_3$) 19.1 (CH*Me*), 52.1 (O*Me*), 53.3 (C*H*Me), 115.6 (C_3 and C_5), 116.8 (C_2 and C_6), 138.7 (C_1), 139.5 (C_4), 175.5 (*C*O_2Me); *m/z* (ESI^+) 195 ($[M+H]^+$, 100%); HRMS (ESI^+) $C_{10}H_{15}N_2O_2^+$ ($[M+H]^+$) requires 195.1128, found 195.1130.

Methyl (*para*-((1,4-dioxo-2-(phenylsulfonamido)1,4-dihydronaphthalen-3-yl)amino)phenyl)-L-alaninate 385



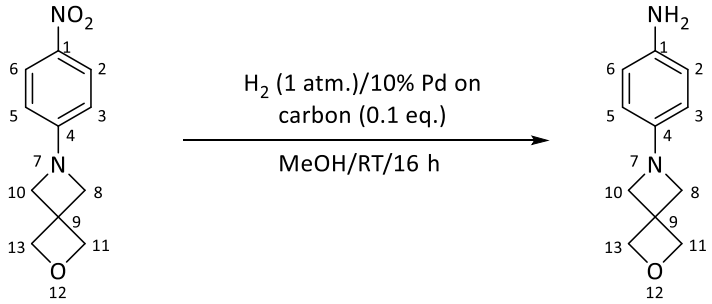
Following *General Procedure 2*, using naphthoquinone **57** (130 mg, 0.374 mmol), methyl (*para*-aminophenyl)-L-alaninate **384** (198 mg, 1.021 mmol) and cerium trichloride heptahydrate (139 mg, 0.374 mmol) in MeOH (7 mL), at 90 °C. Purification *via* column chromatography on silica gel (eluent pet ether:acetone 80:20 then pet ether:EtOAc 50:50) afforded 3-anilinonaphthoquinone **385** as a purple solid (70 mg, 37%). mp 129-130 °C; υ_{max} (thin film) 3282 (N-H), 1736 (ester C=O), 1709 (C=O), 1673 (C=O), 1605, 1570, 1520; $\alpha_D^{[25]}$ -140 (*c* 0.002, $CHCl_3$); δ_H (500 MHz, $CDCl_3$) 1.52 (3H, d, *J* 6.9, CH*Me*), 3.77 (3H, s, O*Me*), 4.19 (1H, q, *J* 6.9, C*H*Me), 6.59-6.64 (2H, m, $H_{3''}$ and $H_{5''}$), 6.68 (1H, s, sulfonamide-N*H*), 6.94-6.99 (2H, m, $H_{2''}$ and $H_{6''}$), 7.31-7.36 (2H, m, $H_{3'}$ and $H_{5'}$), 7.43-7.48 (1H, m, $H_{4'}$), 7.60-7.70 (4H, m, H_6, H_7, $H_{2'}$ and $H_{6'}$), 7.84 (1H, dd, *J* 7.6, 1.4, H_8), 7.97 (1H, s, aniline-N*H*), 8.07 (1H, dd, *J* 7.6, 1.4, H_5); δ_C (125 MHz, $CDCl_3$) 18.9 (CH*Me*), 52.1 (*C*HMe), 52.3 (O*Me*), 111.3 (C_2), 112.9 ($C_{3''}$ and $C_{5''}$), 125.5 ($C_{2''}$ and $C_{6''}$), 126.2 (C_8), 126.8 (C_5), 127.3 ($C_{2'}$ and $C_{6'}$), 128.3 ($C_{1''}$), 128.6 ($C_{3'}$ and $C_{5'}$), 130.4 (C_9), 131.7 (C_{10}), 132.7 (C_6), 132.9 ($C_{4'}$), 134.8 (C_7), 139.0 ($C_{1'}$), 139.3 (C_3), 144.5 ($C_{4''}$), 174.9 (*C*O_2Me), 178.7 (C_1), 182.0 (C_4); *m/z* (ESI^-) 504 ($[M-H]^-$, 100%); HRMS (ESI^-) $C_{26}H_{22}O_6N_3S^-$ ($[M-H]^-$) requires 504.1235, found 504.1246.

7-(*para*-Nitrophenyl)-12-oxa-7-azaspiro[9.9]heptane 386



Following *General Procedure 9*, using 1-fluoro-4-nitrobenzene **381** (657 mg, 4.66 mmol), 2-oxa-6-azaspiro[3.3]heptane oxalate (881 mg, 4.66 mmol), K_2CO_3 (1.93 g, 14.0 mmol) and H_2O (2.5 mL) in EtOH (7.5 mL). Purification *via* column chromatography (eluent pet ether:actone 60:40 then pet ether:EtOAc 80:20 to 0:100) gave *para*-nitrophenyl species **386** as a yellow solid (529 mg, 52%). mp 181-189 ^{o}C; υ_{max} (thin film) 2939 (C-H), 2869 (C-H), 1653, 1602, 1578 (N=O), 1522; δ_H (500 MHz, $CDCl_3$) 4.21 (4H, s, 2 x H_8 and 2 x H_{10}), 4.88 (4H, s, 2 x H_{11} and 2 x H_{13}), 6.30-6.35 (2H, m, H_3 and H_5), 8.09-8.13 (2H, m, H_2 and H_6); δ_C (125 MHz, $CDCl_3$) 38.8 (C_9), 60.9 (C_8 and C_{10}), 80.8 (C_{11} and C_{13}), 109.6 (C_3 and C_5), 126.1 (C_2 and C_6), 138.3 (C_1), 154.0 (C_4); *m/z* (ESI$^+$) 221 ([M+H]$^+$, 30%), 243 ([M+Na]$^+$, 100%); HRMS (ESI$^+$) $C_{11}H_{13}O_3N_2^+$ ([M+H]$^+$) requires 221.0921, found 221.0923.

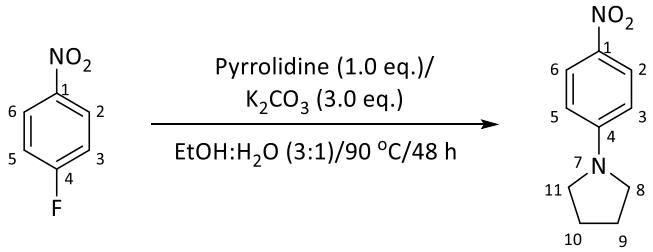
7-(*para*-Aminophenyl)-12-oxa-7-azaspiro[9.9]heptane 387



Following *General Procedure 5*, using 7-(*para*-nitrophenyl)-12-oxa-7-azaspiro[3.3]heptane **386** (360 mg, 1.636 mmol) and 10% Pd/C (17 mg, 0.164 mmol) in MeOH (7 mL). The crude product was filtered through Celite® and the residue concentrated *in vacuo* to give aniline **387** as a red

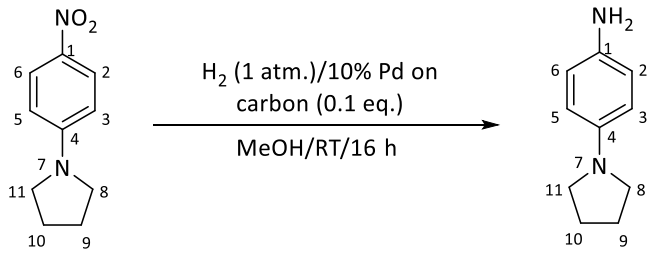
solid (307 mg, quant.), which was observed to undergo decomposition after a few days of standing at RT. δ_H (500 MHz, $CDCl_3$) 3.35 (2H, br. s, NH_2), 3.93 (4H, s, 2 x H_8 and 2 x H_{10}), 4.83 (4H, s, 2 x H_{11} and 2 x H_{13}), 6.34-6.39 (2H, m, H_3 and H_5), 6.62-6.67 (2H, m, H_2 and H_6); *m/z* (ESI$^+$) 191 ([M+H]$^+$, 100%).

4-(1-Nitrophenyl)pyrrolidine 388[382]



Following *General Procedure 9*, using 1-fluoro-4-nitrobenzene **381** (1.00 g, 7.09 mmol), pyrrolidine (516 µL, 7.09 mmol), K_2CO_3 (2.94 g, 21.3 mmol) and H_2O (2.5 mL) in EtOH (7.5 mL). Purification *via* column chromatography (eluent pet ether:actone 80:20) gave 4-arylpyrrolidine **388** as a yellow solid (1.24 g, 91%). mp 166-168 °C (lit. 165 °C);[382] δ_H (400 MHz, $CDCl_3$) 2.04-2.13 (4H, m, 2 x H_9 and 2 x H_{10}), 3.36-3.46 (4H, m, 2 x H_8 and 2 x H_{11}), 6.45-6.52 (2H, H_3 and H_5), 8.09-8.16 (2H, m, H_2 and H_6); *m/z* (ESI$^+$) 193 ([M+H]$^+$, 50%), 215 ([M+Na]$^+$, 100%).

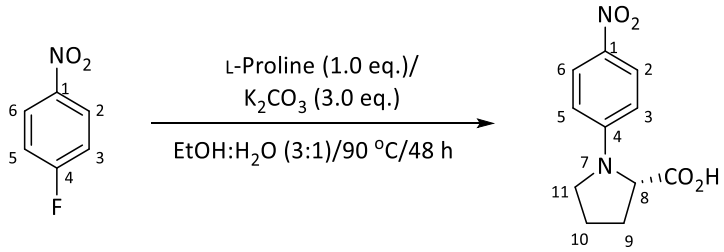
4-(1-Aminophenyl)pyrrolidine 389



Following *General Procedure 5*, using arylpyrrolide **388** (500 mg, 2.60 mmol) and 10% Pd/C (28 mg, 0.26 mmol) in MeOH (6 mL). The crude product was filtered through Celite® and the residue concentrated *in vacuo* to give aniline **389** as a red oil (422 mg, quant.), which was

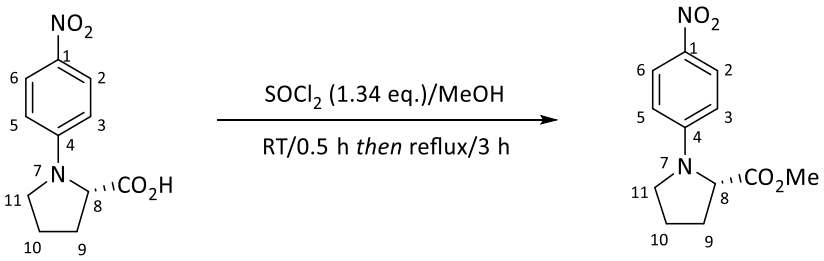
observed to undergo decomposition after a few weeks of standing at RT. δ_H (400 MHz, $CDCl_3$) 1.97-2.02 (4H, m, 2 x H_9 and 2 x H_{10}), 3.20-3.26 (4H, m, 2 x H_8 and 2 x H_{11}), 6.48-6.53 (2H, m, $H_{2''}$ and $H_{6''}$ or $H_{3''}$ and $H_{5''}$), 6.67-6.72 (2H, m, $H_{2''}$ and $H_{6''}$ or $H_{3''}$ and $H_{5''}$); *m/z* (ESI^+) 163 ($[M+H]^+$, 100%).

4-(1-Nitrophenyl)-L-proline 390



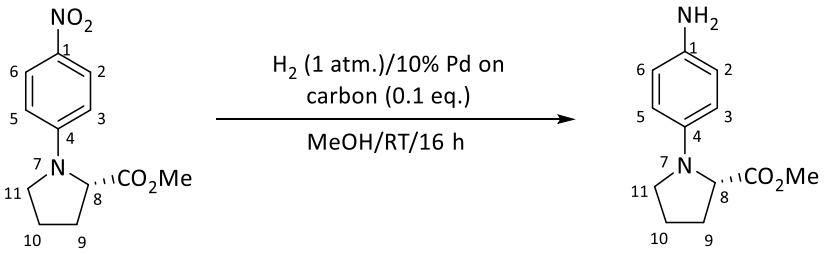
Following *General Procedure 9*, using 1-fluoro-4-nitrobenzene **381** (1.00 g, 7.09 mmol), L-proline (815 mg, 7.09 mmol), K_2CO_3 (2.94 g, 21.3 mmol) and H_2O (2.5 mL) in EtOH (7.5 mL). The crude product was dissolved in EtOAc (10 mL) and then upon the further addition of pet ether (50 mL) a precipitate was formed. This precipitate was collected by suction filtration to yield aryl-L-proline **390** as a yellow solid (1.27 g, 76%). mp 127-132 °C; υ_{max} (thin film) 3489 (O-H), 2978 (C-H), 1707 (C=O), 1598 (N=O), 1513; $\alpha_D^{[25]}$ -201.0 (*c* 0.2, $CHCl_3$); δ_H (400 MHz, DMSO-d_6) 1.90-2.21 (3H, m, H_9 and 2 x H_{10}), 2.26-2.39 (1H, m, H_9), 3.40-3.62 (2H, m, 2 x H_{11}), 4.45 (1H, dd, *J* 8.7, 2.4, H_8), 6.60 (2H, d, *J* 9.1, H_3 and H_5), 8.09 (2H, d, *J* 9.1, H_2 and H_6), 12.96 (1H, br. s, CO_2H); δ_C (100 MHz, DMSO-d_6) 23.2 (C_{10}), 30.2 (C_9), 48.4 (C_{11}), 60.3 (C_8), 111.3 (C_3 and C_5), 125.9 (C_2 and C_6), 136.2 (C_1), 151.5 (C_4), 173.5 (CO_2H); *m/z* (ESI^-) 235 ($[M-H]^-$, 100%); HRMS (ESI^+) $C_{11}H_{12}N_2NaO_4^+$ ($[M+Na]^+$) requires 259.0695, found 259.0690.

Methyl 4-(1-nitrophenyl)-L-prolinate 391



To an ice-cold solution of 4-(1-nitrophenyl)-L-proline **390** (1.00 g, 4.24 mmol) in MeOH (6 mL) was added thionyl chloride (414 µL, 5.68 mmol) dropwise. The solution was warmed to RT and stirred for 30 min before being heated under reflux for 3 h. The reaction mixture was then cooled to RT and concentrated *in vacuo*. EtOAc (30 mL) was added and the solution was washed with H_2O (2 x 20 mL) and brine (2 x 20 mL). The organic layer was then dried, filtered and concentrated *in vacuo* to give methyl L-prolinate **391** as a yellow-brown solid (974 mg, 92%). mp 68-69 ^oC; υ_{max} (thin film) 2956 (C-H), 1732 (C=O), 1711, 1597 (N=O), 1513; $\alpha_D^{[25]}$ -252.5 (*c* 0.2, $CHCl_3$); δ_H (500 MHz, $CDCl_3$) 2.10-2.29 (3H, m, H_9 and 2 x H_{10}), 2.31-2.41 (1H, m, H_9), 3.45-3.52 (1H, m, H_{11}), 3.64-3.70 (1H, m, H_{11}), 3.76 (3H, s, O*Me*), 4.39 (1H, dd, *J* 8.6, 2.3, H_8), 6.49 (2H, d, *J* 9.5, H_3 and H_5), 8.13 (2H, d, *J* 9.5, H_2 and H_6); δ_C (125 MHz, $CDCl_3$) 23.6 (C_{10}), 30.8 (C_9), 48.6 (C_{11}), 52.5 (CO_2Me), 60.7 (C_8), 111.0 (C_3 and C_5), 126.2 (C_2 and C_6), 137.8 (C_1), 151.1 (C_4), 173.1 (CO_2Me); *m/z* (ESI^+) 251 ($[M+H]^+$, 50%), 273 ($[M+Na]^+$, 100%); HRMS (ESI^+) $C_{12}H_{15}O_4N_2^+$ ($[M+H]^+$) requires 251.1026, found 251.1024.

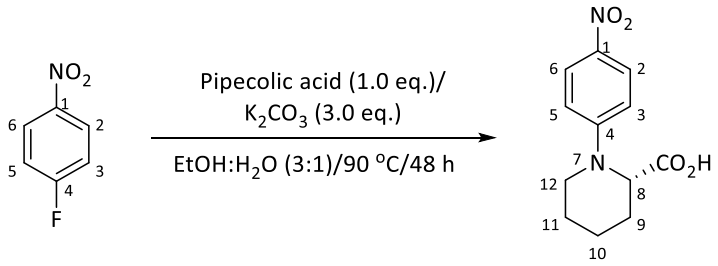
Methyl 4-(1-aminophenyl)-L-prolinate 392



Following *General Procedure 5*, using nitrophenyl **391** (500 mg, 2.00 mmol) and 10% Pd/C (21 mg, 0.20 mmol) in MeOH (5 mL). The crude product was filtered through Celite® and the

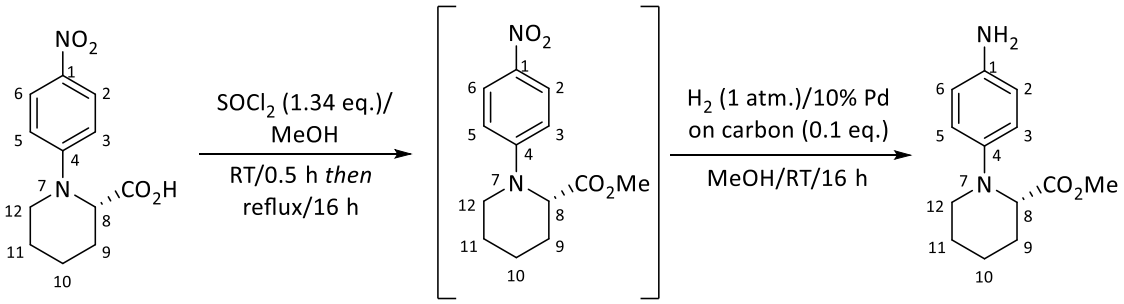
residue concentrated *in vacuo* to give aniline **392** as a red oil (430 mg, 97%), which was observed to undergo decomposition after a few weeks on standing at RT. δ_H (400 MHz, $CDCl_3$) 1.97-2.07 (1H, m, H_{10}), 2.07-2.21 (2H, m, H_9 and H_{10}), 2.21-2.33 (1H, m, H_9), 3.25-3.35 (1H, m, H_{11}), 3.51-3.59 (1H, m, H_{11}), 3.70 (3H, s, O*Me*), 4.17 (1H, d, *J* 8.1, H_8), 6.44 (2H, d, *J* 8.7, H_3 and H_5), 6.66 (2H, d, *J* 8.7, H_2 and H_6); *m/z* (ESI^+) 221 ($[M+H]^+$, 100%).

(*S*)-4-(1-Nitrophenyl)piperidine-8-carboxylic acid 393



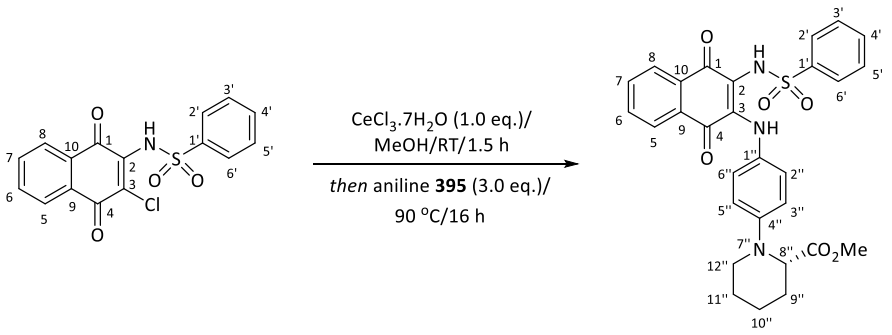
Following *General Procedure 9*, using 1-fluoro-4-nitrobenzene **381** (500 mg, 3.55 mmol), L-pipecolic acid (457 mg, 3.55 mmol), K_2CO_3 (1.47 g, 10.64 mmol) and H_2O (2.5 mL) in EtOH (7.5 mL). Purification *via* column chromatography (eluent pet ether:actone 60:40 to 0:100 before the column was flushed with CH_2Cl_2:MeOH 80:20) gave *para*-nitrophenylpiperidine **393** as an orange-brown oil (684 mg, 77%). υ_{max} (thin film) 2942 (C-H), 1707 (C=O), 1592 (N=O); $\alpha_D^{[25]}$ -20.0 (*c* 0.05, $CHCl_3$); δ_H (500 MHz, $CDCl_3$) 1.38 (1H, qt, *J* 13.1, 3.4, H_{10}(ax)), 1.57 (1H, qt, *J* 13.1, 3.4, H_{11}(ax)), 1.72 (1H, dt, *J* 13.1, 3.4, H_{10}(equ)), 1.77-1.90 (2H, m, H_9(equ) and H_{11}(equ)), 2.25-2.32 (1H, m, H_9(ax)), 3.18 (1H, td, *J* 13.1, 3.4, H_{12}(ax)), 3.67-3.73 (1H, m, H_{12}(equ)), 4.64-4.68 (1H, m, H_8(ax)), 6.72-6.76 (2H, m, H_3 and H_5), 8.03-8.08 (2H, m, H_2 and H_6); δ_C (125 MHz, $CDCl_3$) 20.0 (C_{10}), 24.7 (C_{11}), 27.5 (C_9), 44.3 (C_{12}), 57.0 (C_8), 112.7 (C_3 and C_5), 125.9 (C_2 and C_6), 138.7 (C_1), 155.2 (C_4), 176.9 (CO_2H); *m/z* (ESI^-) 249 ($[M-H]^-$, 100%); HRMS (ESI^+) $C_{12}H_{13}O_4N_2^+$ ($[M+H]^+$) requires 249.0881, found 249.0883.

Methyl (*S*)-4-(1-aminophenyl)piperidine-8-carboxylate 395



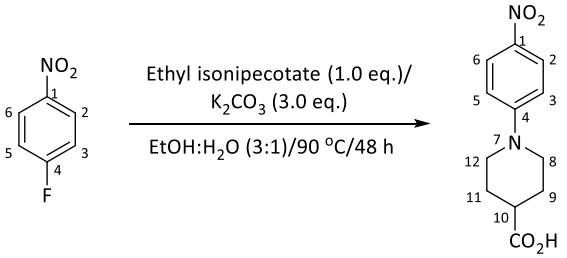
To an ice-cold solution of carboxylic acid **393** (600 mg, 2.40 mmol) in MeOH (15 mL) was added thionyl chloride (350 µL, 4.80 mmol) dropwise. The solution was warmed to RT and stirred for 30 min before being heated under reflux for 16 h. The reaction was then cooled to RT and concentrated *in vacuo* to yield methyl ester **394** as an orange-brown oil (630 mg, quant.), which was used in the next step without further purification. δ_H (500 MHz, $CDCl_3$) 1.42 (1H, qt, *J* 13.3, 3.4, H_{10}(ax)), 1.55-1.70 (1H, m, H_{11}(ax)), 1.78 (1H, dquin, *J* 13.3, 3.4, H_{10}(equ)), 18.5-19.6 (2H, m, H_9(ax) and H_{11}(equ)), 2.33 (1H, dquin, *J* 13.7, 2.1, H_9(equ)), 3.30 (1H, td, *J* 12.6, 3.5, H_{12}(ax)), 3.72 (3H, s, O*Me*), 3.76-3.82 (1H, m, H_{12}(equ)), 4.71 (1H, dd, *J* 5.8, 2.1, H_8), 6.79-6.84 (2H, m, H_3 and H_5), 8.11-8.16 (2H, m, H_2 and H_6); *m/z* (ESI^+) 265 ($[M+H]^+$, 100%). Subsequently, following *General Procedure 5*, using methyl ester **394** (600 mg, 2.27 mmol) and 10% Pd/C (24 mg, 0.23 mmol) in MeOH (7 mL). The crude product was filtered through Celite® and the residue concentrated *in vacuo* to give aniline **395** as a green oil (515 mg, quant.). υ_{max} (thin film) 3358 (N-H), 2939 (C-H), 2857 (C-H), 1736 (C=O), 1711, 1625, 1512; $\alpha_D^{[25]}$ -380.0 (*c* 0.002, $CHCl_3$); δ_H (500 MHz, $CDCl_3$) 1.46-1.56 (1H, m, H_{10}(ax)), 1.56-1.71 (2H, m, H_{10}(equ) and H_{11}(ax)), 1.78-1.86 (1H, m, H_{11}(equ)), 1.92-2.01 (1H, m, H_9(ax)), 2.02-2.09 (1H, m, H_9(equ)), 3.06-3.14 (1H, m, H_{12}(ax) or H_{12}(equ)), 3.31-3.41 (1H, m, H_{12}(ax) or H_{12}(equ)), 3.59 (3H, s, O*Me*), 4.18-4.22 (1H, m, H_8), 6.68 (2H, d, *J* 8.1, H_2 and H_6), 6.83 (2H, d, *J* 8.1, H_3 and H_5); δ_C (125 MHz, $CDCl_3$) 21.2 (C_{10}), 25.5 (C_{11}), 28.8 (C_9), 48.6 (C_{12}), 51.5 (O*Me*), 60.9 (C_8), 116.7 (C_2 and C_6), 119.2 (C_3 and C_5), 138.8 (C_1), 144.6 (C_4), 173.7 (*C*O_2Me); *m/z* (ESI^+) 235 ($[M+H]^+$, 100%); HRMS (ESI^+) $C_{13}H_{19}O_2N_2^+$ ($[M+H]^+$) requires 235.1441, found 235.1437.

Methyl (*S*)-1-(1''-((1,4-dioxo-2-(phenylsulfonamido)-1,4-dihydronaphthalen-3-yl)amino)phenyl)-4''-piperidine-8''-carboxylate 396



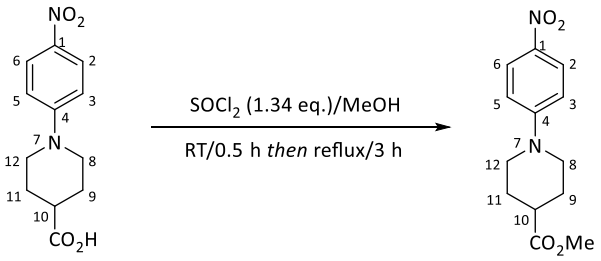
Following *General Procedure 2*, using naphthoquinone **57** (200 mg, 0.576 mmol), aniline **395** (404 mg, 1.73 mmol) and cerium trichloride heptahydrate (214 mg, 0.576 mmol) in MeOH (7 mL), at 90 ^{o}C. Purification *via* column chromatography on silica gel (eluent pet ether:acetone 90:10 to 80:20) gave 3-anilinonaphthoquinone **396** as a purple solid (84 mg, 27%). mp 201-202 ^{o}C; υ_{max} (thin film) 3303 (N-H), 2926 (C-H), 2854 (C-H), 1718 (C=O), 1674 (C=O), 1606, 1570, 1519; $\alpha_D^{[25]}$ -191.6 (*c* 0.002, $CHCl_3$); δ_H (500 MHz, DMSO-d_6) 1.23-1.32 (1H, m, $H_{10''}$(ax)), 1.57 (1H, qt, *J* 12.5, 4.1, $H_{11''}$(ax)), 1.66 (1H, dquin, *J* 13.0, 3.3, $H_{10''}$(equ)), 1.74-1.81 (1H, m, $H_{11''}$(equ)), 1.87 (1H, tdd, *J* 13.2, 5.4, 3.9, $H_{9''}$(ax)), 2.07-2.13 (1H, m, $H_{9''}$(equ)), 3.18 (1H, td, *J* 12.1, 3.3, $H_{12''}$(ax)), 3.47-3.53 (1H, m, $H_{12''}$(equ)), 3.58 (3H, s, O*Me*), 4.70 (1H, dd, *J* 5.4, 2.4, $H_{8''}$), 6.77 (2H, d, *J* 9.0, $H_{3''}$ and $H_{5''}$), 6.89 (2H, d, *J* 9.0, $H_{2''}$ and $H_{6''}$), 7.33-7.38 (2H, m, $H_{3'}$ and $H_{5'}$), 7.46-7.50 (1H, m, $H_{4'}$), 7.54 (1H, dd, *J* 8.4, 1.1, $H_{2'}$ and $H_{6'}$), 7.71-7.80 (3H, m, H_6, H_7 and H_8), 7.98-8.01 (1H, m, H_5), 8.85 (1H, s, sulfonamide-N*H*), 8.89 (1H, s, aniline-N*H*); δ_C (500 MHz, DMSO-d_6) 20.1 ($C_{10''}$), 24.9 ($C_{11''}$), 27.8 ($C_{9''}$), 44.2 ($C_{12''}$), 51.4 (O*Me*), 57.3 ($C_{8''}$), 111.5 (C_2), 113.8 ($C_{3''}$ and $C_{5''}$), 124.7 ($C_{2''}$ and $C_{6''}$), 125.5 (C_8), 126.1 (C_5), 126.6 ($C_{2'}$ and $C_{6'}$), 128.4 ($C_{3'}$ and $C_{5'}$), 129.4 ($C_{1''}$), 130.2 (C_9), 131.8 (C_{10}), 132.0 ($C_{4'}$), 132.7 (C_6), 134.9 (C_7), 141.0 ($C_{1'}$), 142.0 (C_3), 147.3 ($C_{4''}$), 172.8 (CO_2Me), 177.9 (C_1), 182.5 (C_4); *m/z* (ESI^-) 544 ($[M-H]^-$, 100%); HRMS (ESI^-) $C_{29}H_{26}O_6N_3S^-$ ($[M-H]^-$) requires 544.1548, found 544.1560.

4-(1-Nitrophenyl)piperidine-*para*-carboxylic acid 397



1-Fluoro-4-nitrobenzene **381** (1.00 g, 7.09 mmol), ethyl isonipecotate (1.09 mL, 7.09 mmol), K_2CO_3 (2.94 g, 21.3 mmol) and H_2O (2.5 mL) were stirred in EtOH (7.5 mL) at 90 ^oC for 48 h. The solution was cooled to RT, poured onto ice water (20 mL) and 1 M aq. HCl (20 mL) was added. A yellow precipitate formed which was collected *via* suction filtration. Subsequent purification of this precipitate *via* column chromatography on silica gel (eluent pet ether:acetone 20:80 to 0:100) gave *para*-nitrophenylpiperidine **397** as a yellow solid (574 mg, 32%). mp 159-163 ^oC; υ_{max} (thin film) 3457 (O-H), 2016 (C-H), 2970 (C-H), 2947 (C-H), 1739 (C=O); δ_H (500 MHz, DMSO-d_6) 1.58 (2H, qd, *J* 11.9, 3.7, H_9(ax) and H_{11}(ax)), 1.87-1.94 (2H, m, H_9(equ) and H_{11}(equ)), 2.57 (1H, tt, *J* 11.9, 3.7, H_{10}), 3.06-3.14 (2H, m, H_8(ax) and H_{12}(ax)), 3.96 (2H, dt, *J* 11.9, 3.7, H_8(equ) and H_{12}(equ)), 6.99-7.04 (2H, m, H_3 and H_5), 8.01-8.06 (2H, m, H_2 and H_6); δ_C (125 MHz, DMSO-d_6) 27.2 (C_9 and C_{11}), 39.9 (C_{10}), 46.1 (C_8 and C_{12}), 112.6 (C_3 and C_5), 125.9 (C_2 and C_6), 136.4 (C_1), 154.4 (C_4), 175.7 (CO_2H); *m/z* (ESI$^-$) 249 ([M-H]$^-$, 40%), 499 ([2M-H]$^-$, 100%); HRMS (ESI$^+$) $C_{12}H_{14}N_2NaO_4^+$ ([M+Na]$^+$) requires 273.0846, found 273.0847.

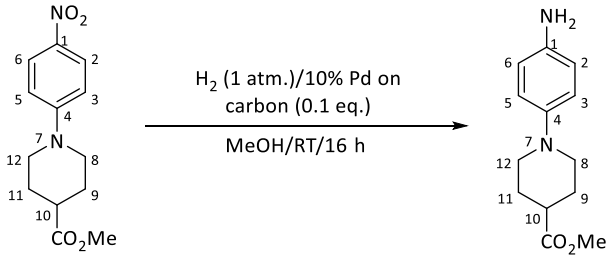
Methyl 4-(1-nitrophenyl)piperidine-*para*-carboxylate 398



To an ice-cold solution of 4-(1-nitrophenyl)piperidine-*para*-carboxylic acid **397** (500 mg, 2.00 mmol) in MeOH (6 mL) was added thionyl chloride (196 µL, 2.68 mmol) dropwise. The

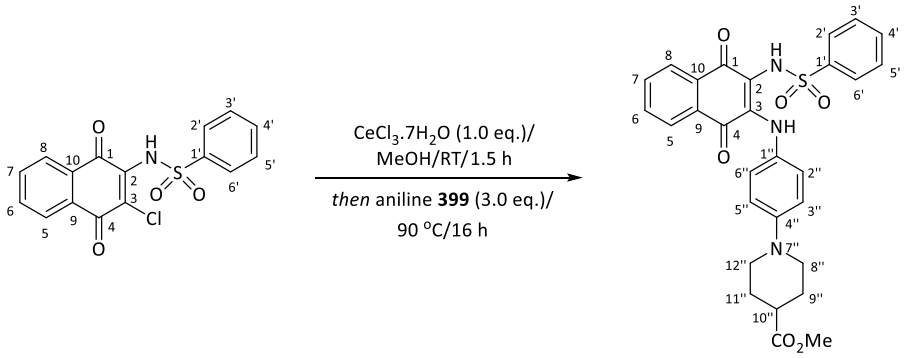
solution was warmed to RT and stirred for 30 min before being heated under reflux for 3 h. The reaction was then cooled to RT and concentrated *in vacuo*. Toluene (10 mL) was added and the solution was again concentrated *in vacuo*; this process was repeated twice more to give methyl ester **398** as a yellow solid (520 mg, 98%). mp 104-106 ^{o}C; υ_{max} (thin film) 2952 (C-H), 2842 (C-H), 1731 (C=O), 1590 (N=O); δ_H (500 MHz, DMSO-d_6) 1.58 (2H, app. qd, *J* 12.0, 3.6, H_9(ax) and H_{11}(ax)), 1.88-1.94 (2H, m, H_9(equ) and H_{11}(equ)), 2.70 (1H, tt, *J* 12.0, 3.6, H_{10}), 3.07-3.14 (2H, m, H_8(ax) and H_{12}(ax)), 3.61 (3H, s, O*Me*), 3.97 (2H, app. dt, *J* 12.0, 3.6, H_8(equ) and H_{12}(equ)), 7.00-7.04 (2H, m, H_3 and H_5), 8.01-8.05 (2H, m, H_2 and H_6); δ_C (125 MHz, DMSO-d_6) 27.1 (C_9 and C_{11}), 39.8 (C_{10}), 46.0 (C_8 and C_{12}), 51.6 (O*Me*), 112.8 (C_3 and C_5), 125.9 (C_2 and C_6), 136.5 (C_1), 154.3 (C_4), 174.4 (*C*O_2Me); *m/z* (ESI$^+$) 265 ([M+H]$^+$, 100%), 287 ([M+Na]$^+$, 25%); HRMS (ESI$^+$) $C_{13}H_{16}N_2NaO_4^+$ ([M+Na]$^+$) requires 287.1002, found 287.1003.

Methyl 4-(1-aminophenyl)piperidine-*para*-carboxyate 399



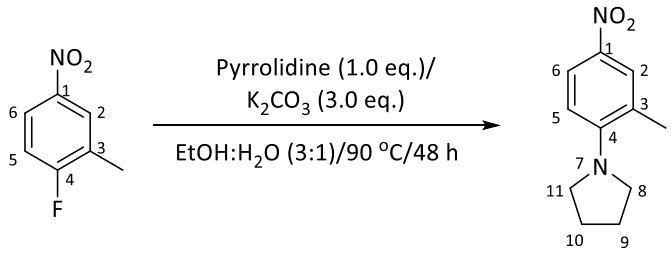
Following *General Procedure 5*, using methyl ester **398** (500 mg, 1.89 mmol) and 10% Pd/C (20 mg, 0.189 mmol) in MeOH (6 mL). The crude product was filtered through Celite® and the residue concentrated *in vacuo* to give aniline **399** as a yellow-brown oil (400 mg, 90%). υ_{max} (thin film) 3393 (N-H), 2953 (C-H), 1730 (C=O), 1607, 1514; δ_H (500 MHz, MeOD) 1.83 (2H, app. qd, *J* 11.7, 3.9, H_9(ax) and H_{11}(ax)), 1.96-2.03 (2H, m, H_9(ax) and H_{11}(equ)), 2.44 (1H, tt, *J* 11.7, 3.9, H_{10}(ax)), 2.65 (2H, app. td, *J* 11.7, 2.2, H_8(ax) and H_{12}(ax)), 3.33-3.39 (2H, m, H_8(equ) and H_{12}(equ)), 3.69 (3H, s, O*Me*), 6.70 (2H, d, *J* 8.8, H_2 and H_6), 6.85 (2H, d, *J* 8.8, H_3 and H_5); δ_C (125 MHz, MeOD) 29.6 (C_9 and C_{11}), 42.0 (C_{10}), 52.4 (O*Me*), 53.0 (C_8 and C_{12}), 117.9 (C_2 and C_6), 121.0 (C_3 and C_5), 143.0 (C_1), 146.0 (C_4), 177.2 (*C*O_2Me); *m/z* (ESI$^+$) 107 (100%), 235 ([M+H]$^+$, 60%); HRMS (ESI$^+$) $C_{13}H_{19}N_2O_2^+$ ([M+Na]$^+$) requires 235.1441, found 235.1443.

Methyl 4''-(1''-((1,4-dioxo-2-(phenylsulfonamido)-1,4-dihydronaphthalen-3-yl)amino)phenyl)piperidine-*para*-carboxylate 400



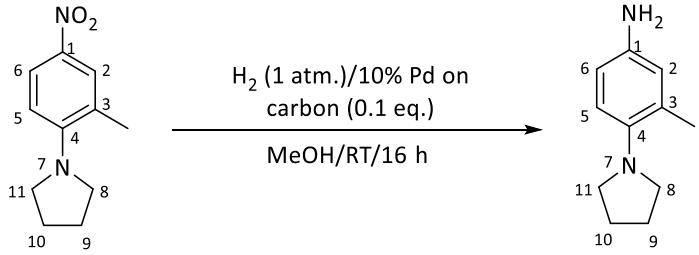
Following *General Procedure 2*, using naphthoquinone **57** (130 mg, 0.374 mmol), aniline **399** (263 mg, 1.12 mmol) and cerium trichloride heptahydrate (139 mg, 0.374 mmol) in MeOH (6 mL), at 90 ^{o}C. Purification *via* column chromatography on silica gel (eluent pet ether:EtOAc 75:25 to 65:35) gave 3-anilinonaphthoquinone **400** as a red solid (58 mg, 28%). mp 192-196 ^{o}C; υ_{max} (thin film) 3330 (N-H), 3258 (N-H), 2953 (C-H), 2925 (C-H), 1729 (ester C=O), 1664 (C=O), 1606 (C=O), 1571, 1514; δ_H (500 MHz, DMSO-d_6) 1.70 (2H, app. qd, *J* 11.0, 4.0, $H_{9''}$(ax) and $H_{11''}$(ax)), 1.87-1.98 (2H, m, $H_{9''}$(equ) and $H_{11''}$(equ)), 2.48-2.57 (1H, m, $H_{10''}$(ax)), 2.77 (2H, app. td, *J* 11.0, 4.0, $H_{8''}$(ax) and $H_{12''}$(ax)), 3.57-3.67 (5H, m, $H_{8''}$(equ), $H_{12''}$(equ) and O*Me*), 6.81 (2H, d, *J* 8.9, $H_{3''}$ and $H_{5''}$), 6.92 (2H, d, *J* 8.9, $H_{2''}$ and $H_{6''}$), 7.32-7.39 (2H, m, $H_{3'}$ and $H_{5'}$), 7.45-7.51 (1H, m, $H_{4'}$), 7.56 (2H, d, *J* 7.6, $H_{2'}$ and $H_{6'}$), 7.70-7.81 (3H, m, H_6, H_7 and H_8), 7.99 (1H, d, *J* 7.2, H_5), 8.88 (1H, s, aniline-N*H*), *sulfonamide-NH not observed*; δ_C (125 MHz, DMSO-d_6) 27.6 (C_9 and C_{11}), 40.1 (C_{10}, obscured under solvent resonance), 48.2 (C_8 and C_{12}), 51.4 (O*Me*), 111.7 (C_2), 114.9 ($C_{3''}$ and $C_{5''}$), 124.7 ($C_{2''}$ and $C_{6''}$), 125.5 (C_8), 126.1 (C_5), 126.6 ($C_{2'}$ and $C_{6'}$), 128.4 ($C_{3'}$ and $C_{5'}$), 129.9 ($C_{1''}$), 130.2 (C_9), 131.7 (C_{10}), 132.0 ($C_{4'}$), 132.7 (C_6), 134.8 (C_7), 141.0 ($C_{1'}$), 142.0 (C_3), 147.7 ($C_{4''}$), 174.7 (*C*O_2Me), 177.9 (C_1), 182.4 (C_4); *m/z* (ESI$^-$) 544 ([M-H]$^-$, 100%); HRMS (ESI$^-$) $C_{29}H_{26}O_6N_3S^-$ ([M-H]$^-$) requires 544.1548, found 544.1559.

4-(3-Methyl-1-nitrophenyl)pyrrolidine 402



2-Fluoro-5-nitrotoluene **401** (1.00 g, 6.45 mmol), pyrollidine (469 µL, 6.45 mmol), K_2CO_3 (2.67 g, 19.35 mmol) and H_2O (5 mL) were heated to reflux in EtOH (15 mL) at 90 ^oC for 48 h. The solution was cooled to RT; suction filtration subsequently yielded 4-arylpyrrolidine **402** as a yellow-brown precipitate (1.02 g, 77%). mp 88 ^oC; υ_{max} (thin film) 2978 (C-H), 1594, 1570 (N=O), 1503; δ_H (500 MHz, $CDCl_3$) 1.97-2.03 (4H, m, 2 x H_9 and 2 x H_{10}), 2.45 (3H, s, *Me*), 3.47-3.52 (4H, m, 2 x H_8 and 2 x H_{11}), 6.63 (1H, d, *J* 9.1, H_5), 7.95-7.99 (2H, m, H_2 and H_6); δ_C (125 MHz, $CDCl_3$) 22.2 (*Me*), 25.7 (C_9 and C_{10}), 51.2 (C_8 and C_{11}), 113.0 (C_5), 123.4 (C_6), 124.0 (C_3), 128.4 (C_2), 138.2 (C_1), 154.3 (C_4); *m/z* (ESI^+) 207 ($[M+H]^+$, 100%), 229 ($[M+Na]^+$, 60%); HRMS (ESI^+) $C_{11}H_{15}O_2N_2^+$ ($[M+H]^+$) requires 207.1128, found 207.1127.

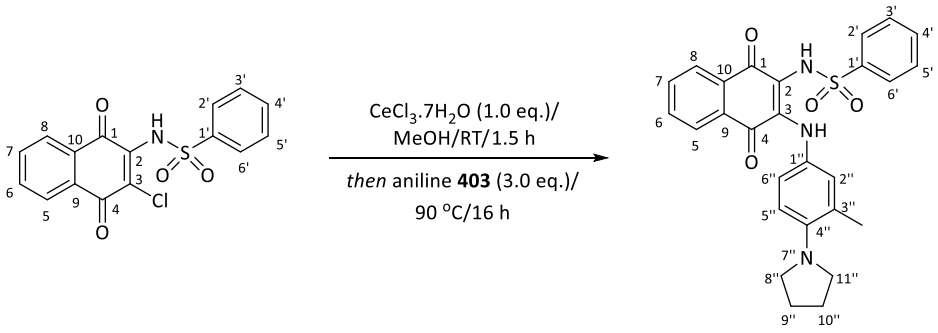
4-(1-Amino-3-methylphenyl)pyrrolidine 403



Following *General Procedure 5*, using 4-arylpyrrolidine **402** (500 mg, 2.427 mmol) and 10% Pd/C (26 mg, 0.243 mmol) in MeOH (7 mL). The crude product was filtered through Celite® and the residue concentrated *in vacuo* to give aniline **403** as a yellow-brown oil (385 mg, 90%). υ_{max} (thin film) 3423 (N-H), 3340 (N-H), 2962 (C-H), 2804 (C-H), 1616, 1500; δ_H (500 MHz, MeOD) 1.86-1.94 (4H, m, 2 x H_9 and 2 x H_{10}), 2.22 (3H, s, *Me*), 2.94-3.02 (4H, m, 2 x H_8 and 2 x H_{11}), 6.53 (1H, dd, *J* 8.5, 1.9, H_6), 6.60 (1H, d, *J* 1.9, H_2), 6.83 (1H, d, *J* 8.5, H_5);

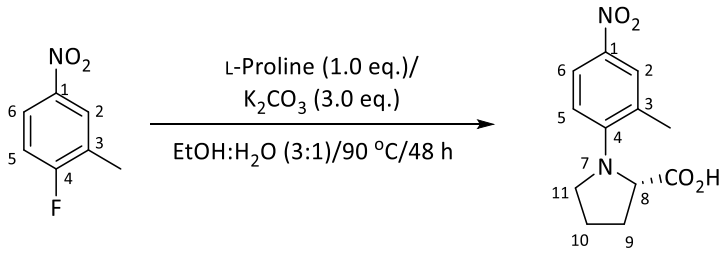
δ_C (125 MHz, MeOD) 19.6 (*Me*), 25.2 (C_9 and C_{10}), 53.1 (C_8 and C_{11}), 115.2 (C_6), 119.2 (C_5), 120.6 (C_2), 133.2 (C_3), 142.8 (C_1 or C_4), 142.9 (C_1 or C_4); *m/z* (ESI^+) 177 ($[M+H]^+$, 100%); HRMS (ESI^+) $C_{11}H_{17}N_2^+$ ($[M+H]^+$) requires 177.1386, found 177.1385.

_N_-(3-((3''-Methyl-4''-(pyrrolidin-7''-yl)phenyl)amino)-1,4-dioxo-1,4-dihydronaphthalen-2-yl)benzenesulfonamide 404



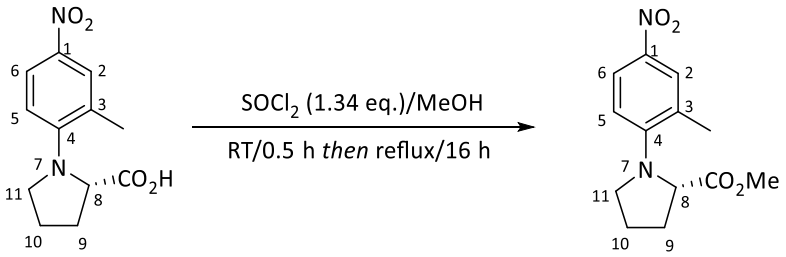
Following *General Procedure 2*, using naphthoquinone **57** (200 mg, 0.576 mmol), 4-(1-amino-3-methylphenyl)pyrrolidine **403** (304 mg, 1.727 mmol) and cerium trichloride heptahydrate (214 mg, 0.576 mmol) in MeOH (7 mL), at 90 °C. Purification *via* column chromatography (eluent pet ether:acetone 95:5 to 90:10) gave 3-anilinonaphthoquinone **404** as a purple solid (105 mg, 37%). mp 188-192 °C; υ_{max} (thin film) 3314 (N-H), 3226 (N-H), 1676 (C=O), 1632 (C=O), 1606, 1576, 1505; δ_H (500 MHz, $CDCl_3$) 1.94-1.98 (4H, m, 2 x $H_{9''}$ and 2 x $H_{10''}$), 2.34 (3H, s, $C_{3''}$-*Me*), 3.23-3.28 (4H, m, 2 x $H_{8''}$ and 2 x $H_{11''}$), 6.73 (1H, br. s, sulfonamide-N*H*), 6.83-6.87 (3H, m, $H_{2''}$, $H_{5''}$ and $H_{6''}$), 7.31-7.36 (2H, m, $H_{3'}$ and $H_{5'}$), 7.46 (1H, app. tt, *J* 7.5, 1.2, $H_{4'}$), 7.61-7.70 (4H, m, H_6, H_7, $H_{2'}$ and $H_{6'}$), 7.87 (1H, dd, *J* 7.5, 1.3, H_8), 8.02 (1H, s, aniline-N*H*), 8.07 (1H, dd, *J* 7.5, 1.3, H_5) δ_C (125 MHz, $CDCl_3$) 20.1 ($C_{3''}$-*Me*), 25.1 ($C_{9''}$ and $C_{10''}$), 51.1 ($C_{8''}$ and $C_{11''}$), 111.7 (C_2), 115.1 ($C_{5''}$), 121.7 ($C_{6''}$), 126.3 (C_8), 126.8 (C_5), 127.1 ($C_{2''}$), 127.4 ($C_{2'}$ and $C_{6'}$), 128.2 ($C_{3''}$), 128.6 ($C_{3'}$ and $C_{5'}$), 130.0 ($C_{1''}$), 130.5 (C_9), 131.7 (C_{10}), 132.7 (C_6), 132.9 ($C_{4'}$), 134.8 (C_7), 138.9 ($C_{1'}$), 139.1 (C_3); *m/z* (ESI^-) 486 ($[M-H]^-$, 100%); HRMS (ESI^-) $C_{27}H_{24}O_4N_3S^-$ ($[M-H]^-$) requires 486.1493, found 486.1503.

4-(3-Methyl-1-nitrophenyl)-L-proline 405



2-Fluoro-5-nitrotoluene **401** (2.00 g, 12.9 mmol), L-proline (1.484 g, 12.90 mmol), K_2CO_3 (5.34 g, 38.7 mmol) and H_2O (5 mL) were heated to reflux in EtOH (15 mL) at 90 °C for 48 h. The solution was cooled to RT, poured onto ice water (50 mL) and 1 M aq. HCl (50 mL) was added. The reaction was extracted with EtOAc (4 x 100 mL) and the organic extracts were combined, dried, filtered and concentrated *in vacuo* to give 4-aryl-L-proline **405** as an orange-brown oil, which was subsequently used without further purification (3.19 g, quant.). υ_{max} (thin film) 2977 (C-H), 1709 (C=O), 1600, 1580 (N=O); $\alpha_D^{[25]}$ +140.0 (*c* 0.1, $CHCl_3$); δ_H (500 MHz, $CDCl_3$) 1.88-2.00 (1H, m, H_{10}), 2.01-2.13 (2H, m, H_9 and H_{10}), 2.34 (3H, s, C_3-*Me*), 2.41-2.50 (1H, m, H_9), 3.37-3.44 (1H, m, H_{11}), 3.71-3.79 (1H, m, H_{11}), 4.57 (1H, app. t, *J* 7.0, H_8), 6.66 (1H, d, *J* 8.5, H_5), 7.83-7.91 (2H, m, H_2 and H_6), 10.01 (1H, br. s, CO_2H); δ_C (125 MHz, $CDCl_3$) 21.4 (C_3-*Me*), 24.2 (C_{10}), 30.8 (C_9), 52.1 (C_{11}), 61.7 (C_8), 114.8 (C_5), 122.7 (C_6), 125.7 (C_3), 127.9 (C_2), 139.4 (C_1), 152.8 (C_4), 178.5 (CO_2H); *m/z* (ESI^+) 251 ($[M+H]^+$, 70%), 273 ($[M+Na]^+$, 100%); HRMS (ESI^+) $C_{12}H_{15}O_4N_2^+$ ($[M+H]^+$) requires 251.1026, found 251.1027.

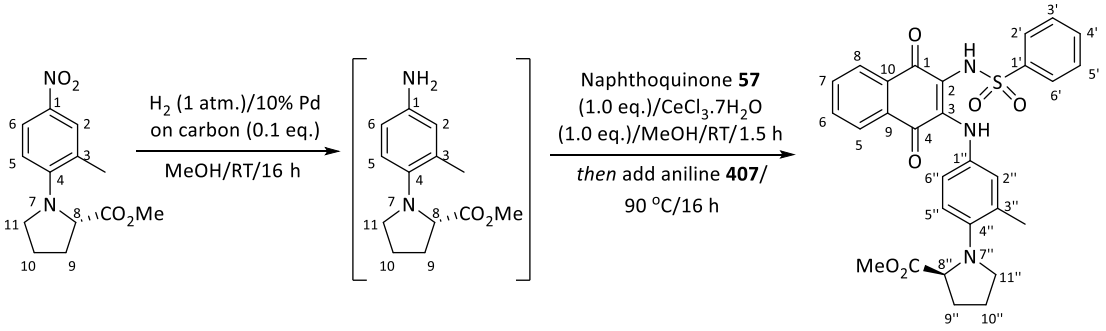
Methyl 4-(3-methyl-1-nitrophenyl)-L-prolinate 406



To an ice-cold solution of 4-(3-methyl-1-nitrophenyl)-L-proline **405** (3.09 g, 12.4 mmol) in MeOH (30 mL) was added thionyl chloride (1.80 mL, 24.7 mmol) dropwise. The solution was

warmed to RT and stirred for 30 min before being heated under reflux for 16 h. The reaction was then cooled to RT and concentrated *in vacuo* to give methyl L-prolinate **406** as an orange-brown oil (3.09 g, 95%). υ_{max} (thin film) 1743 (C=O), 1711, 1600, 1580 (N=O); $\alpha_D^{[25]}$ +122.8 (*c* 0.1, $CHCl_3$); δ_H (500 MHz, MeOD) 1.93-2.11 (3H, m, H_9 and 2 x H_{10}), 2.38 (3H, s, C_3-*Me*), 2.42-2.51 (1H, m, H_9), 3.43-3.50 (1H, m, H_{11}), 3.64 (3H, s, O*Me*), 3.77-3.83 (1H, m, H_{11}), 4.69 (1H, dd, *J* 7.7, 6.3, H_8), 6.76 (1H, d, *J* 9.5, H_5), 7.88-7.93 (2H, m, H_2 and H_6); δ_C (125 MHz, MeOD) 22.0 (C_3-*Me*), 25.5 (C_{10}), 32.1 (C_9), 53.0 (CO_2*Me*), 53.6 (C_{11}), 63.6 (C_8), 116.3 (C_5), 124.0 (C_6), 127.4 (C_3), 129.0 (C_2), 140.6 (C_1), 155.0 (C_4), 175.8 (*C*O_2Me); *m/z* (ESI^+) 265 ($[M+H]^+$, 70%), 287 ($[M+Na]^+$, 100%); HRMS (ESI^+) $C_{13}H_{17}O_4N_2^+$ ($[M+H]^+$) requires 265.1183, found 265.1181.

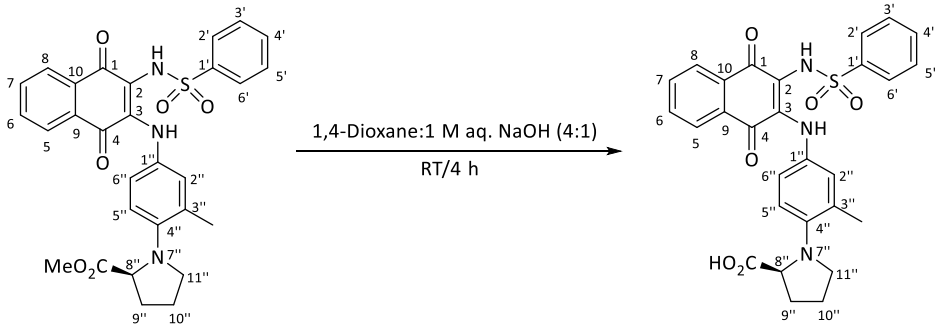
Methyl 4''-(1''-((1,4-dioxo-2-(phenylsulfonamido)-1,4-dihydronaphthalen-3-yl)amino)-3''-methylphenyl)-L-prolinate 408



Following *General Procedure 5*, using methyl L-prolinate **406** (2.50 g, 9.47 mmol) and 10% Pd/C (101 mg, 0.95 mmol) in MeOH (30 mL). The crude product was filtered through Celite® and the residue concentrated *in vacuo* to give aniline **407** as a brown oil (385 mg, 90%), which was used in the next step without further purification. *m/z* (ESI^+) 235 ($[M+H]^+$, 100%). Subsequently, following *General Procedure 2*, using naphthoquinone **57** (600 mg, 1.73 mmol), aniline **407** (1.21 g, 5.18 mmol) and cerium trichloride heptahydrate (643 mg, 1.73 mmol) in MeOH (7 mL), at 90 °C. Purification *via* column chromatography on silica gel (eluent pet ether:acetone 85:15) gave 3-anilinonaphthoquninone **408** as a purple solid (253 mg, 27%). mp 78 °C; υ_{max} (thin film) 3279 (N-H), 2953 (C-H), 1710 (ester C=O), 1674, 1602 (naphthoquinone C=O), 1571 (naphthoquinone C=O), 1504; $\alpha_D^{[25]}$ +300.0 (*c* 0.001, $CHCl_3$);

δ_H (500 MHz, MeOD) 1.93-2.10 (3H, m, $H_{9''}$ and 2 x $H_{10''}$), 2.29 (3H, s, $C_{3''}$-*Me*), 2.35-2.43 (1H, m, $H_{9''}$), 3.07 (1H, td, *J* 8.8, 3.6, $H_{11''}$), 3.59 (3H, s, O*Me*), 3.68-3.74 (1H, m, $H_{11''}$), 4.40 (1H, dd, *J* 8.0, 5.4, $H_{8''}$), 6.78-6.82 (2H, m, $H_{2''}$ and $H_{6''}$), 6.93 (1H, d, *J* 8.2, $H_{5''}$), 7.30-7.35 (2H, m, $H_{3'}$ and $H_{5'}$), 7.44-7.49 (1H, m, $H_{4'}$), 7.57-7.61 (2H, m, $H_{2'}$ and $H_{6'}$), 7.68 (1H, td, *J* 7.4, 1.5, H_6 or H_7), 7.71 (1H, td, *J* 7.4, 1.5, H_6 or H_7), 7.81 (1H, dd, *J* 7.4, 1.5, H_5 or H_8), 8.05 (1H, dd, *J* 7.4, 1.5, H_5 or H_8), *2 x NH not observed*; δ_C (125 MHz, MeOD) 20.2 ($C_{3''}$-*Me*), 23.5 ($C_{10''}$), 31.4 ($C_{9''}$), 52.5 (O*Me*), 53.5 ($C_{11''}$), 64.0 ($C_{8''}$), 112.9 (C_2), 119.0 ($C_{5''}$), 123.3 ($C_{6''}$), 127.1 (C_5 or C_8), 127.7 (C_5 or C_8), 128.2 ($C_{2''}$), 128.4 ($C_{2'}$ and $C_{6'}$), 129.7 ($C_{3'}$ and $C_{5'}$), 131.6 ($C_{3''}$), 132.0 (C_9 or C_{10}), 133.5 ($C_{1''}$), 133.6 ($C_{4'}$), 133.6 (C_9 or C_{10}), 134.0 (C_6 or C_7), 136.0 (C_6 or C_7), 142.0 ($C_{1'}$), 143.0 (C_3), 145.8 ($C_{4''}$), 176.5 (*C*O_2Me), 180.8 (C_1 or C_4), 183.7 (C_1 or C_4); *m/z* (ESI^-) 544 ($[M-H]^-$, 100%); HRMS (ESI^-) $C_{29}H_{26}O_6N_3S^-$ ($[M-H]^-$) requires 544.1548, found 544.1558.

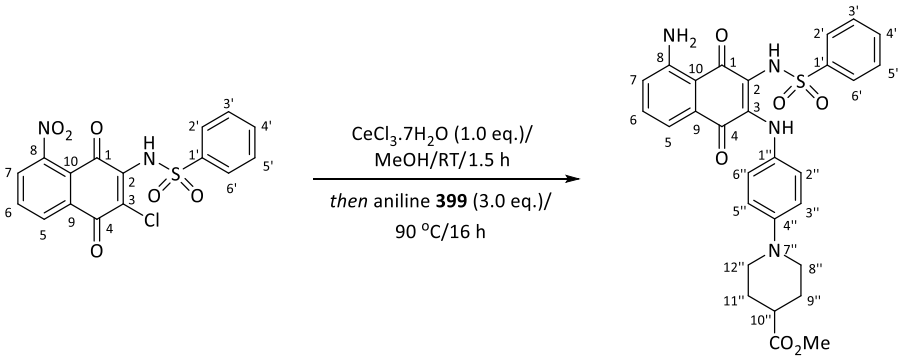
4''-(1''-((1,4-Dioxo-2-(phenylsulfonamido)-1,4-dihydronaphthalen-3-yl)amino)-3''-methylphenyl)-L-proline 409



Methyl ester **408** (110 mg, 0.202 mmol) and 1 M aq. NaOH (2 mL) were stirred in 1,4-dioxane (8 mL) at RT for 4 h. After this time, the *p*H of the solution was adjusted to *c.* 2 with 1 M aq. HCl (10 mL) and the organic product was extracted into EtOAc (3 x 10 mL). The organic layers were combined, washed with brine (3 x 10 mL), dried over Na_2SO_4, filtered and concentrated *in vacuo*. Purification *via* column chromatography (eluent pet ether:acetone 70:30 to 0:100 before the column was flushed with CH_2Cl_2:MeOH 80:20) gave carboxylic acid **409** as a red solid (44 mg, 41%), which was subsequently observed to undergo decomposition after *c.* 1 week of standing at RT. δ_H (400 MHz, MeOD) 1.90-2.09 (3H, m, $H_{9''}$ and 2 x $H_{10''}$), 2.32 (3H,

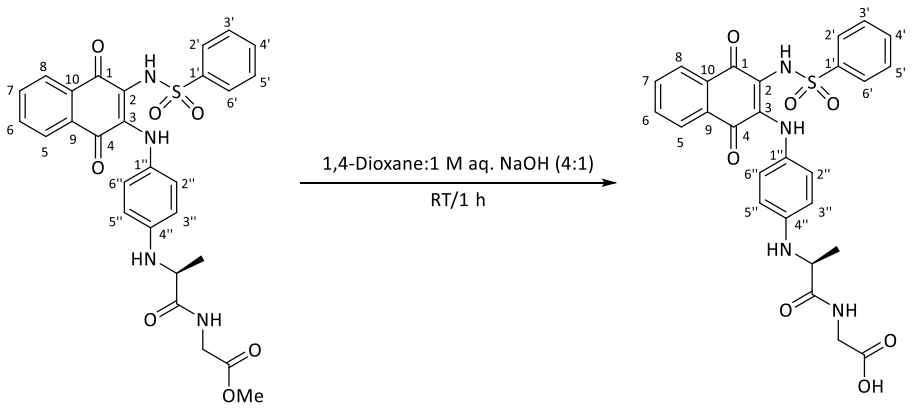
s, $C_{3''}$-*Me*), 2.35-2.42 (1H, m, $H_{9''}$), 3.03-3.10 (1H, m, $H_{11''}$), 3.75-3.83 (1H, m, $H_{11''}$), 4.20 (1H, app. t, *J* 6.9, $H_{8''}$), 6.72-6.77 (2H, m, $H_{2''}$ and $H_{6''}$), 6.89 (1H, d, *J* 8.2, $H_{5''}$), 7.26-7.32 (2H, m, $H_{3'}$ and $H_{5'}$), 7.40-7.46 (1H, m, $H_{4'}$), 7.53-7.57 (2H, m, $H_{2'}$ and $H_{6'}$), 7.60-7.70 (2H, m, H_6 and H_7), 7.76-7.80 (1H, m, H_5 or H_8), 7.97-8.01 (1H, m, H_5 or H_8), *2 x NH and CO_2H not observed*; *m/z* (ESI^-) 530 ($[M-H]^-$, 100%).

Methyl 4''-(1''-((8-amino-1,4-dioxo-2-(phenylsulfonamido)-1,4-dihydronaphthalen-3-yl)amino)phenyl)piperidine-*para*-carboxylate 411



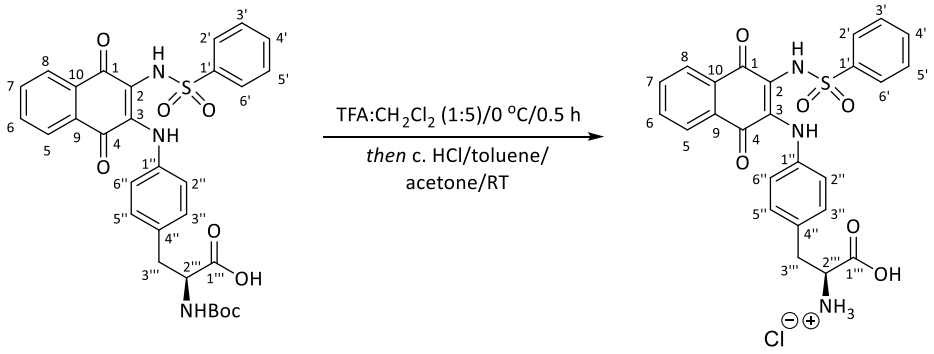
Following *General Procedure 2*, using naphthoquinone **232** (293 mg, 0.746 mmol), aniline **399** (524 mg, 2.24 mmol) and cerium trichloride heptahydrate (278 mg, 0.746 mmol) in MeOH (7 mL), at 90 °C. Purification *via* column chromatography on silica gel (eluent pet ether:acetone 90:10 to 80:20 then pet ether:EtOAc 70:30 to 50:50) gave 8-amino-3-anilinonaphthoquinone **411** as a red solid (16 mg, 4%), which was subsequently observed to undergo decomposition within 48 h of standing at RT. δ_H (400 MHz, MeOD) 1.80-1.92 (2H, m, $H_{9''}$(equ) and $H_{11''}$(equ)), 2.00-2.07 (2H, m, $H_{9''}$(ax) and $H_{11''}$(ax)), 2.53 (1H, app. tt, *J* 11.3, 3.7, $H_{10''}$), 2.82 (2H, app. td, *J* 12.1, 3.9, $H_{8''}$(ax) and $H_{12''}$(ax)), 3.58-3.65 (2H, m, $H_{8''}$(equ) and $H_{12''}$(equ)), 3.71 (3H, s, O*Me*), 6.92-6.96 (4H, m, $H_{2''}$, $H_{3''}$, $H_{5''}$ and $H_{6''}$), 6.98 (1H, dd, *J* 8.4, 1.2, H_5 or H_7), 7.27-7.38 (4H, m, H_6, $H_{3'}$, $H_{5'}$ and H_5 or H_7), 7.45-7.50 (1H, m, $H_{4'}$), 7.59-7.64 (2H, m, $H_{3'}$ and $H_{5'}$), *NH_2 not observed*; *m/z* (ESI^-) 145 (80%), 559 ($[M-H]^-$, 100%).

(*para*-((1,4-Dioxo-2-(phenylsulfonamido)1,4-dihydronaphthalen-3-yl)amino)phenyl)-L-alanylglycine 412



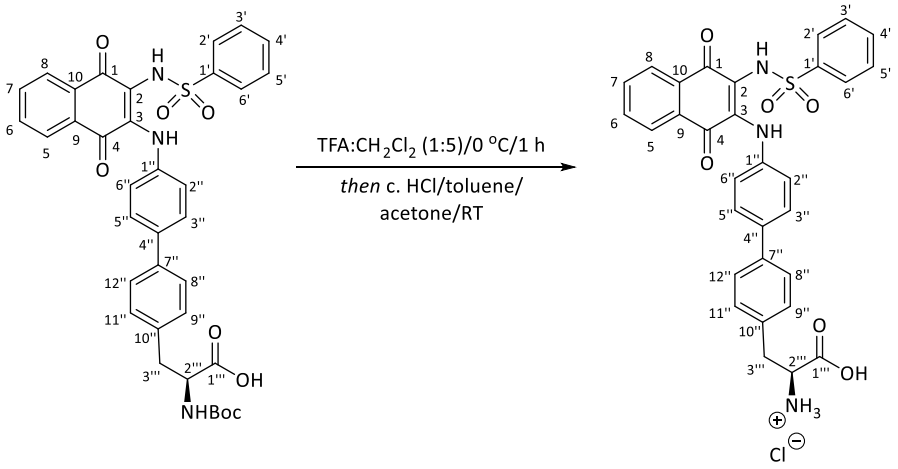
Methyl ester **411** (90 mg, 0.16 mmol) and 1 M aq. NaOH (2 mL) were stirred in 1,4-dioxane (8 mL) at RT for 1 h. After this time, the *p*H of the solution was adjusted to *c.* 2 with 1 M aq. HCl (10 mL) and the organic product was extracted into EtOAc (3 x 10 mL). The organic layers were combined, washed with brine (3 x 10 mL), dried over Na_2SO_4, filtered and concentrated *in vacuo*. Purification *via* column chromatography (eluent CH_2Cl_2:MeOH 98:2 then pet ether:acetone 50:50) gave carboxylic acid **412** as a purple solid (34 mg, 39%). mp 152-155 ^oC; υ_{max} (thin film) 3309 (N-H), 2933 (C-H), 1743 (acid C=O), 1667 (C=O), 1601 (C=O), 1571, 1520; $\alpha_D^{[25]}$ -325.0 (*c* 0.002, $CHCl_3$); δ_H (500 MHz, $CDCl_3$) 1.58 (3H, d, *J* 8.7, CH*Me*), 3.88-3.97 (3H, m, C*H*$_2$ and C*H*Me), 4.02 (1H, d, *J* 3.5, $C_{4''}$-N*H*), 6.64 (2H, d, *J* 8.7, $H_{3''}$ and $H_{5''}$), 6.68 (1H, br. s, sulfonamide-N*H*), 7.00 (2H, d, *J* 8.7, $H_{2''}$ and $H_{6''}$), 7.19-7.23 (1H, m, amide-N*H*), 7.34 (2H, app. t, *J* 8.5, $H_{3'}$ and $H_{5'}$), 7.46 (1H, app. t, *J* 8.5, $H_{4'}$), 7.60-7.71 (4H, m, H_6, H_7, $H_{2'}$ and $H_{6'}$), 7.83 (1H, dd, *J* 7.3, 1.5, H_8), 7.98 (1H, s, aniline-N*H*), 8.07 (1H, dd, *J* 7.3, 1.5, H_5); δ_C (125 MHz, $CDCl_3$) 19.6 (CH*Me*), 21.0 (*C*H$_2$), 55.0 (*C*HMe), 111.4 (C_2), 113.2 ($C_{3''}$ and $C_{5''}$), 125.6 ($C_{2''}$ and $C_{6''}$), 126.2 (C_8), 126.8 (C_5), 127.2 ($C_{2'}$ and $C_{6'}$), 128.7 ($C_{3'}$ and $C_{5'}$), 129.1 ($C_{1''}$), 130.3 (C_9), 131.6 (C_{10}), 132.8 (C_6), 132.9 ($C_{4'}$), 134.9 (C_7), 139.1 ($C_{1'}$), 139.6 (C_3), 144.3 ($C_{4''}$), 169.8 (acid-*C*O), 174.3 (amide-*C*O), 178.7 (C_1), 182.0 (C_4); *required m/z peak was not detectable in either ESI or FI mass spectrometry experiments*.

(*S*)-2'''-Amino-3'''-(4''-((1,4-dioxo-2-(phenylsulfonamido)-1,4-dihydronaphthalen-3-yl)amino)phenyl)propanoic acid 414



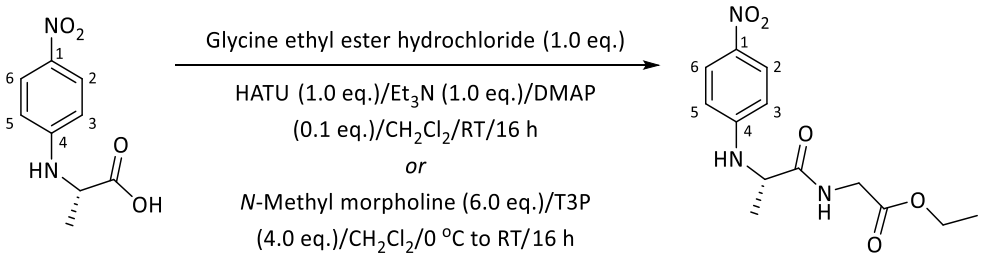
Carboxylic acid **432** (60 mg, 0.102 mmol) was dissolved in CH_2Cl_2 (7.5 mL) at 0 ^{o}C and TFA (1.5 mL) was added dropwise. The solution was stirred at 0 ^{o}C for 30 min, after which time the solvent was removed *in vacuo*. Toluene (10 mL), acetone (10 mL) and c. HCl (0.5 mL) were added and the solvent was removed *in vacuo*. The process of azeotroping was repeated thrice more with toluene (3 x 10 mL) to afford primary amine **414** as an orange solid (53 mg, quant.). mp 189-193 ^{o}C; υ_{max} (thin film) 3430 (N-H), 2924 (C-H), 2853 (C-H), 1707 (acid C=O); $\alpha_D^{[25]}$ -56.0 (*c* 0.01, DMF); δ_H (500 MHz, MeOD) 3.07-3.18 (1H, m, $H_{3'''}$), 3.37-3.47 (1H, m, $H_{3'''}$), 4.13 (1H, br. s, $H_{2'''}$), 7.16 (2H, d, *J* 8.4, $H_{2''}$ and $H_{6''}$), 7.31 (2H, d, *J* 8.4, $H_{3''}$ and $H_{5''}$), 7.38 (2H, app. t, *J* 8.0, $H_{3'}$ and $H_{5'}$), 7.51 (1H, app. t, *J* 8.0, $H_{4'}$), 7.66 (2H, d, *J* 8.0, $H_{2'}$ and $H_{6'}$), 7.70-7.76 (2H, m, H_6 and H_7), 7.78-7.82 (1H, m, H_8), 8.08-8.12 (1H, m, H_5), *5 x NH and CO_2H not observed*; δ_C (125 MHz, MeOD) 37.3 ($C_{3'''}$), 113.6 (C_2), 127.0 ($C_{2''}$ and $C_{6''}$), 127.2 (C_8), 127.7 (C_5), 128.2 ($C_{2'}$ and $C_{6'}$), 129.9 ($C_{3'}$ and $C_{5'}$), 130.0 ($C_{3''}$ and $C_{5''}$), 132.0 (C_9), 133.4 (C_{10}), 133.8 ($C_{4'}$), 134.2 (C_6), 136.1 (C_7), 139.2 (C_3), 142.1 ($C_{1'}$), 143.7 ($C_{1''}$), 167.6 ($C_{1'''}$), 180.8 (C_1), 183.6 (C_4), *$C_{2'''}$ not observed*; *m/z* (ESI^+) 139 (30%), 391 (25%), 413 (35%), 492 ($[M+H]^+$, 100%), 514 ($[M+Na]^+$, 20%); HRMS (ESI^+) $C_{25}H_{21}N_3NaO_6S^+$ ($[M+Na]^+$) requires 514.1043, found 514.1039.

(*S*)-2'''-Carboxy-3'''-(1''-((1,4-dioxo-2-(phenylsulfonamido)-1,4-dihydronaphthalen-3-yl)amino)-[4'',7''-biphenyl]-10''-yl)ethan-2'''-ammonium chloride 415



Methyl ester **455** (28 mg, 0.042 mmol) was dissolved in CH_2Cl_2 (3.75 mL) at 0 °C and TFA (0.75 mL) was added dropwise. The solution was stirred at 0 °C for 1 h, after which time the solvent was removed *in vacuo*. Toluene (5 mL), acetone (5 mL) and c. HCl (0.25 mL) were added and the solvent was removed *in vacuo*. The process of azeotroping was repeated thrice more with toluene (5 mL) to afford carboxylic acid **415** as a purple solid (24 mg, 95%). mp 212-213 °C; υ_{max} (thin film) 3235 (N-H), 2924 (C-H), 2854 (C-H), 1737 (acid C=O), 1603 (naphthoquinone C=O); $\alpha_D^{[25]}$ -132.0 (*c* 0.005, DMF); δ_H (500 MHz, MeOD) 3.14-3.21 (2H, m, C*H*$_2$), 4.18-4.25 (1H, m, C*H*CO$_2$H), 7.11 (2H, d, *J* 8.5, $H_{2''}$ and $H_{6''}$), 7.32-7.40 (4H, m, $H_{3'}$, $H_{5'}$, $H_{9''}$ and $H_{11''}$), 7.46-7.51 (1H, m, $H_{4'}$), 7.54-7.58 (4H, m, $H_{2'}$, $H_{6'}$, $H_{3''}$ and $H_{5''}$), 7.68 (2H, d, *J* 8.2, $H_{8''}$ and $H_{12''}$), 7.75-7.82 (3H, m, H_6, H_7 and H_8), 8.01-8.05 (1H, m, H_5), 8.42 (3H, br. s, N*H*$_3^+$), 9.11 (1H, s, sulfonamide-N*H*), 9.14 (1H, s, aniline-N*H*); δ_C (125 MHz, MeOD) 53.1 (*C*H$_2$), 63.2 (*C*HCO$_2$H), 114.0 (C_2), 123.8 ($C_{2''}$ and $C_{6''}$), 125.4 ($C_{3''}$ and $C_{5''}$), 125.7 (C_8), 126.2 (C_5), 126.3 ($C_{8''}$ and $C_{12''}$), 126.5 ($C_{2'}$ and $C_{6'}$), 128.5 ($C_{3'}$ and $C_{5'}$), 130.1 ($C_{9''}$ and $C_{11''}$), 130.3 (C_9), 131.5 (C_{10}), 132.2 ($C_{4'}$), 133.1 (C_6), 133.6 ($C_{10''}$), 134.4 ($C_{4''}$), 134.9 (C_7), 138.1 ($C_{1''}$), 138.6 ($C_{7''}$), 140.9 ($C_{1'}$), 141.7 (C_3), 170.4 (CH*C*O$_2$H), 178.5 (C_1), 182.3 (C_4); *m/z* (ESI$^-$) 566 ([M-H]$^-$, 100%); HRMS (ESI$^-$) $C_{31}H_{24}N_3O_6S^-$ ([M-H]$^-$) requires 566.1391, found 566.1403.

Ethyl (4-nitrophenyl)-L-alanylgylcinate 418

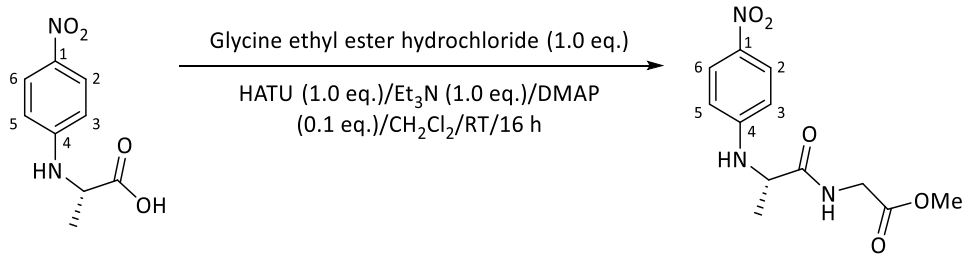


Method A: *para*-Nitrophenyl-L-alanine **382** (210 mg, 1.00 mmol) was dissolved in CH_2Cl_2 (40 mL) at 0 °C. To this solution was added glycine ethyl ester hydrochloride **416** (140 mg, 1.00 mmol), HATU (380 mg, 1.00 mmol), triethylamine (139 µL, 1.00 mmol) and DMAP (12 mg, 0.10 mmol) and the solution was stirred at RT for 16 h. The crude reaction mixture was concentrated *in vacuo*; subsequent purification by column chromatography on silica gel (eluent pet ether:acetone 90:10 to 70:30) gave dipeptide **418** as a yellow solid (174 mg, 59%).

Method B: *para*-Nitrophenyl-L-alanine **382** (210 mg, 1.00 mmol), glycine ethyl ester hydrochloride **416** (140 mg, 1.00 mmol) and *N*-methylmorpholine (660 µL, 6.00 mmol) were dissolved in CH_2Cl_2 (26 mL) and cooled to 0 °C. T3P (50% wt. in EtOAc, 1.19 mL, 4.00 mmol) was added to the solution dropwise and the mixture was stirred for 16 h, over which time the solution was allowed to warm to RT. The crude reaction mixture was concentrated *in vacuo*; subsequent purification by column chromatography on silica gel (eluent pet ether:acetone 90:10 to 70:30) gave dipeptide **418** as a yellow solid (184 mg, 62%).

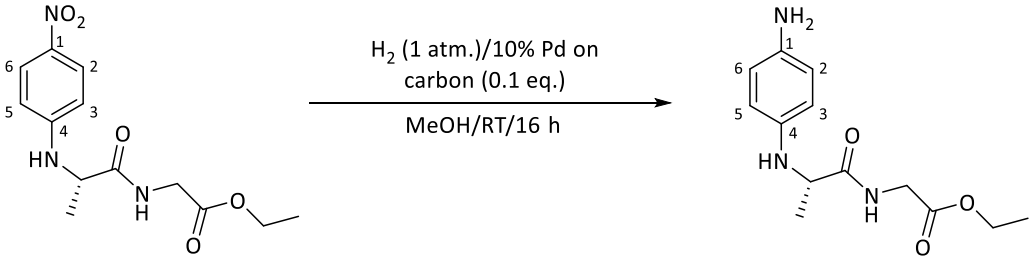
mp 144-146 °C; υ_{max} (thin film) 3353 (N-H), 1749 (C=O), 1709, 1662 (C=O), 1598, 1537, 1504; $[\alpha]_D^{20}$ -17.4 (*c* 0.2, MeOH); δ_H (500 MHz, MeOD) 1.23 (3H, t, *J* 7.1, CH_2*Me*), 1.52 (3H, d, *J* 7.1, CH*Me*), 3.92 (2H, d, *J* 2.8, NHCH_2), 4.40 (1H, q, *J* 7.1, C*H*Me), 4.15 (2H, q, *J* 7.1, OCH_2), 6.63-6.68 (2H, m, H_3 and H_5), 8.02-8.07 (2H, m, H_2 and H_6); δ_C (125 MHz, MeOD) 14.6 (CH_2*Me*), 19.2 (CH*Me*), 42.1 (NH*C*H_2), 54.6 (*C*HMe), 62.4 (O*C*H_2), 113.0 (C_3 and C_5), 127.1 (C_2 and C_6), 139.5 (C_1), 154.8 (C_4), 171.2 (ester-*C*O), 177.0 (amide-*C*O); *m/z* (ESI$^+$) 296 ([M+H]$^+$, 30%), 318 ([M+Na]$^+$, 50%), 613 ([2M+Na]$^+$, 100%); HRMS (ESI$^+$) $C_{13}H_{17}N_3NaO_5^+$ ([M+Na]$^+$) requires 318.1060, found 318.1059.

Methyl (4-nitrophenyl)-L-alanylgylcinate 419



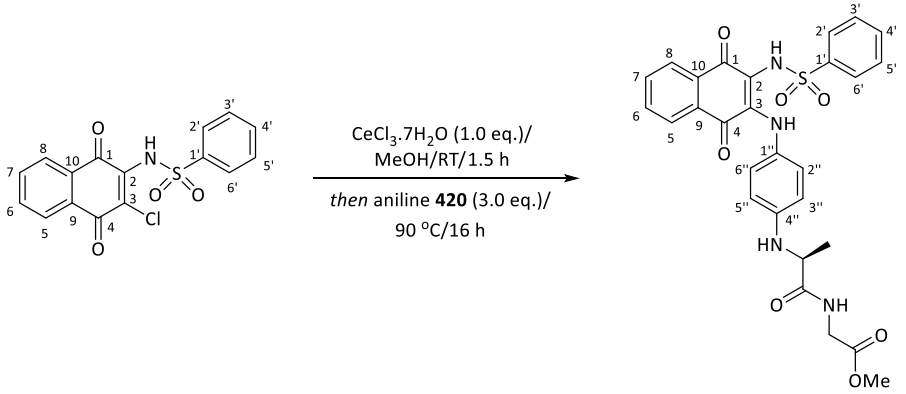
para-Nitrophenyl-L-alanine **382** (210 mg, 1.00 mmol) was dissolved in CH_2Cl_2 (40 mL) at 0 ^oC. To this solution was added glycine methyl ester hydrochloride **417** (126 mg, 1.00 mmol), HATU (380 mg, 1.00 mmol), triethylamine (139 µL, 1.00 mmol) and DMAP (12 mg, 0.10 mmol) and the solution was stirred at RT for 16 h. The crude reaction mixture was concentrated *in vacuo*; subsequent purification by column chromatography on silica gel (eluent pet ether:acetone 90:10 to 70:30) gave dipeptide **419** as a yellow solid (200 mg, 75%). mp 136-138 ^oC; υ_{max} (thin film) 3409 (N-H), 3367 (N-H), 3267 (N-H), 3086 (C-H), 1751 (C=O), 1656 (C=O), 1601, 1582, 1507; $\alpha_D^{[25]}$ -53.6 (*c* 0.1, MeOH); δ_H (500 MHz, $CDCl_3$) 1.59 (3H, d, *J* 7.0, CH*Me*), 3.74 (3H, s, O*Me*), 3.97-4.15 (3H, m, C*H*Me and NHCH_2), 4.91 (1H, d, *J* 4.9, N*H*CH$_2$), 6.58-6.64 (2H, m, H_3 and H_5), 6.73-6.81 (1H, m, aniline-N*H*), 8.07-8.13 (2H, m, H_2 and H_6); δ_C (125 MHz, $CDCl_3$) 19.6 (CH*Me*), 41.4 (NH*C*H$_2$), 52.8 (O*Me*), 54.2 (*C*HMe), 112.6 (C_3 and C_5), 126.6 (C_2 and C_6), 140.0 (C_1), 151.9 (C_4), 170.2 (ester-*C*O), 173.1 (amide-*C*O); *m/z* (ESI$^+$) 282 ([M+H]$^+$, 25%), 304 ([M+Na]$^+$, 60%), 585 ([2M+Na]$^+$, 100%); HRMS (ESI$^+$) $C_{12}H_{15}N_3NaO_5^+$ ([M+Na]$^+$) requires 304.0904, found 304.0902.

Ethyl (4-aminophenyl)-L-alanylgylcinate 420



Following *General Procedure 5*, using ethyl glycinate **418** (1.00 g, 3.39 mmol) and 10% Pd/C (36 mg, 0.339 mmol) in MeOH (15 mL), gave ethyl glycinate **420** as a brown oil (895 mg, quant.). υ_{max} (thin film) 3351 (N-H), 1708 (ester C=O), 1659 (amide C=O); $\alpha_D^{[25]}$ -15.0 (*c* 0.01, $CHCl_3$); δ_H (500 MHz, $CDCl_3$) 1.23 (3H, t, *J* 7.2, CH_2*Me*), 1.43 (3H, d, *J* 6.9, CH*Me*), 3.69 (1H, q, *J* 6.9, C*H*Me), 3.90 (2H, d, *J* 4.6, NHCH_2), 4.14 (2H, q, *J* 7.2, CH_2Me), 6.49-6.53 (2H, m, H_2 and H_6), 6.62-6.67 (2H, m, H_3 and H_5); δ_C (125 MHz, $CDCl_3$) 14.6 (CH_2*Me*), 19.6 (CH*Me*), 42.1 (NH*C*H_2), 56.8 (*C*HMe), 62.4 (O*C*H_2), 116.3 (C_2 and C_6), 118.6 (C_3 and C_5), 139.8 (C_4), 142.1 (C_1), 171.2 (ester-*C*O), 178.9 (amide-*C*O); *m/z* (ESI^+) 266 ($[M+H]^+$, 100%), 553 ($[2M+Na]^+$, 15%); HRMS (ESI^+) $C_{13}H_{20}N_3O_3^+$ ($[M+H]^+$) requires 266.1499, found 266.1499.

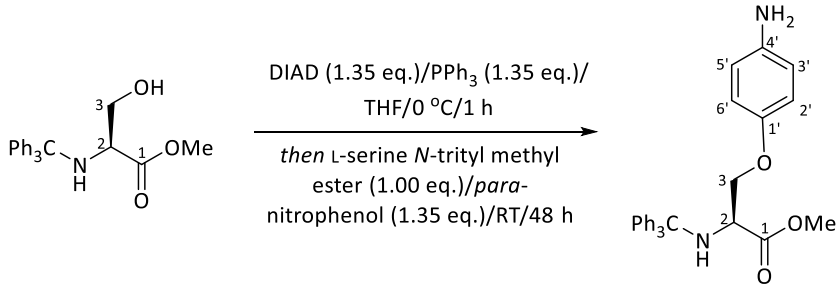
Methyl (*para*-((1,4-dioxo-2-(phenylsulfonamido)1,4-dihydronaphthalen-3-yl)amino)phenyl)-L-alanylglycinate 421



Following *General Procedure 2*, using naphthoquinone **57** (750 mg, 2.16 mmol), aniline **420** (1.82 g, 6.48 mmol) and cerium trichloride heptahydrate (804 mg, 2.16 mmol) in MeOH (15 mL), at 90 °C. Purification *via* column chromatography on silica gel (eluent pet ether:acetone 90:10 to 60:40) gave 3-anilinonaphthoquinone **421** as a purple solid (152 mg, 13%). mp 143-145 °C; υ_{max} (thin film) 3300 (N-H), 1749, 1708, 1700 (ester C=O), 1605 (C=O), 1570, 1519 (C=O); $\alpha_D^{[25]}$ -250.0 (*c* 0.001, $CHCl_3$); δ_H (500 MHz, DMSO-d_6) 1.35 (3H, d, *J* 6.9, CH*Me*), 3.61 (3H, s, O*Me*), 3.78-3.88 (3H, m, CH_2 and C*H*Me), 5.84 (1H, d, *J* 6.8, $C_{4''}$-N*H*), 6.47 (2H, d, *J* 8.8, $H_{3''}$ and $H_{5''}$), 6.82 (2H, d, *J* 8.8, $H_{3''}$ and $H_{5''}$), 7.36 (2H, app. t, *J* 8.0, $H_{3'}$ and $H_{5'}$), 7.45-7.50 (1H, m, $H_{4'}$), 7.52-7.56 (2H, m, $H_{2'}$ and $H_{6'}$), 7.70-7.79 (3H, m, H_6, H_7 and H_8), 7.96-

8.00 (1H, m, H_5), 8.34 (1H, t, *J* 6.8, amide-N*H*), 8.80 (1H, s, sulfonamide-N*H*), 8.84 (1H, s, aniline-N*H*); δ_C (125 MHz, DMSO-d_6) 19.0 (CH*Me*), 40.5 (*C*H_2), 51.7 (O*Me*), 53.0 (*C*HMe), 111.0 (C_2), 111.8 ($C_{3''}$ and $C_{5''}$), 124.8 ($C_{2''}$ and $C_{6''}$), 125.5 (C_8), 126.1 (C_5), 126.6 ($C_{2'}$ and $C_{6'}$), 128.1 ($C_{1''}$), 128.4 ($C_{3'}$ and $C_{5'}$), 130.2 (C_9), 131.9 ($C_{4'}$), 132.0 (C_{10}), 132.6 (C_6), 134.9 (C_7), 141.0 ($C_{1'}$), 142.0 (C_3), 144.7 ($C_{4''}$), 170.3 (ester-*C*O), 174.5 (amide-*C*O), 177.7 (C_1), 182.5 (C_4); *m/z* (ESI^+) 563 ($[M+H]^+$, 90%), 585 ($[M+Na]^+$, 100%); HRMS (ESI^+) $C_{28}H_{27}N_4O_7S^+$ ($[M+H]^+$) requires 563.1595, found 563.1595.

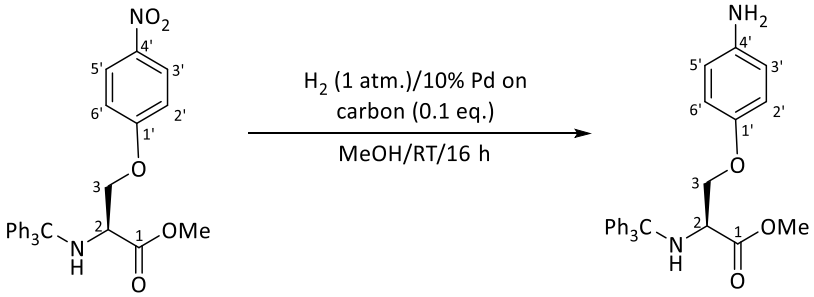
Methyl *O*-(4-nitrophenyl)-*N*-trityl-L-serinate 423



Diisopropyl azodicarboxylate (1.48 mL, 7.51 mmol) was added dropwise to a solution of triphenylphosphine (1.97 g, 7.51 mmol) in THF (60 mL) under argon at 0 °C, and stirred for 1 h. After this time, L-serine-*N*-trityl methyl ester **422** (2.00 g, 5.54 mmol) and *para*-nitrophenol (1.04 g, 7.51 mmol) were added and the mixture was stirred for a further 48 h. The reaction mixture was partitioned between EtOAc (150 mL) and sat. aq. $NaHCO_3$ (100 mL); the organic layer was collected, washed with brine (3 x 50 mL), dried, filtered and concentrated *in vacuo*. Purification *via* column chromatography (eluent pet ether:acetone 95:5 to 85:15) afforded methyl serinate **423** as a yellow oil (2.36 g, 88%). υ_{max} (thin film) 2360, 2342, 1738 (C=O), 1593, 1515; $\alpha_D^{[25]}$ +77.3 (*c* 0.1, $CHCl_3$); δ_H (500 MHz, $CDCl_3$) 2.93 (1H, d, *J* 10.2, N*H*), 3.26 (3H, s, O*Me*), 3.73-3.80 (1H, m, H_2), 4.08 (1H, dd, *J* 9.3, 5.7, H_3), 4.30 (1H, dd, *J* 9.3, 5.7, H_3), 6.89-6.94 (2H, m, $H_{2'}$ and $H_{6'}$), 7.20 (3H, app. t, *J* 7.4, 3 x *para*-Ph), 7.24-7.30 (6H, m, 6 x *meta*-Ph), 7.52 (6H, d, *J* 7.9, 6 x *ortho*-Ph), 8.16-8.21 (2H, m, $H_{3'}$ and $H_{5'}$); δ_C (125 MHz, $CDCl_3$) 52.0 (O*Me*), 55.8 (C_2), 70.8 (C_3), 70.9 (*C*Ph_3), 114.6 ($C_{2'}$ and $C_{6'}$), 125.8 ($C_{3'}$ and $C_{5'}$), 126.6 (3 x *para*-Ph), 128.0 (6 x *meta*-Ph), 128.6 (6 x *ortho*-Ph), 141.7 ($C_{4'}$), 145.5 (3 x *ipso*-Ph), 163.3 ($C_{1'}$), 172.9 (C_1); *m/z*

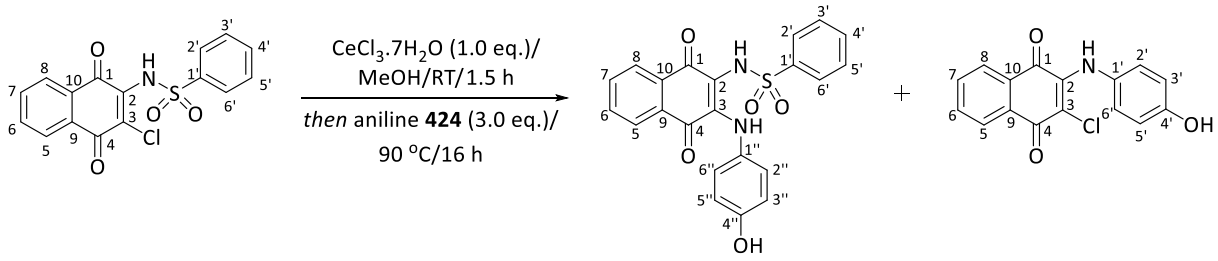
(ESI^+) 243 (100%), 505 ($[M+Na]^+$, 40%); HRMS (ESI^+) $C_{29}H_{26}N_2NaO_5^+$ ($[M+Na]^+$) requires 505.1734, found 505.1734.

Methyl *O*-(4-aminophenyl)-*N*-trityl-L-serinate 424



Following *General Procedure 5*, using methyl serinate **423** (900 mg, 1.87 mmol) and 10% Pd/C (20 mg, 0.187 mmol) in MeOH to give aniline **424** as a yellow oil (840 mg, quant.), which was subsequently used without further purification. υ_{max} (thin film) 3349 (N-H), 1741, 1707 (C=O), 1656, 1514; $\alpha_D^{[25]}$ +265.8 (*c* 0.2, $CHCl_3$); δ_H (500 MHz, $CDCl_3$) 2.88 (1H, d, *J* 10.4, N*H*Trt), 3.22 (3H, s, O*Me*), 3.66-3.73 (1H, m, H_2), 3.94 (1H, dd, *J* 9.0, 6.6, H_3), 4.19 (1H, dd, *J* 9.0, 5.0, H_3), 6.58-6.62 (2H, m, $H_{3'}$ and $H_{5'}$), 6.69-6.73 (2H, m, $H_{2'}$ and $H_{6'}$), 7.15-7.20 (3H, m, 3 x *para*-Ph), 7.23-7.28 (6H, m, 6 x *meta*-Ph), 7.50-7.57 (6H, m, 6 x *ortho*-Ph); δ_C (125 MHz, $CDCl_3$) 51.7 (O*Me*), 56.2 (C_2), 71.2 (C_3), 115.8 ($C_{2'}$ and $C_{6'}$), 116.2 ($C_{3'}$ and $C_{5'}$), 126.4 (3 x *para*-Ph), 127.8 (6 x *meta*-Ph), 128.7 (6 x *ortho*-Ph), 140.4 ($C_{4'}$), 145.7 (3 x *ipso*-Ph), 151.6 ($C_{1'}$), 173.6 (C_1); *m/z* (FI^+) 532 ($[M]^+$, 100%); HRMS (FI^+) $C_{29}H_{28}N_2O_3^+$ ($[M]^+$) requires 452.2100, found 452.2108.

_N_-(3-((4''-Hydroxyphenyl)amino)-1,4-dioxo-1,4-dihydronaphthalen-2-yl) benzenesulfonamide 426 and 2-((4'-Hydroxyphenyl)amino)-3-chloro-1,4-naphthalene-1,4-dione 427



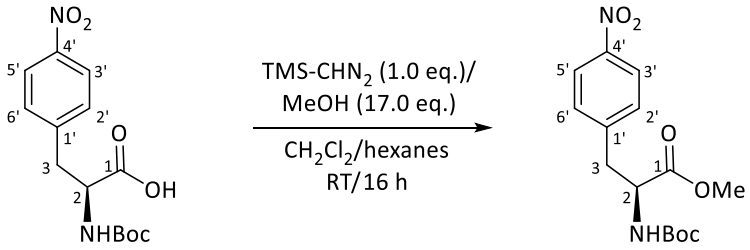
Following *General Procedure 2*, using naphthoquinone **57** (269 mg, 0.774 mmol), aniline **424** (700 mg, 1.55 mmol) and cerium trichloride heptahydrate (289 mg, 0.774 mmol) in MeOH (8 mL), at 90 °C. Purification *via* column chromatography (eluent pet ether:acetone 90:10 to 70:30) gave:

3-anilinonaphthoquinone **426** as a red solid (200 mg, 64%). mp 217-223 °C; υ_{max} (thin film) 3315 (N-H), 1699, 1664, 1605 (C=O), 1572 (C=O), 1516; δ_H (500 MHz, $CDCl_3$) 6.81-6.86 (2H, m, $H_{3''}$ and $H_{5''}$), 6.98-7.03 (2H, m, $H_{2''}$ and $H_{6''}$), 7.32-7.37 (2H, m, $H_{3'}$ and $H_{5'}$), 7.44-7.49 (1H, m, $H_{4'}$), 7.62-7.71 (4H, m, H_6, H_7, $H_{2'}$ and $H_{6'}$), 7.82-7.86 (1H, m, H_8), 7.97 (1H, s, aniline-N*H*), 8.07-8.11 (1H, m, H_5); δ_C (125 MHz, $CDCl_3$) 111.5 (C_2), 115.1 ($C_{3''}$ and $C_{5''}$), 125.6 ($C_{2''}$ and $C_{6''}$), 126.3 (C_8), 126.9 (C_5), 127.3 ($C_{2'}$ and $C_{6'}$), 128.7 ($C_{3'}$ and $C_{5'}$), 130.2 ($C_{1''}$), 130.3 (C_9), 131.5 (C_{10}), 132.9 (C_6), 133.0 ($C_{4'}$), 134.9 (C_7), 138.8 ($C_{1'}$), 139.5 (C_3), 153.7 ($C_{4''}$), 178.9 (C_1), 182.0 (C_4); *m/z* (ESI^+) 107 (100%), 158 (50%), 191 (50%), 421 ($[M+H]^+$, 20%), 443 ($[M+Na]^+$, 50%); HRMS (ESI^+) $C_{22}H_{16}N_2NaO_5S^+$ ($[M+Na]^+$) requires 443.0672, found 443.0673.

2-anilinonaphthoquinone **427** as a red solid (34 mg, 15%). mp 234 °C; υ_{max} (thin film) 3297 (N-H), 1672, 1595 (C=O), 1565 (C=O), 1514; δ_H (500 MHz, DMSO-d_6) 6.70 (2H, d, *J* 8.8, $H_{2'}$ and $H_{6'}$), 6.97 (2H, d, *J* 8.8, $H_{3'}$ and $H_{5'}$), 7.78 (1H, app. td, *J* 7.6, 1.3, H_6 or H_7), 7.85 (1H, app. td, *J* 7.6, 1.3, H_6 or H_7), 7.99-8.04 (2H, m, H_5 and H_8), 9.15 (1H, br. s, O*H*), 9.41 (1H, s, N*H*); δ_C (125 MHz, DMSO-d_6) 111.5 (C_3), 114.5 ($C_{2'}$ and $C_{6'}$), 126.0 (C_5 or C_8), 126.3 ($C_{3'}$ and $C_{5'}$), 126.4

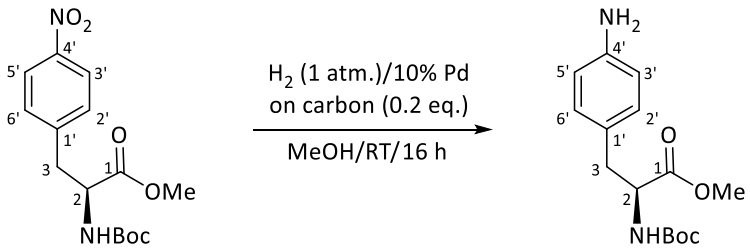
(C_5 or C_8), 130.0 ($C_{4'}$), 130.1 (C_9 or C_{10}), 132.2 (C_9 or C_{10}), 132.9 (C_6 or C_7), 134.8 (C_6 or C_7), 143.4 (C_2), 155.0 ($C_{1'}$), 176.4 (C_1 or C_4), 180.2 (C_1 or C_4); *m/z* (ESI^-) 298 ([M(^{35}Cl)-H]$^-$, 100%), 300 [M(^{37}Cl)-H]$^-$, 33%); HRMS (ESI^-) $C_{16}H_9ClNO_3^-$ ([M(^{35}Cl)-H]$^-$) requires 298.0276, found 298.0283.

Methyl (*S*)-2-((*tert*-butoxycarbonyl)amino)-3-(4'-nitrophenyl)propanoate 429[383]



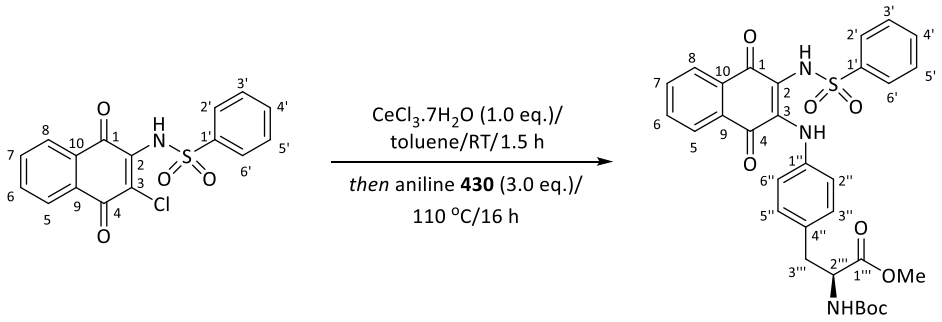
CH_2Cl_2 (26 mL) and MeOH (4.43 mL, 110 mmol) were added to *N*-Boc-4-nitro-L-phenylalanine **428** (2.00 g, 6.45 mmol) under nitrogen. This mixture was stirred until **428** had dissolved completely. 2 M Trimethylsilyldiazomethane in hexanes solution (4.83 mL, 9.67 mmol) was then carefully added to the solution, which was stirred at RT for 16 h. After this time, the reaction was quenched by adding 20% AcOH (50 mL), and then partitioned between CH_2Cl_2 (100 mL) and H_2O (50 mL). The organic layer was collected, washed with brine (2 x 50 mL), dried, filtered and concentrated *in vacuo* to give methyl ester **429** as an off-white solid (2.08 g, quant.). mp 96 ^oC (lit. 99-101 ^oC);[383] $\alpha_D^{[25]}$ +57.6 (*c* 1.0, $CHCl_3$) (lit. +53.0 (*c* 1.0, $CHCl_3$, 22 ^oC));[383] δ_H (400 MHz, $CDCl_3$) 1.42 (9H, s, C*Me*$_3$), 3.13 (1H, dd, *J* 13.7, 6.2, H_3), 3.28 (1H, dd, *J* 13.7, 6.2, H_3), 3.75 (3H, s, O*Me*), 4.61-4.69 (1H, m, H_2), 5.07 (1H, d, *J* 7.9, N*H*), 7.32 (2H, d, *J* 8.5, $H_{2'}$ and $H_{6'}$), 8.17 (2H, d, *J* 8.5, $H_{3'}$ and $H_{5'}$); *m/z* (ESI^+) 347 ([M+Na]$^+$, 100%).

Methyl (*S*) -3-(4'-aminophenyl)-2-((*tert*-butoxycarbonyl)amino)propanoate 430[383]



Following *General Procedure 5*, using methyl ester **429** (1.00 g, 3.09 mmol) and 10% Pd/C (66 mg, 0.618 mmol) in MeOH (20 mL). The crude product was filtered through Celite® and the residue concentrated *in vacuo* to give aniline **430** as a yellow oil (902 mg, quant.). α_D[25] +52.4 (*c* 1.0, $CHCl_3$) (lit. +42.0 (*c* 1.0, $CHCl_3$, 22 °C));[383] δ_H (400 MHz, $CDCl_3$) 1.42 (9H, s, C*Me*$_3$), 2.85 (2H, br. s, N*H*$_2$), 2.95-2.99 (2H, m, 2 x H_3), 3.71 (3H, s, O*Me*), 4.51 (1H, dd, *J* 7.9, 6.0, H_2), 4.97 (1H, d, *J* 7.9, N*H*), 6.59-6.65 (2H, m, $H_{3'}$ and $H_{5'}$), 6.90 (2H, d, *J* 8.2, $H_{2'}$ and $H_{6'}$); *m/z* (ESI$^+$) 317 ([M+Na]$^+$, 100%), 611 ([2M+Na]$^+$, 100%).

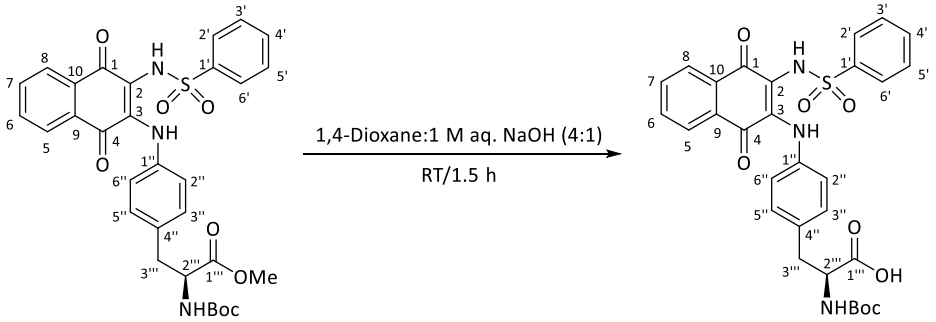
Methyl (*S*)-2'''-((*tert*-butoxycarbonyl)amino)-3'''-(4''-((1,4-dioxo-2-(phenylsulfonamido)-1,4-dihydronaphthalen-3-yl)amino)phenyl)propanoate 431



Following *General Procedure 2*, using naphthoquinone **57** (300 mg, 0.863 mmol), aniline **430** (761 mg, 2.590 mmol) and cerium trichloride heptahydrate (322 mg, 0.863 mmol) in toluene (8 mL), at 110 °C. Purification *via* column chromatography on silica gel (eluent pet ether:EtOAc 70:30 then pet ether:acetone 80:20) gave 3-anilinonaphthoquinone **431** as a red solid (128 mg, 25%). mp 91-94 °C; υ_{max} (thin film) 3292 (N-H), 2976 (C-H), 2929 (C-H), 1704 (C=O), 1603 (C=O), 1574, 1520; α_D[25] +181.5 (*c* 0.02, $CHCl_3$); δ_H (500 MHz, $CDCl_3$) 1.45 (9H, s, C*Me*$_3$), 3.13 (2H, d, *J* 5.7, 2 x $H_{3'''}$), 3.74 (3H, s, O*Me*), 4.57-4.65 (1H, m, $H_{2'''}$), 5.08-5.14 (1H, m, N*H*Boc), 6.76 (1H, br. s, sulfonamide-N*H*), 7.03 (2H, d, *J* 8.2, $H_{2''}$ and $H_{6''}$), 7.14 (2H, d, *J* 8.2, $H_{3''}$ and $H_{5''}$), 7.32-7.37 (2H, m, $H_{3'}$ and $H_{5'}$), 7.44-7.49 (1H, m, $H_{4'}$), 7.63-7.71 (4H, m, H_6, H_7, $H_{2'}$ and $H_{6'}$), 7.83-7.87 (1H, m, H_8), 8.03 (1H, s, aniline-N*H*), 8.07-8.11 (1H, m, H_5); δ_C (125 MHz, $CDCl_3$) 28.3 (C*Me*$_3$), 37.9 ($C_{3'''}$), 52.3 (O*Me*), 54.5 ($C_{2'''}$), 79.9 (*C*Me$_3$), 113.1 (C_2), 123.8 ($C_{2''}$ and $C_{6''}$), 126.4 (C_8), 126.9 (C_5), 127.2 ($C_{3'}$ and $C_{5'}$), 128.8 ($C_{2'}$ and $C_{6'}$), 129.1 ($C_{3''}$ and $C_{5''}$), 130.4 (C_9),

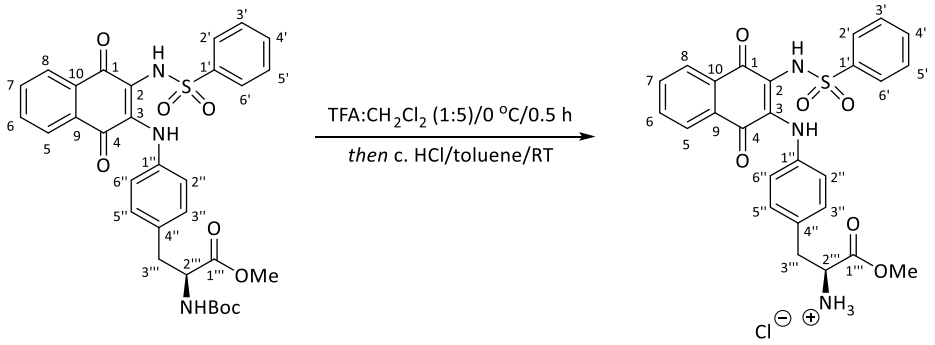
131.3 (C_{10}), 133.1 (C_6), 133.1 ($C_{4'}$), 133.1 ($C_{4''}$), 134.9 (C_7), 136.3 ($C_{1''}$), 138.8 (C_3), 138.8 ($C_{1'}$), 155.1 ($CO_2{}^t$Bu), 172.3 (CO_2Me), 179.0 (C_1), 181.8 (C_4); *m/z* (ESI^-) 604 ($[M-H]^-$, 100%); HRMS (ESI^+) $C_{31}H_{31}N_3NaO_8S^+$ ($[M+Na]^+$) requires 628.1724, found 628.1718.

(*S*)-2'''-((*tert*-Butoxycarbonyl)amino)-3'''-(4''-((1,4-dioxo-2-(phenylsulfonamido)-1,4-dihydronaphthalen-3-yl)amino)phenyl)propanoic acid 432



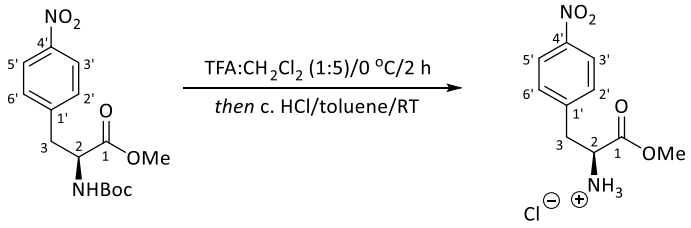
Methyl ester **431** (80 mg, 0.132 mmol) and 1 M aq. NaOH (2 mL) were stirred in 1,4-dioxane (8 mL) at RT for 1.5 h. After this time, the *p*H of the solution was adjusted to *c.* 2 with 1 M aq. HCl (10 mL) and the organic product was extracted into EtOAc (3 x 10 mL). The organic layers were combined, washed with brine (3 x 10 mL), dried over Na_2SO_4, filtered and concentrated *in vacuo* to give carboxylic acid **432** as a purple solid (75 mg, 96%). mp 123-126 ^oC; υ_{max} (thin film) 3285 (N-H), 2928 (C-H), 1708 (acid C=O), 1673, 1603 (naphthoquinone C=O), 1576 (naphthoquinone C=O), 1520; $\alpha_D^{[25]}$ -200.0 (*c* 0.002, DMF); δ_H (500 MHz, MeOD) 1.41 (9H, s, CMe_3), 2.96 (1H, dd, *J* 14.4, 8.6, $H_{3'''}$), 3.15 (1H, dd, *J* 14.4, 4.5, $H_{3'''}$), 4.33-4.40 (1H, m, $H_{2'''}$), 6.97 (2H, d, *J* 7.9, $H_{2''}$ and $H_{6''}$), 7.17 (2H, d, *J* 7.9, $H_{3''}$ and $H_{5''}$), 7.30-7.38 (2H, m, $H_{3'}$ and $H_{5'}$), 7.47 (1H, app. t, *J* 6.7, $H_{4'}$), 7.60 (2H, d, *J* 7.6, $H_{2'}$ and $H_{6'}$), 6.67-6.76 (2H, m, H_6 and H_7), 7.84 (1H, d, *J* 7.2, H_8), 8.08 (1H, d, *J* 6.8, H_5), *3 x NH not observed*; δ_C (125 MHz, MeOD) 28.9 (CMe_3), 38.3 ($C_{3'''}$), 56.5 ($C_{2'''}$), 80.7 (CMe$_3$), 114.0 (C_2), 125.2 ($C_{2''}$ and $C_{6''}$), 127.2 (C_8), 127.7 (C_5), 128.4 ($C_{2'}$ and $C_{6'}$), 129.8 ($C_{3'}$ and $C_{5'}$), 129.9 ($C_{3''}$ and $C_{5''}$), 132.1 (C_9), 133.5 (C_{10}), 133.7 ($C_{4'}$), 134.1 (C_6), 135.1 ($C_{4''}$), 136.0 (C_7), 138.2 ($C_{1''}$), 142.0 ($C_{1'}$), 143.2 (C_3), 158.1 ($CO_2{}^t$Bu), 175.7 (CO_2H), 181.0 (C_1), 183.6 (C_4); *m/z* (ESI^-) 590 ($[M-H]^-$, 100%); HRMS (ESI^-) $C_{30}H_{28}N_3O_8S^-$ ($[M-H]^-$) requires 590.1603, found 590.1612.

(*S*)-3'''-(4''-((1,4-Dioxo-2-(phenylsulfonamido)-1,4-dihydronaphthalen-3-yl)amino)phenyl)-1'''-methoxy-1'''-oxopropan-2'''-ammonium chloride 433



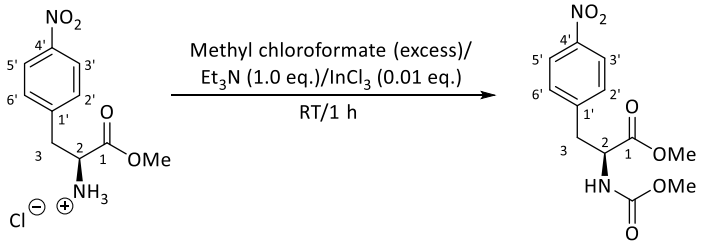
Naphthoquinone **431** (22 mg, 0.036 mmol) was stirred in CH_2Cl_2 (10 mL) at 0 °C. To this solution was added TFA (2 mL) dropwise, and the reaction mixture was stirred at 0 °C for 30 min. After this time, the crude reaction mixture was concentrated *in vacuo*. Toluene (10 mL) and c. HCl (0.5 mL) were added and the solution was concentrated *in vacuo* once more. A further portion of toluene (10 mL) was then added and the solution was concentrated *in vacuo* to give ammonium chloride **433** as an orange solid (19 mg, quant.). mp 179-186 °C; υ_{max} (thin film) 2924 (C-H), 1711 (ester C=O), 1660, 1603 (naphthoquinone C=O), 1572 (naphthoquinone C=O), 1518; $\alpha_D^{[25]}$ -226.6 (*c* 0.005, DMF); δ_H (500 MHz, MeOD) 3.16 (1H, dd, *J* 14.7, 5.8, $H_{3'''}$), 3.36 (1H, dd, *J* 14.7, 5.8, $H_{3'''}$), 3.87 (3H, s, O*Me*), 4.37 (1H, dd, *J* 8.2, 5.3, $H_{2'''}$), 7.15-7.19 (2H, m, $H_{2''}$ and $H_{6''}$), 7.24-7.28 (2H, m, $H_{3''}$ and $H_{5''}$), 7.35-7.40 (2H, m, $H_{3'}$ and $H_{5'}$), 7.48-7.52 (1H, m, $H_{4'}$), 7.64-7.68 (2H, m, $H_{2'}$ and $H_{6'}$), 7.69-7.75 (2H, m, H_6 and H_7), 7.76-7.81 (1H, m, H_8), 8.07-8.12 (1H, m, H_5); δ_C (125 MHz, MeOD) 37.1 ($C_{3'''}$), 54.0 (O*Me*), 55.4 ($C_{2'''}$), 113.8 (C_2), 126.7 ($C_{2''}$ and $C_{6''}$), 127.2 (C_8), 127.8 (C_5), 128.3 ($C_{2'}$ and $C_{6'}$), 129.9 ($C_{3'}$ and $C_{5'}$), 129.9 ($C_{3''}$ and $C_{5''}$), 131.5 ($C_{4''}$), 132.0 (C_9), 133.3 (C_{10}), 133.9 ($C_{4'}$), 134.3 (C_6), 136.1 (C_7), 139.5 ($C_{1''}$), 141.8 ($C_{1'}$), 143.1 (C_3), 170.6 (*C*O_2Me), 180.7 (C_1), 183.5 (C_4); *m/z* (ESI^+) 339 (100%), 506 ($[M+H]^+$, 30%), 528 ($[M+Na]^+$, 10%); HRMS (ESI^+) $C_{26}H_{23}N_3O_6S^+$ ($[M+H]^+$) requires 506.1380, found 506.1382.

(*S*)-1-Methoxy-3-(4'-nitrophenyl)-1-oxopropan-2-ammonium chloride 444[384]



Methyl ester **429** (1.80 mg, 5.56 mmol) was dissolved in TFA (75 mL) and CH_2Cl_2 (75 mL) at 0 °C. The solution was stirred at 0 °C for 2 h, after which time the solvent was removed *in vacuo*. Toluene (20 mL) and c. HCl (1 mL) were added and the solvent was removed *in vacuo*. The process of azeotroping was repeated thrice more with toluene (3 x 20 mL) to afford ammonium chloride **444** as a white solid (1.37 g, 95%). mp 222-223 °C (lit. 221-224 °C);[384] $\alpha_D^{[25]}$ -4.2 (*c* 0.1, EtOH) (lit. +34.2 (*c* 1.0, EtOH, 24 °C) – *NB: **444** appeared to be insoluble in EtOH at this concentration at 24 °C*);[384] δ_H (500 MHz, MeOD) 3.20-3.50 (2H, m, 2 x H_3, obscured by solvent resonance), 3.73 (3H, m, O*Me*), 4.37 (1H, br. s, H_2), 7.44-7.53 (2H, m, $H_{2'}$ and $H_{6'}$), 8.11-8.19 (2H, m, $H_{3'}$ and $H_{5'}$); *m/z* (ESI^+) 225 ($[M+H]^+$, 100%).

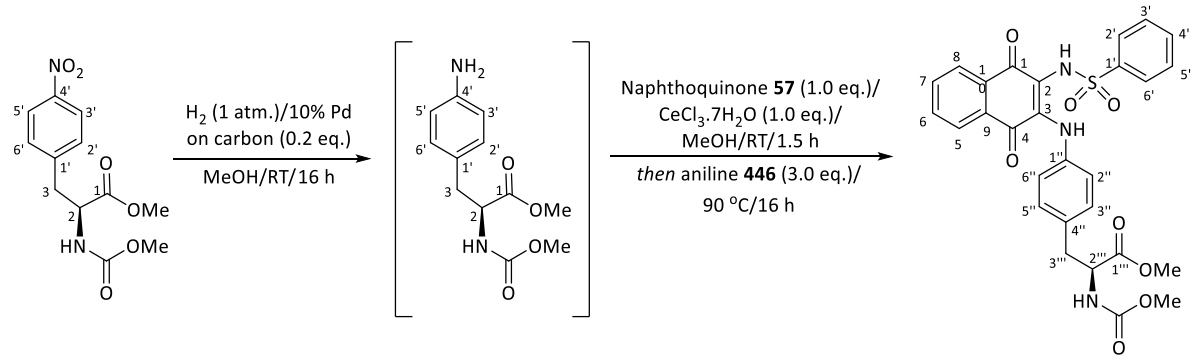
Methyl (*S*)-2-((methoxycarbonyl)amino)-3-(4'-nitrophenyl)propanoate 445



To a suspension of ammonium chloride **444** (1.04 g, 3.99 mmol) and indium trichloride (9 mg, 0.04 mmol) in methyl chloroformate (5 mL), triethylamine (555 µL, 3.99 mmol) was added dropwise at RT. The solution was stirred for a further 1 h at RT before being partitioned between EtOAc (50 mL) and H_2O (50 mL). The organic layer was collected, washed with brine (3 x 20 mL), dried, filtered and concentrated *in vacuo* to give methyl carbamate **445** as a white solid (728 mg, 48%). mp 67 °C; υ_{max} (thin film) 3330 (N-H), 2955 (C-H), 1718 (C=O), 1604, 1517 (N=O); $\alpha_D^{[25]}$ +70.7 (*c* 0.3, $CHCl_3$); δ_H (400 MHz, $CDCl_3$) 3.16 (1H, dd, *J* 13.7, 6.2, H_3), 3.28 (1H,

dd, *J* 13.7, 5.6, H_3), 3.68 (3H, s, O*Me*), 3.75 (3H, s, O*Me*), 4.66-4.74 (1H, m, H_2), 5.20-5.27 (1H, m, N*H*), 7.32 (2H, d, *J* 8.6, $H_{2'}$ and $H_{6'}$), 8.17 (2H, d, *J* 8.6, $H_{3'}$ and $H_{5'}$); δ_C (100 MHz, $CDCl_3$) 38.2 (C_3), 52.2 (O*Me*), 52.6 (O*Me*), 54.4 (C_2), 123.7 (C_2 and C_6), 130.2 (C_3 and C_5), 143.7 (C_4), 147.2 (C_1), 151.2 ($CO_2{}^t$Bu), 171.4 (C_1); *m/z* (ESI^+) 305 ($[M+Na]^+$, 100%); HRMS (ESI^+) $C_{12}H_{14}N_2NaO_6^+$ ($[M+Na]^+$) requires 305.0744, found 305.0744.

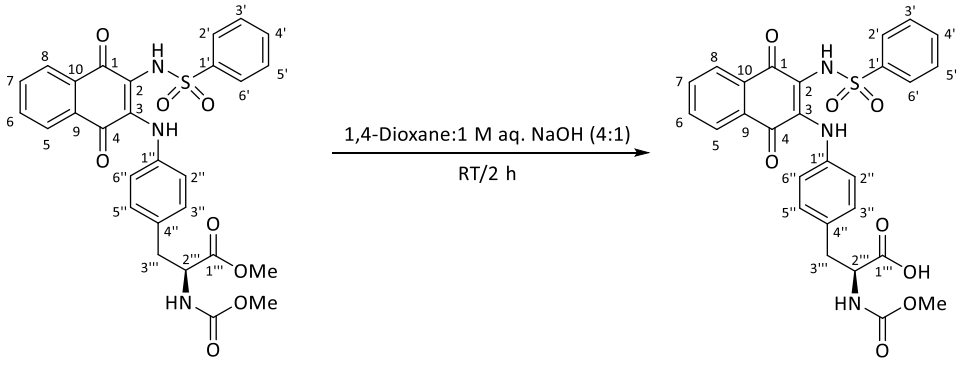
Methyl (*S*)-3'''-(*para*-((1,4-dioxo-2-(phenylsulfonamido)-1,4-dihydronaphthalen-3-yl)amino)phenyl)-2'''-((methoxycarbonyl)amino)propanoate 447



Following *General Procedure 5*, using nitro-substituted **445** (700 mg, 2.48 mmol) and 10% Pd/C (26 mg, 0.248 mmol) in MeOH (20 mL) gave aniline **446** (585 mg, 94%), which was used in the next step without further purification. δ_H (400 MHz, $CDCl_3$) 2.96-3.06 (2H, m, 2 x H_3), 3.65 (3H, s, O*Me*), 3.72 (3H, s, O*Me*), 7.51-7.64 (1H, m, H_2), 5.19 (1H, d, *J* 8.1, N*H*), 6.79 (2H, d, *J* 8.1, $H_{3'}$ and $H_{5'}$), 6.95 (2H, d, *J* 8.1, $H_{2'}$ and $H_{6'}$); *m/z* (FI^+) 252 ($[M]^+$, 100%); HRMS (FI^+) $C_{12}H_{16}N_2O_4^+$ ($[M]^+$) requires 252.1110, found 252.1111. Subsequently, following *General Procedure 2*, using naphthoquinone **57** (200 mg, 0.576 mmol), aniline **446** (290 mg, 1.15 mmol) and cerium trichloride heptahydrate (214 mg, 0.576 mmol) in MeOH (7 mL), at 90 °C. Purification *via* column chromatography on silica gel (eluent pet ether:acetone 85:15 to 65:35) gave 3-anilinonaphthoquinone **447** as a purple solid (141 mg, 44%). mp 190-194 °C; υ_{max} (thin film) 3319 (N-H), 3230 (N-H), 1710 (acid and carbamate C=O), 1603 (naphthoquinone C=O), 1576 (naphthoquinone C=O), 1518; $\alpha_D^{[25]}$ +175.0 (*c* 0.02, $CHCl_3$); δ_H (500 MHz, DMSO-d_6) 2.84 (1H, dd, *J* 14.0, 9.8, $H_{3'''}$), 2.99 (1H, dd, *J* 14.0, 5.7, $H_{3'''}$), 3.50 (3H, s, carbamate-O*Me*), 3.64 (3H, s, ester-O*Me*), 4.20-4.26 (1H, m, $H_{2'''}$), 6.91 (2H, d, *J* 8.3, $H_{2''}$ and $H_{6''}$), 7.09 (2H, d, *J* 8.3, $H_{3''}$ and

$H_{5''}$), 7.33-7.37 (2H, m, $H_{3'}$ and $H_{5'}$), 7.46-7.50 (1H, m, $H_{4'}$), 7.51-7.55 (2H, m, $H_{2'}$ and $H_{6'}$), 7.68-7.72 (1H, m, carbamate-N*H*), 7.73-7.81 (3H, m, H_6, H_7 and H_8), 8.00 (1H, d, *J* 7.6, H_5), 8.93 (1H, br. s, sulfonamide-N*H*), 8.99 (1H, s, aniline-N*H*); δ_C (125 MHz, DMSO-d_6) 36.1 ($C_{3'''}$), 51.5 (carbamate-O*Me*), 51.9 (ester-O*Me*), 55.6 ($C_{2'''}$), 113.5 (C_2), 123.2 ($C_{2''}$ and $C_{6''}$), 125.6 (C_8), 126.2 (C_5), 126.5 ($C_{2'}$ and $C_{6'}$), 128.1 ($C_{3''}$ and $C_{5''}$), 128.5 ($C_{3'}$ and $C_{5'}$), 130.3 (C_9), 131.5 (C_{10}), 132.1 ($C_{4'}$), 132.5 ($C_{4''}$), 133.0 (C_6), 134.9 (C_7), 137.0 ($C_{1''}$), 140.9 ($C_{1'}$), 142.0 (C_3), 156.5 ($CO_2{}^tBu$), 172.6 ($C_{1'''}$), 178.5 (C_1), 182.3 (C_4); *m/z* (ESI^+) 562 ($[M-H]^-$, 100%); HRMS (ESI^-) $C_{28}H_{24}N_3O_8S^-$ ($[M-H]^-$) requires 562.1290, found 562.1290.

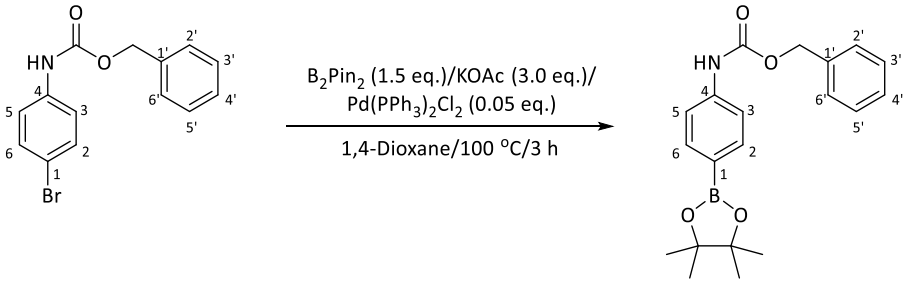
(*S*)-3'''-(*para*-((1,4-Dioxo-2-(phenylsulfonamido)-1,4-dihydronaphthalen-3-yl)amino)phenyl)-2'''-((methoxycarbonyl)amino)propanoic acid 448



Methyl ester **447** (75 mg, 0.132 mmol) and 1 M aq. NaOH (2 mL) were stirred in 1,4-dioxane (8 mL) at RT for 1.5 h. After this time, the *p*H of the solution was adjusted to *c.* 2 with 1 M aq. HCl (10 mL) and the organic product was extracted into EtOAc (3 x 10 mL). The organic layers were combined, washed with brine (3 x 10 mL), dried over Na_2SO_4, filtered and concentrated *in vacuo* to give carboxylic acid **448** as a purple solid (70 mg, 96%). mp 228-230 ^oC; υ_{max} (thin film) 3329 (N-H), 2923 (C-H), 1706 (acid and carbamate C=O), 1603 (naphthoquinone C=O), 1573 (naphthoquinone C=O), 1520; $\alpha_D{}^{[25]}$ -236.0 (*c* 0.01, EtOH); δ_H (500 MHz, MeOD) 2.98 (1H, dd, *J* 13.7, 9.4, $H_{3'''}$), 3.21 (1H, dd, *J* 13.7, 5.1, $H_{3'''}$), 3.62 (3H, s, O*Me*), 4.44 (1H, dd, *J* 9.4, 5.1, $H_{2'''}$), 6.99 (2H, d, *J* 8.2, $H_{2''}$ and $H_{6''}$), 7.18 (2H, d, *J* 8.2, $H_{3''}$ and $H_{5''}$), 7.33-7.38 (2H, m, $H_{3'}$ and $H_{5'}$), 7.46-7.51 (1H, m, $H_{4'}$), 7.59-7.63 (2H, m, $H_{2'}$ and $H_{6'}$), 7.69-7.76 (2H, m, H_6 and H_7), 7.82-7.85 (1H, m, H_8), 8.08-8.11 (1H, m, H_5), *OH and 3 x NH not observed*; δ_C (125 MHz, MeOD) 38.2

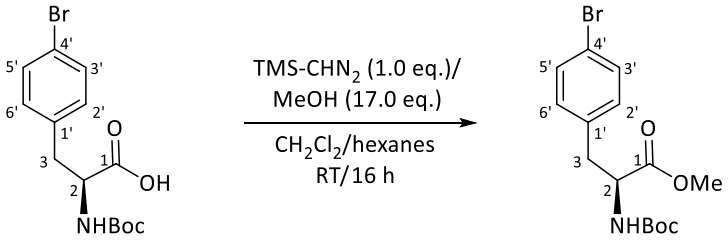
($C_{3'''}$), 52.8 (O*Me*), 56.8 ($C_{2'''}$), 113.9 (C_2), 125.3 ($C_{2''}$ and $C_{6''}$), 127.2 (C_8), 127.7 (C_5), 128.4 ($C_{2'}$ and $C_{6'}$), 129.8 ($C_{3'}$ and $C_{5'}$), 129.9 ($C_{3''}$ and $C_{5''}$), 132.1 (C_9), 133.5 (C_{10}), 133.7 ($C_{4'}$), 134.1 (C_6), 135.0 ($C_{4''}$), 136.0 (C_7), 138.2 ($C_{1''}$), 142.1 ($C_{1'}$), 143.3 (C_3), 159.3 (*C*O_2Me), 175.4 ($C_{1'''}$), 181.0 (C_1), 183.6 (C_4); *m/z* (ESI^+) 391 (30%), 413 (50%), 550 ($[M+H]^+$, 40%), 572 ($[M+Na]^+$, 100%); HRMS (ESI^+) $C_{27}H_{23}N_3NaO_8S^+$ ($[M+Na]^+$) requires 572.1098, found 572.1100.

4-(Benzyl carbamate)phenylboron pinacol ester 449



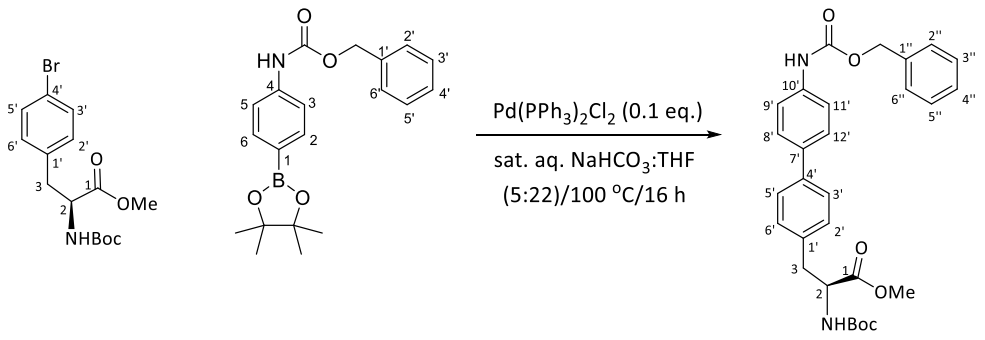
To a solution of benzyl carbamate **372** (2.00 g, 6.534 mmol) in 1,4-dioxane (12 mL) in a microwave vial under N_2 was added $Pd(PPh_3)_2Cl_2$ (0.228 g, 0.327 mmol), *bis*(pinacolato)diboron (2.49 g, 9.804 mmol) and potassium acetate (1.922 g, 19.608 mmol). The vial was sealed and the reaction mixture was heated to 100 °C for 3 h. After cooling, distilled water (50 mL) was added and the organic product was extracted with EtOAc (2 x 50 mL). The combined organic layers were washed with brine (3 x 20 mL), dried, filtered and concentrated *in vacuo* to give the crude product. Purification *via* column chromatography (eluent pet ether:EtOAc 98:2 to 90:10) gave pinacol ester **449** as a white solid (1.323 g, 57%). mp 115-116 °C; υ_{max} (thin film) 3315 (N-H), 2977 (C-H), 1708 (C=O), 1608, 1590, 1531, 1510; δ_H (500 MHz, $CDCl_3$) 1.34 (12H, s, 4 x *Me*), 5.21 (2H, s, CH_2Ph), 6.78 (1H, br. s, N*H*), 7.33-7.43 (7H, m, H_3, H_5, $H_{2'}$, $H_{3'}$, $H_{4'}$, $H_{5'}$ and $H_{6'}$), 7.74-7.78 (2H, m, H_2 and H_6); δ_C (125 MHz, $CDCl_3$) 24.8 (4 x *Me*), 67.1 (*C*H_2Ph), 83.7 (2 x *C*Me_2), 117.4 (C_3 and C_5), 123.6 (br., C_1), 128.3 ($C_{2'}$ and $C_{6'}$, $C_{3'}$ and $C_{5'}$ or $C_{4'}$), 128.4 ($C_{2'}$ and $C_{6'}$, $C_{3'}$ and $C_{5'}$ or $C_{4'}$), 128.6 ($C_{2'}$ and $C_{6'}$, $C_{3'}$ and $C_{5'}$ or $C_{4'}$), 135.9 (C_2 and C_6), 140.4 (C_4), 153.0 (*C*=O); *m/z* (ESI^+) 354 ($[M+H]^+$, 40%), 729 ($[2M+Na]^+$, 100%); HRMS (ESI^+) $C_{20}H_{24}BNNaO_4^+$ ($[M+H]^+$) requires 376.1691, found 376.1676.

Methyl (*S*)-3-(4'-bromophenyl)-2-((*tert*-butoxycarbonyl)amino)propanoate 451[385]



CH_2Cl_2 (5 mL) and MeOH (760 µL, 18.78 mmol) were added to *N*-Boc-4-bromo-L-phenylalanine **450** (380 mg, 1.105 mmol) under argon at RT; this solution was then stirred until all of the solid had dissolved. 2 M Trimethylsilyldiazomethane in hexanes solution (828 µL, 1.66 mmol) was then carefully added to the solution, which was stirred at RT for 16 h. After this time, the reaction was quenched by adding 30% AcOH (5 mL), and then partitioned between EtOAc (50 mL) and H_2O (50 mL). The organic layer was collected, washed with brine (3 x 20 mL), dried, filtered and concentrated *in vacuo* to give methyl ester **451** as a white solid (385 mg, 97%). mp 61-63 ^oC; α_D[25] +44.1 (*c* 1.0, $CHCl_3$) (lit. +29.6 (*c* 1.35, $CHCl_3$, 21 ^oC));[385] δ_H (500 MHz, $CDCl_3$) 1.42 (9H, s, C*Me*$_3$), 3.01 (1H, dd, *J* 13.8, 6.0, H_3), 3.08 (1H, dd, *J* 13.8, 6.0), 3.72 (3H, s, O*Me*), 4.53-4.61 (1H, m, H_2), 4.99 (1H, d, *J* 7.8, N*H*), 7.01 (2H, d, *J* 8.2, $H_{3'}$ and $H_{5'}$), 7.41 (2H, d, *J* 8.2, $H_{2'}$ and $H_{6'}$); *m/z* (ESI$^+$) 380 ([M(^{79}Br)+Na]$^+$, 100%), 382 ([M(^{81}Br)+Na]$^+$, 100%).

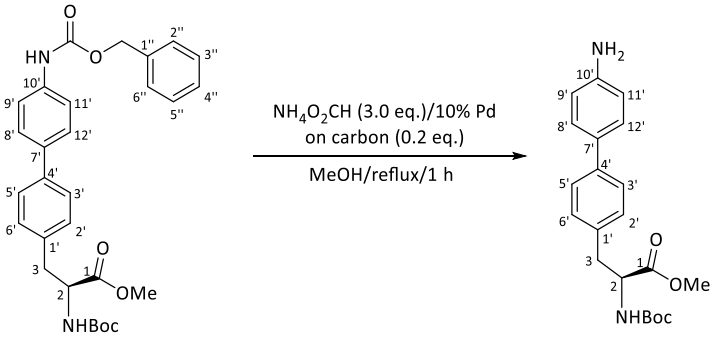
Methyl (*S*)-3-(10'-(((Benzyloxy)carbonyl)amino)-[4',7'-biphenyl]-1'-yl)-2-((*tert*-butoxycarbonyl)amino)propanoate 452



Following *General Procedure 6*, using arylbromide **451** (1.20 g, 3.35 mmol), boronic ester **449** (2.37 g, 6.70 mmol), $Pd(PPh_3)_2Cl_2$ (0.234 g, 0.335 mmol) and sat. aq. $NaHCO_3$ (2.5 mL) in THF

(11 mL). Purification *via* column chromatography on silica gel (eluent pet ether:acetone 95:5 to 80:20) gave biaryl **452** as a white solid (676 mg, 40%). mp 159 ^{o}C; υ_{max} (thin film) 3318 (N-H), 2928 (C-H), 1702 (br., C=O), 1596, 1569, 1535, 1517; $\alpha_D^{[25]}$ +49.5 (*c* 0.25, $CHCl_3$); δ_H (500 MHz, $CDCl_3$) 1.43 (9H, s, C*Me*$_3$), 3.05-3.20 (2H, m, 2 x H_3), 3.74 (3H, s, O*Me*), 4.58-4.67 (1H, m, H_2), 5.02 (1H, d, *J* 7.9, N*H*Boc), 5.23 (2H, s, OC*H*$_2$), 6.77 (1H, br. s, N*H*Cbz), 7.18 (2H, d, *J* 7.7, $H_{2'}$ and $H_{6'}$), 7.32-7.60 (11H, m, $H_{3'}$, $H_{5'}$, $H_{8'}$, $H_{9'}$, $H_{11'}$, $H_{12'}$, $H_{2''}$, $H_{3''}$, $H_{4''}$, $H_{5''}$ and $H_{6''}$); δ_C (125 MHz, $CDCl_3$) 27.3 (C*Me*$_3$), 36.9 (C_3), 51.3 (O*Me*), 53.4 (C_2), 66.1 (O*C*H$_2$), 79.0 (*C*Me$_3$), 117.9 ($C_{9'}$ and $C_{11'}$), 125.9 ($C_{3'}$ and $C_{5'}$), 126.5 ($C_{8'}$ and $C_{12'}$), 127.3 ($C_{3''}$ and $C_{5''}$), 127.4 ($C_{4''}$), 127.6 ($C_{2''}$ and $C_{6''}$), 128.7 ($C_{2'}$ and $C_{6'}$), 133.8 ($C_{1'}$), 135.0 ($C_{7'}$), 135.0 ($C_{1''}$), 136.0 ($C_{10'}$), 138.2 ($C_{4'}$), 152.3 (*C*O$_2$Bn), 154.1 (*C*O$_2$^{t}Bu), 171.3 (*C*O$_2$Me); *m/z* (ESI$^+$) 271 (15%), 405 (20%), 527 ([M+Na]$^+$, 100%); HRMS (ESI$^+$) $C_{29}H_{32}N_2NaO_6^+$ ([M+Na]$^+$) requires 527.2153, found 527.2151.

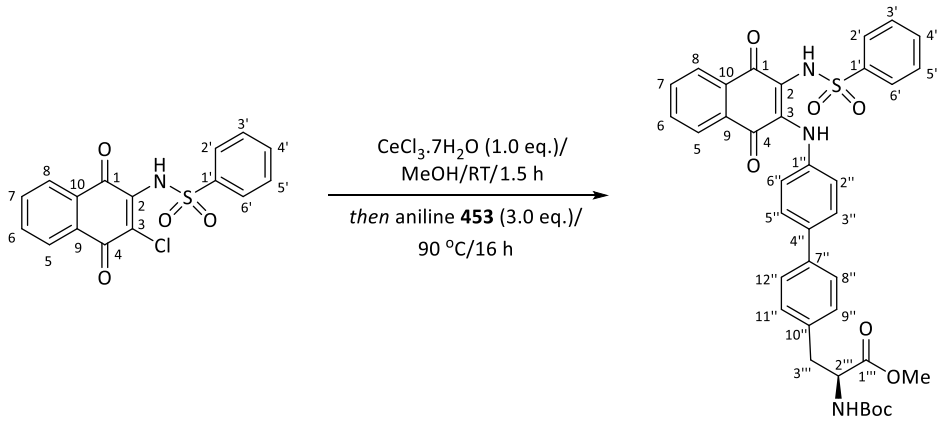
Methyl (*S*)-3-(10'-amino-[4',7'-biphenyl]-1'-yl)-2-((*tert*-butoxycarbonyl)amino)propanoate 453



Benzyl carbamate **452** (650 mg, 1.29 mmol), ammonium formate (244 mg, 3.87 mmol) and 10% Pd/C (28 mg, 0.26 mmol) were stirred in MeOH (65 mL) under an argon atmosphere and heated to reflux for 1 h. After TLC analysis showed complete consumption of starting material, the crude reaction mixture was filtered through Celite® and concentrated *in vacuo*. Purification *via* column chromatography (eluent pet ether:acetone 70:30) gave aniline **453** as a beige solid (326 mg, 68%). mp 95-98 ^{o}C; υ_{max} (thin film) 3368 (N-H), 2976 (C-H), 1742 (C=O), 1705 (C=O), 1610; $\alpha_D^{[25]}$ +155.8 (*c* 0.1, $CHCl_3$); δ_H (500 MHz, $CDCl_3$) 1.43 (9H, s, C*Me*$_3$), 3.07 (1H, dd, *J* 13.4, 7.7, H_3), 3.14 (1H, dd, *J* 13.4, 7.7, H_3), 3.73 (3H, O*Me*), 4.58-4.65 (1H, m, H_2), 5.07 (1H, d, *J* 8.0, N*H*), 6.73-6.76 (2H, m, $H_{9'}$ and $H_{11'}$), 7.15 (2H, d, *J* 7.9, $H_{2'}$ and $H_{6'}$), 7.39 (2H, d,

J 8.4, $H_{8'}$ and $H_{12'}$), 7.44-7.48 (2H, m, $H_{3'}$ and $H_{5'}$), *NH_2 not observed*; δ_C (125 MHz, $CDCl_3$) 28.2 (C*Me*$_3$), 37.8 (C_3), 52.1 (O*Me*), 54.3 (C_2), 79.8 (*C*Me$_3$), 115.3 ($C_{9'}$ and $C_{11'}$), 126.3 ($C_{3'}$ and $C_{5'}$), 127.7 ($C_{8'}$ and $C_{12'}$), 129.5 ($C_{2'}$ and $C_{6'}$), 130.8 ($C_{7'}$), 133.8 ($C_{1'}$), 139.8 ($C_{4'}$), 145.8 ($C_{10'}$), 155.1 (*C*$O_2{}^t$Bu), 172.3 (C_1); *m/z* (ESI$^+$) 271 (100%), 315 (60%), 393 ([M+Na]$^+$, 20%), 763 ([2M+Na]$^+$, 30%); HRMS (ESI$^+$) $C_{21}H_{26}N_2NaO_4{}^+$ ([M+Na]$^+$) requires 393.1785, found 393.1782.

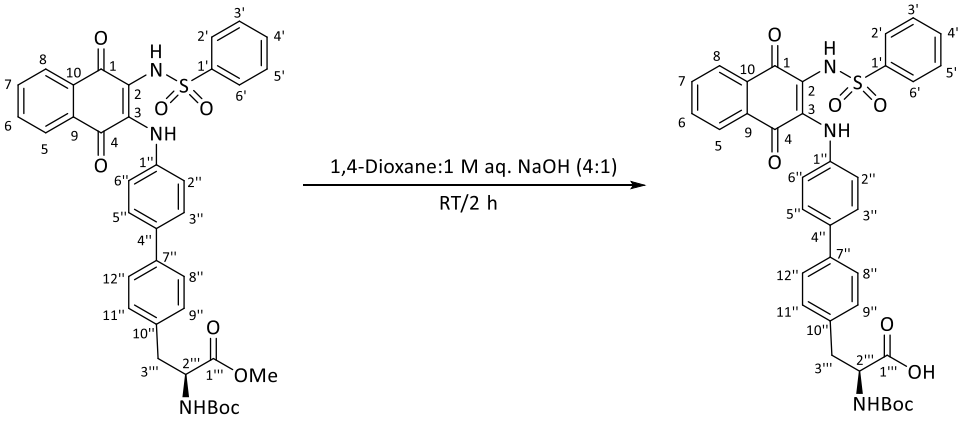
Methyl (*S*)-2'''-((*tert*-butoxycarbonyl)amino)-3'''-(1''-((1,4-dioxo-2-(phenylsulfonamido)-1,4-dihydronaphthalen-3-yl)amino)-[4'',7''-biphenyl]-10''-yl)propanoate 454



Following *General Procedure 2*, using naphthoquinone **57** (150 mg, 0.432 mmol), aniline **453** (319 mg, 0.863 mmol) and cerium trichloride heptahydrate (161 mg, 0.432 mmol) in MeOH (8 mL), at 90 °C. Purification *via* column chromatography on silica gel (eluent pet ether:acetone 95:5 to 75:25) gave naphthoquinone **454** as a red solid (45 mg, 15%). mp 118-122 °C; υ_{max} (thin film) 3330 (N-H), 2924 (C-H), 2854 (C-H), 1739 (C=O), 1714 (C=O), 1680 (C=O), 1603 (C=O), 1574, 1503; $[\alpha]_D{}^{20}$ -106.7 (*c* 0.00625, $CHCl_3$); δ_H (500 MHz, $CDCl_3$) 1.45 (9H, s, C*Me*$_3$), 3.15 (2H, dd, *J* 19.9, 5.8, 2 x $H_{3'''}$), 3.75 (3H, s, O*Me*), 4.59-4.68 (1H, m, $H_{2'''}$), 5.04 (1H, d, *J* 8.2, carbamate-N*H*), 6.85 (1H, br. s, sulfonamide-N*H*), 7.14 (2H, d, *J* 8.5, $H_{2''}$ and $H_{6''}$), 7.21 (2H, d, *J* 8.0, $H_{9''}$ and $H_{11''}$), 7.30-7.35 (2H, m, $H_{3'}$ and $H_{5'}$), 7.43-7.48 (1H, m, $H_{4'}$), 7.54-7.61 (4H, m, $H_{3''}$, $H_{5''}$, $H_{8''}$ and $H_{12''}$), 7.64-7.72 (4H, m, H_6, H_7, $H_{2'}$ and $H_{6'}$), 7.88-7.92 (1H, m, H_8), 8.08-8.14 (2H, m, H_8 and aniline-N*H*); δ_C (125 MHz, $CDCl_3$) 28.3 (C*Me*$_3$), 38.0 ($C_{3'''}$), 52.3 (O*Me*), 54.4 ($C_{2'''}$), 80.0 (*C*Me$_3$), 113.5 (C_2), 123.6 ($C_{2''}$ and $C_{6''}$), 126.4 (C_8), 126.7 ($C_{3''}$ and $C_{5''}$ or $C_{8''}$ and $C_{12''}$), 127.0 (C_5), 127.0 ($C_{3''}$ and $C_{5''}$ or $C_{8''}$ and $C_{12''}$), 127.3 ($C_{2'}$ and $C_{6'}$), 128.7 ($C_{3'}$ and $C_{5'}$), 129.7

($C_{9''}$ and $C_{11''}$), 130.5 (C_9), 131.3 (C_{10}), 133.1 (C_6), 133.1 ($C_{4'}$), 134.9 (C_7 or $C_{10''}$), 135.1 (C_7 or $C_{10''}$), 136.7 ($C_{1''}$), 137.3 ($C_{4''}$), 138.5 (C_3 or $C_{1'}$), 138.6 (C_3 or $C_{1'}$), 139.0 ($C_{7''}$), 155.1 ($CO_2{}^t$Bu), 172.4 ($C_{1'''}$), 179.1 (C_1), 181.8 (C_4); *m/z* (ESI$^-$) 680 ([M-H]$^-$, 100%); HRMS (ESI$^-$) $C_{37}H_{34}O_8N_3S^-$ ([M-H]$^-$) requires 680.2072, found 680.2071.

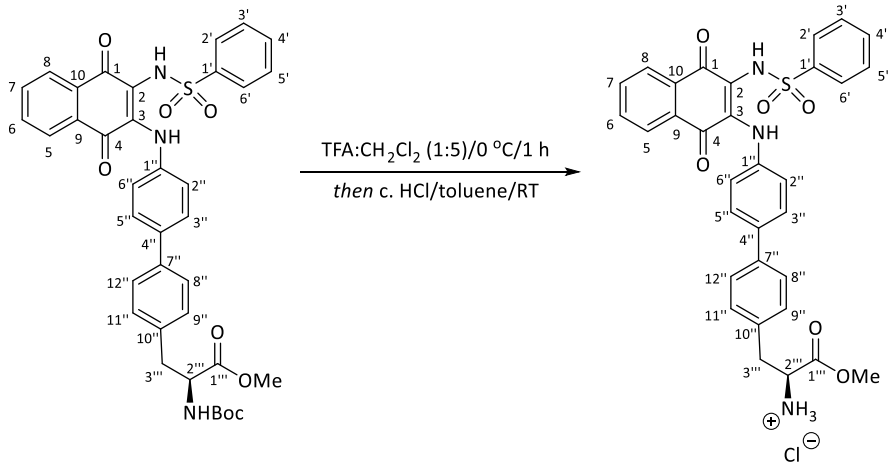
(*S*)-2'''-((*tert*-Butoxycarbonyl)amino)-3'''-(1''-((1,4-dioxo-2-(phenylsulfonamido)-1,4-dihydronaphthalen-3-yl)amino)-[4'',7''-biphenyl]-10''-yl)propanoic acid 455



Methyl ester **454** (37 mg, 0.054 mmol) and 1 M aq. NaOH (2 mL) were stirred in 1,4-dioxane (8 mL) at RT for 2 h. After this time, the *p*H of the solution was adjusted to *c.* 2 with 1 M aq. HCl (10 mL) and the organic product was extracted into EtOAc (3 x 10 mL). The organic layers were combined, washed with brine (3 x 10 mL), dried over Na_2SO_4, filtered and concentrated *in vacuo*. Purification *via* column chromatography on silica gel (eluent CH_2Cl_2:MeOH 100:0 to 70:30) gave carboxylic acid **455** as a red solid (30 mg, 83%). mp 139-143 ^oC; υ_{max} (thin film) 3382 (O-H), 2920 (C-H), 2851 (C-H), 1738 (C=O), 1602 (C=O), 1512; $[\alpha]_D^{20}$ +262.5 (*c* 0.0016, DMF); δ_H (500 MHz, DMF-d_7) 1.37 (9H, s, CMe_3), 3.04-3.11 (1H, m, $H_{3'''}$), 3.20-3.27 (1H, m, $H_{3'''}$), 4.28-4.34 (1H, m, $H_{2'''}$), 6.50 (1H, br. s, N*H*), 7.06 (2H, d, *J* 7.3, $H_{2''}$ and $H_{6''}$), 7.33-7.40 (4H, m, $H_{3'}$, $H_{5'}$, $H_{9''}$ and $H_{11''}$), 7.40-7.45 (1H, m, $H_{4'}$), 7.52 (2H, d, *J* 8.4, $H_{3''}$ and $H_{5''}$), 7.58 (2H, d, *J* 8.0, $H_{8''}$ and $H_{12''}$), 7.72-7.81 (4H, m, H_6, H_7, $H_{2'}$ and $H_{6'}$), 7.81-7.86 (1H, m, H_8), 7.95-7.99 (1H, m, H_5), 8.49 (1H, br. s, N*H*); δ_C (125 MHz, DMF-d_7) 28.1 (CMe_3), 37.4 ($C_{3'''}$), 56.3 ($C_{2'''}$), 78.2 (*C*Me$_3$), 121.6 ($C_{2''}$ and $C_{6''}$), 125.8 (C_5 or C_8), 125.9 (C_5 or C_8), 126.1 ($C_{8''}$ and $C_{12''}$), 126.2 ($C_{3''}$ and $C_{5''}$), 126.7 ($C_{2'}$ and $C_{6'}$), 128.4 ($C_{3'}$ and $C_{5'}$), 129.2 (C_2 or C_3), 130.1 (C_2 or C_3), 130.3 ($C_{9''}$ and

$C_{11''}$), 131.0 ($C_{4'}$), 132.2 (C_9 or C_{10}), 132.4 (C_9 or C_{10}), 133.2 (C_6), 133.8 (C_7), 133.8 ($C_{4''}$), 137.4 ($C_{10''}$), 138.8 ($C_{1'}$), 138.8 ($C_{7''}$), 141.3 ($C_{1''}$), 155.8 ($CO_2{}^t$Bu), 176.0 (CO_2H), 180.1 (C_1), 180.8 (C_4); *m/z* (ESI$^-$) 666 ([M-H]$^-$, 100%); HRMS (ESI$^-$) $C_{36}H_{32}N_3O_8S^-$ ([M-H]$^-$) requires 666.1916, found 666.1920.

(*S*)-3'''-(1''-((1,4-Dioxo-2-(phenylsulfonamido)-1,4-dihydronaphthalen-3-yl)amino)-[4'',7''-biphenyl]-10''-yl)-1'''-methoxy-1'''-oxopropan-2'''-ammonium chloride 456

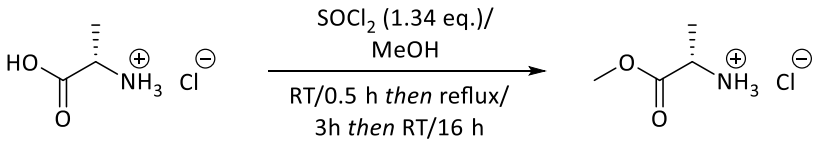


Naphthoquinone **454** (32 mg, 0.047 mmol) was stirred in CH_2Cl_2 (10 mL) at 0 ^oC. To this solution was added TFA (2 mL) dropwise, and the reaction mixture was stirred at 0 ^oC for 1 h. After this time, the crude reaction mixture was concentrated *in vacuo*. The residue was purified *via* column chromatography on silica gel (eluent pet ether:acetone 70:30 to 30:70). Toluene (10 mL) and c. HCl (0.5 mL) were added and the solution was concentrated *in vacuo* once more. A further portion of toluene (10 mL) was then added and the solution was concentrated *in vacuo* to give ammonium chloride **456** as an orange solid (19 mg, 65%). mp 184-192 ^oC; υ_{max} (thin film) 2928 (C-H), 1740 (ester C=O), 1601 (naphthoquinone C=O), 1514; $\alpha_D{}^{[25]}$ -56.7 (*c* 0.01, DMF); δ_H (500 MHz, MeOD) 3.10-3.21 (2H, m, 2 x $H_{3'''}$), 3.73 (3H, s, O*Me*), 4.37 (1H, br. s, $H_{2'''}$), 7.12 (2H, d, *J* 7.9, $H_{2''}$ and $H_{6''}$), 7.31-7.38 (4H, m, $H_{3'}$, $H_{5'}$, $H_{9''}$ and $H_{11''}$), 7.46-7.51 (1H, m, $H_{4'}$), 7.54-7.59 (4H, m $H_{2'}$, $H_{6'}$, $H_{3''}$ and $H_{5''}$), 7.69 (2H, d, *J* 8.2, $H_{8''}$ and $H_{12''}$), 7.75-7.83 (3H, m, H_6, H_7 and H_8), 8.02-8.05 (1H, m, H_5); δ_C (125 MHz, MeOD) 35.5 ($C_{3'''}$), 52.8 (O*Me*), 53.1 ($C_{2'''}$), 113.9 (C_2), 123.9 ($C_{2''}$ and $C_{6''}$), 125.4 ($C_{3''}$ and $C_{5''}$), 125.7 (C_8), 126.2 (C_5),

126.4 ($C_{8''}$ and $C_{12''}$), 126.5 ($C_{2'}$ and $C_{6'}$), 128.5 ($C_{3'}$ and $C_{5'}$), 130.0 ($C_{9''}$ and $C_{11''}$), 130.3 (C_9), 131.5 (C_{10}), 132.2 ($C_{4'}$), 133.1 (C_6), 133.2 ($C_{10''}$), 134.4 ($C_{4''}$), 134.9 (C_7), 138.1 ($C_{1''}$), 138.7 ($C_{7''}$), 140.9 ($C_{1'}$), 141.7 (C_3), 170.4 ($C_{1'''}$), 178.5 (C_1), 182.3 (C_4); *m/z* (ESI^+) 582 ($[M+H]^+$, 100%); HRMS (ESI^+) $C_{32}H_{28}N_3O_6S^+$ ($[M+H]^+$) requires 582.1693, found 582.1685.

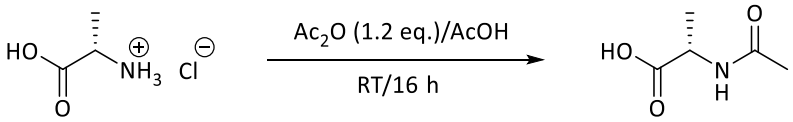
7.7. Preparation and characterisation of compounds reported in Chapter 6

L-Alanine methyl ester hydrochloride 479[386]



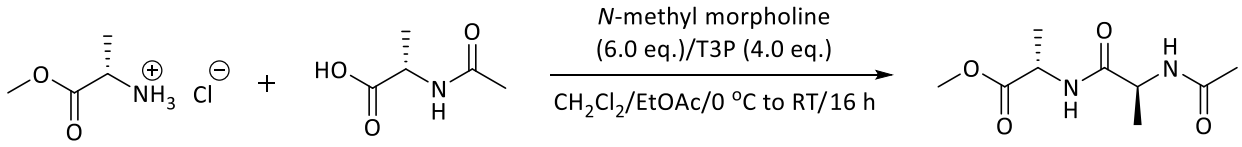
To a solution of L-alanine **478** (5.00 g, 56.2 mmol) in MeOH (30 mL) at 0 °C, $SOCl_2$ (5.49 mL, 75.3 mmol) was slowly added. The mixture was stirred at RT for 30 min before being heated to reflux for 3 h and susbequently left to stir at RT for a further 16 h. MeOH was then removed *in vacuo* and the crude product was washed thrice with toluene (3 x 10 mL). Removal of the toluene *in vacuo* gave methyl ester **479** as a white solid (7.33 g, 93%). mp 110-111 °C (lit. 106-108 °C);[386a] $[\alpha]_D^{25}$ + 9.7 (*c* 2.0, MeOH) (lit. +20.0 (*c* 2.0, MeOH, 7.5 °C));[386b] δ_H (400 MHz, MeOD) 1.55 (3H, d, *J* 7.3, CH*Me*), 3.85 (3H, s, O*Me*), 4.12 (1H, q, *J* 7.3, C*H*Me); *m/z* (ESI^+) 104 ($[M+H]^+$, 100%), 126 ($[M+Na]^+$, 55%).

N-Acetyl-L-alanine 480[387]



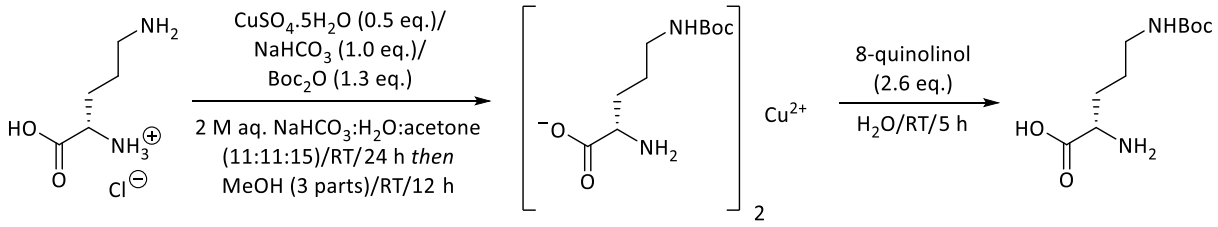
To a suspension of L-alanine **478** (2.50 g, 28.1 mmol) in glacial acetic acid (12.5 mL) was added acetic anhydride (3.15 mL, 33.7 mmol). The initial slurry was allowed to stir at RT for 16 h, resulting in the formation of a clear solution. The reaction was concentrated *in vacuo* to give a viscous yellow oil. This residue was washed with acetone (3 x 20 mL). Removal of the acetone *in vacuo* yielded *N*-acetylated **480** as an off-white solid (2.34 g, 64%). mp 117-119 °C;[387] $[\alpha]_D^{25}$ -53.5 (*c* 1.0, H_2O) (lit. -57.5 (*c* 1.0, H_2O, 25 °C));[387] δ_H (400 MHz, MeOD) 1.39 (3H, d, *J* 7.3, CH*Me*), 1.98 (3H, s, CO*Me*), 4.38 (1H, q, *J* 7.3, C*H*Me), *CO_2H not observed*; *m/z* (ESI^-) 130 ($[M-H]^-$, 100%).

N-Acetyl-L-alaninyl-L-alanine methyl ester 481[388]



L-Alanine methyl ester hydrochloride **479** (100 mg, 1.0 eq.), *N*-acetyl-L-alanine **480** (106 mg, 0.763 mmol) and *N*-methylmorpholine (521 µL, 4.74 mmol) were dissolved in CH_2Cl_2 (13 mL) and cooled to 0 °C. T3P (50% wt. in EtOAc, 982 µL, 3.30 mmol) was added to the solution dropwise and the mixture was stirred for 16 h, over which time the solution was allowed to warm to RT. The crude reaction mixture was concentrated *in vacuo*; subsequent purification by column chromatography on silica gel (eluent CH_2Cl_2:MeOH 98:2 to 95:5) gave dipeptide **481** as a white solid (56 mg, 34%). mp 166-168 °C (lit. 170-171 °C);[388] δ_H (400 MHz, MeOD) 1.33 (3H, d, *J* 7.3, CH*Me*), 1.38 (3H, d, *J* 7.1, CH*Me*), 1.96 (3H, s, CO*Me*), 3.71 (3H, s, O*Me*), 3.30-3.43 (2H, m, 2 x C*H*Me); *m/z* (ESI^+) 157 (100%), 239 ($[M+Na]^+$, 30%).

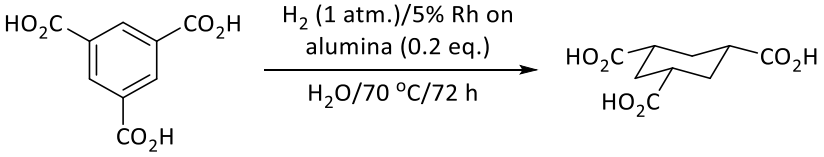
N^{ε}-*tert*-Butoxycarbonyl-L-ornithine 484[389]



To a stirred solution of L-ornithine monohydrochloride **482** (1.85 g, 11.0 mmol) in 2 M aq. $NaHCO_3$ (11 mL), a solution of copper sulfate pentahydrate (1.37 g, 5.48 mmol) in water (11 mL) was added. $NaHCO_3$ (0.92 g, 11.0 mmol) was then added to this solution, followed by 96% di-*tert*-butyl dicarbonate (3.11 g, 14.3 mmol) in acetone (15 mL). The solution was left to stir at RT for 24 h. MeOH (3 mL) was then added and stirring continued at RT for a further 12 h. H_2O (11 mL) and acetone (11 mL) were added and the blue precipitate obtained was collected by suction filtration. This precipitate was suspended in H_2O (50 mL), collected by suction filtration and dessicated overnight to yield the copper salt $[Orn(Boc)]_2Cu$ **483** as a blue

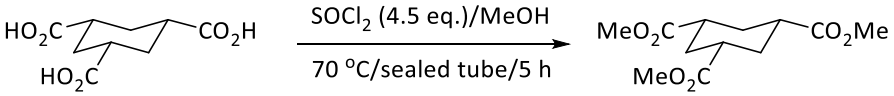
solid (3.10 g, 94%). *m/z* (ESI$^+$) 233 ([M+H]$^+$, 100%). This salt was next suspended in water (18 mL) and 8-quinolinol (2.10 g, 14.5 mmol) was added; the suspension was stirred vigorously at RT for 5 h. After this time, green copper(II) quinolinate, which forms as a precipitate, was removed by suction filtration and washed with water (2 x 10 mL). The precipitate was re-suspended in water (30 mL) and left to stand overnight. Once again the precipitate was removed by suction filtration and washed with water (2 x 10 mL). All the aqueous washings were combined and washed with EtOAc (2 x 20 mL). Concentration of this solution *in vacuo* at a water bath temperature of no greater than 45 ^{o}C yielded N^{ε}-Boc protected L-ornithine **484** as a white solid (1.07 g, 45%). mp 204-206 ^{o}C (lit. 210-213 ^{o}C);[389] $[\alpha]_D^{25}$ +16.1 (*c* 1.0, AcOH) (lit. +15.2 (*c* 1.0, AcOH, 20 ^{o}C));[389] δ_H (400 MHz, MeOD) 1.43 (9H, s, C*Me*$_3$), 1.52-1.66 (2H, m, C*H*$_2$), 1.73-1.94 (2H, m, C*H*$_2$), 3.01-3.15 (2H, m, NHC*H*$_2$), 3.50-3.59 (1H, m, C*H*CO$_2$H), *3 x NH and CO$_2$H not observed*; *m/z* (ESI$^+$) 233 ([M+H]$^+$, 100%), 255 ([M+Na]$^+$, 10%).

cis,*cis*-Cyclohexane-1,3,5-tricarboxylic acid 490[390]



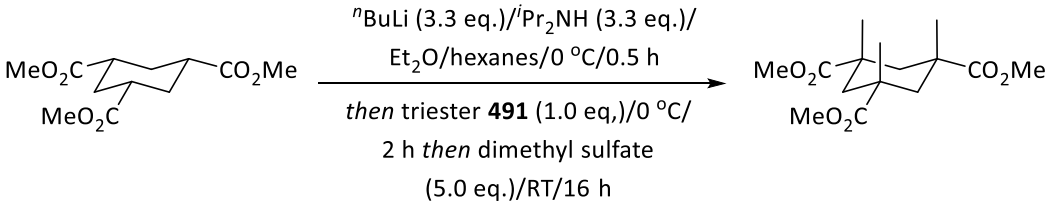
Trimesitic acid **489** (3.00 g, 14.29 mmol) and 5% Rh on Al_2O_3 (660 mg, 0.14 mmol of Rh) were added to water (60 mL) in a round-bottomed flask at RT. The mixture was stirred and then purged with a balloon of H_2 (1 atm.); the resulting solution was heated to 70 ^{o}C for 72 h. The crude reaction mixture was then cooled to RT and filtered through Celite®; concentration of the filtrate *in vacuo* yielded *cis,cis*-cyclohexane-1,3,5-tricarboxylic acid **490** as a white solid (2.94 g, 95%). mp 216 ^{o}C (lit. 218 ^{o}C);[390] δ_H (400MHz, DMSO-d_6) 1.15-1.30 (3H, m 3 x C*H*(H)(ax)), 2.03-2.11 (3H, m, 3 x C*H*(H)(equ)), 2.28-2.39 (3H, m 3 x C*H*CO$_2$H), 12.28 (3H, br. s, 3 x CO$_2$*H*); *m/z* (ESI$^+$) 217 ([M+H]$^+$, 70%), 239 ([M+Na]$^+$, 100%).

Trimethyl-*cis*,*cis*-cyclohexane-1,3,5-tricarboxylate 491



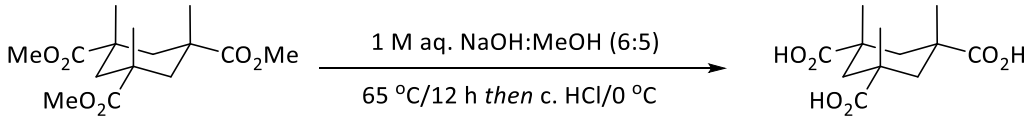
Tricarboxylic acid **490** (2.50 g, 11.6 mmol) was dissolved in MeOH (30 mL) and added dropwise to $SOCl_2$ (5.07 mL, 69.4 mmol) in MeOH (45 mL) at RT. This mixture was heated to 70 °C for 5 h; after this time, the reaction was cooled and the solvent evaporated *in vacuo*. The crude mixture was azeotroped thrice with toluene (3 x 20 mL) to afford trimethyl ester **491** as a white solid (2.96 g, 99%). mp 47-48 °C (lit. 48 °C);[390] δ_H (400MHz, DMSO-d_6) 1.20-1.35 (3H, m, 3 x C*H*(H)(ax)), 2.05-2.16 (3H, m 3 x C*H*(H)(equ)), 2.47-2.57 (3H, m, 3 x C*H*CO_2Me), 3.60 (9H, s, 3 x O*Me*); *m/z* (ESI^+) 259 ($[M+H]^+$, 100%), 281 ($[M+Na]^+$, 30%).

Trimethyl-*cis*,*cis*-1,3,5-trimethylcyclohexane-1,3,5-tricarboxylate 492[390]



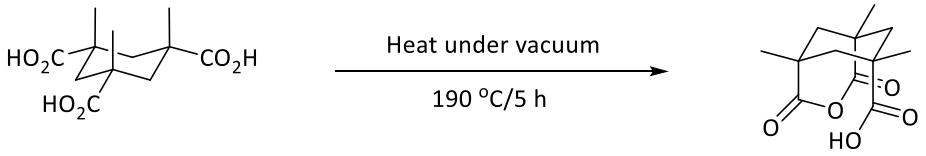
LDA was generated *in situ* by the addition of ^{n}BuLi (2.5 M in hexanes, 12.78 mL, 32.0 mmol) to diisopropylamine (4.50 mL, 32.0 mmol) in Et_2O (25 mL) at 0 °C. To the resulting mixture was added trimethyl tricarboxylate **491** (2.50 g, 9.69 mmol) in Et_2O (25 mL), and the mixture was stirred at 0 °C for 2 h. Subsequently, dimethyl sulfate (4.5 mL, 48.5 mmol) was added and stirring continued at RT for 16 h. The reaction mixture was washed with H_2O (25 mL), 1 M aq. HCl (25 mL) and brine (3 x 20 mL), dried over Na_2SO_4, filtered and concentrated *in vacuo* to give trimethyl tricarboxylate **492** as a yellow oil (1.58 g, 54%). δ_H (400MHz, $CDCl_3$) 0.97 (3H, d, *J* 14.8, 3 x C*H*(H)), 1.22 (9H, s, 3 x C*Me*), 2.74 (3H, d, *J* 14.8, 3 x C*H*(H)), 3.97 (9H, s, 3 x O*Me*); *m/z* (ESI^+) 301 ($[M+H]^+$, 45%), 323 ($[M+Na]^+$, 100%), 623 ($[2M+Na]^+$, 45%).

cis,*cis*-1,3,5-Trimethylcyclohexane-1,3,5-tricarboxylic acid (Kemp's triacid) 493



To a solution of MeOH (13 mL) and 1 M aq. NaOH (15.6 mL) was added trimethyl tricarboxylate **492** (1.55 g, 5.17 mmol) and the mixture was heated to 65 °C and stirred for 12 h. After the solution was cooled, the MeOH was removed by concentration *in vacuo*. The resulting aqueous solution was cooled to 0 °C and the *p*H was adjusted to 1 with c. HCl. Kemp's triacid **493** was obtained as a white precipitate which was collected by suction filtration (948 mg, 71%). mp 236-238 °C (lit. 230-245 °C);[391] δ_H (400MHz, $CDCl_3$) 1.20 (3H, d, *J* 14.9, 3 x C*H*(H)), 1.27 (9H, s, 3 x *Me*), 2.72 (3H, d, *J* 14.9, 3 x C*H*(H)), *3 x CO_2H not observed*; *m/z* (ESI^-) 257 ($[M-H]^-$, 100%).

1,5,7-Trimethyl-2,4-dioxo-3-oxabicyclo[3.3.1]nonane-7-carboxylic acid 494[392]



Kemp's triacid **493** (765 mg, 2.97 mmol) was heated in a sealed flask under vacuum to 190 °C for 5 h to yield anhydride **494** as a white solid (213 mg, 30%). mp 250-251 °C (lit. 243-245 °C);[392] δ_H (400MHz, DMSO-d_6) 1.13 (3H, s, C(*Me*)CO_2H), 1.19 (6H, s, 2 x C(*Me*)CO_2CO), 1.33-1.48 (3H, m, 3 x C*H*(H)), 2.18 (1H, d, *J* 12.6, C*H*(H)), 2.41 (2H, d, *J* 13.6, 2 x C*H*(H)), 12.58 (1H, br. s, CO_2H); *m/z* (ESI^+) 263 ($[M+H]^+$, 15%), 503 ($[2M+Na]^+$, 100%).

7.8. Expression and Purification of MOUSE(NAT2)_WT

LB growth medium was prepared by adding 10 g NaCl, 10 g Bacto® Tryptone and 5 g Bacto® yeast extract per 1000 mL of deionised water. *E. coli* Rosetta®(-DE3)pLysS cells containing pET28b(+), into which the *MOUSE(Nat2)* open-reading frame[393] had been sub-cloned so as to allow the production of recombinant MOUSE(NAT2) with an *N*-terminal hexa-His tag, had been previously prepared by Kawamura *et al.* and stored at -80 °C in LB medium with 10% (*v/v*) glycerol.[257] 10 μL of this thawed stock was used to inoculate 10 mL of LB medium, into which the antibiotic kanamycin (30 μg/mL) was also added; this starter culture was incubated at 37 ^{o}C for 16 h with shaking (180 rpm). A larger-scale culture was then prepared by the addition of 5 mL of starter culture to 1000 mL LB medium; kanamycin (30 μg/mL) and chloramphenicol (34 μg/mL) were also added and the culture incubated at 37 ^{o}C with shaking.

The optical density of the solution at 600 nm (OD_{600}) was monitored at hourly intervals and when the absorbance reached 0.4, IPTG was added to a final concentration of 0.1 mM in order to induce *MOUSE(Nat2)* transcription. After a further incubation period of 20 h at 27 ^{o}C with shaking (180 rpm), the *E. coli* cells were harvested by centrifugation (5000 RCF, 4 ^{o}C, 30 min). These cells were then re-suspended in 20 mL of lysis buffer (300 mM NaCl, 20 mM Tris•HCl (*p*H 8.0), 0.2 mg/mL chicken egg white lysozyme, 0.02 mg/mL deoxyribonuclease I containing one EDTA-free Complete Protease Inhibitor per 20 mL) and flash-frozen in liquid nitrogen. After subsequent thawing in a water bath at 37 ^{o}C, the solution was sonicated on ice (30 cycles of 30 s on, 30 s off at 10 μm). The soluble lysate was then separated from the cell debris by centrifugation (15000 RCF, 4 ^{o}C, 20 min).

To afford pure MOUSE(NAT2) from this soluble lysate *via* column chromatography, 10 mL of Ni-NTA solution was used as the stationary phase and 20 mM Tris•HCl (*p*H 8.0) containing 100 mM NaCl and increasing concentrations of imidazole (0 mM, 10 mM, 25 mM, 50 mM, 250 mM and 500 mM) was used as the mobile phase. 1 mM DTT was added to the 250 mM imidazole solution to prevent enzyme precipitation.

SDS-PAGE gels were run to determine which of the column fractions contained pure MOUSE(NAT2) using a 12% acrylamide separating gel (12.0 mL ProtoGel®, 7.8 mL ProtoGel® resolving buffer, 3.0 mL 1% ammonium phosphate buffer, 7.15 mL deionised water, 0.05 mL TEMED) and a 4% acrylamide stacking gel (3 mL ProtoGel®, 4 mL ProtoGel® stacking buffer, 1.6 mL 1% ammonium phosphate buffer, 8.5 mL deionised water, 0.05 mL TEMED). 5 µL of each column fraction was added to 15 µL of reduced gel loading buffer (10 mM Tris•HCl (*p*H 6.8), 8 M urea, 2% (*w/v*) SDS, 5 mg/mL DTT, 2% (*v/v*) glycerol containing 10 µg/mL bromophenol blue) and heated to 95 °C for 5 min. 10 µL of each cooled solution was then loaded into one of the wells on the gel over air. A reference ladder (High Range Rainbow™ Molecular Weight Markers) was loaded in a well alongside all the sample-containing wells, and electrophoresis was carried out using a 25 mA current in a running buffer (50 mM Tris•HCl (*p*H 8.3), 50 mM glycine, 1% (*w/v*) SDS). The gels were visualised by shaking for 30 min in Coomassie Blue staining buffer and de-stained for 16 h in de-staining buffer (10% EtOH/10% AcOH (*v/v*)). The resulting gels showed that the 50 mM and 250 mM imidazole fractions contained solely MOUSE(NAT2) **(Figure 7.1)**.

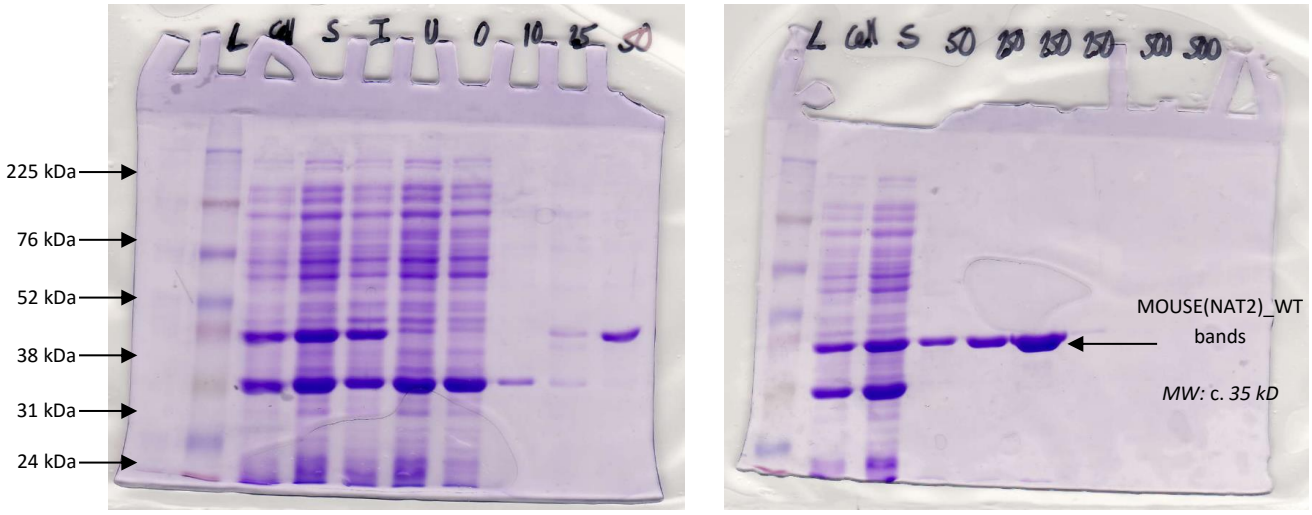


Figure 7.1: SDS-PAGE Gels following purification of the soluble cell lysate *via* Ni-NTA chromatography. Each collected fraction was run against a reference ladder L. Cell = cell lysate; S = soluble fraction; I = insoluble fraction; U = unbound fraction; numbers represent the fractions corresponding to the imidazole washes of those concentrations. The 50 mM and 250 mM imidazole washes are shown to contain pure MOUSE(NAT2)_WT.

The 50 mM and 250 mM fractions were subsequently dialysed for 16 h at 4 °C in 4000 mL of dialysis buffer (20 mM Tris•HCl (*p*H 8.0), 1 mM DTT, 1 mM EDTA). Both fractions were then incubated with thrombin (5 U/mg MOUSE(NAT2)) for 4 h at 4 °C to remove the *N*-terminal hexa-His tag. Complete cleavage was confirmed *via* SDS-PAGE gel electrophoresis **(Figure 7.2)**.

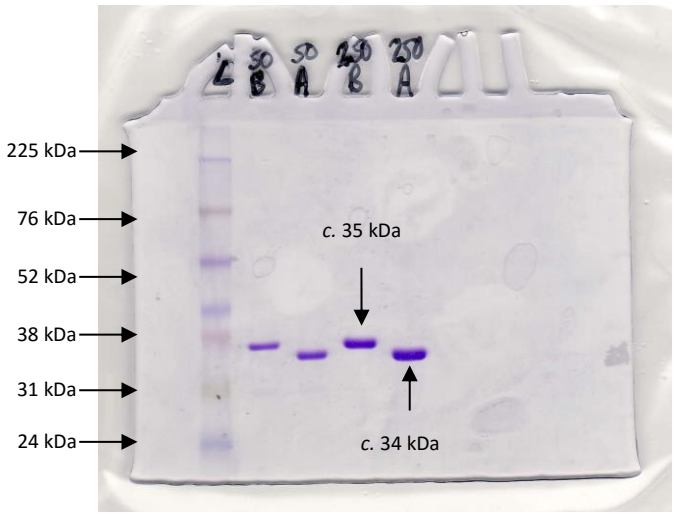


Figure 7.2: SDS-PAGE gel showing samples of the 50 mM and 250 mM fractions pre- and post- thrombin cleavage. B = before thrombin cleavage; A = after thrombin cleavage. The gel clearly shows the loss of the *N*-terminal hexa-His tag upon treatment with thrombin.

The two fractions were then concentrated by centrifugation in a size-exclusion falcon with a filter size of 10 kDa (3050 RCF, 4 °C, 3 x 5 min). The absorbance of each fraction at 280 nm (A_{280}) was measured so the mass of protein collected could be calculated **(Table 7.1)**. 5% (*v/v*) glycerol was added to each concentrated fraction, and the fractions were stored at -80 °C.

Fraction	A_{280}	Dilution Factor	[MOUSE(NAT2)] (mg/mL)	Fraction Volume (mL)	Mass of MOUSE(NAT2) (mg)
50 mM	0.149	30	3.51	4.1	14.4
250 mM	0.333	30	7.85	6.6	51.8
				TOTAL	66.2

Table 7.1: Determination of the concentration and mass of MOUSE(NAT2) in each of the concentrated fractions (ε_{280} = 1.272 for MOUSE(NAT2)).

7.9. Purification of HUMAN(NAT1)_WT

A pellet of *E. coli* cells induced to overexpress HUMAN(NAT1) was kindly supplied by Dr Julien Dairou (Université Denis Diderot, Paris) and stored at -80 ^{o}C. This pellet was thawed in a water bath at 37 ^{o}C and re-suspended in 20 mL of lysis buffer (300 mM NaCl, 20 mM Tris•HCl (*p*H 8.0), 0.2 mg/mL chicken egg white lysozyme, 0.02 mg/mL deoxyribonuclease I containing one EDTA-free Complete Protease Inhibitor per 20 mL). The solution was sonicated on ice (30 cycles of 30 s on, 30 s off at 10 µm) and the soluble lysate was then separated from the cell debris by centrifugation (15000 RCF, 4 ^{o}C, 20 min).

HUMAN(NAT1) was obtained from this soluble lysate *via* column chromatography, as described above **(Section 7.8.)** for MOUSE(NAT2), using 10 mL of Ni-NTA solution as the stationary phase and 20 mM Tris•HCl (*p*H 8.0) containing 100 mM NaCl and increasing concentrations of imidazole as the mobile phase.

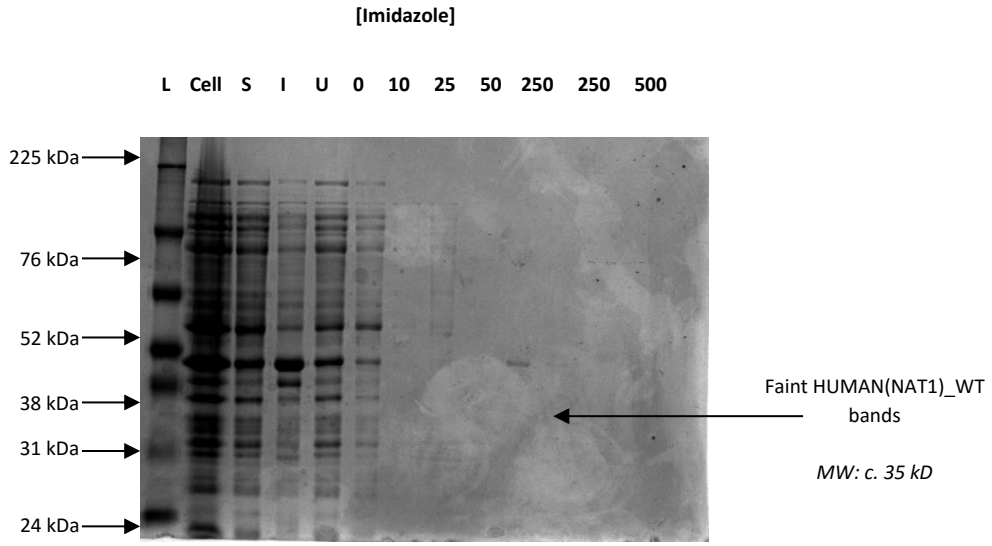


Figure 7.3: SDS-PAGE gel following purification of the soluble cell lysate *via* Ni-NTA chromatography. Each collected fraction was run against a reference ladder L; Cell = cell lysate; S = soluble fraction; I = insoluble fraction; U = unbound fraction; numbers represent the fractions corresponding to the imidazole washes of those concentrations in mM. The 50 mM and 250 mM imidazole washes contain pure HUMAN(NAT1)_WT.

SDS-PAGE gels were run to determine which of the column fractions contained pure HUMAN(NAT1) using an analogous procedure to that outlined in **Section 7.8.** above. The resulting gels showed that the 50 mM and 250 mM imidazole fractions contained solely HUMAN(NAT1) **(Figure 7.3)**. These fractions were therefore dialysed as described in **Section 7.8.** and incubated with thrombin (2 U/mg HUMAN(NAT1)) for 16 h at 4 ^{o}C. The fractions were concentrated by centrifugation in a size-exclusion falcon with a filter size of 10 kDa (3000 RCF, 4 ^{o}C, 5 x 2 min) and the absorbance of each fraction at 280 nm (A_{280}) was measured so the mass of protein collected could be calculated **(Table 7.2)**. 5% (*v/v*) glycerol was added to each concentrated fraction, and the fractions were stored at -80 ^{o}C.

Fraction	A_{280}	Dilution Factor	[HUMAN(NAT1)] (mg/mL)	Fraction Volume (mL)	Mass of HUMAN(NAT1) (mg)
50 mM	0.743	2	1.17	3.6	4.21
250 mM	0.638	3	1.50	1.7	2.56
				TOTAL	6.77

Table 7.2: Determination of the concentration and mass of HUMAN(NAT1) in each of the concentrated fractions (ε_{280} = 1.272 for HUMAN(NAT1)).

7.10. Growth of ZR-75-1 Breast Cancer Cell Line

Cell growth medium was first prepared by mixing 500 mL Roswell Park Memorial Institute (RPMI) 1640 containing L-glutamine, 50 mL heat-inactivated foetal bovine serum (FBS) and 5 mL penicillin-strepomycin solution. Cells from the human breast cancer cell line ZR-75-1, which had been obtained from the American Type Culture Collection (Manassas, VA), were washed with 10 mL of this growth medium and pelleted to remove DMSO in the storage buffer. This pellet was resuspended in 2 mL of growth medium before being added to a cell culture flask (Corning) containing a further 10 mL of medium. The flask was then incubated at 37 ^{o}C in a 5% CO_2 environment.

The cell growth was monitored under a microscope at regular intervals and once almost confluent (every 5-7 days) the cells were split in a 1:2 fashion. Cells were detached from the cell culture flask by removing the growth medium, washing the cell monolayer with 11 mL Dulbecco's phosphate-buffered saline (PBS) and then adding 3 mL trypsin-EDTA solution (0.25%) to cover the cell monolayer. Once the cells were visibly detached from the flask (after about 5 min), 8 mL of growth medium was added and the cells collected by centrifugation (200 RCF, 25 ^{o}C, 5 min). The supernatant solution was decanted and 2 mL growth medium was added to the cell pellet, in which the cells were resuspended. 1 mL of this solution was then added to each of two new cell culture flasks. 10 mL of growth medium was added to each of these two flasks and the flasks incubated at 37 ^{o}C in a 5% CO_2 environment as previously.

After 5 passages, the cells from one of the culture flasks were frozen for future use, and those from all the other flasks were harvested to prepare a cell lysate. The cells in all the flasks were detached and pelleted as usual, although before centrifugation, 100 µL of cell-containing solution was removed and added to 100 µL of trypan blue. The cells in this sample were then counted using a haemocytometer.

For the cells to be frozen, the cell pellet was resuspended in ice-cold cell freezing solution A (50% FBS, 50% growth medium) before adding an equal volume of ice-cold cell freezing solution B (50% FBS, 30% growth medium, 20% DMSO) dropwise, such that the final cell concentration was 1 x 10^7 cells/mL. The solution was dispensed into a 1 mL aliquot in a cryotube, and kept at -80 ^{o}C overnight before being transferred to liquid N_2 for long-term storage.

For the cells to be lysed, the cell pellet was resuspended in complete lysis buffer (100 µL frozen protease inhibitors and 10 µL 100 mM DTT added per 900 µL of lysis buffer (20 mM Tris•HCl (*p*H 8.0), 20 mM NaCl, 0.5% Nonidet P40 containing one EDTA-free Complete Protease Inhibitor per 2.5 mL)) to a final cell concentration of 5 x 10^7 cells/mL. The cell debris was removed by centrifugation in a microfuge (full speed, 4 ^{o}C, 10 min) and the supernatant

retained. The cell lysate was kept on ice and all studies with inhibitors were carried out on the same day.

7.11. Alkylation of the Cys68 Residue of MOUSE(NAT2)_WT

To an aliquot of MOUSE(NAT2) (100 µL at 4 mg/mL) was added 5 µL 2-iodoacetamide (0.105 M solution in DMSO) to a final concentration of 5 mM 2-iodoacetamide. The aliquot was incubated at 4 ^{o}C for 3 h, during which time the alkylating agent covalently modifies the catalytic cysteine residue of MOUSE(NAT2).[247b] Proof of covalent modification was obtained by MS (MALDI) **(Figure 7.4)** and by testing for the loss of catalytic activity in the acetyl CoA hydrolysis assay.

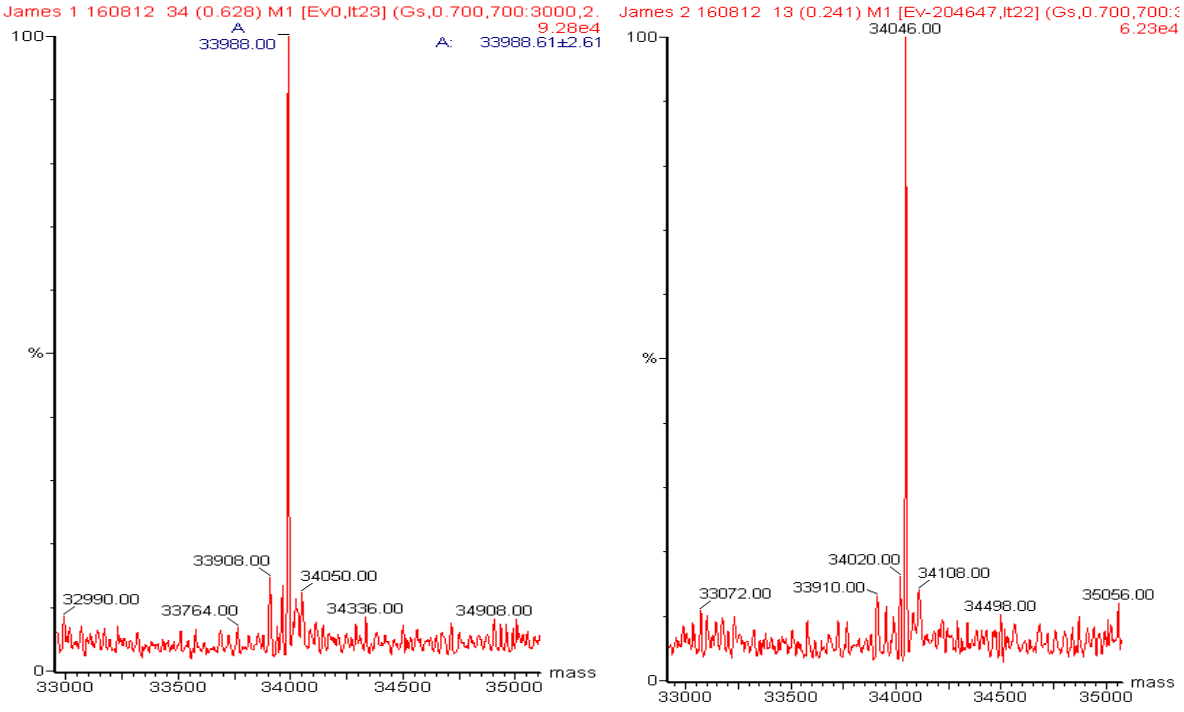


Figure 7.4: MS (MALDI) to show single alkylation of MOUSE(NAT2) after treatment with 2-iodoacetamide. **Left:** MS (MALDI) of unmodified MOUSE(NAT2) (1 mg/mL in 25 µL 95% aq. Tris•HCl (*p*H 8.0)/5% DMSO (*v/v*)). **Right:** MS (MALDI) of modified MOUSE(NAT2) (1 mg/mL in 25 µL 95% aq. Tris•HCl (*p*H 8.0)/5% DMSO (*v/v*)).

7.12. BCA Assay

Standards of bovine serum albumin (BSA) were prepared *via* serial dilutions in double-distilled H_2O to final concentrations of 0, 25, 125, 250, 500, 750, 1000, 1500 and 2000 µg/mL. The two test samples of *E. coli* cell lysate and pure recombinant MOUSE(NAT2) were diluted in double-distilled H_2O by a factor of 20 and 5 respectively. 25 µL of each standard and test solution were pipetted in triplicate into a 96-well plate (Corning). To every well was added 200 µL of working reagent (50:1 BCA Reagent A:BCA Reagent B (supplied in Pierce® BCA Protein Assay Kit, Thermo Scientific); Reagent A contains Na_2CO_3, $NaHCO_3$, bicinchoninic acid and sodium tartrate in 0.1 M aq. NaOH and Reagent B contains 4% aq. $CuSO_4$). The plate was then covered and incubated at 37 ^{o}C for 30 min. During this time, the wells develop a strong purple colour due to reduction of Cu^{2+} ions to Cu^{+} by protein and subsequent chelation of Cu^{+} ions by bicinchoninic acid. The absorbance of the samples was measured at 562 nm, a wavelength at which the absorbance is directly proportional to [protein] over the desired range. A concentration plot of absorbance against [BSA] for the standards was produced **(Figure 7.5)**; from this plot the concentrations of protein in undiluted *E. coli* cell lysate and recombinant MOUSE(NAT2) solutions were determined to be 14200 µg/mL and 3450 µg/mL respectively.

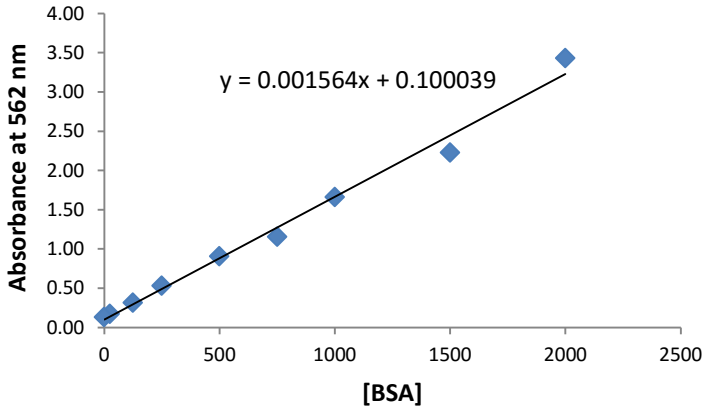


Figure 7.5: Standard plot of [BSA] against absorbance at 562 nm; points plotted at each concentration for the average of three repeat readings.

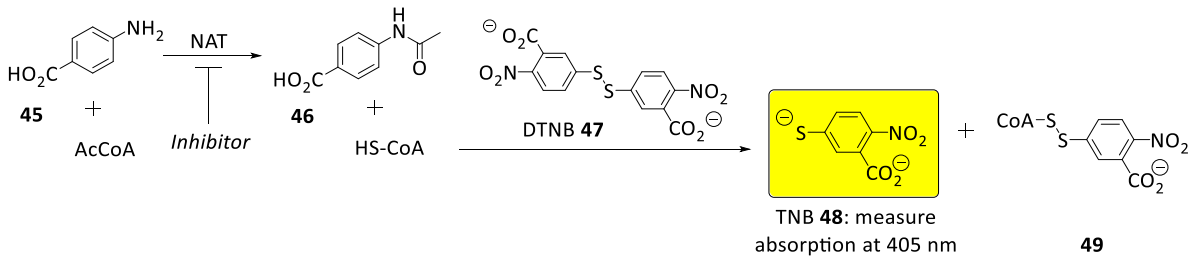
7.13. Protocols for Compound Evaluation

7.13.1. Acetyl CoA Hydrolysis Assay

The acetyl CoA hydrolysis assay monitors the rate of AcCoA hydrolysis by NATs and is based upon the reaction outlined in **Scheme 7.1**. This assay is an end-point assay used to test the inhibitory potency of synthesised compounds against MOUSE(NAT2), HUMAN(NAT1) or HUMAN(NAT2). Assays were carried out in flat-bottomed 96-well plates (Greiner) as outlined in **Table 7.3**, giving a final assay volume of 100 µL containing 5% (*v/v*) DMSO.

For an initial screen of inhibitory potency of a compound at a final concentration of 30 µM, assays were conducted in triplicate and the % specific NAT activity was calculated from a graph of OD_{405} against time. The % specific activity was calculated against a control assay (vehicle only); results in column graphs are reported as average values ± standard deviations.

In IC_{50} tests, a range of ten concentrations was selected for each compound, most often beginning at 10, 30 or 50 µM and diluting by a factor of two in each subsequent well. Assays were conducted in duplicate and % specific activity for each assay was determined relative to a control. KyPlot® software was then used to plot a curve of % specific activity against concentration using the IC50FUN model. This software determines the IC_{50} value, quoted ± one standard deviation, *via* the method of least squares, giving squared correlation coefficients (R^2) and confidence intervals (P).



Scheme 7.1: Acetyl CoA hydrolysis assay used to determine the potency of synthesised inhibitors against NATs.

Stage	Assay Well Component	Stock Concentration	Volume	Final Conditions
Preparation	DMSO (Control) *or* Inhibitor in DMSO	>99% purity *or* Various in >99% purity	5 µL	5% (*v/v*) *or* Various in 5% (*v/v*)
	Enzyme:* HUMAN(NAT1); HUMAN(NAT2); *or* MOUSE(NAT2)	0.015 mg/mL 0.5 mg/mL 0.010 mg/mL	10 µL 10 µL 10 µL	150 ng 5 µg 150 ng
	*p*ABA/5AS^	1.11 mM	45 µL	500 µM
Incubation	*Incubate at 37 °C for 5 min*			
Initiation	AcCoA	1 mM	40 µL	400 µM
Reaction	*Incubate at 37 °C for desired reaction time (various)*[#]			
Quench	DTNB	5mM in 6.4 M Guanidine•HCl, 20mM Tris•HCl (*p*H 7.5)	25 µL	1mM
Observation	*Record absorbance at 405 nm on a FLUORSTAR Omega® Plate Reader*			

Table 7.3: DTNB assay protocol. *"Enzyme" either refers to a $^{1}/_{400}$ dilution of stock MOUSE(NAT2) (4 mg/mL), $^{1}/_{100}$ dilution of stock HUMAN(NAT1) (1.5 mg/mL) or a $^{1}/_{10}$ dilution of stock HUMAN(NAT2) (5 mg/mL); 20 mM Tris•HCl (*p*H 8.0) was used as the dilution buffer. ^*p*ABA was the substrate used in assays against MOUSE(NAT2) or HUMAN(NAT1); 5AS was the substrate used in assays against HUMAN(NAT2). [#]Reaction in different wells on the same plate may be initiated with AcCoA at different time points as desired. For an initial activity test of an inhibitor at a concentration of 30 µM, 4 wells were used in each assay, initiated with AcCoA after 0, 5, 10 and 15 min respectively; quenching with DTNB occurred after 15 min. For an IC_{50} test, a single well was used in each assay, initiated with AcCoA after 0 min and quenched with DTNB after 10 min.

7.13.2. Cytotoxicity Studies Against the ZR-75-1 Cell Line

The ZR-75-1 cells to be used in cytotoxicity studies were split as previously **(Section 7.10.)**, into 25 cm^3 tissue culture flasks, and incubated at 37 °C in a 5% CO_2 environment for 24 h. After this time, 0.5% DMSO was added to each of the flasks containing the requisite inhibitor to a final concentration of 10 µM. Assays were conducted in duplicate. After a further 48 h, the supernatant growth medium from each flask was retained and pelleted, and the cells in each flask were detached and pelleted as previously. Each pellet was resuspended in 1 mL growth medium. 50 µL of this suspension was then added to 125 µL of PBS and 25 µL of trypan blue, and both live and dead cells counted using a haemocytometer.

7.13.3. Spectrophotometry

Visible spectra of each compound were recorded at *p*H 8, *p*H 13 and, for selected compounds, in the presence of MOUSE(NAT2). Unless otherwise stated, the concentrations and volumes of solutions used were as outlined in **Table 7.4**. All spectra were blank-corrected and normalised.

Spectral Conditions	Volume and Type of Buffer Solution Added	Inihibitor (Stock 300 µM in DMSO)		MOUSE(NAT2) (4 mg/mL in 20 mM Tris•HCl (*p*H 8))	
		Volume Added	Final Concentration	Volume Added	Final Concentration
***p*H 8**	95 µL 20mM Tris•HCl	5 µL	15 µM	0 µL	30 µM
***p*H 13.75**	95 µL 1 M NaOH	5 µL	15 µM	0 µL	30 µM
with MOUSE(NAT2)	70 µL 20 mM Tris•HCl	5 µL	15 µM	25 µL	30 µM

Table 7.4: Protocol for spectrophotometry. All samples were made up in 100 µL volumes in wells of a 96-well plate (Corning). The final inhibitor concentration used was 15 µM and the final MOUSE(NAT2) concentration used was 30 µM unless otherwise stated.

7.13.4. Titration Experiments to Determine *p*K_a Values

To determine the *p*K_a of an inhibitor, a full absorbance spectrum was recorded on a plate reader (Omega) for each compound in 14 differently buffered solutions in 5% (*v/v*) DMSO **(Table 7.5)**. 5 µL of the inhibitor in DMSO (stock concentration 2 mM) was added to 95 µL of buffer solution in a flat-bottomed 96-well plate (Corning), giving a final compound concentration of 100 µM. Recorded spectra were blank-corrected and normalised before λ_{max} was determined.

For each inhibitor, a graph of λ_{max} against *p*H was then plotted using GraphPad® software. A sigmoidal dose-response (variable slope) model was used to determine the *p*K_a by the method of least squares; *p*Ka values are quoted ± one standard deviation and squared correlation coefficients (R^2) are stated.

***p*H**	**Buffer**
2.00	4 M Glycine•HCl
4.00	20 mM Acetate•AcOH, 20 mM NaCl
6.00	20 mM MES•AcOH, 20 mM NaCl
7.00	20 mM HEPES•AcOH, 20 mM NaCl
7.50	20 mM Tris•HCl
8.00	20 mM Tris•HCl
8.48	20 mM Tris•HCl, 20 mM NaCl
9.02	20 mM Tris•HCl, 20 mM NaCl
9.54	20 mM CHES•NaOH, 20 mM NaCl
10.00	20 mM CHES•NaOH, 20mM NaCl
10.92	20 mM CAPS•NaOH, 20 mM NaCl
12.10	70 mM Na_2HPO_4•NaOH
12.93	35 mM Na_2HPO_4•NaOH
13.75	1 M NaOH

Table 7.5: Buffer solutions used for different *p*H measurements.

7.13.5. Determination of Absorption Coefficients

To determine molar absorption coefficients at *p*H 8 and 13.75, 5 µL of the inhibitor in DMSO (stock concentrations 4 mM, 2 mM, 1 mM, 0.5 mM) was added to each of four wells in a 96-well flat-bottomed plate (Corning) respectively. To this was added 95 µL 20 mM Tris•HCl (*p*H 8.0) and full visible spectra were recorded on a plate reader (Omega). Experiments were performed in duplicate. Spectra were blank-corrected and normalised and the absorbance at λ_{max} was recorded for each final concentration (200 µM, 100 µM, 50 µM, 25 µM). A plot of absorbance against concentration then yielded ε_N as the gradient divided by the path length of 0.315 cm.

To each of the wells, 10 µL 1 M aq. NaOH was then added and the procedure repeated to yield ε_{CB}, ensuring that a correction factor of $^{11}/_{10}$ was applied to the final inhibitor concentration in each well and to the path length.

7.13.6. Fluorescence Studies

Fluorescence spectra were recorded on a Varian Cary Eclipse Fluorescence Spectrophotometer. 5 µL of a stock solution of 3 mM compound in DMSO was added to 95 µL 20 mM Tris•HCl buffer (*p*H 8.0) to yield a final concentration of 150 µM, unless otherwise stated. Each scan consisted of an initial solvent blank measurement to remove noise or solvent scattering from peak analysis, and was subsequently subtracted from resultant spectra to yield blank-corrected spectra; a negative 95% 20 mM Tris•HCl/5% DMSO (*v/v*) control was also run. Where possible, λ_{ex} and λ_{em} were identified by 'zero order' scans (illumination of the sample with the full available range of electromagnetic radiation simultaneously); otherwise, measurements were recorded at 5 nm increments, starting at λ_{ex} = 200 nm. Spectra were recorded at a sensitivity voltage of 800 V unless otherwise stated. Acidic and basic conditions were achieved by addition of 5 µL of 1 M aq. HCl or NaOH respectively. For fluorescence measurements carried out in the presence of recombinant MOUSE(NAT2), *E. coli* cell extracts or ZR-75-1 cell extracts, 5 µL 0.3 mM compound in DMSO was added to 95 µL of either neat cell extract or the stated dilution of recombinant protein or cell extract in 20 mM Tris•HCl (*p*H 8.0), to yield a final inhibitor concentration of 15 µM; all spectra were blank-corrected with the inhibitor solution in DMSO replaced by DMSO only.

7.13.7. Docking Studies

All images showing protein structures were generated using the software PyMOL (W. L. DeLano (2002) PyMOL, DeLano Scientific, San Carlos, CA). Prior to docking a ligand into the hNAT1 active site (pdb: 2PQT),[247b] the ground state conformation of the ligand was predicted using the molecular editor Avogadro, and the protein was protonated to be consistent with the assay conditions of *p*H 8. The docking simulations and the analysis of the possible interactions between the protein and the ligand were performed using GOLD® v.5.2.[282] The docking site was defined as a region of 10 Å within the active pocket of the enzyme and the generated solutions were ranked using the GOLD® Score Fitness function.

Each docking simulation was repeated ten times to ensure the observed solutions were consistent.

7.13.8. DFT Modelling Studies

The conformational profile resulting from rotation around the selected bonds was obtained by means of DFT calculations at the M06-2X/6-31G* level of theory[285] using the Gaussian09 package.[286] Starting from a conformation of minimal energy, the energy of molecular arrangements obtained by successive 15^{o} rotations around the corresponding bond, from 14.5^{o} to 359.5^{o}, was calculated without any further geometrical restriction in the gas phase.

Bibliography

1. (a) Mahmood, T.; Yang, P.-C., Western blot: technique, theory, and trouble shooting. *N Am J Med Sci* **2012**, *4* (9), 429-434; (b) Jensen, E. C., The basics of western blotting. *Anat Rec* **2012**, *295* (3), 369-371.
2. Pace, C. N.; Vajdos, F.; Fee, L.; Grimsley, G.; Gray, T., How to measure and predict the molar absorption coefficient of a protein. *Protein Sci* **1995**, *4* (11), 2411-2423.
3. (a) Bouguer, P., *Essai d'Optique, sur la gradation de la lumière*. Claude Jombert: Paris, France, **1729**; (b) Lambert, J. H., *Photometria sive de mensure et gradibus luminis, colorum et umbrae*. Eberhardt Klett: Augsburg, Germany, 1760; (c) Beer, A., Bestimmung der Absorption des rothen Lichts in fabrigen Flüssigkeiten. *Annalen der Physik und Chemie* **1852**, *86*, 78-88.
4. Leca - Bouvier, B.; Blum, L. J., Biosensors for protein detection: a review. *Anal Lett* **2005**, *38* (10), 1491-1517.
5. Lowry, O. H.; Rosebrough, N. J.; Farr, A. L.; Randall, R. J., Protein measurement with the folin phenol reagent. *J Biol Chem* **1951**, *193* (1), 265-275.
6. (a) Kresge, N.; Simoni, R. D.; Hill, R. L., The most highly cited paper in publishing history: protein determination by Oliver H. Lowry. *J Biol Chem* **2005**, *280* (28), e25; (b) Van Noorden, R.; Maher, B.; Nuzzo, R., The top 100 papers. *Nature* **2014**, *514* (7524), 550-553.
7. (a) Gornall, A. G.; Bardawill, C. J.; David, M. M., Determination of serum proteins by means of the biuret reaction. *J Biol Chem* **1949**, *177* (2), 751-766; (b) Janairo, G.; Sy, M. L.; Yap, L.; Llanos-Lazaro, N.; Robles, J., Determination of the sensitivity range of biuret test for undergraduate biochemistry experiments. *e-JST* **2011**, *6* (5), 77-83.
8. Folin, O.; Ciocalteu, V., On tyrosine and trytophan determinations in proteins. *J Biol Chem* **1927**, *73* (2), 627-650.
9. Bradford, M. M., A rapid and sensitive method for the quantitation of microgram quantities of protein utilizing the principle of protein-dye binding. *Anal Biochem* **1976**, *72*, 248-254.
10. Smith, P. K.; Krohn, R. I.; Hermanson, G. T.; Mallia, A. K.; Gartner, F. H.; Provenzano, M. D.; Fujimoto, E. K.; Goeke, N. M.; Olson, B. J.; Klenk, D. C., Measurement of protein using bicinchoninic acid. *Anal Biochem* **1985**, *150* (1), 76-85.
11. Guo, Z.-X.; Hao, Y.-M.; Cong, X.; Shen, H.-X., Application of the dibromohydroxyphenylfluorone–molybdenum(VI) complex to the sensitive spectrophotometric determination of protein. *Anal Chim Acta* **2000**, *403* (1–2), 225-233.
12. Capitán-Vallvey, L. F.; Duque, O.; Mirón-García, G.; Checa-Moreno, R., Determination of protein content using a solid phase spectrophotometric procedure. *Anal Chim Acta* **2001**, *433* (1), 155-163.
13. Chen, H.; Wang, L.; Wang, L.; Wang, G.; Li, L.; Xu, F., Preparation of novel composite nanoclusters and their application in the ultrasensitive detection of proteins. *Anal Chim Acta* **2004**, *521* (1), 9-15.
14. Tsukagoshi, K.; Nakahama, K.; Nakajima, R., Direct detection of biomolecules in a capillary electrophoresis-chemiluminescence detection system. *Anal Chem* **2004**, *76* (15), 4410-4415.

15. Jiang, C.; Luo, L., Spectrofluorimetric determination of human serum albumin using a doxycycline-europium probe. *Anal Chim Acta* **2004**, *506* (2), 171-175.
16. Chen, X. W.; Huang, L. L.; Wang, J. H., Studies on the toluidine blue dimer as a fluorescence probe for protein assays. *Anal Lett* **2007**, *40* (16), 3014-3024.
17. Dong, L.; Li, Y.; Zhang, Y.; Chen, X.; Hu, Z., A flow injection sampling resonance light scattering system for total protein determination in human serum. *Spectrochim Acta A* **2007**, *66* (4–5), 1317-1322.
18. Kang, J.; Li, J.; Huang, Z.; Li, X.; Tang, J.; Zhang, Y., Determination of albumin using the chemiluminescence of $Tb^{3+}/K_2S_2O_8$ System. *Anal Lett* **2011**, *44* (4), 626-636.
19. Coulet, P. R., What is a biosensor? In *Biosensor Principles and Applications*, Blum, L. J.; Coulet, P. R., Eds. CRC Press: New York, USA, **1991**; pp 1-7.
20. Gronow, M., Biosensors. *Trends Biochem Sci* **1984**, *9* (8), 336-340.
21. (a) Borisov, S. M.; Wolfbeis, O. S., Optical biosensors. *Chem Rev* **2008**, *108* (2), 423-461; (b) Fan, X.; White, I. M.; Shopova, S. I.; Zhu, H.; Suter, J. D.; Sun, Y., Sensitive optical biosensors for unlabeled targets: a review. *Anal Chim Acta* **2008**, *620* (1–2), 8-26; (c) Cooper, M. A., Optical biosensors in drug discovery. *Nat Rev Drug Discov* **2002**, *1* (7), 515-528.
22. Clark, L. C.; Lyons, C., Electrode systems for continuous monitoring in cardiovascular surgery. *Ann NY Acad Sci* **1962**, *102* (1), 29-45.
23. (a) Soldatkin, O. O.; Peshkova, V. M.; Dzyadevych, S. V.; Soldatkin, A. P.; Jaffrezic-Renault, N.; El'skaya, A. V., Novel sucrose three-enzyme conductometric biosensor. *Mat Sci Eng C* **2008**, *28* (5–6), 959-964; (b) Martinez, R. Prevalence of diabetes in the world, 2013. healthintelligence.drupalgardens.com/content/prevalence-diabetes-world-2013 (accessed 26/12/2014).
24. Silman, I. H.; Katchalski, E., Water-insoluble derivatives of enzymes, antigens, and antibodies. *Annu Rev Biochem* **1966**, *35* (1), 873-908.
25. Updike, S. J.; Hicks, G. P., The enzyme electrode. *Nature* **1967**, *214* (5092), 986-988.
26. Guilbault, G. G.; Montalvo, J. G., Urea-specific enzyme electrode. *J Am Chem Soc* **1969**, *91* (8), 2164-2165.
27. Hedstrom, L., Enzyme specificity and selectivity. In *eLS*, John Wiley & Sons, Ltd., **2001**.
28. (a) Konry, T.; Novoa, A.; Cosnier, S.; Marks, R. S., Development of an "electroptode" immunosensor: indium tin oxide-coated optical fiber tips conjugated with an electropolymerized thin film with conjugated cholera toxin B subunit. *Anal Chem* **2003**, *75* (11), 2633-2639; (b) Leshem, B.; Sarfati, G.; Novoa, A.; Breslav, I.; Marks, R. S., Photochemical attachment of biomolecules onto fibre-optics for construction of a chemiluminescent immunosensor. *Luminescence* **2004**, *19* (2), 69-77; (c) Herrmann, S.; Leshem, B.; Landes, S.; Rager-Zisman, B.; Marks, R. S., Chemiluminescent optical fiber immunosensor for the detection of anti-West Nile virus IgG. *Talanta* **2005**, *66* (1), 6-14; (d) Song, X.; Swanson, B. I., Direct, ultrasensitive, and selective optical detection of protein toxins using multivalent interactions. *Anal Chem* **1999**, *71* (11), 2097-2107.
29. (a) Anderson, F. P.; Miller, W. G., Fiber-optic immunochemical sensor for continuous, reversible measurement of phenytoin. *Clin Chem* **1988**, *34* (7), 1417-1421; (b) Hanbury, C. M.; Miller, W. G.; Harris, R. B., Antibody characteristics for a continuous response fiber optic immunosensor for theophylline. *Biosens Bioelectron* **1996**, *11* (11), 1129-1138; (c) Sheikh, S. H.; Mulchandani, A., Continuous-flow fluoro-immunosensor for paclitaxel measurement. *Biosens Bioelectron* **2001**, *16* (9-12), 647-652.

30. Cummins, C. M.; Koivunen, M. E.; Stephanian, A.; Gee, S. J.; Hammock, B. D.; Kennedy, I. M., Application of europium(III) chelate-dyed nanoparticle labels in a competitive atrazine fluoroimmunoassay on an ITO waveguide. *Biosens Bioelectron* **2006**, *21* (7), 1077-1085.
31. (a) R. Ryan, M.; P. Lowry, J.; D. O'Neill, R., Biosensor for neurotransmitter L-glutamic acid designed for efficient use of L-glutamate oxidase and effective rejection of interference. *Analyst* **1997**, *122* (11), 1419-1424; (b) Baron, R.; Zayats, M.; Willner, I., Dopamine-, L-DOPA-, adrenaline-, and noradrenaline-induced growth of Au nanoparticles: assays for the detection of neurotransmitters and of tyrosinase activity. *Anal Chem* **2005**, *77* (6), 1566-1571; (c) Doong, R.-A.; Shih, H.-M., Glutamate optical biosensor based on the immobilization of glutamate dehydrogenase in titanium dioxide sol-gel matrix. *Biosens Bioelectron* **2006**, *22* (2), 185-191.
32. (a) Thompson, R. B.; Patchan, M. W., Lifetime-based fluorescence energy transfer biosensing of zinc. *Anal Biochem* **1995**, *227* (1), 123-128; (b) Thompson, R. B.; Jones, E. R., Enzyme-based fiber optic zinc biosensor. *Anal Chem* **1993**, *65* (6), 730-734; (c) Zeng, H.-H.; Thompson, R. B.; Maliwal, B. P.; Fones, G. R.; Moffett, J. W.; Fierke, C. A., Real-time determination of picomolar free Cu(II) in seawater using a fluorescence-based fiber optic biosensor. *Anal Chem* **2003**, *75* (24), 6807-6812; (d) Lundgren, J. S.; Salins, L. L. E.; Kaneva, I.; Daunert, S., A dynamical investigation of acrylodan-labeled mutant phosphate binding protein. *Anal Chem* **1998**, *71* (3), 589-595; (e) Shrestha, S.; Salins, L. L.; Mark Ensor, C.; Daunert, S., Rationally designed fluorescently labeled sulfate-binding protein mutants: evaluation in the development of a sensing system for sulfate. *Biotechnol Bioeng* **2002**, *78* (5), 517-526.
33. (a) Blyth, D. J.; Aylott, J. W.; Moir, J. W.; Richardson, D. J.; Russell, D. A., Optical biosensing of nitric oxide using the metalloprotein cytochrome C'. *Analyst* **1999**, *124* (2), 129-134; (b) Barker, S. L.; Kopelman, R.; Meyer, T. E.; Cusanovich, M. A., Fiber-optic nitric oxide-selective biosensors and nanosensors. *Anal Chem* **1998**, *70* (5), 971-976; (c) Zhujun, Z.; Seitz, W. R., Optical sensor for oxygen based on immobilized hemoglobin. *Anal Chem* **1986**, *58* (1), 220-222.
34. (a) Zhang, C.; Wei, Z.-H.; Ye, B.-C., Imaging and tracing of intracellular metabolites utilizing genetically encoded fluorescent biosensors. *Biotechnol J* **2013**, *8* (11), 1280-1291; (b) Li, L.; Wang, Y.; Pan, L.; Shi, Y.; Cheng, W.; Shi, Y.; Yu, G., A nanostructured conductive hydrogels-based biosensor platform for human metabolite detection. *Nano Letters* **2015**, *15* (2), 1146-1151; (c) Boero, C.; Casulli, M. A.; Olivo, J.; Foglia, L.; Orso, E.; Mazza, M.; Carrara, S.; De Micheli, G., Design, development, and validation of an *in situ* biosensor array for metabolite monitoring of cell cultures. *Biosens Bioelectron* **2014**, *61*, 251-259.
35. (a) Schultz, J. S.; Mansouri, S.; Goldstein, I. J., Affinity sensor: a new technique for developing implantable sensors for glucose and other metabolites. *Diabetes Care* **1982**, *5* (3), 245-253; (b) Medintz, I. L.; Clapp, A. R.; Mattoussi, H.; Goldman, E. R.; Fisher, B.; Mauro, J. M., Self-assembled nanoscale biosensors based on quantum dot FRET donors. *Nat Mater* **2003**, *2* (9), 630-638.
36. (a) Graham, C. R.; Leslie, D.; Squirrell, D. J., Gene probe assays on a fibre-optic evanescent wave biosensor. *Biosens Bioelectron* **1992**, *7* (7), 487-493; (b) Watts, H. J.; Yeung, D.; Parkes, H., Real-time detection and quantification of DNA hybridization by an optical biosensor. *Anal Chem* **1995**, *67* (23), 4283-4289; (c) Pilevar, S.; Davis, C. C.;

Portugal, F., Tapered optical fiber sensor using near-infrared fluorophores to assay hybridization. *Anal Chem* **1998**, *70* (10), 2031-2037.

37. (a) Kulagina, N. V.; Lassman, M. E.; Ligler, F. S.; Taitt, C. R., Antimicrobial peptides for detection of bacteria in biosensor assays. *Anal Chem* **2005**, *77* (19), 6504-6508; (b) Kulagina, N. V.; Shaffer, K. M.; Anderson, G. P.; Ligler, F. S.; Taitt, C. R., Antimicrobial peptide-based array for *Escherichia coli* and *Salmonella* screening. *Anal Chim Acta* **2006**, *575* (1), 9-15; (c) Mukundan, H.; Xie, H.; Price, D.; Kubicek-Sutherland, J. Z.; Grace, W. K.; Anderson, A. S.; Martinez, J. S.; Hartman, N.; Swanson, B. I., Quantitative multiplex detection of pathogen biomarkers on multichannel waveguides. *Anal Chem* **2010**, *82* (1), 136-144; (d) Ko, S.; Grant, S. A., A novel FRET-based optical fiber biosensor for rapid detection of *Salmonella typhimurium*. *Biosens Bioelectron* **2006**, *21* (7), 1283-1290.
38. Lodish, H.; Berk, A.; Zipursky, S. L.; Matsudaira, P.; Baltimore, D.; Darnell, J., The molecules of life. In *Molecular Cell Biology*, 4th ed.; W. H. Freeman: New York, USA, **2000**.
39. (a) Soto, C., Unfolding the role of protein misfolding in neurodegenerative diseases. *Nat Rev Neurosci* **2003**, *4* (1), 49-60; (b) Allred, D. C.; Clark, G. M.; Elledge, R.; Fuqua, S. A. W.; Brown, R. W.; Chamness, G. C.; Osborne, C. K.; McGuire, W. L., Association of p53 Protein Expression With Tumor Cell Proliferation Rate and Clinical Outcome in Node-Negative Breast Cancer. *J Natl Cancer I* **1993**, *85* (3), 200-206; (c) Cornford, P. A.; Dodson, A. R.; Parsons, K. F.; Desmond, A. D.; Woolfenden, A.; Fordham, M.; Neoptolemos, J. P.; Ke, Y.; Foster, C. S., Heat shock protein expression independently predicts clinical outcome in prostate cancer. *Cancer Res* **2000**, *60* (24), 7099-7105; (d) Wang, Z.; Moult, J., SNPs, protein structure, and disease. *Hum Mutat* **2001**, *17* (4), 263-270.
40. Zhang, L.; Lv, D.; Su, W.; Liu, Y.; Chen, Y.; Xiang, R., Detection of cancer biomarkers with nanotechnology. *Am J Biochem Biotechnol* **2013**, *9* (1), 71-89.
41. (a) Lee, M. H.; Kim, J. S.; Sessler, J. L., Small molecule-based ratiometric fluorescence probes for cations, anions, and biomolecules. *Chem Soc Rev* **2015**, *44* (13), 4185-4191; (b) Song, D.; Cho, S.; Han, Y.; You, Y.; Nam, W., Ratiometric fluorescent probes for detection of intracellular singlet oxygen. *Org Lett* **2013**, *15* (14), 3582-3585; (c) Huang, C.; Jia, T.; Tang, M.; Yin, Q.; Zhu, W.; Zhang, C.; Yang, Y.; Jia, N.; Xu, Y.; Qian, X., Selective and ratiometric fluorescent trapping and quantification of protein vicinal dithiols and *in situ* dynamic tracing in living cells. *J Am Chem Soc* **2014**, *136* (40), 14237-14244; (d) Lepesheva, G. I.; Azeva, T. N.; Knyukshto, V. N.; Chashchin, V. L.; Usanov, S. A., A model of optical immunosensor for hemoproteins based on Langmuir–Blodgett films of FITC-labelled immunoglobulin G. *Sens Actuat B-Chem* **2000**, *68* (1-3), 27-33.
42. Papkovsky, D. B.; O'Riordan, T. C.; Guilbault, G. G., An immunosensor based on the glucose oxidase label and optical oxygen detection. *Anal Chem* **1999**, *71* (8), 1568-1573.
43. Narang, U.; Anderson, G. P.; Ligler, F. S.; Burans, J., Fiber optic-based biosensor for ricin. *Biosens Bioelectron* **1997**, *12* (9-10), 937-945.
44. (a) Nakagawa, T.; Miyoshi, E.; Yakushijin, T.; Hiramatsu, N.; Igura, T.; Hayashi, N.; Taniguchi, N.; Kondo, A., Glycomic analysis of alpha-fetoprotein L3 in hepatoma cell lines and hepatocellular carcinoma patients. *J Proteome Res* **2008**, *7* (6), 2222-2233; (b) D'Antiga, L.; Vallortigara, F.; Cillo, U.; Talenti, E.; Rugge, M.; Zancan, L.; Dall'Igna, P.;

Salvo, G. L. D.; Perilongo, G., Features predicting unresectability in hepatoblastoma. *Cancer* **2007**, *110* (5), 1050-1058.

45. (a) Fan, A.; Lau, C.; Lu, J., Magnetic bead-based chemiluminescent metal immunoassay with a colloidal gold label. *Anal Chem* **2005**, *77* (10), 3238-3242; (b) Zhang, R.; Nakajima, H.; Soh, N.; Nakano, K.; Masadome, T.; Nagata, K.; Sakamoto, K.; Imato, T., Sequential injection chemiluminescence immunoassay for nonionic surfactants by using magnetic microbeads. *Anal Chim Acta* **2007**, *600* (1–2), 105-113; (c) Stoeva, S. I.; Lee, J.-S.; Smith, J. E.; Rosen, S. T.; Mirkin, C. A., Multiplexed detection of protein cancer markers with biobarcoded nanoparticle probes. *J Am Chem Soc* **2006**, *128* (26), 8378-8379.
46. Bi, S.; Yan, Y.; Yang, X.; Zhang, S., Gold nanolabels for new enhanced chemiluminescence immunoassay of alpha-fetoprotein based on magnetic beads. *Chem-Eur J* **2009**, *15* (18), 4704-4709.
47. Bi, S.; Zhou, H.; Zhang, S., Multilayers enzyme-coated carbon nanotubes as biolabel for ultrasensitive chemiluminescence immunoassay of cancer biomarker. *Biosens Bioelectron* **2009**, *24* (10), 2961-2966.
48. Jokerst, J. V.; Raamanathan, A.; Christodoulides, N.; Floriano, P. N.; Pollard, A. A.; Simmons, G. W.; Wong, J.; Gage, C.; Furmaga, W. B.; Redding, S. W.; McDevitt, J. T., Nano-bio-chips for high performance multiplexed protein detection: determinations of cancer biomarkers in serum and saliva using quantum dot bioconjugate labels. *Biosens Bioelectron* **2009**, *24* (12), 3622-3629.
49. Ambrosi, A.; Airò, F.; Merkoçi, A., Enhanced gold nanoparticle based ELISA for a breast cancer biomarker. *Anal Chem* **2009**, *82* (3), 1151-1156.
50. Zhou, J.; Gan, N.; Hu, F.; Li, T.; Zhou, H.; Li, X.; Zheng, L., A single antibody sandwich electrochemiluminescence immunosensor based on protein magnetic molecularly imprinted polymers mimicking capture probes. *Sens Actuat B-Chem* **2013**, *186*, 300-307.
51. Zhou, J.; Gan, N.; Li, T.; Hu, F.; Li, X.; Wang, L.; Zheng, L., A cost-effective sandwich electrochemiluminescence immunosensor for ultrasensitive detection of HIV-1 antibody using magnetic molecularly imprinted polymers as capture probes. *Biosens Bioelectron* **2014**, *54*, 199-206.
52. Weiss, R. A., How does HIV cause AIDS? *Science* **1993**, *260* (5112), 1273-1279.
53. Cecchin, D.; de la Rica, R.; Bain, R. E. S.; Finnis, M. W.; Stevens, M. M.; Battaglia, G., Plasmonic ELISA for the detection of gp120 at ultralow concentrations with the naked eye. *Nanoscale* **2014**, *6* (16), 9559-9562.
54. Maragos, C. M.; Thompson, V. S., Fiber-optic immunosensor for mycotoxins. *Nat Toxins* **1999**, *7* (6), 371-376.
55. German, I.; Kennedy, R. T., Rapid simultaneous determination of glucagon and insulin by capillary electrophoresis immunoassays. *J Chromatogr B Biomed Sci Appl* **2000**, *742* (2), 353-362.
56. Babu, C. V. S.; Chung, B. C.; Lho, D. S.; Yoo, Y. S., Capillary electrophoretic competitive immunoassay with laser-induced fluorescence detection for methionine-enkephalin. *J Chromatogr A* **2006**, *1111* (2), 133-138.
57. Schmalzing, D.; Nashabeh, W., Capillary electrophoresis based immunoassays: a critical review. *Electrophoresis* **1997**, *18* (12-13), 2184-2193.
58. Hayes, M. A.; Polson, N. A.; Phayre, A. N.; Garcia, A. A., Flow-based microimmunoassay. *Anal Chem* **2001**, *73* (24), 5896-5902.

59. Zhao, X.; Shippy, S. A., Competitive immunoassay for microliter protein samples with magnetic beads and near-infrared fluorescence detection. *Anal Chem* **2004**, *76* (7), 1871-1876.
60. Barnard, S. M.; Walt, D. R., Chemical sensors based on controlled-release polymer systems. *Science* **1991**, *251* (4996), 927-929.
61. (a) Liedberg, B.; Nylander, C.; Lundstrom, I., Biosensing with surface plasmon resonance - how it all started. *Biosens Bioelectron* **1995**, *10* (8), i-ix; (b) Liedberg, B.; Nylander, C.; Lunström, I., Surface plasmon resonance for gas detection and biosensing. *Sens Actuat* **1983**, *4*, 299-304.
62. Matsubara, K.; Kawata, S.; Minami, S., Optical chemical sensor based on surface plasmon measurement. *Appl Opt* **1988**, *27* (6), 1160-1163.
63. Liedberg, B.; Lundström, I.; Stenberg, E., Principles of biosensing with an extended coupling matrix and surface plasmon resonance. *Sens Actuat B-Chem* **1993**, *11* (1-3), 63-72.
64. Sharma, A. K.; Jha, R.; Gupta, B. D., Fiber-optic sensors based on surface plasmon resonance: a comprehensive review. *IEEE Sens J* **2007**, *7* (8), 1118-1129.
65. Alleyne, C. J.; Kirk, A. G.; McPhedran, R. C.; Nicorovici, N. A.; Maystre, D., Enhanced SPR sensitivity using periodic metallic structures. *Opt Express* **2007**, *15* (13), 8163-8169.
66. Biacore Life Sciences. https://www.biacore.com/lifesciences/index.html (accessed 02/01/2015).
67. Haasnoot, W.; Olieman, K.; Cazemier, G.; Verheijen, R., Direct biosensor immunoassays for the detection of nonmilk proteins in milk powder. *J Agric Food Chem* **2001**, *49* (11), 5201-5206.
68. Wink, T.; van Zuilen, S. J.; Bult, A.; van Bennkom, W. P., Self-assembled monolayers for biosensors. *Analyst* **1997**, *122* (4), 43R-50R.
69. Bain, C. D.; Troughton, E. B.; Tao, Y. T.; Evall, J.; Whitesides, G. M.; Nuzzo, R. G., Formation of monolayer films by the spontaneous assembly of organic thiols from solution onto gold. *J Am Chem Soc* **1989**, *111* (1), 321-335.
70. Spinke, J.; Liley, M.; Guder, H. J.; Angermaier, L.; Knoll, W., Molecular recognition at self-assembled monolayers: the construction of multicomponent multilayers. *Langmuir* **1993**, *9* (7), 1821-1825.
71. Lee, J. W.; Sim, S. J.; Cho, S. M.; Lee, J., Characterization of a self-assembled monolayer of thiol on a gold surface and the fabrication of a biosensor chip based on surface plasmon resonance for detecting anti-GAD antibody. *Biosens Bioelectron* **2005**, *20* (7), 1422-1427.
72. Baekkeskov, S.; Aanstoot, H. J.; Christgau, S.; Reetz, A.; Solimena, M.; Cascalho, M.; Folli, F.; Richter-Olesen, H.; De Camilli, P., Identification of the 64K autoantigen in insulin-dependent diabetes as the GABA-synthesizing enzyme glutamic acid decarboxylase. *Nature* **1990**, *347* (6289), 151-156.
73. Choi, S. H.; Lee, J. W.; Sim, S. J., Enhancement of the sensitivity of surface plasmon resonance (SPR) immunosensor for the detection of anti-GAD antibody by changing the *p*H for streptavidin immobilization. *Enzyme Microb Tech* **2004**, *35* (6-7), 683-687.
74. Truong, P. L.; Kim, B. W.; Sim, S. J., Rational aspect ratio and suitable antibody coverage of gold nanorod for ultra-sensitive detection of a cancer biomarker. *Lab Chip* **2012**, *12* (6), 1102-1109.
75. (a) Anker, J. N.; Hall, W. P.; Lyandres, O.; Shah, N. C.; Zhao, J.; Van Duyne, R. P., Biosensing with plasmonic nanosensors. *Nat Mater* **2008**, *7* (6), 442-453; (b) Mock, J. J.;

Smith, D. R.; Schultz, S., Local refractive index dependence of plasmon resonance spectra from individual nanoparticles. *Nano Lett* **2003**, *3* (4), 485-491.

76. Catalona, W. J.; Richie, J. P.; Ahmann, F. R.; Hudson, M. A.; Scardino, P. T.; Flanigan, R. C.; deKernion, J. B.; Ratliff, T. L.; Kavoussi, L. R.; Dalkin, B. L.; et al., Comparison of digital rectal examination and serum prostate specific antigen in the early detection of prostate cancer: results of a multicenter clinical trial of 6,630 men. *J Urol* **1994**, *151* (5), 1283-1290.
77. Gokarna, A.; Jin, L. H.; Hwang, J. S.; Cho, Y. H.; Lim, Y. T.; Chung, B. H.; Youn, S. H.; Choi, D. S.; Lim, J. H., Quantum dot-based protein micro- and nanoarrays for detection of prostate cancer biomarkers. *Proteomics* **2008**, *8* (9), 1809-1818.
78. Aćimović, S. S.; Ortega, M. A.; Sanz, V.; Berthelot, J.; Garcia-Cordero, J. L.; Renger, J.; Maerkl, S. J.; Kreuzer, M. P.; Quidant, R., LSPR chip for parallel, rapid, and sensitive detection of cancer markers in serum. *Nano Letters* **2014**, *14* (5), 2636-2641.
79. Jie, G.; Wang, L.; Zhang, S., Magnetic electrochemiluminescent Fe_3O_4/CdSe-CdS nanoparticle/polyelectrolyte nanocomposite for highly efficient immunosensing of a cancer biomarker. *Chemistry* **2011**, *17* (2), 641-648.
80. Duffy, M. J., Carcinoembryonic antigen as a marker for colorectal cancer: is it clinically useful? *Clin Chem* **2001**, *47* (4), 624-630.
81. Myung, N.; Ding, Z.; Bard, A. J., Electrogenerated chemiluminescence of CdSe nanocrystals. *Nano Lett* **2002**, *2* (11), 1315-1319.
82. Liu, X.; Dai, Q.; Austin, L.; Coutts, J.; Knowles, G.; Zou, J.; Chen, H.; Huo, Q., A one-step homogeneous immunoassay for cancer biomarker detection using gold nanoparticle Probes coupled with dynamic light scattering. *J Am Chem Soc* **2008**, *130* (9), 2780-2782.
83. Huo, Q., Protein complexes/aggregates as potential cancer biomarkers revealed by a nanoparticle aggregation immunoassay. *Colloid Surface B* **2010**, *78* (2), 259-265.
84. Rodríguez-Lorenzo, L.; de la Rica, R.; Álvarez-Puebla, R. A.; Liz-Marzán, L. M.; Stevens, M. M., Plasmonic nanosensors with inverse sensitivity by means of enzyme-guided crystal growth. *Nat Mater* **2012**, *11* (7), 604-607.
85. Tuerk, C.; Gold, L., Systematic evolution of ligands by exponential enrichment: RNA ligands to bacteriophage T4 DNA polymerase. *Science* **1990**, *249* (4968), 505-510.
86. (a) Bunka, D. H.; Stockley, P. G., Aptamers come of age - at last. *Nat Rev Microbiol* **2006**, *4* (8), 588-596; (b) Famulok, M.; Mayer, G., Aptamers and SELEX in Chemistry & Biology. *Chem Biol* **2014**, *21* (9), 1055-1058.
87. (a) Cass, A. E.; Zhang, Y., Nucleic acid aptamers: ideal reagents for point-of-care diagnostics? *Faraday Discuss* **2011**, *149*, 49-61; discussion 63-77; (b) Famulok, M.; Mayer, G., Aptamer modules as sensors and detectors. *Acc Chem Res* **2011**, *44* (12), 1349-1358; (c) Drolet, D. W.; Moon-McDermott, L.; Romig, T. S., An enzyme-linked oligonucleotide assay. *Nat Biotech* **1996**, *14* (8), 1021-1025.
88. Heyduk, T.; Heyduk, E., Molecular beacons for detecting DNA binding proteins. *Nat Biotech* **2002**, *20* (2), 171-176.
89. Heyduk, E.; Heyduk, T., Nucleic acid-based fluorescence sensors for detecting proteins. *Anal Chem* **2005**, *77* (4), 1147-1156.
90. Potyrailo, R. A.; Conrad, R. C.; Ellington, A. D.; Hieftje, G. M., Adapting selected nucleic acid ligands (aptamers) to biosensors. *Anal Chem* **1998**, *70* (16), 3419-3425.

91. McCauley, T. G.; Hamaguchi, N.; Stanton, M., Aptamer-based biosensor arrays for detection and quantification of biological macromolecules. *Anal Biochem* **2003**, *319* (2), 244-250.
92. (a) Elghanian, R.; Storhoff, J. J.; Mucic, R. C.; Letsinger, R. L.; Mirkin, C. A., Selective colorimetric detection of polynucleotides based on the distance-dependent optical properties of gold nanoparticles. *Science* **1997**, *277* (5329), 1078-1081; (b) Cho, M.; Han, M. S.; Ban, C., Detection of mismatched DNAs *via* the binding affinity of MutS using a gold nanoparticle-based competitive colorimetric method. *Chem Commun* **2008**, *38*, 4573-4575; (c) Lin, J.-H.; Chang, C.-W.; Wu, Z.-H.; Tseng, W.-L., Colorimetric assay for *S*-adenosylhomocysteine hydrolase activity and inhibition using fluorosurfactant-capped gold nanoparticles. *Anal Chem* **2010**, *82* (21), 8775-8779; (d) Lin, C.-Y.; Yu, C.-J.; Lin, Y.-H.; Tseng, W.-L., Colorimetric sensing of silver(I) and mercury(II) ions based on an assembly of Tween 20-stabilized gold nanoparticles. *Anal Chem* **2010**, *82* (16), 6830-6837; (e) Liu, J.; Lu, Y., Fast colorimetric sensing of adenosine and cocaine based on a general sensor design involving aptamers and nanoparticles. *Angew Chem Int Ed* **2006**, *45* (1), 90-94; (f) Kim, Y. S.; Kim, J. H.; Kim, I. A.; Lee, S. J.; Jurng, J.; Gu, M. B., A novel colorimetric aptasensor using gold nanoparticle for a highly sensitive and specific detection of oxytetracycline. *Biosens Bioelectron* **2010**, *26* (4), 1644-1649.
93. (a) Sato, K.; Hosokawa, K.; Maeda, M., Rapid aggregation of gold nanoparticles induced by non-cross-linking DNA hybridization. *J Am Chem Soc* **2003**, *125* (27), 8102-8103; (b) Sato, K.; Hosokawa, K.; Maeda, M., Non-cross-linking gold nanoparticle aggregation as a detection method for single-base substitutions. *Nucl Acids Res* **2005**, *33* (1), e4.
94. Lee, S.; Manjunatha, D. H.; Jeon, W.; Ban, C., Cationic surfactant-based colorimetric detection of *Plasmodium* lactate dehydrogenase, a biomarker for malaria, using the specific DNA aptamer. *PLoS ONE* **2014**, *9* (7), e100847.
95. (a) Laromaine, A.; Koh, L.; Murugesan, M.; Ulijn, R. V.; Stevens, M. M., Protease-triggered dispersion of nanoparticle assemblies. *J Am Chem Soc* **2007**, *129* (14), 4156-4157; (b) Zhang, J.; Wang, L.; Zhang, H.; Boey, F.; Song, S.; Fan, C., Aptamer-based multicolor fluorescent gold nanoprobes for multiplex detection in homogeneous solution. *Small* **2010**, *6* (2), 201-204.
96. Dirkzwager, R. M.; Kinghorn, A. B.; Richards, J. S.; Tanner, J. A., APTEC: aptamer-tethered enzyme capture as a novel rapid diagnostic test for malaria. *Chem Commun* **2015**, *51* (22), 4697-4700.
97. (a) Tiede, C.; Tang, A. A.; Deacon, S. E.; Mandal, U.; Nettleship, J. E.; Owen, R. L.; George, S. E.; Harrison, D. J.; Owens, R. J.; Tomlinson, D. C.; McPherson, M. J., Adhiron: a stable and versatile peptide display scaffold for molecular recognition applications. *Protein Eng Des Sel* **2014**, *27* (5), 145-155; (b) Hoffmann, T.; Stadler, L. K. J.; Busby, M.; Song, Q.; Buxton, A. T.; Wagner, S. D.; Davis, J. J.; Ko Ferrigno, P., Structure-function studies of an engineered scaffold protein derived from stefin A. I: Development of the SQM variant. *Protein Eng Des Sel* **2010**, *23* (5), 403-413.
98. Turk, V.; Stoka, V.; Turk, D., Cystatins: biochemical and structural properties, and medical relevance. *Front Biosci* **2008**, 5406-5420.
99. Turk, V.; Bode, W., The cystatins: protein inhibitors of cysteine proteinases. *FEBS Letters* **1991**, *285* (2), 213-219.
100. Dicker, L.; Ford, R.; McMorran, L.; Räuber, C.; Tang, A.; Tiede, C.; Maqbool, A.; Williamson, D.; Esteves, F.; Kampmeier, F.; McPherson, M.; Ferrigno, P. K.; Tomlinson,

D.; Johnson, M. *Affirmers - next generation affinity tools*; published online at: https://www.avactalifesciences.com/wp-content/uploads/2014/05/Screening-Poster-new-branding.pdf (accessed 13/06/2015), **2014**.

101. Lakhin, A. V.; Tarantul, V. Z.; Gening, L. V., Aptamers: problems, solutions and prospects. *Acta Naturae* **2013**, *5* (4), 34-43.
102. (a) Shimomura, O.; Johnson, F. H.; Saiga, Y., Extraction, purification and properties of aequorin, a bioluminescent protein from the luminous hydromedusan, *Aequorea*. *J Cell Comp Physiol* **1962**, *59*, 223-239; (b) Johnson, F. H.; Shimomura, O.; Saiga, Y.; Gershman, L. C.; Reynolds, G. T.; Waters, J. R., Quantum efficiency of *Cypridina* luminescence, with a note on that of *Aequorea*. *J Cell Comp Physiol* **1962**, *60* (1), 85-103; (c) Tsien, R. Y., The green fluorescent protein. *Annu Rev Biochem* **1998**, *67* (1), 509-544.
103. Prasher, D. C.; Eckenrode, V. K.; Ward, W. W.; Prendergast, F. G.; Cormier, M. J., Primary structure of the *Aequorea victoria* green-fluorescent protein. *Gene* **1992**, *111* (2), 229-233.
104. (a) Chalfie, M.; Tu, Y.; Euskirchen, G.; Ward, W. W.; Prasher, D. C., Green fluorescent protein as a marker for gene expression. *Science* **1994**, *263* (5148), 802-805; (b) Inouye, S.; Tsuji, F. I., Aequorea green fluorescent protein. Expression of the gene and fluorescence characteristics of the recombinant protein. *FEBS Lett* **1994**, *341* (2-3), 277-280.
105. Niswender, K. D.; Blackman, S. M.; Rohde, L.; Magnuson, M. A.; Piston, D. W., Quantitative imaging of green fluorescent protein in cultured cells: comparison of microscopic techniques, use in fusion proteins and detection limits. *J Microsc* **1995**, *180* (Pt 2), 109-116.
106. (a) Satori, C. P.; Henderson, M. M.; Krautkramer, E. A.; Kostal, V.; Distefano, M. D.; Arriaga, E. A., Bioanalysis of eukaryotic organelles. *Chem Rev* **2013**, *113* (4), 2733-2811; (b) Cubitt, A. B.; Heim, R.; Adams, S. R.; Boyd, A. E.; Gross, L. A.; Tsien, R. Y., Understanding, improving and using green fluorescent proteins. *Trends Biochem Sci* **1995**, *20* (11), 448-455.
107. Heim, R.; Tsien, R. Y., Engineering green fluorescent protein for improved brightness, longer wavelengths and fluorescence resonance energy transfer. *Curr Biol* **1996**, *6* (2), 178-182.
108. (a) Miyawaki, A.; Llopis, J.; Heim, R.; McCaffery, J. M.; Adams, J. A.; Ikura, M.; Tsien, R. Y., Fluorescent indicators for Ca^{2+} based on green fluorescent proteins and calmodulin. *Nature* **1997**, *388* (6645), 882-887; (b) Persechini, A.; Lynch, J. A.; Romoser, V. A., Novel fluorescent indicator proteins for monitoring free intracellular Ca^{2+}. *Cell Calcium* **1997**, *22* (3), 209-216.
109. Chudakov, D. M.; Matz, M. V.; Lukyanov, S.; Lukyanov, K. A., Fluorescent proteins and their applications in imaging living cells and tissues. *Physiol Rev* **2010**, *90* (3), 1103-1163.
110. Baird, G. S.; Zacharias, D. A.; Tsien, R. Y., Biochemistry, mutagenesis, and oligomerization of DsRed, a red fluorescent protein from coral. *Proc Natl Acad Sci USA* **2000**, *97* (22), 11984-11989.
111. (a) Griffin, B. A.; Adams, S. R.; Tsien, R. Y., Specific covalent labeling of recombinant protein molecules inside live cells. *Science* **1998**, *281* (5374), 269-272; (b) Albert Griffin, B.; Adams, S. R.; Jones, J.; Tsien, R. Y., Fluorescent labeling of recombinant proteins in

living cells with FlAsH. In *Methods in Enzymology*, Jeremy Thorner, S. D. E.; John, N. A., Eds. Academic Press, **2000**, vol. 327, pp 565-578.

112. Lin, M. Z.; Wang, L., Selective labeling of proteins with chemical probes in living cells. **2008**, vol. 23, pp 131-141.
113. Adams, S. R.; Campbell, R. E.; Gross, L. A.; Martin, B. R.; Walkup, G. K.; Yao, Y.; Llopis, J.; Tsien, R. Y., New biarsenical ligands and tetracysteine motifs for protein labeling *in vitro* and *in vivo*: synthesis and biological applications. *J Am Chem Soc* **2002**, *124* (21), 6063-6076.
114. Stroffekova, K.; Proenza, C.; Beam, K. G., The protein-labeling reagent FlAsH-EDT_2 binds not only to CCXXCC motifs but also non-specifically to endogenous cysteine-rich proteins. *Pflugers Arch* **2001**, *442* (6), 859-866.
115. Halo, T. L.; Appelbaum, J.; Hobert, E. M.; Balkin, D. M.; Schepartz, A., Selective recognition of protein tetraserine motifs with a cell-permeable, pro-fluorescent *bis*-boronic acid. *J Am Chem Soc* **2009**, *131* (2), 438-439.
116. (a) Guignet, E. G.; Hovius, R.; Vogel, H., Reversible site-selective labeling of membrane proteins in live cells. *Nat Biotech* **2004**, *22* (4), 440-444; (b) Kapanidis, A. N.; Ebright, Y. W.; Ebright, R. H., Site-specific incorporation of fluorescent probes into protein: hexahistidine-tag-mediated fluorescent labeling with (Ni^{2+}:nitrilotriacetic acid)$_n$-fluorochrome conjugates. *J Am Chem Soc* **2001**, *123* (48), 12123-12125; (c) Lata, S.; Reichel, A.; Brock, R.; Tampe, R.; Piehler, J., High-affinity adaptors for switchable recognition of histidine-tagged proteins. *J Am Chem Soc* **2005**, *127* (29), 10205-10215.
117. Valko, M.; Morris, H.; Cronin, M. T., Metals, toxicity and oxidative stress. *Curr Med Chem* **2005**, *12* (10), 1161-1208.
118. Goldsmith, C. R.; Jaworski, J.; Sheng, M.; Lippard, S. J., Selective labeling of extracellular proteins containing polyhistidine sequences by a fluorescein-nitrilotriacetic acid conjugate. *J Am Chem Soc* **2006**, *128* (2), 418-419.
119. Hauser, C. T.; Tsien, R. Y., A hexahistidine-Zn^{2+}-dye label reveals STIM1 surface exposure. *Proc Nat Acad Sci USA* **2007**, *104* (10), 3693-3697.
120. Ojida, A.; Honda, K.; Shinmi, D.; Kiyonaka, S.; Mori, Y.; Hamachi, I., Oligo-Asp tag/Zn(II) complex probe as a new pair for labeling and fluorescence imaging of proteins. *J Am Chem Soc* **2006**, *128* (32), 10452-10459.
121. (a) Nitz, M.; Franz, K. J.; Maglathlin, R. L.; Imperiali, B., A powerful combinatorial screen to identify high-affinity terbium(III)-binding peptides. *ChemBioChem* **2003**, *4* (4), 272-276; (b) Martin, L. J.; Sculimbrene, B. R.; Nitz, M.; Imperiali, B., Rapid combinatorial screening of peptide libraries for the selection of lanthanide-binding tags (LBTs). *QSAR Comb Sci* **2005**, *24* (10), 1149-1157; (c) Franz, K. J.; Nitz, M.; Imperiali, B., Lanthanide-binding tags as versatile protein coexpression probes. *ChemBioChem* **2003**, *4* (4), 265-271; (d) Sculimbrene, B. R.; Imperiali, B., Lanthanide-binding tags as luminescent probes for studying protein interactions. *J Am Chem Soc* **2006**, *128* (22), 7346-7352.
122. Fricker, S. P., The therapeutic application of lanthanides. *Chem Soc Rev* **2006**, *35* (6), 524-533.
123. (a) Keppler, A.; Gendreizig, S.; Gronemeyer, T.; Pick, H.; Vogel, H.; Johnsson, K., A general method for the covalent labeling of fusion proteins with small molecules *in vivo*. *Nat Biotechnol* **2003**, *21* (1), 86-89; (b) Keppler, A.; Pick, H.; Arrivoli, C.; Vogel, H.; Johnsson, K., Labeling of fusion proteins with synthetic fluorophores in live cells. *Proc Nat Acad Sci USA* **2004**, *101* (27), 9955-9959.

124. Gautier, A.; Juillerat, A.; Heinis, C.; Corrêa Jr, I. R.; Kindermann, M.; Beaufils, F.; Johnsson, K., An engineered protein tag for multiprotein labeling in living cells. *Chem Biol* **2008**, *15* (2), 128-136.
125. Los, G. V.; Encell, L. P.; McDougall, M. G.; Hartzell, D. D.; Karassina, N.; Zimprich, C.; Wood, M. G.; Learish, R.; Ohana, R. F.; Urh, M.; Simpson, D.; Mendez, J.; Zimmerman, K.; Otto, P.; Vidugiris, G.; Zhu, J.; Darzins, A.; Klaubert, D. H.; Bulleit, R. F.; Wood, K. V., HaloTag: a novel protein labeling technology for cell imaging and protein analysis. *ACS Chem Biol* **2008**, *3* (6), 373-382.
126. Lukinavicius, G.; Umezawa, K.; Olivier, N.; Honigmann, A.; Yang, G.; Plass, T.; Mueller, V.; Reymond, L.; Correa, I. R., Jr.; Luo, Z. G.; Schultz, C.; Lemke, E. A.; Heppenstall, P.; Eggeling, C.; Manley, S.; Johnsson, K., A near-infrared fluorophore for live-cell super-resolution microscopy of cellular proteins. *Nat Chem* **2013**, *5* (2), 132-139.
127. Sun, X.; Zhang, A.; Baker, B.; Sun, L.; Howard, A.; Buswell, J.; Maurel, D.; Masharina, A.; Johnsson, K.; Noren, C. J.; Xu, M.-Q.; Corrêa, I. R., Development of SNAP-tag fluorogenic probes for wash-free fluorescence imaging. *ChemBioChem* **2011**, *12* (14), 2217-2226.
128. Lang, K.; Chin, J. W., Fluorescent imaging: shining a light into live cells. *Nat Chem* **2013**, *5* (2), 81-82.
129. Hori, Y.; Nakaki, K.; Sato, M.; Mizukami, S.; Kikuchi, K., Development of protein-labeling probes with a redesigned fluorogenic switch based on intramolecular association for no-wash live-cell imaging. *Angew Chem Int Ed* **2012**, *51* (23), 5611-5614.
130. Miller, L. W.; Cai, Y.; Sheetz, M. P.; Cornish, V. W., In vivo protein labeling with trimethoprim conjugates: a flexible chemical tag. *Nat Methods* **2005**, *2* (4), 255-257.
131. Jing, C.; Cornish, V. W., Chemical tags for labeling proteins inside living cells. *Acc Chem Res* **2011**, *44* (9), 784-792.
132. Gallagher, S. S.; Jing, C.; Peterka, D. S.; Konate, M.; Wombacher, R.; Kaufman, L. J.; Yuste, R.; Cornish, V. W., A trimethoprim-based chemical tag for live cell two-photon imaging. *ChemBioChem* **2010**, *11* (6), 782-784.
133. Gallagher, S. S.; Sable, J. E.; Sheetz, M. P.; Cornish, V. W., An in vivo covalent TMP-tag based on proximity-induced reactivity. *ACS Chem Biol* **2009**, *4* (7), 547-556.
134. Chen, Z.; Jing, C.; Gallagher, S. S.; Sheetz, M. P.; Cornish, V. W., Second-generation covalent TMP-tag for live cell imaging. *J Am Chem Soc* **2012**, *134* (33), 13692-13699.
135. Jing, C.; Cornish, V. W., A fluorogenic TMP-tag for high signal-to-background intracellular live cell imaging. *ACS Chem Biol* **2013**, *8* (8), 1704-1712.
136. Lin, C.-W.; Ting, A. Y., Transglutaminase-catalyzed site-specific conjugation of small-molecule probes to proteins *in vitro* and on the surface of living cells. *J Am Chem Soc* **2006**, *128* (14), 4542-4543.
137. (a) Chen, I.; Howarth, M.; Lin, W.; Ting, A. Y., Site-specific labeling of cell surface proteins with biophysical probes using biotin ligase. *Nat Meth* **2005**, *2* (2), 99-104; (b) Howarth, M.; Takao, K.; Hayashi, Y.; Ting, A. Y., Targeting quantum dots to surface proteins in living cells with biotin ligase. *Proc Nat Acad Sci USA* **2005**, *102* (21), 7583-7588.
138. (a) Fernandez-Suarez, M.; Baruah, H.; Martinez-Hernandez, L.; Xie, K. T.; Baskin, J. M.; Bertozzi, C. R.; Ting, A. Y., Redirecting lipoic acid ligase for cell surface protein labeling with small-molecule probes. *Nat Biotech* **2007**, *25* (12), 1483-1487; (b) Baruah, H.; Puthenveetil, S.; Choi, Y.-A.; Shah, S.; Ting, A. Y., An engineered aryl azide ligase for

site-specific mapping of protein-protein interactions through photo-cross-linking. *Angew Chem Int Ed* **2008**, *47* (37), 7018-7021.

139. (a) Dierks, T.; Schmidt, B.; Borissenko, L. V.; Peng, J.; Preusser, A.; Mariappan, M.; von Figura, K., Multiple sulfatase deficiency is caused by mutations in the gene encoding the human C_α-formylglycine generating enzyme. *Cell* **2003**, *113* (4), 435-444; (b) Carlson, B. L.; Ballister, E. R.; Skordalakes, E.; King, D. S.; Breidenbach, M. A.; Gilmore, S. A.; Berger, J. M.; Bertozzi, C. R., Function and structure of a prokaryotic formylglycine-generating enzyme. *J Biol Chem* **2008**, *283* (29), 20117-20125; (c) Gilmore, J. M.; Scheck, R. A.; Esser-Kahn, A. P.; Joshi, N. S.; Francis, M. B., *N*-Terminal protein modification through a biomimetic transamination reaction. *Angew Chem Int Ed* **2006**, *45* (32), 5307-5311.
140. (a) Chen, I.; Ting, A. Y., Site-specific labeling of proteins with small molecules in live cells. *Curr Opin Biotechnol* **2005**, *16* (1), 35-40; (b) Foley, T. L.; Burkart, M. D., Site-specific protein modification: advances and applications. *Curr Opin Chem Biol* **2007**, *11* (1), 12-19; (c) Sletten, E. M.; Bertozzi, C. R., Bioorthogonal chemistry: fishing for selectivity in a sea of functionality. *Angew Chem Int Ed* **2009**, *48* (38), 6974-6998.
141. (a) Mazmanian, S. K.; Liu, G.; Ton-That, H.; Schneewind, O., *Staphylococcus aureus* sortase, an enzyme that anchors surface proteins to the cell wall. *Science* **1999**, *285* (5428), 760-763; (b) Popp, M. W.; Antos, J. M.; Grotenbreg, G. M.; Spooner, E.; Ploegh, H. L., Sortagging: a versatile method for protein labeling. *Nat Chem Biol* **2007**, *3* (11), 707-708; (c) Johnsson, N.; George, N.; Johnsson, K., Protein chemistry on the surface of living cells. *ChemBioChem* **2005**, *6* (1), 47-52; (d) George, N.; Pick, H.; Vogel, H.; Johnsson, N.; Johnsson, K., Specific labeling of cell surface proteins with chemically diverse compounds. *J Am Chem Soc* **2004**, *126* (29), 8896-8897; (e) Yin, J.; Liu, F.; Li, X.; Walsh, C. T., Labeling proteins with small molecules by site-specific posttranslational modification. *J Am Chem Soc* **2004**, *126* (25), 7754-7755; (f) Yin, J.; Straight, P. D.; McLoughlin, S. M.; Zhou, Z.; Lin, A. J.; Golan, D. E.; Kelleher, N. L.; Kolter, R.; Walsh, C. T., Genetically encoded short peptide tag for versatile protein labeling by Sfp phosphopantetheinyl transferase. *Proc Nat Acad Sci USA* **2005**, *102* (44), 15815-15820.
142. (a) Lang, K.; Chin, J. W., Cellular incorporation of unnatural amino acids and bioorthogonal labeling of proteins. *Chem Rev* **2014**, *114* (9), 4764-4806; (b) Hinner, M. J.; Johnsson, K., How to obtain labeled proteins and what to do with them. *Curr Opin Biotechnol* **2010,** *21* (6), 766-776; (c) Lim, R. K. V.; Lin, Q., Bioorthogonal chemistry: recent progress and future directions. *Chem Commun* **2010**, *46* (10), 1589-1600; (d) Gong, Y.; Pan, L., Recent advances in bioorthogonal reactions for site-specific protein labeling and engineering. *Tetrahedron Lett* **2015**, *56* (17), 2123-2132.
143. (a) Tang, Y.; Wang, P.; Van Deventer, J. A.; Link, A. J.; Tirrell, D. A., Introduction of an aliphatic ketone into recombinant proteins in a bacterial strain that overexpresses an editing-impaired leucyl-tRNA synthetase. *ChemBioChem* **2009**, *10* (13), 2188-2190; (b) Datta, D.; Wang, P.; Carrico, I. S.; Mayo, S. L.; Tirrell, D. A., A designed phenylalanyl-tRNA synthetase variant allows efficient in vivo incorporation of aryl ketone functionality into proteins. *J Am Chem Soc* **2002**, *124* (20), 5652-5653; (c) Ngo, J. T.; Tirrell, D. A., Noncanonical amino acids in the interrogation of cellular protein synthesis. *Acc Chem Res* **2011**, *44* (9), 677-685.
144. (a) Liu, C. C.; Schultz, P. G., Adding new chemistries to the genetic code. *Annu Rev Biochem* **2010**, *79* (1), 413-444; (b) Wang, L.; Zhang, Z.; Brock, A.; Schultz, P. G., Addition of the keto functional group to the genetic code of *Escherichia coli*. *Proc Nat*

Acad Sci USA **2003**, *100* (1), 56-61; (c) Chin, J. W.; Cropp, T. A.; Anderson, J. C.; Mukherji, M.; Zhang, Z.; Schultz, P. G., An expanded eukaryotic genetic code. *Science* **2003**, *301* (5635), 964-967.

145. (a) Sander, E. G.; Jencks, W. P., Equilibria for additions to the carbonyl group. *J Am Chem Soc* **1968**, *90* (22), 6154-6162; (b) Rose, K., Facile synthesis of homogeneous artificial proteins. *J Am Chem Soc* **1994**, *116* (1), 30-33.
146. Zhang, Z.; Smith, B. A. C.; Wang, L.; Brock, A.; Cho, C.; Schultz, P. G., A new strategy for the site-specific modification of proteins *in vivo*. *Biochemistry* **2003**, *42* (22), 6735-6746.
147. Nauman, D. A.; Bertozzi, C. R., Kinetic parameters for small-molecule drug delivery by covalent cell surface targeting. *Biochim Biophys Acta* **2001**, *1568* (2), 147-154.
148. (a) Dirksen, A.; Dirksen, S.; Hackeng, T. M.; Dawson, P. E., Nucleophilic catalysis of hydrazone formation and transimination: implications for dynamic covalent chemistry. *J Am Chem Soc* **2006**, *128* (49), 15602-15603; (b) Dirksen, A.; Hackeng, T. M.; Dawson, P. E., Nucleophilic catalysis of oxime ligation. *Angew Chem Int Ed* **2006**, *45* (45), 7581-7584; (c) Dirksen, A.; Dawson, P. E., Rapid oxime and hydrazone ligations with aromatic aldehydes for biomolecular labeling. *Bioconjugate Chem* **2008**, *19* (12), 2543-2548.
149. Rayo, J.; Amara, N.; Krief, P.; Meijler, M. M., Live cell labeling of native intracellular bacterial receptors using aniline-catalyzed oxime ligation. *J Am Chem Soc* **2011**, *133* (19), 7469-7475.
150. Himo, F.; Lovell, T.; Hilgraf, R.; Rostovtsev, V. V.; Noodleman, L.; Sharpless, K. B.; Fokin, V. V., Copper(I)-catalyzed synthesis of azoles. DFT Study predicts unprecedented reactivity and intermediates. *J Am Chem Soc* **2005**, *127* (1), 210-216.
151. (a) Codelli, J. A.; Baskin, J. M.; Agard, N. J.; Bertozzi, C. R., Second-generation difluorinated cyclooctynes for copper-free click chemistry. *J Am Chem Soc* **2008**, *130* (34), 11486-11493; (b) Ning, X.; Guo, J.; Wolfert, M. A.; Boons, G. J., Visualizing metabolically labeled glycoconjugates of living cells by copper-free and fast Huisgen cycloadditions. *Angew Chem Int Ed* **2008**, *47* (12), 2253-2255; (c) Gordon, C. G.; Mackey, J. L.; Jewett, J. C.; Sletten, E. M.; Houk, K. N.; Bertozzi, C. R., Reactivity of biarylazacyclooctynones in copper-free click chemistry. *J Am Chem Soc* **2012**, *134* (22), 9199-9208; (d) de Almeida, G.; Sletten, E. M.; Nakamura, H.; Palaniappan, K. K.; Bertozzi, C. R., Thiacycloalkynes for copper-free click chemistry. *Angew Chem Int Ed* **2012**, *51* (10), 2443-2447.
152. (a) Ning, X.; Temming, R. P.; Dommerholt, J.; Guo, J.; Ania, D. B.; Debets, M. F.; Wolfert, M. A.; Boons, G.-J.; van Delft, F. L., Protein modification by strain-promoted alkyne-nitrone cycloaddition. *Angew Chem Int Ed* **2010**, *49* (17), 3065-3068; (b) McKay, C. S.; Moran, J.; Pezacki, J. P., Nitrones as dipoles for rapid strain-promoted 1,3-dipolar cycloadditions with cyclooctynes. *Chem Commun* **2010**, *46* (6), 931-933.
153. Griffin, R. J., The medicinal chemistry of the azido group. *Prog Med Chem* **1994**, *31*, 121-232.
154. Kiick, K. L.; Saxon, E.; Tirrell, D. A.; Bertozzi, C. R., Incorporation of azides into recombinant proteins for chemoselective modification by the Staudinger ligation. *Proc Nat Acad Sci USA* **2002**, *99* (1), 19-24.
155. Huisgen, R., 1,3-Dipolar cycloadditions. Past and future. *Angew Chem Int Ed* **1963**, *2* (10), 565-598.
156. (a) Rostovtsev, V. V.; Green, L. G.; Fokin, V. V.; Sharpless, K. B., A stepwise Huisgen cycloaddition process: copper(I)-catalyzed regioselective “ligation” of azides and

terminal alkynes. *Angew Chem Int Ed* **2002**, *41* (14), 2596-2599; (b) Tornøe, C. W.; Christensen, C.; Meldal, M., Peptidotriazoles on solid phase: [1,2,3]-triazoles by regiospecific copper(I)-catalyzed 1,3-dipolar cycloadditions of terminal alkynes to azides. *J Org Chem* **2002**, *67* (9), 3057-3064; (c) Kolb, H. C.; Sharpless, K. B., The growing impact of click chemistry on drug discovery. *Drug Discov Today* **2003**, *8* (24), 1128-1137.

157. Wang, Q.; Chan, T. R.; Hilgraf, R.; Fokin, V. V.; Sharpless, K. B.; Finn, M. G., Bioconjugation by Copper(I)-Catalyzed Azide-Alkyne [3+2] Cycloaddition. *J Am Chem Soc* **2003**, *125* (11), 3192-3193.
158. Deiters, A.; Cropp, T. A.; Mukherji, M.; Chin, J. W.; Anderson, J. C.; Schultz, P. G., Adding amino acids with novel reactivity to the genetic code of *Saccharomyces cerevisiae*. *J Am Chem Soc* **2003**, *125* (39), 11782-11783.
159. Link, A. J.; Tirrell, D. A., Cell surface labeling of *Escherichia coli via* copper(I)-catalyzed [3+2] cycloaddition. *J Am Chem Soc* **2003**, *125* (37), 11164-11165.
160. Kolb, H. C.; Finn, M. G.; Sharpless, K. B., Click chemistry: diverse chemical function from a few good reactions. *Angew Chem Int Ed* **2001**, *40* (11), 2004-2021.
161. Chang, P. V.; Chen, X.; Smyrniotis, C.; Xenakis, A.; Hu, T.; Bertozzi, C. R.; Wu, P., Metabolic labeling of sialic acids in living animals with alkynyl sugars. *Angew Chem Int Ed* **2009**, *48* (22), 4030-4033.
162. Wolbers, F.; ter Braak, P.; Le Gac, S.; Luttge, R.; Andersson, H.; Vermes, I.; van den Berg, A., Viability study of HL60 cells in contact with commonly used microchip materials. *Electrophoresis* **2006**, *27* (24), 5073-5080.
163. Hong, V.; Steinmetz, N. F.; Manchester, M.; Finn, M. G., Labeling live cells by copper-catalyzed alkyne-azide click chemistry. *Bioconjugate Chem* **2010**, *21* (10), 1912-1916.
164. (a) Hong, V.; Presolski, S. I.; Ma, C.; Finn, M. G., Analysis and optimization of copper-catalyzed azide-alkyne cycloaddition for bioconjugation. *Angew Chem Int Ed* **2009**, *48* (52), 9879-9883; (b) Besanceney-Webler, C.; Jiang, H.; Zheng, T.; Feng, L.; Soriano del Amo, D.; Wang, W.; Klivansky, L. M.; Marlow, F. L.; Liu, Y.; Wu, P., Increasing the efficacy of bioorthogonal click reactions for bioconjugation: a comparative study. *Angew Chem Int Ed* **2011**, *50* (35), 8051-8056.
165. (a) Brotherton, W. S.; Michaels, H. A.; Simmons, J. T.; Clark, R. J.; Dalal, N. S.; Zhu, L., Apparent copper(II)-accelerated azide-alkyne cycloaddition. *Org Lett* **2009**, *11* (21), 4954-4957; (b) Kuang, G.-C.; Michaels, H. A.; Simmons, J. T.; Clark, R. J.; Zhu, L., Chelation-assisted, copper(II)-acetate-accelerated azide-alkyne cycloaddition. *J Org Chem* **2010**, *75* (19), 6540-6548; (c) Uttamapinant, C.; Tangpeerachaikul, A.; Grecian, S.; Clarke, S.; Singh, U.; Slade, P.; Gee, K. R.; Ting, A. Y., Fast, cell-compatible click chemistry with copper-chelating azides for biomolecular labeling. *Angew Chem Int Ed* **2012**, *51* (24), 5852-5856.
166. Agard, N. J.; Prescher, J. A.; Bertozzi, C. R., A strain-promoted [3+2] azide-alkyne cycloaddition for covalent modification of biomolecules in living systems. *J Am Chem Soc* **2004**, *126* (46), 15046-15047.
167. Plass, T.; Milles, S.; Koehler, C.; Schultz, C.; Lemke, E. A., Genetically encoded copper-free click chemistry. *Angew Chem Int Ed* **2011**, *50* (17), 3878-3881.
168. Baskin, J. M.; Prescher, J. A.; Laughlin, S. T.; Agard, N. J.; Chang, P. V.; Miller, I. A.; Lo, A.; Codelli, J. A.; Bertozzi, C. R., Copper-free click chemistry for dynamic *in vivo* imaging. *Proc Natl Acad Sci USA* **2007**, *104* (43), 16793-16797.

169. (a) Laughlin, S. T.; Baskin, J. M.; Amacher, S. L.; Bertozzi, C. R., *In vivo* imaging of membrane-associated glycans in developing zebrafish. *Science* **2008**, *320* (5876), 664-667; (b) Dehnert, K. W.; Baskin, J. M.; Laughlin, S. T.; Beahm, B. J.; Naidu, N. N.; Amacher, S. L.; Bertozzi, C. R., Imaging the sialome during zebrafish development with copper-free click chemistry. *ChemBioChem* **2012**, *13* (3), 353-357.
170. McKay, C. S.; Chigrinova, M.; Blake, J. A.; Pezacki, J. P., Kinetics studies of rapid strain-promoted [3+2]-cycloadditions of nitrones with biaryl-aza-cyclooctynone. *Org Biol Chem* **2012**, *10* (15), 3066-3070.
171. McKay, C. S.; Blake, J. A.; Cheng, J.; Danielson, D. C.; Pezacki, J. P., Strain-promoted cycloadditions of cyclic nitrones with cyclooctynes for labeling human cancer cells. *Chem Commun* **2011**, *47* (36), 10040-10042.
172. Lin, F. L.; Hoyt, H. M.; van Halbeek, H.; Bergman, R. G.; Bertozzi, C. R., Mechanistic investigation of the Staudinger ligation. *J Am Chem Soc* **2005**, *127* (8), 2686-2695.
173. Saxon, E.; Armstrong, J. I.; Bertozzi, C. R., A "traceless" Staudinger ligation for the chemoselective synthesis of amide bonds. *Org Lett* **2000**, *2* (14), 2141-2143.
174. Staudinger, H.; Meyer, J., Über neue organische Phosphorverbindungen III. Phosphinmethylenderivate und Phosphinimine. *Helv Chim Acta* **1919**, *2* (1), 635-646.
175. (a) Saxon, E.; Bertozzi, C. R., Cell surface engineering by a modified Staudinger reaction. *Science* **2000**, *287* (5460), 2007-2010; (b) Saxon, E.; Luchansky, S. J.; Hang, H. C.; Yu, C.; Lee, S. C.; Bertozzi, C. R., Investigating cellular metabolism of synthetic azidosugars with the Staudinger ligation. *J Am Chem Soc* **2002**, *124* (50), 14893-14902; (c) Hangauer, M. J.; Bertozzi, C. R., A FRET-based fluorogenic phosphine for live cell imaging with the Staudinger ligation. *Angew Chem Int Ed* **2008**, *47* (13), 2394-2397.
176. Prescher, J. A.; Dube, D. H.; Bertozzi, C. R., Chemical remodelling of cell surfaces in living animals. *Nature* **2004**, *430* (7002), 873-877.
177. (a) Hang, H. C.; Yu, C.; Kato, D. L.; Bertozzi, C. R., A metabolic labeling approach toward proteomic analysis of mucin-type *O*-linked glycosylation. *Proc Nat Acad Sci USA* **2003**, *100* (25), 14846-14851; (b) Vocadlo, D. J.; Hang, H. C.; Kim, E.-J.; Hanover, J. A.; Bertozzi, C. R., A chemical approach for identifying *O*-Glc*N*Ac-modified proteins in cells. *Proc Nat Acad Sci USA* **2003**, *100* (16), 9116-9121.
178. Charron, G.; Zhang, M. M.; Yount, J. S.; Wilson, J.; Raghavan, A. S.; Shamir, E.; Hang, H. C., Robust fluorescent detection of protein fatty-acylation with chemical reporters. *J Am Chem Soc* **2009**, *131* (13), 4967-4975.
179. Watzke, A.; Köhn, M.; Gutierrez-Rodriguez, M.; Wacker, R.; Schröder, H.; Breinbauer, R.; Kuhlmann, J.; Alexandrov, K.; Niemeyer, C. M.; Goody, R. S.; Waldmann, H., Site-selective protein immobilization by Staudinger ligation. *Angew Chem Int Ed* **2006**, *45* (9), 1408-1412.
180. Gobbo, P.; Luo, W.; Cho, S. J.; Wang, X.; Biesinger, M. C.; Hudson, R. H. E.; Workentin, M. S., Small gold nanoparticles for interfacial Staudinger-Bertozzi ligation. *Org Biol Chem* **2015**, *13* (15), 4605-4612.
181. Eustis, S.; El-Sayed, M. A., Why gold nanoparticles are more precious than pretty gold: noble metal surface plasmon resonance and its enhancement of the radiative and nonradiative properties of nanocrystals of different shapes. *Chem Soc Rev* **2006**, *35* (3), 209-217.
182. Lemieux, G. A.; de Graffenried, C. L.; Bertozzi, C. R., A fluorogenic dye activated by the Staudinger ligation. *J Am Chem Soc* **2003**, *125* (16), 4708-4709.

183. Debets, M. F.; van Berkel, S. S.; Dommerholt, J.; Dirks, A. J.; Rutjes, F. P. J. T.; van Delft, F. L., Bioconjugation with strained alkenes and alkynes. *Acc Chem Res* **2011**, *44* (9), 805-815.
184. (a) van Berkel, S. S.; Dirks, A. J.; Debets, M. F.; van Delft, F. L.; Cornelissen, J. J. L. M.; Nolte, R. J. M.; Rutjes, F. P. J. T., Metal-free triazole formation as a tool for bioconjugation. *ChemBioChem* **2007**, *8* (13), 1504-1508; (b) van Berkel, S. S.; Dirks, A. J.; Meeuwissen, S. A.; Pingen, D. L. L.; Boerman, O. C.; Laverman, P.; van Delft, F. L.; Cornelissen, J. J. L. M.; Rutjes, F. P. J. T., Application of metal-free triazole formation in the synthesis of cyclic RGD–DTPA conjugates. *ChemBioChem* **2008**, *9* (11), 1805-1815.
185. (a) Boger, D. L., Diels-Alder reactions of heterocyclic aza dienes. Scope and applications. *Chem Rev* **1986**, *86* (5), 781-793; (b) Sauer, J.; Heldmann, D. K.; Hetzenegger, J.; Krauthan, J.; Sichert, H.; Schuster, J., 1,2,4,5-Tetrazine: synthesis and reactivity in [4+2] cycloadditions. *Eur J Chem* **1998**, *1998* (12), 2885-2896; (c) Blackman, M. L.; Royzen, M.; Fox, J. M., Tetrazine ligation: fast bioconjugation based on inverse-electron-demand Diels-Alder reactivity. *J Am Chem Soc* **2008**, *130* (41), 13518-13519; (d) Devaraj, N. K.; Weissleder, R.; Hilderbrand, S. A., Tetrazine-based cycloadditions: application to pretargeted live cell imaging. *Bioconjugate Chem* **2008**, *19* (12), 2297-2299.
186. (a) Lang, K.; Davis, L.; Wallace, S.; Mahesh, M.; Cox, D. J.; Blackman, M. L.; Fox, J. M.; Chin, J. W., Genetic encoding of bicyclononynes and *trans*-cyclooctenes for site-specific protein labeling in vitro and in live mammalian cells *via* rapid fluorogenic Diels-Alder reactions. *J Am Chem Soc* **2012**, *134* (25), 10317-10320; (b) Plass, T.; Milles, S.; Koehler, C.; Szymański, J.; Mueller, R.; Wießler, M.; Schultz, C.; Lemke, E. A., Amino acids for Diels–Alder reactions in living cells. *Angew Chem Int Ed* **2012**, *51* (17), 4166-4170.
187. (a) Wang, Y.; Rivera Vera, C. I.; Lin, Q., Convenient synthesis of highly functionalized pyrazolines *via* mild, photoactivated 1,3-dipolar cycloaddition. *Org Lett* **2007**, *9* (21), 4155-4158; (b) Wang, Y.; Hu, W. J.; Song, W.; Lim, R. K. V.; Lin, Q., Discovery of long-wavelength photoactivatable diaryltetrazoles for bioorthogonal 1,3-dipolar cycloaddition reactions. *Org Lett* **2008**, *10* (17), 3725-3728; (c) Yu, Z.; Ho, L. Y.; Wang, Z.; Lin, Q., Discovery of new photoactivatable diaryltetrazoles for photoclick chemistry *via* 'scaffold hopping'. *Bioorg Med Chem Lett* **2011**, *21* (17), 5033-5036.
188. Lang, K.; Davis, L.; Torres-Kolbus, J.; Chou, C.; Deiters, A.; Chin, J. W., Genetically encoded norbornene directs site-specific cellular protein labelling *via* a rapid bioorthogonal reaction. *Nat Chem* **2012**, *4* (4), 298-304.
189. Devaraj, N. K.; Hilderbrand, S.; Upadhyay, R.; Mazitschek, R.; Weissleder, R., Bioorthogonal turn-on probes for imaging small molecules inside living cells. *Angew Chem Int Ed* **2010**, *49* (16), 2869-2872.
190. Rossin, R.; Renart Verkerk, P.; van den Bosch, S. M.; Vulders, R. C. M.; Verel, I.; Lub, J.; Robillard, M. S., *In vivo* chemistry for pretargeted tumor imaging in live mice. *Angew Chem Int Ed* **2010**, *49* (19), 3375-3378.
191. Zeglis, B. M.; Mohindra, P.; Weissmann, G. I.; Divilov, V.; Hilderbrand, S. A.; Weissleder, R.; Lewis, J. S., Modular strategy for the construction of radiometalated antibodies for positron emission tomography based on inverse electron demand Diels–Alder click chemistry. *Bioconjugate Chem* **2011**, *22* (10), 2048-2059.
192. Sletten, E. M.; Bertozzi, C. R., A bioorthogonal quadricyclane ligation. *J Am Chem Soc* **2011**, *133* (44), 17570-17573.

193. Stockmann, H.; Neves, A. A.; Stairs, S.; Brindle, K. M.; Leeper, F. J., Exploring isonitrile-based click chemistry for ligation with biomolecules. *Org Biol Chem* **2011**, *9* (21), 7303-7305.
194. (a) Stairs, S.; Neves, A. A.; Stöckmann, H.; Wainman, Y. A.; Ireland-Zecchini, H.; Brindle, K. M.; Leeper, F. J., Metabolic glycan imaging by isonitrile-tetrazine click chemistry. *ChemBioChem* **2013**, *14* (9), 1063-1067; (b) Wainman, Y. A.; Neves, A. A.; Stairs, S.; Stockmann, H.; Ireland-Zecchini, H.; Brindle, K. M.; Leeper, F. J., Dual-sugar imaging using isonitrile and azido-based click chemistries. *Org Biol Chem* **2013**, *11* (42), 7297-7300.
195. Wang, Y.; Song, W.; Hu, W. J.; Lin, Q., Fast alkene functionalization *in vivo* by photoclick chemistry: HOMO lifting of nitrile imine dipoles. *Angew Chem Int Ed Engl* **2009**, *48* (29), 5330-5333.
196. (a) Song, W.; Wang, Y.; Qu, J.; Lin, Q., Selective functionalization of a genetically encoded alkene-containing protein *via* "photoclick chemistry" in bacterial cells. *J Am Chem Soc* **2008**, *130* (30), 9654-9655; (b) Song, W.; Wang, Y.; Qu, J.; Madden, M. M.; Lin, Q., A photoinducible 1,3-dipolar cycloaddition reaction for rapid, selective modification of tetrazole-containing proteins. *Angew Chem Int Ed* **2008**, *47* (15), 2832-2835; (c) Wang, J.; Zhang, W.; Song, W.; Wang, Y.; Yu, Z.; Li, J.; Wu, M.; Wang, L.; Zang, J.; Lin, Q., A biosynthetic route to photoclick chemistry on proteins. *J Am Chem Soc* **2010**, *132* (42), 14812-14818; (d) Song, W.; Wang, Y.; Yu, Z.; Vera, C. I. R.; Qu, J.; Lin, Q., A metabolic alkene reporter for spatiotemporally controlled imaging of newly synthesized proteins in mammalian cells. *ACS Chem Biol* **2010**, *5* (9), 875-885.
197. Lin, Y. A.; Chalker, J. M.; Floyd, N.; Bernardes, G. J. L.; Davis, B. G., Allyl sulfides are privileged substrates in aqueous cross-metathesis: application to site-selective protein modification. *J Am Chem Soc* **2008**, *130* (30), 9642-9643.
198. (a) Chalker, J. M.; Wood, C. S. C.; Davis, B. G., A convenient catalyst for aqueous and protein Suzuki-Miyaura cross-coupling. *J Am Chem Soc* **2009**, *131* (45), 16346-16347; (b) Spicer, C. D.; Davis, B. G., Palladium-mediated site-selective Suzuki-Miyaura protein modification at genetically encoded aryl halides. *Chem Commun* **2011**, *47* (6), 1698-1700; (c) Spicer, C. D.; Triemer, T.; Davis, B. G., Palladium-mediated cell-surface labeling. *J Am Chem Soc* **2012**, *134* (2), 800-803.
199. (a) Hoveyda, A. H.; Zhugralin, A. R., The remarkable metal-catalysed olefin metathesis reaction. *Nature* **2007**, *450* (7167), 243-251; (b) Trnka, T. M.; Grubbs, R. H., The development of L_2X_2RuCHR olefin metathesis catalysts: an organometallic success story. *Acc Chem Res* **2001**, *34* (1), 18-29.
200. Garber, S. B.; Kingsbury, J. S.; Gray, B. L.; Hoveyda, A. H., Efficient and recyclable monomeric and dendritic Ru-based metathesis catalysts. *J Am Chem Soc* **2000**, *122* (34), 8168-8179.
201. van Hest, J. C. M.; Kiick, K. L.; Tirrell, D. A., Efficient incorporation of unsaturated methionine analogues into proteins *in vivo*. *J Am Chem Soc* **2000**, *122* (7), 1282-1288.
202. Lin, Y. A.; Chalker, J. M.; Davis, B. G., Olefin cross-metathesis on proteins: investigation of allylic chalcogen effects and guiding principles in metathesis partner selection. *J Am Chem Soc* **2010**, *132* (47), 16805-16811.
203. Miyaura, N.; Suzuki, A., Palladium-catalyzed cross-coupling reactions of organoboron compounds. *Chem Rev* **1995**, *95* (7), 2457-2483.
204. Spicer, C. D.; Davis, B. G., Rewriting the bacterial glycocalyx *via* Suzuki-Miyaura cross-coupling. *Chem Commun* **2013**, *49* (27), 2747-2749.

205. Sonogashira, K.; Tohda, Y.; Hagihara, N., A convenient synthesis of acetylenes: catalytic substitutions of acetylenic hydrogen with bromoalkenes, iodoarenes and bromopyridines. *Tetrahedron Lett* **1975**, *16* (50), 4467-4470.
206. Li, N.; Lim, R. K. V.; Edwardraja, S.; Lin, Q., Copper-free Sonogashira cross-coupling for functionalization of alkyne-encoded proteins in aqueous medium and in bacterial cells. *J Am Chem Soc* **2011**, *133* (39), 15316-15319.
207. Li, J.; Lin, S.; Wang, J.; Jia, S.; Yang, M.; Hao, Z.; Zhang, X.; Chen, P. R., Ligand-free palladium-mediated site-specific protein labeling inside Gram-negative bacterial pathogens. *J Am Chem Soc* **2013**, *135* (19), 7330-7338.
208. Nakata, E.; Tsukiji, S.; Hamachi, I., Development of new methods to introduce unnatural functional molecules into native proteins for protein engineering. *Bull Chem Sci Jpn* **2007**, *80* (7), 1268-1279.
209. (a) Hamachi, I.; Nagase, T.; Shinkai, S., A general semisynthetic method for fluorescent saccharide-biosensors based on a lectin. *J Am Chem Soc* **2000**, *122* (48), 12065-12066; (b) Nagase, T.; Nakata, E.; Shinkai, S.; Hamachi, I., Construction of artificial signal transducers on a lectin surface by post-photoaffinity-labeling modification for fluorescent saccharide biosensors. *Chem-Eur J* **2003**, *9* (15), 3660-3669.
210. Takaoka, Y.; Tsutsumi, H.; Kasagi, N.; Nakata, E.; Hamachi, I., One-pot and sequential organic chemistry on an enzyme surface to tether a fluorescent probe at the proximity of the active site with restoring enzyme activity. *J Am Chem Soc* **2006**, *128* (10), 3273-3280.
211. (a) Tamura, T.; Tsukiji, S.; Hamachi, I., Native FKBP12 engineering by ligand-directed tosyl chemistry: labeling properties and application to photo-cross-linking of protein complexes *in vitro* and in living cells. *J Am Chem Soc* **2012**, *134* (4), 2216-2226; (b) Takaoka, Y.; Sun, Y.; Tsukiji, S.; Hamachi, I., Mechanisms of chemical protein ^{19}F-labeling and NMR-based biosensor construction in vitro and in cells using self-assembling ligand-directed tosylate compounds. *Chem Sci* **2011**, *2* (3), 511-520.
212. Fujishima, S.-h.; Yasui, R.; Miki, T.; Ojida, A.; Hamachi, I., Ligand-directed acyl imidazole chemistry for labeling of membrane-bound Proteins on live cells. *J Am Chem Soc* **2012**, *134* (9), 3961-3964.
213. Yamaguchi, T.; Asanuma, M.; Nakanishi, S.; Saito, Y.; Okazaki, M.; Dodo, K.; Sodeoka, M., Turn-on fluorescent affinity labeling using a small bifunctional *O*-nitrobenzoxadiazole unit. *Chem Sci* **2014**, *5* (3), 1021-1029.
214. Koshi, Y.; Nakata, E.; Miyagawa, M.; Tsukiji, S.; Ogawa, T.; Hamachi, I., Target-specific chemical acylation of lectins by ligand-tethered DMAP catalysts. *J Am Chem Soc* **2008**, *130* (1), 245-251.
215. Tamura, T.; Kioi, Y.; Miki, T.; Tsukiji, S.; Hamachi, I., Fluorophore labeling of native FKBP12 by ligand-directed tosyl chemistry allows detection of its molecular interactions *in vitro* and in living cells. *J Am Chem Soc* **2013**, *135* (18), 6782-6785.
216. Miki, T.; Fujishima, S.-h.; Komatsu, K.; Kuwata, K.; Kiyonaka, S.; Hamachi, I., LDAI-based chemical labeling of intact membrane proteins and Its pulse-chase analysis under live cell conditions. *Chem Biol* **2014**, *21* (8), 1013-1022.
217. Matsuo, K.; Kioi, Y.; Yasui, R.; Takaoka, Y.; Miki, T.; Fujishima, S.-h.; Hamachi, I., One-step construction of caged carbonic anhydrase I using a ligand-directed acyl imidazole-based protein labeling method. *Chem Sci* **2013**, *4* (6), 2573-2580.

218. Wang, H.; Koshi, Y.; Minato, D.; Nonaka, H.; Kiyonaka, S.; Mori, Y.; Tsukiji, S.; Hamachi, I., Chemical cell-surface receptor engineering using affinity-guided, multivalent organocatalysts. *J Am Chem Soc* **2011**, *133* (31), 12220-12228.
219. Sato, S.; Nakamura, H., Ligand-directed selective protein modification based on local single-electron-transfer catalysis. *Angew Chem Int Ed* **2013**, *52* (33), 8681-8684.
220. (a) Jessani, N.; Cravatt, B. F., The development and application of methods for activity-based protein profiling. *Curr Opin Chem Biol* **2004**, *8* (1), 54-59; (b) Speers, A. E.; Cravatt, B. F., Chemical strategies for activity-based proteomics. *ChemBioChem* **2004**, *5* (1), 41-47.
221. (a) Jessani, N.; Liu, Y.; Humphrey, M.; Cravatt, B. F., Enzyme activity profiles of the secreted and membrane proteome that depict cancer cell invasiveness. *Proc Natl Acad Sci USA* **2002**, *99* (16), 10335-10340; (b) Patricelli, M. P.; Cravatt, B. F., Characterization and manipulation of the acyl chain selectivity of fatty acid amide hydrolase. *Biochemistry* **2001**, *40* (20), 6107-6115.
222. Saghatelian, A.; Jessani, N.; Joseph, A.; Humphrey, M.; Cravatt, B. F., Activity-based probes for the proteomic profiling of metalloproteases. *Proc Natl Acad Sci USA* **2004**, *101* (27), 10000-10005.
223. Liu, Y.; Patricelli, M. P.; Cravatt, B. F., Activity-based protein profiling: the serine hydrolases. *Proc Natl Acad Sci USA* **1999**, *96* (26), 14694-14699.
224. (a) Adam, G. C.; Sorensen, E. J.; Cravatt, B. F., Proteomic profiling of mechanistically distinct enzyme classes using a common chemotype. *Nat Biotechnol* **2002**, *20* (8), 805-809; (b) Adam, G. C.; Burbaum, J.; Kozarich, J. W.; Patricelli, M. P.; Cravatt, B. F., Mapping enzyme active sites in complex proteomes. *J Am Chem Soc* **2004**, *126* (5), 1363-1368.
225. Speers, A. E.; Cravatt, B. F., Profiling enzyme activities *in vivo* using click chemistry methods. *Chem Biol* **2004**, *11* (4), 535-546.
226. Leung, D.; Hardouin, C.; Boger, D. L.; Cravatt, B. F., Discovering potent and selective reversible inhibitors of enzymes in complex proteomes. *Nat Biotechnol* **2003**, *21* (6), 687-691.
227. Xie, H.; Mire, J.; Kong, Y.; Chang, M.; Hassounah, H. A.; Thornton, C. N.; Sacchettini, J. C.; Cirillo, J. D.; Rao, J., Rapid point-of-care detection of the tuberculosis pathogen using a BlaC-specific fluorogenic probe. *Nat Chem* **2012**, *4* (10), 802-809.
228. Li, L.; Li, Z.; Shi, W.; Li, X.; Ma, H., Sensitive and selective near-infrared fluorescent off-on probe and its application to imaging different levels of β-lactamase in *Staphylococcus aureus*. *Anal Chem* **2014**, *86* (12), 6115-6120.
229. Tallman, K. R.; Beatty, K. E., Far-red fluorogenic probes for esterase and lipase detection. *ChemBioChem* **2015**, *16* (1), 70-75.
230. Zhang, L.; Duan, D.; Liu, Y.; Ge, C.; Cui, X.; Sun, J.; Fang, J., Highly selective off-on fluorescent probe for imaging thioredoxin reductase in living cells. *J Am Chem Soc* **2014**, *136* (1), 226-233.
231. Zhang, W.; Ma, Z.; Du, L.; Li, M., Design strategy for photoinduced electron transfer-based small-molecule fluorescent probes of biomacromolecules. *Analyst* **2014**, *139* (11), 2641-2649.
232. Terai, T.; Kikuchi, K.; Urano, Y.; Kojima, H.; Nagano, T., A long-lived luminescent probe to sensitively detect arylamine *N*-acetyltransferase (NAT) activity of cells. *Chem Commun* **2012**, *48* (16), 2234-2236.

233. (a) Gardiner, S. J.; Begg, E. J., Pharmacogenetics, drug-metabolizing enzymes, and clinical practice. *Pharmacol Rev* **2006**, *58* (3), 521-590; (b) McCarver, D. G.; Hines, R. N., The ontogeny of human drug-metabolizing enzymes: phase II conjugation enzymes and regulatory mechanisms. *J Pharmacol Exp Ther* **2002**, *300* (2), 361-366.
234. Husain, A.; Zhang, X.; Doll, M. A.; States, J. C.; Barker, D. F.; Hein, D. W., Identification of *N*-acetyltransferase 2 (*NAT2*) transcription start sites and quantitation of *NAT2*-specific mRNA in human tissues. *Drug Metab Dispos* **2007**, *35* (5), 721-727.
235. Wang, X.; Cui, L.; Zhou, N.; Zhu, W.; Wang, R.; Qian, X.; Xu, Y., A highly selective and sensitive near-infrared fluorescence probe for arylamine *N*-acetyltransferase 2 *in vitro* and *in vivo*. *Chem Sci* **2013**, *4* (7), 2936-2940.
236. (a) Balk, S.; Maitra, U.; Konig, B., Terbium(III)-cholate functionalized vesicles as luminescent indicators for the enzymatic conversion of dihydroxynaphthalene diesters. *Chem Commun* **2014**, *50* (58), 7852-7854; (b) Pershagen, E.; Borbas, K. E., Multiplex detection of enzymatic activity with responsive lanthanide-based luminescent probes. *Angew Chem Int Ed* **2015**, *54* (6), 1787-1790; (c) Terai, T.; Kikuchi, K.; Iwasawa, S.-y.; Kawabe, T.; Hirata, Y.; Urano, Y.; Nagano, T., Modulation of luminescence intensity of lanthanide complexes by photoinduced electron transfer and its application to a long-lived protease probe. *J Am Chem Soc* **2006**, *128* (21), 6938-6946.
237. (a) Fujikawa, Y.; Urano, Y.; Komatsu, T.; Hanaoka, K.; Kojima, H.; Terai, T.; Inoue, H.; Nagano, T., Design and synthesis of highly sensitive fluorogenic substrates for glutathione *S*-transferase and application for activity imaging in living cells. *J Am Chem Soc* **2008**, *130* (44), 14533-14543; (b) Kamiya, M.; Urano, Y.; Ebata, N.; Yamamoto, M.; Kosuge, J.; Nagano, T., Extension of the applicable range of fluorescein: a fluorescein-based probe for western blot analysis. *Angew Chem Int Ed* **2005**, *44* (34), 5439-5441; (c) Kamiya, M.; Kobayashi, H.; Hama, Y.; Koyama, Y.; Bernardo, M.; Nagano, T.; Choyke, P. L.; Urano, Y., An enzymatically activated fluorescence probe for targeted tumor imaging. *J Am Chem Soc* **2007**, *129* (13), 3918-3929; (d) Zhang, S.; Yang, C.; Lu, W.; Huang, J.; Zhu, W.; Li, H.; Xu, Y.; Qian, X., A highly selective space-folded photo-induced electron transfer fluorescent probe for carbonic anhydrase isozymes IX and its applications for biological imaging. *Chem Commun* **2011**, *47* (29), 8301-8303; (e) Zhang, H.; Fan, J.; Wang, J.; Zhang, S.; Dou, B.; Peng, X., An off-on COX-2-specific fluorescent probe: targeting the Golgi apparatus of cancer cells. *J Am Chem Soc* **2013**, *135* (31), 11663-11669; (f) Silvers, W. C.; Prasai, B.; Burk, D. H.; Brown, M. L.; McCarley, R. L., Profluorogenic reductase substrate for rapid, selective, and sensitive visualization and detection of human cancer cells that overexpress NQO1. *J Am Chem Soc* **2013**, *135* (1), 309-314; (g) Sun, Q.; Li, J.; Liu, W.-N.; Dong, Q.-J.; Yang, W.-C.; Yang, G.-F., Non-peptide-based fluorogenic small-molecule probe for elastase. *Anal Chem* **2013**, *85* (23), 11304-11311.
238. Chang, J. W.; Moellering, R. E.; Cravatt, B. F., An activity-based imaging probe for the integral membrane hydrolase KIAA1363. *Angew Chem Int Ed* **2012**, *51* (4), 966-970.
239. Mertens, M. D.; Schmitz, J.; Horn, M.; Furtmann, N.; Bajorath, J.; Mareš, M.; Gütschow, M., A coumarin-labeled vinyl sulfone as tripeptidomimetic activity-based probe for cysteine cathepsins. *ChemBioChem* **2014**, *15* (7), 955-959.
240. Martín-Couce, L.; Martín-Fontecha, M.; Palomares, Ó.; Mestre, L.; Cordomí, A.; Hernangomez, M.; Palma, S.; Pardo, L.; Guaza, C.; López-Rodríguez, M. L.; Ortega-Gutiérrez, S., Chemical probes for the recognition of cannabinoid receptors in native systems. *Angew Chem Int Ed* **2012**, *51* (28), 6896-6899.

241. Anslyn, E. V., Supramolecular and chemical cascade approaches to molecular sensing. *J Am Chem Soc* **2010**, *132* (45), 15833-15835.
242. Laurieri, N.; Crawford, M. H. J.; Kawamura, A.; Westwood, I. M.; Robinson, J.; Fletcher, A. M.; Davies, S. G.; Sim, E.; Russell, A. J., Small molecule colorimetric probes for specific detection of human arylamine *N*-acetyltransferase 1, a potential breast cancer biomarker. *J Am Chem Soc* **2010**, *132* (10), 3238-3239.
243. Russell, A. J.; Westwood, I. M.; Crawford, M. H. J.; Robinson, J.; Kawamura, A.; Redfield, C.; Laurieri, N.; Lowe, E. D.; Davies, S. G.; Sim, E., Selective small molecule inhibitors of the potential breast cancer marker, human arylamine *N*-acetyltransferase 1, and its murine homologue, mouse arylamine *N*-acetyltransferase 2. *Bioorg Med Chem* **2009**, *17* (2), 905-918.
244. Butcher, N. J.; Boukouvala, S.; Sim, E.; Minchin, R. F., Pharmacogenetics of the arylamine *N*-acetyltransferases. *Pharmacogenomics J* **2002**, *2* (1), 30-42.
245. (a) Sim, E.; Walters, K.; Boukouvala, S., Arylamine *N*-acetyltransferases: from structure to function. *Drug Metab Rev* **2008**, *40* (3), 479-510; (b) Weber, W. W.; Hein, D. W., *N*-Acetylation pharmacogenetics. *Pharmacol Rev* **1985**, *37* (1), 25-79.
246. Hein, D. W.; Doll, M. A.; Rustan, T. D.; Gray, K.; Feng, Y.; Ferguson, R. J.; Grant, D. M., Metabolic activation and deactivation of arylamine carcinogens by recombinant human NAT1 and polymorphic NAT2 acetyltransferases. *Carcinogenesis* **1993**, *14* (8), 1633-1638.
247. (a) Sinclair, J. C.; Sandy, J.; Delgoda, R.; Sim, E.; Noble, M. E., Structure of arylamine *N*-acetyltransferase reveals a catalytic triad. *Nat Struct Biol* **2000**, *7* (7), 560-564; (b) Wu, H.; Dombrovsky, L.; Tempel, W.; Martin, F.; Loppnau, P.; Goodfellow, G. H.; Grant, D. M.; Plotnikov, A. N., Structural basis of substrate-binding specificity of human arylamine *N*-acetyltransferases. *J Biol Chem* **2007,** *282* (41), 30189-30197.
248. Riddle, B.; Jencks, W. P., Acetyl coenzyme A: arylamine *N*-acetyltransferase: role of the acetyl-enzyme intermediate and the effects of substituents on the rate. *J Biol Chem* **1971**, *246* (10), 3250-3258.
249. (a) Hickman, D.; Risch, A.; Buckle, V.; Spurr, N. K.; Jeremiah, S. J.; McCarthy, A.; Sim, E., Chromosomal localization of human genes for arylamine *N*-acetyltransferase. *Biochem J* **1994**, *297* (Pt 3), 441-445; (b) Blum, M.; Grant, D. M.; McBride, W.; Heim, M.; Meyer, U. A., Human arylamine *N*-acetyltransferase genes: isolation, chromosomal localization, and functional expression. *DNA Cell Biol* **1990**, *9* (3), 193-203; (c) Franke, S.; Klawitz, I.; Schnakenberg, E.; Rommel, B.; Van de Ven, W.; Bullerdiek, J.; Schloot, W., Isolation and mapping of a cosmid clone containing the human *NAT2* gene. *Biochem Biophys Res Commun* **1994**, *199* (1), 52-55.
250. Walker, K.; Ginsberg, G.; Hattis, D.; Johns, D. O.; Guyton, K. Z.; Sonawane, B., Genetic polymorphism in *N*-acetyltransferase (NAT): Population distribution of NAT1 and NAT2 activity. *J Toxicol Environ Health B Crit Rev* **2009**, *12* (5-6), 440-472.
251. Woosley, R. L.; Drayer, D. E.; Reidenberg, M. M.; Nies, A. S.; Carr, K.; Oates, J. A., Effect of acetylator phenotype on the rate at which procainamide induces antinuclear antibodies and the lupus syndrome. *New Eng J Med* **1978**, *298* (21), 1157-1159.
252. Cartwright, R.; Rogers, H.; Barham-Hall, D.; Glashan, R.; Ahmad, R.; Higgins, E.; Kahn, M., Role of *N*-acetyltransferase phenotypes in bladder carcinogenesis: a pharmacogenetic epidemiological approach to bladder cancer. *Lancet* **1982**, *320* (8303), 842-846.

253. (a) Vatsis, K. P.; Weber, W. W., Structural heterogeneity of caucasian *N*-acetyltransferase at the NAT1 gene locus. *Arch Biochem Biophys* **1993**, *301* (1), 71-76; (b) Grant, D. M.; Hughes, N. C.; Janezic, S. A.; Goodfellow, G. H.; Chen, H. J.; Gaedigk, A.; Yu, V. L.; Grewal, R., Human acetyltransferase polymorphisms. *Mutat Res* **1997**, *376* (1-2), 61-70; (c) Payton, M. A.; Sim, E., Genotyping human arylamine *N*-acetyltransferase type 1 (*NAT1*): the identification of two novel allelic variants. *Biochem Pharmacol* **1998**, *55* (3), 361-366.

254. Bell, D. A.; Stephens, E. A.; Castranio, T.; Umbach, D. M.; Watson, M.; Deakin, M.; Elder, J.; Hendrickse, C.; Duncan, H.; Strange, R. C., Polyadenylation polymorphism in the acetyltransferase 1 gene (NAT1) increases risk of colorectal cancer. *Cancer Res* **1995**, *55* (16), 3537-3542.

255. (a) Wakefield, L.; Cornish, V.; Long, H.; Griffiths, W. J.; Sim, E., Deletion of a xenobiotic metabolizing gene in mice affects folate metabolism. *Biochem Biophys Res Commun* **2007**, *364* (3), 556-560; (b) Minchin, R. F., Acetylation of *p*-aminobenzoylglutamate, a folic acid catabolite, by recombinant human arylamine *N*-acetyltransferase and U937 cells. *Biochem J* **1995**, *307* (Pt 1), 1-3; (c) Ward, A.; Summers, M. J.; Sim, E., Purification of recombinant human *N*-acetyltransferase type 1 (NAT1) expressed in *E. coli* and characterization of its potential role in folate metabolism. *Biochem Pharmacol* **1995**, *49* (12), 1759-1767; (d) Rodrigues-Lima, F.; Dairou, J.; Laurieri, N.; Busi, F.; Dupret, J. M., Pharmacogenomics, biochemistry, toxicology, microbiology and cancer research in one go. *Pharmacogenomics* **2011**, *12* (8), 1091-1093.

256. (a) Wakefield, L.; Cornish, V.; Long, H.; Kawamura, A.; Zhang, X.; Hein, D. W.; Sim, E., Mouse arylamine *N*-acetyltransferase 2 (*Nat2*) expression during embryogenesis: a potential marker for the developing neuroendocrine system. *Biomarkers* **2008**, *13* (1), 106-118; (b) Wakefield, L.; Cornish, V.; Broackes-Carter, F.; Sim, E., Arylamine *N*-acetyltransferase 2 expression in the developing heart. *J Histochem Cytochem* **2005**, *53* (5), 583-592; (c) Cornish, V. A.; Pinter, K.; Boukouvala, S.; Johnson, N.; Labrousse, C.; Payton, M.; Priddle, H.; Smith, A. J. H.; Sim, E., Generation and analysis of mice with a targeted disruption of the arylamine *N*-acetyltransferase type 2 gene. *Pharmacogenomics J* **2003**, *3* (3), 169-177; (d) Mitchell, M. K.; Futscher, B. W.; McQueen, C. A., Developmental expression of *N*-acetyltransferases in C57Bl/6 mice. *Drug Metab Dispos* **1999**, *27* (2), 261-264.

257. Kawamura, A.; Westwood, I.; Wakefield, L.; Long, H.; Zhang, N.; Walters, K.; Redfield, C.; Sim, E., Mouse *N*-acetyltransferase type 2, the homologue of human *N*-acetyltransferase type 1. *Biochem Pharmacol* **2008**, *75* (7), 1550-1560.

258. Laurieri, N., Investigating the endogenous role of human *N*-acetyltransferase 1, as potential breast cancer biomarker, using chemical biology. D.Phil. thesis, Department of Pharmacology, University of Oxford, **2012**.

259. (a) Sim, E.; Abuhammad, A.; Ryan, A., Arylamine *N*-acetyltransferases: from drug metabolism and pharmacogenetics to drug discovery. *Br J Pharmacol* **2014**, *171* (11), 2705-2725; (b) Butcher, N.; Minchin, R., Arylamine *N*-acetyltransferase 1: a novel drug target in cancer development. *Pharmacol Rev* **2012**, *64* (1), 147-165.

260. (a) Cancer Research UK - Breast Cancer Incidence Statistics. http://www.cancerresearchuk.org/cancer-info/cancerstats/types/breast/incidence/uk-breast-cancer-incidence-statistics (accessed 05/04/2015); (b) Sasieni, P. D.; Shelton, J.; Ormiston-Smith, N.; Thomson, C. S.; Silcocks, P. B., What is the lifetime risk of

developing cancer? The effect of adjusting for multiple primaries. *Br J Cancer* **2011**, *105* (3), 460-465.

261. Deroo, B. J.; Korach, K. S., Estrogen receptors and human disease. *J Clin Invest* **2006**, *116* (3), 561-570.
262. Buzdar, A., The place of chemotherapy in the treatment of early breast cancer. *Br J Cancer* **1998**, *78* (Suppl 4), 16-20.
263. Turner, N.; Pearson, A.; Sharpe, R.; Lambros, M.; Geyer, F.; Lopez-Garcia, M. A.; Natrajan, R.; Marchio, C.; Iorns, E.; Mackay, A.; Gillett, C.; Grigoriadis, A.; Tutt, A.; Reis-Filho, J. S.; Ashworth, A., FGFR1 amplification drives endocrine therapy resistance and is a therapeutic target in breast cancer. *Cancer Res* **2010**, *70* (5), 2085-2094.
264. Cancer Research UK - Breast Cancer Survival Statistics. http://www.cancerresearchuk.org/cancer-info/cancerstats/types/breast/survival/ (accessed 05/04/2015).
265. Wolff, A. C.; Hammond, M. E.; Schwartz, J. N.; Hagerty, K. L.; Allred, D. C.; Cote, R. J.; Dowsett, M.; Fitzgibbons, P. L.; Hanna, W. M.; Langer, A.; McShane, L. M.; Paik, S.; Pegram, M. D.; Perez, E. A.; Press, M. F.; Rhodes, A.; Sturgeon, C.; Taube, S. E.; Tubbs, R.; Vance, G. H.; van de Vijver, M.; Wheeler, T. M.; Hayes, D. F., American Society of Clinical Oncology/College of American Pathologists guideline recommendations for human epidermal growth factor receptor 2 testing in breast cancer. *Arch Pathol Lab Med* **2007**, *131* (1), 18-43.
266. Tozlu, S.; Girault, I.; Vacher, S.; Vendrell, J.; Andrieu, C.; Spyratos, F.; Cohen, P.; Lidereau, R.; Bieche, I., Identification of novel genes that co-cluster with estrogen receptor alpha in breast tumor biopsy specimens, using a large-scale real-time reverse transcription-PCR approach. *Endocr Relat Cancer* **2006**, *13* (4), 1109-1120.
267. Adam, P. J.; Berry, J.; Loader, J. A.; Tyson, K. L.; Craggs, G.; Smith, P.; De Belin, J.; Steers, G.; Pezzella, F.; Sachsenmeir, K. F.; Stamps, A. C.; Herath, A.; Sim, E.; O'Hare, M. J.; Harris, A. L.; Terrett, J. A., Arylamine *N*-acetyltransferase 1 Is highly expressed in breast cancers and conveys enhanced growth and resistance to etoposide *in vitro*. *Mol Cancer Res* **2003**, *1* (11), 826-835.
268. Bièche, I.; Girault, I.; Urbain, E.; Tozlu, S.; Lidereau, R., Relationship between intratumoral expression of genes coding for xenobiotic-metabolizing enzymes and benefit from adjuvant tamoxifen in estrogen receptor alpha-positive postmenopausal breast carcinoma. *Breast Cancer Res* **2004**, *6* (3), R252-R263.
269. Johansson, I.; Nilsson, C.; Berglund, P.; Lauss, M.; Ringnér, M.; Olsson, H.; Luts, L.; Sim, E.; Thorstensson, S.; Fjällskog, M.-L.; Hedenfalk, I., Gene expression profiling of primary male breast cancers reveals two unique subgroups and identifies *N*-acetyltransferase-1 (*NAT1*) as a novel prognostic biomarker. *Breast Cancer Research:BCR* **2012**, *14* (1), R31-R31.
270. Endo, Y.; Yamashita, H.; Takahashi, S.; Sato, S.; Yoshimoto, N.; Asano, T.; Hato, Y.; Dong, Y.; Fujii, Y.; Toyama, T., Immunohistochemical determination of the miR-1290 target arylamine *N*-acetyltransferase 1 (NAT1) as a prognostic biomarker in breast cancer. *BMC Cancer* **2014**, *14* (1), 990.
271. Wakefield, L.; Robinson, J.; Long, H.; Ibbitt, J. C.; Cooke, S.; Hurst, H. C.; Sim, E., Arylamine *N*-acetyltransferase 1 expression in breast cancer cell lines: a potential marker in estrogen receptor-positive tumors. *Genes Chromosomes Cancer* **2008**, *47* (2), 118-126.

272. Tiang, J. M.; Butcher, N. J.; Minchin, R. F., Small molecule inhibition of arylamine *N*-acetyltransferase type 1 inhibits proliferation and invasiveness of MDA-MB-231 breast cancer cells. *Biochem Biophys Res Commun* **2010**, *393* (1), 95-100.
273. Tiang, J. M.; Butcher, N. J.; Minchin, R. F., Effects of human arylamine *N*-acetyltransferase 1 knockdown in triple-negative breast cancer cell lines. *Cancer Med* **2015**, *4* (4), 565-574.
274. Tiang, J. M.; Butcher, N. J.; Cullinane, C.; Humbert, P. O.; Minchin, R. F., RNAi-mediated knock-down of arylamine *N*-acetyltransferase 1. Expression induces E-cadherin up-regulation and cell-cell contact growth inhibition. *PLoS ONE* **2011**, *6* (2), e17031.
275. (a) Sim, E.; Pinter, K.; Mushtaq, A.; Upton, A.; Sandy, J.; Bhakta, S.; Noble, M., Arylamine *N*-acetyltransferases: a pharmacogenomic approach to drug metabolism and endogenous function. *Biochem Soc Trans* **2003**, *31* (3), 615-619; (b) Cao, W.; Strnatka, D.; McQueen, C. A.; Hunter, R. J.; Erickson, R. P., *N*-Acetyltransferase 2 activity and folate levels. *Life Sciences* **2010**, *86* (3-4), 103-106.
276. Ragunathan, N.; Dairou, J.; Pluvinage, B.; Martins, M.; Petit, E.; Janel, N.; Dupret, J. M.; Rodrigues-Lima, F., Identification of the xenobiotic-metabolizing enzyme arylamine *N*-acetyltransferase 1 as a new target of cisplatin in breast cancer cells: molecular and cellular mechanisms of inhibition. *Mol Pharmacol* **2008**, *73* (6), 1761-1768.
277. Liu, L.; Wagner, C. R.; Hanna, P. E., Isoform-selective inactivation of human arylamine *N*-acetyltransferases by reactive metabolites of carcinogenic arylamines. *Chem Res Toxicol* **2009**, *22* (12), 1962-1974.
278. Lee, J. H.; Lu, H. F.; Wang, D. Y.; Chen, D. R.; Su, C. C.; Chen, Y. S.; Yang, J. H.; Chung, J. G., Effects of tamoxifen on DNA adduct formation and arylamines *N*-acetyltransferase activity in human breast cancer cells. *Res Commun Mol Pathol Pharmacol* **2004**, *115-116*, 217-233.
279. Deng, Z. J.; Butcher, N. J.; Mortimer, G. M.; Jia, Z.; Monteiro, M. J.; Martin, D. J.; Minchin, R. F., Interaction of human arylamine *N*-acetyltransferase 1 with different nanomaterials. *Drug Metab Dispos* **2014**, *42* (3), 377-383.
280. Tomašić, T.; Peterlin Mašič, L., Rhodanine as a scaffold in drug discovery: a critical review of its biological activities and mechanisms of target modulation. *Exp Opin Drug Discov* **2012**, *7* (7), 549-560.
281. (a) Egleton, J. E., Synthesis and mechanistic evaluation of colorimetric probes for the specific detection of human arylamine *N*-acetyltransferase 1. Part II Thesis, Department of Chemistry, University of Oxford, **2011**; (b) Thinnes, C. C., Synthesis of biosensors as breast cancer diagnostics. Part II Thesis, Department of Chemistry, University of Oxford, **2010**.
282. Verdonk, M. L.; Cole, J. C.; Hartshorn, M. J.; Murray, C. W.; Taylor, R. D., Improved protein-ligand docking using GOLD. *Proteins* **2003**, *52* (4), 609-623.
283. Williams, R. *p*Ka data compiled by R. Williams. http://research.chem.psu.edu/brpgroup/*p*Ka_compilation.pdf (accessed 07/05/2015).
284. Varney, A., Improving breast cancer diagnostics. Part II Thesis, Department of Biochemistry, University of Oxford, **2011**.
285. (a) Zhao, Y.; Truhlar, D. G., Density functionals with broad applicability in chemistry. *Acc Chem Res* **2008**, *41* (2), 157-167; (b) Zhao, Y.; Truhlar, D., The M06 suite of density functionals for main group thermochemistry, thermochemical kinetics, noncovalent interactions, excited states, and transition elements: two new functionals and

systematic testing of four M06-class functionals and 12 other functionals. *Theor Chem Acc* **2008**, *120* (1-3), 215-241.

286. Frisch, M. J. T., G. W.; Schlegel, H. B.; Scuseria, G. E.; Robb, M. A.; Cheeseman, J. R.; Scalmani, G.; Barone, V.; Mennucci, B.; Petersson, G. A.; Nakatsuji, H.; Caricato, M.; Li, X.; Hratchian, H. P.; Izmaylov, A. F.; Bloino, J.; Zheng, G.; Sonnenberg, J. L.; Hada, M.; Ehara, M.; Toyota, K.; Fukuda, R.; Hasegawa, J.; Ishida, M.; Nakajima, T.; Honda, Y.; Kitao, O.; Nakai, H.; Vreven, T.; Montgomery, J. A., Jr.; Peralta, J. E.; Ogliaro, F.; Bearpark, M.; Heyd, J. J.; Brothers, E.; Kudin, K. N.; Staroverov, V. N.; Kobayashi, R.; Normand, J.; Raghavachari, K.; Rendell, A.; Burant, J. C.; Iyengar, S. S.; Tomasi, J.; Cossi, M.; Rega, N.; Millam, J. M.; Klene, M.; Knox, J. E.; Cross, J. B.; Bakken, V.; Adamo, C.; Jaramillo, J.; Gomperts, R.; Stratmann, R. E.; Yazyev, O.; Austin, A. J.; Cammi, R.; Pomelli, C.; Ochterski, J. W.; Martin, R. L.; Morokuma, K.; Zakrzewski, V. G.; Voth, G. A.; Salvador, P.; Dannenberg, J. J.; Dapprich, S.; Daniels, A. D.; Farkas, Ö.; Foresman, J. B.; Ortiz, J. V.; Cioslowski, J.; Fox, D. J. *Gaussian 09, Revision B.01; Gaussian, Inc., Wallingford CT*, **2009**.
287. (a) Dr R. F. Martínez, Chemistry Research Laboratory, 12 Mansfield Road, Oxford, OX1 3TA, UK; (b) The Research & Technological Innovation and Supercomputing Center of Extremadura (CenitS) is gratefully acknowledged for permitting the use of the super-computer LUSITANIA.
288. Fors, B. P.; Krattiger, P.; Strieter, E.; Buchwald, S. L., Water-mediated catalyst preactivation: an efficient protocol for C-N cross-coupling reactions. *Org Lett* **2008**, *10* (16), 3505-3508.
289. Heo, C. K. M.; Bunting, J. W., Rate-determining steps in Michael-type additions and E1cB reactions in aqueous solution. *J Org Chem* **1992**, *57* (13), 3570-3578.
290. (a) Wang, H.; Vath, G. M.; Kawamura, A.; Bates, C. A.; Sim, E.; Hanna, P. E.; Wagner, C. R., Over-expression, purification, and characterization of recombinant human arylamine *N*-acetyltransferase 1. *Protein J* **2005**, *24* (2), 65-77; (b) Dairou, J.; Atmane, N.; Dupret, J. M.; Rodrigues-Lima, F., Reversible inhibition of the human xenobiotic-metabolizing enzyme arylamine *N*-acetyltransferase 1 by *S*-nitrosothiols. *Biochem Biophys Res Commun* **2003**, *307* (4), 1059-1065.
291. Challis, B. C.; Iley, J. N., Pseudomolecular rearrangement of *O*-ethyl-*N*-methyl toluene-4-sulphonimidate to *N*-ethyl-*N*-methyltoluene-4-sulphonamide and its relevance to the nucleophilic properties of neutral sulphonamides. *J Chem Soc Perk T 2* **1985**, *5*, 699-703.
292. Levchenko, E. S.; Markovskii, L. N.; Kirsanov, A. V., *Zh Org Khim+* **1967**, *3*, 1481.
293. Leca, D.; Song, K.; Amatore, M.; Fensterbank, L.; Lacôte, E.; Malacria, M., Iodine(III)-mediated preparations of nitrogen-containing sulfur derivatives: dramatic influence of the sulfur oxidation state. *Chem-Eur J* **2004**, *10* (4), 906-916.
294. Mlostoń, G.; Warkentin, J.; Linden, A.; Heimgartner, H., Reactions of dimethoxycarbene with *N*-tosylated imines. *Helv Chim Acta* **2007**, *90* (10), 2024-2036.
295. S., L. E.; N., M. L.; V., K. A., *Zh Org Khim+* **1967**, *3*, (a) 1481; (b) 1273.
296. Duarte-Ruiz, A.; Nunez-Dallos, N.; Garzon-Tovar, L.; Wurst, K.; Avella-Moreno, E.; Gomez-Baquero, F., Synthesis and structure of $[Na_4(DMSO)_{15}][(I_3)_3(I)]$. Self-assembly of hexacoordinated sodium. *Chem Commun* **2011**, *47* (25), 7110-7112.
297. Lee, S.-P., Investigation on arylamine *N*-acetyltransferases and synthetic inhibitors for diagnostic and therapeutic purposes. Part II Thesis, Department of Biochemistry, University of Oxford, **2009**.

298. (a) Stanley, L. A.; Coroneos, E.; Cuff, R.; Hickman, D.; Ward, A.; Sim, E., Immunochemical detection of arylamine *N*-acetyltransferase in normal and neoplastic bladder. *J Histochem Cytochem* **1996**, *44* (9), 1059-1067; (b) Stanley, L. A.; Copp, A. J.; Pope, J.; Rolls, S.; Smelt, V.; Perry, V. H.; Sim, E., Immunochemical detection of arylamine *N*-acetyltransferase during mouse embryonic development and in adult mouse brain. *Teratology* **1998**, *58* (5), 174-182.
299. Johnson, N., The role of human arylamine *N*-acetyltransferase in development and disease. D.Phil. Thesis, Department of Pharmacology, University of Oxford, **2001**.
300. Hadavizadeh, K. S., Synthesis of colorimetric and fluorescent probes for breast cancer biomarker detection. Part II Thesis, Department of Chemistry, University of Oxford, **2013**.
301. Kawamura, A.; Graham, J.; Mushtaq, A.; Tsiftsoglou, S. A.; Vath, G. M.; Hanna, P. E.; Wagner, C. R.; Sim, E., Eukaryotic arylamine *N*-acetyltransferase. Investigation of substrate specificity by high-throughput screening. *Biochem Pharmacol* **2005**, *69* (2), 347-359.
302. Bordwell, F. G., Equilibrium acidities in dimethyl sulfoxide solution. *Acc Chem Res* **1988**, *21* (12), 456-463.
303. Cresset, provider of chemistry software and consulting services; FORGE, a powerful computational suite to understand SAR and design; www.cresset-group.com.
304. Wang, H.-S.; Wang, Y.-C.; Pan, Y.-M.; Zhao, S.-L.; Chen, Z.-F., Simultaneous reduction of nitro- to amino-group in the palladium-catalyzed Suzuki cross-coupling reaction. *Tetrahedron Lett* **2008**, *49* (16), 2634-2637.
305. Sanz, R.; Guilarte, V.; Pérez, A., Straightforward selective preparation of nitro- or amino-indoles from 2-halonitroanilines and alkynes. First synthesis of 7-amino-5-nitroindoles. *Tetrahedron Lett* **2009**, *50* (31), 4423-4426.
306. Guilbault, G. G., in *Fluorescence Techniques in Cell Biology*. Thaer, A.; Sernetz, M., Eds. Springer Berlin Heidelberg, **1973**; pp 235-242.
307. Bridges, J.; Creaven, P.; Williams, R., The fluorescence of some biphenyl derivatives. **1965**; vol. 96, pp 872-878.
308. Barker, R., Synthesis of Fluorescent Inhibitors of the Breast Cancer Biomarker hNAT1. Part II Thesis, Department of Chemistry, University of Oxford, **2014**.
309. Yu, Y.; Singh, S. K.; Liu, A.; Li, T.-K.; Liu, L. F.; LaVoie, E. J., Substituted dibenzo[*c,h*]cinnolines: topoisomerase I-targeting anticancer agents. *Bioorg Med Chem* **2003**, *11* (7), 1475-1491.
310. (a) Green, J. P., Fluorescence of naphthoquinones. *Nature* **1954**, *174* (4425), 369; (b) Umadevi, M.; Ramasubbu, A.; Vanelle, P.; Ramakrishnan, V., Spectral investigations on 2-methyl-1,4-naphthoquinone: solvent effects, host-guest interactions and SERS. *J Raman Spec* **2003**, *34* (2), 112-120; (c) Jali, B. R.; Masud, K.; Baruah, J. B., Selectivity in changes of fluorescence emission of 1,4-naphthoquinone derivatives by manganese and cadmium ions. *Polyhedron* **2013**, *51*, 75-81.
311. Riedl, J.; Pohl, R.; Rulíšek, L.; Hocek, M., Synthesis and photophysical properties of biaryl-substituted nucleos(t)ides. Polymerase synthesis of DNA probes bearing solvatochromic and *p*H-sensitive dual fluorescent and ^{19}*F*-NMR labels. *J Org Chem* **2012**, *77* (2), 1026-1044.
312. Herman, P.; Murtaza, Z.; Lakowicz, J. R., Sensing of carbon dioxide by a decrease in photoinduced electron transfer quenching. *Anal Biochem* **1999**, *272* (1), 87-93.

313. Schwarz, F. P.; Wasik, S. P., Fluorescence measurements of benzene, naphthalene, anthracene, pyrene, fluoranthene, and benzo[*e*]pyrene in water. *Anal Chem* **1976**, *48* (3), 524-528.
314. Dangerfield, E. M.; Plunkett, C. H.; Win-Mason, A. L.; Stocker, B. L.; Timmer, M. S. M., Protecting-group-free synthesis of amines: synthesis of primary amines from aldehydes *via* reductive amination. *J Org Chem* **2010**, *75* (16), 5470-5477.
315. Razi Naqvi, K.; Donatsch, J.; Wild, U. P., The influence of molecular geometry on the fluorescence spectra of biphenyl and the polyphenyls. *Chem Phys Lett* **1975**, *34* (2), 285-288.
316. Lavis, L. D.; Raines, R. T., Bright ideas for chemical biology. *ACS Chem Biol* **2008**, *3* (3), 142-155.
317. Kathuria, A.; Priya, N.; Chand, K.; Singh, P.; Gupta, A.; Jalal, S.; Gupta, S.; Raj, H. G.; Sharma, S. K., Substrate specificity of acetoxy derivatives of coumarins and quinolones towards calreticulin mediated transacetylation: investigations on antiplatelet function. *Bioorg Med Chem* **2012**, *20* (4), 1624-1638.
318. De, S. K.; Gibbs, R. A., An efficient and practical procedure for the synthesis of 4-substituted coumarins. *Synthesis* **2005**, *2005* (08), 1231-1233.
319. Zorab, R., Synthesis, evaluation and optimisation of fluorescent probes for hNAT1, a breast cancer biomarker. Part II Thesis, Department of Chemistry, University of Oxford, **2015**.
320. Li, Y.-T.; Wang, L.-X.; Pavlova, N. V.; Li, S.-C.; Lee, Y. C., α-KDOase activity in oyster and synthesis of α- and β-4-methylumbelliferyl ketosides of 3-deoxy-D-manno-octulosonic acid (KDO). *J Biol Chem* **1997**, *272* (42), 26419-26424.
321. Vivian, J. T.; Callis, P. R., Mechanisms of tryptophan fluorescence shifts in proteins. *Biophys J* **2001**, *80* (5), 2093-2109.
322. Yao, S.; Schafer-Hales, K. J.; Belfield, K. D., A new water-soluble near-neutral ratiometric fluorescent *p*H indicator. *Org Lett* **2007**, *9* (26), 5645-5648.
323. Berndt, F.; Ioffe, I.; Granovsky, A. A.; Mahrwald, R.; Tannert, S.; Kovalenko, S. A.; Ernsting, N. P., 7-Amino-dibenzofuran-3-carboxylate: a new probe for femtosecond dynamic microsolvation studies of biomolecules. *J Photochem Photobiol A* **2012**, *234*, 164-170.
324. Perry, R. J.; Wilson, B. D., Palladium-mediated carbonylation and coupling reactions of iodobenzene and aniline. Model reactions for the preparation of aromatic polyamides. *Macromolecules* **1993**, *26* (7), 1503-1508.
325. Wils, P.; Warnery, A.; Phung-Ba, V.; Legrain, S.; Scherman, D., High lipophilicity decreases drug transport across intestinal epithelial cells. *J Pharm Exp Ther* **1994**, *269* (2), 654-658.
326. Leeson, P. D.; Springthorpe, B., The influence of drug-like concepts on decision-making in medicinal chemistry. *Nat Rev Drug Discov* **2007**, *6* (11), 881-890.
327. Artursson, P.; Palm, K.; Luthman, K., Caco-2 monolayers in experimental and theoretical predictions of drug transport. *Adv Drug Deliver Rev* **2012**, *64, Supplement*, 280-289.
328. Roughley, S. D.; Jordan, A. M., The medicinal chemist's toolbox: an analysis of reactions used in the pursuit of drug candidates. *J Med Chem* **2011**, *54* (10), 3451-3479.
329. Fish, P. V.; Deur, C.; Gan, X.; Greene, K.; Hoople, D.; Mackenny, M.; Para, K. S.; Reeves, K.; Ryckmans, T.; Stiff, C.; Stobie, A.; Wakenhut, F.; Whitlock, G. A., Design and

synthesis of morpholine derivatives. SAR for dual serotonin & noradrenaline reuptake inhibition. *Bioorg Med Chem Lett* **2008**, *18* (8), 2562-2566.

330. Xu, W.; Gray, D. L.; Glase, S. A.; Barta, N. S., Design and synthesis of reboxetine analogs morpholine derivatives as selective norepinephrine reuptake inhibitors. *Bioorg Med Chem Lett* **2008**, *18* (20), 5550-5553.
331. Allegra, J. C.; Lippman, M. E., The effects of 17β estradiol and tamoxifen on the ZR-75-1 human breast cancer cell line in defined medium. *Eur J Cancer* **1965**, *16* (8), 1007-1015.
332. Fick, A., Über Diffusion. *Ann Phys* **185**, *170* (1), 59-86.
333. (a) Buswell, J. A.; Hamp, S.; Eriksson, K. E., Intracellular quinone reduction in *Sporotrichum pulverulentum* by a NAD(P)H:quinone oxidoreductase. *FEBS Lett* **1979**, *108* (1), 229-232; (b) Han, Y.; Shen, H.; Carr, B. I.; Wipf, P.; Lazo, J. S.; Pan, S. S., NAD(P)H:quinone oxidoreductase-1-dependent and -independent cytotoxicity of potent quinone Cdc25 phosphatase inhibitors. *J Pharmacol Exp Ther* **2004**, *309* (1), 64-70.
334. (a) Palacín, M.; Estévez, R.; Bertran, J.; Zorzano, A., Molecular biology of mammalian plasma membrane amino acid transporters. **1998**; vol. 78, pp 969-1054; (b) Halestrap, A.; Meredith, D., The SLC16 gene family - from monocarboxylate transporters (MCTs) to aromatic amino acid transporters and beyond. *Pflügers Archiv* **2004**, *447* (5), 619-628; (c) Verrey, F.; Closs, E.; Wagner, C.; Palacin, M.; Endou, H.; Kanai, Y., CATs and HATs: the SLC7 family of amino acid transporters. *Pflügers Archiv* **2004**, *447* (5), 532-542; (d) Pineda, M.; Fernández, E.; Torrents, D.; Estévez, R.; López, C.; Camps, M.; Lloberas, J.; Zorzano, A.; Palacín, M., Identification of a membrane protein, LAT-2, that co-expresses with 4F2 heavy chain, an L-type amino acid transport activity with broad specificity for small and large zwitterionic amino acids. *J Biol Chem* **1999**, *274* (28), 19738-19744; (e) Torrents, D.; Estévez, R.; Pineda, M.; Fernández, E.; Lloberas, J.; Shi, Y.-B.; Zorzano, A.; Palacín, M., Identification and characterization of a membrane protein (y+L amino acid transporter-1) that associates with 4F2hc to encode the amino acid transport Activity y+L. A candidate gene for lysinuric protein intolerance. *J Biol Chem* **1998**, *273* (49), 32437-32445.
335. Heubach, G.; Hoerlein, G.; Sachse, B. Fungicidal isoxazole derivatives. German Patent Number DE 2525023, **1967**, published 16/12/1967.
336. Bertolini, G.; Aquino, M.; Biffi, M.; d'Atri, G.; Di Pierro, F.; Ferrario, F.; Mascagni, P.; Somenzi, F.; Zaliani, A.; Leoni, F., A new rational hypothesis for the pharmacophore of the active metabolite of leflunomide, a potent immunosuppressive drug. *J Med Chem* **1997**, *40* (13), 2011-2016.
337. Porcheddu, A.; De Luca, L.; Giacomelli, G., A straightforward route to Piloty's Acid derivatives: a class of potential nitroxyl-generating prodrugs. *Synlett* **2009**, *2009* (13), 2149-2153.
338. Tang, S.; He, J.; Sun, Y.; He, L.; She, X., Efficient and regioselective one-pot synthesis of 3-substituted and 3,5-disubstituted isoxazoles. *Org Lett* **2009**, *11* (17), 3982-3985.
339. Spange, S.; Schreiter, K.; Hofmann, K., Chiral, solvatochromic Schiff bases containing the (*S*)-proline or (*R*)-3-aminopropane-1,2-diol functionality. *Synthesis* **2006**, *2006* (13), 2100-2102.
340. Rozeboom, M. D.; Houk, K. N.; Searles, S.; Seyedrezai, S. E., Photoelectron spectroscopy of *N*-aryl cyclic amines. Variable conformations and relationships to gas- and solution-phase basicities. *J Am Chem Soc* **1982**, *104* (12), 3448-3453.

341. del Amo, E. M.; Urtti, A.; Yliperttula, M., Pharmacokinetic role of L-type amino acid transporters LAT1 and LAT2. *Eur J Pharm Sci* **2008**, *35* (3), 161-174.
342. Walton, J. G. A.; Patterson, S.; Liu, G.; Haraldsen, J. D.; Hollick, J. J.; Slawin, A. M. Z.; Ward, G. E.; Westwood, N. J., Synthesis and biological evaluation of functionalised tetrahydro-β-carboline analogues as inhibitors of *Toxoplasma gondii* invasion. *Org Biol Chem* **2009**, *7* (15), 3049-3060.
343. Berger, V.; Larondelle, Y.; Trouet, A.; Schneider, Y.-J., Transport mechanisms of the large neutral amino acid L-phenylalanine in the human intestinal epithelial Caco-2 cell line. *J Nutr* **2000**, *130* (11), 2780-2788.
344. Lenagh-Snow, G. M. J.; Araújo, N.; Jenkinson, S. F.; Martínez, R. F.; Shimada, Y.; Yu, C.-Y.; Kato, A.; Fleet, G. W. J., Azetidine iminosugars from the cyclization of 3,5-di-*O*-triflates of α-furanosides and of 2,4-di-*O*-triflates of β-pyranosides derived from glucose. *Org Lett* **2012**, *14* (8), 2142-2145.
345. Minchin, R. F.; Hanna, P. E.; Dupret, J.-M.; Wagner, C. R.; Rodrigues-Lima, F.; Butcher, N. J., Arylamine *N*-acetyltransferase 1. *Int J Biochem Cell Biol* **2007**, *39* (11), 1999-2005.
346. Ward, A.; Hickman, D.; Gordon, J. W.; Sim, E., Arylamine *N*-acetyltransferase in human red blood cells. *Biochem Pharmacol* **1992**, *44* (6), 1099-1104.
347. Payton, M.; Smelt, V.; Upton, A.; Sim, E., A method for genotyping murine arylamine *N*-acetyltransferase type 2 (*NAT2*): a gene expressed in preimplantation embryonic stem cells encoding an enzyme acetylating the folate catabolite *p*-aminobenzoylglutamate. *Biochem Pharmacol* **1999**, *58* (5), 779-785.
348. Witham, K. L.; Butcher, N. J.; Sugamori, K. S.; Brenneman, D.; Grant, D. M.; Minchin, R. F., 5-methyl-tetrahydrofolate and the *S*-adenosylmethionine cycle in C57BL/6J mouse tissues: gender differences and effects of arylamine *N*-acetyltransferase-1 deletion. *PLoS ONE* **2013**, *8* (10), e77923.
349. (a) Derewlany, L. O.; Knie, B.; Koren, G., Arylamine *N*-acetyltransferase activity of the human placenta. *J Pharmacol Exp Ther* **1994**, *269* (2), 756-760; (b) Derewlany, L. O.; Knie, B.; Koren, G., Human placental transfer and metabolism of *p*-aminobenzoic acid. *J Pharmacol Exp Ther* **1994**, *269* (2), 761-765; (c) Smelt, V. A.; Upton, A.; Adjaye, J.; Payton, M. A.; Boukouvala, S.; Johnson, N.; Mardon, H. J.; Sim, E., Expression of arylamine *N*-acetyltransferases in pre-term placentas and in human pre-implantation embryos. *Hum Mol Genet* **2000**, *9* (7), 1101-1107.
350. Murphy, M.; Seagroatt, V.; Hey, K.; O'Donnell, M.; Godden, M.; Jones, N.; Botting, B., Neural tube defects 1974-94 - down but not out. *Arch Dis Child Fetal Neonatal Ed* **1996**, *75* (2), F133-F134.
351. Erickson, R. P., Genes, environment, and orofacial clefting: *N*-acetyltransferase and folic acid. *J Craniofac Surg* **2010**, *21* (5), 1384-1387.
352. Jensen, L. E.; Hoess, K.; Mitchell, L. E.; Whitehead, A. S., Loss of function polymorphisms in *NAT1* protect against spina bifida. *Hum Genet* **2006**, *120* (1), 52-57.
353. (a) Cao, W.; Chau, B.; Hunter, R.; Strnatka, D.; McQueen, C. A.; Erickson, R. P., Only low levels of exogenous *N*-acetyltransferase can be achieved in transgenic mice. *Pharmacogenomics J* **2005**, *5* (4), 255-261; (b) Sim, E.; Westwood, I.; Fullam, E., Arylamine *N*-acetyltransferases. *Expert Opin Drug Metab Toxicol* **2007**, *3* (2), 169-184.
354. Erickson, R. P.; Cao, W.; Acuna, D. K.; Strnatka, D. W.; Hunter, R. J.; Chau, B. T.; Wakefield, L. V.; Sim, E.; McQueen, C. A., Confirmation of the role of *N*-acetyltransferase 2 in teratogen-induced cleft palate using transgenics and knockouts. *Mol Reprod Dev* **2008**, *75* (6), 1071-1076.

355. Wakefield, L.; Boukouvala, S.; Sim, E., Characterisation of CpG methylation in the upstream control region of mouse *Nat2*: evidence for a gene-environment interaction in a polymorphic gene implicated in folate metabolism. *Gene* **2010**, *452* (1), 16-21.
356. Kim, S. J.; Kang, H. S.; Chang, H. L.; Jung, Y. C.; Sim, H. B.; Lee, K. S.; Ro, J.; Lee, E. S., Promoter hypomethylation of the *N*-acetyltransferase 1 gene in breast cancer. *Oncol Rep* **2008**, *19* (3), 663-668.
357. (a) Sinclair, J.; Sim, E., A fragment consisting of the first 204 amino-terminal amino acids of human arylamine *N*-acetyltransferase 1 (NAT1) and the first transacetylation step of catalysis. *Biochem Pharmacol* **1997**, *53* (1), 11-16; (b) Mushtaq, A.; Payton, M.; Sim, E., The COOH terminus of arylamine *N*-acetyltransferase from *Salmonella typhimurium* controls enzymic activity. *J Biol Chem* **2002**, *277* (14), 12175-12181.
358. Brooke, E. W.; Davies, S. G.; Mulvaney, A. W.; Pompeo, F.; Sim, E.; Vickers, R. J., An approach to identifying novel substrates of bacterial arylamine *N*-acetyltransferases. *Bioorg Med Chem* **2003**, *11* (7), 1227-1234.
359. Loftsson, T.; Vogensen, S. B.; Brewster, M. E.; Konradsdottir, F., Effects of cyclodextrins on drug delivery through biological membranes. *J Pharm Sci* **2007**, *96* (10), 2532-2546.
360. Lewis, A. M.; Ough, M.; Hinkhouse, M. M.; Tsao, M. S.; Oberley, L. W.; Cullen, J. J., Targeting NAD(P)H:quinone oxidoreductase (NQO1) in pancreatic cancer. *Mol Carcinog* **2005**, *43* (4), 215-224.
361. Berger, S. L., Histone modifications in transcriptional regulation. *Curr Opin Genet Dev* **2002**, *12* (2), 142-148.
362. Dhalluin, C.; Carlson, J. E.; Zeng, L.; He, C.; Aggarwal, A. K.; Zhou, M.-M.; Zhou, M.-M., Structure and ligand of a histone acetyltransferase bromodomain. *Nature* **1999**, *399* (6735), 491-496.
363. (a) Berndsen, C. E.; Albaugh, B. N.; Tan, S.; Denu, J. M., Catalytic mechanism of a MYST family histone acetyltransferase. *Biochemistry* **2007**, *46* (3), 623-629; (b) Tanner, K. G.; Trievel, R. C.; Kuo, M. H.; Howard, R. M.; Berger, S. L.; Allis, C. D.; Marmorstein, R.; Denu, J. M., Catalytic mechanism and function of invariant glutamic acid 173 from the histone acetyltransferase GCN5 transcriptional coactivator. *J Biol Chem* **1999**, *274* (26), 18157-18160.
364. Yan, Y.; Harper, S.; Speicher, D. W.; Marmorstein, R., The catalytic mechanism of the ESA1 histone acetyltransferase involves a self-acetylated intermediate. *Nat Struct Biol* **2002**, *9* (11), 862-869.
365. Ballester, P. J.; Westwood, I.; Laurieri, N.; Sim, E.; Richards, W. G., Prospective virtual screening with Ultrafast Shape Recognition: the identification of novel inhibitors of arylamine *N*-acetyltransferases. *J R Soc Interface* **2010**, *7* (43), 335-342.
366. Filippakopoulos, P.; Knapp, S., Targeting bromodomains: epigenetic readers of lysine acetylation. *Nat Rev Drug Discov* **2014**, *13* (5), 337-356.
367. Wehner, M.; Janssen, D.; Schäfer, G.; Schrader, T., Sequence-selective peptide recognition with designed modules. *Eur J Org Chem* **2006**, *2006* (1), 138-153.
368. Pangborn, A. B.; Giardello, M. A.; Grubbs, R. H.; Rosen, R. K.; Timmers, F. J., Safe and convenient procedure for solvent purification. *Organometallics* **1996**, *15* (5), 1518-1520.
369. Lien, J.-C.; Huang, L.-J.; Teng, C.-M.; Wang, J.-P.; Kuo, S.-C., Synthesis of 2-alkoxy-1,4-naphthoquinone derivatives as antiplatelet, antiinflammatory, and antiallergic agents. *Chem Pharm Bull* **2002**, *50* (5), 672-674.

370. Temtsin-Krayz, G.; Shames, A. I.; Bittner, S., Radical decomposition of *N*,*N*-*bis*-(3-chloro-1,4-naphthoquinon-2-yl) amine in basic conditions followed by EPR. *Res Chem Intermediat* **2003**, *29* (3), 325-333.
371. Wang, X.; Ma, Y.; Ju, T., Regioselective alkylation of saccharin with alcohols under Mitsunobu conditions. *J Chem Res* **2013**, *37* (7), 417-419.
372. Baslé, E.; Jean, M.; Gouault, N.; Renault, J.; Uriac, P., Fluorous scavenger for parallel preparation of tertiary sulfonamides leading to secondary amines. *Tet Lett* **2007**, *48* (46), 8138-8140.
373. Egli, R.; Eugster, C. H., Über die selektive katalytische Reduktion von substituierten Anilinen zu substituierten Cyclohexylaminen und von Benzol- bzw. Phenyl-alkan-sulfonsäuren zu Cyclohexan- bzw. Cyclohexylalkan-sulfonsäuren. *Helv Chim Acta* **1975**, *58* (8), 2321-2346.
374. Scully, J. F.; Brown, E. V., The sulfonation of furan and furan homologs: preparation of furansulfonamides. *J Org Chem* **1954**, *19* (6), 894-901.
375. Lien, J.-C.; Huang, L.-J.; Wang, J.-P.; Teng, C.-M.; Lee, K.-H.; Kuo, S.-C., Synthesis and antiplatelet, antiinflammatory, and antiallergic activities of 2-substituted 3-chloro-1,4-naphthoquinone derivatives. *Bioorg Med Chem* **1997**, *5* (12), 2111-2120.
376. Chankeshwara, S. V.; Chakraborti, A. K., Indium(III) halides as new and highly efficient catalysts for *N*-*tert*-butoxycarbonylation of amines. *Synthesis* **2006**, *16*, 2784-2788.
377. Thinnes, C. C., Synthesis of Biosensors as Breast Cancer Diagnostics. Part II Thesis, Department of Chemistry, University of Oxford, **2010**.
378. Baumann, K.; Flohr, A.; Goetschi, E.; Jacobsen, H.; Jolidon, S.; Luebbers, T, US Patent Application Number US 2009/215759 A1, **2009**.
379. Zhang, C. L.; Zhang, D. F.; Zhao, H. Y.; Lin, Z. Y.; Huang, H. H., A facile protocol for *N*-Cbz protection of amines in PEG-600. *Chinese Chem Lett* **2012**, *23* (7), 789-792.
380. Sah, P. P. T.; Tao, K.-Y., *p*-Bromobenzazide as a reagent for the identification of alcohols. *Recueil Trav Chim Pays-Bas* **1939**, *58* (1), 12-16.
381. Liu, S.; Wang, Y.; Yang, X.; Jiang, J., Selective reduction of nitroarenes to *N*-arylhydroxylamines by use of Zn in a CO_2–H_2O system, promoted by ultrasound. *Res Chem Intermed* **2012**, *38* (9), 2471-2478.
382. Sreedhar, B.; Arundhathi, R.; Reddy, P. L.; Kantam, M. L., CuI nanoparticles for C-N and C-O cross-coupling of heterocyclic amines and phenols with chlorobenzenes. *J Org Chem* **2009**, *74* (20), 7951-7954.
383. Ross, A. J.; Lang, H. L.; Jackson, R. F. W., Much improved conditions for the Negishi cross-coupling of iodoalanine derived zinc reagents with aryl halides. *J Org Chem* **2010**, *75* (1), 245-248.
384. Gerisch, S.; Jakubke, H.-D.; Kreuzfeld, H.-J., Enzymatic peptide synthesis in frozen aqueous systems: Use of N_α-unprotected unusual acyl donors. *Tetrahedron:-Asymmetr* **1995**, *6* (12), 3039-3045.
385. Oswald, C. L.; Carrillo-Márquez, T.; Caggiano, L.; Jackson, R. F. W., Negishi cross-coupling reactions of α-amino acid-derived organozinc reagents and aromatic bromides. *Tetrahedron* **2008**, *64* (4), 681-687.
386. (a) Croft, A. K.; Foley, M. K., Proline-rich proteins-deriving a basis for residue-based selectivity in polyphenolic binding. *Org Biol Chem* **2008**, *6* (9), 1594-1600; (b) Malavašič, Č.; Wagger, J.; Stanovnik, B.; Svete, J., (*S*)-*N*-Benzyl-3(6)-methylpiperazine-2,5-diones as chiral solvating agents for *N*-acylamino acid esters. *Tetrahedron-Asymmetr* **2008**, *19* (13), 1557-1567.

387. Fadnavis, N. W.; Reddy, N. P.; Bhalerao, U. T., Reverse micelles, an alternative to aqueous medium for microbial reactions: yeast mediated resolution of α-amino acids in reverse micelles. *J Org Chem* **1989**, *54* (13), 3218-3221.
388. Jahreis, G.; Smalla, K.; Fittkau, S., Thermitase – eine thermostabile Serinprotease. II. Synthese von substratanalogen Peptidchlormethylketonen als potentielle irreversible Enzyminhibitoren. *J Prakt Chem* **1984**, *326* (1), 41-47.
389. Liu, Y.; Jia, G.; Ling, X.; Lan, N.; Zheng, Y.; Li, S.; Zhang, L.; Liu, L.; Zhang, R.; Xue, Y., Decomposition of copper -amino acid complexes by oxalic acid dihydrate. *Can J Chem* **2012**, *90* (6), 557-559.
390. Ye, Q.; Komarov, I. V.; Kirby, A. J.; Jones, M., 3,5,7-Trimethyl-1-azatricyclo[3.3.1.13,7]decan-2-ylidene, an aminocarbene without π conjugation. *J Org Chem* **2002**, *67* (26), 9288-9294.
391. Kemp, D. S.; Petrakis, K. S., Synthesis and conformational analysis of *cis*,*cis*-1,3,5-trimethylcyclohexane-1,3,5-tricarboxylic acid. *J Org Chem* **1981**, *46* (25), 5140-5143.
392. Schmaderer, H.; Hohenleutner, A.; König, B., Synthesis of a bicyclic diamine derived from Kemp's Acid. *Synth Commun* **2009**, *39* (14), 2596-2604.
393. Kelly, S. L.; Sim, E., Arylamine *N*-acetyltransferase in Balb/c mice: identification of a novel mouse isoenzyme by cloning and expression *in vitro*. *Biochem J* **1994**, *302* (Pt 2), 347-353.